DISSERTATION

ILLUMINATING THE IMPACT OF REPRODUCTIVE EXTRACELLULAR VESICLES: MODELING MATERNAL SIGNALS DURING PREIMPLANTATION EMBRYO DEVELOPMENT

Submitted by

Nico Graham Menjivar

Department of Biomedical Sciences

In partial fulfillment of the requirements

For the Degree of Doctor of Philosophy

Colorado State University

Fort Collins, Colorado

Fall 2024

Doctoral Committee:

Advisor: Dawit Tesfaye
Co-Advisor: Rebecca L. Krisher

Adam Chicco
Fiona K. Hollinshead

Copyright by Nico Graham Menjivar 2024

All Rights Reserved

ABSTRACT

ILLUMINATING THE IMPACT OF REPRODUCTIVE EXTRACELLULAR VESICLES: MODELING MATERNAL SIGNALS DURING PREIMPLANTATION EMBRYO DEVELOPMENT

Pre-implantation embryo development is a complex process beginning around the time of gametic syngamy, the process of two gametes fusing to create a zygote (the first cell of a new organism). Passively transient through the oviduct, the presumptive zygote is then characterized by a series of timely cleavage divisions, activation of the embryonic genome, compaction (morula formation), cavitation (blastocyst formation), and summing in hatching from the encapsulated zona pellucida and implantation to the uterine wall. Unfortunately, the current IVF system that occurs ex vivo, completely bypasses the critical maternal-embryonic crosstalk that would inevitably persist during the primitive stages of pre-implantation development. It is thought that the low yield of developed embryos in vitro, is in part due to the failed ability to recapitulate a suitable system that mimics the maternal environment, shunting early cleavage stage embryos for failure. However, the reservations regarding maternal signals secreted to developing embryos, the reproductively inaccessible nature of the organs, and suboptimal in vitro systems to study replicate in vivo function has limited our complex understanding of these stages.

In this dissertation, I aimed to interrogate multiple aspects of preimplantation embryo development, under the primary premise of modeling maternal signal during the pre-implantation period. Utilizing the intrinsic interest in the growing field of extracellular vesicle (EV) research and their significance in intercellular signaling, particularly their communicative role in selective biological information transfer, my first exertion was developing a source of EVs from in vitro

cultured granulosa cells for use during IVM (necessitating maternal signals amid the follicle microenvironment). Through the analysis of this dataset (in combination with Gebremedhn et al. 2020) together with immunofluorescence and functional experiments, we characterized diverging miRNA profiles of EVs secreted by granulosa cells subjected to polarizing thermal conditions, that are abundantly up taken by COCs and modulate key developmental events that safeguard developing embryos exposed to conditions of stress.

Next, I built upon this work by generating a functional 3D organoid model to study the cellular and extracellular response of the oviduct using a multi-omics approach. Using this atlas as a guide, I characterized the functional undertakings of the oviduct during applied levels of heat stress and found its crucial role in altering the metabolic activity of maternal tissues, which likely in part functionally augment developing embryos and assume failure. Given the functional applicability of reproductive EVs acting as maternal cues, I established this suitable model as a mechanism to generate physiologically relevant EVs (in vivo-like) to offset applied stress during the initial stages of development. These EVs secreted from 3D cultured oviductal organoids were then compared with those secreted from 2D OECs and from in vivo oviductal fluid (miRNAs), and used in an IVC setting, highlighting functional maternal—embryonic crosstalk. Altogether, this dissertation highlights key functional aspects of reproductive extracellular vesicles from both the follicular microenvironment and the oviduct, highlighting the novel and incredible power of suitable in vitro systems to propagate mechanisms to understand maternal signal absent in the current in vitro systems, beginning to illuminate the ‘black box’ of EVs in embryo development.

ACKNOWLEDGEMENTS

To those currently feeling slightly more lost than a little more found, those merely surviving in an imposter-fueled state guided by overwhelming self-doubt, and to those that exist somewhere in between: Remember, life doesn't stay the same for too long; it somehow finds way to change. The days in which you feel that you're treading high water will persist, but one day (soon) the number of good days will unquestionably outnumber the bad. Hang in there, and most importantly hold onto yourself. In the wise words of Dr. Rachel Southard, "Just remember to take care of yourself, to be kind to yourself, and continue to work hard… and all that good stuff." Your story isn't over. It's just beginning. YOU WILL FIND YOUR WAY!

When I began my PhD in the Fall of 2020, I had always envisioned that it would be tough. I didn't think it would be 'being good at your job often attracts more work,' but it was, and today I am eternally grateful. To those individuals, and you know who you are: Endlessly and from the bottom of my heart, thank you. The best parts of who I am, are a direct reflection of each of you.

I want to thank my supervisor, Dr. Dawit Tesfaye, for choosing to believe in my potential and for providing me with the opportunity of a lifetime. Over the past four years, I have had the absolute privilege and honor of participating in establishing our lab here at the Animal Reproduction and Biotechnology Laboratory (ARBL) while duly serving in many extramural roles aside from the traditional tasks of a 'normal' PhD student, been given opportunities to work on particularly important projects in our field, as well as bestowed the ability to bridge deep-rooted connections involving collaborative projects with some of the most pleasant and intelligent scientists across the country and around the globe. As excited as I am for the next chapter of my career, I will miss

our dynamic working environment and your friendship above all. You're undoubtedly the best decision Colorado State University has made in faculty hires and I hope that as your first PhD graduate inside of the U.S., you are proud and continue to achieve great things, while still holding true to your values of 'accountability' and 'contribution' to the fundamental pillars of your program. It has been the biggest blessing of my life thus far, to spend the more primitive stages of my career building character, professionalism, and the opportunity to achieve many accolades as an early scientist, all of which are at the helm of your guidance and direction.

Next, I want to thank my PhD committee: Dr. Rebecca L. Krisher, Dr. Adam Chicco, and Dr. Fiona K. Hollinshead. Attempting to forge the right individuals to collectively contribute to my personal growth as a scientist, was at initial glance, a daunting task. However, I can confidently say that each of you were hand-picked for your various areas of expertise, and my success is in part attributable to each of you. Rebecca, you're my 'scientific idol' in more ways than one… intentionally present, always asking the most important questions in the room, yet your delivery is consistently kind, approachable, and friendly, first (practices, all scientists should adopt). Adam, your perspective, guidance, and ability to recognize potential research avenues addressing pressing issues have always been an instrumental facet to the group and a source of reinvigoration for the work. Fiona, in many regards, you're an inspiration to all of us…your energy, positive attitude, and ambition to achieve 'big wins' in science are the backbone of the collaborative nature of our work. I simply could not have asked for a better team!

Samuel Gebremedhn and Ahmed Gad, since the labs inception you have each stood strong as my initial mentors (teaching me nearly everything I know), turned colleagues, and summing in

confidants/ my scientific family for life. Sam, your infectious energy is what initially piqued my interest in science, and we have missed your presence here immensely! Ahmed (I don't even know where to begin), I am so grateful to have worked with/ alongside you during such an important time in my training at the ARBL. All of the great things that have happened to/ for me, are tied closely to you (reflective that you're my right hand). We have spent countless hours pushing each other to achieve more, yet still finding perspective and a balance to cultivate both extreme passion and ambition for the work, and aside from my unwavering gratitude for all that you have been and done for me, my wish is that you continue to accomplish great things and realize that above all else, you deserve a seat at the table. It is your time to shine, and I hope others have the ability to appreciate all of the great things that you bring to the academic setting. Thank you both for equally contributing to the greatest trifecta that ever was.

Collectively, the research represented here would not have been possible without the help and contribution of several key personnel. Riley Thompson and Mindy Meyers, thank you for being the earliest 'lab mates' that deep down, I knew that I needed. We have accomplished important feats together, over time recognizing that each of us bring diverse strengths to the collaborative aspect of our work, which has resulted in substantial outcomes in which I am very proud to be co-authors of. Additionally, I'd like to thank the members of the Tesfaye and Hollinshead laboratories, as well as the various other groups that compose the ARBL, to include the administrative staff, for their continuous support and friendship throughout my PhD journey.

To my family: Mom, Dad, Kayla, Shelby, and Trevor—In ways different from each other, you have each always supported my wildest dreams, encouraged my drive and passion, understood and

accepted my absence, and most importantly appointed me love without reservation. I know I would not have made it to the end without you. My dearest Mom, you're my reason, my person, and the grounds by which I hold myself in the highest regard and under the brightest light. You're my first phone call, on both the good and the bad days, my source of sunshine on the rainy days, and the individual that 'clapped so loud for me that I never noticed those who didn't.' Your endless support, presence, and persistence, in the times in which I had doubted myself most, are truly the epitome of unconditional love. I love you. Please know that I have achieved this milestone because of you.

Last, and importantly the most preeminent part of my heart, Parker. Sweet girl, you're the best decision that I have ever made. Although you're responsible for harboring all of my deepest secrets, your transmissible love and 'cuddly' demeanor is unreserved and something that brings me constant joy every day. I've realized many things over your short life, but the one that seems to surface to the top is that the world we live in would be a completely different ball game if people were more like you (dogs)…steadfast and loyal, and never wavering from unconditional love! The next chapter of life has me and you taking precedence, so here's to my promise, 'meet ya on the next adventure, Miss Park!'

TABLE OF CONTENTS

ABSTRACT……ii

ACKNOWLEDGEMENTS……iv

CHAPTER I: Current knowledge and the future potential of extracellular vesicles in mammalian reproduction……1

1. Overview……..……1
2. Introduction…….……..……2
3. EVs biogenesis, composition and uptake..…….……4
4. Extracellular vesicles in the follicular microenvironment……9
5. EV-mediated sperm capacitation……11
6. EVs: insightful index for physiological status……12
7. EV-mediated signaling during oviduct/uterine-embryo communication……14
8. Involvement of EVs in mediating stress coping mechanism during mammalian follicular development…….…19
   8.1. EV-mediated molecular signaling during thermal stress……..20
   8.2. EV-coupled molecular cargo as indicators of metabolic stress……23
   8.3. EV-mediated cellular response to oxidative stress……...25
   8.4.The potential of EVs in reproduction and related fields……27
   References……32

CHAPTER II: Granulosa cell-derived extracellular vesicles mitigate the detrimental impact of thermal stress on bovine oocytes and embryos ……..……..52

1. Overview…..……...…….52
2. Introduction……..53
3. Materials and Methods……..……...56
   3.1. Ovary collection and granulosa cell isolation…….……..56
   3.2. Granulosa cell culture and exposure to heat stress……...57
   3.3. Isolation of EVs from spent culture medium ……..57
   3.4. Morphological and molecular characterization of GC-EVs…….……58
   3.5. Fluorescence labeling of GC-EVs and assessing cellular uptake…….59
   3.6. In vitro maturation and exposure to heat stress……..……..60
   3.7. In vitro fertilization and embryo culture…….…….61
   3.8. Quantitative analysis of cumulus cell expansion……..62
   3.9. Total RNA isolation and quality control……...63
   3.10. Quantification of cumulus expansion and stress-associated genes using qRT-PCR……...63
   3.11. Measurement of intracellular ROS accumulation……..……64
   3.12. Analysis of mitochondrial membrane potential (MMP)……65
   3.13. Fluorescent nuclear staining and terminal deoxynucleotidyl transferase-mediated dUTP nick-end labeling (TUNEL) assay……...……66
   3.14. Experimental design……...…67
   3.15. Statistical analysis……..……68
4. Results……..……68

4.1. Characterization of GC-EVs released into the conditioned medium from in vitro cultured follicular GCs……...…69
4.2. GC-EVs shuttle protective messages against heat stress to enhance the thermotolerance of bovine cumulus-oocyte complexes…….69
4.3. GC-EVs prevent ROS accumulation and promote mitochondrial function in oocytes under heat-stress conditions……..73
4.4. The effect of GC-EV supplementation during oocyte maturation on developmental competence of oocytes post IVF……...…74
4.5. GC-EV supplementation modifies the expression of stress-associated transcripts in blastocysts……..78
4.6. Impact of GC-EVs supplementation during oocyte maturation on blastocyst ROS accumulation, mitochondrial function, total cell counts, and apoptotic index..…79
5. Discussion……82
References……90

CHAPTER III: Bovine oviductal organoids: a multi-omics approach to capture the cellular and extracellular molecular response of the oviduct to heat stress…….……102
1. Overview…..……...……...102
Background……...……102
Results……...……102
Conclusions……...…….103
2. Background……...……103
3. Results……...……106
3-D matrix supports dynamic oviductal organoid culture and EV production.....106
Decoding the transcriptome response of oviductal organoids to HS……...…..110
HS alters oviductal organoid-derived EV-coupled miRNAs……...……..114
Quantitative real-time PCR validation of candidate genes and miRNAs…..……....117
MicroRNA sequence motif and RBP identification…….....…117
4. Discussion……..119
HS-induced transcriptomic changes in oviductal organoids…….123
Oviductal organoid-derived EV-miRNA profiles in response to HS…….……...126
5. Conclusions……....130
6. Methods……..130
Collection of bovine oviductal epithelial cells (BOECs)……...……130
Oviductal organoid culture……132
Histology……133
Immunohistochemistry……..……133
Exposure of oviductal organoids to heat stress……..134
Collection of cultured oviductal organoids and conditioned medium for downstream analysis……...…134
Characterization and quantification of oviductal organoid-derived EVs……..135
RNA isolation……....137
RNA library preparation and sequencing……..137
RNA-seq data analysis…….……..138
Target gene prediction, ontological classification and pathway analysis……..139
Quantitative real time PCR validation of candidate mRNA and miRNA……139

MicroRNA sequence motif and RBP identification and analysis……..141
References……..…143

APPENDIX I—Original Publications…..……...156

CHAPTER I—Current knowledge and the future potential of extracellular vesicles in mammalian reproduction[1]

1. Overview

Extracellular vesicles (EVs), which contain various functional classes of vesicles, namely exosomes, microvesicles, and apoptotic bodies, represent the major nano-shuttle to transfer bioactive molecules from donor to recipient cells to facilitate cell-to-cell communication in the follicular, oviduct, and uterine microenvironments. In addition to transferring various molecular cargos in the form of miRNAs, mRNAs, proteins, lipids, and DNA molecules, the relative proportion of those molecular cargos in the reproductive fluids can be associated with the physiological and pathological condition of the host animal. Inside the follicle, EV-mediated circulation of miRNAs has been reported to be associated with the growth status of the enclosed oocytes, the metabolic status, and the advanced maternal aging of the animal. Importantly, EVs have the potential to protect their cargo molecules from extracellular degradation or modification while travelling to the recipient cells. This fact together with the enormous availability in almost all biological fluids and spent culture media make them attractive in the search for biomarkers of oocyte/embryo developmental competence, receptive maternal environment and a multitude of reproductive pathophysiological conditions. One of the key factors that have contributed to the lower efficiency of assisted reproductive technologies (ART) is the absence of several maternal *in vivo* factors in the ART procedures. For this, several studies have been conducted to supplement

---

[1]Tesfaye D, Menjivar N & Gebremedhn S. Current knowledge and the future potential of extracellular vesicles in mammalian reproduction. *Published at Reproduction, Fertility and Development*

various components present in the follicular and oviductal fluids into the existing ART procedures and significant positive impacts have been observed in terms of embryo cleavage rate, blastocyst rate, resistance to stress, and survival after cryopreservation. The potential of EVs in shuttling protective messages against environmental and physiological stressors has been evidenced. The effective use of the EV-coupled molecular signals against stress-associated conditions has the potential to pave the path for the application of these protective signals against oxidative stress-associated pathological conditions including PCOS, ageing, and endometritis. In this review, we provide current knowledge and potential future use of EVs as remedies in reproductive pathophysiological conditions, mainly in follicular and oviductal microenvironments.

2. Introduction

In mammalian reproduction, intercellular communication is an essential process, which occurs indirectly through endocrine, paracrine, and autocrine factors or directly through cell-to-cell contacts (Raposo and Stoorvogel 2013). After their discovery in 1983, membrane- enclosed compartments, which are regarded as extracellular vesicles (EVs) play a significant role in cell-to-cell communication in various reproductive processes. EVs mediate cellular communication via their molecular cargos namely, RNAs (mRNA, miRNA, tRNA, and other long noncoding RNA), proteins, DNA, and lipids, that they transfer to the recipient cells (Valadi et al. 2007; Almiñana et al. 2018; Gatien et al. 2019). Based on their size and mode of biogenesis, EVs are broadly classified as exosomes (50–150 nm), microvesicles (100–1000 nm) and apoptotic bodies (>1000 nm) (Simon et al. 2018). EVs interact with the recipient cells by direct signaling via ligand/receptor molecules in their respective surfaces or through direct fusion of the plasma membrane of the EVs and recipient cells, lipid-raft, clathrin, and caveolae-mediated endocytosis, micropinocytosis, and phagocytosis (Morelli et al. 2004; Montecalvo et al. 2012). Due to the lack of consensus on their

nomenclature, reproductive biologists designate EVs derived from various reproductive fluids as epididmosomes, prostasomes, vaginosomes, uterosomes, and oviductosomes (Al-Dossary et al. 2013; Belleannée et al. 2013; Sullivan and Saez 2013).

Extracellular vesicles are considered as nano shuttles available in various reproductive fluids including follicular, oviductal, and uterine fluids, and are reported to play a role in cell-to-cell, gamete to follicular cells, gamete, or embryo to oviduct/uterine cells communication. Moreover, several studies have demonstrated that EVs are involved in shuttling several bioactive molecules including miRNAs, mRNA, and proteins and their relative abundance could reflect the physiological status of the originating cells or tissues (Valadi et al. 2007; Hailay et al. 2019). EVs from follicular fluid of oocytes under varying growth status (Sohel et al. 2013), different sizes (Hung et al. 2015), and divergent metabolic status (Hailay et al. 2019) are known to carry varying levels of bioactive molecules which might be associated with their functional role. Similarly, bovine granulosa cells subjected to in vitro thermal stress or oxidative stress release protective molecular signals through EVs in form of heat shock proteins, antioxidants, and transcripts associated with endoplasmic reticulum stress (Saeed-Zidane et al. 2017; Gebremedhn et al. 2020b). Interestingly those EVs derived from stressed cultured granulosa cells can shuttle protective messages in the form of miRNA and mRNA or proteins, which upon supplementation in vitro induce tolerance to recipient cells following exposure to recurrent thermal stress (Gebremedhn et al. 2020b). Among the miRNAs enriched in the EVs released from granulosa cells subjected to heat stress are the miR-1246, miR-2904, and miR-374a, which are predicted to coordinately target endoplasmic reticulum genes.

Through its dynamic nature in its luminal fluid composition, the oviduct is an active organ that provides an optimal microenvironment for gamete maturation/activation, fertilization, and

cleavage-stage embryo development (Coy et al. 2012). Several studies indicated the functional variation of oviductal EVs collected from different parts of the oviduct. Supplementation of bovine oviductal EVs collected from the isthmus, but not the ampulla, in the embryo culture positively affect the embryo development (Lopera-Vasquez et al. 2017). This implies that oviductal EVs produced from different regions of the oviduct carry specific molecular signals associated with specific function in supporting gamete and embryo development. This may be associated with the distribution of ciliated and secretory cells in different regions of the oviduct (Harris et al. 2020). This needs to be experimentally validated in future studies. Comparative analysis of the proteome of EVs derived from in vivo oviductal fluid and in vitro cultured oviductal epithelial cells revealed significant differences (Almiñana et al. 2017). In that study, fewer proteins were identified in vitro-derived oviductal EVs (222) compared to those derived from the in vivo counterparts (270). The impact of supplementation of oviductal EVs in vitro culture environment has been evidenced to positively impact sperm activation, prevention of polyspermy, and early embryo development (Machtinger et al. 2016). The data presented in this review also suggest the potential application of oviductal EVs in the current ART to mimic the in vivo oviductal environment.

In the present review, the current knowledge on EVs research in reproduction mainly associated with ovarian functionality, gamete–embryo–oviductal communication, and EVs molecular signaling as indicators of environmental and physiological stress conditions are thoroughly discussed and the future potential of EV research in reproduction will also be highlighted.

3. EVs biogenesis, composition and uptake mechanisms

Extracellular vesicles are a group of heterogenous and membrane-bounded structures released from a variety of cell types in vivo in biological fluids or in vitro in spent culture media. They have

the capacity of transporting various active biomolecules from cells of origin to target recipient cells, thereby modulating the physiology of the recipient cells (Ofir-Birin et al. 2018). Of these three different types of EVs, the majority of interest falls on the microvesicles and exosomes, while the apoptotic bodies are often considered as products of cell death (María et al. 2015). The apoptotic bodies are released when plasma membrane bedding occurs during apoptosis, but microvesicles, which are relatively heterogenous population pinch directly off the plasma membrane. Exosomes, which are intraluminal vesicle contained in multivesicular bodies, are relatively homogenous in size. Exosomes are released to the extracellular space upon fusion of the multi-vesicular bodies (MVBs) with the plasma membrane (Colombo et al. 2014). Despite the fact that initially exosomes were considered to be alternative mechanisms to eliminate waste products from cells interior to maintain cellular homeostasis (Baixauli et al. 2014), a significant number of studies have provided evidence that following the release from the cell surface, exosomes can interact with the extra- cellular matrix or induce cellular response within a specific microenvironment or in distant cells. These evolutionary conserved vesicles are known to exert essential physiological and pathological effects on both recipient and parent cells, via a variety of functional molecules either as structural or cargo components. Currently, because of the absence of widely acceptable specific markers to distinguish exosomes and microvesicles, consensus has been reached to name both with the generic name EV.

In mammals, EVs have been isolated from diverse body fluids, including blood, urine, saliva, breast milk, amniotic fluid, ascites, cerebrospinal fluid, bile, and semen. These vesicles have been named based on their origin, nature and features in many different ways. Many different names have been used in publications depending on their size [with a prefix micro or nano: microparticles, microvesicles (MVs), nanovesicles, nanoparticles], their tissue of origin (prostasomes,

oncosomes), their proposed functions (calcifying matrix vesicles, argosomes, tolerosomes), or simply their presence outside the cells (prefix exo or ecto: ectosomes, exosomes, exovesicles, exosome-like vesicles). Despite the fact that nomenclature of EVs is still under debate (Stephen and Graça 2013), several marker proteins are being used to prove the identity of the vesicles isolated using various techniques including ultracentrifugation and size exclusion chromatography. The protein composition of EVs reflects proteins integrated in or attached to their membrane or those present in their luminal space. Although exosome and microvesicles have different protein profiles due to their different biogenesis pathways, so far no specific protein has been identified to accurately discriminate between the two vesicle populations. This coud partially be due to the fact that plasma membrane-derived EVs and endosome intraluminal vesicles (ILVs) share important features as they bud away from the cytosol in contrast to other intracellular budding events that are required for trafficking between different compartments. Thus, their membrane orientation is identical to that of the cell surface, exposing the extracellular domains of the transmembrane proteins and enclosing cytosolic components. The protein composition of exosomes as components of EVs demonstrated exosomes are enriched with proteins associated with their biogenesis pathway (Villarroya-Beltri et al. 2014). This was further validated by the fact that compared to their cells of origin EVs are enriched with various components of the endosomal sorting complex for transport (ESCRT) machinery and its accessory proteins. The most common exosomal proteins represent those that are associated with membrane transport and fusion and others including cytoskeletal, metabolic, signaling and carrier proteins (Ibrahim and Marbán 2016). The classical biogenesis of exosomes is the most studied one. This classical process of exosome biogenesis involves the inward budding of the plasma membrane and the formation of intracellular MVBs containing ILVs (Kalluri and LeBleu 2020). This most recognized and studied

pathway of exosome biogenesis is driven by ESCRT complexes. The ESCRT is a family of proteins that associate in complexes at the membrane of MVBs to sort cargo and the formation of ILVs (Hanson and Cashikar 2012), which are secreted as exosomes through MVB fusion to the plasma membrane and exocytosis.

The biogenesis of exosomes in vivo is a complex process which involves several proteins including Ras-related protein GTPase Rab, Systenin-1, TSG101, Alix, syndecan-1, ESCRT proteins, phospholipids, teteraspanins, ceramindes, sphingomyelinases and SNARE complex proteins (Simon et al. 2018). Several factors including cell type, culture conditions and the physiological status of the cells are known to determine which putative key regulators of exosome biogenesis will be activated in vivo (Mathieu et al. 2019). As most studies reported mainly focused on the potential function of extracellular vesicles rather than on their origins, it is still unclear which sub-species of vesicles is responsible for a given physiological or functional effect.

Through the EV-mediated cell-to-cell communication, several bioactive molecules are transferred to recipient cells, which may have a significant impact on the phenotype of the recipient cell. These phenotypic changes can be regulation of gene expression through de novo translation and post-translational regulation of target mRNAs (Valadi et al. 2007), and changes in miRNA level during stress response (Jacobs et al. 2013; Sohel et al. 2013; Gebremedhn et al. 2020b). Due to their structural composition EVs can protect their cargo molecules from enzymatic degradation during their transit through extracellular environments (Keller et al. 2011). This capability of EVs signifies their potential conversion to vehicles for delivery of therapeutic proteins, RNA and drugs (Alvarez-Erviti et al. 2011; Tang et al. 2012). For this, EVs need to interact with the recipient cells in several uptake mechanisms (Mulcahy et al. 2014). Both direct and indirect evidence suggests that EVs internalized into recipient cells. Direct visualization using fluorescent lipid membrane

dyes is the most common way for detecting EV uptake. Some of these dyes include PKH67, PKH26, rhodamine B (also called R18), DiI and DiD, which are lipophilic and other membrane permeable chemical compounds are also available including carboxyfluorescein succinimidyl ester (CFSE) and 5(6)-carboxyfluorescein diacetate (CFDA) (reviewed by Mulcahy et al. 2014).

Extracellular vesicles can be uptaken by recipient cells in a variety of endocytic pathways, including clathrin-mediated endocytosis and clathrin-independent pathways such as caveolin-mediated uptake, micropinocytosis, phagocytosis, and lipid raft-mediated internalization. The choice of uptake mechanism used by a specific EV depends on molecular components especially proteins and glycoproteins present on the surface of the EVs and the recipient target cells (Horibe et al. 2018). The significant role of the protein components in EV- recipient cell interaction has been validated by Proteinase K treatment of EVs, which has shown to reduce their uptake in ovarian cancer cells (Escrevente et al. 2011). Among the several proteins playing a role in EV uptake by recipient cells include tetraspanins, which are membrane proteins involved in various processes including cell adhesion, motility, activation and proliferation (Hemler 2005). Tetraspanins are known to be present on EV surfaces suggesting their role in EV function. Among those CD9 and CD81, which are known to be well-established markers of EVs are reported to be involved in oocyte-spermatozoa and phagocyte fusion as reviewed by (Mulcahy et al. 2014). The significant role of tetraspanins in EV uptake by recipient cells has been evidenced by reduced EV uptake after treatment of recipient cells with antibodies against the CD81 or CD9 (Morelli et al. 2004).

Clathrin-mediated endocytosis (CME), which involves internalization of molecules through progressive and sequential assembly of clathrin-coated vesicles containing a range of transmembrane receptors and their ligands, has been reported to be one of the mechanisms in EV

uptake by recipient cells. For example, treatment of cells with chlorpromazine (CME inhibitor) resulted in decreased uptake of EVs by ovarian cancer recipient cells (Escrevente et al. 2011). Similarly, clathrin-mediated endocytosis was found to be the dominant EV uptake pathway in the uptake of syncytiotrophoblast extracellular vesicle by endothelial cells (Cronqvist et al. 2020).

4. Extracellular vesicles in the follicular microenvironment

Initially, described in the late 1980s from the endosomal pathway, EVs were viewed solely as a discarding mechanism for membrane proteins with little to no understanding of their wide range, functional outcome as a conveyor of cellular information (Raposo and Stoorvogel 2013). More recently, EVs natural role in genetic information transfer as carriers of bioactive molecules has propagated their substantial interest as agents for multidirectional crosstalk (Valadi et al. 2007). The increasingly investigated phenomenon of the bidirectional communication of EVs can be summed up directly through gap junctions (GJ)/transzonal projections (TZPs) as well as indirectly through various endocrine, paracrine and autocrine signaling pathways (Bosco et al. 2011). EVs are known to be acted on by Rab GTPases (Rab 27a/Rab 27b) to promote their secretion and release (Ostrowski et al. 2010), which can be validated through the enrichment of protein markers like CD63 and ALIX. Once released into the extracellular space, EVs potential mediation of cellular communication is initiated but not limited to receptor–ligand interactions or even fusion with the target cells membrane to initiate the off-loading of cargo, thereby adjusting the physiological existence of the target cell (Tkach and Théry 2016).

The follicle microenvironment consists of the oocyte and subsequent somatic cells, as well as a variable volume of follicular fluid based on the maturity of the follicle and derived primarily from circulating plasma (Fortune 1994). The bidirectional crosstalk between the oocyte and granulosa cells is dependent on a functional network of gap junctions thought shuttle factors like

proteins (insulin) and hormones (progesterone (P4) and oestradiol (E2)) (O'Shea et al. 2012) necessary for proliferative development (Brower and Schultz 1982). Communication intricacies between the oocyte and subsequent somatic cells have added a supplementary layer of bidirectional crosstalk inducing principal processes like folliculogenesis and meiotic resumption, ultimately leading up to and past early embryonic development (Senbon et al. 2003). A fundamental point of interest currently being evaluated, is the precise molecular content of EVs and the method of molecular transmission mediating cell-to-cell communication. In bovines, it has been shown that follicular fluid (FF) EVs induce the proliferative capacity of granulosa cells to act on the oocyte through Src, PI3K/Akt and MAPK signaling pathways (Hung et al. 2017). Nevertheless, the functional effects noted through increased expression of cumulus expansion marker genes, cultivates such communication within the follicle microenvironment (Da Silveira et al. 2012). The novelty of this finding stems from potentially modulating the developmental competence of oocytes matured in vitro by mimicking the in vivo LH-surge through EV co-incubation (Conti et al. 2012). Interestingly, granulosa cells have the ability to preferentially uptake EVs based on the follicle size, eluding to a differential cargo composition associated with dominant and subordinate follicle size (Hung et al. 2015). Dually noted as prime carriers of bioactive molecules, extra-cellular miRNAs have emerged as a key proponent loaded within EVs. In fact, expression of variable miRNA profiles has been eluded too in humans (Santonocito et al. 2014), bovine (Sohel et al. 2013) and equine (Da Silveira et al. 2012). As transporters of differing miRNA profiles, FF EVs are harnessed with direct targets to mitigate pathways associated with follicular growth and oocyte maturation, such as the wingless signaling pathway (WNT), transforming growth factor beta (TGF-β), mitogen activated protein kinase (MAPK) and epidermal growth factor receptor (ErbB) (Sohel et al. 2013). Interestingly in bovines, miR-640, miR-526b* and miR-381 were

abundantly present in theca cells versus miR-373, miR-30e* and miR-19b-1* being expressed more in cumulus oocyte complexes (COCs) (Sohel et al. 2013). This in fact signifies that differentially expressed miRNAs can be dependent on indicators relevant to basic origin and physiological status, suggesting the ability to pinpoint relative miRNAs via cause and effect relationships associated with reproductive misfunction.

5. EV-mediated sperm capacitation

Ejaculated sperm must pass through the female reproductive tract in order to fertilize an egg. During this transition through the female reproductive track there will be removal of seminal plasma components and exposure to the reproductive tract secretions. Despite the short period, this process is critical for inducing sperm capacitation, which involves an increase of the membrane structure and fluidity due to a removal of cholesterol from the sperm plasma membrane and increase of sperm intracellular calcium and bicarbonate ion permeability (Burton and McKnight 2007). These modifications are associated with induction of the tyrosine phosphorylation of a subset of sperm proteins, which is mediated by the cyclic AMP (cAMP)-dependent protein kinase A (Visconti and Kopf 1998). Supporting a role of the uterine cells in sperm capacitation, human spermatozoa co-incubated with endometrial cell-conditioned medium showed an increase in protein tyrosine phosphorylation (Laflamme et al. 2005). The first exposure of spermatozoa with reproductive tract EVs start in the vagina, where vaginosomes (EVs present in the vaginal luminal fluid) come in contact with the ejaculated sperm, which could have an effect on its functionality. Enhanced progesterone-induced acrosome reaction could be induced by exposure for 30 min to vaginosomes in non-capacitating condition (Fereshteh et al. 2019). In the same study the coincubation of spermatozoa with EVs derived from vaginal luminal fluids results in elevation of cells with highest expression of sperm adhesion molecule 1 (SPAM1), PMCA1/4 and PMCA1

compared to those incubated in phosphate buffered saline solution. A significant level of PCMA4, which is a membrane protein involved in the Ca2+ efflux pump in murine sperm, was detected in the EVs derived from murine vaginal, oviductal and uterine luminal fluid and the flow cytometry analysis of caudal sperm incubated with luminal fluids EVs showed increased expression of PMCA4a, which demonstrated the in vitro uptake of luminal EVs by sperm (Al-Dossary et al. 2013). The coincubation of human spermatozoa in the presence of uterosome-like vesicles derived from conditioned media of endometrial epithelial cells resulted in sperm capacitation as determined by the increase in the level of induced acrosome reaction and induction of protein tyrosine phosphorylation (Franchi et al. 2016). A similar study in humans revealed that spermatozoa can internalize EVs released from cultured primary endometrial cells and result in sperm capacitation and acrosome reaction as manifested by increased protein tyrosine phosphorylation (Murdica et al. 2020). EV internalization was successfully blocked by incubation with filipin suggesting that an energy- dependent process probably attributable to the lipid-raft domain mediated-endocytosis to be the main mechanism of EV uptake by the spermatozoa.

6. EVs: insightful index for physiological status

Stress negatively affects reproductive efficiency, which is seen through an imploding decline in mammalian fertility and overall decrease in livestock productivity. In vitro culture systems have been extensively utilized in attempts to mimic both environmental and metabolic stressors believed to have deleterious effects on oocytes, fertilization, preimplantation, and embryonic development (Edwards and Hansen 1996; Rivera and Hansen 2001). Extracellular miRNAs have also more recently been outlined for their potential role as disease biomarkers, or molecules used for detecting disease/ prognosis progression (Galimberti et al. 2014; Hailay et al. 2019). Found in most biological fluids, and recognizing the stability and ease of access to obtain samples, changes in

circulating miRNA profiles have been noted in human and mice studies correlated to obesity (Can et al. 2016; Castaño et al. 2018), type 2 diabetes (Kong et al. 2011; Higuchi et al. 2015), ageing (Kirkman et al. 2012; Dhahbi et al. 2013; López-Otín et al. 2013), polycystic ovarian syndrome (PCOS) (Hu et al. 2020) and various female reproductive cancers (Liang et al. 2013; Che et al. 2020; Lv et al. 2021). For instance, EVs preferentially loaded with obesity-related miRNA mimics (miR-122, miR-192, miR-27a and miR-27b) and repeatedly injected into lean mice, developed a profound insulin resistance and dyslipidemia, eluding to these specific miRNAs role in indicating the pathophysiology of obesity and potential links to type 2 diabetes (Castaño et al. 2018). Commonly associated with a multi-faceted downregulation in propagating miRNA, specific indications like miR-125b, miR-342; miR-133b, miR-214 are proposed in correlation to neurodegenerative diseases like Alzheimer's and Parkinson's diseases (Galimberti et al. 2014; Cheng et al. 2015; Dong et al. 2016; Rosas-Hernandez et al. 2018). Alternatively, a massive prevalence affecting female infertility is the reproductive abnormality known as Polycystic Ovarian Syndrome (PCOS), whose mechanism of action has yet to be full elucidated. Although, in more recent times, extracellular circulating miRNAs have been analyzed from PCOS follicular fluid at differential expression levels. Furthermore, increased expression levels of miR-146a-5p and miR-126-3p have been dually noted as a direct target of the MAPK and TGF-β signaling pathways, essential for reproductive function (Cheet al. 2020; Jiang et al. 2021). Overall, this suggests that the EVs role in detailed cell-to-cell communication is essential, not only as an indicator of origin, but also as a potential biomarker for various pathophysiological conditions as illustrated in Figure 1.1.

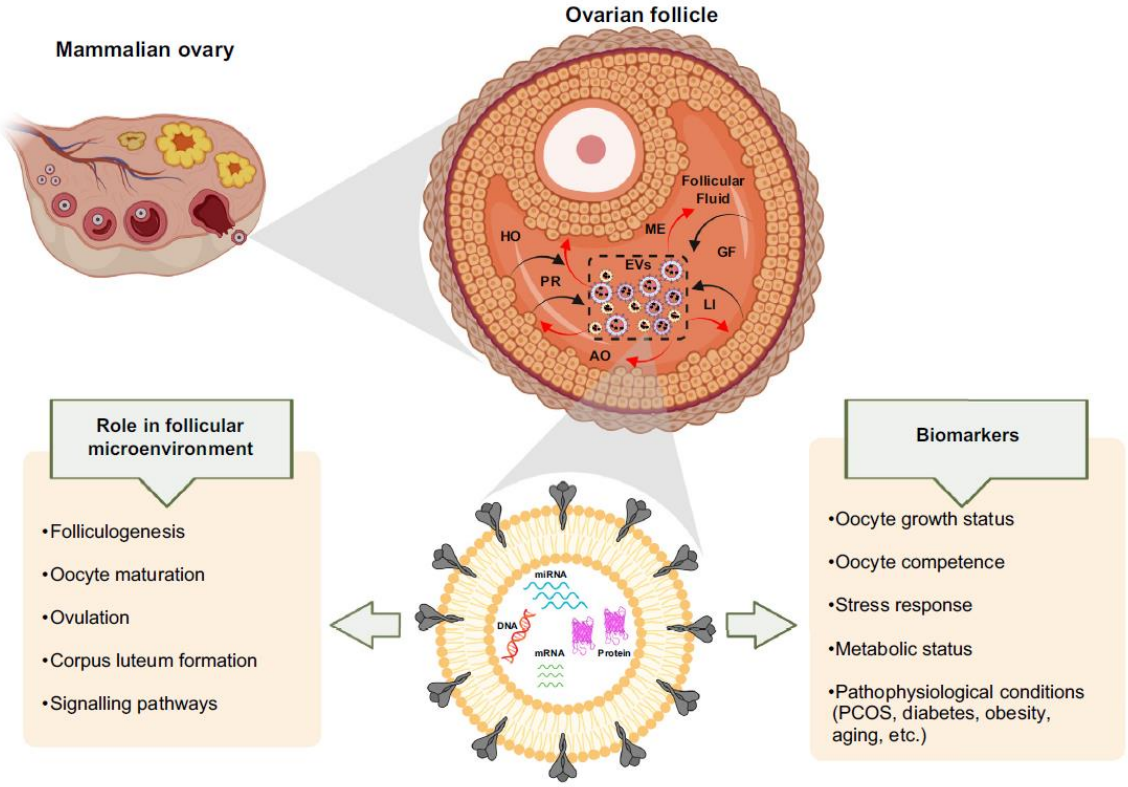


Figure 1.1. Extracellular vesicle-mediated molecular signaling in the ovarian follicle. Schematic representation of extracellular vesicles within the follicle microenvironment, a key proponent of bidirectional crosstalk inducing oocyte growth and maturation, and subsequent physiological index to stress and pathophysiological conditions. Extracellular vesicles serve a mass transit mechanism for bioactive cargo such as miRNA, mRNA, proteins, lipids and metabolites, inducing the proliferative capacity of granulosa cells to act on the oocyte through various signaling pathways (EVs, extracellular vesicles; HO, hormones; PR, proteins; AO, antioxidants; ME, metabolites; GF, growth factors; LI, lipids).

7. EV-mediated signaling during oviduct/uterine-embryo communication

Following ovulation, the oocyte goes to the oviduct for fertilization and subsequent cleavage stage development. The process of sperm capacitation and fertilization and early stage cleavage of mammalian embryos is supported mainly by secretions of the oviduct, which are complex and contain growth factors, hormones, proteases, antioxidant proteins, immune system proteins, metabolites, lipids and heat shock proteins (Avilés et al. 2010; Coy et al. 2012). For this, the oviductal epithelium, which is composed of ciliated and secretory cells, is involved in the secretion

of oviductal fluid that has an important role in gamete maturation, fertilization and embryo developmental competence (Leese et al. 2008; Avilés et al. 2010). Considering their implication for important events in female reproduction including fertilization, early embryo development and implantation, research in the field of intercellular communication in the oviduct and uterine environment has increased exponentially in the last years. During in vivo development the embryo interacts with the surrounding cells in the oviduct and uterus to survive and develop to term (Fazeli 2011). Among the various components of the oviductal fluid, EVs are identified for the first time in murines being designated as oviductosomes (Al-Dossary et al. 2013) and found to mediate embryo and maternal communication (Cruz et al. 2018). The beneficial role of EVs in carrying molecular signals during embryo maternal communication has been evidenced by the fact that EVs from the in vivo oviductal fluid and from conditioned media of bovine oviductal epithelium cells showed a positive impact on embryonic development in vitro (Lopera-Vásquez et al. 2016; Almiñana et al. 2017; Sidrat et al. 2020; Asaadi et al. 2021).

So far, several studies have been conducted focusing on the oviductal fluid EVs in relation to the stage of ovarian cyclicity and the site in the oviduct or EVs secreted by cultured primary oviductal cells. Deciphering the oviductal EV content at different stages of the oestrous cycle including post-ovulatory stage, early luteal phase, late luteal phase and preovulatory stages revealed the content of EVs (miRNAs, rRNA fragments, tRNA fragments, snRNA, snoRNA and other ncRNA) to be under steroid hormone regulation (Almiñana et al. 2018). In that study major differences were observed between post- ovulatory and the rest stages analyzed. Very interestingly, miR-34c and miR-449a, which are known to be involved in defective cilia in the oviduct and associated with infertility, are among the differentially abundant miRNAs. The hormonal regulation of EV content has also been evidenced by the differential protein profile between in

vivo derived oviductal fluid EVs and those EVs secreted by bovine oviductal epithelial cells culture in vitro (Almiñana et al. 2017). A similar study in sheep also indicated that the amount of EVs in the uterine lumen increased after P4 treatment suggesting that P4 may be involved in regulation of the release of EVs from endometrial epithelial to the uterine lumen (Burns et al. 2018). On the contrary, in addition to provision of lipids for cellular growth in elongating conceptus, EVs in the uterine lumen fluid may also be involved in conceptus production of prostaglandins (Burns et al. 2018).

Due to the lack of the female reproductive tract, embryos cultured in vitro are under suboptimal conditions leading to lower blastocyst and pregnancy rates (Pontes et al. 2009). However, embryos are known to support each other during group culture by secreting autocrine factors which act upon the embryo itself or on neighboring embryos (O'Neill 2008). Therefore, culturing embryos in groups has been found to improve embryo developmental rates and quality in various mammalian species, including cattle (Donnay et al. 1997; O'Doherty et al. 1997), pigs (Stokes et al. 2005), and humans (Almagor et al. 1996; Ebner et al. 2010). The importance of autocrine factors for embryo survival and development is evidenced with the development of the well-of-the-well system, which has been successfully applied in bovine (Hoelker et al. 2010), porcine (Taka et al. 2005), mouse and human (Vajta et al. 2008) embryos. In an attempt to compensate the missing signaling factors from the reproductive tract several studies have been performed to investigate the role of coculture of bovine oviductal epithelial cells, cumulus cells and granulosa cells as reviewed by (Wydooghe et al. 2017). The preimplantation embryos are able to secrete the autocrine embryotropins in several ways including active secretion, passive outflow or extracellular vesicles as molecular cargo vehicles. The role of extracellular vesicles in this inter embryo communication has been evidenced in bovine embryos (Pavani et al. 2019). In support of this, fluorescent labelled EVs were

found to be taken up by embryos passing through the glycoprotein layer zona pellucida in bovine (Pavani et al. 2019) and porcine (Saadeldin et al. 2014) preimplantation embryos. Recently, the study conducted by (Burns et al. 2018) demonstrated that EVs isolated from the media conditioned by cultured ovine Day 14 conceptuses can be uptaken by uterine epithelium, but not by other maternal tissues including the ovary, corpus luteum, parametrial lymph nodes or lung, thus serve as a novel form of intercellular communication during the establishment of pregnancy. Proteomic analysis of conceptus secreted EVs revealed the presence of 231 proteins representing those as structural components of EVs and the majority involved in various signaling pathways associated with pregnancy establishment (Burns et al. 2016).

Extracellular vesicles have been identified in the uterine lumen of various species including cattle, sheep, human, pigs and mice (Ng et al. 2013; Vilella et al. 2015; Greening et al. 2016). The EVs in the uterine luminal fluid are likely to have originated from both the luminal epithelium and the glandular epithelium of the uterus (Racicot et al. 2012). The beneficial role of uterine lumen fluid derived EVs in conceptus elongation was evidenced recently (Burns et al. 2018). The way of transmission of EVs to elongated embryos is postulated to follow the mechanisms of direct fusion resulting in provision of lipids, RNA, and proteins cargo and results in stimulation of conceptus elongation via regulation of gene expression. Labeled EVs isolated from the ovine uterine fluid, transferred to ovine trophectodermal cells in vitro within 2 h of co-incubation, resulted in both increased proliferation and release of interferon τ (the ovine pregnancy recognition signal) in a dose-dependent manner (Ruiz-González et al. 2015). In the same study, uterine flushing EVs from cyclic and pregnant ewes revealed the presence of mRNAs for enJSRV-ENV, HSC70, interleukins, and interferon (IFN)-regulatory factors. MicroRNAs 21 and 29a which were found to be present in EVs from the uterine luminal fluid of Day 14 cyclic and pregnant sheep (Burns et al. 2014), are

known to activate the TLR 7/8 (Fabbri et al. 2012). Therefore, EVs in the uterine lumen fluid from the uterine epithelium may be involved in stimulation of IFNT production and subsequent conceptus growth via TLR activation.

Despite substantial differences in EV content depending on the anatomical and functional differences between different parts of the oviduct and stage of the oestrous cycle (Almiñana et al. 2018; Gatien et al. 2019), oviductal proteins are found to be enriched with proteins of protective properties including heat shock proteins and proteins associated with oxidative stress response, which may shuttle these protective messages to the embryos to provide protection against environmental or physiological stressors as a positive bystander effect as observed in bovine granulosa cells (Gebremedhn et al. 2020b). Several studies have evidenced that supple- mentation of oviductal EVs to in vitro cultured embryos enhances the viability and developmental capacity of embryos by modulating the molecular composition and physiology of the embryos. Recent study in rabbits has demonstrated that the oviductal fluid which is enriched with melatonin could reduce reactive oxygen species (ROS) accumulation, 5-methycytosine (5-mC) and increase in blastocysts rate after supplementation in vitro (Qu et al. 2020). In the same study, supplementation of the combination of EVs and melatonin led to similar results as well as a significant decrease in the apoptosis index and increase in inner cell mass (ICM)/ trophectoderm (TE) index. Supplementation of bovine oviductal fluid and/or uterine fluid in a stage-specific manner in vitro at a level of 1.25% resulted in increased blastocyst rate, upregulation of genes related to epigenetics

(DNMT3a and IGF2R), and reduced accumulation of ROS compared to those cultured with SOF + FCS (Hamdi et al. 2018). The positive contribution of EVs from oviductal fluid derived from ampullary or isthmus of the oviduct to early embryo development in vitro has been reported (Lopera- Vasquez et al. 2017). In that study, supplementation of oviductal EVs resulted in

increased survival rate of blastocysts following cryotolerance. Moreover, gene expression analysis of the resulting blastocysts showed elevated expression of water channel AQP3 and DNMT3A and SNRPN transcripts. Similarly, the supplementation of EVs derived from conditioned media of cultured bovine oviductal epithelial cells had no effect on blastocyst yield however, increased trophectoderm cells and modulation of the expression of developmentally related genes (Lopera-Vásquez et al. 2016). The positive impact of bovine oviductal epithelial cells conditioned media and EV supple- mentation in vitro cultured bovine embryos evidenced that molecular signals carried by EVs in conditioned media play the major role in providing factors missing in the in vitro environment.

8. Involvement of EVs in mediating stress coping mechanisms during mammalian follicular development

Throughout the productive lifespan, dairy and beef cows are exposed to several exogenous and endogenous sources of stress, which pose detrimental impacts and contribute to the significant disruption in the physiology of reproduction. Among the key stressors, environmental stressors, including oxidative, heat, cold, and others (Li et al. 2016; Saeed- Zidane et al. 2017; Baddela et al. 2018) and endogenously generated stressors due to the disruption of the various metabolisms (Beam and Butler 1997), are widely reported to impair female reproductive physiologies.

One of the greatest achievements of the past five to six decades in animal farming is the advancements in setting the breeding goals and the intensive selection of farm animals for traits of interest with huge economic implications. For this, the incorporation of genetic scores (i.e genomic selection) into the breeding program and selection procedures has facilitated the genetic gains in a very short period (Meuwissen et al. 2001). It has been reported that the intensive selection of cows for higher milk yield has resulted in a significant increment in the net amount of yields produced.

Nevertheless, a concomitant compromise in the reproductive performance traits is reported, which shades negative consequences to the profitability of farms due to increased culling of less fertile cows in dairy farms (Lucy 2001). It has been reported that the deteriorating reproductive performance of dairy cows is associated with the higher milk yield per cow, which could be attributed to the antagonistic relationship between the fertility and production traits of dairy cows (Hansen 2000). Exposure of cows to both environmental and metabolic stressors are reported to affect the ovarian functions mainly, the steroidogenic capacity of the follicles, leading to disruption of the oestradiol production capacity of the dominant follicle, which in turn impair ovulation and subsequent postovulatory processes (Wolfenson et al. 1997; Roth et al. 2001), reduce the developmental competence of the oocyte and the capacity to reach the blastocyst stage (Roth and Hansen 2005; Nabenishi et al. 2012). One of the fundamental impacts of exposure to both metabolic and environmental stressors is the disruption of intrafollicular bidirectional communication between the follicular cells and the corresponding oocyte. The presence of EVs in the follicular fluid of cows has been reported to be associated with the developmental competence of the oocyte (Sohel et al. 2013). Thus, the exposure to stressors could modify the content of the bioactive molecules encapsulated in the EVs and could also serve as reflectors of the stress exposure. The specific impact of the environmental and metabolic stressors in the cargo of the EVs is discussed below.

8.1 EV-mediated molecular signaling during thermal stress

Summer heat stress is reported to negatively affect the maturation of oocytes, growth, and steroidogenesis of follicular cells, the development of the corpus luteum, and the receptivity of the maternal endometrium (Roth et al. 2001; Roth and Wolfenson 2016). Oocytes collected during the summer period are reported to have impaired microtubule rearrangements and deformed spindle

apparatus, which disrupt the nuclear maturation and reduce the fertilization rate (Roth and Hansen 2005; Nabenishi et al. 2012). In addition, oocytes collected during the summer season are shown to have a higher level of oxidative stress and apoptosis, which is attributed to the lower mitochondrial distribution (Roth 2017). Previously, we showed that bovine granulosa cells subjected to heat stress trigger the expression of heat shock proteins (HSP), mainly the HSP70 and HSP90 accompanied by excessive accumulation of reactive oxygen species (ROS) and reduced viability of cells (Alemu et al. 2018). A similar phenomenon is also reported in other studies that the HSP70 is among the significantly enriched member of the HSPs and apoptosis is induced by the activation of the endoplasmic reticulum and production of excessive ROS (Hou et al. 2014; Li et al. 2016). One of the widely discussed benefits of EVs is their involvement in releasing cellular toxicants into the extracellular space (Kosaka et al. 2013). This was previously shown that EV-mediated pathway is the prime cause of the intracellular β-catenin pool reduction (Chairoungdua et al. 2010), which suggests the crucial role of EVs in selectively encapsulating and releasing cellular contents to maintain cellular hemostasis. In line with this, the elevated cellular reserve of HSPs is also reflected in the EVs released from cells subjected to heat stress and are involved in improving the immune-related cellular responses (Lancaster and Febbraio 2005; Zhan et al. 2009). The release of EVs enriched with HSP from cells subjected to heat stress shows that EVs could be considered as the reflectors of the cellular stress conditions (de Maio 2011). EVs of heat-stressed cells pose a bystander effect to the unstressed neighboring recipient cells, which is reflected by the reduced rate of apoptosis and DNA damage in the recipient cells (Bewicke-Copley et al. 2017). In addition, the result demonstrated that EVs from heat-stressed cells have the potential to protect cells from subsequent heat stress. Recently, we reported the EV-mediated transfer of protective bioactive molecules in bovine granulosa cells (Gebremedhn et al. 2020b). In the same study,

granulosa cells subjected to heat stress release a significantly higher number of EVs enriched with HSPs, antioxidants, and GRPs compared to the cells incubated at normal temperature. Among the other components of the stressed EVs, bta-miR-1246, bta-miR-374a, and bta-miR-2904 are abundantly present, from which the miR-1246 is also reported to be among the miRNAs abundantly present in the circulation of dairy cows subjected to summer heat stress (Zheng et al. 2014). Moreover, we showed that prior priming of granulosa cells with the EVs derived from granulosa cells subjected to heat stress transferred protective molecules to the recipient cells against subsequent heat stress, in which the stress EVs supplemented cells had a significantly lower accumulation of intracellular ROS, improved cell viability and reduced level of apoptosis. The most interesting finding of this experiment is that the protective impact of the stressed EVs is pronounced only when the primed cells are subjected to recurrent heat stress (Gebremedhn et al. 2020b). This suggests, the stress condition at the receiving end determines the type of role that is incurred by the uptaken EVs. Recently, we looked deeper into our recently published data, which is the expression of miRNAs and the dynamics of the abundance of miRNAs between the cells and the corresponding EVs upon exposure to heat stress and we showed that there is no single pattern of release of miRNAs into the extracellular space, rather multiple patterns depending on the cellular function of the miRNAs, which are preferentially enriched upon exposure to stress (Gebremedhn et al. 2020a). Similarly, the beneficial effect of EVs derived from the follicular fluid of cows is also reported in reversing the heat stress damage incurred on oocytes and further improved both the cleavage and blastocyst rates (Rodrigues et al. 2019). The most intriguing fact of this finding is that supplementation of both whole follicular fluid and only EVs derived from the same follicular fluid samples showed to have a positive impact in reversing the heat damage on oocytes. Nevertheless, supple- mentation of follicular fluid devoid of the EVs had not reversed

the heat stress damage. This signifies that EVs in the follicular fluid are the major players of a crucial role in protecting oocytes from heat stress and enhance oocyte maturation and function

8.2 EV-coupled molecular cargo as indicators of metabolic stress

Over the past decades, dramatic changes in the amount of milk produced per cow as a result of combined effects of genetic selection for milk yield, improvements in the management of dairy farms, and nutrition are some of the key achievements in the sector. Nevertheless, this dramatic shift in milk yield has caused a significant decline in reproductive efficacies (Lucy 2001). One of the key aspects of the fertility decline in high-yielding dairy cows is attributed to the imbalances in the energy intake and expenditure, which causes post-partum negative energy balance (NEB) (Beam and Butler 1999). The unfavorable metabolic changes in post-partum cows under NEB impairs follicular development and the developmental competence and quality of the enclosed oocytes (Walters et al. 2002). In addition, downregulation of genes associated with proliferation and steroidogenesis potential, which indicates the impaired maturity of oocyte was reported in granulosa cells derived from the early postpartum period. Interestingly, the p38 mitogen-activated protein kinase path- way is one of the downregulated pathways, which is affected by vitamin A availability, suggesting the important role of vitamin A supplementation in mitigating postpartum NEB (Golini et al. 2014). To tackle the early postpartum energy deficit, high-yielding dairy cows mobilize their adipose tissue reserve, which in turn causes elevation of free fatty acids (FFA) in the circulation (Contreras and Sordillo 2011). The quality of the oocyte and granulosa cells of early postpartum cows is affected by the composition of the follicular fluid and serum, which is characterized by elevated concentrations of non-esterified fatty acid (NEFA) and β-hydroxybutyrate (BHB) concentrations (Leroy et al. 2004). The circulation of cows under NEB is reported to have significantly elevated NEFA, mainly the stearic acid (C18:0), palmitic (C16:0),

and oleic acid (C18:1) (Rukkwamsuk et al. 2000). The toxic effect of NEFA during follicular development was further verified in an in vitro granulosa cells culture, in which the proliferation was significantly reduced and the rate of apoptosis was significantly higher upon treatment with both the palmitic and oleic acids (Vanholder et al. 2005). The content of the EVs in cows' circulation could also be affected by the postpartum energy status.

To examine this, recently we experimented on early lactating dairy cows with divergent metabolic status. For this, sequential follicular fluid and oocyte aspiration was performed in cows from the fifth to the tenth weeks post- partum. The energy status of the cows was assessed by profiling the concentration of the NEFA and BHB. The expression of the miRNAs release via EVs was assessed and it was found that the miRNA profile of EVs released from cows under NEB showed massive deregulation and cows under positive energy balance have a similar expression of miRNAs in the EVs released from the follicular fluid of transient cows (Hailay et al. 2019). The miRNAs that are persistently downregulated in the EVs of cows under NEB, including the miR-132, miR-451, miR-486, miR-874, and miR-2285 are predicted to be involved in biological pathways associated with ovarian function including the TGF-β signaling, lysine degradation, cell cycle, FOXO signaling, mTOR signaling, and others. The difference in miRNAs of the follicular fluid EVs is also reflected in the epigenome profile of the corresponding oocytes, which showed massive differentially methylated regions (DMRs) in oocytes derived from NEB cows compared to cows under positive energy balance (Poirier et al. 2020). Interestingly, among the differentially methylated genomic regions in the oocyte of early postpartum cows, we found genes involved in important pathways including carbon metabolism, and fatty acid metabolism. Moreover, oocytes of postpartum cows are differentially methylated in some imprinted genes namely, MEST and GNAS suggesting the impact of postpartum NEB on the acquisition of imprinting.

8.3 EV-mediated cellular response to oxidative stress

Oxidative stress is a phenomenon, which is caused when the production of ROS overwhelms the cellular production of antioxidants that scavenge the ROS (Burton and Jauniaux 2011). However, it is worth mentioning that a moderate level of ROS production is necessary for maintaining cellular homeostasis and for important stages of follicular development. For instance, ROS produced by the ovary during the follicular stage of the oestrous cycle is reported to induce apoptosis in granulosa and break the wall of the preovulatory follicle and facilitate the ovulation process (Shkolnik et al. 2011). This implies that the amount of ROS production and the ROS scavenging antioxidant production depends on the stage of the follicular development (Agarwal et al. 2012). To understand the impact of the ROS radicals on follicular development, the half-life and ability to be translocated into the nucleus of the cells are important to take into consideration. Among the free radicals, H2O2 is widely utilized as a model for in vitro functional studies (Aprioku 2013). We previously reported that granulosa cells exogenously treated with a mild dose of H2O2 resulted in excessive accumulation of ROS and activation of the key transcription factor and downstream antioxidant genes of the NRF2-mediated oxidative stress signaling pathway: namely NRF2, CAT, TXN1, and PRDX1 (Saeed-Zidane et al. 2017). In the same experiment, examination of the spent culture media revealed that granulosa cells treated with H2O2 released higher number of EVs and those EVs are enriched with some of the antioxidants that were enriched in the cells. This is in agreement with the hypothesis that cells under stress utilize the EVs-mediated pathway to release cellular toxicants (Kosaka et al. 2013). Co-incubation of granulosa cells with these EVs after exposing cells to H2O2 reduced the accumulation of ROS but did not reduce the expression of the oxidative stress-related genes, which could be because of the fact that treatment with H2O2 caused significant transcriptional alteration that could not be reversed by the

supplementation of stressed cells derived EVs (Saeed-Zidane et al. 2017). However, EVs supplemented to cells before the exposure to oxidative stress incurred a protective message to the recipient cells upon subsequent exposure to H2O2 (Eldh et al. 2010). It is worth noting that the time of the EVs supplementation is critical for the delivery of bioactive molecules to either rescue or protect cells from oxidative stress.

Taken all together, EVs of reproductive cells could be essential mediators of environmental and physiological stress. EVs released from reproductive cells subjected to various stressors are enriched with a multitude of bioactive molecules, mainly, miRNAs, stress-associated genes, and methylation modulators. These bioactive molecules could be implicated in improving cellular stress tolerance, improving the outcome of ARTs, and serve as remedies against stress- associated pathophysiological conditions. The aforementioned phenomenon is briefly illustrated in Figure 1.2.

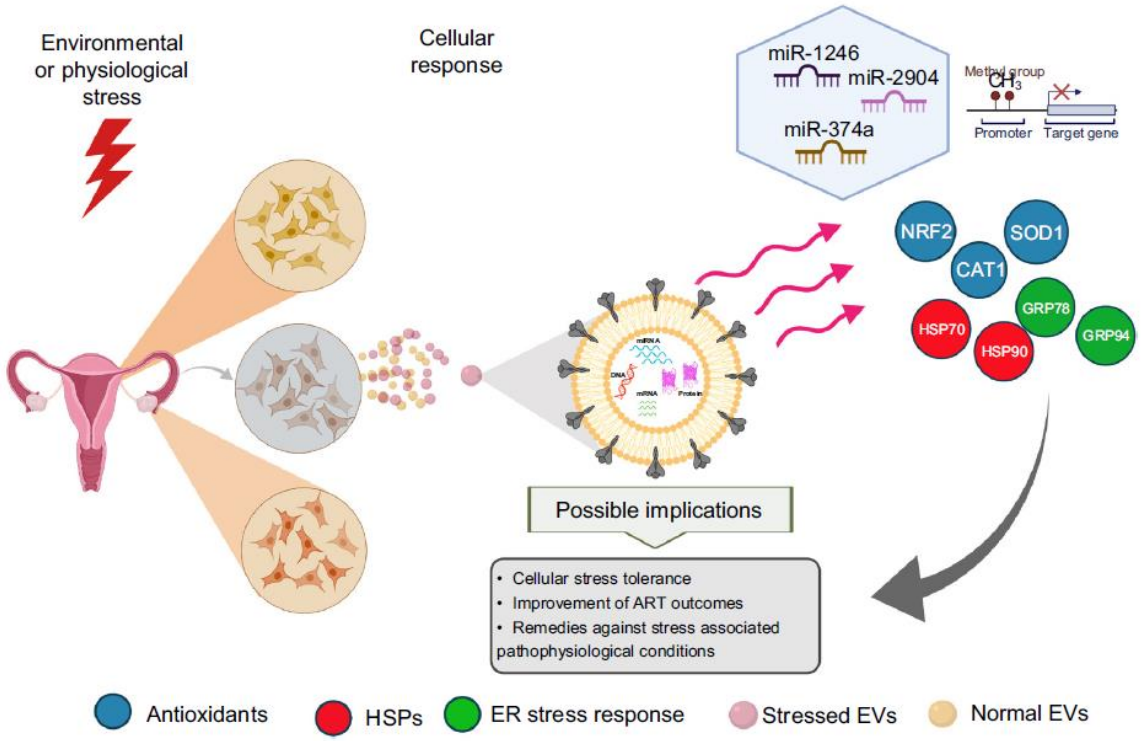


Figure 1.2. A hypothetical model. Reproductive cells respond and release of EVs enriched with stress- associated molecules including, miRNAs and methylation modulators, which could have important implications in improving the stress tolerance, the outcome of ARTs procedures, and possible remedies for stress associated pathophysiological conditions.

8.4 The potential of EVs in reproduction and related fields

Recent developments in modification of EVs facilitated the monitoring and tracking, interaction and transfer in vivo and in vitro (Lai et al. 2015). In that study engineered optical reporters were used to label multiple EV populations for visualization and tracking of tumour EV release, uptake and exchange between cell populations both in vitro and in vivo. Due to the variability in EV internalization mechanisms that exist between cell types, use of specific inhibitors provide a useful tool to study cell specific uptake mechanisms. For this, several inhibitors have been developed, including chlor- promazine to investigate clathrin-mediated uptake (Mulcahy et al. 2014), and specific RDG inhibitory peptides to target integrin-mediated EV uptake (Hoshino et al. 2015). Further research is needed to investigate the precise mechanisms that underline a specific EV entry into selected target cells and, importantly, the way to control the process.

An increasing amount of studies have evidenced the key role of EVs in regulating the different aspects of the reproduction process including gamete (sperm and ova) maturation, sperm capacitation, prevention of polyspermy, oviduct/ uterine-embryo communication and even communication between in vitro-cocultured embryos (Machtinger et al. 2016). Following the preimplantation developmental process, EV production and function continue throughout pregnancy with the placenta and uterine epithelium to be the main source of EVs in maternal-embryo communication (Burns et al. 2016). Follicular microenvironment, which is filled with follicular fluid, is a place for successful maturation of oocytes during the process of folliculogenesis. The easy availability of follicular fluid during oocyte aspiration in human and animals assisted reproductive technology procedures makes it attractive in the search for

biomarkers associated with oocyte quality. Previous studies in bovines demonstrated the presence of specific miRNA signatures coupled in exosomal and nonexosomal portions of the follicular fluid based on the growth status of the oocytes, thereby developmental competence (Sohel et al. 2013). Similarly, EV coupled miRNAs were also found to be associated with advanced maternal aging in mares (Da Silveira et al. 2012). Similarly, comparative analysis of miRNA isolated from EVs derived follicular fluid of young versus older women revealed differential expression of miRNAs targeting genes associated with heparin-sulphate biosynthesis, carbohydrate digestion and absorption, p53 signalling and cytokine– cytokine–receptor interaction (Diez-Fraile et al. 2014).

The use of successful ART is increasingly required to tackle age related infertility problems in humans. Similarly, an increase in selection for production traits in the cattle industry resulted in an increasing decline in fertility. However, the outcome from current ART procedures is far from optimal in terms of pregnancy success after transfer of the resulting blastocysts. Two factors contribute to this low success rate of ART. Firstly, embryo selection for transfer to the recipient has inherent limitations which is mainly dependent on morphological assessment without considering the inherent quality of the embryo in inducing pregnancy (Fragouli et al. 2014). Secondly, the in vitro handling of gametes and embryos under suboptimal culture conditions can induce damage to the functional and structural units of embryos which affect their developmental competence to induce pregnancy after transfer. One of the main reasons for the suboptimal condition of mammalian ART is the absence of reproductive tract factors during in vitro culture of gametes and embryos. To tackle this problem several studies have tried to supplement reproductive tract fluids in the existing ART and could improve the quality of the resulting embryos. Several studies have demonstrated the presence of EVs in bovine follicular fluid and oviductal fluid and

their molecular cargo composition is governed by the physiological status of the host animal. Those changes in molecular cargo carried by EVs is supposed to create optimal conditions for oocyte growth, sperm capacitation, gamete transport, fertilization and preimplantation embryo development. Similarly, the protein content of uterine EVs released by in vitro cultured human endometrial epithelial cells is found to be altered by oestrogen and progesterone treatments suggesting hormonal regulation of EV cargo from uterine cells (Greening et al. 2016). A systematic analysis of bovine reproductive fluid EV contents demonstrated that they carry functional molecules associated with heat shock proteins, antioxidants, energy metabolism, amino acid biosynthesis and regulatory miRNAs targeting genes associated with various functional physiology of the oviduct (Almiñana et al. 2017, 2018; Hailay et al. 2019).

As it is a natural milieu for oocyte maturation in the ovarian follicle, follicular fluid has been utilized as a supplement during IVM procedures and a positive impact has been reported. The positive impact of follicular fluid on oocyte maturation in vitro is attributed to its protein, cytokine, growth factors, steroids, metabolites, and other substances present in the follicular fluid (Sutton et al. 2003). Several studies have been conducted using different levels of follicular fluid and positive impacts in terms of increased blastocysts cell number (Kim et al. 1996), increased inner cell mass number and higher cleavage rate of oocytes matured with follicular fluid collected 20 h after LH surge (Romero-Arredondo and Seidel 1996). In a similar study, supplementation of bovine in vitro maturation media with follicular fluid resulted in enhanced sperm penetration, increased cumulus expansion and ATP levels in oocytes, while blastocyst rate remain the same (Somfai et al. 2012). The functional significance of follicular fluid EVs was found to be dependent on the size of the follicle from which they are isolated. Accordingly, EVs isolated from follicular fluid aspirated from small (3–5 mm) and large (>9 mm) antral follicle were supplemented in IVM of bovine and

mouse oocytes and a significant effect on cumulus expansion and expression of cumulus expansion marker genes was observed by EVs derived from small follicles (Hung et al. 2015). This implies that future research needs to focus on deciphering the molecular content of follicular fluid to identify key molecular cargos which play a significant role to support oocyte growth and maturation with potential application in current ART programs.

Supplementation of in vitro bovine embryo culture with oviductal and uterine fluid supports embryo development and induces the expression of genes related to methylation and oxidative stress (Hamdi et al. 2018). Differential composition of EVs were found in oviductal fluid derived from bovine ampullary and isthmus portion of the oviducts suggesting the differential role of EVs in different parts of the oviduct (Lopera-Vasquez et al. 2017). Moreover, comparative proteomic analysis of EVs derived from in vitro cultured oviductal epithelial cells revealed significant variation in their protein content compared to EVs derived from in vivo oviductal fluid (Almiñana et al. 2017). These differences are most likely to be attributed to the lack of many complex features present in the in vivo microenvironment including in vivo cellular diversity. As generation of enough amount of in vivo oviductal EVs for research and also for ART application is very challenging. Recently, oviductal organoids are being investigated for their suit- ability to generate in vivo-like EVs under in vitro condition as it is a technology to recapitulate the in vivo features of the oviduct (Heidari-Khoei et al. 2020). Therefore, reproductive organoids with other technologies including microfluidics technology would enable scientists to create an organoid-on-a-chip platform which provides new in vitro models to serve as both tissue and organ proxies to bridge the gap between in vitro and in vivo (Lancaster and Knoblich 2014). As organoids are self-organizing structures that can recapitulate the different biological and pathological features of the organ, they represent genetic stability and maintain commitment to their tissue of origin during

long-term culture to get access to an unlimited source of material like EVs to support research in the field. Therefore, reproductive organoids will facilitate the unlimited access to the generation of quantitative and qualitatively acceptable EVs for future research.

The EV-based liquid biopsy tests are under intensive investigation and a strong interest centred around the potential of EVs to serve as targets of the development of biomarkers or therapeutic reagents, especially in the field of cancer research (Théry 2015). In the field of reproduction, the main challenge of development of EV-based biomarker discovery is reproducibility, which is influenced by the various limitations associated with EV isolation, characterization and tracking. In addition, the development as biomarker is dependent on the methods which favors the isolation of highly purified EVs produced in a reproduceable and cost-effective manner. Most research in the field of reproductive EVs are descriptive in their nature without elucidating the actual mechanism of action. A standardized EV isolation method is believed to facilitate the translation and reproducibility of the findings in the clinical diagnostic settings.

References

Agarwal, A, Aponte-Mellado, A, Premkumar, BJ, Shaman, A, and Gupta, S (2012). The effects of oxidative stress on female reproduction: a review. Reproductive Biology and Endocrinology 10, 49.

Al-Dossary, AA, Strehler Emanuel, E, and Martin-Deleon, PA (2013). Expression and secretion of plasma membrane Ca2+-ATPase 4a (PMCA4a) during murine estrus: association with oviductal exosomes and uptake in sperm. PLoS ONE 8, e80181.

Alemu, TW, Pandey, HO, Salilew Wondim, D, Gebremedhn, S, Neuhof, C, Tholen, E, et al. (2018). Oxidative and endoplasmic reticulum stress defense mechanisms of bovine granulosa cells exposed to heat stress. Theriogenology 110, 130–141.

Almagor, M, Bejar, C, Kafka, I, and Yaffe, H (1996). Pregnancy rates after communal growth of preimplantation human embryos in vitro. Fertility and Sterility 66, 394–397.

Almiñana, C, Corbin, E, Tsikis, G, Alcântara-Neto, AS, Labas, V, Reynaud, K, et al. (2017). Oviduct extracellular vesicles protein content and their role during oviduct-embryo cross-talk. Reproduction (Cambridge, England) 154, 153–168.

Almiñana, C, Tsikis, G, Labas, V, Uzbekov, R, da Silveira, JC, Bauersachs, S, and Mermillod, P (2018). Deciphering the oviductal extracellular vesicles content across the estrous cycle: implications for the gametes–oviduct interactions and the environment of the potential embryo. BMC Genomics 19, 622.

Alvarez-Erviti, L, Seow, Y, Yin, H, Betts, C, Lakhal, S, and Wood, MJA (2011). Delivery of siRNA to the mouse brain by systemic injection of targeted exosomes. Nature Biotechnology 29, 341–345.

Aprioku, JS (2013). Pharmacology of free radicals and the impact of reactive oxygen species on the testis. Journal of Reproduction & Infertility 14, 158–172.

Asaadi, A, Dolatabad, NA, Atashi, H, Raes, A, van Damme, P, Hoelker, M, et al. (2021). Extracellular vesicles from follicular and ampullary fluid isolated by density gradient ultracentrifugation improve bovine embryo development and quality. International Journal of Molecular Sciences 22, 578.

Avilés, M, Gutiérrez-Adán, A, and Coy, P (2010). Oviductal secretions: will they be key factors for the future ARTs? In Molecular Human Reproduction 16, 896–906.

Baddela, VS, Sharma, A, Viergutz, T, Koczan, D, and Vanselow, J (2018). Low oxygen levels induce early luteinization associated changes in bovine granulosa cells. Frontiers in Physiology 9, 1066.

Baixauli, F, López-Otín, C, and Mittelbrunn, M (2014). Exosomes and autophagy: coordinated mechanisms for the maintenance of cellular fitness. Frontiers in Immunology 5, 403.

Beam, SW, and Butler, WR (1997). Energy balance and ovarian follicle development prior to the first ovulation postpartum in dairy cows receiving three levels of dietary fat. Biology of Reproduction 56, 133–142.

Beam, SW, and Butler, WR (1999). Effects of energy balance on follicular development and first ovulation in postpartum dairy cows. Journal of Reproduction and Fertility 54, 411–424.

Belleannée, C, Calvo, É, Caballero, J, and Sullivan, R (2013). Epididymosomes convey different repertoires of microRNAs throughout the bovine epididymis. Biology of Reproduction 89, 30.

Bewicke-Copley, F, Mulcahy, LA, Jacobs, LA, Samuel, P, Akbar, N, Pink, RC, and Carter, DRF (2017). Extracellular vesicles released following heat stress induce bystander effect in unstressed populations. Journal of Extracellular Vesicles 6, 1340746.

Bosco, D, Haefliger, J-A, and Meda, P (2011). Connexins: key mediators of endocrine function. Physiological Reviews 91, 1393–1445.

Brower, PT, and Schultz, RM (1982). Intercellular communication between granulosa cells and mouse oocytes: existence and possible nutritional role during oocyte growth. Developmental Biology 90, 144–153.

Burton, GJ, and Jauniaux, E (2011). Oxidative stress. Best Practice & Research Clinical Obstetrics & Gynaecology 25, 287–299.

Burton, KA, and McKnight, GS (2007). PKA, germ cells, and fertility. Physiology (Bethesda, MD) 22, 40–46.

Burns, G, Brooks, K, Wildung, M, Navakanitworakul, R, Christenson, LK, and Spencer, TE (2014). Extracellular vesicles in luminal fluid of the ovine uterus. PLoS ONE 9, e90913.

Burns, GW, Brooks, KE, and Spencer, TE (2016). Extracellular vesicles originate from the conceptus and uterus during early pregnancy in sheep. Biology of Reproduction 94, 56.

Burns, GW, Brooks, KE, O'Neil, EV, Hagen, DE, Behura, SK, and Spencer, TE (2018). Progesterone effects on extracellular vesicles in the sheep uterus. Biology of Reproduction 98, 612–622.

Can, U, Buyukinan, M, and Yerlikaya, FH (2016). The investigation of circulating microRNAs associated with lipid metabolism in childhood obesity. Pediatric Obesity 11, 228–234.

Castaño, C, Kalko, S, Novials, A, and Párrizas, M (2018). Obesity-associated exosomal miRNAs modulate glucose and lipid metabolism in mice. Proceedings of the National Academy of Sciences of the United States of America 115, 12158–12163.

Chairoungdua, A, Smith, DL, Pochard, P, Hull, M, and Caplan, MJ (2010). Exosome release of β-catenin: a novel mechanism that antagonizes Wnt signaling. The Journal of Cell Biology 190, 1079–1091.

Che, X, Jian, F, Chen, C, Liu, C, Liu, G, and Feng, W (2020). PCOS serum-derived exosomal miR-27a-5p stimulates endometrial cancer cells migration and invasion. Journal of Molecular Endocrinology 64, 1–12.

Cheng, L, Doecke, JD, Sharples, RA, Villemagne, VL, Fowler, CJ, Rembach, A, et al. (2015). Prognostic serum miRNA biomarkers associated with Alzheimer's disease shows concordance with neuropsychological and neuroimaging assessment. Molecular Psychiatry 20, 1188–1196.

Colombo, M, Raposo, G, and Théry, C (2014). Biogenesis, secretion, and intercellular interactions of exosomes and other extracellular vesicles. Annual Review of Cell and Developmental Biology 30, 255–289.

Conti, M, Hsieh, M, Zamah, AM, and Oh, JS (2012). Novel signaling mechanisms in the ovary during oocyte maturation and ovulation. Molecular and Cellular Endocrinology 356, 65–73.

Contreras, GA, and Sordillo, LM (2011). Lipid mobilization and inflammatory responses during the transition period of dairy cows. Comparative Immunology, Microbiology and Infectious Diseases 34, 281–289.

Coy, P, García-Vázquez, FA, Visconti, PE, and Avilés, M (2012). Roles of the oviduct in mammalian fertilization. Reproduction (Cambridge, England) 144, 649–660.

Cronqvist, T, Erlandsson, L, Tannetta, D, and Hansson, SR (2020). Placental syncytiotrophoblast extracellular vesicles enter primary endothelial cells through clathrin-mediated endocytosis. Placenta 100, 133–141.

Cruz, L, Romero, JAA, Iglesia, RP, and Lopes, MH (2018). Extracellular vesicles: decoding a new language for cellular communication in early embryonic Development. Frontiers in Cell and Developmental Biology 6, 94.

Da Silveira, JC, Veeramachaneni, DNR, Winger, QA, Carnevale, EM, and Bouma, GJ (2012). Cell-secreted vesicles in equine ovarian follicular fluid contain miRNAs and proteins: a possible new form of cell communication within the ovarian follicle. Biology of Reproduction 86, 71.

de Maio, A (2011). Extracellular heat shock proteins, cellular export vesicles, and the Stress Observation System: a form of communication during injury, infection, and cell damage. It is never known how far a controversial finding will go! Dedicated to Ferruccio Ritossa. Cell Stress & Chaperones 16, 235–249.

Dhahbi, JM, Spindler, SR, Atamna, H, Yamakawa, A, Guerrero, N, Boffelli, D, et al. (2013). Deep sequencing identifies circulating mouse miRNAs that are functionally implicated in manifestations of aging and responsive to calorie restriction. Aging 5, 130–141.

Diez-Fraile, A, Lammens, T, Tilleman, K, Witkowski, W, Verhasselt, B, de Sutter, Petra, et al. (2014). Age-associated differential microRNA levels in human follicular fluid reveal pathways potentially determining fertility and success of in vitro fertilization. Human Fertility (Cambridge, England) 17, 90–98.

Dong, H, Wang, C, Lu, S, Yu, C, Huang, L, Feng, W, et al. (2016). A panel of four decreased serum microRNAs as a novel biomarker for early Parkinson's disease. Biomarkers: Biochemical Indicators of Exposure, Response, and Susceptibility to Chemicals 21, 129–137.

Donnay, I, van Langendonckt, A, Auquier, P, Grisart, B, Vansteenbrugge, A, Massip, A, and Dessy, F (1997). Effects of co-culture and embryo number on the in vitro development of bovine embryos. Theriogenology 47, 1549–1561.

Ebner, T, Shebl, O, Moser, M, Mayer, RB, Arzt, W, and Tews, G (2010). Group culture of human zygotes is superior to individual culture in terms of blastulation, implantation and life birth. Reproductive Biomedicine Online 21, 762–768.

Edwards, JL, and Hansen, PJ (1996). Elevated temperature increases heat shock protein 70 synthesis in bovine two-cell embryos and compromises function of maturing oocytes. Biology of Reproduction 55, 341–346.

Eldh, M, Ekström, K, Valadi, H, Sjöstrand, M, Olsson, B, Jernås, M, and Lötvall, J (2010). Exosomes communicate protective messages during oxidative stress; possible role of exosomal shuttle RNA. PLoS ONE 5, e15353.

Escrevente, C, Keller, S, Altevogt, P, and Costa, J (2011). Interaction and uptake of exosomes by ovarian cancer cells. BMC Cancer 11, 108.

Fabbri, M, Paone, A, Calore, F, Galli, R, Gaudio, E, Santhanam, R, et al. (2012). MicroRNAs bind to Toll-like receptors to induce prometastatic inflammatory response. Proceedings of the National Academy of Sciences of the United States of America 109, E2110–E2116.

Fazeli, A (2011). Maternal communication with gametes and embryo: a personal opinion. Reproduction in Domestic Animals = Zuchthygiene 46, 75–78.

Fereshteh, Z, Bathala, P, Galileo, DS, and Martin-Deleon, PA (2019). Detection of extracellular vesicles in the mouse vaginal fluid: their delivery of sperm proteins that stimulate capacitation and modulate fertility. Journal of Cellular Physiology 234, 12745–12756.

Fortune, JE (1994). Ovarian follicular growth and development in mammals. Biology of Reproduction 50, 225–232.

Fragouli, E, Alfarawati, S, Spath, K, and Wells, D (2014). Morphological and cytogenetic assessment of cleavage and blastocyst stage embryos. Molecular Human Reproduction 20, 117–126.

Franchi, A, Cubilla, M, Guidobaldi, HA, Bravo, AA, and Giojalas, LC (2016). Uterosome-like vesicles prompt human sperm fertilizing capability. Molecular Human Reproduction 22, 833–841.

Galimberti, D, Villa, C, Fenoglio, C, Serpente, M, Ghezzi, L, Cioffi, SMG, et al. (2014). Circulating miRNAs as potential biomarkers in Alzheimer's disease. Journal of Alzheimer's Disease 42, 1261–1267.

Gatien, J, Mermillod, P, Tsikis, G, Bernardi, O, Janati Idrissi, S, Uzbekov, R, et al. (2019). Metabolomic profile of oviductal extracellular vesicles across the estrous cycle in cattle. International Journal of Molecular Sciences 20, .

Gebremedhn, S, Ali, A, Gad, A, Prochazka, R, and Tesfaye, D (2020a). Extracellular vesicles as mediators of environmental and metabolic stress coping mechanisms during mammalian follicular development. Frontiers in Veterinary Science 7, 602043.

Gebremedhn, S, Gad, A, Aglan, HS, Laurincik, J, Prochazka, R, Salilew-Wondim, D, et al. (2020b). Extracellular vesicles shuttle protective messages against heat stress in bovine granulosa cells. Scientific Reports 10, 15824.

Golini, VE, Stradaioli, G, and Sirard, MA (2014). Transcriptome analysis of bovine granulosa cells of preovulatory follicles harvested 30, 60, 90, and 120 days postpartum. Theriogenology 82, 580–591.e5.

Greening, DW, Nguyen, HPT, Elgass, K, Simpson Richard, J, and Salamonsen, LA (2016). Human endometrial exosomes contain hormone-specific cargo modulating trophoblast adhesive capacity: insights into endometrial–embryo interactions. Biology of Reproduction 94, 38.

Hailay, T, Hoelker, M, Poirier, M, Gebremedhn, S, Rings, F, Saeed-Zidane, M, et al. (2019). Extracellular vesicle-coupled miRNA profiles in follicular fluid of cows with divergent post-calving metabolic status. Scientific Reports 9, 12851.

Hamdi, M, Lopera-Vasquez, R, Maillo, V, Sanchez-Calabuig, MJ, Núnez, C, Gutierrez-Adan, A, and Rizos, D (2018). Bovine oviductal and uterine fluid support in vitro embryo development. Reproduction, Fertility, and Development 30, 935–945.

Hansen, LB (2000). Consequences of selection for milk yield from a geneticist's viewpoint. Journal of Dairy Science 83, 1145–1150.

Hanson, PI, and Cashikar, A (2012). Multivesicular body morphogenesis. Annual Review of Cell and Developmental Biology 28, 337–362.

Harris, EA, Stephens, KK, and Winuthayanon, W (2020). Extracellular vesicles and the oviduct function. International Journal of Molecular Sciences 21, 8280.

Heidari-Khoei, H, Esfandiari, F, Hajari, MA, Ghorbaninejad, Z, Piryaei, A, and Baharvand, H (2020). Organoid technology in female reproductive biomedicine. Reproductive Biology and Endocrinology 18, 64.

Hemler, ME (2005). Tetraspanin functions and associated microdomains. Nature Reviews. Molecular Cell Biology 6, 801–811.

Higuchi, C, Nakatsuka, A, Eguchi, J, Teshigawara, S, Kanzaki, M, Katayama, A, et al. (2015). Identification of circulating miR-101, miR-375 and miR-802 as biomarkers for type 2 diabetes. Metabolism: Clinical and Experimental 64, 489–497.

Hoelker, M, Rings, F, Lund, Q, Phatsara, C, Schellander, K, and Tesfaye, D (2010). Effect of embryo density on in vitro developmental characteristics of bovine preimplantative embryos with respect to micro and macroenvironments. Reproduction in Domestic Animals 45, e138–145.

Horibe, S, Tanahashi, T, Kawauchi, S, Murakami, Y, and Rikitake, Y (2018). Mechanism of recipient cell-dependent differences in exosome uptake. BMC Cancer 18, 47.

Hoshino, A, Costa-Silva, B, Shen, T-L, Rodrigues, G, Hashimoto, A, Tesic Mark, M, et al. (2015). Tumour exosome integrins determine organotropic metastasis. Nature 527, 329–335.

Hou, C-H, Lin, F-L, Hou, S-M, and Liu, J-F (2014). Hyperthermia induces apoptosis through endoplasmic reticulum and reactive oxygen species in human osteosarcoma cells. International Journal of Molecular Sciences 15, 17380–17395.

Hu, J, Tang, T, Zeng, Z, Wu, J, Tan, X, and Yan, J (2020). The expression of small RNAs in exosomes of follicular fluid altered in human polycystic ovarian syndrome. PeerJ 8, e8640.

Hung, W-T, Hong, X, Christenson, LK, and McGinnis, LK (2015). Extracellular vesicles from bovine follicular fluid support cumulus expansion. Biology of Reproduction 93, 117.

Hung, W-T, Navakanitworakul, R, Khan, T, Zhang, P, Davis, JS, McGinnis, LK, and Christenson, LK (2017). Stage-specific follicular extracellular vesicle uptake and regulation of bovine granulosa cell proliferation. Biology of Reproduction 97, 644–655.

Ibrahim, A, and Marbán, E (2016). Exosomes: fundamental biology and roles in cardiovascular physiology. Annual Review of Physiology 78, 67–83.

Jacobs, LA, Bewicke-Copley, F, Poolman, MG, Pink, RC, Mulcahy, LA, Baker, I, et al. (2013). Meta-analysis using a novel database, miRStress, reveals miRNAs that are frequently associated with the radiation and hypoxia stress-responses. PLoS ONE 8, e80844.

Jiang, X, Li, J, Zhang, B, Hu, J, Ma, J, Cui, L, and Chen, Z-J (2021). Differential expression profile of plasma exosomal microRNAs in women with polycystic ovary syndrome. Fertility and Sterility 115, 782–792.

Kalluri, R, and LeBleu, VS (2020). The biology, function, and biomedical applications of exosomes. Science (New York, NY) 367, eaau6977.

Keller, S, Ridinger, J, Rupp, A-K, Janssen, JWG, and Altevogt, P (2011). Body fluid derived exosomes as a novel template for clinical diagnostics. Journal of Translational Medicine 9, 86.

Kim, K, Mitsumizo, N, Fujita, K, and Utsumi, K (1996). The effects of follicular fluid on in vitro maturation, oocyte fertilization and the development of bovine embryos. Theriogenology 45, 787–799.

Kirkman, MS, Briscoe, VJ, Clark, N, Florez, H, Haas, LB, Halter, JB, et al. (2012). Diabetes in older adults. Diabetes Care 35, 2650–2664.

Kong, L, Zhu, J, Han, W, Jiang, X, Xu, M, Zhao, Y, et al. (2011). Significance of serum microRNAs in pre-diabetes and newly diagnosed type 2 diabetes: a clinical study. Acta Diabetologica 48, 61–69.

Kosaka, N, Yoshioka, Y, Hagiwara, K, Tominaga, N, Katsuda, T, and Ochiya, T (2013). Trash or treasure: extracellular microRNAs and cell-to-cell communication. Frontiers in Genetics 4, 173.

Laflamme, J, Akoum, A, and Leclerc, P (2005). Induction of human sperm capacitation and protein tyrosine phosphorylation by endometrial cells and interleukin-6. Molecular Human Reproduction 11, 141–150.

Lai, CP, Kim, EY, Badr, CE, Weissleder, R, Mempel, TR, Tannous, BA, and Breakefield, XO (2015). Visualization and tracking of tumour extracellular vesicle delivery and RNA translation using multiplexed reporters. Nature Communications 6, 7029.

Lancaster, GI, and Febbraio, MA (2005). Exosome-dependent trafficking of HSP70: a novel secretory pathway for cellular stress proteins. The Journal of Biological Chemistry 280, 23349–23355.

Lancaster, MA, and Knoblich, JA (2014). Organogenesis in a dish: modeling development and disease using organoid technologies. Science (New York, NY) 345, 1247125.

Leese, HJ, Hugentobler, SA, Gray, SM, Morris, DG, Sturmey, RG, Whitear, S-L, and Sreenan, JM (2008). Female reproductive tract fluids: composition, mechanism of formation and potential role in the developmental origins of health and disease. Reproduction, Fertility, and Development 20, 1–8.

Leroy, JLMR, Vanholder, T, Delanghe, JR, Opsomer, G, van Soom, A, Bols, PEJ, et al. (2004). Metabolic changes in follicular fluid of the dominant follicle in high-yielding dairy cows early post partum. Theriogenology 62, 1131–1143.

Li, J, Gao, H, Tian, Z, Wu, Y, Wang, Y, Fang, Y, et al. (2016). Effects of chronic heat stress on granulosa cell apoptosis and follicular atresia in mouse ovary. Journal of Animal Science and Biotechnology 7, 57.

Liang, B, Peng, P, Chen, S, Li, L, Zhang, M, Cao, D, et al. (2013). Characterization and proteomic analysis of ovarian cancer-derived exosomes. Journal of Proteomics 80, 171–182.

Lopera-Vásquez, R, Hamdi, M, Fernandez-Fuertes, B, Maillo, V, Beltrán-Breña, P, Calle, A, et al. (2016). Extracellular vesicles from BOEC in in vitro embryo development and quality. PLoS ONE 11, e0148083.

Lopera-Vasquez, R, Hamdi, Me, Maillo, V, Gutierrez-Adan, A, Bermejo-Alvarez, P, Ramírez, MÁ, et al. (2017). Effect of bovine oviductal extracellular vesicles on embryo development and quality in vitro. Reproduction (Cambridge, England) 153, 461–470.

López-Otín, C, Blasco, MA, Partridge, L, Serrano, M, and Kroemer, G (2013). The hallmarks of aging. Cell 153, 1194–1217.

Lucy, MC (2001). Reproductive loss in high-producing dairy cattle: where will it end? In Journal of Dairy Science 84, 1277–1293.

Lv, A, Tu, Z, Huang, Y, Lu, W, and Xie, B (2021). Circulating exosomal miR-125a-5p as a novel biomarker for cervical cancer. Oncology Letters 21, 54.

Machtinger, R, Laurent, LC, and Baccarelli, AA (2016). Extracellular vesicles: roles in gamete maturation, fertilization and embryo implantation. Human Reproduction Update 22, 182–193.

María, Y-M, Pia, R-MS, Zoraida, A, Apolonija, BZ, Francesc, EB, Edit, IB, et al. (2015). Biological properties of extracellular vesicles and their physiological functions. Journal of Extracellular Vesicles 4, 27066.

Mathieu, M, Martin-Jaular, L, Lavieu, G, and Théry, C (2019). Specificities of secretion and uptake of exosomes and other extracellular vesicles for cell-to-cell communication. Nature Cell Biology 21, 9–17.

Meuwissen, TH, Hayes, BJ, and Goddard, ME (2001). Prediction of total genetic value using genome-wide dense marker maps. Genetics 157, 1819–1829.

Montecalvo, A, Larregina, AT, Shufesky, WJ, Stolz, DB, Sullivan, MLG, Karlsson, JM, et al. (2012). Mechanism of transfer of functional microRNAs between mouse dendritic cells via exosomes. Blood 119, 756–766.

Morelli, AE, Larregina, AT, Shufesky, WJ, Sullivan, MLG, Stolz, DB, Papworth, GD, et al. (2004). Endocytosis, intracellular sorting, and processing of exosomes by dendritic cells. Blood 104, 3257–3266.

Mulcahy, LA, Pink, RC, and Carter, DRF (2014). Routes and mechanisms of extracellular vesicle uptake. Journal of Extracellular Vesicles 3, 24641.

Murdica, V, Giacomini, E, Makieva, S, Zarovni, N, Candiani, M, Salonia, A, et al. (2020). In vitro cultured human endometrial cells release extracellular vesicles that can be uptaken by spermatozoa. Scientific Reports 10, 8856.

Nabenishi, H, Ohta, H, Nishimoto, T, Morita, T, Ashizawa, K, and Tsuzuki, Y (2012). The effects of cysteine addition during in vitro maturation on the developmental competence, ROS, GSH and apoptosis level of bovine oocytes exposed to heat stress. Zygote (Cambridge, England) 20, 249–259.

Ng, YH, Rome, S, Jalabert, A, Forterre, A, Singh, H, Hincks, CL, and Salamonsen, LA (2013). Endometrial exosomes/microvesicles in the uterine microenvironment: a new paradigm for embryo-endometrial cross talk at implantation. PLoS ONE 8, e58502.

O'Doherty, EM, Wade, MG, Hill, JL, and Boland, MP (1997). Effects of culturing bovine oocytes either singly or in groups on development to blastocysts. Theriogenology 48, 161–169.

Ofir-Birin, Y, Abou Karam, P, Rudik, A, Giladi, T, Porat, Z, and Regev-Rudzki, N (2018). Monitoring extracellular vesicle cargo active uptake by imaging flow cytometry. Frontiers in Immunology 9, 1011.

O'Neill, C (2008). The potential roles for embryotrophic ligands in preimplantation embryo development. Human Reproduction Update 14, 275–288.

O'Shea, LC, Mehta, J, Lonergan, P, Hensey, C, and Fair, T (2012). Developmental competence in oocytes and cumulus cells: candidate genes and networks. Systems Biology in Reproductive Medicine 58, 88–101.

Ostrowski, M, Carmo, NB, Krumeich, S, Fanget, I, Raposo, G, Savina, A, et al. (2010). Rab27a and Rab27b control different steps of the exosome secretion pathway. Nature Cell Biology 12, 19–30.

Pavani, KC, Hendrix, A, van den Broeck, W, Couck, L, Szymanska, K, Lin, X, et al. (2019). Isolation and characterization of functionally active extracellular vesicles from culture medium conditioned by bovine embryos in vitro. International Journal of Molecular Sciences 20, .

Poirier, M, Tesfaye, D, Hailay, T, Salilew-Wondim, D, Gebremedhn, S, Rings, F, et al. (2020). Metabolism-associated genome-wide epigenetic changes in bovine oocytes during early lactation. Scientific Reports 10, 2345.

Pontes, JHF, Nonato-Junior, I, Sanches, BV, Ereno-Junior, JC, Uvo, S, Barreiros, TRR, et al. (2009). Comparison of embryo yield and pregnancy rate between in vivo and in vitro methods in the same Nelore (Bos indicus) donor cows. Theriogenology 71, 690–697.

Qu, P, Luo, S, Du, Y, Zhang, Y, Song, X, Yuan, X, et al. (2020). Extracellular vesicles and melatonin benefit embryonic develop by regulating reactive oxygen species and 5-methylcytosine. Journal of Pineal Research 68, e12635.

Racicot, K, Schmitt, A, and Ott, T (2012). The myxovirus-resistance protein, MX1, is a component of exosomes secreted by uterine epithelial cells. American Journal of Reproductive Immunology 67, 498–505.

Raposo, G, and Stoorvogel, W (2013). Extracellular vesicles: exosomes, microvesicles, and friends. The Journal of Cell Biology 200, 373–383.

Rivera, RM, and Hansen, PJ (2001). Development of cultured bovine embryos after exposure to high temperatures in the physiological range. Reproduction (Cambridge, England) 121, 107–115.

Rodrigues, TA, Tuna, KM, Alli, AA, Tribulo, P, Hansen, PJ, Koh, J, and Paula-Lopes, FF (2019). Follicular fluid exosomes act on the bovine oocyte to improve oocyte competence to support development and survival to heat shock. Reproduction, Fertility, and Development 31, 888–897.

Romero-Arredondo, A, and Seidel, GE (1996). Effects of follicular fluid during in vitro maturation of bovine oocytes on in vitro fertilization and early embryonic development. Biology of Reproduction 55, 1012–1016.

Rosas-Hernandez, H, Chigurupati, S, Raymick, J, Robinson, B, Cuevas, E, Hanig, J, and Sarkar, S (2018). Identification of altered microRNAs in serum of a mouse model of Parkinson's disease. Neuroscience Letters 687, 1–9.

Roth, Z (2017). Effect of heat stress on reproduction in dairy cows: insights into the cellular and molecular responses of the oocyte. Annual Review of Animal Biosciences 5, 151–170.

Roth, Z, and Hansen, PJ (2005). Disruption of nuclear maturation and rearrangement of cytoskeletal elements in bovine oocytes exposed to heat shock during maturation. Reproduction (Cambridge, England) 129, 235–244.

Roth, Z, and Wolfenson, D (2016). Comparing the effects of heat stress and mastitis on ovarian function in lactating cows: basic and applied aspects. Domestic Animal Endocrinology 56, S218–S227.

Roth, Z, Meidan, R, Shaham-Albalancy, A, Braw-Tal, R, and Wolfenson, D (2001). Delayed effect of heat stress on steroid production in medium-sized and preovulatory bovine follicles. Reproduction (Cambridge, England) 121, 745–751.

Ruiz-González, I, Xu, J, Wang, X, Burghardt, RC, Dunlap, KA, and Bazer, FW (2015). Exosomes, endogenous retroviruses and toll-like receptors: pregnancy recognition in ewes. Reproduction (Cambridge, England) 149, 281–291.

Rukkwamsuk, T, Geelen, MJ, Kruip, TA, and Wensing, T (2000). Interrelation of fatty acid composition in adipose tissue, serum, and liver of dairy cows during the development of fatty liver postpartum. Journal of Dairy Science 83, 52–59.

Saadeldin, IM, Kim, SJ, Choi, YB, and Lee, BC (2014). Improvement of cloned embryos development by co-culturing with parthenotes: a possible role of exosomes/microvesicles for embryos paracrine communication. Cellular Reprogramming 16, 223–234.

Saeed-Zidane, M, Linden, L, Salilew-Wondim, D, Held, E, Neuhoff, C, Tholen, E, et al. (2017). Cellular and exosome mediated molecular defense mechanism in bovine granulosa cells exposed to oxidative stress. PLoS ONE 12, e0187569.

Santonocito, M, Vento, M, Guglielmino, MR, Battaglia, R, Wahlgren, J, Ragusa, M, et al. (2014). Molecular characterization of exosomes and their microRNA cargo in human follicular fluid: bioinformatic analysis reveals that exosomal microRNAs control pathways involved in follicular maturation. Fertility and Sterility 102, 1751–1761.e1.

Senbon, S, Hirao, Y, and Miyano, T (2003). Interactions between the oocyte and surrounding somatic cells in follicular development: lessons from in vitro culture. The Journal of Reproduction and Development 49, 259–269.

Shkolnik, K, Tadmor, A, Ben-Dor, S, Nevo, N, Galiani, D, and Dekel, N (2011). Reactive oxygen species are indispensable in ovulation. Proceedings of the National Academy of Sciences of the United States of America 108, 1462–1467.

Sidrat, T, Khan, AA, Joo, M-D, Wei, Y, Lee, K-L, Xu, L, and Kong, Il-K (2020). Bovine oviduct epithelial cell-derived culture media and exosomes improve mitochondrial health by restoring metabolic flux during pre-implantation development. International Journal of Molecular Sciences 21, 7589.

Simon, C, Greening, DW, Bolumar, D, Balaguer, N, Salamonsen, LA, and Vilella, F (2018). Extracellular vesicles in human reproduction in health and disease. Endocrine Reviews 39, 292–332.

Sohel, MMH, Hoelker, M, Noferesti, SS, Salilew-Wondim, D, Tholen, E, Looft, C, et al. (2013). Exosomal and non-exosomal transport of extra-cellular micrornas in follicular fluid: implications for bovine oocyte developmental competence. PLoS ONE 8, e78505.

Somfai, T, Inaba, Y, Watanabe, S, Geshi, M, and Nagai, T (2012). Follicular fluid supplementation during in vitro maturation promotes sperm penetration in bovine oocytes by enhancing cumulus expansion and increasing mitochondrial activity in oocytes. Reproduction, Fertility, and Development 24, 743–752.

Stephen, JG, and Graça, R (2013). As we wait: coping with an imperfect nomenclature for extracellular vesicles. Journal of Extracellular Vesicles 2, 20389.

Stokes, PJ, Abeydeera, LR, and Leese, HJ (2005). Development of porcine embryos in vivo and in vitro; evidence for embryo 'cross talk' in vitro. Developmental Biology 284, 62–71.

Sullivan, R, and Saez, F (2013). Epididymosomes, prostasomes, and liposomes: their roles in mammalian male reproductive physiology. Reproduction (Cambridge, England) 146, R21–R35.

Sutton, ML, Gilchrist, RB, and Thompson, JG (2003). Effects of in-vivo and in-vitro environments on the metabolism of the cumulus-oocyte complex and its influence on oocyte developmental capacity. Human Reproduction Update 9, 35–48.

Taka, M, Iwayama, H, and Fukui, Y (2005). Effect of the well of the well (WOW) system on in vitro culture for porcine embryos after intracytoplasmic sperm injection. The Journal of Reproduction and Development 51, 533–537.

Tang, K, Zhang, Y, Zhang, H, Xu, P, Liu, J, Ma, J, et al. (2012). Delivery of chemotherapeutic drugs in tumour cell-derived microparticles. Nature Communications 3, 1282.

Théry, C (2015). Cancer: diagnosis by extracellular vesicles. Nature 523, 161–162.

Tkach, M, and Théry, C (2016). Communication by extracellular vesicles: where we are and where we need to go. Cell 164, 1226–1232.

Vajta, G, Korösi, T, Du, Y, Nakata, K, Ieda, S, Kuwayama, M, and Nagy, ZP (2008). The well-of-the-well system: an efficient approach to improve embryo development. Reproductive Biomedicine Online 17, 73–81.

Valadi, H, Ekström, K, Bossios, A, Sjöstrand, M, Lee, JJ, and Lötvall, JO (2007). Exosome-mediated transfer of mRNAs and microRNAs is a novel mechanism of genetic exchange between cells. Nature Cell Biology 9, 654–659.

Vanholder, T, Leroy, JLMR, van Soom, A, Opsomer, G, Maes, D, Coryn, M, and de Kruif, A (2005). Effect of non-esterified fatty acids on bovine granulosa cell steroidogenesis and proliferation in vitro. Animal Reproduction Science 87, 33–44.

Vilella, F, Moreno-Moya, JM, Balaguer, N, Grasso, A, Herrero, M, Martínez, S, et al. (2015). Hsa-miR-30d, secreted by the human endometrium, is taken up by the pre-implantation embryo and might modify its transcriptome. Development 142, 3210–3221.

Villarroya-Beltri, C, Baixauli, F, Gutiérrez-Vázquez, C, Sánchez-Madrid, F, and Mittelbrunn, M (2014). Sorting it out: regulation of exosome loading. Seminars in Cancer Biology 28, 3–13.

Visconti, PE, and Kopf, GS (1998). Regulation of protein phosphorylation during sperm capacitation. Biology of Reproduction 59, 1–6.

Walters, AH, Pryor, AW, Bailey, TL, Pearson, RE, and Gwazdauskas, FC (2002). Milk yield, energy balance, hormone, follicular and oocyte measures in early and mid-lactation Holstein cows. Theriogenology 57, 949–961.

Wolfenson, D, Lew, BJ, Thatcher, WW, Graber, Y, and Meidan, R (1997). Seasonal and acute heat stress effects on steroid production by dominant follicles in cows. Animal Reproduction Science 47, 9–19.

Wydooghe, E, Vandaele, L, Heras, S, de Sutter, P, Deforce, D, Peelman, L, et al. (2017). Autocrine embryotropins revisited: how do embryos communicate with each other in vitro when cultured in groups? Biological Reviews 92, 505–520.

Zhan, R, Leng, X, Liu, X, Wang, X, Gong, J, Yan, L, et al. (2009). Heat shock protein 70 is secreted from endothelial cells by a non-classical pathway involving exosomes. Biochemical and Biophysical Research Communications 387, 229–233.

Zheng, Y, Chen, K, Zheng, X, Li, H, and Wang, G (2014). Identification and bioinformatics analysis of microRNAs associated with stress and immune response in serum of heat-stressed and normal Holstein cows. Cell Stress & Chaperones 19, 973–981.

CHAPTER II—Granulosa cell-derived extracellular vesicles mitigate the detrimental impact of thermal stress on bovine oocytes and embryos[2]

1. Overview

Climate change-induced global warming results in rises in body temperatures above normal physiological levels (hyperthermia) with negative impacts on reproductive function in dairy and beef animals. Extracellular vesicles (EVs), commonly described as nano-sized, lipid-enclosed complexes, harnessed with a plethora of bioactive cargoes (RNAs, proteins, and lipids), are crucial to regulating processes like folliculogenesis and the initiation of different signaling pathways. The beneficial role of follicular fluid-derived EVs in inducing thermotolerance to oocytes during in vitro maturation (IVM) has been evidenced. Here we aimed to determine the capacity of in vitro cultured granulosa cell-derived EVs (GC-EVs) to modulate bovine oocytes' thermotolerance to heat stress (HS) during IVM. Moreover, this study tested the hypothesis that EVs released from thermally stressed GCs (S-EVs) shuttle protective messages to provide protection against subsequent HS in bovine oocytes. For this, sub-populations of GC-EVs were generated from GCs subjected to 38.5°C (N-EVs) or 42°C (S-EVs) and supplemented to cumulus-oocyte complexes (COCs) matured in vitro at the normal physiological body temperature of the cow (38.5°C) or HS (41°C) conditions. Results indicate that S-EVs improve the survival of oocytes by reducing ROS accumulation, improving mitochondrial function, and suppressing the expression of stress-associated genes thereby reducing the severity of HS on oocytes. Moreover, our findings indicate

---

[2]Menjivar NG, Gad A, Gebremedhn S, Ghosh S, Tesfaye D. Granulosa cell-derived extracellular vesicles mitigate the detrimental impact of thermal stress on bovine oocytes and embryos. *Published at Frontiers in Cell and Developmental Biology*

a carryover impact from the addition of GC-EVs during oocyte maturation in the development to the blastocyst stage with enhanced viability.

2. Introduction

One of the leading, most consequential interferences to a homeostatic reproductive environment in dairy and beef cattle is elevated summer HS, a prime determinant of fertility and reproductive function (Boni, 2019; Wolfenson and Roth, 2019). Hyperthermia, the abnormal thermal state induced through failed regulatory mechanisms of the body, occurs when endogenous heat production supersedes the subsequent heat loss to the environment (Hansen, 2009). Thermal stress is known to compromise follicular development, ovarian functionality, fertilization, and subsequent early embryonic development (Badinga et al., 1993; Wolfenson et al., 1995; Rivera and Hansen, 2001; Sartori et al., 2002). Of specific interest in reduced fecundity is HS-induced damage to proper oocyte function. It is important to note that oocytes act spontaneously and independently of one another. However, elevated thermal environments are in part responsible for deleterious ramifications on the molecular, functional, and cellular changes to oocytes and their surrounding cumulus cells (CCs) (Abdelnour et al., 2020).

Mammalian oocytes are known to differentially activate various molecules as first-line defense mechanisms including heat shock proteins (HSPs) (Feder and Hofmann, 1999), unfolded protein responses (UPRs), and oxidative stress response pathways to assist cell survival under thermal stress conditions (Alemu et al., 2018; Lin et al., 2019). Additionally, impairments to conventional microtubules and microfilaments due to HS can be correlated to spindle apparatus malfunction and early arrest at metaphase I (MI) (Roth and Hansen, 2005). In order to understand the impact of seasonal thermal stress on follicular function and oocyte physiology, several studies have utilized the in vitro exposure of follicular cells (Li et al., 2016; Alemu et al., 2018; Gebremedhn et al.,

2020) and oocytes (Al-Katanani et al., 2002; Roth and Hansen, 2004; Roth and Hansen, 2005; Nabenishi et al., 2012; Li et al., 2015; Pavani et al., 2016; Rodrigues et al., 2019; Abdelnour et al., 2020) to elevated incubator temperatures. Accordingly, in vitro exposure of oocytes to HS results in impaired developmental potential as evidenced by defective cytoplasmic maturation (Edwards et al., 2005), mitochondrial anomalies (Ferreira et al., 2016), reductions in polar body extrusions (PB) and nuclear maturation (Li et al., 2015; Pavani et al., 2016) as well as increased accumulations of reactive oxygen species (ROS) (Nabenishi et al., 2012), ultimately leading to apoptosis (Nabenishi et al., 2012).

Oocyte growth and maturation occur within the complex follicle microenvironment, involving substantial bi-directional communication between follicular cells (theca, granulosa, and cumulus cells) and the oocyte (Matzuk et al., 2002; Russell et al., 2016). Critical communication and signaling between the varying cell subpopulations during folliculogenesis are paramount to the growth and maturation of developmentally competent oocytes (Matzuk et al., 2002; Alam and Miyano, 2020; Tesfaye et al., 2021). The process by which cells communicate occurs in a multitude of fashions including cytokines (Altan-Bonnet and Mukherjee, 2019), proteins or surface molecules (Ahmed and Xiang, 2011), and gap junctions (Gilula et al., 1978). Of growing interest is cell-to-cell communication via membrane-encapsulated vesicles containing surface markers from the cell of origin, harnessed with an abundant amount of bioactive cargoes (RNAs, proteins, lipids, and metabolites, etc.). Extracellular vesicles (EVs), an all-inclusive term endorsed by the International Society for Extracellular Vesicles (ISEV), is a term used for a heterogenous population of lipid-enclosed nanoparticles with non-replicative function (Théry et al., 2018). Originally depicted as discarding mechanisms of cellular waste, EVs are growing in popularity as

pertinent conveyors of cellular messages via their cargo loads, ultimately leading to modification of cellular activity or key properties of target cells (Valadi et al., 2007).

Several studies involving irradiation (Mothersill and Seymour, 1997; Lyng et al., 2000; Chai and Hei, 2008) and thermal stress (Bewicke-Copley et al., 2017) have demonstrated the potential of EVs present in conditioned medium to induce a bystander effect to recipient cells. In those respective studies, naïve cells treated with a medium conditioned by stressed cells showed increased levels of DNA damage and apoptosis when compared to naïve cells treated with a conditioned medium from control cells. Moreover, naïve cells treated with EVs from irradiated or heat-shocked cells have a higher probability to survive subsequent stress, suggesting that EVs can induce adaptive responses. It has also been shown that the supplementation of follicular fluid-derived EVs enhances the developmental capacity of oocytes to reach the blastocyst stage under HS conditions (Rodrigues et al., 2019). In the same study, it was noted that the supplementation of follicular fluid-derived exosomes were superior when compared to the whole follicular fluid, revealing exosomes' critical role in mitigating HS-induced damage to oocytes. The mechanisms underpinning such bystander effects of EVs are not fully understood, however, it is possible that the changes in protein or RNA contents of EVs may have the capacity to alter the physiology of recipient cells (Bewicke-Copley et al., 2017). MicroRNA profiling of EVs derived from thermally stressed bovine GCs revealed the enrichment of miRNA (miR-1246, miR-2904, and miR-374a), which are known to be involved in pathways associated with cellular response to heat stress, redox status, hypoxia and negative regulation of cell proliferation and inflammatory response (Gebremedhn et al., 2020). In the same study, we demonstrated that the supplementation of thermally stressed EVs to recipient granulosa cells induced tolerance against subsequent thermal stress. Therefore, the current study aimed to test the hypothesis that GC-derived EVs can play a

physiologically relevant role in enhancing the survival and viability of bovine oocytes subjected to thermal stress under in vitro conditions.

3. Materials and Methods

3.1 Ovary collection and granulosa cell isolation

Local abattoir-derived bovine ovaries were collected and transported via an insulated thermos containing physiological saline solution (0.9% NaCl) warmed to 37°C. Upon arrival, ovarian samples were initially washed through a physiological, warmed saline solution and subjected to a 70% ethanol rinse, followed by three repeated washings through a warmed saline solution. Follicular fluid containing granulosa cells and COCs were aspirated from small, growing follicles (3–8 mm in diameter) using a vacuum pump (GenX International; Guelph, ON, Canada) set to approximately 50 mmHg attached to an 18-gauge standard hypodermic needle (Covidien Monoject™; Mansfield, MA, United States) accompanied by a 50 mL sterilized tube (CELLTREAT® Scientific Products; Pepperell, MA, United States). A dense pellet of cellular material containing the COCs was allowed to settle at the bottom of the tube for 10 min, resulting in a visible gradient prior to the collection of cells. The uppermost aqueous portion of the aspirated follicular fluid containing the granulosa cells was then subsequently transferred into a sterile 15 mL tube (Thermo Fisher Scientific; Waltham, MA, United States) with warmed Dulbecco's Phosphate Buffered Saline without calcium and magnesium chloride (DPBS (×1)) (Sigma-Aldrich; St. Louis, MO, United States).

The upper suspension and warmed DPBS (1X) were mechanically homogenized via repetitive pipetting prior to initial centrifugation at 500 xg for 7 min to collect and pelletize the granulosa cells. Next, the supernatant was removed, and the cell pellet was resuspended in red blood cell (RBC) lysis buffer (Sigma-Aldrich; St. Louis, MO, United States) for 3 min. To stop the

reaction, the cell pellet was washed with Dulbecco's Modified Eagle's Medium/Ham's Nutrient Mixture F12 (DMEM/F12) (Sigma-Aldrich; St. Louis, MO, United States) supplemented with 10% Exosome-depleted fetal bovine serum (FBS) (System Biosciences; Palo Alto, CA, United States), 1% Penicillin-Streptomycin (Sigma-Aldrich; St. Louis, MO, United States) and 1% Amphotericin B solution (Sigma-Aldrich; St. Louis, MO, United States). Following centrifugation at 500 xg for 5 min, the supernatant was removed, and the cells were washed in DPBS (1X) and resuspended in DMEM/F12 supplemented medium as described above. Cell counts and viability were determined using a hemocytometer (Hausser Scientific; Horsham, PA, United States) and the trypan blue (Sigma-Aldrich; St. Louis, MO, United States) exclusion method.

3.2 Granulosa cell culture and exposure to heat stress

Granulosa cells were seeded at 2 × 105 cells per well in 24-well, tissue culture-treated plates (United States Scientific, Inc.; Ocala, FL), suspended in DMEM/F12 supplemented medium as described above. In a humidified atmosphere gauged at 38.5°C containing a 5% CO2 environment, cells were cultured for an initial 24 h or until sub-confluent. Following an initial 24 h priming period, the (control) cells continued culture at 38.5°C and the HS cells were transferred to an alternative environment with an elevated thermal temperature of 42°C for the remaining 24 h of the total 48 h culture period. The conditioned spent culture medium was collected and stored at −80°C for EV isolation and downstream application.

3.3 Isolation of EVs from spent culture medium

Two replicates of conditioned spent culture medium containing EVs released from cultured granulosa cells were pooled and initially centrifuged at 500 xg for 10 min, followed by 3,000 xg at 4°C to remove residual cellular debris. Following the initial centrifugations, the supernatant containing EVs were then subjected to centrifugation at increased speeds of 17,200 xg for 30 min,

followed by filtration through a 0.22 µm sterile syringe filter (Sigma-Aldrich; St. Louis, MO, United States), removing particles larger than 200 nm in diameter including apoptotic bodies. Following this, the purified conditioned spent culture medium was subjected to ultracentrifugation as we previously described in (Saeed-Zidane et al., 2017). Briefly, conditioned spent culture medium from each treatment was subjected to ultracentrifugation at 120,000 xg for 70 min using the Optima XE-90 Ultracentrifuge (Beckman Coulter; Pasadena, CA, United States), in 5.2 mL Ultra-Clear™ Centrifuge Tubes (Beckman Coulter; Pasadena, CA, United States) using the Beckman SW 55Ti rotor (Beckman Coulter; Pasadena, CA, United States). After removing the supernatant, the pelletized EVs were washed using DPBS (1X) and ultracentrifuged under the same conditions as described above. Finally, the supernatant was removed and the EVs were then suspended in 500 µL of DPBS (1X) and stored at −80°C until further analysis. Prior to use, all EV samples were thawed at room temperature to sustain high-yield EV recovery (Trummer et al., 2009; Szatanek et al., 2015).

3.4 Morphological and molecular characterization of GC-EVs

Immunoblotting techniques were used to verify the presence of typical EV-specific protein markers (CD63, TSG101, and CD81) in the isolated EVs. Moreover, Cytochrome c (CYCS), a cell-specific marker protein was used to validate the absence of residual cellular debris and cellular protein contaminants in our EV preparations. Full-length blots are provided in (Supplementary Figure S1) and a list of the antibodies used is indicated in (Supplementary Table S1).

Characterizing the size and concentration of EV samples were performed using nanoparticle tracking analysis (NTA). Briefly, 5 µL of purified EVs were diluted in 995 µL of DPBS (1X) and assembled into the ZetaView® QUATT 4 Nanosight Instrument (Particle Metrix; Ammersee, Germany) fitted with four respective lasers (405/488/520/640 nm sources). For each sample, video

measurements were recorded, and 11 positions were analyzed using the Software Zetaview (version 8.05.12 SP1). Similarly, the morphology and size of EVs were determined using a particle beam of electrons for visualization using transmission electron microscopy (TEM). For this, a small volume of isolated EV samples (6–8 µL) was applied to a carbon-coated, copper mesh TEM grid for 1–2 min, followed by negative staining with 2% aqueous uranyl acetate. TEM imaging was done on an FEI/TFS Tecnai T12 Spirit TEM (FEI Company; Hillsboro, OR, United States), operating at 100 kV, with an AMT CCD. We have submitted all relevant data from our experiments to the EV-TRACK knowledgebase (EV-TRACK ID: EV220412) (van Deun et al., 2017).

3.5 Fluorescence labeling of GC-EVs and assessing cellular uptake

EVs were labeled with PKH26 (Mini26-1KT; Sigma-Aldrich; St. Louis, MO, United States), a red fluorescent linker dye responsible for labeling lipid membranes as described in (Da Silveira et al., 2012). Briefly, EVs (3.5 × 1011 particles/mL) were incubated with 1 µL of PKH26 (4 × 10-6 M) for 5 min at room temperature in the dark, followed by immediate quenching with 1% BSA (A6003; Sigma-Aldrich; St. Louis, MO, United States) for 1 min. Samples were precipitated using Exo-spin™ buffer-exosome precipitation reagent (CellGS®; St. Louis. MO, United States) for 60 min in the dark at 4°C, then centrifuged at 16,000 xg for 30 min and resuspended in 100 µL of DPBS (1X) before purification using the Exo-spin™ columns according to the manufacturer's protocol. As a negative control, DPBS (1X) was incubated with PKH26 and treated in the same manner as described above. Labeled EVs or DPBS (1X) (negative control) were used to prove EV uptake by CCs surrounding intact COCs as detailed below.

COCs obtained from follicles ranging in size from 3 to 8 mm in diameter were aspirated from abattoir-derived ovaries. Three COCs were cultured in 20 µL micro drops offset with 20% v/v of GC-EVs suspended in DPBS (1X) measured at 0.3 mg/mL of total protein under oil for a 23 ± 1 h

exposure length. Following incubation, intact COCs were washed in CSU chemically defined medium for the handling of oocytes (HCDM-M) (De La Torre-Sanchez, Jose Fernando et al., 2006), fixed with 4% paraformaldehyde, mounted to a poly-L-lysine coated slide (Newcomer Supply, Inc.; Middleton, WI, United States), and allowed to dry for 24 h at 4°C in the dark. Visualization of fluorescently-labeled EVs within the CCs surrounding the oocyte was ascertained using confocal microscopy (Olympus Fluoview FV10-ASW 4.1) (Olympus; Tokyo, Japan) after excitation of COCs at 559 nm with a ×60 objective lens. Labeled DPBS (1X) was used as negative control within this experiment.

3.6 In vitro maturation and exposure to heat stress

The collection of COCs from slaughterhouse ovaries was done as described above. Once COCs were collected, groups of 50 oocytes were transferred into individual wells, inside 4-well culture dishes (Thermo Fisher Scientific; Waltham, MA, United States) containing 1 mL of CSU chemically defined medium for in vitro maturation of oocytes (IVM) pre-equilibrated at 38.5°C in 5% CO2 (De La Torre-Sanchez, Jose Fernando et al., 2006). At the time IVM medium were set to equilibrate, all mediums irrespective of downstream application were supplemented with 15 ng/mL NIDDK-oFSH-20, 1 μg/mL USDA-LH-B-5, 1 μg/mL estradiol 17β, 50 ng/μL epidermal growth factor, and 0.1 mM cysteamine (De La Torre-Sanchez, Jose Fernando et al., 2006).

For experiments with heat stress, treatments were arranged in a 2 × 4 factorial design with primary effects of incubation temperature during maturation (38.5°C vs. 41°C) and with four culture mediums: non-supplemented control (NC), vehicle [DPBS (1X)], EVs derived from granulosa cells subjected to the normal physiological body temperature of the cow (38.5°C) (normal EVs: N-EVs) or EVs derived from granulosa cells subjected to thermal stress (42°C) (stressed EVs: S-EVs). In brief, COCs were incubated with 20% v/v of DPBS (1X), and treatments

with GC-EVs were offset with equal concentrations of total protein (0.3 mg/mL) assessed using a NanoDrop 2000 Spectrophotometer (Thermo Scientific; Waltham, MA, United States), selected based on previous literature (Almiñana et al., 2017; Alcântara-Neto et al., 2020a; Alcântara-Neto et al., 2020b; Abumaghaid et al., 2022; Mateo-Otero et al., 2022). For all experimental groups, control COCs matured at a temperature of 38.5°C throughout the maturation period (23 ± 1 h), while thermally stressed COCs were subjected to an initial 8 h priming period at 38.5°C and then transferred to 41°C in an atmosphere of 5% CO2 in humidified air for the remaining 15 ± 1 h of the 23 ± 1 h maturation period.

3.7 In vitro fertilization and embryo culture

After maturation, COCs were transferred to 4-well culture dishes containing 430 μL of equilibrated CSU chemically defined medium for in vitro fertilization (F-CDM/well) (De La Torre-Sanchez, Jose Fernando et al., 2006). In a minimal volume of maturation medium, COCs were transferred into F-CDM and held at 38.5°C and 5% CO2 in humidified air until IVF was completed using bull sperm generated from a single ejaculation. Frozen-thawed semen were subjected to a multi-layer, 45%/90% Percoll® (Sigma-Aldrich; St. Louis, MO, United States) gradient and centrifuged at 800 xg for 20 min to separate viable, motile sperm (Parrish et al., 1995). Following this, the supernatant was removed and the remaining sperm pellet was washed with 2 mL of CSU chemically defined medium for the handling of early embryos (HCDM-1) and centrifuged at 300 xg for 5 min (De La Torre-Sanchez, Jose Fernando et al., 2006). The concentration of spermatozoa was determined using a hemocytometer and adjusted to 5 × 106 sperm/mL using equilibrated F-CDM. Finally, sperm were added to COCs at a concentration of 0.5 × 106 sperm/mL, and co-incubated for 18 h at 38.5°C in 5% CO2 in humidified air.

Following exposure with spermatozoa, presumptive zygotes were vortexed at maximum speed for 60–90 s to slough remaining CCs. Denuded zygotes were then transferred through a series of HCDM-1 wash drops, removing residual cells and spermatozoa (De La Torre-Sanchez, Jose Fernando et al., 2006). Zygotes rid of excess cellular debris were then transferred (in groups of 50) to pre-equilibrated 4-well dishes containing 500 µL of CSU chemically defined medium for in vitro culture of early embryos (CDM-1) and cultured for 56 h in a tri-gas incubator regulated to 38.5°C in 5% CO2, 5% O2, and 90% N2. Following an initial culture of 56 h, development was assessed by embryo cleavage in warmed micro drops of CSU chemically defined medium for the handling of late embryos (HCDM-2) (De La Torre-Sanchez, Jose Fernando et al., 2006). Those embryos with ≥2 blastomeres were transferred (in groups ≤35 embryos) to pre-equilibrated 4-well dishes containing 500 µL of CSU chemically defined medium for in vitro culture of late embryos (CDM-2) for an additional 120 h of culture in a humidified chamber at 38.5°C in 5% CO2, 5% O2 and 90% N2 (De La Torre-Sanchez, Jose Fernando et al., 2006). Blastocyst rates were determined on day 7 (168 h) and day 8 (192 h) post-onset of IVF. Blastocysts were evaluated according to their respective stage of development and graded morphologically in accordance with the IETS guidelines (Robertson, 1998).

3.8 Quantitative analysis of cumulus cell expansion

To determine the effect of EV supplementation on cumulus expansion, arbitrary lines were drawn to measure the diameter of single cumulus-oocyte complexes (four replicates; a total of 113–252 COCs per treatment) using the Olympus Cellsens software (Olympus; Tokyo, Japan). Measurements were ascertained from groups of COCs and the mean diameter before maturation was subtracted from the mean diameter after maturation to determine the mean cumulus expansion in µm's. The diameter of COCs was measured before and after maturation at differing ambient

temperatures from recorded images (.jpg) using an inverted microscope (IX73; Olympus; Tokyo, Japan).

3.9 Total RNA isolation and quality control

Total RNA was isolated from three replicates of CCs (each pool contains CCs derived from 50 COCs) using the miRNeasy® mini kit (Qiagen; Hilden, Germany), and on-column DNA digestion was performed using RNase-free DNase (Qiagen; Hilden, Germany). Moreover, total RNA was extracted from three replicate pools of denuded oocytes following the completion of in vitro maturation (each pool consisting of 50 oocytes) and four replicate pools of blastocysts (each pool containing 5 blastocysts) using the RNeasy® plus micro kit (Qiagen; Hilden, Germany). Total RNA sample concentration and integrity were assessed using a NanoDrop 2000 Spectrophotometer (Thermo Scientific; Waltham, MA, United States). RNA samples were stored at −80°C until further use.

3.10 Quantification of cumulus expansion and stress-associated genes using qRT-PCR

The relative abundance of selected cumulus expansion marker genes (PTGS2, EGFR, and PTX3) were quantified in CCs isolated from matured COCs (three replicates; CCs from a pool of 50 COCs per replicate) using qRT-PCR. Cumulus cells were collected immediately following in vitro maturation by recurrent pipetting through a narrow pipette, followed by vortexing and centrifugation. Complete removal of CCs from the oocytes was assessed under a stereo microscope (SZX16; Olympus; Tokyo, Japan) and snap frozen in liquid nitrogen then stored at −80°C until further analysis. For the analysis, synthesized cDNA was reverse transcribed from equal amounts of total RNA (85 ng) using the SuperScript™ III First-Strand Synthesis Super Mix Kit (Invitrogen; Carlsbad, CA, United States) with random hexamer and oligo d(T) 20 primers. Similarly, the transcript abundance of selected stress-related genes (NRF2, SOD1, HSP70, HSP90, GRP78, and

GRP94) were quantified in CCs (three replicates; CCs from a pool of 50 COCs per replicate), in vitro matured denuded oocytes (three replicates; a pool of 50 COCs per replicate) and blastocysts (four replicates; a pool of 5 blastocysts per replicate) using qRT-PCR. For this, cDNA was obtained after reverse transcription of equal amounts of total RNA (85 ng from CCs, 31 ng from oocytes, and 13 ng from blastocysts) as described above. The geometric mean of expression levels of β-ACTIN and GAPDH was used to normalize the expression of candidate genes. Gene-specific primers were designed using Primer-Blast (https://www.ncbi.nlm.nih.gov/tools/primer-blast/) and the list of primers is indicated in Supplementary Table S2. qRT-PCR analysis were performed using the CFX96 Touch Real-Time PCR Detection System (Bio-Rad; Hercules, CA, United States) and data was analyzed using the comparative C(T) method (Schmittgen and Livak, 2008).

3.11 Measurement of intracellular ROS accumulation

The intracellular ROS accumulation in oocytes (three replicates; a total of 15–50 oocytes per treatment) and blastocysts (three replicates; a total of 6-9 blastocysts per treatment) from the various treatment groups was determined as we described previously (Gebremedhn et al., 2020). Briefly, oocytes (n = 32 on average) and embryos (n = 8 on average) from each treatment group were washed twice in phosphate-buffered saline-polyvinylpyrrolidone DPBS (1X)-PVP (0.1%) (P0930; Sigma-Aldrich; St. Louis, MO, United States), placed in 50 µL droplets of 10 µM 2′,7′-Dichlorofluorescin Diacetate (H_2DCFDA) dissolved in H-CDMM or H-2 (oocyte or blastocyst) (287,810; Sigma-Aldrich; St. Louis, MO, United States), and incubated at 38.5°C in the respective culture environment suitable for their specific stage of development for 30 min. After incubation, the oocytes and embryos were washed three times in DPBS (1X)-PVP (0.1%) and then observed under an inverted fluorescent microscope (IX73; Olympus; Tokyo, Japan) using ×20 magnification. The fluorescence of individual specimens was measured from.jpg images and

analyzed using ImageJ software (National Institute of Health; Bethesda, MD, United States) after normalization through subtraction of the background intensity. All images were captured under the same parameters for exposure time and light intensity to avoid fluorescent saturation using a green fluorescent filter with an excitation wavelength of 494 nm and an emission wavelength of 518 nm. Results are plotted as the relative intensity of fluorescence.

3.12 Analysis of mitochondrial membrane potential (MMP)

MMP ($\Delta\Psi m$) in oocytes (duplicates; a total of 12-22 oocytes per treatment) and blastocysts (duplicates; a total of 7-11 blastocysts per treatment) were analyzed by staining with 5,5′,6,6′-tetrachloro-1,1′,3,3′tetraethylbenzimidazolylcarbocyanine iodide (JC-1, Invitrogen; Carlsbad, CA, United States) dissolved in H-CDMM or H-2 (oocyte or blastocyst), as an indicator of mitochondrial activity, as previously described (Pasquariello et al., 2019). Briefly, denuded matured oocytes and blastocysts from the various treatment groups were stained using 2 μM JC-1 for 30 min in the dark at 38.5°C, in the optimal culture environment for their respective stage and development to express two types of fluorescence. Oocytes and blastocysts were then washed three times in DPBS (1X)-PVP (0.1%) and fluorescent images were taken immediately using an inverted laser scanning confocal microscope (ZEISS LSM980, Carl Zeiss Microscopy, Jena, Germany) using a ×20 magnification air objective. Fluorescent images were ascertained using the lowest laser power to give a sufficient signal-to-noise ratio to avoid saturation of the fluorophore. Physiological temperature (37°C) and CO2 level (5%) were maintained inside the incubation chamber amidst imaging. Imaging was performed using a wavelength of 488 nm for J-monomers and excitation/emission at 490/525 nm (FITC filter/green fluorescence) indicating low membrane potential. Similarly, images for J-aggregates were carried out using a wavelength of 561 nm and excitation/emission at 596/615 nm (TRITC filter/red fluorescence) indicating high membrane

potential. Subsequently, the ratio of red to green fluorescence was used to determine mitochondrial membrane potential, expressed as an arbitrary unit as previously described (Silva et al., 2015; Pasquariello et al., 2019). All czi. images were analyzed using ImageJ software (National Institute of Health; Bethesda, MD, United States).

3.13 Fluorescent nuclear staining and terminal deoxynucleotidyl transferase-mediated dUTP nick-end labeling (TUNEL) assay

Blastocyst-stage embryos from the different treatment groups (three replicates; a total of 18-30 blastocysts per treatment) were assessed for proliferative capacity based on total cell counts using a protocol adapted from (Critser and First, 1986) with some modifications. Briefly, blastocysts were washed three times in 100 µL drops of phosphate buffered saline-polyvinylalcohol DPBS (1X)-PVA (0.1%) (P8136; Sigma-Aldrich; St. Louis, MO, United States), for 5 min each time. Blastocysts were then immediately transferred into 1.5 µg/mL Hoechst 33,342 solution (H3570; Thermo Fisher Scientific; Waltham, MA, United States) and stained for 10–15 min at room temperature in the dark. Embryos were then washed as previously described and mounted on a poly-L-lysine coated slide (Newcomer Supply, Inc.; Middleton, WI, United States) with 5–10 µL ProLong Diamond Antifade Mountant (P36966; Invitrogen; Carlsbad, CA, United States). Alternatively, cellular DNA fragmentation in blastocysts from the various treatment groups (three replicates; a total of 19-41 blastocysts per treatment) was determined using an in situ apoptotic cell detection kit, DeadEnd™ Fluorometric TUNEL System according to the manufacturer's instruction (TB235; Promega; Madison, WI, United States). Briefly, blastocysts were fixed in 4% paraformaldehyde (PFA) for 25 min at 4°C. Following fixing, blastocysts were washed twice in 0.1% Tween/PVP in DPBS (1X) (Bio-Rad; Hercules, CA, United States; P0930; Sigma-Aldrich; St. Louis, MO, United States) and permeabilized in 0.3% Triton X-100 in DPBS

(1X) (X100-100ML; Sigma-Aldrich; St. Louis, MO, United States) for 5 min. After permeabilization, blastocysts were washed as detailed previously and incubated in equilibration buffer prior to labeling with the TUNEL assay kit cocktail at 38.5°C for 60 min in a dark humidified chamber as suggested in the manufacturer's protocol. To stop the reaction, blastocysts were moved to 2X SSC for 15 min and washed an additional three times before mounting on a poly-L-lysine coated slide (Newcomer Supply, Inc.; Middleton, WI, United States) with 5–10 µL ProLong Diamond Antifade Mountant (P36966; Invitrogen; Carlsbad, CA, United States) and a coverslip, allowing to dry flat (>24 h). Hoechst/DAPI-labeled or TUNEL-positive nuclei were observed under an inverted fluorescent microscope (IX73; Olympus; Tokyo, Japan) using ×20 magnification, under the same parameters using fitted blue (345/455) and green (494/518) fluorescent filters. For the analysis, fluorescent images were converted to grayscale to accurately adjust what is fluorescently stained (elements in the foreground, as well as elements in the background). Subsequently, the fluorescently labeled cells were then filled appropriately to determine the borders of individual nuclei based on relative size for counting purposes irrespective of the fluorophore utilized (blue/green).

3.14 Experimental design

A schematic overview of the experimental design is shown in (Supplementary Figure S2). Following the generation of GC-EV subsets (N-EVs and S-EVs) for isolation and characterization, their subsequent effect was evaluated on COCs cultured under normal (38.5°C) and HS (41°C) conditions during IVM. For this purpose, COCs were collected by aspirating small-growing follicles (3–8 mm in diameter) from abattoir-derived reproductive ovaries. To avoid result bias, Grade 1 and Grade 2 COCs were selected for further functional studies and placed into 4-well culture dishes containing four distinct equilibrated mediums: non-supplemented control (NC),

vehicle [DPBS (1X)], normal EVs (N-EVs) or stressed EVs (S-EVs) suspeneded in 20% v/v of DPBS (1X), with GC-EV treatments offset with equal concentrations of total protein (0.3mg/ml). Concluding IVM, in vitro matured oocytes were assessed for EV uptake and cumulus expansion. Additionally, selected stress-associated transcripts were investigated among resected cumulus cells and denuded matured oocytes, and confocal microscopy was utilized to determine ROS production and mitochondrial activity among in vitro matured oocytes. In parallel, aside from experiments conducted immediately following IVM, subsequent IVF cycles were carried out to investigate the downstream effects of GC-EV supplementation during oocyte maturation on the resulting blastocyst development. Developmental competence rates were collected, and blastocysts were similarly evaluated for selected stress-associated transcript abundance and dually stained for ROS accumulation, total cell counts, apoptotic indexes, and mitochondrial membrane potential as a means to monitor the quality of the produced blastocysts.

3.15 Statistical analysis

Data were analyzed in GraphPad Prism version 8.4.2 (GraphPad; San Diego, CA, United States). Statistical differences between the mean values of more than two groups under the varying culture conditions were compared using Two-way Analysis of Variance (ANOVA) followed by Tukey's Multiple Comparisons Tests. Alternatively, statistical differences amid gene expression datasets were assessed between the mean values of more than two groups under the same culture conditions using One-way Analysis of Variance (ANOVA) followed by Tukey's Multiple Comparisons Tests. Data are presented as the Mean ± SEM of biological replicates. Statistical significance was identified at $p \leq 0.05$.

4. Results

4.1 Characterization of GC-EVs released into the conditioned medium from in vitro cultured follicular GCs

Vesicle size and concentration differences between N-EVs and S-EVs were assessed using Nanoparticle Tracking Analysis (NTA). The concentration of N-EVs and S-EVs were 6.70E+11 ± 3.50E+11 and 1.00E+12 ± 5.10E+11 particles/mL, with median sizes of 137.75 and 147.95 nm, respectively. Exposure to heat stress resulted in the release of a significantly higher quantity of EVs with a tendency of having larger size particles (Figure 2.1A). Western blotting analysis of N-EVs and S-EVs revealed positive bands for EV- specific transmembrane proteins (CD63, TSG101, and CD81), simultaneously showing negative results for mitochondrial protein marker (CYCS) (Figure 2.1B). Similarly, TEM imaging showed a clear indication that vesicles are encapsulated with the visible appearance of a bilipid membrane (Figure 2.1C).

4.2 GC-EVs shuttle protective messages against heat stress to enhance the thermotolerance of bovine cumulus-oocyte complexes

As a means to validate EVs' capacity to mediate communicative interactions supporting oocyte and embryo development, we confirmed GC-EV uptake by COCs using fluorescence microscopy. After 24 h co-incubation of labeled EVs with COCs, we detected PKH-26 positive EVs in the CCs surrounding the oocyte, but not in the oocyte cytoplasm (Figure 2.2A). Subsequent investigation of the impact of EV supplementation during oocyte maturation revealed that both N-EVs and S-EVs had positive impacts on cumulus expansion compared to non-supplemented controls and vehicle-supplemented groups, irrespective of the presence or absence of thermal stress exposure. Interestingly, under normal physiological temperature

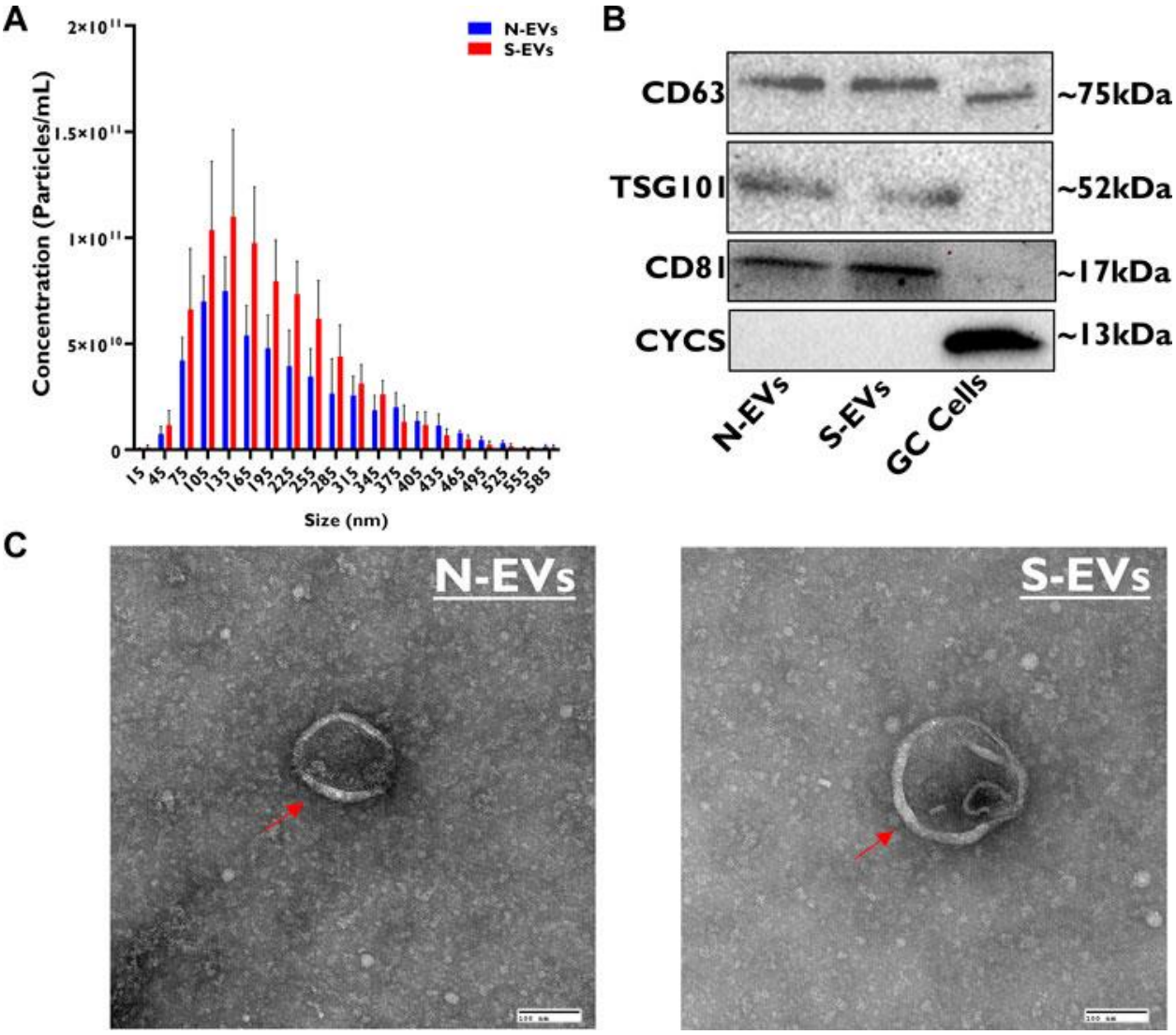


Figure 2.1. Morphological and molecular characterization of GC-EVs. The relative size of EVs isolated from cultured granulosa cells spent culture medium was determined using nanoparticle tracking analysis (NTA). The median size of N-EVs was 137.75 nm (blue) compared to S-EVs 147.95 nm (red). Granulosa cells subjected to thermal stress released a significantly higher quantity of particles (red) and had tendencies to be larger in size (nm) compared to those subjected to normal ambient temperatures (blue) (A). Immunoblotting analysis for EV-specific protein markers (CD63, TSG101, and CD81) and cellular-specific protein marker (CYCS) were verified to determine protein lysate composition in N-EVs, S-EVs, and GCs as a positive control. Full-length blots are presented in Supplementary Figure S1 (B). Transmission electron microscopy (TEM) representative images from N-EVs and S-EVs (marked with red arrows) show the morphology of the lipid bilayer membrane of EV particles. Scale bar, 100 nm (C).

(38.5°C), N-EVs significantly increased cumulus expansion compared to the NC ($p < 0.0001$) and vehicle ($p < 0.0001$). Similar results were found for COCs supplemented with S-EVs during oocyte maturation and cultured under HS conditions when compared to the NC ($p < 0.0001$) and vehicle ($p < 0.0001$) (Figure 2.2B). We further validated differential expression patterns of cumulus expansion marker genes in the CCs from oocytes of the various treatment groups. Results showed that the expression patterns of PTGS2, EGFR, and PTX3 were higher within the CCs from COCs supplemented with N-EVs cultured both under normal and thermal stress conditions. Under HS

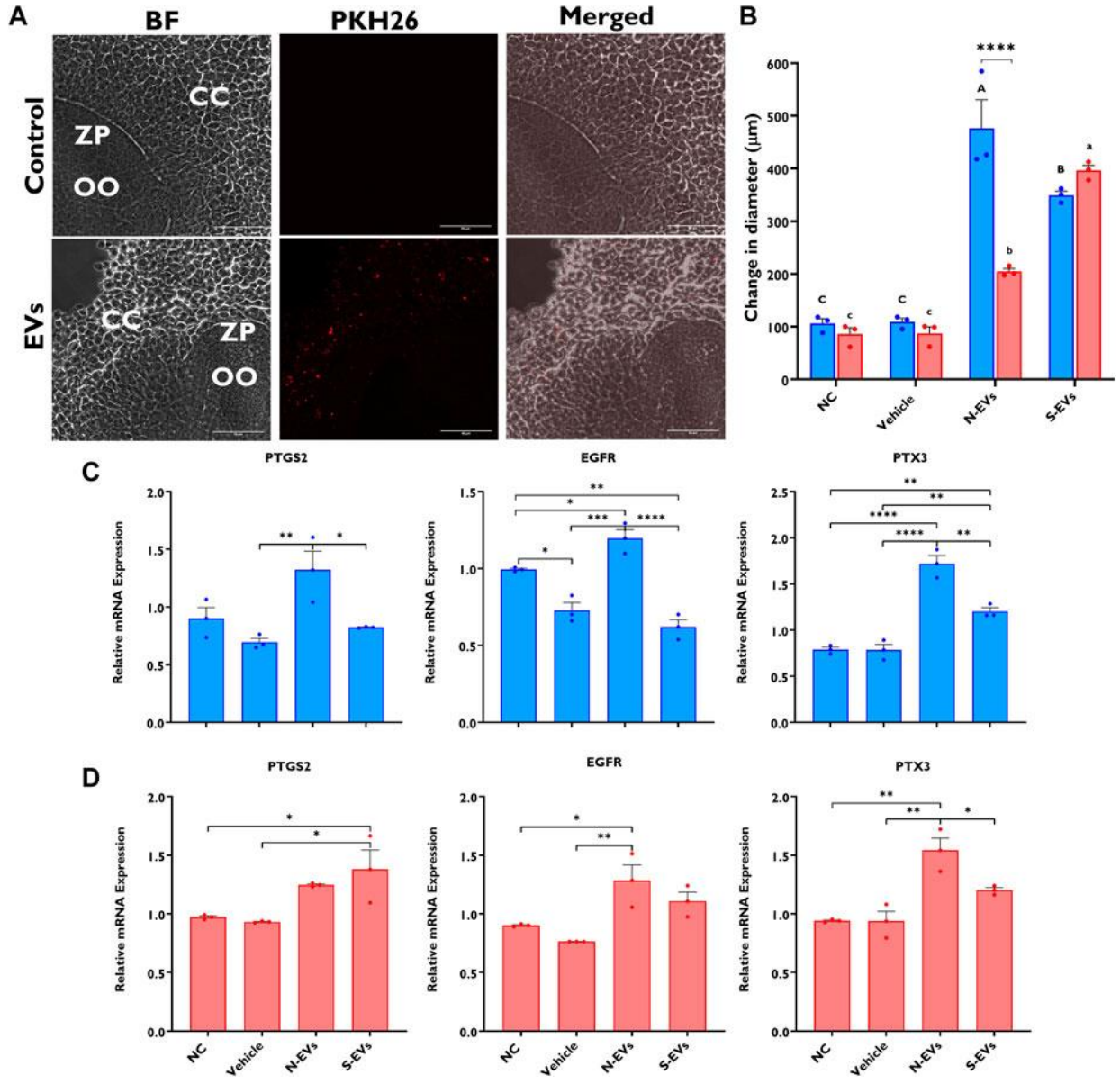


Figure 2.2. Effects of GC-EV supplementation on receptivity of follicular cells EV uptake following maturation at 38.5°C (blue) and 41°C (red) and cumulus expansion. Confocal images of intact cumulus-oocyte complexes co-incubated with PKH26 labeled GC-EVs for 24 h during in vitro maturation. Scale bar, 50 μM (A). Follicular cell uptake of PKH26 labeled EVs is shown in the surrounding cumulus cells (CC), in relation to the oocyte (OO) and respective zona pellucida (ZP). Measurements for cumulus expansion were obtained before and after maturation using the Olympus Cellsens software. The increase in diameter was determined by subtracting the mean diameter before maturation from the mean diameter after maturation (B). Results were carried out in four replicates (a total of 113-252 COCs per treatment). Data among treatments represent the mean±SEM and the differences between means were analyzed using Two-way ANOVA followed by Tukey's Multiple Comparisons Test. Bars with different letters (38.5°C; uppercase) (41°C; lowercase) indicate statistically significant differences of at least ($p < 0.05$) between treatments under the same culture conditions, while (*) indicate statistical differences between the same treatment under different culture environments during IVM (****$p < 0.0001$). The expression of cumulus expansion marker genes was assessed using qRT-PCR from cumulus cells isolated from oocytes in triplicates (a total of 50 COCs per treatment) cultured under thermoneutral (C) and heat stress (D) conditions. Data among treatments cultured under the same environment represent the mean ± SEM and the differences between means were analyzed using One-way ANOVA followed by Tukey's Multiple Comparisons Test. (*$p < 0.05$), (**$p < 0.01$), (***$p < 0.001$), (****$p < 0.0001$).

conditions, N-EVs and S-EVs tended to act cohesively with both expression patterns being upregulated when compared to the NC and vehicle (Figures 2.2C, D). Collectively our data indicate significant differences between GC-EV supplemented treatments ($p < 0.0001$), culture temperatures ($p = 0.0015$), as well as an interaction between temperature and treatment ($p = 0.0002$).

The supplementation of S-EVs to COCs at the time of maturation significantly decreased the relative expression of NRF2, SOD1, HSP70, and HSP90 in CCs from COCs, under both ambient temperatures alike (Figures 2.3A, B). Contrasting evidence showed that N-EVs did not show measurable differences in the suppression of stress-associated transcripts compared to the NC and vehicle under both normal physiological temperature and when subjected to HS (Figures 2.3A, B). As shown in Figure 2.4, the supplementation of both N-EVs and S-EVs resulted in the suppression of the majority of stress-associated genes in oocytes cultured either under normal or thermal stress

conditions. Contrary to these findings, HSP70 was significantly enriched within the oocytes supplemented with S-EVs and cultured at 38.5°C (Figure 2.4A), however, significantly suppressed under thermal stress conditions (Figure 2.4B).

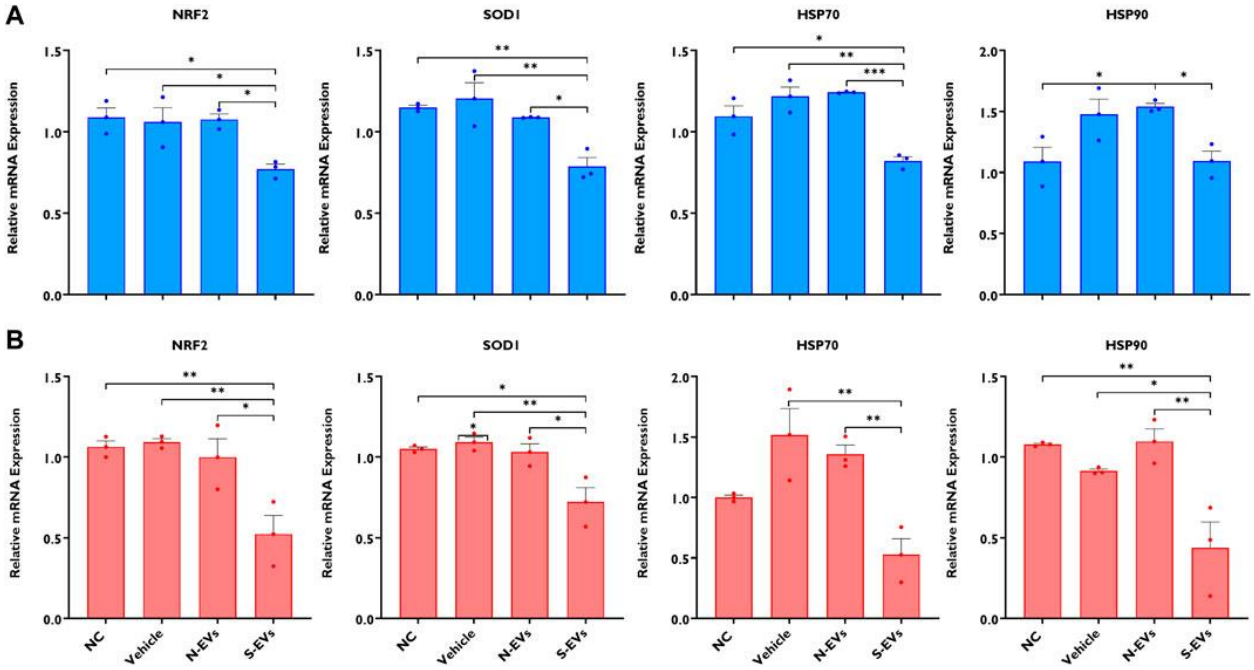


Figure 2.3. The impact of GC-EV supplementation on transcript levels of stress-associated genes in cumulus cells from cumulus-oocyte complexes following maturation at 38.5°C (blue) and 41°C (red). The expression of stress-associated genes was significantly diminished in cumulus cells from oocytes supplemented with S-EVs and matured at 38.5°C (A) and 41°C (B). Results are from cumulus cells removed from a total of three pools of 50 oocytes per pool for each treatment. Data represent the mean ± SEM and the differences between means were analyzed using One-way ANOVA followed by Tukey's Multiple Comparisons Test. (*$p < 0.05$), (**$p < 0.01$), (***$p < 0.001$).

4.3 GC-EVs prevent ROS accumulation and promote mitochondrial function in oocytes under heat-stress conditions

ROS production and mitochondrial membrane potential were investigated in in vitro matured oocytes supplemented with GC-derived EVs via fluorescence microscopy. Diminished fluorescent signals of ROS were seen in those oocytes supplemented with S-EVs and matured at 41°C, compared to the other groups (Figures 2.5B, C). Similarly, under normal ambient temperature, fluorescent ROS signals were substantially reduced in oocytes supplemented with N-EVs and S-

EVs when compared to controls (Figures 2.5A, C). Our data also concur significant differences between GC-EV supplemented treatments ($p = 0.0208$), albeit no measurable differences among temperatures or temperature and treatment interactions. Subsequent investigation of the mitochondrial membrane potential in oocytes by JC-1 staining revealed that under HS conditions, oocytes supplemented with both N-EVs and S-EVs showed markedly high mitochondrial membrane potential ($\Delta\Psi m$) (Figures 2.5E, F). However, under normal physiological conditions, the highest $\Delta\Psi m$ were observed in the treatment group supplemented with N-EVs (Figures 2.5D, F). Statistical comparisons for JC-1 indicated, significant differences between GC-EV supplemented treatments ($p < 0.0001$), however, no statistical differences among culture temperatures, amid a significant interaction between culture temperature and GC-EV supplemented treatments ($p = 0.0002$).

4.4 The effect of GC-EV supplementation during oocyte maturation on developmental competence of oocytes post IVF

Since GC-EVs enhanced the proper function and overall quality of bovine oocytes subjected to HS, we next assessed this correlation on their downstream embryonic developmental potential following in vitro fertilization. As shown in Figure 2.6A, there are no measurable differences in cleavage rates of the oocytes under thermal stress conditions, although, minimal improvements were noted for oocytes supplemented with N-EVs and cultured at 38.5°C. However, HS induces a dramatic decline in the proportion of oocytes capable of developing to the blastocyst stage, whether expressed as the percentage of oocytes developed to blastocyst (Figure 2.6B; $p < 0.0001$) or the percentage of cleaved embryos (Figure 2.6C; $p < 0.0001$). As shown in Figures 2.6B, C, while supplementation of S-EVs during oocyte maturation rescued the majority of oocytes developed to the blastocyst stage under thermal stress conditions, both N-EVs, and S-EVs improve the

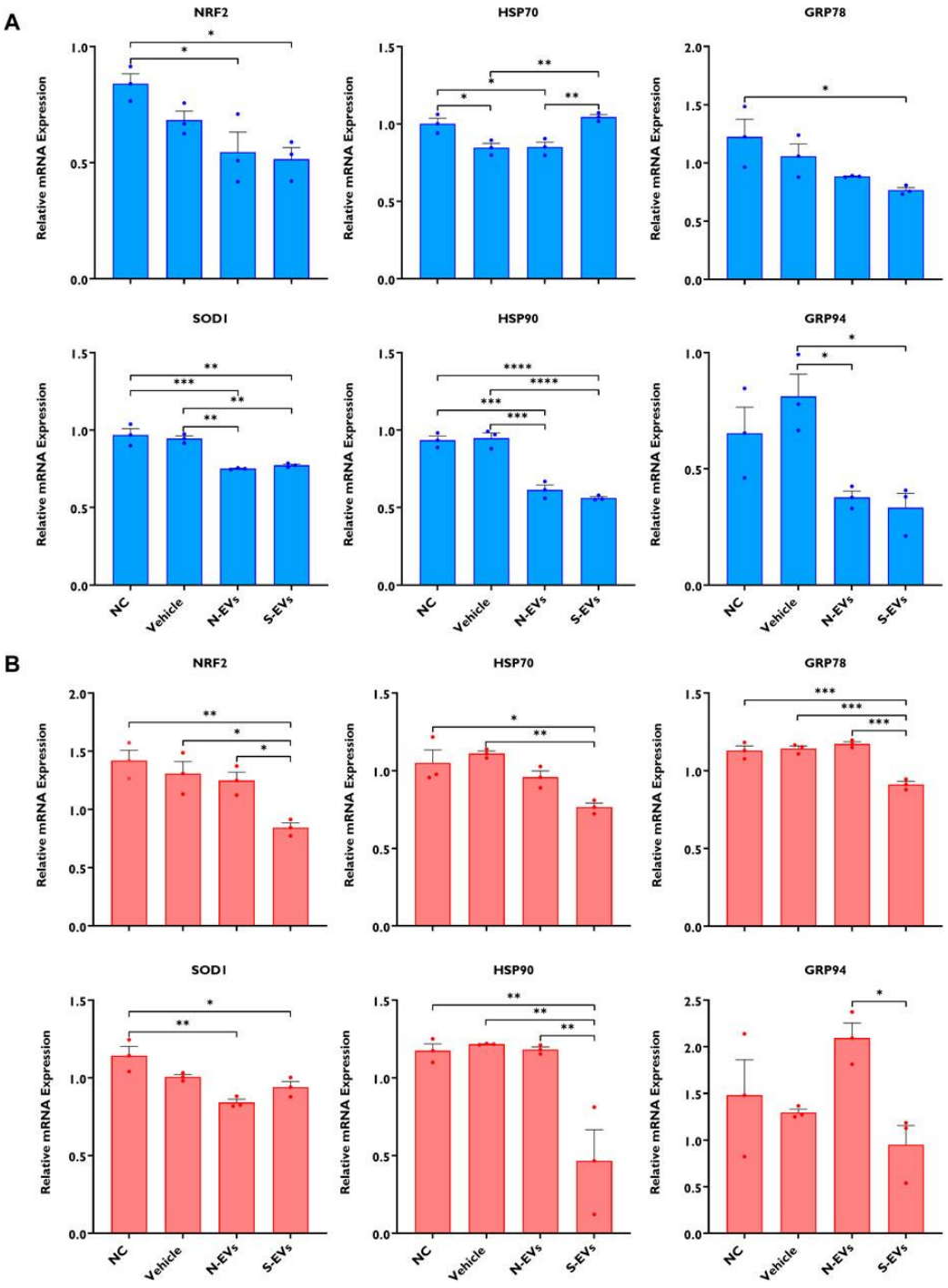


Figure 2.4. The impact of GC-EV supplementation on transcript levels of stress-associated genes in oocytes following maturation at 38.5°C (blue) and 41°C (red). The expression of stress-associated genes were significantly diminished in oocytes supplemented with N-EVs and cultured at 38.5°C (A), and similar decreases in gene expression were visualized in oocytes supplemented with S-EVs and exposed to HS (B). Results are from a total of three pools of 50 oocytes per pool for each treatment. Data represent the mean ± SEM and the differences between means were analyzed using One-way ANOVA followed by Tukey's Multiple Comparisons Test. (*$p < 0.05$), (**$p < 0.01$), (***$p < 0.001$), (****$p < 0.0001$).

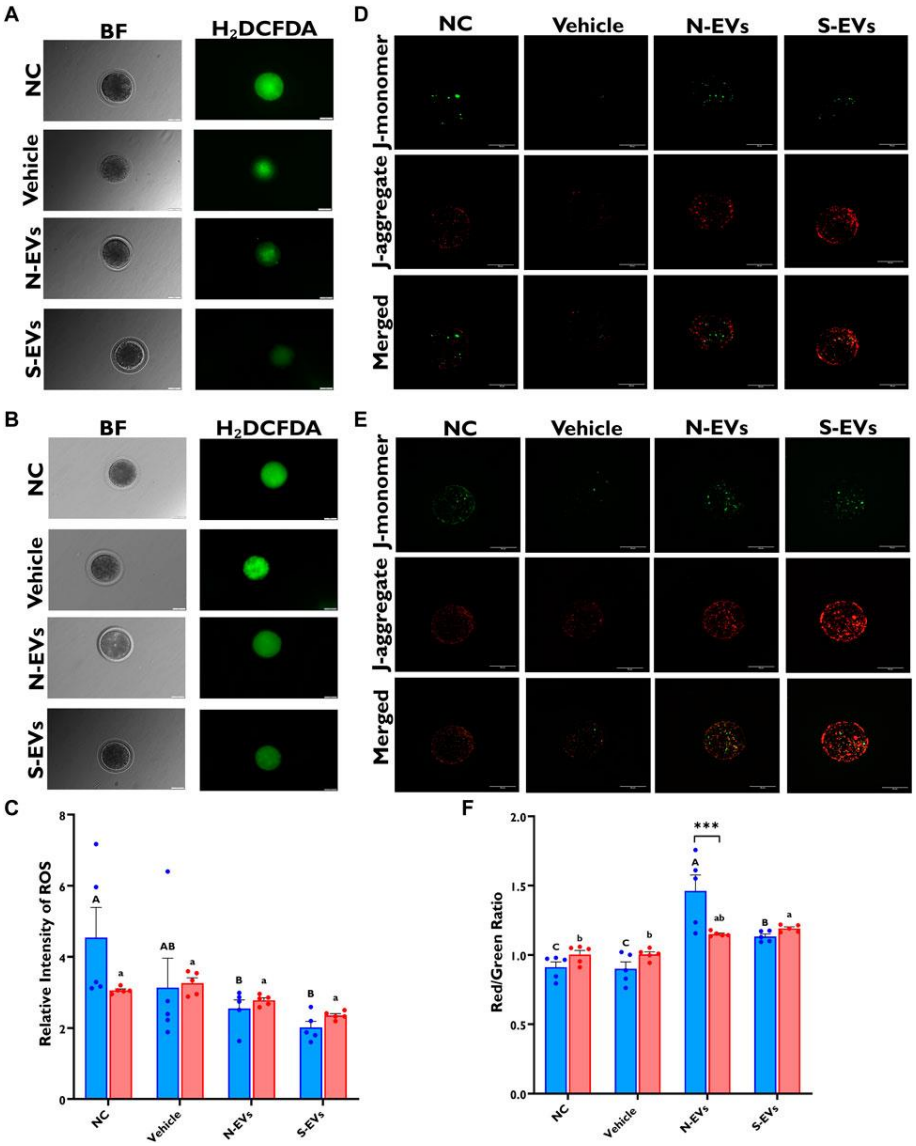


Figure 2.5. The beneficial effects of GC-EVs on oocyte function under in vitro normal physiological (38.5°C; blue) and HS (41°C; red) conditions. Fluorescence images of in vitro matured bovine oocytes treated with 2′,7′-Dichlorofluorescin Diacetate (H_2DCFDA) were captured for the measurement of intracellular ROS levels in single oocytes. Scale bar, 50 µM [38.5°C; (A)] [41°C; (B)]. Quantification of the relative fluorescence intensity in single oocytes were carried out in triplicates (total = of 15–50 oocytes per treatment) (C). Fluorescence images of in vitro matured bovine oocytes treated with 5,5′,6,6′-tetrachloro-1,1′,3,3′tetraethylbenzimidazolylcarbocynanine iodide (JC-1) for the measurement of MMP (ΔΨm), an indicator of mitochondrial activity in single oocytes. Scale bar, 50 µM [38.5°C; (D)] [41°C; (E)]. Quantification of the relative fluorescence intensity (red/green ratio) in single oocytes were carried out in duplicates (total = of 12–22 oocytes per treatment) (F). Data among treatments represent the mean ± SEM and the differences between means were analyzed using Two-way ANOVA followed by Tukey's Multiple Comparisons Test. Bars with different letters (38.5°C; uppercase) (41°C; lowercase) indicate statistically significant differences of at least ($p < 0.05$) between treatments under the same culture conditions, while (*) indicate statistical differences between the same treatment under different culture environments during IVM (***$p < 0.001$).

developmental rate of oocytes becoming blastocysts under normal physiological conditions, when compared to the untreated or vehicle controls. Taken together, our developmental competence data show significant differences between treatments ($p = 0.0002$, $p = 0.0003$) and temperatures ($p < 0.0001$).

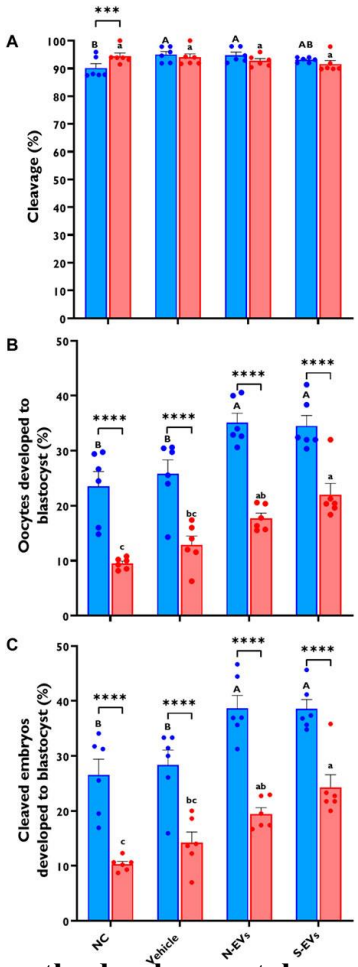


Figure 2.6. The effect of GC-EVs on the developmental capacity of oocytes matured at 38.5°C (blue) and 41°C (red). Results are from a total of six replicates (281–299 total oocytes per treatment). Oocytes supplemented with N-EVs and cultured under 38.5°C showed significant improvements in cleavage percentage compared to the NC, while no visual differences were observed among treatments under HS conditions (A). The percentage of oocytes developed into blastocysts was significantly affected by maturation temperature with significant increases in developmental competence in those treatments supplemented with GC-EVs (B). Similarly, the percentage of cleaved embryos developed into blastocysts was linearly affected by maturation temperature with significant protection from inherent stress visualized in those treatments supplemented with GC-EVs (C). Data among treatments represent the mean ± SEM and the differences between means were analyzed using Two-way ANOVA followed by Tukey's Multiple Comparisons Test. Bars with different letters (38.5°C; uppercase) (41°C; lowercase) indicate statistically significant differences of at least ($p < 0.05$) between treatments under the same culture conditions, while (*) indicate statistical differences between the same treatment under different culture environments during IVM (***$p < 0.001$) (****$p < 0.0001$).

4.5 GC-EV supplementation modifies the expression of stress-associated transcripts in blastocysts

As shown in Figure 2.7A, except for GRP78 and GRP94, the supplementation of both N-EVs and S-EVs during oocyte maturation in the absence of subsequent thermal stress resulted in the cohesive suppression of the tested stress-related genes in blastocysts. Similarly, with an exception for NRF2, the supplementation of both N-EVs and S-EVs during oocyte maturation in the presence of thermal stress exposure resulted in the suppression of all six of the tested stress-associated marker genes within the resulting blastocysts (Figure 2.7B).

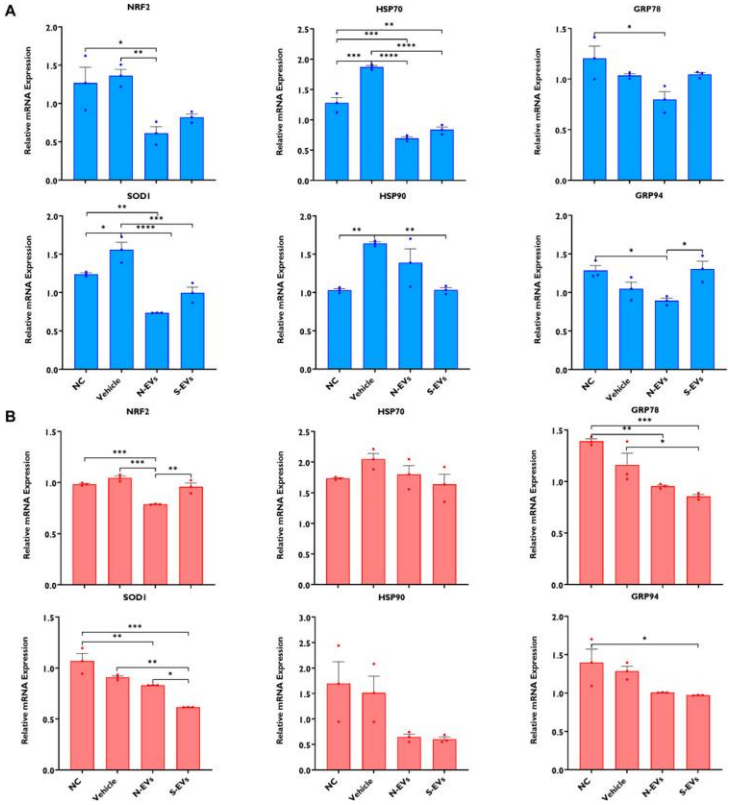


Figure 2.7. The impact of GC-EVs on transcript levels of stress-associated genes in blastocysts derived from oocytes treated with GC-EVs during oocyte maturation at 38.5°C (blue) and 41°C (red). The expressions of stress-associated genes were significantly diminished in blastocysts derived from oocytes supplemented with N-EVs and cultured at 38.5°C (A), and similar decreases in gene expression were visualized in blastocysts derived from oocytes supplemented with S-EVs and exposed to HS (B). Results are from a total of four pools of 5 blastocysts per pool for each treatment. Data represent the mean ± SEM and the differences between means were analyzed using One-way ANOVA followed by Tukey's Multiple Comparisons Test. (*$p < 0.05$), (**$p < 0.01$), (***$p < 0.001$), (****$p < 0.0001$).

4.6 Impact of GC-EVs supplementation during oocyte maturation on blastocyst ROS accumulation, mitochondrial function, total cell counts, and apoptotic index

As shown in Figures 2.88B, C, both qualitative and quantitative ROS levels are markedly lower in blastocysts when S-EVs are supplemented during oocyte maturation under HS exposure. Similarly, when cultured at 38.5°C, blastocysts derived from oocytes supplemented with S-EVs had a significantly lower accumulation of ROS (Figures 2.8A, C). Although our data show no significant differences between temperatures, we show a significant difference among treatments ($p = 0.001$) with a significant interaction between temperature and treatment ($p = 0.0023$). We also assessed the membrane potential of mitochondria amid blastocysts and revealed that under HS conditions, blastocysts derived from both N-EVs and S-EVs supplemented groups had significantly increased mitochondrial function, as evidenced by an increased ratio of fluorescence imaged from J-aggregates vs. J-monomers compared to the NC and vehicle (Figures 2.8E, F). In parallel, blastocysts derived from oocytes supplemented with N-EVs and S-EVs and cultured under normal physiological temperature (38.5°C) showed improved mitochondrial membrane potential compared to the NC and vehicle supplemented groups (Figure 2.8D). Collectively, our data demonstrate a significant difference between GC-EV supplemented treatments ($p = 0.0001$), culture temperatures ($p = 0.0054$), as well as their interaction ($p = 0.0161$).

Alternatively, no measurable differences were observed in total cell numbers among the treatment groups subjected to HS (Figures 2.9B, C). However, there were significant increases in the total cell number in blastocysts derived from oocytes supplemented with N-EVs and cultured at 38.5°C (Figures 2.9A, C). In terms of total cell counts, we show no significant differences between treatments, albeit significant differences between temperatures ($p < 0.0001$), as well as a

significant interaction between temperature and treatment (p = 0.0015). Moreover, as shown in Figures 2.9E, F,

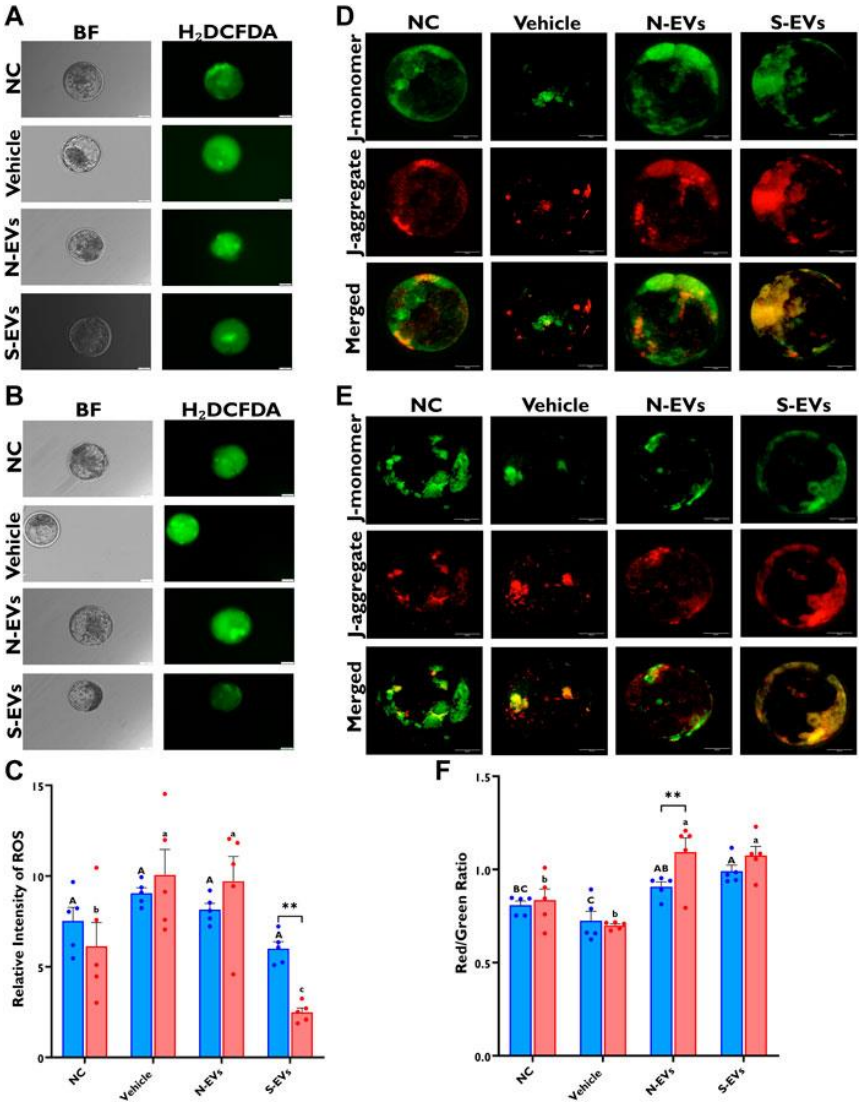


Figure 2.8. Functional alterations of GC-EV supplementation during in vitro maturation on blastocyst quality under in vitro normal physiological (38.5°C; blue) and HS (41°C; red) conditions. Fluorescence images of in vitro cultured bovine blastocysts treated with 2′,7′-Dichlorofluorescin Diacetate (H_2DCFDA) were captured for the measurement of intracellular ROS levels in single blastocysts. Scale bar, 50 µM [38.5°C; (A)] [41°C; (B)]. Quantification of the relative fluorescence intensity in single blastocysts were carried out in triplicates (a total of 6-9 blastocysts per treatment) (C). Fluorescence images of in vitro cultured bovine blastocysts treated with 5,5′,6,6′-tetrachloro-1,1′,3,3′tetraethylbenzimidazolylcarbocyanine iodide (JC-1) for the measurement of MMP (ΔΨm), an indicator of mitochondrial activity in single blastocysts. Scale bar, 50 µM [38.5°C; (D)] [41°C; (E)]. Quantification of the relative fluorescence intensity (red/green ratio) in single blastocysts were carried out in duplicates (a total of 7–11 blastocysts per treatment) (F). Data among treatments represent the mean ± SEM and the differences between means were analyzed using Two-way ANOVA followed by Tukey's Multiple Comparisons Test.

Bars with different letters (38.5°C; uppercase) (41°C; lowercase) indicate statistically significant differences of at least ($p < 0.05$) between treatments under the same culture conditions, while (*) indicate statistical differences between the same treatment under different culture environments during IVM (**$p < 0.01$).

the number of fluorescently labeled nuclei with fragmented DNA (shown in green), is dramatically reduced ($p < 0.0001$) in blastocysts derived from oocytes supplemented with S-EVs and exposed to HS. Additionally, blastocysts derived from oocytes supplemented with N-EVs and S-EVs and cultured under normal physiological temperature (38.5°C) showed diminished apoptotic indexes (Figures 2.9D, F). Importantly, our data indicates a significant difference among treatments ($p < 0.0001$), temperatures ($p = 0.0057$), as well as their interaction ($p = 0.0048$).

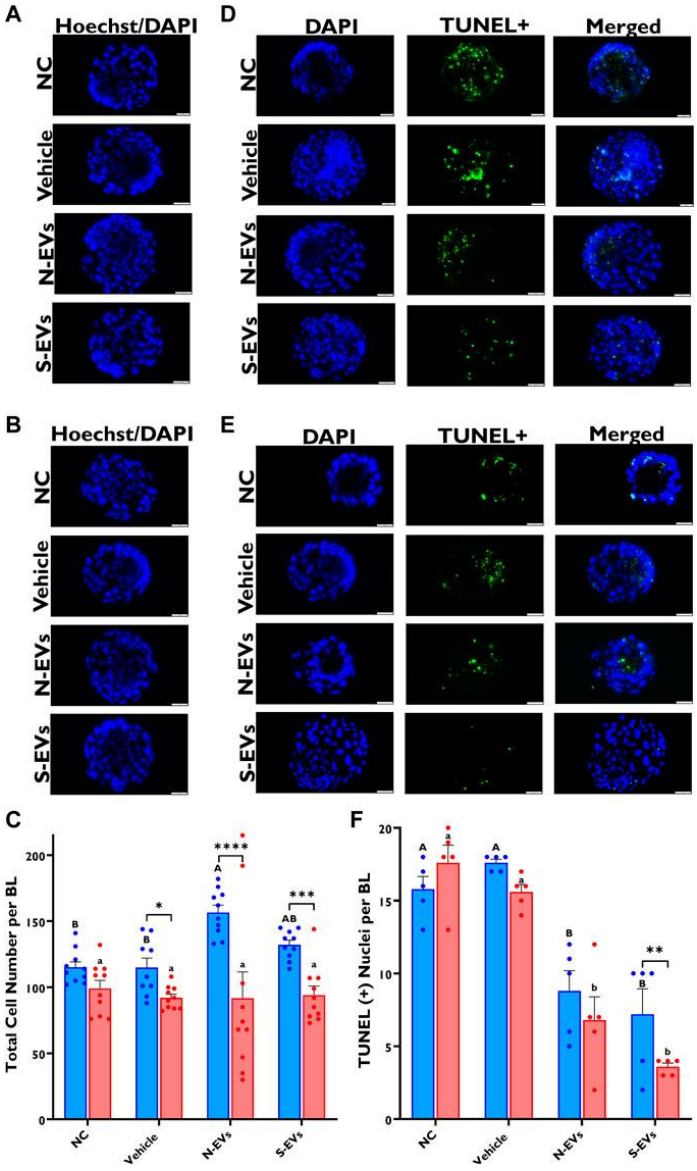


Figure 2.9. The beneficial effect of GC-EV supplementation during in vitro maturation on blastocyst quality under in vitro normal physiological (38.5°C; blue) and HS (41°C; red) conditions. Fluorescence images of in vitro cultured bovine blastocysts treated with Hoechst 33342/DAPI were used to determine total cell numbers in preimplantation embryos. Scale bar, 50 μM [38.5°C; (A)] [41°C; (B)]. Quantification of total cell numbers in single blastocysts were carried out in triplicates (a total of 18–30 blastocysts per treatment) (C). Fluorescence images of in vitro cultured bovine blastocysts subjected to a TUNEL assay were captured for specific detection of apoptotic cells. Scale bar, 50 μM [38.5°C; (D)] [41°C; (E)]. Quantification of TUNEL + cells in single blastocysts were carried out in triplicates (a total of 19–41 blastocysts per treatment) (F). Data among treatments represent the mean ± SEM and the differences between means were analyzed using Two-way ANOVA followed by Tukey's Multiple Comparisons Test. Bars with different letters (38.5°C; uppercase) (41°C; lowercase) indicate statistically significant differences of at least ($p < 0.05$) between treatments under the same culture conditions, while (*) indicate statistical differences between the same treatment under different culture environments during IVM (*$p < 0.05$), (**$p < 0.01$), (***$p < 0.001$), (****$p < 0.0001$).

5. Discussion

Elevated ambient temperatures play a multifaceted role in affecting physiological and cellular functions with direct detrimental impacts on fertility in dairy cattle (Wolfenson et al., 2000). Delineated in a plethora of studies, HS compromises reproductive function by altering follicular dynamics (Badinga et al., 1993; Guzeloglu et al., 2001), afflicting proper granulosa cell function (Li et al., 2016) with impairments in oocyte maturation, fertilization (Roth and Hansen, 2005; Nabenishi et al., 2012) and preimplantation embryo development (Al-Katanani et al., 2002; Roth and Hansen, 2004). Oxidative stress, modeled through HS, is evidenced by the harmful effects elicited at the cellular level by inducing DNA damage, protein modifications, and lipid peroxidation (Alvarez, 2003; Kitagawa et al., 2004). We and others have recently shown that GCs exposed to HS release EVs containing protective signals which can be beneficial in eliciting positive responses or increased protection against stress in recipient or bystander cells (Bewicke-Copley et al., 2017; Gebremedhn et al., 2020). Hence, given the physiological relevance of the whereabouts of the oocyte in vivo at the time of maturation, in the present study, we generated subsets of EVs released from in vitro cultured follicular GCs subjected to the normal ambient body

temperature of the cow (38.5°C) and HS (42°C) conditions. Throughout this work, we sufficiently demonstrate the capacity of GC-derived N-EVs and S-EVs in modulating a multitude of factors associated with oocyte quality when cultured under suboptimal conditions.

It has been shown previously that the addition of follicular fluid exosomes to the maturation medium can increase cumulus expansion with projections to modulate developmental competence under HS conditions (Rodrigues et al., 2019). In addition, exosomes isolated from bovine follicular fluid of small follicles have been reported to support cumulus expansion of bovine and mouse COCs cultured without fetal calf serum (Hung et al., 2015). Similarly, we found that GC-derived EVs can support cumulus expansion in COCs during maturation in the presence or absence of thermal stress. This was evidenced by the induction of the expression of cumulus expansion-associated genes (PTGS2, EGFR, and PTX3) in COCs supplemented with GC-EVs and subsequently subjected to thermal stress compared to the NC and vehicle groups. Interestingly, the impact of N-EVs in inducing the expression of cumulus expansion marker genes was prominent in COCs cultured under normal conditions following EV supplementation (Figure 2.2B). On the contrary, S-EVs suppressed the expression of cumulus expansion marker genes in the absence of HS (Figure 2.2C). Statistically comparing treatments under differing ambient culture environments, we collectively show the beneficial effects of N-EVs under normal physiological temperature compared to HS, while S-EVs showed similar effects on cumulus expansion under HS versus normal temperature. Moreover, expression analysis of stress-associated genes in CCs and oocytes revealed the role of GC-derived EVs in reducing the expression of stress-associated transcripts, thereby the severity of thermal stress in those cells. Irrespective of environmental culture conditions, S-EVs in particular, clearly repressed the expression of HSP70, HSP90, NRF2, and SOD1 in CCs, signifying the inherent presence of other stress factors in our in vitro culture

environment, even under normal culture conditions. To date, the precise molecular pathways in which GC-EVs promote thermotolerance in COCs are not fully understood. However, it is postulated that donor cell cytoplasmic proteins and RNA-enriched EVs can have the potential to modulate the stress response mechanisms of recipient cells. Moreover, EVs are widely accepted for their physiochemical traits to foster therapeutic applications primarily on EV-delivered bioactive compounds (mRNA, miRNA, long non-coding RNAs, DNAs, proteins, and lipids) with biological regulatory functions (Liu et al., 2022). Exosome-mediated transfer of miRNA in bovine follicular GCs has been evidenced in our previous study (Sohel et al., 2013). Collectively, as it has been demonstrated in previous studies (Mothersill and Seymour, 1997; Lyng et al., 2000; Chai and Hei, 2008; Bewicke-Copley et al., 2017), results from this study demonstrate the capabilities of GC-EVs to support cumulus expansion and conventional physiology underpinning proper oocyte function by reducing the severity of thermal stress during in vitro oocyte maturation.

Oocyte competence is largely determined by the quality and subsequent accumulation of organelles, metabolites, and maternal RNAs acquired during the period of growth and maturation determining the success of fertilization, embryo development, and pregnancy establishment. Following confirmation of GC-EVs' impact on CCs, we examined the expression of stress-associated transcripts in the presence or absence of subsequent thermal stress. Under HS exposure, the expression of NRF2, SOD1, HSP70, HSP90, GRP78, and GRP94 was dramatically reduced in oocytes supplemented with S-EVs. These observations are similar to our previous report showing that priming of naïve GCs using EVs derived from thermally stressed bovine GCs could provide protection against thermal stress by suppressing the expression of stress-associated genes as a means of inducing thermotolerance (Gebremedhn et al., 2020). Previous reports well document overexpressed levels of HSPs to be especially detrimental to cells undergoing developmental

growth and rapid divisions (Krebs and Feder, 1997). The chaperoning functions of HSPs inhibit Caspase processing, a heat-sensitive target leading to heat shock-induced apoptosis (Mosser et al., 1997). Inhibition of heat-shock-induced apoptosis using a caspase inhibitor has been shown to effectively mitigate the detrimental impacts of HS on oocyte competence for fertilization and subsequent embryo development (Roth and Hansen, 2004). Taken together, as functionally evidenced in part by others, S-EVs inherently contain high expression of HSPs (Gebremedhn et al., 2020), which likely in part inhibit caspase activity and provide resistance to stress-induced apoptosis, modulating the thermoprotective role of the CCs (Tatemoto et al., 2000) surrounding the oocyte and perhaps the integrity and function of the oocyte under HS conditions. In addition, S-EVs' inherent capacity to induce a beneficial "bystander effect," may potentially underpin the transfer of specific cargoes (possibly miRNA transfer), which serve to post-transcriptionally regulate gene expression via degradation and/or translational repression. Conclusively, S-EV-coupled miRNAs may be involved in the posttranscriptional regulation of HSPs under thermal stress conditions, resulting in the downregulation of HSP transcripts compared to the control counterparts.

Exposure to thermal stress is known to have direct implications on cellular function as it leads to the accumulation of intracellular ROS causing oxidative damage (Azad et al., 2010), mitochondrial dysfunction, and autophagy (Scherz-Shouval and Elazar, 2011; Shen et al., 2017), resulting in a continued decline in fertility (Guérin et al., 2001). The overwhelming importance of mitochondria for the development of oocytes and embryos as an apoptotic regulator and importantly a prominent source of energy in the form of ATP is widely accepted (van Blerkom, 2009). Mitochondrial dysfunction has been suggested to be a major factor in chromosomal anomalies during meiotic divisions in oocytes and mitosis in embryos affecting the developmental

competence of oocytes and embryos (Schon et al., 2000; Eichenlaub-Ritter et al., 2004; Desler et al., 2007). Studies in mice and humans using JC-1 have shown the relationship between mitochondrial activity and the developmental competence of oocytes and embryos (Acton et al., 2004). In addition to reductions in ROS accumulation, supplementation of S-EVs at the time of oocyte maturation and subsequent exposure to HS, notably increased the ratio of red to green fluorescence after JC-1 staining, indicating improved mitochondrial activity. On the other hand, under normal physiological temperatures, GC-EV supplementation synergistically reduced the accumulation of ROS with the highest mitochondrial activity coming from oocytes derived from the treatment supplemented with N-EVs during IVM. Comparisons between treatments under differing ambient culture environments showed increased mitochondrial activity in oocytes supplemented with N-EVs under normal physiological temperature compared to HS conditions. Similarly, the supplementation of S-EVs also had a similar impact on mitochondrial function in oocytes under HS conditions versus normal ambient temperature. The positive impacts of GC-EVs during oocyte maturation in the absence of thermal stress exposure may be in part due to the intrinsic quality of oocytes derived from local slaughterhouse ovaries and indicative that certain levels of stress are inherently present within the in vitro environment.

To investigate the downstream effect of GC-EVs supplementation during bovine IVM, we performed IVF and IVC of the resulting oocytes for development until the blastocyst stage. Supplementation of both N-EVs and S-EVs during oocyte maturation showed to improve blastocyst rates both in the presence or absence of thermal stress exposure, indicating the positive impact of GC-EVs in supporting oocyte development to the blastocyst stage (Figures 2.6B, C). Moreover, a significant reduction in the expression of stress-associated genes (SOD1, HSP70, HSP90, GRP78, and GRP94) was observed in blastocysts derived from COCs supplemented with

N-EVs and S-EVs. However, in the absence of HS, blastocysts from GC-EVs'-supplemented treatment groups tended to suppress the relative abundance of stress-associated genes, with exceptions to the expression of GRP78 and GRP94, which showed increases in expression in S-EVs supplemented treatment groups. This indicates the differential impact of GC-EVs in modulating the stress response of oocytes to environmental stressors. In the present study, it is shown that blastocysts derived from COCs supplemented with S-EVs and exposed to HS during maturation have increased embryo quality due to reduced ROS accumulation, decreased TUNEL+ apoptotic nuclei, and increased mitochondrial activity compared to their NC counterparts. Interestingly, as shown in oocytes, S-EVs significantly reduced the amount of accumulated ROS in blastocysts under HS compared to those cultured under normal ambient temperature. These results partly support our hypothesis that S-EVs derived from GCs mitigate the detrimental effects of HS during oocyte maturation, which may have an impact on the further developmental potential of oocytes in giving rise to developmentally competent blastocysts. Our data also suggests that GC-EV supplementation amid HS exposure during IVM may not induce the proliferative capacity of bovine embryos, however, GC-EVs effectively modulate the inherent quality of resulting blastocysts. To leverage our findings, a similar study showed that EVs isolated via density gradient ultracentrifugation and size-exclusion chromatography from Holstein heifer follicular fluid, improve embryo quality based primarily on differential apoptotic cell counts (Asaadi et al., 2021). Similarly, the addition of bovine oviduct epithelial cell EVs had a positive impact on the quality of in vitro produced bovine embryos, signifying EVs' functional and physiological relevance to support the development of viable and competent blastocysts under in vitro environments to enhance the pregnancy outcome after transfer (Lopera-Vásquez et al., 2016).

Taken together, the current study demonstrated that GC-EVs play a pivotal regulatory role against HS during in vitro maturation of bovine oocytes by reducing ROS accumulation, enhancing proper mitochondrial function, and altering the expression of stress-associated genes, thereby reducing the severity of thermal stress, improving oocyte survival and viability (Figure 2.10). Despite the fact that EVs are uptaken only by CCs, the impact of EV supplementation seems to be through changing the physiology of the CCs, which ultimately lends impact on oocyte physiology, particularly ROS accumulation, mitochondrial activity, and gene expression profiles. Furthermore, the beneficial role of EVs and their capabilities to modulate the detrimental effects of HS during maturation can have long-lasting impacts on the development and quality of blastocysts, potentially in the establishment of pregnancy and the generation of healthy offspring. As GC-EVs are known to shuttle protective signals in the form of RNAs, proteins, and/or lipids, further studies are needed to determine the exact mechanisms of action of EVs in modulating stress response for potential application in assisted reproductive technologies involving IVM, IVF, and IVC of mammalian oocytes and embryos.

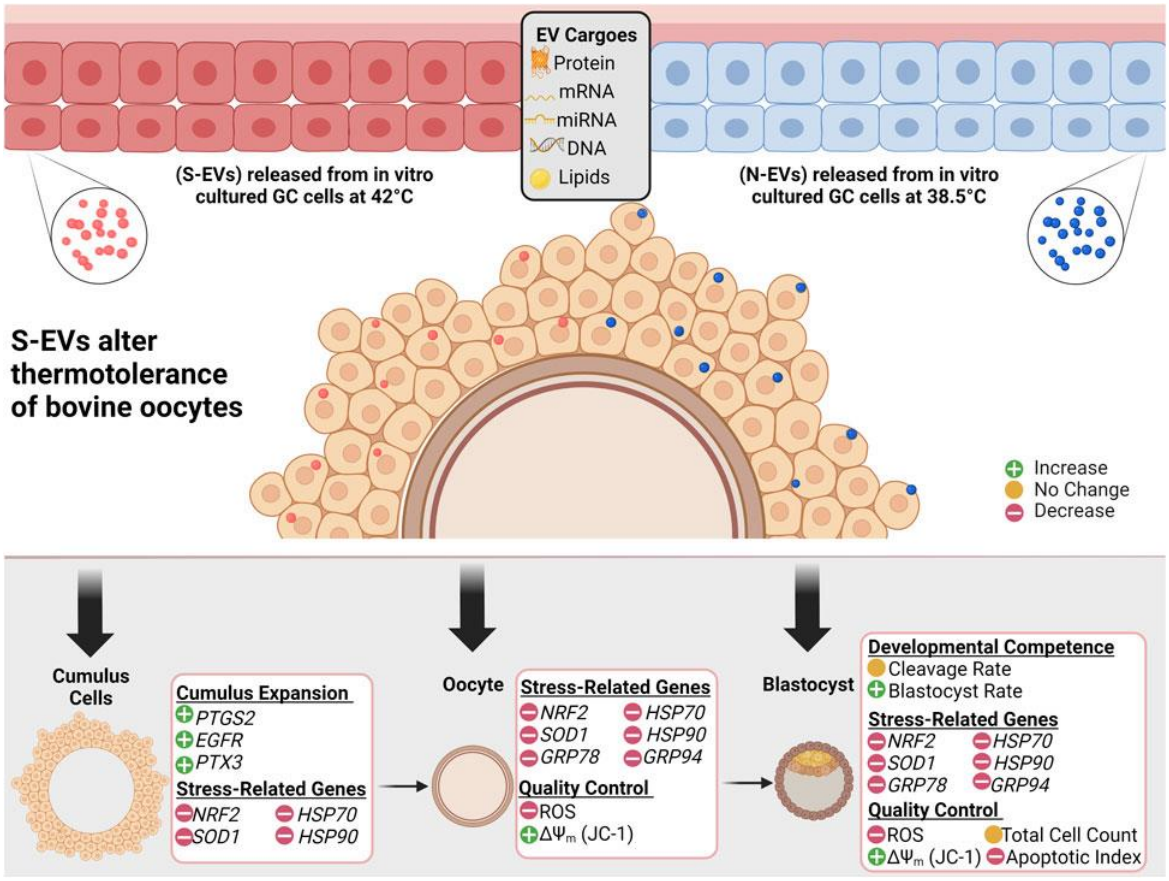


Figure 2.10. Graphical Synopsis. Schematic illustration showing EVs secreted from follicular granulosa cultured in vitro under 38.5°C (N-EVs) and 42°C (S-EVs), preferentially uptaken in the cumulus cells in intact cumulus-oocyte complexes following co-incubation during in vitro oocyte maturation. Results indicate that S-EVs effectively modulate the thermotolerance of bovine oocytes to elevated temperatures shown through the functional analysis conducted in the cumulus cells, oocytes, and developed blastocysts.

References

Abdelnour, S.A., Yang, C.-Y., Swelum, A.A., Abd El-Hack, M.E., Khafaga, A.F. & Abdo, M. et al. (2020) Molecular, functional, and cellular alterations of oocytes and cumulus cells induced by heat stress and shock in animals. Environmental Science and Pollution Research International, 27(31), 38472–38490. Available from: https://doi.org/10.1007/s11356-020-10302-4.

Abumaghaid, M.M., Abdelazim, A.M., Belali, T.M., Alhujaily, M. & Saadeldin, I.M. (2022) Shuttle Transfer of mRNA Transcripts via Extracellular Vesicles From Male Reproductive Tract Cells to the Cumulus-Oocyte Complex in Rabbits (Oryctolagus cuniculus). Frontiers in Veterinary Science, 9, 816080. Available from: https://doi.org/10.3389/fvets.2022.816080.

Acton, B.M., Jurisicova, A., Jurisica, I. & Casper, R.F. (2004) Alterations in mitochondrial membrane potential during preimplantation stages of mouse and human embryo development. Molecular Human Reproduction, 10(1), 23–32. Available from: https://doi.org/10.1093/molehr/gah004.

Ahmed, K.A. & Xiang, J. (2011) Mechanisms of cellular communication through intercellular protein transfer. Journal of Cellular and Molecular Medicine, 15(7), 1458–1473. Available from: https://doi.org/10.1111/j.1582-4934.2010.01008.x.

Alam, M.H. & Miyano, T. (2020) Interaction between growing oocytes and granulosa cells in vitro. Reproductive Medicine and Biology, 19(1), 13–23. Available from: https://doi.org/10.1002/rmb2.12292.

Alcântara-Neto, A.S., Fernandez-Rufete, M., Corbin, E., Tsikis, G., Uzbekov, R. & Garanina, A.S. et al. (2020) Oviduct fluid extracellular vesicles regulate polyspermy during porcine in vitro

fertilisation. Reproduction, Fertility, and Development, 32(4), 409–418. Available from: https://doi.org/10.1071/RD19058.

Alcântara-Neto, A.S., Schmaltz, L., Caldas, E., Blache, M.-C., Mermillod, P. & Almiñana, C. (2020) Porcine oviductal extracellular vesicles interact with gametes and regulate sperm motility and survival. Theriogenology, 155, 240–255. Available from: https://doi.org/10.1016/j.theriogenology.2020.05.043.

Alemu, T.W., Pandey, H.O., Salilew Wondim, D., Gebremedhn, S., Neuhof, C. & Tholen, E. et al. (2018) Oxidative and endoplasmic reticulum stress defense mechanisms of bovine granulosa cells exposed to heat stress. Theriogenology, 110, 130–141. Available from: https://doi.org/10.1016/j.theriogenology.2017.12.042.

Al-Katanani, Y.M., Paula-Lopes, F.F. & Hansen, P.J. (2002) Effect of season and exposure to heat stress on oocyte competence in Holstein cows. Journal of Dairy Science, 85(2), 390–396. Available from: https://doi.org/10.3168/jds.s0022-0302(02)74086-1.

Almiñana, C., Corbin, E., Tsikis, G., Alcântara-Neto, A.S., Labas, V. & Reynaud, K. et al. (2017) Oviduct extracellular vesicles protein content and their role during oviduct-embryo cross-talk. Reproduction (Cambridge, England), 154(3), 153–168. Available from: https://doi.org/10.1530/REP-17-0054.

Altan-Bonnet, G. & Mukherjee, R. (2019) Cytokine-mediated communication: a quantitative appraisal of immune complexity. Nature Reviews. Immunology, 19(4), 205–217. Available from: https://doi.org/10.1038/s41577-019-0131-x.

Alvarez, J.G. (2003) DNA fragmentation in human spermatozoa: significance in the diagnosis and treatment of infertility. Minerva Ginecologica, 55(3), 233–239.

Asaadi, A., Dolatabad, N.A., Atashi, H., Raes, A., van Damme, P. & Hoelker, M. et al. (2021) Extracellular Vesicles from Follicular and Ampullary Fluid Isolated by Density Gradient Ultracentrifugation Improve Bovine Embryo Development and Quality. International Journal of Molecular Sciences, 22(2). Available from: https://doi.org/10.3390/ijms22020578.

Azad, M.A.K., Kikusato, M., Sudo, S., Amo, T. & Toyomizu, M. (2010) Time course of ROS production in skeletal muscle mitochondria from chronic heat-exposed broiler chicken. Comparative Biochemistry and Physiology. Part A, Molecular & Integrative Physiology, 157(3), 266–271. Available from: https://doi.org/10.1016/j.cbpa.2010.07.011.

Badinga, L., Thatcher, W.W., Diaz, T., Drost, M. & Wolfenson, D. (1993) Effect of environmental heat stress on follicular development and steroidogenesis in lactating Holstein cows. Theriogenology, 39(4), 797–810. Available from: https://doi.org/10.1016/0093-691X(93)90419-6.

Bewicke-Copley, F., Mulcahy, L.A., Jacobs, L.A., Samuel, P., Akbar, N. & Pink, R.C. et al. (2017) Extracellular vesicles released following heat stress induce bystander effect in unstressed populations. Journal of Extracellular Vesicles, 6(1), 1340746. Available from: https://doi.org/10.1080/20013078.2017.1340746.

Boni, R. (2019) Heat stress, a serious threat to reproductive function in animals and humans. Molecular Reproduction and Development, 86(10), 1307–1323. Available from: https://doi.org/10.1002/mrd.23123.

Chai, Y. & Hei, T.K. (2008) Radiation Induced Bystander Effect in vivo. Acta Medica Nagasakiensia, 53, S65-S69.

Critser, E.S. & First, N.L. (1986) Use of a fluorescent stain for visualization of nuclear material in living oocytes and early embryos. Stain Technology, 61(1), 1–5. Available from: https://doi.org/10.3109/10520298609110697.

Da Silveira, J.C., Veeramachaneni, D.N.R., Winger, Q.A., Carnevale, E.M. & Bouma, G.J. (2012) Cell-secreted vesicles in equine ovarian follicular fluid contain miRNAs and proteins: a possible new form of cell communication within the ovarian follicle. Biology of Reproduction, 86(3), 71. Available from: https://doi.org/10.1095/biolreprod.111.093252.

De La Torre-Sanchez, Jose Fernando, Preis, K. & Seidel, G.E., JR (2006) Metabolic regulation of in-vitro-produced bovine embryos. I. Effects of metabolic regulators at different glucose concentrations with embryos produced by semen from different bulls. Reproduction, Fertility, and Development, 18(5), 585–596. Available from: https://doi.org/10.1071/rd05063.

Desler, C., Munch-Petersen, B., Stevnsner, T., Matsui, S.-I., Kulawiec, M. & Singh, K.K. et al. (2007) Mitochondria as determinant of nucleotide pools and chromosomal stability. Mutation Research, 625(1-2), 112–124. Available from: https://doi.org/10.1016/j.mrfmmm.2007.06.002.

Edwards, J.L., Saxton, A.M., Lawrence, J.L., Payton, R.R. & Dunlap, J.R. (2005) Exposure to a physiologically relevant elevated temperature hastens in vitro maturation in bovine oocytes. Journal of Dairy Science, 88(12), 4326–4333. Available from: https://doi.org/10.3168/jds.S0022-0302(05)73119-2.

Eichenlaub-Ritter, U., Vogt, E., Yin, H. & Gosden, R. (2004) Spindles, mitochondria and redox potential in ageing oocytes. Reproductive Biomedicine Online, 8(1), 45–58. Available from: https://doi.org/10.1016/s1472-6483(10)60497-x.

Feder, M.E. & Hofmann, G.E. (1999) Heat-shock proteins, molecular chaperones, and the stress response: evolutionary and ecological physiology. Annual Review of Physiology, 61, 243–282. Available from: https://doi.org/10.1146/annurev.physiol.61.1.243.

Ferreira, R.M., Chiaratti, M.R., Macabelli, C.H., Rodrigues, C.A., Ferraz, M.L. & Watanabe, Y.F. et al. (2016) The Infertility of Repeat-Breeder Cows During Summer Is Associated with Decreased Mitochondrial DNA and Increased Expression of Mitochondrial and Apoptotic Genes in Oocytes. Biology of Reproduction, 94(3), 66. Available from: https://doi.org/10.1095/biolreprod.115.133017.

Gebremedhn, S., Gad, A., Aglan, H.S., Laurincik, J., Prochazka, R. & Salilew-Wondim, D. et al. (2020) Extracellular vesicles shuttle protective messages against heat stress in bovine granulosa cells. Scientific Reports, 10(1), 15824. Available from: https://doi.org/10.1038/s41598-020-72706-z.

Gilula, N.B., Epstein, M.L. & Beers, W.H. (1978) Cell-to-cell communication and ovulation. A study of the cumulus-oocyte complex. The Journal of Cell Biology, 78(1), 58–75. Available from: https://doi.org/10.1083/jcb.78.1.58.

Guérin, P., El Mouatassim, S. & Ménézo, Y. (2001) Oxidative stress and protection against reactive oxygen species in the pre-implantation embryo and its surroundings. Human Reproduction Update, 7(2), 175–189. Available from: https://doi.org/10.1093/humupd/7.2.175.

Guzeloglu, A., Ambrose, J.D., Kassa, T., Diaz, T., Thatcher, M.J. & Thatcher, W.W. (2001) Long-term follicular dynamics and biochemical characteristics of dominant follicles in dairy cows subjected to acute heat stress. Animal Reproduction Science, 66(1-2), 15–34. Available from: https://doi.org/10.1016/s0378-4320(01)00082-3.

Hansen, P.J. (2009) Effects of heat stress on mammalian reproduction. Philosophical Transactions of the Royal Society of London. Series B, Biological Sciences, 364(1534), 3341–3350. Available from: https://doi.org/10.1098/rstb.2009.0131.

Hung, W.-T., Hong, X., Christenson, L.K. & McGinnis, L.K. (2015) Extracellular Vesicles from Bovine Follicular Fluid Support Cumulus Expansion. Biology of Reproduction, 93(5), 117. Available from: https://doi.org/10.1095/biolreprod.115.132977.

Kitagawa, Y., Suzuki, K., Yoneda, A. & Watanabe, T. (2004) Effects of oxygen concentration and antioxidants on the in vitro developmental ability, production of reactive oxygen species (ROS), and DNA fragmentation in porcine embryos. Theriogenology, 62(7), 1186–1197. Available from: https://doi.org/10.1016/j.theriogenology.2004.01.011.

Krebs, R.A. & Feder, M.E. (1997) Deleterious consequences of Hsp70 overexpression in Drosophila melanogaster larvae. Cell Stress & Chaperones, 2(1), 60–71. Available from: https://doi.org/10.1379/1466-1268(1997)002<0060:dcohoi>2.3.co;2.

Li, J., Gao, H., Tian, Z., Wu, Y., Wang, Y. & Fang, Y. et al. (2016) Effects of chronic heat stress on granulosa cell apoptosis and follicular atresia in mouse ovary. Journal of Animal Science and Biotechnology, 7, 57. Available from: https://doi.org/10.1186/s40104-016-0116-6.

Li, Y., Zhang, Z., He, C., Zhu, K., Xu, Z. & Ma, T. et al. (2015) Melatonin protects porcine oocyte in vitro maturation from heat stress. Journal of Pineal Research, 59(3), 365–375. Available from: https://doi.org/10.1111/jpi.12268.

Lin, T., Lee, J.E., Kang, J.W., Shin, H.Y., Lee, J.B. & Jin, D.I. (2019) Endoplasmic Reticulum (ER) Stress and Unfolded Protein Response (UPR) in Mammalian Oocyte Maturation and

Preimplantation Embryo Development. International Journal of Molecular Sciences, 20(2). Available from: https://doi.org/10.3390/ijms20020409.

Liu, H., Liang, J., Ye, X., Huang, M., Ma, L. & Xie, X. et al. (2022) The potential role of extracellular vesicles in bioactive compound-based therapy: A review of recent developments. Critical Reviews in Food Science and Nutrition, 1–15. Available from: https://doi.org/10.1080/10408398.2022.2081667.

Lopera-Vásquez, R., Hamdi, M., Fernandez-Fuertes, B., Maillo, V., Beltrán-Breña, P. & Calle, A. et al. (2016) Extracellular Vesicles from BOEC in In Vitro Embryo Development and Quality. PloS One, 11(2), e0148083. Available from: https://doi.org/10.1371/journal.pone.0148083.

Lyng, F.M., Seymour, C.B. & Mothersill, C. (2000) Production of a signal by irradiated cells which leads to a response in unirradiated cells characteristic of initiation of apoptosis. British Journal of Cancer, 83(9), 1223–1230. Available from: https://doi.org/10.1054/bjoc.2000.1433.

Mateo-Otero, Y., Yeste, M., Roca, J., Llavanera, M., Bucci, D. & Galeati, G. et al. (2022) Seminal extracellular vesicles subsets modulate gene expression in cumulus cells of porcine in vitro matured oocytes. Scientific Reports, 12(1), 19096. Available from: https://doi.org/10.1038/s41598-022-22004-7.

Matzuk, M.M., Burns, K.H., Viveiros, M.M. & Eppig, J.J. (2002) Intercellular communication in the mammalian ovary: oocytes carry the conversation. Science (New York, N.Y.), 296(5576), 2178–2180. Available from: https://doi.org/10.1126/science.1071965.

Mosser, D.D., Caron, A.W., Bourget, L., Denis-Larose, C. & Massie, B. (1997) Role of the human heat shock protein hsp70 in protection against stress-induced apoptosis. Molecular and Cellular Biology, 17(9), 5317–5327. Available from: https://doi.org/10.1128/MCB.17.9.5317.

Mothersill, C. & Seymour, C. (1997) Medium from irradiated human epithelial cells but not human fibroblasts reduces the clonogenic survival of unirradiated cells. International Journal of Radiation Biology, 71(4), 421–427. Available from: https://doi.org/10.1080/095530097144030.

Nabenishi, H., Ohta, H., Nishimoto, T., Morita, T., Ashizawa, K. & Tsuzuki, Y. (2012) The effects of cysteine addition during in vitro maturation on the developmental competence, ROS, GSH and apoptosis level of bovine oocytes exposed to heat stress. Zygote (Cambridge, England), 20(3), 249–259. Available from: https://doi.org/10.1017/S0967199411000220.

Parrish, J.J., Krogenaes, A. & Susko-Parrish, J.L. (1995) Effect of bovine sperm separation by either swim-up or Percoll method on success of in vitro fertilization and early embryonic development. Theriogenology, 44(6), 859–869. Available from: https://doi.org/10.1016/0093-691x(95)00271-9.

Pasquariello, R., Ermisch, A.F., Silva, E., McCormick, S., Logsdon, D. & Barfield, J.P. et al. (2019) Alterations in oocyte mitochondrial number and function are related to spindle defects and occur with maternal aging in mice and humans†. Biology of Reproduction, 100(4), 971–981. Available from: https://doi.org/10.1093/biolre/ioy248.

Pavani, K.C., Baron, E., Correia, P., Lourenço, J., Bettencourt, B.F. & Sousa, M. et al. (2016) Gene expression, oocyte nuclear maturation and developmental competence of bovine oocytes and embryos produced after in vivo and in vitro heat shock. Zygote (Cambridge, England), 24(5), 748–759. Available from: https://doi.org/10.1017/S0967199416000071.

Rivera, R.M. & Hansen, P.J. (2001) Development of cultured bovine embryos after exposure to high temperatures in the physiological range. Reproduction (Cambridge, England), 121(1), 107–115.

Robertson, I. (1998) Certification and identification of the embryo. Manual of the International Embryo Transfer Society, 103–134.

Rodrigues, T.A., Tuna, K.M., Alli, A.A., Tribulo, P., Hansen, P.J. & Koh, J. et al. (2019) Follicular fluid exosomes act on the bovine oocyte to improve oocyte competence to support development and survival to heat shock. Reproduction, Fertility, and Development, 31(5), 888–897. Available from: https://doi.org/10.1071/RD18450.

Roth, Z. & Hansen, P.J. (2004) Involvement of apoptosis in disruption of developmental competence of bovine oocytes by heat shock during maturation. Biology of Reproduction, 71(6), 1898–1906. Available from: https://doi.org/10.1095/biolreprod.104.031690.

Roth, Z. & Hansen, P.J. (2005) Disruption of nuclear maturation and rearrangement of cytoskeletal elements in bovine oocytes exposed to heat shock during maturation. Reproduction (Cambridge, England), 129(2), 235–244. Available from: https://doi.org/10.1530/rep.1.00394.

Russell, D.L., Gilchrist, R.B., Brown, H.M. & Thompson, J.G. (2016) Bidirectional communication between cumulus cells and the oocyte: Old hands and new players? Theriogenology, 86(1), 62–68. Available from: https://doi.org/10.1016/j.theriogenology.2016.04.019.

Saeed-Zidane, M., Linden, L., Salilew-Wondim, D., Held, E., Neuhoff, C. & Tholen, E. et al. (2017) Cellular and exosome mediated molecular defense mechanism in bovine granulosa cells

exposed to oxidative stress. PloS One, 12(11), e0187569. Available from: https://doi.org/10.1371/journal.pone.0187569.

Sartori, R., Sartor-Bergfelt, R., Mertens, S.A., Guenther, J.N., Parrish, J.J. & Wiltbank, M.C. (2002) Fertilization and early embryonic development in heifers and lactating cows in summer and lactating and dry cows in winter. Journal of Dairy Science, 85(11), 2803–2812. Available from: https://doi.org/10.3168/jds.S0022-0302(02)74367-1.

Scherz-Shouval, R. & Elazar, Z. (2011) Regulation of autophagy by ROS: physiology and pathology. Trends in Biochemical Sciences, 36(1), 30–38. Available from: https://doi.org/10.1016/j.tibs.2010.07.007.

Schmittgen, T.D. & Livak, K.J. (2008) Analyzing real-time PCR data by the comparative C(T) method. Nature Protocols, 3(6), 1101–1108. Available from: https://doi.org/10.1038/nprot.2008.73.

Schon, E.A., Kim, S.H., Ferreira, J.C., Magalhães, P., Grace, M. & Warburton, D. et al. (2000) Chromosomal non-disjunction in human oocytes: is there a mitochondrial connection? Human Reproduction (Oxford, England), 15 Suppl 2, 160–172. Available from: https://doi.org/10.1093/humrep/15.suppl_2.160.

Shen, M., Jiang, Y., Guan, Z., Cao, Y., Li, L. & Liu, H. et al. (2017) Protective mechanism of FSH against oxidative damage in mouse ovarian granulosa cells by repressing autophagy. Autophagy, 13(8), 1364–1385. Available from: https://doi.org/10.1080/15548627.2017.1327941.

Silva, E., Greene, A.F., Strauss, K., Herrick, J.R., Schoolcraft, W.B. & Krisher, R.L. (2015) Antioxidant supplementation during in vitro culture improves mitochondrial function and

development of embryos from aged female mice. Reproduction, Fertility, and Development, 27(6), 975–983. Available from: https://doi.org/10.1071/RD14474.

Sohel, M.M.H., Hoelker, M., Noferesti, S.S., Salilew-Wondim, D., Tholen, E. & Looft, C. et al. (2013) Exosomal and Non-Exosomal Transport of Extra-Cellular microRNAs in Follicular Fluid: Implications for Bovine Oocyte Developmental Competence. PloS One, 8(11), e78505. Available from: https://doi.org/10.1371/journal.pone.0078505.

Szatanek, R., Baran, J., Siedlar, M. & Baj-Krzyworzeka, M. (2015) Isolation of extracellular vesicles: Determining the correct approach (Review). International Journal of Molecular Medicine, 36(1), 11–17. Available from: https://doi.org/10.3892/ijmm.2015.2194.

Tatemoto, H., Sakurai, N. & Muto, N. (2000) Protection of porcine oocytes against apoptotic cell death caused by oxidative stress during In vitro maturation: role of cumulus cells. Biology of Reproduction, 63(3), 805–810. Available from: https://doi.org/10.1095/biolreprod63.3.805.

Tesfaye, D., Menjivar, N. & Gebremedhn, S. (2021) Current knowledge and the future potential of extracellular vesicles in mammalian reproduction. Reproduction, Fertility, and Development, 34(2), 174–189. Available from: https://doi.org/10.1071/RD21277.

Théry, C., Witwer, K.W., Aikawa, E., Alcaraz, M.J., Anderson, J.D. & Andriantsitohaina, R. et al. (2018) Minimal information for studies of extracellular vesicles 2018 (MISEV2018): a position statement of the International Society for Extracellular Vesicles and update of the MISEV2014 guidelines. Journal of Extracellular Vesicles, 7(1), 1535750. Available from: https://doi.org/10.1080/20013078.2018.1535750.

Trummer, A., Rop, C. de, Tiede, A., Ganser, A. & Eisert, R. (2009) Recovery and composition of microparticles after snap-freezing depends on thawing temperature. Blood Coagulation &

Fibrinolysis : an International Journal in Haemostasis and Thrombosis, 20(1), 52–56. Available from: https://doi.org/10.1097/MBC.0b013e32831be9c5.

Valadi, H., Ekström, K., Bossios, A., Sjöstrand, M., Lee, J.J. & Lötvall, J.O. (2007) Exosome-mediated transfer of mRNAs and microRNAs is a novel mechanism of genetic exchange between cells. Nature Cell Biology, 9(6), 654–659. Available from: https://doi.org/10.1038/ncb1596.

van Blerkom, J. (2009) Mitochondria in early mammalian development. Seminars in Cell & Developmental Biology, 20(3), 354–364. Available from: https://doi.org/10.1016/j.semcdb.2008.12.005.

van Deun, J., Mestdagh, P., Agostinis, P., Akay, Ö., Anand, S. & Anckaert, J. et al. (2017) EV-TRACK: transparent reporting and centralizing knowledge in extracellular vesicle research. Nature Methods, 14(3), 228–232. Available from: https://doi.org/10.1038/nmeth.4185.

Wolfenson, D. & Roth, Z. (2019) Impact of heat stress on cow reproduction and fertility. Animal Frontiers : the Review Magazine of Animal Agriculture, 9(1), 32–38. Available from: https://doi.org/10.1093/af/vfy027.

Wolfenson, D., Roth, Z. & Meidan, R. (2000) Impaired reproduction in heat-stressed cattle: basic and applied aspects. Animal Reproduction Science, 60-61, 535–547. Available from: https://doi.org/10.1016/s0378-4320(00)00102-0.

Wolfenson, D., Thatcher, W.W., Badinga, L., Savi0, J.D., Meidan, R. & Lew, B.J. et al. (1995) Effect of Heat Stress on Follicular Development during the Estrous Cycle in Lactating Dairy Cattle1. Biology of reproduction, 52(5), 1106–1113. Available from: https://doi.org/10.1095/biolreprod52.5.1106.

CHAPTER III—Bovine oviductal organoids: a multi-omics approach to capture the cellular and extracellular molecular response of the oviduct to heat stress[3]

1. Overview

Background

The mammalian oviduct is a complex, fibromuscular organ known for its role in orchestrating a series of timely and dynamic changes to suitably support early embryogenesis. Climate change-induced heat stress (HS) is one of the largest single stressors compromising reproductive function in humans and farm animals via systemic changes in the redox status of the maternal environment, adversely affecting fertilization and early embryonic development. Oviductal organoids represent a unique 3-dimensional, biomimetic model to study the physiology of the oviduct and its subsequent impact on embryo development under various environmental conditions.

Results

Our study is the first to demonstrate an innovative approach to understanding the cascade of molecular changes sustained by bovine oviductal organoids under HS and the subsequent maternal signals harnessed within their secreted extracellular vesicles (EVs). Transcriptomic analysis of oviductal organoids exposed to HS revealed 2,570 differentially expressed genes (1,222 up- and 1,348 downregulated), while EV-coupled miRNome analysis disclosed 18 miRNAs with significant differential expression (12 up- and 6 downregulated) in EVs from thermally stressed organoids compared to EVs released from organoids cultured under thermoneutral conditions.

---

[3]Menjivar NG, Gad A, Thompson RE, Meyers MA, Hollinshead FK, Tesfaye D. Bovine oviductal organoids: a multi-omics approach to capture the cellular and extracellular molecular response of the oviduct to heat stress. *Published at BMC Genomics*

Genes activated in oviductal organoids in response to thermal stress, include: COX1, ACTB, CST6, TPT1, and HSPB1, while miR-1246, miR-148a, miR21-5p, miR-451, and miR-92a represent the top highly abundant EV-coupled miRNAs released in response to HS. Pathway analysis of genes enriched in organoids exposed to thermal stress showed the enrichment of endocrine resistance, cellular senescence, and notch signaling pathways. Similarly, EV-coupled miRNAs released from thermally stressed organoids showed their potential regulation of genes involved in cellular senescence, p53 signaling, and TGF-beta signaling pathways.

Conclusions

In conclusion, the cellular and extracellular response of bovine oviductal organoids to in vitro HS conditions reveal the prospective impact of environmental HS on the physiology of the oviduct and the probable subsequent impacts on oocyte fertilization and early embryo development. Future studies elucidating the potential impact of HS-associated EVs from oviductal organoids on oocyte fertilization and preimplantation embryo development, would justify the use of an organoid model to optimally understand the oviduct-embryo communication under suboptimal environments.

2. Background

The mammalian oviduct comprises an advantageous microenvironment with biochemical and biophysical support to sustain the formation of life as the ‘site’ of fertilization and preimplantation embryo development [1]. Effective measures of communication are cohesively required from the embryo itself and the maternal environment to establish a periconceptional milieu to support conception and early embryonic development [2]. Tangible evidence exists demonstrating an unequivocal two-way signaling interaction at the embryo–maternal interface [3, 4], suggesting reciprocal crosstalk leading to a successful pregnancy provides a significant basis for physiological implantation [3,4,5]. Classically, cell–cell communications’ paramount role in regulating

physiological processes were commonly defined either via direct contact through membrane signaling (juxtracrine) or by secreting various molecules (growth factors, hormones, cytokines, metabolites, etc.) with ensuing signaling function (autocrine, paracrine, and endocrine). More recently, extracellular vesicles (EVs) which exist in almost all biological fluids, have been implicated as emerging bi-directional, putative messengers to nano-shuttle regulatory bioactive molecules (lipids, proteins, nucleic acids, etc.) with biologically plausible functions [6,7,8,9]. Irrespective of their origin, previous reports have shown that EVs released following external stress stimuli induce bystander tolerance in naïve cells treated with 'stressed EVs,' [10,11,12,13,14,15] indicating their potential to transfer 'protective' molecules (protectosomes).

The large-scale impacts of elevated ambient temperatures resulting from climate change on animal production and reproductive performance have been extensively studied [16, 17]. External heat acting on a homeothermic animal impede fertility, affecting the physiological and cellular function of several reproductive tissues [18, 19]. In vivo and in vitro studies have demonstrated the direct effects of heat stress (HS)-induced dysfunction through impairments to mammalian oocyte maturation, fertilization, and early embryo development [20,21,22,23]. However, the complexity to investigate the impact of HS in regard to oviduct physiology and the embryo-oviduct dialog in later stage embryos have been largely stunted due to its inaccessible location without surgery or necropsy post-slaughter. Therefore, novel approaches to recapitulate the in vivo physiology and function of the oviduct in vitro, would provide an innovative mechanism to validate the system's functional response to HS.

Despite the extensive work carried out to understand the effects of HS on reproductive function, its underlying impacts on oviduct physiology remain largely unknown. Initial attempts to study the embryo-oviduct dialogue via EVs from oviductal fluid [24] and monolayer-bovine

oviductal epithelial cell (BOEC) conditioned culture medium [25], demonstrated promising improvements in embryo quality and cryotolerance following their addition during embryo culture. Regardless of the beneficial roles of EVs, the potential transfer of identified embryotropic molecules eliciting such positive responses in embryo development was not studied. However, Almiñana and colleagues have shown major discrepancies in the protein cargo signatures from in vivo vs. in vitro derived EVs of oviductal origin, revealing that in vitro monolayer-BOECs inadequately mimic the in vivo oviductal environment, likely resulting from a lack of paracrine signaling amid reduced cellular diversity [26].

Organoids represent biomimetic, three-dimensional, in vitro cell clusters that organizationally self-regenerate into complex structures to mirror the physiological function of their tissue of origin [27]. Generally, organoid cell clusters are encapsulated within a jelly-like extracellular matrix and function similar to their native in vivo organ in terms of gene and protein expression, metabolic function and microscale tissue architecture [28]. Studies in humans [29] and mice [30, 31] have recently outlined advantages over existing traditional cell culture models through the establishment and long-term stability of fallopian tube organoids that faithfully recapitulate the phenotype of their in vivo tissue. Thus, in this study, we aimed to utilize bovine oviductal organoids to decrypt the oviducts' differential response to HS in terms of cellular transcriptome and secreted EV-miRNome, to elucidate the potential downstream impacts on fertilization and early embryo development. Furthermore, several studies have revealed the regulatory role of miRNA sequence motifs and their corresponding RNA binding proteins in EV-miRNA secretion versus cellular retention under specific environmental conditions [32,33,34,35,36]. Therefore, investigating the interplay between miRNA sequence motifs and RNA binding proteins in the packaging and release

of specific miRNAs into EVs by subjecting organoids to thermal stress, would shine light upon the molecular mechanisms behind the oviductal response to HS via EV-coupled miRNA signaling.

3. Results

The experimental design outlining the different groups of organoid cultures and EVs used in the RNA-seq analyses are summarized in Fig. 3.1.

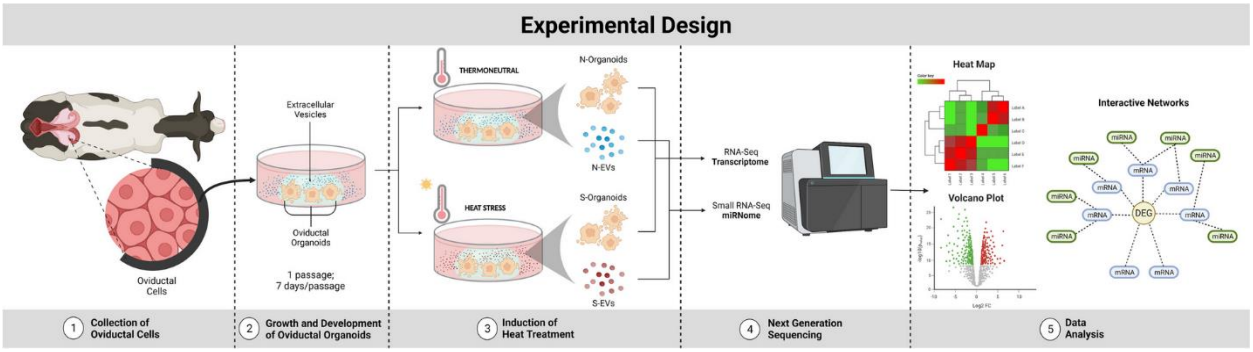


Figure 3.1. Schematic Illustration of the Experimental Design. Oviductal cells were collected from abattoir-derived reproductive material for the establishment of bovine oviductal organoids. Organoids were subsequently grown and developed under thermoneutral conditions for 14 days prior to exposing to heat treatment. Following HS exposure, organoid cells and the corresponding EVs were collected, isolated, and subjected to genome-wide transcriptomic and miRNomic profiling, respectively.

3.1 3-D matrix supports dynamic oviductal organoid culture and EV production

Oviductal organoids generated from bovine oviducts resected from diestrus reproductive tracts (n = 10) were grown for 14 days (one passage, 7 days per passage; Fig. 3.2A), prior to suspension in a xeno-free, synthetic matrix for experiments with HS. Representative histological and immunohistochemical (Fig. 3.2B) images of in tact oviduct and in vitro cultured oviductal organoids (P1D7) demonstrate the architectural morphology (hematoxylin and eosin; H&E) and presence of oviduct-specific glycoprotein 1 (OVPG1), zonula occludens-1 (ZO1), and forkhead box J1 (FOXJ1), respectively. H&E staining showed that crosssections of oviductal organoids contain a monolayer of oviductal epithelial cells encircling a centralized lumen. Also, mature organoids maintained through extended culture persistently express hallmark protein OVGP1, as

well as epithelial cell tight junctions (ZO1), and ciliated cells (FOXJ1). Comprehensively, the organoid cellular morphology contain both partially differentiated and polarized cuboidal cells, as well as columnar shaped cells, which precisely represent the established structure of functional organoids. Additionally, we used a gene panel to functionally characterize the expression patterns of in vitro produced oviductal organoids (37 °C and 42 °C) compared to naïve in vivo BOECs. The panel was comprised of cell proliferation and adhesion (MKI67 and CDH1), ciliated cell function and differentiation (LRRC6, TUBA1A, TUBA1B and TUBA1C), and hormonal prostaglandin function (PTGS2, PTGES and OXTR) gene expression signatures. Overall, minimal statistical differences presided between in vitro produced organoids and in vivo derived cells, strengthening the biomimicry of extended culture in a 3-D matrix (Fig. 3.3). In addition, a dual-targeted approach to isolate EVs using ultracentrifugation and size exclusion chromatography (SEC) was employed to isolate a relatively homogenous population of oviductal organoid-derived EVs. The molecular and morphological characterization of oviductal organoid-derived EVs validated the integrity of our procedure to isolate molecular analysis grade EVs from conditioned culture medium of in vitro-cultured bovine oviductal organoids. Representative TEM images (Fig. 3.4A), indicate the presence of membrane-enveloped vesicles released from oviductal organoids. Moreover, nanoparticle tracking analysis revealed a higher particle concentration in the S-EVs (derived from organoids cultured at 42 °C; 1.29E + 10 particles/mL), when compared to the N-EVs (derived from organoids cultured at 37 °C; 1.01E + 10 particles/mL), with median sizes of 120.01 and 133.99 nm, respectively (Fig. 3.4B). Western blot analysis (Fig. 3.4C) indicated the presence of EV marker proteins (TSG101, FLOT1, and CD63) in the EV samples derived from oviductal organoids, while CYCS, a cellular contaminant and negative marker of EVs, was absent. In addition, RNA quality control for integrity, prior to RNA sequencing, revealed the presence of

18S and 28S ribosomal RNA peaks in the oviductal organoid RNA and their absence in oviductal organoid-derived EV-RNA samples (Fig. 3.4D & E).

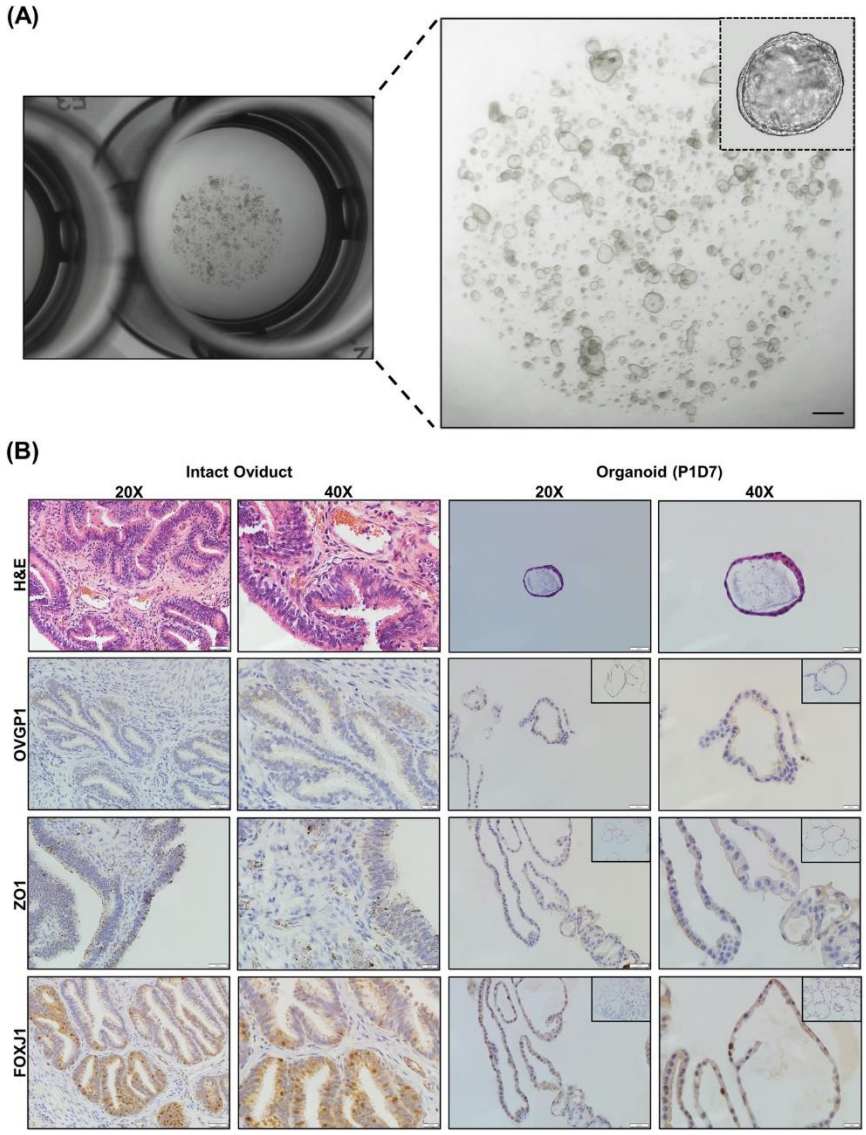


Figure 3.2. Establishment of Oviductal Organoid Culture System. Representative morphology of cultured bovine oviductal organoids after 14 days in culture. Scale bar, 1 mm (A). Immunostaining of in vitro cultured bovine oviductal organoids at passage 1, day 7 (P1D7). Histological oviductal samples with H&E staining, and immunohistochemical (OVGP1, ZO1, and FOXJ1) at 20 × and 40 × magnification, respectively. Scale bar = 50 μm at 20 × magnification and 20 μm at 40 × magnification. Controls shown in insets represent a negative reagent control (OVGP1, ZO1 and FOXJ1).

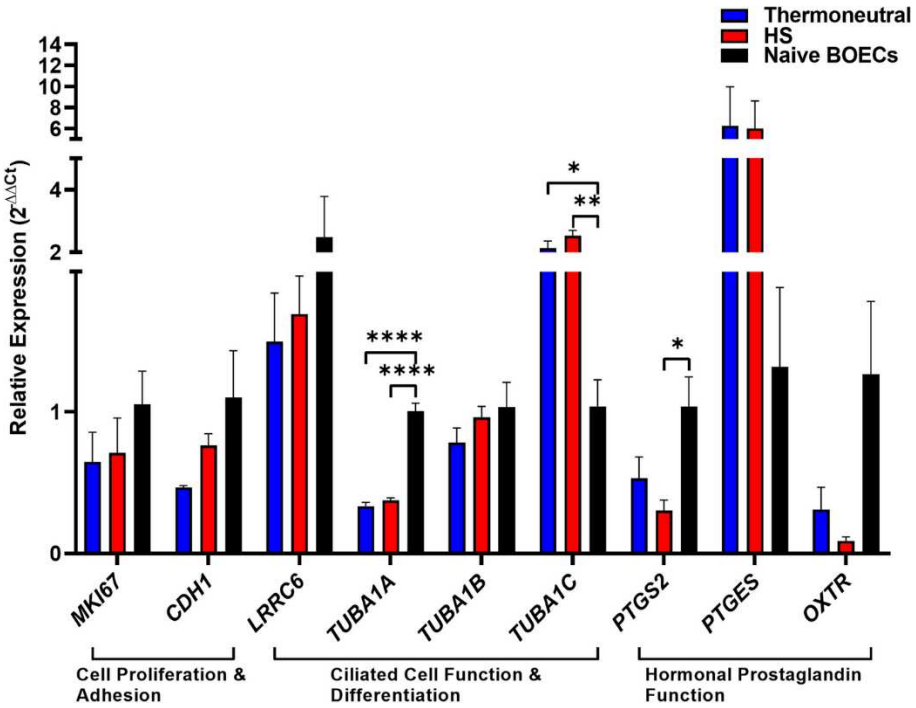


Figure 3.3. In vitro Produced Organoid Retention of the In vivo Oviduct. Quantitative real time PCR analysis of selected genes outlining the mRNA expression of markers for cell proliferation and adhesion, ciliated cell function and differentiation, and hormonal prostaglandin function in in vitro produced organoids (37 °C and 42 °C) and naïve bovine oviductal epithelial cells (BOEC). Data are shown as the mean ± SEM and the differences between means were analyzed using one-way ANOVA followed by Tukey's Multiple Comparisons Test in biologically independent samples (n = 3). Statistical significance (*) between groups were determined at ($p < 0.05$).

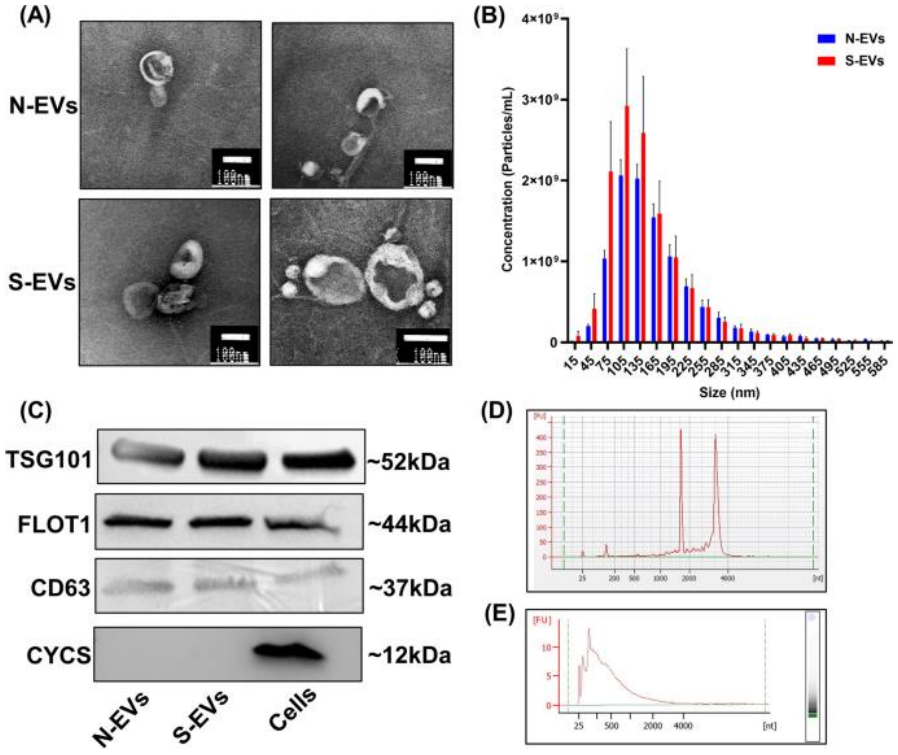


Figure 3.4. Characterization of Oviductal Organoid-derived EVs. Transmission Electron Microscopy (TEM) images depicting a clear bilipid enclosed complex in oviductal organoid-derived EVs. Scale bar, 100 nm (A). Size distribution and concentration of N-EVs (blue bars) and S-EVs (red bars) resulting from Nanoparticle Tracking Analysis (NTA) (B). Cropped blots for Western Blotting (WB) analysis in EVs shows traditionally expressed EV-associated protein markers (TSG101, FLOT1, CD63) and the absence of expression for non-EV, mitochondrial associated cellular marker protein (CYCS) in lanes indicated by N-EVs and S-EVs (C). Representative RNA quality control and size distribution from oviductal organoids (D) and the corresponding EVs indicating the absence of 18 s and 28 s cellular RNA components (E).

3.2 Decoding the transcriptome response of oviductal organoids to HS

To understand the changes in molecular physiology of the bovine oviduct under HS conditions, this study examines the first comprehensive transcriptome analysis revealing the cellular response of oviductal organoids to elevated thermal stress. A total of ten RNA libraries were prepared from the organoid cells cultured under HS (42 °C) and thermoneutral conditions (37 °C). Approximately 536 million raw reads were sequenced from both groups. After adapter trimming and quality filtering, approximately 53.6 million reads per library were retained with an average of 99% of the quality-controlled (QC) reads mapped to the bovine reference genome (ARS-UCD1.2). A summary of the total number of reads and the mapping results for each group is presented in Additional file 1: Table S1. Principal component analysis (PCA) and the accompanied hierarchical heatmap revealed that biological replicates for each group clustered together except for one replicate amid the HS groups (Fig. 3.5A & B), which has been excluded from further analysis. A stringent criterion was set to avoid bias for low expression in which, expressed genes represent zFPKM > -3 amongst all replicates. In total, 11,935 and 12,564 genes were detected in the HS and thermoneutral cultured organoid groups, respectively, with 11,725 genes mutually expressed in both groups (Fig. 3.5C). Of the most highly expressed genes in both groups, the top 20 genes most abundantly expressed amongst all organoid samples include: COX1, ACTB, CST6, TPT1, RPLP1, RPLP0, FTH1, COX2, EEF1A1, UBA52, RPS15 (Table 1).

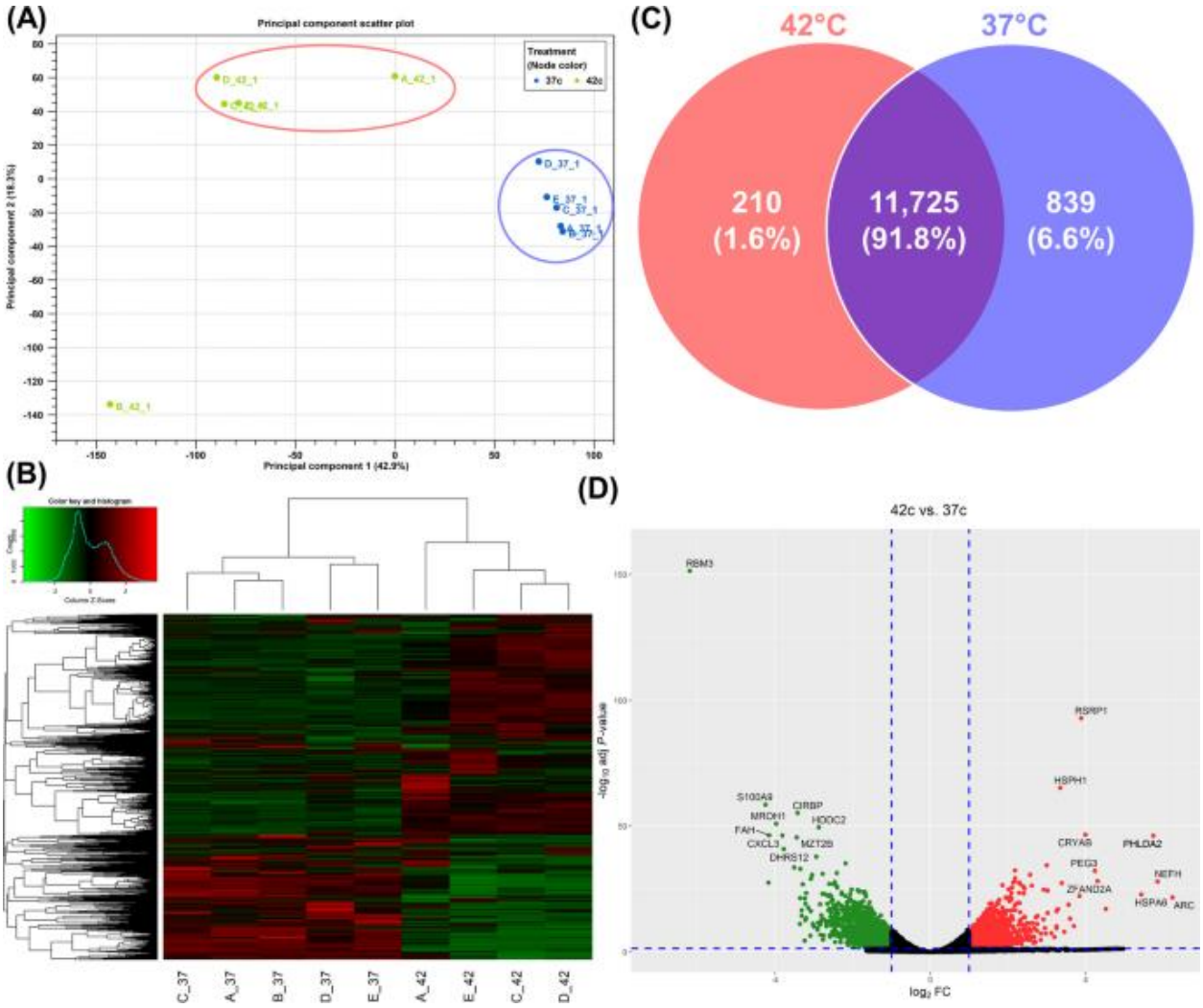


Figure 3.5. Impact of HS on Oviductal Organoids: Transcriptomic Cellular Response. Principal component analysis (PCA) (A) and heatmap/hierarchical clustering of oviductal organoid samples (B) cultured under HS (42 °C; A_42-D_42) or thermoneutral conditions (37 °C; A_37-D_37). Venn diagram indicating exclusively and commonly expressed genes in the 42 °C and 37 °C groups (C). Volcano plot displaying differentially expressed genes, up- and downregulated in oviductal organoids cultured under HS (42 °C) compared to those cultured under thermoneutral conditions (37 °C) (D).

Considering a false discovery rate (FDR) < 0.05 and a fold change (FC) ≥ 2, a total of 2,570 differentially expressed genes (DEGs) (1,222 up- and 1,348 downregulated) were identified in the oviductal organoids subjected to HS compared to the thermoneutral groups, including 170 genes with unknown function (Additional file 2: Table S2). The volcano plot (Fig. 3.5D) illustrates the distribution of DEGs, up- and downregulated, in the HS compared to the thermoneutral groups. The top 20 known DEGs (upregulated include: CRISPLD2, HSPA6, SERPINE1; downregulated

include: RBM3, MROH1, FAH) identified in the HS compared with the thermoneutral cultured groups are listed in Table 2. Gene ontology (GO) enrichment analysis of the upregulated genes in the HS groups revealed that endocrine resistance, cellular senescence, and notch signaling pathway to be the top significant pathways (Fig. 3.6A; Additional file 3A: Table S3A). Alternatively, metabolic pathways, oxidative phosphorylation, nucleotide metabolism, carbon metabolism, and thermogenesis were the top significant pathways dominated by the downregulated genes (Fig. 3.6B; Additional file 3B: Table S3B). Biological processes in which genes upregulated in thermally stressed organoids involve cell migration, transcription regulation, and protein phosphorylation (Fig. 3.6C; Additional file 4A: Table S4A), while cholesterol biosynthetic processes, mitochondrial electron transport and ATP synthesis were the processes in which involve downregulated genes (Fig. 3.6D; Additional file 4B: Table S4B). Interaction networks of DEGs commonly involved in highly enriched pathways are presented in Fig. 3.6E. The highlighted genes amid the interaction networks are involved in various signaling pathways, gene expression regulation, and functions regulating cellular senescence and pregnancy homeostasis.

Table 1 Top 20 expressed genes in oviductal organoids from the HS (42 °C) and thermoneutral (37 °C) groups

Genes	42 °C Group TPM	%[a]	Genes	37 °C Group TPM	%[a]
COX1	12,134.48	10.36	*COX1*	18,703.53	14.63
ACTB	9851.64	8.41	*COX3*	12,044.18	9.42
CST6	7866.93	6.71	*COX2*	9073.11	7.10
TPT1	6996.46	5.97	*FTH1*	8633.91	6.76
HSPB1	6814.69	5.82	*RPLP1*	6970.11	5.45
RPLP1	6408.56	5.47	*GAPDH*	6133.64	4.80
RPLP0	6155.16	5.25	*RPLP0*	5702.06	4.46
CLU	5635.77	4.81	*ATP6*	5258.80	4.11
CRYAB	5519.48	4.71	*KRT19*	5247.57	4.11
FTL	5403.90	4.61	*FTL*	5217.36	4.08
ACTG1	5399.25	4.61	*TPT1*	5153.81	4.03
COX3	5017.02	4.28	*ACTB*	4863.59	3.81
FTH1	5004.65	4.27	*ACTG1*	4709.11	3.68
COX2	4958.39	4.23	*EEF1A1*	4561.17	3.57
EEF1A1	4524.72	3.86	*RPS15*	4490.25	3.51
UBA52	4411.87	3.77	*CST6*	4456.38	3.49
HSPA1A	4367.03	3.73	*ND3*	4434.30	3.47
ANXA2	3736.05	3.19	*ND1*	4104.32	3.21
HSPA8	3531.16	3.01	*MSLN*	4025.36	3.15
RPS15	3418.48	2.92	*UBA52*	4018.46	3.14

TPM average Transcript Per Million mapped reads

[a] Percentage of the genes sequence reads

Table 2 Top 20 DEGs in HS (42 °C) oviductal organoids compared to the thermoneutral (37 °C) groups

Upregulated Genes	FC	FDR	Downregulated Genes	FC	FDR
RAB39A	85.71	3.56E-03	*MFAP4*	-14.38	3.37E-11
ARC	75.04	1.91E-22	*PPP1R32*	-15.65	1.65E-09
CRISPLD2	64.85	1.25E-32	*MROH1*	-15.68	1.10E-51
NEFH	57.56	9.69E-29	*ACSM1*	-17.54	8.85E-19
PHLDA2	53.28	6.75E-47	*FAH*	-17.80	4.22E-47
ENSBTAG00000001219	52.94	1.64E-08	*RHBDD3*	-18.01	2.75E-28
HSPA6	42.95	1.46E-23	*NOS2*	-18.02	1.52E-19
ENSBTAG00000052847	36.38	1.28E-07	*S100A9*	-18.97	2.65E-59
PURG	31.95	3.79E-09	*ASB9*	-19.67	1.96E-11
FAM71F1	26.14	2.53E-08	*HERC3*	-19.85	6.46E-60
NPB	22.86	8.62E-18	*DIRAS3*	-21.65	3.80E-10
GAS2	20.03	9.82E-10	*HNMT*	-22.45	2.36E-10
ZFAND2A	19.72	6.73E-29	*ETNPPL*	-24.09	5.00E-10
PEG3	18.76	5.88E-33	*SERPINB13*	-32.57	9.11E-15
CRYAB	15.90	2.22E-47	*ENSBTAG00000003661*	-32.99	1.55E-20
ENSBTAG00000049003	14.77	2.45E-16	*CSF3*	-34.72	2.48E-17
RSRP1	14.73	1.16E-93	*LRCOL1*	-36.95	1.50E-05
SERPINE1	14.29	5.61E-23	*DAPL1*	-60.38	1.61E-08
ENSBTAG00000050861	12.67	2.26E-06	*RBM3*	-73.40	3.10E-152
TEX49	12.64	9.61E-08	*SERPINE3*	-163.84	1.87E-63

FC Fold Change, *FDR* False Discovery Rate

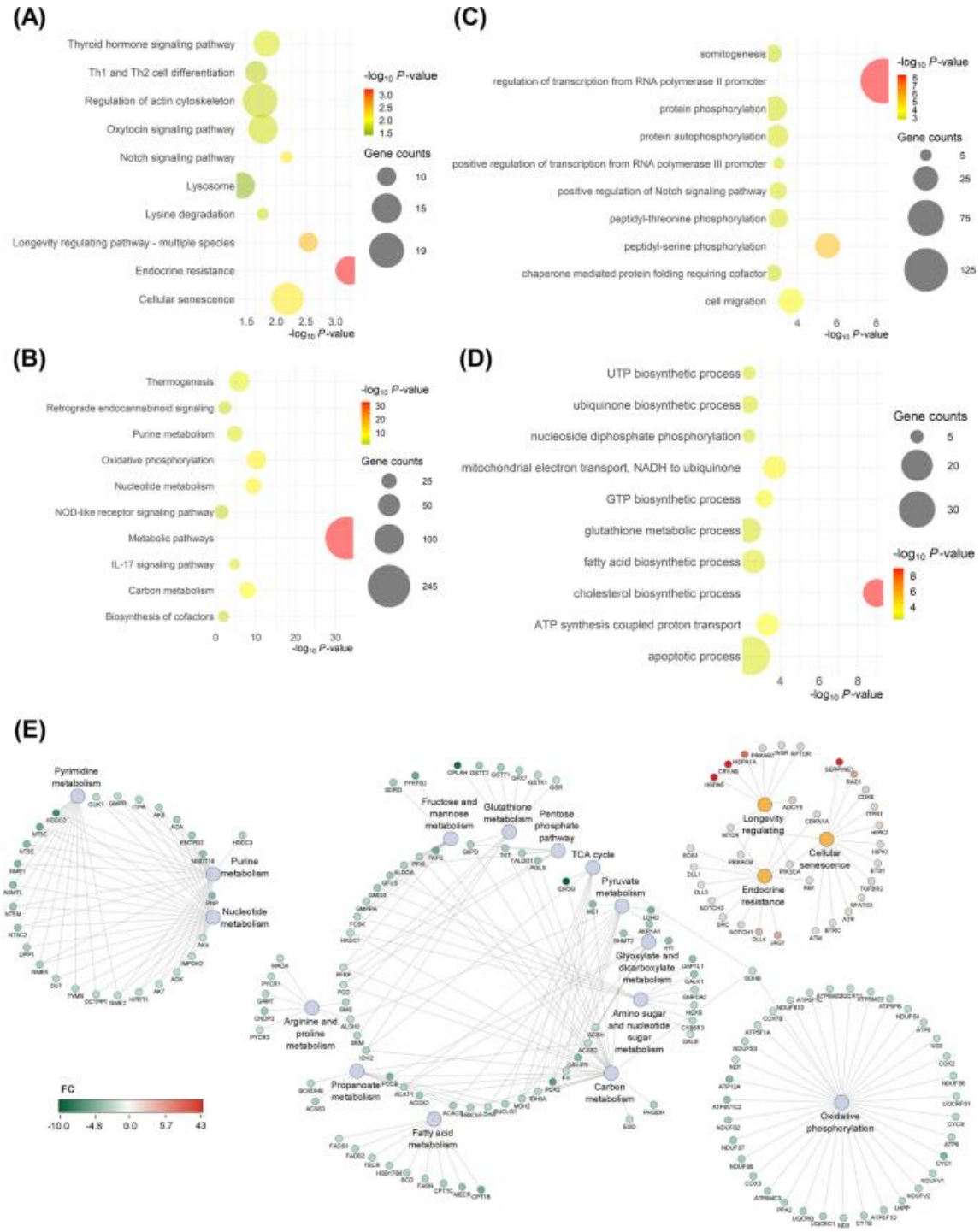


Figure 3.6. Oviductal Organoids: Ontological Classification and Interactive Networking. Bubble plots, revealing the top 10 pathways and biological processes targeted by the up- (A and C) and downregulated genes (B and D) in the 42 °C compared to the 37 °C groups, respectively. The color and size of each bubble represent the P-value and number of gene counts. Interactive networking of the differentially expressed genes commonly involved in highly enriched pathways including the up- (red) and downregulated (green) genes in the 42 °C compared to the 37 °C groups (E).

3.3 HS alters oviductal organoid-derived EV-coupled miRNAs

To understand the extracellular response of oviductal organoids to HS, organoid-secreted EVs were investigated for their miRNA content using small RNA sequencing technology. Three small RNA libraries were prepared from the EVs derived from each of the organoid cultures under 37 °C and 42 °C. Approximately 135 million raw reads were sequenced from both EV groups. After adapter trimming and quality control, an average of 21 million reads per library was retained. An average of 87% and 89% of these reads from the HS and thermoneutral EV groups, respectively, were mapped to the bovine reference genome (Additional file 5: Table S5). Based on the miRNA expression patterns, the PCA (Fig. 3.7A) and hierarchical heatmap (Fig. 3.7B) exhibited a clear clustering of the replicates from each group. Sequencing data analysis revealed a total of 251 known miRNAs amongst both groups with at least 10 counts per million (CPM) (Fig. 3.7C). While a complete list of all the expressed miRNAs detected is presented in Additional file 6: Table S6, a list of the top 20 expressed miRNAs from each group are presented in Table 3. Among the top 20 expressed miRNAs, 15 were commonly detected amongst both groups.

Differential expression analysis of EV-miRNAs released from oviductal organoids subjected to divergent ambient temperatures indicated a total of 18 miRNAs as significantly-differentially expressed between the two groups ($FC > 2$, $FDR < 0.05$). EVs from HS oviductal organoids exhibited the enrichment of 12 miRNAs (including: miR-150, miR-92a, miR-223, and miR-202) and 6 downregulated miRNAs (including: miR-221, miR-11980, miR-23a and miR-370) compared to the EVs released from thermoneutral cultured organoids (Table 4 and Fig. 3.7D). Interestingly, two differentially expressed (DE)-miRNAs (miR-10b and miR-92a) were also noted in the top 20 expressed miRNAs list. Pathway analysis revealed that genes potentially targeted by the upregulated EV-miRNAs were involved in cellular senescence, p53, and TGF-beta signaling

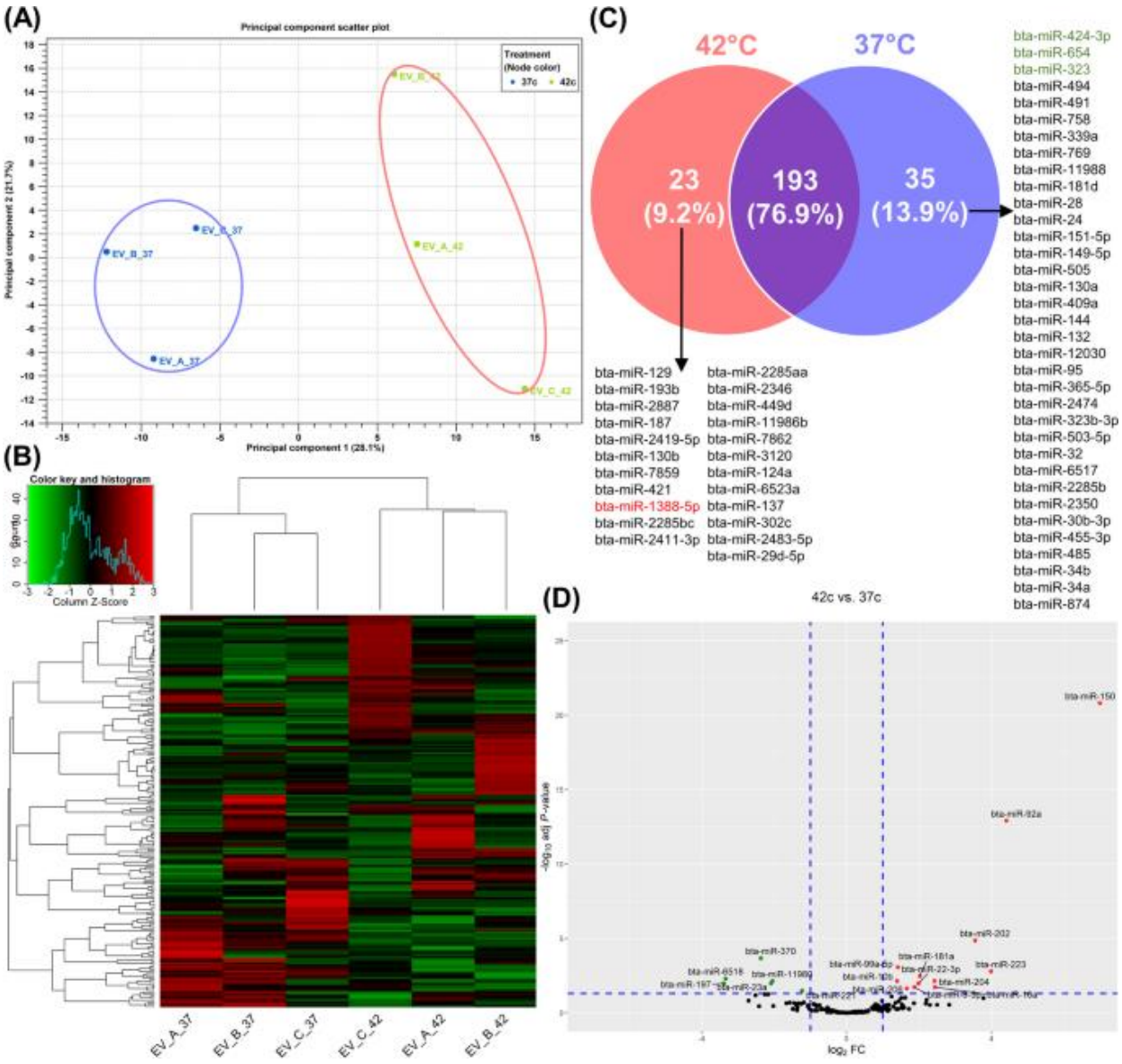


Figure 3.7. HS Alters Oviductal Organoid-derived EVs Molecular Cargo: miRNome Extracellular Response. Principal component analysis (PCA) (A) and heatmap/hierarchical clustering of oviductal organoid-derived EVs (B). Venn diagram indicating exclusively and commonly expressed miRNAs in the 42 °C and 37 °C groups (C), red and green miRNAs are significantly different (FDR < 0.05) between the two groups. Volcano plot displaying differentially expressed miRNAs, up- (red) and downregulated (green) in oviductal organoid-derived EVs from the 42 °C compared to 37 °C groups (D)

pathways (Fig. 3.8A; Additional file 7A: Table S7A), while those potentially targeted by the downregulated EV-miRNAs were involved in MAPK and FoxO signaling pathways (Fig. 3.8B; Additional file 7B: Table S7B). Transcription and cell cycle regulation were among the top

abundant biological processes targeted by the upregulated miRNAs (Fig. 3.8C; Additional file 8A: Table S8A), while protein phosphorylation and regulation of cell cycle and proliferation were among the top biological processes targeted by the downregulated miRNAs in the HS compared to the thermoneutral groups (Fig. 3.8D; Additional file 8B: Table S8B). Interaction networks between common experimentally validated target genes of the DE-EV-miRNAs and the organoids DEGs, are presented in Fig. 3.9A. Additionally, a focus on the DEGs involved in the cellular senescence pathway network and the DE-EV-miRNAs potentially targeting their function are represented in Fig. 3.9B.

Table 3 Top 20 expressed miRNAs in oviductal organoid-derived EVs from the HS (42 °C) and thermoneutral (37 °C) groups

miRNA	42 °C Group CPM	%[a]	miRNA	37 °C Group CPM	%[a]
bta-miR-1246	714,796.52	52.39	bta-miR-1246	363,004.63	44.35
bta-miR-148a	91,700.77	6.72	bta-miR-148a	63,584.52	7.77
bta-miR-21-5p	66,565.11	4.88	bta-miR-21-5p	43,902.13	5.36
bta-miR-451	63,787.82	4.68	bta-let-7a-5p	38,199.05	4.67
bta-miR-92a	52,778.22	3.87	bta-miR-378	33,327.83	4.07
bta-miR-122	39,526.19	2.90	bta-miR-451	26,116.20	3.19
bta-let-7a-5p	35,926.19	2.63	bta-let-7i	22,986.77	2.81
bta-let-7i	25,351.78	1.86	bta-let-7f	20,881.75	2.55
bta-miR-378	23,826.87	1.75	bta-miR-122	19,106.09	2.33
bta-let-7f	19,848.71	1.45	bta-let-7b	17,898.58	2.19
bta-miR-26a	19,314.54	1.42	bta-miR-26a	16,336.63	2.00
bta-let-7b	17,836.14	1.31	bta-miR-151-3p	10,162.43	1.24
bta-miR-10b	12,289.04	0.90	bta-miR-200b	8044.04	0.98
bta-miR-151-3p	12,105.22	0.89	bta-miR-320a	6426.09	0.79
bta-miR-99a-5p	10,290.88	0.75	bta-miR-200c	5618.62	0.69
bta-miR-200b	9131.74	0.67	bta-let-7 g	5587.82	0.68
bta-miR-10a	7387.11	0.54	bta-miR-100	5124.45	0.63
bta-miR-143	6627.53	0.49	bta-miR-30d	5002.99	0.61
bta-miR-30d	6243.01	0.46	bta-miR-10b	4666.79	0.57
bta-miR-486	6147.07	0.45	bta-miR-192	4474.81	0.55

CPM average Counts Per Million mapped reads

[a] Percentage of the miRNA sequence reads

Table 4 DE-miRNAs in oviductal organoid-derived EVs from the HS (42 °C) compared to the thermoneutral (37 °C) groups

Upregulated miRNA	FC	FDR	*FC* Fold Change, *FDR* False Discovery Rate Downregulated miRNA	FC	FDR
bta-miR-150	127.29	1.56E-21	bta-miR-221	-2.35	3.27E-02
bta-miR-92a	21.28	1.24E-13	bta-miR-11980	-4.13	7.36E-03
bta-miR-223	15.82	1.61E-03	bta-miR-23a	-4.26	1.04E-02
bta-miR-202	11.69	1.38E-05	bta-miR-370	-5.17	2.14E-04
bta-miR-16a	5.42	1.89E-02	bta-miR-6518	-10.17	5.05E-03
bta-miR-204	5.36	7.36E-03	bta-miR-197	-10.51	1.04E-02
bta-miR-181a	4.06	3.43E-03			
bta-miR-22-3p	3.96	1.04E-02			
bta-miR-9-5p	3.65	1.89E-02			
bta-miR-206	3.16	2.27E-02			
bta-miR-99a-5p	2.66	8.58E-04			
bta-miR-10b	2.62	7.36E-03			

FC Fold Change, *FDR* False Discovery Rate

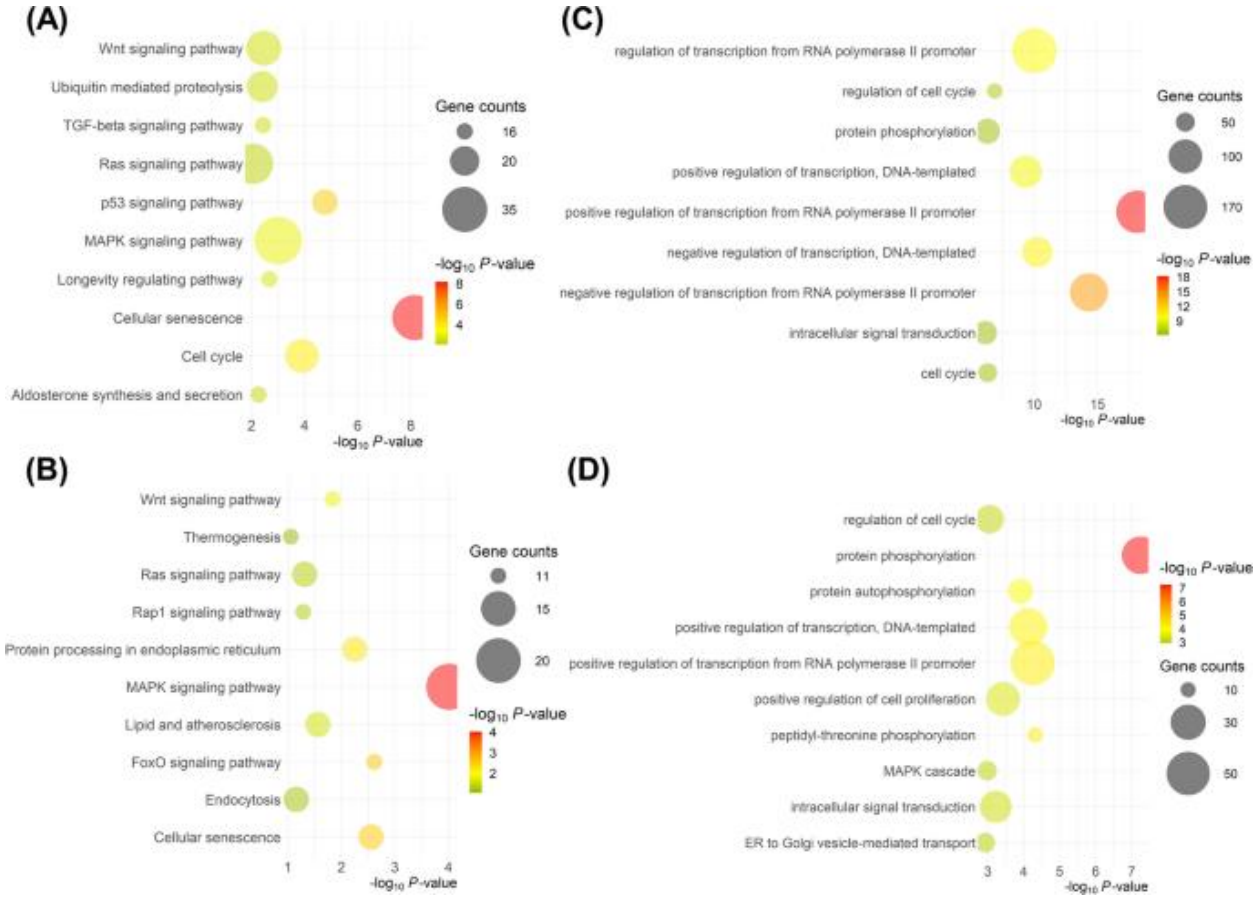


Figure 3.8. Oviductal Organoid-derived EV-miRNAs: Ontological Classification. Bubble plots, revealing the top 10 pathways and biological processes targeted by the up- (A and C) and downregulated miRNAs (B and D), respectively in the 42 °C compared to the 37 °C groups. The color and size of each bubble represent the P-value and number of miRNA target genes, respectively.

3.4 Quantitative real-time PCR validation of candidate genes and miRNAs

To validate the sequencing data, 10 DE-genes (5 up- and 5 downregulated in the HS compared to the thermoneutral groups) and 4 upregulated miRNAs were selected for validation in 4 independent, biological replicates using quantitative real-time PCR. Selected candidate genes in oviductal organoids (Fig. 3.10A) and miRNAs in oviductal organoid-secreted EVs (Fig. 3.10B) show the same expression pattern consistent with the RNA-seq data.

3.5 MicroRNA sequence motif and RBP identification

To investigate the potential mechanism of miRNA sorting and packaging into EVs by oviductal organoids in response to thermal stress, miRNA sequence motif analysis was performed for the

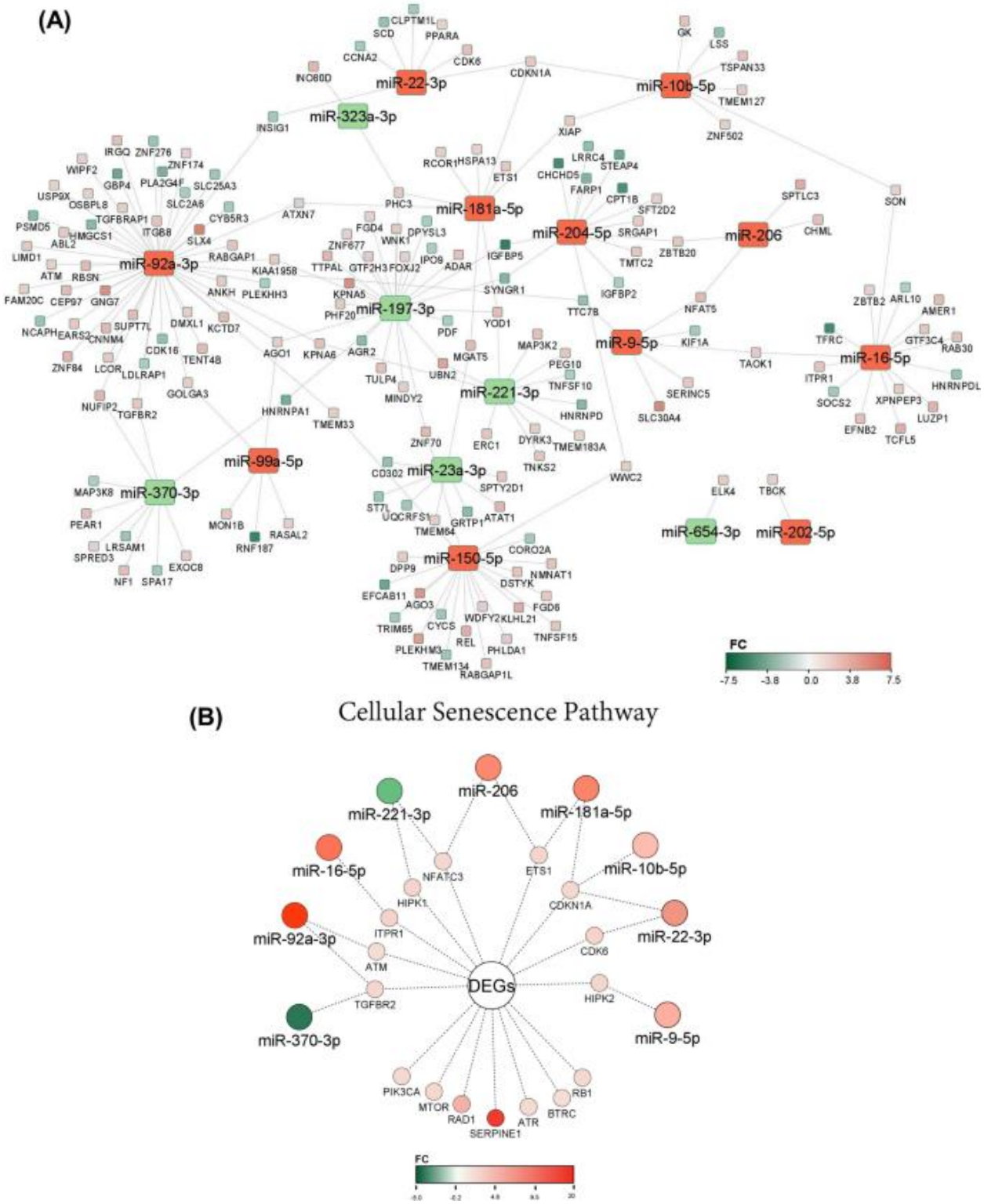


Figure 3.9. Oviductal Organoid DE-EV-miRNAs and DEGs Interaction Network. Interactive networking of common experimentally validated target genes of the DE-EV-miRNAs and the organoids DEGs in the 42 °C compared to the 37 °C groups (A). A network of the DEGs involved in the cellular senescence pathway and targeted by the DE-EV-miRNAs (B).

miRNAs significantly enriched in EVs released in response to thermal stress using low abundant miRNAs (enriched in EVs released from organoids cultured under thermoneutral conditions) as controls. Accordingly, we have identified two miRNA motifs [U/A][C/U][C/A][U/G/A/C]A and [C/U][U/A]GU to be shared by 69% (9 of the 13) and 62% (8 out of 13) of the upregulated miRNAs, respectively (Fig. 3.11A). Moreover, an additional two motifs UG[U/A][A/G] and ACCC were identified and shared by 46% (6 of the 13) and 23% (3 out of 13) of the upregulated miRNAs, respectively. The sequence position and distribution of the identified motifs among the candidate miRNAs is indicated in Table 5 and Fig. 3.11B, respectively. Submission of the initial two significantly conserved motifs to the TOMTOM RBP identification tool showed that sequence motif ([U/A][C/U][C/A][U/G/A/C]A) is potentially targeted and bound by the RNA binding motif 6 (RBM6) protein (Fig. 3.11C), while sequence motif ([C/U][U/A]GU) is potentially targeted and bound by human antigen R (HuR) and zinc finger CysCysCysHis domain-containing protein 14 (ZC3H14) proteins (Fig. 3.11D).

4. Discussion

Oviductal fluid containing EVs have been identified as a major component safeguarding gametes from environmental stress [37, 38] and is regarded as the optimal milieu in which its composition reflects oviductal physiology [39]. Recent efforts have aimed to study the effects of HS on the oviduct both in vivo [40] and in vitro [41] through BOECs and EVs known to largely contribute and responsibly impact the composition of the oviductal fluid. In vivo, alterations in oviductal cells' gene expression and EV concentrations have been reported, while similar significant alterations in HSP70 and OVGP1 expression were reported in vitro. OVGP1 is a hormonally-regulated, carbohydrate-rich and traditionally-expressed protein-coding gene known to regulate receptivity and trophoblast adhesion. Alimiñana et al. [26], investigated the differential

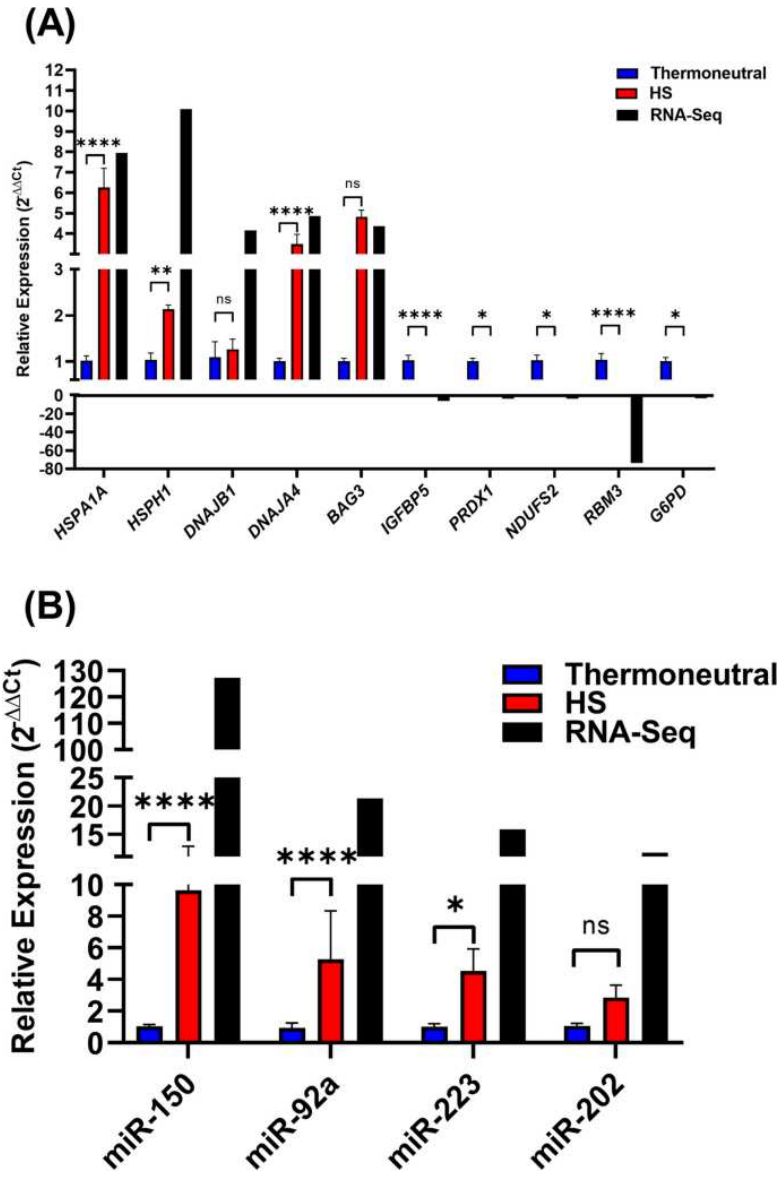


Figure 3.10. Quantitative Real Time PCR Validation. Expression validation of the selected DE-genes (A) and -miRNAs (B) compared against values calculated via RNA-seq analysis. Data are shown as the mean ± SEM and the differences between means were analyzed using one-way ANOVA followed by Tukey's Multiple Comparisons Test in biologically independent samples (n = 4). Statistical significance (*) between the 42 °C compared to the 37 °C groups were determined at ($p < 0.05$)

protein contents in BOECs and oviduct-derived EVs from in vivo and in vitro origin and revealed the absence of OVGP1 in in vitro cultured BOECs and corresponding EVs. Alternatively, in the present study oviductal organoids morphologically mirror their original tissue by forming round, cystic structures accompanied with an apical polarity in regard to a central lumen exhibiting

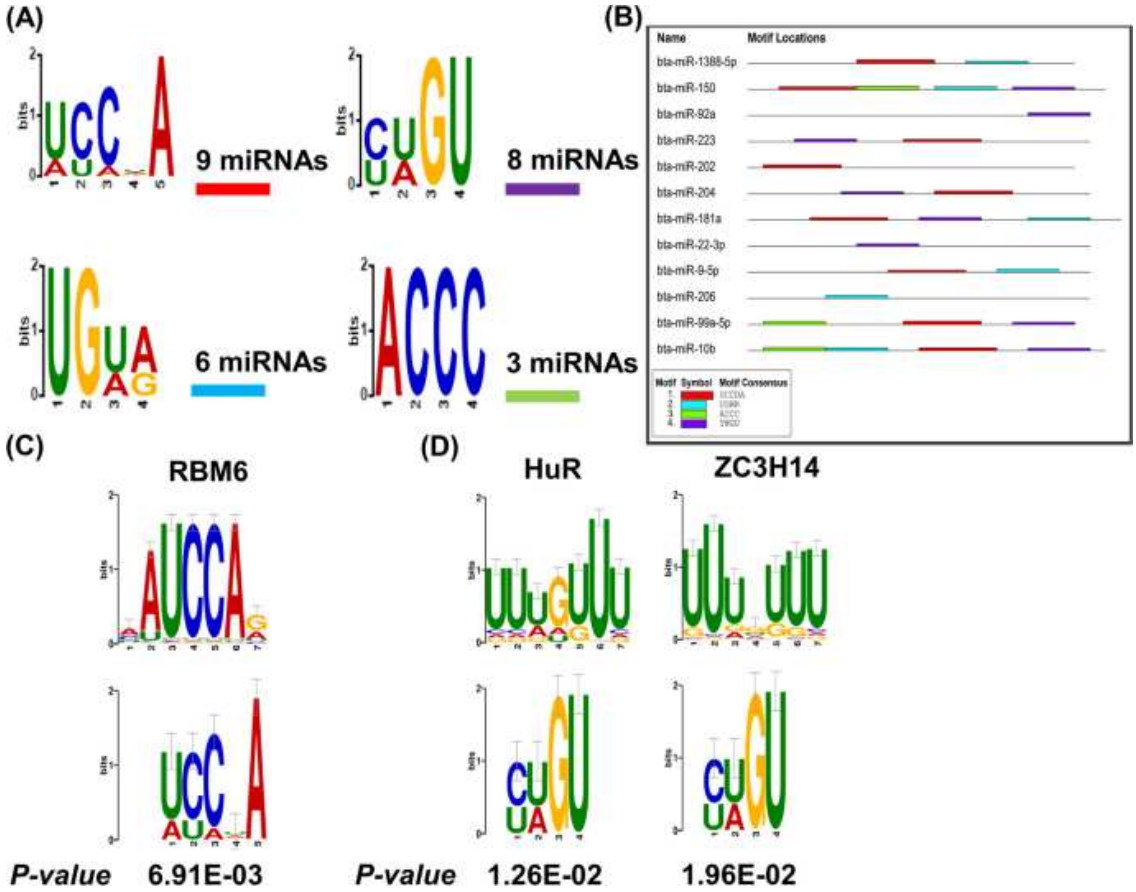


Figure 3.11. miRNA sequence motif analysis. Four identified, over-represented miRNA sequence motifs located amongst the upregulated miRNAs in differing numbers in the 42 °C compared to the 37 °C groups (A). Table depicting the location and distribution of the over-represented miRNA sequence motifs positioning on the upregulated miRNAs (B). Alignments of the ([U/A][C/U][C/A][U/G/A/C]A(C) and the [C/U][U/A]GU (D) miRNA sequence motifs with known RNA-binding proteins. ($p < 0.05$).

Table 5 Identified motif positioning on the upregulated miRNAs in the HS (42 °C) compared to the thermoneutral (37 °C) groups

miRNA	*p*-value		miRNA	*p*-value	
bta-miR-1388-5p	8.73E-04	AGGACUGUCCAACCUGAGAAU	bta-miR-181a	5.59E-03	AACAUUCAACGCUGUCGGUGAGUU
bta-miR-99a-5p	1.70E-03	AACCCGUAGAUCCGAUCUUGU	bta-miR-92a	5.59E-03	UAUUGCACUUGUCCCGGCCUGU
bta-miR-204	3.06E-03	UUCCCUUUGUCAUCCUAUGCCU	bta-miR-22-3p	9.20E-03	AGUUCUUCAGUGGCAAGCUUUA
bta-miR-202	3.06E-03	UUCCUAUGCAUAUACUUCUUU	bta-miR-223	9.20E-03	UGUCAGUUUGUCAAAUACCCCA
bta-miR-10b	5.07E-03	UACCCUGUAGAACCGAAUUUGUG	bta-miR-150	9.20E-03	UCUCCCAACCCUUGUACCAGUGU
bta-miR-150	5.07E-03	UCUCCCAACCCUUGUACCAGUGU	bta-miR-10b	1.75E-02	UACCCUGUAGAACCGAAUUUGUG
bta-miR-181a	7.23E-03	AACAUUCAACGCUGUCGGUGAGUU	bta-miR-99a-5p	1.75E-02	AACCCGUAGAUCCGAUCUUGU
bta-miR-223	1.19E-02	UGUCAGUUUGUCAAAUACCCCA	bta-miR-204	1.75E-02	UUCCCUUUGUCAUCCUAUGCCU
bta-miR-9-5p	1.88E-02	UCUUUGGUUAUCUAGCUGUAUG			

encircling microvilli, consistent with previous reports of fallopian/oviductal organoids in mice [30, 31] and humans [29]. Moreover, our study revealed the detection of OVGP1, ZO1, and FOXJ1 in in vitro cultured organoids after passaging, indicating the suitability of our 3-D extended culture model to persist naïve-like identity, vital for the interpretation of the results in regard to oviductal physiology. Similarly, our gene panel revealed minimal differences amid in vitro cultured organoids in the mRNA expression of genes regulating cell proliferation and adhesion (MKI67 and CDH1), ciliated cell function and differentiation (LRRC6, TUBA1A, TUBA1B and TUBA1C), and hormonal prostaglandin function (PTGS2, PTGES and OXTR) compared to naïve in vivo BOECs. Collectively, interspersed FOXJ1 + cells indicate ciliated cell presence, while stable MKI67 mRNA levels amid in vitro cultured oviductal organoids and naïve in vivo BOECs reveal their active proliferation capacity. Similar to our previous work in endometrial organoids [42], in the present study ZO1 was found to be localized in both the nucleus and the cytoplasm. Such findings have been previously reported in monlayer cultures and several cell lines, and is posed to be correlated to the stage of cell growth and inversely connected to the extent and/or maturity of intercellular contacts [43]. Our study dually noted a significant increase in the transcript abundance for TUBA1C, which was also shown to be upregulated in oviductal fluid collected from the contra- versus ipsilateral bovine oviduct [44]. Additionally, in in vitro cultured HS oviductal organoids, the mRNA expression of PTGS2 was signifncatly lower than in naïve in vivo BOECs, potentially indicating that the organoid cultures are not highly affected by in vitro ‘culture shock,’ which formally leads to an overproduction of reactive oxygen species (ROS) amidst cells [45], which has been shown in vivo [46] and in vitro [47] in regard to the oviduct. Additionally, in other studies the 3-D reproductive structures (organoids) have been shown to tolerably respond to exogenous hormonal stimuli [29, 48,49,50], a hallmark feature of mimicking

in vivo function. In support of this notion, it was previously shown that small RNA profiles from 3-D culture-derived EVs of cervical cancer HeLa cells also showed to exhibit striking similarity (~96%) to circulating EVs found in vivo [51]. In this study, we have demonstrated for the first time the potential of oviductal organoids to systematically study the physiological and dynamic response of the oviduct to seasonal heat stress.

HS-induced transcriptomic changes in oviductal organoids

High-throughput transcriptomic analysis of oviductal organoids cultured in vitro under thermoneutral and HS conditions revealed clear temperature-dependent clustering, indicative of a substantial physiological change governing oviductal organoids under HS conditions. In view of the oviduct and considering damaged cellular activity is prompted through HS (i.e. redox status and mitochondrial function, as well as protein folding), it is likely that the cellular response to the environment, acting as a dynamic machine, continuously diversifies and shifts an optimal milieu to a substandard microenvironment. These findings are in consonance with a recent in vivo study showing alterations in oviductal cells' (ipsilateral and contralateral) gene expression from dairy cows under HS conditions [40]. Notably in our study, we found that of the 12,774 expressed genes, 11,725 genes were mutually expressed amongst both groups. Importantly, in terms of oviductal organoids long-term maintenance of naive-like physiology, in the present study, the RNA-sequencing dataset validated the presence of marker genes for BOEC function (OVGP1, GPX4 and HMGCR) [52,53,54,55], which were stably expressed amid both groups of oviductal organoids following passaging during in vitro culture. Hence, the presented long-term 3-D organoid culture system functionally recapitulates certain validated aspects of the in vivo oviduct to satisfy novel descriptive studies, exemplified here, needed to address challenges in comprehending the early embryo–maternal interactions to conduct further functional studies.

Comparative analysis revealed, among the top highly abundant genes in both groups, we found genes related to early embryonic development (ACTB and UBA52), prostaglandin biosynthesis and the establishment/maintenance of pregnancy (COX1, COX2 and CST6), as well as embryonic cellular senescence (RPLP1 and RPS15). Uniquely, COX1 is found to be upregulated as the transient embryo is present within the oviduct, suggesting synthesized prostaglandins interact with the embryo and facilitate embryo–maternal communication [56]. However, HS has been shown to largely disrupt the balance of vaginal prostaglandins (PGE2 and PGF2a), reducing oviductal smooth muscle motility, which is an important catalyst for the transportation of the gamete/embryo [57]. Correspondingly, in high abundance, were genes encoding functions in the sperm-oviduct interactions preceding early embryo development (HSPA8 and HSPA1A), as well as genes reported to exert cryoprotective and anti-apoptotic effects as a consequence of stress (HSPB1). It is widely known that environmental cellular stress is directly connected to an immediate rapid induction of various heat shock proteins (HSPs). Convincing reports suggest HSPs (especially HSPA1 and HSPB1), cohesively act as protective proteins through potentially downregulating signaling events leading to apoptosis [58]. Although, HSPs act as molecular chaperones critical for the maintenance of cellular homeostasis, increased amounts of HSPs can facilitate the suppression of overexpressed/mutated genes resulting from a loss of p53 function [59].

Upregulated genes (CRISPLD2, HSPA6, SERPINE1) in the thermal stressed groups could serve as potential indicators of the response of oviductal organoids to environmental heat stress. Higher expression of CRISPLD2, a secreted glycoprotein and target gene regulated by the P4-PR response, has been shown to potentially mediate the stromal-epithelial cross-talk during implantation and decidualization, largely dependent upon hormonal regulation [60]. Similarly, the

HSP family member, HSPA6, shown to be involved in cellular response to stress, has been reported to be highly expressed in the ipsilateral oviduct likely in preparation for the presence of gametes and to facilitate embryo development [44]. Notably in our study, SERPINE1, which encodes a proteinase inhibitor, is shown to be involved in functional pathways governing cellular senescence. Cellular senescence contributes to the age-related decline in reproductive function and is known as a cellular response to stress aimed at inhibiting the proliferation of damaged cells, ultimately leading to a state of permanent growth arrest [61, 62]. Additionally, reports using SERINE1 protease inhibitors to suppress oviductal protease activity through mediating the estrogen-epithelial ERa signaling, have been shown to be preeminent for fertilization and preimplantation embryo development [63].

In mammalian reproduction, it is widely known that mitochondria are inherited maternally and serve as energy factories, synthesizing the majority of the cells' ATP predominantly through oxidative phosphorylation, in part, holding pertinent roles in metabolic functions governing embryonic development [64]. Results from the current study revealed the suppression of 1,348 genes in oviductal organoids following exposure to thermal stress, found to be involved in pathways related to oxidative phosphorylation and metabolic processes. Among the genes downregulated in oviductal organoids as a result of exposure to HS, NDUFS8, NDUFS7, NDUFS6, NDUFS3, NDUFS2, COQ9, NDUFV2, ND3, NDUFV1, ND2 and ATP5F1A, ATP5PB, ATP8, ATP6, ATP5MC2, ATP5MC3, ATP5F1C, ATP5F1D, ATP5MC1 are found to be involved in biological processes associated with mitochondrial function and ATP synthesis. Previous reports indicate that NADPH, supplies an antioxidant defense, while NADH promotes an increase in the oxidant load, generating ROS and sustained oxidative stress [65]. Therefore, genes suppressing the metabolic activity of high-functioning pathways (TCA cycle, pyruvate metabolism, fatty acid

metabolism, etc.), promote an imbalance in mitochondrial NADH and NADPH, effecting ATP production, which leads to impairments in mitochondrial function, partly due to suppressed oxidative phosphorylation function. Interestingly, highly downregulated (FC = -73.4) RBM3, a stress-responsive gene, was shown to potentially have a mechanistic function to counteract the regulatory role of miRNAs by increasing inefficiencies in global protein synthesis under conditions of stress [66]. On the other hand, in agreeance with Stamperna and colleagues, our study concurred among the DEGs, the downregulation of LOC512548 and HP (contralateral), as well as SOCS3 (ipsilateral) in oviductal epithelial cells from dairy cows during the summer versus spring season [40]. Antileukoproteinase's (LOC512548) role in inhibiting serine proteases, have been found to have antibiotic and anti-inflammatory functions in the human endometrium [67], as well as a coincidental function amidst the sperm-oocyte interaction in the human oviduct [68]. Taken together, our results demonstrate that the potential impact of seasonal heat stress on oviductal physiology is mediated by the dysregulation of genes responsible for mitochondrial function and energy metabolism, as well as reproductive and immune system responses.

Oviductal organoid-derived EV-miRNA profiles in response to HS

Previous studies from our lab demonstrated the divergent EV-mediated molecular response of bovine granulosa cells to HS through their encapsulated miRNA cargoes, revealing their subsequent protective capacity against recurrent HS following co-incubation among naïve granulosa cells [14], as well as oocytes and embryos [15]. Similarly, in the present study, we detected a total of 251 EV-coupled miRNAs with 193 mutually expressed and 3 miRNAs (bta-miR-1246, bta-miR-148a, bta-miR-21-5p) sequentially expressed as the first, second and third most abundant among both groups. In vitro functional analysis in a previously reported study demonstrated the antiapoptotic measures of bta-miR-1246 by targeting PCBP2 and CREBL2 in

HEK293 cells [69]. In accordance with others [70, 71], our study revealed a high prevalence of bta-miR-148a, which is found to target DNMT1 and improve the developmental capacity of porcine somatic cell nuclear transfer embryos [72]. Furthermore, studies in mice showed that miR-21 targets PTEN [73], leading to the hypothesis that bta-miR-21-5p activity may activate AKT and ERK1/2 signaling pathways in the bovine corpus luteum to promote angiogenesis [74].

Specialized miRNAs packaged into EVs (23 exclusively expressed), reveal temperature-dependent variations in EV-encapsulated bioactive cargo resulting from oviductal organoids subjected to either HS or thermoneutral conditions. Among the miRNAs enriched in EVs released in response to HS, bta-miR-150, bta-miR-92a, bta-miR223 and bta-miR-202 were at minimum tenfold higher than in the thermoneutral groups. Pathway analysis of genes enriched by upregulated miRNAs include cellular senesce and p53 signaling pathways, which are critical in cell cycle processes involving proliferation and the maintenance of genomic and cellular integrity. Interestingly, in the present study, pathways related to cellular senescence are also the most significant pathways enriched by the DEGs in the oviductal organoids in response to HS. To our knowledge, this is the first evidence indicating bovine oviductal organoids use cellular senescence as a stress response mechanism to prevent stress-induced damage including oxidative stress, genotoxic damages and inflammation [75]. Notably, previous reports show that increased expression of miR-150 downregulates pro-apoptotic P2X7 mRNA expression in human cervical epithelial cancer cells [76]. Furthermore, as indicated in zebrafish, miR-92a-3p [77] and miR-202-5P [78], are maternally-derived miRNAs with critical functions in gametogenesis. It was shown that miR-92a-3p targets wee2, a cyclin-dependent kinase 1 inhibitor, regulating the cell cycle prior to the maternal-zygotic transition in cleavage-stage zebrafish embryos [77]. Additionally, miR-202-5P, which is enriched in EVs released in response to HS was also found to be highly abundant

in early zebrafish embryos, suggesting its role in regulating primordial germ cell development throughout embryogenesis [78]. Therefore, although precautionary measures should be taken into account interpreting the species phylogenetic relationship, it is possible that oviductal organoids release EVs with the potential to shuttle specific miRNAs having a physiological role in early embryo development. Further functional studies to investigate the role of oviductal stress-associated EV-coupled miRNAs in regulating oviductal cells survival and potential to mediate early embryo development, is of great biological value.

In contrast to those miRNAs enriched in EVs released from oviductal organoids in response to HS, 35 miRNAs were found to be exclusively detected in EVs released from oviductal organoids cultured under thermoneutral conditions. Among the miRNAs downregulated in EVs from the HS groups compared to the thermoneutral groups were: bta-miR-197, bta-miR-6518, bta-miR-370, bta-miR-23a, bta-miR-11980 and bta-miR-221; with bta-miR-424-3P, bta-miR-654 and bta-miR-323 exclusively-differentially expressed in the EVs from thermoneutral cultured oviductal organoids. We found genes targeted by the downregulated miRNAs involve pathways regulating cellular senescence, as well as MAPK and FoxO signaling, with functions in cell-cycle arrest and intracellular signal transduction. Recent studies show miR-197-3p to be dramatically downregulated in ovarian tissues of patients with polycystic ovarian syndrome and in KGN human granulosa cell lines [79]. It was also confirmed that miR-197-3p targets CUL3, and its overexpression induces apoptosis by modulating caspase 3 and Bax (apoptotic) and bcl-2 (anti-apoptotic) protein expressions [79]. Similar reports indicate miR-370-3p inhibits cell proliferation and induces apoptosis in endometriotic cyst stromal cells by suppressing SF-1 [80]. These findings along with ours suggests the dysregulation of the aforementioned miRNAs due to HS might lead

to the development of novel therapeutic targets underlying reproductive anomalies, organismal aging and human diseases.

We have previously shown the relevance of EV-coupled miRNA signaling in reproductive cells, in which certain miRNA species are selectively enriched in EVs in response to various stressors [14]. It seems clear that selective enrichment of EV-miRNAs stems in part from the physiological response of oviductal organoids to HS, with potential negative impacts on bystander cells and the gamete/embryo. However, detailed mechanisms underpinning how specific miRNAs are enriched in EVs released in response to HS are largely unknown. Recent reports indicated the involvement of specific RNA binding proteins (RBPs) and unique miRNA sequence motifs in EV-miRNA sorting versus cellular retention in a tissue/cell dependent manner [33,34,35,36]. To this point, in order to shed light on the potential mechanisms involved in miRNA sorting into EVs by oviductal organoids in response to HS, we employed computational technologies to identify miRNA sequence motifs and their target RBPs for 12 miRNAs enriched in EVs released from oviductal organoids following exposure to HS. Accordingly, two miRNA sequence motifs shared by 9 out of the 12 miRNAs were found in EV-coupled miRNAs released in response to HS. Further in silico analysis revealed that the identified motifs are recognized by RBPs, namely: RBM6, HuR and ZC3H14. Among these previous studies, it has been revealed that HuR, a regulator of cytoplasmic mRNA fate, alters the cellular response to proliferative, stress, apoptotic, differentiation, senescence, inflammatory and immune stimuli [81]. Moreover, cellular oxidative stress has implicated HuR to impair responses to oxidant damage that characterizes cellular senescence and advancing age [32]. Phosphorylated HuR using an ATP analog activated PKCα, promoted the export of HuR to the cytoplasm, where its target COX2, became more stable [32]. Notably, COX1 and COX2 play important roles in the smooth muscle layer and epithelial cells

within the oviduct [56]. Regardless, further studies are required to investigate the interplay between miRNA motifs and RBPs in mediating the oviductal response to external stimuli, such as HS and their impacts on cellular survival and function during the maternal-embryo interaction.

5. Conclusions

Our study incorporates both an innovative approach and novel techniques pushing the threshold to: 1) generate a new viewpoint on the oviducts' capacity to undergo critical changes to external stimuli to safeguard the resulting gamete/embryo; 2) establish multifaceted, functional studies focused on oviduct signaling (organoids/EVs) and signatures potentially regulating stress response; 3) a potential platform to generate physiologically relevant EVs for implementation in current assisted reproductive technologies systems, aiming to enhance embryo survival and viability under various environmental and pathophysiological conditions (i.e. bystander effect). Finally, we have provided a comprehensive insight into the cellular and extracellular response of oviductal organoids to HS, yielding a structural footing to investigate the functional applicability and regulatory role of RNA cargoes (mRNA and miRNA) in modulating the fine-tuned oviductal microenvironment, essential for early stages of life. Further studies stemming from this work are needed to focus on the functional analysis of genes and EV-coupled miRNAs and their involvement in mediating the impact of physiological changes amid the oviduct microenvironment on the developing gamete/embryo and subsequent establishment of pregnancy. Taken together, oviductal organoids thusly provide a non-invasive approach to investigate normal and pathological reproductive processes, from a traditionally inaccessible organ.

6. Methods

Collection of bovine oviductal epithelial cells (BOECs)

Complete reproductive tracts including oviducts and ovaries (n = 10; a pool of 2 animals per replicate) were obtained from a local slaughterhouse (JBS Foods, USA) at the discretion of BPO Parts LLC (La Salle, CO) and transported within 1 h following collection via an insulated box containing physiological saline solution (0.9% NaCl) warmed to 37 °C to the Animal Reproduction and Biotechnology Laboratory for processing. Upon arrival, reproductive tracts were evaluated for the stage of the estrous cycle, dependent on the presence or absence of a fully formed, active corpus luteum with visible vasculature around its periphery. Resected ovaries containing complete contra- and ipsilateral oviducts from assessed stage II, diestrus tracts were initially washed through a physiological, warmed saline solution and subjected to a 70% ethanol rinse, followed by repetitive washings through a warmed saline solution. To offset the variability in abattoir-derived reproductive material, the same oviducts were represented in samples subjected to the differing ambient culture conditions (37 °C and 42 °C). Oviducts were trimmed from surrounding the tissues,opened longitudinally and processed according to previously defined measures [82, 83] by exposing the oviductal lumen, followed by scraping with a scalpel blade (Hill-Rom Holdings 371,120) in Handling Medium (HM) [HM; MEM Eagle with Earle's Salts (Sigma-Aldrich M2279) containing 25 mM HEPES (Sigma-Aldrich H0887), 100 U/ml Penicillin-0.1 mg/ml Streptomycin (Sigma-Aldrich P4333), 0.1 mM Pyruvate (Gibco 11,360–070), 2 mM Glutamax (Gibco 35,050–061) and Bovine Serum Albumin (5% v/v) (Sigma-Aldrich A9418)] to collect epithelial cells from the entire length of the oviduct for dissociation by enzymatic digestion. Subsequently, the solutions were passed through a 40 μm cell strainer (Greiner 542,040) to remove residual stromal and inflammatory cells then backwashed with RPMI-1640 medium (Gibco 11,875–085). The ensuing suspensions were then pelletized through centrifugation at 1000 xg for 10 min, washed in 1 mL

DMEM/F-12 (Gibco 21,041–025), and finally resuspended in 20x (v/v) phenol red-free, growth factor reduced UltiMatrix (Cultrex; Boitechne BME001-05).

Oviductal organoid culture

Parameters to establish organoid cultures were determined as we have previously described [50]. Unless indicated otherwise, all chemicals were manufactured by Sigma-Aldrich. Briefly, the homogenized UltiMatrix suspension, as described above, was aliquoted in 25 µL microdrops in a 48-well culture plate (Corning 3548), and allowed to strengthen formation for 30 min at 37 °C. The 3-D suspensions were then overlayed with 250 µL of Organoid Medium (OM) (OM; DMEM/F-12 without phenol red (Gibco 21,041–025), 100 µg/mL primocin (Invivogen ant-pm-1), 2.5 mM L-glutamine, 2% B27 Plus (Gibco A35828-01), 1% N2 (Gibco 17,502–048), 1% Insulin–transferrin–selenium (Gibco 41,400–045), 1 mM nicotinamide (N0636), 50 ng/mL recombinant human EGF (R&D Systems 236-EG), 50 ng/mL recombinant human FGF-10 (PeproTech 100–26), 100 ng/mL recombinant human Noggin (R&D systems 6057-NG/CF), 0.5 µM TGFβ/Alk inhibitor A83-01 (Tocris 2939), 1.25 mM N-acetyl-L-cysteine (EMD Millipore 106,425), 10 µM SB202190 (S7067), 10 µM Y27632 (EMD Millipore 688,000) as previously described [50, 82, 83]. For all experiments, organoid culture suspensions were in a confined chamber regulated to 37 °C and 5% CO2 in humidified air for growth and development prior to exposure to 42 °C to induce thermal stress. The OM was refreshed by half (v/v) every two to three days with passaging occurring weekly every 7th day. For passaging, the UltiMatrix containing the organoids were collected and pelletized via centrifugation at 1,000 xg for 10 min, washed in 1 mL of DMEM/F-12 with agitation applied from vigorous pipetting to induce dissociation and yield mostly single cells, followed by replating according to the same procedure described above. Organoids of low passage number (P1D7) were used for the experiments described.

Histology

Histological preparation of intact oviduct and oviductal organoids was performed as we have previously described [82, 83]. Briefly, organoid VitroGel® suspensions were soaked in 250 µL of VitroGel® Cell Recovery Solution and washed with DMEM/F-12 followed by DPBS (1X) and centrifuged at 600 xg for 6 min. After centrifugation, organoid pellets were fixed in 4% paraformaldehyde for 30 min and embedded in 2% agarose gel (Bio-Rad 1,613,101). Agarose-embedded organoids were stored in 70% ethanol until processing, then embedded in paraffin wax, sectioned (6 µm), and stained using hematoxylin and eosin (H&E) and assessed for normal oviductal epithelial cell architecture.

Immunohistochemistry

Organoid preparation for immunohistochemistry was performed as we have previously described [50, 82, 83]. Briefly, paraffin wax embedded organoids were mounted on Superfrost Plus slides, deparaffinized then rehydrated through graded alcohols until distilled water. Antigen retrieval was then accomplished by subjection to citrate buffer (pH 6; 96 °C for 20 min) and blocked with hydrogen peroxide then washed in distilled water. Slides were then incubated with primary (4 °C overnight) and HRP-conjugated and/or biotinylated secondary antibodies (OVGP1; Biotin Ms IgG, ZO1; Rb IgG HRP, and FOXJ1; Biotin Rb IgG), respectively. A list of the antibodies and dilutions is indicated in (Additional file 9: Table S9). Negative reagent controls provided utilized the same staining procedures in the absence of the primary antobody incubation step. Prior to microscopy evaluation, slides were activated using the RTU Vectastain kit (Vector Laboratories) for 30 min and visualized using Vectastain ABC-HRP and DAB substrate solution (Vector Laboratories) counterstained with hematoxylin. Incubations took place at a room temperature

environment with TBS-T solution used as a washing buffer. Slides were assessed for localization and presence of OVGP1, ZO1, and FOXJ1 staining.

Exposure of oviductal organoids to heat stress

Following the culmination of the first passage (14 days from initial collection), organoids were removed from UltiMatrix using Organoid Harvesting Solution (Cultrex; Biotechne 3700–100-01) and transferred to VitroGel® (TheWell Bioscience VHM04-K), a synthetic, xeno-free extracellular matrix. At this point, the 3-D matrices were incubated for 30 min at 37 °C to become less fluidic, according to the procedure described above. Finally, the OM was replenished followed by culturing for an initial 24 h priming period at 37 °C and 5% CO2 in humidified air. Thermoneutral organoids remained at 37 °C for an additional 24 h, while for experiments with heat stress organoids were transferred to a confined chamber regulated to 42 °C in an atmosphere of 5% CO2 in humidified air for the remaining 24 h. Experiments were replicated a total of eight times to gauge variability in abattoir-derived reproductive material for both culture environments.

Collection of cultured oviductal organoids and conditioned medium for downstream analysis

Following the collection of conditioned OM, the 3-D organoid suspensions were collected and suspended in VitroGel® Cell Recovery Solution (TheWell Bioscience MS03-100), washed with DMEM/F-12 and pelletized by centrifugation at 600 xg for 6 min. Organoid pellets were snap frozen in liquid nitrogen and stored at -80 °C for downstream use. The EV-containing conditioned OM were then centrifuged in sequential order at 500 xg for 10 min, 3,000 xg for 10 min and 17,200 xg for 30 min and filtered through a 0.22 μm sterile filter (Millex® SLGPR33RB) to remove residual cellular contaminants, large particles and protein aggregates. All centrifugation steps were performed at 4 °C. Bovine oviductal organoid-derived EVs were isolated from ~ 10 mL of conditioned OM (8 replicates/treatment group) using ultracentrifugation followed by size

exclusion chromatography (SEC). Briefly, OM were subjected to two consecutive rounds of ultracentrifugation at 120,000 xg for 70 min in the Optima XE-90 Ultracentrifuge using the SW 55Ti rotor (Beckman Coulter A94471). Isolated EVs were further standardized by elution in 180 µL of sterile DPBS (1X) (ThermoFisher Scientific 14,190–144) using the Exo-spin™ mini columns (CELL guidance systems EX03-50) according to the manufacturer's protocol. Isolated EVs were then stored at -80 °C for further characterization and molecular analysis.

Characterization and quantification of oviductal organoid-derived EVs

EV identification and characterization were carried out according to guidelines detailed by the International Society for Extracellular Vesicles [84], including EV marker protein validation, nanoparticle concentration/size distribution and morphological visualization as described below. Detailed information regarding experimental procedures has been submitted to the EV-TRACK knowledgebase (https://evtrack.org/) (EVTRACK ID: EV230000)[85].

Western blotting (WB)

Immunoblotting technique was performed for isolated EVs to detect EV and cellular protein markers. For this, proteins were extracted from oviductal organoid cells and the corresponding EVs using RIPA buffer (Marker Gene™ Technologies M2777). Protein lysates were then boiled with 4 × Laemmli Sample Buffer (Bio-Rad 1,610,747) and 2-Mercaptoethanol (Bio-Rad 1,610,710) at 95 °C for 5 min prior to loading on a 4–15% (w/v) Tris–Glycine Stain Free Gel (Bio-Rad 4,568,084). Electrophoresis was performed for 15 min at 90 V followed by 30 min at 200 V with Precision Plus Protein Dual Color Standards as a molecular weight marker (Bio-Rad 1,610,374). Separated proteins were transferred (100 V for 60 min at 4 °C) to a 0.20-µm pore nitrocellulose membrane (Bio-Rad 1,620,112) and blocked for 1 h at room temperature in 5% (w/v)

Non-Fat Dry Milk (Bio-Rad 1,706,404) and further incubated over night at 4 °C with a primary antibody against each marker protein (System Biosciences; rabbit polyclonal TSG101 EXOAB-TSG101-1, rabbit polyclonal FLOT1 EXOAB-FLOT1-1, rabbit polyclonal CD63 EXOAB-CD63A-1) (Sino Biological rabbit polyclonal Cytochrome C 102139-T42). Afterwards, membranes were washed 5 times with TBS-T solution and exposed to the secondary antibody (System Biosciences; Goat anti Rabbit HRP) for 1 h at room temperature. Bands and signals were enhanced using SuperSignal™ West Pico PLUS Chemiluminescent Substrate (ThermoFisher Scientific 34,579) and imaged using the ChemiDoc XRS + chemiluminescence system with Image Lab™ Software (version 6.0.1 build 34) (Bio-Rad). A list of the antibodies and dilutions is indicated in (Additional file 9: Table S9) with full length blots provided (Additional file 10: Fig. S1).

Nanoparticle tracking analysis (NTA)

A ZetaView® QUATT 4 Nanosight Instrument (Particle Metrix) was used to determine the particle concentration and size distribution in all EV samples. Briefly, isolated EVs were diluted in sterile DPBS (1X) and loaded into the device and analyzed. Measurements were taken at 11 positions via scatter mode using a 488 nm laser to determine the size distribution and concentration within a sample. Analysis of EV concentrations were calculated using the Zetaview Software (version 8.05.12 SP1) before and after sample dilution.

Transmission electron microscopy (TEM)

For morphological evaluation of oviductal organoid-derived EVs, we performed negative staining TEM of EVs by adsorption onto mesh copper grids with carbon-coated formvar film (Electron

Microscopy Sciences FCF 400-Cu). For this, grids were placed film side down on parafilm containing drops of 1% Alcinan Blue 8GX (Sigma-Aldrich 33,864–99-2) for 5 min, followed by washing with ddH2O for 15 s. Afterwards, the grids were floated on a 5 µL drop of isolated EVs for 10 min, prior to fixing in 2.4% uranyl acetate (Electron Microscopy Sciences 22,400) for 30 s. After fixing, samples were set to dry for imaging on a JEOL JEM-1200 EX transmission electron microscope.

RNA isolation

Total RNA was isolated from organoid cells (5 replicates/treatment group, a pool of samples from 2 animals per replicate) using an RNeasy® Plus Micro Kit (Qiagen 74,034). To remove genomic DNA contaminants, on-column DNA digestion was performed using RNase-free DNase (Qiagen; Hilden, Germany). Similarly, an Exosomal RNA Isolation Kit (Norgen Biotek Corp. 58,000) was used to isolate total RNA enriched with small RNA from oviductal organoid-derived EVs (3 replicates/treatment group, a pool of 2 animals per replicate) according to the manufacturer's protocol. In both cases, RNA quality control and concentration were assessed using an Agilent 2100 Bioanalyzer (Agilent Technologies G2939BA) and NanoDrop™ 2000 Spectrophotometer (ThermoFisher Scientific ND-2000), respectively.

RNA library preparation and sequencing

RNA libraries and next-generation sequencing (NGS) were conducted by Novogene Co., LTD (California, USA). For mRNA transcriptome profiling, RNA libraries were generated using a NEBNext® Ultra™ RNA Library Prep Kit for Illumina (NEB E7530L) and for miRNA profiling, small-RNA libraries were prepared using a TruSeq Small RNA Library Prep Kit (Illumina RS-200) according to the manufacturer's instructions. Library quantity and quality assessments were performed using a Qubit® DNA HS Assay Kit on a Qubit® 2.0 Fluorometer and an Agilent DNA

High Sensitivity Kit in an Agilent 2100 Bioanalyzer, respectively. Library concentrations were calculated using quantitative PCR measures then pooled in equimolar ratios and sequenced in a NovaSeq6000 sequencing instrument (Illumina) as paired (150 bases) or single-end (50 bases) reads for the transcriptome and miRNA sequencing, respectively.

RNA-seq data analysis

FASTQ files were generated for each sample using the software bcl2fastq (Illumina) with FastQC tool version 0.11.9 assessing their quality. Data were analyzed using the CLC Genomics Workbench software, version 21 (www.qiagenbioinformatics.com). Trimming of raw sequencing reads was based on quality score (Q-score > 30), ambiguous nucleotides (maximum two nucleotides allowed), read length (≥ 15 nucleotides), and removal of adapter sequences. Reads were mapped to the bovine reference genome (ARS-UCD1.2) and small-RNA reads were annotated against bovine precursor and mature miRNAs listed in the mirBase database (release 22) using the CLC Genomics Workbench RNA-seq Analysis and Quantify miRNA tools, respectively, with default software parameters applied. Normalization of raw expression data was performed using the trimmed mean of M-values (TMM) normalization method [86] and presented as either transcripts per million (TPM) or TMM-adjusted counts per million (CPM), for genes and miRNAs, respectively. For genes, the expression threshold was determined by the zFPKM method using the zFPKM R package v.1.16.0 [87]. The zFPKM transform/normalization method is used to determine, with high consistency, the threshold of expressed transcripts avoiding the low-abundance and biological noise transcripts due to sequencing errors, and/or off-target read mapping. zFPKM values are calculated from the distribution of the log2 (TPM values) after fitting to the right side of the major peaks of each gene expression curve to a half-Gaussian curve, mirrored into a full Gaussian distribution, and then transformed log2(TPM) into zFPKM from this

fit. Based on the recommended zFPKM score that considers the expressed/active genes [79], genes with zFPKM > −3 in all replicates were considered as expressed. A miRNA with an average value of CPM ≥ 10 was considered to be expressed. The CLC Genomics Workbench Differential Expression tool was used for the expression analysis comparison of the two groups. Differential expression was considered based on a negative binomial Generalized Linear Model (GLM) function. DEGs and DE-miRNAs were filtered based on FC ≥ 2 and P-adjusted value FDR < 0.05 [88]. The raw FASTQ and processed CSV files for the transcriptome and miRNA sequencing data have been deposited in the NCBI's Gene Expression Omnibus (GEO) (https://www.ncbi.nlm.nih.gov/geo/) with the accession numbers GSE221929 and GSE221895, respectively.

Target gene prediction, ontological classification and pathway analysis

Genes targeted by the DE-miRNAs were identified using the miRWalk database [89]. Within miRWalk, validated target genes from miRTarBase (version 7.0) and commonly targeted genes predicted by TargetScan (version 7.1) and miRDB (release 5.0) were selected for ontological classification and pathway analysis. Both targeted genes and DEG lists were submitted to the Database for Annotation, Visualization, and Integrated Discovery (DAVID) Bioinformatics web tool v. 2021 (http://david.abcc.ncifcrf.gov/) for pathways and ontological classification enrichment analysis using the EASE Score (a modified Fisher Exact p-value) with a threshold of less than or equal to 0.05. Pathways and biological processes (BPs) were determined from the KEGG database [90], and GOTERM_BP_DIRECT annotation set, respectively. The interaction networks of the miRNAs, targeted genes, and DEGs were constructed with Cytoscape software [91].

Quantitative real time PCR validation of candidate mRNA and miRNA

In order to validate the in vivo biomimicry of in vitro produced organoids, as well as the NGS data for DEGs and DE-miRNAs, quantitative real-time PCR (qRT-PCR) expression analysis was performed for selected transcripts and miRNAs in oviductal organoid cells and oviductal organoid-derived EVs, respectively. Additionally, naïve BOEC samples were used as a control in the organoid characterization experiment. For the functional characterization of in vitro produced organoids and validation of candidate DEGs, equal amounts of total RNA (~ 638 ng/µL and ~ 1024 ng/µL, respectively) extracted from independent organoid samples was reverse transcribed to generate cDNA, using the SuperScript™ III First-Strand Synthesis Super Mix Kit (Invitrogen 18,080,400) with random hexamer and oligo d(T) 20 primers, according to the manufacturer's instructions. The gene panel were strategically constructed to characterize the functionality of in vitro produced organoids (n = 3), while ten candidate genes for the validation of the DEGs (n = 4) were randomly selected, with gene-specific primers designed using the Primer-Blast tool (https://www.ncbi.nlm.nih.gov/tools/primer-blast/). All primers are indicated in Additional file 11: Table S10. Quantification of each candidate gene was performed in 20 µl reaction volumes containing 0.5 µL of each primer (10 µM), 10 µL of iQ SYBR Green Supermix (Bio-Rad 1,708,880), 7 µL of ddH2O and 2 µL of the cDNA template. The following thermocycling conditions were applied for amplification: initial denaturation at 95 °C for 3 min, followed by 40 cycles of amplification at 95 °C for 15 s., 60 °C for 30 s., 72 °C for 30 s. The specificity of the amplification was determined from the melting curve analysis generated following each run. The geometric mean of expression levels of β-ACTIN and GAPDH was used to normalize the expression of the candidate genes.

Four DE-miRNAs (bta-miR-150, bta-miR-92a, bta-miR-223 and bta-miR-202) were chosen for quantification in the samples described above using TaqMan™ miRNA Assays

(Applied Biosystems™) according to the manufacturer's instructions. Briefly, 5 ng/μL of total RNA were reverse-transcribed using a TaqMan™ microRNA Reverse Transcription Kit (Applied Biosystems™ 4,366,596). The reaction mixture (7.5 μL) constituted 0.75 μL dNTP mix w/dTTp (100 M total), 0.075 μL 10X RT buffer, 0.095 μL RNase inhibitor (20U/μL), 0.5 μL Multiscribe™ RT enzyme (50U/μL), 1.5 μL of the given miRNA-specific stem-loop primer, and 2.5 μL of RNA (5 ng/μL). The miRNA-specific cDNA reaction mixture was incubated at 16 °C for 30 min, 42 °C for 30 min then followed by 85 °C for 5 min For miRNA quantification, 20 μL qRT-PCR mixtures were prepared in a 96-well PCR plate with 10 μL TaqMan™ Universal PCR Master Mix, no AmpErase™ UNG (Applied Biosystems™ 4,324,018), 1 μL miRNA-specific TaqMan microRNA probe (FAM, 250 nM), 7 μL ddH2O and 2 μL of the RT product. The following thermocycling conditions were applied for amplification: initial denaturation at 95 °C for 10 min, followed by 40 cycles of amplification at 95 °C for 15 s. and 60 °C for 1 min Expression normalization was performed against small nuclear RNA (U6), as it stably resembled the mean expression values for all miRNAs. All qRT-PCR validation analyses were performed using the CFX96 Touch Real-Time PCR Detection System (Bio-Rad) and expression data analysis was performed using a comparative threshold cycle (CT) method [92]. All data are shown as the mean ± SEM and the differences between means were analyzed using one-way ANOVA followed by Tukey's Multiple Comparisons Test in biologically independent samples ($n = 4$). Statistical significance (*) between the 42 °C compared to the 37 °C groups were determined at ($p < 0.05$).

MicroRNA sequence motif and RBP identification and analysis

Sequence-specific miRNA motifs (4–6 nucleotides), enriched in the upregulated miRNAs (including the significantly, exclusively expressed miRNAs; $n = 13$) versus the downregulated miRNAs (including the significantly, exclusively expressed miRNAs; $n = 9$ as control sequences)

in EVs derived from oviductal organoids exposed to HS, were identified using Multiple Expectation Maximization for Motif Elicitation (MEME) suite v. 5.5.0 https://meme-suite.org [93]. Motifs commonly detected in at least 50% of the submitted miRNAs were selected for further analysis to determine the motif-associated RBPs using a TOMTOM motif comparison tool [94].

References

1. Pérez-Cerezales S, Ramos-Ibeas P, Acuña OS, Avilés M, Coy P, Rizos D, Gutiérrez-Adán A. The oviduct: from sperm selection to the epigenetic landscape of the embryo. Biol Reprod. 2018;98:262–76. doi:10.1093/biolre/iox173.

2. Fazeli A. Maternal Communication with Gametes and Embryo: A Personal Opinion. Reproduction in Domestic Animals. 2011;46:75–8. doi:10.1111/j.1439-0531.2011.01870.x.

3. Almiñana C, Heath PR, Wilkinson S, Sanchez-Osorio J, Cuello C, Parrilla I, et al. Early developing pig embryos mediate their own environment in the maternal tract. PLoS One. 2012;7:e33625. doi:10.1371/journal.pone.0033625.

4. Maillo V, Gaora PÓ, Forde N, Besenfelder U, Havlicek V, Burns GW, et al. Oviduct-Embryo Interactions in Cattle: Two-Way Traffic or a One-Way Street?1. Biol Reprod 2015. doi:10.1095/biolreprod.115.127969.

5. Herrler A, Rango U von, Beier HM. Embryo-maternal signalling: how the embryo starts talking to its mother to accomplish implantation. Reprod Biomed Online. 2003;6:244–56. doi:10.1016/s1472-6483(10)61717-8.

6. Valadi H, Ekström K, Bossios A, Sjöstrand M, Lee JJ, Lötvall JO. Exosome-mediated transfer of mRNAs and microRNAs is a novel mechanism of genetic exchange between cells. Nat Cell Biol. 2007;9:654–9. doi:10.1038/ncb1596.

7. Sohel MMH, Hoelker M, Noferesti SS, Salilew-Wondim D, Tholen E, Looft C, et al. Exosomal and Non-Exosomal Transport of Extra-Cellular microRNAs in Follicular Fluid: Implications for Bovine Oocyte Developmental Competence. PLoS One. 2013;8:e78505. doi:10.1371/journal.pone.0078505.

8. Pavani KC, Alminana C, Wydooghe E, Catteeuw M, Ramírez MA, Mermillod P, et al. Emerging role of extracellular vesicles in communication of preimplantation embryos in vitro. Reprod Fertil Dev. 2016;29:66–83. doi:10.1071/RD16318.

9. Tesfaye D, Menjivar N, Gebremedhn S. Current knowledge and the future potential of extracellular vesicles in mammalian reproduction. Reprod Fertil Dev. 2021;34:174–89. doi:10.1071/RD21277.

10. Eldh M, Ekström K, Valadi H, Sjöstrand M, Olsson B, Jernås M, Lötvall J. Exosomes communicate protective messages during oxidative stress; possible role of exosomal shuttle RNA. PLoS One. 2010;5:e15353. doi:10.1371/journal.pone.0015353.

11. Bewicke-Copley F, Mulcahy LA, Jacobs LA, Samuel P, Akbar N, Pink RC, Carter DRF. Extracellular vesicles released following heat stress induce bystander effect in unstressed populations. J Extracell Vesicles. 2017;6:1340746. doi:10.1080/20013078.2017.1340746.

12. Saeed-Zidane M, Linden L, Salilew-Wondim D, Held E, Neuhoff C, Tholen E, et al. Cellular and exosome mediated molecular defense mechanism in bovine granulosa cells exposed to oxidative stress. PLoS One. 2017;12:e0187569. doi:10.1371/journal.pone.0187569.

13. Rodrigues TA, Tuna KM, Alli AA, Tribulo P, Hansen PJ, Koh J, Paula-Lopes FF. Follicular fluid exosomes act on the bovine oocyte to improve oocyte competence to support development and survival to heat shock. Reprod Fertil Dev. 2019;31:888–97. doi:10.1071/RD18450.

14. Gebremedhn S, Gad A, Aglan HS, Laurincik J, Prochazka R, Salilew-Wondim D, et al. Extracellular vesicles shuttle protective messages against heat stress in bovine granulosa cells. Sci Rep. 2020;10:15824. doi:10.1038/s41598-020-72706-z.

15. Menjivar NG, Gad A, Gebremedhn S, Ghosh S, Tesfaye D. Granulosa cell-derived extracellular vesicles mitigate the detrimental impact of thermal stress on bovine oocytes and embryos. Front Cell Dev Biol. 2023;11:1142629. doi:10.3389/fcell.2023.1142629.

16. Nardone A, Ronchi B, Lacetera N, Ranieri MS, Bernabucci U. Effects of climate changes on animal production and sustainability of livestock systems. Livestock Science. 2010;130:57–69. doi:10.1016/j.livsci.2010.02.011.

17. Boni R. Heat stress, a serious threat to reproductive function in animals and humans. Mol Reprod Dev. 2019;86:1307–23. doi:10.1002/mrd.23123.

18. Hansen PJ. Effects of heat stress on mammalian reproduction. Philos Trans R Soc Lond B Biol Sci. 2009;364:3341–50. doi:10.1098/rstb.2009.0131.

19. Takahashi M. Heat stress on reproductive function and fertility in mammals. Reprod Med Biol. 2011;11:37–47. doi:10.1007/s12522-011-0105-6.

20. Edwards JL, Hansen PJ. Differential responses of bovine oocytes and preimplantation embryos to heat shock. Mol Reprod Dev. 1997;46:138–45. doi:10.1002/(SICI)1098-2795(199702)46:2<138::AID-MRD4>3.0.CO;2-R.

21. Paula Lopes F, Lima RS, Risolia P, Ispada J, Assumpção ME, Visintin JA. Heat stress induced alteration in bovine oocytes: Functional and cellular aspects. Anim Reprod. 2012;9:395–403.

22. Sartori R, Sartor-Bergfelt R, Mertens SA, Guenther JN, Parrish JJ, Wiltbank MC. Fertilization and early embryonic development in heifers and lactating cows in summer and lactating and dry cows in winter. J Dairy Sci. 2002;85:2803–12. doi:10.3168/jds.S0022-0302(02)74367-1.

23. Pavani KC, Baron E, Correia P, Lourenço J, Bettencourt BF, Sousa M, Da Silva FM. Gene expression, oocyte nuclear maturation and developmental competence of bovine oocytes and embryos produced after in vivo and in vitro heat shock. Zygote. 2016;24:748–59. doi:10.1017/S0967199416000071.

24. Lopera-Vasquez R, Hamdi M, Maillo V, Gutierrez-Adan A, Bermejo-Alvarez P, Ramírez MÁ, et al. Effect of bovine oviductal extracellular vesicles on embryo development and quality in vitro. Reproduction. 2017;153:461–70. doi:10.1530/REP-16-0384.

25. Lopera-Vásquez R, Hamdi M, Fernandez-Fuertes B, Maillo V, Beltrán-Breña P, Calle A, et al. Extracellular Vesicles from BOEC in In Vitro Embryo Development and Quality. PLoS One. 2016;11:e0148083. doi:10.1371/journal.pone.0148083.

26. Almiñana C, Corbin E, Tsikis G, Alcântara-Neto AS, Labas V, Reynaud K, et al. Oviduct extracellular vesicles protein content and their role during oviduct-embryo cross-talk. Reproduction. 2017;154:153–68. doi:10.1530/REP-17-0054.

27. Clevers H. Modeling Development and Disease with Organoids. Cell. 2016;165:1586–97. doi:10.1016/j.cell.2016.05.082.

28. Hofer M, Lutolf MP. Engineering organoids. Nature Reviews Materials. 2021;6:402–20. doi:10.1038/s41578-021-00279-y.

29. Kessler M, Hoffmann K, Brinkmann V, Thieck O, Jackisch S, Toelle B, et al. The Notch and Wnt pathways regulate stemness and differentiation in human fallopian tube organoids. Nat Commun. 2015;6:8989. doi:10.1038/ncomms9989.

30. Xie Y, Park E-S, Xiang D, Li Z. Long-term organoid culture reveals enrichment of organoid-forming epithelial cells in the fimbrial portion of mouse fallopian tube. Stem Cell Res. 2018;32:51–60. doi:10.1016/j.scr.2018.08.021.

31. Lõhmussaar K, Kopper O, Korving J, Begthel H, Vreuls CPH, van Es JH, Clevers H. Assessing the origin of high-grade serous ovarian cancer using CRISPR-modification of mouse organoids. Nat Commun. 2020;11:2660. doi:10.1038/s41467-020-16432-0.

32. Abdelmohsen K, Kuwano Y, Kim HH, Gorospe M. Posttranscriptional gene regulation by RNA-binding proteins during oxidative stress: implications for cellular senescence. Biol Chem. 2008;389:243–55. doi:10.1515/BC.2008.022.

33. Villarroya-Beltri C, Gutiérrez-Vázquez C, Sánchez-Cabo F, Pérez-Hernández D, Vázquez J, Martin-Cofreces N, et al. Sumoylated hnRNPA2B1 controls the sorting of miRNAs into exosomes through binding to specific motifs. Nat Commun. 2013;4:2980. doi:10.1038/ncomms3980.

34. Shurtleff MJ, Temoche-Diaz MM, Karfilis KV, Ri S, Schekman R. Y-box protein 1 is required to sort microRNAs into exosomes in cells and in a cell-free reaction. Elife 2016. doi:10.7554/eLife.19276.

35. Teng Y, Ren Y, Hu X, Mu J, Samykutty A, Zhuang X, et al. MVP-mediated exosomal sorting of miR-193a promotes colon cancer progression. Nat Commun. 2017;8:14448. doi:10.1038/ncomms14448.

36. Garcia-Martin R, Wang G, Brandão BB, Zanotto TM, Shah S, Kumar Patel S, et al. MicroRNA sequence codes for small extracellular vesicle release and cellular retention. Nature. 2022;601:446–51. doi:10.1038/s41586-021-04234-3.

37. Guérin P, El Mouatassim S, Ménézo Y. Oxidative stress and protection against reactive oxygen species in the pre-implantation embryo and its surroundings. Human Reproduction Update. 2001;7:175–89. doi:10.1093/humupd/7.2.175.

38. Li S, Winuthayanon W. Oviduct: roles in fertilization and early embryo development. J Endocrinol. 2017;232:R1-R26. doi:10.1530/JOE-16-0302.

39. Saint-Dizier M, Schoen J, Chen S, Banliat C, Mermillod P. Composing the Early Embryonic Microenvironment: Physiology and Regulation of Oviductal Secretions. Int J Mol Sci 2019. doi:10.3390/ijms21010223.

40. Stamperna K, Giannoulis T, Cañon-Beltrán K, Dovolou E, Kalemkeridou M, Nanas I, et al. Oviductal epithelial cells transcriptome and extracellular vesicles characterization during thermoneutral and heat stress conditions in dairy cows. Theriogenology. 2022;187:152–63. doi:10.1016/j.theriogenology.2022.04.011.

41. Rąpała Ł, Starzyński RR, Trzeciak PZ, Dąbrowski S, Gajewska M, Jurka P, et al. Influence of elevated temperature on bovine oviduct epithelial cells (BOECs). PLoS One. 2018;13:e0198843. doi:10.1371/journal.pone.0198843.

42. Thompson RE, Meyers MA, Pukazhenthi BS, Hollinshead FK. Evaluation of growth, viability, and structural integrity of equine endometrial organoids following cryopreservation. Cryobiology. 2022;104:56–62. doi:10.1016/j.cryobiol.2021.11.003.

43. Gottardi CJ, Arpin M, Fanning AS, Louvard D. The junction-associated protein, zonula occludens-1, localizes to the nucleus before the maturation and during the remodeling of cell-cell contacts. Proc Natl Acad Sci U S A. 1996;93:10779–84. doi:10.1073/pnas.93.20.10779.

44. Lamy J, Labas V, Harichaux G, Tsikis G, Mermillod P, Saint-Dizier M. Regulation of the bovine oviductal fluid proteome. Reproduction. 2016;152:629–44. doi:10.1530/REP-16-0397.

45. Sherr CJ, DePinho RA. Cellular Senescence: Minireview Mitotic Clock or Culture Shock? Cell. 2000;102:407–10. doi:10.1016/S0092-8674(00)00046-5.

46. Gabler C, Odau S, Muller K, Schon J, Bondzio A, Einspanier R. Exploring cumulus-oocyte-complex-oviductal cell interactions: gene profiling in the bovine oviduct. J Physiol Pharmacol. 2008;59 Suppl 9:29–42.

47. Danesh Mesgaran S, Sharbati J, Einspanier R, Gabler C. mRNA expression pattern of selected candidate genes differs in bovine oviductal epithelial cells in vitro compared with the in vivo state and during cell culture passages. Reprod Biol Endocrinol. 2016;14:44. doi:10.1186/s12958-016-0176-7.

48. Fitzgerald HC, Dhakal P, Behura SK, Schust DJ, Spencer TE. Self-renewing endometrial epithelial organoids of the human uterus. Proc Natl Acad Sci U S A. 2019;116:23132–42. doi:10.1073/pnas.1915389116.

49. Turco MY, Gardner L, Hughes J, Cindrova-Davies T, Gomez MJ, Farrell L, et al. Long-term, hormone-responsive organoid cultures of human endometrium in a chemically defined medium. Nat Cell Biol. 2017;19:568–77. doi:10.1038/ncb3516.

50. Thompson RE, Johnson AK, Dini P, Turco MY, Prado TM, Premanandan C, et al. Hormone-responsive organoids from domestic mare and endangered Przewalski's horse endometrium. Reproduction. 2020;160:819–31. doi:10.1530/REP-20-0266.

51. Thippabhotla S, Zhong C, He M. 3D cell culture stimulates the secretion of in vivo like extracellular vesicles. Sci Rep. 2019;9:13012. doi:10.1038/s41598-019-49671-3.

52. Rottmayer R, Ulbrich SE, Kölle S, Prelle K, Neumueller C, Sinowatz F, et al. A bovine oviduct epithelial cell suspension culture system suitable for studying embryo-maternal interactions: morphological and functional characterization. Reproduction. 2006;132:637–48. doi:10.1530/rep.1.01136.

53. Bauersachs S, Blum H, Mallok S, Wenigerkind H, Rief S, Prelle K, Wolf E. Regulation of ipsilateral and contralateral bovine oviduct epithelial cell function in the postovulation period: a transcriptomics approach. Biol Reprod. 2003;68:1170–7. doi:10.1095/biolreprod.102.010660.

54. Bauersachs S, Rehfeld S, Ulbrich SE, Mallok S, Prelle K, Wenigerkind H, et al. Monitoring gene expression changes in bovine oviduct epithelial cells during the oestrous cycle. J Mol Endocrinol. 2004;32:449–66. doi:10.1677/jme.0.0320449.

55. Ulbrich SE, Kettler A, Einspanier R. Expression and localization of estrogen receptor alpha, estrogen receptor beta and progesterone receptor in the bovine oviduct in vivo and in vitro. J Steroid Biochem Mol Biol. 2003;84:279–89. doi:10.1016/s0960-0760(03)00039-6.

56. Odau S, Gabler C, Holder C, Einspanier R. Differential expression of cyclooxygenase 1 and cyclooxygenase 2 in the bovine oviduct. J Endocrinol. 2006;191:263–74. doi:10.1677/joe.1.06761.

57. Kobayashi Y, Wakamiya K, Kohka M, Yamamoto Y, Okuda K. Summer heat stress affects prostaglandin synthesis in the bovine oviduct. Reproduction. 2013;146:103–10. doi:10.1530/REP-12-0479.

58. Huang L, Min J-N, Masters S, Mivechi NF, Moskophidis D. Insights into function and regulation of small heat shock protein 25 (HSPB1) in a mouse model with targeted gene disruption. Genesis. 2007;45:487–501. doi:10.1002/dvg.20319.

59. Calderwood SK, Khaleque MA, Sawyer DB, Ciocca DR. Heat shock proteins in cancer: chaperones of tumorigenesis. Trends Biochem Sci. 2006;31:164–72. doi:10.1016/j.tibs.2006.01.006.

60. Yoo J-Y, Shin H, Kim TH, Choi W-S, Ferguson SD, Fazleabas AT, et al. CRISPLD2 is a target of progesterone receptor and its expression is decreased in women with endometriosis. PLoS One. 2014;9:e100481. doi:10.1371/journal.pone.0100481.

61. Velarde MC, Menon R. Positive and negative effects of cellular senescence during female reproductive aging and pregnancy. J Endocrinol. 2016;230:R59-76. doi:10.1530/JOE-16-0018.

62. Calcinotto A, Kohli J, Zagato E, Pellegrini L, Demaria M, Alimonti A. Cellular Senescence: Aging, Cancer, and Injury. Physiol Rev. 2019;99:1047–78. doi:10.1152/physrev.00020.2018.

63. Winuthayanon W, Bernhardt ML, Padilla-Banks E, Myers PH, Edin ML, Lih FB, et al. Oviductal estrogen receptor α signaling prevents protease-mediated embryo death. Elife. 2015;4:e10453. doi:10.7554/eLife.10453.

64. Dumollard R, Duchen M, Carroll J. The role of mitochondrial function in the oocyte and embryo. Curr Top Dev Biol. 2007;77:21–49. doi:10.1016/S0070-2153(06)77002-8.

65. Balaban RS, Nemoto S, Finkel T. Mitochondria, oxidants, and aging. Cell. 2005;120:483–95. doi:10.1016/j.cell.2005.02.001.

66. Dresios J, Aschrafi A, Owens GC, Vanderklish PW, Edelman GM, Mauro VP. Cold stress-induced protein Rbm3 binds 60S ribosomal subunits, alters microRNA levels, and enhances global protein synthesis. Proc Natl Acad Sci U S A. 2005;102:1865–70. doi:10.1073/pnas.0409764102.

67. King AE, Critchley HO, Kelly RW. Presence of secretory leukocyte protease inhibitor in human endometrium and first trimester decidua suggests an antibacterial protective role. Mol Hum Reprod. 2000;6:191–6. doi:10.1093/molehr/6.2.191.

68. Ota Y, Shimoya K, Zhang Q, Moriyama A, Chin R, Tenma K, et al. The expression of secretory leukocyte protease inhibitor (SLPI) in the fallopian tube: SLPI protects the acrosome

reaction of sperm from inhibitory effects of elastase. Hum Reprod. 2002;17:2517–22. doi:10.1093/humrep/17.10.2517.

69. Hu Y, Cai M-C, Wang L, Zhang T-H, Luo Z-G, Zhang G-W, Zuo F-Y. MiR-1246 is upregulated and regulates lung cell apoptosis during heat stress in feedlot cattle. Cell Stress Chaperones. 2018;23:1219–28. doi:10.1007/s12192-018-0927-9.

70. Burns G, Brooks K, Wildung M, Navakanitworakul R, Christenson LK, Spencer TE. Extracellular vesicles in luminal fluid of the ovine uterus. PLoS One. 2014;9:e90913. doi:10.1371/journal.pone.0090913.

71. Almiñana C, Tsikis G, Labas V, Uzbekov R, Da Silveira JC, Bauersachs S, Mermillod P. Deciphering the oviductal extracellular vesicles content across the estrous cycle: implications for the gametes-oviduct interactions and the environment of the potential embryo. BMC Genomics. 2018;19:622. doi:10.1186/s12864-018-4982-5.

72. Wang P, Li X, Cao L, Huang S, Li H, Zhang Y, et al. MicroRNA-148a overexpression improves the early development of porcine somatic cell nuclear transfer embryos. PLoS One. 2017;12:e0180535. doi:10.1371/journal.pone.0180535.

73. Liu L-Z, Li C, Chen Q, Jing Y, Carpenter R, Jiang Y, et al. MiR-21 induced angiogenesis through AKT and ERK activation and HIF-1α expression. PLoS One. 2011;6:e19139. doi:10.1371/journal.pone.0019139.

74. Gecaj RM, Schanzenbach CI, Kirchner B, Pfaffl MW, Riedmaier I, Tweedie-Cullen RY, Berisha B. The Dynamics of microRNA Transcriptome in Bovine Corpus Luteum during Its Formation, Function, and Regression. Front Genet. 2017;8:213. doi:10.3389/fgene.2017.00213.

75. Pérez-Mancera PA, Young ARJ, Narita M. Inside and out: the activities of senescence in cancer. Nat Rev Cancer. 2014;14:547–58. doi:10.1038/nrc3773.

76. Zhou L, Qi X, Potashkin JA, Abdul-Karim FW, Gorodeski GI. MicroRNAs miR-186 and miR-150 down-regulate expression of the pro-apoptotic purinergic P2X7 receptor by activation of instability sites at the 3'-untranslated region of the gene that decrease steady-state levels of the transcript. J Biol Chem. 2008;283:28274–86. doi:10.1074/jbc.M802663200.

77. Presslauer CE, Bizuayehu TT, Fernandes JM, Babiak IS. miR-92a-3p controls cell cycle progression in zebrafish. bioRxiv 2019. doi:10.1101/680991.

78. Zhang J, Liu W, Jin Y, Jia P, Jia K, Yi M. MiR-202-5p is a novel germ plasm-specific microRNA in zebrafish. Sci Rep. 2017;7:7055. doi:10.1038/s41598-017-07675-x.

79. Shen X, Gong A. The expression of microRNA-197-3p regulates the proliferation of ovarian granulosa cells through CUL3 in polycystic ovarian syndrome. Acta Biochim Pol. 2022;69:599–604. doi:10.18388/abp.2020_5951.

80. Hu Z, Mamillapalli R, Taylor HS. Increased circulating miR-370-3p regulates steroidogenic factor 1 in endometriosis. Am J Physiol Endocrinol Metab. 2019;316:E373-E382. doi:10.1152/ajpendo.00244.2018.

81. Srikantan S, Gorospe M. HuR function in disease. Front Biosci (Landmark Ed). 2012;17:189–205. doi:10.2741/3921.

82. Thompson RE, Meyers MA, Veeramachaneni DNR, Pukazhenthi BS, Hollinshead FK. Equine Oviductal Organoid Generation and Cryopreservation. Methods Protoc 2022. doi:10.3390/mps5030051.

83. Thompson RE, Meyers MA, Premanandan C, Hollinshead FK. Generation and cryopreservation of feline oviductal organoids. Theriogenology. 2023;196:167–73. doi:10.1016/j.theriogenology.2022.11.020.

84. Théry C, Witwer KW, Aikawa E, Alcaraz MJ, Anderson JD, Andriantsitohaina R, et al. Minimal information for studies of extracellular vesicles 2018 (MISEV2018): a position statement of the International Society for Extracellular Vesicles and update of the MISEV2014 guidelines. J Extracell Vesicles. 2018;7:1535750. doi:10.1080/20013078.2018.1535750.

85. van Deun J, Mestdagh P, Agostinis P, Akay Ö, Anand S, Anckaert J, et al. EV-TRACK: transparent reporting and centralizing knowledge in extracellular vesicle research. Nat Methods. 2017;14:228–32. doi:10.1038/nmeth.4185.

86. Robinson MD, Oshlack A. A scaling normalization method for differential expression analysis of RNA-seq data. Genome Biol. 2010;11:R25. doi:10.1186/gb-2010-11-3-r25.

87. Hart T, Komori HK, LaMere S, Podshivalova K, Salomon DR. Finding the active genes in deep RNA-seq gene expression studies. BMC Genomics. 2013;14:778. doi:10.1186/1471-2164-14-778.

88. Benjamini Y, Hochberg Y. Controlling the False Discovery Rate: A Practical and Powerful Approach to Multiple Testing. Journal of the Royal Statistical Society: Series B (Methodological). 1995;57:289–300. doi:10.1111/j.2517-6161.1995.tb02031.x.

89. Sticht C, La Torre C de, Parveen A, Gretz N. miRWalk: An online resource for prediction of microRNA binding sites. PLoS One. 2018;13:e0206239. doi:10.1371/journal.pone.0206239.

90. Ogata H, Goto S, Sato K, Fujibuchi W, Bono H, Kanehisa M. KEGG: Kyoto Encyclopedia of Genes and Genomes. Nucleic Acids Research. 1999;27:29–34. doi:10.1093/nar/27.1.29.

91. Shannon P, Markiel A, Ozier O, Baliga NS, Wang JT, Ramage D, et al. Cytoscape: a software environment for integrated models of biomolecular interaction networks. Genome Res. 2003;13:2498–504. doi:10.1101/gr.1239303.

92. Schmittgen TD, Livak KJ. Analyzing real-time PCR data by the comparative C(T) method. Nat Protoc. 2008;3:1101–8. doi:10.1038/nprot.2008.73.

93. Bailey TL, Johnson J, Grant CE, Noble WS. The MEME Suite. Nucleic Acids Research. 2015;43:W39-49. doi:10.1093/nar/gkv416.

94. Gupta S, Stamatoyannopoulos JA, Bailey TL, Noble WS. Quantifying similarity between motifs. Genome Biol. 2007;8:R24. doi:10.1186/gb-2007-8-2-r24.

CSIRO PUBLISHING

SPECIAL ISSUE | REVIEW
https://doi.org/10.1071/RD21277

Reproduction, Fertility and Development

Current knowledge and the future potential of extracellular vesicles in mammalian reproduction

Dawit Tesfaye[A,*], Nico Menjivar[A] and Samuel Gebremedhn[B]

For full list of author affiliations and declarations see end of paper

*Correspondence to:
Dawit Tesfaye
Animal Reproduction and Biotechnology Laboratory, Department of Biomedical Sciences, Colorado State University, 3051 Rampart Road, Fort Collins, CO 80521, USA
Email: Dawit.Tesfaye@Colostate.edu

Published: 12 October 2021

Cite this:
Tesfaye D *et al.* (2021)
Reproduction, Fertility and Development
doi:10.1071/RD21277

© 2021 The Author(s) (or their employer(s)). Published by CSIRO Publishing on behalf of the IETS.

ABSTRACT

Extracellular vesicles (EVs), which contain various functional classes of vesicles, namely exosomes, microvesicles, and apoptotic bodies, represent the major nano-shuttle to transfer bioactive molecules from donor to recipient cells to facilitate cell-to-cell communication in the follicular, oviduct, and uterine microenvironments. In addition to transferring various molecular cargos in the form of miRNAs, mRNAs, proteins, lipids, and DNA molecules, the relative proportion of those molecular cargos in the reproductive fluids can be associated with the physiological and pathological condition of the host animal. Inside the follicle, EV-mediated circulation of miRNAs has been reported to be associated with the growth status of the enclosed oocytes, the metabolic status, and the advanced maternal aging of the animal. Importantly, EVs have the potential to protect their cargo molecules from extracellular degradation or modification while travelling to the recipient cells. This fact together with the enormous availability in almost all biological fluids and spent culture media make them attractive in the search for biomarkers of oocyte/embryo developmental competence, receptive maternal environment and a multitude of reproductive pathophysiological conditions. One of the key factors that have contributed to the lower efficiency of assisted reproductive technologies (ART) is the absence of several maternal *in vivo* factors in the ART procedures. For this, several studies have been conducted to supplement various components present in the follicular and oviductal fluids into the existing ART procedures and significant positive impacts have been observed in terms of embryo cleavage rate, blastocyst rate, resistance to stress, and survival after cryopreservation. The potential of EVs in shuttling protective messages against environmental and physiological stressors has been evidenced. The effective use of the EV-coupled molecular signals against stress-associated conditions has the potential to pave the path for the application of these protective signals against oxidative stress-associated pathological conditions including PCOS, ageing, and endometritis. In this review, we provide current knowledge and potential future use of EVs as remedies in reproductive pathophysiological conditions, mainly in follicular and oviductal microenvironments.

Keywords: assisted reproductive technology, DNA, extracellular vesicles, reproduction, RNA, stress response.

Introduction

In mammalian reproduction, intercellular communication is an essential process, which occurs indirectly through endocrine, paracrine, and autocrine factors or directly through cell-to-cell contacts (Raposo and Stoorvogel 2013). After their discovery in 1983, membrane-enclosed compartments, which are regarded as extracellular vesicles (EVs) play a significant role in cell-to-cell communication in various reproductive processes. EVs mediate cellular communication via their molecular cargos namely, RNAs (mRNA, miRNA, tRNA, and other long noncoding RNA), proteins, DNA, and lipids, that they transfer to the recipient cells (Valadi *et al.* 2007; Almiñana *et al.* 2018; Gatien *et al.* 2019). Based on their size and mode of biogenesis, EVs are broadly classified as exosomes (50–150 nm), microvesicles (100–1000 nm) and apoptotic bodies (>1000 nm) (Simon *et al.* 2018). EVs interact with

the recipient cells by direct signalling via ligand/receptor molecules in their respective surfaces or through direct fusion of the plasma membrane of the EVs and recipient cells, lipid-raft, clathrin, and caveolae-mediated endocytosis, micropinocytosis, and phagocytosis (Morelli *et al.* 2004; Montecalvo *et al.* 2012). Due to the lack of consensus on their nomenclature, reproductive biologists designate EVs derived from various reproductive fluids as epididmosomes, prostasomes, vaginosomes, uterosomes, and oviductosomes (Al-Dossary *et al.* 2013; Belleannée *et al.* 2013; Sullivan and Saez 2013).

Extracellular vesicles are considered as nano shuttles available in various reproductive fluids including follicular, oviductal, and uterine fluids, and are reported to play a role in cell-to-cell, gamete to follicular cells, gamete, or embryo to oviduct/uterine cells communication. Moreover, several studies have demonstrated that EVs are involved in shuttling several bioactive molecules including miRNAs, mRNA, and proteins and their relative abundance could reflect the physiological status of the originating cells or tissues (Valadi *et al.* 2007; Hailay *et al.* 2019). EVs from follicular fluid of oocytes under varying growth status (Sohel *et al.* 2013), different sizes (Hung *et al.* 2015), and divergent metabolic status (Hailay *et al.* 2019) are known to carry varying levels of bioactive molecules which might be associated with their functional role. Similarly, bovine granulosa cells subjected to *in vitro* thermal stress or oxidative stress release protective molecular signals through EVs in form of heat shock proteins, antioxidants, and transcripts associated with endoplasmic reticulum stress (Saeed-Zidane *et al.* 2017; Gebremedhn *et al.* 2020*b*). Interestingly those EVs derived from stressed cultured granulosa cells can shuttle protective messages in the form of miRNA and mRNA or proteins, which upon supplementation *in vitro* induce tolerance to recipient cells following exposure to recurrent thermal stress (Gebremedhn *et al.* 2020*b*). Among the miRNAs enriched in the EVs released from granulosa cells subjected to heat stress are the miR-1246, miR-2904, and miR-374a, which are predicted to coordinately target endoplasmic reticulum genes.

Through its dynamic nature in its luminal fluid composition, the oviduct is an active organ that provides an optimal microenvironment for gamete maturation/activation, fertilisation, and cleavage-stage embryo development (Coy *et al.* 2012). Several studies indicated the functional variation of oviductal EVs collected from different parts of the oviduct. Supplementation of bovine oviductal EVs collected from the isthmus, but not the ampulla, in the embryo culture positively affect the embryo development (Lopera-Vasquez *et al.* 2017). This implies that oviductal EVs produced from different regions of the oviduct carry specific molecular signals associated with specific function in supporting gamete and embryo development. This may be associated with the distribution of ciliated and secretory cells in different regions of the oviduct (Harris *et al.* 2020). This needs to be experimentally validated in future studies. Comparative analysis of the proteome of EVs derived from *in vivo* oviductal fluid and *in vitro* cultured oviductal epithelial cells revealed significant differences (Almiñana *et al.* 2017). In that study, fewer proteins were identified *in vitro* derived oviductal EVs (222) compared to those derived from the *in vivo* counterparts (270). The impact of supplementation of oviductal EVs *in vitro* culture environment has been evidenced to positively impact sperm activation, prevention of polyspermy, and early embryo development (Machtinger *et al.* 2016). The data presented in this review also suggest the potential application of oviductal EVs in the current ART to mimic the *in vivo* oviductal environment.

In the present review, the current knowledge on EVs research in reproduction mainly associated with ovarian functionality, gamete–embryo–oviductal communication, and EVs molecular signalling as indicators of environmental and physiological stress conditions are thoroughly discussed and the future potential of EV research in reproduction will also be highlighted.

EVs biogenesis, composition and uptake mechanisms

Extracellular vesicles are a group of heterogenous and membrane-bounded structures released from a variety of cell types *in vivo* in biological fluids or *in vitro* in spent culture media. They have the capacity of transporting various active biomolecules from cells of origin to target recipient cells, thereby modulating the physiology of the recipient cells (Ofir-Birin *et al.* 2018). Of these three different types of EVs, the majority of interest falls on the microvesicles and exosomes, while the apoptotic bodies are often considered as products of cell death (María *et al.* 2015). The apoptotic bodies are released when plasma membrane bedding occurs during apoptosis, but microvesicles, which are relatively heterogenous population pinch directly off the plasma membrane. Exosomes, which are intraluminal vesicle contained in multivesicular bodies, are relatively homogenous in size. Exosomes are released to the extracellular space upon fusion of the multivesicular bodies (MVBs) with the plasma membrane (Colombo *et al.* 2014). Despite the fact that initially exosomes were considered to be alternative mechanisms to eliminate waste products from cells interior to maintain cellular homeostasis (Baixauli *et al.* 2014), a significant number of studies have provided evidence that following the release from the cell surface, exosomes can interact with the extracellular matrix or induce cellular response within a specific microenvironment or in distant cells. These evolutionary conserved vesicles are known to exert essential physiological and pathological effects on both recipient and parent cells, via a variety of functional molecules either as structural or cargo components. Currently, because of the absence of widely acceptable specific markers to distinguish exosomes and

microvesicles, consensus has been reached to name both with the generic name EV.

In mammals, EVs have been isolated from diverse body fluids, including blood, urine, saliva, breast milk, amniotic fluid, ascites, cerebrospinal fluid, bile, and semen. These vesicles have been named based on their origin, nature and features in many different ways. Many different names have been used in publications depending on their size [with a prefix micro or nano: microparticles, microvesicles (MVs), nanovesicles, nanoparticles], their tissue of origin (prostasomes, oncosomes), their proposed functions (calcifying matrix vesicles, argosomes, tolerosomes), or simply their presence outside the cells (prefix exo or ecto: ectosomes, exosomes, exovesicles, exosome-like vesicles). Despite the fact that nomenclature of EVs is still under debate (Stephen and Graça 2013), several marker proteins are being used to prove the identity of the vesicles isolated using various techniques including ultracentrifugation and size exclusion chromatography. The protein composition of EVs reflects proteins integrated in or attached to their membrane or those present in their luminal space. Although exosome and microvesicles have different protein profiles due to their different biogenesis pathways, so far no specific protein has been identified to accurately discriminate between the two vesicle populations. This coud partially be due to the fact that plasma membrane-derived EVs and endosome intraluminal vesicles (ILVs) share important features as they bud away from the cytosol in contrast to other intracellular budding events that are required for trafficking between different compartments. Thus, their membrane orientation is identical to that of the cell surface, exposing the extracellular domains of the transmembrane proteins and enclosing cytosolic components. The protein composition of exosomes as components of EVs demonstrated exosmones are enriched with proteins associated with their biogenesis pathway (Villarroya-Beltri *et al.* 2014). This was further validated by the fact that compared to their cells of origin EVs are enriched with various components of the endosomal sorting complex for transport (ESCRT) machinery and its accessory proteins. The most common exosomal proteins represent those that are associated with membrane transport and fusion and others including cytoskeletal, metabolic, signalling and carrier proteins (Ibrahim and Marbán 2016). The classical biogenesis of exosomes is the most studied one. This classical process of exosome biogenesis involves the inward budding of the plasma membrane and the formation of intracellular MVBs containing ILVs (Kalluri and LeBleu 2020). This most recognised and studied pathway of exosome biogenesisis is driven by ESCRT complexes. The ESCRT is a family of proteins that associate in complexes at the membrane of MVBs to sort cargo and the formation of ILVs (Hanson and Cashikar 2012), which are secreted as exosomes through MVB fusion to the plasma membrane and exocytosis.

The biogenesis of exosomes *in vivo* is a complex process which involves several proteins including Ras-related protein GTPase Rab, Systenin-1, TSG101, Alix, syndecan-1, ESCRT proteins, phospholipids, teteraspanins, ceramindes, sphingomyelinases and SNARE complex proteins (Simon *et al.* 2018). Several factors including cell type, culture conditions and the physiological status of the cells are known to determine which putative key regulators of exosome biogenesis will be activated *in vivo* (Mathieu *et al.* 2019). As most studies reported mainly focused on the potential function of extracellular vesicles rather than on their origins, it is still unclear which sub-species of vesicles is responsible for a given physiological or functional effect.

Through the EV-mediated cell-to-cell communication, several bioactive molecules are transferred to recipient cells, which may have a significant impact on the phenotype of the recipient cell. These phenotypic changes can be regulation of gene expression through de novo translation and post-translational regulation of target mRNAs (Valadi *et al.* 2007), and changes in miRNA level during stress response (Jacobs *et al.* 2013; Sohel *et al.* 2013; Gebremedhn *et al.* 2020*b*). Due to their structural composition EVs can protect their cargo molecules from enzymatic degradation during their transit through extracellular environments (Keller *et al.* 2011). This capability of EVs signifies their potential conversion to vehicles for delivery of therapeutic proteins, RNA and drugs (Alvarez-Erviti *et al.* 2011; Tang *et al.* 2012). For this, EVs need to interact with the recipient cells in several uptake mechanisms (Mulcahy *et al.* 2014). Both direct and indirect evidence suggests that EVs internalised into recipient cells. Direct visualisation using flourescent lipid membrane dyes is the most common way for detecting EV uptake. Some of these dyes include PKH67, PKH26, rhodamine B (also called R18), DiI and DiD, which are lipophilic and other membrane permeable chemical compounds are also available including carboxyfluorescein succinimidyl ester (CFSE) and 5(6)-carboxyfluorescein diacetate (CFDA) (reviewed by Mulcahy *et al.* 2014).

Extracellular vesicles can be uptaken by recipient cells in a variety of endocytic pathways, including clathrin-mediated endocytosis and clathrin-independent pathways such as caveolin-mediated uptake, micropinocytosis, phagocytosis and lipid raft-mediated internalisation. The choice of uptake mechanism used by a specific EV depends on molecular components especially proteins and glycoproteins present on the surface of the EVs and the recipient target cells (Horibe *et al.* 2018). The significant role of the protein components in EV-recipient cell interaction has been validated by Proteinase K treatment of EVs, which has shown to reduce their uptake in ovarian cancer cells (Escrevente *et al.* 2011). Among the several proteins playing a role in EV uptake by recipient cells include tetraspanins, which are membrane proteins involved in various processes including cell adhesion, motility, activation and proliferation (Hemler 2005). Tetraspanins are known to be present on EV surfaces suggesting their role in EV function. Among those CD9 and CD81, which are known to be well-established markers of EVs are reported to be

involved in oocyte-spermatozoa and phagocyte fusion as reviewed by (Mulcahy *et al.* 2014). The significant role of tetraspanins in EV uptake by recipient cells has been evidenced by reduced EV uptake after treatment of recipient cells with antibodies against the CD81 or CD9 (Morelli *et al.* 2004).

Clathrin-mediated endocytosis (CME), which involves internalisation of molecules through progressive and sequential assembly of clathrin-coated vesicles containing a range of transmembrane receptors and their ligands, has been reported to be one of the mechanisms in EV uptake by recipient cells. For example, treatment of cells with chlorpromazine (CME inhibitor) resulted in decreased uptake of EVs by ovarian cancer recipient cells (Escrevente *et al.* 2011). Similarly, clathrin-mediated endocytosis was found to be the dominant EV uptake pathway in the uptake of syncytiotrophoblast extracellular vesicle by endothelial cells (Cronqvist *et al.* 2020).

Extracellular vesicles in the follicular microenvironment

Initially, described in the late 1980s from the endosomal pathway, EVs were viewed solely as a discarding mechanism for membrane proteins with little to no understanding of their wide range, functional outcome as a conveyor of cellular information (Raposo and Stoorvogel 2013). More recently, EVs natural role in genetic information transfer as carriers of bioactive molecules has propagated their substantial interest as agents for multidirectional crosstalk (Valadi *et al.* 2007). The increasingly investigated phenomenon of the bidirectional communication of EVs can be summed up directly through gap junctions (GJ)/transzonal projections (TZPs) as well as indirectly through various endocrine, paracrine and autocrine signalling pathways (Bosco *et al.* 2011). EVs are known to be acted on by Rab GTPases (Rab 27a/Rab 27b) to promote their secretion and release (Ostrowski *et al.* 2010), which can be validated through the enrichment of protein markers like CD63 and ALIX. Once released into the extracellular space, EVs potential mediation of cellular communication is initiated but not limited to receptor–ligand interactions or even fusion with the target cells membrane to initiate the off-loading of cargo, thereby adjusting the physiological existence of the target cell (Tkach and Théry 2016).

The follicle microenvironment consists of the oocyte and subsequent somatic cells, as well as a variable volumes of follicular fluid based on the maturity of the follicle and derived primarily from circulating plasma (Fortune 1994). The bidirectional crosstalk between the oocyte and granulosa cells is dependent on a functional network of gap junctions thought shuttle factors like proteins (insulin) and hormones (progesterone (P4) and oestradiol (E2)) (O'Shea *et al.* 2012) necessary for proliferative development (Brower and Schultz 1982). Communication intricacies between the oocyte and subsequent somatic cells have added a supplementary layer of bidirectional crosstalk inducing principal processes like folliculogenesis and meiotic resumption, ultimately leading up to and past early embryonic development (Senbon *et al.* 2003). A fundamental point of interest currently being evaluated, is the precise molecular content of EVs and the method of molecular transmission mediating cell-to-cell communication. In bovines, it has been shown that follicular fluid (FF) EVs induce the proliferative capacity of granulosa cells to act on the oocyte through Src, PI3K/Akt and MAPK signalling pathways (Hung *et al.* 2017). Nevertheless, the functional effects noted through increased expression of cumulus expansion marker genes, cultivates such communication within the follicle microenvironment (Da Silveira *et al.* 2012). The novelty of this finding stems from potentially modulating the developmental competence of oocytes matured *in vitro* by mimicking the *in vivo* LH-surge through EV co-incubation (Conti *et al.* 2012). Interestingly, granulosa cells have the ability to preferentially uptake EVs based on the follicle size, eluding to a differential cargo composition associated with dominant and subordinate follicle size (Hung *et al.* 2015). Dually noted as prime carriers of bioactive molecules, extra-cellular miRNAs have emerged as a key proponent loaded within EVs. In fact, expression of variable miRNA profiles has been eluded too in humans (Santonocito *et al.* 2014), bovine (Sohel *et al.* 2013) and equine (Da Silveira *et al.* 2012). As transporters of differing miRNA profiles, FF EVs are harnessed with direct targets to mitigate pathways associated with follicular growth and oocyte maturation, such as the wingless signalling pathway (WNT), transforming growth factor beta (TGF-β), mitogen activated protein kinase (MAPK) and epidermal growth factor receptor (ErbB) (Sohel *et al.* 2013). Interestingly in bovines, miR-640, miR-526b* and miR-381 were abundantly present in theca cells versus miR-373, miR-30e* and miR-19b-1* being expressed more in cumulus oocyte complexes (COCs) (Sohel *et al.* 2013). This in fact signifies that differentially expressed miRNAs can be dependent on indicators relevant to basic origin and physiological status, suggesting the ability to pinpoint relative miRNAs via cause and effect relationships associated with reproductive misfunction.

EV-mediated sperm capacitation

Ejaculated sperm must pass through the female reproductive tract in order to fertilize an egg. During this transition through the female reproductive track there will be removal of seminal plasma components and exposure to the reproductive tract secretions. Despite the short period, this process is critical for inducing sperm capacitation, which involves an increase of the membrane structure and fluidity due to a removal of cholesterol from the sperm plasma membrane and increase of sperm intracellular calcium and bicarbonate ion permeability

(Burton and McKnight 2007). These modifications are associated with induction of the tyrosine phosphorylation of a subset of sperm proteins, which is mediated by the cyclic AMP (cAMP)-dependent protein kinase A (Visconti and Kopf 1998). Supporting a role of the uterine cells in sperm capacitation, human spermatozoa co-incubated with endometrial cell-conditioned medium showed an increase in protein tyrosine phosphorylation (Laflamme *et al.* 2005). The first exposure of spermatozoa with reproductive tract EVs start in the vagina, where vaginosomes (EVs present in the vaginal luminal fluid) come in contact with the ejaculated sperm, which could have an effect on its functionality. Enhanced progesterone-induced acrosome reaction could be induced by exposure for 30 min to vaginosomes in non-capacitating condition (Fereshteh *et al.* 2019). In the same study the coincubation of spermatozoa with EVs derived from vaginal luminal fluids results in elevation of cells with highest expression of sperm adhesion molecule 1 (SPAM1), PMCA1/4 and PMCA1 compared to those incubated in phosphate buffered saline solution. A significant level of PCMA4, which is a membrane protein involved in the Ca^{2+} efflux pump in murine sperm, was detected in the EVs derived from murine vaginal, oviductal and uterine luminal fluid and the flow cytometry analysis of caudal sperm incubated with luminal fluids EVs showed increased expression of PMCA4a, which demonstrated the *in vitro* uptake of luminal EVs by sperm (Al-Dossary *et al.* 2013). The coincubation of human spermatozoa in the presence of uterosome-like vesicles derived from conditioned media of endometrial epithelial cells resulted sperm capacitation as determined by the increase in the level of induced acrosome reaction and induction of protein tyrosine phosphorylation (Franchi *et al.* 2016). A similar study in humans revealed that spermatozoa can internalise EVs released from cultured primary endometrial cells and result in sperm capacitation and acrosome reaction as manifested by increased protein tyrosine phosphorylation (Murdica *et al.* 2020). EV internalisation was successfully blocked by incubation with filipin suggesting that an energy-dependent process probably attributable to the lipid-raft domain mediated-endocytosis to be the main mechanism of EV uptake by the spermatozoa.

EVs: insightful index for physiological status

Stress negatively affects reproductive efficiency, which is seen through an imploding decline in mammalian fertility and overall decrease in livestock productivity. *In vitro* culture systems have been extensively utilised in attempts to mimic both environmental and metabolic stressors believed to have deleterious effects on oocytes, fertilisation, preimplantation, and embryonic development (Edwards and Hansen 1996; Rivera and Hansen 2001). Extracellular miRNAs have also more recently been outlined for their potential role as disease biomarkers, or molecules used for detecting disease/prognosis progression (Galimberti *et al.* 2014; Hailay *et al.* 2019). Found in most biological fluids, and recognising the stability and ease of access to obtain samples, changes in circulating miRNA profiles have been noted in human and mice studies correlated to obesity (Can *et al.* 2016; Castaño *et al.* 2018), type 2 diabetes (Kong *et al.* 2011; Higuchi *et al.* 2015), ageing (Kirkman *et al.* 2012; Dhahbi *et al.* 2013; López-Otín *et al.* 2013), polycystic ovarian syndrome (PCOS) (Hu *et al.* 2020) and various female reproductive cancers (Liang *et al.* 2013; Che *et al.* 2020; Lv *et al.* 2021). For instance, EVs preferentially loaded with obesity-related miRNA mimics (miR-122, miR-192, miR-27a and miR-27b) and repeatedly injected into lean mice, developed a profound insulin resistance and dyslipidemia, eluding to these specific miRNAs role in indicating the pathophysiology of obesity and potential links to type 2 diabetes (Castaño *et al.* 2018). Commonly associated with a multi-faceted downregulation in propagating miRNA, specific indications like miR-125b, miR-342; miR-133b, miR-214 are proposed in correlation to neurodegenerative diseases like Alzheimer's and Parkinson's diseases (Galimberti *et al.* 2014; Cheng *et al.* 2015; Dong *et al.* 2016; Rosas-Hernandez *et al.* 2018). Alternatively, a massive prevalence affecting female infertility is the reproductive abnormality known as Polycystic Ovarian Syndrome (PCOS), whose mechanism of action has yet to be full elucidated. Although, in more recent times, extracellular circulating miRNAs have been analyzed from PCOS follicular fluid at differential expression levels. Furthermore, increased expression levels of miR-146a-5p and miR-126-3p have been dually noted as a direct target of the MAPK and TGF-β signalling pathways, essential for reproductive function (Che *et al.* 2020; Jiang *et al.* 2021). Overall, this suggests that the EVs role in detailed cell-to-cell communication is essential, not only as an indicator of origin, but also as a potential biomarker for various pathophysiological conditions as illustrated in Fig. 1.

EV-mediated signalling during oviduct/uterine-embryo communication

Following ovulation, the oocyte goes to the oviduct for fertilisation and subsequent cleavage stage development. The process of sperm capacitation and fertilisation and early stage cleavage of mammalian embryos is supported mainly by secretions of the oviduct, which are complex and contain growth factors, hormones, proteases, antioxidant proteins, immune system proteins, metabolites, lipids and heat shock proteins (Avilés *et al.* 2010; Coy *et al.* 2012). For this, the oviductal epithelium, which is composed of ciliated and secretory cells, is involved in the secretion of oviductal fluid that has an important role in gamete maturation, fertilisation and embryo developmental competence (Leese *et al.* 2008;

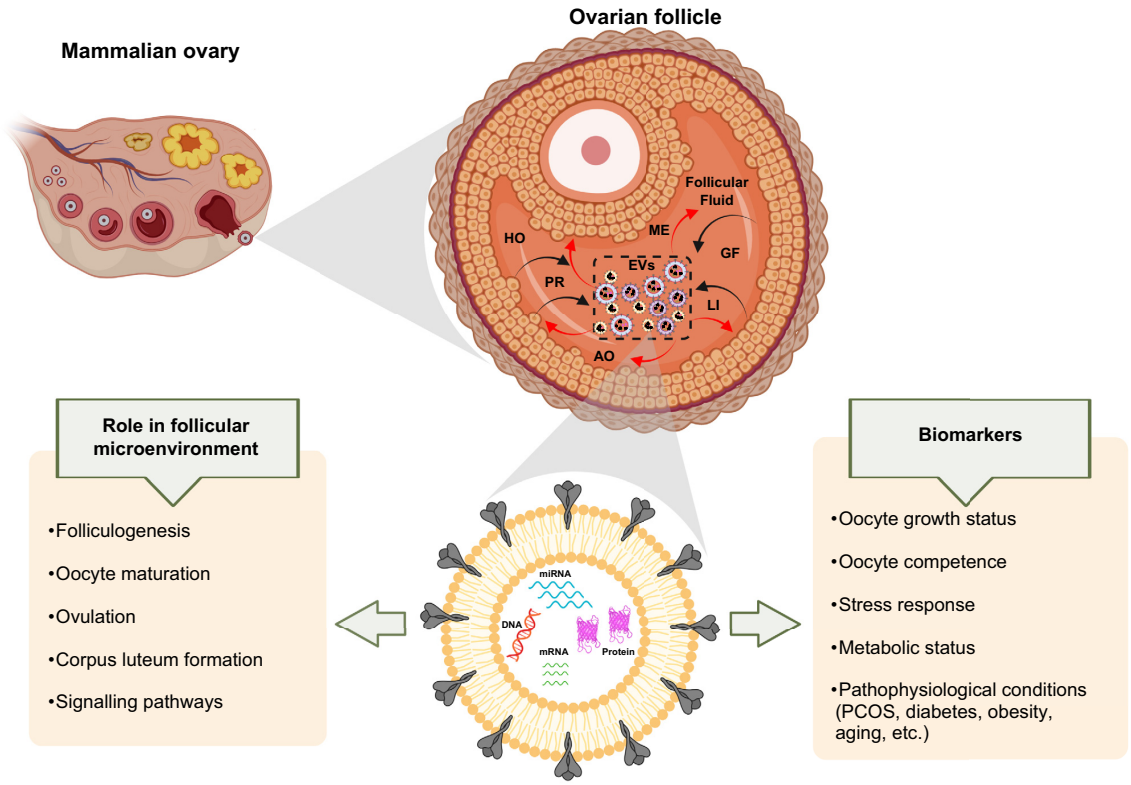


Fig. 1. Extracellular vesicle mediated molecular signalling in the ovarian follicle. Schematic representation of extracellular vesicles within the follicle microenvironment, a key proponent of bidirectional crosstalk inducing oocyte growth and maturation, and subsequent physiological index to stress and pathophysiological conditions. Extracellular vesicles serve a mass transit mechanism for bioactive cargo such as miRNA, mRNA, proteins, lipids and metabolites, inducing the proliferative capacity of granulosa cells to act on the oocyte through various signaling pathways (EVs, extracellular vesicles; HO, hormones; PR, proteins; AO, antioxidants; ME, metabolites; GF, growth factors; LI, lipids).

Avilés *et al.* 2010). Considering their implication for important events in female reproduction including fertilisation, early embryo development and implantation, research in the field of intercellular communication in the oviduct and uterine environment has increased exponentially in the last years. During *in vivo* development the embryo interacts with the surrounding cells in the oviduct and uterus to survive and develop to term (Fazeli 2011). Among the various components of the oviductal fluid, EVs are identified for the first time in murines being designated as oviductosomes (Al-Dossary *et al.* 2013) and found to mediate embryo and maternal communication (Cruz *et al.* 2018). The beneficial role of EVs in carrying molecular signals during embryo maternal communication has been evidenced by the fact that EVs from the *in vivo* oviductal fluid and from conditioned media of bovine oviductal epithelium cells showed a positive impact on embryonic development *in vitro* (Lopera-Vásquez *et al.* 2016; Almiñana *et al.* 2017; Sidrat *et al.* 2020; Asaadi *et al.* 2021).

So far, several studies have been conducted focusing on the oviductal fluid EVs in relation to the stage of ovarian cyclicity and the site in the oviduct or EVs secreted by cultured primary oviductal cells. Deciphering the oviductal EV content at different stages of the oestrous cycle including post-ovulatory stage, early luteal phase, late luteal phase and preovulatory stages revealed the content of EVs (miRNAs, rRNA fragments, tRNA fragments, snRNA, snoRNA and other ncRNA) to be under steroid hormone regulation (Almiñana *et al.* 2018). In that study major differences were observed between post-ovulatory and the rest stages analyzed. Very interestingly, miR-34c and miR-449a, which are known to be involved in defective cilia in the oviduct and associated with infertility, are among the differentially abundant miRNAs. The hormonal regulation of EV content has also been evidenced by the differential protein profile between *in vivo* derived oviductal fluid EVs and those EVs secreted by bovine oviductal epithelial cells culture *in vitro* (Almiñana *et al.* 2017). A similar study in sheep also indicated that the amount of EVs

in the uterine lumen increased after P4 treatment suggesting that P4 may be involved in regulation of the release of EVs from endometrial epithelial to the uterine lumen (Burns *et al.* 2018). On the contrary, in addition to provision of lipids for cellular growth in elongating conceptus, EVs in the uterine lumen fluid may also be involved in conceptus production of prostaglandins (Burns *et al.* 2018).

Due to the lack of the female reproductive tract, embryos cultured *in vitro* are under suboptimal conditions leading to lower blastocyst and pregnancy rates (Pontes *et al.* 2009). However, embryos are known to support each other during group culture by secreting autocrine factors which act upon the embryo itself or on neighboring embryos (O'Neill 2008). Therefore, culturing embryos in groups has been found to improve embryo developmental rates and quality in various mammalian species, including cattle (Donnay *et al.* 1997; O'Doherty *et al.* 1997), pigs (Stokes *et al.* 2005), and humans (Almagor *et al.* 1996; Ebner *et al.* 2010). The importance of autocrine factors for embryo survival and development is evidenced with the development of the well-of-the-well system, which has been successfully applied in bovine (Hoelker *et al.* 2010), porcine (Taka *et al.* 2005), mouse and human (Vajta *et al.* 2008) embryos. In an attempt to compensate the missing signalling factors from the reproductive tract several studies have been performed to investigate the role of coculture of bovine oviductal epithelial cells, cumulus cells and granulosa cells as reviewed by (Wydooghe *et al.* 2017). The preimplantation embryos are able to secrete the autocrine embryotropins in several ways including active secretion, passive outflow or extracellular vesicles as molecular cargo vehicles. The role of extracellular vesicles in this inter embryo communication has been evidenced in bovine embryos (Pavani *et al.* 2019). In support of this, fluorescent labelled EVs were found to be taken up by embryos passing through the glycoprotein layer zona pellucida in bovine (Pavani *et al.* 2019) and porcine (Saadeldin *et al.* 2014) preimplantation embryos. Recently, the study conducted by (Burns *et al.* 2018) demonstrated that EVs isolated from the media conditioned by cultured ovine Day 14 conceptuses can be up taken by uterine epithelium, but not by other maternal tissues including the ovary, corpus luteum, parametrial lymph nodes or lung, thus serve as a novel form of intercellular communication during the establishment of pregnancy. Proteomic analysis of conceptus secreted EVs revealed the presence of 231 proteins representing those as structural components of EVs and the majority involved in various signalling pathways associated with pregnancy establishment (Burns *et al.* 2016).

Extracellular vesicles have been identified in the uterine lumen of various species including cattle, sheep, human, pigs and mice (Ng *et al.* 2013; Vilella *et al.* 2015; Greening *et al.* 2016). The EVs in the uterine luminal fluid are likely to have originated from both the luminal epithelium and the glandular epithelium of the uterus (Racicot *et al.* 2012). The beneficial role of uterine lumen fluid derived EVs in conceptus elongation was evidenced recently (Burns *et al.* 2018). The way of transmission of EVs to elongated embryos is postulated to follow the mechanisms of direct fusion resulting in provision of lipids, RNA, and proteins cargo and results in stimulation of conceptus elongation via regulation of gene expression. Labelled EVs isolated from the ovine uterine fluid, transferred to ovine trophectodermal cells *in vitro* within 2 h of co-incubation, resulted in both increased proliferation and release of interferon τ (the ovine pregnancy recognition signal) in a dose dependent manner (Ruiz-González *et al.* 2015). In the same study, uterine flushing EVs from cyclic and pregnant ewes revealed the presence of mRNAs for enJSRV-ENV, HSC70, interleukins, and interferon (IFN)-regulatory factors. MicroRNAs 21 and 29a which were found to be present in EVs from the uterine luminal fluid of Day 14 cyclic and pregnant sheep (Burns *et al.* 2014), are known to activate the TLR 7/8 (Fabbri *et al.* 2012). Therefore, EVs in the uterine lumen fluid from the uterine epithelium may be involved in stimulation of IFNT production and subsequent conceptus growth via TLR activation.

Despite substantial differences in EV content depending on the anatomical and functional differences between different parts of the oviduct and stage of the oestrous cycle (Almiñana *et al.* 2018; Gatien *et al.* 2019), oviductal proteins are found to be enriched with proteins of protective properties including heat shock proteins and proteins associated with oxidative stress response, which may shuttle these protective messages to the embryos to provide protection against environmental or physiological stressors as a positive by-stander effect as observed in bovine granulosa cells (Gebremedhn *et al.* 2020*b*). Several studies have evidenced that supplementation of oviductal EVs to *in vitro* cultured embryos enhances the viability and developmental capacity of embryos by modulating the molecular composition and physiology of the embryos. Recent study in rabbits has demonstrated that the oviductal fluid which is enriched with melatonin could reduce reactive oxygen species (ROS) accumulation, 5-methycytosine (5-mC) and increase in blastocysts rate after supplementation *in vitro* (Qu *et al.* 2020). In the same study, supplementation of the combination of EVs and melatonin led to similar results as well as a significant decrease in the apoptosis index and increase in inner cell mass (ICM)/trophectoderm (TE) index. Supplementation of bovine oviductal fluid and/or uterine fluid in a stage specific manner *in vitro* at a level of 1.25% resulted in increased blastocyst rate, upregulation of genes related to epigenetics (DNMT3a and IGF2R), and reduced accumulation of ROS compared to those cultured with SOF + FCS (Hamdi *et al.* 2018). The positive contribution of EVs from oviductal fluid derived from ampillary or isthmus of the oviduct to early embryo development *in vitro* has been reported (Lopera-Vasquez *et al.* 2017). In that study, supplementation of oviductal EVs resulted in increased survival rate of blastocysts following cryotolerance. Moreover, gene expression analysis of the resulting blastocysts showed elevated expression of water

channel AQP3 and DNMT3A and SNRPN transcripts. Similarly, the supplementation of EVs derived from conditioned media of cultured bovine oviductal epithelial cells had no effect on blastocyst yield however, increased trophectoderm cells and modulation of the expression of developmentally related genes (Lopera-Vásquez *et al.* 2016). The positive impact of bovine oviductal epithelial cells conditioned media and EV supplementation *in vitro* cultured bovine embryos evidenced that molecular signals carried by EVs in conditioned media play the major role in providing factors missing in the *in vitro* environment.

Involvement of EVs in mediating stress coping mechanisms during mammalian follicular development

Throughout the productive lifespan, dairy and beef cows are exposed to several exogenous and endogenous sources of stress, which pose detrimental impacts and contribute to the significant disruption in the physiology of reproduction. Among the key stressors, environmental stressors, including oxidative, heat, cold, and others (Li *et al.* 2016; Saeed-Zidane *et al.* 2017; Baddela *et al.* 2018) and endogenously generated stressors due to the disruption of the various metabolisms (Beam and Butler 1997), are widely reported to impair female reproductive physiologies.

One of the greatest achievements of the past five to six decades in animal farming is the advancements in setting the breeding goals and the intensive selection of farm animals for traits of interest with huge economic implications. For this, the incorporation of genetic scores (i.e genomic selection) into the breeding program and selection procedures has facilitated the genetic gains in a very short period (Meuwissen *et al.* 2001). It has been reported that the intensive selection of cows for higher milk yield has resulted in a significant increment in the net amount of yields produced. Nevertheless, a concomitant compromise in the reproductive performance traits is reported, which shades negative consequences to the profitability of farms due to increased culling of less fertile cows in dairy farms (Lucy 2001). It has been reported that the deteriorating reproductive performance of dairy cows is associated with the higher milk yield per cow, which could be attributed to the antagonistic relationship between the fertility and production traits of dairy cows (Hansen 2000). Exposure of cows to both environmental and metabolic stressors are reported to affect the ovarian functions mainly, the steroidogenic capacity of the follicles, leading to disruption of the oestradiol production capacity of the dominant follicle, which in turn impair ovulation and subsequent postovulatory processes (Wolfenson *et al.* 1997; Roth *et al.* 2001), reduce the developmental competence of the oocyte and the capacity to reach the blastocyst stage (Roth and Hansen 2005; Nabenishi *et al.* 2012). One of the fundamental impacts of exposure to both metabolic and environmental stressors is the disruption of intrafollicular bidirectional communication between the follicular cells and the corresponding oocyte. The presence of EVs in the follicular fluid of cows has been reported to be associated with the developmental competence of the oocyte (Sohel *et al.* 2013). Thus, the exposure to stressors could modify the content of the bioactive molecules encapsulated in the EVs and could also serve as reflectors of the stress exposure. The specific impact of the environmental and metabolic stressors in the cargo of the EVs is discussed below.

EV-mediated molecular signaling during thermal stress

Summer heat stress is reported to negatively affect the maturation of oocytes, growth, and steroidogenesis of follicular cells, the development of the corpus luteum, and the receptivity of the maternal endometrium (Roth *et al.* 2001; Roth and Wolfenson 2016). Oocytes collected during the summer period are reported to have impaired microtubule rearrangements and deformed spindle apparatus, which disrupt the nuclear maturation and reduce the fertilization rate (Roth and Hansen 2005; Nabenishi *et al.* 2012). In addition, oocytes collected during the summer season are shown to have a higher level of oxidative stress and apoptosis, which is attributed to the lower mitochondrial distribution (Roth 2017). Previously, we showed that bovine granulosa cells subjected to heat stress trigger the expression of heat shock proteins (HSP), mainly the HSP70 and HSP90 accompanied by excessive accumulation of reactive oxygen species (ROS) and reduced viability of cells (Alemu *et al.* 2018). A similar phenomenon is also reported in other studies that the HSP70 is among the significantly enriched member of the HSPs and apoptosis is induced by the activation of the endoplasmic reticulum and production of excessive ROS (Hou *et al.* 2014; Li *et al.* 2016). One of the widely discussed benefits of EVs is their involvement in releasing cellular toxicants into the extracellular space (Kosaka *et al.* 2013). This was previously shown that EV-mediated pathway is the prime cause of the intracellular β-catenin pool reduction (Chairoungdua *et al.* 2010), which suggests the crucial role of EVs in selectively encapsulating and releasing cellular contents to maintain cellular hemostasis.

In line with this, the elevated cellular reserve of HSPs is also reflected in the EVs released from cells subjected to heat stress and are involved in improving the immune-related cellular responses (Lancaster and Febbraio 2005; Zhan *et al.* 2009). The release of EVs enriched with HSP from cells subjected to heat stress shows that EVs could be considered as the reflectors of the cellular stress conditions (de Maio 2011). EVs of heat-stressed cells pose a bystander effect to the unstressed neighbouring recipient cells, which is reflected by the reduced rate of apoptosis and DNA damage in the recipient cells (Bewicke-Copley *et al.* 2017). In addition, the result demonstrated that EVs from heat-stressed cells have

the potential to protect cells from subsequent heat stress. Recently, we reported the EV-mediated transfer of protective bioactive molecules in bovine granulosa cells (Gebremedhn *et al.* 2020*b*). In the same study, granulosa cells subjected to heat stress release a significantly higher number of EVs enriched with HSPs, antioxidants, and GRPs compared to the cells incubated at normal temperature. Among the other components of the stressed EVs, bta-miR-1246, bta-miR-374a, and bta-miR-2904 are abundantly present, from which the miR-1246 is also reported to be among the miRNAs abundantly present in the circulation of dairy cows subjected to summer heat stress (Zheng *et al.* 2014). Moreover, we showed that prior priming of granulosa cells with the EVs derived from granulosa cells subjected to heat stress transferred protective molecules to the recipient cells against subsequent heat stress, in which the stress EVs supplemented cells had a significantly lower accumulation of intracellular ROS, improved cell viability and reduced level of apoptosis. The most interesting finding of this experiment is that the protective impact of the stressed EVs is pronounced only when the primed cells are subjected to recurrent heat stress (Gebremedhn *et al.* 2020*b*). This suggests, the stress condition at the receiving end determines the type of role that is incurred by the uptaken EVs. Recently, we looked deeper into our recently published data, which is the expression of miRNAs and the dynamics of the abundance of miRNAs between the cells and the corresponding EVs upon exposure to heat stress and we showed that there is no single pattern of release of miRNAs into the extracellular space, rather multiple patterns depending on the cellular function of the miRNAs, which are preferentially enriched upon exposure to stress (Gebremedhn *et al.* 2020a). Similarly, the beneficial effect of EVs derived from the follicular fluid of cows is also reported in reversing the heat stress damage incurred on oocytes and further improved both the cleavage and blastocyst rates (Rodrigues *et al.* 2019). The most intriguing fact of this finding is that supplementation of both whole follicular fluid and only EVs derived from the same follicular fluid samples showed to have a positive impact in reversing the heat damage on oocytes. Nevertheless, supplementation of follicular fluid devoid of the EVs had not reversed the heat stress damage. This signifies that EVs in the follicular fluid are the major players of a crucial role in protecting oocytes from heat stress and enhance oocyte maturation and function.

EV-coupled molecular cargo as indicators of metabolic stress

Over the past decades, dramatic changes in the amount of milk produced per cow as a result of combined effects of genetic selection for milk yield, improvements in the management of dairy farms, and nutrition are some of the key achievements in the sector. Nevertheless, this dramatic shift in milk yield has caused a significant decline in reproductive efficacies (Lucy 2001). One of the key aspects of the fertility decline in high-yielding dairy cows is attributed to the imbalances in the energy intake and expenditure, which causes post-partum negative energy balance (NEB) (Beam and Butler 1999). The unfavourable metabolic changes in post-partum cows under NEB impairs follicular development and the developmental competence and quality of the enclosed oocytes (Walters *et al.* 2002). In addition, downregulation of genes associated with proliferation and steroidogenesis potential, which indicates the impaired maturity of oocyte was reported in granulosa cells derived from the early postpartum period. Interestingly, the p38 mitogen-activated protein kinase pathway is one of the downregulated pathways, which is affected by vitamin A availability, suggesting the important role of vitamin A supplementation in mitigating postpartum NEB (Golini *et al.* 2014). To tackle the early postpartum energy deficit, high-yielding dairy cows mobilise their adipose tissue reserve, which in turn causes elevation of free fatty acids (FFA) in the circulation (Contreras and Sordillo 2011). The quality of the oocyte and granulosa cells of early postpartum cows is affected by the composition of the follicular fluid and serum, which is characterised by elevated concentration of non-esterified fatty acid (NEFA) and β-hydroxybutyrate (BHB) concentrations (Leroy *et al.* 2004). The circulation of cows under NEB is reported to have significantly elevated NEFA, mainly the stearic acid (C18:0), palmitic (C16:0), and oleic acid (C18:1) (Rukkwamsuk *et al.* 2000). The toxic effect of NEFA during follicular development was further verified in an *in vitro* granulosa cells culture, in which the proliferation was significantly reduced and the rate of apoptosis was significantly higher upon treatment with both the palmitic and oleic acids (Vanholder *et al.* 2005). The content of the EVs in cows' circulation could also be affected by the postpartum energy status.

To examine this, recently we experimented on early lactating dairy cows with divergent metabolic status. For this, sequential follicular fluid and oocyte aspiration was performed in cows from the fifth to the tenth weeks postpartum. The energy status of the cows was assessed by profiling the concentration of the NEFA and BHB. The expression of the miRNAs release via EVs was assessed and it was found that the miRNA profile of EVs released from cows under NEB showed massive deregulation and cows under positive energy balance have a similar expression of miRNAs in the EVs released from the follicular fluid of transient cows (Hailay *et al.* 2019). The miRNAs that are persistently downregulated in the EVs of cows under NEB, including the miR-132, miR-451, miR-486 and miR-874 and miR-2285 are predicted to be involved in biological pathways associated with ovarian function including the TGF-β signalling, lysine degradation, cell cycle, FOXO signalling, mTOR signalling and others. The difference in miRNAs of the follicular fluid EVs is also reflected in the epigenome profile of the corresponding oocytes, which showed massive differentially methylated regions (DMRs) in oocytes derived from NEB

cows compared to cows under positive energy balance (Poirier *et al.* 2020). Interestingly, among the differentially methylated genomic regions in the oocyte of early potpartum cows, we found genes involved in important pathways including carbon metabolism, and fatty acid metabolism. Moreover, oocytes of postpartum cows are differentially methylated in some imprinted genes namely, MEST and GNAS suggesting the impact of postpartum NEB on the acquisition of imprinting.

EV-mediated cellular response to oxidative stress

Oxidative stress is a phenomenon, which is caused when the production of ROS overwhelms the cellular production of antioxidants that scavenge the ROS (Burton and Jauniaux 2011). However, it is worth mentioning that a moderate level of ROS production is necessary for maintaining cellular homeostasis and for important stages of follicular development. For instance, ROS produced by the ovary during the follicular stage of the oestrous cycle is reported to induce apoptosis in granulosa and break the wall of the preovulatory follicle and facilitate the ovulation process (Shkolnik *et al.* 2011). This implies that the amount of ROS production and the ROS scavenging antioxidants production depends on the stage of the follicular development (Agarwal *et al.* 2012). To understand the impact of the ROS radicals on follicular development, the half-life and ability to be translocated into the nucleus of the cells are important to take into consideration. Among the free radicals, H_2O_2 is widely utilised as a model for *in vitro* functional studies (Aprioku 2013). We previously reported that granulosa cells exogenously treated with a mild dose of H_2O_2 resulted in excessive accumulation of ROS and activation of the key transcription factor and downstream antioxidant genes of the NRF2-mediated oxidative stress signalling pathway: namely NRF2, CAT, TXN1, and PRDX1 (Saeed-Zidane *et al.* 2017). In the same experiment, examination of the spent culture media revealed that granulosa cells treated with H_2O_2 released higher number of EVs and those EVs are enriched with some of the antioxidants that were enriched in the cells. This is in agreement with the hypothesis that cells under stress utilise the EVs-mediated pathway to release cellular toxicants (Kosaka *et al.* 2013). Co-incubation of granulosa cells with these EVs after exposing cells to H_2O_2 reduced the accumulation of ROS but did not reduce the expression of the oxidative stress-related genes, which could be because of the fact that treatment with H_2O_2 caused significant transcriptional alteration that could not be reversed by the supplementation of stressed cells derived EVs (Saeed-Zidane *et al.* 2017). However, EVs supplemented to cells before the exposure to oxidative stress incurred a protective message to the recipient cells upon subsequent exposure to H_2O_2 (Eldh *et al.* 2010). It is worth noting that the time of the EVs supplementation is critical for the delivery of bioactive molecules to either rescue or protect cells from oxidative stress.

Taken all together, EVs of reproductive cells could be essential mediators of environmental and physiological stress. EVs released from reproductive cells subjected to various stressors are enriched with a multitude of bioactive molecules, mainly, miRNAs, stress-associated genes, and methylation modulators. These bioactive molecules could be implicated in improving cellular stress tolerance, improving the outcome of ARTs, and serve as remedies against stress-associated pathophysiological conditions. The aforementioned phenomenon is briefly illustrated in Fig. 2.

The potential of EVs in reproduction and related fields

Recent developments in modification of EVs facilitated the monitoring and tracking, interaction and transfer *in vivo* and *in vitro* (Lai *et al.* 2015). In that study engineered optical reporters were used to label multiple EV populations for visualization and tracking of tumour EV release, uptake and exchange between cell populations both *in vitro* and *in vivo*. Due to the variability in EV internalization mechanisms that exist between cell types, use of specific inhibitors provide a useful tool to study cell specific uptake mechanisms. For this, several inhibitors have been developed, including chlorpromazine to investigate clathrin-mediated uptake (Mulcahy *et al.* 2014), and specific RDG inhibitory peptides to target integrin-mediated EV uptake (Hoshino *et al.* 2015). Further research is needed to investigate the precise mechanisms that underline a specific EV entry into selected target cells and, importantly, the way to control the process.

An increasing amount of studies have evidenced the key role of EVs in regulating the different aspects of the reproduction process including gamete (sperm and ova) maturation, sperm capacitation, prevention of polyspermy, oviduct/uterine-embryo communication and even communication between *in vitro*-cocultured embryos (Machtinger *et al.* 2016). Following the preimplantation developmental process, EV production and function continue throughout pregnancy with the placenta and uterine epithelium to be the main source of EVs in maternal-embryo communication (Burns *et al.* 2016). Follicular microenvironment, which is filled with follicular fluid, is a place for successful maturation of oocytes during the process of folliculogenesis. The easy availability of follicular fluid during oocyte aspiration in human and animals assisted reproductive technology procedures makes it attractive in the search for biomarkers associated with oocyte quality. Previous studies in bovines demonstrated the presence of specific miRNA signatures coupled in exosomal and nonexosomal portions of the follicular fluid based on the growth status of the oocytes, thereby developmental competence (Sohel *et al.* 2013). Similarly, EV coupled miRNAs were also found to be associated with advanced maternal aging in mares (Da Silveira *et al.* 2012). Similarly, comparative analysis of miRNA isolated from EVs derived follicular fluid of young versus older women

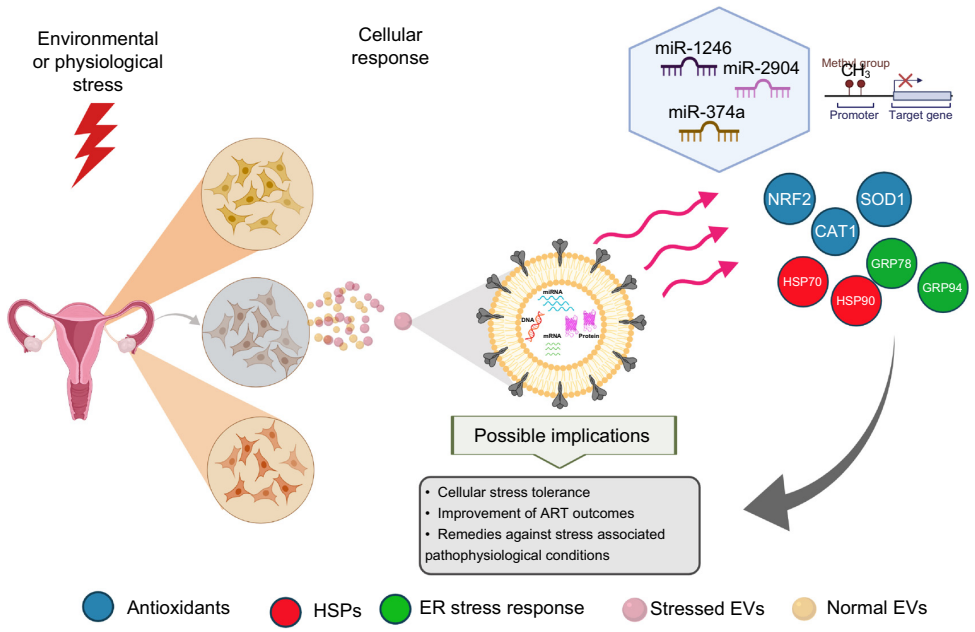


Fig. 2. A hypothetical model showing the response of reproductive cells the release of EVs enriched with stress-associated molecules including, miRNAs and methylation modulators, which could have important implications in improving the stress tolerance, the outcome of ARTs procedures, and possible remedies for stress associated pathophysiological conditions.

revealed differential expression of miRNAs targeting genes associated with heparin-sulphate biosynthesis, carbohydrate digestion and absorption, p53 signalling and cytokine–cytokine–receptor interaction (Diez-Fraile *et al.* 2014).

The use of successful ART is increasingly required to tackle age related infertility problems in humans. Similarly, an increase in selection for production traits in the cattle industry resulted in an increasing decline in fertility. However, the outcome from current ART procedures is far from optimal in terms of pregnancy success after transfer of the resulting blastocysts. Two factors contribute to this low success rate of ART. Firstly, embryo selection for transfer to recipient has inherent limitation which is mainly dependent on morphological assessment without considering the inherent quality of the embryo in inducing pregnancy (Fragouli *et al.* 2014). Secondly, the *in vitro* handling of gametes and embryos under suboptimal culture conditions can induce damage to the functional and structural units of embryos which affect their developmental competence to induce pregnancy after transfer. One of the main reasons for the suboptimal condition of mammalian ART is the absence of reproductive tract factors during *in vitro* culture of gametes and embryos. To tackle this problem several studies have tried to supplement reproductive tract fluids in the existing ART and could improve the quality of the resulting embryos. Several studies have demonstrated the presence of EVs in bovine follicular fluid and oviductal fluid and their molecular cargo composition is governed by the physiological status of the host animal. Those changes in molecular cargo carried by EVs is supposed to create optimal conditions for oocyte growth, sperm capacitation, gamete transport, fertilisation and preimplantation embryo development. Similarly, the protein content of uterine EVs released by *in vitro* cultured human endometrial epithelial cells is found to be altered by oestrogen and progesterone treatments suggesting hormonal regulation of EV cargo from uterine cells (Greening *et al.* 2016). A systematic analysis of bovine reproductive fluid EV contents demonstrated that they carry functional molecules associated with heat shock proteins, antioxidants, energy metabolism, amino acid biosynthesis and regulatory miRNAs targeting genes associated with various functional physiology of the oviduct (Almiñana *et al.* 2017, 2018; Hailay *et al.* 2019).

As it is a natural milieu for oocyte maturation in the ovarian follicle, follicular fluid has been utilised as supplement during IVM procedures and positive impact has been reported. The positive impact of follicular fluid on oocyte maturation *in vitro* is attributed to its protein, cytokine, growth factors, steroids, metabolites and other substances present in the follicular fluid (Sutton *et al.* 2003). Several studies have been conducted using different levels of follicular fluid and positive impacts in terms of increased blastocysts cell number (Kim *et al.* 1996), increased inner cell mass number and higher

cleavage rate of oocytes matured with follicular fluid collected 20 h after LH surge (Romero-Arredondo and Seidel 1996). In a similar study, supplementation of bovine *in vitro* maturation media with follicular fluid resulted in enhanced sperm penetration, increased cumulus expansion and ATP levels in oocytes, while blastocyst rate remain the same (Somfai *et al.* 2012). The functional significance of follicular fluid EVs was found to be dependent on the size of the follicle from which they are isolated. Accordingly, EVs isolated from follicular fluid aspirated from small (3–5 mm) and large (>9 mm) antral follicle were supplemented in IVM of bovine and mouse oocytes and a significant effect on cumulus expansion and expression of cumulus expansion marker genes was observed by EVs derived from small follicles (Hung *et al.* 2015). This implies that future research needs to focus on deciphering the molecular content of follicular fluid to identify key molecular cargos which play a significant role to support oocyte growth and maturation with potential application in current ART programs.

Supplementation of *in vitro* bovine embryo culture with oviductal and uterine fluid supports embryo development and induces the expression of genes related to methylation and oxidative stress (Hamdi *et al.* 2018). Differential composition of EVs were found in oviductal fluid derived from bovine ampullary and isthmus portion of the oviducts suggesting the differential role of EVs in different parts of the oviduct (Lopera-Vasquez *et al.* 2017). Moreover, comparative proteomic analysis of EVs derived from *in vitro* cultured oviductal epithelial cells revealed significant variation in their protein content compared to EVs derived from *in vivo* oviductal fluid (Almiñana *et al.* 2017). These differences are most likely to be attributed to the lack of many complex features present in the *in vivo* microenvironment including *in vivo* cellular diversity. As generation of enough amount of *in vivo* oviductal EVs for research and also for ART application is very challenging. Recently, oviductal organoids are being investigated for their suitability to generate *in vivo*-like EVs under *in vitro* condition as it is a technology to recapitulate the *in vivo* features of the oviduct (Heidari-Khoei *et al.* 2020). Therefore, reproductive organoids with other technologies including microfluidics technology would enable scientists to create an organoid-on-a-chip platform which provides new *in vitro* models to serve as both tissue and organ proxies to bridge the gap between *in vitro* and *in vivo* (Lancaster and Knoblich 2014). As organoids are self-organising structures that can recapitulate the different biological and pathological features of the organ, they represent genetic stability and maintain commitment to their tissue of origin during long-term culture to get access to an unlimited source of material like EVs to support research in the field. Therefore, reproductive organoids will facilitate the unlimited access to the generation of quantitative and qualitatively acceptable EVs for future research.

The EV-based liquid biopsy tests are under intensive investigation and a strong interest centred around the potential of EVs to serve as targets of the development of biomarkers or therapeutic reagents, especially in the field of cancer research (Théry 2015). In the field of reproduction, the main challenge of development of EV-based biomarker discovery is reproducibility, which is influenced by the various limitations associated with EV isolation, characterisation and tracking. In addition, the development as biomarker is dependent on the methods which favors the isolation of highly purified EVs produced in reproduceable and cost-effective manner. Most research in the field of reproductive EVs are descriptive in their nature without elucidating the actual mechanism of action. A standardised EV isolation method is believed to facilitate the translation and reproducibility of the findings in the clinical diagnostic settings.

References

Agarwal A, Aponte-Mellado A, Premkumar BJ, Shaman A, Gupta S (2012) The effects of oxidative stress on female reproduction: a review. *Reproductive Biology and Endocrinology* **10**, 49. doi:10.1186/1477-7827-10-49

Al-Dossary AA, Strehler Emanuel E, Martin-Deleon PA (2013) Expression and secretion of plasma membrane Ca^{2+}-ATPase 4a (PMCA4a) during murine estrus: association with oviductal exosomes and uptake in sperm. *PLoS ONE* **8**(11), e80181. doi:10.1371/journal.pone.0080181

Alemu TW, Pandey HO, Salilew Wondim D, Gebremedhn S, Neuhof C, Tholen E, *et al.* (2018) Oxidative and endoplasmic reticulum stress defense mechanisms of bovine granulosa cells exposed to heat stress. *Theriogenology* **110**, 130–141. doi:10.1016/j.theriogenology.2017.12.042

Almagor M, Bejar C, Kafka I, Yaffe H (1996) Pregnancy rates after communal growth of preimplantation human embryos in vitro. *Fertility and Sterility* **66**(3), 394–397. doi:10.1016/s0015-0282(16)58507-0

Almiñana C, Corbin E, Tsikis G, Alcântara-Neto AS, Labas V, Reynaud K, *et al.* (2017) Oviduct extracellular vesicles protein content and their role during oviduct-embryo cross-talk. *Reproduction (Cambridge, England)* **154**(3), 153–168. doi:10.1530/REP-17-0054

Almiñana C, Tsikis G, Labas V, Uzbekov R, da Silveira JC, Bauersachs S, Mermillod P (2018) Deciphering the oviductal extracellular vesicles content across the estrous cycle: implications for the gametes–oviduct interactions and the environment of the potential embryo. *BMC Genomics* **19**(1), 622. doi:10.1186/s12864-018-4982-5

Alvarez-Erviti L, Seow Y, Yin H, Betts C, Lakhal S, Wood MJA (2011) Delivery of siRNA to the mouse brain by systemic injection of targeted exosomes. *Nature Biotechnology* **29**(4), 341–345. doi:10.1038/nbt.1807

Aprioku JS (2013) Pharmacology of free radicals and the impact of reactive oxygen species on the testis. *Journal of Reproduction & Infertility* **14**(4), 158–172.

Asaadi A, Dolatabad NA, Atashi H, Raes A, van Damme P, Hoelker M, *et al.* (2021) Extracellular vesicles from follicular and ampullary fluid isolated by density gradient ultracentrifugation improve bovine embryo development and quality. *International Journal of Molecular Sciences* **22**(2), 578. doi:10.3390/ijms22020578

Avilés M, Gutiérrez-Adán A, Coy P (2010) Oviductal secretions: will they be key factors for the future ARTs? *In Molecular Human Reproduction* **16**(12), 896–906. doi:10.1093/molehr/gaq056

Baddela VS, Sharma A, Viergutz T, Koczan D, Vanselow J (2018) Low oxygen levels induce early luteinization associated changes in bovine granulosa cells. *Frontiers in Physiology* **9**, 1066. doi:10.3389/fphys.2018.01066

Baixauli F, López-Otín C, Mittelbrunn M (2014) Exosomes and autophagy: coordinated mechanisms for the maintenance of cellular fitness. *Frontiers in Immunology* **5**, 403. doi:10.3389/fimmu.2014.00403

Beam SW, Butler WR (1997) Energy balance and ovarian follicle development prior to the first ovulation postpartum in dairy cows receiving three levels of dietary fat. *Biology of Reproduction* **56**(1), 133–142. doi:10.1095/biolreprod56.1.133

Beam SW, Butler WR (1999) Effects of energy balance on follicular development and first ovulation in postpartum dairy cows. *Journal of Reproduction and Fertility*. **54**, 411–424.

Belleannée C, Calvo É, Caballero J, Sullivan R (2013) Epididymosomes convey different repertoires of microRNAs throughout the bovine epididymis. *Biology of Reproduction* **89**(2), 30. doi:10.1095/biolreprod.113.110486

Bewicke-Copley F, Mulcahy LA, Jacobs LA, Samuel P, Akbar N, Pink RC, Carter DRF (2017) Extracellular vesicles released following heat stress induce bystander effect in unstressed populations. *Journal of Extracellular Vesicles* **6**(1), 1340746. doi:10.1080/20013078.2017.1340746

Bosco D, Haefliger J-A, Meda P (2011) Connexins: key mediators of endocrine function. *Physiological Reviews* **91**(4), 1393–1445. doi:10.1152/physrev.00027.2010

Brower PT, Schultz RM (1982) Intercellular communication between granulosa cells and mouse oocytes: existence and possible nutritional role during oocyte growth. *Developmental Biology* **90** (1), 144–153. doi:10.1016/0012-1606(82)90219-6

Burton GJ, Jauniaux E (2011) Oxidative stress. *Best Practice & Research Clinical Obstetrics & Gynaecology* **25**(3), 287–299. doi:10.1016/j.bpobgyn.2010.10.016

Burton KA, McKnight GS (2007) PKA, germ cells, and fertility. *Physiology (Bethesda, MD)* **22**, 40–46. doi:10.1152/physiol.00034.2006

Burns G, Brooks K, Wildung M, Navakanitworakul R, Christenson LK, Spencer TE (2014) Extracellular vesicles in luminal fluid of the ovine uterus. *PLoS ONE* **9**(3), e90913. doi:10.1371/journal.pone.0090913

Burns GW, Brooks KE, Spencer TE (2016) Extracellular vesicles originate from the conceptus and uterus during early pregnancy in sheep. *Biology of Reproduction* **94**(3), 56. doi:10.1095/biolreprod.115.134973

Burns GW, Brooks KE, O'Neil EV, Hagen DE, Behura SK, Spencer TE (2018) Progesterone effects on extracellular vesicles in the sheep uterus. *Biology of Reproduction* **98**(5), 612–622. doi:10.1093/biolre/ioy011

Can U, Buyukinan M, Yerlikaya FH (2016) The investigation of circulating microRNAs associated with lipid metabolism in childhood obesity. *Pediatric Obesity* **11**(3), 228–234. doi:10.1111/ijpo.12050

Castaño C, Kalko S, Novials A, Párrizas M (2018) Obesity-associated exosomal miRNAs modulate glucose and lipid metabolism in mice. *Proceedings of the National Academy of Sciences of the United States of America* **115**(48), 12158–12163. doi:10.1073/pnas.1808855115

Chairoungdua A, Smith DL, Pochard P, Hull M, Caplan MJ (2010) Exosome release of β-catenin: a novel mechanism that antagonizes Wnt signaling. *The Journal of Cell Biology* **190**(6), 1079–1091. doi:10.1083/jcb.201002049

Che X, Jian F, Chen C, Liu C, Liu G, Feng W (2020) PCOS serum-derived exosomal miR-27a-5p stimulates endometrial cancer cells migration and invasion. *Journal of Molecular Endocrinology* **64**(1), 1–12. doi:10.1530/JME-19-0159

Cheng L, Doecke JD, Sharples RA, Villemagne VL, Fowler CJ, Rembach A, *et al.* (2015) Prognostic serum miRNA biomarkers associated with Alzheimer's disease shows concordance with neuropsychological and neuroimaging assessment. *Molecular Psychiatry* **20**(10), 1188–1196. doi:10.1038/mp.2014.127

Colombo M, Raposo G, Théry C (2014) Biogenesis, secretion, and intercellular interactions of exosomes and other extracellular vesicles. *Annual Review of Cell and Developmental Biology* **30**(1), 255–289. doi:10.1146/annurev-cellbio-101512-122326

Conti M, Hsieh M, Zamah AM, Oh JS (2012) Novel signaling mechanisms in the ovary during oocyte maturation and ovulation. *Molecular and Cellular Endocrinology* **356**(1–2), 65–73. doi:10.1016/j.mce.2011.11.002

Contreras GA, Sordillo LM (2011) Lipid mobilization and inflammatory responses during the transition period of dairy cows. *Comparative Immunology, Microbiology and Infectious Diseases* **34**(3), 281–289. doi:10.1016/j.cimid.2011.01.004

Coy P, García-Vázquez FA, Visconti PE, Avilés M (2012) Roles of the oviduct in mammalian fertilization. *Reproduction (Cambridge, England)* **144**(6), 649–660. doi:10.1530/REP-12-0279

Cronqvist T, Erlandsson L, Tannetta D, Hansson SR (2020) Placental syncytiotrophoblast extracellular vesicles enter primary endothelial cells through clathrin-mediated endocytosis. *Placenta* **100**, 133–141. doi:10.1016/j.placenta.2020.07.006

Cruz L, Romero JAA, Iglesia RP, Lopes MH (2018) Extracellular vesicles: decoding a new language for cellular communication in early embryonic Development. *Frontiers in Cell and Developmental Biology* **6**, 94. doi:10.3389/fcell.2018.00094

Da Silveira JC, Veeramachaneni DNR, Winger QA, Carnevale EM, Bouma GJ (2012) Cell-secreted vesicles in equine ovarian follicular fluid contain miRNAs and proteins: a possible new form of cell communication within the ovarian follicle. *Biology of Reproduction* **86**(3), 71. doi:10.1095/biolreprod.111.093252

de Maio A (2011) Extracellular heat shock proteins, cellular export vesicles, and the Stress Observation System: a form of communication during injury, infection, and cell damage. It is never known how far a controversial finding will go! Dedicated to Ferruccio Ritossa. *Cell Stress & Chaperones* **16**(3), 235–249. doi:10.1007/s12192-010-0236-4

Dhahbi JM, Spindler SR, Atamna H, Yamakawa A, Guerrero N, Boffelli D, *et al.* (2013) Deep sequencing identifies circulating mouse miRNAs that are functionally implicated in manifestations of aging and responsive to calorie restriction. *Aging* **5**(2), 130–141. doi:10.18632/aging.100540

Diez-Fraile A, Lammens T, Tilleman K, Witkowski W, Verhasselt B, de Sutter Petra, *et al.* (2014) Age-associated differential microRNA levels in human follicular fluid reveal pathways potentially determining fertility and success of in vitro fertilization. *Human Fertility (Cambridge, England)* **17**(2), 90–98. doi:10.3109/14647273.2014.897006

Dong H, Wang C, Lu S, Yu C, Huang L, Feng W, *et al.* (2016) A panel of four decreased serum microRNAs as a novel biomarker for early Parkinson's disease. *Biomarkers: Biochemical Indicators of Exposure, Response, and Susceptibility to Chemicals* **21**(2), 129–137. doi:10.3109/1354750X.2015.1118544

Donnay I, van Langendonckt A, Auquier P, Grisart B, Vansteenbrugge A, Massip A, Dessy F (1997) Effects of co-culture and embryo number on the in vitro development of bovine embryos. *Theriogenology* **47**(8), 1549–1561. doi:10.1016/s0093-691x(97)00160-x

Ebner T, Shebl O, Moser M, Mayer RB, Arzt W, Tews G (2010) Group culture of human zygotes is superior to individual culture in terms of blastulation, implantation and life birth. *Reproductive Biomedicine Online* **21**(6), 762–768. doi:10.1016/j.rbmo.2010.06.038

Edwards JL, Hansen PJ (1996) Elevated temperature increases heat shock protein 70 synthesis in bovine two-cell embryos and compromises function of maturing oocytes. *Biology of Reproduction* **55**(2), 341–346. doi:10.1095/biolreprod55.2.341

Eldh M, Ekström K, Valadi H, Sjöstrand M, Olsson B, Jernås M, Lötvall J (2010) Exosomes communicate protective messages during oxidative stress; possible role of exosomal shuttle RNA. *PLoS ONE* **5**(12), e15353. doi:10.1371/journal.pone.0015353

Escrevente C, Keller S, Altevogt P, Costa J (2011) Interaction and uptake of exosomes by ovarian cancer cells. *BMC Cancer* **11**, 108. doi:10.1186/1471-2407-11-108

Fabbri M, Paone A, Calore F, Galli R, Gaudio E, Santhanam R, *et al.* (2012) MicroRNAs bind to Toll-like receptors to induce prometastatic inflammatory response. *Proceedings of the National Academy of Sciences of the United States of America* **109**(31), E2110–E2116. doi:10.1073/pnas.1209414109

Fazeli A (2011) Maternal communication with gametes and embryo: a personal opinion. *Reproduction in Domestic Animals = Zuchthygiene* **46**(Suppl 2), 75–78. doi:10.1111/j.1439-0531.2011.01870.x

Fereshteh Z, Bathala P, Galileo DS, Martin-Deleon PA (2019) Detection of extracellular vesicles in the mouse vaginal fluid: their delivery of sperm proteins that stimulate capacitation and modulate fertility. *Journal of Cellular Physiology* **234**(8), 12745–12756. doi:10.1002/jcp.27894

Fortune JE (1994) Ovarian follicular growth and development in mammals. *Biology of Reproduction* **50**(2), 225–232. doi:10.1095/biolreprod50.2.225

Fragouli E, Alfarawati S, Spath K, Wells D (2014) Morphological and cytogenetic assessment of cleavage and blastocyst stage embryos. *Molecular Human Reproduction* **20**(2), 117–126. doi:10.1093/molehr/gat073

Franchi A, Cubilla M, Guidobaldi HA, Bravo AA, Giojalas LC (2016) Uterosome-like vesicles prompt human sperm fertilizing capability. *Molecular Human Reproduction* **22**(12), 833–841. doi:10.1093/molehr/gaw066

Galimberti D, Villa C, Fenoglio C, Serpente M, Ghezzi L, Cioffi SMG, *et al.* (2014) Circulating miRNAs as potential biomarkers in Alzheimer's disease. *Journal of Alzheimer's Disease* **42**(4), 1261–1267. doi:10.3233/JAD-140756

Gatien J, Mermillod P, Tsikis G, Bernardi O, Janati Idrissi S, Uzbekov R, *et al.* (2019) Metabolomic profile of oviductal extracellular vesicles across the estrous cycle in cattle. *International Journal of Molecular Sciences* **20**(24). doi:10.3390/ijms20246339

Gebremedhn S, Ali A, Gad A, Prochazka R, Tesfaye D (2020a) Extracellular vesicles as mediators of environmental and metabolic stress coping mechanisms during mammalian follicular development. *Frontiers in Veterinary Science* **7**, 602043. doi:10.3389/fvets.2020.602043

Gebremedhn S, Gad A, Aglan HS, Laurincik J, Prochazka R, Salilew-Wondim D, *et al.* (2020b) Extracellular vesicles shuttle protective messages against heat stress in bovine granulosa cells. *Scientific Reports* **10**(1), 15824. doi:10.1038/s41598-020-72706-z

Golini VE, Stradaioli G, Sirard MA (2014) Transcriptome analysis of bovine granulosa cells of preovulatory follicles harvested 30, 60, 90, and 120 days postpartum. *Theriogenology* **82**(4), 580–591.e5. doi:10.1016/j.theriogenology.2014.05.019

Greening DW, Nguyen HPT, Elgass K, Simpson Richard J, Salamonsen LA (2016) Human endometrial exosomes contain hormone-specific cargo modulating trophoblast adhesive capacity: insights into endometrial–embryo interactions. *Biology of Reproduction* **94**(2), 38. doi:10.1095/biolreprod.115.134890

Hailay T, Hoelker M, Poirier M, Gebremedhn S, Rings F, Saeed-Zidane M, *et al.* (2019) Extracellular vesicle-coupled miRNA profiles in follicular fluid of cows with divergent post-calving metabolic status. *Scientific Reports* **9**(1), 12851. doi:10.1038/s41598-019-49029-9

Hamdi M, Lopera-Vasquez R, Maillo V, Sanchez-Calabuig MJ, Núnez C, Gutierrez-Adan A, Rizos D (2018) Bovine oviductal and uterine fluid support in vitro embryo development. *Reproduction, Fertility, and Development* **30**(7), 935–945. doi:10.1071/RD17286

Hansen LB (2000) Consequences of selection for milk yield from a geneticist's viewpoint. *Journal of Dairy Science* **83**(5), 1145–1150. doi:10.3168/jds.S0022-0302(00)74980-0

Hanson PI, Cashikar A (2012) Multivesicular body morphogenesis. *Annual Review of Cell and Developmental Biology* **28**, 337–362. doi:10.1146/annurev-cellbio-092910-154152

Harris EA, Stephens KK, Winuthayanon W (2020) Extracellular vesicles and the oviduct function. *International Journal of Molecular Sciences* **21**(21), 8280. doi:10.3390/ijms21218280

Heidari-Khoei H, Esfandiari F, Hajari MA, Ghorbaninejad Z, Piryaei A, Baharvand H (2020) Organoid technology in female reproductive biomedicine. *Reproductive Biology and Endocrinology* **18**(1), 64. doi:10.1186/s12958-020-00621-z

Hemler ME (2005) Tetraspanin functions and associated microdomains. *Nature Reviews. Molecular Cell Biology* **6**(10), 801–811. doi:10.1038/nrm1736

Higuchi C, Nakatsuka A, Eguchi J, Teshigawara S, Kanzaki M, Katayama A, *et al.* (2015) Identification of circulating miR-101, miR-375 and miR-802 as biomarkers for type 2 diabetes. *Metabolism: Clinical and Experimental* **64**(4), 489–497. doi:10.1016/j.metabol.2014.12.003

Hoelker M, Rings F, Lund Q, Phatsara C, Schellander K, Tesfaye D (2010) Effect of embryo density on in vitro developmental characteristics of bovine preimplantative embryos with respect to micro and macroenvironments. *Reproduction in Domestic Animals* **45**(5), e138–145. doi:10.1111/j.1439-0531.2009.01535.x

Horibe S, Tanahashi T, Kawauchi S, Murakami Y, Rikitake Y (2018) Mechanism of recipient cell-dependent differences in exosome uptake. *BMC Cancer* **18**(1), 47. doi:10.1186/s12885-017-3958-1

Hoshino A, Costa-Silva B, Shen T-L, Rodrigues G, Hashimoto A, Tesic Mark M, *et al.* (2015) Tumour exosome integrins determine organotropic metastasis. *Nature* **527**(7578), 329–335. doi:10.1038/nature15756

Hou C-H, Lin F-L, Hou S-M, Liu J-F (2014) Hyperthermia induces apoptosis through endoplasmic reticulum and reactive oxygen species in human osteosarcoma cells. *International Journal of Molecular Sciences* **15**(10), 17380–17395. doi:10.3390/ijms151017380

Hu J, Tang T, Zeng Z, Wu J, Tan X, Yan J (2020) The expression of small RNAs in exosomes of follicular fluid altered in human polycystic ovarian syndrome. *PeerJ* **8**, e8640. doi:10.7717/peerj.8640

Hung W-T, Hong X, Christenson LK, McGinnis LK (2015) Extracellular vesicles from bovine follicular fluid support cumulus expansion. *Biology of Reproduction* **93**(5), 117. doi:10.1095/biolreprod.115.132977

Hung W-T, Navakanitworakul R, Khan T, Zhang P, Davis JS, McGinnis LK, Christenson LK (2017) Stage-specific follicular extracellular vesicle uptake and regulation of bovine granulosa cell proliferation. *Biology of Reproduction* **97**(4), 644–655. doi:10.1093/biolre/iox106

Ibrahim A, Marbán E (2016) Exosomes: fundamental biology and roles in cardiovascular physiology. *Annual Review of Physiology* **78**, 67–83. doi:10.1146/annurev-physiol-021115-104929

Jacobs LA, Bewicke-Copley F, Poolman MG, Pink RC, Mulcahy LA, Baker I, *et al.* (2013) Meta-analysis using a novel database, miRStress, reveals miRNAs that are frequently associated with the radiation and hypoxia stress-responses. *PLoS ONE* **8**(11), e80844. doi:10.1371/journal.pone.0080844

Jiang X, Li J, Zhang B, Hu J, Ma J, Cui L, Chen Z-J (2021) Differential expression profile of plasma exosomal microRNAs in women with polycystic ovary syndrome. *Fertility and Sterility* **115**(3), 782–792. doi:10.1016/j.fertnstert.2020.08.019

Kalluri R, LeBleu VS (2020) The biology, function, and biomedical applications of exosomes. *Science (New York, NY)* **367**(6478), eaau6977. doi:10.1126/science.aau6977

Keller S, Ridinger J, Rupp A-K, Janssen JWG, Altevogt P (2011) Body fluid derived exosomes as a novel template for clinical diagnostics. *Journal of Translational Medicine* **9**, 86. doi:10.1186/1479-5876-9-86

Kim K, Mitsumizo N, Fujita K, Utsumi K (1996) The effects of follicular fluid on in vitro maturation, oocyte fertilization and the development of bovine embryos. *Theriogenology* **45** (4), 787–799. doi:10.1016/0093-691x(96)00008-8

Kirkman MS, Briscoe VJ, Clark N, Florez H, Haas LB, Halter JB, *et al.* (2012) Diabetes in older adults. *Diabetes Care* **35**(12), 2650–2664. doi:10.2337/dc12-1801

Kong L, Zhu J, Han W, Jiang X, Xu M, Zhao Y, *et al.* (2011) Significance of serum microRNAs in pre-diabetes and newly diagnosed type 2 diabetes: a clinical study. *Acta Diabetologica* **48**(1), 61–69. doi:10.1007/s00592-010-0226-0

Kosaka N, Yoshioka Y, Hagiwara K, Tominaga N, Katsuda T, Ochiya T (2013) Trash or treasure: extracellular microRNAs and cell-to-cell communication. *Frontiers in Genetics* **4**, 173. doi:10.3389/fgene.2013.00173

Laflamme J, Akoum A, Leclerc P (2005) Induction of human sperm capacitation and protein tyrosine phosphorylation by endometrial cells and interleukin-6. *Molecular Human Reproduction* **11**(2), 141–150. doi:10.1093/molehr/gah142

Lai CP, Kim EY, Badr CE, Weissleder R, Mempel TR, Tannous BA, Breakefield XO (2015) Visualization and tracking of tumour extracellular vesicle delivery and RNA translation using multiplexed reporters. *Nature Communications* **6**, 7029. doi:10.1038/ncomms8029

Lancaster GI, Febbraio MA (2005) Exosome-dependent trafficking of HSP70: a novel secretory pathway for cellular stress proteins. *The Journal of Biological Chemistry* **280**(24), 23349–23355. doi:10.1074/jbc.M502017200

Lancaster MA, Knoblich JA (2014) Organogenesis in a dish: modeling development and disease using organoid technologies. *Science (New York, NY)* **345**(6194), 1247125. doi:10.1126/science.1247125

Leese HJ, Hugentobler SA, Gray SM, Morris DG, Sturmey RG, Whitear S-L, Sreenan JM (2008) Female reproductive tract fluids: composition, mechanism of formation and potential role in the developmental origins of health and disease. *Reproduction, Fertility, and Development* **20**(1), 1–8. doi:10.1071/rd07153

Leroy JLMR, Vanholder T, Delanghe JR, Opsomer G, van Soom A, Bols PEJ, *et al.* (2004) Metabolic changes in follicular fluid of the dominant follicle in high-yielding dairy cows early post partum. *Theriogenology* **62**(6), 1131–1143. doi:10.1016/j.theriogenology.2003.12.017

Li J, Gao H, Tian Z, Wu Y, Wang Y, Fang Y, *et al.* (2016) Effects of chronic heat stress on granulosa cell apoptosis and follicular atresia in mouse ovary. *Journal of Animal Science and Biotechnology* **7**, 57. doi:10.1186/s40104-016-0116-6

Liang B, Peng P, Chen S, Li L, Zhang M, Cao D, *et al.* (2013) Characterization and proteomic analysis of ovarian cancer-derived exosomes. *Journal of Proteomics* **80**, 171–182. doi:10.1016/j.jprot.2012.12.029

Lopera-Vásquez R, Hamdi M, Fernandez-Fuertes B, Maillo V, Beltrán-Breña P, Calle A, *et al.* (2016) Extracellular vesicles from BOEC in *in vitro* embryo development and quality. *PLoS ONE* **11**(2), e0148083. doi:10.1371/journal.pone.0148083

Lopera-Vasquez R, Hamdi Me, Maillo V, Gutierrez-Adan A, Bermejo-Alvarez P, Ramírez MÁ, *et al.* (2017) Effect of bovine oviductal extracellular vesicles on embryo development and quality in vitro. *Reproduction (Cambridge, England)* **153**(4), 461–470. doi:10.1530/REP-16-0384

López-Otín C, Blasco MA, Partridge L, Serrano M, Kroemer G (2013) The hallmarks of aging. *Cell* **153**(6), 1194–1217. doi:10.1016/j.cell.2013.05.039

Lucy MC (2001) Reproductive loss in high-producing dairy cattle: where will it end? *In Journal of Dairy Science* **84**(6), 1277–1293. doi:10.3168/jds.S0022-0302(01)70158-0

Lv A, Tu Z, Huang Y, Lu W, Xie B (2021) Circulating exosomal miR-125a-5p as a novel biomarker for cervical cancer. *Oncology Letters* **21**(1), 54. doi:10.3892/ol.2020.12316

Machtinger R, Laurent LC, Baccarelli AA (2016) Extracellular vesicles: roles in gamete maturation, fertilization and embryo implantation. *Human Reproduction Update* **22**(2), 182–193. doi:10.1093/humupd/dmv055

María Y-M, Pia R-MS, Zoraida A, Apolonija BZ, Francesc EB, Edit IB, *et al.* (2015) Biological properties of extracellular vesicles and their physiological functions. *Journal of Extracellular Vesicles* **4**(1), 27066. doi:10.3402/jev.v4.27066

Mathieu M, Martin-Jaular L, Lavieu G, Théry C (2019) Specificities of secretion and uptake of exosomes and other extracellular vesicles for cell-to-cell communication. *Nature Cell Biology* **21**(1), 9–17. doi:10.1038/s41556-018-0250-9

Meuwissen TH, Hayes BJ, Goddard ME (2001) Prediction of total genetic value using genome-wide dense marker maps. *Genetics* **157**(4), 1819–1829.

Montecalvo A, Larregina AT, Shufesky WJ, Stolz DB, Sullivan MLG, Karlsson JM, *et al.* (2012) Mechanism of transfer of functional microRNAs between mouse dendritic cells via exosomes. *Blood* **119**(3), 756–766. doi:10.1182/blood-2011-02-338004

Morelli AE, Larregina AT, Shufesky WJ, Sullivan MLG, Stolz DB, Papworth GD, *et al.* (2004) Endocytosis, intracellular sorting, and processing of exosomes by dendritic cells. *Blood* **104**(10), 3257–3266. doi:10.1182/blood-2004-03-0824

Mulcahy LA, Pink RC, Carter DRF (2014) Routes and mechanisms of extracellular vesicle uptake. *Journal of Extracellular Vesicles* **3**, 24641 doi:10.3402/jev.v3.24641

Murdica V, Giacomini E, Makieva S, Zarovni N, Candiani M, Salonia A, *et al.* (2020) In vitro cultured human endometrial cells release extracellular vesicles that can be uptaken by spermatozoa. *Scientific Reports* **10**(1), 8856. doi:10.1038/s41598-020-65517-9

Nabenishi H, Ohta H, Nishimoto T, Morita T, Ashizawa K, Tsuzuki Y (2012) The effects of cysteine addition during in vitro maturation on the developmental competence, ROS, GSH and apoptosis level of bovine oocytes exposed to heat stress. *Zygote (Cambridge, England)* **20**(3), 249–259. doi:10.1017/S0967199411000220

Ng YH, Rome S, Jalabert A, Forterre A, Singh H, Hincks CL, Salamonsen LA (2013) Endometrial exosomes/microvesicles in the uterine microenvironment: a new paradigm for embryo-endometrial cross talk at implantation. *PLoS ONE* **8**(3), e58502. doi:10.1371/journal.pone.0058502

O'Doherty EM, Wade MG, Hill JL, Boland MP (1997) Effects of culturing bovine oocytes either singly or in groups on development to blastocysts. *Theriogenology* **48** (1), 161–169. doi:10.1016/S0093-691X(97)00199-4

Ofir-Birin Y, Abou Karam P, Rudik A, Giladi T, Porat Z, Regev-Rudzki N (2018) Monitoring extracellular vesicle cargo active uptake by imaging flow cytometry. *Frontiers in Immunology* **9**, 1011. doi:10.3389/fimmu.2018.01011

O'Neill C (2008) The potential roles for embryotrophic ligands in preimplantation embryo development. *Human Reproduction Update* **14**, 275–288.

O'Shea LC, Mehta J, Lonergan P, Hensey C, Fair T (2012) Developmental competence in oocytes and cumulus cells: candidate genes and networks. *Systems Biology in Reproductive Medicine* **58**(2), 88–101. doi:10.3109/19396368.2012.656217

Ostrowski M, Carmo NB, Krumeich S, Fanget I, Raposo G, Savina A, *et al.* (2010) Rab27a and Rab27b control different steps of the exosome secretion pathway. *Nature Cell Biology* **12**(1), 19–30. doi:10.1038/ncb2000

Pavani KC, Hendrix A, van den Broeck W, Couck L, Szymanska K, Lin X, *et al.* (2019) Isolation and characterization of functionally active extracellular vesicles from culture medium conditioned by bovine embryos *in vitro*. *International Journal of Molecular Sciences* **20**(1). doi:10.3390/ijms20010038

Poirier M, Tesfaye D, Hailay T, Salilew-Wondim D, Gebremedhn S, Rings F, *et al.* (2020) Metabolism-associated genome-wide epigenetic changes in bovine oocytes during early lactation. *Scientific Reports* **10**(1), 2345. doi:10.1038/s41598-020-59410-8

Pontes JHF, Nonato-Junior I, Sanches BV, Ereno-Junior JC, Uvo S, Barreiros TRR, *et al.* (2009) Comparison of embryo yield and pregnancy rate between in vivo and in vitro methods in the same Nelore (*Bos indicus*) donor cows. *Theriogenology* **71**(4), 690–697. doi:10.1016/j.theriogenology.2008.09.031

Qu P, Luo S, Du Y, Zhang Y, Song X, Yuan X, *et al.* (2020) Extracellular vesicles and melatonin benefit embryonic develop by regulating reactive oxygen species and 5-methylcytosine. *Journal of Pineal Research* **68**(3), e12635. doi:10.1111/jpi.12635

Racicot K, Schmitt A, Ott T (2012) The myxovirus-resistance protein, MX1, is a component of exosomes secreted by uterine epithelial cells. *American Journal of Reproductive Immunology* **67**(6), 498–505. doi:10.1111/j.1600-0897.2012.01109.x

Raposo G, Stoorvogel W (2013) Extracellular vesicles: exosomes, microvesicles, and friends. *The Journal of Cell Biology* **200**(4), 373–383. doi:10.1083/jcb.201211138

Rivera RM, Hansen PJ (2001) Development of cultured bovine embryos after exposure to high temperatures in the physiological range. *Reproduction (Cambridge, England)* **121**(1), 107–115.

Rodrigues TA, Tuna KM, Alli AA, Tribulo P, Hansen PJ, Koh J, Paula-Lopes FF (2019) Follicular fluid exosomes act on the bovine oocyte to improve oocyte competence to support development and survival to heat shock. *Reproduction, Fertility, and Development* **31**(5), 888–897. doi:10.1071/RD18450

Romero-Arredondo A, Seidel Jr GE (1996) Effects of follicular fluid during in vitro maturation of bovine oocytes on in vitro fertilization and early embryonic development. *Biology of Reproduction* **55**(5), 1012–1016. doi:10.1095/biolreprod55.5.1012

Rosas-Hernandez H, Chigurupati S, Raymick J, Robinson B, Cuevas E, Hanig J, Sarkar S (2018) Identification of altered microRNAs in serum of a mouse model of Parkinson's disease. *Neuroscience Letters* **687**, 1–9. doi:10.1016/j.neulet.2018.07.022

Roth Z (2017) Effect of heat stress on reproduction in dairy cows: insights into the cellular and molecular responses of the oocyte. *Annual Review of Animal Biosciences* **5**, 151–170. doi:10.1146/annurev-animal-022516-022849

Roth Z, Hansen PJ (2005) Disruption of nuclear maturation and rearrangement of cytoskeletal elements in bovine oocytes exposed to heat shock during maturation. *Reproduction (Cambridge, England)* **129**(2), 235–244. doi:10.1530/rep.1.00394

Roth Z, Wolfenson D (2016) Comparing the effects of heat stress and mastitis on ovarian function in lactating cows: basic and applied aspects. *Domestic Animal Endocrinology* **56**(Suppl), S218–S227. doi:10.1016/j.domaniend.2016.02.013

Roth Z, Meidan R, Shaham-Albalancy A, Braw-Tal R, Wolfenson D (2001) Delayed effect of heat stress on steroid production in medium-sized and preovulatory bovine follicles. *Reproduction (Cambridge, England)* **121**(5), 745–751.

Ruiz-González I, Xu J, Wang X, Burghardt RC, Dunlap KA, Bazer FW (2015) Exosomes, endogenous retroviruses and toll-like receptors: pregnancy recognition in ewes. *Reproduction (Cambridge, England)* **149**(3), 281–291. doi:10.1530/REP-14-0538

Rukkwamsuk T, Geelen MJ, Kruip TA, Wensing T (2000) Interrelation of fatty acid composition in adipose tissue, serum, and liver of dairy cows during the development of fatty liver postpartum. *Journal of Dairy Science* **83**(1), 52–59. doi:10.3168/jds.S0022-0302(00)74854-5

Saadeldin IM, Kim SJ, Choi YB, Lee BC (2014) Improvement of cloned embryos development by co-culturing with parthenotes: a possible role of exosomes/microvesicles for embryos paracrine communication. *Cellular Reprogramming* **16**(3), 223–234. doi:10.1089/cell.2014.0003

Saeed-Zidane M, Linden L, Salilew-Wondim D, Held E, Neuhoff C, Tholen E, *et al.* (2017) Cellular and exosome mediated molecular defense mechanism in bovine granulosa cells exposed to oxidative stress. *PLoS ONE* **12** (11), e0187569. doi:10.1371/journal.pone.0187569

Santonocito M, Vento M, Guglielmino MR, Battaglia R, Wahlgren J, Ragusa M, *et al.* (2014) Molecular characterization of exosomes and their microRNA cargo in human follicular fluid: bioinformatic analysis reveals that exosomal microRNAs control pathways involved in follicular maturation. *Fertility and Sterility* **102**(6), 1751–1761.e1. doi:10.1016/j.fertnstert.2014.08.005

Senbon S, Hirao Y, Miyano T (2003) Interactions between the oocyte and surrounding somatic cells in follicular development: lessons from in vitro culture. *The Journal of Reproduction and Development* **49**(4), 259–269. doi:10.1262/jrd.49.259

Shkolnik K, Tadmor A, Ben-Dor S, Nevo N, Galiani D, Dekel N (2011) Reactive oxygen species are indispensable in ovulation. *Proceedings of the National Academy of Sciences of the United States of America* **108**(4), 1462–1467. doi:10.1073/pnas.1017213108

Sidrat T, Khan AA, Joo M-D, Wei Y, Lee K-L, Xu L, Kong Il-K (2020) Bovine oviduct epithelial cell-derived culture media and exosomes improve mitochondrial health by restoring metabolic flux during pre-implantation development. *International Journal of Molecular Sciences* **21**(20), 7589. doi:10.3390/ijms21207589

Simon C, Greening DW, Bolumar D, Balaguer N, Salamonsen LA, Vilella F (2018) Extracellular vesicles in human reproduction in health and disease. *Endocrine Reviews* **39**(3), 292–332. doi:10.1210/er.2017-00229

Sohel MMH, Hoelker M, Noferesti SS, Salilew-Wondim D, Tholen E, Looft C, *et al.* (2013) Exosomal and non-exosomal transport of extra-cellular micrornas in follicular fluid: implications for bovine oocyte developmental competence. *PLoS ONE* **8**(11), e78505. doi:10.1371/journal.pone.0078505

Somfai T, Inaba Y, Watanabe S, Geshi M, Nagai T (2012) Follicular fluid supplementation during in vitro maturation promotes sperm penetration in bovine oocytes by enhancing cumulus expansion and increasing mitochondrial activity in oocytes. *Reproduction, Fertility, and Development* **24**(5), 743–752. doi:10.1071/RD11251

Stephen JG, Graça R (2013) As we wait: coping with an imperfect nomenclature for extracellular vesicles. *Journal of Extracellular Vesicles* **2**(1), 20389. doi:10.3402/jev.v2i0.20389

Stokes PJ, Abeydeera LR, Leese HJ (2005) Development of porcine embryos in vivo and in vitro; evidence for embryo 'cross talk' in vitro. *Developmental Biology* **284**(1), 62–71. doi:10.1016/j.ydbio.2005.05.001

Sullivan R, Saez F (2013) Epididymosomes, prostasomes, and liposomes: their roles in mammalian male reproductive physiology. *Reproduction (Cambridge, England)* **146**(1), R21–R35. doi:10.1530/REP-13-0058

Sutton ML, Gilchrist RB, Thompson JG (2003) Effects of in-vivo and in-vitro environments on the metabolism of the cumulus-oocyte complex and its influence on oocyte developmental capacity. *Human Reproduction Update* **9**(1), 35–48. doi:10.1093/humupd/dmg009

Taka M, Iwayama H, Fukui Y (2005) Effect of the well of the well (WOW) system on in vitro culture for porcine embryos after intracytoplasmic sperm injection. *The Journal of Reproduction and Development* **51**(4), 533–537. doi:10.1262/jrd.17005

Tang K, Zhang Y, Zhang H, Xu P, Liu J, Ma J, *et al.* (2012) Delivery of chemotherapeutic drugs in tumour cell-derived microparticles. *Nature Communications* **3**, 1282. doi:10.1038/ncomms2282

Théry C (2015) Cancer: diagnosis by extracellular vesicles. *Nature* **523**(7559), 161–162. doi:10.1038/nature14626

Tkach M, Théry C (2016) Communication by extracellular vesicles: where we are and where we need to go. *Cell* **164**(6), 1226–1232. doi:10.1016/j.cell.2016.01.043

Vajta G, Korösi T, Du Y, Nakata K, Ieda S, Kuwayama M, Nagy ZP (2008) The well-of-the-well system: an efficient approach to improve embryo development. *Reproductive Biomedicine Online* **17**(1), 73–81. doi:10.1016/s1472-6483(10)60296-9

Valadi H, Ekström K, Bossios A, Sjöstrand M, Lee JJ, Lötvall JO (2007) Exosome-mediated transfer of mRNAs and microRNAs is a novel mechanism of genetic exchange between cells. *Nature Cell Biology* **9**(6), 654–659. doi:10.1038/ncb1596

Vanholder T, Leroy JLMR, van Soom A, Opsomer G, Maes D, Coryn M, de Kruif A (2005) Effect of non-esterified fatty acids on bovine granulosa cell steroidogenesis and proliferation in vitro. *Animal Reproduction Science* **87**(1–2), 33–44. doi:10.1016/j.anireprosci.2004.09.006

Vilella F, Moreno-Moya JM, Balaguer N, Grasso A, Herrero M, Martínez S, *et al.* (2015) Hsa-miR-30d, secreted by the human endometrium, is taken up by the pre-implantation embryo and might modify its transcriptome. *Development* **142**(18), 3210–3221. doi:10.1242/dev.124289

Villarroya-Beltri C, Baixauli F, Gutiérrez-Vázquez C, Sánchez-Madrid F, Mittelbrunn M (2014) Sorting it out: regulation of exosome loading. *Seminars in Cancer Biology* **28**, 3–13. doi:10.1016/j.semcancer.2014.04.009

Visconti PE, Kopf GS (1998) Regulation of protein phosphorylation during sperm capacitation. *Biology of Reproduction* **59**(1), 1–6. doi:10.1095/biolreprod59.1.1

Walters AH, Pryor AW, Bailey TL, Pearson RE, Gwazdauskas FC (2002) Milk yield, energy balance, hormone, follicular and oocyte measures in early and mid-lactation Holstein cows. *Theriogenology* **57**(2), 949–961. doi:10.1016/s0093-691x(01)00688-4

Wolfenson D, Lew BJ, Thatcher WW, Graber Y, Meidan R (1997) Seasonal and acute heat stress effects on steroid production by dominant follicles in cows. *Animal Reproduction Science* **47**(1–2), 9–19. doi:10.1016/s0378-4320(96)01638-7

Wydooghe E, Vandaele L, Heras S, de Sutter P, Deforce D, Peelman L, *et al.* (2017) Autocrine embryotropins revisited: how do embryos communicate with each other in vitro when cultured in groups? *Biological Reviews* **92**(1), 505–520. doi:10.1111/brv.12241

Zhan R, Leng X, Liu X, Wang X, Gong J, Yan L, *et al.* (2009) Heat shock protein 70 is secreted from endothelial cells by a non-classical pathway involving exosomes. *Biochemical and Biophysical Research Communications* **387**(2), 229–233. doi:10.1016/j.bbrc.2009.06.095

Zheng Y, Chen K, Zheng X, Li H, Wang G (2014) Identification and bioinformatics analysis of microRNAs associated with stress and immune response in serum of heat-stressed and normal Holstein cows. *Cell Stress & Chaperones* **19**(6), 973–981. doi:10.1007/s12192-014-0521-8

Data availability. Data sharing is not applicable as no new data were generated or analysed during this study.

Conflicts of interest. The authors declare that they have no conflicts of interest.

Declaration of funding. This research did not receive any specific funding.

Author affiliations

[A]Animal Reproduction and Biotechnology Laboratory, Department of Biomedical Sciences, Colorado State University, 3051 Rampart Road, Fort Collins, CO 80521, USA.

[B]Genus plc, 1525 River Road, DeForest, WI 53532, USA.

Molecular Human Reproduction, Vol.29, No.4, gaad009, 2023
Advance Access Publication on February 28, 2023 https://doi.org/10.1093/molehr/gaad009

molecular human reproduction

ORIGINAL RESEARCH

Dynamics of extracellular vesicle-coupled microRNAs in equine follicular fluid associated with follicle selection and ovulation

Samuel Gebremedhn[1,2,†], Ahmed Gad[1,3,†], Ghassan M. Ishak[4,5], Nico G. Menjivar[1], Melba O. Gastal[5], Jean M. Feugang[6], Radek Prochazka[7], Dawit Tesfaye [1,*], and Eduardo L. Gastal [5]

[1]Animal Reproduction and Biotechnology Laboratory (ARBL), Department of Biomedical Sciences, College of Veterinary Medicine and Biomedical Sciences, Colorado State University, Fort Collins, CO, USA [2]Division of IVF Research, Genus Plc, DeForest, WI, USA [3]Department of Animal Production, Faculty of Agriculture, Cairo University, Giza, Egypt [4]Department of Surgery and Obstetrics, College of Veterinary Medicine, University of Baghdad, Baghdad, Iraq [5]Department of Animal Science, School of Agricultural Sciences, Southern Illinois University, Carbondale, IL, USA [6]Department of Animal and Dairy Sciences, Mississippi State University, Mississippi State, MS, USA [7]Laboratory of Developmental Biology, Institute of Animal Physiology and Genetics, Czech Academy of Sciences, Libĕchov, Czech Republic

*Correspondence address. Animal Reproduction and Biotechnology Laboratory (ARBL), Department of Biomedical Sciences, Colorado State University, Fort Collins, CO 80523, USA. E-mail: dawit.tesfaye@colostate.edu https://orcid.org/0000-0001-8166-0606

Submitted on November 21, 2022; resubmitted on February 16, 2023; editorial decision on February 23, 2023

ABSTRACT: Innumerable similarities in reproductive cyclicity and hormonal alterations highlight the considerable utility of the mare to study aspects of follicular dynamics and reproductive function in view of the largely constricted, human research subjects. The bi-directional communication between the growing oocyte and the surrounding somatic cells embodies the hallmark of mammalian follicular development, partially mediated by extracellular vesicles (EVs) encapsulated with microRNAs (miRNAs) and present in the follicular fluid (FF). Here, we aimed to decipher the dynamics of the miRNAs in EVs from equine FF aspirated *in vivo* during different stages of follicular development, namely, predeviation (PreDev; 18–20 mm), deviation (Dev; 22–25 mm), postdeviation (PostDev; 26–29 mm), preovulatory (PreOV; 30–35 mm), and impending ovulation (IMP; ∼40 mm). Approximately 176 known miRNAs were found in all groups with 144 mutually detected among all groups. Cluster analysis exhibited 15 different expression patterns during follicular development. Among these patterns, a group of 22 miRNAs (including miR-146b-5p, miR-140, and miR-143) exhibited a sharp reduction in expression from the PreDev until the PreOV stage. Another cluster of 23 miRNAs (including miR-106b, miR-199a-5p, and miR-125a-5p) exhibited a stable expression pattern at the PreDev stage until the PostDev stage, with a significant increase at the PreOV stage followed by a significant decrease at the IMP stage. In conclusion, this study provides greater insights into the stage-specific expression dynamics of FF EV-miRNAs during equine follicular development, which may propose novel approaches to improve ART and provide new biomarkers to facilitate the assessment of ovarian pathophysiological conditions.

Key words: follicular fluid / extracellular vesicles / microRNAs / folliculogenesis / equine / ovary / oocytes / noncoding RNA

Introduction

Ovarian follicle development in mono-ovulatory species (e.g. mares, cows, and women) is characterized by follicular dominance of a single follicle in a given ovulatory wave. Selection of a dominant follicle is established by diameter deviation, in which the future dominant follicle continually maintains constant growth until ovulation, whereas the remaining (subordinate) follicles grow at a reduced rate and eventually regress (Baerwald *et al.*, 2003a,b; Ginther *et al.*, 2004a,b, 2005; Baerwald, 2009; Adams *et al.*, 2012; Ginther, 2017a; Bashir *et al.*, 2018; Garcia-Guerra *et al.*, 2018). The mechanisms of follicle development, selection, dominance, and ovulation are a series of long and complex processes involving systemic interactions of hormones (e.g. FSH and LH) and intrafollicular components such as insulin-like growth factor 1 (IGF1), insulin-like growth factor-binding proteins (IGFBPs), IGFBP protease, vascular endothelial growth factor, inhibin-A, activin-A, and estradiol (Donadeu and Ginther, 2002; Ginther *et al.*, 2004c; Beg and Ginther, 2006; Bashir *et al.*, 2016b; Ginther, 2017b; Wischral

†These authors should be considered joint first authors.

© The Author(s) 2023. Published by Oxford University Press on behalf of European Society of Human Reproduction and Embryology. All rights reserved.
For permissions, please email: journals.permissions@oup.com

Downloaded from https://academic.oup.com/molehr/article/29/4/gaad009/7059535 by Colorado State University user on 30 November 2023

et al., 2022). Several studies have shown the importance of the mare as a relevant experimental model for understanding ovarian follicular dynamics, anovulatory dysfunction, and oocyte aging in women (Ginther et al., 2004b, 2005; Carnevale, 2008; Baerwald, 2009; Ginther, 2012; Bashir et al., 2016a, 2018; Benammar et al., 2021). In this regard, mares and women, for example, are both mono-ovulatory species, having similar patterns of follicular waves and temporal relationships between follicular events and hormonal concentrations (Ginther et al., 2004b,c, 2005). Additionally, because equine are among the most long-lived domestic animals with easily assessable reproductive anatomy excellent for monitoring and manipulation, they have been largely used as study models for reproductive aging in women (Carnevale, 2008; Baerwald, 2009; Benammar et al., 2021).

Despite the extensive work that has been carried out to understand the different aspects of follicle selection in mono-ovulatory species, the underlying regulatory mechanisms at the molecular level are still largely unknown. The presence and involvement of active biochemical substances within the follicular fluid (FF) (e.g. hormones, growth factors, and proteins) in regulating the bi-directional communications between follicular cells and the oocyte is of utmost importance for the selection and development of a healthy dominant follicle and consequently, ovulation of a competent oocyte (Gilchrist et al., 2004; Campos-Chillon et al., 2015). The recent discovery of extracellular vesicles (EVs) has added a new layer of cell–cell communication amid the follicular microenvironment for a better understanding of folliculogenesis and oogenesis, as well as revealing the potential association of cargo molecules with oocyte competence and animal fertility (Sohel et al., 2013; Noferesti et al., 2015; Hailay et al., 2019). Currently, little information is available on the role of EVs during specific stages of follicle development including before, during, and after follicle deviation (i.e. 'selection' of the dominant follicle), as well as during the ovulation process. Knowledge regarding the intrafollicular milieu *in vivo* may offer unique insights into the mechanisms governing the development of a healthy follicle. It also serves as the foundation for perfecting the diagnosis and treatment of ovulatory failures associated with various ovarian pathophysiological conditions.

EVs are nano-sized, membrane-bound, and evolutionarily conserved structures secreted from almost all cell types through exocytosis into the surrounding extracellular space (György et al., 2011). Broadly categorized into three main subpopulations according to their size and mode of biogenesis, EVs consist of exosomes, microvesicles, and apoptotic bodies (Taylor and Gercel-Taylor, 2013). Even though EVs were initially considered as merely mediators to shuttle cellular toxicants into the extracellular space for cellular homeostasis and maintenance, recent studies have shed light upon their role in cellular crosstalk mechanisms with neighboring cells posing both beneficial and deleterious effects (Yáñez-Mó et al., 2015). This was further consolidated by the phenotypic changes attained in recipient cells arising from the transfer of an array of functional bioactive molecules, including mRNA, microRNAs (miRNAs), and proteins, upon EV interaction with the cellular matrix (O'Brien et al., 2020).

EVs are reported to be abundantly present in the FF of various mammalian species, including bovine, equine, and humans (Santonocito et al., 2014; Tesfaye et al., 2020). In equine FF, distinct miRNA cargoes in EVs were shown to be dependent upon the age of the mare, showing differentially expressed EV-miRNAs predicted to target members of the TGF-β pathway (da Silveira et al., 2015). In addition, miRNAs released via EVs were also abundantly expressed in mare granulosa cells (GCs), implicating a strong involvement of EVs in cell–cell communication in the mare ovarian follicle microenvironment (da Silveira et al., 2012). Similarly, in humans, FF EV-miRNAs were reported to play a role in cellular communication among follicular cells and oocytes, and could be associated with oocyte developmental competence after IVF (Scalici et al., 2016; Martinez et al., 2018). Moreover, EV-coupled miRNAs could be used as potential diagnostic markers for several ovarian pathophysiological conditions, such as polycystic ovary syndrome (PCOS), premature ovarian insufficiency (POI), and ovarian cancer (Sang et al., 2013; Roth et al., 2014; Montazerian et al., 2018).

In this regard, characterization of the expression and dynamics of EV-miRNAs in FF creates an opportunity for novel biomarker discoveries vital for oocyte developmental competence acquisition or potential strategies for intrafollicular treatment using the mare as a model for human studies. Therefore, the objective of this work was to characterize the EV-miRNAs expression and dynamics in equine FF collected *in vivo* during five specific stages of follicular development (i.e. predeviation, deviation, postdeviation, preovulatory, and impending ovulation). The present study has identified for the first-time various clusters of EV-coupled miRNAs with dynamic alterations throughout follicular development. These miRNA clusters could potentially be used as a molecular control profile to investigate the impact of various pathophysiological conditions on follicular development, causes of infertility and to identify EV-coupled molecular signals that could be targets of future intervention to improve ART outcome and enhance pregnancy success.

Materials and methods

Animals

Quarter horse mares ($n = 19$; 8 to 14 ± 1.8 (SD) years old) with normal reproductive tracts as determined by ultrasonographic examination were used during the ovulatory season (June and July) in the northern hemisphere (latitude, 37.7°N) for *in vivo* collection of FF samples. Mares were kept under natural light on pasture with free access to water and trace-mineralized salt. All experimental procedures were performed in accordance with the United States Department of Agriculture Guide for Care and Use of Agricultural Animals in Research and were approved by the Institutional Animal Care and Use Committee of Southern Illinois University.

Ultrasonography, follicle tracking, and groups

Ultrasound-guided ablations of all follicles ≥6 mm were performed on Days 10–11 of the estrous cycle (ovulation = Day 0) to induce a new follicular wave as described previously (Gastal et al., 1997). Thereafter, daily ultrasonographic follicle examinations were performed using a duplex B-mode and color-Doppler ultrasound machine (Aloka SSD-3500; Hitachi Aloka Medical America, Inc., Wallingford, CT, USA) equipped with a finger-mounted 3.5–10 MHz convex-array transducer (UST-995-7.5) until follicles reached the targeted group diameter. Follicles that were ultrasonographically healthy and grew for at

Downloaded from https://academic.oup.com/molehr/article/29/4/gaad009/7059535 by Colorado State University user on 30 November 2023

least three consecutive days were assigned to five groups based on the targeted diameters: predeviation (PreDev; 18–20 mm), deviation (Dev; 22–25 mm), postdeviation (PostDev; 26–29 mm), preovulatory (PreOV; 30–35 mm), and impending ovulation (IMP; ~40 mm) follicles with signs of imminent ovulation, as described previously (Gastal *et al.*, 2006). The complete experimental design is illustrated in Fig. 1.

Follicular fluid sample collection

For follicular ablation and FF sampling procedures, mares were prepared and sedated (Haag *et al.*, 2013; Ishak *et al.*, 2018). Samples of FF were collected *in vivo* by ultrasound-guided transvaginal follicle aspiration as previously described (Ishak *et al.*, 2018). Briefly, antral follicles were measured and aspirated using a sterile 12-G needle mounted on a 5–10 MHz transvaginal ultrasound-guided convex array transducer (Aloka UST-987-7.5). Once the targeted follicle was presented on the ultrasound screen, only the tip of the 12-G needle was introduced into the follicle's antrum, and immediately the leaking FF was collected into a sterile vial. Only clear FF samples without any visible trace of blood contamination were used in the present study. Therefore, a total of 42 clear FF samples were obtained from 19 mares, with 6–8 mares being considered for each follicle group. To obtain enough FF samples during the ovulatory season and avoid the effects of the autumn transition/anovulatory season on follicle dynamics and milieu, each mare was sampled once or twice within the same cycle. Therefore, to minimize biological noise in the different FF samples collected from the same mares, the second follicle aspiration within the same cycle was performed using a different follicle group that was far apart from the first aspirated follicle type (e.g. PreDev versus PreOV or IMP). Collected FF samples were immediately centrifuged (1600×*g*

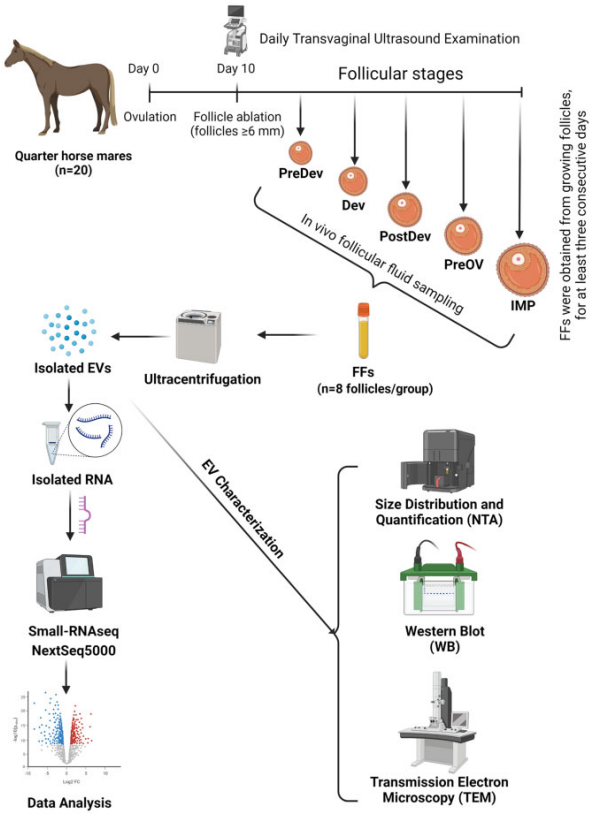


Figure 1. Experimental design for the analysis of extracellular vesicle-coupled miRNAs in equine follicular fluid. Quarter horse mares were used during the ovulatory season for *in vivo* collection of follicular fluid (FF) samples. Ultrasound-guided ablations of all follicles ≥6 mm were performed on Days 10–11 of the estrous cycle (ovulation = Day 0) to induce a new follicular wave. Thereafter, daily ultrasonographic follicle examinations were performed until follicles reached the targeted group diameter. Follicles that were healthy and grew for at least three consecutive days were assigned to five groups based on the targeted diameters: predeviation (PreDev; 18–20 mm), deviation (Dev; 22–25 mm), postdeviation (PostDev; 26–29 mm), preovulatory (PreOV; 30–35 mm), and impending ovulation (IMP; ~40). Samples of FF were collected *in vivo* by ultrasound-guided transvaginal follicle aspiration and used for extracellular vesicle (EV) isolation. Isolated EVs were characterized using three different approaches and then used for total RNA isolation and small-RNAseq analysis.

Downloaded from https://academic.oup.com/molehr/article/29/4/gaad009/7059535 by Colorado State University user on 30 November 2023

for 10 min at 4°C), and the supernatants were subjected to a second centrifugation (3200×g for 15 min at 4°C) and stored at –80°C for later evaluation.

Isolation of EVs from FF of mares

In each experimental group, two or three frozen-thawed FF samples of different origins (follicles and animals) were pooled, and four different pools were used for EV isolation. FF samples were subjected to a series of centrifugations after removing from –80°C storage starting at 500×g for 5 min to remove cells, followed by 4000×g to remove the cellular debris. Samples of FF were filtered through a 0.22 µM sterile filter to remove particles larger than 200 nm. Thereafter, EVs were isolated by centrifuging samples at 25 000×g for 30 min at 4°C. For the EV isolation, 2 ml of pre-centrifuged follicular samples were subjected to an ultracentrifugation procedure at 120 000×g for 70 min at 4°C using the Beckman SWTi55 rotor (Beckman Coulter; Pasadena, CA, USA). The EV pellet was washed with sterile PBS and then centrifuged again at 120 000×g for 70 min. Finally, EVs were resuspended in 500 µl of PBS and stored at −80°C until further characterization and analysis.

Morphological and molecular characterization of EVs

The presence of EV-specific proteins (CD63 antigen molecule, tumor susceptibility gene 101 (TSG101), and flotillin 1 (FLOT1)) in the isolated EVs and the absence of a cell-specific marker protein, cytochrome C (CYTC), were verified by the immunoblotting technique as previously described (Gebremedhn *et al.*, 2020). Briefly, 100 µl of isolated EVs were lysed in 50 µl 1 × RIPA buffer and the protein extract samples were centrifuged at 12 000×g for 30 min at 4°C. Following this, protein lysates were separated by electrophoresis in a 10–12% gradient sodium dodecyl sulphate–polyacrylamide gel (Bio-Rad Laboratories, Hercules, CA, USA) at 90 volts for 15 min then 125 volts for 60 min and transferred onto a nitrocellulose membrane (Bio-Rad) for 1 h at 100 volts. Membranes were blocked in 5% non-fat dry milk dissolved in TBST (100 ml of 10× TBS (Bio-Rad), 1 ml of Tween (Bio-Rad), and 900 mL of Nanopure water) for 1 h on a shaker at room temperature. Following the blocking, membranes were incubated with the following anti-CD63 rabbit polyclonal (1:250; System Biosciences, Palo Alto, CA, USA): Anti-TSG101 rabbit polyclonal (1:250; System Biosciences), Anti-FLOT1 rabbit polyclonal (1:250; System Biosciences), and Anti-CYCS goat polyclonal (1:350; Sino Biological; Wayne, PA, USA) primary antibodies overnight at 4°C. After the membranes were washed with 1× TBST, they were incubated with appropriate secondary antibodies conjugated with horseradish peroxidase for 1 h at room temperature protected from light. After the membranes were washed with 1× TBST, protein bands were visualized using an enhanced chemiluminescence substrate (Bio-Rad), and images were acquired using Chemi Doc XRS + chemiluminescence imaging system (Bio-Rad Laboratories). The size and concentration of isolated EVs were determined using the Zetaview Particle Metrix (Particle Metrix, Ammersee, Germany). Briefly, 10 µl of purified EVs was diluted in 990 µl of sterile PBS and assembled into the Zetaview Laser scattering microscope (Particle Metrix) fitted with an LM14C laser. For each sample, 11 independent video measurements were recorded at 11 independent positions, and video files were analyzed with ZetaView software version 8.05.12 (Particle Metrix).

The morphology and size of the purified EVs were analyzed using a transmission electron microscope (TEM) according to the methods previously reported (Gebremedhn *et al.*, 2020). Briefly, a drop of 30 µl purified EVs was placed on parafilm. The EV drops were covered with Formvar/carbon-coated grids and allowed to stand for 5 min to absorb the EVs. The grids that contained the EVs were washed with drops of ddH_2O and fixed by placing them on a 30 µl drop of 2% uranyl acetate. The presence of the EVs on the carbon-coated grids was examined under an electron microscope. We have submitted all relevant data of our experiments to the EV-TRACK knowledgebase (EV-TRACK ID: EV220406; van Deun *et al.*, 2017).

Total RNA extraction, library preparation, and sequencing

Total RNA, including miRNAs, was isolated from EVs using a Norgen Exosomal RNA Isolation kit (Norgen, Thorold, ON, Canada) according to the manufacturer's instructions. On-column DNA digestion was performed to remove genomic DNA contaminants. The RNA concentration and size distribution were analyzed using an Agilent RNA 6000 Pico kit in an Agilent 2100 Bioanalyzer (Agilent Technologies, Santa Clara, CA, USA). Small-RNA libraries were prepared for next-generation sequencing using a TruSeq Small RNA Library Prep Kit (Illumina) according to the manufacturer's instructions. Library quantity and quality assessments were performed using a Qubit DNA HS Assay Kit in a Qubit 2.0 Fluorometer (Thermo Fisher Scientific, Waltham, MA, USA) and an Agilent DNA High Sensitivity kit in an Agilent 2100 Bioanalyzer (Agilent Technologies), respectively. The precise concentration of the libraries was calculated using a quantitative PCR. The libraries were pooled in equimolar ratios and then sequenced in a NovaSeq6000 sequencing instrument (Illumina, Inc., San Diego, CA, USA) as single-end reads.

Sequencing data analysis and miRNA clustering

FASTQ files were generated for each sample using the software bcl2fastq (Illumina Inc.), and their quality was checked using the FastQC tool version 0.11.9 (Babraham Institute, Cambridge, UK). Data were analyzed using the software CLC Genomics Workbench, version 21 (Qiagen, Redwood City, CA, USA). Raw sequencing reads were trimmed based on quality score (Q-score >30), ambiguous nucleotides (maximum two nucleotides allowed), read length (≥15 nucleotides), and removing adapter sequences. Reads were mapped to the equine (*Equus caballus*) reference genome (EquCab3.0) and annotated against equine precursor and mature miRNAs listed in the mirBase database (release 22) using the CLC Genomics Workbench RNA-Seq Analysis and Quantify miRNA tools, respectively, applying the default software parameters and considering the presence of different isomiRs by allowing 2 up- or downstream additional or missing bases, as well as a maximum of 2 mismatches within the read. Raw expression data were normalized using the trimmed mean of M-values normalization method (TMM normalization) (Robinson and Oshlack, 2010) and presented as TMM-adjusted counts per million (CPM). The CLC Genomics Workbench Differential Expression tool was used for

Downloaded from https://academic.oup.com/molehr/article/29/4/gaad009/7059535 by Colorado State University user on 30 November 2023

the expression analysis comparison of the two groups. Those miRNAs with a fold change (FC) ≥2 and *P*-adjusted value (FDR) (Benjamini and Hochberg, 1995) <0.1 were considered differentially expressed (DE). The raw FASTQ files and processed comma-separated value (CSV) files have been deposited in the NCBI Gene Expression Omnibus (GEO) with the accession number GSE211179. miRNAs were grouped in different cluster patterns according to their expression profiles among the different developmental stages using the Mfuzz Bioconductor package (Kumar and Futschik, 2007).

Target gene prediction and ontological classification

Genes targeted by the DE-miRNA were identified using the human homologous miRNAs in the miRWalk database (Sticht *et al.*, 2018). Within the miRWalk, validated target genes from miRTarBase (version 7.0) and commonly target genes predicted by TargetScan (version 7.1) and miRDB (release 5.0) were selected for pathway analysis using the DAVID bioinformatics web tool (https://david.abcc.ncifcrf.gov/) and the KEGG pathway database (Ogata *et al.*, 1999). Interaction networks of the DE-miRNAs and targeted genes were constructed with Cytoscape (Shannon *et al.*, 2003).

Results

FF samples of mares are enriched with EVs

The FF samples derived from mares with different stages of follicular development were subjected to isolation of the EVs and further molecular and morphological characterization based on the recommendations set by the International Society of Extracellular Vesicles (ISEV; https://www.isev.org/). The western blot analysis showed that EVs of the mare FF from all the developmental stages are enriched with the transmembrane proteins CD63 and FLOT1 and the TSG101 protein. Moreover, the mitochondrial protein marker, cytochrome C, was absent from the EV samples but present in samples derived from mare GCs (Fig. 2A), confirming both the identity of the EVs and the absence of cellular contaminations during the EV preparations (the full uncropped blot is presented in Supplementary Fig. S1). Similarly, TEM imaging showed the presence of EVs with visible bilipid membranes within the acceptable size ranges (Fig. 2B). The NTA analysis showed that the EV samples from the FF fall within the range of 91–111 nm diameter (Fig. 2C). The analysis revealed that the EVs derived from the PostDev stage of follicular development had a relatively large proportion of small-size EVs compared to the preceding stages of development. Similarly, the concentration of the EVs showed a range of 6.2×10^7 to 1.4×10^8 particles/ml and, contrary to the size of the EVs, no statistically significant differences were observed in the concentration of the particles among the EV samples derived from all stages of follicular development (Fig. 2D). The RNAs isolated from the EV samples were analyzed for their integrity, and electropherogram analysis showed the absence of cellular RNA peaks (18 s and 28 s) and the presence of peaks around the small RNA size ranges, which indicate the presence of small RNAs in the EV samples (Fig. 2E).

The miRNA profile of EVs derived from FF showed clear distinctions among stages of follicular development

A total of 20 small-RNA sequence libraries, with four libraries for each stage, were constructed and after the trimming procedures of the adaptors and low-quality reads, on average, 23 million reads per library passed the quality control parameters and were used for the mapping (Supplementary Table SI) against the reference genome. Results showed that an average of 74% of the quality-passed reads (16 million reads per library) were mapped against the equine (*Equus caballus*) reference genome (EquCab3.0). On average, 3% of the mapped sequences were annotated to miRNAs (Supplementary Table SI). Principal component analysis showed that the miRNA profile of the EVs was distinctly different in the PreDev stage compared to the rest of the following follicular developmental stages. The separation of the stages of follicular development was consistent as we proceed from the PreDev stage toward the Dev, PostDev, PreOV, and IMP stages (Fig. 3A). Similarly, the hierarchical clustering analysis showed a similar pattern of clustering following the sequential stages of follicular development (Fig. 3B). During the analysis of the sequence data, we set a stringent parameter to consider a miRNA as detected if it was detected in a minimum of three of the four sequence libraries with a minimum of 10 CPM. The result showed that a total of 176 known mature miRNAs were detected in all groups, of which 144 miRNAs were commonly detected in all stages of follicular development (Fig. 3C). Among the top 20 miRNAs that exhibited the highest read counts in all follicular development stages, 14 miRNAs, including members of the Let-7 family (let-7c and let-7g), miR-148a, miR-21, miR-99a, miR-10b, miR-10a, miR-143, miR-423-5p, miR-192, let-7c, let-7g, miR-24, miR-486-5p, miR-215, and miR-128, were commonly detected in all stages of follicular development (Table I). The complete list of miRNAs detected in each stage and the corresponding CPM values are indicated in Supplementary Table SII.

Differentially expressed miRNAs

Differential expression analysis indicated 66 miRNAs as significantly differentially expressed in 10 different comparisons (Fig. 4; Supplementary Table SIII). The highest number of DE-miRNAs has been found in the comparison of the PreOV versus PreDev stages with 29 and 14 up- and downregulated miRNAs, respectively. Moreover, comparing PreDev versus IMP stage showed a total of 24 DE-miRNAs (4 up- and 20 downregulated miRNAs). The lowest number of DE-miRNAs was found in the PostDev versus Dev and PreOV versus PostDev comparisons with five and four DE-miRNAs, respectively (Fig. 4; Supplementary Table SIII). Interestingly, six DE-miRNAs (miR-9a, miR-204b, miR-206, miR-34c, miR-483, and miR-485-3p) appeared in at least 5 out of the 10 different stage comparisons (Table II). The validated targeted genes by these miRNAs, as well as the corresponding pathways, are presented in Fig. 5.

MicroRNAs released into FF via EVs are temporally clustered according to the stages of follicular development

The abundance of EV-coupled miRNAs across the stages of follicular development was sorted according to the abundance in each stage of

Downloaded from https://academic.oup.com/molehr/article/29/4/gaad009/7059535 by Colorado State University user on 30 November 2023

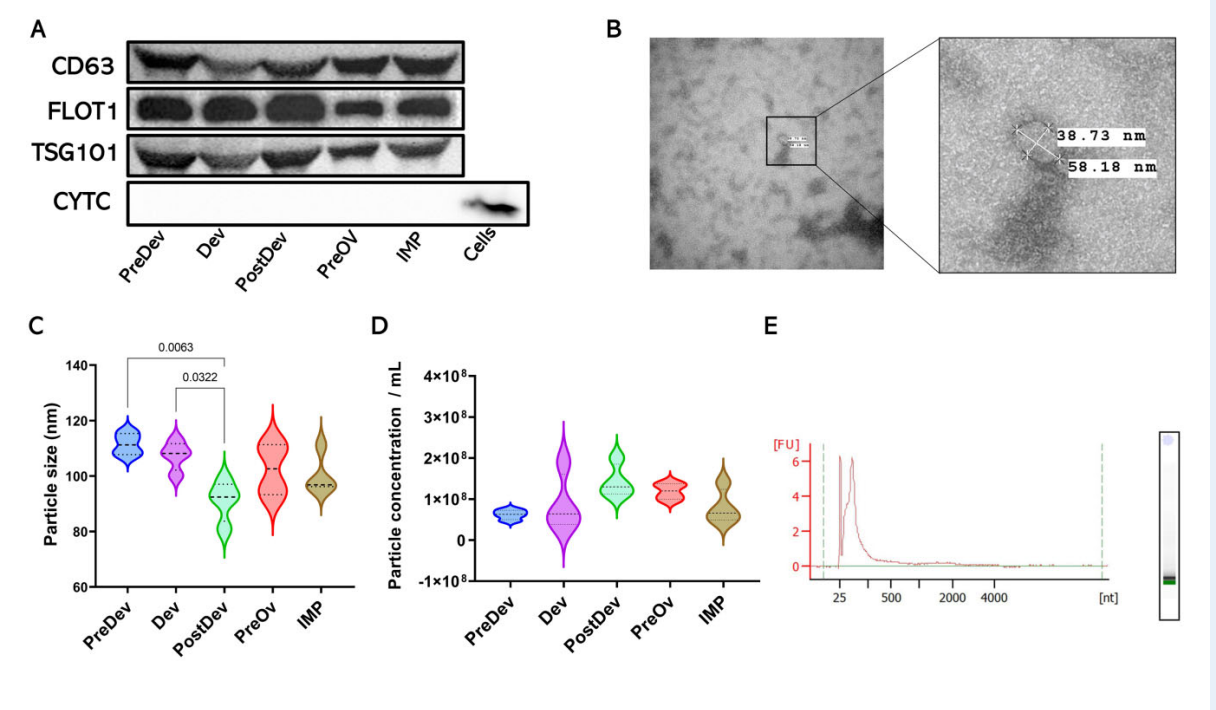


Figure 2. Morphological and molecular characterization of extracellular vesicles isolated from equine follicular fluid. (**A**) Western blot analysis of extracellular vesicle (EV) marker proteins (CD63 antigen molecule, flotillin 1 (FLOT1), and tumor susceptibility gene 101 (TSG101)) and cellular protein contamination indicator (cytochrome C (CYTC)) (cells = granulosa cells, as positive control). The full, uncropped blot is presented in Supplementary Fig. S1. (**B**) Transmission electron microscope imaging showing a clear morphology of EVs with a cross-sectional size of the diameter. (**C**) The median size of the EVs isolated from the mare follicular fluid (FF) using the nano tracking analysis (NTA). (**D**) The concentration of EVs isolated from the follicular fluid using the NTA analysis. (**E**) The RNA size distribution (left) and the gel-like image (right) of EVs showing the presence of the peak of small RNA and the absence of the 18s and 28s ribosomal RNA peaks. FU: fluorescence unit; nt: nucleotide. Data for EV size and concentration are presented as mean ± SEM, and the mean differences were analyzed using one-way ANOVA followed by the Tukey multiple comparison test. *P*-values <0.05 were considered statistically significant differences between groups. PreDev: predeviation; Dev: deviation; PostDev: postdeviation; PreOV: preovulatory; IMP: impending ovulation.

development and shown to have distinct clustering patterns. Cluster analysis showed that the miRNAs released via EVs were clustered into 15 different patterns (Fig. 6A; Supplementary Table SIV). Each cluster pattern was composed of a variable number of miRNAs, in which clusters 3 and 14 contained a higher number of miRNAs compared to the other clusters (Fig. 6B).

A microRNA cluster exhibited a consistent declining expression pattern through the later stages of follicular development

Among the multiple clusters of miRNAs that exhibited variable expression patterns across the stages of development, cluster 14, which comprises 22 miRNAs, showed a consistent declining expression pattern from the PreDev toward the PreOV and IMP stages (Fig. 7A). In this cluster, seven miRNAs were among the differentially expressed miRNAs in the different stage comparisons, and one was exclusively expressed in the PreDev stage (Fig. 7B). Among the DE-miRNAs in this cluster, miR-146b-5p was significantly upregulated in the PreDev stage compared to the PostDev, PreOV, and IMP stages. Similarly, miR-34b-5p appeared to be exclusively expressed in the PreDev stage (Fig. 7B). Pathway analysis on the predicted target genes of the exclusive and DE-miRNAs of this cluster showed pathways related to oocyte meiosis, fatty acid biosynthesis, cell cycle, mechanistic target of rapamycin (mTOR) signaling, mitogen-activated protein kinase (MAPK) signaling, and AMP-activated protein kinase (AMPK) signaling were among the top significantly targeted pathways (Fig. 7C).

A microRNA cluster exhibited a significant abundance during the preovulatory stage of follicular development

A cluster of 23 miRNAs exhibited significantly higher abundance during the PreOV stage of follicular development (Fig. 8A) compared to the other stages. In this cluster, 10 miRNAs were among the DE-miRNAs in the different stage comparisons, and three were exclusively expressed in the PreOV stage (Fig. 8B). Among these miRNAs, miR-106, miR-199a-5p, miR-199b-5p, and miR-218 were significantly

Downloaded from https://academic.oup.com/molehr/article/29/4/gaad009/7059535 by Colorado State University user on 30 November 2023

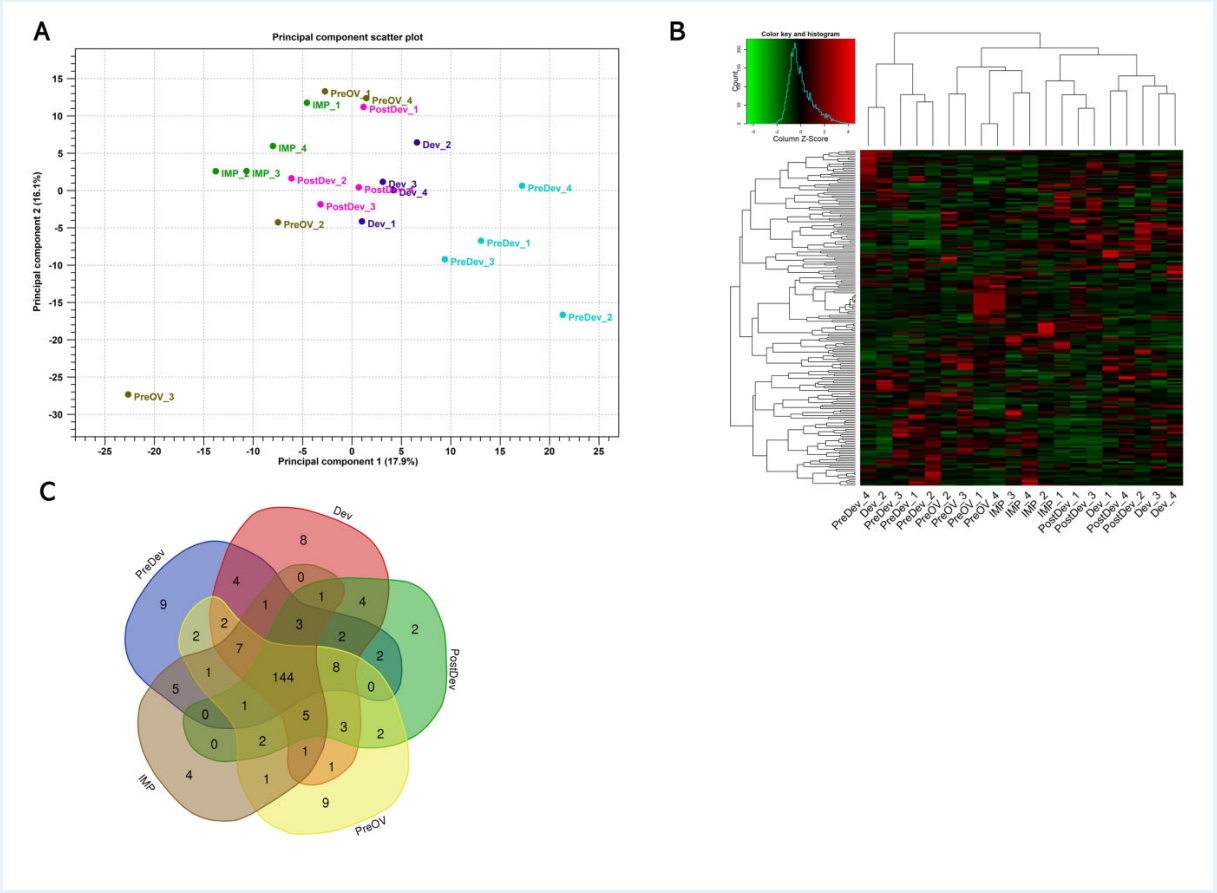


Figure 3. Small-RNA sequence data overview. (**A**) Principal component analysis. (**B**) Heatmap and hierarchical clustering of expressed microRNAs (miRNAs). Red and green colors represent high and low expressed miRNAs, respectively. (**C**) Venn diagram for commonly and exclusively expressed miRNAs in the follicular fluid extracellular vesicles at different stages of follicular development. A miRNA with a value of CPM >10 in at least three replicates of the four biological replicates was considered detected. PreDev: predeviation; Dev: deviation; PostDev: postdeviation; PreOV: preovulatory; IMP: impending ovulation.

upregulated in the PreOV stage compared to the other stages, while miR-490-3P, miR-598, and miR-708 were exclusively detected during the PreOV stage (Fig. 8B). Pathway analysis revealed that these miRNAs are regulating genes involved in pathways associated with TGF-signaling, endocytosis, and circadian rhythm (Fig. 8C).

A cluster of microRNAs was found to have a sharp increment during the ovulation stages

The EVs obtained from FF of equine ovulatory follicles are endowed with 11 miRNAs enriched during the impending ovulation stage (IMP group) compared to the preceding stages of development (Fig. 9A). In this cluster, four miRNAs (miR-206, miR-204b, miR-183, and miR-362-5p) were significantly upregulated in the IMP stage compared to the other stages of follicular development (Fig. 9B). Additionally, two of them (miR-206 and miR-204b) were also upregulated in the PostDev compared to PreDev and Dev stages. The predicted target genes of these differentially expressed miRNAs in the impending ovulatory follicles are involved in pathways related to gap junction, estrogen, Rap1, and GnRH signaling pathways (Fig. 9C).

Discussion

The presence and potential involvement of EV-coupled miRNAs in mare and human FFs in mediating cell–cell communication in association with oocyte developmental competence has been reported previously (da Silveira *et al.*, 2012, 2015; Martinez *et al.*, 2018). However, those studies considered specific stages of follicular development while using small-scale miRNA expression technology, which may not provide the complete picture of EV-miRNAs mediating follicular and oocyte development. Therefore, in the current study, we constructed

Downloaded from https://academic.oup.com/molehr/article/29/4/gaad009/7059535 by Colorado State University user on 30 November 2023

Downloaded from https://academic.oup.com/molehr/article/29/4/gaad009/7059535 by Colorado State University user on 30 November 2023

Table I List of top 20 most abundant microRNAs in the extracellular vesicles obtained from equine follicular fluids at different follicular stages.

Name	PreDev CPM	Name	Dev CPM	Name	PostDev CPM	Name	PreOV CPM	Name	IMP CPM
eca-miR-148a	409 806.46	**eca-miR-148a**	277 969.22	**eca-miR-148a**	206 178.04	**eca-miR-148a**	152 965.15	**eca-miR-148a**	169 838.89
eca-miR-21	194 891.59	**eca-miR-21**	135 755.66	**eca-miR-192**	92 665.57	**eca-miR-21**	95 901.47	**eca-miR-192**	81 230.16
eca-miR-99a	89 666.93	**eca-miR-99a**	84 174.55	**eca-miR-21**	72 389.67	**eca-miR-99a**	71 623.18	**eca-miR-21**	77 134.05
eca-miR-10b	66 218.20	**eca-miR-10b**	63 145.15	**eca-miR-99a**	54 958.62	**eca-miR-192**	51 373.46	**eca-miR-10a**	52 998.08
eca-miR-10a	60 677.32	**eca-miR-192**	57 725.74	**eca-miR-10b**	48 179.59	**eca-miR-10b**	49 761.65	**eca-miR-423-5p**	49 064.92
eca-miR-143	44 643.29	**eca-miR-10a**	55 601.35	**eca-miR-423-5p**	45 372.59	**eca-miR-423-5p**	39 955.41	**eca-miR-10b**	48 652.41
eca-miR-423-5p	33 408.40	**eca-miR-423-5p**	38 494.35	**eca-miR-10a**	43 382.60	**eca-miR-10a**	32 691.44	**eca-miR-99a**	38 118.68
eca-miR-192	29 890.37	**eca-miR-486-5p**	24 016.11	**eca-miR-215**	38 287.41	**eca-miR-486-5p**	24 713.88	**eca-miR-215**	27 490.33
eca-miR-100	23 916.29	**eca-miR-215**	23 578.38	**eca-miR-22**	25 803.64	**eca-miR-218**	21 250.09	**eca-miR-100**	21 564.89
eca-let-7c	21 197.74	**eca-miR-143**	22 493.12	**eca-miR-24**	21 075.65	**eca-miR-215**	18 943.79	**eca-miR-22**	19 754.83
eca-let-7g	18 603.44	**eca-miR-24**	21 927.39	**eca-miR-128**	19 638.04	**eca-let-7g**	17 988.93	**eca-miR-128**	19 450.89
eca-miR-27b	17 700.45	**eca-miR-27b**	19 126.45	**eca-miR-143**	15 821.05	**eca-miR-128**	17 875.35	**eca-miR-24**	17 208.97
eca-miR-24	15 907.17	**eca-miR-100**	17 140.29	**eca-miR-27b**	15 704.95	**eca-miR-26a**	16 816.53	**eca-miR-486-5p**	16 539.04
eca-miR-486-5p	15 309.42	**eca-let-7c**	16 728.22	**eca-miR-486-5p**	14 674.94	**eca-miR-143**	16 704.88	**eca-miR-143**	16 396.20
eca-miR-26a	15 047.80	**eca-miR-128**	16 083.20	**eca-miR-27a**	13 579.20	**eca-miR-27b**	16 077.11	**eca-let-7g**	16 114.67
eca-miR-215	12 010.99	**eca-miR-22**	13 850.70	**eca-miR-409-3p**	13 136.62	**eca-miR-22**	15 668.66	**eca-miR-7**	12 918.37
eca-miR-378	10 869.25	**eca-miR-27a**	12 916.35	**eca-let-7c**	11 905.89	**eca-miR-24**	14 686.37	**eca-let-7c**	12 566.43
eca-let-7f	10 072.44	**eca-let-7g**	11 417.87	**eca-miR-122**	11 485.03	**eca-miR-7**	14 500.99	**eca-let-7a**	12 493.91
eca-miR-409-3p	8942.59	**eca-miR-378**	10 646.15	**eca-let-7g**	11 369.86	**eca-let-7c**	11 931.11	**eca-miR-26a**	12 312.08
eca-miR-128	8814.08	**eca-miR-26a**	10 192.51	**eca-miR-378**	9602.69	**eca-let-7a**	10 613.72	**eca-miR-27a**	12 149.54

miRNA: microRNA; PreDev: predeviation; Dev: deviation; PostDev: postdeviation; PreOV: preovulatory; IMP: impending ovulation; CPM: counts per million.

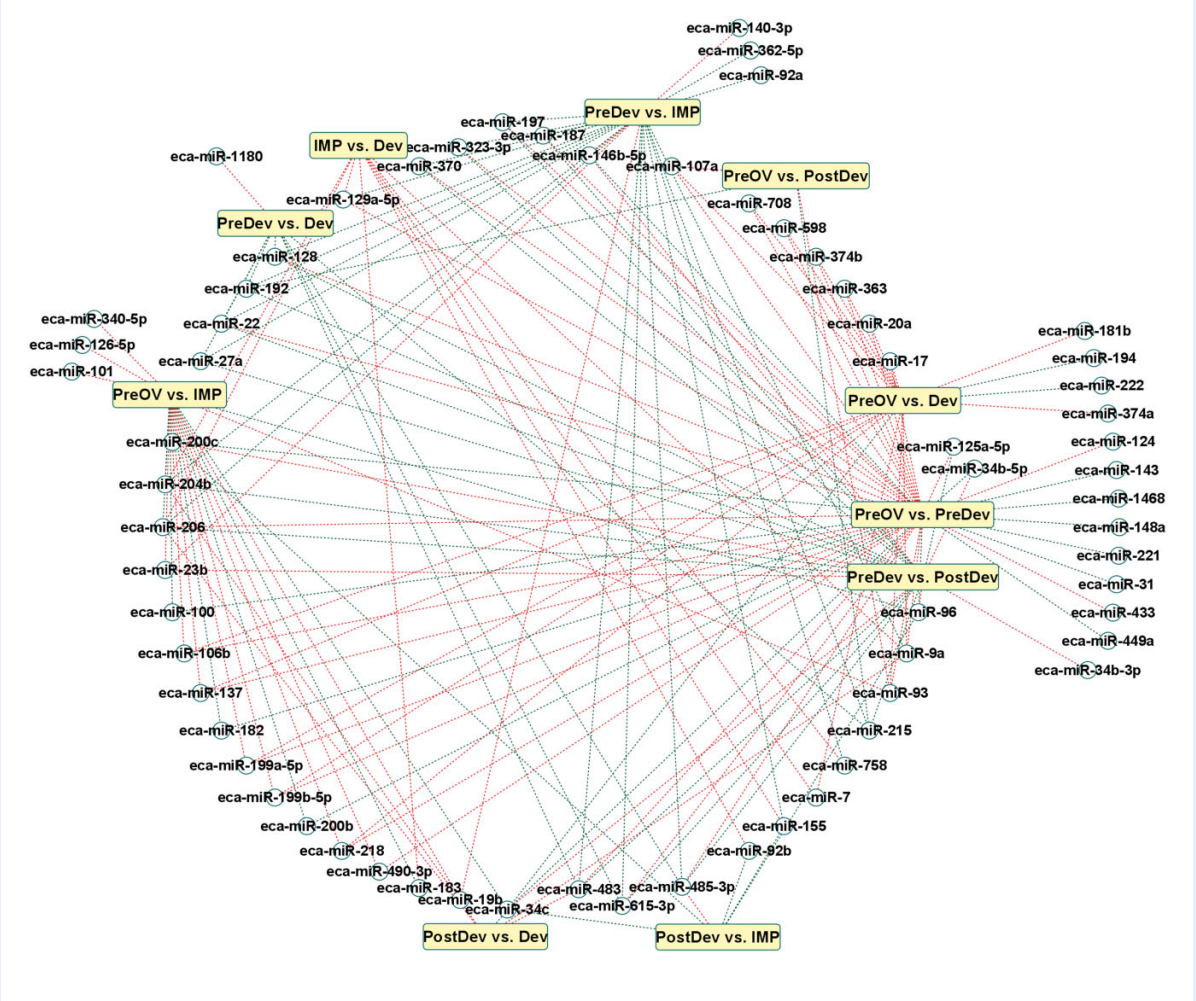


Figure 4. Differentially expressed microRNAs in extracellular vesicles isolated from equine follicular fluid. Commonly and exclusively differentially expressed (DE)-microRNAs from the 10 different stage comparisons (yellow boxes). Red and green edges emerged from each comparison indicating the up- and downregulated microRNAs, respectively. PreDev: predeviation; Dev: deviation; PostDev: postdeviation; PreOV: preovulatory; IMP: impending ovulation.

Table II Expression fold changes of differentially expressed microRNAs commonly appearing in at least five different equine follicular-stage comparisons.

Name	PreDev versus Dev	PostDev versus Dev	PreOV versus Dev	IMP versus Dev	PreDev versus PostDev	PreDev versus IMP	PostDev versus IMP	PreOV versus PreDev	PreOV versus PostDev	PreOV versus IMP
eca-miR-9a	–	19.9	26.0	42.6	–	−14.8	–	9.0	–	–
eca-miR-204b	–	8.0	–	17.0	−3.4	−7.2	–	–	–	−5.3
eca-miR-206	–	5.5	–	10.8	−7.0	−13.9	–	3.5	–	−3.9
eca-miR-34c	–	−55.3	−10.0	–	268.4	–	−63.3	−48.7	–	−11.5
eca-miR-483	−6.8	4.0	–	–	−27.1	−16.1	–	16.4	–	–
eca-miR-485-3p	−21.2	–	–	–	−42.6	−9.0	4.8	25.6	–	–

miRNA: microRNA, PreDev: predeviation; Dev: deviation; PostDev: postdeviation; PreOV: preovulatory; IMP: impending ovulation; –: not applicable.

Downloaded from https://academic.oup.com/molehr/article/29/4/gaad009/7059535 by Colorado State University user on 30 November 2023

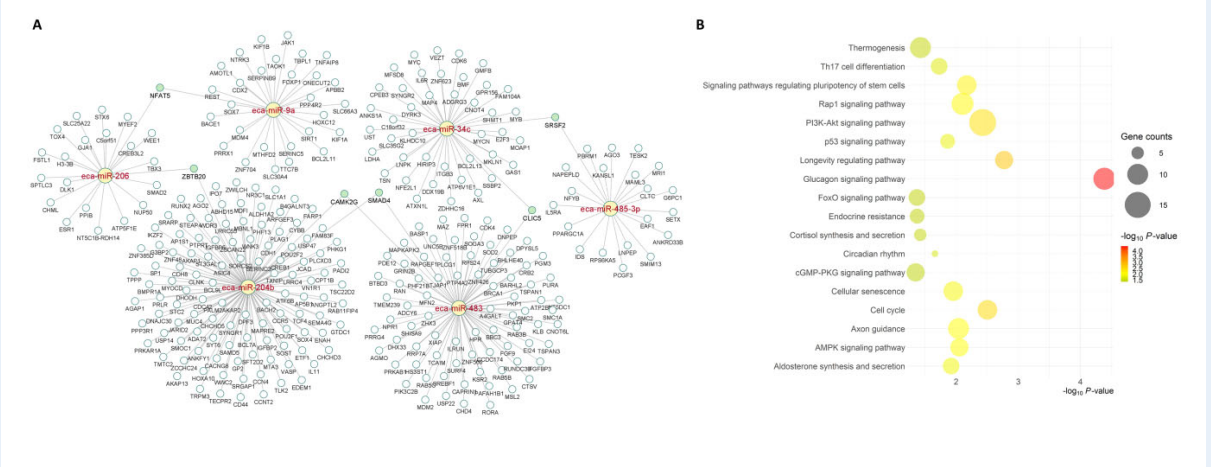
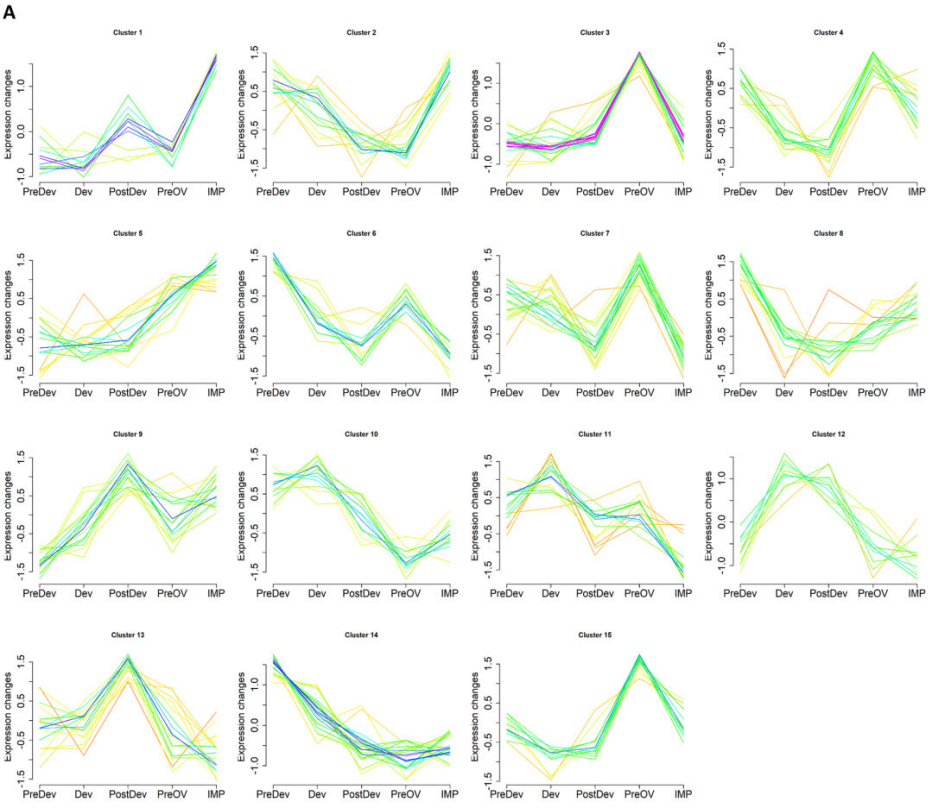


Figure 5. Gene network and pathways targeted by six differentially expressed miRNAs. (**A**) Network of the validated targeted genes by the six differentially expressed (DE)-miRNAs that appeared in at least 5 out of the 10 different stage comparisons. The commonly targeted genes are presented as green nodes. (**B**) Pathways associated with the validated targeted genes.

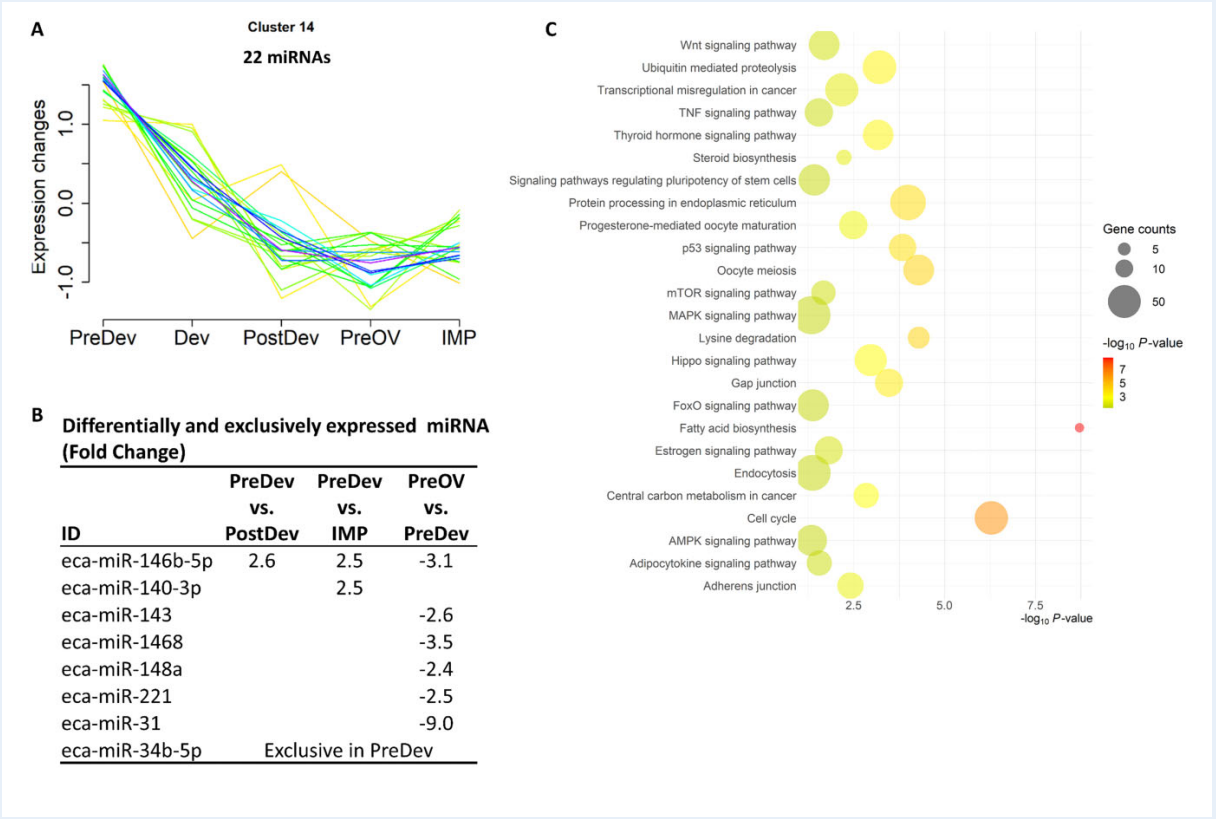


B

Cluster	Counts	%
1	11	4.7
2	16	6.8
3	23	9.8
4	15	6.4
5	17	7.3
6	13	5.6
7	19	8.1
8	15	6.4
9	16	6.8
10	13	5.6
11	15	6.4
12	10	4.3
13	17	7.3
14	22	9.4
15	12	5.1
Total	**234**	**100**

Figure 6. Clustering analysis of extracellular vesicle-coupled microRNAs across the stages of equine follicular development. (**A**) Fifteen different miRNA expression patterns in the follicular fluid extracellular vesicles during follicular development. (**B**) The counts and percentage of microRNAs (miRNAs) in each cluster. PreDev: predeviation; Dev: deviation; PostDev: postdeviation; PreOV: preovulatory; IMP: impending ovulation.

Downloaded from https://academic.oup.com/molehr/article/29/4/gaad009/7059535 by Colorado State University user on 30 November 2023



B

Differentially and exclusively expressed miRNA (Fold Change)

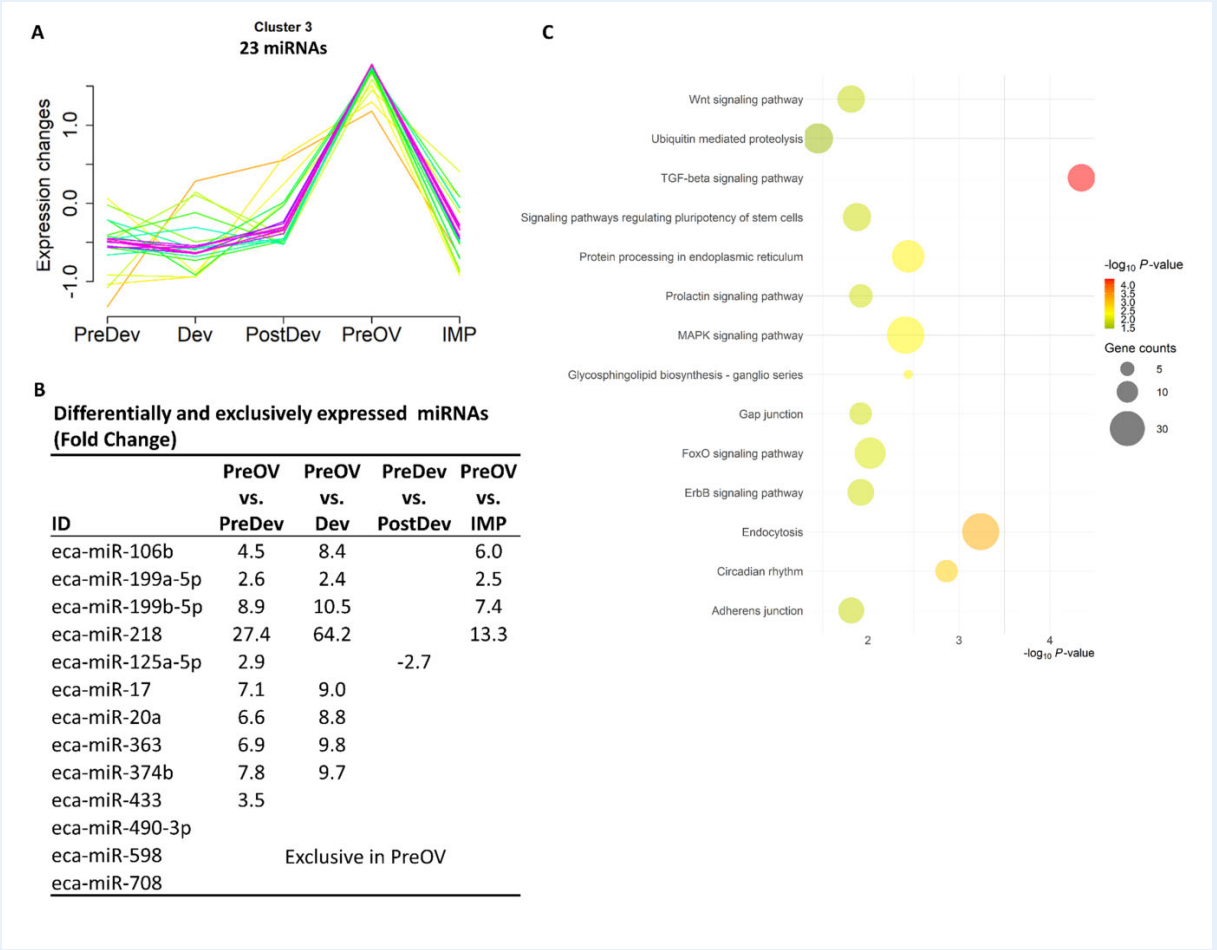
ID	PreDev vs. PostDev	PreDev vs. IMP	PreOV vs. PreDev
eca-miR-146b-5p	2.6	2.5	-3.1
eca-miR-140-3p		2.5	
eca-miR-143			-2.6
eca-miR-1468			-3.5
eca-miR-148a			-2.4
eca-miR-221			-2.5
eca-miR-31			-9.0
eca-miR-34b-5p	Exclusive in PreDev		

Figure 7. Cluster 14 consists of 22 microRNAs. (**A**) A group of 22 microRNAs (miRNAs) exhibited a sharp reduction in their expression from the PreDev until the PreOV stage. (**B**) Among this cluster, seven miRNAs were differentially expressed (DE), and one miRNA was exclusively expressed in the PreDev group. (**C**) Pathways associated with the exclusive and DE-miRNAs target genes of this cluster. PreDev: predeviation; Dev: deviation; PostDev: postdeviation; PreOV: preovulatory; IMP: impending ovulation.

stage-specific expression profile dynamics of EV-miRNAs in FF during equine follicular development using high-throughput miRNA sequencing in order to elucidate the patterns of EV-miRNAs and their potential involvement during specific stages of follicular and oocyte development in the mare. Our findings will contribute to establishing standard EV-miRNA expression patterns across the follicular developmental stages as a baseline to facilitate the diagnosis and assessment of ovarian-related pathophysiological conditions in mares, with potential application in humans. Moreover, in addition to the identification of critical miRNAs for follicular development, results from this study may suggest novel approaches using EV-mediated miRNA signaling applications to improve the IVF cycles of humans and other mammalian species.

In the present study, all examined follicular stages exhibited miR-148a as the top highly expressed miRNA in FF-isolated EVs, with no significant differences among the different stages except for the PreOV versus PreDev comparison, in which it was downregulated in the PreOV stage. The same miRNA has been reported as the most abundant in FF-EVs of small and large follicles in goats (Ding *et al.*, 2021). Additionally, miR-148 was significantly upregulated in the FFs of hyperstimulated compared to unstimulated heifers, suggesting its regulation via the hormonal profile of the cow during follicular development (Noferesti *et al.*, 2015). Although its exact role is still unclear, the expression of miR-148a in human FF-EVs was highly associated with Day-3 embryo quality (Martinez *et al.*, 2018) and its overexpression improved the development of porcine somatic cell nuclear transfer embryos (Wang *et al.*, 2017). Another interesting miRNA that was among the top highly abundant miRNAs in all groups was miR-21, which has been reported as one of the most abundant miRNAs in FF exosomes of pigs (Yuan *et al.*, 2021) and humans (Santonocito *et al.*, 2014). In the mare, miR-21 has been reported to play a role in GC survival and consequently in follicle development (Schauer *et al.*, 2013). The antiapoptotic role of miR-21 has been confirmed in mouse periovulatory GCs (Carletti *et al.*, 2010). Moreover, miR-21 was reported to be involved in oocyte maturation, embryo development, and blastocyst formation (Dehghan *et al.*, 2021). The high abundance of these candidate miRNAs in FF-EVs across all stages of follicular development implies their housekeeping role in maintaining basic cellular function and intercellular communication during follicular selection and development in the mare. Moreover, these miRNAs could be good candidates to improve the developmental competence of oocytes undergoing IVM.

Downloaded from https://academic.oup.com/molehr/article/29/4/gaad009/7059535 by Colorado State University user on 30 November 2023



B

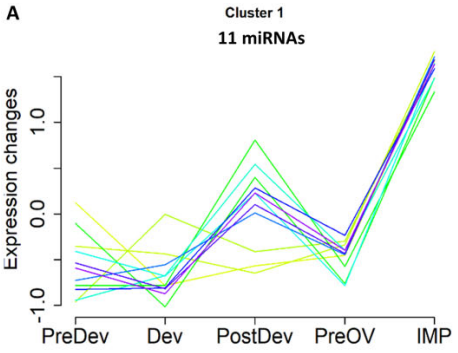
Differentially and exclusively expressed miRNAs (Fold Change)

ID	PreOV vs. PreDev	PreOV vs. Dev	PreDev vs. PostDev	PreOV vs. IMP
eca-miR-106b	4.5	8.4		6.0
eca-miR-199a-5p	2.6	2.4		2.5
eca-miR-199b-5p	8.9	10.5		7.4
eca-miR-218	27.4	64.2		13.3
eca-miR-125a-5p	2.9		-2.7	
eca-miR-17	7.1	9.0		
eca-miR-20a	6.6	8.8		
eca-miR-363	6.9	9.8		
eca-miR-374b	7.8	9.7		
eca-miR-433	3.5			
eca-miR-490-3p				
eca-miR-598		Exclusive in PreOV		
eca-miR-708				

Figure 8. Cluster 3 consists of 23 microRNAs. (**A**) A group of 23 microRNAs (miRNAs) exhibited stable expression at the PreDev until the PostDev stage, a significant increase at the PreOV stage, and then a significant decrease at the IMP stage. (**B**) Among this cluster, 10 miRNAs were differentially expressed (DE), and three were exclusively expressed in the PreOV group. (**C**) Pathways associated with the exclusive and DE-miRNAs target genes of this cluster. PreDev: predeviation; Dev: deviation; PostDev: postdeviation; PreOV: preovulatory; IMP: impending ovulation.

The cluster analysis performed herein identified several clusters of miRNAs with distinct expression dynamics during the entire follicular developmental stages, ranging from the PreDev to IMP stages. A cluster group of 22 miRNAs (cluster 14) showed a consistent declining expression pattern from the PreDev stage to the PreOV and IMP stages. Among the miRNAs in this cluster, miR-146b-5p was significantly upregulated in the PreDev stage compared to the PostDev, PreOV, and IMP stages. This miRNA appears to play a significant role in GC survival, as its downregulation inhibits GCs apoptosis (Chen *et al.*, 2015). Previously, it has been reported that miR-146a was significantly higher in the plasma and GCs of patients with POI, a disorder resulting from an increased rate of follicle loss or a reduced number of follicles formed during ovarian development and characterized by increased apoptosis of ovarian GCs (Yang *et al.*, 2012). In the same cluster, miR-31 and miR-143 exhibited a significant reduction in the PreOV stage compared to the PreDev stage. Both miRNAs were shown to decrease steroid hormone synthesis in bovine GCs by targeting the FSH receptor, therefore affecting follicular development and follicular atresia (Zhang *et al.*, 2019b). In the mare, intrafollicular estradiol concentrations increase along with follicle development, reaching their peak during the preovulatory stage (Bashir *et al.*, 2016b). Interestingly, the reduction of miR-31 and miR-143 in the PreOV stage is consistent with the increase in FF estradiol concentrations previously reported, since these two miRNAs seem to be involved in the control of steroid hormone biosynthesis. Additionally, pathway analysis of genes targeted by this group of miRNAs includes fatty acid biosynthesis, which was the top targeted pathway and is crucial for oocyte, GC, and follicular development (Uzbekova *et al.*, 2021; Shi and Sirard, 2022). Our findings support the concept that the reduction of these miRNAs may have potential implications in the preservation, functionality, and viability of GCs and follicle/oocyte maturation.

Downloaded from https://academic.oup.com/molehr/article/29/4/gaad009/7059535 by Colorado State University user on 30 November 2023



B

Differentially expressed miRNAs (Fold Change)

ID	PostDev vs. Dev	IMP vs. Dev	PreDev vs. PostDev	PreDev vs. IMP	PreOV vs. PreDev	PreOV vs. IMP
eca-miR-206	5.5	10.8	-7.0	-13.9	3.5	-3.9
eca-miR-204b	8.0	17.0	-3.4	-7.2		-5.3
eca-miR-183		2.6				-2.4
eca-miR-362-5p				-19.7		

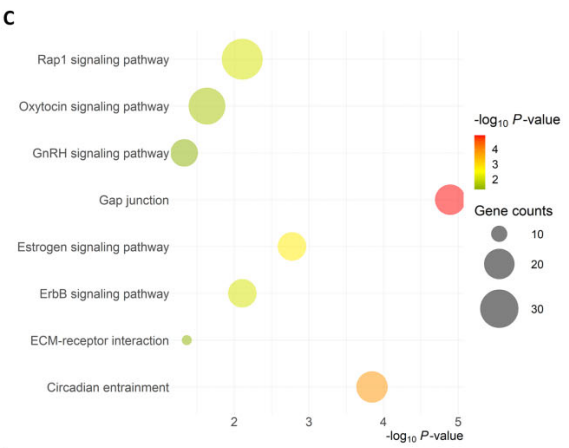


Figure 9. Cluster 1 consists of 11 microRNAs. (**A**) A group of 11 microRNAs (miRNAs) exhibited an expression increase at the PostDev and IMP stages. (**B**) Among this cluster, four miRNAs were differentially expressed (DE). (**C**) Pathways associated with the DE-miRNAs target genes of this cluster. PreDev: predeviation; Dev: deviation; PostDev: postdeviation; PreOV: preovulatory; IMP: impending ovulation.

Another interesting finding in our study was the expression pattern of 23 miRNAs, which had significantly higher abundance during the PreOV stage (cluster 3). Among this group, 10 miRNAs were differentially expressed in the different stage comparisons, and three miRNAs were exclusively expressed in the PreOV stage (miR-490-3p, miR-598, and miR-708). Among the DE-miRNAs, miR-125a-5p and miR-199a have been previously reported to be highly expressed in preovulatory compared to medium follicles, and in luteal tissues in ovine ovaries (McBride *et al.*, 2012). Moreover, in agreement with our finding, miR-125a was found to be highly expressed in mouse preovulatory follicles, decreasing toward ovulation through an intrafollicular intercellular regulation mechanism that facilitates the ovulation process (Grossman *et al.*, 2020). However, miRNAs from the same cluster (i.e. miR-125a and miR-106b) have also been suggested to play roles in follicular atresia (Zhang *et al.*, 2019a).

In the current study, the highest number of DE-miRNAs have been identified, as expected, in two different comparisons (PreOV versus PreDev; PreDev versus IMP). This indicates that miRNA expression dynamics differ along with follicle development, which may be attributed to the hormonal profile differences between the respective stages of follicular development. Interestingly, miR-206 and miR-204b were among the DE-miRNAs that appeared in at least five different stage comparisons. Moreover, both miRNAs exhibited the same expression pattern (cluster 1) with a significant increase during the IMP stage, which may justify the potential involvement of these miRNAs in modulating cell viability (Sun *et al.*, 2019; Cui *et al.*, 2020; Zhou *et al.*, 2021). Pathway analysis revealed that both miRNAs target genes related to the gap junction pathway. In this regard, it is well known that at the time of ovulation, intercellular communication between the oocyte and GCs via gap junctions is alleviated to allow the completeness of meiosis (Sela-Abramovich *et al.*, 2006). In addition, miR-206 was proven to target and reduce the expression level of the estrogen (E2) receptor-α (ERα) mRNA and protein in human cells (Adams *et al.*, 2007). ERα has a dominant role in maintaining oocyte meiotic arrest by regulating the expression of natriuretic peptide C and natriuretic peptide receptor 2 (Liu *et al.*, 2017). Therefore, the significant upregulation of miR-206 and miR-204b at the ovulatory stage may indicate their potential role in oocyte maturation prior to ovulation. Further functional studies on the potential role of EV-coupled miR-206 and miR-204b may pave the way for the development of novel approaches to supplement EVs enriched with these candidate miRNAs during IVM to enhance the outcome of ART in animals and humans.

The present study enhances our understanding of the intrafollicular milieu during follicle growth and maturation. The results described herein offer unique insights into the mechanisms governing follicular growth and ovulation in women, and may have implications to understand anovulation processes as well as optimize ovarian stimulation protocols and oocyte IVM for assisted reproduction. Moreover, the characterization of the EV-miRNA expression and dynamics in FF of

Downloaded from https://academic.oup.com/molehr/article/29/4/gaad009/7059535 by Colorado State University user on 30 November 2023

livestock and women may lead to opportunities for the development of diagnostic markers for abnormal pathophysiological conditions leading to defective follicular development and ovarian function. Most importantly, results from the current study identify EV-coupled miRNAs as targets for the future development of therapeutic treatments for ovarian pathologies.

In conclusion, this study provides, for the first time, EV-coupled miRNA expression dynamics in equine FF at specific stages of follicle development, which might be translated to other species, including humans, to improve or control fertility. The clusters of miRNAs identified during different stages of follicular development provide more insight into the potential role of EV-miRNA-mediated cell–cell communication in supporting folliculogenesis. Moreover, the EV-miRNA fingerprints observed during follicular development have the potential to be used as a standard to investigate the impact of various pathophysiological conditions, including metabolic syndromes associated with obesity, maternal aging, and PCOS, on follicular physiology and its subsequent influence on fertility.

Supplementary data

Supplementary data are available at *Molecular Human Reproduction* online.

Data availability

The data underlying this article are available in NCBI's Gene Expression Omnibus (GEO) repository with the accession number GSE211179. Moreover, data related to EV experiment are available on the EV-TRACK knowledgebase (EV-TRACK ID: EV220406).

Acknowledgments

We acknowledge the University of Colorado, Boulder EM Services Core Facility in the MCDB Department, for their help and support with TEM imaging. Nanoparticle tracking analysis was performed by Ms. Melinda Meyers from the Department of Clinical Sciences at Colorado State University.

Authors' roles

Conceptualization: D.T., E.L.G., and J.F. Experimental work: S.G., N.M., G.M.I., M.O.G., and E.L.G. Data analysis: A.G., S.G., and R.P. Interpretation of data: A.G., S.G., and G.M.I. Writing of original draft: A.G., S.G., E.L.G., and G.M.I. Manuscript editing: D.T., E.L.G., G.M.I., A.G., S.G., and N.M. Supervision: D.T., E.L.G., and J.F. Funding acquisition: E.L.G. and D.T. All authors have read and agreed to the published version of this manuscript.

Funding

This research was supported in part by Southern Illinois University, Carbondale, IL; Ministry of Higher Education & Scientific Research, Baghdad, Iraq; USDA-ARS project 6066-31000-015-00D; and NIH MS-IDeA Network of Biomedical Research Excellence award 5P20GM103476-19. G.M.I. was the recipient of a PhD scholarship from the Ministry of Higher Education & Scientific Research, Baghdad, Iraq.

Conflict of interest

There is no conflict of interest to declare.

References

Adams BD, Furneaux H, White BA. The micro-ribonucleic acid (miRNA) miR-206 targets the human estrogen receptor-alpha (ERalpha) and represses ERalpha messenger RNA and protein expression in breast cancer cell lines. *Mol Endocrinol* 2007;**21**:1132–1147.

Adams GP, Singh J, Baerwald AR. Large animal models for the study of ovarian follicular dynamics in women. *Theriogenology* 2012;**78**:1733–1748.

Baerwald AR. Human antral folliculogenesis: What we have learned from the bovine and equine models. *Anim Reprod* 2009;**6**:20–29.

Baerwald AR, Adams GP, Pierson RA. A new model for ovarian follicular development during the human menstrual cycle. *Fertil Steril* 2003a;**80**:116–122.

Baerwald AR, Adams GP, Pierson RA. Characterization of ovarian follicular wave dynamics in women. *Biol Reprod* 2003b;**69**:1023–1031.

Bashir ST, Baerwald AR, Gastal MO, Pierson RA, Gastal EL. Follicle growth and endocrine dynamics in women with spontaneous luteinized unruptured follicles versus ovulation. *Hum Reprod* 2018;**33**:1130–1140.

Bashir ST, Gastal MO, Tazawa SP, Tarso SGS, Hales DB, Cuervo-Arango J, Baerwald AR, Gastal EL. The mare as a model for luteinized unruptured follicle syndrome: intrafollicular endocrine milieu. *Reproduction* 2016a;**151**:271–283.

Bashir ST, Ishak GM, Gastal MO, Roser JF, Gastal EL. Changes in intrafollicular concentrations of free IGF-1, activin A, inhibin A, VEGF, estradiol, and prolactin before ovulation in mares. *Theriogenology* 2016b;**85**:1491–1498.

Beg MA, Ginther OJ. Follicle selection in cattle and horses: role of intrafollicular factors. *Reproduction* 2006;**132**:365–377.

Benammar A, Derisoud E, Vialard F, Palmer E, Ayoubi JM, Poulain M, Chavatte-Palmer P. The mare: a pertinent model for human assisted reproductive technologies? *Animals (Basel)* 2021;**11**:2304.

Benjamini Y, Hochberg Y. Controlling the false discovery rate: a practical and powerful approach to multiple testing. *J R Stat Soc Ser B Methodol*1995;**57**:289–300.

Campos-Chillon F, Farmerie TA, Bouma GJ, Clay CM, Carnevale EM. Effects of aging on gene expression and mitochondrial DNA in the equine oocyte and follicle cells. *Reprod Fertil Dev* 2015;**27**:925–933.

Carletti MZ, Fiedler SD, Christenson LK. MicroRNA 21 blocks apoptosis in mouse periovulatory granulosa cells. *Biol Reprod* 2010;**83**:286–295.

Downloaded from https://academic.oup.com/molehr/article/29/4/gaad009/7059535 by Colorado State University user on 30 November 2023

Carnevale EM. The mare model for follicular maturation and reproductive aging in the woman. *Theriogenology* 2008;**69**:23–30.

Chen X, Xie M, Liu D, Shi K. Downregulation of microRNA-146a inhibits ovarian granulosa cell apoptosis by simultaneously targeting interleukin-1 receptor-associated kinase and tumor necrosis factor receptor-associated factor 6. *Mol Med Rep* 2015;**12**:5155–5162.

Cui Z, Liu L, Kwame Amevor F, Zhu Q, Wang Y, Li D, Shu G, Tian Y, Zhao X. High expression of miR-204 in chicken atrophic ovaries promotes granulosa cell apoptosis and inhibits autophagy. *Front Cell Dev Biol* 2020;**8**:580072.

da Silveira JC, Veeramachaneni DNR, Winger QA, Carnevale EM, Bouma GJ. Cell-secreted vesicles in equine ovarian follicular fluid contain miRNAs and proteins: a possible new form of cell communication within the ovarian follicle. *Biol Reprod* 2012;**86**:71.

da Silveira JC, Winger QA, Bouma GJ, Carnevale EM. Effects of age on follicular fluid exosomal microRNAs and granulosa cell transforming growth factor-β signalling during follicle development in the mare. *Reprod Fertil Dev* 2015;**27**:897–905.

Dehghan Z, Mohammadi-Yeganeh S, Rezaee D, Salehi M. MicroRNA-21 is involved in oocyte maturation, blastocyst formation, and pre-implantation embryo development. *Dev Biol* 2021; **480**:69–77.

Ding Q, Jin M, Kalds P, Meng C, Wang H, Zhong J, Wang X, Chen Y. Comparison of microRNA profiles in extracellular vesicles from small and large goat follicular fluid. *Animals (Basel)* 2021;**11**:3190.

Donadeu FX, Ginther OJ. Changes in concentrations of follicular fluid factors during follicle selection in mares. *Biol Reprod* 2002;**66**: 1111–1118.

Garcia-Guerra A, Wiltbank MC, Battista SE, Kirkpatrick BW, Sartori R. Mechanisms regulating follicle selection in ruminants: Lessons learned from multiple ovulation models. *Anim Reprod* 2018;**15**: 660–679.

Gastal EL, Gastal MO, Bergfelt DR, Ginther OJ. Role of diameter differences among follicles in selection of a future dominant follicle in mares. *Biol Reprod* 1997;**57**:1320–1327.

Gastal EL, Gastal MO, Ginther OJ. Serrated granulosa and other discrete ultrasound indicators of impending ovulation in mares. *J Equine Vet Sci* 2006;**26**:67–73.

Gebremedhn S, Gad A, Aglan HS, Laurincik J, Prochazka R, Salilew-Wondim D, Hoelker M, Schellander K, Tesfaye D. Extracellular vesicles shuttle protective messages against heat stress in bovine granulosa cells. *Sci Rep* 2020;**10**:15824.

Gilchrist RB, Ritter LJ, Armstrong DT. Oocyte-somatic cell interactions during follicle development in mammals. *Anim Reprod Sci* 2004;**82-83**:431–446.

Ginther OJ. The mare: a 1000-pound Guinea pig for study of the ovulatory follicular wave in women. *Theriogenology* 2012;**77**: 818–828.

Ginther OJ. Follicle selection in mares: 90 years from observation to theory. *J Equine Vet Sci* 2017a;**54**:24–31.

Ginther OJ. Systemic and intrafollicular components of follicle selection in mares. *Domest Anim Endocrinol* 2017b;**59**:116–133.

Ginther OJ, Beg MA, Gastal EL, Gastal MO, Baerwald AR, Pierson RA. Systemic concentrations of hormones during the development of follicular waves in mares and women: a comparative study. *Reproduction* 2005;**130**:379–388.

Ginther OJ, Bergfelt DR, Beg MA, Meira C, Kot K. In vivo effects of an intrafollicular injection of insulin-like growth factor I on the mechanism of follicle deviation in heifers and mares. *Biol Reprod* 2004a;**70**:99–105.

Ginther OJ, Gastal EL, Gastal MO, Bergfelt DR, Baerwald AR, Pierson RA. Comparative study of the dynamics of follicular waves in mares and women. *Biol Reprod* 2004b;**71**:1195–1201.

Ginther OJ, Gastal MO, Gastal EL. Follicle dynamics and selection in mares. *Anim Reprod* 2004c;**1**:45–63.

Grossman H, Har-Paz E, Gindi N, Miller I, Shalgi R. Pre-ovulatory intercellular regulation of miR-125a-3p within mouse ovarian follicles. *Reproduction* 2020;**159**:215–225.

György B, Szabó TG, Pásztói M, Pál Z, Misják P, Aradi B, László V, Pállinger E, Pap E, Kittel A *et al.* Membrane vesicles, current state-of-the-art: emerging role of extracellular vesicles. *Cell Mol Life Sci* 2011;**68**:2667–2688.

Haag KT, Magalhães-Padilha DM, Fonseca GR, Wischral A, Gastal MO, King SS, Jones KL, Figueiredo JR, Gastal EL. Quantification, morphology, and viability of equine preantral follicles obtained via the Biopsy Pick-Up method. *Theriogenology* 2013;**79**:599–609.

Hailay T, Hoelker M, Poirier M, Gebremedhn S, Rings F, Saeed-Zidane M, Salilew-Wondim D, Dauben C, Tholen E, Neuhoff C et al Extracellular vesicle-coupled miRNA profiles in follicular fluid of cows with divergent post-calving metabolic status. *Sci Rep* 2019; **9**:12851.

Ishak GM, Bashir ST, Dutra GA, Gastal GDA, Gastal MO, Cavinder CA, Feugang JM, Gastal EL. In vivo antral follicle wall biopsy: a new research technique to study ovarian function at the cellular and molecular levels. *Reprod Biol Endocrinol* 2018;**16**:71.

Kumar LE, Futschik M. Mfuzz: a software package for soft clustering of microarray data. *Bioinformation* 2007;**2**:5–7.

Liu W, Xin Q, Wang X, Wang S, Wang H, Zhang W, Yang Y, Zhang Y, Zhang Z, Wang C *et al.* Estrogen receptors in granulosa cells govern meiotic resumption of pre-ovulatory oocytes in mammals. *Cell Death Dis* 2017;**8**:e2662.

Martinez RM, Liang L, Racowsky C, Dioni L, Mansur A, Adir M, Bollati V, Baccarelli AA, Hauser R, Machtinger R. Extracellular microRNAs profile in human follicular fluid and IVF outcomes. *Sci Rep* 2018;**8**:17036.

McBride D, Carré W, Sontakke SD, Hogg CO, Law A, Donadeu FX, Clinton M. Identification of miRNAs associated with the follicular-luteal transition in the ruminant ovary. *Reproduction* 2012;**144**: 221–233.

Montazerian M, Yasari F, Aghaalikhani N. Ovarian extracellular MicroRNAs as the potential non-invasive biomarkers: an update. *Biomed Pharmacother* 2018;**106**:1633–1640.

Noferesti SS, Sohel MMH, Hoelker M, Salilew-Wondim D, Tholen E, Looft C, Rings F, Neuhoff C, Schellander K, Tesfaye D. Controlled ovarian hyperstimulation induced changes in the expression of circulatory miRNA in bovine follicular fluid and blood plasma. *J Ovarian Res* 2015;**8**:81.

O'Brien K, Breyne K, Ughetto S, Laurent LC, Breakefield XO. RNA delivery by extracellular vesicles in mammalian cells and its applications. *Nat Rev Mol Cell Biol* 2020;**21**:585–606.

Ogata H, Goto S, Sato K, Fujibuchi W, Bono H, Kanehisa M. KEGG: Kyoto Encyclopedia of Genes and Genomes. *Nucleic Acids Res* 1999;**27**:29–34.

Downloaded from https://academic.oup.com/molehr/article/29/4/gaad009/7059535 by Colorado State University user on 30 November 2023

Robinson MD, Oshlack A. A scaling normalization method for differential expression analysis of RNA-seq data. *Genome Biol* 2010;**11**: R25.

Roth LW, McCallie B, Alvero R, Schoolcraft WB, Minjarez D, Katz-Jaffe MG. Altered microRNA and gene expression in the follicular fluid of women with polycystic ovary syndrome. *J Assist Reprod Genet* 2014;**31**:355–362.

Sang Q, Yao Z, Wang H, Feng R, Wang H, Zhao X, Xing Q, Jin L, He L, Wu L *et al.* Identification of microRNAs in human follicular fluid: Characterization of microRNAs that govern steroidogenesis in vitro and are associated with polycystic ovary syndrome in vivo. *J Clin Endocrinol Metab* 2013;**98**:3068–3079.

Santonocito M, Vento M, Guglielmino MR, Battaglia R, Wahlgren J, Ragusa M, Barbagallo D, Borzì P, Rizzari S, Maugeri M *et al.* Molecular characterization of exosomes and their microRNA cargo in human follicular fluid: Bioinformatic analysis reveals that exosomal microRNAs control pathways involved in follicular maturation. *Fertil Steril* 2014;**102**:1751–1761.e1.

Scalici E, Traver S, Mullet T, Molinari N, Ferrières A, Brunet C, Belloc S, Hamamah S. Circulating microRNAs in follicular fluid, powerful tools to explore in vitro fertilization process. *Sci Rep* 2016;**6**:24976.

Schauer SN, Sontakke SD, Watson ED, Esteves CL, Donadeu FX. Involvement of miRNAs in equine follicle development. *Reproduction* 2013;**146**:273–282.

Sela-Abramovich S, Edry I, Galiani D, Nevo N, Dekel N. Disruption of gap junctional communication within the ovarian follicle induces oocyte maturation. *Endocrinology* 2006;**147**:2280–2286.

Shannon P, Markiel A, Ozier O, Baliga NS, Wang JT, Ramage D, Amin N, Schwikowski B, Ideker T. Cytoscape: a software environment for integrated models of biomolecular interaction networks. *Genome Res* 2003;**13**:2498–2504.

Shi M, Sirard M-A. Metabolism of fatty acids in follicular cells, oocytes, and blastocysts. *Reprod Fertil* 2022;**3**:R96–R108.

Sohel MMH, Hoelker M, Noferesti SS, Salilew-Wondim D, Tholen E, Looft C, Rings F, Uddin MJ, Spencer TE, Schellander K *et al.* Exosomal and non-exosomal transport of extra-cellular microRNAs in follicular fluid: implications for bovine oocyte developmental competence. *PLoS One* 2013;**8**:e78505.

Sticht C, La Torre C D, Parveen A, Gretz N. miRWalk: an online resource for prediction of microRNA binding sites. *PLoS One* 2018; **13**:e0206239.

Sun X, Su S, Zhang G, Zhang H, Yu X. MiR-204 suppresses cell proliferation and promotes apoptosis in ovarian granulosa cells via targeting TPT1 in polycystic ovary syndrome. *Biochem Cell Biol* 2019; **97**:554–562.

Taylor DD, Gercel-Taylor C. The origin, function, and diagnostic potential of RNA within extracellular vesicles present in human biological fluids. *Front Genet* 2013;**4**:142.

Tesfaye D, Hailay T, Salilew-Wondim D, Hoelker M, Bitseha S, Gebremedhn S. Extracellular vesicle mediated molecular signaling in ovarian follicle: implication for oocyte developmental competence. *Theriogenology* 2020;**150**:70–74.

Uzbekova S, Bertevello PS, Dalbies-Tran R, Elis S, Labas V, Monget P, Teixeira-Gomes A-P. Metabolic exchanges between the oocyte and its environment: focus on lipids. *Reprod Fertil Dev* 2021;**34**: 1–26.

van Deun J, Mestdagh P, Agostinis P, Akay Ö, Anand S, Anckaert J, Martinez ZA, Baetens T, Beghein E, Bertier L *et al.* EV-TRACK: Transparent reporting and centralizing knowledge in extracellular vesicle research. *Nat Methods* 2017;**14**:228–232.

Wang P, Li X, Cao L, Huang S, Li H, Zhang Y, Yang T, Jiang J, Shi D. MicroRNA-148a overexpression improves the early development of porcine somatic cell nuclear transfer embryos. *PLoS One* 2017; **12**:e0180535.

Wischral A, Pastorello M, Gastal MO, Beg MA, Gastal EL. Hemodynamic, endocrine, and gene expression mechanisms regulating equine ovarian follicular and cellular development. *Mol Reprod Dev* 2022;**89**:23–38.

Yáñez-Mó M, Siljander PR-M, Andreu Z, Zavec AB, Borràs FE, Buzas EI, Buzas K, Casal E, Cappello F, Carvalho J *et al.* Biological properties of extracellular vesicles and their physiological functions. *J Extracell Vesicles* 2015;**4**:27066.

Yang X, Zhou Y, Peng S, Wu L, Lin H-Y, Wang S, Wang H. Differentially expressed plasma microRNAs in premature ovarian failure patients and the potential regulatory function of mir-23a in granulosa cell apoptosis. *Reproduction* 2012;**144**:235–244.

Yuan C, Li Z, Zhao Y, Wang X, Chen L, Zhao Z, Cao M, Chen T, Iqbal T, Zhang B *et al.* Follicular fluid exosomes: Important modulator in proliferation and steroid synthesis of porcine granulosa cells. *FASEB J* 2021;**35**:e21610.

Zhang J, Xu Y, Liu H, Pan Z. MicroRNAs in ovarian follicular atresia and granulosa cell apoptosis. *Reprod Biol Endocrinol* 2019a; **17**:9.

Zhang Z, Chen C-Z, Xu M-Q, Zhang L-Q, Liu J-B, Gao Y, Jiang H, Yuan B, Zhang J-B. MiR-31 and miR-143 affect steroid hormone synthesis and inhibit cell apoptosis in bovine granulosa cells through FSHR. *Theriogenology* 2019b;**123**:45–53.

Zhou J, Jin X, Sheng Z, Zhang Z. miR-206 serves an important role in polycystic ovary syndrome through modulating ovarian granulosa cell proliferation and apoptosis. *Exp Ther Med* 2021;**21**:179.

Downloaded from https://academic.oup.com/molehr/article/29/4/gaad009/7059535 by Colorado State University user on 30 November 2023

frontiers | Frontiers in Cell and Developmental Biology

TYPE Original Research
PUBLISHED 06 April 2023
DOI 10.3389/fcell.2023.1142629

Check for updates

OPEN ACCESS

EDITED BY
Renee J. Chosed,
University of South Carolina,
United States

REVIEWED BY
Celina Checura,
Clemson University, United States
Ahmed Balboula,
University of Missouri, United States

*CORRESPONDENCE
Dawit Tesfaye,
dawit.tesfaye@colostate.edu

SPECIALTY SECTION
This article was submitted to Molecular and Cellular Reproduction, a section of the journal Frontiers in Cell and Developmental Biology

RECEIVED 11 January 2023
ACCEPTED 09 March 2023
PUBLISHED 06 April 2023

CITATION
Menjivar NG, Gad A, Gebremedhn S, Ghosh S and Tesfaye D (2023), Granulosa cell-derived extracellular vesicles mitigate the detrimental impact of thermal stress on bovine oocytes and embryos.
Front. Cell Dev. Biol. 11:1142629.
doi: 10.3389/fcell.2023.1142629

COPYRIGHT
© 2023 Menjivar, Gad, Gebremedhn, Ghosh and Tesfaye. This is an open-access article distributed under the terms of the Creative Commons Attribution License (CC BY). The use, distribution or reproduction in other forums is permitted, provided the original author(s) and the copyright owner(s) are credited and that the original publication in this journal is cited, in accordance with accepted academic practice. No use, distribution or reproduction is permitted which does not comply with these terms.

Granulosa cell-derived extracellular vesicles mitigate the detrimental impact of thermal stress on bovine oocytes and embryos

Nico G. Menjivar[1], Ahmed Gad[1,2], Samuel Gebremedhn[1,3], Soham Ghosh[4] and Dawit Tesfaye[1]*

[1]Animal Reproduction and Biotechnology Laboratory (ARBL), Department of Biomedical Sciences, College of Veterinary Medicine and Biomedical Sciences, Colorado State University, Fort Collins, CO, United States, [2]Department of Animal Production, Faculty of Agriculture, Cairo University, Giza, Egypt, [3]Genus Plc, Deforest, WI, United States, [4]Cellular Engineering and Mechanobiology Laboratory (CEML), Department of Mechanical Engineering, Translational Medicine Institute (TMI), Colorado State University, Fort Collins, CO, United States

Climate change-induced global warming results in rises in body temperatures above normal physiological levels (hyperthermia) with negative impacts on reproductive function in dairy and beef animals. Extracellular vesicles (EVs), commonly described as nano-sized, lipid-enclosed complexes, harnessed with a plethora of bioactive cargoes (RNAs, proteins, and lipids), are crucial to regulating processes like folliculogenesis and the initiation of different signaling pathways. The beneficial role of follicular fluid-derived EVs in inducing thermotolerance to oocytes during *in vitro* maturation (IVM) has been evidenced. Here we aimed to determine the capacity of *in vitro* cultured granulosa cell-derived EVs (GC-EVs) to modulate bovine oocytes' thermotolerance to heat stress (HS) during IVM. Moreover, this study tested the hypothesis that EVs released from thermally stressed GCs (S-EVs) shuttle protective messages to provide protection against subsequent HS in bovine oocytes. For this, sub-populations of GC-EVs were generated from GCs subjected to 38.5°C (N-EVs) or 42°C (S-EVs) and supplemented to cumulus-oocyte complexes (COCs) matured *in vitro* at the normal physiological body temperature of the cow (38.5°C) or HS (41°C) conditions. Results indicate that S-EVs improve the survival of oocytes by reducing ROS accumulation, improving mitochondrial function, and suppressing the expression of stress-associated genes thereby reducing the severity of HS on oocytes. Moreover, our findings indicate a carryover impact from the addition of GC-EVs during oocyte maturation in the development to the blastocyst stage with enhanced viability.

KEYWORDS

extracellular vesicles, granulosa cells, cumulus-oocyte complex, oocyte maturation, heat stress, embryo development

1 Introduction

One of the leading, most consequential interferences to a homeostatic reproductive environment in dairy and beef cattle is elevated summer HS, a prime determinant of fertility and reproductive function (Boni, 2019; Wolfenson and Roth, 2019). Hyperthermia, the abnormal thermal state induced through failed regulatory mechanisms of the body, occurs when endogenous heat production supersedes the subsequent heat loss to the environment (Hansen, 2009). Thermal stress is known to compromise follicular development, ovarian functionality, fertilization, and subsequent early embryonic development (Badinga et al., 1993; Wolfenson et al., 1995; Rivera and Hansen, 2001; Sartori et al., 2002). Of specific interest in reduced fecundity is HS-induced damage to proper oocyte function. It is important to note that oocytes act spontaneously and independently of one another. However, elevated thermal environments are in part responsible for deleterious ramifications on the molecular, functional, and cellular changes to oocytes and their surrounding cumulus cells (CCs) (Abdelnour et al., 2020).

Mammalian oocytes are known to differentially activate various molecules as first-line defense mechanisms including heat shock proteins (HSPs) (Feder and Hofmann, 1999), unfolded protein responses (UPRs), and oxidative stress response pathways to assist cell survival under thermal stress conditions (Alemu et al., 2018; Lin et al., 2019). Additionally, impairments to conventional microtubules and microfilaments due to HS can be correlated to spindle apparatus malfunction and early arrest at metaphase I (MI) (Roth and Hansen, 2005). In order to understand the impact of seasonal thermal stress on follicular function and oocyte physiology, several studies have utilized the *in vitro* exposure of follicular cells (Li et al., 2016; Alemu et al., 2018; Gebremedhn et al., 2020) and oocytes (Al-Katanani et al., 2002; Roth and Hansen, 2004; Roth and Hansen, 2005; Nabenishi et al., 2012; Li et al., 2015; Pavani et al., 2016; Rodrigues et al., 2019; Abdelnour et al., 2020) to elevated incubator temperatures. Accordingly, *in vitro* exposure of oocytes to HS results in impaired developmental potential as evidenced by defective cytoplasmic maturation (Edwards et al., 2005), mitochondrial anomalies (Ferreira et al., 2016), reductions in polar body extrusions (PB) and nuclear maturation (Li et al., 2015; Pavani et al., 2016) as well as increased accumulations of reactive oxygen species (ROS) (Nabenishi et al., 2012), ultimately leading to apoptosis (Nabenishi et al., 2012).

Oocyte growth and maturation occur within the complex follicle microenvironment, involving substantial bi-directional communication between follicular cells (theca, granulosa, and cumulus cells) and the oocyte (Matzuk et al., 2002; Russell et al., 2016). Critical communication and signaling between the varying cell subpopulations during folliculogenesis are paramount to the growth and maturation of developmentally competent oocytes (Matzuk et al., 2002; Alam and Miyano, 2020; Tesfaye et al., 2021). The process by which cells communicate occurs in a multitude of fashions including cytokines (Altan-Bonnet and Mukherjee, 2019), proteins or surface molecules (Ahmed and Xiang, 2011), and gap junctions (Gilula et al., 1978). Of growing interest is cell-to-cell communication *via* membrane-encapsulated vesicles containing surface markers from the cell of origin, harnessed with an abundant amount of bioactive cargoes (RNAs, proteins, lipids, and metabolites, *etc.*). Extracellular vesicles (EVs), an all-inclusive term endorsed by the International Society for Extracellular Vesicles (ISEV), is a term used for a heterogenous population of lipid-enclosed nanoparticles with non-replicative function (Théry et al., 2018). Originally depicted as discarding mechanisms of cellular waste, EVs are growing in popularity as pertinent conveyors of cellular messages *via* their cargo loads, ultimately leading to modification of cellular activity or key properties of target cells (Valadi et al., 2007).

Several studies involving irradiation (Mothersill and Seymour, 1997; Lyng et al., 2000; Chai and Hei, 2008) and thermal stress (Bewicke-Copley et al., 2017) have demonstrated the potential of EVs present in conditioned medium to induce a bystander effect to recipient cells. In those respective studies, naïve cells treated with a medium conditioned by stressed cells showed increased levels of DNA damage and apoptosis when compared to naïve cells treated with a conditioned medium from control cells. Moreover, naïve cells treated with EVs from irradiated or heat-shocked cells have a higher probability to survive subsequent stress, suggesting that EVs can induce adaptive responses. It has also been shown that the supplementation of follicular fluid-derived EVs enhances the developmental capacity of oocytes to reach the blastocyst stage under HS conditions (Rodrigues et al., 2019). In the same study, it was noted that the supplementation of follicular fluid-derived exosomes were superior when compared to the whole follicular fluid, revealing exosomes' critical role in mitigating HS-induced damage to oocytes. The mechanisms underpinning such bystander effects of EVs are not fully understood, however, it is possible that the changes in protein or RNA contents of EVs may have the capacity to alter the physiology of recipient cells (Bewicke-Copley et al., 2017). MicroRNA profiling of EVs derived from thermally stressed bovine GCs revealed the enrichment of miRNA (miR-1246, miR-2904, and miR-374a), which are known to be involved in pathways associated with cellular response to heat stress, redox status, hypoxia and negative regulation of cell proliferation and inflammatory response (Gebremedhn et al., 2020). In the same study, we demonstrated that the supplementation of thermally stressed EVs to recipient granulosa cells induced tolerance against subsequent thermal stress. Therefore, the current study aimed to test the hypothesis that GC-derived EVs can play a physiologically relevant role in enhancing the survival and viability of bovine oocytes subjected to thermal stress under *in vitro* conditions.

2 Materials and methods

2.1 Ovary collection and granulosa cell isolation

Local abattoir-derived bovine ovaries were collected and transported *via* an insulated thermos containing physiological saline solution (0.9% NaCl) warmed to 37°C. Upon arrival, ovarian samples were initially washed through a physiological, warmed saline solution and subjected to a 70% ethanol rinse, followed by three repeated washings through a warmed saline solution. Follicular fluid containing granulosa cells and COCs were aspirated from small, growing follicles (3–8 mm in diameter) using a vacuum pump (GenX International; Guelph,

ON, Canada) set to approximately 50 mmHg attached to an 18-gauge standard hypodermic needle (Covidien Monoject™; Mansfield, MA, United States) accompanied by a 50 mL sterilized tube (CELLTREAT® Scientific Products; Pepperell, MA, United States). A dense pellet of cellular material containing the COCs was allowed to settle at the bottom of the tube for 10 min, resulting in a visible gradient prior to the collection of cells. The uppermost aqueous portion of the aspirated follicular fluid containing the granulosa cells was then subsequently transferred into a sterile 15 mL tube (Thermo Fisher Scientific; Waltham, MA, United States) with warmed Dulbecco's Phosphate Buffered Saline without calcium and magnesium chloride (DPBS (×1)) (Sigma-Aldrich; St. Louis, MO, United States).

The upper suspension and warmed DPBS (1X) were mechanically homogenized *via* repetitive pipetting prior to initial centrifugation at 500 xg for 7 min to collect and pelletize the granulosa cells. Next, the supernatant was removed, and the cell pellet was resuspended in red blood cell (RBC) lysis buffer (Sigma-Aldrich; St. Louis, MO, United States) for 3 min. To stop the reaction, the cell pellet was washed with Dulbecco's Modified Eagle's Medium/Ham's Nutrient Mixture F12 (DMEM/F12) (Sigma-Aldrich; St. Louis, MO, United States) supplemented with 10% Exosome-depleted fetal bovine serum (FBS) (System Biosciences; Palo Alto, CA, United States), 1% Penicillin-Streptomycin (Sigma-Aldrich; St. Louis, MO, United States) and 1% Amphotericin B solution (Sigma-Aldrich; St. Louis, MO, United States). Following centrifugation at 500 xg for 5 min, the supernatant was removed, and the cells were washed in DPBS (1X) and resuspended in DMEM/F12 supplemented medium as described above. Cell counts and viability were determined using a hemocytometer (Hausser Scientific; Horsham, PA, United States) and the trypan blue (Sigma-Aldrich; St. Louis, MO, United States) exclusion method.

2.2 Granulosa cell culture and exposure to heat stress

Granulosa cells were seeded at 2×10^5 cells per well in 24-well, tissue culture-treated plates (United States Scientific, Inc.; Ocala, FL), suspended in DMEM/F12 supplemented medium as described above. In a humidified atmosphere gauged at 38.5°C containing a 5% CO_2 environment, cells were cultured for an initial 24 h or until sub-confluent. Following an initial 24 h priming period, the (control) cells continued culture at 38.5°C and the HS cells were transferred to an alternative environment with an elevated thermal temperature of 42°C for the remaining 24 h of the total 48 h culture period. The conditioned spent culture medium was collected and stored at −80°C for EV isolation and downstream application.

2.3 Isolation of EVs from spent culture medium

Two replicates of conditioned spent culture medium containing EVs released from cultured granulosa cells were pooled and initially centrifuged at 500 xg for 10 min, followed by 3,000 xg at 4°C to remove residual cellular debris. Following the initial centrifugations, the supernatant containing EVs were then subjected to centrifugation at increased speeds of 17,200 xg for 30 min, followed by filtration through a 0.22 µm sterile syringe filter (Sigma-Aldrich; St. Louis, MO, United States), removing particles larger than 200 nm in diameter including apoptotic bodies. Following this, the purified conditioned spent culture medium was subjected to ultracentrifugation as we previously described in (Saeed-Zidane et al., 2017). Briefly, conditioned spent culture medium from each treatment was subjected to ultracentrifugation at 120,000 xg for 70 min using the Optima XE-90 Ultracentrifuge (Beckman Coulter; Pasadena, CA, United States), in 5.2 mL Ultra-Clear™ Centrifuge Tubes (Beckman Coulter; Pasadena, CA, United States) using the Beckman SW 55Ti rotor (Beckman Coulter; Pasadena, CA, United States). After removing the supernatant, the pelletized EVs were washed using DPBS (1X) and ultracentrifuged under the same conditions as described above. Finally, the supernatant was removed and the EVs were then suspended in 500 µL of DPBS (1X) and stored at −80°C until further analysis. Prior to use, all EV samples were thawed at room temperature to sustain high-yield EV recovery (Trummer et al., 2009; Szatanek et al., 2015).

2.4 Morphological and molecular characterization of GC-EVs

Immunoblotting techniques were used to verify the presence of typical EV-specific protein markers (CD63, TSG101, and CD81) in the isolated EVs. Moreover, Cytochrome c (CYCS), a cell-specific marker protein was used to validate the absence of residual cellular debris and cellular protein contaminants in our EV preparations. Full-length blots are provided in (Supplementary Figure S1) and a list of the antibodies used is indicated in (Supplementary Table S1).

Characterizing the size and concentration of EV samples were performed using nanoparticle tracking analysis (NTA). Briefly, 5 µL of purified EVs were diluted in 995 µL of DPBS (1X) and assembled into the ZetaView® QUATT 4 Nanosight Instrument (Particle Metrix; Ammersee, Germany) fitted with four respective lasers (405/488/520/640 nm sources). For each sample, video measurements were recorded, and 11 positions were analyzed using the Software Zetaview (version 8.05.12 SP1). Similarly, the morphology and size of EVs were determined using a particle beam of electrons for visualization using transmission electron microscopy (TEM). For this, a small volume of isolated EV samples (6–8 µL) was applied to a carbon-coated, copper mesh TEM grid for 1–2 min, followed by negative staining with 2% aqueous uranyl acetate. TEM imaging was done on an FEI/TFS Tecnai T12 Spirit TEM (FEI Company; Hillsboro, OR, United States), operating at 100 kV, with an AMT CCD. We have submitted all relevant data from our experiments to the EV-TRACK knowledgebase (EV-TRACK ID: EV220412) (van Deun et al., 2017).

2.5 Fluorescence labeling of GC-EVs and assessing cellular uptake

EVs were labeled with PKH26 (Mini26-1KT; Sigma-Aldrich; St. Louis, MO, United States), a red fluorescent linker dye responsible for labeling lipid membranes as described in (Da Silveira et al., 2012). Briefly, EVs (3.5×10^{11} particles/mL) were incubated with

1 μL of PKH26 (4×10^{-6} M) for 5 min at room temperature in the dark, followed by immediate quenching with 1% BSA (A6003; Sigma-Aldrich; St. Louis, MO, United States) for 1 min. Samples were precipitated using Exo-spin™ buffer-exosome precipitation reagent (CellGS®; St. Louis. MO, United States) for 60 min in the dark at 4°C, then centrifuged at 16,000 xg for 30 min and resuspended in 100 μL of DPBS (1X) before purification using the Exo-spin™ columns according to the manufacturer's protocol. As a negative control, DPBS (1X) was incubated with PKH26 and treated in the same manner as described above. Labeled EVs or DPBS (1X) (negative control) were used to prove EV uptake by CCs surrounding intact COCs as detailed below.

COCs obtained from follicles ranging in size from 3 to 8 mm in diameter were aspirated from abattoir-derived ovaries. Three COCs were cultured in 20 μL micro drops offset with 20% v/v of GC-EVs suspended in DPBS (1X) measured at 0.3 mg/mL of total protein under oil for a 23 ± 1 h exposure length. Following incubation, intact COCs were washed in CSU chemically defined medium for the handling of oocytes (HCDM-M) (De La Torre-Sanchez, Jose Fernando et al., 2006), fixed with 4% paraformaldehyde, mounted to a poly-L-lysine coated slide (Newcomer Supply, Inc.; Middleton, WI, United States), and allowed to dry for 24 h at 4°C in the dark. Visualization of fluorescently-labeled EVs within the CCs surrounding the oocyte was ascertained using confocal microscopy (Olympus Fluoview FV10-ASW 4.1) (Olympus; Tokyo, Japan) after excitation of COCs at 559 nm with a ×60 objective lens. Labeled DPBS (1X) was used as negative control within this experiment.

2.6 *In vitro* maturation and exposure to heat stress

The collection of COCs from slaughterhouse ovaries was done as described above. Once COCs were collected, groups of 50 oocytes were transferred into individual wells, inside 4-well culture dishes (Thermo Fisher Scientific; Waltham, MA, United States) containing 1 mL of CSU chemically defined medium for *in vitro* maturation of oocytes (IVM) pre-equilibrated at 38.5°C in 5% CO_2 (De La Torre-Sanchez, Jose Fernando et al., 2006). At the time IVM medium were set to equilibrate, all mediums irrespective of downstream application were supplemented with 15 ng/mL NIDDK-oFSH-20, 1 μg/mL USDA-LH-B-5, 1 μg/mL estradiol 17β, 50 ng/μL epidermal growth factor, and 0.1 mM cysteamine (De La Torre-Sanchez, Jose Fernando et al., 2006).

For experiments with heat stress, treatments were arranged in a 2 × 4 factorial design with primary effects of incubation temperature during maturation (38.5°C vs. 41°C) and with four culture mediums: non-supplemented control (NC), vehicle [DPBS (1X)], EVs derived from granulosa cells subjected to the normal physiological body temperature of the cow (38.5°C) (normal EVs: N-EVs) or EVs derived from granulosa cells subjected to thermal stress (42°C) (stressed EVs: S-EVs). In brief, COCs were incubated with 20% v/v of DPBS (1X), and treatments with GC-EVs were offset with equal concentrations of total protein (0.3 mg/mL) assessed using a NanoDrop 2000 Spectrophotometer (Thermo Scientific; Waltham, MA, United States), selected based on previous literature (Almiñana et al., 2017; Alcântara-Neto et al., 2020a; Alcântara-Neto et al., 2020b; Abumaghaid et al., 2022; Mateo-Otero et al., 2022). For all experimental groups, control COCs matured at a temperature of 38.5°C throughout the maturation period (23 ± 1 h), while thermally stressed COCs were subjected to an initial 8 h priming period at 38.5°C and then transferred to 41°C in an atmosphere of 5% CO_2 in humidified air for the remaining 15 ± 1 h of the 23 ± 1 h maturation period.

2.7 *In vitro* fertilization and embryo culture

After maturation, COCs were transferred to 4-well culture dishes containing 430 μL of equilibrated CSU chemically defined medium for *in vitro* fertilization (F-CDM/well) (De La Torre-Sanchez, Jose Fernando et al., 2006). In a minimal volume of maturation medium, COCs were transferred into F-CDM and held at 38.5°C and 5% CO_2 in humidified air until IVF was completed using bull sperm generated from a single ejaculation. Frozen-thawed semen were subjected to a multi-layer, 45%/90% Percoll® (Sigma-Aldrich; St. Louis, MO, United States) gradient and centrifuged at 800 xg for 20 min to separate viable, motile sperm (Parrish et al., 1995). Following this, the supernatant was removed and the remaining sperm pellet was washed with 2 mL of CSU chemically defined medium for the handling of early embryos (HCDM-1) and centrifuged at 300 xg for 5 min (De La Torre-Sanchez, Jose Fernando et al., 2006). The concentration of spermatozoa was determined using a hemocytometer and adjusted to 5×10^6 sperm/mL using equilibrated F-CDM. Finally, sperm were added to COCs at a concentration of 0.5×10^6 sperm/mL, and co-incubated for 18 h at 38.5°C in 5% CO_2 in humidified air.

Following exposure with spermatozoa, presumptive zygotes were vortexed at maximum speed for 60–90 s to slough remaining CCs. Denuded zygotes were then transferred through a series of HCDM-1 wash drops, removing residual cells and spermatozoa (De La Torre-Sanchez, Jose Fernando et al., 2006). Zygotes rid of excess cellular debris were then transferred (in groups of 50) to pre-equilibrated 4-well dishes containing 500 μL of CSU chemically defined medium for *in vitro* culture of early embryos (CDM-1) and cultured for 56 h in a tri-gas incubator regulated to 38.5°C in 5% CO_2, 5% O_2, and 90% N_2. Following an initial culture of 56 h, development was assessed by embryo cleavage in warmed micro drops of CSU chemically defined medium for the handling of late embryos (HCDM-2) (De La Torre-Sanchez, Jose Fernando et al., 2006). Those embryos with ≥2 blastomeres were transferred (in groups ≤35 embryos) to pre-equilibrated 4-well dishes containing 500 μL of CSU chemically defined medium for *in vitro* culture of late embryos (CDM-2) for an additional 120 h of culture in a humidified chamber at 38.5°C in 5% CO_2, 5% O_2 and 90% N_2 (De La Torre-Sanchez, Jose Fernando et al., 2006). Blastocyst rates were determined on day 7 (168 h) and day 8 (192 h) post-onset of IVF. Blastocysts were evaluated according to their respective stage of development and graded morphologically in accordance with the IETS guidelines (Robertson, 1998).

2.8 Quantitative analysis of cumulus cell expansion

To determine the effect of EV supplementation on cumulus expansion, arbitrary lines were drawn to measure the diameter of single cumulus-oocyte complexes (four replicates; a total of 113–252 COCs per treatment) using the Olympus Cellsens software

(Olympus; Tokyo, Japan). Measurements were ascertained from groups of COCs and the mean diameter before maturation was subtracted from the mean diameter after maturation to determine the mean cumulus expansion in μm's. The diameter of COCs was measured before and after maturation at differing ambient temperatures from recorded images (.jpg) using an inverted microscope (IX73; Olympus; Tokyo, Japan).

2.9 Total RNA isolation and quality control

Total RNA was isolated from three replicates of CCs (each pool contains CCs derived from 50 COCs) using the miRNeasy® mini kit (Qiagen; Hilden, Germany), and on-column DNA digestion was performed using RNase-free DNase (Qiagen; Hilden, Germany). Moreover, total RNA was extracted from three replicate pools of denuded oocytes following the completion of *in vitro* maturation (each pool consisting of 50 oocytes) and four replicate pools of blastocysts (each pool containing 5 blastocysts) using the RNeasy® plus micro kit (Qiagen; Hilden, Germany). Total RNA sample concentration and integrity were assessed using a NanoDrop 2000 Spectrophotometer (Thermo Scientific; Waltham, MA, United States). RNA samples were stored at −80°C until further use.

2.10 Quantification of cumulus expansion and stress-associated genes using qRT-PCR

The relative abundance of selected cumulus expansion marker genes (PTGS2, EGFR, and PTX3) were quantified in CCs isolated from matured COCs (three replicates; CCs from a pool of 50 COCs per replicate) using qRT-PCR. Cumulus cells were collected immediately following *in vitro* maturation by recurrent pipetting through a narrow pipette, followed by vortexing and centrifugation. Complete removal of CCs from the oocytes was assessed under a stereo microscope (SZX16; Olympus; Tokyo, Japan) and snap frozen in liquid nitrogen then stored at −80°C until further analysis. For the analysis, synthesized cDNA was reverse transcribed from equal amounts of total RNA (85 ng) using the SuperScript™ III First-Strand Synthesis Super Mix Kit (Invitrogen; Carlsbad, CA, United States) with random hexamer and oligo d(T) 20 primers. Similarly, the transcript abundance of selected stress-related genes (NRF2, SOD1, HSP70, HSP90, GRP78, and GRP94) were quantified in CCs (three replicates; CCs from a pool of 50 COCs per replicate), *in vitro* matured denuded oocytes (three replicates; a pool of 50 COCs per replicate) and blastocysts (four replicates; a pool of 5 blastocysts per replicate) using qRT-PCR. For this, cDNA was obtained after reverse transcription of equal amounts of total RNA (85 ng from CCs, 31 ng from oocytes, and 13 ng from blastocysts) as described above. The geometric mean of expression levels of β-ACTIN and GAPDH was used to normalize the expression of candidate genes. Gene-specific primers were designed using Primer-Blast (https://www.ncbi.nlm.nih.gov/tools/primer-blast/) and the list of primers is indicated in Supplementary Table S2. qRT-PCR analysis were performed using the CFX96 Touch Real-Time PCR Detection System (Bio-Rad; Hercules, CA, United States) and data was analyzed using the comparative C(T) method (Schmittgen and Livak, 2008).

2.11 Measurement of intracellular ROS accumulation

The intracellular ROS accumulation in oocytes (three replicates; a total of 15–50 oocytes per treatment) and blastocysts (three replicates; a total of 6-9 blastocysts per treatment) from the various treatment groups was determined as we described previously (Gebremedhn et al., 2020). Briefly, oocytes (n = 32 on average) and embryos (n = 8 on average) from each treatment group were washed twice in phosphate-buffered saline-polyvinylpyrrolidone DPBS (1X)-PVP (0.1%) (P0930; Sigma-Aldrich; St. Louis, MO, United States), placed in 50 μL droplets of 10 μM 2′,7′-Dichlorofluorescin Diacetate (H_2DCFDA) dissolved in H-CDMM or H-2 (oocyte or blastocyst) (287,810; Sigma-Aldrich; St. Louis, MO, United States), and incubated at 38.5°C in the respective culture environment suitable for their specific stage of development for 30 min. After incubation, the oocytes and embryos were washed three times in DPBS (1X)-PVP (0.1%) and then observed under an inverted fluorescent microscope (IX73; Olympus; Tokyo, Japan) using ×20 magnification. The fluorescence of individual specimens was measured from.jpg images and analyzed using ImageJ software (National Institute of Health; Bethesda, MD, United States) after normalization through subtraction of the background intensity. All images were captured under the same parameters for exposure time and light intensity to avoid fluorescent saturation using a green fluorescent filter with an excitation wavelength of 494 nm and an emission wavelength of 518 nm. Results are plotted as the relative intensity of fluorescence.

2.12 Analysis of mitochondrial membrane potential (MMP)

MMP ($\Delta\Psi_m$) in oocytes (duplicates; a total of 12-22 oocytes per treatment) and blastocysts (duplicates; a total of 7-11 blastocysts per treatment) were analyzed by staining with 5,5′,6,6′-tetrachloro-1,1′,3,3′tetraethylbenzimidazolylcarbocynanine iodide (JC-1, Invitrogen; Carlsbad, CA, United States) dissolved in H-CDMM or H-2 (oocyte or blastocyst), as an indicator of mitochondrial activity, as previously described (Pasquariello et al., 2019). Briefly, denuded matured oocytes and blastocysts from the various treatment groups were stained using 2 μM JC-1 for 30 min in the dark at 38.5°C, in the optimal culture environment for their respective stage and development to express two types of fluorescence. Oocytes and blastocysts were then washed three times in DPBS (1X)-PVP (0.1%) and fluorescent images were taken immediately using an inverted laser scanning confocal microscope (ZEISS LSM980, Carl Zeiss Microscopy, Jena, Germany) using a ×20 magnification air objective. Fluorescent images were ascertained using the lowest laser power to give a sufficient signal-to-noise ratio to avoid saturation of the fluorophore. Physiological temperature (37°C) and CO_2 level (5%) were maintained inside the incubation chamber amidst imaging. Imaging was performed using a wavelength of 488 nm for J-monomers and excitation/emission at 490/525 nm (FITC filter/green fluorescence) indicating low membrane potential. Similarly, images for J-aggregates were carried out using a wavelength of 561 nm and excitation/emission at 596/615 nm (TRITC filter/red

fluorescence) indicating high membrane potential. Subsequently, the ratio of red to green fluorescence was used to determine mitochondrial membrane potential, expressed as an arbitrary unit as previously described (Silva et al., 2015; Pasquariello et al., 2019). All czi. images were analyzed using ImageJ software (National Institute of Health; Bethesda, MD, United States).

2.13 Fluorescent nuclear staining and terminal deoxynucleotidyl transferase-mediated dUTP nick-end labeling (TUNEL) assay

Blastocyst-stage embryos from the different treatment groups (three replicates; a total of 18-30 blastocysts per treatment) were assessed for proliferative capacity based on total cell counts using a protocol adapted from (Critser and First, 1986) with some modifications. Briefly, blastocysts were washed three times in 100 µL drops of phosphate buffered saline-polyvinylalcohol DPBS (1X)-PVA (0.1%) (P8136; Sigma-Aldrich; St. Louis, MO, United States), for 5 min each time. Blastocysts were then immediately transferred into 1.5 µg/mL Hoechst 33,342 solution (H3570; Thermo Fisher Scientific; Waltham, MA, United States) and stained for 10–15 min at room temperature in the dark. Embryos were then washed as previously described and mounted on a poly-L-lysine coated slide (Newcomer Supply, Inc.; Middleton, WI, United States) with 5–10 µL ProLong Diamond Antifade Mountant (P36966; Invitrogen; Carlsbad, CA, United States). Alternatively, cellular DNA fragmentation in blastocysts from the various treatment groups (three replicates; a total of 19-41 blastocysts per treatment) was determined using an *in situ* apoptotic cell detection kit, DeadEnd™ Fluorometric TUNEL System according to the manufacturer's instruction (TB235; Promega; Madison, WI, United States). Briefly, blastocysts were fixed in 4% paraformaldehyde (PFA) for 25 min at 4°C. Following fixing, blastocysts were washed twice in 0.1% Tween/PVP in DPBS (1X) (Bio-Rad; Hercules, CA, United States; P0930; Sigma-Aldrich; St. Louis, MO, United States) and permeabilized in 0.3% Triton X-100 in DPBS (1X) (X100-100ML; Sigma-Aldrich; St. Louis, MO, United States) for 5 min. After permeabilization, blastocysts were washed as detailed previously and incubated in equilibration buffer prior to labeling with the TUNEL assay kit cocktail at 38.5°C for 60 min in a dark humidified chamber as suggested in the manufacturer's protocol. To stop the reaction, blastocysts were moved to 2X SSC for 15 min and washed an additional three times before mounting on a poly-L-lysine coated slide (Newcomer Supply, Inc.; Middleton, WI, United States) with 5–10 µL ProLong Diamond Antifade Mountant (P36966; Invitrogen; Carlsbad, CA, United States) and a coverslip, allowing to dry flat (>24 h). Hoechst/DAPI-labeled or TUNEL-positive nuclei were observed under an inverted fluorescent microscope (IX73; Olympus; Tokyo, Japan) using ×20 magnification, under the same parameters using fitted blue (345/455) and green (494/518) fluorescent filters. For the analysis, fluorescent images were converted to grayscale to accurately adjust what is fluorescently stained (elements in the foreground, as well as elements in the background). Subsequently, the fluorescently labeled cells were then filled appropriately to determine the borders of individual nuclei based on relative size for counting purposes irrespective of the fluorophore utilized (blue/green).

2.14 Experimental design

A schematic overview of the experimental design is shown in (Supplementary Figure S2). Following the generation of GC-EV subsets (N-EVs and S-EVs) for isolation and characterization, their subsequent effect was evaluated on COCs cultured under normal (38.5°C) and HS (41°C) conditions during IVM. For this purpose, COCs were collected by aspirating small-growing follicles (3–8 mm in diameter) from abattoir-derived reproductive ovaries. To avoid result bias, Grade 1 and Grade 2 COCs were selected for further functional studies and placed into 4-well culture dishes containing four distinct equilibrated mediums: non-supplemented control (NC), vehicle [DPBS (1X)], normal EVs (N-EVs) or stressed EVs (S-EVs) suspeneded in 20% v/v of DPBS (1X), with GC-EV treatments offset with equal concentrations of total protein (0.3mg/ml). Concluding IVM, *in vitro* matured oocytes were assessed for EV uptake and cumulus expansion. Additionally, selected stress-associated transcripts were investigated among resected cumulus cells and denuded matured oocytes, and confocal microscopy was utilized to determine ROS production and mitochondrial activity among *in vitro* matured oocytes. In parallel, aside from experiments conducted immediately following IVM, subsequent IVF cycles were carried out to investigate the downstream effects of GC-EV supplementation during oocyte maturation on the resulting blastocyst development. Developmental competence rates were collected, and blastocysts were similarly evaluated for selected stress-associated transcript abundance and dually stained for ROS accumulation, total cell counts, apoptotic indexes, and mitochondrial membrane potential as a means to monitor the quality of the produced blastocysts.

2.15 Statistical analysis

Data were analyzed in GraphPad Prism version 8.4.2 (GraphPad; San Diego, CA, United States). Statistical differences between the mean values of more than two groups under the varying culture conditions were compared using Two-way Analysis of Variance (ANOVA) followed by Tukey's Multiple Comparisons Tests. Alternatively, statistical differences amid gene expression datasets were assessed between the mean values of more than two groups under the same culture conditions using One-way Analysis of Variance (ANOVA) followed by Tukey's Multiple Comparisons Tests. Data are presented as the Mean ± SEM of biological replicates. Statistical significance was identified at $p \leq 0.05$.

3 Results

3.1 Characterization of GC-EVs released into the conditioned medium from *in vitro* cultured follicular GCs

Vesicle size and concentration differences between N-EVs and S-EVs were assessed using Nanoparticle Tracking Analysis (NTA). The

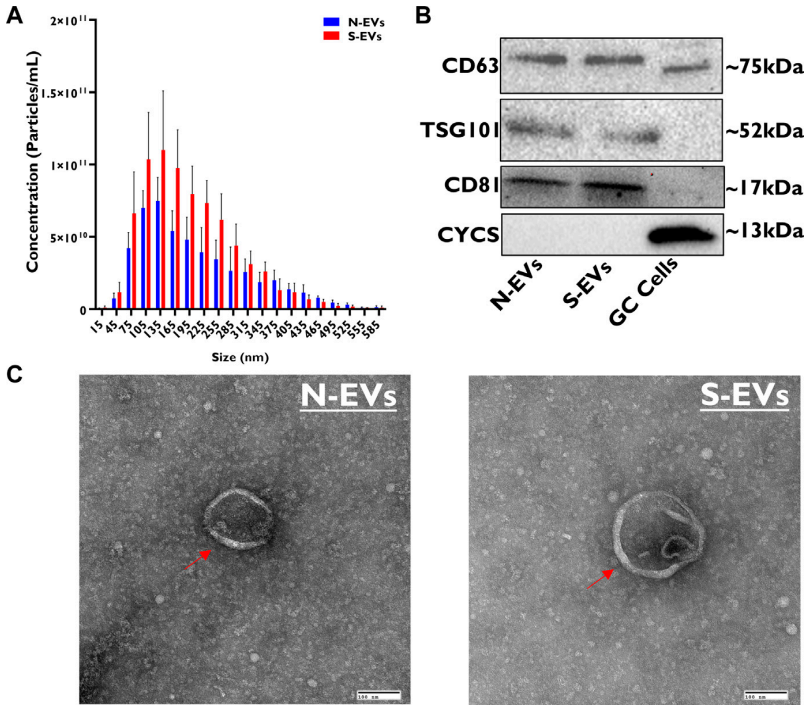


FIGURE 1
Morphological and molecular characterization of GC-EVs. The relative size of EVs isolated from cultured granulosa cells spent culture medium was determined using nanoparticle tracking analysis (NTA). The median size of N-EVs was 137.75 nm (blue) compared to S-EVs 147.95 nm (red). Granulosa cells subjected to thermal stress released a significantly higher quantity of particles (red) and had tendencies to be larger in size (nm) compared to those subjected to normal ambient temperatures (blue) **(A)**. Immunoblotting analysis for EV-specific protein markers (CD63, TSG101, and CD81) and cellular-specific protein marker (CYCS) were verified to determine protein lysate composition in N-EVs, S-EVs, and GCs as a positive control. Full-length blots are presented in Supplementary Figure S1 **(B)**. Transmission electron microscopy (TEM) representative images from N-EVs and S-EVs (marked with red arrows) show the morphology of the lipid bilayer membrane of EV particles. Scale bar, 100 nm **(C)**.

concentration of N-EVs and S-EVs were 6.70E+11 ± 3.50E+11 and 1.00E+12 ± 5.10E+11 particles/mL, with median sizes of 137.75 and 147.95 nm, respectively. Exposure to heat stress resulted in the release of a significantly higher quantity of EVs with a tendency of having larger size particles (Figure 1A). Western blotting analysis of N-EVs and S-EVs revealed positive bands for EV- specific transmembrane proteins (CD63, TSG101, and CD81), simultaneously showing negative results for mitochondrial protein marker (CYCS) (Figure 1B). Similarly, TEM imaging showed a clear indication that vesicles are encapsulated with the visible appearance of a bilipid membrane (Figure 1C).

3.2 GC-EVs shuttle protective messages against heat stress to enhance the thermotolerance of bovine cumulus-oocyte complexes

As a means to validate EVs' capacity to mediate communicative interactions supporting oocyte and embryo development, we confirmed GC-EV uptake by COCs using fluorescence microscopy. After 24 h co-incubation of labeled EVs with COCs, we detected PKH-26 positive EVs in the CCs surrounding the oocyte, but not in the oocyte cytoplasm (Figure 2A). Subsequent investigation of the impact of EV supplementation during oocyte maturation revealed that both N-EVs and S-EVs had positive impacts on cumulus expansion compared to non-supplemented controls and vehicle-supplemented groups, irrespective of the presence or absence of thermal stress exposure. Interestingly, under normal physiological temperature (38.5°C), N-EVs significantly increased cumulus expansion compared to the NC ($p < 0.0001$) and vehicle ($p < 0.0001$). Similar results were found for COCs supplemented with S-EVs during oocyte maturation and cultured under HS conditions when compared to the NC ($p < 0.0001$) and vehicle ($p < 0.0001$) (Figure 2B). We further validated differential expression patterns of cumulus expansion marker genes in the CCs from oocytes of the various treatment groups. Results showed that the expression patterns of PTGS2, EGFR, and PTX3 were higher within the CCs from COCs supplemented with N-EVs cultured both under normal and thermal stress conditions. Under HS conditions, N-EVs and S-EVs tended to act cohesively with both expression patterns being upregulated when compared to the NC and vehicle (Figures 2C, D). Collectively our data indicate significant differences between GC-EV supplemented treatments ($p < 0.0001$), culture temperatures ($p =$

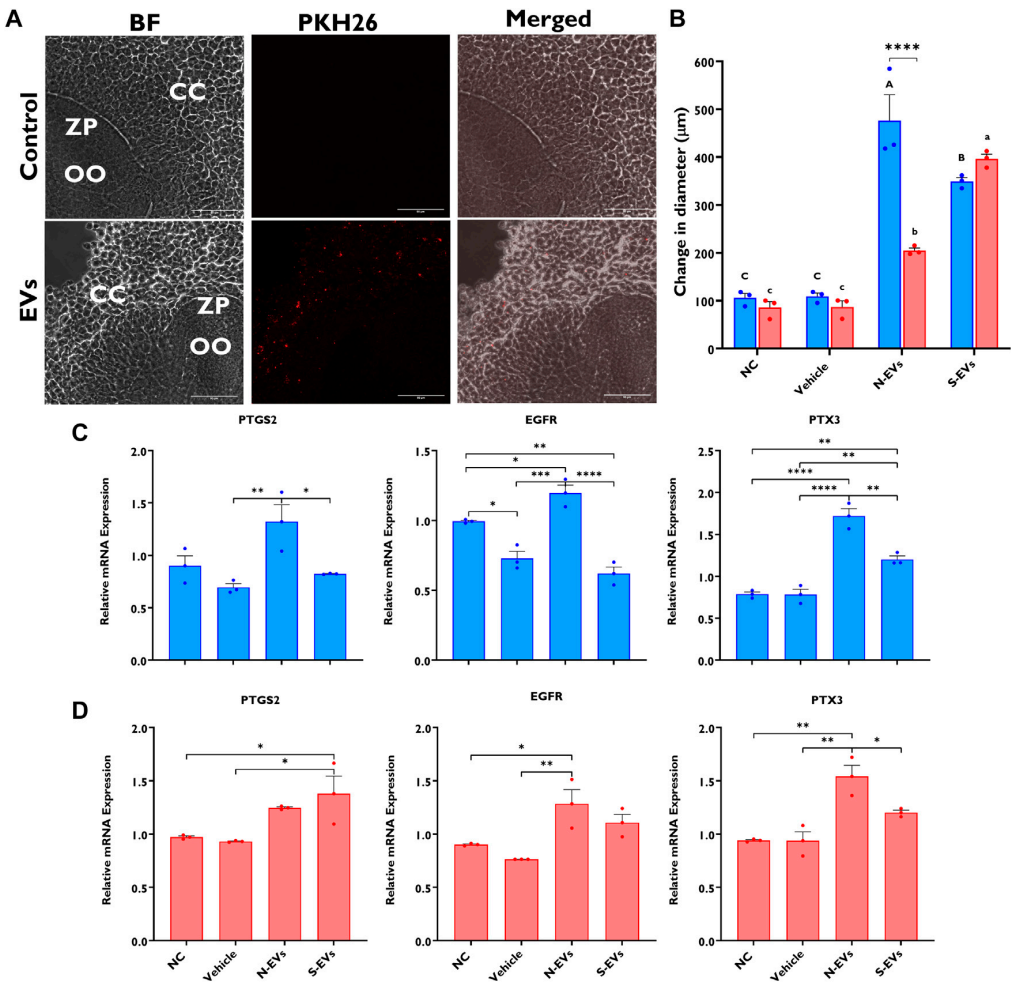


FIGURE 2
Effects of GC-EV supplementation on receptivity of follicular cells EV uptake following maturation at 38.5°C (blue) and 41°C (red) and cumulus expansion. Confocal images of intact cumulus-oocyte complexes co-incubated with PKH26 labeled GC-EVs for 24 h during in vitro maturation. Scale bar, 50 µM **(A)**. Follicular cell uptake of PKH26 labeled EVs is shown in the surrounding cumulus cells (CC), in relation to the oocyte (OO) and respective zona pellucida (ZP). Measurements for cumulus expansion were obtained before and after maturation using the Olympus Cellsens software. The increase in diameter was determined by subtracting the mean diameter before maturation from the mean diameter after maturation **(B)**. Results were carried out in four replicates (a total of 113-252 COCs per treatment). Data among treatments represent the mean±SEM and the differences between means were analyzed using Two-way ANOVA followed by Tukey's Multiple Comparisons Test. Bars with different letters (38.5°C; uppercase) (41°C; lowercase) indicate statistically significant differences of at least ($p < 0.05$) between treatments under the same culture conditions, while (*) indicate statistical differences between the same treatment under different culture environments during IVM (****$p < 0.0001$). The expression of cumulus expansion marker genes was assessed using qRT-PCR from cumulus cells isolated from oocytes in triplicates (a total of 50 COCs per treatment) cultured under thermoneutral **(C)** and heat stress **(D)** conditions. Data among treatments cultured under the same environment represent the mean ± SEM and the differences between means were analyzed using One-way ANOVA followed by Tukey's Multiple Comparisons Test. (*$p < 0.05$), (**$p < 0.01$), (***$p < 0.001$), (****$p < 0.0001$).

0.0015), as well as an interaction between temperature and treatment ($p = 0.0002$).

The supplementation of S-EVs to COCs at the time of maturation significantly decreased the relative expression of NRF2, SOD1, HSP70, and HSP90 in CCs from COCs, under both ambient temperatures alike (Figures 3A, B). Contrasting evidence showed that N-EVs did not show measurable differences in the suppression of stress-associated transcripts compared to the NC and vehicle under both normal physiological temperature and when subjected to HS (Figures 3A, B). As shown in Figure 4, the supplementation of both N-EVs and S-EVs resulted in the suppression of the majority of stress-associated genes in oocytes cultured either under normal or thermal stress conditions. Contrary to these findings, *HSP70* was significantly enriched within the oocytes supplemented with S-EVs and cultured at 38.5°C (Figure 4A), however, significantly suppressed under thermal stress conditions (Figure 4B).

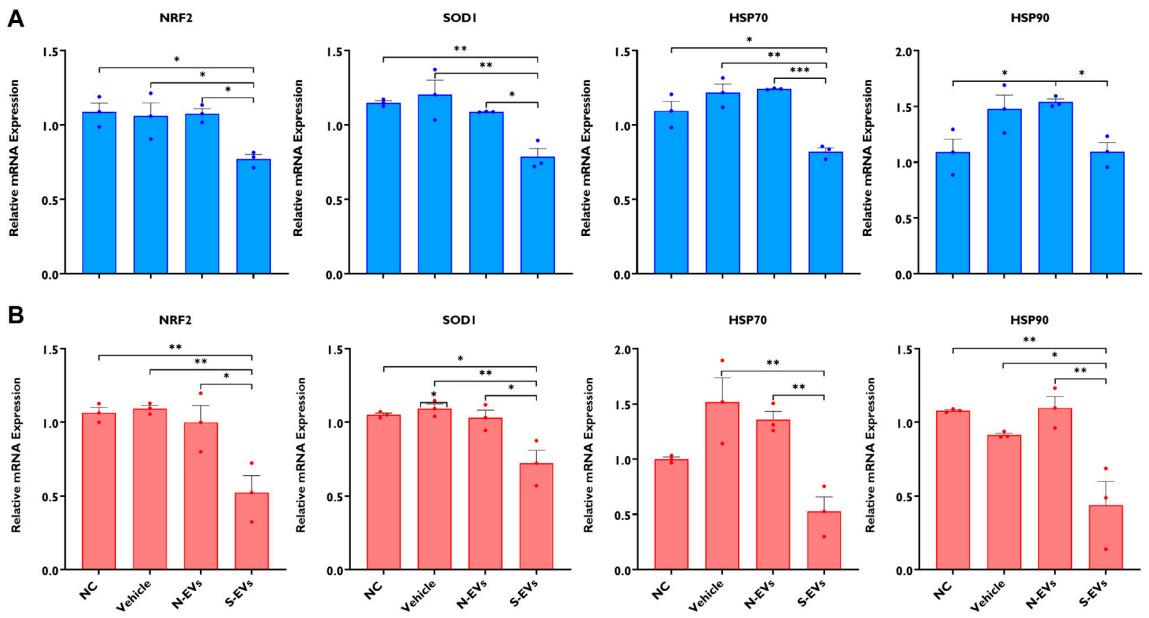


FIGURE 3
The impact of GC-EV supplementation on transcript levels of stress-associated genes in cumulus cells from cumulus-oocyte complexes following maturation at 38.5°C (blue) and 41°C (red). The expression of stress-associated genes was significantly diminished in cumulus cells from oocytes supplemented with S-EVs and matured at 38.5°C **(A)** and 41°C **(B)**. Results are from cumulus cells removed from a total of three pools of 50 oocytes per pool for each treatment. Data represent the mean ± SEM and the differences between means were analyzed using One-way ANOVA followed by Tukey's Multiple Comparisons Test. (*$p < 0.05$), (**$p < 0.01$), (***$p < 0.001$).

3.3 GC-EVs prevent ROS accumulation and promote mitochondrial function in oocytes under heat-stress conditions

ROS production and mitochondrial membrane potential were investigated in *in vitro* matured oocytes supplemented with GC-derived EVs *via* fluorescence microscopy. Diminished fluorescent signals of ROS were seen in those oocytes supplemented with S-EVs and matured at 41°C, compared to the other groups (Figures 5B, C). Similarly, under normal ambient temperature, fluorescent ROS signals were substantially reduced in oocytes supplemented with N-EVs and S-EVs when compared to controls (Figures 5A, C). Our data also concur significant differences between GC-EV supplemented treatments ($p = 0.0208$), albeit no measurable differences among temperatures or temperature and treatment interactions. Subsequent investigation of the mitochondrial membrane potential in oocytes by JC-1 staining revealed that under HS conditions, oocytes supplemented with both N-EVs and S-EVs showed markedly high mitochondrial membrane potential ($\Delta\Psi_m$) (Figures 5E, F). However, under normal physiological conditions, the highest $\Delta\Psi_m$ were observed in the treatment group supplemented with N-EVs (Figures 5D, F). Statistical comparisons for JC-1 indicated, significant differences between GC-EV supplemented treatments ($p < 0.0001$), however, no statistical differences among culture temperatures, amid a significant interaction between culture temperature and GC-EV supplemented treatments ($p = 0.0002$).

3.4 The effect of GC-EV supplementation during oocyte maturation on developmental competence of oocytes post IVF

Since GC-EVs enhanced the proper function and overall quality of bovine oocytes subjected to HS, we next assessed this correlation on their downstream embryonic developmental potential following *in vitro* fertilization. As shown in Figure 6A, there are no measurable differences in cleavage rates of the oocytes under thermal stress conditions, although, minimal improvements were noted for oocytes supplemented with N-EVs and cultured at 38.5°C. However, HS induces a dramatic decline in the proportion of oocytes capable of developing to the blastocyst stage, whether expressed as the percentage of oocytes developed to blastocyst (Figure 6B; $p < 0.0001$) or the percentage of cleaved embryos (Figure 6C; $p < 0.0001$). As shown in Figures 6B, C, while supplementation of S-EVs during oocyte maturation rescued the majority of oocytes developed to the blastocyst stage under thermal stress conditions, both N-EVs, and S-EVs improve the developmental rate of oocytes becoming blastocysts under normal physiological conditions, when compared to the untreated or vehicle controls. Taken together, our developmental competence data show significant differences

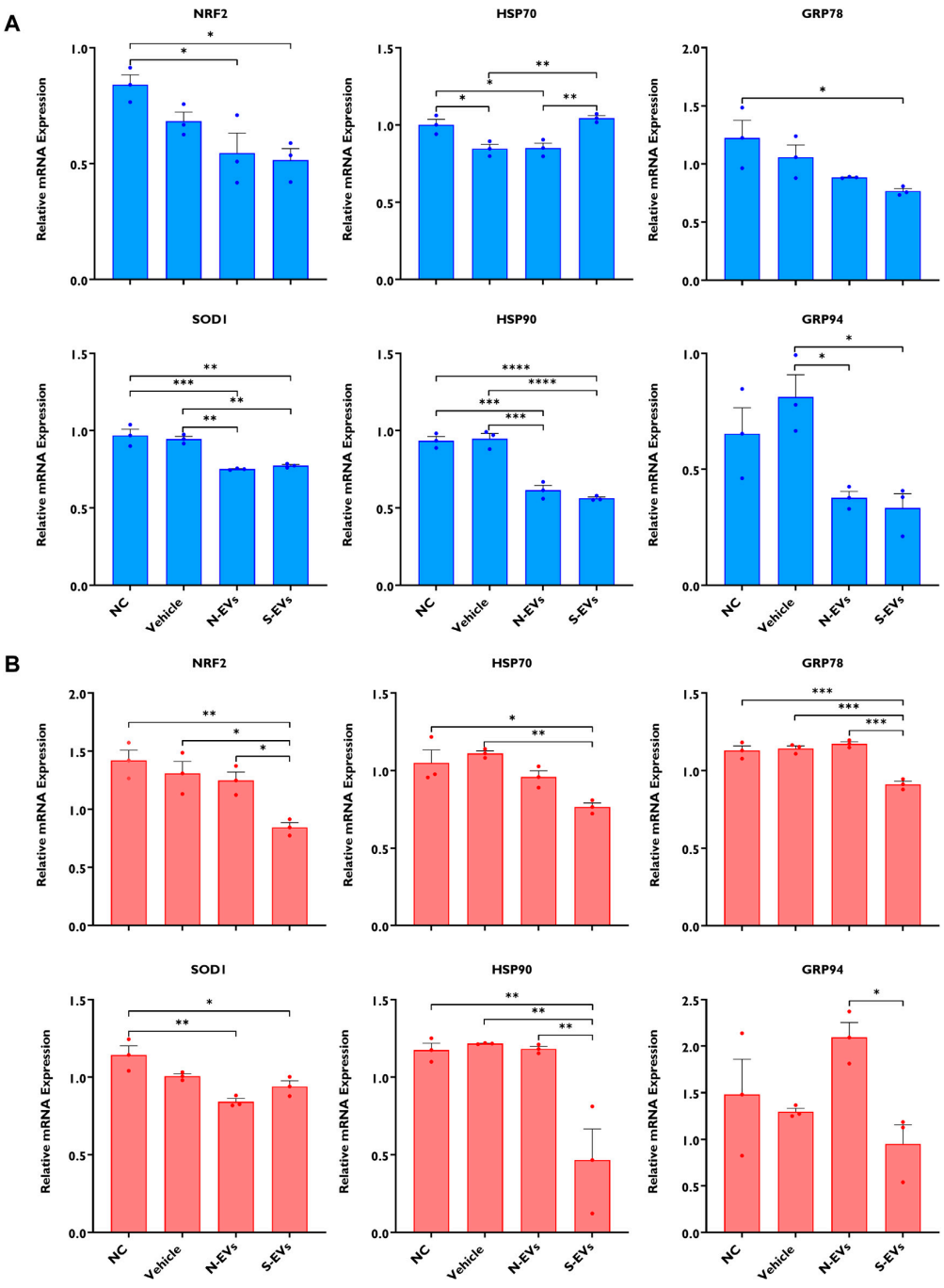


FIGURE 4
The impact of GC-EV supplementation on transcript levels of stress-associated genes in oocytes following maturation at 38.5°C (blue) and 41°C (red). The expression of stress-associated genes were significantly diminished in oocytes supplemented with N-EVs and cultured at 38.5°C **(A)**, and similar decreases in gene expression were visualized in oocytes supplemented with S-EVs and exposed to HS **(B)**. Results are from a total of three pools of 50 oocytes per pool for each treatment. Data represent the mean ± SEM and the differences between means were analyzed using One-way ANOVA followed by Tukey's Multiple Comparisons Test. (*$p < 0.05$), (**$p < 0.01$), (***$p < 0.001$), (****$p < 0.0001$).

10.3389/fcell.2023.1142629

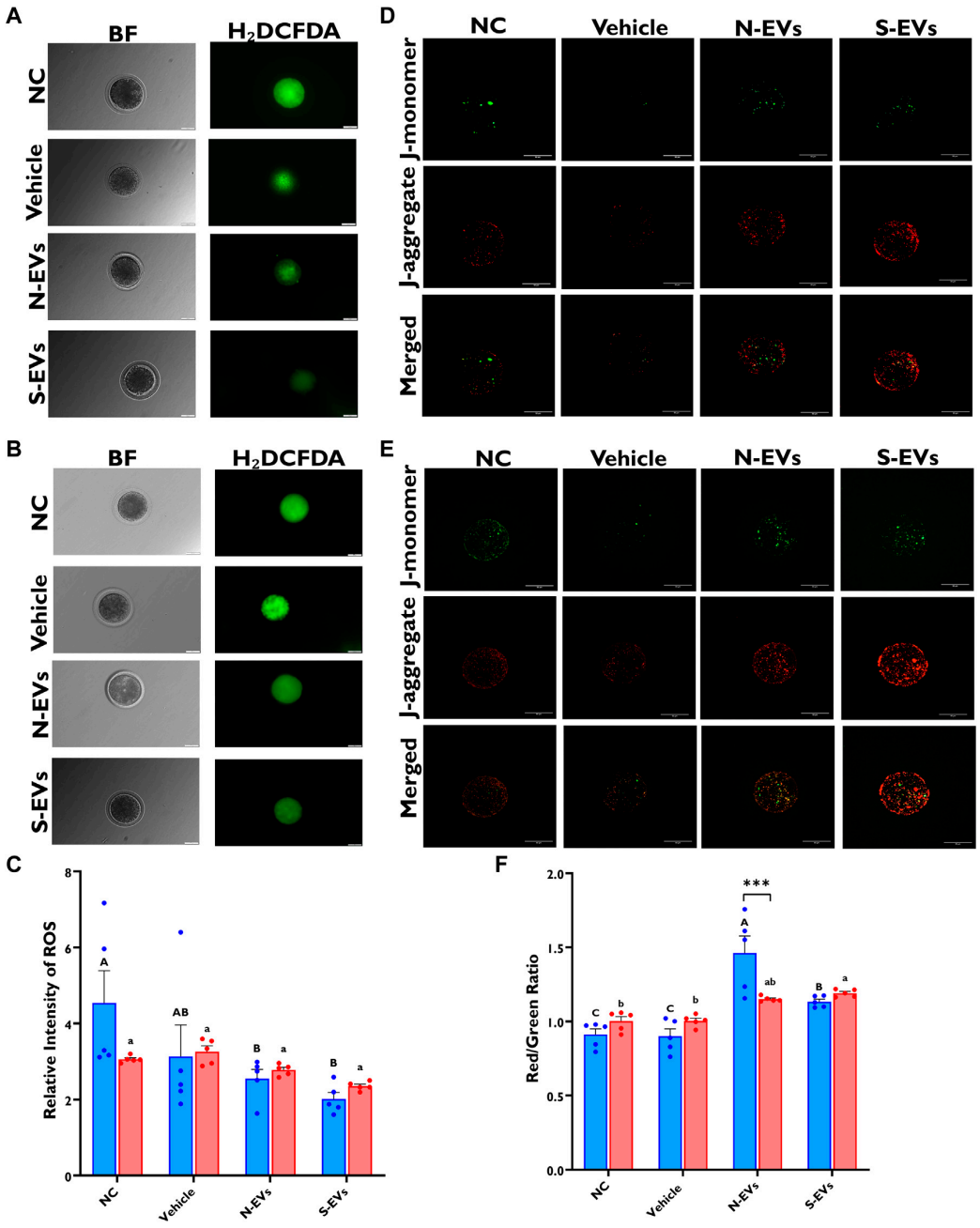


FIGURE 5
The beneficial effects of GC-EVs on oocyte function under *in vitro* normal physiological (38.5°C; blue) and HS (41°C; red) conditions. Fluorescence images of *in vitro* matured bovine oocytes treated with 2′,7′-Dichlorofluorescin Diacetate (H_2DCFDA) were captured for the measurement of intracellular ROS levels in single oocytes. Scale bar, 50 μM [38.5°C; **(A)**] [41°C; **(B)**]. Quantification of the relative fluorescence intensity in single oocytes were carried out in triplicates (total = of 15–50 oocytes per treatment) **(C)**. Fluorescence images of *in vitro* matured bovine oocytes treated with 5,5′,6,6′-tetrachloro-1,1′,3,3′tetraethylbenzimidazolylcarbocynanine iodide (JC-1) for the measurement of MMP ($\Delta\Psi$m), an indicator of mitochondrial activity in single oocytes. Scale bar, 50 μM [38.5°C; **(D)**] [41°C; **(E)**]. Quantification of the relative fluorescence intensity (red/green ratio) in single oocytes were carried out in duplicates (total = of 12–22 oocytes per treatment) **(F)**. Data among treatments represent the mean ± SEM and the differences between means were analyzed using Two-way ANOVA followed by Tukey's Multiple Comparisons Test. Bars with different letters (38.5°C; uppercase) (41°C; lowercase) indicate statistically significant differences of at least ($p < 0.05$) between treatments under the same culture conditions, while (*) indicate statistical differences between the same treatment under different culture environments during IVM (***$p < 0.001$).

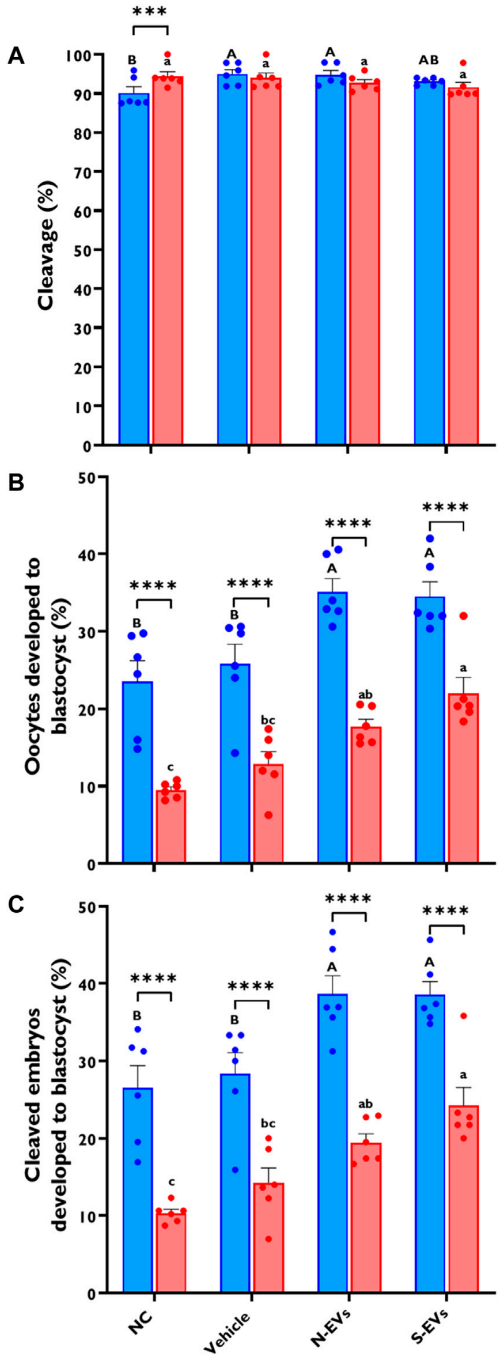


FIGURE 6
The effect of GC-EVs on the developmental capacity of oocytes matured at 38.5°C (blue) and 41°C (red). Results are from a total of six replicates (281–299 total oocytes per treatment). Oocytes supplemented with N-EVs and cultured under 38.5°C showed significant improvements in cleavage percentage compared to the NC, while no visual differences were observed among treatments under HS conditions **(A)**. The percentage of oocytes developed into blastocysts was significantly affected by maturation temperature with significant increases in developmental competence in those

(*Continued*)

FIGURE 6 (Continued)
treatments supplemented with GC-EVs **(B)**. Similarly, the percentage of cleaved embryos developed into blastocysts was linearly affected by maturation temperature with significant protection from inherent stress visualized in those treatments supplemented with GC-EVs **(C)**. Data among treatments represent the mean ± SEM and the differences between means were analyzed using Two-way ANOVA followed by Tukey's Multiple Comparisons Test. Bars with different letters (38.5°C; uppercase) (41°C; lowercase) indicate statistically significant differences of at least ($p < 0.05$) between treatments under the same culture conditions, while (*) indicate statistical differences between the same treatment under different culture environments during IVM (***$p < 0.001$) (****$p < 0.0001$).

between treatments ($p = 0.0002$, $p = 0.0003$) and temperatures ($p < 0.0001$).

3.5 GC-EV supplementation modifies the expression of stress-associated transcripts in blastocysts

As shown in Figure 7A, except for GRP78 and GRP94, the supplementation of both N-EVs and S-EVs during oocyte maturation in the absence of subsequent thermal stress resulted in the cohesive suppression of the tested stress-related genes in blastocysts. Similarly, with an exception for NRF2, the supplementation of both N-EVs and S-EVs during oocyte maturation in the presence of thermal stress exposure resulted in the suppression of all six of the tested stress-associated marker genes within the resulting blastocysts (Figure 7B).

3.6 Impact of GC-EVs supplementation during oocyte maturation on blastocyst ROS accumulation, mitochondrial function, total cell counts, and apoptotic index

As shown in Figures 8B, C, both qualitative and quantitative ROS levels are markedly lower in blastocysts when S-EVs are supplemented during oocyte maturation under HS exposure. Similarly, when cultured at 38.5°C, blastocysts derived from oocytes supplemented with S-EVs had a significantly lower accumulation of ROS (Figures 8A, C). Although our data show no significant differences between temperatures, we show a significant difference among treatments ($p = 0.001$) with a significant interaction between temperature and treatment ($p = 0.0023$). We also assessed the membrane potential of mitochondria amid blastocysts and revealed that under HS conditions, blastocysts derived from both N-EVs and S-EVs supplemented groups had significantly increased mitochondrial function, as evidenced by an increased ratio of fluorescence imaged from J-aggregates vs. J-monomers compared to the NC and vehicle (Figures 8E, F). In parallel, blastocysts derived from oocytes supplemented with N-EVs and S-EVs and cultured under normal physiological temperature (38.5°C) showed improved mitochondrial membrane potential compared to the NC and

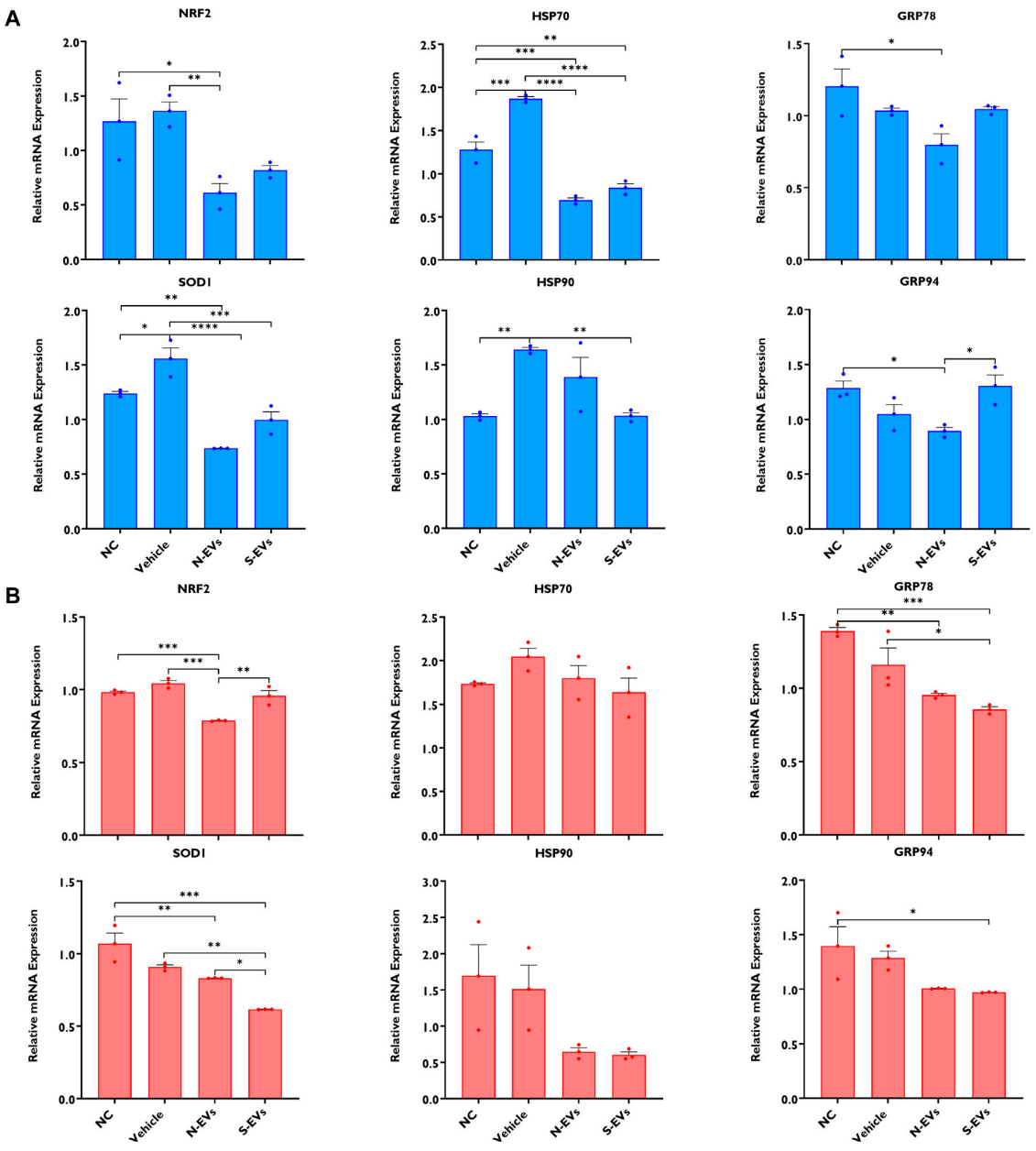


FIGURE 7
The impact of GC-EVs on transcript levels of stress-associated genes in blastocysts derived from oocytes treated with GC-EVs during oocyte maturation at 38.5°C (blue) and 41°C (red). The expressions of stress-associated genes were significantly diminished in blastocysts derived from oocytes supplemented with N-EVs and cultured at 38.5°C **(A)**, and similar decreases in gene expression were visualized in blastocysts derived from oocytes supplemented with S-EVs and exposed to HS **(B)**. Results are from a total of four pools of 5 blastocysts per pool for each treatment. Data represent the mean ± SEM and the differences between means were analyzed using One-way ANOVA followed by Tukey's Multiple Comparisons Test. (*$p < 0.05$), (**$p < 0.01$), (***$p < 0.001$), (****$p < 0.0001$).

vehicle supplemented groups (Figure 8D). Collectively, our data demonstrate a significant difference between GC-EV supplemented treatments ($p = 0.0001$), culture temperatures ($p = 0.0054$), as well as their interaction ($p = 0.0161$).

Alternatively, no measurable differences were observed in total cell numbers among the treatment groups subjected to HS (Figures 9B, C). However, there were significant increases in the total cell number in blastocysts derived from oocytes supplemented with

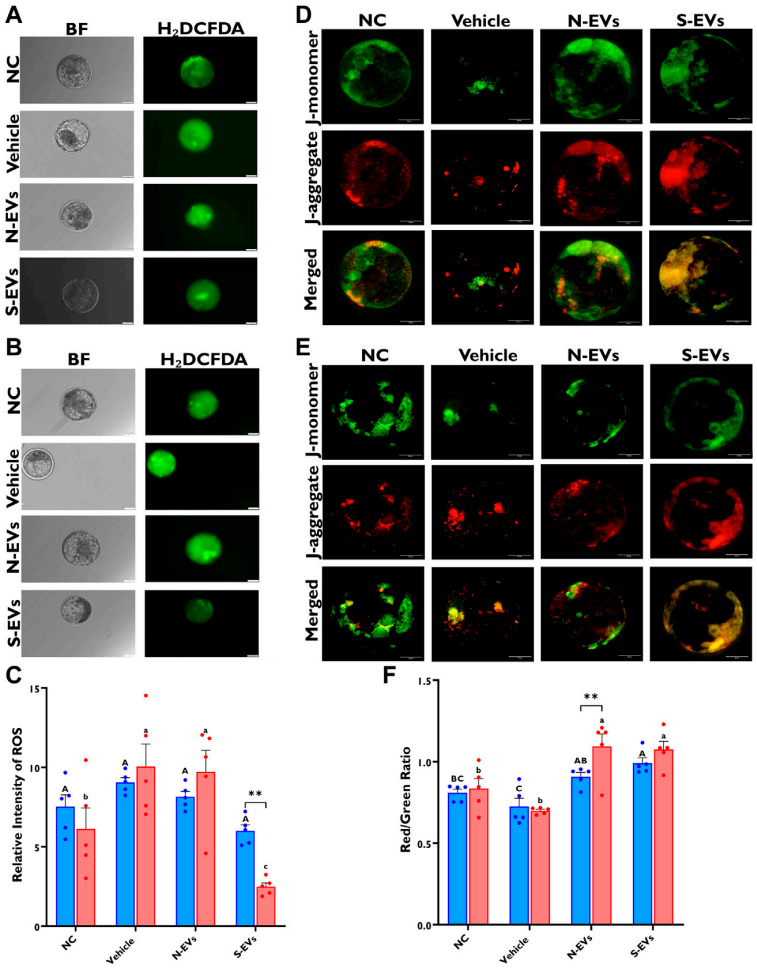


FIGURE 8
Functional alterations of GC-EV supplementation during *in vitro* maturation on blastocyst quality under *in vitro* normal physiological (38.5°C; blue) and HS (41°C; red) conditions. Fluorescence images of *in vitro* cultured bovine blastocysts treated with 2′,7′-Dichlorofluorescin Diacetate (H_2DCFDA) were captured for the measurement of intracellular ROS levels in single blastocysts. Scale bar, 50 μM [38.5°C; **(A)**] [41°C; **(B)**]. Quantification of the relative fluorescence intensity in single blastocysts were carried out in triplicates (a total of 6–9 blastocysts per treatment) **(C)**. Fluorescence images of *in vitro* cultured bovine blastocysts treated with 5,5′,6,6′-tetrachloro-1,1′,3,3′tetraethylbenzimidazolylcarbocynanine iodide (JC-1) for the measurement of MMP (ΔΨm), an indicator of mitochondrial activity in single blastocysts. Scale bar, 50 μM [38.5°C; **(D)**] [41°C; **(E)**]. Quantification of the relative fluorescence intensity (red/green ratio) in single blastocysts were carried out in duplicates (a total of 7–11 blastocysts per treatment) **(F)**. Data among treatments represent the mean ± SEM and the differences between means were analyzed using Two-way ANOVA followed by Tukey's Multiple Comparisons Test. Bars with different letters (38.5°C; uppercase) (41°C; lowercase) indicate statistically significant differences of at least ($p < 0.05$) between treatments under the same culture conditions, while (*) indicate statistical differences between the same treatment under different culture environments during IVM (**$p < 0.01$).

N-EVs and cultured at 38.5°C (Figures 9A, C). In terms of total cell counts, we show no significant differences between treatments, albeit significant differences between temperatures ($p < 0.0001$), as well as a significant interaction between temperature and treatment ($p = 0.0015$). Moreover, as shown in Figures 9E, F, the number of fluorescently labeled nuclei with fragmented DNA (shown in green), is dramatically reduced ($p < 0.0001$) in blastocysts derived from oocytes supplemented with S-EVs and exposed to HS. Additionally, blastocysts derived from oocytes supplemented with N-EVs and S-EVs and cultured under normal physiological temperature (38.5°C) showed diminished apoptotic indexes (Figures 9D, F). Importantly, our data indicates a significant difference among treatments ($p < 0.0001$), temperatures ($p = 0.0057$), as well as their interaction ($p = 0.0048$).

4 Discussion

Elevated ambient temperatures play a multifaceted role in affecting physiological and cellular functions with direct

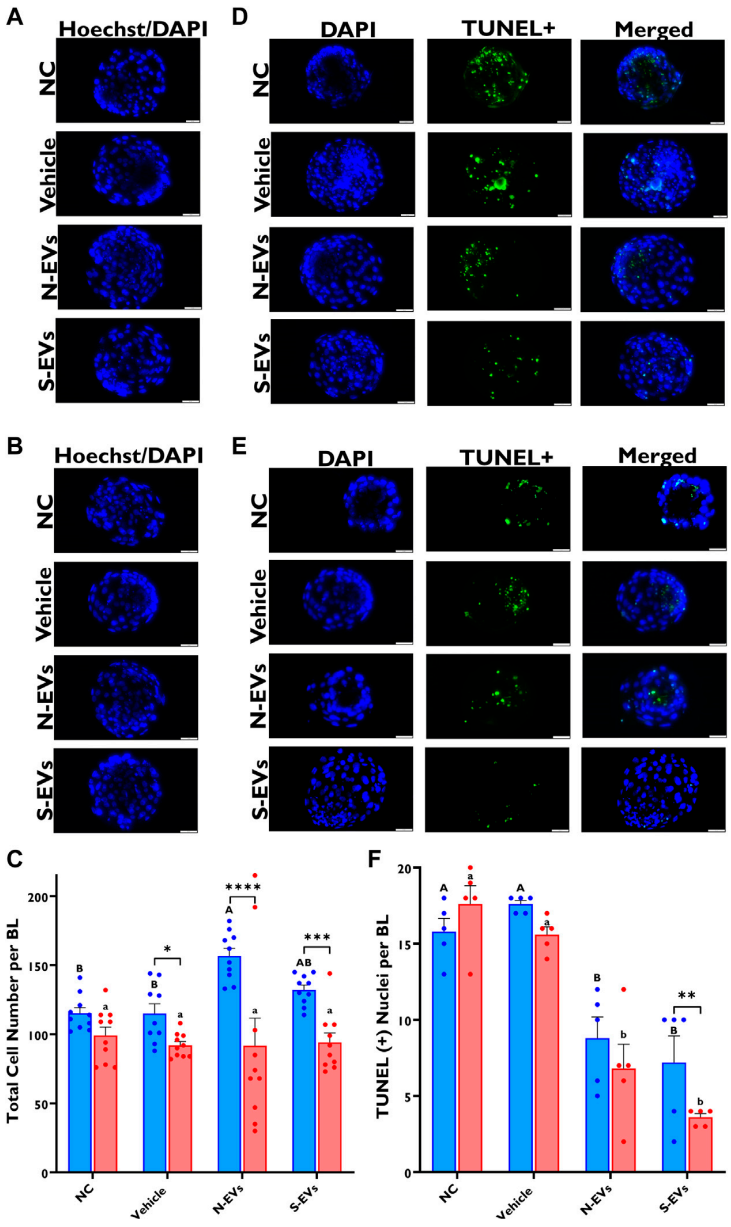


FIGURE 9
The beneficial effect of GC-EV supplementation during *in vitro* maturation on blastocyst quality under *in vitro* normal physiological (38.5°C; blue) and HS (41°C; red) conditions. Fluorescence images of *in vitro* cultured bovine blastocysts treated with Hoechst 33342/DAPI were used to determine total cell numbers in preimplantation embryos. Scale bar, 50 μM [38.5°C; **(A)**] [41°C; **(B)**]. Quantification of total cell numbers in single blastocysts were carried out in triplicates (a total of 18–30 blastocysts per treatment) **(C)**. Fluorescence images of *in vitro* cultured bovine blastocysts subjected to a TUNEL assay were captured for specific detection of apoptotic cells. Scale bar, 50 μM [38.5°C; **(D)**] [41°C; **(E)**]. Quantification of TUNEL + cells in single blastocysts were carried out in triplicates (a total of 19–41 blastocysts per treatment) **(F)**. Data among treatments represent the mean ± SEM and the differences between means were analyzed using Two-way ANOVA followed by Tukey's Multiple Comparisons Test. Bars with different letters (38.5°C; uppercase) (41°C; lowercase) indicate statistically significant differences of at least ($p < 0.05$) between treatments under the same culture conditions, while (*) indicate statistical differences between the same treatment under different culture environments during IVM (*$p < 0.05$), (**$p < 0.01$), (***$p < 0.001$), (****$p < 0.0001$).

detrimental impacts on fertility in dairy cattle (Wolfenson et al., 2000). Delineated in a plethora of studies, HS compromises reproductive function by altering follicular dynamics (Badinga et al., 1993; Guzeloglu et al., 2001), afflicting proper granulosa

cell function (Li et al., 2016) with impairments in oocyte maturation, fertilization (Roth and Hansen, 2005; Nabenishi et al., 2012) and preimplantation embryo development (Al-Katanani et al., 2002; Roth and Hansen, 2004). Oxidative stress, modeled through HS, is evidenced by the harmful effects elicited at the cellular level by inducing DNA damage, protein modifications, and lipid peroxidation (Alvarez, 2003; Kitagawa et al., 2004). We and others have recently shown that GCs exposed to HS release EVs containing protective signals which can be beneficial in eliciting positive responses or increased protection against stress in recipient or bystander cells (Bewicke-Copley et al., 2017; Gebremedhn et al., 2020). Hence, given the physiological relevance of the whereabouts of the oocyte *in vivo* at the time of maturation, in the present study, we generated subsets of EVs released from *in vitro* cultured follicular GCs subjected to the normal ambient body temperature of the cow (38.5°C) and HS (42°C) conditions. Throughout this work, we sufficiently demonstrate the capacity of GC-derived N-EVs and S-EVs in modulating a multitude of factors associated with oocyte quality when cultured under suboptimal conditions.

It has been shown previously that the addition of follicular fluid exosomes to the maturation medium can increase cumulus expansion with projections to modulate developmental competence under HS conditions (Rodrigues et al., 2019). In addition, exosomes isolated from bovine follicular fluid of small follicles have been reported to support cumulus expansion of bovine and mouse COCs cultured without fetal calf serum (Hung et al., 2015). Similarly, we found that GC-derived EVs can support cumulus expansion in COCs during maturation in the presence or absence of thermal stress. This was evidenced by the induction of the expression of cumulus expansion-associated genes (PTGS2, EGFR, and PTX3) in COCs supplemented with GC-EVs and subsequently subjected to thermal stress compared to the NC and vehicle groups. Interestingly, the impact of N-EVs in inducing the expression of cumulus expansion marker genes was prominent in COCs cultured under normal conditions following EV supplementation (Figure 2B). On the contrary, S-EVs suppressed the expression of cumulus expansion marker genes in the absence of HS (Figure 2C). Statistically comparing treatments under differing ambient culture environments, we collectively show the beneficial effects of N-EVs under normal physiological temperature compared to HS, while S-EVs showed similar effects on cumulus expansion under HS *versus* normal temperature. Moreover, expression analysis of stress-associated genes in CCs and oocytes revealed the role of GC-derived EVs in reducing the expression of stress-associated transcripts, thereby the severity of thermal stress in those cells. Irrespective of environmental culture conditions, S-EVs in particular, clearly repressed the expression of HSP70, HSP90, NRF2, and SOD1 in CCs, signifying the inherent presence of other stress factors in our *in vitro* culture environment, even under normal culture conditions. To date, the precise molecular pathways in which GC-EVs promote thermotolerance in COCs are not fully understood. However, it is postulated that donor cell cytoplasmic proteins and RNA-enriched EVs can have the potential to modulate the stress response mechanisms of recipient cells. Moreover, EVs are widely accepted for their physiochemical traits to foster therapeutic applications primarily on EV-delivered bioactive compounds (mRNA, miRNA, long non-coding RNAs, DNAs, proteins, and lipids) with biological regulatory functions (Liu et al., 2022). Exosome-mediated transfer of miRNA in bovine follicular GCs has been evidenced in our previous study (Sohel et al., 2013). Collectively, as it has been demonstrated in previous studies (Mothersill and Seymour, 1997; Lyng et al., 2000; Chai and Hei, 2008; Bewicke-Copley et al., 2017), results from this study demonstrate the capabilities of GC-EVs to support cumulus expansion and conventional physiology underpinning proper oocyte function by reducing the severity of thermal stress during *in vitro* oocyte maturation.

Oocyte competence is largely determined by the quality and subsequent accumulation of organelles, metabolites, and maternal RNAs acquired during the period of growth and maturation determining the success of fertilization, embryo development, and pregnancy establishment. Following confirmation of GC-EVs' impact on CCs, we examined the expression of stress-associated transcripts in the presence or absence of subsequent thermal stress. Under HS exposure, the expression of NRF2, SOD1, HSP70, HSP90, GRP78, and GRP94 was dramatically reduced in oocytes supplemented with S-EVs. These observations are similar to our previous report showing that priming of naïve GCs using EVs derived from thermally stressed bovine GCs could provide protection against thermal stress by suppressing the expression of stress-associated genes as a means of inducing thermotolerance (Gebremedhn et al., 2020). Previous reports well document overexpressed levels of HSPs to be especially detrimental to cells undergoing developmental growth and rapid divisions (Krebs and Feder, 1997). The chaperoning functions of HSPs inhibit Caspase processing, a heat-sensitive target leading to heat shock-induced apoptosis (Mosser et al., 1997). Inhibition of heat-shock-induced apoptosis using a caspase inhibitor has been shown to effectively mitigate the detrimental impacts of HS on oocyte competence for fertilization and subsequent embryo development (Roth and Hansen, 2004). Taken together, as functionally evidenced in part by others, S-EVs inherently contain high expression of HSPs (Gebremedhn et al., 2020), which likely in part inhibit caspase activity and provide resistance to stress-induced apoptosis, modulating the thermoprotective role of the CCs (Tatemoto et al., 2000) surrounding the oocyte and perhaps the integrity and function of the oocyte under HS conditions. In addition, S-EVs' inherent capacity to induce a beneficial "bystander effect," may potentially underpin the transfer of specific cargoes (possibly miRNA transfer), which serve to post-transcriptionally regulate gene expression *via* degradation and/or translational repression. Conclusively, S-EV-coupled miRNAs may be involved in the posttranscriptional regulation of HSPs under thermal stress conditions, resulting in the downregulation of HSP transcripts compared to the control counterparts.

Exposure to thermal stress is known to have direct implications on cellular function as it leads to the accumulation of intracellular ROS causing oxidative damage (Azad et al., 2010), mitochondrial dysfunction, and autophagy (Scherz-Shouval and Elazar, 2011; Shen et al., 2017), resulting in a continued decline in fertility (Guérin et al., 2001). The overwhelming importance of mitochondria for the development of oocytes and embryos as an apoptotic regulator and importantly a prominent source of energy in the form of ATP is widely accepted (van Blerkom, 2009). Mitochondrial dysfunction has been suggested to be a major factor in chromosomal anomalies during meiotic divisions in oocytes and

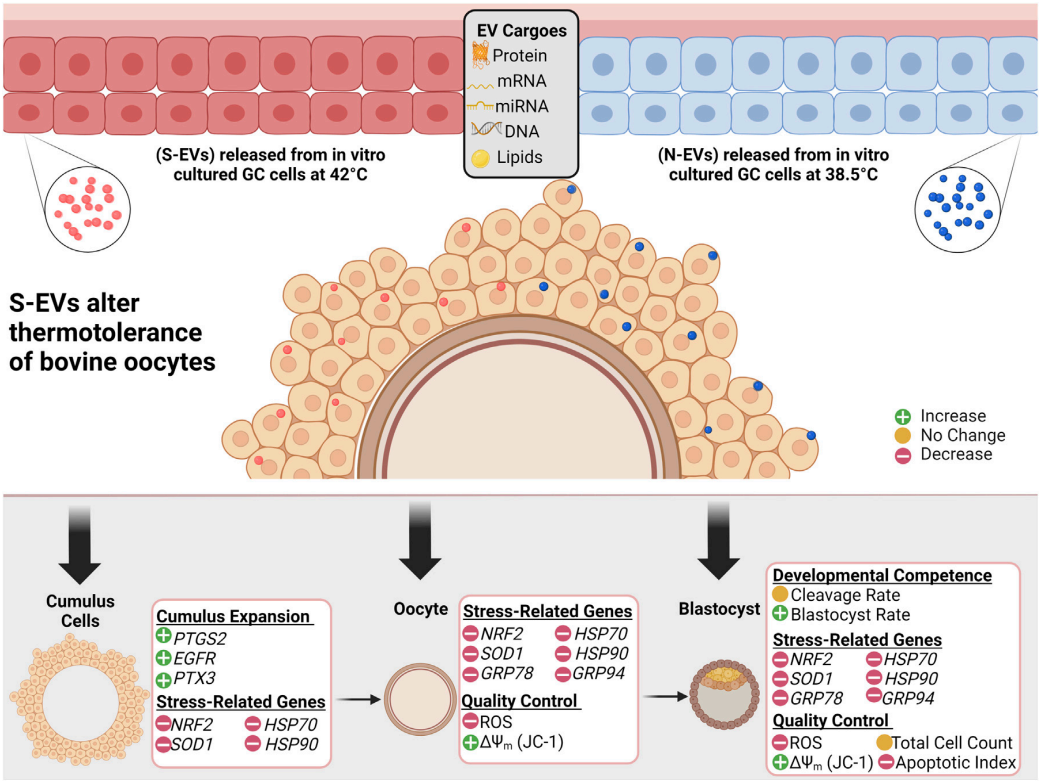


FIGURE 10
Graphical Synopsis. Schematic illustration showing EVs secreted from follicular granulosa cultured *in vitro* under 38.5°C (N-EVs) and 42°C (S-EVs), preferentially uptaken in the cumulus cells in intact cumulus-oocyte complexes following co-incubation during *in vitro* oocyte maturation. Results indicate that S-EVs effectively modulate the thermotolerance of bovine oocytes to elevated temperatures shown through the functional analysis conducted in the cumulus cells, oocytes, and developed blastocysts.

mitosis in embryos affecting the developmental competence of oocytes and embryos (Schon et al., 2000; Eichenlaub-Ritter et al., 2004; Desler et al., 2007). Studies in mice and humans using JC-1 have shown the relationship between mitochondrial activity and the developmental competence of oocytes and embryos (Acton et al., 2004). In addition to reductions in ROS accumulation, supplementation of S-EVs at the time of oocyte maturation and subsequent exposure to HS, notably increased the ratio of red to green fluorescence after JC-1 staining, indicating improved mitochondrial activity. On the other hand, under normal physiological temperatures, GC-EV supplementation synergistically reduced the accumulation of ROS with the highest mitochondrial activity coming from oocytes derived from the treatment supplemented with N-EVs during IVM. Comparisons between treatments under differing ambient culture environments showed increased mitochondrial activity in oocytes supplemented with N-EVs under normal physiological temperature compared to HS conditions. Similarly, the supplementation of S-EVs also had a similar impact on mitochondrial function in oocytes under HS conditions *versus* normal ambient temperature. The positive impacts of GC-EVs during oocyte maturation in the absence of thermal stress exposure may be in part due to the intrinsic quality of oocytes derived from local slaughterhouse ovaries and indicative that certain levels of stress are inherently present within the *in vitro* environment.

To investigate the downstream effect of GC-EVs supplementation during bovine IVM, we performed IVF and IVC of the resulting oocytes for development until the blastocyst stage. Supplementation of both N-EVs and S-EVs during oocyte maturation showed to improve blastocyst rates both in the presence or absence of thermal stress exposure, indicating the positive impact of GC-EVs in supporting oocyte development to the blastocyst stage (Figures 6B, C). Moreover, a significant reduction in the expression of stress-associated genes (SOD1, HSP70, HSP90, GRP78, and GRP94) was observed in blastocysts derived from COCs supplemented with N-EVs and S-EVs. However, in the absence of HS, blastocysts from GC-EVs'-supplemented treatment groups tended to suppress the relative abundance of stress-associated genes, with exceptions to the expression of GRP78 and GRP94, which showed increases in expression in S-EVs supplemented treatment groups. This indicates the differential impact of GC-EVs in modulating the stress response of oocytes to environmental stressors. In the present study, it is shown that blastocysts derived from COCs supplemented with S-EVs and exposed to HS during maturation have increased embryo quality due to

reduced ROS accumulation, decreased TUNEL+ apoptotic nuclei, and increased mitochondrial activity compared to their NC counterparts. Interestingly, as shown in oocytes, S-EVs significantly reduced the amount of accumulated ROS in blastocysts under HS compared to those cultured under normal ambient temperature. These results partly support our hypothesis that S-EVs derived from GCs mitigate the detrimental effects of HS during oocyte maturation, which may have an impact on the further developmental potential of oocytes in giving rise to developmentally competent blastocysts. Our data also suggests that GC-EV supplementation amid HS exposure during IVM may not induce the proliferative capacity of bovine embryos, however, GC-EVs effectively modulate the inherent quality of resulting blastocysts. To leverage our findings, a similar study showed that EVs isolated *via* density gradient ultracentrifugation and size-exclusion chromatography from Holstein heifer follicular fluid, improve embryo quality based primarily on differential apoptotic cell counts (Asaadi et al., 2021). Similarly, the addition of bovine oviduct epithelial cell EVs had a positive impact on the quality of *in vitro* produced bovine embryos, signifying EVs' functional and physiological relevance to support the development of viable and competent blastocysts under *in vitro* environments to enhance the pregnancy outcome after transfer (Lopera-Vásquez et al., 2016).

Taken together, the current study demonstrated that GC-EVs play a pivotal regulatory role against HS during *in vitro* maturation of bovine oocytes by reducing ROS accumulation, enhancing proper mitochondrial function, and altering the expression of stress-associated genes, thereby reducing the severity of thermal stress, improving oocyte survival and viability (Figure 10). Despite the fact that EVs are uptaken only by CCs, the impact of EV supplementation seems to be through changing the physiology of the CCs, which ultimately lends impact on oocyte physiology, particularly ROS accumulation, mitochondrial activity, and gene expression profiles. Furthermore, the beneficial role of EVs and their capabilities to modulate the detrimental effects of HS during maturation can have long-lasting impacts on the development and quality of blastocysts, potentially in the establishment of pregnancy and the generation of healthy offspring. As GC-EVs are known to shuttle protective signals in the form of RNAs, proteins, and/or lipids, further studies are needed to determine the exact mechanisms of action of EVs in modulating stress response for potential application in assisted reproductive technologies involving IVM, IVF, and IVC of mammalian oocytes and embryos.

Data availability statement

The original contributions presented in the study are included in the article/Supplementary Material, further inquiries can be directed to the corresponding author. Written details on experimental procedures have been submitted to the EV-TRACK knowledgebase and can be accessed under (EV-TRACK ID: EV220412).

Author contributions

Conceptualization: NM and DT. Experimental work: NM, AG, SaG, and SoG. Data analysis: NM. Writing of original draft: NM, AG, SoG, and DT. Supervision: DT. Funding acquisition: DT. All authors have read and agreed to the published version of this manuscript.

Funding

NM is supported by grant funds from the United States Department of Agriculture (USDA), National Needs Fellowship (NNF): 2021-38420-34040.

Acknowledgments

The authors thank the staff at BPO Parts LLC for their assistance in collection of reproductive materials. We acknowledge the University of Colorado, Boulder EM Services Core Facility in the MCDB Department, for their help and support with TEM imaging. Nano-particle tracking analysis was performed by Ms. Mindy A. Meyers from the Department of Clinical Sciences at Colorado State University. Support for confocal imaging was provided by Samantha Kaonis, a member of the Cellular Engineering and Mechanobiology Laboratory at Colorado State University. Semen used for this experiment was provided to our laboratory by Teixeira Cattle Company (Pismo Beach, CA) and prepared by JLG Enterprises (Oakdale, CA).

Conflict of interest

Author SaG was employed by Genus Plc.

The remaining authors declare that the research was conducted in the absence of any commercial or financial relationships that could be construed as a potential conflict of interest.

Publisher's note

All claims expressed in this article are solely those of the authors and do not necessarily represent those of their affiliated organizations, or those of the publisher, the editors and the reviewers. Any product that may be evaluated in this article, or claim that may be made by its manufacturer, is not guaranteed or endorsed by the publisher.

Supplementary material

The Supplementary Material for this article can be found online at: https://www.frontiersin.org/articles/10.3389/fcell.2023.1142629/full#supplementary-material

References

Abdelnour, S. A., Yang, C. Y., Swelum, A. A., Abd El-Hack, M. E., Khafaga, A. F., Abdo, M., et al. (2020). Molecular, functional, and cellular alterations of oocytes and cumulus cells induced by heat stress and shock in animals. *Environ. Sci. Pollut. Res. Int.* 27 (31), 38472–38490. doi:10.1007/s11356-020-10302-4

Abumaghaid, M. M., Abdelazim, A. M., Belali, T. M., Alhujaily, M., and Saadeldin, I. M. (2022). Shuttle transfer of mRNA transcripts via extracellular vesicles from male reproductive tract cells to the cumulus-oocyte complex in rabbits (*Oryctolagus cuniculus*). *Front. Veterinary Sci.* 9, 816080. doi:10.3389/fvets.2022.816080

Acton, B. M., Jurisicova, A., Jurisica, I., and Casper, R. F. (2004). Alterations in mitochondrial membrane potential during preimplantation stages of mouse and human embryo development. *Mol. Hum. Reprod.* 10 (1), 23–32. doi:10.1093/molehr/gah004

Ahmed, K. A., and Xiang, J. (2011). Mechanisms of cellular communication through intercellular protein transfer. *J. Cell. Mol. Med.* 15 (7), 1458–1473. doi:10.1111/j.1582-4934.2010.01008.x

Al-Katanani, Y. M., Paula-Lopes, F. F., and Hansen, P. J. (2002). Effect of season and exposure to heat stress on oocyte competence in Holstein cows. *J. Dairy Sci.* 85 (2), 390–396. doi:10.3168/jds.s0022-0302(02)74086-1

Alam, M. H., and Miyano, T. (2020). Interaction between growing oocytes and granulosa cells *in vitro*. *Reproductive Med. Biol.* 19 (1), 13–23. doi:10.1002/rmb2.12292

Alcântara-Neto, A. S., Fernandez-Rufete, M., Corbin, E., Tsikis, G., Uzbekov, R., Garanina, A. S., et al. (2020a). Oviduct fluid extracellular vesicles regulate polyspermy during porcine *in vitro* fertilisation. *Reproduction, Fertil. Dev.* 32 (4), 409–418. doi:10.1071/RD19058

Alcântara-Neto, A. S., Schmaltz, L., Caldas, E., Blache, M. C., Mermillod, P., and Almiñana, C. (2020b). Porcine oviductal extracellular vesicles interact with gametes and regulate sperm motility and survival. *Theriogenology* 155, 240–255. doi:10.1016/j.theriogenology.2020.05.043

Alemu, T. W., Pandey, H. O., Salilew Wondim, D., Gebremedhn, S., Neuhof, C., Tholen, E., et al. (2018). Oxidative and endoplasmic reticulum stress defense mechanisms of bovine granulosa cells exposed to heat stress. *Theriogenology* 110, 130–141. doi:10.1016/j.theriogenology.2017.12.042

Almiñana, C., Corbin, E., Tsikis, G., Alcântara-Neto, A. S., Labas, V., Reynaud, K., et al. (2017). Oviduct extracellular vesicles protein content and their role during oviduct-embryo cross-talk. *Reprod. Camb. Engl.* 154 (3), 153–168. doi:10.1530/REP-17-0054

Altan-Bonnet, G., and Mukherjee, R. (2019). Cytokine-mediated communication: A quantitative appraisal of immune complexity. *Nat. Rev. Immunol.* 19 (4), 205–217. doi:10.1038/s41577-019-0131-x

Alvarez, J. G. (2003). DNA fragmentation in human spermatozoa: Significance in the diagnosis and treatment of infertility. *Minerva Ginecol.* 55 (3), 233–239.

Asaadi, A., Dolatabad, N. A., Atashi, H., Raes, A., van Damme, P., Hoelker, M., et al. (2021). Extracellular vesicles from follicular and ampullary fluid isolated by density gradient ultracentrifugation improve bovine embryo development and quality. *Int. J. Mol. Sci.* 22, 578. doi:10.3390/ijms22020578

Azad, M. A. K., Kikusato, M., Sudo, S., Amo, T., and Toyomizu, M. (2010). Time course of ROS production in skeletal muscle mitochondria from chronic heat-exposed broiler chicken. *Comp. Biochem. Physiology. Part A, Mol. Integr. Physiology* 157 (3), 266–271. doi:10.1016/j.cbpa.2010.07.011

Badinga, L., Thatcher, W. W., Diaz, T., Drost, M., and Wolfenson, D. (1993). Effect of environmental heat stress on follicular development and steroidogenesis in lactating Holstein cows. *Theriogenology* 39 (4), 797–810. doi:10.1016/0093-691X(93)90419-6

Bewicke-Copley, F., Mulcahy, L. A., Jacobs, L. A., Samuel, P., Akbar, N., Pink, R. C., et al. (2017). Extracellular vesicles released following heat stress induce bystander effect in unstressed populations. *J. Extracell. Vesicles* 6 (1), 1340746. doi:10.1080/20013078.2017.1340746

Boni, R. (2019). Heat stress, a serious threat to reproductive function in animals and humans. *Mol. Reproduction Dev.* 86 (10), 1307–1323. doi:10.1002/mrd.23123

Chai, Y., and Hei, T. K. (2008). Radiation induced bystander effect *in vivo*. *Acta Medica Nagasaki.* 53, S65–S69.

Critser, E. S., and First, N. L. (1986). Use of a fluorescent stain for visualization of nuclear material in living oocytes and early embryos. *Stain Technol.* 61 (1), 1–5. doi:10.3109/10520298609110697

Da Silveira, J. C., Veeramachaneni, D. N. R., Winger, Q. A., Carnevale, E. M., and Bouma, G. J. (2012). Cell-secreted vesicles in equine ovarian follicular fluid contain miRNAs and proteins: A possible new form of cell communication within the ovarian follicle. *Biol. Reproduction* 86 (3), 71. doi:10.1095/biolreprod.111.093252

De La Torre-Sanchez, S., Fernando, J., Preis, K., and Seidel, G. E., J. R. (2006). Metabolic regulation of *in-vitro*-produced bovine embryos. I. Effects of metabolic regulators at different glucose concentrations with embryos produced by semen from different bulls. *Reproduction, Fertil. Dev.* 18 (5), 585–596. doi:10.1071/rd05063

Desler, C., Munch-Petersen, B., Stevnsner, T., Matsui, S. I., Kulawiec, M., Singh, K. K., et al. (2007). Mitochondria as determinant of nucleotide pools and chromosomal stability. *Mutat. Res.* 625 (1-2), 112–124. doi:10.1016/j.mrfmmm.2007.06.002

Edwards, J. L., Saxton, A. M., Lawrence, J. L., Payton, R. R., and Dunlap, J. R. (2005). Exposure to a physiologically relevant elevated temperature hastens *in vitro* maturation in bovine oocytes. *J. Dairy Sci.* 88 (12), 4326–4333. doi:10.3168/jds.S0022-0302(05)73119-2

Eichenlaub-Ritter, U., Vogt, E., Yin, H., and Gosden, R. (2004). Spindles, mitochondria and redox potential in ageing oocytes. *Reprod. Biomed. Online* 8 (1), 45–58. doi:10.1016/s1472-6483(10)60497-x

Feder, M. E., and Hofmann, G. E. (1999). Heat-shock proteins, molecular chaperones, and the stress response: Evolutionary and ecological physiology. *Annu. Rev. Physiology* 61, 243–282. doi:10.1146/annurev.physiol.61.1.243

Ferreira, R. M., Chiaratti, M. R., Macabelli, C. H., Rodrigues, C. A., Ferraz, M. L., Watanabe, Y. F., et al. (2016). The infertility of repeat-breeder cows during summer is associated with decreased mitochondrial DNA and increased expression of mitochondrial and apoptotic genes in oocytes. *Biol. Reproduction* 94 (3), 66. doi:10.1095/biolreprod.115.133017

Gebremedhn, S., Gad, A., Aglan, H. S., Laurincik, J., Prochazka, R., Salilew-Wondim, D., et al. (2020). Extracellular vesicles shuttle protective messages against heat stress in bovine granulosa cells. *Sci. Rep.* 10 (1), 15824. doi:10.1038/s41598-020-72706-z

Gilula, N. B., Epstein, M. L., and Beers, W. H. (1978). Cell-to-cell communication and ovulation. A study of the cumulus-oocyte complex. *J. Cell. Biol.* 78 (1), 58–75. doi:10.1083/jcb.78.1.58

Guérin, P., El Mouatassim, S., and Ménézo, Y. (2001). Oxidative stress and protection against reactive oxygen species in the pre-implantation embryo and its surroundings. *Hum. Reprod. Update* 7 (2), 175–189. doi:10.1093/humupd/7.2.175

Guzeloglu, A., Ambrose, J. D., Kassa, T., Diaz, T., Thatcher, M. J., and Thatcher, W. W. (2001). Long-term follicular dynamics and biochemical characteristics of dominant follicles in dairy cows subjected to acute heat stress. *Animal Reproduction Sci.* 66 (1-2), 15–34. doi:10.1016/s0378-4320(01)00082-3

Hansen, P. J. (2009). Effects of heat stress on mammalian reproduction. *Philosophical Trans. R. Soc. Lond. Ser. B, Biol. Sci.* 364 (1534), 3341–3350. doi:10.1098/rstb.2009.0131

Hung, W. T., Hong, X., Christenson, L. K., and McGinnis, L. K. (2015). Extracellular vesicles from bovine follicular fluid support cumulus expansion. *Biol. Reproduction* 93 (5), 117. doi:10.1095/biolreprod.115.132977

Kitagawa, Y., Suzuki, K., Yoneda, A., and Watanabe, T. (2004). Effects of oxygen concentration and antioxidants on the *in vitro* developmental ability, production of reactive oxygen species (ROS), and DNA fragmentation in porcine embryos. *Theriogenology* 62 (7), 1186–1197. doi:10.1016/j.theriogenology.2004.01.011

Krebs, R. A., and Feder, M. E. (1997). Deleterious consequences of Hsp70 overexpression in *Drosophila melanogaster* larvae. *Cell. Stress & Chaperones* 2 (1), 60–71. doi:10.1379/1466-1268(1997)002<0060:dcohoi>2.3.co;2

Li, J., Gao, H., Tian, Z., Wu, Y., Wang, Y., Fang, Y., et al. (2016). Effects of chronic heat stress on granulosa cell apoptosis and follicular atresia in mouse ovary. *J. Animal Sci. Biotechnol.* 7, 57. doi:10.1186/s40104-016-0116-6

Li, Y., Zhang, Z., He, C., Zhu, K., Xu, Z., Ma, T., et al. (2015). Melatonin protects porcine oocyte *in vitro* maturation from heat stress. *J. Pineal Res.* 59 (3), 365–375. doi:10.1111/jpi.12268

Lin, T., Lee, J. E., Kang, J. W., Shin, H. Y., Lee, J. B., and Jin, D. I. (2019). Endoplasmic reticulum (ER) stress and unfolded protein response (UPR) in mammalian oocyte maturation and preimplantation embryo development. *Int. J. Mol. Sci.* 20, 409. doi:10.3390/ijms20020409

Liu, H., Liang, J., Ye, X., Huang, M., Ma, L., Xie, X., et al. (2022). The potential role of extracellular vesicles in bioactive compound-based therapy: A review of recent developments. *Crit. Rev. Food Sci. Nutr.* 1–15, 1–15. doi:10.1080/10408398.2022.2081667

Lopera-Vásquez, R., Hamdi, M., Fernandez-Fuertes, B., Maillo, V., Beltrán-Breña, P., Calle, A., et al. (2016). Extracellular vesicles from BOEC in *in vitro* embryo development and quality. *PloS One* 11 (2), e0148083. doi:10.1371/journal.pone.0148083

Lyng, F. M., Seymour, C. B., and Mothersill, C. (2000). Production of a signal by irradiated cells which leads to a response in unirradiated cells characteristic of initiation of apoptosis. *Br. J. Cancer* 83 (9), 1223–1230. doi:10.1054/bjoc.2000.1433

Mateo-Otero, Y., Yeste, M., Roca, J., Llavanera, M., Bucci, D., Galeati, G., et al. (2022). Seminal extracellular vesicles subsets modulate gene expression in cumulus cells of porcine *in vitro* matured oocytes. *Sci. Rep.* 12 (1), 19096. doi:10.1038/s41598-022-22004-7

Matzuk, M. M., Burns, K. H., Viveiros, M. M., and Eppig, J. J. (2002). Intercellular communication in the mammalian ovary: Oocytes carry the conversation. *Sci. (New York, N.Y.)* 296 (5576), 2178–2180. doi:10.1126/science.1071965

Mosser, D. D., Caron, A. W., Bourget, L., Denis-Larose, C., and Massie, B. (1997). Role of the human heat shock protein hsp70 in protection against stress-induced apoptosis. *Mol. Cell. Biol.* 17 (9), 5317–5327. doi:10.1128/MCB.17.9.5317

Mothersill, C., and Seymour, C. (1997). Medium from irradiated human epithelial cells but not human fibroblasts reduces the clonogenic survival of unirradiated cells. *Int. J. Radiat. Biol.* 71 (4), 421–427. doi:10.1080/095530097144030

Nabenishi, H., Ohta, H., Nishimoto, T., Morita, T., Ashizawa, K., and Tsuzuki, Y. (2012). The effects of cysteine addition during *in vitro* maturation on the developmental competence, ROS, GSH and apoptosis level of bovine oocytes exposed to heat stress. *Zygote Camb. Engl.* 20 (3), 249–259. doi:10.1017/S0967199411000220

Parrish, J. J., Krogenaes, A., and Susko-Parrish, J. L. (1995). Effect of bovine sperm separation by either swim-up or Percoll method on success of *in vitro* fertilization and early embryonic development. *Theriogenology* 44 (6), 859–869. doi:10.1016/0093-691x(95)00271-9

Pasquariello, R., Ermisch, A. F., Silva, E., McCormick, S., Logsdon, D., Barfield, J. P., et al. (2019). Alterations in oocyte mitochondrial number and function are related to spindle defects and occur with maternal aging in mice and humans. *Biol. Reproduction* 100 (4), 971–981. doi:10.1093/biolre/ioy248

Pavani, K. C., Baron, E., Correia, P., Lourenço, J., Bettencourt, B. F., Sousa, M., et al. (2016). Gene expression, oocyte nuclear maturation and developmental competence of bovine oocytes and embryos produced after *in vivo* and *in vitro* heat shock. *Zygote Camb. Engl.* 24 (5), 748–759. doi:10.1017/S0967199416000071

Rivera, R. M., and Hansen, P. J. (2001). Development of cultured bovine embryos after exposure to high temperatures in the physiological range. *Reprod. Camb. Engl.* 121 (1), 107–115. doi:10.1530/rep.0.1210107

Robertson, I. (1998). Certification and identification of the embryo. *Man. Intermational Embryo Transf. Soc.* 6, 103–134.

Rodrigues, T. A., Tuna, K. M., Alli, A. A., Tribulo, P., Hansen, P. J., Koh, J., et al. (2019). Follicular fluid exosomes act on the bovine oocyte to improve oocyte competence to support development and survival to heat shock. *Reproduction, Fertil. Dev.* 31 (5), 888–897. doi:10.1071/RD18450

Roth, Z., and Hansen, P. J. (2005). Disruption of nuclear maturation and rearrangement of cytoskeletal elements in bovine oocytes exposed to heat shock during maturation. *Reprod. Camb. Engl.* 129 (2), 235–244. doi:10.1530/rep.1.00394

Roth, Z., and Hansen, P. J. (2004). Involvement of apoptosis in disruption of developmental competence of bovine oocytes by heat shock during maturation. *Biol. Reproduction* 71 (6), 1898–1906. doi:10.1095/biolreprod.104.031690

Russell, D. L., Gilchrist, R. B., Brown, H. M., and Thompson, J. G. (2016). Bidirectional communication between cumulus cells and the oocyte: Old hands and new players? *Theriogenology* 86 (1), 62–68. doi:10.1016/j.theriogenology.2016.04.019

Saeed-Zidane, M., Linden, L., Salilew-Wondim, D., Held, E., Neuhoff, C., Tholen, E., et al. (2017). Cellular and exosome mediated molecular defense mechanism in bovine granulosa cells exposed to oxidative stress. *PloS One* 12 (11), e0187569. doi:10.1371/journal.pone.0187569

Sartori, R., Sartor-Bergfelt, R., Mertens, S. A., Guenther, J. N., Parrish, J. J., and Wiltbank, M. C. (2002). Fertilization and early embryonic development in heifers and lactating cows in summer and lactating and dry cows in winter. *J. Dairy Sci.* 85 (11), 2803–2812. doi:10.3168/jds.S0022-0302(02)74367-1

Scherz-Shouval, R., and Elazar, Z. (2011). Regulation of autophagy by ROS: Physiology and pathology. *Trends Biochem. Sci.* 36 (1), 30–38. doi:10.1016/j.tibs.2010.07.007

Schmittgen, T. D., and Livak, K. J. (2008). Analyzing real-time PCR data by the comparative C(T) method. *Nat. Protoc.* 3 (6), 1101–1108. doi:10.1038/nprot.2008.73

Schon, E. A., Kim, S. H., Ferreira, J. C., Magalhães, P., Grace, M., Warburton, D., et al. (2000). Chromosomal non-disjunction in human oocytes: Is there a mitochondrial connection? *Hum. Reprod. Oxf. Engl.* 15 (2), 160–172. doi:10.1093/humrep/15.suppl_2.160

Shen, M., Jiang, Y., Guan, Z., Cao, Y., Li, L., Liu, H., et al. (2017). Protective mechanism of FSH against oxidative damage in mouse ovarian granulosa cells by repressing autophagy. *Autophagy* 13 (8), 1364–1385. doi:10.1080/15548627.2017.1327941

Silva, E., Greene, A. F., Strauss, K., Herrick, J. R., Schoolcraft, W. B., and Krisher, R. L. (2015). Antioxidant supplementation during *in vitro* culture improves mitochondrial function and development of embryos from aged female mice. *Reproduction, Fertil. Dev.* 27 (6), 975–983. doi:10.1071/RD14474

Sohel, M. M. H., Hoelker, M., Noferesti, S. S., Salilew-Wondim, D., Tholen, E., Looft, C., et al. (2013). Exosomal and non-exosomal transport of extra-cellular microRNAs in follicular fluid: Implications for bovine oocyte developmental competence. *PloS One* 8 (11), e78505. doi:10.1371/journal.pone.0078505

Szatanek, R., Baran, J., Siedlar, M., and Baj-Krzyworzeka, M. (2015). Isolation of extracellular vesicles: Determining the correct approach (Review). *Int. J. Mol. Med.* 36 (1), 11–17. doi:10.3892/ijmm.2015.2194

Tatemoto, H., Sakurai, N., and Muto, N. (2000). Protection of porcine oocytes against apoptotic cell death caused by oxidative stress during *in vitro* maturation: Role of cumulus cells. *Biol. Reproduction* 63 (3), 805–810. doi:10.1095/biolreprod63.3.805

Tesfaye, D., Menjivar, N., and Gebremedhn, S. (2021). Current knowledge and the future potential of extracellular vesicles in mammalian reproduction. *Reproduction, Fertil. Dev.* 34 (2), 174–189. doi:10.1071/RD21277

Théry, C., Witwer, K. W., Aikawa, E., Alcaraz, M. J., Anderson, J. D., Andriantsitohaina, R., et al. (2018). Minimal information for studies of extracellular vesicles 2018 (MISEV2018): A position statement of the international society for extracellular vesicles and update of the MISEV2014 guidelines. *J. Extracell. Vesicles* 7 (1), 1535750. doi:10.1080/20013078.2018.1535750

Trummer, A., Rop, C. D., Tiede, A., Ganser, A., and Eisert, R. (2009). Recovery and composition of microparticles after snap-freezing depends on thawing temperature. *Blood Coagulation Fibrinolysis Int. J. Haemostasis Thrombosis* 20 (1), 52–56. doi:10.1097/MBC.0b013e32831be9c5

Valadi, H., Ekström, K., Bossios, A., Sjöstrand, M., Lee, J. J., and Lötvall, J. O. (2007). Exosome-mediated transfer of mRNAs and microRNAs is a novel mechanism of genetic exchange between cells. *Nat. Cell. Biol.* 9 (6), 654–659. doi:10.1038/ncb1596

van Blerkom, J. (2009). Mitochondria in early mammalian development. *Seminars Cell. & Dev. Biol.* 20 (3), 354–364. doi:10.1016/j.semcdb.2008.12.005

van Deun, J., Mestdagh, P., Agostinis, P., Akay, Ö., Anand, S., Anckaert, J., et al. (2017) EV-TRACK: Transparent reporting and centralizing knowledge in extracellular vesicle research. *Nat. Methods* 14 (3), 228–232. doi:10.1038/nmeth.4185

Wolfenson, D., and Roth, Z. (2019). Impact of heat stress on cow reproduction and fertility. *Animal Front. Rev. Mag. Animal Agric.* 9 (1), 32–38. doi:10.1093/af/vfy027

Wolfenson, D., Roth, Z., and Meidan, R. (2000). Impaired reproduction in heat-stressed cattle: Basic and applied aspects. *Animal Reproduction Sci.* 60-61, 535–547. doi:10.1016/s0378-4320(00)00102-0

Wolfenson, D., Thatcher, W. W., Badinga, L., Savi0, J. D., Meidan, R., Lew, B. J., et al. (1995). Effect of heat stress on follicular development during the estrous cycle in lactating dairy cattle. *Biol. reproduction* 52 (5), 1106–1113. doi:10.1095/biolreprod52.5.1106

Gad *et al. Journal of Ovarian Research* (2023) 16:101
https://doi.org/10.1186/s13048-023-01181-7

Journal of Ovarian Research

RESEARCH

Open Access

Extracellular vesicle-microRNAs mediated response of bovine ovaries to seasonal environmental changes

Ahmed Gad[1,2], Kamryn Joyce[3], Nico Graham Menjivar[1], Daniella Heredia[3], Camila Santos Rojas[3], Dawit Tesfaye[1*] and Angela Gonella-Diaza[3]

Abstract

Background Among the various seasonal environmental changes, elevated ambient temperature during the summer season is a main cause of stress in dairy and beef cows, leading to impaired reproductive function and fertility. Follicular fluid extracellular vesicles (FF-EVs) play an important role in intrafollicular cellular communication by, in part, mediating the deleterious effects of heat stress (HS). Here we aimed to investigate the changes in FF-EV miRNA cargoes in beef cows in response to seasonal changes: summer (SUM) compared to the winter (WIN) season using high throughput sequencing of FF-EV-coupled miRNAs. In addition to their biological relevance, the potential mechanisms involved in the packaging and release of those miRNAs as a response to environmental HS were elucidated.

Results Sequencing analysis revealed that an average of 6.6% of the EV-RNA mapped reads were annotated to bovine miRNAs. Interestingly, miR-148a, miR-99a-5p, miR-10b, and miR-143 were the top four miRNAs in both groups accounting for approximately 52 and 62% of the total miRNA sequence reads in the SUM and WIN groups, respectively. A group of 16 miRNAs was up-regulated and 8 miRNAs were down-regulated in the SUM compared to the WIN group. Five DE-miRNAs (miR-10a, miR-10b, miR-26a, let-7f, and miR-1246) were among the top 20 expressed miRNA lists. Sequence motif analysis revealed the appearance of two specific motifs in 13 out of the 16 upregulated miRNAs under HS conditions. Both motifs were found to be potentially bonded by specific RNA binding proteins including Y-box binding proteins (YBX1 and YBX2) and RBM42.

Conclusion Our findings indicate that FF EV-coupled miRNA profile varies under seasonal changes. These miRNAs could be a good indicator of the cellular mechanism in mediating HS response and the potential interplay between miRNA motifs and RNA binding proteins can be one of the mechanisms governing the packaging and release of miRNAs via EVs to facilitate cellular survival.

Keywords Follicular fluid, Extracellular vesicles, miRNA, Heat stress, Beef cows

*Correspondence:
Dawit Tesfaye
dawit.tesfaye@colostate.edu
Full list of author information is available at the end of the article

This is a U.S. Government work and not under copyright protection in the US; foreign copyright protection may apply 2023. **Open Access** This article is licensed under a Creative Commons Attribution 4.0 International License, which permits use, sharing, adaptation, distribution and reproduction in any medium or format, as long as you give appropriate credit to the original author(s) and the source, provide a link to the Creative Commons licence, and indicate if changes were made. The images or other third party material in this article are included in the article's Creative Commons licence, unless indicated otherwise in a credit line to the material. If material is not included in the article's Creative Commons licence and your intended use is not permitted by statutory regulation or exceeds the permitted use, you will need to obtain permission directly from the copyright holder. To view a copy of this licence, visit http://creativecommons.org/licenses/by/4.0/. The Creative Commons Public Domain Dedication waiver (http://creativecommons.org/publicdomain/zero/1.0/) applies to the data made available in this article, unless otherwise stated in a credit line to the data.

Background

Global climate change directly impacts the livestock sector due to continued increases in atmospheric temperatures and as a result, animals are exposed to more adverse conditions of heat stress (HS). The global economic losses amid the dairy and beef industry due to HS are estimated to be between $14.89 – 39.94 billion per year by the end of the century [1]. This primarily stems from the significant impact of HS on animal productivity and the continued decline in fertility and reproductive performance [2]. The harmful effects of HS on ovarian functions and subsequent oocyte developmental competence are one of the main reasons driving reduced fertility [3]. The development of novel alternative strategies to mitigate the negative impacts of HS on reproductive function requires a more comprehensive understanding of heat-induced molecular alterations at the cellular level.

In bovine, follicular development is a lengthy process starting from the growth of primordial follicles to the preovulatory stage. Effects of maternal hyperthermia during specific stages of follicular growth and development may significantly affect follicular growth [4], in which the carryover effects of HS have the capacity to linger for months into the cool season resulting in long-term impacts on the reproductive performance of animals [5].

Seasonal effects on cows' reproduction include different factors (e.g., feeding, daylight hours, etc.), however, the most important factor is the consequence of increased temperature and humidity that result in inadequate regulation of the cow's body temperature, a reduction in appetite and dry matter intake, reduction in duration and intensity of estrus, as well as disruption in hormonal levels [6, 7]. Several seasonal studies have reported the sensitivity of the ovarian pool of oocytes to elevated temperatures expressed as reduced developmental competence [8, 9]. Seasonal HS is known to alter steroid production and the biochemical composition of the follicular fluid (FF). For instance, FF obtained from large follicles of cows during the hot season is evidenced by lowered steroid concentrations, reduced granulosa cell (GC) viability, and impaired aromatase activity [10]. Moreover, the biochemical changes in the FF of the dominant follicle from high-producing cows exposed to HS post-partum have been evidenced by reduced concentrations of glucose, IGF-1, and cholesterol [11]. At the cellular level, cells activate heat shock proteins (HSPs) and oxidative stress response machinery as a defensive mechanism in response to HS that could ultimately lead to cell apoptosis [12]. Activated HSPs, as well as RNA transcripts, could be released by stressed cells and uptaken by other recipient cells to modulate their immunological responses against stress [13–15]. In the intrafollicular microenvironment, such cellular communication is facilitated by the FF containing various paracrine factors important for cell–cell communication during follicular growth [16].

In the follicular microenvironment, one of the more recently discovered mechanisms that facilitate and modulate communicative measures between various cells and the oocyte is extracellular vesicles (EVs). EVs are nano-sized, membrane-bound, and evolutionarily conserved structures secreted from almost all cell types into the surrounding extracellular space and are preferentially found among almost all body fluids [17]. EVs are broadly categorized as exosomes, microvesicles, and apoptotic bodies according to their size and mode of biogenesis [18]. Their capacity to modulate intercellular crosstalk is largely through their ability to transfer various bioactive molecules, including mRNA, miRNAs, and proteins, between neighboring cells following secretion into body fluids [19]. We have recently shown that bovine GCs subjected to in vitro thermal stress release EVs harnessed with protective molecular signals that induce tolerance to recurrent thermal stress in naïve recipient cells [20]. In addition, those EVs were found to contain different miRNA profiles in response to HS. The emerging regulatory role of miRNAs in mediating the stress response in different species [21–24] sheds light on their use as potential biomarkers and/or tools to modulate the cellular stress response. Therefore, understanding the follicular responses, in terms of EV-coupled miRNAs, to HS in cows during the summer seasons will aid in determining the specific role of these miRNAs in mediating the HS response amid intrafollicular cellular communication. Here we aimed to investigate the follicular level response of beef cows to seasonal changes with regard to the FF-EV miRNA profiles. Moreover, miRNA motifs and the corresponding RNA binding proteins were identified and their potential involvement in the packaging and release of miRNAs into EVs as it relevantly correlates to cellular survival under HS conditions is elucidated.

Materials and methods

Animals and sample collection

The experiment was conducted at the UF/IFAS North Florida Research and Education Center (Marianna, Flora, USA). Eleven *Bos taurus* crossbreed open cows were included in the experiment after clinical and gynecological examinations. Transrectal ultrasound was conducted to evaluate ovaries and it was determined that all cows were cycling (bearing at least one CL or preovulatory follicle in one of the ovaries) and without any ovarian abnormalities (cysts, tumors, etc.) before each OPU session. The cows remain open, maintained in outdoor pens with bahia grass and fed bermudagrass hay to meet the

nutritional requirements of mature cows. Also, cows had ad libitum access to water and mineralized salt during the whole study (from winter until summer). Body weight and Body condition score (scored from 1 (thin) to 9 (fat)) were not different between winter and summer (Winter: 580.2 ± 20.5 kg and BCS of 5.0 ± 0.0; Summer: 571.1 ± 18.1 kg and BCS of 5.0 ± 0.0; P > 0.05). Ovum pick-up (OPU) sessions were conducted by a single operator in two different seasons: Winter (January 2021) and Summer (August 2021). Before each OPU session cows were stimulated to increase the number of follicles. Briefly, on a random day of the estrus cycle (Day 0) a progesterone device (Eazi-Breed CIDR Cattle Insert; Pfizer Animal Health, New York, NY, USA) was inserted in the vagina and a single dose of a GnRH analog (Factrel, 2 mL, im, Pfizer Animal Health) was administrated. Follicular growth stimulation was conducted by giving 3 injections of FSH (Folltropin V, im, Vetoquinol, Bertinoro, Italy). On day 3, 3 ml (equivalent to 105 IU) of FSH were administrated in the morning and afternoon. On day 4, 2 ml of FSH were administrated in the morning (equivalent to 70 IU). Finally, on day 5, the CIDR was removed and OPU was conducted in the morning. Ultrasound examinations (Esaote ultrasound, MyLabDelta Vet, with 10–5 MHz transducer) were conducted to evaluate the presence of a corpus luteum and the number of follicles at days 0 and 5.

OPU was performed using a real-time B-mode ultrasound scanner (Mindray 2200; Mindray Bio-Medical Electronics, Shenzhen, China) equipped with a 5-MHz micro-convex transducer (Mindray model 65C15EAV, Mindray Bio-Medical Electronics, Shenzhen, China) and coupled to a follicular aspiration guide (WTA, São Paulo, Brazil) and a stainless-steel guide. The follicular puncture was performed using a disposable 18 G hypodermic needle connected to a 50-mL conical tube via a suitable silicon tubing system (WTA). The pressure for aspiration was maintained using a vacuum pump (WTA model BV-003, WTA) with negative pressure adjusted between 60 and 80 mmHg. After the OPU of both ovaries, the aspiration system was replaced with a new one before conducting OPU for the next cow. The complete experimental design is presented in Fig. 1.

Summer vs. winter environmental conditions

As previously stated, OPU was conducted on the same animals in two different seasons. Environmental data (average minimum and maximum temperature and relative humidity) from the 3 weeks before each OPU session was collected using the Florida Automated Weather Network (FAWN; https://fawn.ifas.ufl.edu/data/reports/). For the winter OPU, data were collected from February 2 to 23 of 2021, and for the summer OPU, data were collected from July 23 to August 13 of 2021. Next, the temperature humidity index (THI) was calculated using the following equation: THI = (1.8 × T + 32)—[(0.55—0.0055 × RH) × (1.8 × T—26)], where T = air temperature (°C) and RH = relative humidity (%) [25]. As expected, average temperature (summer: 27.48 °C; winter: 11.46 °C), minimum temperature (summer: 23.14 °C; winter: 6.45 °C), maximum temperature (summer: 33.66 °C; winter: 16.14 °C), and relative humidity (summer: 82%; winter: 83%) were contrasting in the summer compared with the winter. Also, when estimating the THI, the average THI in the summer was 79 while in the winter was 53. In Bos taurus beef cattle, a THI equivalent to 75 is an indicator of heat stress [26, 27]. Three weeks before the summer OPU session THI was always over 75, ranging from 75.47 to 82.45.

Isolation of extracellular vesicles from follicular fluid

Four different FF samples (pool of two animals in each) from each group were used for EV isolation. Follicular fluid samples were subjected to a series of centrifugations starting at 500 xg for 10 min to remove cells, followed by 3000 xg for 10 min to remove the cellular debris, and at 12,000 xg for 30 min to remove protein aggregates and large particles. All centrifugation steps were performed at 4 °C. The supernatant of FF samples was filtered through a 0.22 μM sterile filter to remove particles larger than 200 nm. For the EV isolation, 2 ml of pre-centrifuged follicular samples were subjected to an ultracentrifugation procedure at 120,000 xg for 70 min at 4 ^{O}C using the Beckman SWTi55 rotor. The EVs pellet was washed with sterile PBS and then centrifuged again at 120,000 xg for 70 min. Finally, EVs were resuspended in 500 μL of PBS and stored at − 80 °C until further characterization and analysis.

Morphological and molecular characterization of EVs

The presence of EV-specific proteins (CD63, TSG101, FLOT1) in the isolated EVs and the absence of a cell-specific marker protein, cytochrome C (CYCS), were verified by the immunoblotting technique as we previously described [20]. Briefly, 100 μL of isolated EVs were lysed in 50 μL 1 × RIPA buffer and the protein extract samples were centrifuged at 12,000 × *g* for 30 min at 4 °C. Following this, protein lysates were separated in 10–12% gradient SDS-PAGE gel (Bio-Rad Laboratories, USA) at 90 V for 15 min and 125 V for 60 min and transferred onto a nitrocellulose membrane (Bio-Rad Laboratories, USA) for 1 h at 100 V. Membranes were blocked in 5% non-fat dry milk dissolved in TBST for 1 h on a shaker at room temperature. Following blocking, membranes were incubated with anti-CD63 rabbit polyclonal (1:250 System Biosciences, USA), Anti-TSG101 rabbit polyclonal (1:250

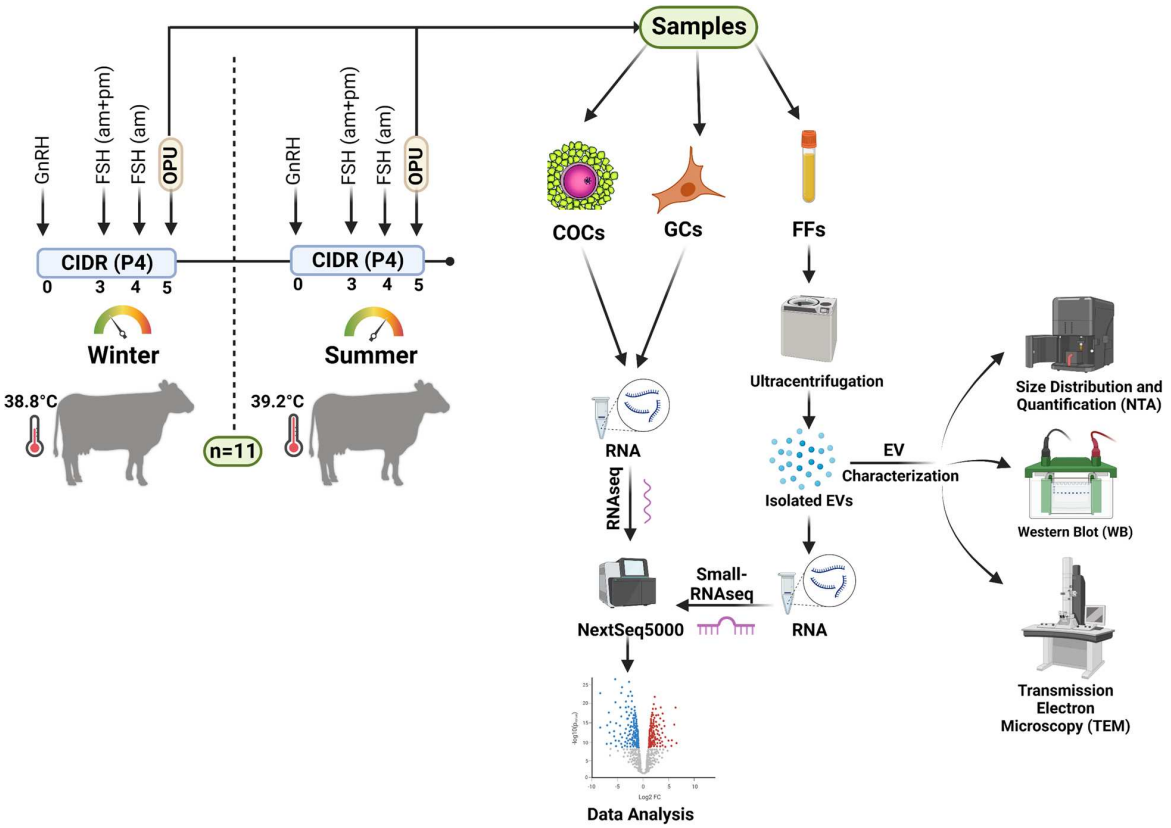


Fig. 1 Experimental Design. Dry beef cows ($n=11$) were subjected to synchronization and stimulation for follicular dynamics. Ovum pick-up (OPU) was conducted on all animals in the summer and winter seasons by ultrasound-guided transvaginal follicle aspiration. The follicular fluids (FFs) were collected from each target group (4 biological replicates/group; 8 mL FF/replicate). EVs were then isolated from the FFs using high-speed ultracentrifugation. Isolated EVs were characterized using NanoSight Tracking Analysis, western blot for EV and cellular marker proteins, and transmission electron microscopy. Total RNA was isolated from FF-EVs and small-RNA library preparation and RNAseq (NextSeq500; Illumina) were performed

System Biosciences, USA), Anti-FLOT1 rabbit polyclonal (1:250 System Biosciences, USA), and Anti-CYTc goat polyclonal (1:350 Santa Cruz Biotechnology, Germany) primary antibodies overnight at 4^0C. After washing the membranes with 1×TBST, membranes were incubated with appropriate secondary antibodies conjugated with horseradish peroxidase for 1 h at room temperature protected from light. After washing the membranes, protein bands were visualized using an enhanced chemiluminescence substrate (Bio-Rad Laboratories, USA) and images were acquired using Chemi Doc XRS+chemiluminescence imaging system (Bio-Rad Laboratories, USA).

The morphology of the purified EVs were analyzed using a transmission electron microscope (TEM) according to the methods previously reported [20]. Briefly, a drop of 30 µl purified EVs was placed on parafilm. The EVs drops were covered with Formvar/carbon-coated grids and allowed to stand for 5 min to absorb the EVs. The grids that contained the EVs were washed with drops of ddH_2O and fixed by placing them on a 30 µL drop of 2% uranyl acetate. The presence of the EVs on the carbon-coated grids was examined under an electron microscope. TEM imaging was done on a FEI/TFS Tecnai T12 Spirit TEM (FEI Company; Hillsboro, OR, USA), operating at 100 kV, with an AMT CCD.

The concentration and size distribution of isolated EVs were determined using the Zetaview Particle Metrix (Particle Metrix, Germany). Briefly, 10 µl of purified EVs was diluted in 990 µl of sterile PBS and assembled into the Zetaview Laser scattering microscope (Particle Metrix, Germany) fitted with an LM14C laser. For each sample, 11 independent video measurements were recorded at 11 independent positions, and video files were analyzed with ZetaView software version 8.05.12.

All experimental parameters related to EV isolation and characterization have been submitted to the EV-TRACK knowledgebase (https://evtrack.org) under the EV-TRACK ID EV220402.

Total RNA extraction, library preparation, and sequencing

Total RNA including miRNAs was isolated from EVs using a Norgen Exosomal RNA Isolation kit (Norgen, Canada), according to the manufacturer's instructions. On-column DNA digestion was performed to remove genomic DNA contaminants. The RNA concentration and size distribution were analyzed using an Agilent RNA 6000 Pico kit in an Agilent 2100 Bioanalyzer (Agilent Technologies, Santa Clara, CA, USA). Small-RNA libraries were prepared for next-generation sequencing (NGS) using a TruSeq Small RNA Library Prep Kit (Illumina) according to the manufacturer's instructions. Library quantity and quality assessments were performed using a Qubit DNA HS Assay Kit in a Qubit 2.0 Fluorometer (Thermo Fisher Scientific) and an Agilent DNA High Sensitivity kit in an Agilent 2100 Bioanalyzer (Agilent Technologies), respectively. The precise concentration of the libraries was calculated using a quantitative PCR. The libraries were pooled in equimolar ratios and then sequenced in a NovaSeq6000 sequencing instrument (Illumina, Inc., San Diego, CA, USA) as single-end reads (50 bases).

Sequencing data analysis

FASTQ files were generated for each sample using the software bcl2fastq (Illumina Inc., San Diego, CA), and their quality was checked using the FastQC tool version 0.11.9. Data were analyzed using the software CLC Genomics Workbench, version 21. Raw sequence reads were trimmed based on quality score (Q-score > 30), ambiguous nucleotides (maximum two nucleotides allowed), read length (≥ 15 nucleotides), and adapter sequences were also removed. Reads were mapped to the bovine reference genome (ARS-UCD1.2) and annotated against bovine precursor and mature miRNAs listed in the miRBase database (release 22) using the CLC Genomics Workbench RNA-Seq Analysis and Quantify miRNA tools, respectively, applying the default software parameters. Raw expression data were normalized using the trimmed mean of M-values normalization method (TMM normalization) [28] and presented as TMM-adjusted Counts Per Million (CPM). The CLC Genomics Workbench Differential Expression tool was used for the expression analysis comparison of the two groups. MiRNAs with fold change (FC) > 1.5, p-adjusted value (FDR < 0.1 [29]), and average CPM > 10 were considered differentially expressed (DE). The raw FASTQ files and processed CSV files have been deposited in the NCBI's Gene Expression Omnibus (GEO) with the accession number GSE221198.

qRT-PCR validation

To validate the miRNA sequencing data, five DE-miRNAs (three from SUM upregulated and two from downregulated), as representative candidates, were selected for expression validation using qRT-PCR. For this, three independent EV samples from three different animals were used for total RNA including miRNAs isolation as mentioned above, and selected miRNAs were quantified using specific TaqMan miRNA Assays (Applied Biosystems, Foster City, CA, USA) using a real-time PCR (Bio-Rad Inc.) according to the manufacturer's instructions. In brief, for each miRNA, a total of 5 ng RNA was reverse transcribed (RT) using a TaqMan microRNA Reverse Transcription Kit (Thermo Fisher Scientific, Waltham, MA) and miRNA-specific stem-loop primer (Applied Biosystems). RT reaction mixtures were incubated at 16 °C then 42 °C for 30 min each, followed by 85 °C for 5 min. The qRT-PCR was conducted in a 20 µl reaction mixture containing 2 µl cDNA sample, 1 µl FAM-labeled TaqMan assay, 10 µl TaqMan Universal PCR Master Mix (Applied Biosystems), and 7 µl nuclease-free water. Reaction conditions were as follows: initial denaturation at 95 °C for 10 min, followed by 40 cycles consisting of denaturation at 95 °C for 15 s, annealing, and extension at 60 °C for 60 s. Expression values were normalized to the geometric mean of miR-125 and miR-191 expression levels, the most stably expressed miRNA across all samples based on the NormFinder analysis. Statistical analysis of miRNA expression data was performed using Student's t-test and statistical significance was identified at $P \leq 0.05$.

Target gene prediction and ontological classification

Genes targeted by the DE-miRNA were identified using the human homologous miRNAs in the miRWalk database [30] to enhance the target prediction. Within the miRWalk, validated target genes from miRTarBase (version 7.0) and commonly target genes predicted by TargetScan (version 7.1) and miRDB (release 5.0) were selected for ontological classification analysis using the DAVID bioinformatics web tool (https://david.abcc.ncifcrf.gov/). Pathways and biological processes (BP) were determined from the KEGG pathway database [31], and GOTERM_BP_DIRECT annotation set, respectively. Terms with low gene count (< 5 genes) were filtered out from the pathways and BP lists. The interaction networks of the targeted genes and the identified pathways were constructed with Cytoscape [32].

Sequence motif analysis

Sequence-specific miRNA motifs (4–6 base) that are enriched in the up-regulated miRNAs compared to the down-regulated miRNAs (control sequences) were identified using Multiple Expectation Maximization for Motif Elicitation (MEME) suite v. 5.5.0 [33]. Motifs that commonly appeared in at least 50% of the submitted miRNAs were selected for further analysis. To determine the motif-associated RNA binding proteins (RBPs), the selected motifs were submitted to the TOMTOM motif comparison tool [34] using the RNA database.

Results

Identification and characterizations of isolated EVs

Follicular fluid-derived EVs from SUM and WIN groups were characterized morphologically and molecularly according to the recommendations set by the International Society of Extracellular Vesicles (ISEV) [35]. The western blot analysis showed that the FF-EVs from both groups are enriched with the transmembrane proteins FLOT1, CD63, and TSG101 protein. Moreover, the mitochondrial protein marker, Cytochrome C was absent in the EV samples, but present in bovine GCs (Fig. 2A), confirming the purity of the EVs and the absence of cellular contaminants in the EV preparation. TEM imaging showed the presence of EVs with visible bilipid membranes within the acceptable size ranges (Fig. 2B). The NTA analysis showed that the concentration of EV samples from both groups was within the range of 3.5×10^{11} to 1.75×10^{12} particles/mL with no significant differences between the groups. Similarly, the EVs median size was around 114 nm in both groups with no significant differences (Fig. 2C). The total RNA isolated from the EV samples were analyzed for their integrity and the electropherogram analysis showed a clear peak for the small RNA size ranges and the absence of rRNA subunit peaks (18 s and 28 s) which characterize the cellular RNA, indicating no cellular contamination in the isolated EV samples (Fig. 2E).

MiRNA expression profiles and differential expression analysis

A total of eight small-RNA libraries were constructed with approximately 20 million reads per library that passed the QC parameters with an average of 85% mapped to the bovine reference genome. Out of the mapped reads, an average of 6.6% were annotated to the bovine miRNAs from the miRBase database (Supplementary Table S1). Based on the miRNA expression profiles, principal component analysis (PCA) and heatmap exhibited a clear clustering of the replicates of each group (Fig. 3). A total of 243 and 248 miRNAs were considered as expressed (> 10 CPM) in the SUM and WIN groups, respectively, with 232 miRNAs being expressed in common and a total of 11 and 16 miRNAs were found to be exclusively detected in SUM and WIN groups,

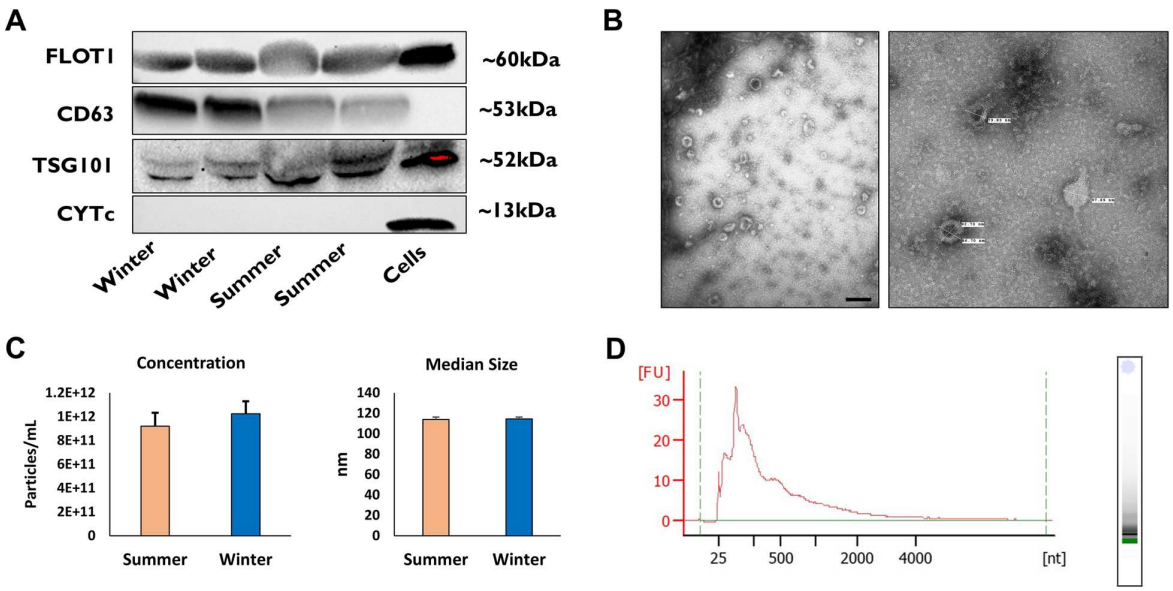


Fig. 2 Morphological and molecular characterization of EVs. Western blot analysis of EVs marker proteins FLOT1, CD63, and TSG101 and cellular protein contamination indicator CYTc **(A)**. Transmission electron microscope (TEM) imaging shows a clear morphology of EVs with a cross-sectional size of the diameter, scale bar = 200 nm **(B)**. The concentration and median size of the isolated EVs using the NTA analysis **(C)**. The RNA size distribution of EVs shows the presence of the peak of small RNA and the absence of the 18 s and 28 s ribosomal RNA peaks **(D)**

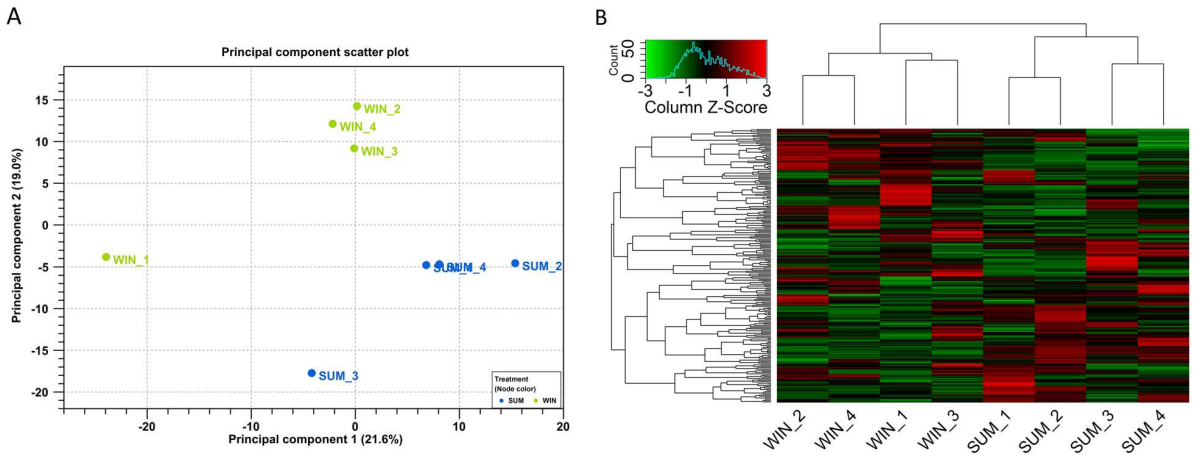


Fig. 3 Small-RNA sequence data overview. Principal Component Analysis (**A**). Heatmap and hierarchical clustering of expressed miRNAs. Red and green colors represent high and low expressed miRNAs, respectively **(B)**. SUM: summer group; WIN: winter group

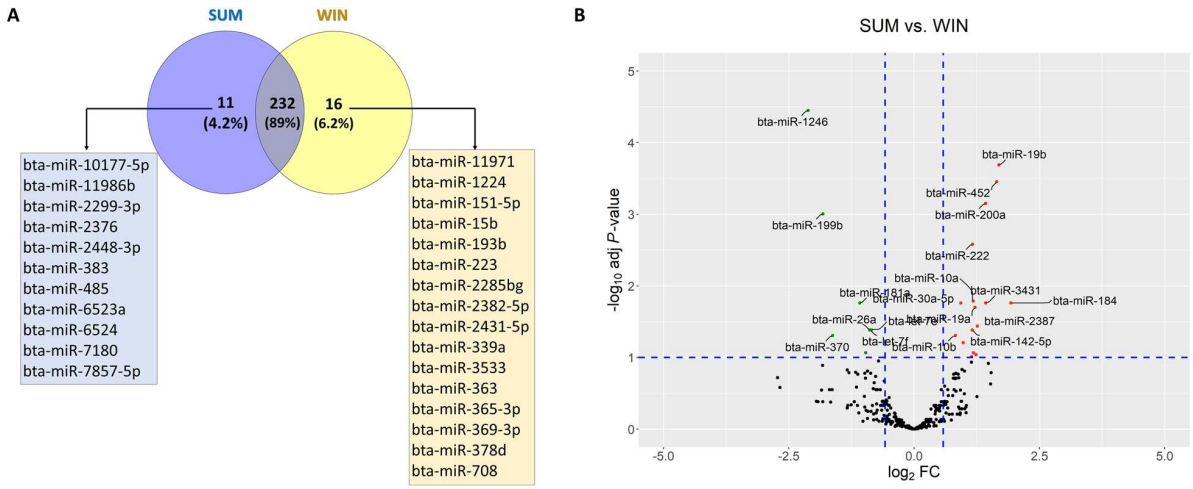


Fig. 4 Differentially expressed miRNAs. Venn diagram for commonly and exclusively expressed miRNAs in the FF-EVs of summer (SUM) and winter (WIN) groups **(A)**. Volcano plot of expressed miRNAs. Up- and downregulated miRNAs in the SUM compared to the WIN FF-EV groups are labeled with red and green points, respectively **(B)**

respectively (Fig. 4A). The top 20 highly expressed miRNAs are presented in Table 1 and the complete list of all expressed miRNAs is presented in Supplementary Table S2. Among the top 20 expressed miRNAs, 18 miRNAs were commonly detected in both groups. Interestingly, miR-148a, miR-99a-5p, miR-10b, and miR-143 were the top four miRNAs in both groups and accounting for approximately 52 and 62% of the total miRNA sequence reads in the SUM and WIN groups, respectively (Table 1).

Differential expression analysis indicated a total of 24 miRNAs as significantly differentially expressed between the two groups (FC > 1.5, FDR < 0.1, CPM > 10). A group of 16 miRNAs was up-regulated and 8 miRNAs were down-regulated in the SUM compared to the WIN group (Table 2 and Fig. 4B). MiR-184, miR-19b, and miR-452 were up-regulated and miR-1246, miR-199b, and miR-370 were downregulated with more than three folds in the SUM compared to the WIN group. Interestingly, five

Table 1 List of top 20 most abundant miRNAs in the extracellular vesicles obtained from follicular fluids from SUM and WIN groups

Name	SUM	Name	WIN
bta-miR-148a	335,249	bta-miR-148a	265,292.7
bta-miR-99a-5p	146,729.6	bta-miR-99a-5p	100,948.9
bta-miR-10b	131,675.5	bta-miR-10b	74,287.82
bta-miR-143	48,985.58	bta-miR-143	46,764.92
bta-let-7b	29,996.77	bta-miR-26a	43,106.6
bta-miR-10a	28,665.65	bta-let-7a-5p	35,540.64
bta-miR-26a	23,293.75	bta-miR-1246	35,452.23
bta-let-7a-5p	21,727.87	bta-let-7b	28,978.75
bta-miR-320a	20,767.93	bta-let-7i	23,237.47
bta-miR-21-5p	15,787.62	bta-miR-320a	22,398.35
bta-let-7i	15,370.83	bta-let-7f	21,824.77
bta-miR-151-3p	13,991.34	bta-let-7c	15,041.31
bta-miR-27b	12,268.99	bta-miR-21-5p	14,597.74
bta-miR-128	11,920.15	bta-miR-10a	12,673.24
bta-let-7f	11,891.01	bta-miR-423-5p	10,828.92
bta-miR-25	11,251.66	bta-miR-151-3p	10,629.91
bta-miR-378	10,807.93	bta-miR-146b	10,133.07
bta-let-7c	10,641.53	bta-miR-128	9588.558
bta-miR-423-5p	10,115.64	bta-let-7 g	9309.91
bta-miR-146b	9761.571	bta-miR-27b	9140.885

The expression values indicated as the mean of TMM-adjusted Counts Per Million (CPM)

Table 2 Differentially expressed (DE) miRNAs in extracellular vesicles obtained from follicular fluids of SUM compared to WIN group

Name	Sequence	FC	FDR
bta-miR-184	TGGACGGAGAACTGATAAGGGT	3.81	0.017351
bta-miR-19b	TGTGCAAATCCATGCAAAACTGA	3.23	0.000205
bta-miR-452	TGTTTGCAGAGGAAACTGAGAC	3.14	0.000351
bta-miR-200a	TAACACTGTCTGGTAACGATGTT	2.69	0.000704
bta-miR-3431	CCTCAGTCAGCCTTGTGGATGT	2.69	0.017329
bta-miR-2387	TGGAAGGCCTGGCTTTGCAGCG	2.40	0.036309
bta-miR-2408	CACGTGTGTGAGCTCAGCCGG	2.35	0.091029
bta-miR-19a	TGTGCAAATCTATGCAAAACTGA	2.32	0.019879
bta-miR-95	TTCAACGGGTATTTATTGAGCA	2.27	0.085596
bta-miR-10a	TACCCTGTAGATCCGAATTTGTG	2.26	0.0162
bta-miR-222	AGCTACATCTGGCTACTGGGT	2.25	0.00262
bta-miR-142-5p	CATAAAGTAGAAAGCACTAC	2.23	0.041243
bta-miR-24-3p	TGGCTCAGTTCAGCAGGAACAG	2.21	0.097153
bta-miR-2483-3p	AAACATCTGGTTGGTTGAGAGA	1.97	0.062057
bta-miR-30a-5p	TGTAAACATCCTCGACTGGAAGCT	1.91	0.017351
bta-miR-10b	TACCCTGTAGAACCGAATTTGTG	1.77	0.049396
bta-let-7e	TGAGGTAGGAGGTTGTATAGT	-1.81	0.041243
bta-let-7f	TGAGGTAGTAGATTGTATAGTT	-1.83	0.041243
bta-miR-26a	TTCAAGTAATCCAGGATAGGCT	-1.85	0.041243
bta-miR-126-3p	CGTACCGTGAGTAATAATGCG	-1.95	0.085596
bta-miR-181a	AACATTCAACGCTGTCGGTGAGTT	-2.12	0.017351
bta-miR-370	GCCTGCTGGGGTGGAACCTGGT	-3.09	0.049396
bta-miR-199b	CCCAGTGTTTAGACTATCTGTTC	-3.53	0.000985
bta-miR-1246	AATGGATTTTTGGAGCAGG	-4.33	3.54E-05

FC Fold Change, *FDR* False Discovery Rate

DE-miRNAs (miR-10a, miR-10b, miR-26a, let-7f, and miR-1246) were also among the top 20 expressed miRNA lists.

qRT-PCR validation

To validate the sequencing data, a group of 5 DE-miRNAs was selected and quantified using qRT-PCR. All miRNAs exhibited the same expression pattern as in the miRNAseq data ($P < 0.05$) except for miR-222, which showed the same pattern but with no statistical significance between the two groups (Fig. 5).

Target gene prediction and gene ontology

Target gene analysis revealed a total of 871 and 909 genes as potential targets of up and downregulated miRNAs, in SUM group respectively, with 140 genes commonly targeted by both groups of miRNAs. Ontological classification of these genes showed that EGFR tyrosine kinase inhibitor resistance, ErbB signaling, p53 signaling, and endocrine resistance were the top significant pathways targeted by the upregulated miRNAs in the SUM compared to the WIN group. On the other hand, cellular senescence, JAK-STAT signaling, FoxO signaling, and hippo signaling were the top significant pathways targeted by the downregulated miRNAs (Fig. 6, Supplementary Table S3). Regulation of transcription and gene expression were the top significant biological processes targeted by the elevated miRNAs in the SUM compared to the WIN group while regulation of cell proliferation and cell cycle were the top significant biological processes targeted by the downregulated miRNAs (Fig. 6, Supplementary Table S4). The interaction networks of the top 5 pathways and their corresponding genes targeted by the DE miRNAs are presented in Fig. 7.

miRNA sequence motif analysis

To identify potential sequence motifs and the corresponding RNA binding proteins associated with the regulation of the packaging and release of the candidate miRNAs into EVs in response to thermal stress, we performed motif sequence analysis of the miRNAs that were enriched in SUM FF-EVs compared to the miRNAs that were enriched in WIN FF-EVs group. We identified four different motifs (4–5 bases). Two of them significantly appeared on more than 80% (13 out of 16) of the

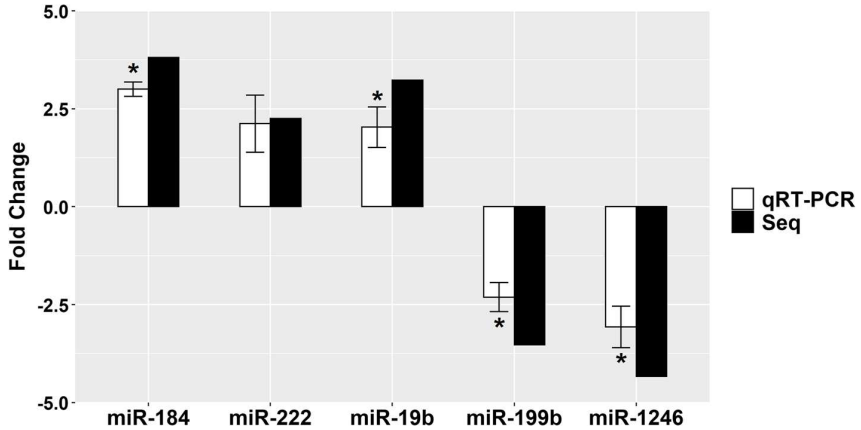


Fig. 5 qRT-PCR analysis. Expression validation of the selected DE-miRNAs in comparison to the RNAseq (Seq) analysis. *Statistical significance between the summer and winter FF-EV groups ($P < 0.05$)

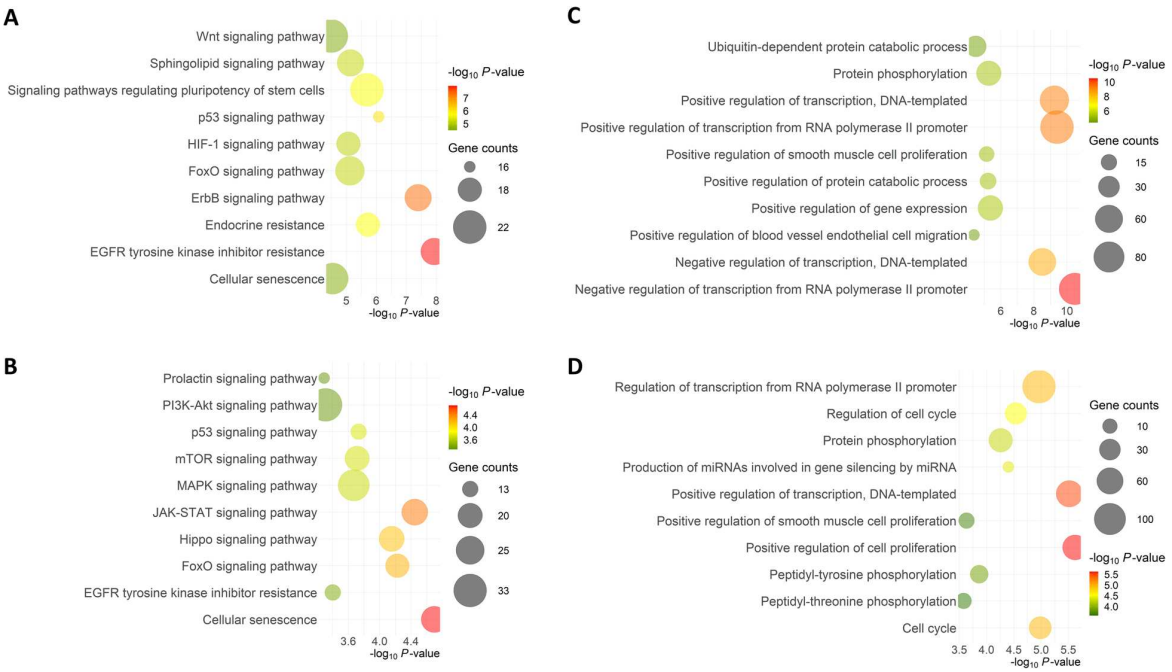


Fig. 6 Ontological Classification. Top 10 pathways and biological processes targeted by the up- **(A** and **C**, respectively**)** and down-regulated miRNAs (**B** and **D**, respectively**)** in the summer compared to the winter FF-EV groups

up-regulated miRNAs (Fig. 8A and B; Table 3). RBP-specific motif matching showed that the first motif (AACU) is potentially targeted by RBM42, YBX2, and YBX1 proteins (Fig. 8C) while the second motif (CUGG) is potentially targeted by SAMD4A, MBNL1, MATR3, and HuR proteins (Fig. 8D).

Discussion

Extracellular vesicles are known to shuttle ample bioactive molecules (mRNA, miRNA, proteins, and lipids) reflecting the physiological status of the secreting cells, [36, 37] leading to alterations in gene expression and function in recipient cells [38]. Our previous studies

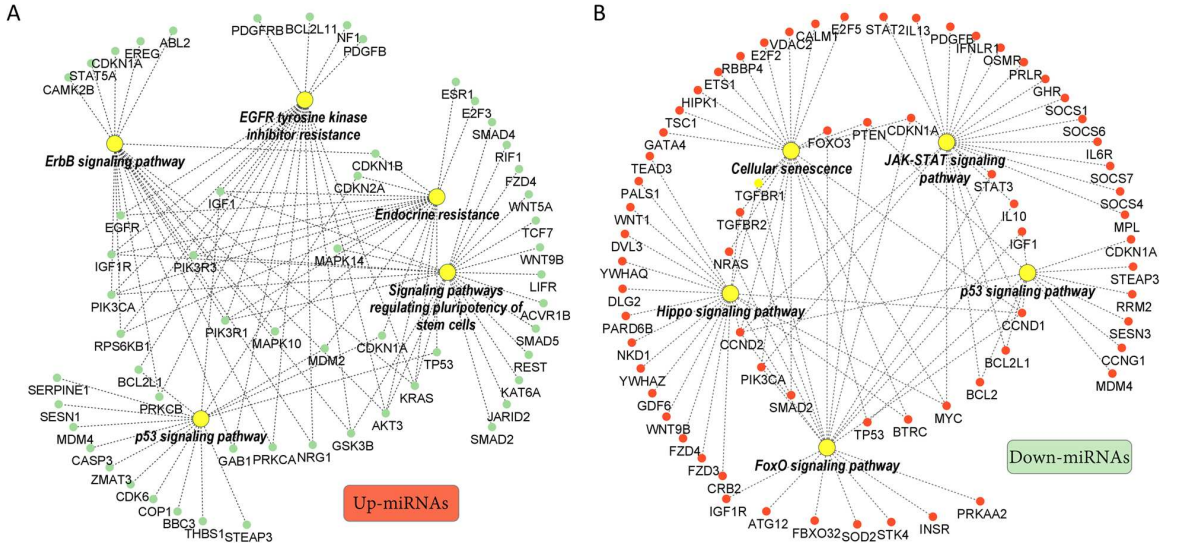


Fig. 7 Interaction networking. The top 5 pathways and their corresponding genes targeted by up **(A)** or downregulated **(B)** miRNAs in the summer compared to the winter group

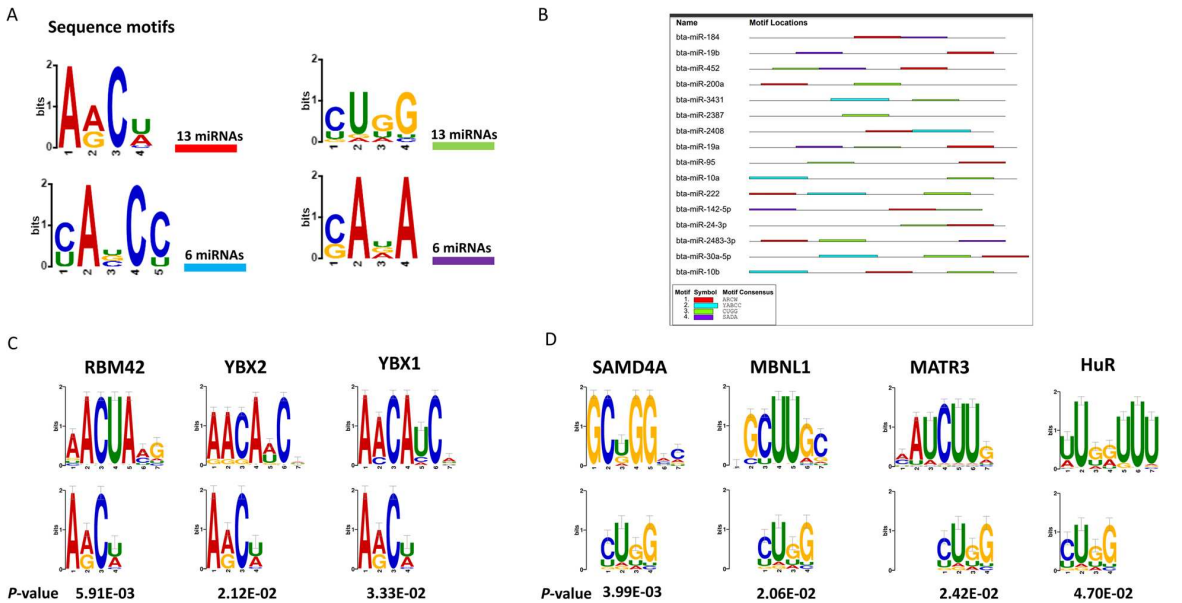


Fig. 8 miRNA sequence motif analysis. Four identified motifs in different numbers of the up-regulated miRNAs in the summer compared to the winter group **(A)**. The locations and distribution of the identified motifs on the up-regulated miRNAs **(B)**. The alignments of the AACU **(C)** and CUGG **(D)** motifs with the known RNA binding protein motifs ($P < 0.05$)

indicated that the bovine FF-EVs-miRNA profiles are associated with oocyte developmental competence [39] and the post-calving metabolic status of dairy cows [40]. We have also reported that, under in vitro conditions, bovine granulosa cells subjected to thermal stress release EVs with different miRNA cargo have the potential to shuttle protective messages to recipient cells inducing thermotolerance against subsequent HS [20]. Therefore, unveiling the ovarian FF-EV cargoes in response to environmental thermal stress conditions in vivo will aid to elucidate the EV-mediated molecular response and potential impact on follicular development and oocyte

Table 3 The identified motif positions on the up-regulated miRNAs in the SUM compared to the WIN group

miRNA	*P*-Value		miRNA	*P*-Value	
bta-miR-19a	3.89E-03	UGUGCAAAUCUAUGCAAAACUGA	bta-miR-30a-5p	3.66E-03	UGUAAACAUCCUCGACUGGAAGCU
bta-miR-452	3.89E-03	UGUUUGCAGAGGAAACUGAGAC	bta-miR-2483-3p	3.66E-03	AAACAUCUGGUUGGUUGAGAGA
bta-miR-19b	3.89E-03	UGUGCAAAUCCAUGCAAAACUGA	bta-miR-222	3.66E-03	AGCUACAUCUGGCUACUGGGU
bta-miR-184	3.89E-03	UGGACGGAGAACUGAUAAGGGU	bta-miR-2387	3.66E-03	UGGAAGGCCUGGCUUUGCAGCG
bta-miR-30a-5p	1.18E-02	UGUAAACAUCCUCGACUGGAAGCU	bta-miR-200a	3.66E-03	UAACACUGUCUGGUAACGAUGUU
bta-miR-2483-3p	1.18E-02	AAACAUCUGGUUGGUUGAGAGA	bta-miR-10b	2.31E-02	UACCCUGUAGAACCGAAUUUGUG
bta-miR-24-3p	1.18E-02	UGGCUCAGUUCAGCAGGAACAG	bta-miR-10a	2.31E-02	UACCCUGUAGAUCCGAAUUUGUG
bta-miR-222	1.18E-02	AGCUACAUCUGGCUACUGGGU	bta-miR-452	2.31E-02	UGUUUGCAGAGGAAACUGAGAC
bta-miR-2408	1.18E-02	CACGUGUGUGAGCUCAGCCGG	bta-miR-24-3p	3.44E-02	UGGCUCAGUUCAGCAGGAACAG
bta-miR-200a	1.18E-02	UAACACUGUCUGGUAACGAUGUU	bta-miR-95	3.44E-02	UUCAACGGGUAUUUAUUGAGCA
bta-miR-142-5p	1.58E-02	CAUAAAGUAGAAAGCACUAC	bta-miR-3431	3.94E-02	CCUCAGUCAGCCUUGUGGAUGU
bta-miR-95	1.58E-02	UUCAACGGGUAUUUAUUGAGCA	bta-miR-142-5p	6.89E-02	CAUAAAGUAGAAAGCACUAC
bta-miR-10b	1.88E-02	UACCCUGUAGAACCGAAUUUGUG	bta-miR-19a	8.74E-02	UGUGCAAAUCUAUGCAAAACUGA

growth. Here we aimed to investigate the changes in FF-EV-coupled miRNAs in beef cows when comparing winter and summer seasons. The deviation in EV-miRNA profiles in summer compared to the winter season may in part explain the abnormal ovarian function, follicular development, and infertility-associated problems due to climate change-induced thermal stress in dairy and beef animals [41, 42].

Among the top 20 highly abundant miRNAs, 18 were commonly expressed in both groups including miR-148a and miR-99a, the top highly expressed miRNAs in the FF-EVs with no significant differences between the groups. Similarly, miR-148 was reported as the top expressed miRNA in FF-EVs from large and small follicles in goats [43]. In human FFs, miR-99a was specifically enriched in the FF-EVs and considered as a regulator of the ovarian follicle developmental process to include meiosis resumption [44]. In another study, the expression of miR-148a and miR-99a in FF-EVs was highly correlated with IVF outcomes, specifically day-3 embryo quality [45]. The detection of these candidate miRNAs at a higher level in both seasons indicates their potential housekeeping role in ovarian function. In the same top 20 miRNAs list, miR-10a and miR-10b were expressed amid both groups and were significantly upregulated in the SUM compared to the WIN group. Both miRNAs belong to the conserved mir-10 family and are known to play key roles in inducing apoptosis and repressing cell proliferation in ovarian GCs through suppressing the brain-derived neurotrophic factor (BDNF) and TGF-β pathways [46]. Additionally, miR-10a has been reported to promote human GC tumor development by targeting PTEN-AKT/Wnt pathways [47] and regulating lipid metabolism and steroid hormone synthesis in sheep GCs [48]. Previously, it has been validated that miR-10a directly recognizes and targets the *BCL6* transcript and negatively regulates its expression leading to cellular apoptosis [49]. In correlation with HS, miR-10a was suggested to be involved in the stress response pathway regulation via its repression of a number of p53/Rb networks' key genes [50]. Therefore, our results indicate the negative impact of seasonal HS on ovarian function is mediated by the enrichment of miR-10a and miR-10b in EVs released in response to thermal stress. Another interesting miRNA from the same top 20 miRNAs list was miR-26a which exhibited a significant downregulation in the SUM compared to the WIN group. A similar study in heat-stressed Holstein cows showed that the expression of miR-26a was downregulated in serum and found to be involved in stress and immune response-related processes [51]. Moreover, a HS-induced increase in corticosterone hormone is similarly found to be associated with the reduction in miR-26a in rat serum EVs [52]. In addition, it has been confirmed that miR-26a targets Exh2 and plays a critical role in regulating apoptosis in mouse ovarian GCs [53].

In the current study, we found a total of 24 DE-miRNAs in the FF-EVs between the SUM and WIN groups. Among the upregulated miRNAs, four (miR-19a, miR-19b, miR-30a-5p, and miR-200a) were commonly identified as highly expressed in the serum of heat-stressed Holstein cows [51]. In another study, miR-19a and miR-19b were identified among the circulatory miRNAs that were highly expressed in lactating Holstein cows under summer HS conditions and were correlated with functions governing responses to stress and oxidative damage [54]. Moreover, heat shock during in vitro maturation of bovine oocytes was shown to increase the expression of miR-19b in embryos, indicating a carryover impact of HS on miRNAs in the cellular response [55]. In humans, miR-19b has been reported as an inhibitor of GC proliferation by directly targeting *IGF-1* and the reduction in its expression could reverse the results [56] suggesting the important regulatory and specific role of miR-19b in GCs and could explain the oocyte quality and fertility

reduction during the summer season. The top-upregulated miRNA in the SUM group was miR-184. This miRNA is associated with an inhibitory effect on GC estradiol production [57] and was found to be increased in bovine GCs at day 7 compared to day 3 of the estrous cycle [58].

On the other hand, a cluster of eight miRNAs was downregulated in the SUM FF-EVs compared to the WIN group including miR-181a and miR-1246. Both miRNAs showed a clear reduction in buffalo GCs cultured under thermal stress conditions [59] and are known to be involved in stress and immune responses [51, 60]. Inhibition of miR-181a expression suppresses apoptosis and ROS production in human chondrocyte cells [61] and reduces heat stress damage through the upregulation of antioxidant-related genes and the downregulation of apoptotic genes in bovine peripheral blood mononuclear cells [62]. Contrary to our findings, miR-1246 was found to be highly enriched in the serum of dairy cows under environmental HS [51, 54], as well as, in the GC-released EVs under in vitro elevated culture temperature [20]. However, the expression of miR-1246 in correlation with HS seems to be time-dependent, as in cattle and buffalo fibroblast cells, the expression of miR-1246 declined immediately after HS and then increased gradually during the recovery period post-HS [60]. This discrepancy in the differential expression results of EV-miRNA-1246 might be associated with the timing of exposure and recovery to thermal stress. Taken together, our data revealed that seasonal HS can induce the enrichment of FF-EV-coupled miRNAs, with a potential negative impact on ovarian function (i.e. miR-10 family) and the depletion of candidate miRNAs (i.e. miR-26a) with the potential beneficial role in ovarian physiology.

Although EV miRNA abundance is altered under suboptimal physiological conditions to include HS, little is known about the mechanism associated with their sorting into EVs versus their cellular retention. Recently, the regulatory role of RBPs in the packaging of particular RNA molecules into EVs following the recognition and binding of specific sequence motifs is emerging among different models [63, 64]. Sequence motif analysis for EV-coupled miRNAs enriched in SUM samples revealed two specific motifs appearing on 13 out of the 16 upregulated miRNAs and recognized by specific RBPs. One of those motifs was found to be potentially recognized and bound by Y-box binding proteins (YBX1 and YBX2). These proteins are members of a large family of proteins with the cold shock domain that play roles in several cellular processes including proliferation and stress response [65, 66]. A study by Guarino et al. reported that oxidative stress enhances the secretion of YBX1 protein from stressed cells which significantly inhibits proliferation and leads to cell cycle arrest in receiving cells [67]. Y-box proteins have been identified as the main components in the formation of ribonucleoprotein particles with the different types of RNA including mRNA and miRNA [68] and play a role in sorting these RNA molecules into EVs [69]. Regarding miRNAs, it has been evidenced that YBX1 binds to and is required for the sorting of specific miRNAs into EVs released from the HEK293T human cell line [70]. Another interesting RBP that matched with the same sequence motif was RBM42, which together with the hnRNP K is part of the stress granules. Under stress conditions, both proteins co-localize and interact to form cytoplasmic foci in order to maintain cellular ATP levels [71]. The expression of these proteins in correlation to stress conditions, as well as, their matching of common sequence motifs among the upregulated miRNAs in the SUM group could explain a potential mechanism involved in sorting and releasing of these FF-EV-miRNAs under HS conditions. However, further studies are required to specifically investigate the role of miRNA motifs and RBPs in regulating the sorting and packaging of stress associated miRNAs into EVs and the role that this interplay drives on follicular cells stress response and survival under various environmental and physiological suboptimal conditions.

Conclusions

Overall, the current study revealed that FF-EV-miRNA profiles can be explored to investigate the follicular level response of cows to seasonal changes and this might partially explain altered ovarian physiology, follicular development, and infertility-associated issues resulting from climate change-induced seasonal thermal stress in the dairy and beef industry. Based on the differentially expressed miRNAs, we suggest that the negative impact of HS on ovarian function is mediated by abnormal alterations in EV-coupled molecular signaling within the follicular microenvironment, as shown by the contrasting finding when comparing summer and winter EV-miRNAs. However, further studies are needed to confirm and investigate the exact role of these EV-miRNAs concerning seasonal effects and fertility. The current study also identified potential targets of future therapeutic and managerial intervention to tackle the negative impact of environmental thermal stress in cattle with potential translation to seasonal human infertility problems.

Supplementary Information

The online version contains supplementary material available at https://doi.org/10.1186/s13048-023-01181-7.

Additional file 1: Table S1. Summary of sequence reads mapped to the bovine reference genome and annotated against bovine miRNAs listed in the mirBase database. **Table S2.** A complete list of all expressed miRNAs indicated as the mean of TMM-adjusted Counts Per Million (CPM) value. **Table S3.** KEGG pathway analysis for genes targted by the differentially expressed miRNAs in SUM vs. WIN group. **Table S4.** Biological process (BP) analysis for genes targted by the differentially expressed miRNAs in SUM vs. WIN group.

Acknowledgements
The authors acknowledge the University of Colorado, Boulder EM Services Core Facility in the MCDB Department as well as D.N. Rao Veeramachaneni and Jennifer S. Palmer at Colorado State University, for their assistance with TEM imaging. Nano-particle tracking analysis was performed by Ms. Mindy A. Meyers from the Department of Clinical Sciences at Colorado State University. The authors thank Jhon Fredy Rodriguez and Edna Ballesteros from Breeding Tech LLC (Madisonville – Texas) for their technical assistance during the OPU procedures.

Authors' contributions
Conceptualization: D.T., A.G.D., Experimental work: A.G., K.J., N.G.M., D.H., C.S.R., Data analysis: A.G, N.G.M., Interpretation of data: A.G, D.T., A.G.D., Writing of original draft: A.G, Manuscript editing: D.T., A.G.D., N.G.M., Supervision: D.T., A.G.D., Funding acquisition: D.T., A.G.D., All authors have read and agreed to the published version of this manuscript.

Availability of data and materials
The raw FASTQ files and processed CSV files of the miRNA sequencing data have been deposited in the NCBI's Gene Expression Omnibus (GEO) repository with the accession number GSE221198. All parameters related to EV experiments are available on the EV-TRACK knowledgebase (EV-TRACK ID: EV220402).

Declarations

Ethics approval and consent to participate
All procedures involving cows were approved by the Animal Care and Use Committee of the University of Florida with the approval number IACUC202200000706.

Competing interests
There is no conflict of interest to declare.

Author details
[1]Department of Biomedical Sciences, Animal Reproduction and Biotechnology Laboratory (ARBL), Department of Biomedical Sciences, Colorado State University, Fort Collins, CO, USA. [2]Department of Animal Production, Faculty of Agriculture, Cairo University, Giza 12613, Egypt. [3]North Florida Research and Education Center, Institute of Food and Agricultural Sciences, University of Florida, Marianna, FL, USA.

Received: 19 January 2023 Accepted: 5 May 2023
Published online: 23 May 2023

References

1. Thornton P, Nelson G, Mayberry D, Herrero M. Impacts of heat stress on global cattle production during the 21st century: a modelling study. Lancet Planet Heal. 2022;6:e192–201. Available from: http://www.thelancet.com/article/S254251962200002X/fulltext. [cited 2022 Dec 15].
2. Rojas-Downing MM, Nejadhashemi AP, Harrigan T, Woznicki SA. Climate change and livestock: Impacts, adaptation, and mitigation. Clim Risk Manag. 2017;16:145–63. Available from: https://linkinghub.elsevier.com/retrieve/pii/S221209631730027X. [cited 2022 Dec 15].
3. Khan A, Dou J, Wang Y, Jiang X, Khan MZ, Luo H, et al. Evaluation of heat stress effects on cellular and transcriptional adaptation of bovine granulosa cells. J Anim Sci Biotechnol. 2020;11:25. Available from: https://jasbsci.biomedcentral.com/articles/10.1186/s40104-019-0408-8.
4. Roth Z. Effect of Heat Stress on Reproduction in Dairy Cows: Insights into the Cellular and Molecular Responses of the Oocyte. Annu Rev Anim Biosci. 2017;5:151–70. Available from: https://pubmed.ncbi.nlm.nih.gov/27732786/. [cited 2022 Nov 11].
5. Friedman E, Voet H, Reznikov D, Wolfenson D, Roth Z. Hormonal treatment before and after artificial insemination differentially improves fertility in subpopulations of dairy cows during the summer and autumn. J Dairy Sci. 2014;97:7465–75. Available from: https://pubmed.ncbi.nlm.nih.gov/25306276/. [cited 2022 Nov 14].
6. Rensis F De, Scaramuzzi RJ. Heat stress and seasonal effects on reproduction in the dairy cow—a review. Theriogenology. 2003;60:1139–51. Available from: https://linkinghub.elsevier.com/retrieve/pii/S0093691X03001262. [cited 2023 Mar 3].
7. Herbut P, Angrecka S, Walczak J. Environmental parameters to assessing of heat stress in dairy cattle-a review. Int J Biometeorol. 2018;62:2089–97. Available from: https://link.springer.com/article/10.1007/s00484-018-1629-9. [cited 2023 Mar 3].
8. Rocha A, Randel RD, Broussard JR, Lim JM, Blair RM, Roussel JD, et al. High environmental temperature and humidity decrease oocyte quality in Bos taurus but not in Bos indicus cows. Theriogenology. 1998;49:657–65. Available from: https://pubmed.ncbi.nlm.nih.gov/10732044/. [cited 2022 Nov 14].
9. Al-Katanani YM, Paula-Lopes FF, Hansen PJ. Effect of Season and Exposure to Heat Stress on Oocyte Competence in Holstein Cows. J Dairy Sci. 2002;85:390–6. Available from: https://pubmed.ncbi.nlm.nih.gov/11913699/. [cited 2022 Nov 14].
10. Roth Z. Heat stress, the follicle, and its enclosed oocyte: mechanisms and potential strategies to improve fertility in dairy cows. Reprod Domest Anim. 2008;43 Suppl 2:238–44. Available from: http://doi.wiley.com/10.1111/j.1439-0531.2008.01168.x. [cited 2018 Jan 10].
11. Shehab-El-Deen MAMM, Fadel MS, van Soom A, Saleh SY, Maes D, Leroy JLMR. Circadian rhythm of metabolic changes associated with summer heat stress in high-producing dairy cattle. Trop Anim Health Prod. 2010;42:1119–25. Available from: https://pubmed.ncbi.nlm.nih.gov/20221690/. [cited 2022 Nov 14].
12. Shan Q, Ma F, Wei J, Li H, Ma H, Sun P. Physiological Functions of Heat Shock Proteins. Curr Protein Pept Sci. 2020;21:751–60. Available from: https://pubmed.ncbi.nlm.nih.gov/31713482/. [cited 2022 Dec 12].
13. Saeed-Zidane M, Linden L, Salilew-Wondim D, Held E, Neuhoff C, Tholen E, et al. Cellular and exosome mediated molecular defense mechanism in bovine granulosa cells exposed to oxidative stress. PLoS One. 2017;12:e0187569. https://journals.plos.org/plosone/article?id=10.1371/journal.pone.0187569. [cited 2022 Dec 12].
14. Tsutsumi S, Neckers L. Extracellular heat shock protein 90: A role for a molecular chaperone in cell motility and cancer metastasis. Cancer Sci. 2007;98:1536–9. Available from: https://onlinelibrary.wiley.com/doi/full/10.1111/j.1349-7006.2007.00561.x. [cited 2022 Dec 12].
15. Hightower LE, Guidon PT. Selective release from cultured mammalian cells of heat-shock (stress) proteins that resemble glia-axon transfer proteins. J Cell Physiol. 1989;138:257–66. Available from: https://onlinelibrary.wiley.com/doi/full/10.1002/jcp.1041380206. [cited 2022 Dec 12].
16. Gilchrist R., Ritter L., Armstrong D. Oocyte–somatic cell interactions during follicle development in mammals. Anim Reprod Sci. 2004;82–83:431–46. Available from: https://pubmed.ncbi.nlm.nih.gov/15271471/. [cited 2022 Nov 17].
17. György B, Szabó TG, Pásztói M, Pál Z, Misják P, Aradi B, et al. Membrane vesicles, current state-of-the-art: emerging role of extracellular vesicles. Cell Mol Life Sci. 2011;68:2667–88. Available from: https://link.springer.com/article/10.1007/s00018-011-0689-3. [cited 2022 Nov 17].
18. Taylor DD, Gercel-Taylor C. The origin, function, and diagnostic potential of RNA within extracellular vesicles present in human biological fluids. Front Genet. 2013;4. Available from: https://pubmed.ncbi.nlm.nih.gov/23908664/. [cited 2022 Dec 9].

19. Yáñez-Mó M, Siljander PR-M, Andreu Z, Zavec AB, Borràs FE, Buzas EI, et al. Biological properties of extracellular vesicles and their physiological functions. J Extracell Vesicles. 2015;4:27066. Available from: http://www.ncbi.nlm.nih.gov/pubmed/25979354. [cited 2020 Apr 6].
20. Gebremedhn S, Gad A, Aglan HS, Laurincik J, Prochazka R, Salilew-Wondim D, et al. Extracellular vesicles shuttle protective messages against heat stress in bovine granulosa cells. Sci Rep. 2020;10:1–19. https://doi.org/10.1038/s41598-020-72706-z. [cited 2020 Sep 25].
21. Nehammer C, Podolska A, Mackowiak SD, Kagias K, Pocock R. Specific microRNAs Regulate Heat Stress Responses in Caenorhabditis elegans. Sci Rep. 2015;5:8866. Available from: https://www.nature.com/articles/srep08866. [cited 2022 Dec 12].
22. Li Q, Yang C, Du J, Zhang B, He Y, Hu Q, et al. Characterization of miRNA profiles in the mammary tissue of dairy cattle in response to heat stress. BMC Genomics. 2018;19:1–11. Available from: https://bmcgenomics.biomedcentral.com/articles/10.1186/s12864-018-5298-1. [cited 2022 Dec 12].
23. Leung AKL, Sharp PA. MicroRNA Functions in Stress Responses. Mol Cell. 2010;40:205–15. Available from: https://linkinghub.elsevier.com/retrieve/pii/S1097276510007550.
24. Leung AKL, Sharp PA. Molecular Cell Review MicroRNA Functions in Stress Responses. 2010. Available from: http://www.mirbase.org/. [cited 2022 Dec 12].
25. Sarlo Davila KM, Hamblen H, Hansen PJ, Dikmen S, Oltenacu PA, Mateescu RG. Genetic parameters for hair characteristics and core body temperature in a multibreed Brahman–Angus herd1. J Anim Sci. 2019;97:3246–52. [cited 2023 Jan 13]. Available from: https://academic.oup.com/jas/article/97/8/3246/5520432.
26. Mateescu RG, Sarlo-Davila KM, Dikmen S, Rodriguez E, Oltenacu PA. The effect of Brahman genes on body temperature plasticity of heifers on pasture under heat stress. J Anim Sci. 2020;98:1–9. Available from: https://academic.oup.com/jas/article/98/5/skaa126/5823257. [cited 2023 Jan 13].
27. St-Pierre NR, Cobanov B, Schnitkey G. Economic Losses from Heat Stress by US Livestock Industries. J Dairy Sci. 2003;86:E52–77. Available from: https://linkinghub.elsevier.com/retrieve/pii/S0022030203740405. [cited 2023 Jan 13].
28. Robinson MD, Oshlack A. A scaling normalization method for differential expression analysis of RNA-seq data. Genome Biol. 2010;11:R25. Available from: http://genomebiology.biomedcentral.com/articles/10.1186/gb-2010-11-3-r25. [cited 2018 Oct 2].
29. Benjamini Y, Hochberg Y. Controlling the false discovery rate: a practical and powerful approach to multiple testing. J R Stat Soc Ser B. 1995;57:289–300. https://doi.org/10.1111/j.2517-6161.1995.tb02031.x. [cited 2019 Feb 25].
30. Sticht C, De La Torre C, Parveen A, Gretz N. miRWalk: An online resource for prediction of microRNA binding sites. PLoS One. 2018;13:e0206239. https://doi.org/10.1371/journal.pone.0206239. [cited 2021 Aug 24].
31. Ogata H, Goto S, Sato K, Fujibuchi W, Bono H, Kanehisa M. KEGG: Kyoto Encyclopedia of Genes and Genomes. Nucleic Acids Res. 1999;27:29–34. Available from: http://www.ncbi.nlm.nih.gov/pubmed/9847135. [cited 2018 Oct 4].
32. Shannon P. Cytoscape: A Software Environment for Integrated Models of Biomolecular Interaction Networks. Genome Res. 2003;13:2498–504. Available from: http://www.genome.org/cgi/doi/10.1101/gr.1239303. [cited 2018 Oct 4].
33. Bailey TL, Johnson J, Grant CE, Noble WS. The MEME Suite. Nucleic Acids Res. 2015;43:W39–49. Available from: https://pubmed.ncbi.nlm.nih.gov/25953851/. [cited 2022 Oct 18].
34. Gupta S, Stamatoyannopoulos JA, Bailey TL, Noble WS. Quantifying similarity between motifs. Genome Biol. 2007;8. Available from: https://pubmed.ncbi.nlm.nih.gov/17324271/. [cited 2022 Oct 18].
35. Théry C, Witwer KW, Aikawa E, Alcaraz MJ, Anderson JD, Andriantsitohaina R, et al. Minimal information for studies of extracellular vesicles 2018 (MISEV2018): a position statement of the International Society for Extracellular Vesicles and update of the MISEV2014 guidelines. J Extracell Vesicles. 2018;7:1535750. Available from: https://www.tandfonline.com/doi/abs/10.1080/20013078.2018.1535750. [cited 2021 Oct 11].
36. Valadi H, Ekström K, Bossios A, Sjöstrand M, Lee JJ, Lötvall JO. Exosome-mediated transfer of mRNAs and microRNAs is a novel mechanism of genetic exchange between cells. Nat Cell Biol. 2007;9:654–9. Available from: http://www.nature.com/articles/ncb1596. [cited 2020 Mar 22].
37. Godakumara K, Dissanayake K, Hasan MM, Kodithuwakku SP, Fazeli A. Role of extracellular vesicles in intercellular communication during reproduction. Reprod Domest Anim. 2022;57:14–21. Available from: https://pubmed.ncbi.nlm.nih.gov/35837748/. [cited 2022 Nov 30].
38. Thomou T, Mori MA, Dreyfuss JM, Konishi M, Sakaguchi M, Wolfrum C, et al. Adipose-derived circulating miRNAs regulate gene expression in other tissues. Nature. 2017;542:450–5. Available from: https://www.nature.com/articles/nature21365. [cited 2022 Dec 1].
39. Sohel MMH, Hoelker M, Noferesti SS, Salilew-Wondim D, Tholen E, Looft C, et al. Exosomal and Non-Exosomal Transport of Extra-Cellular microRNAs in Follicular Fluid: Implications for Bovine Oocyte Developmental Competence. PLoS One. 2013;8:e78505. Available from: https://journals.plos.org/plosone/article?id=10.1371/journal.pone.0078505. [cited 2022 Nov 30].
40. Hailay T, Hoelker M, Poirier M, Gebremedhn S, Rings F, Saeed-Zidane M, et al. Extracellular vesicle-coupled miRNA profiles in follicular fluid of cows with divergent post-calving metabolic status. Sci Rep. 2019;9:12851. Available from: http://www.nature.com/articles/s41598-019-49029-9. [cited 2020 Apr 15].
41. Miretti S, Lecchi C, Ceciliani F, Baratta M. MicroRNAs as Biomarkers for Animal Health and Welfare in Livestock. Front Vet Sci. 2020;7:985.
42. Reza AMMT, Choi Y-J, Han SG, Song H, Park C, Hong K, et al. Roles of microRNAs in mammalian reproduction: from the commitment of germ cells to peri-implantation embryos. Biol Rev. 2019;94:415–38. Available from: https://onlinelibrary.wiley.com/doi/10.1111/brv.12459. [cited 2023 Mar 30].
43. Ding Q, Jin M, Kalds P, Meng C, Wang H, Zhong J, et al. Comparison of MicroRNA Profiles in Extracellular Vesicles from Small and Large Goat Follicular Fluid. Animals. 2021;11:3190. Available from: https://pubmed.ncbi.nlm.nih.gov/34827922/. [cited 2022 Aug 12].
44. Santonocito M, Vento M, Guglielmino MR, Battaglia R, Wahlgren J, Ragusa M, et al. Molecular characterization of exosomes and their microRNA cargo in human follicular fluid: bioinformatic analysis reveals that exosomal microRNAs control pathways involved in follicular maturation. Fertil Steril. 2014;102:1751–1761.e1. Available from: https://linkinghub.elsevier.com/retrieve/pii/S0015028214020640. [cited 2020 Apr 20].
45. Martinez RM, Liang L, Racowsky C, Dioni L, Mansur A, Adir M, et al. Extracellular microRNAs profile in human follicular fluid and IVF outcomes. Sci Rep. 2018;8:17036. Available from: http://www.nature.com/articles/s41598-018-35379-3. [cited 2020 Feb 13].
46. Jiajie T, Yanzhou Y, Hoi-Hung AC, Zi-Jiang C, Wai-Yee C. Conserved miR-10 family represses proliferation and induces apoptosis in ovarian granulosa cells. Sci Rep. 2017;7:41304. Available from: https://www.nature.com/articles/srep41304. [cited 2022 Nov 28].
47. Tu J, Cheung H-H, Lu G, Chen Z, Chan W-Y. MicroRNA-10a promotes granulosa cells tumor development via PTEN-AKT/Wnt regulatory axis. Cell Death Dis. 2018;9:1076. Available from: https://www.nature.com/articles/s41419-018-1117-5. [cited 2023 Mar 2].
48. Dai T, Kang X, Yang C, Mei S, Wei S, Guo X, et al. Integrative Analysis of miRNA-mRNA in Ovarian Granulosa Cells Treated with Kisspeptin in Tan Sheep. Animals. 2022;12:2989. Available from:https://www.mdpi.com/2076-2615/12/21/2989.
49. Fan Q, Meng X, Liang H, Zhang H, Liu X, Li L, et al. miR-10a inhibits cell proliferation and promotes cell apoptosis by targeting BCL6 in diffuse large B-cell lymphoma. Protein Cell. 2016;7:899–912. Available from: https://link.springer.com/article/10.1007/s13238-016-0316-z. [cited 2022 Nov 28].
50. Ovcharenko D, Stölzel F, Poitz D, Fierro F, Schaich M, Neubauer A, et al. miR-10a overexpression is associated with NPM1 mutations and MDM4 downregulation in intermediate-risk acute myeloid leukemia. Exp Hematol. 2011;39. Available from: https://pubmed.ncbi.nlm.nih.gov/21784052/. [cited 2022 Nov 28].
51. Zheng Y, Chen K, Zheng X, Li H, Wang G. Identification and bioinformatics analysis of microRNAs associated with stress and immune response in serum of heat-stressed and normal Holstein cows. Cell Stress Chaperones. 2014;19:973–81. [cited 2020 Sep 23]. Available from: http://link.springer.com/10.1007/s12192-014-0521-8.
52. Lafourcade CA, Fernández A, Ramírez JP, Corvalán K, Carrasco MÁ, Iturriaga A, et al. A role for mir-26a in stress: a potential sEV Biomarker and

modulator of excitatory neurotransmission. Cells. 2020;9. [cited 2022 Nov 30]. Available from: https://www.mdpi.com/2073-4409/9/6/1364.
53. Huo S, Qi H, Si Y, Li C, Du W. MicroRNA 26a targets Ezh2 to regulate apoptosis in mouse ovarian granulosa cells. Syst Biol Reprod Med. 2021;67:221–9.https://doi.org/10.1080/19396368.2021.1895362.
54. Lee J, Lee S, Son J, Lim H, Kim E, Kim D, et al. Analysis of circulating-microRNA expression in lactating Holstein cows under summer heat stress. PLoS One. 2020;15:e0231125. https://doi.org/10.1371/journal.pone.0231125. [cited 2020 Sep 23].
55. Souza V das GP de, Souza GT de, Lemos DR de, Guimarães JM de O, Quintão CCR, Munk M, et al. Heat shock during in vitro maturation of bovine oocytes disturbs bta-miR-19b and DROSHA transcripts abundance after in vitro fertilization. Reprod Domest Anim. 2021;56:1128–36. Available from: https://onlinelibrary.wiley.com/doi/full/10.1111/rda.13956. [cited 2022 Dec 6].
56. Zhong Z, Li F, Li Y, Qin S, Wen C, Fu Y, et al. Inhibition of microRNA-19b promotes ovarian granulosa cell proliferation by targeting IGF-1 in polycystic ovary syndrome. Mol Med Rep. 2018;17:4889. Available from: /pmc/articles/PMC5865948/. [cited 2023 Mar 2].
57. Sirotkin A V., Ovcharenko D, Grossmann R, Lauková M, Mlynček M. Identification of MicroRNAs controlling human ovarian cell steroidogenesis via a genome-scale screen. J Cell Physiol. 2009;219:415–20. Available from: https://onlinelibrary.wiley.com/doi/full/10.1002/jcp.21689. [cited 2023 Mar 2].
58. Salilew-Wondim D, Ahmad I, Gebremedhn S, Sahadevan S, Hossain MM, Rings F, et al. The Expression Pattern of microRNAs in Granulosa Cells of Subordinate and Dominant Follicles during the Early Luteal Phase of the Bovine Estrous Cycle. PLoS One. 2014;9:e106795. Available from: https://journals.plos.org/plosone/article?id=10.1371/journal.pone.0106795. [cited 2023 Mar 2].
59. Faheem MS, Ghanem N, Gad A, Procházka R, Dessouki SM. Adaptive and Biological Responses of Buffalo Granulosa Cells Exposed to Heat Stress under In Vitro Condition. Animals. 2021;11:794. Available from: https://pubmed.ncbi.nlm.nih.gov/33809236/. [cited 2022 Dec 6].
60. Shandilya UK, Sharma A, Sodhi M, Mukesh M. Heat stress modulates differential response in skin fibroblast cells of native cattle (Bos indicus) and riverine buffaloes (Bubalus bubalis). Biosci Rep. 2020;40. [cited 2020 Sep 22]. Available from: https://portlandpress.com/bioscirep/article/40/2/BSR20191544/221965/Heat-stress-modulates-differential-response-in.
61. Cheleschi S, Tenti S, Mondanelli N, Corallo C, Barbarino M, Giannotti S, et al. MicroRNA-34a and MicroRNA-181a Mediate Visfatin-Induced Apoptosis and Oxidative Stress via NF-κB Pathway in Human Osteoarthritic Chondrocytes. Cells. 2019;8:874. [cited 2022 Dec 6]. Available from: https://pubmed.ncbi.nlm.nih.gov/31405216/.
62. Chen K-L, Fu Y-Y, Shi M-Y, Li H-X. Down-regulation of miR-181a can reduce heat stress damage in PBMCs of Holstein cows. Vitr Cell Dev Biol - Anim. 2016;52:864–71. Available from: https://pubmed.ncbi.nlm.nih.gov/27130682/. [cited 2020 Sep 23].
63. Fabbiano F, Corsi J, Gurrieri E, Trevisan C, Notarangelo M, D'Agostino VG. RNA packaging into extracellular vesicles: An orchestra of RNA-binding proteins? J Extracell Vesicles. 2020;10. Available from: https://pubmed.ncbi.nlm.nih.gov/33391635/. [cited 2022 Feb 22].
64. Garcia-Martin R, Wang G, Brandão BB, Zanotto TM, Shah S, Kumar Patel S, et al. MicroRNA sequence codes for small extracellular vesicle release and cellular retention. Nature. 2022;601:446–51. Available from: https://www.nature.com/articles/s41586-021-04234-3. [cited 2022 Feb 17].
65. Mordovkina D, Lyabin DN, Smolin EA, Sogorina EM, Ovchinnikov LP, Eliseeva I. Y-Box Binding Proteins in mRNP Assembly, Translation, and Stability Control. Biomolecules. 2020;10:591. Available from: https://www.mdpi.com/2218-273X/10/4/591/htm. [cited 2022 Dec 1].
66. Eliseeva IA, Kim ER, Guryanov SG, Ovchinnikov LP, Lyabin DN. Y-box-binding protein 1 (YB-1) and its functions. Biochem. 2011;76:1402–33. Available from: https://pubmed.ncbi.nlm.nih.gov/22339596/. [cited 2022 Dec 1].
67. Guarino AM, Troiano A, Pizzo E, Bosso A, Vivo M, Pinto G, et al. Oxidative Stress Causes Enhanced Secretion of YB-1 Protein that Restrains Proliferation of Receiving Cells. Genes (Basel). 2018;9:513. Available from: https://pubmed.ncbi.nlm.nih.gov/30360431/. [cited 2022 Dec 1].
68. Mordovkina D, Lyabin DN, Smolin EA, Sogorina EM, Ovchinnikov LP, Eliseeva I. Y-Box Binding Proteins in mRNP Assembly, Translation, and Stability Control. Biomolecules. 2020;10:591. Available from:/pmc/articles/PMC7226217/. [cited 2022 Dec 5].
69. Yanshina DD, Kossinova OA, Gopanenko A V., Krasheninina OA, Malygin AA, Venyaminova AG, et al. Structural features of the interaction of the 3′-untranslated region of mRNA containing exosomal RNA-specific motifs with YB-1, a potential mediator of mRNA sorting. Biochimie. 2018;144:134–43. Available from: https://pubmed.ncbi.nlm.nih.gov/29133115/. [cited 2022 Dec 5].
70. Shurtleff MJ, Temoche-Diaz MM, Karfilis K V., Ri S, Schekman R. Y-box protein 1 is required to sort microRNAs into exosomes in cells and in a cell-free reaction. Elife. 2016;5. Available from: https://elifesciences.org/articles/19276. [cited 2022 Dec 1].
71. Fukuda T, Naiki T, Saito M, Irie K. hnRNP K interacts with RNA binding motif protein 42 and functions in the maintenance of cellular ATP level during stress conditions. Genes to Cells. 2009;14:113–28. Available from: https://pubmed.ncbi.nlm.nih.gov/19170760/. [cited 2022 Dec 1].

Publisher's Note

Springer Nature remains neutral with regard to jurisdictional claims in published maps and institutional affiliations.

Ready to submit your research? Choose BMC and benefit from:

- fast, convenient online submission
- thorough peer review by experienced researchers in your field
- rapid publication on acceptance
- support for research data, including large and complex data types
- gold Open Access which fosters wider collaboration and increased citations
- maximum visibility for your research: over 100M website views per year

At BMC, research is always in progress.

Learn more biomedcentral.com/submissions



BMC Genomics

RESEARCH

Open Access

Bovine oviductal organoids: a multi-omics approach to capture the cellular and extracellular molecular response of the oviduct to heat stress

Nico G. Menjivar[1], Ahmed Gad[1,2], Riley E. Thompson[3], Mindy A. Meyers[3], Fiona K. Hollinshead[3] and Dawit Tesfaye[1*]

Abstract

Background The mammalian oviduct is a complex, fibromuscular organ known for its role in orchestrating a series of timely and dynamic changes to suitably support early embryogenesis. Climate change-induced heat stress (HS) is one of the largest single stressors compromising reproductive function in humans and farm animals via systemic changes in the redox status of the maternal environment, adversely affecting fertilization and early embryonic development. Oviductal organoids represent a unique 3-dimensional, biomimetic model to study the physiology of the oviduct and its subsequent impact on embryo development under various environmental conditions.

Results Our study is the first to demonstrate an innovative approach to understanding the cascade of molecular changes sustained by bovine oviductal organoids under HS and the subsequent maternal signals harnessed within their secreted extracellular vesicles (EVs). Transcriptomic analysis of oviductal organoids exposed to HS revealed 2,570 differentially expressed genes (1,222 up- and 1,348 downregulated), while EV-coupled miRNome analysis disclosed 18 miRNAs with significant differential expression (12 up- and 6 downregulated) in EVs from thermally stressed organoids compared to EVs released from organoids cultured under thermoneutral conditions. Genes activated in oviductal organoids in response to thermal stress, include: *COX1*, *ACTB*, *CST6*, *TPT1*, and *HSPB1*, while miR-1246, miR-148a, miR21-5p, miR-451, and miR-92a represent the top highly abundant EV-coupled miRNAs released in response to HS. Pathway analysis of genes enriched in organoids exposed to thermal stress showed the enrichment of endocrine resistance, cellular senescence, and notch signaling pathways. Similarly, EV-coupled miRNAs released from thermally stressed organoids showed their potential regulation of genes involved in cellular senescence, p53 signaling, and TGF-beta signaling pathways.

Conclusions In conclusion, the cellular and extracellular response of bovine oviductal organoids to in vitro HS conditions reveal the prospective impact of environmental HS on the physiology of the oviduct and the probable subsequent impacts on oocyte fertilization and early embryo development. Future studies elucidating the potential impact of HS-associated EVs from oviductal organoids on oocyte fertilization and preimplantation embryo development, would justify the use of an organoid model to optimally understand the oviduct-embryo communication under suboptimal environments.

*Correspondence:
Dawit Tesfaye
Dawit.Tesfaye@colostate.edu
Full list of author information is available at the end of the article

© The Author(s) 2023. **Open Access** This article is licensed under a Creative Commons Attribution 4.0 International License, which permits use, sharing, adaptation, distribution and reproduction in any medium or format, as long as you give appropriate credit to the original author(s) and the source, provide a link to the Creative Commons licence, and indicate if changes were made. The images or other third party material in this article are included in the article's Creative Commons licence, unless indicated otherwise in a credit line to the material. If material is not included in the article's Creative Commons licence and your intended use is not permitted by statutory regulation or exceeds the permitted use, you will need to obtain permission directly from the copyright holder. To view a copy of this licence, visit http://creativecommons.org/licenses/by/4.0/. The Creative Commons Public Domain Dedication waiver (http://creativecommons.org/publicdomain/zero/1.0/) applies to the data made available in this article, unless otherwise stated in a credit line to the data.

Keywords Organoids, Extracellular vesicles, Oviduct, Heat stress, Transcriptome, miRNA

Background

The mammalian oviduct comprises an advantageous microenvironment with biochemical and biophysical support to sustain the formation of life as the 'site' of fertilization and preimplantation embryo development [1]. Effective measures of communication are cohesively required from the embryo itself and the maternal environment to establish a periconceptional milieu to support conception and early embryonic development [2]. Tangible evidence exists demonstrating an unequivocal two-way signaling interaction at the embryo–maternal interface [3, 4], suggesting reciprocal crosstalk leading to a successful pregnancy provides a significant basis for physiological implantation [3–5]. Classically, cell–cell communications' paramount role in regulating physiological processes were commonly defined either via direct contact through membrane signaling (juxtracrine) or by secreting various molecules (growth factors, hormones, cytokines, metabolites, etc.) with ensuing signaling function (autocrine, paracrine, and endocrine). More recently, extracellular vesicles (EVs) which exist in almost all biological fluids, have been implicated as emerging bi-directional, putative messengers to nano-shuttle regulatory bioactive molecules (lipids, proteins, nucleic acids, etc.) with biologically plausible functions [6–9]. Irrespective of their origin, previous reports have shown that EVs released following external stress stimuli induce bystander tolerance in naïve cells treated with 'stressed EVs,' [10–15] indicating their potential to transfer 'protective' molecules (protectosomes).

The large-scale impacts of elevated ambient temperatures resulting from climate change on animal production and reproductive performance have been extensively studied [16, 17]. External heat acting on a homeothermic animal impede fertility, affecting the physiological and cellular function of several reproductive tissues [18, 19]. In vivo and in vitro studies have demonstrated the direct effects of heat stress (HS)-induced dysfunction through impairments to mammalian oocyte maturation, fertilization, and early embryo development [20–23]. However, the complexity to investigate the impact of HS in regard to oviduct physiology and the embryo-oviduct dialog in later stage embryos have been largely stunted due to its inaccessible location without surgery or necropsy post-slaughter. Therefore, novel approaches to recapitulate the in vivo physiology and function of the oviduct in vitro, would provide an innovative mechanism to validate the system's functional response to HS.

Despite the extensive work carried out to understand the effects of HS on reproductive function, its underlying impacts on oviduct physiology remain largely unknown. Initial attempts to study the embryo-oviduct dialogue via EVs from oviductal fluid [24] and monolayer-bovine oviductal epithelial cell (BOEC) conditioned culture medium [25], demonstrated promising improvements in embryo quality and cryotolerance following their addition during embryo culture. Regardless of the beneficial roles of EVs, the potential transfer of identified embryotropic molecules eliciting such positive responses in embryo development was not studied. However, Almiñana and colleagues have shown major discrepancies in the protein cargo signatures from in vivo vs. in vitro derived EVs of oviductal origin, revealing that in vitro monolayer-BOECs inadequately mimic the in vivo oviductal environment, likely resulting from a lack of paracrine signaling amid reduced cellular diversity [26].

Organoids represent biomimetic, three-dimensional, in vitro cell clusters that organizationally self-regenerate into complex structures to mirror the physiological function of their tissue of origin [27]. Generally, organoid cell clusters are encapsulated within a jelly-like extracellular matrix and function similar to their native in vivo organ in terms of gene and protein expression, metabolic function and microscale tissue architecture [28]. Studies in humans [29] and mice [30, 31] have recently outlined advantages over existing traditional cell culture models through the establishment and long-term stability of fallopian tube organoids that faithfully recapitulate the phenotype of their in vivo tissue. Thus, in this study, we aimed to utilize bovine oviductal organoids to decrypt the oviducts' differential response to HS in terms of cellular transcriptome and secreted EV-miRNome, to elucidate the potential downstream impacts on fertilization and early embryo development. Furthermore, several studies have revealed the regulatory role of miRNA sequence motifs and their corresponding RNA binding proteins in EV-miRNA secretion versus cellular retention under specific environmental conditions [32–36]. Therefore, investigating the interplay between miRNA sequence motifs and RNA binding proteins in the packaging and release of specific miRNAs into EVs by subjecting organoids to thermal stress, would shine light upon the molecular mechanisms behind the oviductal response to HS via EV-coupled miRNA signaling.

Results

The experimental design outlining the different groups of organoid cultures and EVs used in the RNA-seq analyses are summarized in Fig. 1.

3-D matrix supports dynamic oviductal organoid culture and EV production

Oviductal organoids generated from bovine oviducts resected from diestrus reproductive tracts ($n=10$) were grown for 14 days (one passage, 7 days per passage; Fig. 2A), prior to suspension in a xeno-free, synthetic matrix for experiments with HS. Representative histological and immunohistochemical (Fig. 2B) images of in tact oviduct and in vitro cultured oviductal organoids (P1D7) demonstrate the architectural morphology (hematoxylin and eosin; H&E) and presence of oviduct-specific glycoprotein 1 (OVPG1), zonula occludens-1 (ZO1), and forkhead box J1 (FOXJ1), respectively. H&E staining showed that crosssections of oviductal organoids contain a monolayer of oviductal epithelial cells encircling a centralized lumen. Also, mature organoids maintained through extended culture persistently express hallmark protein OVGP1, as well as epithelial cell tight junctions (ZO1), and ciliated cells (FOXJ1). Comprehensively, the organoid cellular morphology contain both partially differentiated and polarized cuboidal cells, as well as columnar shaped cells, which precisely represent the established structure of functional organoids. Additionally, we used a gene panel to functionally characterize the expression patterns of in vitro produced oviductal organoids (37 °C and 42 °C) compared to naïve in vivo BOECs. The panel was comprised of cell proliferation and adhesion (*MKI67* and *CDH1*), ciliated cell function and differentiation (*LRRC6*, *TUBA1A*, *TUBA1B* and *TUBA1C*), and hormonal prostaglandin function (*PTGS2*, *PTGES* and *OXTR*) gene expression signatures. Overall, minimal statistical differences presided between in vitro produced organoids and in vivo derived cells, strengthening the biomimicry of extended culture in a 3-D matrix (Fig. 3). In addition, a dual-targeted approach to isolate EVs using ultracentrifugation and size exclusion chromatography (SEC) was employed to isolate a relatively homogenous population of oviductal organoid-derived EVs. The molecular and morphological characterization of oviductal organoid-derived EVs validated the integrity of our procedure to isolate molecular analysis grade EVs from conditioned culture medium of in vitro-cultured bovine oviductal organoids. Representative TEM images (Fig. 4A), indicate the presence of membrane-enveloped vesicles released from oviductal organoids. Moreover, nanoparticle tracking analysis revealed a higher particle concentration in the S-EVs (derived from organoids cultured at 42 °C; 1.29E + 10 particles/mL), when compared to the N-EVs (derived from organoids cultured at 37 °C; 1.01E + 10 particles/mL), with median sizes of 120.01 and 133.99 nm, respectively (Fig. 4B). Western blot analysis (Fig. 4C) indicated the presence of EV marker proteins (TSG101, FLOT1, and CD63) in the EV samples derived from oviductal organoids, while CYCS, a cellular contaminant and negative marker of EVs, was absent. In addition, RNA quality control for integrity, prior to RNA sequencing, revealed the presence of 18S and 28S ribosomal RNA peaks in the oviductal organoid RNA and their absence in oviductal organoid-derived EV-RNA samples (Fig. 4D & E).

Decoding the transcriptome response of oviductal organoids to HS

To understand the changes in molecular physiology of the bovine oviduct under HS conditions, this study examines the first comprehensive transcriptome analysis revealing the cellular response of oviductal organoids

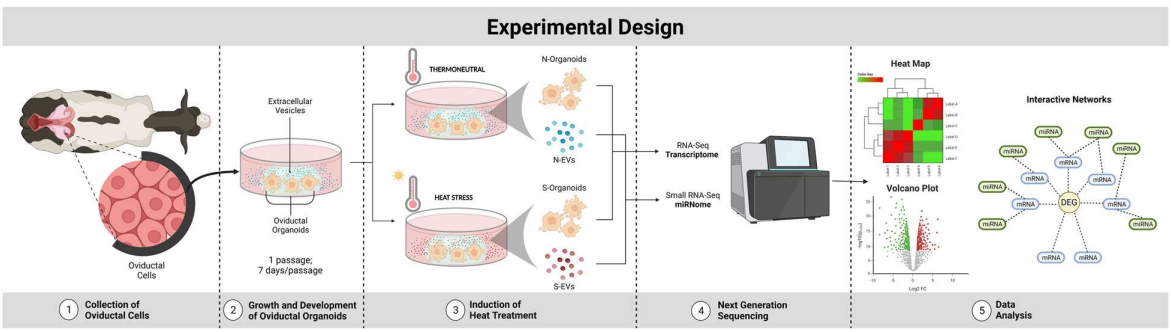


Fig. 1 Schematic Illustration of the Experimental Design. Oviductal cells were collected from abattoir-derived reproductive material for the establishment of bovine oviductal organoids. Organoids were subsequently grown and developed under thermoneutral conditions for 14 days prior to exposing to heat treatment. Following HS exposure, organoid cells and the corresponding EVs were collected, isolated and subjected to genome-wide transcriptomic and miRNomic profiling, respectively

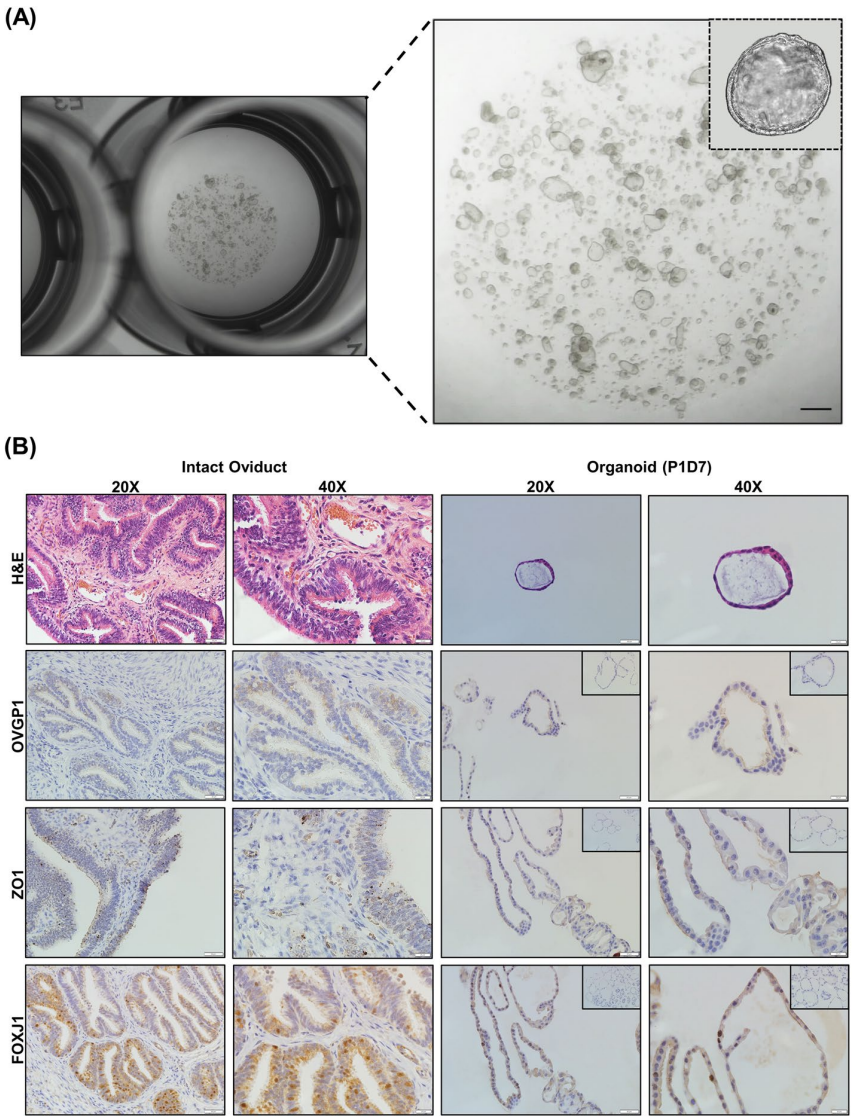


Fig. 2 Establishment of Oviductal Organoid Culture System. Representative morphology of cultured bovine oviductal organoids after 14 days in culture. Scale bar, 1 mm (**A**). Immunostaining of in vitro cultured bovine oviductal organoids at passage 1, day 7 (P1D7). Histological oviductal samples with H&E staining, and immunohistochemical (OVGP1, ZO1, and FOXJ1) at 20× and 40× magnification, respectively. Scale bar = 50 µm at 20× magnification and 20 µm at 40× magnification. Controls shown in insets represent a negative reagent control (OVGP1, ZO1 and FOXJ1)

to elevated thermal stress. A total of ten RNA libraries were prepared from the organoid cells cultured under HS (42 °C) and thermoneutral conditions (37 °C). Approximately 536 million raw reads were sequenced from both groups. After adapter trimming and quality filtering, approximately 53.6 million reads per library were retained with an average of 99% of the quality-controlled (QC) reads mapped to the bovine reference genome (ARS-UCD1.2). A summary of the total number of reads and the mapping results for each group is presented in Additional file 1: Table S1. Principal component analysis (PCA) and the accompanied hierarchical heatmap revealed that biological replicates for each group clustered together except for one replicate amid the HS groups (Fig. 5A & B), which has been excluded from further analysis. A stringent criterion was set to avoid bias for low expression in which, expressed genes represent zFPKM > −3 amongst all replicates. In total, 11,935 and

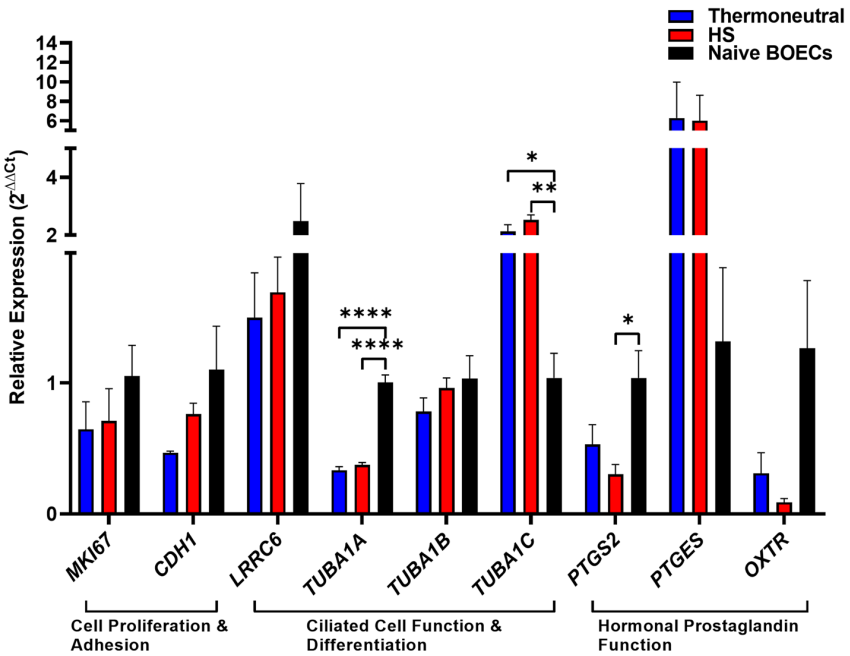


Fig. 3 In vitro Produced Organoid Retention of the In vivo Oviduct. Quantitative real time PCR analysis of selected genes outlining the mRNA expression of markers for cell proliferation and adhesion, ciliated cell function and differentiation, and hormonal prostaglandin function in in vitro produced organoids (37 °C and 42 °C) and naïve bovine oviductal epithelial cells (BOEC). Data are shown as the mean ± SEM and the differences between means were analyzed using one-way ANOVA followed by Tukey's Multiple Comparisons Test in biologically independent samples ($n = 3$). Statistical significance (*) between groups were determined at ($p < 0.05$)

12,564 genes were detected in the HS and thermoneutral cultured organoid groups, respectively, with 11,725 genes mutually expressed in both groups (Fig. 5C). Of the most highly expressed genes in both groups, the top 20 genes most abundantly expressed amongst all organoid samples include: *COX1*, *ACTB*, *CST6*, *TPT1*, *RPLP1*, *RPLP0*, *FTH1*, *COX2*, *EEF1A1*, *UBA52*, *RPS15* (Table 1).

Considering a false discovery rate (FDR) < 0.05 and a fold change (FC) ≥ 2, a total of 2,570 differentially expressed genes (DEGs) (1,222 up- and 1,348 downregulated) were identified in the oviductal organoids subjected to HS compared to the thermoneutral groups, including 170 genes with unknown function (Additional file 2: Table S2). The volcano plot (Fig. 5D) illustrates the distribution of DEGs, up- and downregulated, in the HS compared to the thermoneutral groups. The top 20 known DEGs (upregulated include: *CRISPLD2*, *HSPA6*, *SERPINE1*; downregulated include: *RBM3*, *MROH1*, *FAH*) identified in the HS compared with the thermoneutral cultured groups are listed in Table 2. Gene ontology (GO) enrichment analysis of the upregulated genes in the HS groups revealed that endocrine resistance, cellular senescence, and notch signaling pathway to be the top significant pathways (Fig. 6A; Additional file 3A: Table S3A). Alternatively, metabolic pathways, oxidative phosphorylation, nucleotide metabolism, carbon metabolism, and thermogenesis were the top significant pathways dominated by the downregulated genes (Fig. 6B; Additional file 3B: Table S3B). Biological processes in which genes upregulated in thermally stressed organoids involve cell migration, transcription regulation, and protein phosphorylation (Fig. 6C; Additional file 4A: Table S4A), while cholesterol biosynthetic processes, mitochondrial electron transport and ATP synthesis were the processes in which involve downregulated genes (Fig. 6D; Additional file 4B: Table S4B). Interaction networks of DEGs commonly involved in highly enriched pathways are presented in Fig. 6E. The highlighted genes amid the interaction networks are involved in various signaling pathways, gene expression regulation, and functions regulating cellular senescence and pregnancy homeostasis.

HS alters oviductal organoid-derived EV-coupled miRNAs

To understand the extracellular response of oviductal organoids to HS, organoid-secreted EVs were investigated for their miRNA content using small RNA sequencing technology. Three small RNA libraries were prepared from the EVs derived from each of the organoid cultures under 37 °C and 42 °C. Approximately 135

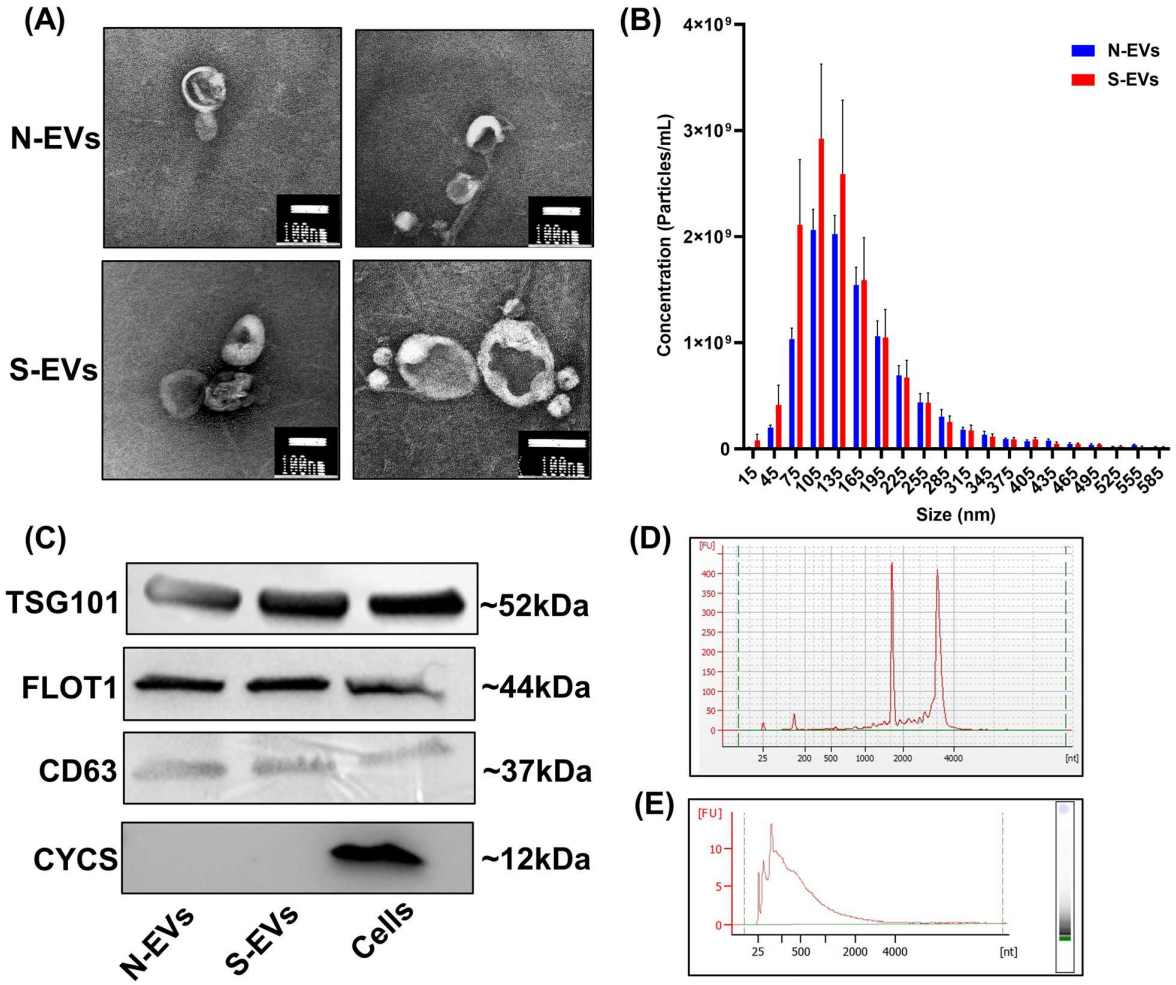


Fig. 4 Characterization of Oviductal Organoid-derived EVs. Transmission Electron Microscopy (TEM) images depicting a clear bilipid enclosed complex in oviductal organoid-derived EVs. Scale bar, 100 nm (**A**). Size distribution and concentration of N-EVs (blue bars) and S-EVs (red bars) resulting from Nanoparticle Tracking Analysis (NTA) (**B**). Cropped blots for Western Blotting (WB) analysis in EVs shows traditionally expressed EV-associated protein markers (TSG101, FLOT1, CD63) and the absence of expression for non-EV, mitochondrial associated cellular marker protein (CYCS) in lanes indicated by N-EVs and S-EVs (**C**). Representative RNA quality control and size distribution from oviductal organoids (**D**) and the corresponding EVs indicating the absence of 18 s and 28 s cellular RNA components (**E**)

million raw reads were sequenced from both EV groups. After adapter trimming and quality control, an average of 21 million reads per library was retained. An average of 87% and 89% of these reads from the HS and thermoneutral EV groups, respectively, were mapped to the bovine reference genome (Additional file 5: Table S5). Based on the miRNA expression patterns, the PCA (Fig. 7A) and hierarchical heatmap (Fig. 7B) exhibited a clear clustering of the replicates from each group. Sequencing data analysis revealed a total of 251 known miRNAs amongst both groups with at least 10 counts per million (CPM) (Fig. 7C). While a complete list of all the expressed miRNAs detected is presented in Additional file 6: Table S6, a list of the top 20 expressed miRNAs from each group are presented in Table 3. Among the top 20 expressed miRNAs, 15 were commonly detected amongst both groups.

Differential expression analysis of EV-miRNAs released from oviductal organoids subjected to divergent ambient temperatures indicated a total of 18 miRNAs as significantly-differentially expressed between the two groups (FC > 2, FDR < 0.05). EVs from HS oviductal organoids exhibited the enrichment of 12 miRNAs (including: miR-150, miR-92a, miR-223, and

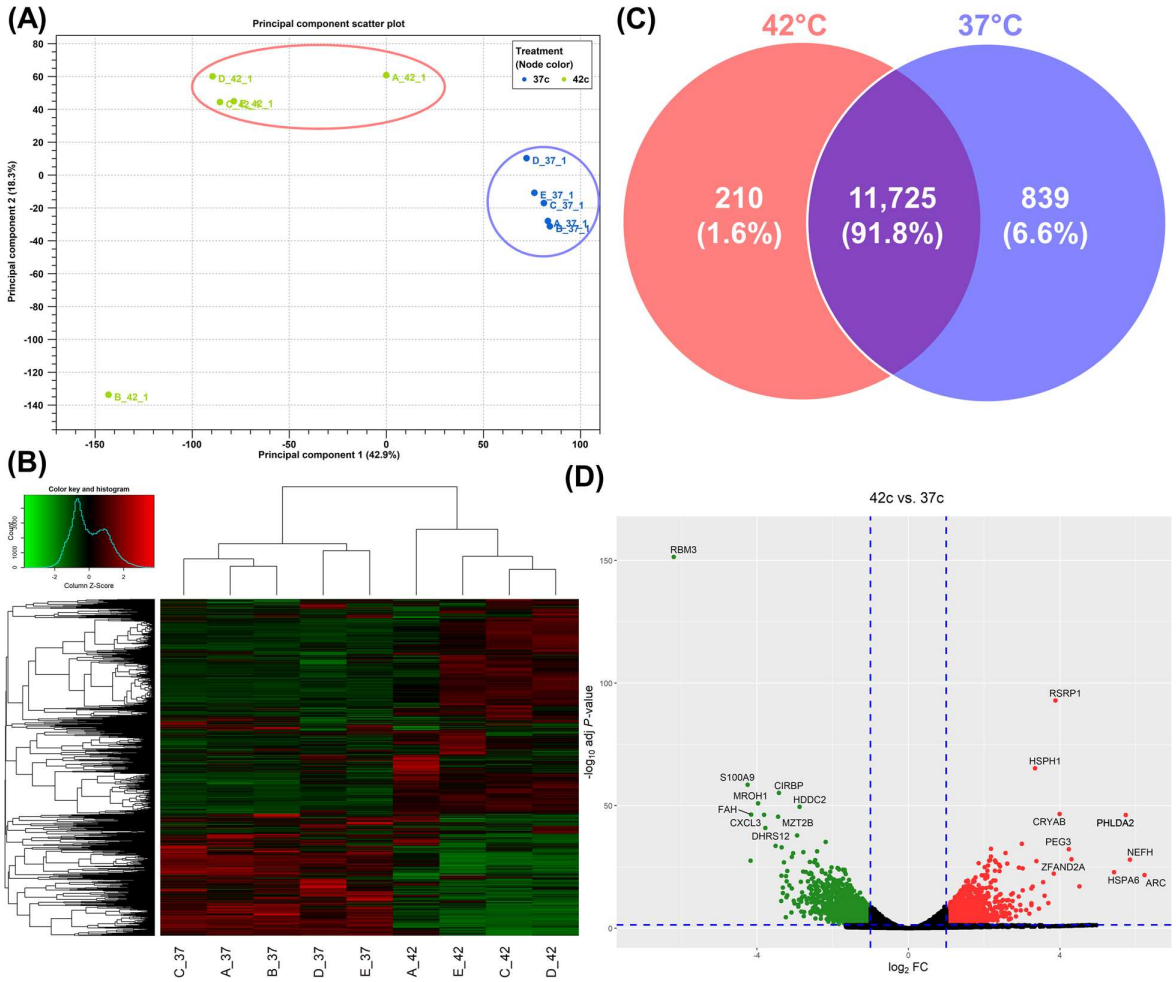


Fig. 5 Impact of HS on Oviductal Organoids: Transcriptomic Cellular Response. Principal component analysis (PCA) (**A**) and heatmap/hierarchical clustering of oviductal organoid samples (**B**) cultured under HS (42 °C; A_42-D_42) or thermoneutral conditions (37 °C; A_37-D_37). Venn diagram indicating exclusively and commonly expressed genes in the 42 °C and 37 °C groups (**C**). Volcano plot displaying differentially expressed genes, up- and downregulated in oviductal organoids cultured under HS (42 °C) compared to those cultured under thermoneutral conditions (37 °C) (**D**)

miR-202) and 6 downregulated miRNAs (including: miR-221, miR-11980, miR-23a and miR-370) compared to the EVs released from thermoneutral cultured organoids (Table 4 and Fig. 7D). Interestingly, two differentially expressed (DE)-miRNAs (miR-10b and miR-92a) were also noted in the top 20 expressed miRNAs list. Pathway analysis revealed that genes potentially targeted by the upregulated EV-miRNAs were involved in cellular senescence, p53, and TGF-beta signaling pathways (Fig. 8A; Additional file 7A: Table S7A), while those potentially targeted by the downregulated EV-miRNAs were involved in MAPK and FoxO signaling pathways (Fig. 8B; Additional file 7B: Table S7B). Transcription and cell cycle regulation were among the top abundant biological processes targeted by the upregulated miRNAs (Fig. 8C; Additional file 8A: Table S8A), while protein phosphorylation and regulation of cell cycle and proliferation were among the top biological processes targeted by the downregulated miRNAs in the HS compared to the thermoneutral groups (Fig. 8D; Additional file 8B: Table S8B). Interaction networks between common experimentally validated target genes of the DE-EV-miRNAs and the organoids DEGs, are presented in Fig. 9A. Additionally, a focus on the DEGs involved in the cellular senescence pathway network and the DE-EV-miRNAs potentially targeting their function are represented in Fig. 9B.

Table 1 Top 20 expressed genes in oviductal organoids from the HS (42 °C) and thermoneutral (37 °C) groups

Genes	42 °C Group TPM	%[a]	Genes	37 °C Group TPM	%[a]
COX1	12,134.48	10.36	*COX1*	18,703.53	14.63
ACTB	9851.64	8.41	*COX3*	12,044.18	9.42
CST6	7866.93	6.71	*COX2*	9073.11	7.10
TPT1	6996.46	5.97	*FTH1*	8633.91	6.76
HSPB1	6814.69	5.82	*RPLP1*	6970.11	5.45
RPLP1	6408.56	5.47	*GAPDH*	6133.64	4.80
RPLP0	6155.16	5.25	*RPLP0*	5702.06	4.46
CLU	5635.77	4.81	*ATP6*	5258.80	4.11
CRYAB	5519.48	4.71	*KRT19*	5247.57	4.11
FTL	5403.90	4.61	*FTL*	5217.36	4.08
ACTG1	5399.25	4.61	*TPT1*	5153.81	4.03
COX3	5017.02	4.28	*ACTB*	4863.59	3.81
FTH1	5004.65	4.27	*ACTG1*	4709.11	3.68
COX2	4958.39	4.23	*EEF1A1*	4561.17	3.57
EEF1A1	4524.72	3.86	*RPS15*	4490.25	3.51
UBA52	4411.87	3.77	*CST6*	4456.38	3.49
HSPA1A	4367.03	3.73	*ND3*	4434.30	3.47
ANXA2	3736.05	3.19	*ND1*	4104.32	3.21
HSPA8	3531.16	3.01	*MSLN*	4025.36	3.15
RPS15	3418.48	2.92	*UBA52*	4018.46	3.14

TPM average Transcript Per Million mapped reads

[a] Percentage of the genes sequence reads

Quantitative real-time PCR validation of candidate genes and miRNAs

To validate the sequencing data, 10 DE-genes (5 up- and 5 downregulated in the HS compared to the thermoneutral groups) and 4 upregulated miRNAs were selected for validation in 4 independent, biological replicates using quantitative real-time PCR. Selected candidate genes in oviductal organoids (Fig. 10A) and miRNAs in oviductal organoid-secreted EVs (Fig. 10B) show the same expression pattern consistent with the RNA-seq data.

MicroRNA sequence motif and RBP identification

To investigate the potential mechanism of miRNA sorting and packaging into EVs by oviductal organoids in response to thermal stress, miRNA sequence motif analysis was performed for the miRNAs significantly enriched in EVs released in response to thermal stress using low abundant miRNAs (enriched in EVs released from organoids cultured under thermoneutral conditions) as controls. Accordingly, we have identified two miRNA motifs [U/A][C/U][C/A][U/G/A/C]A and [C/U][U/A]GU to be shared by 69% (9 of the 13) and 62% (8 out of 13) of the upregulated miRNAs, respectively (Fig. 11A). Moreover, an additional two motifs UG[U/A][A/G] and ACCC were identified and shared by 46% (6 of the 13) and 23% (3 out of 13) of the upregulated miRNAs, respectively. The sequence position and distribution of the identified motifs among the candidate miRNAs is indicated in

Table 2 Top 20 DEGs in HS (42 °C) oviductal organoids compared to the thermoneutral (37 °C) groups

Upregulated Genes	FC	FDR	Downregulated Genes	FC	FDR
RAB39A	85.71	3.56E-03	*MFAP4*	-14.38	3.37E-11
ARC	75.04	1.91E-22	*PPP1R32*	-15.65	1.65E-09
CRISPLD2	64.85	1.25E-32	*MROH1*	-15.68	1.10E-51
NEFH	57.56	9.69E-29	*ACSM1*	-17.54	8.85E-19
PHLDA2	53.28	6.75E-47	*FAH*	-17.80	4.22E-47
ENSBTAG00000001219	52.94	1.64E-08	*RHBDD3*	-18.01	2.75E-28
HSPA6	42.95	1.46E-23	*NOS2*	-18.02	1.52E-19
ENSBTAG00000052847	36.38	1.28E-07	*S100A9*	-18.97	2.65E-59
PURG	31.95	3.79E-09	*ASB9*	-19.67	1.96E-11
FAM71F1	26.14	2.53E-08	*HERC3*	-19.85	6.46E-60
NPB	22.86	8.62E-18	*DIRAS3*	-21.65	3.80E-10
GAS2	20.03	9.82E-10	*HNMT*	-22.45	2.36E-10
ZFAND2A	19.72	6.73E-29	*ETNPPL*	-24.09	5.00E-10
PEG3	18.76	5.88E-33	*SERPINB13*	-32.57	9.11E-15
CRYAB	15.90	2.22E-47	*ENSBTAG00000003661*	-32.99	1.55E-20
ENSBTAG00000049003	14.77	2.45E-16	*CSF3*	-34.72	2.48E-17
RSRP1	14.73	1.16E-93	*LRCOL1*	-36.95	1.50E-05
SERPINE1	14.29	5.61E-23	*DAPL1*	-60.38	1.61E-08
ENSBTAG00000050861	12.67	2.26E-06	*RBM3*	-73.40	3.10E-152
TEX49	12.64	9.61E-08	*SERPINE3*	-163.84	1.87E-63

FC Fold Change, *FDR* False Discovery Rate

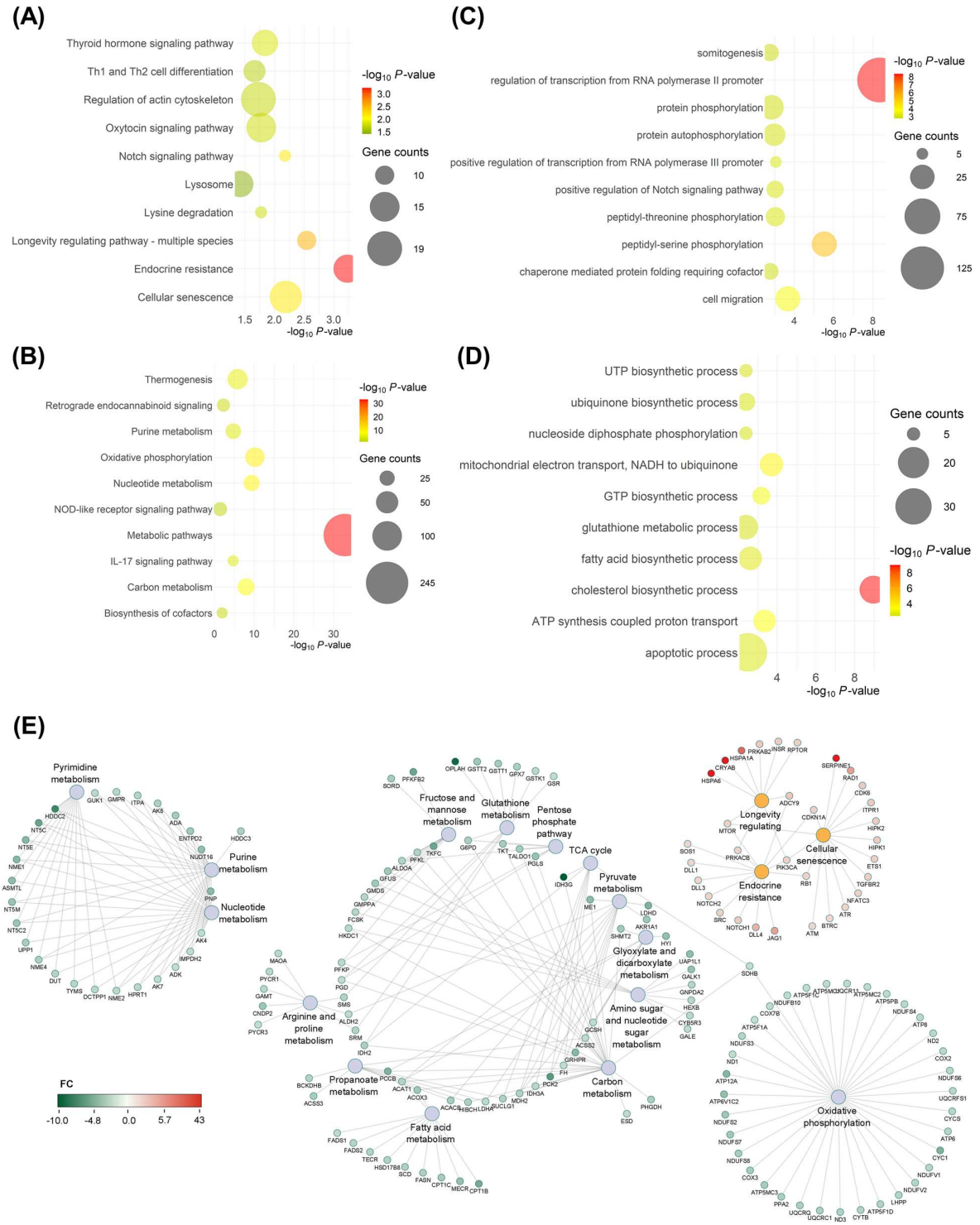


Fig. 6 Oviductal Organoids: Ontological Classification and Interactive Networking. Bubble plots, revealing the top 10 pathways and biological processes targeted by the up- (**A** and **C**) and downregulated genes (**B** and **D**) in the 42 °C compared to the 37 °C groups, respectively. The color and size of each bubble represent the P-value and number of gene counts. Interactive networking of the differentially expressed genes commonly involved in highly enriched pathways including the up- (red) and downregulated (green) genes in the 42 °C compared to the 37 °C groups (**E**)

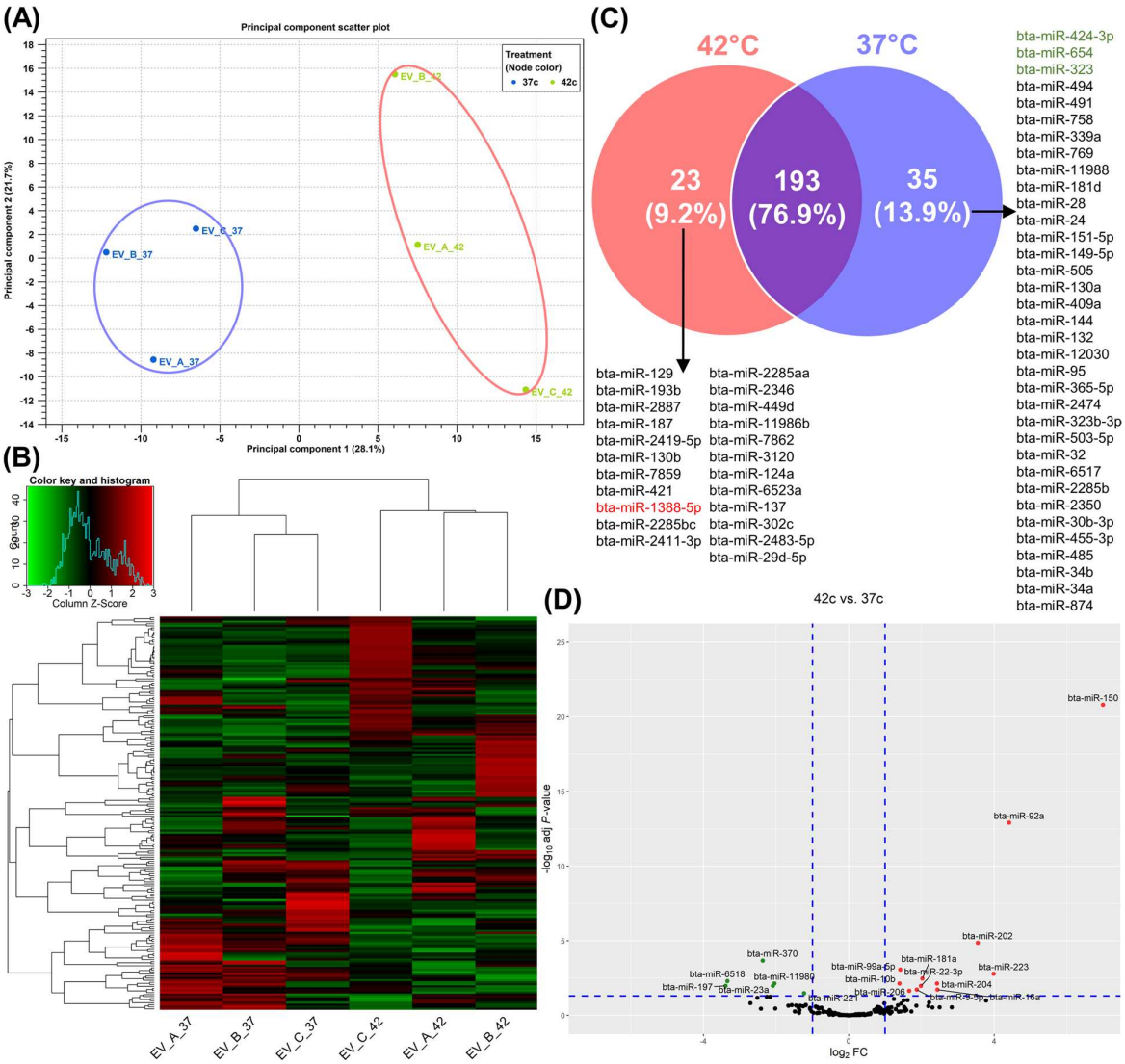


Fig. 7 HS Alters Oviductal Organoid-derived EVs Molecular Cargo: miRNome Extracellular Response. Principal component analysis (PCA) (**A**) and heatmap/hierarchical clustering of oviductal organoid-derived EVs (**B**). Venn diagram indicating exclusively and commonly expressed miRNAs in the 42 °C and 37 °C groups (**C**), red and green miRNAs are significantly different (FDR < 0.05) between the two groups. Volcano plot displaying differentially expressed miRNAs, up- (red) and downregulated (green) in oviductal organoid-derived EVs from the 42 °C compared to 37 °C groups (**D**)

Table 5 and Fig. 11B, respectively. Submission of the initial two significantly conserved motifs to the TOMTOM RBP identification tool showed that sequence motif ([U/A][C/U][C/A][U/G/A/C]A) is potentially targeted and bound by the RNA binding motif 6 (RBM6) protein (Fig. 11C), while sequence motif ([C/U][U/A]GU) is potentially targeted and bound by human antigen R (HuR) and zinc finger CysCysCysHis domain-containing protein 14 (ZC3H14) proteins (Fig. 11D).

Discussion

Oviductal fluid containing EVs have been identified as a major component safeguarding gametes from environmental stress [37, 38] and is regarded as the optimal milieu in which its composition reflects oviductal physiology [39]. Recent efforts have aimed to study the effects of HS on the oviduct both in vivo [40] and in vitro [41] through BOECs and EVs known to largely contribute and responsibly impact the composition

Table 3 Top 20 expressed miRNAs in oviductal organoid-derived EVs from the HS (42 °C) and thermoneutral (37 °C) groups

miRNA	42 °C Group CPM	%[a]	miRNA	37 °C Group CPM	%[a]
bta-miR-1246	714,796.52	52.39	bta-miR-1246	363,004.63	44.35
bta-miR-148a	91,700.77	6.72	bta-miR-148a	63,584.52	7.77
bta-miR-21-5p	66,565.11	4.88	bta-miR-21-5p	43,902.13	5.36
bta-miR-451	63,787.82	4.68	bta-let-7a-5p	38,199.05	4.67
bta-miR-92a	52,778.22	3.87	bta-miR-378	33,327.83	4.07
bta-miR-122	39,526.19	2.90	bta-miR-451	26,116.20	3.19
bta-let-7a-5p	35,926.19	2.63	bta-let-7i	22,986.77	2.81
bta-let-7i	25,351.78	1.86	bta-let-7f	20,881.75	2.55
bta-miR-378	23,826.87	1.75	bta-miR-122	19,106.09	2.33
bta-let-7f	19,848.71	1.45	bta-let-7b	17,898.58	2.19
bta-miR-26a	19,314.54	1.42	bta-miR-26a	16,336.63	2.00
bta-let-7b	17,836.14	1.31	bta-miR-151-3p	10,162.43	1.24
bta-miR-10b	12,289.04	0.90	bta-miR-200b	8044.04	0.98
bta-miR-151-3p	12,105.22	0.89	bta-miR-320a	6426.09	0.79
bta-miR-99a-5p	10,290.88	0.75	bta-miR-200c	5618.62	0.69
bta-miR-200b	9131.74	0.67	bta-let-7 g	5587.82	0.68
bta-miR-10a	7387.11	0.54	bta-miR-100	5124.45	0.63
bta-miR-143	6627.53	0.49	bta-miR-30d	5002.99	0.61
bta-miR-30d	6243.01	0.46	bta-miR-10b	4666.79	0.57
bta-miR-486	6147.07	0.45	bta-miR-192	4474.81	0.55

CPM average Counts Per Million mapped reads

[a] Percentage of the miRNA sequence reads

Table 4 DE-miRNAs in oviductal organoid-derived EVs from the HS (42 °C) compared to the thermoneutral (37 °C) groups

Upregulated miRNA	FC	FDR	*FC* Fold Change, *FDR* False Discovery Rate Downregulated miRNA	FC	FDR
bta-miR-150	127.29	1.56E-21	bta-miR-221	-2.35	3.27E-02
bta-miR-92a	21.28	1.24E-13	bta-miR-11980	-4.13	7.36E-03
bta-miR-223	15.82	1.61E-03	bta-miR-23a	-4.26	1.04E-02
bta-miR-202	11.69	1.38E-05	bta-miR-370	-5.17	2.14E-04
bta-miR-16a	5.42	1.89E-02	bta-miR-6518	-10.17	5.05E-03
bta-miR-204	5.36	7.36E-03	bta-miR-197	-10.51	1.04E-02
bta-miR-181a	4.06	3.43E-03			
bta-miR-22-3p	3.96	1.04E-02			
bta-miR-9-5p	3.65	1.89E-02			
bta-miR-206	3.16	2.27E-02			
bta-miR-99a-5p	2.66	8.58E-04			
bta-miR-10b	2.62	7.36E-03			

FC Fold Change, *FDR* False Discovery Rate

of the oviductal fluid. In vivo, alterations in oviductal cells' gene expression and EV concentrations have been reported, while similar significant alterations in *HSP70* and *OVGP1* expression were reported in vitro. *OVGP1* is a hormonally-regulated, carbohydrate-rich and traditionally-expressed protein-coding gene known to regulate receptivity and trophoblast adhesion. Alimiñana et al. [26], investigated the differential protein contents in BOECs and oviduct-derived EVs from in vivo and in vitro origin and revealed the absence of OVGP1 in in vitro cultured BOECs and corresponding EVs. Alternatively, in the present study oviductal organoids morphologically mirror their original tissue by forming round, cystic structures accompanied with

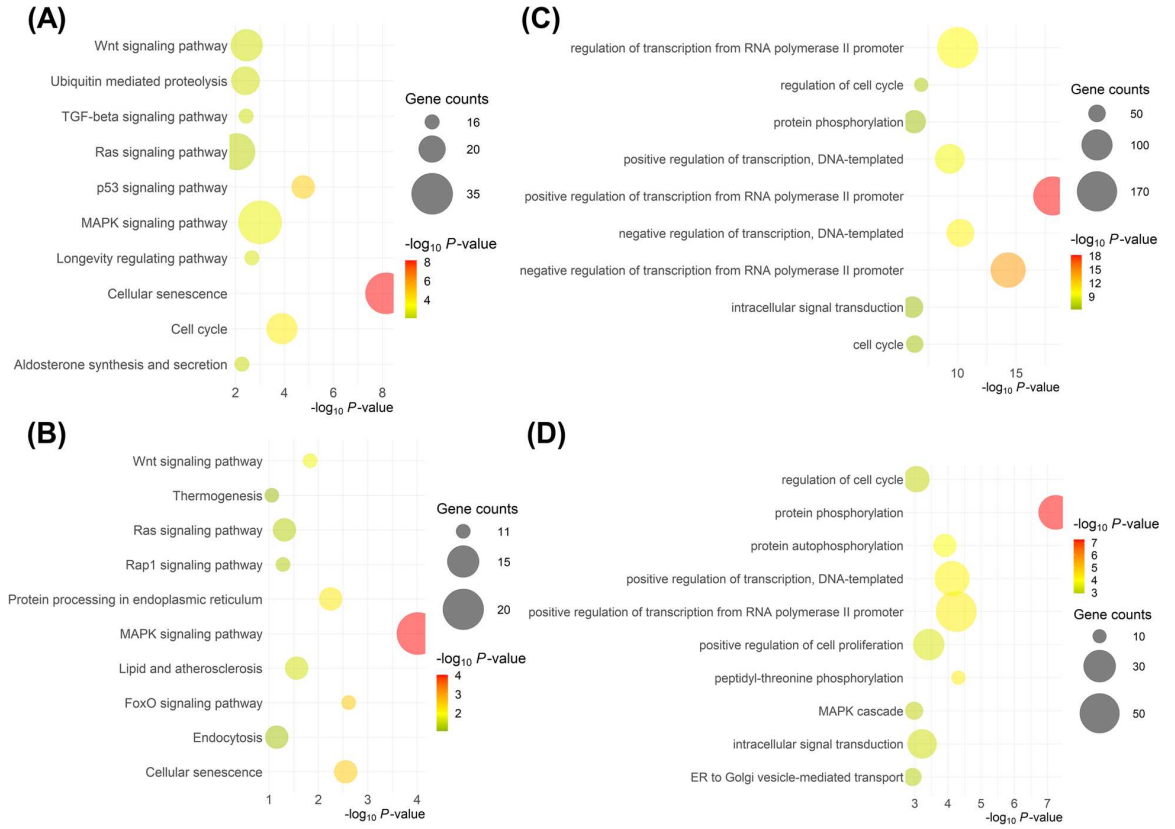


Fig. 8 Oviductal Organoid-derived EV-miRNAs: Ontological Classification. Bubble plots, revealing the top 10 pathways and biological processes targeted by the up- (**A** and **C**) and downregulated miRNAs (**B** and **D**), respectively in the 42 ℃ compared to the 37 ℃ groups. The color and size of each bubble represent the P-value and number of miRNA target genes, respectively

an apical polarity in regard to a central lumen exhibiting encircling microvilli, consistent with previous reports of fallopian/oviductal organoids in mice [30, 31] and humans [29]. Moreover, our study revealed the detection of OVGP1, ZO1, and FOXJ1 in in vitro cultured organoids after passaging, indicating the suitability of our 3-D extended culture model to persist naïve-like identity, vital for the interpretation of the results in regard to oviductal physiology. Similarly, our gene panel revealed minimal differences amid in vitro cultured organoids in the mRNA expression of genes regulating cell proliferation and adhesion (*MKI67* and *CDH1*), ciliated cell function and differentiation (*LRRC6*, *TUBA1A*, *TUBA1B* and *TUBA1C*), and hormonal prostaglandin function (*PTGS2*, *PTGES* and *OXTR*) compared to naïve in vivo BOECs. Collectively, interspersed FOXJ1 + cells indicate ciliated cell presence, while stable *MKI67* mRNA levels amid in vitro cultured oviductal organoids and naïve in vivo BOECs reveal their active proliferation capacity. Similar to our previous work in endometrial organoids [42], in the present study ZO1 was found to be localized in both the nucleus and the cytoplasm. Such findings have been previously reported in monlayer cultures and several cell lines, and is posed to be correlated to the stage of cell growth and inversely connected to the extent and/or maturity of intercellular contacts [43]. Our study dually noted a significant increase in the transcript abundance for *TUBA1C*, which was also shown to be upregulated in oviductal fluid collected from the contra- versus ipsilateral bovine oviduct [44]. Additionally, in in vitro cultured HS oviductal organoids, the mRNA expression of *PTGS2* was signifncatly lower than in naïve in vivo BOECs, potentially indicating that the organoid cultures are not highly affected by in vitro 'culture shock,' which formally leads to an overproduction of reactive oxygen species (ROS) amidst cells [45], which has been shown in vivo [46] and in vitro [47] in regard to the oviduct. Additionally, in other studies the 3-D reproductive

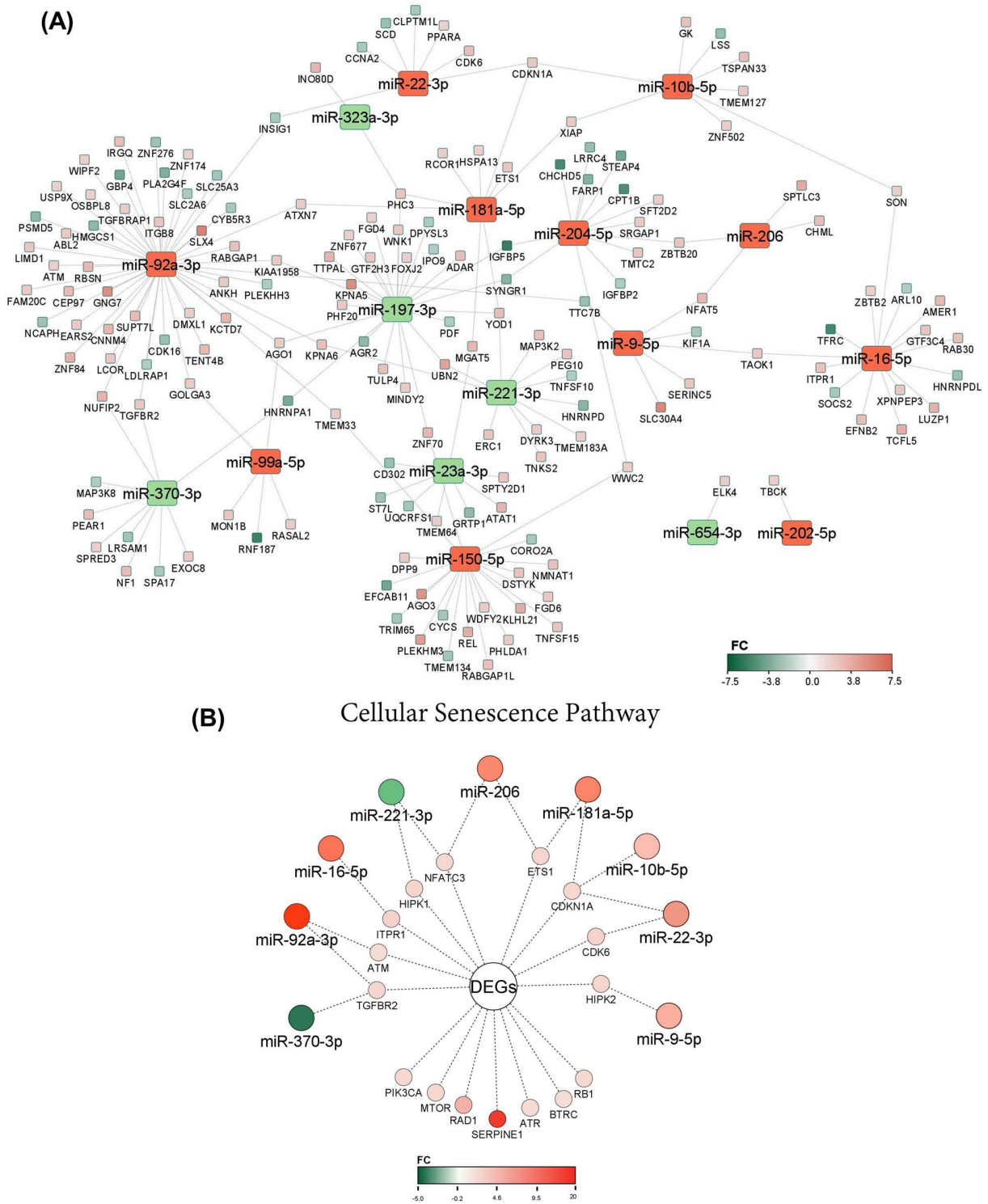


Fig. 9 Oviductal Organoid DE-EV-miRNAs and DEGs Interaction Network. Interactive networking of common experimentally validated target genes of the DE-EV-miRNAs and the organoids DEGs in the 42 °C compared to the 37 °C groups (**A**). A network of the DEGs involved in the cellular senescence pathway and targeted by the DE-EV-miRNAs (**B**)

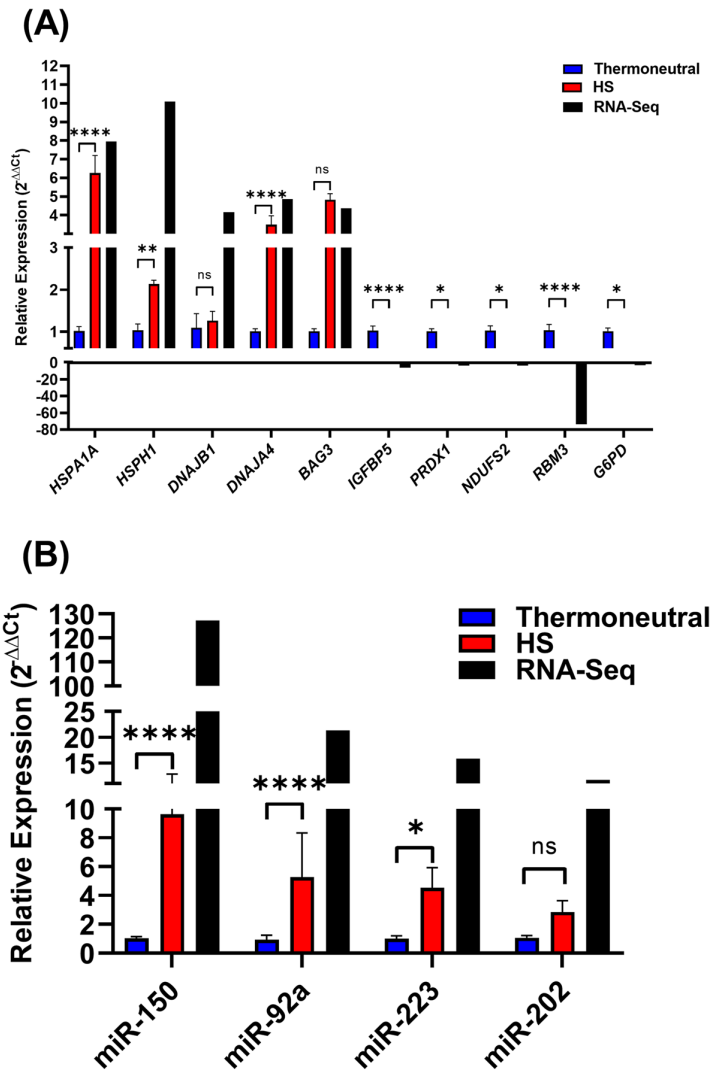


Fig. 10 Quantitative Real Time PCR Validation. Expression validation of the selected DE-genes (**A**) and -miRNAs (**B**) compared against values calculated via RNA-seq analysis. Data are shown as the mean ± SEM and the differences between means were analyzed using one-way ANOVA followed by Tukey's Multiple Comparisons Test in biologically independent samples ($n = 4$). Statistical significance (*) between the 42 °C compared to the 37 °C groups were determined at ($p < 0.05$)

structures (organoids) have been shown to tolerably respond to exogenous hormonal stimuli [29, 48–50], a hallmark feature of mimicking in vivo function. In support of this notion, it was previously shown that small RNA profiles from 3-D culture-derived EVs of cervical cancer HeLa cells also showed to exhibit striking similarity (~ 96%) to circulating EVs found in vivo [51]. In this study, we have demonstrated for the first time the potential of oviductal organoids to systematically study the physiological and dynamic response of the oviduct to seasonal heat stress.

HS-induced transcriptomic changes in oviductal organoids

High-throughput transcriptomic analysis of oviductal organoids cultured in vitro under thermoneutral and HS conditions revealed clear temperature-dependent clustering, indicative of a substantial physiological change governing oviductal organoids under HS conditions. In view of the oviduct and considering damaged cellular activity is prompted through HS (i.e. redox status and mitochondrial function, as well as protein folding), it is likely that the cellular response to the environment, acting as a dynamic machine, continuously diversifies and

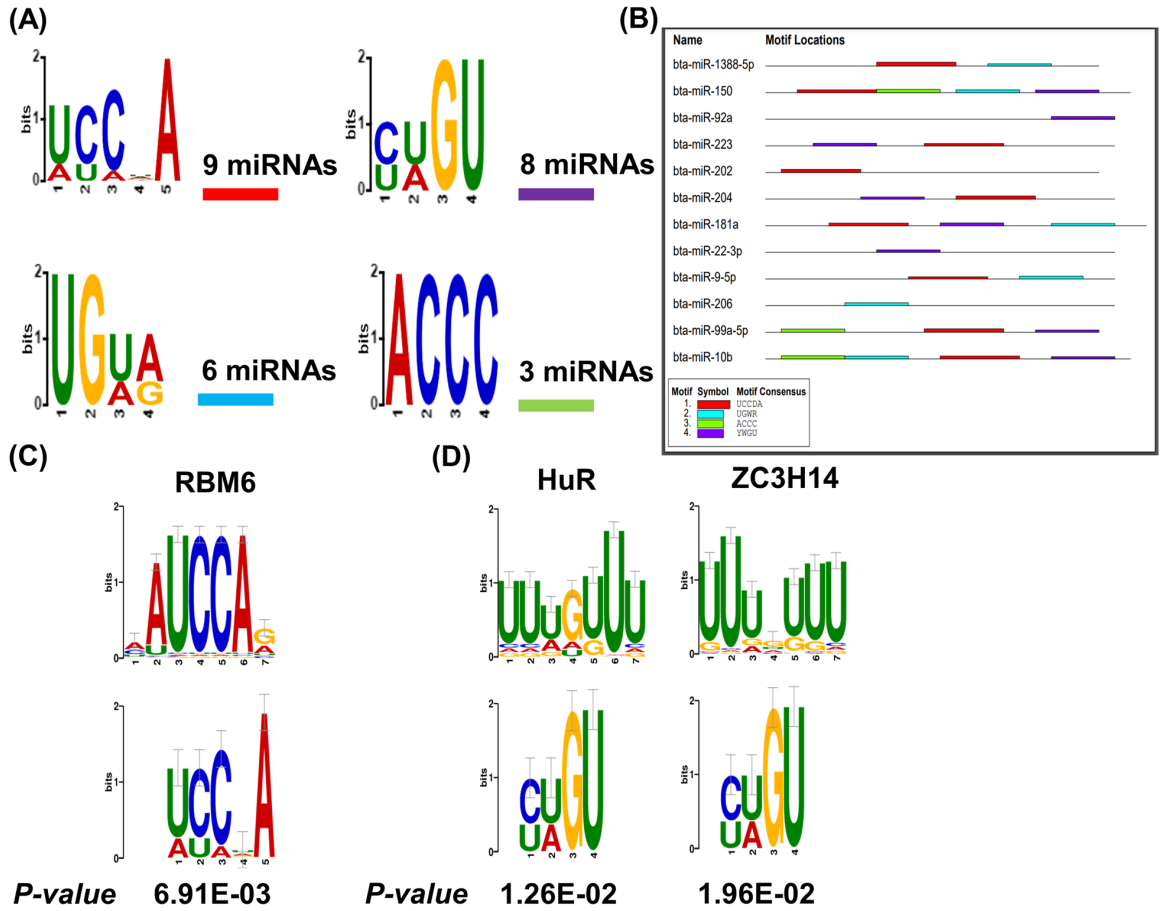
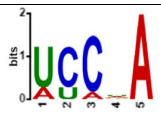
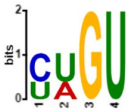


Fig. 11 miRNA sequence motif analysis. Four identified, over-represented miRNA sequence motifs located amongst the upregulated miRNAs in differing numbers in the 42 °C compared to the 37 °C groups (**A**). Table depicting the location and distribution of the over-represented miRNA sequence motifs positioning on the upregulated miRNAs (**B**). Alignments of the ([U/A][C/U][C/A][U/G/A/C]A(**C**) and the [C/U][U/A]GU (**D**) miRNA sequence motifs with known RNA-binding proteins. ($p < 0.05$)

shifts an optimal milieu to a substandard microenvironment. These findings are in consonance with a recent in vivo study showing alterations in oviductal cells' (ipsilateral and contralateral) gene expression from dairy cows under HS conditions [40]. Notably in our study, we found that of the 12,774 expressed genes, 11,725 genes were mutually expressed amongst both groups. Importantly, in terms of oviductal organoids long-term maintenance of naive-like physiology, in the present study, the RNA-sequencing dataset validated the presence of marker genes for BOEC function (*OVGP1*, *GPX4* and *HMGCR*) [52–55], which were stably expressed amid both groups of oviductal organoids following passaging during in vitro culture. Hence, the presented long-term 3-D organoid culture system functionally recapitulates certain validated aspects of the in vivo oviduct to satisfy novel descriptive studies, exemplified here, needed to address challenges in comprehending the early embryo–maternal interactions to conduct further functional studies.

Comparative analysis revealed, among the top highly abundant genes in both groups, we found genes related to early embryonic development (*ACTB* and *UBA52*), prostaglandin biosynthesis and the establishment/maintenance of pregnancy (*COX1*, *COX2* and *CST6*), as well as embryonic cellular senescence (*RPLP1* and *RPS15*). Uniquely, *COX1* is found to be upregulated as the transient embryo is present within the oviduct, suggesting synthesized prostaglandins interact with the embryo and facilitate embryo–maternal communication [56]. However, HS has been shown to largely disrupt the balance of vaginal prostaglandins (PGE2 and PGF2a), reducing oviductal smooth muscle motility, which is an important catalyst for the transportation of the gamete/

Table 5 Identified motif positioning on the upregulated miRNAs in the HS (42 °C) compared to the thermoneutral (37 °C) groups

miRNA	*p*-value		miRNA	*p*-value	
bta-miR-1388-5p	8.73E-04	AGGACUGUCCAACCUGAGAAU	bta-miR-181a	5.59E-03	AACAUUCAACGCUGUCGGUGAGUU
bta-miR-99a-5p	1.70E-03	AACCCGUAGAUCCGAUCUUGU	bta-miR-92a	5.59E-03	UAUUGCACUUGUCCCGGCCUGU
bta-miR-204	3.06E-03	UUCCCUUUGUCAUCCUAUGCCU	bta-miR-22-3p	9.20E-03	AGUUCUUCAGUGGCAAGCUUUA
bta-miR-202	3.06E-03	UUCCUAUGCAUAUACUUCUUU	bta-miR-223	9.20E-03	UGUCAGUUUGUCAAAUACCCCA
bta-miR-10b	5.07E-03	UACCCUGUAGAACCGAAUUUGUG	bta-miR-150	9.20E-03	UCUCCCAACCCUUGUACCAGUGU
bta-miR-150	5.07E-03	UCUCCCAACCCUUGUACCAGUGU	bta-miR-10b	1.75E-02	UACCCUGUAGAACCGAAUUUGUG
bta-miR-181a	7.23E-03	AACAUUCAACGCUGUCGGUGAGUU	bta-miR-99a-5p	1.75E-02	AACCCGUAGAUCCGAUCUUGU
bta-miR-223	1.19E-02	UGUCAGUUUGUCAAAUACCCCA	bta-miR-204	1.75E-02	UUCCCUUUGUCAUCCUAUGCCU
bta-miR-9-5p	1.88E-02	UCUUUGGUUAUCUAGCUGUAUG			

embryo [57]. Correspondingly, in high abundance, were genes encoding functions in the sperm-oviduct interactions preceding early embryo development (*HSPA8* and *HSPA1A*), as well as genes reported to exert cryoprotective and anti-apoptotic effects as a consequence of stress (*HSPB1*). It is widely known that environmental cellular stress is directly connected to an immediate rapid induction of various heat shock proteins (HSPs). Convincing reports suggest HSPs (especially *HSPA1* and *HSPB1*), cohesively act as protective proteins through potentially downregulating signaling events leading to apoptosis [58]. Although, HSPs act as molecular chaperones critical for the maintenance of cellular homeostasis, increased amounts of HSPs can facilitate the suppression of overexpressed/mutated genes resulting from a loss of p53 function [59].

Upregulated genes (*CRISPLD2*, *HSPA6*, *SERPINE1*) in the thermal stressed groups could serve as potential indicators of the response of oviductal organoids to environmental heat stress. Higher expression of *CRISPLD2*, a secreted glycoprotein and target gene regulated by the P4-PR response, has been shown to potentially mediate the stromal-epithelial cross-talk during implantation and decidualization, largely dependent upon hormonal regulation [60]. Similarly, the HSP family member, *HSPA6*, shown to be involved in cellular response to stress, has been reported to be highly expressed in the ipsilateral oviduct likely in preparation for the presence of gametes and to facilitate embryo development [44]. Notably in our study, *SERPINE1*, which encodes a proteinase inhibitor, is shown to be involved in functional pathways governing cellular senescence. Cellular senescence contributes to the age-related decline in reproductive function and is known as a cellular response to stress aimed at inhibiting the proliferation of damaged cells, ultimately leading to a state of permanent growth arrest [61, 62]. Additionally, reports using *SERINE1* protease inhibitors to suppress oviductal protease activity through mediating the estrogen-epithelial ERa signaling, have been shown to be preeminent for fertilization and preimplantation embryo development [63].

In mammalian reproduction, it is widely known that mitochondria are inherited maternally and serve as energy factories, synthesizing the majority of the cells' ATP predominantly through oxidative phosphorylation, in part, holding pertinent roles in metabolic functions governing embryonic development [64]. Results from the current study revealed the suppression of 1,348 genes in oviductal organoids following exposure to thermal stress, found to be involved in pathways related to oxidative phosphorylation and metabolic processes. Among the genes downregulated in oviductal organoids as a result of exposure to HS, *NDUFS8*, *NDUFS7*, *NDUFS6*, *NDUFS3*, *NDUFS2*, *COQ9*, *NDUFV2*, *ND3*, *NDUFV1*, *ND2* and *ATP5F1A*, *ATP5PB*, *ATP8*, *ATP6*, *ATP5MC2*, *ATP5MC3*, *ATP5F1C*, *ATP5F1D*, *ATP5MC1* are found to be involved in biological processes associated with mitochondrial function and ATP synthesis. Previous reports indicate that NADPH, supplies an antioxidant defense, while NADH promotes an increase in the oxidant load,

generating ROS and sustained oxidative stress [65]. Therefore, genes suppressing the metabolic activity of high-functioning pathways (TCA cycle, pyruvate metabolism, fatty acid metabolism, etc.), promote an imbalance in mitochondrial NADH and NADPH, effecting ATP production, which leads to impairments in mitochondrial function, partly due to suppressed oxidative phosphorylation function. Interestingly, highly downregulated (FC = -73.4) *RBM3*, a stress-responsive gene, was shown to potentially have a mechanistic function to counteract the regulatory role of miRNAs by increasing inefficiencies in global protein synthesis under conditions of stress [66]. On the other hand, in agreeance with Stamperna and colleagues, our study concurred among the DEGs, the downregulation of *LOC512548* and *HP* (contralateral), as well as *SOCS3* (ipsilateral) in oviductal epithelial cells from dairy cows during the summer versus spring season [40]. Antileukoproteinase's (*LOC512548)* role in inhibiting serine proteases, have been found to have antibiotic and anti-inflammatory functions in the human endometrium [67], as well as a coincidental function amidst the sperm-oocyte interaction in the human oviduct [68]. Taken together, our results demonstrate that the potential impact of seasonal heat stress on oviductal physiology is mediated by the dysregulation of genes responsible for mitochondrial function and energy metabolism, as well as reproductive and immune system responses.

Oviductal organoid-derived EV-miRNA profiles in response to HS

Previous studies from our lab demonstrated the divergent EV-mediated molecular response of bovine granulosa cells to HS through their encapsulated miRNA cargoes, revealing their subsequent protective capacity against recurrent HS following co-incubation among naïve granulosa cells [14], as well as oocytes and embryos [15]. Similarly, in the present study, we detected a total of 251 EV-coupled miRNAs with 193 mutually expressed and 3 miRNAs (bta-miR-1246, bta-miR-148a, bta-miR-21-5p) sequentially expressed as the first, second and third most abundant among both groups. In vitro functional analysis in a previously reported study demonstrated the antiapoptotic measures of bta-miR-1246 by targeting *PCBP2* and *CREBL2* in HEK293 cells [69]. In accordance with others [70, 71], our study revealed a high prevalence of bta-miR-148a, which is found to target *DNMT1* and improve the developmental capacity of porcine somatic cell nuclear transfer embryos [72]. Furthermore, studies in mice showed that miR-21 targets *PTEN* [73], leading to the hypothesis that bta-miR-21-5p activity may activate AKT and ERK1/2 signaling pathways in the bovine corpus luteum to promote angiogenesis [74].

Specialized miRNAs packaged into EVs (23 exclusively expressed), reveal temperature-dependent variations in EV-encapsulated bioactive cargo resulting from oviductal organoids subjected to either HS or thermoneutral conditions. Among the miRNAs enriched in EVs released in response to HS, bta-miR-150, bta-miR-92a, bta-miR223 and bta-miR-202 were at minimum tenfold higher than in the thermoneutral groups. Pathway analysis of genes enriched by upregulated miRNAs include cellular senesce and p53 signaling pathways, which are critical in cell cycle processes involving proliferation and the maintenance of genomic and cellular integrity. Interestingly, in the present study, pathways related to cellular senescence are also the most significant pathways enriched by the DEGs in the oviductal organoids in response to HS. To our knowledge, this is the first evidence indicating bovine oviductal organoids use cellular senescence as a stress response mechanism to prevent stress-induced damage including oxidative stress, genotoxic damages and inflammation [75]. Notably, previous reports show that increased expression of miR-150 downregulates pro-apoptotic $P2X_7$ mRNA expression in human cervical epithelial cancer cells [76]. Furthermore, as indicated in zebrafish, miR-92a-3p [77] and miR-202-5P [78], are maternally-derived miRNAs with critical functions in gametogenesis. It was shown that miR-92a-3p targets wee2, a cyclin-dependent kinase 1 inhibitor, regulating the cell cycle prior to the maternal-zygotic transition in cleavage-stage zebrafish embryos [77]. Additionally, miR-202-5P, which is enriched in EVs released in response to HS was also found to be highly abundant in early zebrafish embryos, suggesting its role in regulating primordial germ cell development throughout embryogenesis [78]. Therefore, although precautionary measures should be taken into account interpreting the species phylogenetic relationship, it is possible that oviductal organoids release EVs with the potential to shuttle specific miRNAs having a physiological role in early embryo development. Further functional studies to investigate the role of oviductal stress-associated EV-coupled miRNAs in regulating oviductal cells survival and potential to mediate early embryo development, is of great biological value.

In contrast to those miRNAs enriched in EVs released from oviductal organoids in response to HS, 35 miRNAs were found to be exclusively detected in EVs released from oviductal organoids cultured under thermoneutral conditions. Among the miRNAs downregulated in EVs from the HS groups compared to the thermoneutral groups were: bta-miR-197, bta-miR-6518, bta-miR-370, bta-miR-23a, bta-miR-11980 and bta-miR-221; with bta-miR-424-3P, bta-miR-654 and bta-miR-323 exclusively-differentially expressed in the EVs from thermoneutral

cultured oviductal organoids. We found genes targeted by the downregulated miRNAs involve pathways regulating cellular senescence, as well as MAPK and FoxO signaling, with functions in cell-cycle arrest and intracellular signal transduction. Recent studies show miR-197-3p to be dramatically downregulated in ovarian tissues of patients with polycystic ovarian syndrome and in KGN human granulosa cell lines [79]. It was also confirmed that miR-197-3p targets *CUL3*, and its overexpression induces apoptosis by modulating caspase 3 and Bax (apoptotic) and bcl-2 (anti-apoptotic) protein expressions [79]. Similar reports indicate miR-370-3p inhibits cell proliferation and induces apoptosis in endometriotic cyst stromal cells by suppressing SF-1 [80]. These findings along with ours suggests the dysregulation of the aforementioned miRNAs due to HS might lead to the development of novel therapeutic targets underlying reproductive anomalies, organismal aging and human diseases.

We have previously shown the relevance of EV-coupled miRNA signaling in reproductive cells, in which certain miRNA species are selectively enriched in EVs in response to various stressors [14]. It seems clear that selective enrichment of EV-miRNAs stems in part from the physiological response of oviductal organoids to HS, with potential negative impacts on bystander cells and the gamete/embryo. However, detailed mechanisms underpinning how specific miRNAs are enriched in EVs released in response to HS are largely unknown. Recent reports indicated the involvement of specific RNA binding proteins (RBPs) and unique miRNA sequence motifs in EV-miRNA sorting versus cellular retention in a tissue/cell dependent manner [33–36]. To this point, in order to shed light on the potential mechanisms involved in miRNA sorting into EVs by oviductal organoids in response to HS, we employed computational technologies to identify miRNA sequence motifs and their target RBPs for 12 miRNAs enriched in EVs released from oviductal organoids following exposure to HS. Accordingly, two miRNA sequence motifs shared by 9 out of the 12 miRNAs were found in EV-coupled miRNAs released in response to HS. Further in silico analysis revealed that the identified motifs are recognized by RBPs, namely: RBM6, HuR and ZC3H14. Among these previous studies, it has been revealed that HuR, a regulator of cytoplasmic mRNA fate, alters the cellular response to proliferative, stress, apoptotic, differentiation, senescence, inflammatory and immune stimuli [81]. Moreover, cellular oxidative stress has implicated HuR to impair responses to oxidant damage that characterizes cellular senescence and advancing age [32]. Phosphorylated HuR using an ATP analog activated PKCα, promoted the export of HuR to the cytoplasm, where its target *COX2*, became more stable [32]. Notably, *COX1* and *COX2* play important roles in the smooth muscle layer and epithelial cells within the oviduct [56]. Regardless, further studies are required to investigate the interplay between miRNA motifs and RBPs in mediating the oviductal response to external stimuli, such as HS and their impacts on cellular survival and function during the maternal-embryo interaction.

Conclusions

Our study incorporates both an innovative approach and novel techniques pushing the threshold to: 1) generate a new viewpoint on the oviducts' capacity to undergo critical changes to external stimuli to safeguard the resulting gamete/embryo; 2) establish multifaceted, functional studies focused on oviduct signaling (organoids/EVs) and signatures potentially regulating stress response; 3) a potential platform to generate physiologically relevant EVs for implementation in current assisted reproductive technologies systems, aiming to enhance embryo survival and viability under various environmental and pathophysiological conditions (i.e. bystander effect). Finally, we have provided a comprehensive insight into the cellular and extracellular response of oviductal organoids to HS, yielding a structural footing to investigate the functional applicability and regulatory role of RNA cargoes (mRNA and miRNA) in modulating the fine-tuned oviductal microenvironment, essential for early stages of life. Further studies stemming from this work are needed to focus on the functional analysis of genes and EV-coupled miRNAs and their involvement in mediating the impact of physiological changes amid the oviduct microenvironment on the developing gamete/embryo and subsequent establishment of pregnancy. Taken together, oviductal organoids thusly provide a non-invasive approach to investigate normal and pathological reproductive processes, from a traditionally inaccessible organ.

Methods

Collection of bovine oviductal epithelial cells (BOECs)

Complete reproductive tracts including oviducts and ovaries ($n=10$; a pool of 2 animals per replicate) were obtained from a local slaughterhouse (JBS Foods, USA) at the discretion of BPO Parts LLC (La Salle, CO) and transported within 1 h following collection via an insulated box containing physiological saline solution (0.9% NaCl) warmed to 37 °C to the Animal Reproduction and Biotechnology Laboratory for processing. Upon arrival, reproductive tracts were evaluated for the stage of the estrous cycle, dependent on the presence or absence of a fully formed, active corpus luteum with visible vasculature around its periphery. Resected ovaries containing complete contra- and ipsilateral oviducts from assessed stage II, diestrus tracts were initially washed

through a physiological, warmed saline solution and subjected to a 70% ethanol rinse, followed by repetitive washings through a warmed saline solution. To offset the variability in abattoir-derived reproductive material, the same oviducts were represented in samples subjected to the differing ambient culture conditions (37 °C and 42 °C). Oviducts were trimmed from surrounding the tissues,opened longitudinally and processed according to previously defined measures [82, 83] by exposing the oviductal lumen, followed by scraping with a scalpel blade (Hill-Rom Holdings 371,120) in Handling Medium (HM) [HM; MEM Eagle with Earle's Salts (Sigma-Aldrich M2279) containing 25 mM HEPES (Sigma-Aldrich H0887), 100 U/ml Penicillin-0.1 mg/ml Streptomycin (Sigma-Aldrich P4333), 0.1 mM Pyruvate (Gibco 11,360–070), 2 mM Glutamax (Gibco 35,050–061) and Bovine Serum Albumin (5% v/v) (Sigma-Aldrich A9418)] to collect epithelial cells from the entire length of the oviduct for dissociation by enzymatic digestion. Subsequently, the solutions were passed through a 40 µm cell strainer (Greiner 542,040) to remove residual stromal and inflammatory cells then backwashed with RPMI-1640 medium (Gibco 11,875–085). The ensuing suspensions were then pelletized through centrifugation at 1000 xg for 10 min, washed in 1 mL DMEM/F-12 (Gibco 21,041–025), and finally resuspended in 20x (v/v) phenol red-free, growth factor reduced UltiMatrix (Cultrex; Boitechne BME001-05).

Oviductal organoid culture

Parameters to establish organoid cultures were determined as we have previously described [50]. Unless indicated otherwise, all chemicals were manufactured by Sigma-Aldrich. Briefly, the homogenized UltiMatrix suspension, as described above, was aliquoted in 25 µL microdrops in a 48-well culture plate (Corning 3548), and allowed to strengthen formation for 30 min at 37 °C. The 3-D suspensions were then overlayed with 250 µL of Organoid Medium (OM) (OM; DMEM/F-12 without phenol red (Gibco 21,041–025), 100 µg/mL primocin (Invivogen ant-pm-1), 2.5 mM L-glutamine, 2% B27 Plus (Gibco A35828-01), 1% N2 (Gibco 17,502–048), 1% Insulin–transferrin–selenium (Gibco 41,400–045), 1 mM nicotinamide (N0636), 50 ng/mL recombinant human EGF (R&D Systems 236-EG), 50 ng/mL recombinant human FGF-10 (PeproTech 100–26), 100 ng/mL recombinant human Noggin (R&D systems 6057-NG/CF), 0.5 µM TGFβ/Alk inhibitor A83-01 (Tocris 2939), 1.25 mM N-acetyl-L-cysteine (EMD Millipore 106,425), 10 µM SB202190 (S7067), 10 µM Y27632 (EMD Millipore 688,000) as previously described [50, 82, 83]. For all experiments, organoid culture suspensions were in a confined chamber regulated to 37 °C and 5% CO_2 in humidified air for growth and development prior to exposure to 42 °C to induce thermal stress. The OM was refreshed by half (v/v) every two to three days with passaging occurring weekly every 7th day. For passaging, the UltiMatrix containing the organoids were collected and pelletized via centrifugation at 1,000 xg for 10 min, washed in 1 mL of DMEM/F-12 with agitation applied from vigorous pipetting to induce dissociation and yield mostly single cells, followed by replating according to the same procedure described above. Organoids of low passage number (P1D7) were used for the experiments described.

Histology

Histological preparation of intact oviduct and oviductal organoids was performed as we have previously described [82, 83]. Briefly, organoid VitroGel® suspensions were soaked in 250 µL of VitroGel® Cell Recovery Solution and washed with DMEM/F-12 followed by DPBS (1X) and centrifuged at 600 xg for 6 min. After centrifugation, organoid pellets were fixed in 4% paraformaldehyde for 30 min and embedded in 2% agarose gel (Bio-Rad 1,613,101). Agarose-embedded organoids were stored in 70% ethanol until processing, then embedded in paraffin wax, sectioned (6 µm), and stained using hematoxylin and eosin (H&E) and assessed for normal oviductal epithelial cell architecture.

Immunohistochemistry

Organoid preparation for immunohistochemistry was performed as we have previously described [50, 82, 83]. Briefly, paraffin wax embedded organoids were mounted on Superfrost Plus slides, deparaffinized then rehydrated through graded alcohols until distilled water. Antigen retrieval was then accomplished by subjection to citrate buffer (pH 6; 96 °C for 20 min) and blocked with hydrogen peroxide then washed in distilled water. Slides were then incubated with primary (4 °C overnight) and HRP-conjugated and/or biotinylated secondary antibodies (OVGP1; Biotin Ms IgG, ZO1; Rb IgG HRP, and FOXJ1; Biotin Rb IgG), respectively. A list of the antibodies and dilutions is indicated in (Additional file 9: Table S9). Negative reagent controls provided utilized the same staining procedures in the absence of the primary antobody incubation step. Prior to microscopy evaluation, slides were activated using the RTU Vectastain kit (Vector Laboratories) for 30 min and visualized using Vectastain ABC-HRP and DAB substrate solution (Vector Laboratories) counterstained with hematoxylin. Incubations took place at a room temperature environment with TBS-T solution used as a washing buffer. Slides were assessed for localization and presence of OVGP1, ZO1, and FOXJ1 staining.

Exposure of oviductal organoids to heat stress

Following the culmination of the first passage (14 days from initial collection), organoids were removed from UltiMatrix using Organoid Harvesting Solution (Cultrex; Biotechne 3700–100-01) and transferred to VitroGel® (TheWell Bioscience VHM04-K), a synthetic, xeno-free extracellular matrix. At this point, the 3-D matrices were incubated for 30 min at 37 °C to become less fluidic, according to the procedure described above. Finally, the OM was replenished followed by culturing for an initial 24 h priming period at 37 °C and 5% CO_2 in humidified air. Thermoneutral organoids remained at 37 °C for an additional 24 h, while for experiments with heat stress organoids were transferred to a confined chamber regulated to 42 °C in an atmosphere of 5% CO_2 in humidified air for the remaining 24 h. Experiments were replicated a total of eight times to gauge variability in abattoir-derived reproductive material for both culture environments.

Collection of cultured oviductal organoids and conditioned medium for downstream analysis

Following the collection of conditioned OM, the 3-D organoid suspensions were collected and suspended in VitroGel® Cell Recovery Solution (TheWell Bioscience MS03-100), washed with DMEM/F-12 and pelletized by centrifugation at 600 xg for 6 min. Organoid pellets were snap frozen in liquid nitrogen and stored at -80 °C for downstream use. The EV-containing conditioned OM were then centrifuged in sequential order at 500 xg for 10 min, 3,000 xg for 10 min and 17,200 xg for 30 min and filtered through a 0.22 µm sterile filter (Millex® SLGPR33RB) to remove residual cellular contaminants, large particles and protein aggregates. All centrifugation steps were performed at 4 °C. Bovine oviductal organoid-derived EVs were isolated from ~ 10 mL of conditioned OM (8 replicates/treatment group) using ultracentrifugation followed by size exclusion chromatography (SEC). Briefly, OM were subjected to two consecutive rounds of ultracentrifugation at 120,000 xg for 70 min in the Optima XE-90 Ultracentrifuge using the SW 55Ti rotor (Beckman Coulter A94471). Isolated EVs were further standardized by elution in 180 µL of sterile DPBS (1X) (ThermoFisher Scientific 14,190–144) using the Exo-spin™ mini columns (CELL guidance systems EX03-50) according to the manufacturer's protocol. Isolated EVs were then stored at -80 °C for further characterization and molecular analysis.

Characterization and quantification of oviductal organoid-derived EVs

EV identification and characterization were carried out according to guidelines detailed by the International Society for Extracellular Vesicles [84], including EV marker protein validation, nanoparticle concentration/size distribution and morphological visualization as described below. Detailed information regarding experimental procedures has been submitted to the EV-TRACK knowledgebase (https://evtrack.org/) (EVTRACK ID: EV230000)[85].

Western blotting (WB)

Immunoblotting technique was performed for isolated EVs to detect EV and cellular protein markers. For this, proteins were extracted from oviductal organoid cells and the corresponding EVs using RIPA buffer (Marker Gene™ Technologies M2777). Protein lysates were then boiled with 4×Laemmli Sample Buffer (Bio-Rad 1,610,747) and 2-Mercaptoethanol (Bio-Rad 1,610,710) at 95 °C for 5 min prior to loading on a 4–15% (w/v) Tris–Glycine Stain Free Gel (Bio-Rad 4,568,084). Electrophoresis was performed for 15 min at 90 V followed by 30 min at 200 V with Precision Plus Protein Dual Color Standards as a molecular weight marker (Bio-Rad 1,610,374). Separated proteins were transferred (100 V for 60 min at 4 °C) to a 0.20-µm pore nitrocellulose membrane (Bio-Rad 1,620,112) and blocked for 1 h at room temperature in 5% (w/v) Non-Fat Dry Milk (Bio-Rad 1,706,404) and further incubated over night at 4 °C with a primary antibody against each marker protein (System Biosciences; rabbit polyclonal TSG101 EXOAB-TSG101-1, rabbit polyclonal FLOT1 EXOAB-FLOT1-1, rabbit polyclonal CD63 EXOAB-CD63A-1) (Sino Biological rabbit polyclonal Cytochrome C 102139-T42). Afterwards, membranes were washed 5 times with TBS-T solution and exposed to the secondary antibody (System Biosciences; Goat anti Rabbit HRP) for 1 h at room temperature. Bands and signals were enhanced using SuperSignal™ West Pico PLUS Chemiluminescent Substrate (ThermoFisher Scientific 34,579) and imaged using the Chemi-Doc XRS + chemiluminescence system with Image Lab™ Software (version 6.0.1 build 34) (Bio-Rad). A list of the antibodies and dilutions is indicated in (Additional file 9: Table S9) with full length blots provided (Additional file 10: Fig. S1).

Nanoparticle tracking analysis (NTA)

A ZetaView® QUATT 4 Nanosight Instrument (Particle Metrix) was used to determine the particle concentration and size distribution in all EV samples. Briefly, isolated EVs were diluted in sterile DPBS (1X) and loaded into the device and analyzed. Measurements were taken at 11 positions via scatter mode using a 488 nm laser to determine the size distribution and concentration within a sample. Analysis of EV concentrations were calculated using the Zetaview Software (version 8.05.12 SP1) before and after sample dilution.

Transmission electron microscopy (TEM)

For morphological evaluation of oviductal organoid-derived EVs, we performed negative staining TEM of EVs by adsorption onto mesh copper grids with carbon-coated formvar film (Electron Microscopy Sciences FCF 400-Cu). For this, grids were placed film side down on parafilm containing drops of 1% Alcinan Blue 8GX (Sigma-Aldrich 33,864–99-2) for 5 min, followed by washing with ddH_2O for 15 s. Afterwards, the grids were floated on a 5 µL drop of isolated EVs for 10 min, prior to fixing in 2.4% uranyl acetate (Electron Microscopy Sciences 22,400) for 30 s. After fixing, samples were set to dry for imaging on a JEOL JEM-1200 EX transmission electron microscope.

RNA isolation

Total RNA was isolated from organoid cells (5 replicates/treatment group, a pool of samples from 2 animals per replicate) using an RNeasy® Plus Micro Kit (Qiagen 74,034). To remove genomic DNA contaminants, on-column DNA digestion was performed using RNase-free DNase (Qiagen; Hilden, Germany). Similarly, an Exosomal RNA Isolation Kit (Norgen Biotek Corp. 58,000) was used to isolate total RNA enriched with small RNA from oviductal organoid-derived EVs (3 replicates/treatment group, a pool of 2 animals per replicate) according to the manufacturer's protocol. In both cases, RNA quality control and concentration were assessed using an Agilent 2100 Bioanalyzer (Agilent Technologies G2939BA) and NanoDrop™ 2000 Spectrophotometer (ThermoFisher Scientific ND-2000), respectively.

RNA library preparation and sequencing

RNA libraries and next-generation sequencing (NGS) were conducted by Novogene Co., LTD (California, USA). For mRNA transcriptome profiling, RNA libraries were generated using a NEBNext® Ultra™ RNA Library Prep Kit for Illumina (NEB E7530L) and for miRNA profiling, small-RNA libraries were prepared using a TruSeq Small RNA Library Prep Kit (Illumina RS-200) according to the manufacturer's instructions. Library quantity and quality assessments were performed using a Qubit® DNA HS Assay Kit on a Qubit® 2.0 Fluorometer and an Agilent DNA High Sensitivity Kit in an Agilent 2100 Bioanalyzer, respectively. Library concentrations were calculated using quantitative PCR measures then pooled in equimolar ratios and sequenced in a NovaSeq6000 sequencing instrument (Illumina) as paired (150 bases) or single-end (50 bases) reads for the transcriptome and miRNA sequencing, respectively.

RNA-seq data analysis

FASTQ files were generated for each sample using the software bcl2fastq (Illumina) with FastQC tool version 0.11.9 assessing their quality. Data were analyzed using the CLC Genomics Workbench software, version 21 (www.qiagenbioinformatics.com). Trimming of raw sequencing reads was based on quality score (Q-score > 30), ambiguous nucleotides (maximum two nucleotides allowed), read length (≥ 15 nucleotides), and removal of adapter sequences. Reads were mapped to the bovine reference genome (ARS-UCD1.2) and small-RNA reads were annotated against bovine precursor and mature miRNAs listed in the mirBase database (release 22) using the CLC Genomics Workbench RNA-seq Analysis and Quantify miRNA tools, respectively, with default software parameters applied. Normalization of raw expression data was performed using the trimmed mean of M-values (TMM) normalization method [86] and presented as either transcripts per million (TPM) or TMM-adjusted counts per million (CPM), for genes and miRNAs, respectively. For genes, the expression threshold was determined by the zFPKM method using the zFPKM R package v.1.16.0 [87]. The zFPKM transform/normalization method is used to determine, with high consistency, the threshold of expressed transcripts avoiding the low-abundance and biological noise transcripts due to sequencing errors, and/or off-target read mapping. zFPKM values are calculated from the distribution of the log2 (TPM values) after fitting to the right side of the major peaks of each gene expression curve to a half-Gaussian curve, mirrored into a full Gaussian distribution, and then transformed log2(TPM) into zFPKM from this fit. Based on the recommended zFPKM score that considers the expressed/active genes [79], genes with zFPKM > −3 in all replicates were considered as expressed. A miRNA with an average value of CPM ≥ 10 was considered to be expressed. The CLC Genomics Workbench Differential Expression tool was used for the expression analysis comparison of the two groups. Differential expression was considered based on a negative binomial Generalized Linear Model (GLM) function. DEGs and DE-miRNAs were filtered based on FC ≥ 2 and *P*-adjusted value FDR < 0.05 [88]. The raw FASTQ and processed CSV files for the transcriptome and miRNA sequencing data have been deposited in the NCBI's Gene Expression Omnibus (GEO) (https://www.ncbi.nlm.nih.gov/geo/) with the accession numbers GSE221929 and GSE221895, respectively.

Target gene prediction, ontological classification and pathway analysis

Genes targeted by the DE-miRNAs were identified using the miRWalk database [89]. Within miRWalk, validated target genes from miRTarBase (version 7.0) and commonly targeted genes predicted by TargetScan (version 7.1) and miRDB (release 5.0) were selected for ontological classification and pathway analysis. Both targeted genes and DEG lists were submitted to the Database for Annotation, Visualization, and Integrated Discovery (DAVID) Bioinformatics web tool v. 2021 (http://david.abcc.ncifcrf.gov/) for pathways and ontological classification enrichment analysis using the EASE Score (a modified Fisher Exact p-value) with a threshold of less than or equal to 0.05. Pathways and biological processes (BPs) were determined from the KEGG database [90], and GOTERM_BP_DIRECT annotation set, respectively. The interaction networks of the miRNAs, targeted genes, and DEGs were constructed with Cytoscape software [91].

Quantitative real time PCR validation of candidate mRNA and miRNA

In order to validate the in vivo biomimicry of in vitro produced organoids, as well as the NGS data for DEGs and DE-miRNAs, quantitative real-time PCR (qRT-PCR) expression analysis was performed for selected transcripts and miRNAs in oviductal organoid cells and oviductal organoid-derived EVs, respectively. Additionally, naïve BOEC samples were used as a control in the organoid characterization experiment. For the functional characterization of in vitro produced organoids and validation of candidate DEGs, equal amounts of total RNA (~638 ng/µL and ~1024 ng/µL, respectively) extracted from independent organoid samples was reverse transcribed to generate cDNA, using the SuperScript™ III First-Strand Synthesis Super Mix Kit (Invitrogen 18,080,400) with random hexamer and oligo d(T) 20 primers, according to the manufacturer's instructions. The gene panel were strategically constructed to characterize the functionality of in vitro produced organoids ($n=3$), while ten candidate genes for the validation of the DEGs ($n=4$) were randomly selected, with gene-specific primers designed using the Primer-Blast tool (https://www.ncbi.nlm.nih.gov/tools/primer-blast/). All primers are indicated in Additional file 11: Table S10. Quantification of each candidate gene was performed in 20 µl reaction volumes containing 0.5 µL of each primer (10 µM), 10 µL of iQ SYBR Green Supermix (Bio-Rad 1,708,880), 7 µL of ddH_2O and 2 µL of the cDNA template. The following thermocycling conditions were applied for amplification: initial denaturation at 95 °C for 3 min, followed by 40 cycles of amplification at 95 °C for 15 s., 60 °C for 30 s., 72 °C for 30 s. The specificity of the amplification was determined from the melting curve analysis generated following each run. The geometric mean of expression levels of *β-ACTIN* and *GAPDH* was used to normalize the expression of the candidate genes.

Four DE-miRNAs (bta-miR-150, bta-miR-92a, bta-miR-223 and bta-miR-202) were chosen for quantification in the samples described above using TaqMan™ miRNA Assays (Applied Biosystems™) according to the manufacturer's instructions. Briefly, 5 ng/µL of total RNA were reverse-transcribed using a TaqMan™ microRNA Reverse Transcription Kit (Applied Biosystems™ 4,366,596). The reaction mixture (7.5 µL) constituted 0.75 µL dNTP mix w/dTTp (100 M total), 0.075 µL 10X RT buffer, 0.095 µL RNase inhibitor (20U/µL), 0.5 µL Multiscribe™ RT enzyme (50U/µL), 1.5 µL of the given miRNA-specific stem-loop primer, and 2.5 µL of RNA (5 ng/µL). The miRNA-specific cDNA reaction mixture was incubated at 16 °C for 30 min, 42 °C for 30 min then followed by 85 °C for 5 min For miRNA quantification, 20 µL qRT-PCR mixtures were prepared in a 96-well PCR plate with 10 µL TaqMan™ Universal PCR Master Mix, no AmpErase™ UNG (Applied Biosystems™ 4,324,018), 1 µL miRNA-specific TaqMan microRNA probe (FAM, 250 nM), 7 µL ddH_2O and 2 µL of the RT product. The following thermocycling conditions were applied for amplification: initial denaturation at 95 °C for 10 min, followed by 40 cycles of amplification at 95 °C for 15 s. and 60 °C for 1 min Expression normalization was performed against small nuclear RNA (U6), as it stably resembled the mean expression values for all miRNAs. All qRT-PCR validation analyses were performed using the CFX96 Touch Real-Time PCR Detection System (Bio-Rad) and expression data analysis was performed using a comparative threshold cycle (CT) method [92]. All data are shown as the mean ± SEM and the differences between means were analyzed using one-way ANOVA followed by Tukey's Multiple Comparisons Test in biologically independent samples ($n=4$). Statistical significance (*) between the 42 °C compared to the 37 °C groups were determined at ($p<0.05$).

MicroRNA sequence motif and RBP identification and analysis

Sequence-specific miRNA motifs (4–6 nucleotides), enriched in the upregulated miRNAs (including the significantly, exclusively expressed miRNAs; $n=13$) versus the downregulated miRNAs (including the significantly, exclusively expressed miRNAs; $n=9$ as control sequences) in EVs derived from oviductal organoids exposed to HS, were identified using Multiple Expectation Maximization for Motif Elicitation (MEME) suite v. 5.5.0 https://meme-suite.org [93].

Motifs commonly detected in at least 50% of the submitted miRNAs were selected for further analysis to determine the motif-associated RBPs using a TOMTOM motif comparison tool [94].

Abbreviations

HS	Heat stress
EV	Extracellular vesicle
BOEC	Bovine oviductal epithelial cell
HSP	Heat shock protein
ROS	Reactive oxygen species
RBP	RNA-binding protein
HM	Handling medium
OM	Organoid medium
SEC	Size exclusion chromatography
NTA	Nanoparticle tracking analysis
TEM	Transmission electron microscopy
FC	Fold change
QC	Quality control
NGS	Next-generation sequencing
PCA	Principal component analysis
GO	Gene ontology
TMM	Trimmed mean of M-values
TPM	Transcripts per million
CPM	Counts per million
GLM	Generalized linear model
DEG	Differentially expressed genes
DE-miRNAs	Differentially expressed miRNAs
GEO	Gene expression omnibus
DAVID	Database for annotation, visualization, and integrated discovery
BP	Biological processes
MEME	Multiple expectation maximization for motif elicitation
NCBI	National center for biotechnology information

Supplementary Information

The online version contains supplementary material available at https://doi.org/10.1186/s12864-023-09746-y.

Additional file 1: Table S1. Summary of sequence reads for oviductal organoids mapped to the bovine reference genome.

Additional file 2: Table S2. Differentially expressed genes in 42°C compared to 37°C group.

Additional file 3: Table S3A. KEGG pathway analysis for differentially expressed genes enriched in 42°C compared to 37°C group. **Table S3B.** KEGG pathway analysisfor differentially expressed genes enriched in 42°C compared to 37°C group.

Additional file 4: Table S4A. Biological process (BP) analysis for differentially expressed genes enriched in 42°C compared to 37°C group. **Table S4B.** Biological process (BP) analysis for differentially expressed genes enriched in 42°C compared to 37°C group.

Additional file 5: Table S5. Summary of sequence reads for oviductal organoid EVs mapped to the bovine reference genome and annotated against bovine miRNAs listed in the mirBase database.

Additional file 6: Table S6. A complete list of all expressed miRNAs indicated as the mean of TMM-adjusted Counts Per Million (CPM) value.

Additional file 7: Table S7A. KEGG pathway analysis for genes targted by the differentially expressed miRNAs in 42°C compared to 37°C group. **Table S7B.** KEGG pathway analysis for genes targted by the differentially expressed miRNAs in 42°C compared to 37°C group.

Additional file 8: Table S8A. Biological process (BP) analysis for genes targted by the differentially expressed miRNAs in 42°C compared to 37°C group. **Table S8B.** Biological process (BP) analysis for genes targted by the differentially expressed miRNAs in 42°C compared to 37°C group.

Additional file 9: Table S9. List of Antibodies used.

Additional file 10: Figure S1. Western blot analysis of extracellular vesicle and cellular protein markers.

Additional file 11: Table S10. Sequence specific primers used for qRT-PCR analysis.

Acknowledgements
We acknowledge D.N. Rao Veeramachaneni and Jennifer S. Palmer at Colorado State University for their excellent technical assistance with TEM imaging. The authors also thank the staff at BPO Parts LLC for their assistance in collection of reproductive materials.

Author's contributions
Conceptualization: N.M., D.T., F.H., Experimental design: N.M., Data curation: N.M., A.G., R.T., M. M., Data analysis: N.M., A.G., Validation: N.M, Writing- original draft: N.M., Writing- review & editing: A.G., R.T., M.M., F.H., D.T., Supervision: F.H., D.T., Funding acquisition: F.H., D.T. All authors have read and approved the published version of this manuscript.

Funding
This study is supported by grant funds from the College Research Council (CRC), Office of the Vice President for Research (OVPR) at Colorado State University. NGM is financially supported by USDA National Needs Fellowship grant number 2021–38420-34040 and USDA-NIFA-AFRI Predoctoral Fellowship grant number 2022–11297.

Availability of data and materials
Datasets generated during the current study including the raw FASTQ files and processed CSV files for genes and miRNAs were deposited in the National Center for Biotechnology Information (NCBI) Gene Expression Omnibus (GEO) database (https://www.ncbi.nlm.nih.gov/geo/) and can be accessed with accession numbers GSE221929 and GSE221895, respectively. Experimental procedures related to EV experiments have been submitted to the EV-TRACK knowledgebase (https://evtrack.org/) (EVTRACK ID: EV230000).

Declarations

Ethics approval and consent to participate
Not applicable.

Consent for publication
Not applicable.

Competing interests
The authors declare no competing interests.

Author details
[1]Animal Reproduction and Biotechnology Laboratory (ARBL), Department of Biomedical Sciences, College of Veterinary Medicine and Biomedical Sciences, Colorado State University, 3107 Rampart Rd, Fort Collins, CO 80521, USA. [2]Department of Animal Production, Faculty of Agriculture, Cairo University, Giza 12613, Egypt. [3]Animal Reproduction and Biotechnology Laboratory (ARBL), Department of Clinical Sciences, College of Veterinary Medicine and Biomedical Sciences, Colorado State University, Fort Collins, CO 80523, USA.

Received: 13 January 2023 Accepted: 16 October 2023
Published online: 27 October 2023

References

1. Pérez-Cerezales S, Ramos-Ibeas P, Acuña OS, Avilés M, Coy P, Rizos D, Gutiérrez-Adán A. The oviduct: from sperm selection to the epigenetic landscape of the embryo. Biol Reprod. 2018;98:262–76. https://doi.org/10.1093/biolre/iox173.

2. Fazeli A. Maternal Communication with Gametes and Embryo: A Personal Opinion. Reprod Domest Anim. 2011;46:75–8. https://doi.org/10.1111/j.1439-0531.2011.01870.x.
3. Almiñana C, Heath PR, Wilkinson S, Sanchez-Osorio J, Cuello C, Parrilla I, et al. Early developing pig embryos mediate their own environment in the maternal tract. PLoS ONE. 2012;7: e33625. https://doi.org/10.1371/journal.pone.0033625.
4. Maillo V, Gaora PÓ, Forde N, Besenfelder U, Havlicek V, Burns GW, et al. Oviduct-Embryo Interactions in Cattle: Two-Way Traffic or a One-Way Street?1. Biol Reprod. 2015. https://doi.org/10.1095/biolreprod.115.127969.
5. Herrler A, von Rango U, Beier HM. Embryo-maternal signalling: how the embryo starts talking to its mother to accomplish implantation. Reprod Biomed Online. 2003;6:244–56. https://doi.org/10.1016/s1472-6483(10)61717-8.
6. Valadi H, Ekström K, Bossios A, Sjöstrand M, Lee JJ, Lötvall JO. Exosome-mediated transfer of mRNAs and microRNAs is a novel mechanism of genetic exchange between cells. Nat Cell Biol. 2007;9:654–9. https://doi.org/10.1038/ncb1596.
7. Sohel MMH, Hoelker M, Noferesti SS, Salilew-Wondim D, Tholen E, Looft C, et al. Exosomal and Non-Exosomal Transport of Extra-Cellular microRNAs in Follicular Fluid: Implications for Bovine Oocyte Developmental Competence. PLoS ONE. 2013;8: e78505. https://doi.org/10.1371/journal.pone.0078505.
8. Pavani KC, Alminana C, Wydooghe E, Catteeuw M, Ramírez MA, Mermillod P, et al. Emerging role of extracellular vesicles in communication of preimplantation embryos in vitro. Reprod Fertil Dev. 2016;29:66–83. https://doi.org/10.1071/RD16318.
9. Tesfaye D, Menjivar N, Gebremedhn S. Current knowledge and the future potential of extracellular vesicles in mammalian reproduction. Reprod Fertil Dev. 2021;34:174–89. https://doi.org/10.1071/RD21277.
10. Eldh M, Ekström K, Valadi H, Sjöstrand M, Olsson B, Jernås M, Lötvall J. Exosomes communicate protective messages during oxidative stress; possible role of exosomal shuttle RNA. PLoS ONE. 2010;5: e15353. https://doi.org/10.1371/journal.pone.0015353.
11. Bewicke-Copley F, Mulcahy LA, Jacobs LA, Samuel P, Akbar N, Pink RC, Carter DRF. Extracellular vesicles released following heat stress induce bystander effect in unstressed populations. J Extracell Vesicles. 2017;6:1340746. https://doi.org/10.1080/20013078.2017.1340746.
12. Saeed-Zidane M, Linden L, Salilew-Wondim D, Held E, Neuhoff C, Tholen E, et al. Cellular and exosome mediated molecular defense mechanism in bovine granulosa cells exposed to oxidative stress. PLoS ONE. 2017;12: e0187569. https://doi.org/10.1371/journal.pone.0187569.
13. Rodrigues TA, Tuna KM, Alli AA, Tribulo P, Hansen PJ, Koh J, Paula-Lopes FF. Follicular fluid exosomes act on the bovine oocyte to improve oocyte competence to support development and survival to heat shock. Reprod Fertil Dev. 2019;31:888–97. https://doi.org/10.1071/RD18450.
14. Gebremedhn S, Gad A, Aglan HS, Laurincik J, Prochazka R, Salilew-Wondim D, et al. Extracellular vesicles shuttle protective messages against heat stress in bovine granulosa cells. Sci Rep. 2020;10:15824. https://doi.org/10.1038/s41598-020-72706-z.
15. Menjivar NG, Gad A, Gebremedhn S, Ghosh S, Tesfaye D. Granulosa cell-derived extracellular vesicles mitigate the detrimental impact of thermal stress on bovine oocytes and embryos. Front Cell Dev Biol. 2023;11:1142629. https://doi.org/10.3389/fcell.2023.1142629.
16. Nardone A, Ronchi B, Lacetera N, Ranieri MS, Bernabucci U. Effects of climate changes on animal production and sustainability of livestock systems. Livest Sci. 2010;130:57–69. https://doi.org/10.1016/j.livsci.2010.02.011.
17. Boni R. Heat stress, a serious threat to reproductive function in animals and humans. Mol Reprod Dev. 2019;86:1307–23. https://doi.org/10.1002/mrd.23123.
18. Hansen PJ. Effects of heat stress on mammalian reproduction. Philos Trans R Soc Lond B Biol Sci. 2009;364:3341–50. https://doi.org/10.1098/rstb.2009.0131.
19. Takahashi M. Heat stress on reproductive function and fertility in mammals. Reprod Med Biol. 2011;11:37–47. https://doi.org/10.1007/s12522-011-0105-6.
20. Edwards JL, Hansen PJ. Differential responses of bovine oocytes and preimplantation embryos to heat shock. Mol Reprod Dev. 1997;46:138–45. https://doi.org/10.1002/(SICI)1098-2795(199702)46:2%3c138::AID-MRD4%3e3.0.CO;2-R.
21. Paula Lopes F, Lima RS, Risolia P, Ispada J, Assumpção ME, Visintin JA. Heat stress induced alteration in bovine oocytes: Functional and cellular aspects. Anim Reprod. 2012;9:395–403.
22. Sartori R, Sartor-Bergfelt R, Mertens SA, Guenther JN, Parrish JJ, Wiltbank MC. Fertilization and early embryonic development in heifers and lactating cows in summer and lactating and dry cows in winter. J Dairy Sci. 2002;85:2803–12. https://doi.org/10.3168/jds.S0022-0302(02)74367-1.
23. Pavani KC, Baron E, Correia P, Lourenço J, Bettencourt BF, Sousa M, Da Silva FM. Gene expression, oocyte nuclear maturation and developmental competence of bovine oocytes and embryos produced after in vivo and in vitro heat shock. Zygote. 2016;24:748–59. https://doi.org/10.1017/S0967199416000071.
24. Lopera-Vasquez R, Hamdi M, Maillo V, Gutierrez-Adan A, Bermejo-Alvarez P, Ramírez MÁ, et al. Effect of bovine oviductal extracellular vesicles on embryo development and quality in vitro. Reproduction. 2017;153:461–70. https://doi.org/10.1530/REP-16-0384.
25. Lopera-Vásquez R, Hamdi M, Fernandez-Fuertes B, Maillo V, Beltrán-Breña P, Calle A, et al. Extracellular Vesicles from BOEC in In Vitro Embryo Development and Quality. PLoS ONE. 2016;11: e0148083. https://doi.org/10.1371/journal.pone.0148083.
26. Almiñana C, Corbin E, Tsikis G, Alcântara-Neto AS, Labas V, Reynaud K, et al. Oviduct extracellular vesicles protein content and their role during oviduct-embryo cross-talk. Reproduction. 2017;154:153–68. https://doi.org/10.1530/REP-17-0054.
27. Clevers H. Modeling Development and Disease with Organoids. Cell. 2016;165:1586–97. https://doi.org/10.1016/j.cell.2016.05.082.
28. Hofer M, Lutolf MP. Engineering organoids Nature Reviews Materials. 2021;6:402–20. https://doi.org/10.1038/s41578-021-00279-y.
29. Kessler M, Hoffmann K, Brinkmann V, Thieck O, Jackisch S, Toelle B, et al. The Notch and Wnt pathways regulate stemness and differentiation in human fallopian tube organoids. Nat Commun. 2015;6:8989. https://doi.org/10.1038/ncomms9989.
30. Xie Y, Park E-S, Xiang D, Li Z. Long-term organoid culture reveals enrichment of organoid-forming epithelial cells in the fimbrial portion of mouse fallopian tube. Stem Cell Res. 2018;32:51–60. https://doi.org/10.1016/j.scr.2018.08.021.
31. Lõhmussaar K, Kopper O, Korving J, Begthel H, Vreuls CPH, van Es JH, Clevers H. Assessing the origin of high-grade serous ovarian cancer using CRISPR-modification of mouse organoids. Nat Commun. 2020;11:2660. https://doi.org/10.1038/s41467-020-16432-0.
32. Abdelmohsen K, Kuwano Y, Kim HH, Gorospe M. Posttranscriptional gene regulation by RNA-binding proteins during oxidative stress: implications for cellular senescence. Biol Chem. 2008;389:243–55. https://doi.org/10.1515/BC.2008.022.
33. Villarroya-Beltri C, Gutiérrez-Vázquez C, Sánchez-Cabo F, Pérez-Hernández D, Vázquez J, Martin-Cofreces N, et al. Sumoylated hnRNPA2B1 controls the sorting of miRNAs into exosomes through binding to specific motifs. Nat Commun. 2013;4:2980. https://doi.org/10.1038/ncomms3980.
34. Shurtleff MJ, Temoche-Diaz MM, Karfilis KV, Ri S, Schekman R. Y-box protein 1 is required to sort microRNAs into exosomes in cells and in a cell-free reaction. Elife. 2016. https://doi.org/10.7554/eLife.19276.
35. Teng Y, Ren Y, Hu X, Mu J, Samykutty A, Zhuang X, et al. MVP-mediated exosomal sorting of miR-193a promotes colon cancer progression. Nat Commun. 2017;8:14448. https://doi.org/10.1038/ncomms14448.
36. Garcia-Martin R, Wang G, Brandão BB, Zanotto TM, Shah S, Kumar Patel S, et al. MicroRNA sequence codes for small extracellular vesicle release and cellular retention. Nature. 2022;601:446–51. https://doi.org/10.1038/s41586-021-04234-3.
37. Guérin P, El Mouatassim S, Ménézo Y. Oxidative stress and protection against reactive oxygen species in the pre-implantation embryo and its surroundings. Hum Reprod Update. 2001;7:175–89. https://doi.org/10.1093/humupd/7.2.175.
38. Li S, Winuthayanon W. Oviduct: roles in fertilization and early embryo development. J Endocrinol. 2017;232:R1–26. https://doi.org/10.1530/JOE-16-0302.
39. Saint-Dizier M, Schoen J, Chen S, Banliat C, Mermillod P. Composing the Early Embryonic Microenvironment: Physiology and Regulation of Oviductal Secretions. Int J Mol Sci. 2019. https://doi.org/10.3390/ijms21010223.

40. Stamperna K, Giannoulis T, Cañon-Beltrán K, Dovolou E, Kalemkeridou M, Nanas I, et al. Oviductal epithelial cells transcriptome and extracellular vesicles characterization during thermoneutral and heat stress conditions in dairy cows. Theriogenology. 2022;187:152–63. https://doi.org/10.1016/j.theriogenology.2022.04.011.
41. Rąpała Ł, Starzyński RR, Trzeciak PZ, Dąbrowski S, Gajewska M, Jurka P, et al. Influence of elevated temperature on bovine oviduct epithelial cells (BOECs). PLoS ONE. 2018;13: e0198843. https://doi.org/10.1371/journal.pone.0198843.
42. Thompson RE, Meyers MA, Pukazhenthi BS, Hollinshead FK. Evaluation of growth, viability, and structural integrity of equine endometrial organoids following cryopreservation. Cryobiology. 2022;104:56–62. https://doi.org/10.1016/j.cryobiol.2021.11.003.
43. Gottardi CJ, Arpin M, Fanning AS, Louvard D. The junction-associated protein, zonula occludens-1, localizes to the nucleus before the maturation and during the remodeling of cell-cell contacts. Proc Natl Acad Sci U S A. 1996;93:10779–84. https://doi.org/10.1073/pnas.93.20.10779.
44. Lamy J, Labas V, Harichaux G, Tsikis G, Mermillod P, Saint-Dizier M. Regulation of the bovine oviductal fluid proteome. Reproduction. 2016;152:629–44. https://doi.org/10.1530/REP-16-0397.
45. Sherr CJ, DePinho RA. Cellular Senescence: Minireview Mitotic Clock or Culture Shock? Cell. 2000;102:407–10. https://doi.org/10.1016/S0092-8674(00)00046-5.
46. Gabler C, Odau S, Muller K, Schon J, Bondzio A, Einspanier R. Exploring cumulus-oocyte-complex-oviductal cell interactions: gene profiling in the bovine oviduct. J Physiol Pharmacol. 2008;59(Suppl 9):29–42.
47. Danesh Mesgaran S, Sharbati J, Einspanier R, Gabler C. mRNA expression pattern of selected candidate genes differs in bovine oviductal epithelial cells in vitro compared with the in vivo state and during cell culture passages. Reprod Biol Endocrinol. 2016;14:44. https://doi.org/10.1186/s12958-016-0176-7.
48. Fitzgerald HC, Dhakal P, Behura SK, Schust DJ, Spencer TE. Self-renewing endometrial epithelial organoids of the human uterus. Proc Natl Acad Sci U S A. 2019;116:23132–42. https://doi.org/10.1073/pnas.1915389116.
49. Turco MY, Gardner L, Hughes J, Cindrova-Davies T, Gomez MJ, Farrell L, et al. Long-term, hormone-responsive organoid cultures of human endometrium in a chemically defined medium. Nat Cell Biol. 2017;19:568–77. https://doi.org/10.1038/ncb3516.
50. Thompson RE, Johnson AK, Dini P, Turco MY, Prado TM, Premanandan C, et al. Hormone-responsive organoids from domestic mare and endangered Przewalski's horse endometrium. Reproduction. 2020;160:819–31. https://doi.org/10.1530/REP-20-0266.
51. Thippabhotla S, Zhong C, He M. 3D cell culture stimulates the secretion of in vivo like extracellular vesicles. Sci Rep. 2019;9:13012. https://doi.org/10.1038/s41598-019-49671-3.
52. Rottmayer R, Ulbrich SE, Kölle S, Prelle K, Neumueller C, Sinowatz F, et al. A bovine oviduct epithelial cell suspension culture system suitable for studying embryo-maternal interactions: morphological and functional characterization. Reproduction. 2006;132:637–48. https://doi.org/10.1530/rep.1.01136.
53. Bauersachs S, Blum H, Mallok S, Wenigerkind H, Rief S, Prelle K, Wolf E. Regulation of ipsilateral and contralateral bovine oviduct epithelial cell function in the postovulation period: a transcriptomics approach. Biol Reprod. 2003;68:1170–7. https://doi.org/10.1095/biolreprod.102.010660.
54. Bauersachs S, Rehfeld S, Ulbrich SE, Mallok S, Prelle K, Wenigerkind H, et al. Monitoring gene expression changes in bovine oviduct epithelial cells during the oestrous cycle. J Mol Endocrinol. 2004;32:449–66. https://doi.org/10.1677/jme.0.0320449.
55. Ulbrich SE, Kettler A, Einspanier R. Expression and localization of estrogen receptor alpha, estrogen receptor beta and progesterone receptor in the bovine oviduct in vivo and in vitro. J Steroid Biochem Mol Biol. 2003;84:279–89. https://doi.org/10.1016/s0960-0760(03)00039-6.
56. Odau S, Gabler C, Holder C, Einspanier R. Differential expression of cyclooxygenase 1 and cyclooxygenase 2 in the bovine oviduct. J Endocrinol. 2006;191:263–74. https://doi.org/10.1677/joe.1.06761.
57. Kobayashi Y, Wakamiya K, Kohka M, Yamamoto Y, Okuda K. Summer heat stress affects prostaglandin synthesis in the bovine oviduct. Reproduction. 2013;146:103–10. https://doi.org/10.1530/REP-12-0479.
58. Huang L, Min J-N, Masters S, Mivechi NF, Moskophidis D. Insights into function and regulation of small heat shock protein 25 (HSPB1) in a mouse model with targeted gene disruption. Genesis. 2007;45:487–501. https://doi.org/10.1002/dvg.20319.
59. Calderwood SK, Khaleque MA, Sawyer DB, Ciocca DR. Heat shock proteins in cancer: chaperones of tumorigenesis. Trends Biochem Sci. 2006;31:164–72. https://doi.org/10.1016/j.tibs.2006.01.006.
60. Yoo J-Y, Shin H, Kim TH, Choi W-S, Ferguson SD, Fazleabas AT, et al. CRISPLD2 is a target of progesterone receptor and its expression is decreased in women with endometriosis. PLoS ONE. 2014;9: e100481. https://doi.org/10.1371/journal.pone.0100481.
61. Velarde MC, Menon R. Positive and negative effects of cellular senescence during female reproductive aging and pregnancy. J Endocrinol. 2016;230:R59-76. https://doi.org/10.1530/JOE-16-0018.
62. Calcinotto A, Kohli J, Zagato E, Pellegrini L, Demaria M, Alimonti A. Cellular Senescence: Aging, Cancer, and Injury. Physiol Rev. 2019;99:1047–78. https://doi.org/10.1152/physrev.00020.2018.
63. Winuthayanon W, Bernhardt ML, Padilla-Banks E, Myers PH, Edin ML, Lih FB, et al. Oviductal estrogen receptor α signaling prevents protease-mediated embryo death. Elife. 2015;4: e10453. https://doi.org/10.7554/eLife.10453.
64. Dumollard R, Duchen M, Carroll J. The role of mitochondrial function in the oocyte and embryo. Curr Top Dev Biol. 2007;77:21–49. https://doi.org/10.1016/S0070-2153(06)77002-8.
65. Balaban RS, Nemoto S, Finkel T. Mitochondria, oxidants, and aging. Cell. 2005;120:483–95. https://doi.org/10.1016/j.cell.2005.02.001.
66. Dresios J, Aschrafi A, Owens GC, Vanderklish PW, Edelman GM, Mauro VP. Cold stress-induced protein Rbm3 binds 60S ribosomal subunits, alters microRNA levels, and enhances global protein synthesis. Proc Natl Acad Sci U S A. 2005;102:1865–70. https://doi.org/10.1073/pnas.0409764102.
67. King AE, Critchley HO, Kelly RW. Presence of secretory leukocyte protease inhibitor in human endometrium and first trimester decidua suggests an antibacterial protective role. Mol Hum Reprod. 2000;6:191–6. https://doi.org/10.1093/molehr/6.2.191.
68. Ota Y, Shimoya K, Zhang Q, Moriyama A, Chin R, Tenma K, et al. The expression of secretory leukocyte protease inhibitor (SLPI) in the fallopian tube: SLPI protects the acrosome reaction of sperm from inhibitory effects of elastase. Hum Reprod. 2002;17:2517–22. https://doi.org/10.1093/humrep/17.10.2517.
69. Hu Y, Cai M-C, Wang L, Zhang T-H, Luo Z-G, Zhang G-W, Zuo F-Y. MiR-1246 is upregulated and regulates lung cell apoptosis during heat stress in feedlot cattle. Cell Stress Chaperones. 2018;23:1219–28. https://doi.org/10.1007/s12192-018-0927-9.
70. Burns G, Brooks K, Wildung M, Navakanitworakul R, Christenson LK, Spencer TE. Extracellular vesicles in luminal fluid of the ovine uterus. PLoS ONE. 2014;9: e90913. https://doi.org/10.1371/journal.pone.0090913.
71. Almiñana C, Tsikis G, Labas V, Uzbekov R, Da Silveira JC, Bauersachs S, Mermillod P. Deciphering the oviductal extracellular vesicles content across the estrous cycle: implications for the gametes-oviduct interactions and the environment of the potential embryo. BMC Genomics. 2018;19:622. https://doi.org/10.1186/s12864-018-4982-5.
72. Wang P, Li X, Cao L, Huang S, Li H, Zhang Y, et al. MicroRNA-148a overexpression improves the early development of porcine somatic cell nuclear transfer embryos. PLoS ONE. 2017;12: e0180535. https://doi.org/10.1371/journal.pone.0180535.
73. Liu L-Z, Li C, Chen Q, Jing Y, Carpenter R, Jiang Y, et al. MiR-21 induced angiogenesis through AKT and ERK activation and HIF-1α expression. PLoS ONE. 2011;6: e19139. https://doi.org/10.1371/journal.pone.0019139.
74. Gecaj RM, Schanzenbach CI, Kirchner B, Pfaffl MW, Riedmaier I, Tweedie-Cullen RY, Berisha B. The Dynamics of microRNA Transcriptome in Bovine Corpus Luteum during Its Formation, Function, and Regression. Front Genet. 2017;8:213. https://doi.org/10.3389/fgene.2017.00213.
75. Pérez-Mancera PA, Young ARJ, Narita M. Inside and out: the activities of senescence in cancer. Nat Rev Cancer. 2014;14:547–58. https://doi.org/10.1038/nrc3773.
76. Zhou L, Qi X, Potashkin JA, Abdul-Karim FW, Gorodeski GI. MicroRNAs miR-186 and miR-150 down-regulate expression of the pro-apoptotic purinergic P2X7 receptor by activation of instability sites at the 3′-untranslated region of the gene that decrease steady-state levels of the transcript. J Biol Chem. 2008;283:28274–86. https://doi.org/10.1074/jbc.M802663200.

77. Presslauer CE, Bizuayehu TT, Fernandes JM, Babiak IS. miR-92a-3p controls cell cycle progression in zebrafish. bioRxiv 2019. https://doi.org/10.1101/680991.
78. Zhang J, Liu W, Jin Y, Jia P, Jia K, Yi M. MiR-202-5p is a novel germ plasm-specific microRNA in zebrafish. Sci Rep. 2017;7:7055. https://doi.org/10.1038/s41598-017-07675-x.
79. Shen X, Gong A. The expression of microRNA-197-3p regulates the proliferation of ovarian granulosa cells through CUL3 in polycystic ovarian syndrome. Acta Biochim Pol. 2022;69:599–604. https://doi.org/10.18388/abp.2020_5951.
80. Hu Z, Mamillapalli R, Taylor HS. Increased circulating miR-370-3p regulates steroidogenic factor 1 in endometriosis. Am J Physiol Endocrinol Metab. 2019;316:E373–82. https://doi.org/10.1152/ajpendo.00244.2018.
81. Srikantan S, Gorospe M. HuR function in disease. Front Biosci (Landmark Ed). 2012;17:189–205. https://doi.org/10.2741/3921.
82. Thompson RE, Meyers MA, Veeramachaneni DNR, Pukazhenthi BS, Hollinshead FK. Equine Oviductal Organoid Generation and Cryopreservation. Methods Protoc. 2022. https://doi.org/10.3390/mps5030051.
83. Thompson RE, Meyers MA, Premanandan C, Hollinshead FK. Generation and cryopreservation of feline oviductal organoids. Theriogenology. 2023;196:167–73. https://doi.org/10.1016/j.theriogenology.2022.11.020.
84. Théry C, Witwer KW, Aikawa E, Alcaraz MJ, Anderson JD, Andriantsitohaina R, et al. Minimal information for studies of extracellular vesicles 2018 (MISEV2018): a position statement of the International Society for Extracellular Vesicles and update of the MISEV2014 guidelines. J Extracell Vesicles. 2018;7:1535750. https://doi.org/10.1080/20013078.2018.1535750.
85. van Deun J, Mestdagh P, Agostinis P, Akay Ö, Anand S, Anckaert J, et al. EV-TRACK: transparent reporting and centralizing knowledge in extracellular vesicle research. Nat Methods. 2017;14:228–32. https://doi.org/10.1038/nmeth.4185.
86. Robinson MD, Oshlack A. A scaling normalization method for differential expression analysis of RNA-seq data. Genome Biol. 2010;11:R25. https://doi.org/10.1186/gb-2010-11-3-r25.
87. Hart T, Komori HK, LaMere S, Podshivalova K, Salomon DR. Finding the active genes in deep RNA-seq gene expression studies. BMC Genomics. 2013;14:778. https://doi.org/10.1186/1471-2164-14-778.
88. Benjamini Y, Hochberg Y. Controlling the False Discovery Rate: A Practical and Powerful Approach to Multiple Testing. J Roy Stat Soc: Ser B (Methodol). 1995;57:289–300. https://doi.org/10.1111/j.2517-6161.1995.tb02031.x.
89. Sticht C, La Torre C, de, Parveen A, Gretz N. miRWalk: An online resource for prediction of microRNA binding sites. PLoS ONE. 2018;13: e0206239. https://doi.org/10.1371/journal.pone.0206239.
90. Ogata H, Goto S, Sato K, Fujibuchi W, Bono H, Kanehisa M. KEGG: Kyoto Encyclopedia of Genes and Genomes. Nucleic Acids Res. 1999;27:29–34. https://doi.org/10.1093/nar/27.1.29.
91. Shannon P, Markiel A, Ozier O, Baliga NS, Wang JT, Ramage D, et al. Cytoscape: a software environment for integrated models of biomolecular interaction networks. Genome Res. 2003;13:2498–504. https://doi.org/10.1101/gr.1239303.
92. Schmittgen TD, Livak KJ. Analyzing real-time PCR data by the comparative C(T) method. Nat Protoc. 2008;3:1101–8. https://doi.org/10.1038/nprot.2008.73.
93. Bailey TL, Johnson J, Grant CE, Noble WS. The MEME Suite. Nucleic Acids Res. 2015;43:W39-49. https://doi.org/10.1093/nar/gkv416.
94. Gupta S, Stamatoyannopoulos JA, Bailey TL, Noble WS. Quantifying similarity between motifs. Genome Biol. 2007;8:R24. https://doi.org/10.1186/gb-2007-8-2-r24.

Publisher's Note

Springer Nature remains neutral with regard to jurisdictional claims in published maps and institutional affiliations.

Ready to submit your research? Choose BMC and benefit from:

- fast, convenient online submission
- thorough peer review by experienced researchers in your field
- rapid publication on acceptance
- support for research data, including large and complex data types
- gold Open Access which fosters wider collaboration and increased citations
- maximum visibility for your research: over 100M website views per year

At BMC, research is always in progress.

Learn more biomedcentral.com/submissions



Received: 15 December 2023 | Revised: 15 December 2023 | Accepted: 19 December 2023

DOI: 10.1002/jev2.12404

POSITION PAPER

Minimal information for studies of extracellular vesicles (MISEV2023): From basic to advanced approaches

Joshua A. Welsh[1,†,‡,§,‖] | Deborah C. I. Goberdhan[2,†,‡,§,‖] | Lorraine O'Driscoll[3,4,5,†,‡,‖] | Edit I. Buzas[6,7,8,‡,§] | Cherie Blenkiron[9,‡] | Benedetta Bussolati[10,§] | Houjian Cai[11,§] | Dolores Di Vizio[12,‡] | Tom A. P. Driedonks[13,§] | Uta Erdbrügger[14,‡,‖] | Juan M. Falcon-Perez[15,16,17,‡,‖] | Qing-Ling Fu[18,19,‡,§] | Andrew F. Hill[20,‡] | Metka Lenassi[21,‡,§] | Sai Kiang Lim[22,23,24,§] | Mỹ G. Mahoney[25,§] | Sujata Mohanty[26,§] | Andreas Möller[27,28,§] | Rienk Nieuwland[29,30,‡,§,‖] | Takahiro Ochiya[31,‡,§] | Susmita Sahoo[32,‡,§] | Ana C. Torrecilhas[33,§] | Lei Zheng[34,‡] | Andries Zijlstra[35,36,‡] | Sarah Abuelreich[37,‖] | Reem Bagabas[37,‖] | Paolo Bergese[38,39,40,‖] | Esther M. Bridges[41,‖] | Marco Brucale[42,43,‖] | Dylan Burger[44,45,46,‖] | Randy P. Carney[47,‖] | Emanuele Cocucci[48,49,‖] | Rossella Crescitelli[50,51,‖] | Edveena Hanser[52,53,‖] | Adrian L. Harris[54,‖] | Norman J. Haughey[55,‖] | An Hendrix[56,57,‖] | Alexander R. Ivanov[58,‖] | Tijana Jovanovic-Talisman[59,‖] | Nicole A. Kruh-Garcia[60,‖] | Vroniqa Ku'ulei-Lyn Faustino[37,‖] | Diego Kyburz[53,61,‖] | Cecilia Lässer[62,‖] | Kathleen M. Lennon[37,‖] | Jan Lötvall[63,‖] | Adam L. Maddox[37,‖] | Elena S. Martens-Uzunova[64,‖] | Rachel R. Mizenko[47,‖] | Lauren A. Newman[65,‖] | Andrea Ridolfi[66,‖] | Eva Rohde[67,68,69,‖] | Tatu Rojalin[47,70,‖] | Andrew Rowland[65,‖] | Andras Saftics[37,‖] | Ursula S. Sandau[71,‖] | Julie A. Saugstad[71,‖] | Faezeh Shekari[72,73,‖] | Simon Swift[74,‖] | Dmitry Ter-Ovanesyan[75,‖] | Juan P. Tosar[76,77,‖] | Zivile Useckaite[65,‖] | Francesco Valle[42,43,‖] | Zoltan Varga[78,79,‖] | Edwin van der Pol[80,81,30,‖] | Martijn J. C. van Herwijnen[82,‖] | Marca H. M. Wauben[82,‖] | Ann M. Wehman[83,‖] | Sarah Williams[84,‖] | Andrea Zendrini[38,39,‖] | Alan J. Zimmerman[58,‖] | MISEV Consortium | Clotilde Théry[85,86,†,‡,§,‖] | Kenneth W. Witwer[87,88,89,†,‡,§,‖]

Correspondence
Joshua A. Welsh, Email: joadwe@outlook.com; Deborah C. I. Goberdhan, Email: deborah.goberdhan@wrh.ox.ac.uk; Lorraine O'Driscoll, Email: lodrisc@tcd.ie; Clotilde Théry, Email: Clotilde.Thery@curie.fr; Kenneth W. Witwer, Email: kwitwer1@jhmi.edu

Abstract

Extracellular vesicles (EVs), through their complex cargo, can reflect the state of their cell of origin and change the functions and phenotypes of other cells. These features indicate strong biomarker and therapeutic potential and have generated broad interest, as evidenced by the steady year-on-year increase in the numbers of scientific

This is an open access article under the terms of the Creative Commons Attribution License, which permits use, distribution and reproduction in any medium, provided the original work is properly cited.

© 2024 The Authors. *Journal of Extracellular Vesicles* published by Wiley Periodicals, LLC on behalf of the International Society for Extracellular Vesicles.

†MISEV Organizing Committee.
‡ISEV Board 2020-2022.
§ISEV Board 2022-2024.
‖Original section drafting contribution.

publications about EVs. Important advances have been made in EV metrology and in understanding and applying EV biology. However, hurdles remain to realising the potential of EVs in domains ranging from basic biology to clinical applications due to challenges in EV nomenclature, separation from non-vesicular extracellular particles, characterisation and functional studies. To address the challenges and opportunities in this rapidly evolving field, the International Society for Extracellular Vesicles (ISEV) updates its 'Minimal Information for Studies of Extracellular Vesicles', which was first published in 2014 and then in 2018 as MISEV2014 and MISEV2018, respectively. The goal of the current document, MISEV2023, is to provide researchers with an updated snapshot of available approaches and their advantages and limitations for production, separation and characterisation of EVs from multiple sources, including cell culture, body fluids and solid tissues. In addition to presenting the latest state of the art in basic principles of EV research, this document also covers advanced techniques and approaches that are currently expanding the boundaries of the field. MISEV2023 also includes new sections on EV release and uptake and a brief discussion of in vivo approaches to study EVs. Compiling feedback from ISEV expert task forces and more than 1000 researchers, this document conveys the current state of EV research to facilitate robust scientific discoveries and move the field forward even more rapidly.

KEYWORDS
ectosomes, exosomes, extracellular vesicles, extracellular particles, guidelines, microparticles, microvesicles, minimal information requirements, MISEV, reproducibility, rigor, standardisation

1 | AN INTRODUCTION TO ISEV AND MISEV

1.1 | Extracellular vesicles and MISEV

Extracellular vesicles (EVs) serve diverse and important roles in most biological systems, arising in part from their compositional complexity. EVs are lipid bilayer membrane-delimited, nano- to micro-sized particles that appear to be released by all cell types. The molecular and structural heterogeneity of EVs mean that many discoveries remain to be made in fundamental biology and development of biomarker and therapeutic applications, yet this same complexity also poses challenges at every stage of EV studies. From definition and categorisation to separation, characterisation, engineering and clinical applications, the 'Minimum Information for Studies of Extracellular Vesicles' (MISEV) aims to help all practitioners of EV research and application to follow best practices for each specific question and indication.

Now in its third iteration, MISEV2023, as a field consensus document seeks to provide recommendations and guidance on EV-related studies that encourage enhanced research design and reporting of experimental details, building on the criteria and guidelines set out in the previous two iterations. MISEV is produced by the International Society for Extracellular Vesicles (ISEV) (https://www.isev.org). Founded in 2011 with the mission to enhance EV research globally, ISEV is the leading professional society for scientists and clinicians involved in the study and use of extracellular vesicles. ISEV engages a diverse group of researchers across the world through its annual meeting, thematic workshops and other meetings (in-person and virtual), peer-reviewed journals, online learning platforms, and partnerships with other societies. ISEV is thus uniquely positioned to shepherd the development and dissemination of expert consensus on best-practice guidelines and scientific considerations.

MISEV2014 (Lotvall et al., 2014) was the first EV position paper produced by ISEV and designed to give robustness to EV analysis. MISEV2018 (Thery et al., 2018) gave a more in-depth and critical assessment of the approaches and methods used to move the field forward, much of which still holds today. MISEV2018 also includes suggested experimental approaches to address some of the remaining challenges and to provide robust EV characterisation. The earlier MISEV recommendations remain largely or entirely valid, and MISEV2023 should be read in the context of the previous documents.

Like the iterations before it, MISEV2023 provides succinct recommendations and guidance for EV researchers, with refinement of points raised in MISEV2018 and addition of recommendations and guidance for newer areas of development. MISEV2023 broadly covers the nomenclature, pre-processing variables, separation and characterisation of EVs, as well as in vitro and in vivo analysis of EV release, uptake and functions.

In addition to previous MISEV guidelines (Lotvall et al., 2014; Thery et al., 2018), ISEV has prompted and coordinated development and dissemination of expert consensus on best-practice guidelines and scientific considerations including inter-society

20013078, 2024, 2, Downloaded from https://isevjournals.onlinelibrary.wiley.com/doi/10.1002/jev2.12404 by Colorado State University, Wiley Online Library on [09/10/2024]. See the Terms and Conditions (https://onlinelibrary.wiley.com/terms-and-conditions) on Wiley Online Library for rules of use; OA articles are governed by the applicable Creative Commons License

TABLE 1 Journal of Extracellular Vesicles: ISEV position papers and statements.

Title	Year	Ref.
Standardization of sample collection, isolation and analysis methods in extracellular vesicle research	2013	(Witwer et al., 2013)
ISEV position paper: extracellular vesicle RNA analysis and bioinformatics	2013	(Hill et al., 2013)
Minimal experimental requirements for definition of extracellular vesicles and their functions: a position statement from the International Society for Extracellular Vesicles	2014	(Lotvall et al., 2014)
Applying extracellular vesicles-based therapeutics in clinical trials—an ISEV position paper	2015	(Lener et al., 2015)
Obstacles and opportunities in the functional analysis of extracellular vesicle RNA—an ISEV position paper	2017	(Mateescu et al., 2017)
Minimal information for studies of extracellular vesicles 2018 (MISEV2018): a position statement of the International Society for Extracellular Vesicles and update of the MISEV2014 guidelines	2018	(Thery et al., 2018)
Biological membranes in EV biogenesis, stability, uptake, and cargo transfer: an ISEV position paper arising from the ISEV membranes and EVs workshop	2019	(Russell et al., 2019)
MIFlowCyt-EV: a framework for standardized reporting of extracellular vesicle flow cytometry experiments	2020	(Welsh, Van Der Pol, Arkesteijn, et al., 2020)
Urinary extracellular vesicles: A position paper by the Urine Task Force of the International Society for Extracellular Vesicles	2021	(Erdbrügger et al., 2021)

position papers (Welsh, Van Der Pol, Arkesteijn, et al., 2020), and focused recommendations of topic-specific experts (Erdbrügger et al., 2021; Hill et al., 2013; Lener et al., 2015; Mateescu et al., 2017; Russell et al., 2019; Verweij et al., 2021; Witwer et al., 2013) (Table 1). More recently, the ISEV Rigor and Standardisation Subcommittee oversees appointment and activities of thematic task forces and special interest groups on specific sources of EVs and other EV-related topics. ISEV also recommends adoption of other reporting and atlas tools, such as the 'Minimum Information for the Publication of Quantitative Real-Time PCR Experiments' (MIQE) for real-time reverse transcriptase-quantitative polymerase chain reaction (qPCR) analyses (Bustin et al., 2009) and EV-TRACK (EV-TRACK Consortium et al., 2017; Roux et al., 2020). Overall, the activities and recommendations of ISEV share the aim of increasing rigor, reproducibility and transparency in EV research. The goal of this MISEV document is to help practitioners in all areas of EV research and application to implement or develop best practices for each individual EV source, type, research question or application.

1.2 | What MISEV IS and IS NOT

Since MISEV2018 appeared, there has been much discussion of what the guidelines mean and how they should or should not be applied. Informed by that discussion, what MISEV IS, and IS NOT, is summarised below.

MISEV IS:

1. An introduction to EV research.
2. A set of recommendations that are meant to increase rigor, reproducibility, and transparency during EV study design, execution and reporting.
3. A tool to assist reviewers and editors, using their own expert knowledge, in assessing the strengths and weaknesses of EV-related proposals, funding applications, abstracts and manuscripts.
4. A non-exhaustive set of examples of various useful EV techniques and platforms.
5. A rigor and standardisation framework that supports innovative EV research and applications and parties ranging from product developers to regulators.
6. An indication of current, broad consensus in the EV field as well as some areas of uncertainty and growth.
7. Relevant to translational and clinical research and applications, including production and initial evaluation of therapeutic EVs.
8. Applicable to all sorts of EV research and applications, not just those involving mammalian EVs. Although examples provided in MISEV may be specific to mammalian EVs, the basic principles are most likely applicable to all EV sources. These include

20013078, 2024, 2, Downloaded from https://isevjournals.onlinelibrary.wiley.com/doi/10.1002/jev2.12404 by Colorado State University, Wiley Online Library on [09/10/2024]. See the Terms and Conditions (https://onlinelibrary.wiley.com/terms-and-conditions) on Wiley Online Library for rules of use; OA articles are governed by the applicable Creative Commons License

informative nomenclature, definition of sources, description of separation/concentration techniques, and characterisation of EVs, properly controlled functional studies, and comprehensive reporting.

By contrast, MISEV IS NOT:

1. A one-size-fits-all blueprint, a comprehensive checklist of 'dos and don'ts', or a substitute for careful expert judgement. There is no technique or platform that is absolutely required or prohibited by MISEV. Similarly, MISEV does not mandate use of any particular marker or markers, enriched or depleted. Chosen techniques and targets should be fit for purpose, appropriate for the experimental system, contributing to overall MISEV compliance, and properly reported. Importantly, no research group has access to all techniques and platforms.
2. A barrier to innovation. When introducing a new technique or new application of EVs, it is possible that some aspects of the approach do not fit perfectly into the existing MISEV framework, or more likely, into a reviewer's interpretation of it. See above on absolute mandates and invoke the exceptions if you must. MISEV should not stifle innovation, but rather inform how innovative or new techniques are presented and validated.
3. A means to prevent publication or funding of a particular project. Just as MISEV should not stifle innovation, it should not be used to prevent research from being shared with the community. For example, an 'exosome' or 'ectosome' study that does not prove biogenesis can be presented instead as about EVs, or an 'EV' report without full characterisation as a broader extracellular particle study. Proper controls might be needed to prove the contribution of EVs to an effect, but if they cannot be done, it might suffice to acknowledge the caveats.
4. A comprehensive collection of citations, each of which entirely embodies the recommendations of MISEV. The MISEV document is not a literature review or compendium. Only a small percentage of the EV literature is cited here, and each citation is made for a specific purpose. Citation in MISEV does not imply endorsement of a report, author team, journal or publisher by ISEV, nor does it suggest primacy or perfection of the cited study. Some cited studies may contain aspects that are inconsistent with MISEV recommendations. Also, many excellent studies are not cited in this document.

In summary, the spirit of MISEV is embodied in just a handful of questions:

1. What terms do you use, and what do they mean?
2. From what/where did you obtain your EVs?
3. How did you separate, concentrate, characterise and store them?
4. How confidently can you attribute a function or biomarker to EVs versus other components?
5. Have you shared data and reported methods in sufficient detail to enable others to replicate or reproduce your results?

1.3 | How to use MISEV2023

MISEV2023 is intended to aid any and all EV researchers: from those just starting their EV journey to more established investigators who wish to understand the current state of the art and/or cutting-edge problems faced by the EV community. However, the result is a large document that may require some help to navigate.

Nomenclature (Section 2) is applicable to all EV studies. Clear and consistent language will help to ensure that results are understandable and comparable.

For those who are newer to EV research, we consider Sections 3–5 to be vital, covering minimum considerations for sample collection/processing, EV separation methods and EV characterisation, respectively.

Sections 6–9 provide further technique-specific guidance for EV characterisation, approaches to modulate EV release and uptake, EV functional studies, and the EV analysis in vivo. These sections provide the reader with up-to-date information to support informed decisions, but, for the most part, do not give specific recommendations.

The information and guidelines presented in MISEV2023 thus promote rigor, reproducibility and transparency in EV science, with the goal to ensure that conclusions are supported by the experiments performed and the information reported.

> Consensus: 89.3% (891) of MISEV2023 survey respondents agreed "completely," and 10.7% (107) agreed "mostly" with Section 1: An introduction to ISEV and MISEV. No respondents disagreed ("mostly" or "completely"), and no respondents stated that they had no opinion and/or expertise.

20013078, 2024, 2, Downloaded from https://isevjournals.onlinelibrary.wiley.com/doi/10.1002/jev2.12404 by Colorado State University, Wiley Online Library on [09/10/2024]. See the Terms and Conditions (https://onlinelibrary.wiley.com/terms-and-conditions) on Wiley Online Library for rules of use; OA articles are governed by the applicable Creative Commons License

20013078, 2024, 2, Downloaded from https://isevjournals.onlinelibrary.wiley.com/doi/10.1002/jev2.12404 by Colorado State University, Wiley Online Library on [09/10/2024]. See the Terms and Conditions (https://onlinelibrary.wiley.com/terms-and-conditions) on Wiley Online Library for rules of use; OA articles are governed by the applicable Creative Commons License

2 | NOMENCLATURE

2.1 | EV definition and EV subtypes

Definition: The term 'extracellular vesicles' (EVs) refers to particles that are released from cells, are delimited by a lipid bilayer, and cannot replicate on their own (i.e., do not contain a functional nucleus). The current definition of EV is retained from MISEV2018, except that the 2018 use of the word 'naturally' (as in 'naturally released') has been removed to avoid unintended exclusion of engineered EVs or EVs produced under various cell culture conditions. In general, ISEV recommends use of the generic term 'EV' and operational extensions of this term instead of inconsistently defined and sometimes misleading terms such as 'exosomes' and 'ectosomes' that are associated with biogenesis pathways that are difficult to establish.

Regarding 'operational terms' that can be added as a prefix to 'EV' (Table 2), their use continues to be encouraged *with caution* if one or more EV subtypes are separated on the basis of characteristics such as size, density, molecular composition or cellular origin. We urge careful and clear definition of these operational terms. For example, terms such as 'small' and 'large' have been commonly used to denote EV populations over the last few years, usually after presumed size-based populations of EVs have been separated with methods such as filtration or differential ultracentrifugation (differential UC, dUC). However, although 'small' might generally refer to EVs <200 nm in diameter, there is no strict consensus on upper and lower size cut-offs, and it has also become clear that many separation methods, such as dUC, yield EV populations with overlapping size profiles. Thus, while such terminology may still be used, researchers should be aware of its limitations and strive to define terms as clearly as possible.

As mentioned above, terms related to presumed biogenesis pathways should be used only with caution and strong evidence. The term 'exosome' refers to EVs from internal compartments of the cell that are released via the multivesicular body (MVB), while the term 'ectosome' (a.k.a., microvesicle, microparticle) refers to EVs from the cell surface. Numerous specialised terms have also been used to denote EVs that arise during specific cellular processes such as cell migration ('migrasomes') or programmed cell death ('apoptotic bodies'). In some cases, biogenesis or release of specific EV subtypes may be inhibited or stimulated by pharmacological or genetic intervention (see also 7.1). Unfortunately, most EV separation techniques do not enrich for EVs produced by different mechanisms, and definitive characterisation of biogenesis-based subtypes is also difficult, with no universal molecular markers of ectosomes, exosomes or other EV subtypes. Therefore, ISEV discourages the use of biogenesis-based terms unless such an EV population is specifically separated and characterised. Of note, 'sEV' (for small EV) and 'exosome' are not synonymous: small EV populations include both small ectosomes and exosomes. For the reasons above, most of the existing 'exosome' and 'ectosome/microvesicle' literature refers to a broad population of EVs, and not to EVs that are released via specific biogenesis pathways. Some EV-like particles may not fully meet the definition of EVs as given above. For example, if a cell is extruded, the resulting particles have not been strictly 'released' from the cell.

2.2 | EV mimetics

A term such as 'EV mimetics' (EVMs) can be used to denote EV-like particles that are produced through direct disruption of cells, by de novo synthesis from molecular components, or by fusion of native EVs with, for example, liposomes. Whatever nomenclature is used for such particles, it will ideally indicate the general production process, differentiate the particles from native EVs, and not claim resemblance to EVs from a specific biogenesis pathway. That is, avoid 'exosome-like vesicles' and similar terms that incorrectly imply specific biogenesis-related properties. Some examples of possible terms, but without strict endorsement, are artificial cell-derived vesicles (ACDVs) for vesicles from extruded cells and synthetic vesicles (SVs) for EV mimetics that are synthesised de novo from molecular components or made as hybrid entities, for example, fusions between liposomes and native EVs (Table 2).

2.3 | How to approach non-vesicular extracellular particles (NVEPs)

There is a growing awareness of a wide diversity of non-vesicular extracellular particles that often co-separate with EVs, and the ISEV community specifically requested guidance in the run-up to MISEV2023 on how to handle and name these particles. Since ISEV is a society of EV experts, we cannot presume to establish a nomenclature for other types of extracellular particles, such as lipoprotein particles (LPPs), ribonucleoprotein particles (RNPs), viruses, or various newly proposed particle types like exomeres and supermeres. Nevertheless, how EVs relate to other particles—and how they can be separated from them and characterised along with them in complex mixtures—is of great relevance to the EV field. Therefore, MISEV2023 provides the following nomenclature proposals while recognising that other terms may be required for increased clarity (Figure 1, Table 2).

Extracellular particles (EPs) is the preferred overarching term for cell-derived multimolecular assemblies in the nanometre to micron size range, including both EVs and non-vesicular entities:

TABLE 2 Quick-reference card on EV nomenclature and related terms.

Term	Definition	Usage
Extracellular vesicles (EVs)	Particles that are released from cells, are delimited by a lipid bilayer, and cannot replicate on their own.	Recommended
Non-vesicular extracellular particles (NVEPs)	Multimolecular assemblies that are released from cells and do not have a lipid bilayer (non-vesicular extracellular particle fraction).	Recommended
Extracellular particles (EPs)	Umbrella term for all particles outside the cell, including EVs and NVEPs.	Recommended
EV mimetic	EV-like particles that are produced through direct artificial manipulation. This term is preferred over 'exosome-like vesicles' and similar terms that imply specific biogenesis-related properties.	Recommended
Artificial cell-derived vesicles (ACDVs)	EV mimetics that are produced in the laboratory under conditions of induced cell disruption, such as extrusion.	Recommended
Synthetic vesicles (SVs)	EV mimetics that are synthesized de novo from molecular components or made as hybrid entities, e.g., fusions between liposomes and native EVs.	Recommended
Small EVs (operational term)	Based on the diameter of the separated particles, small EVs are often described as <200 nm in diameter. However, measured diameter is related to the specific characterization method.	Recommended, but caution required
Large EVs (operational term)	Based on the diameter of the separated particles, large EVs are often described as >200 nm in diameter. However, measured diameter is related to the specific characterization method.	Recommended, but caution required
Other 'operational terms'	Physical characteristics: e.g., diameter: small extracellular vesicles (sEVs), large EVs (lEVs), density: low, medium, high (defined ranges). Biochemical composition: e.g., contains a specific (macro)molecule, such as a protein. Cellular origin and/or conditions under which EVs were generated: terms that highlight specific aspects of biogenesis such as molecular mechanisms, energy-dependence (or lack thereof) and functional state of the parent cell related to stress or death.	Recommended, but caution required
Exosome	Biogenesis-related term indicating origin from the endosomal system. Unless subcellular origin can be demonstrated, it is likely that a broad population of EVs is being studied, not exosomes specifically. Exosomes represent a subtype of small EVs: the diameter of intraluminal vesicles of endosomes is generally smaller than 200 nm.	Discouraged unless subcellular origin can be demonstrated
Ectosome	Biogenesis-related term indicating origin from the plasma membrane. Unless subcellular origin can be demonstrated it is likely that a broad population of EVs is being studied, not ectosomes specifically. Ectosomes can have a wide range of sizes, including sizes similar to those of exosomes.	Discouraged unless subcellular origin can be demonstrated
Microvesicle	Biogenesis-related term indicating origin from the plasma membrane. However, historically, the term has often been used to designate large EVs or all EVs, whatever their subcellular origin. This term can therefore lead to confusion.	Discouraged
Exosome-like vesicles	As 'exosome' is a biogenesis-related term indicating origin from the endosomal system, this and similar terms are discouraged for synthesized EV mimetics.	Discouraged

Non-vesicular extracellular particles (NVEPs) are all non-EV particles made from cell-derived components of one or more molecular classes (e.g., proteins, nucleic acids); lipids, if present, do not form a delimiting bilayer membrane. NVEPs and EVs may have overlapping physicochemical properties, and NVEPs may greatly outnumber EVs in biological matrices. As a result, most EP separation methods result in NVEP/EV co-isolation. Similarly, many EP characterisation methods do not identify EVs specifically. NVEPs that are smaller than EVs may not be detected by some EV characterisation methods, thus their quantity in an EP preparation may remain unknown. Therefore, when EVs and NVEPs cannot be fully distinguished from each other, the term 'EP' may be appropriate, or the use of 'EV preparation' or 'EV-containing preparation'.

Table 2 is a quick-reference card of recommended nomenclature.

20013078, 2024, 2, Downloaded from https://isevjournals.onlinelibrary.wiley.com/doi/10.1002/jev2.12404 by Colorado State University, Wiley Online Library on [09/10/2024]. See the Terms and Conditions (https://onlinelibrary.wiley.com/terms-and-conditions) on Wiley Online Library for rules of use; OA articles are governed by the applicable Creative Commons License

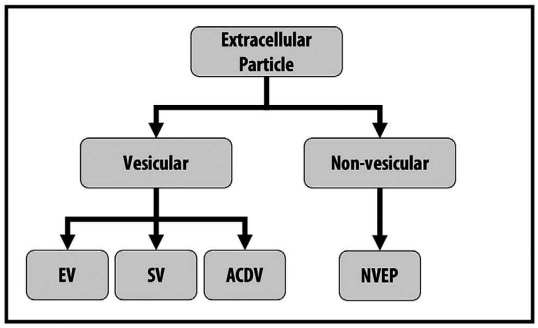


FIGURE 1 Hierarchy of EP nomenclature. Extracellular particles include vesicular and non-vesicular particles. This figure presents several distinctions that can be made between classes of EPs, as well as examples of possible nomenclature. EP: extracellular particle; EV: extracellular vesicle; SV: synthetic vesicle; ACDV: artificial cell-derived vesicle; NVEP: non-vesicular extracellular particle. See also Section 2 and Table 2.

Recommendations:

- **'Extracellular vesicles'** is the term for particles that are delimited by a lipid bilayer and cannot replicate on their own (vesicular component of extracellular particles).
- Operational terms are encouraged, but with caution, as these can be influenced by separation methods.
- Biogenesis terms are discouraged unless subcellular origin can be demonstrated for the specific EV source and condition. With few exceptions, a broad population of EVs is studied, not ectosomes or exosomes specifically.
- **'Extracellular particles'** is the overarching term for cell-derived multimolecular assemblies in the nanometer to micron size range, including both vesicular and non-vesicular entities.
- **'Non-vesicular extracellular particles'** is an accurate term for cell-derived multimolecular assemblies that are non-vesicular in nature (i.e., the non-vesicular fraction of extracellular particles).

> Consensus: 79.5% (793) of MISEV2023 survey respondents agreed "completely," and 19.9% (199) agreed "mostly" with Section 2: Nomenclature. 0.4% (4) "mostly" disagreed, and 0.2% (2) stated that they had no opinion and/or expertise. No respondents disagreed "completely."

3 | COLLECTION AND PRE-PROCESSING: PRE-ANALYTICAL VARIABLES THROUGH TO STORAGE

An array of factors in sample collection, pre-processing (i.e., before specific EV separation/concentration steps), and storage of EV-containing sources and their derivatives may affect EVs quantitatively and qualitatively. Some considerations related to these factors are common between many EV source materials, such as how to maximise (and measure) the quality of starting material; reporting all relevant donor characteristics for biofluid/solid tissue samples; measures of the quantity and quality of the source material as the baseline for the data collected during EV characterisation; and standardising and reporting pre-processing variables. In contrast, other recommendations may be specific to the starting source, such as approaches to remove source-specific contaminants/co-isolates and to confirm their removal.

3.1 | Common recommendations

- Describe the source of EV-containing materials. For materials from human and non-human animal donors, report relevant donor characteristics, including but not limited to age, biological sex, substance exposures (medications, substance use) and disease.
- Report the quantity (e.g., sample volume, mass) and quality of source material.
- Provide all methodologic details of sample collection.
- Consider how pre-separation storage may influence the EVs that are eventually separated. Where relevant, avoid repeated freeze-thaw cycles or assess effects of freeze-thaw.

20013078, 2024, 2, Downloaded from https://isevjournals.onlinelibrary.wiley.com/doi/10.1002/jev2.12404 by Colorado State University, Wiley Online Library on [09/10/2024]. See the Terms and Conditions (https://onlinelibrary.wiley.com/terms-and-conditions) on Wiley Online Library for rules of use; OA articles are governed by the applicable Creative Commons License

- Report all storage parameters pre- and post-EV separation (including use of preservatives or cryoprotectants, temperature, time, freezing procedure, storage vessel, number of freeze-thaw cycles and thawing method).
- Remove cells from all EV source materials as early as possible in pre-processing. Cell disruption can form particles resembling native EVs, and post-collection cellular processes like activation and death can alter EV composition and function.
- Assess and report the degree of depletion of cells and source-specific, common EV co-isolates during pre-processing and, later, after EV separation/concentration.
- Implement quality control measures throughout the sample collection, pre-processing and EV separation.
- If samples must be pooled to obtain sufficient EVs for study, report the number of individual samples in a pool, the donor demographics contributing to the pool, the quantity (e.g., volume) of each individual sample and final quantity. Where possible, follow up with individual samples.
- In studies that seek to determine if EVs or EV cargo can serve as biomarkers of a disease or condition, also test whether non-enriched materials, for example, NVEPs or whole biofluid, may have similar associations.
- For those EV sources for which ISEV has a Task Force (isev.org/taskforces), we recommend that researchers keep themselves updated and informed on outputs of that Task Force. See also the next sections with some specific recommendations.

3.2 | Cell culture-conditioned medium

All types of cells cultured in vitro release EVs and other factors into their culture medium, thus creating cell culture-conditioned medium [CCM; Shekari et al., 2023]. This includes eukaryotic cells from multi- and unicellular organisms and prokaryotic cells including gram-positive and -negative bacteria and *Mycobacteria*. Most recommendations in this section apply to CCM from all cell types; additional and more specific details on bacterial EVs are provided in Section 3.3.

Cell culture parameters for both eukaryotic and prokaryotic cells include the producing cells (e.g., name, viability, passage number and seeding and harvest density); medium components (e.g., basal medium, complex additives such as serum, nutrients, micronutrients, antibiotics/mycotics and any other additives); culture conditions, including 2D/3D/suspension culture, temperature, pH, gas concentrations and any physical stimuli; duration of conditioning; harvesting approaches; and any detected contaminations or infections. Cell culture conditions directly and indirectly affect EV yield, composition, and function. Culture media components can contain EVs or may be taken up by cells and repackaged into EVs (Lehrich et al., 2021; Palviainen et al., 2019). Complex supplements such as blood serum [e.g., foetal bovine/calf serum (FBS/FCS)] and platelet lysate (PL) are often used in mammalian cell culture, but they are rich in EVs, NVEPs, and various, often undefined entities, including DNA fragments and micronutrients (Arigony et al., 2013; Lehrich et al., 2021). Depleting EVs from these supplements can be difficult to accomplish and verify (Erdbrügger et al., 2021; Lehrich et al., 2018), and depletion of complex supplements, for example, by ultracentrifugation, may depend on degree of dilution. Commercial 'EV-free' products should also not be assumed to be devoid of EVs without verification. Use of both EV-depleted medium and 'defined' (serum/PL-free) media may alter cell physiology and EV production (Lehrich et al., 2021). Since viable and dying cells may release different subtypes of EVs (Crescitelli et al., 2013; Shlomovitz et al., 2021), and since EVs produced by only a few percent of dying cells may outnumber EVs generated by healthy cells, the proportion of live and dying cells in a culture affects proportions of EV subtypes and EV quantity. Unwanted microbial contamination (common: *Mycoplasma*), should be checked and reported. These microbes affect many characteristics of producing cells (Zhang et al., 2000); they or their constituents may be repackaged into EVs of the host culture (Yang et al., 2012); and some may also release their own EVs (Gaurivaud et al., 2018).

Recommendations:

- CCM recommendations made in MISEV2018 (Thery et al., 2018) are still relevant. These include, but are not limited to, reporting medium composition and preparation; characteristics of producing cells including identity, seeding and harvest density and viability at harvest; culture conditions including vessel/system, surface coating (if any), temperature, and gas concentrations; physical or chemical stimulants/treatments, if any; frequency, intervals and method of CCM harvest; and any CCM storage before EV separation. If cells are from a primary source, rather than an established cell line, report harvesting and pre-culturing conditions such as enzymatic digestion.
- If serum, PL or other complex additives are used, report the source and the percent of the total medium. If EV depletion of such additives is done, report method and degree of depletion (including dilution, which may be necessary prior to depletion methods involving centrifugation) using the same methods used to characterise released EVs. Vendors of EV-depleted supplements are also encouraged to report method and degree of EV depletion.
- Non-conditioned medium controls should be processed and characterised to assess the contribution of the medium itself to putative EV measurements.

20013078, 2024, 2, Downloaded from https://isevjournals.onlinelibrary.wiley.com/doi/10.1002/jev2.12404 by Colorado State University, Wiley Online Library on [09/10/2024]. See the Terms and Conditions (https://onlinelibrary.wiley.com/terms-and-conditions) on Wiley Online Library for rules of use; OA articles are governed by the applicable Creative Commons License

20013078, 2024, 2, Downloaded from https://isevjournals.onlinelibrary.wiley.com/doi/10.1002/jev2.12404 by Colorado State University, Wiley Online Library on [09/10/2024]. See the Terms and Conditions (https://onlinelibrary.wiley.com/terms-and-conditions) on Wiley Online Library for rules of use; OA articles are governed by the applicable Creative Commons License

3.3 | Bacteria

The diversity of bacteria, bacterial EVs and source material characteristics makes it difficult to issue universal recommendations on sample type, pre-processing, separation, collection and characterisation. Bacterial EVs arise from outer and inner membranes of gram-negative bacteria and cytoplasmic membranes of gram-positive bacteria through blebbing and lytic biogenesis pathways (Toyofuku et al., 2023). Different species, strains (Bitto, Cheng, et al., 2021; Bitto, Zavan, et al. 2021; McMillan & Kuehn, 2023; Zavan et al., 2023), and growth conditions (Hong et al., 2019; Keenan & Allardyce, 2000) affect EV heterogeneity on multiple levels, including function (Turner et al., 2018). Bacterial EVs can be harvested from mono- or polymicrobial culture in vitro, in vivo/ex vivo sources such as body fluids or faeces, and environmental samples ranging from soil to seawater. Despite this diversity, some recommendations are possible.

For most bacterial species, studies of the influence of culture conditions on the yield and composition of bacterial EVs are in their infancy, but most considerations for culture-derived eukaryotic EVs also apply to bacterial EVs (Bose et al., 2020; Brown et al., 2015). These include effects of media composition, oxygenation/aeration and culture format (for bacteria: standing, shaking, roller bottle, bioreactor, planktonic cell or biofilm) and growth phase (Bitto, Cheng, et al., 2021; Bitto, Zavan, et al. 2021; Kuehn & Kesty, 2005; Mehanny et al., 2022; Zavan et al., 2019). Thus, culture details should be reported.

Following sample collection, as for eukaryotic EVs, all methodologic details of separation/concentration should be reported. Non-specific methods like precipitation and ultracentrifugation may co-isolate and/or aggregate unwanted non-EV materials. For bacteria, these may include pili, flagellae, phage, and protein, lipoprotein, and nucleoprotein complexes. Filtration and chromatography methods are gentler alternatives (Bitto & Kaparakis-Liaskos, 2022; Liangsupree et al., 2021). In density gradient ultracentrifugation, densities of EV-rich fractions should be determined for each bacterium and growth condition, with clear reporting of fractions (Bitto & Kaparakis-Liaskos, 2022; Singorenko et al., 2017). Consider that different separation methods may enrich or deplete subtypes of bacterial EVs.

Detailed characterisation of bacterial EV preparations beyond core measurements of size distribution and macromolecular content is limited by the availability of validated, commercially available affinity reagents to bacterial markers for only a limited number of species. In many cases, markers of co-isolating materials require further definition. Lipopolysaccharide [LPS, gram-negative bacteria, Tulkens et al., 2020], lipotechoic acid [LTA, gram-positive bacteria, Champagne-Jorgensen et al., 2021] and mycobacterial lipids (Prados-Rosales et al., 2011) are universal markers for these broad classes of bacterial EVs. LPS and LTA have the advantage of commercially available antibodies. However, LPS can be present in NVEPs including LPS micelles and complexes with LPS binding protein that may be present in in vivo samples (Page et al., 2022), so appropriate controls should be included. Finally, for functional assays, normalisation methods for bacterial EV input should be accurately reported, e.g., different protein assay types can return different values (Bitto, Zavan, et al., 2021).

Recommendations:

- In addition to other culture parameters, report bacterial growth phase at harvest.
- Limit storage prior to EV separation/concentration, especially if samples are left unfiltered.
- When obtaining bacterial EVs from in vivo and environmental sources, consider that host EVs or EVs from non-target species are likely present.
- LPS and LTA are broad markers of gram-negative and -positive bacteria, respectively, with well-characterised, commercially-available affinity reagents. In many species, specific markers of EVs and non-EV materials remain unavailable.
- Non-vesicular co-isolates of bacterial EVs may include pili, flagellae, phage and protein, lipoprotein and nucleoprotein complexes.

3.4 | Blood

Blood is the most studied biofluid in EV research, and most studies involve human blood. Previous MISEV guidelines, ISEV position papers and other publications (Clayton et al., 2019; Coumans et al., 2017; Thery et al., 2018; Witwer et al., 2013) highlighted the importance of standardisation and reporting of (i) donor variables, for example, age, biological sex, circadian rhythm, diet, exercise level and medication, and (ii) pre-analytical processing variables such as blood collection, preparation, handling, storage, anticoagulants, centrifugation protocols and handling time (Buntsma et al., 2022; Dhondt et al., 2020, 2023; Lacroix et al., 2012; López-Guerrero et al., 2023; Gyorgy et al., 2014; Palviainen et al., 2020), which remain valid. Here, we focus on the complexity of blood, which contains cells, lipoproteins, proteins and other factors that may be retained in EV preparations and confound downstream analysis. The degree to which blood samples are processed and EVs are separated from common co-isolates depends on the study aim and the downstream analysis. The MIBlood-EV was developed by the ISEV Blood Task Force to enable scientists

to report the traceability of blood-derived samples used for EV studies (Lucien et al., 2023). The MIBlood-EV is divided into categories of: (a) general study information, (b) blood collection, processing, storage, (c) qualitative and quantitative evaluation of haemolysis, platelets and lipoproteins, three major confounding factors in blood EV research.

Blood cells account for about 45% of the blood volume, so removal of cells before any cell-disruptive processing such as freeze/thawing (which forms EV-like cell fragments) and avoidance of cell activation (and thus release of EVs post-collection) is particularly important. Red blood cells are dense and thus relatively easy to separate from EVs by low-speed centrifugation. However, red blood cells may lyse ('haemolysis') during blood collection and processing, releasing internal contents such as haemoglobin, which turns the plasma or serum a reddish instead of yellow colour. Most other blood cells can also be efficiently removed by centrifugation. In contrast, 1–3 μm platelets are derived from megakaryocytes, highly abundant in blood, and overlap in size range and/or density with EVs. The presence of even a few platelets may affect downstream EV analysis, and activated platelets will release large numbers of EVs. Although various centrifugation protocols are used to deplete platelets from plasma and serum (Bracht et al., 2023; Karimi et al., 2022), these protocols incompletely separate platelets from EVs, and extent of platelet depletion is typically unreported. Additional depletion of residual platelets from plasma and serum can be achieved by filtration (Bettin et al., 2022; Bracht et al., 2023).

Lipoproteins are another main confounding class of NVEPs, including high-density, low-density, intermediate-density, and very low-density lipoproteins (HDL, LDL, IDL, VLDL) as well as larger chylomicrons. They overlap in size (all but HDL), density (HDL), and/or molecular composition with blood EVs, and some lipoprotein subtypes outnumber blood EVs by orders of magnitude (Johnsen et al., 2019; Simonsen, 2017). Because neither density- nor size-based separation can separate all lipoproteins from EVs, a combination of methods that exploit different physical and biochemical properties (here reported in Chapter 4) is recommended when more pure EV populations are required (Karimi et al., 2018; Ter-Ovanesyan et al., 2023; Van Deun et al., 2020; Vergauwen et al., 2021; Zhang, Borg, et al., 2020).

Blood also contains high concentrations of free, 'soluble' proteins such as serum albumin, immunoglobulins and fibrinogen, as well as protein and ribonucleoprotein (RNP) aggregates, that may co-isolate with EVs and affect downstream analysis. These proteins are generally smaller and denser than EVs, allowing separation from EVs by size exclusion chromatography (SEC), density gradient centrifugation, or combinations thereof.

Of note, the surface of EVs, especially in complex environments such as blood, is covered with a biomolecular corona of various molecules and particles [(Palviainen et al., 2020; Tóth et al., 2021; Wolf et al., 2022; Yerneni et al., 2022) and see also Section 4.7]. Hence, some blood proteins and lipoproteins, previously defined as contaminants of the EV preparation, may be truly associated with EVs and remain even after the EVs have been rigorously but gently separated from blood.

Recommendations:

- Effects of donor characteristics on blood and EV properties are better studied for blood than for many other EV sources and are thus especially important to consider and report. For example, large lipoprotein particles such as chylomicrons have elevated concentrations after dietary intake, so to minimise their influence, collect blood from overnight-fasted donors.
- When blood is collected by venipuncture, use the largest feasible needle gauge to minimise platelet activation and haemolysis. To minimise bacterial and skin cell contamination and to avoid tissue factor-mediated platelet activation, it may also be a good practice to discard a small volume of the blood draw (e.g., for human blood draws, the first 2–3 mL).
- Select blood collection tubes/anticoagulants that are compatible with downstream analyses.
- Following collection, minimise platelet activation and EV release by avoiding excessive agitation and low temperatures and processing to plasma or serum as quickly as possible.
- Use a plasma or serum preparation protocol that efficiently removes platelets but not EVs. If centrifugation is used, draw supernatant from the top down with a pipette, leaving a specified amount of plasma or serum on top of the pellet to avoid disturbing the pellet and releasing platelets.
- Major contaminants/co-isolates of blood EVs are platelets, lipoproteins, haemolysis products, and a host of soluble/aggregated proteins including RNPs. Determine and report relative enrichment of EVs over whichever of these materials is important in a given study.
- Complete the MIBlood-EV reporting tool and attach it as supplementary material for any manuscript with research using blood specimens. The completed document should also be added to the MIBlood-EV shared folder (details at: https://www.isev.org/rigor-standardization)

3.5 | Urine

Urine is the second most-analysed biofluid after blood and can be obtained non-invasively, serially and in large quantities. Urinary EV (uEVs) and their contents are promising biomarkers and bio-regulators in health and disease of the kidney, the urogenital tract and possibly other organs and systems (Burger et al., 2014; Carreras-Planella et al., 2021; Erdbrügger et al., 2021; Morikawa et al., 2019; Ramirez-Garrastacho et al., 2022). Challenges in uEV studies arise from the diverse cellular origin of uEVs and the

20013078, 2024, 2, Downloaded from https://isevjournals.onlinelibrary.wiley.com/doi/10.1002/jev2.12404 by Colorado State University, Wiley Online Library on [09/10/2024]. See the Terms and Conditions (https://onlinelibrary.wiley.com/terms-and-conditions) on Wiley Online Library for rules of use; OA articles are governed by the applicable Creative Commons License

20013078, 2024, 2, Downloaded from https://isevjournals.onlinelibrary.wiley.com/doi/10.1002/jev2.12404 by Colorado State University, Wiley Online Library on [09/10/2024]. See the Terms and Conditions (https://onlinelibrary.wiley.com/terms-and-conditions) on Wiley Online Library for rules of use; OA articles are governed by the applicable Creative Commons License

dynamic composition of urine, which varies by fluid intake, time of collection, diet, exercise, age, biological sex, medication and health and disease status. Please refer to previous, specific recommendations of the Urine Task Force of ISEV for all stages of uEV research: a position paper (Erdbrügger et al., 2021) and a 'Quick Reference Card' (van Royen et al., 2023).

Here, we focus on considerations specific for urine as an EV source. For urine collection and storage, many biobanked urine samples have not been processed to remove cells prior to storage, so uEV-specific biobanks or new collections may be needed. For any urine sample, urine proteins are the most common co-isolates/contaminants of uEV preparations (Dhondt et al., 2020). Protein abundance in urine spans five orders of magnitude. Amongst the highest-abundance urinary proteins (Tamm-Horsfall protein (THP), albumin and 20 other serum-filtered proteins) THP can not only co-isolate with uEVs, reducing uEV purity, but also polymerise into lattice-like networks that trap uEVs, reducing uEV yield. THP can be depolymerised and reduced by changing urine ionic strength or pH or by treating with reducing reagents (Correll et al., 2022; Liu, Cauvi, et al., 2018; Pisitkun et al., 2004). Removal of THP may be needed for downstream characterisation procedures such as mass spectrometry, but it is less necessary for other approaches (e.g., single-EV analysis by immunolabelling).

uEV studies in particular require careful normalisation approaches because of the magnitude of inter- and intra-individual variation in urine concentrations (i.e., of solutes in the urine; specific gravity), resulting from changes in the external environment, water and salt homeostasis, and circadian patterns. Because uEV levels may vary with urine concentration, normalisation between samples is necessary to counterbalance data variance. Unfortunately, there is no consensus method or marker(s) accounting for excretion rate and uEV processing that can be used for the robust normalisation of uEV quantity and/or content. Currently, normalisation for excretion rate is done based on absolute (total protein, uEV number, uEV biomarker) or relative (time collection, relative to urinary creatinine, osmolality) measures. In studies of organ-specific uEVs, organ-specific markers can be used; for example, prostate-specific antigen (PSA) concentrations can account for the proportion of prostate fluid in urine.

Recommendations:

- Follow previously published ISEV recommendations (Erdbrügger et al., 2021; van Royen et al., 2023).
- Perform uEV research using cell-free urine and cell-free urine biobanks.
- Where appropriate, report methodology and outcome of uEV co-isolate/contaminant depletion (THP, albumin and other serum-filtered proteins).
- For normalisation, collect data both on uEVs and non-EV urine parameters (e.g., creatinine, PSA or others as applicable) to estimate absolute or relative excretion rates.

3.6 | Cerebrospinal fluid

Cerebrospinal fluid (CSF) bathes the central nervous system (CNS) and contains biomarkers of CNS health and disease (Gaetani et al., 2019; Hühmer et al., 2006; Jack et al., 2018; Rao et al., 2013). Several CSF- specific factors must be considered in CSF EV studies. CSF is produced in the brain ventricles and circulates through the brain and spinal cord in a continuous flow (Czarniak et al., 2023). This flow establishes a rostro-caudal gradient, with lower levels of some brain proteins (e.g., S-100β, total or phosphorylated Tau), but higher levels of others (e.g., neurofilament, amyloid-β40 or β42) in the lumbar region relative to the brain (Jingami et al., 2019; Rostgaard et al., 2023). Hence, collection site (e.g., lumbar/spinal canal vs. brain) and volume may affect CSF composition (Cameron et al., 2019; Teunissen et al., 2009). Common confounders of CSF studies include residual cells and blood contamination, since protein concentrations in blood are 200–400 times greater than in CSF (You et al., 2005). Useful measurements of contaminants include cell counts (e.g., CSF samples that contain >500 erythrocytes/μL might be excluded (Teunissen et al., 2009) and protein assays for hemoglobin, catalase, peroxiredoxin, carbonic anhydrase I, apolipoprotein B-100, IgM, apolipoprotein B-100, fibrinogen or haptoglobin (Aasebø et al., 2014; You et al., 2005). Human donor characteristics reported to affect CSF biomarkers (Klener et al., 2014; Lewczuk et al., 2006; Mattsson et al., 2011) include sex (Li et al., 2017), ethnicity (Howell et al., 2017), disease-relevant genotypes (Li et al., 2017), medications (Riekse et al., 2006; Wong, 2007) and substance use (Liu et al., 2020; Wang et al., 2021). Age (Shah et al., 2011; Wong et al., 2000; Zhang et al., 2005) may be particularly important for cohort design and normalisation considerations, since human CSF protein concentrations are high in neonates, decline through childhood and increase from adolescence through adulthood (Howell et al., 2017; Shah et al., 2011; Zhang et al., 2005). For biomarkers that cycle with circadian rhythm, the time of day for collection is important (Lucey et al., 2017). However, these effects of pre-analytical variables may or may not affect EVs.

CSF EV studies are also challenged by very low concentration of EVs in CSF and the precious nature of CSF samples. Since CSF collection is relatively invasive, total CSF volume is limited for most patients, and sampling is usually done only for specific disease indications, the total number of samples and their volumes are small. For example, most established human CSF biorepositories are able to share 1.0 mL or less of each sample. As a result, high-yield separation approaches and high-sensitivity characterisation assays are especially needed for CSF EV studies (Krušić Alić et al., 2022; Sandau et al., 2020; Ter-Ovanesyan et al., 2021). Pooling

samples from multiple donors may be an option to optimise new protocols or to perform omics characterisation, with or without follow-up with higher-sensitivity specific molecular assays for individual samples.

Recommendations:

- Report anatomic collection site and volume of CSF drawn because of possible influence of the rostral-caudal CSF gradient.
- Measure levels of specific co-isolates/contaminants, such as blood cells and blood proteins, and establish exclusion criteria where appropriate, for example, >500 erythrocytes/μL from biomarker studies.
- High-yield separations and high-sensitivity characterisation methods are especially important for studying CSF EVs, and sample pooling may be needed.

3.7 | Saliva

Healthy adult humans produce 500–1500 mL saliva per day, varying with pathological and physiological conditions (Chiappin et al., 2007). Saliva is non-invasively accessed, making it an attractive source of biomarkers, EV-associated or not, especially for oral and periodontal conditions (Nonaka & Wong, 2022; Ogawa et al., 2008). In saliva EV studies, common co-isolates include salivary components such as eukaryotic cells and subcellular structures, proteins such as enzymes and antibodies, electrolytes, food debris, bacterial cells and bacterial EVs (Aps & Martens, 2005; Chiappin et al., 2007; Han, Bartold, et al., 2021; Kaczor-Urbanowicz et al., 2019; Ngamchuea et al., 2017; Ogawa et al., 2008). The overall composition of saliva depends on the relative activity and contributions of the three major pairs of salivary glands—parotid, submandibular and sublingual—as well as 300–750 minor salivary glands (Aps & Martens, 2005; Khurshid et al., 2016), which may secrete different amounts of salivary enzymes and mucins.

Parameters to report in saliva studies are whether whole saliva or saliva from one type of gland only is collected; the method of saliva collection (Beale et al., 2016; Khurshid et al., 2016; Navazesh, 1993); salivation stimulus, if any (Gomar-Vercher et al., 2018). Recency of food and drink intake may have outsized effects on saliva quantity and quality and should be standardised if possible or assessed at collection. From studies of whole saliva, age (Xu et al., 2019), biological sex (Li-Hui et al., 2016), smoking (Rad et al., 2010), stress (Keremi et al., 2017), exercise (Ligtenberg et al., 2016), oral hygiene, medical conditions and medications, and mental health status (Aps & Martens, 2005; Bhattarai et al., 2018) may be associated with differences in one or more of viscosity, pH, concentrations of different proteins, and saliva flow rate. However, it is not known if these factors affect or are associated with the concentration and composition of saliva EVs, so additional studies are needed.

Recommendations:

- Report the source of saliva clearly (whole or from a specific gland), the method used for collection, and any stimulus used.
- Standardise allowed food and drink intake prior to collection or, at minimum, assess these factors at collection.

3.8 | Synovial fluid

Synovial fluid (SF) is a viscous fluid within the spaces of joints. SF EVs have potential as biomarkers and therapeutic agents for joint disorders (Boere et al., 2019) since SF is in direct contact with affected tissues (Michael et al., 2019). The viscosity of SF is due to large amounts of protein and the glycosaminoglycan hyaluronic acid (HA). This viscosity poses several hurdles to reproducible SF EV studies, for example, making it challenging to pellet cells/debris prior to freezing and hampering EV recovery. Indeed, most reported samples have been frozen and thawed before EV separation and characterisation, with inconsistent pre-freezing removal of cells and debris (Gao et al., 2020; Rüwald et al., 2020). Hyaluronidase treatment of SF is required for accurate detection of inflammatory cells and soluble mediators (Boere et al., 2019). Most research groups use hyaluronidase to decrease SF viscosity before EV separation, but others do not (Mustonen et al., 2021). SEC may outperform UC in removal of proteins such as albumin, fibronectin and apolipoprotein A-I (Foers et al., 2018). Donor characteristics that may associate with differences in SF variables and possibly EVs include biological sex (Kolhe et al., 2020) and disease identity and stage (Foers et al., 2020; Schioppo et al., 2021).

Recommendations:

- Consider the use of hyaluronidase to reduce viscosity and obtain homogenised synovial fluid before EV separation and characterisation.

20013078, 2024, 2, Downloaded from https://isevjournals.onlinelibrary.wiley.com/doi/10.1002/jev2.12404 by Colorado State University, Wiley Online Library on [09/10/2024]. See the Terms and Conditions (https://onlinelibrary.wiley.com/terms-and-conditions) on Wiley Online Library for rules of use; OA articles are governed by the applicable Creative Commons License

20013078, 2024, 2, Downloaded from https://isevjournals.onlinelibrary.wiley.com/doi/10.1002/jev2.12404 by Colorado State University, Wiley Online Library on [09/10/2024]. See the Terms and Conditions (https://onlinelibrary.wiley.com/terms-and-conditions) on Wiley Online Library for rules of use; OA articles are governed by the applicable Creative Commons License

3.9 | Milk

Milk is a rich and complex source of nutritional and immunological components, which include cells, milk fat globules (MFGs), casein micelles, soluble molecules and EVs (Ballard & Morrow, 2013). EVs separated from milk of at least 16 different species have thus far been reported, chiefly human and bovine. To allow separation of relatively pure EVs, milk components that share EV characteristics such as density and size [MFGs and cellular debris (Busatto et al., 2019)] should be removed, for example, by centrifugation), and milk should be kept at body temperature for short-term storage (Zonneveld et al., 2014). Casein micelles, which overlap in size with EVs, are the biggest challenge, especially for milk of ruminant species. Casein micelles can be precipitated by pelleting after acidifying milk to pH 4.6 (Mukhopadhya, Santoro, Moran, et al., 2021; Rahman et al., 2019; Santoro et al., 2023; Somiya et al., 2018), aggregated by enzymatic treatment (Gao et al., 2019), or dissociated by sequestering calcium with EDTA (Gao et al., 2019) or sodium citrate (Benmoussa et al., 2020). Currently, there is no preferred method, but acidification and EDTA are used most often. Following pre-processing, cleared milk supernatant can be stored until EV separation. Methods such as UC, dgUC and SEC may be combined for higher purity, since single-step approaches will yield a low purity. Colloidal properties and acceptable storage times until processing may be different for raw, homogenised, pasteurised, ultra-high temperature-treated, and dried/powdered milk (Mukhopadhya, Santoro, & O'Driscoll, 2021). Furthermore, the effects of storage length and temperatures have yet to be comprehensively determined.

Recommendations:

- Keep milk at body temperature for short-term storage prior to storage or EV separation.
- Common EV co-isolates include cells/components, milk fat globules, and casein micelles. These should be removed (and/or, in the case of micelles, disrupted), and their presence tracked through the EV separation process.

3.10 | Solid tissue

Cell-EV interactions in solid tissues may primarily involve EVs that are released near the site of action. It is thus important to study EVs in tissue. However, greatly complicating the study of tissue EVs is the interrelated diversity of tissue harvesting and storage methods, cellular and extracellular matrix composition, and physical properties. Despite these challenges, two basic approaches to tissue EV studies have been developed and applied mostly to brain or tumor tissues.

Tissues can be used for EV studies by keeping tissues/cells 'alive' in culture after harvesting or by harvesting EVs directly from tissue before or after storage. Some tissues can be cultured ex vivo over several days and culture medium harvested for EV separation (Lunavat et al., 2017; Jeurissen et al., 2017; Jingushi et al., 2018). EV preparations may include tissue EVs present in the original tissue, EVs released during culture (perhaps with different properties from the native EVs), and products of cell death in culture like apoptotic bodies (Carrel & Burrows, 1911). Keeping tissue under conditions as close to their in situ environment as possible may be very important, such as maintaining tissue hydrated prior to culturing and avoiding high oxygen concentrations, although limited evidence has been gathered for the influence of these factors on collected EVs. Alternatively, tissue is processed immediately after resection (Cianciaruso et al., 2019; Crescitelli et al., 2020; Crescitelli et al., 2021; Gallart-Palau et al., 2016; Huang et al., 2020; Jang et al., 2019; Jeppesen et al., 2019; Perez-Gonzalez et al., 2012; Steenbeek et al., 2018) or after prior storage, usually freezing (Hurwitz et al., 2018; Hurwitz et al., 2019; Huang et al., 2020; Perez-Gonzalez et al., 2012; Vella et al., 2017; Yelamanchili et al., 2015). A preliminary study found no major differences in EV composition in fresh versus frozen tissues (Shen et al., 2023). Tissues are typically divided into small pieces [using tissue homogenizers (Gallart-Palau et al., 2016; Hurwitz et al., 2018; Hurwitz et al., 2019; Yelamanchili et al., 2015), vortexing (Banigan et al., 2013) or slicing (Huang et al., 2020; Jeppesen et al., 2019; Polanco et al., 2016; Vella et al., 2017)], followed by enzymatic treatment to disrupt the extracellular matrix (ECM) (Jingushi et al., 2018). These methods result in different degrees of cell damage, potentially introducing EV-like artefacts.

Recommendations:

- For ex vivo culturing approaches, keep the tissue as close as possible to its 'native' conditions, including maintaining hydration and nutrition. Consider also the influence of cell death processes on the EV preparation.
- For separating EVs directly from tissue (without ex vivo culturing), establish or follow best practices for the specific tissue in harvesting (e.g., perfusion or not of an animal model to minimise effects of blood); storage (does freezing affect outcome?); physical and enzymatic tissue separation (if done) and influence of specific EV separation/concentration methods.

- Tissue EV characterisation should focus in particular on tracing the presence of cellular components that may be expected to be depleted in EVs, since cells and cellular artefacts may be the key contaminants of tissue EV preparations.

3.11 | Other sources

Not all sources of EVs are covered above; only those for which ISEV recently had or currently has a Task Force. ISEV members are welcome to propose formation of new task forces where no ISEV task force yet exists. These, in turn, may help to inform best practice.

3.12 | Pre-separation and post-separation storage

Storage conditions of both pre-separation sources and post-separation EVs may also affect EV yields, contents, functionality, and the ratio of single particles and aggregates. For most EV sources, pre-processing is advisable prior to pre-separation storage to remove potentially interfering entities such as cells. However, stringent pre-processing is not always possible. Details of whatever steps are performed should be reported, and an explanation given if pre-processing cannot be done. Acceptable storage prior to EV separation varies by source. Storage conditions, including any additives [e.g., bactericidal agents (Lucas et al., 2021)], should be fully reported and the influence on EV quantity and quality investigated if not already known.

Following separation of EVs, EVs should be studied in as native a form as possible. However, for most studies, stored EVs are used. Here, several considerations apply. All storage vessels and their materials should be reported, as EVs can be lost by attaching to surfaces (Evtushenko et al., 2020). Separated EVs may be stable without freezing for some time, but this may vary by EV composition and source and of course information on storage of EVs from some matrices is more comprehensive to date compared to information on EVs from other matrices. Long-term storage is typically at −80°C, although other temperatures have been examined. For example, saliva EVs were reportedly stable at 4°C for up to 20 months, retaining membrane integrity and protein content (Kumeda et al., 2017). Urinary EVs have reportedly been stored at −20°C for up to four years (Barreiro et al., 2021). Lyophilisation of EVs is also possible (Trenkenschuh et al., 2022). There is conflicting evidence on the effects of freeze-thaw cycles on EV properties. A study of saliva EVs found minimal effects of freeze-thawing on membrane integrity (defined as dipeptidyl peptidase IV activity) (Kumeda et al., 2017). However, studies of various sources of EVs have reported particle concentration and other changes with freeze-thawing (Gelibter et al., 2022; Görgens et al., 2022). Cryoprotectants may reduce effects of freeze-thaw (Le Saux et al., 2020; Lőrincz Á et al., 2014); for example, supplementing phosphate buffered saline (PBS) with human albumin and trehalose (PBS-HAT) reportedly improved short- and long-term stability for EVs stored at −80°C and through several freeze-thaw cycles (Görgens et al., 2022). Since optimal storage conditions may vary by EV composition and source, the freezing method (e.g., snap-freezing in liquid nitrogen, gradual freezing), suspension buffer (including cryoprotectants and other additives), temperature, duration of storage until use, thawing method (speed, temperature) and number of freeze-thaw cycles should be reported. Freeze-thaw cycles should be minimised, for example, by a careful aliquoting strategy, and samples with different numbers of freeze cycles may not be directly comparable.

> Consensus: 70.4% (703) of MISEV2023 survey respondents agreed "completely," and 28.5% (284) agreed "mostly" with Section 3: Collection and pre-processing: pre-analytical variables through to storage. 0.1% (1) "mostly" disagreed, and 1.0% (10) stated that they had no opinion and/or expertise. No respondents disagreed "completely."

4 | EV SEPARATION AND CONCENTRATION

EVs are typically characterised and used after one or more separation or concentration procedures. Trends in these approaches have been previously assessed by ISEV (Gardiner et al., 2016; Royo et al., 2020). Separation/concentration can be performed according to the EV biophysical characteristics of size, density, charge and surface composition (specific surface molecules). Other terms that are sometimes used for these procedures include 'enrichment', 'purification' and 'isolation'. The material captured after separation/concentration is an 'EV-containing preparation' or 'EV preparation' that may require storage prior to analysis or use. Any separation method should be chosen based on the known properties of the specific EV sources and the desired EV yield and specificity. When separating complex biofluids, quantification of yield and specificity for total EVs will likely be estimates, since particle number quantification is not always EV-specific and/or typically relies on surrogates of EV abundance such as spike-in populations or measurement of detectable subpopulations. Figure 2 shows the position of some commonly used methods for EV preparation on a yield (recovery) versus specificity grid. This section provides information and suggestions on some of these methods. More detailed information can be found in the literature (Hendrix et al., 2023).

20013078, 2024, 2, Downloaded from https://isevjournals.onlinelibrary.wiley.com/doi/10.1002/jev2.12404 by Colorado State University, Wiley Online Library on [09/10/2024]. See the Terms and Conditions (https://onlinelibrary.wiley.com/terms-and-conditions) on Wiley Online Library for rules of use; OA articles are governed by the applicable Creative Commons License

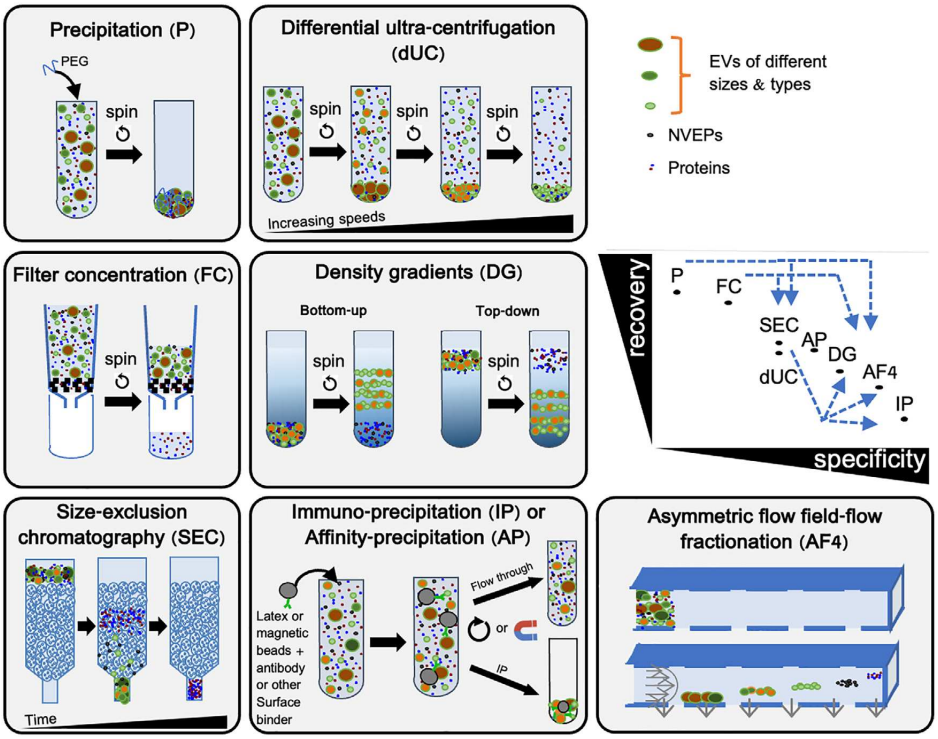


FIGURE 2 Position of some EV separation and concentration methods on a recovery (yield) versus specificity grid. Dashed blue arrows indicate combinations of methods resulting in increased specificity. Specificity can be of different types: Size exclusion chromatography (SEC) separates EVs by size from many (but not all) NVEPs, but all EV types are recovered together, while differential ultracentrifugation (dUC) separates EV subtypes based on their size/weight, but also co-isolates NVEPs at high speeds. Note that many 'exosome purification' kits use precipitation (P), thus do not isolate pure exosomes or even EVs but a mixture of EPs, while some use affinity precipitation (AP), which may be more specific to EVs but not exosomes. Those who develop new methods should consider positioning their EV outcomes on such a graph.

EVs can sometimes be studied or used directly and immediately in the source matrix. In biomarker studies, for example, there may be no need to separate or concentrate EVs from a biological matrix if sufficient specificity and sensitivity are reached with the unfractionated sample. In some cases, EVs can also be analysed specifically and directly in a biological fluid (Duijvesz et al., 2015; Woud et al., 2022). However, to show exclusive EV association of a proposed biomarker or function, separation may be required in the first instance, and further guidance on this is provided here.

4.1 | EV concentration

Concentration in EV studies is the act of increasing the particle number:sample volume ratio. Concentration may be needed in various settings. Large volumes of source materials like CCM, urine, milk may require concentration before EVs can be separated from other EPs. For example, chromatography columns may have a maximum loading volume, while some separation methods may be more efficient if material is first concentrated (e.g., some immunoisolation procedures). Concentration methods may, but do not necessarily, also achieve some degree of separation of particle types.

Concentration can be done by several approaches. Polymer-based methods of precipitation reduce the availability of biomolecules to solvent, 'crowding out' water molecules. This allows suspended/dissolved materials including EPs to be pelleted by low-speed centrifugation. Some commercial kits that are described as 'exosome isolation' kits in fact rely on such polymer precipitation and do not strictly 'isolate' EVs, much less subtypes of EVs. Precipitation methods may not achieve any appreciable separation of EPs (Gámez-Valero et al., 2016; Karttunen et al., 2019; Lobb et al., 2015; Paolini et al., 2016).

In filtration, a suspension passes through a filter by, for example, gravity, centrifugation or vacuum: water and molecules smaller than the molecular weight cut-off of the filter pass through, while EPs larger than the cut-off are recovered in the concentrated

20013078, 2024, 2, Downloaded from https://isevjournals.onlinelibrary.wiley.com/doi/10.1002/jev2.12404 by Colorado State University, Wiley Online Library on [09/10/2024]. See the Terms and Conditions (https://onlinelibrary.wiley.com/terms-and-conditions) on Wiley Online Library for rules of use; OA articles are governed by the applicable Creative Commons License

fluid compartment of the filter. A variety of filter cut-offs are available, including 3, 10, 100 and 1000 kDa, allowing filtration to achieve some degree of size separation, not just concentration. A cut-off of 100 kDa retains EVs while removing many proteins, while a cut-off of 1000 kDa may allow passage of some smaller EVs. However, another consideration is recovery, since different filters/tubes may allow different levels of EV 'sticking' and thus recovery (Vergauwen et al., 2017). Please note that filtration may also be performed to retain microbes ('sterilization') or large EVs/EPs in the pre-filter compartment; although care should be taken to avoid extrusion. Tangential flow filtration (TFF, also called cross-flow filtration) is a filter-based concentration method in which liquid and molecules smaller than the pores pass through the filter perpendicularly to the flow applied to the EV-containing fluid. This allows continuous flow and repeated passages of the fluid unless and until the filter is clogged, and thus allows processing of large volumes of fluid. As for other filtration methods, size-based separation can be achieved based on the molecular weight cut-off of the filter. TFF has been successfully and reproducibly used for large-scale EV production, for example, for therapeutic applications (Busatto et al., 2018; Lamparski et al., 2002). Finally, concentration can also be obtained by (ultra)centrifugation, for which parameters are described in the next section.

Summary: Concentration

- Can be done by polymer-based precipitation, filtration including tangential flow filtration, and (ultra)centrifugation.
- Leads to EV-containing preparations containing variable amounts of NVEPs and proteins, depending on the exact method and variables such as filter cut-off (size or molecular weight).

Reporting recommendations: for concentration, report the following:

- nature of the material used for concentration;
- initial and final volumes of biofluid;
- time of processing (incubation with polymer, centrifugation through filters or directly);
- flow rate (for TFF);
- size or molecular weight cut-off (for filtration/concentration);
- temperature during concentration.

4.2 | Differential (ultra)centrifugation

The principle of differential ultracentrifugation (dUC) is to apply increasing relative centrifugal forces (RCF = g-force) to the EV-containing fluid, from which intact donor cells or tissues have first been eliminated by one or more low speed centrifugations. The aim is to pellet sequentially EPs of decreasing sedimentation coefficients. Since the sedimentation velocity of a sphere is proportional to its diameter squared and to the density contrast between the particle and the medium (Stokes' law equation), the largest and/or densest EPs tend to be pelleted in the first (medium speed/short time) steps, while the smallest and/or least dense are recovered predominantly after higher speed/longer centrifugation. However, in practice, perfect EV separations are not achieved by this method, and pellets from different centrifugation speed have overlapping properties and variable biochemical and physical parameters.

Whatever the centrifugation steps used, as detailed in MISEV2018, report speed in rpm and rotor type (to allow calculation of adjusted k-factor), time of centrifugation (to allow calculation of the sedimentation coefficient of the pelleted particles), and temperature. Instrument acceleration and deceleration settings should also be reported. In typical dUC workflows reported in the literature, a maximal force of around 10,000 to 20,000 × *g* is applied for between 10 and 90 min to enrich putatively larger/denser EVs, while a maximal force of around 100,000 to 200,000 × *g* is applied for 45 to 150 min to pellet putatively smaller/lighter EVs. These figures can be used to calculate the sedimentation coefficient (S) of the particles recovered by these different protocols: S = adjusted K factor of the rotor/Time of centrifugation. Theoretically, particles with S coefficients in the range of 15–150 are recovered by the 'larger EV' centrifugation conditions, and those in the range of 2 to 5 by the 'smaller EV' conditions. Particles with smaller S can be recovered by extending the speed and time of centrifugation, at the cost of increasing NVEP/free protein co-isolation. Depending on the centrifugation parameters, the resulting pellets may be enriched for large/dense or for small/light EVs, but complete separation of these populations is not achieved. Yield of smaller EVs may also be low, especially when suspended in protein-rich fluids such as blood products and complex culture medium components, and this problem may not be resolved by simply increasing centrifugation time or speed (Driedonks et al., 2019; Zhang, Borg, et al., 2020). Examples of dUC protocols (with or without density gradient, see next section) and downstream comparison of EVs include (Jeppesen et al., 2019; Kowal et al., 2016; Lischnig et al., 2022; Martin-Jaular et al., 2021).

The majority of published studies have focused on smaller EVs and thus discard and/or do not analyse the pellet(s) obtained with lower-speed centrifugation. To allow comparison between studies and to avoid pelleting larger particles and potentially introducing artefacts, however, it is recommended to perform these first centrifugations. The strong g-force of high-speed UC has also been shown to induce aggregation of EVs (Linares et al., 2015), but this may not be observed for all sources of EVs. When

20013078, 2024, 2, Downloaded from https://isevjournals.onlinelibrary.wiley.com/doi/10.1002/jev2.12404 by Colorado State University, Wiley Online Library on [09/10/2024]. See the Terms and Conditions (https://onlinelibrary.wiley.com/terms-and-conditions) on Wiley Online Library for rules of use; OA articles are governed by the applicable Creative Commons License

analysing a new source of EVs, retain the intermediate centrifugation pellets and analyse them side-by-side at least once with the final, highest-speed pellet to determine whether the molecules or activity of interest are specifically enriched in small EVs or are also present in other subtypes.

Summary: dUC

- Enriches for EV subtypes that are separated according to their sedimentation coefficient, proportional to their diameter and density.
- Co-isolates NVEPs that have the same sedimentation coefficient as EVs, especially after high-speed and lengthy ultracentrifugation.
- May induce aggregation of EVs.

Reporting recommendations: for differential (ultra)centrifugation, report the following:

- speed, rotor type, and time of centrifugation, to allow calculation of the adjusted k-factor (to apply to other rotors) and the sedimentation coefficient of the pelleted EPs;
- tube type and sample volume in the tube;
- temperature during centrifugation;
- acceleration and deceleration (brake) settings.

4.3 | Density gradient/cushion

Density gradients or cushions can be used to separate certain NVEPs and proteins from EVs based on the characteristic densities of different classes of EPs (Raposo et al., 1996). Gradients are prepared of layers consisting of different ratios of a selected dense medium (like sucrose, iodixanol or iohexol) and aqueous buffers, with density decreasing from bottom to top of the gradient, whereas cushions consist of a homogeneous layer of dense material below an aqueous column. EV-containing materials can be loaded beneath a gradient ('bottom-up') or onto the top of a gradient or cushion ('top-down') and then ultracentrifuged. In the bottom-up approach, the EV-containing preparation is mixed with high-density medium, loaded at the bottom of a centrifuge tube, and overlayed with layers of decreasing density; the preparation may also be underlaid under a prepared gradient. As ultracentrifugation proceeds, particles that are less dense than the surrounding medium float upwards. With sufficient time, particles will ultimately reach a density fraction corresponding to their buoyant density. Since smaller EVs travel at a relatively slower rate than larger EVs, especially in viscous media, the bottom-up approach in velocity sucrose density gradient UC can also be used to separate EVs according to size (Aalberts et al., 2012). In top-down settings, the EV-containing preparation in a low-density medium is loaded onto the top of a gradient or cushion: for gradients, particles travel into the gradient at a rate corresponding to their density and size until their equilibrium buoyant density is reached; for cushions, particles that reach the cushion remain at the interface if less dense than the cushion material but continue into and through the cushion if they are denser. The cushion approach is thus easier to implement but separates EPs by a threshold of density. Importantly, for gradients, lengthy ultracentrifugation may be needed for optimal separation [e.g., longer than 48 h (Aalberts et al., 2012; Palma et al., 2012)], but shorter spins may suffice for some applications [e.g., 1–2 h (Kowal et al., 2016), 16 h (Aalberts et al., 2012; Liao et al., 2019)].

Following separation by gradient, fractions must be collected carefully to avoid disrupting the gradient. It is good practice to confirm density of final fractions, for example, by weighing given volumes or measuring refractive index. Before performing most downstream assays, the density medium must be removed. This can be done, for example, by diluting the fractions with buffer and ultracentrifuging, or by using SEC. Recovery after density gradient and fraction washing is relatively low.

Summary: density gradients and cushions

- Can be implemented in different settings (top-down, bottom-up) depending on the aim, that is, to separate EVs from proteins, or from NVEPs, or to separate EV subtypes.
- Leads to low recovery of high-purity material (based on density).

Reporting recommendations. For density gradients and cushions, report the following:

- density material, buffer composition, and exact method of gradient/cushion preparation;
- volume and concentration of material loaded, as well as method of loading onto or at the bottom of the column;
- exhaustive description of centrifugation parameters (same as for dUC);
- details of collection procedure, final densities of fractions (where relevant), and washing.

20013078, 2024, 2, Downloaded from https://isevjournals.onlinelibrary.wiley.com/doi/10.1002/jev2.12404 by Colorado State University, Wiley Online Library on [09/10/2024]. See the Terms and Conditions (https://onlinelibrary.wiley.com/terms-and-conditions) on Wiley Online Library for rules of use; OA articles are governed by the applicable Creative Commons License

4.4 | Size exclusion chromatography

SEC separates nanoparticles including EVs based on size (Boing et al., 2014; Karimi et al., 2018). In SEC, a sample is placed onto the top of a column loaded with a matrix that contains passages with defined pore size. Driven by gravity or by pressure from a pump, larger particles pass through the matrix quickly, without entering the pores, and can be collected as early fractions, while smaller particles (smaller than the matrix pore size) are retained longer and elute predominantly in later fractions. Certain SEC matrices allow separation of EV-sized particles (EVs, viruses, larger lipoprotein particles) from small NVEPs and free proteins.

Variables that affect the degree of separation by SEC include the matrix composition and pore size, column packing method, the ratio of column length to diameter (or volume), flow rate (gravity vs. defined pressure), and applied sample concentration and volume. Size exclusion columns can be home-made or purchased. Commercial columns are often packed under strictly controlled conditions and may allow more reproducible results than home-made columns. Abundance and purity of EVs and other NVEPs in collected fractions must be established through careful characterisation, as for all other methods. SEC dilutes the sample, increasing volume compared with the input material, so concentration of a sample before or after SEC may thus be needed. SEC size separation can be combined with affinity methods by modifying the matrix. The related method of bind-elute chromatography combines size-based separation with selection by charge or molecular affinity and permits a single elution (with retention of unwanted materials) that may be amenable to high-throughput separations, for example, in multi-well plates. In some cases, SEC matrices can be reused after thorough cleaning.

Summary: SEC

- SEC is an easily accessible technique for size-based separation of particles.
- Columns can be packed with a variety of matrices and at different scales, depending on desired capacity and resolution of separation.

Reporting recommendations. For SEC, report the following:

- type of matrix and pore size; height and diameter (or volume) of matrix-containing column;
- method of column packing (or source of commercially-available columns);
- source, volume and particle concentration of pre-SEC sample, including any prior separation/concentration steps;
- buffer composition;
- specify gravity flow or pressure. If pressure, indicate pump system and pressure parameters;
- void volume and numbers and volume of fractions collected;
- any post-SEC concentration methods;
- if columns are re-used, method of column regeneration and number of times the column has been used.

4.5 | Fluid flow-based separation

Fluid flow-based techniques separate EVs and other particles based on one or more particle properties, but without relying on a 'matrix' or stationary phase. The two main categories of flow-based techniques currently used in EV studies are field-flow fractionation (FFF, Giddings et al., 1976) and free-flow electrophoresis (FFE, Preußer et al., 2022). These techniques can be applied to highly heterogeneous input materials, and the absence of a solid phase allows high particle recovery. They are also among the gentlest of separation methods and may thus be used to study molecules that are loosely associated with EVs.

The most prevalent FFF approach in EV studies is asymmetric flow FFF (AF4, Sitar et al., 2015), in which particles in a sample are transported by fluid flow with a parabolic pattern through a long, thin channel, while a field perpendicular to the direction of transport tends to concentrate particles against the bottom of the channel. Smaller particles, diffusing more rapidly, are more likely to enter the higher-velocity flow regions in the middle of the channel, and particles are thus separated by hydrodynamic size. Some degree of purification may also be achieved by a channel bottom consisting of a molecular weight cut-off filter. Although AF4 can precisely separate particle populations with small differences in size (Hood et al., 2014; Zhang et al., 2018), it is not specific to EVs in its standard configuration. AF4 is also not a preparative technique. In contrast, FFE combines flow with electrophoresis, adding separation by, for example, isoelectric point (Preußer et al., 2022). Introducing separation buffers with different pH or other characteristics across the separation channel allows high-resolution separation of different EV and other EP populations. FFE can be done at various scales.

Summary:

- Fluid flow-based separations such as AF4 can achieve size-based separations with high resolution.
- Lacking a solid phase and with limited applied forces, flow is gentler than most EV separation techniques.

20013078, 2024, 2, Downloaded from https://isevjournals.onlinelibrary.wiley.com/doi/10.1002/jev2.12404 by Colorado State University, Wiley Online Library on [09/10/2024]. See the Terms and Conditions (https://onlinelibrary.wiley.com/terms-and-conditions) on Wiley Online Library for rules of use; OA articles are governed by the applicable Creative Commons License

- Size-based separation can be combined with separation by other principles by applying different types of fields.
- Preparative scales can be reached with flow techniques such as free-flow electrophoresis.

Reporting recommendations. For flow-based separations, report the following:

- all instrumentation, including pumps and collection devices;
- composition of all buffers and their filtration. Especially in FFE: how properties of the buffers were confirmed;
- all field characteristics such as flow rates and pressures, pH gradients, electric field;
- dimensions and composition of separation chambers, including any molecular weight cutoff plates;
- all relevant details of fraction collection.

4.6 | Charge and molecular recognition-based separations

The common principle of all affinity methods is to capture EVs based on their surface charge or molecular composition. Ion-exchange chromatography takes advantage of a very simple affinity of particles/surfaces of opposite charge: EVs and/or NVEPs have affinity for a matrix based on negative (anion-exchange) or positive (cation-exchange) surface charge (Saari et al., 2023). In contrast, the term 'affinity separation' as commonly used in molecular biology refers to methods that harness the specific recognition of one macromolecular complex for another. In this context, affinity probes include heparin and various lectins (which bind glycans, Balaj et al., 2015); specific full-length proteins with affinity for a particular lipid or protein (e.g., Tim4 for phosphatidylserine, (Nakai et al., 2016); peptides that bind specific EV surface proteins (Bai et al., 2014; Gao et al., 2018; Gobbo et al., 2016; Joy et al., 2018; Liu et al., 2019; Pham et al., 2021; Suwatthanarak et al., 2021) or the membrane more generally (Gori et al., 2020; Ishida et al., 2020; Yang et al., 2022), including curvature-sensing peptides that select for EVs in certain size ranges (Saludes et al., 2012); aptamers [short single-stranded DNA or RNA molecules that are developed to bind specific targets (Zhang, Yue et al., 2019)]. Antibodies that are raised to recognise specific EV surface molecules are the most commonly used affinity reagents, and their most-used targets are the tetraspanins (Kowal et al., 2016; Mathieu et al., 2021).

In molecular recognition-based affinity approaches, the EV-containing fluid (which may have first been concentrated according to Section 4.1) is introduced to affinity probes before or after the latter are bound to a matrix, such as a membrane or beads. Beads, in turn, can be placed in a column or tube to facilitate binding and washing. Molecular target-displaying materials are bound by affinity probes to the matrix ('pull-down'), while unbound material flows away ('flow-through'). Non-specifically bound materials may be removed by one or more washes. If EVs are the intended target, detergent should not be present in the dilution and washing buffers unless at very small concentrations (0.001% or less) to minimise non-specific binding to the capturing matrix or between EVs. To evaluate the efficiency and specificity of recovery of the targeted EVs, it is recommended, at least during protocol development, to compare side-by-side the flow-through and the pull-down by biochemical analyses, measuring the affinity motif and a few EV markers (see Section 5).

Bound EVs can be dissociated from the matrix and recovered by a variety of techniques, ranging from changing the properties of the buffer, to adding an excess of target molecules (e.g., sugars or lipids), to eliminating factors required for efficient binding (e.g., using EDTA to chelate calcium). However, some affinity reagents may bind tightly to their EV target and require removal by, for example proteases. In some cases, the EV-binding molecule and/or the matrix may be recovered together with the EVs. This may not be an issue if downstream analyses are not affected by these materials (e.g., nucleic acid analysis of EVs contaminated with a protein-based affinity probe), but it may be in other cases, (e.g., in functional uses, since the EV surface is modified by an EV-binding molecule). Antibodies are particularly difficult to separate from EVs. Low pH treatment classically used to separate antibodies and antigens will likely affect the structure of EVs, and protease treatments may also digest proteins on the surface of the EVs.

In any molecular affinity approach, it is important to understand the degree to which the target molecule is associated with EVs versus NVEPs, or with one EV subtype versus others, and to assess the specificity of the capture reagent. For example, the use of CD9 or CD63 affinity capture for urinary EVs (uEVs) excludes uEVs from cells of the proximal nephron (Blijdorp et al., 2021; Limbutara et al., 2020). In another example, the literature on L1CAM affinity (a putative neuronal EV marker) has developed substantially since MISEV2018. Although L1CAM has been investigated as a membrane-associated antigen to separate putative neuronal EVs from peripheral blood samples, it has more recently been described as being in a cleaved, mostly soluble form in certain EV sources (Norman et al., 2021). It is also found on EVs from a variety of sources, not just neurons, and a widely-used anti-L1CAM antibody might also recognise other targets (Gomes & Witwer, 2022; Norman et al., 2021).

Summary: charge and molecular recognition affinity-based methods

- Separate components of EV preparations according to surface charge or exposure of a specific molecular determinant.
- Will co-isolate all EV subtypes or NVEPs which expose a given charge or molecular determinant: specificity and recovery depend on the specificity versus universality of exposure of the chosen molecular determinant.

20013078, 2024, 2, Downloaded from https://isevjournals.onlinelibrary.wiley.com/doi/10.1002/jev2.12404 by Colorado State University, Wiley Online Library on [09/10/2024]. See the Terms and Conditions (https://onlinelibrary.wiley.com/terms-and-conditions) on Wiley Online Library for rules of use; OA articles are governed by the applicable Creative Commons License

- Antibody-based affinity separation leads to co-isolation of the determinant-exposing EPs with the antibody and/or isolation beads.
- Efficiency and selectivity must be quantified when establishing the protocol by quantifying material recovered in pull-down versus flow-through.

Reporting recommendations: for affinity-based separation, report the following:

- molecule used as affinity probe (nature, source);
- matrix (beads, gel, column);
- incubation times;
- buffer and number of washes;
- elution process (such as elution buffer composition, time).

4.7 | General considerations and caution on kit-based approaches

Due to overlapping biophysical characteristics of EPs (Geeurickx et al., 2019; Karimi et al., 2018) and the abundance of many NVEPs in various EV sources, complementary separation techniques are increasingly applied sequentially (Benedikter et al., 2017; Stam et al., 2021; Zhang, Borg, et al., 2020) (arrows in Figure 2), which allows increased specificity. Examples of methods used to separate EVs from protein aggregates and other NVEPs include size exclusion chromatography, density gradient ultracentrifugation (Jeppesen et al., 2019), asymmetric flow field-flow fractionation (AF4) (Zhang et al., 2018) and ultra-high-speed ultracentrifugation (Zhang, Higginbotham, et al., 2019; Zhang et al., 2021). However, some of these studies suggest that several proteins previously proposed to be sEV markers are equally, if not more, abundant in NVEPs, thus calling for re-evaluation of the achieved EV selectivity.

Conversely, a growing realization since MISEV2018 is that some molecules that co-isolate with EVs, including proteins, nucleic acids, sugars, and lipids, could be viewed not as 'contaminants', but rather as a part of a dynamic EV 'corona' (Buzas, 2022; Palviainen et al., 2020; Tóth et al., 2021). Molecules and even biological nanoparticles such as lipoproteins (Busatto et al., 2022; Sódar et al., 2016) may adsorb to the EV surface where they may serve as biomarkers or contribute to EV function (Musicò et al., 2023; Radeghieri et al., 2022). The EV corona may be removed in part or in full by separation processes including dUC and SEC (Singh et al., 2020; Wolf et al., 2022). Ongoing studies of the EV corona may change how we view contaminants and the perceived need for highly pure EVs; this point is also relevant for the next MISEV section, on EV characterization.

Only methods using readily (i.e., commercially) available devices and instruments are described in this section. However, new developments of separation methods, including those involving equipment built in individual laboratories, are occurring constantly and are strongly encouraged by ISEV. When establishing a new separation/concentration workflow, a good practice is to assess the extent of EV separation/concentration with methods discussed in Sections 5 and 6 and with careful and complete book-keeping. Comparing the results with those of another already established method is also recommended. For example, EV marker proteins can be tracked and related to total isolated protein to determine fold enrichment over total protein reported and account for EV marker losses (Geeurickx et al., 2019; Zhang, Borg, et al., 2020). Results will indicate recovery and degree of enrichment and will also show whether the separated EV population is representative of the original population or has been selectively obtained.

Finally, some cautionary notes on commercial kits. Numerous kits are advertised as obtaining specific types of EVs (usually 'exosomes') or EVs from specific types of sources. These kits may or may not achieve EV separation or concentration based on a variety of principles, including polymer precipitation, membrane affinity, antibody capture and filtration. These kits may be helpful under certain circumstances, but EV researchers should be aware of several major caveats. Kits that do not disclose details of the principles of EV separation/concentration may produce results that are difficult to interpret, not least because they may introduce unknown contaminants (e.g., polyethylene glycol for some polymer precipitation kits). Extra work may be needed to compare these methods with results from other techniques and to place the results on the recovery/specificity grid (Figure 2) for better interpretation. Precipitation-based kits in particular will concentrate all EPs in a mixture, even many free proteins, resulting in a highly impure preparation, especially from complex, NVEP-rich sources such as blood plasma and serum. Use of such kits is strongly discouraged unless for volume reduction alone (Gámez-Valero et al., 2016; Karttunen et al., 2019; Lobb et al., 2015; Paolini et al., 2016). In contrast, affinity-based methods may isolate only subtypes of EVs, and the specificity of the affinity reagents may be difficult to assess if the exact reagents are not disclosed. Generally, kits that disclose contents and principles should be preferred over kits that make unsubstantiated claims (e.g., 'exosome' isolation) and do not provide details.

20013078, 2024, 2, Downloaded from https://isevjournals.onlinelibrary.wiley.com/doi/10.1002/jev2.12404 by Colorado State University, Wiley Online Library on [09/10/2024]. See the Terms and Conditions (https://onlinelibrary.wiley.com/terms-and-conditions) on Wiley Online Library for rules of use; OA articles are governed by the applicable Creative Commons License

20013078, 2024, 2, Downloaded from https://isevjournals.onlinelibrary.wiley.com/doi/10.1002/jev2.12404 by Colorado State University, Wiley Online Library on [09/10/2024]. See the Terms and Conditions (https://onlinelibrary.wiley.com/terms-and-conditions) on Wiley Online Library for rules of use; OA articles are governed by the applicable Creative Commons License

Recommendations

- If separation/concentration is not done, indicate why. Otherwise, justify why each separation/concentration method was selected in terms of yield and specificity.
- Provide sufficient methodologic detail to allow replication of each separation and concentration step.
- Report any measurements that are used to assess the separation/concentration process(es). Where applicable and feasible, and especially when establishing a new workflow, check EVs before and after each step. For example, track EV marker protein levels relative to total protein to estimate fold enrichment and yield for each step.
- For affinity-based EV separation approaches, establish molecular specificity of reagents and EV/EV subtype-specificity of all targeted markers.

> Consensus: 74.4% (743) of MISEV2023 survey respondents agreed "completely," and 24.8% (248) agreed "mostly" with Section 4: EV separation and concentration. 0.1% (1) "mostly" disagreed, and 0.6% (6) stated that they had no opinion and/or expertise. No respondents disagreed "completely."

5 | EV CHARACTERIZATION

EV characterization is needed for estimation of EV quantity, to establish the presence of EVs, and to assess the contributions of non-EV components to an EV preparation. Characterization is challenged by small particle size, heterogeneity of EV size and molecular heterogeneity, a lack of universal EV identification methods, and the non-EV-specificity of many measurement techniques. As a result, no single measurement or method is able to satisfy all EV characterization requirements, and use of orthogonal methods (those that do not have the same measurement limitations) is recommended.

If making claims about an EV preparation, the extent to which a sample will need to be characterised to justify the claims may depend upon the source of the material (see Section 4). This may mean additional characterization steps are needed with different samples and may also mean that additional reporting information is required to allow the influence of other preanalytical variables on EVs to be assessed.

Overall EV composition (contribution to total mass of proteins, lipids, nucleic acids and other biomolecules) varies by EV source. While measurement of these individual molecular classes can be used to estimate EV abundance, these values do not necessarily perfectly correlate with EV concentration, nor is there universality across source materials; thus, they should not be used as a sole measure of EV concentration.

Just as no single molecular class measurement can quantify all EVs, there are also no universal molecular markers of EVs or EV subtypes. Markers must be chosen based on source- and type-specific evidence. Currently, no generic marker is known to identify all EVs irrespective of source. Although several proteins have been proposed as putative markers of EV biogenesis pathways (e.g., Annexin A1 (Jeppesen et al., 2019), SLC3A2, and BSG (Mathieu et al., 2019) for purported ectosomes, and Lamp1 (Mathieu et al., 2021)) for purported exosomes, the universality of these markers is not yet clear or accepted. Note that affinity-based protocols involving the tetraspanins CD9, CD63 and CD81 are not specific for exosomes as an EV subtype; using antibodies to each of these tetraspanins enriches EV populations that do not completely overlap in molecular composition (Kowal et al., 2016; Mathieu et al., 2021). Additionally, not all EVs display these tetraspanins, therefore tetraspanin enrichment does not capture all EVs.

Orthogonal methods measurements of the same parameter are unlikely to have the same biases; for example, the derivation of diameter from optical versus non-optical methods. Characterization of EV samples using orthogonal methods is critical to provide evidence that co-isolates are not responsible for biomarker or functional findings. Due to many EV characterization methods being either not EV specific or unable to detect all EVs, transparent reporting of methods and results is needed for reproducibility of EV data. A framework for reporting EV data has been previously developed and updated in the form of EV-TRACK (EV-TRACK Consortium et al., 2017; Roux et al., 2020). Standardization of EV characterization has been supported by ISEV workshops, the ISEV Rigor and Standardization Task Forces, and ISEV position papers (Clayton et al., 2018; Nieuwland et al., 2020; Welsh, Van Der Pol, Arkesteijn, et al., 2020).

In the following sections different approaches to EV characterization are discussed, with each section providing recommendations if that characterization approach is taken. Overall recommendations for characterization, regardless of the method, are summarised below.

Recommendations

- Each EV preparation should be defined by quantitative measures of the source of EVs (e.g., number of secreting cells, volume of biofluid, mass of tissue).
- Approximations of the abundance of EVs should be made (particle number, protein, and/or lipid content).

- EV preparations should be tested for the presence of components associated with EV subtypes or EVs generically, depending on desired specificity one wishes to achieve.
- Establish the degree to which non-vesicular, co-isolated components are present.
- Provide an indication of the instrument/method limit of detection (LOD) when EVs are characterised with quantitative metrics.

5.1 | Quantification of particle number concentration

EV number can be used along with volume measurement to define the number concentration (in particles/mL), a metric that is widely reported and used for assay input standardization, assay output measurements, and in vivo dosing. However, it is often unreliable, since many techniques lack specificity for EVs and sensitivity for all EVs.

The ISEV Rigor and Standardization EV Reference Material Task Force recently outlined the considerations in measurement techniques, along with the challenges faced by the field in moving towards traceable measurements, for the development and reporting of well-characterised EV reference materials (Welsh, van der Pol, Bettin, et al., 2020). A key highlight of this work is the need to report assay LOD, allowing others to validate findings irrespective of the sensitivity limit. Note that reported EV concentration in blood plasma spans six orders of magnitude depending on the measurement method (Johnsen et al., 2019). Greater confidence in EV concentration measurements may be achieved by using orthogonal methods, each with defined LODs, for example, detecting light scattering intensity, fluorescence intensity and physical size, since orthogonal methods do not share the same measurement limitations (Arab et al., 2021; Silva et al., 2021). For example, for resistive pulse sensing (RPS) techniques that are calibrated with size-standards, a LOD can be reported in diameter. The lower LOD for RPS will most likely be due to sensitivity limitations, while the upper LOD will be influenced by the pore size. For optical techniques such as flow cytometry, the LOD may be reported in diameter, derived from light-scattering optical models, or molecules of equivalent soluble fluorophore (MESF), derived from fluorescence intensities. These approaches result in concordant data across instruments and sensitivities (Welsh, Van Der Pol, Arkesteijn, et al., 2020; Welsh, Jones, et al., 2020; van der Pol, Sturk, et al., 2018). Currently, there is no method to derive a traceable LOD for nanoparticle tracking analysis (NTA), DLS, or imaging flow cytometry, due to the number of variables involved in particle detectability. Techniques that output concentration measurements without any phenotypic characterization, such as the use of membrane dyes, can lead to overestimation of EV concentration due to dye self-aggregation and an inability to differentiate between EVs and other co-isolates (Takov et al., 2017). A membrane dye lacking these problems could lead to underestimation unless it universally stained all EVs, irrespective of composition and derivation, and such a dye has not yet been reported. Further instrument and assay-specific recommendations can be found in Section 6.

For techniques that cannot differentiate EVs from other potential co-isolates or suspension contaminates, it is recommended that concentration be reported as 'particle or EP concentration' and not 'EV concentration', regardless of upstream separation steps.

Recommendations

- Report the LOD of each assay, or state that it is not quantifiable or known.
- Where possible, report data from dilution series to demonstrate that concentration derivations were in the linear region of system measurement.
- Where possible, use orthogonal methods to determine particle number.
- Unless methods are highly specific for EVs, the output of these measures should be described as pertaining to 'particles' or 'EPs'.

5.2 | Quantification of particle size

Measurements of EV size (in nm radius or diameter) rely on assumptions, such as of sphericity or mobility, and output can be influenced by upstream variables (Tian et al., 2020). Common high-throughput methods assume that EVs are spherical. These include flow cytometry, NTA, RPS, multi-angle light scattering and dynamic light scattering (DLS). While 'size' and 'diameter' are often used interchangeably between measurement methodologies, the way in which they are derived can also result in consistent differences in measurement techniques. For example, techniques relying on the mobility of particles, such as NTA or DLS, measure hydrodynamic diameter, resulting in an overestimation of size compared with an imaging method such as cryo-EM (Chernyshev et al., 2015; Skliar et al., 2018). Few if any methods are able to measure EV size accurately throughout the entire possible EV diameter range, from tens of nanometres to microns. For example, while high-resolution imaging by cryo-EM is one of the most accurate methods (Yuana et al., 2013), it is relatively low-throughput, and many larger EVs that tend to be orders of

20013078, 2024, 2, Downloaded from https://isevjournals.onlinelibrary.wiley.com/doi/10.1002/jev2.12404 by Colorado State University, Wiley Online Library on [09/10/2024]. See the Terms and Conditions (https://onlinelibrary.wiley.com/terms-and-conditions) on Wiley Online Library for rules of use; OA articles are governed by the applicable Creative Commons License

magnitude less abundant may not be quantified. The ability to quantify low contrast EVs below 100 nm may also be a limiting factor.

As more researchers use dedicated single-particle techniques with increased sensitivity, it is becoming increasingly clear that many EV preparations display an asymmetric right-skewed distribution, for example, a log-normal distribution, with the majority of EVs <100 nm in diameter (Bachurski et al., 2019; Dong et al., 2020; Lennon et al., 2019; Tian et al., 2018, 2020; van der Pol, Coumans, Grootemaat, et al., 2014). Most single-particle analysis techniques cannot resolve the full population of EVs, so the detected EV diameter distribution should be shared, not just a summary metric such as mean, mode, or median size, which can be easily skewed depending on the LOD and the asymmetric size distribution (Welsh, van der Pol, Bettin, et al., 2020). Be aware that the modal size statistic, as measured, for example, by NTA for low refractive index particles, may better approximate the instrument LOD than the true modal diameter of the EV population (Bachurski et al., 2019). Techniques using software with proprietary algorithms to determine particle diameter may also result in variation between software versions or software platforms (van der Pol, Coumans, Grootemaat, et al., 2014); software and version should therefore be reported. Techniques deriving size from refractive index assumptions may result in variation due to differing compositions and cargo. Derivation of size from fluorescent probes, such as membrane intercalating dyes, may result in variation due to different dye intercalation based on different membrane lipid compositions. For techniques that cannot differentiate EVs from co-isolates/contaminants, it is recommended that diameter be reported as 'particle' or 'EP' diameter and not 'EV diameter', regardless of upstream separation steps.

Recommendations

- Where possible, make orthogonal measurements to increase confidence in size distribution.
- EV diameter distribution of a population should be shared, not just mean, mode, or median.
- Consider the LOD of the method chosen and how this may influence the data.
- Report instrument settings, software platforms and versions and possible influence of measurement reagents, especially intercalating dye.

5.3 | Quantification of total protein

Total protein (in μg, or μg/mL for concentration) in an EV preparation can be approximated by colorimetric assays, fluorometric assays, global protein stain on SDS-PAGE, or absorbance readings, each with differing sensitivities and accuracies (Vergauwen et al., 2017). As a bulk analysis technique, total protein quantification often overestimates EV concentration due to co-isolated protein, especially for less specific methods of EV separation or complex biofluids. Conversely, highly purified, low-yield EV preparations may challenge assay sensitivity. Since measured protein concentration may vary depending upon whether intact or disrupted EVs are measured, details of physical disruption and the nature and concentration of any detergent should be indicated.

Protein concentration as a surrogate of EV concentration should be used with caution and is generally not recommended, as enrichment of some proteins per EV may occur with different cellular phenotypes or stimulations. Since protein:particle ratios also depend on the LODs lower concentration limit of detection or lower size limit of detection of each assay/instrument, it is recommended to provide absolute protein and particle concentrations separately if ratios are reported.

Recommendations

- Report output by 'particles' or 'EPs' unless evidence of upstream processing is highly specific for EVs.
- Report the lower concentration limit of detection of each assay to facilitate interpretation.
- For ratios, report the original constituent measurements, not just the ratio.
- Protein concentration should be within the linear range of the reference curve, which should also be reported.
- Report whether intact or disrupted preparations are used.

5.4 | Quantification of total lipids

Total lipid quantification of EV samples can be achieved by colorimetric assays (Visnovitz et al., 2019), fluorescence of membrane intercalating dyes, total reflection Fourier-transform infrared spectroscopy (FTIR) or chromatography (Mihaly et al., 2017). However, intercalating dye methods and FTIR may be insufficiently sensitive for small amounts of EVs, and some methods require highly specialised equipment. It remains unknown whether these techniques detect all EVs independent of lipid composition. Total lipid measurements may overestimate EVs due to co-isolated NVEPs such as lipoproteins.

20013078, 2024, 2, Downloaded from https://isevjournals.onlinelibrary.wiley.com/doi/10.1002/jev2.12404 by Colorado State University, Wiley Online Library on [09/10/2024]. See the Terms and Conditions (https://onlinelibrary.wiley.com/terms-and-conditions) on Wiley Online Library for rules of use; OA articles are governed by the applicable Creative Commons License

Recommendations

- Consider the LOD of your assay.
- Consider how co-isolated NVEPs may influence your measurement.

5.5 | Quantification of total RNA

RNA is a frequently studied EV-associated molecule (see Section 6.5), so basic characterization of EV preparations may include total RNA quantification as a quality control component or for normalization in profiling and functional studies. Quantification of total EV RNA can be done by capillary electrophoresis and other methods. However, using total RNA as a surrogate for EV concentration or purity is difficult to recommend due to vastly more abundant extra-EV RNA in many EV sources. Some methods of RNA quantification do not distinguish between RNA and DNA. Isolation kits have also been demonstrated to influence downstream results (Eldh et al., 2012). An early ISEV RNA position paper recommended the use of sensitive techniques such as Agilent Bioanalyzer pico chip or Quant-iT RiboGreen RNA Assay for EV RNA quantification over less sensitive methods such as NanoDrop (Hill et al., 2013). However, several nucleic acids dyes, such as RiboGreen, are not specific for RNA over DNA. Additionally, small RNAs require specialised Bioanalyzer kits. Other sensitive methods include the Qubit microRNA Assay kit, which has sensitivity for small RNAs. Pre-treatment with RNase-free DNase may be useful for accurate RNA quantification since many techniques are sensitive to DNA contamination. However, DNase treatment may not completely remove all DNA contamination (Verwilt et al., 2020).

Recommendations

- Consider the ability of your assay to discriminate between RNA and DNA, and the limits of detection of your chosen method.
- Report any enzymatic pre-treatments of the sample, for example, with DNase.

5.6 | Characterization of EV morphology

EV morphology is currently best assessed for smaller EVs using high-resolution imaging techniques such as: scanning electron microscopy (SEM) (Cavallaro, Hååg, et al., 2021) , transmission electron microscopy (TEM) (Théry et al., 2006), cryo-EM (Arraud et al., 2014; Stoner et al., 2016; Wu et al., 2015); and scanning-probe microscopy (SPM), including atomic force microscopy (AFM) (Sharma et al., 2011). EVs that are much larger than the light diffraction limit ($\gtrsim$200 nm diameter) might be assessed by conventional light microscopy. These techniques are not necessarily interchangeable or capable of attaining comparable image quality. For example, desiccated conditions may cause EVs to form an artefactual cup shape, not seen under hydrated conditions. Imaging techniques may allow assessment of EV purity, at least at the particle level, if they can visualise co-isolated NVEPs equally well. Imaging techniques are often limited by low throughput and the potential for bias based on field-of-view selection (Rikkert et al., 2019).

Recommendations

- Irrespective of imaging technique, report all experimental details. These include the instrument, software version, acquisition and analysis settings, sample preparation processes, how the imaged areas were selected, and controls and calibration information where relevant. Further details can be found in Sections 6.4.1 and 6.4.4.

5.7 | Characterization of EVs by protein composition

Because of the heterogeneity of EVs, MISEV2023, like MISEV2018, cannot recommend molecular markers of specific EV subtypes. MISEV2023 recommends the five-component framework introduced in MISEV2018 for reporting claims about the protein content of EVs (Table 3). Categories 1 and 2 assess the presence of EVs features. Category 3 assesses purity from common contaminants. Categories 4 and 5 provide additional information on possible intracellular origins of EVs (4) or co-isolates (5). Ideally, enrichment or depletion of markers in EV preparations versus unfractionated source material should be shown. To avoid perceived restrictions on which EV proteins should be analysed, MISEV2023 gives only a few nominative examples (Table 3). Other putative marker proteins can be assigned to one of the categories using databases such as Uniprot (https://www.uniprot.org/), where the section 'Subcellular location' indicates subcellular compartments or extracellular location, and 'features' indicates

20013078, 2024, 2, Downloaded from https://isevjournals.onlinelibrary.wiley.com/doi/10.1002/jev2.12404 by Colorado State University, Wiley Online Library on [09/10/2024]. See the Terms and Conditions (https://onlinelibrary.wiley.com/terms-and-conditions) on Wiley Online Library for rules of use; OA articles are governed by the applicable Creative Commons License

TABLE 3 Protein content-based EV characterisation.

Category				
1- Transmembrane (or GPI-anchored) proteins associated with plasma membrane and/or endosomes All EVs Non-exhaustive examples, categorized a, b, c: by decreasing strength of membrane association.	**2- Cytosolic proteins in EVs** All EVs	**3- Major components of non-EV co-isolated structures (NVEPs)** All EVs as purity control	**4- Transmembrane, lipid-bound and soluble proteins associated with intracellular compartments other than PM/endosomes** Subtypes of EVs and/or pathologic/atypical state, and/or novel separation method	**5- Secreted proteins recovered with EVs** Corona or functional component of EVs
1a: multi-pass transmembrane proteins. Tetraspanins (CD9, CD63, CD81, CD82); other multi-pass membrane proteins (CD47; heterotrimeric G proteins GNA*, TSAP6)	**2a: with lipid or membrane protein-binding ability**. ESCRT-I/II/III (TSG101, CHMP*) and accessory proteins: ALIX (PDCD6IP), VPS4A/B; ARRDC1; Flotillins (FLOT1/2); caveolins (CAV*); syntenin (SDCBP)	**3a: lipoproteins**. Produced mostly by liver, abundant in plasma, serum. Apolipoproteins	**4a: nucleus**. Histones (HIST1H**); Lamin A/C (LMNA/C)	**5a: blood-derived corona proteins**. Partially overlapping with 3a/3b: apolipoproteins, complement, fibrinogen
1b: single-pass transmembrane proteins. Major Histocompatibility Class I or II, Integrins (ITGA*/ITGB*), transferrin receptor (TFR2); LAMP1/2; heparan sulphate proteoglycans including syndecans (SDC*); EMMPRIN (BSG); ADAM10	**2b: promiscuous incorporation into EVs (and possibly NVEPs)**. Heat shock proteins HSC70 (HSPA8), and HSP84 (HSP90AB1) note that both are abundant also in NVEPs; cytoskeleton: actin (ACT*), tubulin (TUB*); enzymes (GAPDH)	**3b: protein and protein/nucleic acid aggregates**. Immunoglobulins (blood); Tamm-Horsfall protein (Uromodulin/UMOD; urine); albumin. YWAH* (14-3-3*) and AGO* (can be present in EVs but generally more abundant in NVEPs).	**4b: mitochondria**. VDAC, cytochrome C (CYC1); TOMM20	**5b: cytokines and growth factors**. e.g., TGFB1/2; IFNG, VEGFA, FGF1/2, PDGF*, EGF, interleukins (IL*)
1c: GPI- or lipid-anchored proteins. Glypicans (GPC1), 5′nucleotidase CD73 (NT5E), complement-binding protein CD59		**3c: exomere or supermere-enriched components**. HSP90AA/B, TGFBI, HSPA13, LDHA/B	**4c: secretory pathway**. Endoplasmic reticulum, Golgi apparatus: calnexin (CANX); Grp94 (HSP90B1); BIP (HSPA5), GM130 (GOLGA2)	**5c: adhesion and extracellular matrix proteins**. Fibronectin (FN1), Collagens (COL**), MFGE8; galectin3-binding protein (LGALS3BP), CD5L; fetuin-A (AHSG)
			4d: others. Autophagosomes, cytoskeleton… LC3 (MAP1LC3A), Actinin1/4 (ACTN1/4)	

At least one protein of categories 1, 2 and 3 should be analysed as EV hallmarks and to assess the presence of NVEPs in an EV preparation. Analysis of proteins of category 4 is optional, as they may be present in some subtypes of EVs, or under certain conditions, with no general rule. Proteins of category 5 may bind to EVs after their release and may be part of the recently described EV 'corona'. ***Please note that this table provides a limited number of examples only*** for proteins commonly found in mammalian cell-derived EVs. Other proteins that fall into the given categories may be equally valid, particularly for analysis of EVs from prokaryotic (bacteria) or non-mammalian eukaryotic sources (including parasites and plants). For most proteins of interest, their subcellular location in intracellular compartments (for categories 1 and 4), or their transmembrane or lipid-anchored nature (for categories 1 and 2), is provided in the Uniprot database (www.uniprot.org). *XX* = human gene names. *XX** or *XX*** used for families of multiple proteins, for example, for integrins: *ITGA** indicates any integrin alpha chain.

20013078, 2024, 2, Downloaded from https://isevjournals.onlinelibrary.wiley.com/doi/10.1002/jev2.12404 by Colorado State University, Wiley Online Library on [09/10/2024]. See the Terms and Conditions (https://onlinelibrary.wiley.com/terms-and-conditions) on Wiley Online Library for rules of use; OA articles are governed by the applicable Creative Commons License

topological and transmembrane domains. Although these categories apply to EVs regardless of analysis method, some of these markers may not be technically usable in some single-EV analysis techniques, which may require other controls. A variety of methods exist to determine the presence of protein markers. The sensitivity, specificity, and reliability of these methods can vary. Current assay- and instrument-specific reporting considerations are outlined in Section 6.

Recommendation

- Utilise the five-component framework (Table 3) for reporting claims about EV protein content.

5.8 | Non-protein markers of EVs

Non-protein markers, such as phosphatidylserine, glycans or specific nucleic acids, are seldom EV-specific but in some cases may add support for the presence of a lipid bilayer or cytosolic components. Co-localization with protein markers may also provide stronger evidence for the presence of EVs, for example, a membrane-intercalating dye and a tetraspanin-positive event, especially for single-particle measurements. Non-protein markers may be detected directly with techniques such as lipid mass spectrometry or Raman spectroscopy (Section 6.7), or indirectly using fluorescent probes such as membrane labels or intraluminal dyes. Recommendations for the reporting of EV labelling with non-protein markers is outlined in Section 6.6. The non-EV-specificity of most non-protein component markers urges caution. Membrane dyes may complex with any lipids, including those of NVEPs; dyes that are activated by intraluminal enzymes such as esterases may not be present in all EV preparations or subtypes; nucleic acid dyes have been used for EVs, but recommendations on controls and specificity are still needed (Liu et al., 2022).

Recommendations:

- If non-protein markers are used, consider using protein colocalization.

5.9 | Localization of EV-associated components

EV-associated components such as proteins, nucleic acids and glycans, may be luminal, in the membrane, or external to the EV. Knowledge of topology may be important for understanding the biology. For example, must an EV fuse with a recipient cell to deliver a luminal cargo, or can the EV simply present a surface-associated molecule to a receptor? The location of putative active components should therefore be determined by performing mild digestions, permeabilizations or affinity reagent accessibility by adopting or adapting previously published methods (Bonsergent & Lavieu, 2019; Cvjetkovic et al., 2016; Lai et al., 2015; Mateescu et al., 2017; McKenzie et al., 2016; Osteikoetxea et al., 2015; Sharma et al., 2010; Sung & Weaver, 2017).

Recommendations:

- Consider how topology can be determined in method design.

> Consensus: 72.3% (722) of MISEV2023 survey respondents agreed "completely," and 27.0% (269) agreed "mostly" with Section 5: EV characterization. 0.3% (3) "mostly" disagreed, and 0.4% (4) stated that they had no opinion and/or expertise. No respondents disagreed "completely."

6 | TECHNIQUE-SPECIFIC REPORTING CONSIDERATIONS FOR EV CHARACTERIZATION

As utilization and expertise has expanded across a broad range of EV detection assays and instrumentation, the identification of pertinent reporting criteria has also grown to ensure reliable and reproducible interpretation of data. A collated list of minimal assay and instrument-specific reporting considerations are detailed here. These are generally applicable irrespective of experiment design. The techniques listed in the following section are not exhaustive, and many detection technologies are under development or being actively researched. The techniques listed are, however, all commercially available, with existing literature from multiple researchers. These recommendations are not exhaustive, and further criteria are likely required due to subjective experimental parameters.

20013078, 2024, 2, Downloaded from https://isevjournals.onlinelibrary.wiley.com/doi/10.1002/jev2.12404 by Colorado State University, Wiley Online Library on [09/10/2024]. See the Terms and Conditions (https://onlinelibrary.wiley.com/terms-and-conditions) on Wiley Online Library for rules of use; OA articles are governed by the applicable Creative Commons License

6.1 | Flow cytometry-based methods

6.1.1 | Bead-based flow cytometry

Bead-based flow cytometry has been used widely to interrogate EV surface proteins. Large beads capture particles regardless of their surface composition (e.g., surfactant-free aldehyde/sulphate beads) (Théry et al., 2006), or antibody-conjugated beads capture particles exposing the corresponding antigen. Commercially available EV multiplex kits allow interrogation of 30 or more surface antigens (Koliha et al., 2016; Wiklander et al., 2018). After capture, bead-associated particles are labelled with a fluorescently conjugated affinity reagent (or mixture of several) for detection. Differences in staining intensity are semi-quantitative only, since signal derives from multiple particles captured by individual beads. A difference in signal intensity might thus mean different particle concentration, epitope density, diameter distribution or relative abundances of EV subsets.

When reporting bead-based approaches, controls should include isotypes as detection antibodies, or isotype-conjugated capture beads, and capture beads with detection antibody alone (for antibody-coated capture beads). Multiple EV input concentrations may be used to demonstrate titration of signal and rule out non-specific binding (Wiklander et al., 2018; Welsh et al., 2022). Stained beads as a percentage is not a valid statistic; reporting normalised bead median fluorescence intensities is recommended (Welsh et al., 2022). Reporting data and median fluorescent intensity statistics in molecules of equivalent soluble fluorophore (MESF) (as with single EV flow cytometry) from singlet gated beads is recommended to allow standardization of data across instrument platforms and settings. If preparing beads in-house, reagents and conjugation chemistry should be reported, while for commercial capture bead reagents, catalogue and lot numbers should be reported. Other reporting parameters include: total bead number, the sample-bead incubation time, post-bead incubation wash methodology, detection reagent staining time and post-staining wash methodology.

Recommendations:

- Controls should include isotypes as detection antibodies, or isotype-conjugated capture beads, and capture beads with detection antibody alone (for antibody-coated capture beads).
- Multiple input EV concentrations should be used to demonstrate titration of signal.
- If making beads, reagents and conjugation chemistry should be reported. For commercial capture beads reagent catalogue and lot numbers should be reported.
- Report normalised bead median fluorescence intensities.
- Report data and median fluorescent intensity statistics in molecules of equivalent soluble fluorophore (MESF) (as with single EV flow cytometry) from singlet gated beads.
- Report full and detailed methodology.

6.1.2 | Single-EV flow cytometry

Flow cytometry is an optical technique that has demonstrated detection of vesicles down to ~40 nm in specialised cases (Zhu et al., 2014) and ~100 nm using many modern conventional cytometers by light scatter and fluorescence (Morales-Kastresana et al., 2019; Sandau et al., 2020; Stoner et al., 2016; Welsh, Killingsworth, et al., 2021). Through calibration of data, flow cytometry has been demonstrated to be capable of characterising particle diameter (Stoner et al., 2016; Tian et al., 2020; van der Pol, de Rond, et al., 2018; Welsh, Horak, et al., 2020), epitope abundance (Gorgens et al., 2019; Welsh, Jones, et al., 2020), epitope density (Welsh, Jones, et al., 2020), effective refractive index (Pleet et al., 2023; van der Pol, de Rond, et al., 2018) and number concentration within standardised size ranges (van der Pol, Sturk, et al., 2018). In 2023, a tri-society working group (EV Flow Cytometry Working Group) initiative involving the International Society for Extracellular Vesicles, International Society for Advancement of Cytometry, International Society for Thrombosis & Haemostasis, published a single-EV flow cytometry compendium to comprehensively address the considerations for developing a single-EV flow cytometry assay (Welsh et al., 2023).

Calibration of fluorescent and light scatter parameters is critical for interpretation and replication of single-EV flow cytometry results. If particle concentrations are reported using single-EV flow cytometry, define the upper and lower LOD to allow replication and interpretation of data using orthogonal techniques. Currently, imaging cytometers use a dynamic triggering method that makes determination of the lower LOD difficult to define and therefore standardise.

In 2020, a comprehensive experiment and reporting framework was developed (MIFlowCyt-EV) and published as a position paper by the EV Flow Cytometry Working Group (van der Pol et al., 2022; Welsh, Tang, et al., 2021; Welsh, Van Der Pol, Arkesteijn, et al. 2020). The MIFlowCyt-EV reporting framework is split into categories of: preanalytical variables and experimental design, sample preparation, assay controls, instrument calibration & data acquisition, EV characterization, FC data reporting and FC data sharing. This reporting framework and learning resources for implementing the MIFlowCyt-EV framework can be found on the

20013078, 2024, 2, Downloaded from https://isevjournals.onlinelibrary.wiley.com/doi/10.1002/jev2.12404 by Colorado State University, Wiley Online Library on [09/10/2024]. See the Terms and Conditions (https://onlinelibrary.wiley.com/terms-and-conditions) on Wiley Online Library for rules of use; OA articles are governed by the applicable Creative Commons License

EV Flow Cytometry Working Group website (www.evflowcytometry.org). Complete the MIFlowCyt-EV spreadsheet and attach it as supplementary material for any manuscript with single-EV flow cytometry. The MIFlowCyt-EV framework is applicable to all flow cytometers, including conventional, spectral, imaging and single-photon-detecting cytometers.

Recommendations:

- Refer to the ISEV-ISAC-ISTH MIFlowCyt-EV framework Position Paper and utilise the reporting framework as supplementary material for any manuscript utilising single-EV flow cytometry.
- Ensure correct calibration of volume and fluorescent and light scatter parameters.
- Define upper and lower limits of detection to allow others to validate your work.

6.2 | Genetic protein tagging

EV proteins can be genetically labelled by introducing a genetic construct from which a tag, such as GFP, is ultimately co-translated with a protein or protein domain of interest (Corso et al., 2019; Heusermann et al., 2016; Joshi et al., 2020; Mittelbrunn et al., 2011). The tagged protein may be chosen based on its status as a general EV or EV subtype marker (Section 5.7), and numerous markers have been labelled (Corso et al., 2019; Dooley et al., 2021). Tagged proteins have been used to interrogate EV/subtype release and uptake pathways (Mathieu et al., 2019; Mathieu et al., 2021) and to enable overall biodistribution and pharmacokinetics studies. Importantly, the tag itself or alterations in expression of the tagged protein may affect EV biogenesis (Fan et al., 2020), loading, release, or function, so unlabelled EVs are recommended as a control to assess these possibilities. The fusion protein may also affect subcellular localization or cellular functions. Localization of the chimeric versus wildtype protein should be confirmed. Certain tags (e.g., GFP) may be subject to quenching in acidic compartments (Corrigan et al., 2014). Construct maps should be provided and, where possible, plasmids deposited in Addgene (www.addgene.org) or other repositories.

Recommendations:

- Carefully consider the selection of the tagged protein and its suitability as an EV or EV subtype marker.
- Assess the subcellular localization and function of the chimeric versus wildtype protein in the cell and the EV by comparing engineered and wildtype cells and labelled/unlabelled EVs.
- Report construct maps and deposit plasmids with a repository.

6.3 | Mass spectrometry proteomics

Mass spectrometry (MS) measures mass-to-charge ratio of molecules and, in EV studies, is commonly used to detect and characterises EV-associated proteins in both discovery and targeted applications (Aebersold & Mann, 2003; Hoshino et al., 2020; Pocsfalvi, Stanly, Vilasi, et al., 2016; Sodar et al., 2017). Targeted analyses are typically performed on a triple quadrupole (QQQ) liquid chromatography (LC)-MS platform, while untargeted proteomics is commonly performed using Time-of-Flight (ToF) or Orbitrap MS platforms (Liebler & Zimmerman, 2013). Targeted and untargeted proteomic approaches have nuances in terms of applications, advantages and limitations in sample processing, data acquisition, and analysis (Granvogl et al., 2007; Klont et al., 2018). Untargeted proteomic studies are used to identify all detectable ions within the sample, whether from EV-related proteins or contaminant matrix proteins. This approach provides a comprehensive understanding of the sample protein composition and is ideal for applications such as biomarker discovery (Nakayasu et al., 2021). For characterization of MISEV EV purity (Category 1, 2) and matrix contamination (Category 3) markers (Section 5.7), targeted peptide analysis may be more suitable, demonstrating the presence or absence of each analyte above a pre-specified detection threshold. It can also quantify absolute protein abundance. Multiplexing, for example, as in LC-MS workflows, can provide high sensitivity for limited sample volumes, such as for samples from clinical trials (Newman et al., 2022). Targeted proteomics may be more suitable to quantify changes in protein abundances, such as in a disease or therapeutic intervention (Pocsfalvi, Stanly, Fiumeet, al., 2016; Rodrigues et al., 2021). Inclusion of stable isotope labelled (SIL) peptide standards enables absolute quantification of the corresponding endogenous analyte when used in combination with 'light' peptide calibrators prepared in a matched matrix (Liebler & Zimmerman, 2013).

Instrument settings, including collision energy, gas flow and temperature, and capillary voltage, are platform and analyte-specific and, as such, should be optimised and then kept constant for the duration of a project. MS instruments are sensitive to contamination by ion-pairing reagents, buffer salts, and detergents, reducing sensitivity and assay performance. As such, EV peptide samples for targeted LC-MS analysis should be prepared in low-salt buffer/MS-compatible solvent matrix and an appropriate concentration of SIL peptide standard. Positive controls containing proteins of interest and negative controls, such as EVs from alternative species or cell lysates not expressing a protein of interest, should be included in targeted analyses (Abbatiello et al.,

20013078, 2024, 2, Downloaded from https://isevjournals.onlinelibrary.wiley.com/doi/10.1002/jev2.12404 by Colorado State University, Wiley Online Library on [09/10/2024]. See the Terms and Conditions (https://onlinelibrary.wiley.com/terms-and-conditions) on Wiley Online Library for rules of use; OA articles are governed by the applicable Creative Commons License

2013; Bereman, 2015; Nakayasu et al., 2021). Report the sequences of target peptides and the strategy for peptide selection. The linearity of response and limits of detection and quantification should be defined using synthetic light and heavy-labelled peptides spiked into an appropriate matrix. Report normalization, for example, by total protein, volume of starting material or particle count from which proteins were digested and injected for MS analysis. When reporting results from either targeted or untargeted proteomic studies, follow the Minimal Information About a Proteomic Experiment (MIAPE) guidelines for harmonization of methodology and rigor/reproducibility (Gandham et al., 2020; Kreimer et al., 2015; Taylor et al., 2007). All sample preparation techniques should be reported with reproducible experimental descriptions for each step. All data software and versions used should be reported to understand how data were processed. Filters, scores and confidence levels for both identifications and quantitation should also be reported, as well as the method used for quantitation if relevant (Martinez-Bartolome et al., 2013). Data and metadata should be uploaded to a data repository to ensure that data generation and reporting remain rigorous and potentially reproducible for EV experiments.

Recommendations:

- Optimise instrument settings and keep them constant for the duration of a project.
- In targeted LC-MS protein analyses, include both positive controls (containing proteins of interest) and negative controls, such as EVs from alternative species or cell lysates not expressing a protein of interest.
- Spike SIL peptide standards into the EV matrix to assess matrix effects and to demonstrate the concordance of retention times and quantifier-to-qualifier ion transition ratios between standards and endogenous analytes.
- For targeted MRM analyses, monitor at least one quantifier and one (preferably two) qualifier ion transitions.
- Define linearity of response and limits of detection and quantification using synthetic light and heavy-labelled peptides spiked into an appropriate matrix.
- Report sequences of target peptides and the strategy for peptide selection, as well as the isotopic purity and source of synthetic peptides.
- Sample preparation techniques, including the normalisation approach used, should be reported with detailed experimental descriptions for each step in the workflow.
- Follow the reporting recommendations of the Minimal Information About a Proteomic Experiment (MIAPE).
- Upload data and metadata to a data repository.

6.4 | Microscopy-based methods

6.4.1 | Atomic force microscopy

Atomic Force Microscopy (AFM) provides label- and stain-free imaging of individual EVs and co-isolated nanoparticles (Bordanaba-Florit et al., 2021; Obeid et al., 2019; Sharma et al., 2018). AFM imaging requires analytes to be deposited on a solid surface (substrate). Measurements can then be performed after either drying the sample or keeping it submerged in liquid, such as saline or cell culture media. AFM morphometry can be used to obtain EV size distribution and ultrastructural details and to check for the presence and relative amounts of contaminants (Cavallaro, Pevere, et al., 2021; Paolini et al., 2016, 2020; Parisse et al., 2017). In addition, AFM is one of the very few techniques capable of measuring single-vesicle nanomechanical properties (Gautron et al., 2021; Piontek et al., 2021), which were found to correlate with EV identity and function (Bortot et al., 2021; LeClaire et al., 2021; Romanò et al., 2022; Sorkin et al., 2018; Vorselen et al., 2018; Whitehead et al., 2015; Ye et al., 2021). The unique mechanical fingerprint of EVs can also be used to discriminate them from NVEPs of similar size and shape (Ridolfi et al., 2020).

Minimal reporting requirements for the AFM imaging of EV samples comprise detailed information on the preliminary sample deposition procedure, substrate type and pre-treatment, immobilization method, sample concentration and deposition times, plus details on any rinsing and/or drying steps. AFM imaging mode, acquisition conditions, and probe information including expected tip curvature radius and spring constant should also be provided. If quantitative morphometry is performed, the heuristics employed to select the measured objects, as well as the procedure to extract morphological descriptors from them, should be described. Reporting the height of the detected particles, for example, greater than or less than the thickness of two lipid bilayers (~8 nm) may help distinguish between deformed EVs and non-EVs/collapsed EVs. In addition, EV mechanical studies should describe the assumed contact mechanic model (Calò et al., 2014; Ridolfi et al., 2021; Vorselen et al., 2017), and, ideally, provide enough data for the reader to be able to test alternative models.

20013078, 2024, 2, Downloaded from https://isevjournals.onlinelibrary.wiley.com/doi/10.1002/jev2.12404 by Colorado State University, Wiley Online Library on [09/10/2024]. See the Terms and Conditions (https://onlinelibrary.wiley.com/terms-and-conditions) on Wiley Online Library for rules of use; OA articles are governed by the applicable Creative Commons License

Recommendations

- Report preliminary sample deposition procedure, substrate type and pre-treatment, immobilization method, sample concentration and deposition times, plus details on any rinsing and/or drying steps.
- Provide AFM imaging mode, acquisition conditions and probe information, including expected tip curvature radius and spring constant.
- If quantitative morphometry is performed, describe the heuristics used to select the measured objects, as well as the procedure to extract morphological descriptors.
- EV mechanical studies should describe the assumed contact mechanic model (Calò et al., 2014; Ridolfi et al., 2021; Vorselen et al., 2017), and, ideally, provide enough data for the reader to be able to test alternative models.

6.4.2 | Diffraction-limited fluorescence microscopy

Applications of fluorescence microscopy techniques can range from live cell imaging to single-molecule localization. These approaches, including Total Internal Reflection Microscopy (TIRF-M), confocal microscopy and more recently, light-sheet microscopy, have been used to evaluate cell-EV interactions such as EV release and uptake (Christianson et al., 2013; Elgamal et al., 2020; Feng et al., 2010; Heusermann et al., 2016; Joshi et al., 2020; Lai et al., 2015; Mittelbrunn et al., 2011), as well as the composition of single EVs (Corso et al., 2019; Han, Kang, et al., 2021). As a general consideration, since TIRF microscopy is limited to imaging the surface at the glass interface and has high signal-to-noise ratio that facilitates single molecule detection, it may be the most suitable system for analysing EV content (Han, Kang, et al., 2021). Confocal and light-sheet microscopes, especially the most recent models, are capable of single-molecule detection for calibration (Willy et al., 2021) and dynamic studies, but are more suitable for live cell imaging experiments (Elgamal et al., 2020; Mittelbrunn et al., 2011). These methods and potential drawbacks have been extensively reviewed (Chuo et al., 2018; Colombo et al., 2021; Gallego-Perez et al., 2016; Panagopoulou et al., 2020).

In microscopy experiments, report the type of microscope, magnification, laser power and exposure time because fluorescently labelled samples have a limited number of labelled molecules. Each labelled sample can provide only a finite number of photons before photobleaching, so each experiment must be optimised to maximise the amount of information obtained from a limited 'photon budget' (Li et al., 2015). Consequently, the sample is exposed for a short time using minimal excitation to perform live-cell experiments (Coffman & Wu, 2014; Heddleston et al., 2021) or at higher excitation power and longer camera exposure for single-molecule detection (Elgamal et al., 2020). While calibration of the system is mandatory for quantitative microscopy experiments (Montero Llopis et al., 2021; Willy et al., 2021), we recommend where possible to extend it to any microscopy approach to obtain unbiased evaluation of sensitivity of the instrument. Calibration to a single fluorescent dye or labelled protein molecules is a well-established approach that permits one to infer the total number of proteins or RNAs present on or in EVs (de Voogt et al., 2021; Higginbotham et al., 2011) and ensure that even molecules retained in few copies in EV can be detected. The software used to detect EVs should be reported including the specific parameters used to threshold the object intensities. Code developed for these purposes should be deposited and made accessible to the community. Available algorithms (Aguet et al., 2013; Elgamal et al., 2020; Jaqaman et al., 2008) take advantage of the small size of EVs, which are in general diffraction-limited objects. These assume the same shape as the point spread function (PSF) of the imaging system and can be approximated to a Gaussian function in confocal, TIRF and light-sheet microscopy.

Recommendations

- Report the type of microscope, magnification, laser power and exposure time.
- Calibration of the system is mandatory for quantitative microscopy experiments, but is also recommended for any microscopy approach to obtain unbiased evaluation of the sensitivity of the instrument.
- The software used to detect EVs should be reported, including the specific parameters used to recognise the objects and, if applicable, threshold the object intensities. Any code written for these procedures should be made publicly available.

6.4.3 | Dynamic light scattering

DLS, also known as photon correlation spectroscopy (PCS) and quasi-elastic light scattering (QELS), is a technique capable of determining the hydrodynamic diameter of sufficiently monodisperse particles in dilute aqueous dispersions (Berne & Pecora, 1976; Hackley & Clogston, 2011; "Particle size analysis — Dynamic light scattering (DLS)" 2017; Stetefeld et al., 2016). DLS can be performed as a cuvette analysis or as an inline analysis when connected to a fluidic pump, such as high-performance liquid chromatography (HPLC). The hydrodynamic diameter is defined as the diameter of a solid sphere that would exhibit the same

20013078, 2024, 2, Downloaded from https://isevjournals.onlinelibrary.wiley.com/doi/10.1002/jev2.12404 by Colorado State University, Wiley Online Library on [09/10/2024]. See the Terms and Conditions (https://onlinelibrary.wiley.com/terms-and-conditions) on Wiley Online Library for rules of use; OA articles are governed by the applicable Creative Commons License

diffusion coefficient as the measured particle of interest. DLS measures the autocorrelation function of the intensity of laser light scattered by multiple particles in solution. The autocorrelation function carries information about the diffusion coefficient of the particles, which is related to the hydrodynamic diameter via the Stokes-Einstein theory of Brownian motion.

Various algorithms can be used to derive the diffusion coefficient from the measured autocorrelation function. The most common method, the cumulant analysis, assumes a monodisperse size distribution, which EV samples do not have. Other approaches, such as the CONTIN algorithm, attempt to handle the drawbacks of the cumulant analysis (Provencher, 1982), but for polydisperse size distributions of EV samples (van der Pol, Coumans, Grootemaat et al., 2014), derivation of the diffusion coefficient distribution from the autocorrelation function becomes an ill-posed mathematical problem. This implies that DLS should not be used to determine quantitative properties, such as the average hydrodynamic diameter, of EV samples, unless DLS is applied to a monodisperse size fraction of EVs, such as an EV sample fractionated by flow field-flow fractionation using an inline analysis. On the other hand, DLS can be used to qualitatively confirm the presence of submicrometer particles and possible aggregates that may be present in EV samples (Palmieri et al., 2014). In either case, please follow the recommendations on nomenclature and reporting of DLS measurements from the international standard ISO 22412:2017 ("Particle size analysis — Dynamic light scattering (DLS)" 2017).

Recommendations

- DLS should not be used to determine quantitative properties, such as the average hydrodynamic diameter, of EV samples, unless applied to a monodisperse size fraction of EVs.
- DLS can be used to qualitatively confirm the presence of submicrometer particles and possible aggregates that may be present in EV samples.
- Follow the recommendations on nomenclature and reporting of DLS measurements from the international standard ISO 22412:2017 ("Particle size analysis — Dynamic light scattering (DLS)", 2017).

6.4.4 | Electron microscopy

Electron microscopy (EM) variants are among the few techniques capable of detecting EVs irrespective of size. The throughput of EM, however, means that larger EVs are statistically underestimated as compared with smaller EVs (van der Pol et al., 2022). While EV characterization by SEM (Cavallaro, Hååg, et al., 2021; Wu et al., 2015), TEM (van der Pol, Coumans, Grootemaat, et al., 2014), and cryo-EM (de Vrij et al., 2013; Hoog & Lotvall, 2015; Linares et al., 2015) are all high-resolution methods, they are not necessarily interchangeable or capable of providing images of comparable quality. For example, cryo-EM clearly shows the lipid bilayer, better maintains EV morphology than the dehydrating conditions used to fix samples for TEM, and may be more quantitative, as all particles in a given volume can be imaged, not just those that adhere to a surface (the grid). TEM should be performed with a protocol adapted to EVs, which includes contrasting and embedding in a mixture of uranyl compounds and methylcellulose to maintain the lipid bilayer morphology (Théry et al., 2006). SEM shows the surface aspect of EVs of any size, but images obtained at the highest magnification required to visualise the smallest EVs may be more difficult to analyse.

There have been limited standardization studies across EM methods to determine minimal reporting requirements. For TEM, three major parameters should be reported: fixation, adsorption, and negative staining methods (Rikkert et al., 2019). Fixation includes: the fixative used, its concentration, and incubation time. Adsorption includes the grid material, mesh size, film type, coating, incubation time, and wash details. Negative staining details should include substance, concentration, and incubation time. Both low- and high-magnification images should be shared, along with selection criteria.

Recommendations

- TEM should be performed with a protocol adapted to EVs, which includes contrasting and embedding in a mixture of uranyl compounds and methylcellulose to maintain the bilayer morphology.
- Three major criteria should be reported for any electron microscopy technique used: fixation, adsorption, and negative staining methods.
- High- and low-magnification images should be supplied for both high-resolution EV images and an assessment of the broader quality of the sample.

6.4.5 | Nanoparticle tracking analysis

NTA, also known as single particle tracking, is a widely utilised optical technique in the EV field to estimate particle size and concentration. The use of NTA to determine effective refractive index and epitope existence has also been demonstrated (Gardiner

20013078, 2024, 2, Downloaded from https://isevjournals.onlinelibrary.wiley.com/doi/10.1002/jev2.12404 by Colorado State University, Wiley Online Library on [09/10/2024]. See the Terms and Conditions (https://onlinelibrary.wiley.com/terms-and-conditions) on Wiley Online Library for rules of use; OA articles are governed by the applicable Creative Commons License

et al., 2014; van der Pol, Coumans, Sturk, et al., 2014). NTA derives hydrodynamic diameter by measuring a particle's diffusion coefficient, usually implementing an algorithm that reduces variation in diameter distribution. It should be noted that the FTLA algorithm used on some platforms was developed to better represent monodisperse mixtures, of which EVs are not, and can result in artefactual multi-modal distribution (van der Pol, Coumans, Grootemaat, et al., 2014; Walker, 2012). Currently, there is no method of determining or reporting a set LOD for NTA. Several standardization studies have been conducted comparing results between users and instruments (Bachurski et al., 2019; Hole et al., 2013; Vestad et al., 2017). The use of NTA to measure the diameter distributions and concentration of complex biofluids should be interpreted with caution due to counting of co-isolates such as lipoproteins and large protein complexes, and EVs larger than a few hundred nanometers in diameter are difficult to quantify. Detection of particles with NTA can be done using light scattering, relying on refractive index and diameter, or fluorescence. Fluorescence NTA depends on removal of unbound label, photobleaching resistance of the dye, and the presence of detectable levels of dye per particle.

For NTA reporting, include instrument model, camera type, camera settings, laser wavelength, laser power, software version, analysis settings, and particles per frame. As outlined in Section 5.2, NTA diameter distributions are preferred over a single diameter statistic, since NTA statistics are easily skewed by the LOD. If known, the algorithm used to produce diameter distributions should be reported due to potential for differing results depending on the algorithm used (Kestens et al., 2017; Walker, 2012). A buffer-only control is recommended in the case of light scatter or fluorescence detection modes. For fluorescent NTA, report the number of total particles in light scatter mode along with the number of labelled particles in fluorescence mode, along with label removal method and a buffer/reagent control to assess labelling artefacts. Report sample injection fluidics and settings if used.

Recommendations

- Instrument model, camera type, camera settings, laser wavelength, laser power, software version, analysis settings and particles per frame should be reported.
- Report NTA diameter distributions rather than a single diameter statistic.
- If known, report the algorithm used to produce diameter distributions.
- A buffer-only control is recommended for both light scatter and fluorescence detection modes.
- When using fluorescent NTA, it is recommended to report the number of total particles in light scatter mode, the number of labelled particles in fluorescence mode, along with label removal method, Use a buffer-only/reagent control to assess labelling artefacts.
- Report injection fluidics and settings if used.

6.4.6 | Single-particle interferometric reflectance imaging sensing

Combined interferometric imaging/fluorescence imaging (Bachurski et al., 2019; Crescitelli et al., 2021; Daaboul et al., 2016; Dogrammatzis et al., 2021) involves particle capture by affinity agents (e.g., antibodies, peptides, aptamers) onto a multiplexed array of micron-sized spots. In interference reflectance imaging sensor (IRIS) mode, interference patterns from scattered light are used to derive the size and number of captured particles (Young et al., 2018). Converting interference to nominal size depends on refractive index (RI), which can vary across EV populations (de Rond, Coumans, et al., 2018). Current SP-IRIS platforms assume a constant RI (~1.45), which may result in variation across orthogonal measurements and may undersize EVs with lower RI. It is thus recommended that software version and estimated refractive index parameter be reported.

In fluorescence mode, captured particles labelled with fluorescent probes are detected in one or more color channels. Some aspects of this mode require careful consideration of calibrations and control experiments to obtain rigorous results. For particles smaller than the diffraction limit, for example, <~250 nm in diameter for visible light, validate the detected events to confirm that single particles were detected, for example, with a dilution series to ensure that fluorescence intensity per particle does not scale with solution concentration. To confirm that fluorescence is associated specifically with EVs, vesicle-disrupting surfactant treatments can be used; however, consider that surfactants can also disrupt lipoprotein particles (Botha et al., 2022). For fluorophore detection, reporting recommendations are indicated below.

Recommendations

- Report details of affinity reagent(s) printed onto the chip.
- Report software version and estimated refractive index parameter.
- For particles smaller than the diffraction limit, detection of single events should be validated.
- To confirm that fluorescence is associated specifically with EVs, surfactants can be used to disrupt vesicles (although they may also disrupt certain NVEPs).

20013078, 2024, 2, Downloaded from https://isevjournals.onlinelibrary.wiley.com/doi/10.1002/jev2.12404 by Colorado State University, Wiley Online Library on [09/10/2024]. See the Terms and Conditions (https://onlinelibrary.wiley.com/terms-and-conditions) on Wiley Online Library for rules of use; OA articles are governed by the applicable Creative Commons License

20013078, 2024, 2, Downloaded from https://isevjournals.onlinelibrary.wiley.com/doi/10.1002/jev2.12404 by Colorado State University, Wiley Online Library on [09/10/2024]. See the Terms and Conditions (https://onlinelibrary.wiley.com/terms-and-conditions) on Wiley Online Library for rules of use; OA articles are governed by the applicable Creative Commons License

- For fluorophore detection, report affinity reagent (e.g., antibody clone), conjugated fluorophore type, incubation concentration, light-source wavelength, bandpass filter cut-offs, analysis software version and fluorescence cut-offs along with the method of choosing these cut-offs. Negative controls such as nonspecific IgG capture spots or chips incubated with EV-depleted materials are recommended for choosing these cut-offs.

6.4.7 | Super-resolution microscopy

To resolve fluorescence emitters events that are closer together than the diffraction limit of light, fluorescent super-resolution microscopy methods modulate the light to ensure that neighbouring molecules do not emit simultaneously. A resolution 10-fold below the diffraction limit can be achieved using two main approaches: (1) stimulated emission depletion (STED) (Hell & Wichmann, 1994; Klar & Hell, 1999), which spatially regulates activation of an ensemble of fluorophores using a synchronised two-laser system with a phase plate; and (2) single molecule localization microscopy (SMLM) techniques, such as (d)STORM (Rust et al., 2006; Wombacher et al., 2010) and (f)PALM (Betzig et al., 2006; Hess et al., 2006), which temporally regulate stochastic activation of single fluorophores. The nanometer scale resolution of STED and SMLM is well suited for detecting and characterising individual EVs and their components, including EV membranes (Nizamudeen et al., 2018; Sharma et al., 2020; Zong et al., 2018), proteins (Avalos-Padilla et al., 2021; Chen et al., 2016; Lennon et al. 2019; Maire et al. 2021; Mondal et al., 2019; Sanada et al., 2017; Wang et al., 2018; Zong et al., 2018), DNA fragments (Maire et al. 2021) and miRNAs (Chen et al., 2018; Oleksiuk et al., 2015). Using quantitative analysis, these methods have been further used to define EV size (Mondal et al., 2019; Zong et al., 2018; Nizamudeen et al. 2018; Lennon et al. 2019; Sharma et al., 2020) and to quantify protein content (Lennon et al., 2019) and number of localizations of miRNA (Oleksiuk et al., 2015) and DNA fragments in EVs (Maire et al., 2021). Additionally, STED and SMLM have been used to image cellular uptake (Chen et al., 2016; Chen et al., 2018; Polanco et al., 2018; Pfeiler et al., 2019; Toda et al., 2020) and release of EVs (Ambrose et al., 2020) or EV clusters (Valcz et al., 2019).

Super-resolution microscopy methods comprise tailored approaches for sample preparation, sample imaging, and data analysis. To prepare samples for SMLM and STED imaging, EV membranes or cargo molecules are labelled with reagents that contain appropriate photo-controllable fluorophores. Four typical strategies for labelling EVs are affinity labelling, genetic labelling, covalent labelling, and uptake of lipophilic molecules/lipid analogues. Reported details of labelling should include type of labelling, appropriate reagent controls and/or references, reagent concentration, incubation times/buffers, and method for removal of excess fluorescent reagents). If applicable (e.g., for isolated EVs), reporting should include coverslip modifications/coatings, the protocol for incubation of EVs on coverslips, fixation protocol, and controls for affinity separation (e.g., isotype or non-fouling surface). Reported imaging parameters should include the major microscope components: laser lines, camera, filters, objectives and other relevant optical path components. Descriptions of protocols should include detailed imaging parameters such as laser powers, relevant microscope configuration and imaging conditions (including buffer for SMLM). Reports on multicolour imaging should detail the alignment between channels and any applied correction for chromatic aberration (Churchman & Spudich, 2012; Hebisch et al., 2017).

In STED, the resulting images consist of intensity maps, and analysis typically relies on approaches established in confocal microscopy (Gould et al., 2012); relevant processing/analysis parameters should be reported. SMLM images are reconstructed from the determined coordinates (i.e., localizations) of single molecules, and EV analysis typically employs segmentation and/or clustering algorithms (Khater et al., 2020). To quantify detected molecular densities and molecular organization with SMLM, it is important to define the photophysical properties of fluorescent reporters (e.g., average number of localizations per molecule, maximal dark time) (Khater et al., 2020). Thus, SMLM reporting should include details on image processing parameters, photophysical characterization of relevant fluorescent reporters, and data analysis parameters/algorithms. Newly developed analysis methods should be evaluated (e.g., using simulations or another validated approach), and custom written codes should be made publicly available.

Recommendations

- Reporting details of the EV labelling protocol.
- Where applicable, report coverslip modifications/coatings, the protocol for incubation of EVs on coverslips, fixation protocol and controls for affinity separation.
- Report the major microscope components and imaging protocol parameters such as laser power, relevant microscope configuration and imaging conditions.
- Reports on multicolor imaging should detail the alignment between channels and any applied correction for chromatic aberration.
- SMLM reporting should also include details of image processing parameters, photophysical characterization of relevant fluorescent reporters and data analysis parameters/algorithms.
- Newly developed analysis methods should be evaluated, and custom written codes should be made publicly available.

6.5 | Nucleic acid characterization

Nucleic acids (NAs) are among the most commonly assayed EV constituents because of perceived biomarker potential and functional roles. RNA has been studied much more frequently than DNA, although there are more recent reports on EV DNA in intercellular communication (Clancy et al., 2022; Sansone et al., 2017) and as disease biomarkers (Cambier et al., 2021; García-Silva et al., 2019; Möhrmann et al., 2018; Qu et al., 2019; Vagner et al., 2018) including in microbial infections (Bitto et al., 2017; Kameli et al., 2021). Some early EV studies reported DNA inside the EV lumen (Cai et al., 2013; Kahlert et al., 2014; Lee et al., 2014; Thakur et al., 2014), whereas some recent studies have suggested mostly EV surface-association of DNA (Bitto et al., 2017; Lázaro-Ibáñez et al., 2019; Liu et al., 2022; Maire et al., 2021; Saari et al., 2020). These seemingly contradictory findings might be due to the lack of standardised methods for protecting EV surface DNA from digestion during EV separation and characterization (Lázaro-Ibáñez et al., 2019). Whether the major type of EV DNA is ssDNA or dsDNA is also still debated (Balaj et al., 2011; Lázaro-Ibáñez et al., 2019; Liu et al., 2022; Thakur et al., 2014).

Challenges for RNA studies including input quantities, normalization and sensitivity are also relevant for EV DNA research. Most characterization of EV RNAs involves one or more of: detection, identification, quantification, localization (inside or outside the EV) and enrichment (packaging). Low-input RNA sequencing (RNA-Seq) and quantitative PCR (qPCR) are commonly used to identify specific sequences in EV preparations. ISEV has previously provided guidance on aspects of EV RNA studies ranging from sample collection to bioinformatic analysis (Hill et al., 2013; Soekmadji et al., 2018; Witwer et al., 2013), as has the US NIH Extracellular RNA Communication Consortium (ERCC) (Ainsztein et al., 2015; Das et al., 2019).

Regardless of RNA characterization method, biases may be introduced by RNA purification and pre-assay preparations. Some RNA purification methods isolate mostly longer RNAs (>200 nt), while others are biased by design to concentrate short RNAs. For RNA-Seq, library preparation methods may select for RNAs or inserts within a particular size range. Reverse transcription protocols may also select for specific RNAs such as polyA-tailed transcripts. Tiled probe-based imaging of longer RNAs becomes less sensitive for shorter/degraded transcripts. Adapter ligation-based small RNA library preparation methods optimised for miRNAs will also enrich other RNAs containing 5′-phosphates and 3′-OH, while RNAs bearing different end-chemistries will be underrepresented. Highly structured RNAs such as full-length tRNAs are not efficiently reverse-transcribed unless using thermostable enzymes. Accurate interpretation and reporting of results thus depend on understanding and reporting techniques with enough detail to assess biases.

Due to its ability to detect and measure small amounts of nucleic acids, reverse transcription real-time quantitative PCR (qPCR) is widely used in the EV field. We recommend that qPCR experiments follow the Minimum Information for Publication of Quantitative Real-Time PCR Experiments (MIQE) guidelines (Bustin et al., 2009) where possible, and the ISEV EV RNA checklist in the 2017 ISEV position paper (Mateescu et al., 2017). When sharing qPCR results, raw cycle of quantitation (Cq) values should be reported in addition to normalised or processed data for readers to assess abundance of the target RNA and reliability of the assay. Although Cq values depend on many variables and may not by themselves be informative, they tend to correlate with abundance, especially in liquid samples, and where the input sample volume can be reported. Possibly, not all MIQE principles broadly apply to extracellular samples. For example, when samples contain only minute amounts of carrier-specific RNA, having identical input RNA levels in every sample might not always be possible. Some prefer to normalise by sample input volume, given the liquid nature of extracellular samples. Normalization strategy can greatly impact interpretation of the results and should be reported. Digital PCR, including droplet digital PCR (ddPCR), provides absolute quantification and has been shown to improve reproducibility and accuracy of EV RNA detection compared with conventional qPCR (Wang et al., 2019). Absolute quantification may also circumvent issues with normalization.

Recommendations

- For qPCR-based analysis, report sequences of reverse transcription adapters or primers as well as primers and probes (where relevant) for amplification steps; experimental design with biological and technical replicates; exact cycling conditions; and data inclusion and exclusion criteria.
- For RNA-Seq, report all details of nucleic acid fragmentation, reverse transcription, adapters and adapter attachment (ligation or ligation-free), amplification and multiplexing, as well as clean-up or size selection.
- For sequencing data analysis, report pre-processing, read mapping, overlapping annotations and database quality, quantification and normalization/differential expression analysis.

6.6 | Protein- and non-protein labelling of EVs

Most EV labelling reagents include fluorescence moieties, but other modes of detection are available and should share similar controls. Due the small size and thus limited cargo capacity of EVs, the detection of protein and non-protein markers is diffi-

20013078, 2024, 2, Downloaded from https://isevjournals.onlinelibrary.wiley.com/doi/10.1002/jev2.12404 by Colorado State University, Wiley Online Library on [09/10/2024]. See the Terms and Conditions (https://onlinelibrary.wiley.com/terms-and-conditions) on Wiley Online Library for rules of use; OA articles are governed by the applicable Creative Commons License

20013078, 2024, 2, Downloaded from https://isevjournals.onlinelibrary.wiley.com/doi/10.1002/jev2.12404 by Colorado State University, Wiley Online Library on [09/10/2024]. See the Terms and Conditions (https://onlinelibrary.wiley.com/terms-and-conditions) on Wiley Online Library for rules of use; OA articles are governed by the applicable Creative Commons License

cult and can easily be confounded by unbound reagents from the labelling process or co-isolates from the separation method. The degree to which unbound label requires removal increases with the sensitivity of the techniques. For techniques that can detect <10 molecules of a reagent, for example, super-resolution microscopy, SP-IRIS and single EV flow cytometry, the presence of unbound dye may easily lead to false positive events.

Lipid dyes are routinely used to bind to/insert into the EV membrane (de Rond, van der Pol, et al., 2018; Feng et al., 2010; Lundy et al., 2015; Sandau et al., 2020; Stoner et al., 2016). Lipid-specificity does not guarantee EV-specificity, since NVEPs such as lipoproteins may be co-isolated and stained, and some reagents may also label proteins. Supplementation with an EV protein marker is therefore recommended. Lipid labels may also self-aggregate (de Rond, van der Pol, et al., 2018; Pužar Dominkuš et al., 2018) and vary in affinity for EVs with different membrane composition.

Protein-reactive dyes that label the EV surface (Lim et al., 2021; Roberts-Dalton et al., 2017; Tian et al., 2010) may also label free protein and protein-containing NVEPs. If the EV separation method does not completely remove non-EV components, this possibility should be recognised and/or assessed. As above, a lipid marker might be used to complement protein labelling. When protein artefacts are a possibility, a low-concentration detergent can be used to assess the lability of the EV membrane and reduction of associated signal (Gyorgy et al., 2011).

For antibodies, manufacturer-matched isotype controls, used at the same concentration as the specific antibody, are one way to support specificity. Negative EV controls, for example, from cells that do not express the antibody epitope, are also useful controls.

In assays where purification is required after staining, procedural controls should be used to demonstrate before/after consistency of the EV population, that the purification procedure did not introduce artefacts, and that the dye was removed. For example:

1. Analyse a buffer with reagent control before and after label depletion method (e.g., SEC) to assess free/aggregated label removal.
2. Analyse unstained EVs before and after the label depletion method to demonstrate that it does not change or selectively enrich the EV population.
3. Analyse the reagent-stained sample after label removal and compare with unstained results (above) to assess possible dye-induced changes. Staining may noticeably increase the diameter or density of small EVs in particular.

Recommendations

- Use a buffer/label-only control to identify false-positive artefacts arising from unbound label. However, label-only artefacts are not the only potential labelling artefacts.
- For antibodies, manufacturer-matched isotype controls may be used at the same concentration as the specific antibody to evaluate binding specificity. Negative EV controls (lacking the antibody epitope) may also be used.
- Be aware that EV protein labelling methods may also label free proteins and protein-containing NVEPs, and that lipid dyes may label lipid-containing NVEPs. Ensure that the EV separation method is appropriate for the downstream analysis. If the EV separation method does not completely remove non-EV components, this possibility should be recognised and/or assessed.
- To identify the contribution of non-EV labelling artefacts, consider using protein and lipid labelling concurrently.
- In assays where purification is required after staining, procedural controls should be used to demonstrate before/after consistency of the EV population, that the purification procedure did not introduce artefacts, and that excess dye was removed.

6.7 | Raman spectroscopy

Raman spectroscopy (RS) is a label-free analytical optical technique capable of qualitatively and quantitatively resolving the chemical composition of a small volume of a sample based on inelastically scattered photons originating from the sample upon irradiation with a narrow-linewidth laser (Smith & Dent, 2005). A Raman spectrum is essentially a chemical fingerprint of the interrogated small volume of the sample within the focus of the laser beam. RS enables chemical specific, non-destructive probing, minimal to no sample pre-processing, and it is relatively inert to aqueous content of the measured sample (Smith & Dent, 2005). A strategy to overcome the weak signals of RS is the use of surface-enhanced Raman scattering (SERS), which is a nano plasmonic-assisted amplification derivative of RS (Langer et al., 2020; Jones et al., 2019). This method uses metal nanostructures to boost Raman scattering by many orders of magnitude. Both spontaneous and surface-enhanced Raman methods have demonstrated utility for basic research and translational EV analyses (Carlomagno et al., 2021; Enciso-Martinez et al., 2020; Gualerzi et al., 2017; Gualerzi et al., 2019; Kwizera et al., 2018; Lee et al., 2018; Ma et al., 2018; Park et al., 2017; Rojalin et al., 2020; Smith et al., 2015).

Inter- and intra-device variability in Raman spectra can arise for several reasons, including laser variations and non-uniform response of each of the optical elements, including the detector, to different light energies (known as spectral response). Raman systems should therefore be carefully calibrated (Raj et al., 2020). Modern commercial Raman systems have automatic calibration routines, but older and lab-built systems do not, thus adding to the issue of reproducibility. Several aspects of the measurement should be reported, including laser wavelength and power, calibration routines, make/model of major optical components, numerical aperture and magnification of the objective (if applicable), probe type and specifications (typically for non-microscope setups and measurements), and physical size of the laser spot. Spectra acquisition parameters should also be mentioned, for example, total number of spectra collected on each sample or sampled spot, signal collection time per one spectrum (also called as integration or acquisition time), and for scanning, the dimensions of the scanned area/volume (e.g., 100 × 100 area, step size of 400 nm, total scanned area 40 μm × 40 μm). Lastly, it is recommended to report all pertinent parameters of sample preparation. As EV samples are typically suspended in aqueous solutions with different concentrations of dissolved compounds, and thus osmotic pressures, there is a need to consider and report the EV formulation and whether the EVs were measured in suspension or dry. For example, EVs can be measured in suspension using SERS nanoprobes or dried onto a quartz glass slide for RS spectra acquisition (Cameron et al., 2018). It is unclear if there is an advantage to wet versus dry measurements (Butler et al., 2016), so both approaches are considered feasible provided that the EV sample preparation steps are detailed.

Along with instrument and sample considerations, data analysis and statistical procedures can impact the endpoints and conclusions of RS studies. All data analysis software and versions should be reported. If custom-made program suites and algorithms are employed, it is recommended that the code be deposited in an online data repository for transparency and re-usability. After acquisition (and before downstream analyses), spectra that are meant to be compared with each other should be postprocessed using identical data manipulation parameters. For example, if baseline correction and/or background subtraction is implemented, all related parameters should be kept constant for all spectra. All downstream spectral analyses and further statistical testing (e.g., multivariate analysis, machine learning, statistical hypothesis testing) should be reported in full and with data openly available.

Recommendations

- Report all instrument and measurement parameters.
- Report sample preparation/application parameters including buffer composition and wet/dry measurement.
- Report data analysis software and versions. Deposit any code for custom-made program suites and algorithms in an online data repository for transparency and re-usability.
- Report downstream spectral analyses and further statistical testing.

6.8 | Resistive pulse sensing

Resistive pulse sensing (RPS) is a non-optical technique utilising the Coulter principle to determine the concentration and diameter of particles (Hogg & Coulter, 1967), along with zeta potential on some platforms. Current implementations of RPS include pre-calibrated fixed pores in a microfluidic cartridge format and uncalibrated stretchable pores, both with detection limits down to ~50 nm in diameter and the capability to measure particles up to several microns. The use of RPS to measure the diameter distributions and concentration of EVs in complex biofluids should be interpreted with caution, since co-isolates, such as lipoproteins and large protein complexes, are also counted and cannot be differentiated from EVs. RPS measurements do, however, have very high concordance with TEM data (van der Pol, Coumans, Grootemaat, et al., 2014).

When reporting RPS data it is recommended that instrument model, pore size, calibration bead diameter and source, and software version be reported. For stretchable pores, the applied voltage, applied stretch, and procedure to optimise settings should be shared (Coumans et al., 2014). For microfluidic RPS, appropriate dilution buffer to lower the surface tension of water should be considered and reported (Cimorelli et al., 2021). As outlined in Section 5.2, it is preferable to report RPS diameter distributions rather than a single diameter statistic for EV data, due to RPS statistics being easily skewed by the LOD. The inclusion of buffer-only controls to identify background, along with detergent-lysed samples run at the same concentration to determine label events is also recommended (Osteikoetxea et al., 2015). Due to RPS techniques being easily clogged by larger particles, preanalytical steps such as centrifugation or filtration may be used to remove larger particles. Since these approaches may alter the EV population being analysed and affect comparison with orthogonal methods, any preanalytical procedures should be clearly stated.

Recommendations

- Report any preanalytical procedures applied prior to RPS.
- For microfluidic RPS, appropriate dilution buffer should be considered and reported.
- Include buffer-only controls and detergent-lysed samples run at the same concentration as the untreated sample.

20013078, 2024, 2, Downloaded from https://isevjournals.onlinelibrary.wiley.com/doi/10.1002/jev2.12404 by Colorado State University, Wiley Online Library on [09/10/2024]. See the Terms and Conditions (https://onlinelibrary.wiley.com/terms-and-conditions) on Wiley Online Library for rules of use; OA articles are governed by the applicable Creative Commons License

- Report all instrument and software details.
- Report RPS diameter distributions rather than a single diameter statistic.

6.9 | Western blotting

Western blotting is a commonly used method to detect proteins in EV-containing preparations. Proteins are first separated by gel electrophoresis, then transferred to a membrane and probed with affinity reagents, usually antibodies. Input is often normalised by some aspect of the EV preparation (total protein, particle count) or some aspect of the EV source (biofluid volume, cultured cell number): the former allows comparison of amounts of EV cargo between similar groups of EVs, while the latter might also assess overall differences in EV production/uptake balance in the source system. For cell culture EVs, cell lysates, either in specified protein amount or in cell-equivalent amounts, should be loaded onto the same gel to assess enrichment/depletion in EVs versus producing cells. This comparison, however, can be easily performed only for analysis of EVs from cell culture-conditioned medium, since for other sources of EVs (e.g., biological samples), the source cells cannot be easily identified or recovered.

Where possible, known antigen-positive and -negative control samples should be included beside the experimental samples. Controls for assessing the purity of the sample preparation should also be included if claiming the protein is present on or in EVs; see Section 5.7. Antibody information (specificity, clone, source, labelling concentration, incubation time), sample denaturing conditions, presence, and nature of reducing agent, transfer methodology, membrane type, buffers, and imaging equipment and parameters should all be reported. For transparency, it is recommended that uncropped images of Western blots (including controls and a molecular weight ladder) be provided at a minimum as supplementary information.

Recommendations

- Provide details of protein enrichment and quantification.
- Where possible, include antigen-positive and -negative controls
- If claiming EV-association of a protein, include measures of the purity of the EV preparation.
- Report all details of input normalization, gel electrophoresis, transfer methodology, probing and imaging/analysis. These include but are not limited to antibody information, sample denaturing and reducing conditions, transfer methodology, membrane type, buffers, and imaging equipment and parameters.
- Provide uncropped images of all Western blots (e.g., as supplementary information if published in a journal).

> Consensus: 70.6% (705) of MISEV2023 survey respondents agreed "completely," and 27.5% (274) agreed "mostly" with Section 6: Technique-specific reporting considerations for EV characterization. 0.4% (4) "mostly" disagreed, and 1.5% (15) stated that they had no opinion and/or expertise. No respondents disagreed "completely."

7 | EV RELEASE AND UPTAKE

7.1 | Approaches to modulate EV release

EV release can be visualised by a range of methods, including those employing fluorescent tags and dyes (Sections 6.2, 6.6), which permit real-time imaging [reviewed in (Verweij et al., 2021)]. MISEV2018 discussed inhibition of EV release with a range of genetic manipulations and drugs, for example, *RAB27A/B* knockdown (Ostrowski et al., 2010), neutral sphingomyelinase inhibition (Trajkovic et al., 2008) and ARRDC1 inhibition (Mackenzie et al., 2016; Wang & Lu, 2017). More recent genetic and pharmacological manipulations are reviewed elsewhere (Catalano & O'Driscoll, 2020; Dixson et al., 2023; Zhang, Lu, et al., 2020). Some cellular manipulations can also stimulate EV release (Taher et al., 2019). While these treatments are often claimed to be specific for EVs of particular biogenesis pathways, they may affect EV formation and membrane trafficking more generally. It is thus difficult to exclude an impact on other EVs and/or non-EV cellular processes (Izumi, 2021; Mathieu et al., 2019; Puca et al., 2013; Xiang et al., 2021). MISEV2018 highlighted the importance of identifying biogenesis machinery that is confined to particular EV subtypes, and this remains a priority, with very few specific additional regulators identified. Using complementary methods to attenuate and/or enhance the production of specific EV subtypes can add strength to data suggesting their association with specific functions. The resulting EVs and control preparations should be analysed using the physical and molecular methods described in Sections 5 and 6, with particular attention to normalization methods (e.g., based on the number/protein mass of secreting cells, or EV number, etc.), identification of unchanged as well as altered markers, where possible, for specificity, and the use of multiple cell types to test whether the mechanism is generic or cell type-specific.

20013078, 2024, 2, Downloaded from https://isevjournals.onlinelibrary.wiley.com/doi/10.1002/jev2.12404 by Colorado State University, Wiley Online Library on [09/10/2024]. See the Terms and Conditions (https://onlinelibrary.wiley.com/terms-and-conditions) on Wiley Online Library for rules of use; OA articles are governed by the applicable Creative Commons License

Recommendations

- For genetic and pharmacological manipulations used to inhibit or stimulate EV secretion, report potential effects on other secretory or cell biological processes. For example, confirm that there is no change in cell viability, proliferation and secretion of non-EV-associated factors.
- Where possible, assess whether inhibiting a specific EV production pathway leads to a change in other EV release mechanisms by assessing EV-specific cargoes or activities.
- Identification of unchanged markers and the use of appropriate normalization methods are important for rigorous comparative analysis of EV preparations.

7.2 | EV interaction with cells

EVs can interact with target cells at different levels: binding, internalization, and fusion/content delivery. EVs contact the surface of cells, which might be referred to as 'EV binding'. In contrast, 'EV uptake' encompasses several outcomes. It can mean fusion of the EV with the cell membrane and release of contents into the cytoplasm. It can also mean internalization into the endocytic and/or other intracellular compartments of the cell, with or without EV-cellular membrane fusion. EV-mediated effects on the recipient cell might thus be occasioned by EV binding to receptors at the cell surface or internally and/or by release of contents into the cell at the surface or internally. The relative importance of these different interactions remains unclear, even though most reports of EV function have assumed content delivery. However, EV uptake may occur only at a low rate (Bonsergent et al., 2021; Somiya & Kuroda, 2021a, 2021b) in some target cells, necessitating a high ratio of EVs to target cells to visualise this process (Jurgielewicz et al., 2020; Ragni et al., 2019).

How can these different modes of action be interrogated? Some fluorescence microscopy methods can identify subcellular fluorescent events associated with cells, while flow cytometry mostly detects EV 'capture' without discriminating between binding and uptake. For all methods, the long-lived nature of EV labelling substances may not accurately reflect the presence of EVs in target cells, lipophilic dyes might change EV properties (Section 6.6), and detection of downstream receptor-mediated cell signalling induced by EVs does not discriminate between different modes of action. While covalently bound dyes cannot be exchanged between EVs and cell membranes without fusion, lipophilic dyes can be exchanged without actual EV transfer, resulting in false positive signals (Simonsen, 2019). New approaches for assaying cargo delivery (including endosomal escape) have been developed since MISEV2018, for example, anti-GFP fluobodies (Joshi et al., 2020), proteolytic cargo cleavage (Perrin et al., 2021), split-luciferase reporters (Somiya & Kuroda, 2021a), CRISPR-Cas9 reporters (de Jong et al., 2020), Cre reporters (Borghesan et al., 2019), trans-activator delivery (Somiya & Kuroda, 2021b) and knockout of a cargo gene in recipient cells (Taha et al., 2020). By labelling specific EV subtypes, blocking their biogenesis and assaying cargo delivery, it may be possible to determine how EV-target cell interaction mechanisms vary between different EV subtypes and EV donor-acceptor combinations. Going forward, inhibition of specific EV ligand-receptor interactions may establish discrete phenotypic effects: for example, by genetic approaches or addition of blocking antibodies or inhibitory compounds. Blockade of specific intracellular trafficking pathways will suggest which are critical for EV function.

Recommendations

- Assess the suitability of the labelling/reporting system in terms of the impact on normal cellular processes, the stability of the EV-cell association, and longevity within an intracellular environment.
- Report EV:recipient cell ratios and the physiological relevance of the delivered dose.
- Report incubation conditions, exposure time, cell densities, and configuration, for example, 2D/3D.
- Evaluate binding, uptake and content transfer to identify critical mechanistic elements driving the cellular response(s).

> Consensus: 69.6% (695) of MISEV2023 survey respondents agreed "completely," and 24.3% (243) agreed "mostly" with Section 7: EV release and uptake. 0.2% (2) "mostly" disagreed, and 5.8% (58) stated that they had no opinion and/or expertise. No respondents disagreed "completely."

8 | FUNCTIONAL STUDIES

MISEV2018 recommendations on functional studies of EVs continue to hold for MISEV2023. Because of the great diversity of functional studies in vivo and in vitro, we provide only general recommendations. First, physiologically informed dose-response and time-course studies are encouraged. Second, carefully selected EV negative controls are needed to assess the contribution of 'background' EV activity (such as EVs present in culture medium components) and/or non-specific activity of EVs other than those of interest. For cell culture-derived EVs, this might mean unconditioned medium that has been processed in the same way

20013078, 2024, 2, Downloaded from https://isevjournals.onlinelibrary.wiley.com/doi/10.1002/jev2.12404 by Colorado State University, Wiley Online Library on [09/10/2024]. See the Terms and Conditions (https://onlinelibrary.wiley.com/terms-and-conditions) on Wiley Online Library for rules of use; OA articles are governed by the applicable Creative Commons License

20013078, 2024, 2, Downloaded from https://isevjournals.onlinelibrary.wiley.com/doi/10.1002/jev2.12404 by Colorado State University, Wiley Online Library on [09/10/2024]. See the Terms and Conditions (https://onlinelibrary.wiley.com/terms-and-conditions) on Wiley Online Library for rules of use; OA articles are governed by the applicable Creative Commons License

as conditioned medium (i.e., to separate any EVs that may be present in culture medium components). For EVs from a specific cell type, EVs from another cell type might serve as an appropriate control. For engineered EVs, consider EVs from unmanipulated cells or cells engineered with an irrelevant component (cell engineering) or EVs that have not been modified (post-production engineering). For patient disease studies, use EVs sourced from healthy, matched or untreated donors. Third, controls consisting of non-EV-containing, EV-depleted or enzymatically treated EV separation fractions can help to identify if a function is specific to EVs or associated with co-isolating materials. Possibly complicating this analysis, evidence has emerged since MISEV2018 for a functional role of certain loosely tethered coronal elements, as discussed in Sections 3.4 and 4.7, and EV co-isolates may indeed contribute along with EVs, additively or synergistically, to effects. Finally, the influence of EV separation/concentration, storage and formulation factors on EV activity should be studied, with the goal of maximising activity. Importantly, it is not expected that all conceivable controls will be studied simultaneously in any given system. Instead, potency assays (Gimona et al., 2021; Nguyen et al., 2020) can be used (or developed) to identify the most informative controls for pre-clinical and clinical studies.

Recommendations

- Perform dose-response and time-course studies to assess specificity, kinetics and saturability.
- Report and justify the method(s) used to normalise input.
- Evaluate negative EV controls where possible to rule out effects of 'background' EVs (e.g., from culture medium) and to evaluate the specific effects of EVs from a certain source or of specific EV elements.
- Evaluate appropriate non-EV (e.g., NVEP, soluble protein) negative controls to understand the EV-association of specific activities.
- Assess the effects of pre-analysis factors, especially storage and formulation, on EV activity.

> Consensus: 71.1% (710) of MISEV2023 survey respondents agreed "completely," and 25.1% (250) agreed "mostly" with Section 8: Functional studies. 0.3% (3) "mostly" disagreed, and 0.1% (1) "completely" disagreed. 3.4% (34) stated that they had no opinion and/or expertise.

9 | EV ANALYSIS IN VIVO

In vivo EV studies can provide mechanistic insights into EV release, biodistribution, pharmacokinetics and function (Verweij et al., 2021) and may be performed in a wide variety of species, including but not limited to model organisms that recapitulate aspects of human health and disease. In genetically tractable organisms, progress may be facilitated by EV tags and cellular reporter systems (Section 6.2). The relative ease of genetic manipulation of invertebrate and vertebrate model organisms allows hypothesis testing and specific EV labelling approaches (Beckett et al., 2013; Budnik et al., 2016; Fan et al., 2020; Gross et al., 2012; Verweij et al., 2019), including for EV subtype-specific mechanisms (Beer et al., 2018; Fan et al., 2020). Table 4 presents non-exhaustive examples of in vivo models for EV studies, each of which has specific strengths and limitations. For example, enlarged endosomal compartments in secondary cells of the fruit fly *Drosophila melanogaster* allow visualization of intraluminal vesicle biogenesis (Corrigan et al., 2014; Fan et al., 2020), while larval motor neurons express multiple EV cargoes with known physiological roles, such that EV regulatory mechanisms can be tested through functional assays (Koles et al., 2012; Korkut et al., 2013; Walsh et al., 2021). The transparent nematode *Caenorhabditis elegans* has also provided insights into the cellular, developmental, and behavioral roles of EVs in addition to EV biogenesis (Beer & Wehman, 2017; Wang et al., 2014; Wehman et al., 2011). EV separation and concentration are challenging for small invertebrates but have been reported from nematode worms (Nikonorova et al., 2022; Russell et al., 2020) and fruit flies, (Thomas et al., 2018; Tsai et al., 2019). By virtue of its transparency, the zebrafish embryo can be used for real-time biodistribution and uptake studies (Hyenne et al., 2019; Verweij et al., 2019). In contrast, larger mammalian models may be needed to recapitulate some aspects of human physiology and disease processes. A key strength of in vivo models is the opportunity to assess the release of physiological levels of EVs and their interaction with target cells.

Some in vivo studies examine endogenous EVs, usually using fluorescent (Estrada et al., 2022; Hegyesi et al., 2022; Neckles et al., 2019; Nørgård et al., 2022) or bioluminescent tags (Gupta et al., 2020; Luo et al., 2020; Rufino-Ramos et al., 2022). Pre-clinical studies with syngeneic models and human cancer cell line xenograft models have allowed tumour and other EVs to be specifically labelled and traced (Driedonks et al., 2022; Hyenne et al., 2019; Liu et al., 2016; Pucci et al., 2016; Wiklander et al., 2015). Functions have been assigned to these EVs, such as roles in metastasis, by pharmacologically or genetically manipulating putative EV biogenesis regulators (Costa-Silva et al., 2015; Peinado et al., 2012; Wen et al., 2016); however, see caveats on blocking biogenesis that are discussed in Section 7.1 and on the relationship between uptake and function discussed in Section 7.2. Attempts to assess cytoplasmic delivery of EV cargo have involved, for example, EV-loaded mRNA for the DNA recombinase Cre and its detection in target reporter cells (Zomer et al., 2015). Parabiosis, whereby the circulations of two animals are joined, permits labelled EVs from one mouse to be visualised in the other (Liu, Kou, et al., 2018; Zhang et al., 2022).

TABLE 4 Studying EV biology in vivo.

In vivo models	EV-releasing cells or other EV source	Other specific strengths	Genetic tractability	Genetic similarity to humans
Budding yeast *Saccharomyces cerevisiae*	Unicellular yeast (Oliveira et al., 2010; Zhao et al., 2019)	Whole organism analysis in vivo	++++	+
Green algae *Chlamydomonas reinhardtii*	Flagellated unicellular algae (Wood et al., 2013)	Cilia biology	++++	+
Flowering plant *Arabadopsis thaliana*	Leaf cells (Baldrich et al., 2019; He et al., 2021)	Plant immunity	++++	+
Nematode *Caenorhabditis elegans*	Embryonic cells (Beer et al., 2018; Wehman et al., 2011)	EV release mechanisms; whole organism analysis in vivo	++++	++
	Larval epithelial cells (Liégeois et al., 2006; Hyenne et al., 2015)	EV release mechanisms; whole organism analysis in vivo		
	Ciliated sensory neurons (Clupper et al., 2022; Nikonorova et al., 2022; Razzauti & Laurent, 2021; Wang et al., 2015)	Cilia biology; whole organism analysis in vivo; reproductive functions		
Fly *Drosophila melanogaster*	Larval wing imaginal disc (Beckett et al., 2013; Gradilla et al., 2014; Gross et al., 2012; Matusek et al., 2014)	Wnt/Hedgehog morphogen signalling	++++	++
	Larval motor neuron axon terminals (Koles et al., 2012; Korkut et al., 2013; Walsh et al., 2021)	Synaptic function		
	Larval haemocytes (Tassetto et al., 2017)	Adaptive immune system		
	Adult male secondary cells (Corrigan et al., 2014; Fan et al., 2020; Marie et al., 2023)	Large MVBs: exosome subtype biogenesis; reproductive functions		
	Adult muscle cells (Jewett et al., 2021)	Neurodegeneration		
Zebrafish *Dario rerio*	Embryonic yolk syncytial layer (Verweij et al., 2019)	Transparent embryos: EV imaging in bloodstream; target cell biodistribution; metabolic functions	+++	+++
	Adult osteoblasts (Kobayashi-Sun et al., 2020)	Fracture healing		
	Larval and adult cardiomyocytes (Scott et al., 2021)	Cardiovascular disease		
	Tumor cell lines (Hyenne et al., 2019)	Melanoma		
Chicken *Gallus gallus domesticus*	Chorioallantoic membrane (CAM) cells (Sung et al., 2015)	High-resolution live imaging of cell migration	+	+++
Mouse *Mus musculus*	Endothelial cells (McCann et al., 2020)	Cell type-specific EVs in plasma	++	++++
	Red blood cells; heart (Valkov et al., 2021)	Ischaemic heart		
	Mouse tumour cells	Pre-clinical metastasis (syngeneic grafts) (Ge et al., 2021; Ghoroghi et al., 2021)		
	Human tumour xenografts (Costa-Silva et al., 2015; Hoshino et al., 2015; Peinado et al., 2012; Zomer et al., 2015; Zomer et al., 2016)	Metastasis		

A non-exhaustive list of cellular models from different organisms, with particular emphasis on those that are widely used in genetic studies. Nomenclature: genetic tractability and genetic similarity to humans are rated from: weak ('+') to strong ('++++'). Please note that citations are examples only.

20013078, 2024, 2, Downloaded from https://isevjournals.onlinelibrary.wiley.com/doi/10.1002/jev2.12404 by Colorado State University, Wiley Online Library on [09/10/2024]. See the Terms and Conditions (https://onlinelibrary.wiley.com/terms-and-conditions) on Wiley Online Library for rules of use; OA articles are governed by the applicable Creative Commons License

20013078, 2024, 2, Downloaded from https://isevjournals.onlinelibrary.wiley.com/doi/10.1002/jev2.12404 by Colorado State University, Wiley Online Library on [09/10/2024]. See the Terms and Conditions (https://onlinelibrary.wiley.com/terms-and-conditions) on Wiley Online Library for rules of use; OA articles are governed by the applicable Creative Commons License

Other in vivo studies introduce exogenous EVs into an organism. These EV may be unlabelled when a disease or physiologic outcome is targeted and imaging is not done. For studies with imaging, EVs are often fluorescently or bioluminescently labelled (Alexander et al., 2015; García-Silva et al., 2021; Kang et al., 2021; Long et al., 2017; Royo et al., 2019). Exogenous EVs have also been labelled, for example, with species-specific RNAs (Ciullo et al., 2022) and by substances compatible with magnetic resonance imaging (MRI), X-ray computed tomography (CT) imaging, magnetic particle imaging (MPI), single-photon emission computed tomography (SPECT) or positron emission tomography (PET) (Arifin et al., 2022; Skotland et al., 2022). There are several caveats to the exogenous approach. Specific labels may affect biodistribution patterns and detectability thresholds (Lázaro-Ibáñez et al., 2021), necessitating standardization (Herrmann et al., 2021). Exogenous EVs may also differ from endogenous EVs in route and timing of administration (bolus/continuous), dose, non-EV components of the administered preparation, and of course composition, and physiologic relevance should be carefully pondered (see also Section 8) (Ridder et al., 2014).

For detection and tracking endogenous and exogenous EVs, several additional technical considerations apply. In vivo EV tracking and ex vivo detection will be limited by technique-specific sensitivity and spatial resolution, for example, a fluorescent signal may represent a single EV, clustered EVs or non-EV labelled substances. Caveats associated with genetic labels such as the common CD63-GFP approaches are discussed in Section 6.2 and elsewhere (Verweij et al., 2021). They include the potential disruption of protein, EV or cellular biology through fusion protein (over)expression; possible quenching in acidic compartments; labelling of only specific EV subtypes; labelling of different EV subtypes by a specific marker in different cell types and species; and possible separation of the tag from its host protein. A knock-in strategy, by which a fluorescently tagged fusion construct (e.g., CD63-GFP) replaces the respective EV gene in its endogenous locus, or the use of multiple EV markers, provide possible solutions to some of these problems.

Recommendations *(Note: These recommendations are broad, as this section of MISEV2023 is meant to raise awareness of the diversity of in vivo studies and not to make prescriptive guidelines. Innovative new approaches should thrive in diverse organisms to move the field forward.)*

- Report all details of labelling and detection/imaging technologies to allow replication studies.
- For exogenous EV administration, report all parameters of administration, including anatomical site, timing (bolus/continuous) and dose.
- Consider and control for the possible effects of EV labelling on EV biodistribution, pharmacokinetics and function.
- Consider that pharmacologic or genetic manipulations meant to block EV production in vivo may have off-target consequences.
- Consider the possibility of different behaviour of endogenous and exogenous EVs.

> Consensus: 65.5% (654) of MISEV2023 survey respondents agreed "completely," and 21.6% (216) agreed "mostly" with Section 9: EV analysis in vivo. 0.1% (1) "mostly" disagreed, and 12.7% (127) stated that they had no opinion and/or expertise. No respondents disagreed "completely."

10 | CONCLUSIONS

Consensus building was achieved for MISEV2023 through a lengthy process. Suggestions for the new MISEV were gathered from the ISEV community and MISEV2018 authorship through a 2020 survey that received >750 responses (Witwer et al., 2021). A five-member MISEV2023 organising committee was then formed during the strategic planning session of the ISEV Board of Directors in November 2020, consisting of Deborah Goberdhan, Lorraine O'Driscoll, Clotilde Théry, Joshua Welsh and Kenneth Witwer. An initial MISEV2023 draft went through rounds of review and revision by members of the ISEV board and other individuals, including task force members, who were invited by the organising team because of their subject expertise relevant to specific sections. An exhaustive MISEV2023 survey was circulated to ~5700 EV researchers, and 1025 responses were received. Refinements were made to the manuscript by the organising committee and invited co-authors based on these responses. The manuscript was then submitted to the Journal of Extracellular Vesicles. The journal selected more than 30 individual experts to review the manuscript, and reviews were shared with the organising committee along with editorial suggestions. The manuscript was then revised by the organising committee and subject experts, and the ISEV Board of Directors was consulted on matters of timing and logistics. At the request of the ISEV Board, the revised manuscript was sent via survey to all who were involved in developing the guidelines and who had indicated willingness to accept co-authorship. The results of this authorship survey were used to gauge consensus on each section and to determine the final author lists before resubmission to the journal. The consensus statements at the end of Sections 1 through 9 reflect the complete answers of 998 unique MISEV2023 authorship confirmation survey respondents. There were 1039 responses in total, including several duplicates, one triplicate, three declines, and several incomplete responses. Note that several confirmed authors did not complete the survey for reasons that were deemed valid, including technical issues.

MISEV2023 has compiled recommendations for EV research, from basic to advanced, state-of-the-art technologies and methodologies. As such, it can serve both as a handbook for those new to EV research and also as an inspiration for more advanced science in the field. In generating this document, an overarching goal has been to reach a high degree of agreement from a large group of scientists within the EV community. As with any consensus document, not every co-author necessarily agrees with every section or every recommendation. We also recognise that new methods will appear, while some advanced techniques may become easier to use: the field is dynamic, not static. Nevertheless, we propose that MISEV2023 describes the current best practice in the field and represents the current consensus position of the extracellular vesicle community.

AFFILIATIONS

[1]Translational Nanobiology Section, Laboratory of Pathology, National Cancer Institute, National Institutes of Health, Bethesda, Maryland, USA

[2]Nuffield Department of Women's and Reproductive Health, University of Oxford, Women's Centre, John Radcliffe Hospital, Oxford, UK

[3]School of Pharmacy and Pharmaceutical Sciences, Trinity College Dublin, Dublin, Ireland

[4]Trinity Biomedical Sciences Institute, Trinity College Dublin, Dublin, Ireland

[5]Trinity St. James's Cancer Institute, Trinity College Dublin, Dublin, Ireland

[6]Department of Genetics, Cell- and Immunobiology, Semmelweis University, Budapest, Hungary

[7]HCEMM-SU Extracellular Vesicle Research Group, Semmelweis University, Budapest, Hungary

[8]HUN-REN-SU Translational Extracellular Vesicle Research Group, Semmelweis University, Budapest, Hungary

[9]Faculty of Medical and Health Sciences, The University of Auckland, Auckland, New Zealand

[10]Department of Molecular Biotechnology and Health Sciences, University of Turin, Turin, Italy

[11]University of Georgia, Athens, Georgia, USA

[12]Department of Surgery, Division of Cancer Biology and Therapeutics, Cedars-Sinai Medical Center, Los Angeles, California, USA

[13]Department CDL Research, University Medical Center Utrecht, Utrecht, The Netherlands

[14]University of Virginia Health System, Charlottesville, Virginia, USA

[15]Exosomes Laboratory, Center for Cooperative Research in Biosciences, Basque Research and Technology Alliance, Derio, Spain

[16]Metabolomics Platform, Center for Cooperative Research in Biosciences, Basque Research and Technology Alliance, Derio, Spain

[17]IKERBASQUE, Basque Foundation for Science, Bilbao, Spain

[18]Otorhinolaryngology Hospital, The First Affiliated Hospital, Sun Yat-sen University, Guangzhou, China

[19]Extracellular Vesicle Research and Clinical Translational Center, The First Affiliated Hospital, Sun Yat-sen University, Guangzhou, China

[20]Institute for Health and Sport, Victoria University, Melbourne, Australia

[21]Faculty of Medicine, University of Ljubljana, Ljubljana, Slovenia

[22]Institute of Molecular and Cell Biology (IMCB), Agency for Science, Technology and Research (A*STAR), Singapore, Singapore

[23]Paracrine Therapeutics Pte. Ltd., Singapore, Singapore

[24]Department of Surgery, YLL School of Medicine, National University Singapore, Singapore, Singapore

[25]Thomas Jefferson University, Philadelphia, Pennsylvania, USA

[26]Stem Cell Facility, All India Institute of Medical Sciences, New Delhi, India

[27]Chinese University of Hong Kong, Hong Kong, Hong Kong S.A.R.

[28]QIMR Berghofer Medical Research Institute, Brisbane, Australia

[29]Laboratory of Experimental Clinical Chemistry, Amsterdam University Medical Centers, Location AMC, University of Amsterdam, Amsterdam, The Netherlands

[30]Amsterdam Vesicle Center, Amsterdam University Medical Centers, Location AMC, University of Amsterdam, Amsterdam, The Netherlands

[31]Tokyo Medical University, Tokyo, Japan

[32]Icahn School of Medicine at Mount Sinai, New York, New York, USA

[33]Laboratório de Imunologia Celular e Bioquímica de Fungos e Protozoários, Departamento de Ciências Farmacêuticas, Instituto de Ciências Ambientais, Químicas e Farmacêuticas, Universidade Federal de São Paulo (UNIFESP) Campus Diadema, Diadema, Brazil

[34]Department of Laboratory Medicine, Nanfang Hospital, Southern Medical University, Guangzhou, China

[35]Department of Pathology, Vanderbilt University Medical Center, Nashville, Tennessee, USA

[36]Genentech, South San Francisco, California, USA

[37]Department of Molecular Medicine, Beckman Research Institute, City of Hope Comprehensive Cancer Center, Duarte, California, USA

[38]Department of Molecular and Translational Medicine, University of Brescia, Brescia, Italy

[39]Center for Colloid and Surface Science (CSGI), Florence, Italy

[40]National Center for Gene Therapy and Drugs based on RNA Technology, Padua, Italy

20013078, 2024, 2, Downloaded from https://isevjournals.onlinelibrary.wiley.com/doi/10.1002/jev2.12404 by Colorado State University, Wiley Online Library on [09/10/2024]. See the Terms and Conditions (https://onlinelibrary.wiley.com/terms-and-conditions) on Wiley Online Library for rules of use; OA articles are governed by the applicable Creative Commons License

[41]Weatherall Institute of Molecular Medicine, University of Oxford, Oxford, UK

[42]Consiglio Nazionale delle Ricerche - Istituto per lo Studio dei Materiali Nanostrutturati, Bologna, Italy

[43]Consorzio Interuniversitario per lo Sviluppo dei Sistemi a Grande Interfase, Florence, Italy

[44]Kidney Research Centre, Ottawa Hopsital Research Institute, Ottawa, Canada

[45]Department of Cellular and Molecular Medicine, University of Ottawa, Ottawa, Canada

[46]School of Pharmaceutical Sciences, University of Ottawa, Ottawa, Canada

[47]Department of Biomedical Engineering, University of California, Davis, California, USA

[48]Division of Pharmaceutics and Pharmacology, College of Pharmacy, The Ohio State University, Columbus, Ohio, USA

[49]Comprehensive Cancer Center, The Ohio State University, Columbus, Ohio, USA

[50]Sahlgrenska Center for Cancer Research, Department of Surgery, Institute of Clinical Sciences, Sahlgrenska Academy, University of Gothenburg, Gothenburg, Sweden

[51]Wallenberg Centre for Molecular and Translational Medicine, Institute of Clinical Sciences, Sahlgrenska Academy, University of Gothenburg, Gothenburg, Sweden

[52]Department of Biomedicine, University Hospital Basel, Basel, Switzerland

[53]Department of Biomedicine, University of Basel, Basel, Switzerland

[54]Department of Oncology, University of Oxford, Oxford, UK

[55]Departments of Neurology and Psychiatry, Johns Hopkins University School of Medicine, Baltimore, Maryland, USA

[56]Laboratory of Experimental Cancer Research, Department of Human Structure and Repair, Ghent University, Ghent, Belgium

[57]Cancer Research Institute Ghent, Ghent, Belgium

[58]Barnett Institute of Chemical and Biological Analysis, Department of Chemistry and Chemical Biology, Northeastern University, Boston, Massachusetts, USA

[59]Department of Cancer Biology and Molecular Medicine, Beckman Research Institute, City of Hope Comprehensive Cancer Center, Duarte, California, USA

[60]Bio-pharmaceutical Manufacturing and Academic Resource Center (BioMARC), Infectious Disease Research Center, Colorado State University, Fort Collins, Colorado, USA

[61]Department of Rheumatology, University Hospital Basel, Basel, Switzerland

[62]Krefting Research Centre, Department of Internal Medicine and Clinical Nutrition, Institute of Medicine at Sahlgrenska Academy, University of Gothenburg, Gothenburg, Sweden

[63]Krefting Research Centre, Institute of Medicine at Sahlgrenska Academy, University of Gothenburg, Gothenburg, Sweden

[64]Erasmus MC Cancer Institute, University Medical Center Rotterdam, Department of Urology, Rotterdam, The Netherlands

[65]College of Medicine and Public Health, Flinders University, Adelaide, Australia

[66]Department of Physics and Astronomy, and LaserLaB Amsterdam, Vrije Universiteit Amsterdam, Amsterdam, The Netherlands

[67]Department of Transfusion Medicine, University Hospital, Salzburger Landeskliniken GmbH of Paracelsus Medical University, Salzburg, Austria

[68]GMP Unit, Paracelsus Medical University, Salzburg, Austria

[69]Transfer Centre for Extracellular Vesicle Theralytic Technologies, EV-TT, Salzburg, Austria

[70]Expansion Therapeutics, Structural Biology and Biophysics, Jupiter, Florida, USA

[71]Department of Anesthesiology & Perioperative Medicine, Oregon Health & Science University, Portland, Oregon, USA

[72]Department of Stem Cells and Developmental Biology, Cell Science Research Center, Royan Institute for Stem Cell Biology and Technology, ACECR, Tehran, Iran

[73]Celer Diagnostics, Toronto, Canada

[74]Waipapa Taumata Rau University of Auckland, Auckland, New Zealand

[75]Wyss Institute for Biologically Inspired Engineering, Harvard University, Boston, Massachusetts, USA

[76]Universidad de la República, Montevideo, Uruguay

[77]Institut Pasteur de Montevideo, Montevideo, Uruguay

[78]Biological Nanochemistry Research Group, Institute of Materials and Environmental Chemistry, Research Centre for Natural Sciences, Budapest, Hungary

[79]Department of Biophysics and Radiation Biology, Semmelweis University, Budapest, Hungary

[80]Biomedical Engineering and Physics, Amsterdam UMC, location AMC, University of Amsterdam, Amsterdam, The Netherlands

[81]Laboratory of Experimental Clinical Chemistry, Amsterdam UMC, location AMC, University of Amsterdam, Amsterdam, The Netherlands

[82]Department of Biomolecular Health Sciences, Faculty of Veterinary Medicine, Utrecht University, Utrecht, The Netherlands

[83]University of Denver, Denver, USA

[84]International Society for Extracellular Vesicles

[85]Institut Curie, INSERM U932, PSL University, Paris, France

[86]CurieCoreTech Extracellular Vesicles, Institut Curie, Paris, France

[87]Department of Molecular and Comparative Pathobiology, Johns Hopkins University School of Medicine, Baltimore, Maryland, USA

[88]EV Core Facility "EXCEL", Institute for Basic Biomedical Sciences, Johns Hopkins University School of Medicine, Baltimore, Maryland, USA

[89]The Richman Family Precision Medicine Center of Excellence in Alzheimer's Disease, Johns Hopkins University School of Medicine, Baltimore, Maryland, USA

20013078, 2024, 2, Downloaded from https://isevjournals.onlinelibrary.wiley.com/doi/10.1002/jev2.12404 by Colorado State University, Wiley Online Library on [09/10/2024]. See the Terms and Conditions (https://onlinelibrary.wiley.com/terms-and-conditions) on Wiley Online Library for rules of use; OA articles are governed by the applicable Creative Commons License

20013078, 2024, 2, Downloaded from https://isevjournals.onlinelibrary.wiley.com/doi/10.1002/jev2.12404 by Colorado State University, Wiley Online Library on [09/10/2024]. See the Terms and Conditions (https://onlinelibrary.wiley.com/terms-and-conditions) on Wiley Online Library for rules of use; OA articles are governed by the applicable Creative Commons License

AUTHOR CONTRIBUTIONS

Joshua A. Welsh: Project administration; visualization; writing—original draft; writing—review and editing. **Deborah C. I. Goberdhan**: Project administration; writing—original draft; writing—review and editing. **Lorraine O'Driscoll**: Project administration; writing—original draft; writing—review and editing. **Edit I. Buzas**: Writing—review and editing. **Cherie Blenkiron**: Writing—review and editing. **Benedetta Bussolati**: Writing—review and editing. **Houjian Cai**: Writing—review and editing. **Dolores Di Vizio**: Writing—review and editing. **Tom A. P. Driedonks**: Writing—review and editing. **Uta Erdbrügger**: Writing—review and editing. **Juan M. Falcon-Perez**: Writing—review and editing. **Qing-Ling Fu**: Writing—review and editing. **Andrew F. Hill**: Writing—review and editing. **Metka Lenassi**: Writing—review and editing. **Sai Kiang Lim**: Writing—review and editing. **Mỹ G. Mahoney**: Writing—review and editing. **Sujata Mohanty**: Writing—review and editing. **Andreas Möller**: Writing—review and editing. **Rienk Nieuwland**: Writing—review and editing. **Takahiro Ochiya**: Writing—review and editing. **Susmita Sahoo**: Writing—review and editing. **Ana C. Torrecilhas**: Writing—review and editing. **Lei Zheng**: Writing—review and editing. **Andries Zijlstra**: Writing—review and editing. **Sarah Abuelreich**: Writing—review and editing. **Reem Bagabas**: Writing—review and editing. **Paolo Bergese**: Writing—review and editing. **Esther M. Bridges**: Writing—review and editing. **Marco Brucale**: Writing—review and editing. **Dylan Burger**: Writing—review and editing. **Randy P. Carney**: Writing—review and editing. **Emanuele Cocucci**: Writing—review and editing. **Rossella Crescitelli**: Writing—review and editing. **Edveena Hanser**: Writing—review and editing. **Adrian L. Harris**: Writing—review and editing. **Norman J. Haughey**: Writing—review and editing. **An Hendrix**: Writing—review and editing. **Alexander R. Ivanov**: Writing—review and editing. **Tijana Jovanovic-Talisman**: Writing—review and editing. **Nicole A. Kruh-Garcia**: Writing—review and editing. **Diego Kyburz**: Writing—review and editing. **Cecilia Lässer**: Writing—review and editing. **Kathleen M. Lennon**: Writing—review and editing. **Jan Lötvall**: Writing—review and editing. **Elena S. Martens-Uzunova**: Writing—review and editing. **Rachel R. Mizenko**: Writing—review and editing. **Lauren A. Newman**: Writing—review and editing. **Andrea Ridolfi**: Writing—review and editing. **Eva Rohde**: Writing—review and editing. **Tatu Rojalin**: Writing—review and editing. **Andrew Rowland**: Writing—review and editing. **Andras Saftics**: Writing—review and editing. **Ursula S. Sandau**: Writing—review and editing. **Julie A. Saugstad**: Writing—review and editing. **Faezeh Shekari**: Writing—review and editing. **Simon Swift**: Writing—review and editing. **Dmitry Ter-Ovanesyan**: Writing—review and editing. **Juan P. Tosar**: Writing—review and editing. **Zivile Useckaite**: Writing—review and editing. **Francesco Valle**: Writing—review and editing. **Zoltan Varga**: Writing—review and editing. **Edwin van der**: Writing—review and editing. **Martijn J. C. van Herwijnen**: Writing—review and editing. **Marca H. M. Wauben**: Writing—review and editing. **Ann M. Wehman**: Writing—review and editing. **Sarah Williams**: Writing—review and editing. **Andrea Zendrini**: Writing—review and editing. **Alan J. Zimmerman**: Writing—review and editing. **Clotilde Théry**: Project administration; writing—original draft; writing—review and editing. **Kenneth W. Witwer**: Project administration; writing—original draft; writing—review and editing.

ACKNOWLEDGEMENTS

The authors thank all members of the international EV research community for their support throughout the process of producing this document.

AUTHORSHIP AND PARTICIPATION

MISEV Consortium: **Sarah Abuelreich** (Department of Molecular Medicine, Beckman Research Institute, City of Hope Comprehensive Cancer Center, Duarte, CA, USA), **Samar Ahmad** (Department of Biochemistry, University of Toronto, Toronto, Canada), **Dina AK Ahmed** (University of Westminster, London, UK; Egypt Center for Research and Regenerative Medicine, Cairo, Egypt), **Sarah H Ahmed** (Biotechnology Department, Faculty of Science, Cairo University, Cairo, Egypt; Center of Excellence for Stem Cells and Regenerative Medicine, Zewail City for Science and Technology, Cairo, Egypt), **Elena Aikawa** (Brigham and Women's Hospital, Boston, MA, USA; Harvard Medical School, Boston, MA, USA), **Naveed Akbar** (Division of Cardiovascular Medicine, Radcliffe Department of Medicine, University of Oxford, Oxford, UK), **Kazunari Akiyoshi** (Kyoto University, Kyoto, Japan), **David P Al-Adra** (Division of Transplantation, Department of Surgery, University of Wisconsin, Madison, WI, USA), **Maimonah E Al-Masawa** (Centre for Tissue Engineering and Regenerative Medicine, Faculty of Medicine, Universiti Kebangsaan Malaysia Medical Centre, Jalan Yaacob Latif, Kuala Lumpur, Malaysia), **Manuel Albanese** (Department for Clinical Sciences and Community Health (DISCCO), University of Milan, Milan, Italy; National Institute of Molecular Genetics (INGM), Milan, Italy), **Ainhoa Alberro** (Multiple Sclerosis Group, Biogipuzkoa Health Research Institute, San Sebastian, Spain), **María José Alcaraz** (Department of Pharmacology, University of Valencia, Spain), **Jen Alexander-Brett** (Washington University School of Medicine, St. Louis, MO, USA), **Kimberley L Alexander** (Neurosurgery Department, Chris O'Brien Lifehouse, Camperdown, Australia; Neuropathology Department, Royal Prince Alfred Hospital, Camperdown, Australia; School of Medical Sciences, Faculty of Medicine and Health, The University of Sydney, Australia), **Nilufar Ali** (Boise State University, Boise, ID, USA; Azymus Therapeutics Inc., Boise, ID, USA), **Faisal J Alibhai** (University Health Network, Toronto, Canada), **Susann Allelein** (Fraunhofer Institut for Cell Therapy and Immunology IZI, Leipzig, Germany), **Mark C Allenby** (BioMimetic Systems Engineering Laboratory, School of Chemical Engineering, Faculty of Engineering, Architecture and Information Technology, The University of Queensland, St Lucia, Australia; Centre for Biomedical Technologies, School of Mechanical, Medical, and Process Engineering, Faculty of Engineering, Queensland University of Technology, Brisbane, Australia), **Fausto Almeida** (University of Sao Paulo,

Ribeirao Preto Medical School, Sao Paulo, Brazil), **Luis Pereira de Almeida** (Center for Neuroscience and Cell Biology, University of Coimbra, Coimbra, Portugal; Center for Innovative Biomedicine and Biotechnology, University of Coimbra, Coimbra, Portugal; Faculty of Pharmacy, University of Coimbra, Coimbra, Portugal), **Sameh W Almousa** (Wake Forest School of Medicine, Winston-Salem, NC, USA), **Nihal Altan-Bonnet** (National Institutes of Health, Bethesda, MD, USA), **Wanessa F Altei** (Molecular Oncology Research Center, Barretos Cancer Hospital, Barretos, Brazil; Radiation Oncology Department, Barretos Cancer Hospital, Barretos, Brazil), **Gloria Alvarez-Llamas** (Immunology Department, IIS-Fundacion Jimenez Diaz, Fundacion Jimenez Diaz University Hospital-UAM, Madrid, Spain; Department of Biochemistry and Molecular Biology, Complutense University, Madrid, Spain), **Cora L Alvarez** (Instituto de Química y Fisicoquímica Biológicas "Prof. Alejandro C. Paladini", Buenos Aires, Argentina; Consejo Nacional de Investigaciones Científicas y Tecnicas, Argentina; Facultad de Ciencias Exactas y Naturales, University of Buenos Aires, Buenos Aires, Argentina), **Hyo Jung An** (Department of Pathology, Gyeongsang National University Changwon Hospital, Changwon, Republic of Korea; lnstitute of Medical Sciences, Gyeongsang National University, Jinju, Republic of Korea; Department of Pathology, Gyeongsang National University School of Medicine, Jinju, Republic of Korea), **Krishnan Anand** (Department of Chemical Pathology, School of Pathology, Faculty of Health Sciences, University of the Free State, Bloemfontein, South Africa), **Samir EL Andaloussi** (Department of Laboratory Medicine, Karolinska Institutet, Stockholm, Sweden; ME Cell Therapy and Allogenic Stem Cell Transplantation CAST, Karolinska University Hospital, Stockholm, Sweden), **Johnathon D Anderson** (University of California, Davis School of Medicine, Sacramento, CA, USA), **Ramaroson Andriantsitohaina** (INSERM U1046, UMR CNRS 9214, University of Montpellier, Montpellier, France), **Khairul I Ansari** (Inoviq Limited, Notting Hill, Australia), **Achille Anselmo** (FRACTAL—Flow Cytometry Resource, Advanced Cytometry Technical Applications Laboratory, IRCCS Ospedale San Raffaele Scientific Institute, Milan, Italy; Università Vita-Salute San Raffaele, Milan, Italy), **Anna Antoniou** (Department for Neurodegenerative Diseases and Geriatric Psychiatry, University of Bonn Medical Center, Bonn, Germany; German Center for Neurodegenerative Diseases, Bonn, Germany), **Farrukh Aqil** (Department of Medicine, University of Louisville, Louisville, KY, USA; Brown Cancer Center, University of Louisville, Louisville, KY, USA), **Tanina Arab** (Department of Molecular and Comparative Pathobiology, Johns Hopkins University School of Medicine, Baltimore, MD, USA), **Fabienne Archer** (IVPC UMR754, INRAE, EPHE, Universite Claude Bernard Lyon 1, Lyon, France), **Syrine Arif** (Faculté de Médecine, Université Laval, Quebec, Canada; Centre de Recherche du Centre Hospitalier Universitaire de Québec, Université Laval, Quebec, Canada; Centre de Recherche en Organogénèse Expérimentale de l'Université Laval/LOEX, Quebec, Canada), **David A Armstrong** (Dartmouth Health, Lebanon, NH, USA; Veterans Affairs Medical Center, White River Junction, VT, USA), **Onno J Arntz** (Experimental Rheumatology, Radboud University Medical Center, Nijmegen, The Netherlands), **Pierre Arsène** (Mursla Ltd, Cambridge, UK; Exosla Ltd, Cambridge, UK), **Luis Arteaga-Blanco** (Laboratory on Thymus Research, Oswaldo Cruz Institute/Fiocruz, Rio de Janeiro, Brazil), **Nandini Asokan** (INSERM U1109, Strasbourg France; Center Research Biomedicine De Strasbourg, France), **Trude Aspelin** (Department of Medical Biochemistry, Oslo University Hospital, Oslo, Norway), **Georgia K Atkin-Smith** (Walter and Eliza Hall Institute of Medical Research, Melbourne, Australia; La Trobe Institute for Molecular Science, La Trobe University, Melbourne, Australia), **Dimitri Aubert** (Vesiculab Ltd, Nottingham, UK), **Kanchana K Ayyar** (Boston Medical Center, Boston, MA, USA), **Maryam Azlan** (School of Health Sciences, Universiti Sains Malaysia, George Town, Malaysia), **Ioannis Azoidis** (Johns Hopkins University School of Medicine, Baltimore, MD, USA; University of Birmingham, Birmingham, UK), **Anaïs Bécot** (INSERM U1266, Institute of Psychiatry and Neurosciences of Paris, Paris, France), **Jean-Marie Bach** (Oniris, INRAE, IECM, Nantes, France), **Daniel Bachurski** (Center for Integrated Oncology Aachen Bonn Cologne Duesseldorf, Department I of Internal Medicine, Faculty of Medicine, University of Cologne, and University Hospital Cologne, Cologne, Germany; CECAD Center of Excellence on Cellular Stress Responses in Aging-Associated Diseases, University of Cologne, Cologne, Germany; Center for Molecular Medicine Cologne, University of Cologne, Cologne, Germany), **Seoyoon Bae** (Department of Life Sciences, Pohang University of Science and Technology, Pohang, Republic of Korea), **Reem Bagabas** (Department of Molecular Medicine, Beckman Research Institute, City of Hope Comprehensive Cancer Center, Duarte, CA, USA), **Roger Olofsson Bagge** (Sahlgrenska Center for Cancer Research, Department of Surgery, Institute of Clinical Sciences, Sahlgrenska Academy, University of Gothenburg, Gothenburg, Sweden; Department of Surgery, Sahlgrenska University Hospital, Gothenburg, Sweden; Wallenberg Centre for Molecular and Translational Medicine, Institute of Clinical Sciences, Sahlgrenska Academy, University of Gothenburg, Gothenburg, Sweden), **Monika Baj-Krzyworzeka** (Department of Clinical Immunology, Medical College, Jagiellonian University, Krakow, Poland), **Leonora Balaj** (Department of Neurosurgery, Massachusetts General Hospital, Harvard Medical School, Boston, MA, USA), **Carolina Balbi** (Center for Molecular Cardiology, University of Zurich, Zurich, Switzerland; Laboratory of Cellular and Molecular Cardiology, Istituto Cardiocentro Ticino-EOC, Lugano, Switzerland), **Bas WM van Balkom** (Department of Nephrology and Hypertension, University Medical Center Utrecht, Utrecht, The Netherlands), **Abhijna R Ballal** (Centre for Molecular Neurosciences, Kasturba Medical College Manipal, Manipal Academy of Higher Education, Manipal, India), **Afsareen Bano** (Maharshi Dayanand University, Rohtak, Haryana, India), **Sébastien Banzet** (Institut de Recherche Biomédicale des Armées, Brétigny sur Orge, France; INSERM UMR-MD-1197, Clamart, France; Centre de Transfusion des Armées, Clamart, France), **Yonis Bare** (Institut de Recherche en Infectiologie de Montpellier (IRIM), UMR9004 CNRS, Montpellier, France; University of Montpellier, Montpellier, France), **Lucio Barile** (Cardiovascular Theranostics, Istituto Cardiocentro Ticino, Ente Ospedaliero Cantonale, Bellinzona, Switzerland; Euler Institute, Faculty of Biomedical Sciences, Università Svizzera Italiana, Lugano, Switzerland), **Bahnisikha Barman** (Vanderbilt University School

20013078, 2024, 2, Downloaded from https://isevjournals.onlinelibrary.wiley.com/doi/10.1002/jev2.12404 by Colorado State University, Wiley Online Library on [09/10/2024]. See the Terms and Conditions (https://onlinelibrary.wiley.com/terms-and-conditions) on Wiley Online Library for rules of use; OA articles are governed by the applicable Creative Commons License

of Medicine, Nashville, TN, USA), **Isabel Barranco** (Department of Medicine and Animal Surgery, Veterinary Science, University of Murcia, Murcia, Spain), **Valeria Barreca** (Istituto Superiore di Sanità, Rome, Italy), **Geneviève Bart** (Developmental Biology Laboratory, Disease Networks RU, Faculty of Biochemistry and Molecular Medicine, University Oulu, Oulu, Finland), **Natasha S Barteneva** (Nazarbayev University, Astana, Kazakhstan), **Manuela Basso** (Department of Cellular, Computational and Integrative Biology (CIBIO), University of Trento, Trento, Italy), **Mona Batish** (Department of Medical and Molecular Sciences, University of Delaware, Newark, DE,USA), **Natalie R Bauer** (Frederick P. Whiddon College of Medicine, University of South Alabama, Mobile, AL, USA), **Amy A Baxter** (La Trobe University, Melbourne, Australia), **Wilfried W Bazié** (Axe de Recherche Maladies Infectieuses et Immunitaires, Centre de Recherche du CHU de Québec, Université Laval, Quebec, Canada; Programme de Recherche sur les Maladies Infectieuses, Centre Muraz, Institut National de Santé Publique, Bobo-Dioulasso, Burkina Faso), **Erica Bazzan** (Department of Cardiac, Thoracic, Vascular Sciences and Public Health, University of Padua, Padua, Italy), **Joel EJ Beaumont** (Department of Radiotherapy, GROW-School for Oncology and Reproduction, Maastricht University Medical Centre+, Maastricht, The Netherlands), **Mary Bebawy** (Private consultant), **Maarten P Bebelman** (Max Planck Institute of Molecular Cell Biology and Genetics, Dresden, Germany; Amsterdam UMC, Amsterdam, The Netherlands), **Apolonija Bedina-Zavec** (National Institute of Chemistry, Ljubljana, Slovenia), **Danielle J Beetler** (Mayo Clinic Center for Clinical and Translational Science, Rochester, MN, USA; Mayo Clinic Department of Cardiovascular Medicine, Jacksonville, Florida, USA; Mayo Clinic Graduate School of Biomedical Sciences, Rochester, Minnesota, USA), **Tamás Beke-Somfai** (Institute of Materials and Environmental Chemistry, Biomolecular Self-assembly Research Group, Reserach Centre for Natural Sciences, Budapest, Hungary), **Clémence Belleannée** (Faculty of Medicine, Université Laval, Quebec, Canada; CHU de Quebec Research Center, Quebec, Canada), **Birke J Benedikter** (University Eye Clinic Maastricht, MHeNs School for Mental Health and Neuroscience, Maastricht University Medical Center+, Maastricht, The Netherlands), **Berglind E Benediktsdóttir** (Faculty of Pharmaceutical Sciences, School of Health Sciences, University of Iceland, Reykjavik, Iceland), **Anna C Berardi** (Ospedale Santo Spirito, Pescara, Italy), **Mathilde Bergamelli** (Division of Obstetrics and Gynecology, Department of Clinical Science, Intervention and Technology, Karolinska Institutet, Stockholm, Sweden; Department of Gynecology and Reproductive Medicine, Karolinska University Hospital, Stockholm, Sweden), **Paolo Bergese** (Department of Molecular and Translational Medicine, University of Brescia, Brescia, Italy; Center for Colloid and Surface Science (CSGI), Florence, Italy; National Center for Gene Therapy and Drugs based on RNA Technology, Padua, Italy), **Irene Bertolini** (Immunology, Microenvironment and Metastasis Program, The Wistar Institute, Philadelphia, PA, USA), **Asima Bhattacharyya** (School of Biological Sciences, National Institute of Science Education and Research (NISER) Bhubaneswar, An OCC of Homi Bhabha National Institute, Odisha, India), **Suvendra N Bhattacharyya** (CSIR-Indian Institute of Chemical Biology, Kolkata, India; Department of Pharmacology and Experimental Neuroscience, University of Nebraska Medical Center, Omaha, NE, USA), **Steven J Biller** (Wellesley College, Wellesley, MA, USA), **Clotilde Billottet** (BRIC- Bordeaux Institute of Oncology-Inserm U1312, University of Bordeaux, Bordeaux, France), **John J Bissler** (St. Jude Children's Reseach Hospital, Memphis, TN, USA; Le Bonheur Children's Hospital, Memphis, TN, USA; University of Tennessee Health Sciences Center, Memphis, TN, USA), **Olivier Blanc-Brude** (INSERM, Paris Center for Cardiovascular Research-ParCC, Université Paris Cité, Paris, France), **Cherie Blenkiron** (Faculty of Medical and Health Sciences, The University of Auckland, Auckland, New Zealand), **Charles J Blijdorp** (Erasmus MC, Rotterdam, The Netherlands), **Sylwia Bobis-Wozowicz** (Department of Cell Biology, Faculty of Biochemistry, Biophysics and Biotechnology, Jagiellonian University, Krakow, Poland), **Victor Bodart-Santos** (Department of Neuroscience, Mayo Clinic Florida, Jacksonville, FL, USA), **Bernadett R Bodnár** (Department of Genetics, Cell- and Immunobiology, Semmelweis University, Budapest, Hungary; HCEMM-SU Extracellular Vesicle Research Group, Semmelweis University, Budapest, Hungary), **Eric Boilard** (Centre de Recherche du Centre Hospitalier Universitaire de Québec, Université Laval, Quebec, Canada; Centre de Recherche ARThrite (Arthrite Recherche Traitements) de l'Université Laval, Quebec, Canada), **Wilfrid Boireau** (Institut Femto-ST, CNRS, Université de Franche-Comté, Besançon, France), **Vladimir Bokun** (Department of Metabolism, Digestion and Reproduction, Imperial College London, London, UK), **Stephanie M Bollard** (School of Medicine, University College Dublin, Dublin, Ireland), **Sveva Bollini** (Department of Experimental Medicine (DIMES), University of Genova, Genova, Italy; IRCCS Ospedale Policlinico San Martino, Genova, Italy), **Antonella Bongiovanni** (Cell-Tech HUB at Institute for Research and Biomedical Innovation, National Research Council of Italy (CNR), Palermo, Italy), **Laura Bongiovanni** (Department of Veterinary Medicine, University of Teramo, Teramo, Italy; Department of Biomolecular Health Sciences, Faculty of Veterinary Medicine, Utrecht University, Utrecht, The Netherlands), **Amandine Bonifay** (C2VN, INSERM 1263, INRAE 1260, Aix-Marseille University, Marseille, France), **Marni D Boppart** (University of Illinois at Urbana-Champaign, Urbana-Champaign, IL, USA; Beckman Institute for Advanced Science and Technology, University of Illinois at Urbana-Champaign, Urbana-Champaign, IL, USA), **Francesc E Borràs** (REMAR-IVECAT Group, Germans Trias i Pujol Research Institute (IGTP) & Nephrology Department, University Hospital Germans Trias i Pujol (HUGTiP), Can Ruti Campus, Badalona, Spain; Department of Cell Biology, Physiology and Immunology, Universitat de Barcelona (UB), Barcelona, Spain), **Steffi Bosch** (Oniris IECM Laboratory, INRAE, USC1383, Nantes, France), **Daniela Boselli** (FRACTAL—Flow Cytometry Resource, Advanced Cytometry Technical Applications Laboratory, IRCCS Ospedale San Raffaele Scientific Institute, Milan, Italy), **Massimo Bottini** (Department of Experimental Medicine, University of Rome Tor Vergata, Rome, Italy; Sanford Burnham Prebys, La Jolla, CA, USA), **Jeff Bouffard** (Concordia University, Montreal, Canada), **Chantal M Boulanger** (Paris-Cardiovascular Research Center, INSERM, Université Paris Cité, Paris, France), **Paul C Boutros** (Department of Human

20013078, 2024, 2, Downloaded from https://isevjournals.onlinelibrary.wiley.com/doi/10.1002/jev2.12404 by Colorado State University, Wiley Online Library on [09/10/2024]. See the Terms and Conditions (https://onlinelibrary.wiley.com/terms-and-conditions) on Wiley Online Library for rules of use; OA articles are governed by the applicable Creative Commons License

20013078, 2024, 2, Downloaded from https://isevjournals.onlinelibrary.wiley.com/doi/10.1002/jev2.12404 by Colorado State University, Wiley Online Library on [09/10/2024]. See the Terms and Conditions (https://onlinelibrary.wiley.com/terms-and-conditions) on Wiley Online Library for rules of use; OA articles are governed by the applicable Creative Commons License

Genetics, University of California, Los Angeles, Los Angeles, CA, USA; Department of Urology, University of California, Los Angeles, Los Angeles, CA, USA; Jonsson Comprehensive Cancer Center, University of California Los Angeles, Los Angeles, CA, USA), **Oscar Boyadjian** (McGill University, Montreal, Canada), **Anders T Boysen** (Department of Clinical Medicine, Aarhus University, Aarhus, Denmark), **Batuhan T Bozkurt** (Department of Biomedical Engineering, University of California, Davis, Davis, CA, USA), **Kyle P Bramich** (La Trobe Institute for Molecular Science, La Trobe University, Melbourne, Australia), **Fabian Braun** (III. Department of Medicine, University Medical Center Hamburg-Eppendorf, Hamburg, Germany; Hamburg Center for Kidney Health (HCKH), University Medical Center Hamburg-Eppendorf, Hamburg, Germany; Martin Zeitz Centre for Rare Diseases, University Medical Center Hamburg-Eppendorf, Hamburg, Germany), **Rocío del Carmen Bravo-Miana** (Multiple Sclerosis Group, Biogipuzkoa Health Research Institute, San Sebastian, Spain), **Xandra O Breakefield** (Massachusetts General Hospital and Harvard Medical School, Boston, MA, USA), **Santra Brenna** (Neurology Department, Experimental Research in Stroke and Inflammation (ERSI), University Medical Center Hamburg-Eppendorf, Hamburg, Germany), **Kieran Brennan** (School of Biomolecular and Biomedical Science, University College Dublin, Dublin, Ireland; Conway Institute of Biomolecular and Biomedical Research, University College Dublin, Dublin, Ireland), **Meadhbh Á Brennan** (University of Galway, Galway, Ireland), **Koen Breyne** (Molecular Neurogenetics Unit, Department of Neurology, Massachusetts General Hospital, Harvard Medical School, Boston, MA, USA), **Esther M Bridges** (Weatherall Institute of Molecular Medicine, University of Oxford, Oxford, UK), **David R Brigstock** (Center for Clinical and Translational Research, The Research Institute at Nationwide Children's Hospital, Columbus, OH, USA; Department of Surgery, Wexner Medical Center, The Ohio State University, Columbus OH, USA), **Alain R Brisson** (University of Bordeaux, Pessac, France), **Chaya Brodie** (Mina and Everard Goodman Faculty of Life Sciences, Bar-Ilan University, Ramat-Gan, Israel; Institute of Nanotechnology and Advanced Materials (BINA), Bar-Ilan University, Ramat-Gan , Israel; Hermelin Brain Tumor Center, Henry Ford Health, Detroit, MI 48202, USA), **Marco Brucale** (Consiglio Nazionale delle Ricerche—Istituto per lo Studio dei Materiali Nanostrutturati, Bologna, Italy; Consorzio Interuniversitario per lo Sviluppo dei Sistemi a Grande Interfase, Florence, Italy), **Katelyn A Bruno** (University of Florida, Gainesville, FL, USA; Mayo Clinic, Jacksonville, FL, USA), **Cecilia Bucci** (Department of Experimental Medicine, University of Salento, Lecce, Italy), **Shilpa Buch** (University of Nebraska Medical Center, Omaha, NE, USA), **Amy H Buck** (Institute of Immunology & Infection Research, University of Edinburgh, Edinburgh, UK), **Mátyás Bukva** (Laboratory of Microscopic Image Analysis and Machine Learning, Hungarian Research Network (HUN-REN), Biological Research Centre, Szeged, Hungary; Department of Immunology, University of Szeged, Szeged, Hungary; Doctoral School of Interdisciplinary Medicine, University of Szeged, Szeged, Hungary), **Jeff WM Bulte** (Russell H. Morgan Dept. of Radiology and Radiological Science, Division of MR Research, Johns Hopkins University School of Medicine, Baltimore, MD, USA; Cellular Imaging Section and Vascular Biology Program, Institute for Cell Engineering, Johns Hopkins University School of Medicine, Baltimore, MD, USA), **Sandra Buratta** (Department of Chemistry, Biology and Biotechnology, University of Perugia, Perugia, Italy), **Dylan Burger** (Kidney Research Centre, Ottawa Hopsital Research Institute, Ottawa, Canada; Department of Cellular and Molecular Medicine, University of Ottawa, Ottawa, Canada; School of Pharmaceutical Sciences, University of Ottawa, Ottawa, Canada), **Olivier Burgy** (INSERM U1231, Faculty of Medicine and Pharmacy, University of Bourgogne-Franche Comté, Dijon, France), **Julia V Burnier** (Cancer Research Program, Research Institute of the McGill University Health Centre, Montreal, Canada; Gerald Bronfman Department of Oncology, McGill University, Montreal, Canada; Department of Pathology, McGill University, Montreal, Canada), **Kaiping Burrows** (Laureate Institute for Brain Research, Tulsa, OK, USA), **Sara Busatto** (Vascular Biology Program, Boston Children's Hospital, Boston, MA, USA; Department of Surgery, Boston Children's Hospital and Harvard Medical School, Boston, MA, USA), **Benedetta Bussolati** (Department of Molecular Biotechnology and Health Sciences, University of Turin, Turin, Italy), **Edit I Buzas** (Department of Genetics, Cell- and Immunobiology, Semmelweis University, Budapest, Hungary; HCEMM-SU Extracellular Vesicle Research Group, Semmelweis University, Budapest, Hungary; HUN-REN-SU Translational Extracellular Vesicle Research Group, Semmelweis University, Budapest, Hungary), **Krisztina Buzas** (HUN-REN Biological Research Centre, Szeged, Hungary; Department of Immunology, University of Szeged, Szeged, Hungary), **J Brian Byrd** (Department of Medicine, University of Michigan, Ann Arbor, MI, USA), **Albano Cáceres-Verschae** (Department of Oncology-Pathology, Karolinska Institutet, Stockholm, Sweden; Centro de Innovación e Investigación Biomédica, Universidad de Los Andes, Santiago, Chile; Centro de Biología Celular y Biomedicina, Universidad San Sebastián, Santiago, Chile), **Houjian Cai** (University of Georgia, Athens, GA, USA), **Hugo R Caires** (i3S-Institute for Research and Innovation in Health, University of Porto, Porto, Portugal), **Carmen Campos-Silva** (Universidad Loyola, Sevilla, España), **Giovanni Camussi** (Department of Medical Sciences, University of Turin, Turin, Italy), **Paola de Candia** (Dipartimento di Medicina Molecolare e Biotecnologie Mediche, Università degli Studi di Napoli Federico II, Napoli, Italy), **Carmen Carceller** (Department of Dentistry, Faculty of Health Sciences, Universidad Europea de Valencia, Valencia, Spain), **Carmen Fernandez-Becerra** (ISGlobal, Barcelona Institute for Global Health, Hospital Clínic-Universitat de Barcelona, Barcelona, Spain; IGTP, Germans Trias i Pujol Health Research Institute, Badalona, Spain; CIBERINFEC, ISCIII-CIBER de Enfermedades Infecciosas, Instituto de Salud Carlos III, Madrid, Spain), **Randy P Carney** (Department of Biomedical Engineering, University of California, Davis, Davis, CA, USA), **Alexis G Murillo Carrasco** (Centro de Investigação Translacional em Oncologia, Instituto do Câncer do Estado de São Paulo, São Paulo, Brazil; Comprehensive Center for Precision Oncology, Universidade de São Paulo, São Paulo, Brazil), **David RF Carter** (Evox Therapeutics Limited, Oxford, UK; Department of Biological and Medical Sciences, Faculty of Health and Life Sciences, Oxford Brookes

University, Oxford, UK), **Sara Cavallaro** (Krantz Family Center for Cancer Research, Massachusetts General Hospital, Boston, MA, USA; Department of Medicine, Harvard Medical School, Boston, MA, USA), **Serena Cavallero** (Department of Public Health and Infectious Diseases, Sapienza University of Rome, Rome, Italy; Pasteur Institute Italy Fondazione Cenci Bolognetti, Rome,Italy), **Sophie Cavallero** (Département des Effets Biologiques des Rayonnements, Institut de Recherche Biomédicale des Armées (IRBA), Bretigny sur orge, France), **Cristóbal Cerda-Troncoso** (Centro de Biología Celular y Biomedicina, Facultad de Medicina y Ciencia, Universidad San Sebastián, Santiago, Chile; Centro Ciencia & Vida, Fundación Ciencia & Vida, Santiago, Chile; Department of Human Genetics, KU Leuven, Leuven, Belgium), **Richard Chahwan** (Institute of Experimental Immunology, University of Zurich, Zurich, Switzerland; Faculty of Medicine, University of Zurich, Zurich, Switzerland; Faculty of Science, University of Zurich, Zurich, Switzerland), **Renata Chalupská** (AstraZeneca, Mölndal, Sweden), **Lawrence W Chamley** (Department of Obstetrics and Gynaecology, University of Auckland, New Zealand; Hub for Extracellular Investigations, University of Auckland, New Zealand), **Partha K Chandra** (Department of Pharmacology, Tulane University School of Medicine, New Orleans, LA, USA), **Wen-Wei Chang** (Department of Biomedical Sciences, Chung Shan Medical University, Taichung City, Taiwan), **Al Charest** (Department of Medicine, Beth Israel Deaconess Medical Center, Boston, MA, USA; Harvard Medical School, Boston, MA, USA), **Chihchen Chen** (Institute of Nanoengineering and Microsystems, Department of Power Mechanical Engineering, National Tsing Hua University, Hsinchu, Taiwan), **Hao Chen** (Medical School of Nantong University, Nantong, China; Guangzhou Medical University, Guangzhou, China), **Qiang Chen** (Cancer Center, Faculty of Health Sciences, University of Macau, Taipa, Macau SAR, China; MOE Frontier Science Centre for Precision Oncology, University of Macau, Taipa, Macau SAR, China), **Shuai Chen** (Department of Reproduction Biology/Leibniz-Institute for Zoo and Wildlife Research (IZW), Berlin, Germany), **Siyu Chen** (The University of Queensland, Brisbane, Australia; The University of California, Los Angeles, Los Angeles, CA, USA), **Yunxi Chen** (Research Institute of McGill University Health Centre, Montreal, Canada), **Lesley Cheng** (Department of Biochemistry and Chemistry, La Trobe Institute for Molecular Science, La Trobe University, Melbourne, Australia), **Vasiliy S Chernyshev** (National Medical Research Center for Obstetrics, Gynecology and Perinatology named after Academician V.I. Kulakov, Moscow, Russia), **Venkatesh Kumar Chetty** (University Hospital Essen, Essen, Germany), **Sai V Chitti** (Department of Biochemistry, La Trobe Institute for Molecular Science, La Trobe University, Melbourne, Australia), **Ssang-Goo Cho** (Department of Stem Cell and Regenerative Biotechnology, Molecular & Cellular Reprogramming Center and Institute of Advanced Regenerative Science, Konkuk University, Seoul, Republic of Korea; StemExOne Co., Ltd., Seoul, Republic of Korea), **Yoon-Kyoung Cho** (Department of Biomedical Engineering, Ulsan National Institute of Science and Technology, Ulsan, Republic of Korea; Center for Soft and Living Matter, Institute for Basic Science, Ulsan, Republic of Korea), **Byeong Hyeon Choi** (Department of Thoracic and Cardiovascular Surgery, Korea University Guro Hospital, College of Medicine, Korea University, Seoul, Republic of Korea; Image Guided Precision Cancer Surgery Institute, Korea University, Seoul, Republic of Korea), **Somchai Chutipongtanate** (MILCH and Novel Therapeutics Lab, Division of Epidemiology, Department of Environmental and Public Health Sciences, University of Cincinnati College of Medicine, Cincinnati, OH, USA), **Maria Elena Cicardi** (Jefferson Weinberg Center for ALS, Department of Neuroscience, Thomas Jefferson University, Philadelphia, PA, USA), **Anna Cifuentes-Rius** (Exopharm Ltd, Melbourne, Australia), **Alessandra Ciullo** (Smidt Heart Institute, Cedars-Sinai Medical Center, Los Angeles, CA, USA), **Aled Clayton** (Division of Cancer and Genetics, School of Medicine, Cardiff University, Cardiff, UK), **Jacob A Cleary** (Wake Forest School of Medicine, Winston-Salem, NC, USA), **Federico Cocozza** (INSERM U932, Institut Curie Centre de Recherche, PSL Research University, Paris, France), **Emanuele Cocucci** (Division of Pharmaceutics and Pharmacology, College of Pharmacy, The Ohio State University, Columbus, OH, USA; Comprehensive Cancer Center, The Ohio State University, Columbus, OH, USA), **Robert J Coffey** (Epithelial Biology Center, Department of Medicine, Vanderbilt University Medical Center, Nashville, TN, USA), **Federica Collino** (Department of Clinical Sciences and Community Health, University of Milano, Milan, Italy.; Pediatric Nephrology, Dialysis and Transplant Unit, Fondazione IRCCS Ca' Granda-Ospedale Maggiore Policlinico, Milano, Italy), **Federico Colombo** (Division of Pharmaceutics and Pharmacology, College of Pharmacy, The Ohio State University, Columbus, OH, USA), **Pascal Colosetti** (CarMeN Laboratory, UMR INRAE 1397/INSERM 1060, University of Lyon, Lyon, France), **Alvaro Compañ-Bertomeu** (Universitat de Valencia, Valencia, Spain; Farmacia María Luisa Bertomeu Navajas, Valencia, Spain; Universidad Internacional de Valencia, Valencia, Spain), **Julie Constanzo** (Institut de Recherche en Cancérologie de Montpellier (IRCM), INSERM U1194, Nuclear Medicine Department, Institut régional du Cancer de Montpellier (ICM), University of Montpellier, Montpellier, France), **Denis Corbeil** (Biotechnology Center (BIOTEC) and Center for Molecular and Cellular Bioengineering, Technische Universität Dresden, Dresden, Germany; Tissue Engineering Laboratories, Medizinische Fakultät der Technischen Universität Dresden, Dresden, Germany), **Anabela Cordeiro-da-Silva** (Faculty of Pharmacy, University of Porto, Porto, Portugal; Institute for Research and Innovation in Health, University of Porto, Porto, Portugal), **Júlia Costa** (Instituto de Tecnologia Química e Biológica António Xavier, Universidade Nova de Lisboa, Lisbon, Portugal), **Yvonne Couch** (St Hilda's College, University of Oxford, Oxford, UK; Somerville College, University of Oxford, Oxford, UK), **Yvan Courageux** (ICREC Research Program, Health Science Research Institute Germans Trias i Pujol (IGTP), Badalona, Spain; Heart Institute (iCor), Germans Trias i Pujol University Hospital, Badalona, Spain; Department of Biochemistry, Molecular Biology and Biomedicine, Universitat Autònoma de Barcelona (UAB), Barcelona, Spain), **Kelly Coutant** (Faculté de Médecine, Université Laval, Quebec, Canada), **Beth Coyle** (Children's Brain Tumour Research Centre, School of Medicine, University of Nottingham Biodiscovery Institute, University of Nottingham, University Park, Nottingham, UK), **Rossella Crescitelli** (Sahlgrenska Center

20013078, 2024, 2, Downloaded from https://isevjournals.onlinelibrary.wiley.com/doi/10.1002/jev2.12404 by Colorado State University, Wiley Online Library on [09/10/2024]. See the Terms and Conditions (https://onlinelibrary.wiley.com/terms-and-conditions) on Wiley Online Library for rules of use; OA articles are governed by the applicable Creative Commons License

for Cancer Research, Department of Surgery, Institute of Clinical Sciences, Sahlgrenska Academy, University of Gothenburg, Gothenburg, Sweden; Wallenberg Centre for Molecular and Translational Medicine, Institute of Clinical Sciences, Sahlgrenska Academy, University of Gothenburg, Gothenburg, Sweden), **Marina Cretich** (Istituto di Scienze e Tecnologie Chimiche "Giulio Natta", Consiglio Nazionale delle Ricerche, Milan, Italy), **André Cronemberger-Andrade** (MSC—Matière et Systèmes Complexes/CNRS, Université Paris Cité, Paris, France), **Rachel E Crossland** (Translational and Clinical Research Institute, Faculty of Medical Science, Newcastle University, Newcastle upon Tyne, UK), **Marcela A Cucher** (Department of Microbiology, School of Medicine, University of Buenos Aires, Buenos Aires, Argentina; Institute of Research on Microbiology and Medical Parasitology (IMPaM, UBA-CONICET), University of Buenos Aires, Buenos Aires, Argentina.), **Malgorzata Czystowska-Kuzmicz** (Department of Biochemistry, Medical University of Warsaw, Warsaw, Poland), **Pasquale D'Acunzo** (Center for Dementia Research, Nathan S. Kline Institute for Psychiatric Research, Orangeburg, NY, USA; Department of Psychiatry, New York University Grossman School of Medicine, New York, NY, USA), **Igea D'Agnano** (Institute for Biomedical Technologies-CNR, Segrate, Italy), **Vito G D'Agostino** (Department of Cellular, Computational and Integrative Biology (CIBIO), University of Trento, Trento, Italy), **Gisela D'Angelo** (Institut Curie, PSL University, Paris, France; CNRS UMR144, Paris, France), **Daniele D'Arrigo** (Laboratoire Matière et Systèmes Complexes , CNRS UMR 7057, Université Paris Cité, Paris, France; Abbelight, Cachan, France), **Crislyn D'Souza-Schorey** (Department of Biological Sciences, University of Notre Dame, Notre Dame, IN, USA), **Raghubendra S Dagur** (SciBiz consulting, LLC, Sacramento, CA, USA), **Kirsty M Danielson** (University of Otago, Wellington, New Zealand), **Saumya Das** (Massachusetts General Hospital, Boston, MA, USA), **Thibaud Dauphin** (Oniris VetAgroBio Nantes, INRAE, IECM, Nantes, France), **Sean M Davidson** (University College London, London, UK), **Owen G Davies** (School of Sport Exercise and Health Sciences, Loughborough University, Loughborough, UK), **Rebecca L Davies** (Centre for Regenerative Medicine Research, School of Medicine, Keele University, Keele, UK; Robert Jones and Agnes Hunt Orthopaedic Hospital, Oswestry, UK), **Chelsea N Davis** (Aberystwyth University, Aberystwyth, UK), **Gagan Deep** (Department of Cancer Biology, Wake Forest University School of Medicine, Winston-Salem, NC, USA; Sticht Center for Healthy Aging and Alzheimer's Prevention, Wake Forest School of Medicine, Winston-Salem, North Carolina, USA; Atirum Health Wake Forest Baptist Comprehensive Cancer Center, Wake Forest University School of Medicine, Winston-Salem, North Carolina, USA), **Jonathan Degosserie** (Department of Laboratory Medicine, CHU UCL Namur, Université Catholique de Louvain, Yvoir, Belgium; Namur Molecular Tech, CHU UCL Namur, Université Catholique de Louvain, Yvoir, Belgium; Namur Research Institute of Life Sciences, CHU UCL Namur, Université de Namur, Yvoir, Belgium), **Mats Van Delen** (Laboratory of Experimental Hematology, Vaccine and Infectious Disease Institute (Vaxinfectio), University of Antwerp, Antwerp, Belgium; Health Department, Flemish Institute for Technological Research (VITO), Mol, Belgium), **Vatsal Deliwala** (Australian Institute for Bioengineering and Nanotechnology, The University of Queensland, Brisbane, Australia; Centre for Advanced Imaging, The University of Queensland, Brisbane, Australia; School of Chemical Engineering, The University of Queensland, Brisbane, Australia), **Elizabeth R Dellar** (Nuffield Department of Clinical Neurosciences, John Radcliffe Hospital, University of Oxford, Oxford, UK), **Jan Van Deun** (Department of Dermatology, Universitätsklinikum Erlangen, Friedrich-Alexander-Universität Erlangen-Nürnberg, Erlangen, Germany), **Apurba Dev** (Uppsala University, Uppsala, Sweden; KTH Royal Institute of Technology, Stockholm, Sweden), **Sarah Deville** (Ghent University, Ghent, Belgium), **Andrew Devitt** (School of Biosciences, College of Health & Life Sciences, Aston University, Birmingham, UK), **Bert Dhondt** (Department of Human Structure and Repair, Ghent University, Ghent, Belgium), **Lothar C Dieterich** (European Center of Angioscience, Medical Faculty Mannheim, Heidelberg University, Mannheim, Germany), **Dirk P Dittmer** (Lineberger Comprehensive Cancer Center, Department of Microbiology and Immunology, The University of North Carolina at Chapel Hill, Chapel Hill, NC, USA), **Brian Dobosh** (Department of Pediatrics, Emory University School of Medicine, Atlanta, GA, USA; Center for CF and Airways Disease Research, Children's Healthcare of Atlanta, Atlanta, GA, USA), **Gabriella Dobra** (Laboratory of Microscopic Image Analysis and Machine Learning, Hungarian Research Network (HUN-REN), Biological Research Centre, Szeged, Hungary; Department of Immunology, University of Szeged, Szeged, Hungary), **Navneet Dogra** (Department of Pathology, Molecular and Cell-Based Medicine, Icahn Genomics Institute, New York, NY, USA), **Eisuke Dohi** (Department of Mental Disorder Research, National Institute of Neuroscience, National Center of Neurology and Psychiatry, Tokyo, Japan), **Vincenza Dolo** (Department of Life, Health and Environmental Sciences, University of L'Aquila, L'Aquila, Italy), **Timothy V Domashevich** (Departments of Ophthalmology, University of Colorado Anschutz Medical Campus, Aurora, CO, USA), **Massimo Dominici** (Laboratory of Cellular Therapy, Division of Oncology, Department of Medical and Surgical Sciences for Children & Adults, University of Modena and Reggio Emilia, Modena, Italy; Division of Oncology, Department of Oncology and Hematology, University Hospital of Modena, Modena, Italy), **Liang Dong** (Department of Urology, Renji Hospital, Shanghai Jiao Tong University School of Medicine, Shanghai, China), **Etienne Doré** (Centre de Recherche du Centre Hospitalier Universitaire de Québec, Université Laval, Quebec, Canada; Centre de Recherche ARThrite (Arthrite Recherche Traitements) de l'Université Laval, Quebec, Canada), **Rebecca A Dragovic** (Nuffield Department of Women's and Reproductive Health, Oxford Endometriosis CaRe Centre, University of Oxford, Oxford, UK), **Tom AP Driedonks** (Department CDL Research, University Medical Center Utrecht, Utrecht, The Netherlands), **Lila Drittanti** (AGS Therapeutics, Paris, France; Markets & Listing, Paris, France), **Marvin Droste** (Department of Pediatrics II, Pediatric Nephrology, University Hospital Essen, University of Duisburg-Essen, Essen, Germany), **Wei Duan** (Deakin University, Geelong, Australia), **Esmahan Durmaz** (School of Optometry and Vision Sciences, Cardiff University, Cardiff, UK), **Suman Dutta** (Nuffield Department of Clinical Neurosciences, John Radcliffe Hospital, University of Oxford,

20013078, 2024, 2, Downloaded from https://isevjournals.onlinelibrary.wiley.com/doi/10.1002/jev2.12404 by Colorado State University, Wiley Online Library on [09/10/2024]. See the Terms and Conditions (https://onlinelibrary.wiley.com/terms-and-conditions) on Wiley Online Library for rules of use; OA articles are governed by the applicable Creative Commons License

Oxford, UK; Kavli Institute for Nanoscience Discovery, Dorothy Crowfoot Hodgkin Building, University of Oxford, Oxford, UK), **Takanori Eguchi** (Department of Dental Pharmacology, Faculty of Medicine, Dentistry and Pharmaceutical Sciences, Okayama University, Okayama, Japan; Advanced Research Center for Oral and Craniofacial Sciences, Okayama University, Okayama, Japan), **Ramon M Eichenberger** (Institute of Chemistry and Biotechnology, Zurich University of Applied Sciences, Wädenswil, Switzerland), **Erez Eitan** (NeuroDex INC, Natick, MA, USA), **Karin Ekström** (Sahlgrenska Center for Cancer Research, Department of Surgery, Institute of Clinical Sciences, Sahlgrenska Academy, University of Gothenburg, Gothenburg, Sweden; Wallenberg Centre for Molecular and Translational Medicine, Institute of Clinical Sciences, Sahlgrenska Academy, University of Gothenburg, Gothenburg, Sweden), **Maria Eldh** (Division of Immunology and Allergy, Department of Medicine Solna, Karolinska Institutet, Stockholm, Sweden), **Celine Elie-Caille** (FEMTO-ST Institute, CNRS UMR-6174, Université de Bourgogne Franche-Comté, Besançon, France), **Agustin Enciso-Martinez** (Ten Dijke/Chemical Signaling Laboratory, Department of Cell and Chemical Biology, Leiden University Medical Center and Oncode Institute, Leiden, The Netherlands; Department of Biomedical Engineering and Physics, Amsterdam University Medical Centers, Amsterdam, The Netherlands; Amsterdam Vesicle Center, Amsterdam University Medical Centers, Location AMC, University of Amsterdam, Amsterdam, The Netherlands), **Uta Erdbrügger** (University of Virginia Health System, Charlottesville, VA, USA), **Rezvan Esmaeili** (Genetics Department, Breast Cancer Research Center, Motamed Cancer Institute, Academic Center for Education Culture and Research, Tehran, Iran; Department of Experimental Radiation Oncology, The University of Texas MD Anderson Cancer Center, Houston, TX, USA), **Camille Ettelaie** (Biomedical Science, Hull-York Medical School, Hull, UK), **András I Försönits** (Department of Genetics, Cell- and Immunobiology, Semmelweis University, Budapest, Hungary), **Muller Fabbri** (Center for Cancer and Immunology Research, Children's National Hospital, Washington, DC, USA; GW Cancer Center, George Washington University, Washington, DC, USA), **Marco Falasca** (Department of Medicine and Surgery, University of Parma, Parma, Italy; Metabolic Signalling Group, Curtin Medical School, Curtin Health and Innovation Research Institute, Curtin University, Bentley, Australia), **Juan M Falcon-Perez** (Exosomes Laboratory, Center for Cooperative Research in Biosciences, Basque Research and Technology Alliance, Derio, Spain; Metabolomics Platform, Center for Cooperative Research in Biosciences, Basque Research and Technology Alliance, Derio, Spain; IKERBASQUE, Basque Foundation for Science, Bilbao, Spain), **Hongkuan Fan** (Department of Pathology and Laboratory Medicine, Medical University of South Carolina, Charleston, USA), **Farah Fatima** (Chalmers University of Technology, Gothenburg, Sweden), **Vroniqa Ku'ulei-Lyn Faustino** (Department of Molecular Medicine, Beckman Research Institute, City of Hope Comprehensive Cancer Center, Duarte, CA, USA), **Alireza Fazeli** (Estonian University of Life Sciences, Tartu, Estonia; University of Tartu, Tartu, Estonia; University of Sheffield, Sheffield, UK), **María Fernández-Rhodes** (Biomedical Research Institute of Lleida Dr. Pifarré Foundation (IRBLLEIDA), University Hospital Arnau de Vilanova (HUAV), Lleida, Spain; Department of Medical Basic Sciences, University of Lleida (UdL), Lleida, Spain), **Christopher Fernandez-Prada** (Faculty of Veterinary Medicine, Université de Montréal, Montreal, Canada), **Mariola J Ferraro** (Department of Microbiology and Cell Science, University of Florida, Gainesville, FL, USA), **Joao N Ferreira** (Avatar Biotechnologies for Oral Health and Health Longevity Research Unit, Faculty of Dentistry, Chulalongkorn University, Bangkok, Thailand; Department of Research Affairs, Faculty of Dentistry, Chulalongkorn University, Bangkok, Thailand), **Rafaela F Ferreira** (Institute of Animal Science and Physiology, University of Bonn, Bonn, Germany), **Leandra K Figueroa-Hall** (Laureate Institute for Brain Research, Tulsa, OK, USA; The University of Tulsa, Tulsa, OK, USA), **Aliosha I Figueroa-Valdés** (IMPACT, Center of Interventional Medicine for Precision and Advanced Cellular Therapy, Santiago, Chile; Laboratory of Nano-Regenerative Medicine, Centro de Investigación e Innovación Biomédica (CiiB), Universidad de los Andes, Santiago, Chile; Cells for Cells, Santiago, Chile), **Paolo V Fioretti** (University of Trento, Trento, Italy), **Sabine Flenady** (StemXo, Melbourne, Australia; Melbourne University, Melbourne, Australia; Central Queensland University, Norman Gardens, Australia), **Miguel Flores-Bellver** (CellSight Ocular Stem Cell and Regeneration Program, Department of Ophthalmology, Sue Anschutz-Rodgers Eye Center, University of Colorado Anschutz Medical Campus, Aurora, CO, USA), **Ellis K Fok** (School of Biomedical Sciences, Faculty of Medicine, The Chinese University of Hong Kong, Hong Kong SAR; Sichuan University-The Chinese University of Hong Kong Joint Laboratory for Reproductive Medicine, West China Second University Hospital, Chengdu, China; School of Biomedical Sciences Core Laboratory, Shenzhen Research Institute, The Chinese University of Hong Kong, Shenzhen, China), **Pamali Fonseka** (Department of Biochemistry, La Trobe Institute for Molecular Science, La Trobe University, Melbourne, Australia), **Karen Forbes** (Leeds Institute of Cardiovascular and Metabolic Medicine, University of Leeds, Leeds, UK), **Verity J Ford** (Clinical Center, National Institutes of Health, Bethesda, MD, USA), **Cristina Fornaguera** (Grup d'Enginyeria de Materials (Gemat), Institut Químic de Sarrià (IQS), Universitat Ramon Llull (URL), Barcelona, Spain), **Dorian Forte** (Department of Medical and Surgical Sciences, Institute of Hematology "L. and A. Seràgnoli", University of Bologna, Bologna, Italy), **Stefano Forte** (IOM Ricerca, Viagrande, Italy; Mediterranean Institute of Oncology, Viagrande, Italy), **Orazio Fortunato** (Fondazione IRCCS Istituto Nazionale dei Tumori, Milan, Italy), **Jeffrey L Franklin** (Department of Medicine, Gastroenterology, Vanderbilt University Medical Center, Nashville, TN, USA; Department of Cell and Developmental Biology, Vanderbilt University, Nashville, TN, USA; Epithelial Biology Center, Department of Medicine, Vanderbilt University Medical Center, Nashville, TN, USA), **Daniela Freitas** (i3S-Institute for Research and Innovation in Health, University of Porto, Porto, Portugal; IPATIMUP-Institute of Molecular Pathology and Immunology, University of Porto, Porto, Portugal), **Annie Frelet-Barrand** (Institute FEMTO-ST, Université de Franche-Comté, CNRS, Besançon, France), **Qing-Ling Fu** (Otorhinolaryngology Hospital, The First Affiliated Hospital, Sun Yat-sen University, Guangzhou, China; Extracellular Vesicle Research and

20013078, 2024, 2, Downloaded from https://isevjournals.onlinelibrary.wiley.com/doi/10.1002/jev2.12404 by Colorado State University, Wiley Online Library on [09/10/2024]. See the Terms and Conditions (https://onlinelibrary.wiley.com/terms-and-conditions) on Wiley Online Library for rules of use; OA articles are governed by the applicable Creative Commons License

20013078, 2024, 2, Downloaded from https://isevjournals.onlinelibrary.wiley.com/doi/10.1002/jev2.12404 by Colorado State University, Wiley Online Library on [09/10/2024]. See the Terms and Conditions (https://onlinelibrary.wiley.com/terms-and-conditions) on Wiley Online Library for rules of use; OA articles are governed by the applicable Creative Commons License

Clinical Translational Center, The First Affiliated Hospital, Sun Yat-sen University, Guangzhou, China), **Yu Fujita** (The Jikei University Shool of Medicine, Tokyo, Japan), **Kathrin Gärtner** (Eximmium Biotechnologies GmbH, Munich, Germany), **André Görgens** (Department of Laboratory Medicine, Karolinska Institutet, Stockholm, Sweden; Department of Cellular Therapy and Allogeneic Stem Cell Transplantation (CAST), Karolinska University Hospital Huddinge and Karolinska Comprehensive Cancer Center, Stockholm, Sweden; Institute for Transfusion Medicine, University Hospital Essen, University of Duisburg-Essen, Essen, Germany), **Áurea M Gabriel** (Institute of Hygiene and Tropical Medicine, NOVA University of Lisbon, Lisbon, Portugal; Institute of Biological Sciences, Federal University of Pará, Belém, Brazil), **Martina Gabrielli** (CNR Institute of Neuroscience, Vedano al Lambro, Italy), **Susanne Gabrielsson** (Division of Immunology and Allergy, Department of Medicine Solna, Karolinska Institutet, Stockholm, Sweden; Center for Molecular Medicine, Karolinska University Hospital, Stockholm, Sweden; Department of Clinical Immunology and Transfusion Medicine, Karolinska University Hospital, Stockholm, Sweden), **Alicia Galinsoga** (Department of Genetics, Cell- and Immunobiology, Semmelweis University, Budapest, Hungary), **Andrea Galisova** (Institute for Clinical and Experimental Medicine, Prague, Czech Republic), **Teena KJB Gamage** (Department of Obstetrics and Gynaecology, University of Auckland, New Zealand; Department of Physiology, Faculty of Medical and Health Sciences, The University of Auckland, Auckland, New Zealand), **Yingtang Gao** (Tianjin Key Laboratory of Extracorporeal Life Support for Critical Diseases, Tianjin Institute of Hepatobiliary Disease, Nankai University Affiliated the Third Center Hospital, Tianjin, China), **Marta Garcia-Contreras** (MGH/Harvard Medical School, Boston, MA, USA), **M Madhy Garcia Garcia** (University of California Irvine, Irvine, CA, USA), **Maria Noé Garcia** (Institute of Studies of the Humoral Immunity (IDEHU), National Council of Science and Technology (CONICET), University of Buenos Aires, Buenos Aires, Argentina), **Ernesto Gargiulo** (Department of Hematology, Rigshospitalet, Copenhagen University Hospital, Copenhagen, Denmark), **Hernán González-King Garibotti** (Research and Early Development, Cardiovascular, Renal and Metabolism, BioPharmaceuticals R&D, AstraZeneca, Mölndal, Sweden), **Margaret M Mc Gee** (School of Biomolecular and Biomedical Science, University College Dublin, Dublin, Ireland; Conway Institute of Biomolecular and Biomedical Research, University College Dublin, Dublin, Ireland), **Géraldine C Genard** (Division of Biomedical Physics in Radiation Oncology, German Cancer Research Center (DKFZ), Heidelberg, Germany), **Fabiana Geraci** (Department of Biological, Chemical and Pharmaceutical Sciences and Technologies, University of Palermo, Palermo, Italy), **Jamal Ghanam** (Department of Pediatrics III, University Hospital Essen, Essen, Germany), **Subhadip Ghatak** (McGowan Center for Regenerative Medicine, Department of Surgery, University of Pittsburgh, Pittsburgh, PA, USA), **Mahlegha Ghavami** (Pathology Department, Dalhousie University, Halifax, Canada), **Raluca E Ghebosu** (Australian Institute for Bioengineering and Nanotechnology, The University of Queensland, Brisbane, Australia), **Yong Song Gho** (Pohang University of Science and Technology, Pohang, Republic of Korea), **Sayam Ghosal** (Department of Genetics, Cell- and Immunobiology, Semmelweis University, Budapest, Hungary; HCEMM-SU Extracellular Vesicle Research Group, Semmelweis University, Budapest, Hungary), **Georgios Giamas** (Department of Biochemistry and Biomedicine, School of Life Sciences, University of Sussex, Brighton, UK), **Bernd Giebel** (Institute for Transfusion Medicine, University Hospital Essen, University of Duisburg-Essen, Essen, Germany), **Caroline Gilbert** (Division of Infectious and Immune Diseases, CHU de Quebec Research Center, Quebec, Canada; Department of Microbiology, Infectious Disease and Immunology, Faculty of Medicine, Université Laval, Quebec, Canada), **Mario Gimona** (Paracelsus Medical University, Salzburg, Austria), **Henrique Girão** (Coimbra Institute for Clinical and Biomedical Research (iCBR), Faculty of Medicine, University of Coimbra, Coimbra, Portugal; Center for Innovative Biomedicine and Biotechnology, University of Coimbra, Coimbra, Portugal; Academic and Clinical Center of Coimbra, Coimbra, Portugal), **Ilaria Giusti** (Department of Life, Health and Environmental Sciences, University of L'Aquila, L'Aquila, Italy), **Evan A Gizzie** (Meso Scale Diagnostics, LLC., Rockville, MD, USA), **Sofija Glamočlija** (Institute for the Application of Nuclear Energy, Belgrade, Serbia), **Sarah E Glass** (Vanderbilt University Medical Center, Nashville, TN, USA), **Jessica Gobbo** (Department of Medical Oncology, Centre Georges-François Leclerc, Dijon, France; INSERM UMR 1231, «Equipe labellisée» Ligue National contre le Cancer and Laboratoire d'Excellence LipSTIC, Dijon, France; University of Bourgogne, Dijon, France), **Deborah CI Goberdhan** (Nuffield Department of Women's and Reproductive Health, University of Oxford, Women's Centre, John Radcliffe Hospital, Oxford, UK), **Nihar Godbole** (Translational Extracellular Vesicles in Obstetrics and Gynae-Oncology Group, University of Queensland Centre for Clinical Research, Faculty of Medicine, Royal Brisbane and Women's Hospital, The University of Queensland, Brisbane, Australia), **Jacky G Goetz** (Tumor Biomechanics, INSERM UMR_S1109, Strasbourg, France; University of Strasbourg, Strasbourg, France; Equipe Labellisée Ligue Contre le Cancer), **Olesia Gololobova** (Department of Molecular and Comparative Pathobiology, Johns Hopkins University School of Medicine, Baltimore, MD, USA; EV Core Facility "EXCEL", Institute for Basic Biomedical Sciences, Johns Hopkins University School of Medicine, Baltimore, MD, USA), **Manuel Gomez-Florit** (Health Research Institute of the Balearic Islands (IdISBa), Palma, Spain; Cell Therapy and Tissue Engineering Group, Research Institute on Health Sciences (IUNICS), University of the Balearic Islands, Palma, Spain), **Jenifer Pendiuk Goncalves** (Australian Institute for Bioengineering and Nanotechnology, The University of Queensland, Brisbane, Australia), **Cansu Gorgun** (School of Pharmacy and Biomolecular Sciences, Royal College of Surgeons in Ireland, Dublin, Ireland; Trinity Centre for Biomedical Engineering, Trinity Biomedical Sciences Institute, Trinity College, Dublin, Ireland; Advanced Materials and Bioengineering Research Centre, Trinity College Dublin and Royal College of Surgeons in Ireland, Dublin, Ireland), **Alessandro Gori** (Institute of Chemical Sciences and Technologies, National Research Council of Italy, Milan, Italy), **Sabina Gorska** (Hirszfeld Institute of Immunology and Experimental Therapy, Polish Academy of Sciences, Wroclaw, Poland), **Michael W Graner** (University

of Colorado Anschutz Medical Campus, Aurora, CO, USA), **Georges E Grau** (Vascular Immunology Unit, School of Medical Sciences, The University of Sydney, Sydney, Australia; Sydney Nano Institute, The University of Sydney, Australia; Sydney Infectious Diseases Institute, The University of Sydney, Australia), **Laura Grech** (Faculty of Medicine and Surgery, University of Malta, Msida, Malta), **David W Greening** (Baker Heart & Diabetes Institute, Melbourne, Australia; La Trobe University, Melbourne, Australia; The University of Melbourne, Melbourne, Australia), **Rüdiger M Groß** (Institute of Molecular Virology, Ulm University Medical Center, Ulm, Germany), **Julia C Gross** (Institute of Molecular Medicine, Health and Medical University, Potsdam, Germany), **Jens Gruber** (Curexsys GmbH, Goettingen, Germany), **Alice Gualerzi** (IRCCS Fondazione Don Carlo Gnocchi Onlus, Milan, Italy), **Dominic Guanzon** (The University of Queensland, Brisbane, Australia), **Johann M Gudbergsson** (Department of Biomedicine, Aarhus University, Aarhus, Denmark), **Coralie L Guerin** (Cytometry Platform, Institut Curie, Paris, France; Extracellular Vesicles Platform, Institut Curie, Paris, France), **Flora Guerra** (Department of Biological and Environmental Sciences and Technologies, Università del Salento, Lecce, Italy), **Maria I Guillén** (Faculty of Health Sciences, Cardenal Herrera CEU University, Alfara del Patriarca, Valencia, Spain; Interuniversity Research Institute for Molecular Recognition and Technological Development (IDM), University of Valencia, Polytechnic University of Valencia, Valencia, Spain), **Vikramsingh Gujar** (Oklahoma State University Center for Health Sciences, Tulsa, OK, USA), **Wei Guo** (Department of Biology, University of Pennsylvania, Philadelphia, PA, USA), **Veer Bala Gupta** (Faculty of Heath, School of Medicine, Deakin University, Geelong, Australia), **Vivek Kumar Gupta** (Faculty of Medicine, Health and Human Sciences, Macquarie Medical School, Macquarie University, Sydney, Australia; School of Life Sciences, Pooja Bhagwat Memorial Mahajana Education Centre, Mysore, Karnataka, India), **Dakota Gustafson** (Department of Laboratory Medicine & Pathobiology, University of Toronto, Toronto, ON, Canada; Faculty of Health Sciences, Queen's University, Kingston, ON, Canada), **Edina Gyukity-Sebestyén** (Laboratory of Microscopic Image Analysis and Machine Learning, Hungarian Research Network (HUN-REN), Biological Research Centre, Szeged, Hungary; Department of Immunology, Albert Szent-Györgyi Medical School, Faculty of Science and Informatics, University of Szeged, Szeged, Hungary), **Patrick Hölker** (University Hospital Cologne, Cologne, Germany), **Mangesh D Hade** (Nationwide Children's Hospital, Columbus, OH, USA; The Ohio State University, Columbus, OH, USA), **Daniel W Hagey** (Department of Laboratory Medicine, Karolinska Institutet, Stockholm, Sweden; Department of Cellular Therapy and Allogeneic Stem Cell Transplantation (CAST), Karolinska University Hospital Huddinge and Karolinska Comprehensive Cancer Center, Stockholm, Sweden), **Chungmin Han** (Wyss Institute for Biologically Inspired Engineering, Harvard University, Boston, MA, USA; Brigham and Women's Hospital, Boston, MA, USA; Harvard Medical School, Boston, MA, USA), **Pingping Han** (School of Dentistry, The University of Queensland, Brisbane, Australia), **Rikinari Hanayama** (WPI Nano Life Science Institute (NanoLSI), Kanazawa University, Kanazawa, Japan; Department of Immunology, Graduate School of Medical Sciences, Kanazawa University, Kanazawa, Japan), **Aase Handberg** (Department of Clinical Biochemistry, Aalborg University Hospital, Aalborg, Denmark; Department of Clinical Medicine, Aarhus University, Aarhus, Denmark), **Edveena Hanser** (Department of Biomedicine, University Hospital Basel, Basel, Switzerland; Department of Biomedicine, University of Basel, Basel, Switzerland), **Masako Harada** (Department of Biomedical Engineering, Michigan State University, East Lansing, MI, USA; Institute for Quantitative Health Science and Engineering (IQ), Department of Pharmacology & Toxicology, Michigan State University, East Lansing, MI, USA), **Maria Harmati** (Laboratory of Microscopic Image Analysis and Machine Learning, Hungarian Research Network (HUN-REN), Biological Research Centre, Szeged, Hungary; Department of Immunology, University of Szeged, Szeged, Hungary), **Adrian L Harris** (Department of Oncology, University of Oxford, Oxford, UK), **Paul Harrison** (Institute of Inflammation and Ageing, University of Birmingham, Birmingham, UK), **Rane A Harrison** (Hemab Therapeutics, Cambridge, MA, USA), **Norman J Haughey** (Departments of Neurology and Psychiatry, Johns Hopkins University School of Medicine, Baltimore, MD, USA), **Paul A Haynes** (School of Natural Sciences, Macquarie University, Sydney, Australia), **Mei He** (Department of Pharmaceutics, College of Pharmacy, University of Florida, Gainesville, FL, USA; University of Florida Health Cancer Center, Gainesville, FL, USA), **Hargita Hegyesi** (Department of Genetics, Cell- and Immunobiology, Semmelweis University, Budapest, Hungary), **An Hendrix** (Laboratory of Experimental Cancer Research, Department of Human Structure and Repair, Ghent University, Ghent, Belgium; Cancer Research Institute Ghent, Ghent, Belgium), **Martijn JC van Herwijnen** (Department of Biomolecular Health Sciences, Faculty of Veterinary Medicine, Utrecht University, Utrecht, The Netherlands), **Andrew F Hill** (Institute for Health and Sport, Victoria University, Melbourne, Australia), **Colin L Hisey** (Department of Biomedical Engineering, The Ohio State University, Columbus, OH, USA; Department of Chemical and Biomolecular Engineering, The Ohio State University, Columbus, OH, USA; Northwestern University, Department of Biomedical Engineering, Evanston, IL, USA), **Fred H Hochberg** (Massachusetts General Hospital, Boston, MA, USA (retired); Scintillon Institute, San Diego, CA, USA; PIOMA, Sarasota, FL, USA), **Esther NM Nolte-'t Hoen** (Department of Biomolecular Health Sciences, Faculty of Veterinary Medicine, Utrecht University, Utrecht, The Netherlands), **Marija Holcar** (Institute for Biochemistry and Molecular Genetics, Faculty of Medicine, University of Ljubljana, Ljubljana, Slovenia), **Beth Holder** (Imperial College London, London, UK), **Wolfgang Holnthoner** (Ludwig Boltzmann Institute for Traumatology, The Research Centre in Cooperation with AUVA, Vienna, Austria; Austrian Cluster for Tissue Regeneration, Vienna, Austria), **Harry Holthofer** (Finnish Institute of Molecular Medicine (FIMM), University of Helsinki, Helsinki, Finland), **D Craig Hooper** (Thomas Jefferson University, Philadelphia, PA, USA), **Elham Hosseini-Beheshti** (Asbestos and Dust Diseases Research Institute, Sydney, Australia), **Baharak Hosseinkhani** (Laboratory of Angiogenesis and Vascular Metabolism, Center for Cancer Biology (CCB), VIB and Department of Oncology, Leuven Cancer Institute (LKI), KU Leuven, Leuven, Belgium), **Jane**

20013078, 2024, 2, Downloaded from https://isevjournals.onlinelibrary.wiley.com/doi/10.1002/jev2.12404 by Colorado State University, Wiley Online Library on [09/10/2024]. See the Terms and Conditions (https://onlinelibrary.wiley.com/terms-and-conditions) on Wiley Online Library for rules of use; OA articles are governed by the applicable Creative Commons License

Howard (UCD School of Medicine, College of Health, and Agricultural Sciences (CHAS), University College Dublin, Dublin, Ireland; UCD Conway Institute of Biomolecular and Biomedical Research, University College Dublin, Dublin, Ireland), **Kathryn L Howe** (University Health Network, Toronto, Canada; University of Toronto, Toronto, Canada; Peter Munk Cardiac Centre, Toronto, Canada), **Nicholas R Hoyle** (ClinBioConsulting FRG, Eschenlohe, Germany), **Jiri Hrdy** (Institute of Immunology and Microbiology, First Faculty of Medicine, Charles University and General University Hospital in Prague, Prague, Czech Republic), **Guoku Hu** (University of Nebraska Medical Center, Omaha, NE, USA), **Yiyao Huang** (Department of Molecular and Comparative Pathobiology, Johns Hopkins University School of Medicine, Baltimore, MD, USA; Department of Laboratory Medicine, Nanfang Hospital, Southern Medical University, Guangzhou, China), **Veronica Huber** (Translational Immunology Unit, Fondazione IRCCS Istituto Nazionale dei Tumori, Milan, Italy), **Samo Hudoklin** (Institute of Cell Biology, Faculty of Medicine, University of Ljubljana, Ljubljana, Slovenia), **Antonia Hufnagel** (Novo Nordisk Foundation Center for Basic Metabolic Research, Faculty of Health and Medical Sciences, University of Copenhagen, Copenhagen, Denmark), **Mark D Hulett** (Department of Biochemistry and Chemistry, La Trobe Institute for Molecular Science, La Trobe University, Melbourne, Australia), **Stuart Hunt** (The University of Sheffield, Sheffield, UK), **Vincent Hyenne** (INSERM UMR_S1109, Tumor Biomechanics, Strasbourg, France; University of Strasbourg, Strasbourg, France; CNRS SNC5055, Strasbourg, France), **Emilio Di Ianni** (Department of Neurology, Massachusetts General Hospital, Harvard Medical School, Boston, MA, USA), **Dalila Iannotta** (School of Chemical Engineering, The University of Queensland, Brisbane, Australia), **Ahmed GE Ibrahim** (Smidt Heart Institute, Cedars-Sinai Medical Center, Los Angeles, CA, USA), **Sherif A Ibrahim** (AviceRNA, Konya, Turkey; Department of Pediatrics and Human Development, Michigan State University, East Lansing, MI, USA; Department of Histology and Cell Biology, Faculty of Medicine, Mansoura University, Mansoura, Egypt), **Seiko Ikezu** (Department of Neuroscience, Mayo Clinic Florida, Jacksonville, FL, USA), **Tsuneya Ikezu** (Department of Neuroscience, Mayo Clinic Florida, Jacksonville, FL, USA), **Hyungsoon Im** (Center for Systems Biology, Massachusetts General Hospital, Boston, MA, USA; Department of Radiology, Massachusetts General Hospital, Boston, MA, USA), **Jameel M Inal** (London Metropolitan University, School of Human Sciences, Cell Communication in Disease Pathology, London, UK; University of Hertfordshire, School of Life and Medical Sciences, Biosciences Research Group, Hatfield, UK), **Aleksandra Inic-Kanada** (Institute of Specific Prophylaxis and Tropical Medicine, Center for Pathophysiology, Infectiology, and Immunology, Medical University of Vienna, Vienna, Austria), **Marit Inngjerdingen** (Department of Pharmacology, University of Oslo, Oslo, Norway), **Yasuo Inoshima** (Gifu University, Gifu, Japan), **Alexander R Ivanov** (Barnett Institute of Chemical and Biological Analysis, Department of Chemistry and Chemical Biology, Northeastern University, Boston, MA, USA), **Alena Ivanova** (Discovery Biology, Discovery Sciences, BioPharmaceuticals R&D, AstraZeneca, Mölndal, Sweden), **Elena Izquierdo** (Departamento de Ciencias Médicas Básicas, Instituto de Medicina Molecular Aplicada (IMMA) Nemesio Díez, Facultad de Medicina, Universidad San Pablo-CEU, CEU Universities, Madrid, Spain), **Malene Møller Jørgensen** (Department of Clinical Immunology, Aalborg University Hospital, Aalborg, Denmark; Department of Clinical Medicine, Aalborg University, Aalborg, Denmark), **Hannah K Jackson** (Pain Centre Versus Arthritis, School of Life Sciences, Queen's Medical Centre, University of Nottingham, Nottingham, UK; Children's Brain Tumour Research Centre, Biodiscovery Institute, University of Nottingham, Nottingham, UK), **Soren Jacobsen** (COPEACT, Department of Rheumatology, Rigshospitalet, Copenhagen, Denmark; Department of Clinical Medicine, University of Copenhagen, Denmark), **Fernanda Jadue** (Universidad de Los Andes, Santiago, Chile; Universidad del Desarrollo, Santiago, Chile), **Naureen Javeed** (Mayo Clinic, Rochester, MN, USA), **Steven M Jay** (University of Maryland, College Park, MD, USA), **Muthuvel Jayachandran** (Mayo Clinic College of Medicine and Science, Rochester, MN, USA), **Migara K Jayasinghe** (Department of Pharmacology, Yong Loo Lin School of Medicine, National University of Singapore, Singapore), **Guido Jenster** (Erasmus Medical Center, Department of Urology, Rotterdam, The Netherlands), **Dennis K Jeppesen** (Department of Medicine, Vanderbilt University Medical Center, Nashville, TN, USA), **Carmen Jerónimo** (Cancer Biology and Epigenetics Group, Research Center, Portuguese Oncology Institute of Porto (IPO Porto), Porto, Portugal; Department of Pathology and Molecular Immunology, ICBAS- School of Medicine and Biomedical Sciences, University of Porto, Porto, Portugal), **Linglei Jiang** (CNBG-Virogin Biotech (Shanghai) Co., Ltd., Shanghai, China), **Jing Jin** (Beijing Jizhongke Biotechnology Co., LTD, Beijing, China), **Kentaro Jingushi** (Laboratory of Molecular and Cellular Physiology, Graduate School of Pharmaceutical Sciences, Osaka University, Osaka, Japan), **Dong-Gyu Jo** (School of Pharmacy, Sungkyunkwan University, Seoul, Republic of Korea; Institute of Quantum Biophysics, Sungkyunkwan University, Seoul, Republic of Korea; Biomedical Institute for Convergence, Sungkyunkwan University, Seoul, Republic of Korea), **Marianne S Joerger-Messerli** (Department for BioMedical Research (DBMR), University of Bern, Bern, Switzerland; Department of Obstetrics and Feto-maternal Medicine, University Women's Hospital, Inselspital, Bern University Hospital, Bern, Switzerland), **Jennifer C Jones** (Center for Cancer Research, National Cancer Institute, National Institutes of Health, Bethesda, MD, USA; Translational Nanobiology Section, Laboratory of Pathology, National Cancer Institute, National Institutes of Health, Bethesda, MD, USA), **Melissa K Jones** (IFAS, University of Florida, Gainesville, FL, USA), **Olivier G de Jong** (Department of Pharmaceutics, Utrecht Institute of Pharmaceutical Sciences (UIPS), Utrecht University, Utrecht, The Netherlands), **Tijana Jovanovic-Talisman** (Department of Cancer Biology and Molecular Medicine, Beckman Research Institute, City of Hope Comprehensive Cancer Center, Duarte, CA, USA), **Anthony W Ferrante, Jr** (Naomi Berrie Diabetes Center, Columbia University, New York, NY, USA), **Leon G Coleman Jr** (Bowles Center for Alcohol Studies, Department of Pharmacology, University of North Carolina at Chapel Hill School of Medicine, Chapel Hill, NC, USA), **David Juncker** (McGill University, Montreal, Canada), **Stephanie Jung** (Institute of Cardiovascular Immunology,

20013078, 2024, 2, Downloaded from https://isevjournals.onlinelibrary.wiley.com/doi/10.1002/jev2.12404 by Colorado State University, Wiley Online Library on [09/10/2024]. See the Terms and Conditions (https://onlinelibrary.wiley.com/terms-and-conditions) on Wiley Online Library for rules of use; OA articles are governed by the applicable Creative Commons License

University Hospital Bonn, University of Bonn, Bonn, Germany), **Benjamin Jurek** (Max-Planck Insitute for Psychiatry, Munich, Germany), **Marcin Jurga** (EXO Biologics SA, Liège, Belgium), **Verline Justilien** (Department of Cancer Biology, Mayo Clinic, Jacksonville, FL, USA), **Mehdi Kabani** (CNRS, CEA, Laboratoire des Maladies Neurodégénératives, Université Paris-Saclay, Fontenay-aux-Roses, France), **Raghu Kalluri** (The University of Texas MD Anderson Cancer Center, Houston, TX, USA), **Masood Kamali-Moghaddam** (Department of Immunology, Genetics and Pathology, Science for Life Laboratory, Uppsala University, Uppsala, Sweden), **Masamitsu Kanada** (Institute for Quantitative Health Science and Engineering (IQ), Department of Pharmacology & Toxicology, Michigan State University, East Lansing, MI, USA), **Taeyoung Kang** (Department of Biochemistry, La Trobe Institute for Molecular Science, La Trobe University, Melbourne, Australia), **Shin-ichi Kano** (University of Alabama at Birmingham, Birmingham, AL, USA), **Maria Kaparakis-Liaskos** (Department of Microbiology, Anatomy, Physiology and Pharmacology, La Trobe University, Melbourne, Australia), **Elżbieta Karnas** (Department of Cell Biology, Faculty of Biochemistry, Biophysics and Biotechnology, Jagiellonian University, Krakow, Poland), **Antoine Karoichan** (Faculty of Dental Medicine and Oral Health Sciences, McGill University, Montreal, Canada), **Fatah Kashanchi** (Laboratory of Molecular Virology, George Mason University, Manassas, VA, USA), **Sara Assar Kashani** (Centre for Motor Neuron Disease Research, Macquarie Medical School, Macquarie University, Sydney, Australia), **Namita N Kashyap** (Centre for Molecular Neurosciences, Kasturba Medical College Manipal, Manipal Academy of Higher Education, Manipal, India), **Miroslava Katsur** (The Hatter Cardiovascular Institute, University College London, London, UK), **Silvio Kau-Strebinger** (Department of Pathobiology, University of Veterinary Medicine Vienna, Vienna, Austria), **Amy C Kauffman** (Corning Life Sciences, Kennebunk, ME, USA), **Sukhbir Kaur** (Laboratory of Pathology, National Cancer Institute, National Institutes of Health, Bethesda, MD, USA), **Oksana Kehoe** (Centre for Regenerative Medicine Research, School of Medicine, Keele University, Keele, UK; Robert Jones and Agnes Hunt Orthopaedic Hospital, Oswestry, UK), **Richard JR Kelwick** (Imperial College London, London, UK), **Amirmohammad Nasiri Kenari** (Research Centre for Advanced Science and Technology, The University of Tokyo, Tokyo, Japan), **Brachyahu M Kestecher** (Department of Genetics, Cell- and Immunobiology, Semmelweis University, Budapest, Hungary; HCEMM-SU Extracellular Vesicle Research Group, Semmelweis University, Budapest, Hungary; HUN-REN-SU Translational Extracellular Vesicle Research Group, Semmelweis University, Budapest, Hungary), **Tom G Keulers** (Department of Radiotherapy, GROW-School for Oncology and Reproduction, Maastricht University Medical Centre+, Maastricht, The Netherlands), **Kendall R Van Keuren-Jensen** (Neurogenomics, TGen, Phoenix, AZ, USA), **Kasra Khalaj** (The Hospital for Sick Children, Toronto, Canada; University of Toronto, Toronto, Canada), **Delaram Khamari** (Department of Genetics, Cell- and Immunobiology, Semmelweis University, Budapest, Hungary), **Ramin Khanabdali** (Inoviq Limited, Notting Hill, Australia), **Elena Khomyakova** (Exosome Analytics, Evry, France), **Amanda Khoo** (Department of Medical Biophysics, University of Toronto, Toronto, Canada; Princess Margaret Cancer Centre, University Health Network, Toronto, Canada), **Daniel H Kim** (University of California, Santa Cruz, Santa Cruz, CA, USA; Canary Center at Stanford for Cancer Early Detection, Palo Alto, USA; Stanford RNA Medicine Program, Palo Alto, USA), **Dongin Kim** (College of Pharmacy, Oklahoma University Health Sciences Center, Oklahoma City, OK, USA), **Han Sang Kim** (Division of Medical Oncology, Department of Internal Medicine, Graduate School of Medical Science, Brain Korea 21 Project, Yonsei University College of Medicine, Seoul, Korea), **In-San Kim** (Chemical and Biological Integrative Research Center, Biomedical Research Division, Korea Institute of Science and Technology (KIST), Seoul, Republic of Korea; KU-KIST Graduate School of Converging Science and Technology, Korea University, Seoul, Republic of Korea), **Soo Kim** (Brexogen Inc., Seoul, Republic of Korea), **Yohan Kim** (Nathan S. Kline Institute for Psychiatric Research, Orangeburg, NY, USA; Department of Psychiatry, New York University School of Medicine, New York, NY, USA), **Peter E Kima** (Microbiology and Cell Science, University of Florida, Gainesville, FL, USA), **Thomas Kislinger** (Princess Margaret Cancer Centre, University Health Network, Toronto, ON, Canada; University of Toronto, Department of Medical Biophysics, Toronto, Canada), **Mikael Klingeborn** (McLaughlin Research Institute, Great Falls, MT, USA), **Rob Knight** (Cellese Inc., Irvine, CA, USA), **Hiroaki Komuro** (Smidt Heart Institute, Cedars-Sinai Medical Center, Los Angeles, CA, USA; Department of Cardiovascular Medicine, Tokyo Medical and Dental University, Tokyo, Japan), **Anna Koncz** (Department of Genetics, Cell- and Immunobiology, Semmelweis University, Budapest, Hungary), **Timothea Konstantinou** (Cardiff University, Cardiff, UK), **Luke van der Koog** (Department of Molecular Pharmacology, Groningen Research Institute of Pharmacy, Faculty of Science and Engineering, University of Groningen, Groningen, The Netherlands; GRIAC, Groningen Research Institute for Asthma and COPD, University Medical Center Groningen, Groningen, The Netherlands), **Sander AA Kooijmans** (CDL Research, University Medical Center Utrecht, Utrecht, The Netherlands), **Miroslaw T Kornek** (Department of Internal Medicine I, University Hospital Bonn of the Rheinische Friedrich-Wilhelms-University, Bonn, Germany; Department of General, Visceral and Thoracic Surgery, German Armed Forces Central Hospital, Koblenz, Germany), **Maja Kosanović** (Institute for the Application of Nuclear Energy, INEP, University of Belgrade, Belgrade, Serbia), **Enis Kostallari** (Division of Gastroenterology and Hepatology, Mayo Clinic, Rochester, MN, USA), **Tiana F Koukoulis** (The Florey Institute of Neuroscience and Mental Health, The University of Melbourne, Parkville, Australia), **Stella Kourembanas** (Division of Newborn Medicine, Boston Children's Hospital, Boston, MA, USA; Harvard Medical School, Boston, MA, USA), **Eva-Maria Krämer-Albers** (Institute for Developmental Biology and Neurobiology, Johannes Gutenberg University Mainz, Mainz, Germany), **Veronika Kralj-Iglic** (Laboratory of Clinical Biophysics, Faculty of Health Sciences, University of Ljubljana, Ljubljana, Slovenia), **Susanne Krasemann** (Institute of Neuropathology, University Medical Center Hamburg-Eppendorf, Hamburg, Germany; Core Facility for Pathology, University Medical Center Hamburg-Eppendorf, Hamburg, Germany), **Anna D Krasnodembskaya**

20013078, 2024, 2, Downloaded from https://isevjournals.onlinelibrary.wiley.com/doi/10.1002/jev2.12404 by Colorado State University, Wiley Online Library on [09/10/2024]. See the Terms and Conditions (https://onlinelibrary.wiley.com/terms-and-conditions) on Wiley Online Library for rules of use; OA articles are governed by the applicable Creative Commons License

(Queen's University Belfast, Belfast, UK), **Natalia J Krawczynska** (Beckman Institute for Advanced Science and Technology, University of Illinois at Urbana-Champaign, Urbana-Champaign, IL, USA; Department of Molecular and Integrative Physiology, University of Illinois at Urbana-Champaign, IL, USA), **Mateja E Kreft** (Institute of Cell Biology, Faculty of Medicine, University of Ljubljana, Ljubljana, Slovenia), **Nicole A Kruh-Garcia** (Bio-pharmaceutical Manufacturing and Academic Resource Center (BioMARC), Infectious Disease Research Center, Colorado State University, Fort Collins, CO, USA), **Meta J Kuehn** (Duke University Medical Center, Durham, NC, USA), **Marije E Kuipers** (Department of Biomolecular Health Sciences, Faculty of Veterinary Medicine, Utrecht University, Utrecht, The Netherlands; Department of Parasitology, Leiden University Medical Center, Leiden, The Netherlands), **Konxhe Kulaj** (Molecular Cell Biology, Institute for Theoretical Medicine, Medical Faculty, University of Augsburg, Augsburg, Germany; Institute for Diabetes and Obesity, Helmholtz Zentrum München, Neuherberg, Germany; German Center for Diabetes Research (DZD), Neuherberg, Germany), **Julia Kuligowski** (Health Research Institute La Fe, Valencia, Spain), **Yumi Kumagai** (Juntendo University, Tokyo, Japan), **Ashish Kumar** (Department of Cancer Biology, Wake Forest School of Medicine, Winston-Salem, NC, USA), **Saroj Kumar** (Department of Biophysics, All India Institute of Medical Sciences, New Delhi, India; Department of Health Science, Lulea University of Technology, Lulea, Sweden), **Sharad Kumar** (Centre for Cancer Biology, University of South Australia, Adelaide, Australia; Adelaide Medical School, Faculty of Health and Medical Sciences, The University of Adelaide, Adelaide, Australia), **Meena Kumari** (Kansas State University, Manhattan, KS, USA), **Gabrielis Kundrotas** (EXO Biologics SA, Liège, Belgium), **Igor V Kurochkin** (Central Research Laboratories, Sysmex Co., Kobe, Japan), **Masahiko Kuroda** (Department of Molecular Pathology, Tokyo Medical University, Tokyo, Japan), **Marzena Kurzawa-Akanbi** (Biosciences Institute, Faculty of Medical Sciences, Newcastle University, Newcastle upon Tyne, UK), **Sasha J Kweskin** (Bayer AG, St. Louis, MO, USA), **Diego Kyburz** (Department of Biomedicine, University of Basel, Basel, Switzerland; Department of Rheumatology, University Hospital Basel, Basel, Switzerland), **Elisa Lázaro-Ibáñez** (Advanced Drug Delivery, Pharmaceutical Sciences, Biopharmaceutics R&D, AstraZeneca, Gothenburg, Sweden), **Cecilia Lässer** (Krefting Research Centre, Department of Internal Medicine and Clinical Nutrition, Institute of Medicine at Sahlgrenska Academy, University of Gothenburg, Gothenburg, Sweden), **Jan Lötvall** (Krefting Research Centre, Institute of Medicine at Sahlgrenska Academy, University of Gothenburg, Gothenburg, Sweden), **Ákos M Lőrincz** (Department of Physiology, Semmelweis University, Budapest, Hungary; Second Department of Internal Medicine, Szent György Hospital, Székesfehérvár, Hungary), **Andrew Lai** (Translational Extracellular Vesicles in Obstetrics and Gynae-Oncology Group, University of Queensland Centre for Clinical Research, Faculty of Medicine, Royal Brisbane and Women's Hospital, The University of Queensland, Brisbane, Australia), **Charles P Lai** (Institute of Atomic and Molecular Sciences, Academia Sinica, Taipei, Taiwan; Chemical Biology and Molecular Biophysics Program, TIGP, Academia Sinica, Taipei, Taiwan; Genome and Systems Biology Degree Program, National Taiwan University, Taipei, Taiwan), **Saara Laitinen** (Finnish Red Cross Blood Service, Helsinki, Finland), **Solange Landreville** (Université Laval, Quebec, Canada; Centre de Recherche du Centre Hospitalier Universitaire de Québec, Université Laval, Quebec, Canada), **Sigrun Lange** (Pathobiology and Extracellular Vesicles Research Group, School of Life Sciences, University of Westminster, London, UK), **Scott M Langevin** (University of Vermont Larner College of Medicine, Burlington, VT, USA; University of Vermont Cancer Center, Burlington, VT, USA), **Marc-André Langlois** (Department of Biochemistry, Microbiology & Immunology, Faculty of Medicine, University of Ottawa, Ottawa, Canada), **Lucia R Languino** (Thomas Jefferson University, Philadelphia, PA, USA), **Joanne Lannigan** (Flow Cytometry Support Services, LLC, Alexandria, VA, USA), **Daniel S Lark** (Colorado State University, Fort Collins, CO, USA), **Adriana T Larregina** (University of Pittsburgh School of Medicine, Pittsburgh, PA, USA), **Louise C Laurent** (Division of Maternal Fetal Medicine, Department of Obstetrics, Gynecology, and Reproductive Sciences, University of California, San Diego, San Diego, CA, USA), **David Laurin** (Research Center INSERM U1209/CNRS UMR 5309, Etablissement Français du Sang, Université Grenoble Alpes, Grenoble, France), **Gregory Lavieu** (INSERM U1316, CNRS UMR7057, Université Paris Cité, Paris, France), **Charlotte Lawson** (Department of Comparative Biomedical Sciences, Royal Veterinary College, London, UK; School of Pharmacy and Biomedical Sciences, University of Central Lancashire, Preston, UK), **Soazig Le Lay** (CNRS, INSERM, l'institut du thorax, Nantes University, Nantes, France; Univ Angers, SFR ICAT, Angers, France), **Kevin Leandro** (Center for Neuroscience and Cell Biology, University of Coimbra, Coimbra, Portugal; Center for Innovative Biomedicine and Biotechnology, University of Coimbra, Coimbra, Portugal; Faculty of Pharmacy, University of Coimbra, Coimbra, Portugal), **Aurélie Ledreux** (Department of Neurosurgery, School of Medicine, University of Colorado Anschutz Medical Campus, Aurora, CO, USA), **Changjin Lee** (SL Bigen, Inc., Incheon, Republic of Korea), **Dong-Sup Lee** (Seoul National University College of Medicine, Seoul, Republic of Korea), **Hakho Lee** (Center for Systems Biology, Massachusetts General Hospital, Boston, MA, USA; Department of Radiology, Massachusetts General Hospital, Harvard Medical School, Boston, MA, USA), **Heon-Jin Lee** (Department of Microbiology and Immunology, School of Dentistry, Kyungpook National University, Daegu, Republic of Korea), **Sun Young Lee** (Department of Ophthalmology and Physiology & Neuroscience , University of Southern California, Los Angeles, CA, USA), **Tae Ryong Lee** (SL Bigen, Inc., Incheon, Republic of Korea), **Wai-Leng Lee** (School of Science, Monash University Malaysia, Bandar Sunway, Malaysia), **Iliya Lefterov** (University of Pittsburgh, Pittsburgh, PA, USA; Medical University Varna, Varna, Bulgaria), **Xinhua Lei** (Beijing Jizhongke Biotechnology Co., LTD, Beijing, China), **Janne Leivo** (Department of Life Technologies, University of Turku, Turku, Finland; InFLAMES Research Flagship, University of Turku, Turku, Finland), **Quentin Lemaire** (CNRS, UMR 8576 - UGSF—Unité de Glycobiologie Structurale et Fonctionnelle, University of Lille, Lille, France), **Adriana F Paes Leme** (Laboratório Nacional de Biociências—LNBio, Centro Nacional de Pesquisa em

20013078, 2024, 2, Downloaded from https://isevjournals.onlinelibrary.wiley.com/doi/10.1002/jev2.12404 by Colorado State University, Wiley Online Library on [09/10/2024]. See the Terms and Conditions (https://onlinelibrary.wiley.com/terms-and-conditions) on Wiley Online Library for rules of use; OA articles are governed by the applicable Creative Commons License

Energia e Materiais—CNPEM, Campinas, Brazil), **Stanley M Lemon** (Lineberger Comprehensive Cancer Center and Departments of Medicine and Microbiology & Immunology, The University of North Carolina at Chapel Hill, Chapel Hill, NC, USA), **Metka Lenassi** (University of Ljubljana, Faculty of Medicine, Ljubljana, Slovenia), **Kathleen M. Lennon** (Department of Molecular Medicine, Beckman Research Institute, City of Hope Comprehensive Cancer Center, Duarte, CA, USA), **Stephen Lenzini** (RoosterBio, Frederick, MD, USA), **Jonathan Leor** (Neufeld Cardiac Research Institute, School of Medicine, Tel Aviv University, Tel Aviv, Israel; Tamman Cardiovascular Research Institute, Heart Center, Sheba Medical Center, Ramat Gan, Israel), **Efrat levy** (New York University Langone Health, New York, NY, USA; Nathan S. Kline Institute for Psychiatric Research, Orangeburg, NY, USA), **Bo Li** (Department of Laboratory Medicine, Nanfang Hospital, Southern Medical University, Guangzhou, China; Guangdong Engineering and Technology Research Center for Rapid Diagnostic Biosensors, Nanfang Hospital, Southern Medical University, Guangzhou, China), **Guoping Li** (Cardiovascular Research Center, Massachusetts General Hospital, Boston, MA, USA; Harvard Medical School, Boston, MA, USA), **Jiao Jiao Li** (University of Technology Sydney, Sydney, Australia; Kolling Institute, Sydney, Australia), **Qiubai Li** (Department of Rheumatology and Immunology, Union Hospital, Tongji Medical College, Huazhong University of Science and Technology, Wuhan, China; Hubei Engineering Research Center for Application of Extracelluar Vesicle, Hubei University of Science and Technology, Xianning, China), **Xinlei Li** (The Abigail Wexner Research Institute, Nationwide Children's Hospital, Columbus, OH, USA), **Xiuming Liang** (Biomolecular Medicine, Clinical Research Center, Department of Laboratory Medicine, Karolinska Institutet, Stockholm, Sweden; Cancer Research Laboratory, Shandong University-Karolinska Institutet Collaborative Laboratory, School of Basic Medical Science, Shandong University, Jinan, China), **Rebecca Lim** (Hudson Institute, Melbourne, Australia; Monash University, Melbourne, Australia), **Sai Kiang Lim** (Institute of Molecular and Cell Biology (IMCB), Agency for Science, Technology and Research (A*STAR), Singapore; Paracrine Therapeutics Pte. Ltd., Singapore; Department of Surgery, YLL School of Medicine, National University Singapore, Singapore), **Tania Limongi** (Department of Applied Science and Technology, Politecnico di Torino, Turin, Italy), **Aija Linē** (Latvian Biomedical Research and Study Centre, Riga, Latvia), **Paula Pincela Lins** (Hasselt University, Faculty of Medicine and Life Sciences, Biomedical Research Institute, Diepenbeek, Belgium; Health Department, Flemish Institute for Technological Research (VITO), Mol, Belgium), **Lien Lippens** (Laboratory of Experimental Cancer Research, Department of Human Structure and Repair, Ghent University, Ghent, Belgium; Cancer Research Institute Ghent, Ghent, Belgium), **Guanshu Liu** (Department of Radiology, Johns Hopkins University School of Medicine, Baltimore, MD, USA; FM Kirby Center, Kennedy Krieger Institute, Baltimore, MD, USA), **Alicia Llorente** (Department of Molecular Cell Biology, Institute for Cancer Research, Oslo University Hospital, Oslo, Norway; Department for Mechanical, Electrical and Chemical Engineering, Oslo Metropolitan University, Oslo, Norway; Centre for Cancer Cell Reprogramming, University of Oslo, Oslo, Norway), **Modeline N Longjohn** (Faculty of Medicine, Memorial University of Newfoundland and Labrador, St. John's, NL, Canada), **Fons AJ van de Loo** (Experimental Rheumatology, Radboud University Medical Center, Nijmegen, The Netherlands), **Magdalena J Lorenowicz** (Biomedical Primate Research Centre, Rijswijk, The Netherlands), **Aurelio Lorico** (Touro University Nevada College of Medicine, Henderson, NV, USA), **Olivier Loudig** (Center for Discovery and Innovation, Hackensack Meridian Health, Nutley, NJ, USA), **Xavier Loyer** (PARCC, INSERM, Université de Paris, Paris, France), **Estefanía Lozano-Andrés** (Department of Biomolecular Health Sciences, Faculty of Veterinary Medicine, Utrecht University, Utrecht, The Netherlands), **Biao Lu** (Department of Bioengineering, School of Engineering, Santa Clara University, Santa Clara, CA, USA), **Quan Lu** (Department of Environmental Health, Harvard T.H. Chan School of Public Health, Boston, MA, USA), **Quentin Lubart** (Abbelight, Cachan, France), **Fabrice Lucien** (Department of Urology, Mayo Clinic, Rochester, MN, USA; Department of Immunology, Mayo Clinic, Rochester, MN, USA), **Taral R Lunavat** (Department of Biomedicine, University of Bergen, Bergen, Norway), **Ludwig Ermann Lundberg** (Swedish University of Agricultural Sciences, Uppsala, Sweden; BioGaia AB, Stockholm, Sweden), **David J Lundy** (College of Biomedical Engineering, Taipei Medical University, Taipei, Taiwan; Center for Cell Therapy, Taipei Medical University Hospital, Taipei, Taiwan), **Jens C Luoto** (Åbo Akademi University, Turku, Finland; Turku Bioscience, Turku, Finland), **David C Lyden** (Departments of Pediatrics and Cell and Developmental Biology, Meyer Cancer Center, Weill Cornell Medicine, New York, NY, USA), **Andreas Möller** (Chinese University of Hong Kong, Hong Kong, Hong Kong SAR; QIMR Berghofer Medical Research Institute, Brisbane, Australia), **Janis A Müller** (Institute of Virology, Philipps University Marburg, Marburg, Germany), **Daniel J MacPhee** (Department of Veterinary Biomedical Sciences, Western College of Veterinary Medicine, Saskatoon, Canada; University of Saskatchewan, Saskatoon, Canada), **Adam L. Maddox** (Department of Molecular Medicine, Beckman Research Institute, City of Hope Comprehensive Cancer Center, Duarte, CA, USA), **Elise Madec** (MSC-med, Paris, France; EverZom, Paris, France), **Setty M Magaña** (The Abigail Wexner Research Institute, Nationwide Children's Hospital, Columbus, OH, USA), **Vasiliki Mahairaki** (Department of Genetic Medicine, Johns Hopkins University School of Medicine, Baltimore, MD, USA; The Richman Family Precision Medicine Center of Excellence in Alzheimer's Disease, Johns Hopkins University School of Medicine, Baltimore, MD, USA), **Mỹ G Mahoney** (Thomas Jefferson University, Philadelphia, PA, USA), **Harmeet Malhi** (Mayo Clinic, Rochester, MN, USA), **Cécile E Malnou** (Institut Toulousain des Maladies Infectieuses et Inflammatoires, INSERM, CNRS, UPS, Université de Toulouse, Toulouse, France), **Doste R Mamand** (Biomolecular and Cellular Medicine, Clinical Research Center, Department of Laboratory Medicine, Karolinska Institutet, Huddinge, Sweden), **Kenny Man** (Department of Oral and Maxillofacial Surgery & Special Dental Care, University Medical Center Utrecht, Utrecht, The Netherlands; UMC Utrecht Regenerative Medicine Center, Circulatory Health Research Center, University Medical Center Utrecht, Utrecht, The Netherlands), **Mauro Manno** (National Research Council of

20013078, 2024, 2, Downloaded from https://isevjournals.onlinelibrary.wiley.com/doi/10.1002/jev2.12404 by Colorado State University, Wiley Online Library on [09/10/2024]. See the Terms and Conditions (https://onlinelibrary.wiley.com/terms-and-conditions) on Wiley Online Library for rules of use; OA articles are governed by the applicable Creative Commons License

20013078, 2024, 2, Downloaded from https://isevjournals.onlinelibrary.wiley.com/doi/10.1002/jev2.12404 by Colorado State University, Wiley Online Library on [09/10/2024]. See the Terms and Conditions (https://onlinelibrary.wiley.com/terms-and-conditions) on Wiley Online Library for rules of use; OA articles are governed by the applicable Creative Commons License

Italy, Institute of Biophysics, Palermo, Italy), **Pierre-Yves Mantel** (Christine Kühne—Center for Allergy Research and Education, Davos, Switzerland; Department of Oncology, Microbiology, and Immunology, University of Fribourg, Fribourg, Switzerland), **Tecla Marangon** (Biomedical Engineering, College of Science and Engineering, University of Galway, Galway, Ireland), **Eduardo Marbán** (Smidt Heart Institute, Cedars-Sinai Medical Center, Los Angeles, CA ,USA), **Antonio Marcilla** (Área de Parasitología, Dept. Farmacia y Tecnología Farmacéutica y Parasitología, F. Farmàcia, Universitat de València, Valencia, Spain; Joint Unit on Endocrinology, Nutrition and Clinical Dietetics, IIS La Fe-Universitat de València, Valencia, Spain), **Krishna P Maremanda** (Department of Biochemistry and Biophysics, Texas A&M University, College Station, TX, USA), **Leonid Margolis** (National Institutes of Health, Bethesda, MD, USA (retired)), **Luis Mariñas-Pardo** (Universidad Internacional de Valencia, Valencia, Spain; Instituto de Salud Carlos III, Majadahonda, Spain), **Ivica Marić** (Faculty of Medicine, University of Ljubljana, Ljubljana, Slovenia), **Silvia Sánchez Martín** (Institut d'Investigació Sanitària Pere Virgili, Tarragona, España), **Eduardo Martínez-Martínez** (Instituto Nacional de Medicina Genómica, Mexico City, Mexico), **Catherine Martel** (Faculty of Medicine, Université de Montréal, Montreal, Canada; Montreal Heart Institute, Montreal, Canada), **Elena S Martens-Uzunova** (Erasmus MC Cancer Institute, University Medical Center Rotterdam, Department of Urology, Rotterdam, The Netherlands), **Pilar Martin-Duque** (Instituto de Salud Carlos III, Majadahonda, Spain; IIS Aragón, Zaragoza, Spain), **Lorena Martin-Jaular** (Institut Curie, INSERM U932, PSL University, Paris, France; CurieCoreTech Extracellular Vesicles, Institut Curie, Paris, France), **Paola A Martinez-Murillo** (CK-CARE, Davos, Switzerland), **Sarai Martinez-Pacheco** (School of Pharmacy and Pharmaceutical Sciences, Panoz Institute, Trinity College Dublin, Dublin, Ireland; Trinity Biomedical Sciences Institute, Trinity College Dublin, Dublin, Ireland; Trinity St. James's Cancer Institute, Trinity College Dublin, Dublin, Ireland), **Tania Martins-Marques** (Coimbra Institute for Clinical and Biomedical Research (iCBR), Faculty of Medicine, University of Coimbra, Coimbra, Portugal; Center for Innovative Biomedicine and Biotechnology, University of Coimbra, Coimbra, Portugal), **Benjamin Mary** (Tumor Biomechanics, INSERM UMR_S1109, Centre de Recherche en Biomédecine de Strasbourg, Strasbourg, France), **Akbar L Marzan** (La Trobe Institute for Molecular Science, La Trobe University, Melbourne, Australia), **Andreu Matamoros-Angles** (Institute of Neuropathology, University Medical Center Hamburg-Eppendorf, Hamburg, Germany), **Suresh Mathivanan** (La Trobe Institute for Molecular Science, La Trobe University, Melbourne, Australia), **Juntaro Matsuzaki** (Division of Pharmacotherapeutics, Keio University Faculty of Pharmacy, Tokyo, Japan), **Maria D Mayan** (CellCOM Research Group, Instituto de Investigación Biomédica de A Coruña (INIBIC), University Hospital Complex A Coruña, Coruña, Spain; Servizo Galego de Saúde (SERGAS), Galicia, Spain), **Carla Mazzeo** (Boston University, Boston, MA, USA), **Mariama Mbengue** (Cardiff University, Cardiff, UK), **Mark J McCann** (The New Zealand Institute for Plant and Food Research Limited, Palmerston North, New Zealand; Te Ohu Rangahau Kai, AgResearch Limited, Palmerston North, New Zealand), **Luke C McIlvenna** (Blizard Institute, Barts and the London School of Medicine and Dentistry, Queen Mary University of London, London, UK), **Mark J McVey** (Department of Anesthesia and Pain Medicine Hospital for Sick Children, Toronto, ON, Canada; Anesthesiology and Pain Medicine, University of Toronto, Toronto, ON, Canada; Department of Physics, Toronto Metropolitan University, Toronto, ON, Canada), **Nicole Meisner-Kober** (Department of Biosciences and Medical Biology, Paris-Lodron University Salzburg, Salzburg, Austria), **Maiken Mellergaard** (Department of Clinical Biochemistry, Aalborg University Hospital, Aalborg, Denmark; Department of Clinical Medicine, Aalborg University, Aalborg, Denmark), **Giorgia Melli** (Neurocenter of Southern Switzerland, Ente Ospedaliero Cantonale, Lugano, Switzerland; Laboratories for Translational Research, Ente Ospedaliero Cantonale, Bellinzona, Switzerland; Faculty of Biomedical Sciences, Università della Svizzera Italiana, Lugano, Switzerland), **Kerstin Menck** (Department of Medicine A, University of Muenster, Muenster, Germany), **Nico G Menjivar** (Colorado State University, Fort Collins, CO, USA), **Ramkumar Menon** (Department of Obstetrics and Gynecology, The University of Texas Medical Branch at Galveston, Galveston, TX, USA), **Kyle I Mentkowski** (Massachusetts General Hospital, Boston, MA, USA), Flemish Institute for Technological Research (VITO), Mol, Belgium (University of Antwerp, Antwerp, Belgium), **John J Miklavcic** (Chapman University, Orange, CA, USA), **Andras G Miklosi** (ONI (Oxford Nanoimaging Ltd), Oxford, UK), **Bojana Milutinovic** (MD Anderson Cancer Center, University of Texas, Houston, TX, USA), **Valentina R Minciacchi** (Center for Thrombosis and Hemostasis, Johannes Gutenberg University Medical Center, Mainz, Germany), **Mehdi Mirzaei** (Macquarie Medical School, Macquarie University, Sydney, Australia), **Shalini Mishra** (Wake Forest School of Medicine, Winston-Salem, NC, USA), **Megan I Mitchell** (Center for Discovery and Innovation, Hackensack Meridian Health, Nutley, NJ, USA), **Rachel R Mizenko** (Department of Biomedical Engineering, University of California, Davis, Davis, CA, USA), **Danilo Mladenović** (HansaBioMed Life Sciences, Tallinn, Estonia; Tallinn University, Tallinn, Estonia), **Eqbal Mohamadi** (NIGEB, Tehran, Iran; KNT, Javanrud, Iran), **Sujata Mohanty** (Stem Cell Facility, All India Institute of Medical Sciences, New Delhi, India), **Fatemeh Momen-Heravi** (Cancer Biology and Immunology Laboratory, Columbia University Irving Medical Center, New York, NY, USA; Herbert Irving Comprehensive Cancer Center, Columbia University Irving Medical Center, New York, NY, USA; College of Dental Medicine, Columbia University, New YorkCity, NY, USA), **Sujan K Mondal** (Michigan State University, East Lansing, MI, USA), **Marta Monguió-Tortajada** (Department of Immunobiology, University of Lausanne, Epalinges, Switzerland), **Jisook Moon** (College of Life Science, Department of Biotechnology, CHA University, Seoul, Republic of Korea), **Mattia I Morandi** (Institute of Organic Chemistry and Biochemistry of the Czech Academy of Science, Prague, Czech Republic), **Violaine Moreau** (INSERM, BRIC, U1312, University of Bordeaux, Bordeaux, France), **Lissette Retana Moreira** (Departamento de Parasitología, Facultad de Microbiología, Universidad de Costa Rica, San José, Costa Rica; Centro de Investigación en Enfermedades Tropicales (CIET), Universidad de Costa Rica, San José, Costa Rica), **Adrian E Morelli**

(Thomas E Starzl Transplantation Institute, Department of Surgery, University of Pittsburgh, Pittsburgh, PA, USA), **Marcelo A Mori** (Universidade Estadual de Campinas (UNICAMP), Campinas, Brazil), **Masahiro Morimoto** (Department of Oral Diagnosis and Medicine, Hokkaido University Faculty of Dental Medicine, Sapporo, Japan), **Mathilde Mosser** (Oniris VetAgroBio Nantes, INRAE, IECM, Nantes, France), **Thabiso E Motaung** (Forestry and Agricultural Biotechnology Institute, University of Pretoria, Pretoria, South Africa), **Etienne Moussay** (Tumor Stroma Interactions, Department of Cancer Research, Luxembourg Institute of Health, Luxembourg, Luxembourg), **Vera Mugoni** (Department of Cellular, Computational and Integrative Biology (CIBIO), University of Trento, Trento, Italy), **Francois Mullier** (Université catholique de Louvain, CHU UCL Namur, Namur Thrombosis and Hemostasis Center (NTHC), Namur Research Institute for Life Sciences (NARILIS), Hematology Laboratory, Yvoir, Belgium; Institut de Recherche Expérimentale et Clinique (IREC), Pôle Mont, Université catholique de Louvain (UCLouvain), Yvoir, Belgium), **Maurizio Muraca** (University of Padua, Padua, Italy; Istituto di Ricerca Pediatrica "Città della Speranza", Padua, Italy), **Saravanakumar Murugesan** (University of Alabama at Birmingham, Birmingham, AL, USA), **Luca Musante** (School of Veterinary Medicine, University of Pennsylvania, Philadelphia, PA, USA), **Angelo Musicò** (Department of Molecular and Translational Medicine, University of Brescia, Brescia, Italy; CSGI, Center for Colloid and Surface Science, Florence, Italy), **Afrodité Németh** (Pázmány Péter Catholic University, Budapest, Hungary), **Krisztina Németh** (Department of Genetics, Cell- and Immunobiology, Semmelweis University, Budapest, Hungary; HUN-REN-SU Translational Extracellular Vesicle Research Group, Semmelweis University, Budapest, Hungary), **Amélie Nadeau** (Research Institute of McGill University Health Centre, Montreal, Canada; Department of Pathology, McGill University, Montreal, Canada), **Gi-Hoon Nam** (Department of Biochemistry and Molecular Biology, Korea University College of Medicine, Seoul, Republic of Korea; SHIFTBIO.INC, Seoul, Republic of Korea), **Honami Naora** (University of Texas MD Anderson Cancer Center, Houston, TX, USA), **Riccardo Natoli** (Clear Vision Research Group, Eccles Institute of Neuroscience, John Curtin School of Medical Research, College of Health and Medicine, The Australian National University, Acton, ACT, Australia; School of Medicine and Psychology, College of Health and Medicine, The Australian National University, Acton, ACT, Australia), **Muhammad Nawaz** (Department of Rheumatology and Inflammation Research, Institute of Medicine, Sahlgrenska Academy, University of Gothenburg, Gothenburg, Sweden), **Irina Nazarenko** (Institute for Infection Prevention and Control, Faculty of Medicine, Medical Center—University of Freiburg, Freiburg, Germany; Hahn-Schikard Institute, Freiburg, Germany), **Justus C Ndukaife** (Department of Electrical and Computer Engineering, Vanderbilt University, Nashville, TN, USA; Department of Mechanical Engineering, Vanderbilt University, Nashville, TN, USA; The Vanderbilt Center for Extracellular Vesicle Research, School of Medicine, Vanderbilt University, Nashville, TN, USA), **Christina Nedeva** (La Trobe Institute for Molecular Science, La Trobe University, Melbourne, Australia), **Peter Nejsum** (Department of Clinical Medicine, Aarhus University, Aarhus, Denmark), **Inge Nelissen** (Health Department, Flemish Institute for Technological Research (VITO), Mol, Belgium), **Christian Neri** (Institute of Biology Paris-Seine, Sorbonne Université, Paris, France; Centre National de la Recherche Scientifique, Paris, France; Institut National de la Santé et de la Recherche Médicale, Paris, France), **Tommaso Neri** (Centro Dipartimentale di Biologia Cellulare Cardiorespiratoria, Dipartimento di Patologia Chirurgica, Medica, Molecolare e dell'Area Critica, Università di Pisa, Pisa, Italy), **Paolo Neviani** (The Saban Research Institute of Children's Hospital Los Angeles, University of Southern California, Los Angeles, CA, USA), **Lauren A Newman** (College of Medicine and Public Health, Flinders University, Adelaide, Australia), **Chiew Yong Ng** (Universiti Kebangsaan Malaysia Medical Centre, Kuala Lumpur, Malaysia; National University of Singapore, Singapore), **Guillaume van Niel** (Institute of Psychiatry and Neuroscience of Paris (IPNP), INSERM U1266, Université Paris Cité, Paris, France; GHU-Paris Psychiatrie et Neurosciences, Hôpital Sainte Anne, Paris, France), **Rienk Nieuwland** (Laboratory of Experimental Clinical Chemistry, Amsterdam University Medical Centers, Location AMC, University of Amsterdam, Amsterdam, The Netherlands; Amsterdam Vesicle Center, Amsterdam University Medical Centers, Location AMC, University of Amsterdam, Amsterdam, The Netherlands), **Nadezhda Nikiforova** (Rochester Institute of Technology, Rochester, NY, USA), **Leonardo Nimrichter** (Instituto de Microbiologia Paulo de Góes, Universidade Federal do Rio de Janeiro, Rio de Janeiro, Brazil), **Chitranshi Nitin** (Macquarie University, Sydney, Australia), **Makon-Sébastien Njock** (Department of Pneumology, University Hospital of Liège, Liège, Belgium; University of Liège/GIGA Research Centre/Laboratory of Pneumology, Liège, Belgium), **Daniele Noël** (IRMB, INSERM, University of Montpellier, Montpellier, France), **Alessio Noghero** (Lovelace Biomedical Research Institute, Albuquerque, NM, USA), **John P Nolan** (Scintillon Institute, San Diego, CA, USA), **Sam Noppen** (Department of Microbiology, Immunology and Transplantation, Rega Institute, Laboratory of Virology and Chemotherapy, KU Leuven, Leuven, Belgium), **Nicole Noren Hooten** (National Institute on Aging, National Institutes of Health, Baltimore, MD, USA), **Antonio da Silva Novaes** (Department of Medicine, Federal University of Sao Paulo, Sao Paulo, Brazil; Department of Medicine, State University of New York at Stony Brook, Stony Brook, NY, USA), **Lorraine O'Driscoll** (School of Pharmacy and Pharmaceutical Sciences, Trinity College Dublin, Dublin, Ireland; Trinity Biomedical Sciences Institute, Trinity College Dublin, Dublin, Ireland; Trinity St. James's Cancer Institute, Trinity College Dublin, Dublin, Ireland), **Ana O'Loghlen** (Centre for Biological Research (CIB), Spanish National Research Council (CSIC), Madrid, Spain), **Takahiro Ochiya** (Tokyo Medical University, Tokyo, Japan), **Johannes Oesterreicher** (Ludwig Boltzmann Institute for Traumatology, The Research Centre in Cooperation with AUVA, Vienna, Austria; Austrian Cluster for Tissue Regeneration, Vienna, Austria), **Seung W Oh** (MDimune Inc., Seoul, Republic of Korea; BioDrone Therapeutics Inc., Seattle, WA, USA), **Attila Oláh** (Department of Physiology, Faculty of Medicine, University of Debrecen, Debrecen, Hungary), **Martin Olivier** (McGill University, Montreal, Canada; Research Institute of McGill University Health Centre, Montreal, Canada), **Siew Ling Ong** (New Zealand

20013078, 2024, 2, Downloaded from https://isevjournals.onlinelibrary.wiley.com/doi/10.1002/jev2.12404 by Colorado State University, Wiley Online Library on [09/10/2024]. See the Terms and Conditions (https://onlinelibrary.wiley.com/terms-and-conditions) on Wiley Online Library for rules of use; OA articles are governed by the applicable Creative Commons License

Leather & Shoe Research Association (LASRA), Palmerston North, New Zealand; AgResearch Limited, Palmerston North, New Zealand), **Angelica Ortiz** (New York University Grossman School of Medicine, New York, NY, USA), **Luis A Ortiz** (Department of Environmental and Occupational Health, Graduate School of Public Health, University of Pittsburgh, Pittsburgh, PA, USA), **Ole Østergaard** (Novo Nordisk Foundation, Center for Protein Research, Faculty of Health and Medical Sciences, University of Copenhagen, Copenhagen, Denmark), **Omar A Osorio** (Department of Medicine, Division of Pulmonary and Critical Care Medicine, Washington University School Of Medicine, St. Louis, MO, USA), **Xabier Osteikoetxea** (Semmelweis University, Budapest, Hungary; Hungarian Centre of Excellence for Molecular Medicine, Szeged, Hungary), **Matias Ostrowski** (INBIRS Institute, CONICET, University of Buenos Aires, Buenos Aires, Argentina), **David Otaegui** (Biogipuzkoa Health Research Institute, San Sebastián, Spain), **Alexander Otahal** (Center for Regenerative Medicine, University for Continuing Education Krems, Krems, Austria), **Patricia M M Ozawa** (Vanderbilt University, Nashville, TN, USA), **Dilara C Ozkocak** (Department of Biochemistry and Chemistry, La Trobe Institute for Molecular Science, La Trobe University, Melbourne, Australia; Research Centre for Extracellular Vesicles, La Trobe University, Melbourne, Australia), **Krisztina Pálóczi** (Semmelweis University, Budapest, Hungary), **Rocío Pérez-González** (Alicante Institute for Health and Biomedical Research (ISABIAL), Alicante, Spain; Institute of Neuroscience (IN), University Miguel Hernández-CSIC, San Juan de Alicante, Alicante, Spain), **Bianca C Pachane** (Universidade Federal de São Carlos—UFSCar, São Carlos, Brazil), **Hafiza Padinharayil** (Jubilee Mission Medical College and Research Institute, Thrissur, India), **Daan Paget** (Division of Cardiovascular Medicine, Radcliffe Department of Medicine, University of Oxford, Oxford, UK; Department of Pharmacology, University of Oxford, Oxford, UK; Department of Physiology and Pharmacology, Karolinska Institutet, Stockholm, Sweden), **Jerome Paggetti** (Tumor Stroma Interactions, Department of Cancer Research, Luxembourg Institute of Health, Luxembourg, Luxembourg), **Paola C Loreto Palacio** (Abigail Wexner Research Institute, Nationwide Children's Hospital, Columbus, OH, USA), **Christian P Pallasch** (Department I of Internal Medicine, Centre for Integrated Oncology (CIO) Aachen-Bonn- Cologne Duesseldorf, University of Cologne, Cologne, Germany; Cologne Excellence Cluster for Cellular Stress Responses in Ageing-Associated Diseases (CECAD), University of Cologne, Cologne, Germany; Centre for Molecular Medicine Cologne (CMMC), University of Cologne, Cologne, Germany), **Roberta Palmulli** (Department of Pathology, University of Cambridge, Cambridge, UK; Department of Biochemistry, University of Cambridge, Cambridge, UK), **Bairen Pang** (The First Affiliated Hospital of Ningbo University, Ningbo, China), **Liliia Paniushkina** (ExCT, PMU, Salzburg, Austria; Micalis, Inrae, Paris, France), **Paschalia Pantazi** (Institute of Reproductive and Developmental Biology, Imperial College London, London, UK), **Lucia Paolini** (Department of Medical and Surgical Specialties, Radiological Sciences and Public Health (DSMC), University of Brescia, Brescia, Italy ; Center for Colloid and Surface Science (CSGI), Florence, Italy), **Daniela L Papademetrio** (Departamento de Inmunología, Facultad de Farmacia y Bioquímica, University of Buenos Aires, Buenos Aires, Argentina; Hospital de Alta Complejidad del Bicentenario Esteban Echeverría, Unidad de Conocimiento Traslacional, Buenos Aires, Argentina), **Pietro Parisse** (Istituto Officina dei Materiali, National Research Council of Italy, Trieste, Italy; Elettra Sincrotrone Trieste S.C.p.A., Trieste, Italy), **Dong Jun Park** (University of California, San Diego, San Diego, CA, USA), **Juhee Park** (Center for Soft and Living Matter, Institute for Basic Science, Ulsan, Republic of Korea), **Young-Gyun Park** (Korea Advanced Institute of Science and Technology, Daejeon, Republic of Korea), **James G Patton** (Department of Biological Sciences, Vanderbilt University, Nashville, TN, USA), **Nicholas J Peake** (Sheffield Hallam University, Sheffield, UK), **D Michiel Pegtel** (Department of Pathology, Amsterdam UMC, Vrije Universiteit Amsterdam, Amsterdam, The Netherlands; Cancer Center Amsterdam, Imaging and Biomarkers, Amsterdam, The Netherlands), **Héctor Peinado** (Microenvironment and Metastasis Laboratory, Molecular Oncology Programme, Spanish National Cancer Research Center (CNIO), Madrid, Spain), **Francesca Perut** (Biomedical Science and Technologies and Nanobiotechnology Laboratory, IRCCS Istituto Ortopedico Rizzoli, Bologna, Italy), **Michael W Pfaffl** (Division of Animal Physiology and Immunology, School of Life Sciences Weihenstephan, Technical University of Munich, Freising, Germany), **Annika Pfeiffer** (Laboratory of Allergic Diseases, Division of Intramural Research, National Institute of Allergy and Infectious Diseases, National Institutes of Health, Bethesda, MD, USA), **Thanh Kha Phan** (Department of Biochemistry and Chemistry, La Trobe Institute for Molecular Science, La Trobe University, Melbourne, Australia), **Donald G Phinney** (Department of Molecular Medicine, The Herbert Wertheim UF Scripps Institute for Biomedical Innovation and Technology, Jupiter, FL, USA), **Leonidas A Phylactou** (The Cyprus Institute of Neurology & Genetics, Nicosia, Cyprus), **Silvia Picciolini** (IRCCS Fondazione Don Carlo Gnocchi Onlus, Milan, Italy), **Monika Pietrowska** (Maria Sklodowska-Curie National Research Institute of Oncology, Gliwice, Poland), **Max Piffoux** (Centre Léon Bérard, Lyon, France; Hospices civils de Lyon, Lyon, France), **Cláudio Pinheiro** (Laboratory of Experimental Cancer Research, Department of Human Structure and Repair, Ghent University, Ghent, Belgium; Cancer Research Institute Ghent, Ghent, Belgium), **Ryan C Pink** (Department of Biological and Medical Sciences, Faculty of Health and Life Sciences, Oxford Brookes University, Oxford, UK), **Michelle L Pleet** (Viral Immunology Section, Neuroimmunology Branch, National Institute of Neurological Disorders and Stroke, National Institutes of Health, Bethesda, MD, USA), **Gabriella Pocsfalvi** (Institute of Biosciences and BioResourses, National Research Council, Napoli, Italy), **Qi Hui Poh** (La Trobe University, Melbourne, Australia; Baker Heart & Diabetes Institute, Melbourne, Australia), **Edwin van der Pol** (Biomedical Engineering and Physics, Amsterdam UMC, location AMC, University of Amsterdam, Amsterdam, The Netherlands; Laboratory of Experimental Clinical Chemistry, Amsterdam UMC, location AMC, University of Amsterdam, Amsterdam, The Netherlands; Amsterdam Vesicle Center, Amsterdam University Medical Centers, Location AMC, University of Amsterdam, Amsterdam, The Netherlands), **Ganesha Poojary** (Department of Physiotherapy, Manipal College of Health Professions,

20013078, 2024, 2, Downloaded from https://isevjournals.onlinelibrary.wiley.com/doi/10.1002/jev2.12404 by Colorado State University, Wiley Online Library on [09/10/2024]. See the Terms and Conditions (https://onlinelibrary.wiley.com/terms-and-conditions) on Wiley Online Library for rules of use; OA articles are governed by the applicable Creative Commons License

Manipal Academy of Higher Education, Manipal, Karnataka, India), **Ivan KH Poon** (Department of Biochemistry and Chemistry, La Trobe Institute for Molecular Science, La Trobe University, Melbourne, Australia; Research Centre for Extracellular Vesicles, La Trobe University, Melbourne, Australia), **Giuseppina Poppa** (Department of Life, Health and Environmental Sciences, University of L'Aquila, L'Aquila, Italy), **Hernando A del Portillo** (ISGlobal, Barcelona Institute for Global Health, Hospital Clínic-Universitat de Barcelona, Barcelona, Spain; IGTP, Germans Trias i Pujol Health Research Institute, Badalona, Spain; Catalan Institution for Research and Advanced Studies (ICREA), Barcelona, Spain), **Vendula Pospichalova** (Faculty of Science, Masaryk University, Brno, Czech Republic), **Shirley Potter** (Mater Misericordiae University Hospital Dublin, Dublin, Ireland; The Conway Institute of Biomedical Science, University College Dublin, Dublin, Ireland; Irish Cancer Society, Dublin, Ireland), **Bonita H Powell** (Johns Hopkins University, Baltimore, MD, USA), **Simon J Powis** (University of St Andrews, St Andrews, UK), **Ilaria Prada** (Axxam S.p.A., Bresso, Milan, Italy), **Indira Prasadam** (Centre for Biomedical Technologies, School of Mechanical, Medical, and Process Engineering, Faculty of Engineering, Queensland University of Technology, Brisbane, Australia), **Christian Preußer** (Institute for Tumor Immunology, Philipps University Marburg, Marburg, Germany; EV Core Facility, Philipps University Marburg, Marburg, Germany), **Heather H Pua** (Department of Pathology, Microbiology, and Immunology, Vanderbilt University Medical Center, Nashville, TN, USA; Vanderbilt Center for Immunobiology, Vanderbilt University Medical Center, Nashville, TN, USA), **Ferdinando Pucci** (Department of Otolaryngology, Head & Neck Surgery, Oregon Health & Science University, Portland, OR, USA; Cell, Developmental and Cancer Biology, Oregon Health & Science University, Portland, OR, USA), **Florian Puhm** (Département de microbiologie et immunologie, Faculté de Médecine de l'Université Laval, Université Laval, Quebec, Canada; Centre de Recherche ARThrite (Arthrite Recherche Traitements) de l'Université Laval, Quebec, Canada), **Berta Puig** (Experimental Research in Stroke and Inflammation (ERSI) Group, Neurology Department, University Medical Center Hamburg-Eppendorf, Hamburg, Germany), **Lynn Pulliam** (University of California, San Francisco, San Francisco, CA, USA; Veterans Affairs Health Care, San Francisco, San Francisco, CA, USA), **Adityas Purnianto** (The University of Melbourne, Parkville, Australia; The Florey Institute of Neuroscience and Mental Health, The University of Melbourne, Parkville, Australia), **Johanna MM Puutio** (EV Group, Molecular and Integrative Biosciences Research Programme, Faculty of Biological and Environmental Sciences, University of Helsinki, Helsinki, Finland; EV Core, Molecular and Integrative Biosciences Research Programme, Faculty of Biological and Environmental Sciences, University of Helsinki, Helsinki, Finland), **Rachel C Quilang** (Leiden University Medical Center, Leiden, The Netherlands), **Piul S Rabbani** (New York University School of Medicine, New York, NY, USA), **Gorjana Rackov** (BioMed X GmbH, Heidelberg, Germany), **Annalisa Radeghieri** (University of Brescia, Department of Molecular and Translational Medicine, Brescia, Italy; CSGI—Research Center for Colloids and Nanoscience, Florence, Italy), **Claudia M Radu** (Department of Medicine, University of Padua, Padua, Italy), **Robert L Raffai** (University of California, San Francisco, San Francisco, CA, USA; Department of Veterans Affairs, San Francisco, CA, USA), **Alok Raghav** (Department of Anatomy and Cell Biology, Lee Gill Ya Cancer and Diabetes Institute, Gachon University, Incheon, Republic of Korea; Multidisciplinary Research Unit, GSVM Medical College Kanpur, Uttar Pradesh, India), **Mohammad Rahbari** (German Cancer Research Center, Division of Chronic Inflammation and Cancer, Heidelberg, Germany; Department of Surgery, University Mannheim, Medical Faculty Mannheim, University Hospital Heidelberg, Mannheim, Germany), **MD Matiur Rahman** (Department of Medicine, Faculty of Veterinary, Animal and Biomedical Sciences, Sylhet Agricultural University, Sylhet, Bangladesh; Laboratory of Food and Environmental Hygiene, Gifu University, Gifu, Japan), **Md Mostafizur Rahman** (South Asian University, New Delhi, India), **Alex J Rai** (Department of Pathology & Cell Biology, Columbia University Irving Medical Center, New York, NY, USA), **Stefania Raimondo** (Department of Biomedicine, Neuroscience and Advanced Diagnostics (Bi.N.D.), University of Palermo, Palermo, Italy), **Sneha Raju** (Faculty of Medicine, University of Toronto, Toronto, Canada), **Janusz Rak** (McGill University, Montreal, Canada), **Lausonia Ramaswamy** (Sysmex Corporation, Kobe, Japan), **Javier Ramirez-Ricardo** (Department of Pathology, Microbiology, and Immunology, Vanderbilt University Medical Center, Nashville, TN, USA), **Marcel I Ramirez** (Carlos Chagas Institute, Oswaldo Cruz Foundation (Fiocruz), Curitiba, Brazil), **Shikha Rani** (The University of Queensland, Brisbane, Australia), **Graca Raposo** (Institut Curie, PSL University, Paris, France; CNRS UMR144, Paris, France), **Hilal A Rather** (Wake Forest School of Medicine, Winston-Salem, NC, USA; Duke University, Durham, NC, USA), **Agnieszka Razim** (Medical University of Vienna, Vienna, Austria; Hirszfeld Institute of Immunology and Experimental Therapy, Polish Academy of Sciences, Wroclaw, Poland), **Antonia Reale** (Myeloma Research Group, Australian Centre for Blood Diseases, Central Clinical School, Monash University—The Alfred, Melbourne, Australia; Medical Oncology, Cabrini Malvern, Melbourne, Australia), **Eduardo Reategui** (William G. Lowrie Department of Chemical and Biomolecular Engineering, The Ohio State University, Columbus, OH, USA; Comprehensive Cancer Center, The Ohio State University, Columbus, OH, USA), **Caroline J Reddel** (ANZAC Research Institute, Concord Repatriation General Hospital, Concord, Australia; The University of Sydney, Camperdown, Australia), **Shivakumar K Reddy** (Centre for Molecular Neurosciences, Kasturba Medical College Manipal, Manipal Academy of Higher Education, Manipal, India), **Stephen Redenti** (Department of Biology, Lehman College, City University of New York, New York, NY, USA; Biochemistry and Biology Doctoral Programs, City University of New York, New York, NY, USA), **Samantha L Reed** (Emory University Department of Human Genetics, Atlanta, GA, USA), **Neta Regev-Rudzki** (Department of Biomolecular Sciences, Weizmann Institute of Science, Rehovot, Israel), **Katrin S Reiners** (Institute of Clinical Chemistry and Clinical Pharmacology, University Hospital Bonn, Bonn, Germany), **Nataša Resnik** (Institute of Cell Biology, Faculty of Medicine, University of Ljubljana, Ljubljana, Slovenia), **Gregory E Rice** (Centre for Clinical Research, The

20013078, 2024, 2, Downloaded from https://isevjournals.onlinelibrary.wiley.com/doi/10.1002/jev2.12404 by Colorado State University, Wiley Online Library on [09/10/2024]. See the Terms and Conditions (https://onlinelibrary.wiley.com/terms-and-conditions) on Wiley Online Library for rules of use; OA articles are governed by the applicable Creative Commons License

20013078, 2024, 2, Downloaded from https://isevjournals.onlinelibrary.wiley.com/doi/10.1002/jev2.12404 by Colorado State University, Wiley Online Library on [09/10/2024]. See the Terms and Conditions (https://onlinelibrary.wiley.com/terms-and-conditions) on Wiley Online Library for rules of use; OA articles are governed by the applicable Creative Commons License

University of Queensland, Herston, Australia; Inoviq Limited, Notting Hill, Australia), **Franz L Ricklefs** (Department of Neurosurgery, University Medical Center Hamburg-Eppendorf, Hamburg, Germany), **Andrea Ridolfi** (Department of Physics and Astronomy, and LaserLaB Amsterdam, Vrije Universiteit Amsterdam, Amsterdam, The Netherlands), **Kirsi Rilla** (University of Eastern Finland, Kuopio, Finland), **Michael P Rimmer** (Institute of Regeneration and Repair, Centre for Reproductive Health, University of Edinburgh, Edinburgh, UK; School of Medicine, University of St Andrews, Fife, UK), **Kelly CS Roballo** (Edward Via College of Osteopathic Medicine, Blacksburg, VA, USA; Virginia Maryland College of Veterinary Medicine, Virginia Tech, Blacksburg, Virginia, USA), **Paul D Robbins** (Institute on the Biology of Aging, University of Minnesota, Minneapolis, MN, USA), **David D Roberts** (Laboratory of Pathology, Center for Cancer Research, National Cancer Institute, National Institutes of Health, Bethesda, MD, USA), **Jordi Roca** (Department of Medicine and Animal Surgery, Veterinary Science, University of Murcia, Murcia, Spain), **Avital A Rodal** (Brandeis University, Waltham, MA, USA), **Dorival M Rodrigues-Junior** (Department of Medical Biochemistry and Microbiology, Science for Life Laboratory, Biomedical Center, Uppsala University, Uppsala, Sweden), **Marcio L Rodrigues** (Carlos Chagas Institute, Oswaldo Cruz Foundation (Fiocruz), Curitiba, Brazil; Paulo de Goes Microbiology Institute, Federal University of Rio de Janeiro (UFRJ), Rio de Janeiro, Brazil), **Marieke T Roefs** (Evercyte GmbH, Vienna, Austria), **Russell G Rogers** (Smidt Heart Institute, Cedars-Sinai Medical Center, Los Angeles, CA, USA), **Eva Rohde** (Department of Transfusion Medicine, University Hospital, Salzburger Landeskliniken GmbH of Paracelsus Medical University, Salzburg, Austria; GMP Unit, Paracelsus Medical University, Salzburg, Austria; Transfer Centre for Extracellular Vesicle Theralytic Technologies, EV-TT, Salzburg, Austria), **Tatu Rojalin** (Department of Biomedical Engineering, University of California, Davis, Davis, CA, USA; Expansion Therapeutics, Structural Biology and Biophysics, Jupiter, FL, USA), **Rita Romani** (Department of Medicine and Surgery, University of Perugia, Perugia, Italy), **Miriam Romano** (Center for Colloid and Surface Science (CSGI), Florence, Italy; Department of Molecular and Translational Medicine, University of Brescia, Brescia, Italy), **Sophie Rome** (CarMeN Laboratory, UMR INRAE 1397/INSERM 1060, University of Lyon, Lyon, France), **Rok Romih** (Institute of Cell Biology, Faculty of Medicine, University of Ljubljana, Ljubljana, Slovenia), **Anna Romolo** (Laboratory of Clinical Biophysics, Faculty of Health Sciences, University of Ljubljana, Ljubljana, Slovenia), **Tatiane De Rossi** (Brazilian Biosciences National Laboratory, Brazilian Center for Research in Energy and Materials (CNPEM), Campinas, Brazil), **Kasper M Rouschop** (Department of Radiotherapy, GROW-School for Oncology and Reproduction, Maastricht University Medical Centre+, Maastricht, The Netherlands), **David A Routenberg** (Meso Scale Diagnostics, LLC., Rockville, MD, USA), **Quentin Roux** (Centre de Recherche en Cancérologie et Immunologie Intégrée Nantes Angers, INSERM U1307, CNRS UMR6075, Nantes University, Nantes, France), **Andrew Rowland** (College of Medicine and Public Health, Flinders University, Adelaide, Australia), **Martin E van Royen** (Department of Pathology, Erasmus MC, Rotterdam, The Netherlands), **Annaïg J Rozo** (Aston University, Birmingham, UK), **David Rufino-Ramos** (Center for Neuroscience and Cell Biology, University of Coimbra, Coimbra, Portugal; Center for Innovative Biomedicine and Biotechnology, University of Coimbra, Coimbra, Portugal; Center for Genomic Medicine, Massachusetts General Hospital, Boston, MA, USA), **Aurelia Rughetti** (Department Experimental Medicine, Sapienza University of Rome, Rome, Italy), **Ashley E Russell** (Department of Biology, School of Science, Penn State Erie, The Behrend College, Erie, PA, USA), **Stephanie F Rutter** (La Trobe Institute for Molecular Science, La Trobe University, Melbourne, Australia), **Myltykbay S Rysmakhanov** (West-Kazakhstan Medical University, Aktobe, Kazakhstan), **Catherine A Sánchez** (Academic Department, Clínica Las Condes, Santiago, Chile; Faculty of Medicine, Universidad de Chile, Santiago, Chile), **Yoel Sadovsky** (Magee Womens Research Institute, University of Pittsburgh, Pittsburgh, PA, USA), **Reihaneh Safavi-Sohi** (Department of Chemistry and Biochemistry, University of Notre Dame, Notre Dame, IN, USA; Harper Cancer Research Institute, University of Notre Dame, Notre Dame, IN, USA; Department of Chemistry and Biochemistry, Seton Hall University, South Orange, NJ, USA), **Andras Saftics** (Department of Molecular Medicine, Beckman Research Institute, City of Hope Comprehensive Cancer Center, Duarte, CA, USA), **Ram Sagar** (Department of Genetic Medicine, Johns Hopkins University School of Medicine, Baltimore, MD, USA), **Susmita Sahoo** (Icahn School of Medicine at Mount Sinai, New York, NY, USA), **Nathaniel EB Saidu** (Department of Cancer Immunology, Institute of Cancer Research, Oslo University Hospital, Oslo, Norway), **Julien Saint-Pol** (Blood-Brain Barrier Laboratory (LBHE), UR 2465, University of Artois, Lens, France), **Edison Salas-Huenuleo** (Advanced Integrated Technologies, Santiago, Chile), **Ana I Salazar-Puerta** (The Ohio State University, Columbus, OH, USA), **Ayesha Saleem** (Faculty of Kinesiology, University of Manitoba, Winnipeg, Canada; Children's Hospital Research Institute of Manitoba (CHRIM), Winnipeg, Canada), **Ghasem Hosseini Salekdeh** (School of Natural Sciences, Macquarie University, Sydney, Australia), **Carlos Salomon** (Translational Extracellular Vesicles in Obstetrics and Gynae-Oncology Group, University of Queensland Centre for Clinical Research, Faculty of Medicine, Royal Brisbane and Women's Hospital, The University of Queensland, Brisbane, Australia; Departamento de Investigación, Postgrado y Educación Continua (DIPEC), Facultad de Ciencias de la Salud, Universidad del Alba, Santiago, Chile), **Amanda Salviano-Silva** (Department of Neurosurgery, University Medical Center Hamburg-Eppendorf, Hamburg, Germany), **Amankeldi A Salybekov** (Qazaq Institute of Innovative Medicine, Regenerative Medicine Division, Cell and Gene Therapy Department, Astana, Kazakhstan; Kidney Disease and Transplant Center, Shonan Kamakura General Hospital, Kamakura, Japan), **Mark Samuels** (Department of Biochemistry and Biomedicine, School of Life Sciences, University of Sussex, Brighton, UK), **Ursula S Sandau** (Department of Anesthesiology & Perioperative Medicine, Oregon Health & Science University, Portland, OR, USA), **Jascinta P Santavanond** (Department of Biochemistry and Chemistry, La Trobe Institute for Molecular Science, La Trobe University, Melbourne, Australia; Research Centre for Extracellular Vesicles, La Trobe University, Melbourne,

Australia), **Jessie Santoro** (School of Pharmacy and Pharmaceutical Sciences & Trinity Biomedical Sciences Institute, Trinity College Dublin, Dublin, Ireland), **Mark Santos** (Touro University Nevada, Henderson, NV, USA), **Rahul Sanwlani** (La Trobe Institute for Molecular Science, La Trobe University, Melbourne, Australia; Faculty of Health and Medical Sciences, School of Biosciences, University of Surrey, Surrey, UK), **Julie A Saugstad** (Department of Anesthesiology & Perioperative Medicine, Oregon Health & Science University, Portland, OR, USA), **Meike J Saul** (II. Medical Clinic and Polyclinic, University Medical Center Hamburg-Eppendorf, Hamburg, Germany), **Tine Hiorth Schøyen** (Cardiovascular Research Group, Department of Clinical Medicine, University of Tromsø—The Arctic University of Norway, Tromsø, Norway), **Irma Schabussova** (Institute of Specific Prophylaxis and Tropical Medicine, Center for Pathophysiology, Infectiology, and Immunology, Medical University of Vienna, Vienna, Austria), **Emilia Scharrig** (Thomas Jefferson University, Philadelphia, PA, USA), **Randy Schekman** (Department of Molecular and Cell Biology and Howard Hughes Medical Institute, University of California, Berkeley, Berkeley, CA, USA), **Jessica Schiavi-Tritz** (CNRS, LRGP, University of Lorraine, Nancy, France), **Raymond M Schiffelers** (CDL Research, University Medical Center Utrecht, Utrecht, The Netherlands), **Anna M Schmid** (Institute of Specific Prophylaxis and Tropical Medicine, Center for Pathophysiology, Infectiology, and Immunology, Medical University of Vienna, Vienna, Austria), **Raphael Schneider** (University of Toronto, Toronto, Canada), **Stefan Schneider** (Curexsys GmbH, Goettingen, Germany), **Andreina Schoeberlein** (Department of Obstetrics and Feto-maternal Medicine, University Women's Hospital, Inselspital, Bern University Hospital, Bern, Switzerland; Department for BioMedical Research (DBMR), University of Bern, Bern, Switzerland), **Jeffrey S Schorey** (Department of Biological Sciences, University of Notre Dame, Notre Dame, IN, USA), **Naohiro Seo** (Nanobio Device Laboratory, Graduate School of Bioengineering, The University of Tokyo, Tokyo, Japan), **Joaquin Seras-Franzoso** (Clinical Biochemistry, Drug Delivery & Therapy (CB-DDT), Vall d'Hebron Institut de Recerca (VHIR), Universitat Autònoma de Barcelona (UAB), Barcelona, Spain; Networking Research Center on Bioengineering, Biomaterials and Nanomedicine (CIBER-BBN), Instituto de Salud Carlos III, Madrid, Spain; Department of Genetics and Microbiology, Universitat Autònoma de Barcelona (UAB), Bellaterra, Spain), **Sanjay Shahi** (Department of Biochemistry and Genetics, La Trobe Institute for Molecular Science, La Trobe University, Melbourne, Australia), **Olga Shatnyeva** (Cell Therapy, Evotec International GmbH, Goettingen, Germany), **Deanna F Shea** (School of Biological Sciences, University of Auckland, Auckland, New Zealand), **Faezeh Shekari** (Department of Stem Cells and Developmental Biology, Cell Science Research Center, Royan Institute for Stem Cell Biology and Technology, ACECR, Tehran, Iran; Celer Diagnostics, Toronto, Canada), **Ganesh V Shelke** (Neurosciences and Cellular and Structural Biology Division, Eunice Kennedy Shriver National Institute of Child Health and Human Development, National Institutes of Health, Bethesda, MD, USA), **Ashok K Shetty** (Institute for Regenerative Medicine, Texas A&M University School of Medicine, College Station, Texas, USA; Department of Cell Biology and Genetics, Texas A&M University School of Medicine, College Station, Texas, USA), **Kiyotaka Shiba** (Cancer Institute, Japanese Foundation for Cancer Research, Tokyo, Japan), **Thomas Michael Shiju** (Cole Eye Institute, Cleveland Clinic, Cleveland, OH, USA), **Surya Shrivastava** (Novartis Biomedical Research, San Diego, CA, USA), **Sachin Shukla** (L V Prasad Eye Institute, Hyderabad, India), **Pia R-M Siljander** (EV Group, Molecular and Integrative Biosciences Research Programme, Faculty of Biological and Environmental Sciences, University of Helsinki, Helsinki, Finland; EV Core, Molecular and Integrative Biosciences Research Programme, Faculty of Biological and Environmental Sciences, University of Helsinki, Helsinki, Finland), **Andreia M Silva** (Anjarium Biosciences AG, Schlieren, Switzerland), **Ajay P Singh** (Department of Pathology and Mitchell Cancer Institute, Frederick P. Whiddon College of Medicine, University of South Alabama, Mobile, AL, USA), **Sangeeta Singh** (Wake Forest University, Winston-Salem, NC, USA), **Mikhail Skliar** (The University of Utah, Salt Lake City, UT, USA), **Johan Skog** (Exosome Diagnostics, a Bio-Techne brand, Boston, MA, USA), **Joost PG Sluijter** (Laboratory of Experimental Cardiology, Department of Cardiology, University Medical Center Utrecht, The Netherlands; UMC Utrecht Regenerative Medicine Center, Circulatory Health Research Center, University Medical Center Utrecht, Utrecht, The Netherlands), **Orman L Snyder** (Kansas State University, Manhattan, KS, USA), **Carolina Soekmadji** (School of Biomedical Sciences, Faculty of Medicine, The University of Queensland, Brisbane, Australia), **Ahmed Somaida** (Department of Pharmaceutics and Biopharmaceutics, Philipps University Marburg, Marburg, Germany), **Masaharu Somiya** (SANKEN, Osaka University, Ibaraki, Japan), **Karolina Soroczyńska** (Department of Biochemistry, Medical University of Warsaw, Warsaw, Poland; Postgraduate School of Molecular Medicine, Medical University of Warsaw, Warsaw, Poland), **Javier Sotillo** (Instituto de Salud Carlos III, Majadahonda, Spain), **Fernando Souza-Fonseca-Guimaraes** (Frazer Institute, The University of Queensland, Woolloongabba, Australia), **Sheila Spada** (Tumor of Immunology and Immunotherapy Unit, IRCCS Regina Elena National Cancer Institute, Rome, Italy), **Harry VM Spiers** (Department of Surgery, University of Cambridge, Cambridge, UK; Wellcome-MRC Cambridge Stem Cell Unit, University of Cambridge, Cambridge, UK; Department of Transplantation, Addenbrooke's Hospital, Cambridge, UK), **Joshua D Spitzberg** (Center for Systems Biology, Massachusetts General Hospital, Boston, MA, USA), **Akhil Srivastava** (Ellis Fischel Cancer Center, University of Missouri School of Medicine, Columbia, MO, USA), **Amit K Srivastava** (Department of Medicine, Sidney Kimmel Medical College, Thomas Jefferson University, Cardeza Foundation for Hematologic Research, Philadelphia, PA, USA), **Ewa Ł Stępień** (Department of Medical Physics, M. Smoluchowski Institute of Physics, Faculty of Physics, Astronomy and Applied Computer Science, Jagiellonian University, Krakow, Poland; Center for Theranostics, Jagiellonian University, Krakow, Poland), **Frederic St-Denis-Bissonnette** (Health Canada, Ontario, Canada; University of Ottawa, Ottawa, Canada), **Philip D Stahl** (Washington University, St. Louis, MO, USA), **Janine Stam** (Department of Analytical Biochemistry, Groningen Research Institute of Pharmacy, University of Groningen, Groningen, The Netherlands), **Oumaima**

20013078, 2024, 2, Downloaded from https://isevjournals.onlinelibrary.wiley.com/doi/10.1002/jev2.12404 by Colorado State University, Wiley Online Library on [09/10/2024]. See the Terms and Conditions (https://onlinelibrary.wiley.com/terms-and-conditions) on Wiley Online Library for rules of use; OA articles are governed by the applicable Creative Commons License

Stambouli (Institute for Transfusion Medicine, University Hospital Essen, University of Duisburg-Essen, Essen, Germany), **Bruce A Stanton** (Geisel School of Medicine at Dartmouth, Hanover, NH, USA), **Frank RM Stassen** (Maastricht University, Maastricht, The Netherlands), **Oskar Staufer** (INM—Leibniz Institute for New Materials, Saarbruecken, Germany; Max Planck Bristol Center for Minimal Biology, Bristol, UK; Center for Biophysics, Saarbruecken University, Saarbruecken, Germany), **Loïc Steiner** (Division of Immunology and Allergy, Department of Medicine, Karolinska Institutet, Stockholm, Sweden; Department of Clinical Immunology and Transfusion Medicine, Karolinska University Hospital, Stockholm, Sweden), **Ganna Stepanova** (Faculty of Medicine, Institute of Translational Medicine, Semmelweis University, Budapest, Hungary), **Veronika Stoka** (J. Stefan Institute, Ljubljana, Slovenia), **Willem Stoorvogel** (Department Biomolecular Health Sciences, Faculty of Veterinary Medicine, Utrecht University, Utrecht, The Netherlands), **Elke Pogge von Strandmann** (Institute for Tumor Immunology, Philipps University Marburg, Marburg, Germany; EV Core Facility, Philipps University Marburg, Marburg, Germany), **Dirk Strunk** (Cell Therapy Institute, Paracelsus Medical University, Salzburg, Austria), **Stanley S Stylli** (Department of Surgery (RMH), The University of Melbourne, Parkville, Australia; Department of Neurosurgery, Royal Melbourne Hospital, Parkville, Australia), **Huaqi Su** (The Florey Institute of Neuroscience and Mental Health, The University of Melbourne, Parkville, Australia), **Subbaya Subramanian** (Department of Surgery, University of Minnesota, Minneapolis, MN, USA; Center for Immunology, University of Minnesota, Minneapolis, MN, USA; Masonic Cancer Center, University of Minnesota, Minneapolis, MN, USA), **Bingdong Sui** (The Fourth Military Medical University, Xi'an, China), **Sonal Sukreet** (University of California, San Diego, San Diego, CA, USA; University of Nebraska-Lincoln, Lincoln, NE, USA), **Elias Sulaiman** (The Hatter Cardiovascular Institute, University College London, London, UK), **Bong Hwan Sung** (Department of Cell and Developmental Biology, School of Medicine, Vanderbilt University, Nashville, TN, USA; The Vanderbilt Center for Extracellular Vesicle Research, School of Medicine, Vanderbilt University, Nashville, TN, USA), **Vijaya Sunkara** (Ulsan National Institute of Science & Technology, Ulsan, Republic of Korea; Center for Soft and Living Matter, Institute for Basic Science, Ulsan, Republic of Korea), **Zucai Suo** (Department of Biomedical Sciences, Florida State University College of Medicine, Tallahassee, FL, USA), **Per Svenningsen** (Department of Molecular Medicine, University of Southern Denmark, Odense, Denmark), **Julian Swatler** (Nencki Institute of Experimental Biology, Warsaw, Poland; IRCCS Humanitas Research Hospital, Rozzano, Milan, Italy), **Simon Swift** (Waipapa Taumata Rau University of Auckland, Auckland, New Zealand), **Emma KC Symonds** (University of Otago, Wellington, New Zealand), **Viktoria Szeifert** (Stanford University, Department of Pathology, Stanford, CA, USA), **Imola Cs Szigyártó** (Research Centre for Natural Sciences, Institute of Materials and Environmental Chemistry, Budapest, Hungary), **Eszter Á Tóth** (Department of Genetics, Cell- and Immunobiology, Semmelweis University, Budapest, Hungary), **Neslihan P Taşlı** (Department of Genetics and Biotechnology, Yeditepe University, İstanbul, Turkey), **Hidetoshi Tahara** (Institute of Biomedical & Health Sciences, Department of Cellular and Molecular Biology, Hiroshima University, Hiroshima, Japan), **Ryou-u Takahashi** (Department of Cellular and Molecular Biology, Graduate School of Biomedical and Health Science, Hiroshima University, Hiroshima, Japan), **Yoshinobu Takakura** (Graduate School of Pharmaceutical Sciences, Kyoto University, Kyoto, Japan), **Osamu Takikawa** (National Center for Geriatrics and Gerontology, Aichi, Japan), **Kaloyan Takov** (National Heart and Lung Institute, Imperial College London, London, UK), **Vera A Tang** (Flow Cytometry & Virometry Core Facility, Department of Biochemistry, Microbiology, & Immunology, University of Ottawa, Ottawa, Canada), **Simona Taverna** (Institute of Translational Pharmacology (IFT), National Research Council of Italy (CNR), Palermo, Italy), **Nadim Tawil** (Research Institute of McGill University Health Centre, Montreal, Canada), **Loes Teeuwen** (Karolinska Institutet, Solna, Sweden), **Sandra Tejedor** (System Biology Research Center, University of Skövde, Skövde, Sweden ; Research and Early Development, Cardiovascular, Renal and Metabolism (CVRM), Biopharmaceuticals R&D, AstraZeneca, Gothenburg, Sweden), **Dmitry Ter-Ovanesyan** (Wyss Institute for Biologically Inspired Engineering, Harvard University, Boston, MA, USA), **Tobias Tertel** (Institute for Transfusion Medicine, University Hospital Essen, University of Duisburg-Essen, Essen, Germany), **Clotilde Théry** (Institut Curie, INSERM U932, PSL University, Paris, France; CurieCoreTech Extracellular Vesicles, Institut Curie, Paris, France), **Abhimanyu Thakur** (Pritzker School of Molecular Engineering, Ben May Department for Cancer Research, University of Chicago, Chicago, IL, USA; Department of Neurosurgery, Massachusetts General Hospital, Harvard Medical School, Boston, MA, USA), **Tara Thompson-Felix** (Yale University, New Haven, CT, USA), **Changhai Tian** (Department of Toxicology and Cancer Biology, University of Kentucky College of Medicine, Lexington, KY, USA), **Aleksei Tikhonov** (Gustave Roussy, Villejuif, France), **Swasti Tiwari** (Sanjay Gandhi Postgraduate Institute of Medical Sciences, Lucknow, India; Georgetown University, Washington, DC, USA), **Wei Seong Toh** (Department of Orthopaedic Surgery, Yong Loo Lin School of Medicine, National University of Singapore, Singapore), **John J Tomes** (Aberystwyth University, Aberystwyth, UK), **Elisa Tonoli** (Nottingham Trent University, Nottingham, UK), **Ana C Torrecilhas** (Laboratório de Imunologia Celular e Bioquímica de Fungos e Protozoários, Departamento de Ciências Farmacêuticas, Instituto de Ciências Ambientais, Químicas e Farmacêuticas, Universidade Federal de São Paulo (UNIFESP) Campus Diadema, Diadema, Brazil), **Juan P Tosar** (Universidad de la República, Montevideo, Uruguay; Institut Pasteur de Montevideo, Montevideo, Uruguay), **Camille V Trinidad** (University of Kansas Medical Center, Kansas City, KS, USA), **Lucienne Tritten** (Swiss Tropical and Public Health Institute, Allschwil, Switzerland; University of Basel, Basel, Switzerland; Institute of Parasitology, University of Zurich, Zurich, Switzerland), **Rucha Trivedi** (School of Biomedical Science, University of North Texas Health Science Center, Fort Worth, TX, USA), **Zach Troyer** (Department of Molecular and Comparative Pathobiology, Johns Hopkins University School of Medicine, Baltimore, MD, USA), **Migmar Tsamchoe** (Department of Anatomy and Cell Biology, McGill University, Quebec, Canada; McGill University Health

20013078, 2024, 2, Downloaded from https://isevjournals.onlinelibrary.wiley.com/doi/10.1002/jev2.12404 by Colorado State University, Wiley Online Library on [09/10/2024]. See the Terms and Conditions (https://onlinelibrary.wiley.com/terms-and-conditions) on Wiley Online Library for rules of use; OA articles are governed by the applicable Creative Commons License

Centre Research Institute, Quebec, Canada), **Vera Tscherrig** (Department of Obstetrics and Feto-maternal Medicine, University Women's Hospital, Inselspital, Bern University Hospital, Bern, Switzerland; Graduate School for Cellular and Biomedical Sciences (GCB), University of Bern, Bern, Switzerland; Department for BioMedical Research (DBMR), University of Bern, Bern, Switzerland), **Thupten Tsering** (Research Institute of McGill University Health Centre, Montreal, Canada; Department of Pathology, McGill University, Montreal, Canada), **Kristyna Turkova** (Institute of Biophysics of the Czech Academy of Sciences, Brno, Czech Republic; St. Anne's University Hospital Brno, International Clinical Research Center,Brno, Czech Republic), **Oleg S Tutanov** (Vanderbilt University Medical Center, Nashville, TN, USA), **Koji Ueda** (Japanese Foundation for Cancer Research, Tokyo, Japan), **Dinesh Upadhya** (Centre for Molecular Neurosciences, Kasturba Medical College Manipal, Manipal Academy of Higher Education, Manipal, India), **Fumihiko Urabe** (Department of Urology, The Jikei University School of Medicine, Tokyo, Japan), **Lorena Urbanelli** (Department of Chemistry, Biology and Biotechnology, University of Perugia, Perugia, Italy), **Ornella Urzì** (Dipartimento di Biomedicina, Neuroscienze e Diagnostica Avanzata (Bi.N.D), sezione di Biologia e Genetica, University of Palermo, Palermo, Italy; Sahlgrenska Center for Cancer Research and Wallenberg Centre for Molecular and Translational Medicine, Department of Surgery, Institute of Clinical Sciences, Sahlgrenska Academy, University of Gothenburg, Gothenburg, Sweden), **Zivile Useckaite** (College of Medicine and Public Health, Flinders University, Adelaide, Australia), **Elena Vacchi** (Neurodegenerative Diseases Group, Laboratory for Translational Research, Ente Ospedaliero Cantonale, Bellinzona, Switzerland), **Pieter Vader** (University Medical Center Utrecht, Utrecht, The Netherlands), **Riccardo Vago** (IRCCS San Raffaele Scientific Institute, Milan, Italy; Università Vita-Salute San Raffaele, Milan, Italy), **Hadi Valadi** (Department of Rheumatology and Inflammation Research, Institute of Medicine, Sahlgrenska Academy, University of Gothenburg, Gothenburg, Sweden), **Sami Valkonen** (Division of Pharmaceutical Biosciences, Faculty of Pharmacy, University of Helsinki, Helsinki, Finland; School of Pharmacy, University of Eastern Finland, Kuopio, Finland), **Francesco Valle** (Consiglio Nazionale delle Ricerche—Istituto per lo Studio dei Materiali Nanostrutturati, Bologna, Italy; Consorzio Interuniversitario per lo Sviluppo dei Sistemi a Grande Interfase, Florence, Italy), **Manuel Varas-Godoy** (Centro de Biología Celular y Biomedicina, Facultad de Medicina y Ciencia, Universidad San Sebastián, Santiago, Chile; Centro Ciencia & Vida, Fundación Ciencia & Vida, Santiago, Chile; Advanced Center for Chronic Diseases, Santiago, Chile), **Zoltán Varga** (Biological Nanochemistry Research Group, Institute of Materials and Environmental Chemistry, Research Centre for Natural Sciences, Budapest, Hungary; Department of Physical Chemistry and Materials Science, Faculty of Chemical Technology and Biotechnology, Budapest University of Technology and Economics, Budapest, Hungary), **Zoltan Varga** (Biological Nanochemistry Research Group, Institute of Materials and Environmental Chemistry, Research Centre for Natural Sciences, Budapest, Hungary; Department of Biophysics and Radiation Biology, Semmelweis University, Budapest, Hungary), **M Helena Vasconcelos** (Faculty of Pharmacy, University of Porto, Porto, Portugal; Institute for Research and Innovation in Health, University of Porto, Porto, Portugal), **Ivan J Vechetti** (University of Nebraska-Lincoln, Lincoln, NE, USA), **Sara I Veiga** (Krantz Family Center for Cancer Research, Massachusetts General Hospital, Boston, MA, USA; Department of Medicine, Harvard Medical School, Boston, MA, USA), **Laura J Vella** (The Florey Institute of Neuroscience and Mental Health, The University of Melbourne, Parkville, Australia; Department of Surgery, The Royal Melbourne Hospital, Melbourne, Australia; The University of Melbourne, Parkville, Australia), **Émilie Velot** (French National Center for Scientific Research, Molecular Engineering and Physiopathology, University of Lorraine, Nancy, France), **Frederik J Verweij** (Department of Cell Biology, Neurobiology and Biophysics, Utrecht University, Utrecht, The Netherlands; Centre for Living Technologies, Alliance Eindhoven University of Technology, Wageningen University & Research, University Medical Center Utrecht, The Netherlands), **Beate Vestad** (Research Institute of Internal Medicine, Oslo University Hospital Rikshospitalet, Oslo, Norway; Norwegian PSC Research Center, Oslo University Hospital Rikshospitalet, Oslo, Norway), **Ludovic Vinay** (Faculty of Medicine, Université Laval, Quebec, Canada; CHU de Quebec Research Center, Quebec, Canada), **Margarida Viola** (University Medical Center Utrecht, Utrecht, The Netherlands), **Tamás Visnovitz** (Department of Genetics, Cell- and Immunobiology, Semmelweis University, Budapest, Hungary; Department of Plant Physiology and Molecular Plant Biology, ELTE Eötvös Loránd University, Budapest, Hungary), **Dolores Di Vizio** (Department of Surgery, Division of Cancer Biology and Therapeutics, Cedars-Sinai Medical Center, Los Angeles, CA, USA), **Wyatt N Vreeland** (National Institute of Standards & Technology, Gaithersburg, MD, USA), **Krisztina V Vukman** (Department of Genetics, Cell- and Immunobiology, Semmelweis University, Budapest, Hungary), **Philippa K Wade** (Centre for Biomolecular Sciences, Biodiscovery Institute 3, School of Medicine, University of Nottingham, Nottingham, UK), **Simonides I van de Wakker** (UMC Utrecht Regenerative Medicine Center, Circulatory Health Research Center, University Medical Center Utrecht, Utrecht, The Netherlands), **Lucas Walther** (Transgene SA, Illkirch-Graffenstaden, France; INSERM UMR_S1109, Tumor Biomechanics, Strasbourg, France; University of Strasbourg, Strasbourg, France), **Tong Wang** (MOE Key Laboratory of Tumor Molecular Biology, Institute of Life and Health Engineering, College of Life Science and Technology, The First Affiliated Hospital, Jinan University, Guangzhou, China), **Xiaoqin Wang** (Advanced Drug Delivery, Pharmaceutical Sciences, Biopharmaceutics R&D, AstraZeneca, Gothenburg, Sweden), **Dionysios C Watson** (Sylvester Comprehensive Cancer Center, University of Miami, Miami, FL, USA), **Marca HM Wauben** (Department of Biomolecular Health Sciences, Faculty of Veterinary Medicine, Utrecht University, Utrecht, The Netherlands), **Alissa M Weaver** (Vanderbilt University School of Medicine, Nashville, TN, USA), **Jason P Webber** (Institute of Life Science, Swansea University Medical School, Swansea University, Swansea, UK), **Viktoria Weber** (Department for Biomedical Research, University for Continuing Education Krems, Krems, Austria), **Ann M Wehman** (University of Denver, Denver, USA), **Luisa Weiss** (School of Biomolecular and Biomedical Science, University College Dublin, Dublin,

20013078, 2024, 2, Downloaded from https://isevjournals.onlinelibrary.wiley.com/doi/10.1002/jev2.12404 by Colorado State University, Wiley Online Library on [09/10/2024]. See the Terms and Conditions (https://onlinelibrary.wiley.com/terms-and-conditions) on Wiley Online Library for rules of use; OA articles are governed by the applicable Creative Commons License

Ireland; Conway SPHERE Research Group, Conway Institute, University College Dublin, Dublin, Ireland), **Mark L Weiss** (Kansas State University, Manhattan, KS, USA), **René Weiss** (Center for Biomedical Technology, Department for Biomedical Research, University for Continuing Education Krems, Krems, Austria), **Ralph Weissleder** (Center for Systems Biology, Harvard Medical School, Boston, MA, USA; Interventional Radiology, Massachusetts General Hospital, Boston, MA, USA), **Joshua A Welsh** (Translational Nanobiology Section, Laboratory of Pathology, National Cancer Institute, National Institutes of Health, Bethesda, MD, USA), **Yi Wen** (Kansas State University College of Veterinary Medicine, Manhattan, KS, USA; Department of Molecular and Comparative Pathobiology, Johns Hopkins University School of Medicine, Baltimore, MD, USA), **Olivier de Wever** (Laboratory of Experimental Cancer Research, Department of Human Structure and Repair, Ghent University, Ghent, Belgium; Cancer Research Institute Ghent, Ghent, Belgium), **Asa M Wheelock** (Respiratory Medicine Unit, Department of Medicine Solna & Centre for Molecular Medicine, Karolinska Institutet, Stockholm, Sweden; Department of Respiratory Medicine and Allergy, Karolinska University Hospital Solna, Stockholm, Sweden), **Katherine E White** (University of Nottingham, Nottingham, UK), **Bradley Whitehead** (Department of Clinical Medicine, Aarhus University, Aarhus, Denmark), **Theresa L Whiteside** (University of Pittsburgh Medical Center, Pittsburgh, PA, USA), **Joseph Whitley** (Department of Pharmaceutical and Biomedical Sciences, University of Georgia, Athens, GA, USA), **Zoltán Wiener** (Department of Genetics, Cell- and Immunobiology, Semmelweis University, Budapest, Hungary), **Andre J van Wijnen** (Department of Biochemistry, University of Vermont, Burlington, VT, USA), **Oscar PB Wiklander** (Department of Laboratory Medicine, Karolinska Institutet, Stockholm, Sweden), **Sarah Williams** (International Society for Extracellular Vesicles), **Charisse N Winston** (Alzheimer's Therapeutic Research Institute, University of Southern California, Los Angeles, CA, USA), **Kenneth W Witwer** (Department of Molecular and Comparative Pathobiology, Johns Hopkins University School of Medicine, Baltimore, MD, USA; EV Core Facility "EXCEL", Institute for Basic Biomedical Sciences, Johns Hopkins University School of Medicine, Baltimore, MD, USA; The Richman Family Precision Medicine Center of Excellence in Alzheimer's Disease, Johns Hopkins University School of Medicine, Baltimore, MD, USA), **Martin Wolf** (Cell Therapy Institute, Paracelsus Medical University, Salzburg, Austria), **Joy Wolfram** (School of Chemical Engineering, The University of Queensland, Brisbane, Australia; Australian Institute for Bioengineering and Nanotechnology, The University of Queensland, Brisbane, Australia; Department of Nanomedicine, Houston Methodist Research Institute, Houston, TX, USA), **Liang Wu** (Department of Nephrology, The First Affiliated Hospital of Shaoyang University, Shaoyang, Hunan, China; Erasmus MC Transplant Institute, University Medical Center Rotterdam, Department of Internal Medicine, Division of Nephrology and Transplantation, Rotterdam, The Netherlands), **Yunjie Wu** (Department of Pharmacology, University of Oslo, Oslo, Norway), **Magdalena E Wysmołek** (Division of Parasitology, Department of Preclinical Sciences, Institute of Veterinary Medicine, Warsaw University of Life Sciences-SGGW, Warsaw, Poland; Institute of Specific Prophylaxis and Tropical Medicine, Center for Pathophysiology, Infectiology, and Immunology, Medical University of Vienna, Vienna, Austria), **Patricia Xander** (Instituto de Ciências Ambientais, Químicas e Farmacêuticas, Departamento de Ciências Farmacêuticas, Universidade Federal de São Paulo Campus Diadema, Diadema, Brazil; Instituto de Ciências Ambientais, Químicas e Farmacêuticas, Programa de Pós-Graduação Biologia-Química, Universidade Federal de São Paulo Campus Diadema, Diadema, Brazil), **Cristina PR Xavier** (Instituto de Investigação e Inovação em Saúde (i3S), University of Porto, Porto, Portugal; Cancer Drug Resistance Group, Institute of Molecular Pathology and Immunology (IPATIMUP), University of Porto, Porto, Portugal), **Yu Xiao** (School of Pharmaceutical Sciences, Tsinghua University, Beijing, China; Tsinghua University-Peking University Joint Center for Life Sciences, Tsinghua University, Beijing, China; Beijing Advanced Innovation Center for Structural Biology, Tsinghua University, Beijing, China), **Rong Xu** (Australian Centre for Blood Diseases, Central Clinical School, Monash University, Melbourne, Australia; Victorian Heart Institute, Monash University, Melbourne, Australia), **María Yáñez-Mó** (Dept Biología Molecular, Instituto Universitario de Biología Molecular, Universidad Autónoma de Madrid, Madrid, Spain; Centro de Biología Molecular Severo Ochoa, Instituto de Investigaciones Sanitarias Princesa, Madrid, Spain), **Tomofumi Yamamoto** (Tokyo Medical University, Tokyo, Japan; National Institute of Health Sciences, Kanagawa, Japan), **Yuki Yamamoto** (Department of Cellular and Molecular Biology, Graduate School of Biomedical and Health Science, Hiroshima University, Hiroshima, Japan), **Yusuke Yamamoto** (Laboratory of Integrative Oncology, National Cancer Center Research Institute, Tokyo, Japan), **Xiaomei Yan** (Department of Chemical Biology, Xiamen University, Xiamen, China), **Lifang Yang** (Eastern Virginia Medical School, Norfolk, VA, USA), **Yongkang Yang** (Institute for Cell Engineering, Johns Hopkins University School of Medicine, Baltimore, MD, USA; The Johns Hopkins University School of Medicine, Sidney Kimmel Comprehensive Cancer Center, Baltimore, MD, USA), **Reza Yarani** (Translational Type 1 Diabetes Research, Department of Clinical Research, Steno Diabetes Center Copenhagen, Herlev, Denmark), **Kyungmoo Yea** (Department of New Biology, DGIST, Daegu, Republic of Korea.; New Biology Research Center, DGIST, Daegu 43024, Republic of Korea.), **Laura Yedigaryan** (Translational Cardiomyology Laboratory, Stem Cell and Developmental Biology, Department of Development and Regeneration, KU Leuven, Leuven, Belgium), **Vengala Rao Yenuganti** (Department of Animal Biology, School of Life Sciences, University of Hyderabad, Hyderabad, India), **Saigopalakrishna S Yerneni** (Carnegie Mellon University, Pittsburgh, PA, USA), **Vincent Yeung** (Harvard Medical School, Boston, MA, USA; Schepens Eye Research Institute of Mass Eye and Ear, Boston, MA, USA), **Yagmur Yildizhan** (Rega Institute for Medical Research, KU Leuven, Leuven, Belgium), **Hang Yin** (School of Pharmaceutical Sciences, Tsinghua University, Beijing, China), **Akira Yokoi** (Nagoya University Graduate School of Medicine, Nagoya, Japan; Nagoya University Institute for Advanced Research, Nagoya, Japan), **Yusuke Yoshioka** (Department of Molecular and Cellular Medicine, Institute of Medical Science, Tokyo Medical University, Tokyo, Japan), **Yang**

20013078, 2024, 2, Downloaded from https://isevjournals.onlinelibrary.wiley.com/doi/10.1002/jev2.12404 by Colorado State University, Wiley Online Library on [09/10/2024]. See the Terms and Conditions (https://onlinelibrary.wiley.com/terms-and-conditions) on Wiley Online Library for rules of use; OA articles are governed by the applicable Creative Commons License

You (Department of Neuroscience, Mayo Clinic Florida, Jacksonville, FL, USA), **Ling-Qing Yuan** (Department of Metabolism and Endocrinology, National Clinical Research Center for Metabolic Diseases, the Second Xiangya Hospital, Central South University, Changsha, China), **Samuel Tassi Yunga** (Cancer Early Detection Advanced Research Center (CEDAR), Knight Cancer Institute, School of Medicine, Oregon Health & Science University, Portland, OR, USA; Department of Biomedical Engineering, School of Medicine, Oregon Health & Science University, Portland, OR, USA), **Amin Zakeri** (Department of Clinical Medicine, Aarhus University, Aarhus, Denmark), **Augusto Zani** (Developmental and Stem Cell Biology Program, SickKids Research institute, Toronto, Canada; Division of General and Thoracic Surgery, Hospital for Sick Children, Toronto, Canada; Department of Surgery, University of Toronto, Toronto, Canada), **Michele Zanoni** (IRCCS Istituto Romagnolo per lo Studio dei Tumori (IRST) "Dino Amadori", Meldola, Italy), **Valentina Zappulli** (Department of Comparative Biomedicine and Food Science, University of Padua, Padua, Italy), **Natasa Zarovni** (Day One Srl, Rome, Italy), **Jana Zarubova** (Department of Bioengineering, University of California, Los Angeles, Los Angeles, CA, USA), **Janos Zempleni** (University of Nebraska-Lincoln, Lincoln, NE, USA), **Vytautas Žėkas** (Department of Physiology, Biochemistry, Microbiology and Laboratory Medicine, Institute of Biomedical Sciences, Faculty of Medicine, Vilnius University, Vilnius, Lithuania), **Andrea Zendrini** (Center for Colloid and Surface Science (CSGI), Florence, Italy; Department of Molecular and Translational Medicine, University of Brescia, Brescia, Italy), **Hao Zhang** (Institute of Precision Cancer Medicine and Pathology, School of Medicine, Jinan University, Guangzhou, China), **Qin Zhang** (Department of Medicine, Vanderbilt University Medical Center, Nashville, TN, USA), **Zheng Zhao** (Sartorius Stedim North America, Ann Arbor, MI, USA), **Lei Zheng** (Department of Laboratory Medicine, Nanfang Hospital, Southern Medical University, Guangzhou, China), **Yinghong Zhou** (School of Dentistry, The University of Queensland, Brisbane, Australia), **Antje M Zickler** (Department of Laboratory Medicine, Karolinska Institutet, Stockholm, Sweden; ME Cell Therapy and Allogenic Stem Cell Transplantation CAST, Karolinska University Hospital, Stockholm, Sweden), **Andries Zijlstra** (Department of Pathology, Vanderbilt University Medical Center, Nashville, TN, USA; Genentech, South San Francisco, CA, USA), **Alan J Zimmerman** (Barnett Institute of Chemical and Biological Analysis, Department of Chemistry and Chemical Biology, Northeastern University, Boston, MA, USA), **Pascale Zimmermann** (KU Leuven, Leuven, Belgium; Centre de Recherche en Cancérologie de Marseille, Merseille, France), **Angela M Zivkovic** (Department of Nutrition, University of California, Davis, Davis, CA, USA), **Davide Zocco** (Lonza Siena, Siena, Italy), **Ewa K Zuba-Surma** (Department of Cell Biology, Faculty of Biochemistry, Biophysics and Biotechnology, Jagiellonian University, Krakow, Poland), **Haseeb Zubair** (Surgical Sciences Division, Department of Surgery, School of Medicine, University of Maryland, Baltimore, MD, USA; Program in Oncology, UM Greenebaum Comprehensive Cancer Center, Baltimore, MD, USA).

CONFLICT OF INTEREST STATEMENT

Pierre Arsène is CEO of Mursla Ltd. and Chair of Exosla Ltd; Antonella Bongiovanni has filed the patent (PCT/EP2020/086622) related to microalgal-derived extracellular vesicles and is co-founder and CEO of the spin-off company EVEBiofactory srl; Paul C Boutros sits on the scientific advisory boards of Sage Bionetworks, Intersect Diagnostics Inc and BioSymetrics Inc; Xandra O Breakefield is Scientific Advisor for Evox and MGB-Cannon; Edit I Buzas is a member of the Scientific Advisory Boards of Sphere Gene Therapeutics Inc (Boston, MA, USA) and ReNeuron (UK); David RF Carter is an Evox Therapeutics Ltd, employee and stock option holder; Anna Cifuentes-Rius was employed by Exopharm Ltd when the survey was conducted ACR is a shareholder of Exopharm Ltd; Rossella Crescitelli has developed multiple EV-associated patents for putative clinical utilisation and they own equity in Exocure Sweden AB; Andrew Devitt is Chief Technical Officer, co-founder, and director of EVolution Therapeutics; Erez Eitan works and has equity in NeuroDex, a company that develops EV-based diagnostics; Samir EL Andaloussi is co-founder of Evox Therapeutics; Ludwig Ermann Lundberg is an employee of BioGaia; Susanne Gabrielsson has a patent on B cell derived EVs in immune therapy and is part of the Scientific Advisory Board of Anjarium Biosciences; Ernesto Gargiulo is a medical writer at Novo Nordisk A/S; Bernd Giebel is a member of the Scientific Advisory Boards of Mursla Ltd, ReNeuron, and PLBioscience and is the founding director of Exosla Ltd; André Görgens is a consultant for and has equity interest in Evox Therapeutics (Oxford, UK) and is an inventor on several patent applications and patents related to EV isolation, modification, and analytics; Ahmed GE Ibrahim owns stock in Capricor Therapeutics; Marzena Kurzawa-Akanbi Kurzawa-Akanbi is an academic founder and Chief Scientific Officer at ESP Diagnostics Limited; Quentin Lubart is an employee of Abbelight (Cachan, France), which constructs and sells super-resolution microscopes to characterize EVs; Fabrice Lucien receives consulting fees from Mursla Bio and Early is Good; Elisa Lázaro-Ibáñez is employed by AstraZeneca R&D; Jan Lötvall is co-founder of two companies aiming to develop EV-based therapeutics, Exocure Sweden AB and Nexo Therapeutics AB, has been or is a scientific consultant for NanoSight, Clara Biotech and ExoCoBio, and was Editor-in-Chief of the Journal of Extracellular Vesicles during the development and publication of MISEV2023; Eduardo Marbán has founder's equity in Capricor Therapeutics Inc; Maurizio Muraca is a consultant for EXO Biologics (Liège, Belgium); Irina Nazarenko is a scientific adviser of CapCO Bio GmbH; D Michiel Pegtel has research funding from Takeda, Amgen, Abbvie, and Gilead, is an advisor of Y2Y BV, and has equity in Y2Y BV; Janusz Rak is inventor on a patent on oncogene-carrying EVs that is licensed to NXPharmaGene; Gregory E Rice is Chief Scientific Officer, Inoviq Ltd; Andrew Rowland is a recipient of investigator-initiated research funding outside of the scope of this publication from AstraZeneca, Boehringer Ingelheim, and Pfizer and is a recipient of speakers fees from Boehringer Ingelheim and Genentech; Susmita Sahoo performs research funded by Evox Therapeutics; Randy Schekman is a member of the Scientific Advisory Boards

20013078, 2024, 2, Downloaded from https://isevjournals.onlinelibrary.wiley.com/doi/10.1002/jev2.12404 by Colorado State University, Wiley Online Library on [09/10/2024]. See the Terms and Conditions (https://onlinelibrary.wiley.com/terms-and-conditions) on Wiley Online Library for rules of use; OA articles are governed by the applicable Creative Commons License

of companies involved in the analysis and diagnostic/therapeutic application of various forms of synthetic or native extracellular vesicles in diagnostics: Sail (formerly Senda) Biomedicines, Invaio Sciences, Mercy BioAnalytics, and Esperovax; Raymond M Schiffelers is CSO of Excytex bv; Johan Skog is an employee of Bio-Techne and an inventor on patents for exosome isolation and analysis; Vera A Tang is a consultant for Beckman Coulter on small particle flow cytometry; Clotilde Théry is an inventor on a submitted patent on therapeutic use of EVs; Edwin van der Pol is cofounder and shareholder of Exometry, Amsterdam, The Netherlands; Joshua A Welsh is an inventor on patents and patent applications related to EV analysis; Oscar PB Wiklander has stock options with Evox Therapeutics; Kenneth W Witwer is or has been an advisory board member of ShiftBio, Exopharm, NeuroDex, NovaDip, and ReNeuron; holds NeuroDex options; privately consults as Kenneth Witwer Consulting; and conducts research under a sponsored research agreement with Ionis Pharmaceuticals.

ORCID

Joshua A. Welsh https://orcid.org/0000-0002-1097-9756
Deborah C. I. Goberdhan https://orcid.org/0000-0003-0645-6714
Edit I. Buzas https://orcid.org/0000-0002-3744-206X
Benedetta Bussolati https://orcid.org/0000-0002-3663-5134
Houjian Cai https://orcid.org/0000-0003-4887-2652
Juan M. Falcon-Perez https://orcid.org/0000-0003-3133-0670
Andrew F. Hill https://orcid.org/0000-0001-5581-2354
Metka Lenassi https://orcid.org/0000-0002-9488-6855
Sujata Mohanty https://orcid.org/0000-0002-0047-4914
Rienk Nieuwland https://orcid.org/0000-0002-5671-3400
Takahiro Ochiya https://orcid.org/0000-0002-0776-9918
Susmita Sahoo https://orcid.org/0000-0002-7279-1564
Ana C. Torrecilhas https://orcid.org/0000-0001-5724-2199
Lei Zheng https://orcid.org/0000-0003-2576-8780
Andries Zijlstra https://orcid.org/0000-0001-8460-8803
Marco Brucale https://orcid.org/0000-0001-7244-4389
Randy P. Carney https://orcid.org/0000-0001-8193-1664
Rossella Crescitelli https://orcid.org/0000-0002-1714-3169
Norman J. Haughey https://orcid.org/0000-0001-5194-4122
Elena S. Martens-Uzunova https://orcid.org/0000-0002-5363-2525
Lauren A. Newman https://orcid.org/0000-0003-3303-1666
Eva Rohde https://orcid.org/0000-0001-8692-886X
Ursula S. Sandau https://orcid.org/0000-0002-3646-7089
Julie A. Saugstad https://orcid.org/0000-0002-2996-9611
Faezeh Shekari https://orcid.org/0000-0001-6026-5412
Juan P. Tosar https://orcid.org/0000-0002-2021-2479
Marca H. M. Wauben https://orcid.org/0000-0003-0360-0311
Ann M. Wehman https://orcid.org/0000-0001-9826-4132
Alan J. Zimmerman https://orcid.org/0000-0001-6280-4790
Clotilde Théry https://orcid.org/0000-0001-8294-6884
Kenneth W. Witwer https://orcid.org/0000-0003-1664-4233

REFERENCES

Aalberts, M., van Dissel-Emiliani, F. M., van Adrichem, N. P., van Wijnen, M., Wauben, M. H., Stout, T. A., & Stoorvogel, W. (2012). Identification of distinct populations of prostasomes that differentially express prostate stem cell antigen, annexin A1, and GLIPR2 in humans. *Biology of Reproduction*, *86*, 82.

Aasebø, E., Opsahl, J. A., Bjørlykke, Y., Myhr, K. M., Kroksveen, A. C., & Berven, F. S. (2014). Effects of blood contamination and the rostro-caudal gradient on the human cerebrospinal fluid proteome. *PLoS ONE*, *9*, e90429.

Abbatiello, S. E., Mani, D. R., Schilling, B., Maclean, B., Zimmerman, L. J., Feng, X., Cusack, M. P., Sedransk, N., Hall, S. C., Addona, T., Allen, S., Dodder, N. G., Ghosh, M., Held, J. M., Hedrick, V., Inerowicz, H. D., Jackson, A., Keshishian, H., Kim, J. W., … Carr, S. A. (2013). Design, implementation and multisite evaluation of a system suitability protocol for the quantitative assessment of instrument performance in liquid chromatography-multiple reaction monitoring-MS (LC-MRM-MS). *Molecular & Cellular Proteomics*, *12*, 2623–2639.

Aebersold, R., & Mann, M. (2003). Mass spectrometry-based proteomics. *Nature*, *422*, 198–207.

Aguet, F., Antonescu, C. N., Mettlen, M., Schmid, S. L., & Danuser, G. (2013). Advances in analysis of low signal-to-noise images link dynamin and AP2 to the functions of an endocytic checkpoint. *Developmental Cell*, *26*, 279–291.

Ainsztein, A. M., Brooks, P. J., Dugan, V. G., Ganguly, A., Guo, M., Howcroft, T. K., Kelley, C. A., Kuo, L. S., Labosky, P. A., Lenzi, R., McKie, G. A., Mohla, S., Procaccini, D., Reilly, M., Satterlee, J. S., Srinivas, P. R., Church, E. S., Sutherland, M., Tagle, D. A., … Venkatachalam, S. (2015). The NIH extracellular RNA communication consortium. *Journal of Extracellular Vesicles*, *4*, 27493.

20013078, 2024, 2, Downloaded from https://isevjournals.onlinelibrary.wiley.com/doi/10.1002/jev2.12404 by Colorado State University, Wiley Online Library on [09/10/2024]. See the Terms and Conditions (https://onlinelibrary.wiley.com/terms-and-conditions) on Wiley Online Library for rules of use; OA articles are governed by the applicable Creative Commons License

Alexander, M., Hu, R., Runtsch, M. C., Kagele, D. A., Mosbruger, T. L., Tolmachova, T., Seabra, M. C., Round, J. L., Ward, D. M., & O'Connell, R. M. (2015). Exosome-delivered microRNAs modulate the inflammatory response to endotoxin. *Nature Communications*, *6*, 7321.

Ambrose, A. R., Dechantsreiter, S., Shah, R., Montero, M. A., Quinn, A. M., Hessel, E. M., Beinke, S., Tannahill, G. M., & Davis, D. M. (2020). Corrected super-resolution microscopy enables nanoscale imaging of autofluorescent lung macrophages. *Biophysical Journal*, *119*, 2403–2417.

Aps, J. K., & Martens, L. C. (2005). Review: The physiology of saliva and transfer of drugs into saliva. *Forensic Science International*, *150*, 119–131.

Arab, T., Mallick, E. R., Huang, Y., Dong, L., Liao, Z., Zhao, Z., Gololobova, O., Smith, B., Haughey, N. J., Pienta, K. J., Slusher, B. S., Tarwater, P. M., Tosar, J. P., Zivkovic, A. M., Vreeland, W. N., Paulaitis, M. E., & Witwer, K. W. (2021). Characterization of extracellular vesicles and synthetic nanoparticles with four orthogonal single-particle analysis platforms. *Journal of Extracellular Vesicles*, *10*, e12079.

Arifin, D. R., Witwer, K. W., & Bulte, J. W. M. (2022). Non-Invasive imaging of extracellular vesicles: Quo vaditis in vivo? *Journal of Extracellular Vesicles*, *11*, e12241.

Arigony, A. L., de Oliveira, I. M., Machado, M., Bordin, D. L., Bergter, L., Prá, D., & Henriques, J. A. (2013). The influence of micronutrients in cell culture: A reflection on viability and genomic stability. *BioMed Research International*, *2013*, 597282.

Arraud, N., Linares, R., Tan, S., Gounou, C., Pasquet, J. M., Mornet, S., & Brisson, A. R. (2014). Extracellular vesicles from blood plasma: Determination of their morphology, size, phenotype and concentration. *Journal of Thrombosis and Haemostasis*, *12*, 614–627.

Avalos-Padilla, Y., Georgiev, V. N., Lantero, E., Pujals, S., Verhoef, R., Borgheti-Cardoso L, N., Albertazzi, L., Dimova, R., & Fernàndez-Busquets, X. (2021). The ESCRT-III machinery participates in the production of extracellular vesicles and protein export during *Plasmodium falciparum* infection. *Plos Pathogens*, *17*, e1009455.

Bachurski, D., Schuldner, M., Nguyen, P. H., Malz, A., Reiners, K. S., Grenzi, P. C., Babatz, F., Schauss, A. C., Hansen, H. P., Hallek, M., & Pogge von Strandmann, E. (2019). Extracellular vesicle measurements with nanoparticle tracking analysis – An accuracy and repeatability comparison between NanoSight NS300 and ZetaView. *Journal of Extracellular Vesicles*, *8*, 1596016.

Bai, L., Du, Y., Peng, J., Liu, Y., Wang, Y., Yang, Y., & Wang, C. (2014). Peptide-based isolation of circulating tumor cells by magnetic nanoparticles. *Journal of Materials Chemistry B*, *2*, 4080–4088.

Balaj, L., Atai, N. A., Chen, W., Mu, D., Tannous, B. A., Breakefield, X. O., Skog, J., & Maguire, C. A. (2015). Heparin affinity purification of extracellular vesicles. *Scientific Reports*, *5*, 10266.

Balaj, L., Lessard, R., Dai, L., Cho, Y. J., Pomeroy, S. L., Breakefield, X. O., & Skog, J. (2011). Tumour microvesicles contain retrotransposon elements and amplified oncogene sequences. *Nature Communications*, *2*, 180.

Baldrich, P., Rutter, B. D., Karimi, H. Z., Podicheti, R., Meyers, B. C., & Innes, R. W. (2019). Plant extracellular vesicles contain diverse small RNA species and are enriched in 10- to 17-nucleotide "Tiny" RNAs. *Plant Cell*, *31*, 315–324.

Ballard, O., & Morrow, A. L. (2013). Human milk composition: Nutrients and bioactive factors. *Pediatric Clinics of North America*, *60*, 49–74.

Banigan, M. G., Kao, P. F., Kozubek, J. A., Winslow, A. R., Medina, J., Costa, J., Schmitt, A., Schneider, A., Cabral, H., Cagsal-Getkin, O., Vanderburg, C. R., & Delalle, I. (2013). Differential expression of exosomal microRNAs in prefrontal cortices of schizophrenia and bipolar disorder patients. *PLoS ONE*, *8*, e48814.

Barreiro, K., Dwivedi, O. P., Valkonen, S., Groop, P. H., Tuomi, T., Holthofer, H., Rannikko, A., Yliperttula, M., Siljander, P., Laitinen, S., Serkkola, E., Af Hallstrom, T., Forsblom, C., Groop, L., & Puhka, M. (2021). Urinary extracellular vesicles: Assessment of pre-analytical variables and development of a quality control with focus on transcriptomic biomarker research. *Journal of Extracellular Vesicles*, *10*, e12158.

Beale, D. J., Jones, O. A., Karpe, A. V., Dayalan, S., Oh, D. Y., Kouremenos, K. A., Ahmed, W., & Palombo, E. A. (2016). A review of analytical techniques and their application in disease diagnosis in breathomics and salivaomics research. *International Journal of Molecular Sciences*, *18*, 24.

Beckett, K., Monier, S., Palmer, L., Alexandre, C., Green, H., Bonneil, E., Raposo, G., Thibault, P., Borgne, R. L., & Vincent, J. P. (2013). Drosophila S2 cells secrete wingless on exosome-like vesicles but the wingless gradient forms independently of exosomes. *Traffic (Copenhagen, Denmark)*, *14*, 82–96.

Beer, K. B., Rivas-Castillo, J., Kuhn, K., Fazeli, G., Karmann, B., Nance, J. F., Stigloher, C., & Wehman, A. M. (2018). Extracellular vesicle budding is inhibited by redundant regulators of TAT-5 flippase localization and phospholipid asymmetry. *PNAS*, *115*, E1127–E1136.

Beer, K. B., & Wehman, A. M. (2017). Mechanisms and functions of extracellular vesicle release in vivo-What we can learn from flies and worms. *Cell Adhesion & Migration*, *11*, 135–150.

Benedikter, B. J., Bouwman, F. G., Vajen, T., Heinzmann, A. C. A., Grauls, G., Mariman, E. C., Wouters, E. F. M., Savelkoul, P. H., Lopez-Iglesias, C., Koenen, R. R., Rohde, G. G. U., & Stassen, F. R. M. (2017). Ultrafiltration combined with size exclusion chromatography efficiently isolates extracellular vesicles from cell culture media for compositional and functional studies. *Scientific Reports*, *7*, 15297.

Benmoussa, A., Michel, S., Gilbert, C., & Provost, P. (2020). Isolating multiple extracellular vesicles subsets, including exosomes and membrane vesicles, from bovine milk using sodium citrate and differential ultracentrifugation. *Bio-Protocol*, *10*, e3636.

Bereman, M. S. (2015). Tools for monitoring system suitability in LC MS/MS centric proteomic experiments. *Proteomics*, *15*, 891–902.

Berne, B. J., & Pecora, R. (1976). *Dynamic light scattering: With applications to chemistry, biology, and physics*. Wiley.

Bettin, B., Gasecka, A., Li, B., Dhondt, B., Hendrix, A., Nieuwland, R., & van der Pol, E. (2022). Removal of platelets from blood plasma to improve the quality of extracellular vesicle research. *Journal of Thrombosis and Haemostasis*, *20*, 2679–2685.

Betzig, E., Patterson, G. H., Sougrat, R., Lindwasser, O. W., Olenych, S., Bonifacino, J. S., Davidson, M. W., Lippincott-Schwartz, J., & Hess, H. F. (2006). Imaging intracellular fluorescent proteins at nanometer resolution. *Science*, *313*, 1642–1645.

Bhattarai, K. R., Kim, H. R., & Chae, H. J. (2018). Compliance with saliva collection protocol in healthy volunteers: strategies for managing risk and errors. *International journal of Medical Sciences*, *15*, 823–831.

Bitto, N. J., Chapman, R., Pidot, S., Costin, A., Lo, C., Choi, J., D'Cruze, T., Reynolds, E. C., Dashper, S. G., Turnbull, L., Whitchurch, C. B., Stinear, T. P., Stacey, K. J., & Ferrero, R. L. (2017). Bacterial membrane vesicles transport their DNA cargo into host cells. *Scientific Reports*, *7*, 7072.

Bitto, N. J., Cheng, L., Johnston, E. L., Pathirana, R., Phan, T. K., Poon, I. K. H., O'Brien-Simpson, N. M., Hill, A. F., Stinear, T. P., & Kaparakis-Liaskos, M. (2021). Staphylococcus aureus membrane vesicles contain immunostimulatory DNA, RNA and peptidoglycan that activate innate immune receptors and induce autophagy. *Journal of Extracellular Vesicles*, *10*, e12080.

Bitto, N. J., & Kaparakis-Liaskos, M. (2022). Methods of bacterial membrane vesicle production, purification, quantification, and examination of their immunogenic functions. *Methods in Molecular Biology*, *2523*, 43–61.

Bitto, N. J., Zavan, L., Johnston, E. L., Stinear, T. P., Hill, A. F., & Kaparakis-Liaskos, M. (2021). Considerations for the analysis of bacterial membrane vesicles: Methods of vesicle production and quantification can influence biological and experimental outcomes. *Microbiology Spectrum*, *9*, e0127321.

Blijdorp, C. J., Tutakhel, O. A. Z., Hartjes, T. A., van den Bosch, T. P. P., van Heugten, M. H., Rigalli, J. P., Willemsen, R., Musterd-Bhaggoe, U. M., Barros, E. R., Carles-Fontana, R., Carvajal, C. A., Arntz, O. J., van de Loo, F. A. J., Jenster, G., Clahsen-van Groningen, M. C., Cuevas, C. A., Severs, D., Fenton, R. A., van Royen, M. E., … Hoorn, E. J. (2021). Comparing approaches to normalize, quantify, and characterize urinary extracellular vesicles. *Journal of the American Society of Nephrology*, *32*, 1210–1226.

20013078, 2024, 2, Downloaded from https://isevjournals.onlinelibrary.wiley.com/doi/10.1002/jev2.12404 by Colorado State University, Wiley Online Library on [09/10/2024]. See the Terms and Conditions (https://onlinelibrary.wiley.com/terms-and-conditions) on Wiley Online Library for rules of use; OA articles are governed by the applicable Creative Commons License

Boere, J., van de Lest, C. H. A., de Grauw, J. C., Plomp, S. G. M., Libregts, S., Arkesteijn, G. J. A., Malda, J., Wauben, M. H. M., & van Weeren, P. R. (2019). Extracellular vesicles in synovial fluid from juvenile horses: No age-related changes in the quantitative profile. *Veterinary Journal*, *244*, 91–93.
Boing, A. N., van der Pol, E., Grootemaat, A. E., Coumans, F. A., Sturk, A., & Nieuwland, R. (2014). Single-step isolation of extracellular vesicles by size-exclusion chromatography. *Journal of Extracellular Vesicles*, *3*, 00–00.
Bonsergent, E., Grisard, E., Buchrieser, J., Schwartz, O., Théry, C., & Lavieu, G. (2021). Quantitative characterization of extracellular vesicle uptake and content delivery within mammalian cells. *Nature Communications*, *12*, 1864.
Bonsergent, E., & Lavieu, G. (2019). Content release of extracellular vesicles in a cell-free extract. *Febs Letters*, *593*, 1983–1992.
Bordanaba-Florit, G., Royo, F., Kruglik, S. G., & Falcón-Pérez, J. M. (2021). Using single-vesicle technologies to unravel the heterogeneity of extracellular vesicles. *Nature Protocols*, *16*, 3163–3185.
Borghesan, M., Fafián-Labora, J., Eleftheriadou, O., Carpintero-Fernández, P., Paez-Ribes, M., Vizcay-Barrena, G., Swisa, A., Kolodkin-Gal, D., Ximénez-Embún, P., Lowe, R., Martín-Martín, B., Peinado, H., Muñoz, J., Fleck, R. A., Dor, Y., Ben-Porath, I., Vossenkamper, A., Muñoz-Espin, D., & O'Loghlen, A. (2019). Small extracellular vesicles are key regulators of non-cell autonomous intercellular communication in senescence via the interferon protein IFITM3. *Cell Reports*, *27*, 3956–3971.e6.
Bortot, B., Apollonio, M., Rampazzo, E., Valle, F., Brucale, M., Ridolfi, A., Ura, B., Addobbati, R., Di Lorenzo, G., Romano, F., Buonomo, F., Ripepi, C., Ricci, G., & Biffi, S. (2021). Small extracellular vesicles from malignant ascites of patients with advanced ovarian cancer provide insights into the dynamics of the extracellular matrix. *Molecular Oncology*, *15*, 3596–3614.
Bose, S., Aggarwal, S., Singh, D. V., & Acharya, N. (2020). Extracellular vesicles: An emerging platform in gram-positive bacteria. *Microbial Cell*, *7*, 312–322.
Botha, J., Handberg, A., & Simonsen, J. B. (2022). Lipid-based strategies used to identify extracellular vesicles in flow cytometry can be confounded by lipoproteins: Evaluations of annexin V, lactadherin, and detergent lysis. *Journal of Extracellular Vesicles*, *11*, e12200.
Bracht, J. W. P., Los, M., van Eijndhoven, M. A. J., Bettin, B., van der Pol, E., Pegtel, D. M., & Nieuwland, R. (2023). Platelet removal from human blood plasma improves detection of extracellular vesicle-associated miRNA. *Journal of Extracellular Vesicles*, *12*, e12302.
Brown, L., Wolf, J. M., Prados-Rosales, R., & Casadevall, A. (2015). Through the wall: Extracellular vesicles in Gram-positive bacteria, mycobacteria and fungi. *Nature Reviews Microbiology*, *13*, 620–630.
Budnik, V., Ruiz-Cañada, C., & Wendler, F. (2016). Extracellular vesicles round off communication in the nervous system. *Nature Reviews Neuroscience*, *17*, 160–172.
Buntsma, N. C., Gąsecka, A., Roos, Y., van Leeuwen, T. G., van der Pol, E., & Nieuwland, R. (2022). EDTA stabilizes the concentration of platelet-derived extracellular vesicles during blood collection and handling. *Platelets*, *33*, 764–771.
Burger, D., Thibodeau, J. F., Holterman, C. E., Burns, K. D., Touyz, R. M., & Kennedy, C. R. (2014). Urinary podocyte microparticles identify prealbuminuric diabetic glomerular injury. *Journal of the American Society of Nephrology*, *25*, 1401–1407.
Busatto, S., Vilanilam, G., Ticer, T., Lin, W. L., Dickson, D. W., Shapiro, S., Bergese, P., & Wolfram, J. (2018). Tangential flow filtration for highly efficient concentration of extracellular vesicles from large volumes of fluid. *Cells*, *7*(12), 273.
Busatto, S., Yang, Y., Iannotta, D., Davidovich, I., Talmon, Y., & Wolfram, J. (2022). Considerations for extracellular vesicle and lipoprotein interactions in cell culture assays. *Journal of Extracellular Vesicles*, *11*, e12202.
Busatto, S., Zendrini, A., Radeghieri, A., Paolini, L., Romano, M., Presta, M., & Bergese, P. (2019). The nanostructured secretome. *Biomaterials Science*, *8*, 39–63.
Bustin, S. A., Benes, V., Garson, J. A., Hellemans, J., Huggett, J., Kubista, M., Mueller, R., Nolan, T., Pfaffl, M. W., Shipley, G. L., Vandesompele, J., & Wittwer, C. T. (2009). The MIQE Guidelines: Minimum information for publication of quantitative real-time PCR experiments. *Clinical Chemistry*, *55*, 611–622.
Butler, H. J., Ashton, L., Bird, B., Cinque, G., Curtis, K., Dorney, J., Esmonde-White, K., Fullwood, N. J., Gardner, B., Martin-Hirsch, P. L., Walsh, M. J., McAinsh, M. R., Stone, N., & Martin, F. L. (2016). Using Raman spectroscopy to characterize biological materials. *Nature Protocols*, *11*, 664–687.
Buzas, E. I. (2022). Opportunities and challenges in studying the extracellular vesicle corona. *Nature Cell Biology*, *24*, 1322–1325.
Cai, J., Han, Y., Ren, H., Chen, C., He, D., Zhou, L., Eisner, G. M., Asico, L. D., Jose, P. A., & Zeng, C. (2013). Extracellular vesicle-mediated transfer of donor genomic DNA to recipient cells is a novel mechanism for genetic influence between cells. *Journal of Molecular Cell Biology*, *5*, 227–238.
Calò, A., Reguera, D., Oncins, G., Persuy, M. A., Sanz, G., Lobasso, S., Corcelli, A., Pajot-Augy, E., & Gomila, G. (2014). Force measurements on natural membrane nanovesicles reveal a composition-independent, high Young's modulus. *Nanoscale*, *6*, 2275–2285.
Cambier, L., Stachelek, K., Triska, M., Jubran, R., Huang, M., Li, W., Zhang, J., Li, J., & Cobrinik, D. (2021). Extracellular vesicle-associated repetitive element DNAs as candidate osteosarcoma biomarkers. *Scientific Reports*, *11*, 94.
Cameron, J. M., Butler, H. J., Palmer, D. S., & Baker, M. J. (2018). Biofluid spectroscopic disease diagnostics: A review on the processes and spectral impact of drying. *Journal of Biophotonics*, *11*, e201700299.
Cameron, S., Gillio-Meina, C., Ranger, A., Choong, K., & Fraser, D. D. (2019). Collection and analyses of cerebrospinal fluid for pediatric translational research. *Pediatric Neurology*, *98*, 3–17.
Carlomagno, C., Giannasi, C., Niada, S., Bedoni, M., Gualerzi, A., & Brini, A. T. (2021). Raman fingerprint of extracellular vesicles and conditioned media for the reproducibility assessment of cell-free therapeutics. *Frontiers in Bioengineering and Biotechnology*, *9*, 640617.
Carrel, A., & Burrows, M. T. (1911). Cultivation of tissues in vitro and its technique. *Journal of Experimental Medicine*, *13*, 387–396.
Carreras-Planella, L., Cucchiari, D., Cañas, L., Juega, J., Franquesa, M., Bonet, J., Revuelta, I., Diekmann, F., Taco, O., Lauzurica, R., & Borràs, F. E. (2021). Urinary vitronectin identifies patients with high levels of fibrosis in kidney grafts. *Journal of Nephrology*, *34*, 861–874.
Catalano, M., & O'Driscoll, L. (2020). Inhibiting extracellular vesicles formation and release: A review of EV inhibitors. *Journal of Extracellular Vesicles*, *9*, 1703244.
Cavallaro, S., Pevere, F., Stridfeldt, F., Görgens, A., Paba, C., Sahu, S. S., Mamand, D. R., Gupta, D., El Andaloussi, S., Linnros, J., & Dev, A. (2021). Multiparametric profiling of single nanoscale extracellular vesicles by combined atomic force and fluorescence microscopy: Correlation and heterogeneity in their molecular and biophysical features. *Small*, *17*, e2008155.
Cavallaro, S., Hååg, P., Viktorsson, K., Krozer, A., Fogel, K., Lewensohn, R., Linnros, J., & Dev, A. (2021). Comparison and optimization of nanoscale extracellular vesicle imaging by scanning electron microscopy for accurate size-based profiling and morphological analysis. *Nanoscale Advances*, *3*(11), 3053–3063.
Champagne-Jorgensen, K., Mian, M. F., McVey Neufeld, K. A., Stanisz, A. M., & Bienenstock, J. (2021). Membrane vesicles of *Lacticaseibacillus rhamnosus* JB-1 contain immunomodulatory lipoteichoic acid and are endocytosed by intestinal epithelial cells. *Scientific Reports*, *11*, 13756.
Chen, C., Zong, S., Wang, Z., Lu, J., Zhu, D., Zhang, Y., & Cui, Y. (2016). Imaging and intracellular tracking of cancer-derived exosomes using single-molecule localization-based super-resolution microscope. *ACS Applied Materials & Interfaces*, *8*, 25825–25833.
Chen, C., Zong, S., Wang, Z., Lu, J., Zhu, D., Zhang, Y., Zhang, R., & Cui, Y. (2018). Visualization and intracellular dynamic tracking of exosomes and exosomal miRNAs using single molecule localization microscopy. *Nanoscale*, *10*, 5154–5162.
Chernyshev, V. S., Rachamadugu, R., Tseng, Y. H., Belnap, D. M., Jia, Y., Branch, K. J., Butterfield, A. E., Pease, L. F., Bernard, P. S., & Skliar, M. (2015). Size and shape characterization of hydrated and desiccated exosomes. *Analytical and Bioanalytical Chemistry*, *407*, 3285–3301.

20013078, 2024, 2, Downloaded from https://isevjournals.onlinelibrary.wiley.com/doi/10.1002/jev2.12404 by Colorado State University, Wiley Online Library on [09/10/2024]. See the Terms and Conditions (https://onlinelibrary.wiley.com/terms-and-conditions) on Wiley Online Library for rules of use; OA articles are governed by the applicable Creative Commons License

Chiappin, S., Antonelli, G., Gatti, R., & De Palo, E. F. (2007). Saliva specimen: A new laboratory tool for diagnostic and basic investigation. *Clinica Chimica Acta*, *383*, 30–40.
Christianson, H. C., Svensson, K. J., van Kuppevelt, T. H., Li, J. P., & Belting, M. (2013). Cancer cell exosomes depend on cell-surface heparan sulfate proteoglycans for their internalization and functional activity. *PNAS*, *110*, 17380–17385.
Chuo, S. T., Chien, J. C., & Lai, C. P. (2018). Imaging extracellular vesicles: Current and emerging methods. *Journal of Biomedical Science*, *25*, 91.
Churchman, L. S, & Spudich, J. A. (2012). Colocalization of fluorescent probes: Accurate and precise registration with nanometer resolution. *Cold Spring Harbor Protocols*, *2012*, 141–149.
Cianciaruso, C., Beltraminelli, T., Duval, F., Nassiri, S., Hamelin, R., Mozes, A., Gallart-Ayala, H., Ceada Torres, G., Torchia, B., Ries, C. H., Ivanisevic, J., & De Palma, M. (2019). Molecular profiling and functional analysis of macrophage-derived tumor extracellular vesicles. *Cell Reports*, *27*, 3062–3080.e11.
Cimorelli, M., Nieuwland, R., Varga, Z., & van der Pol, E. (2021). Standardized procedure to measure the size distribution of extracellular vesicles together with other particles in biofluids with microfluidic resistive pulse sensing. *PLoS ONE*, *16*, e0249603.
Ciullo, A., Li, C., Li, L., Ungerleider, K. C., Peck, K., Marbán, E., & Ibrahim, A. G. E. (2022). Biodistribution of unmodified cardiosphere-derived cell extracellular vesicles using single RNA tracing. *Journal of Extracellular Vesicles*, *11*, e12178.
Clancy, J. W., Sheehan, C. S., Boomgarden, A. C., & D'Souza-Schorey, C. (2022). Recruitment of DNA to tumor-derived microvesicles. *Cell Reports*, *38*, 110443.
Clayton, A., Boilard, E., Buzas, E. I., Cheng, L., Falcón-Perez, J. M., Gardiner, C., Gustafson, D., Gualerzi, A., Hendrix, A., Hoffman, A., Jones, J., Lässer, C., Lawson, C., Lenassi, M., Nazarenko, I., O'Driscoll, L., Pink, R., Siljander, P. R., Soekmadji, C., … Nieuwland, R. (2019). Considerations towards a roadmap for collection, handling and storage of blood extracellular vesicles. *Journal of Extracellular Vesicles*, *8*, 1647027.
Clayton, A., Buschmann, D., Byrd, J. B., Carter, D. R. F., Cheng, L., Compton, C., Daaboul, G., Devitt, A., Falcon-Perez, J. M., Gardiner, C., Gustafson, D., Harrison, P., Helmbrecht, C., Hendrix, A., Hill, A., Hoffman, A., Jones, J. C., Kalluri, R., Kang, J. Y., … Nieuwland, R. (2018). Summary of the ISEV workshop on extracellular vesicles as disease biomarkers, held in Birmingham, UK, during December 2017. *Journal of Extracellular Vesicles*, *7*, 1473707.
Clupper, M., Gill, R., Elsayyid, M., Touroutine, D., Caplan, J. L., & Tanis, J. E. (2022). Kinesin-2 motors differentially impact biogenesis of extracellular vesicle subpopulations shed from sensory cilia. *Iscience*, *25*, 105262.
Coffman, V. C., & Wu, J. Q. (2014). Every laboratory with a fluorescence microscope should consider counting molecules. *Molecular Biology of the Cell*, *25*, 1545–1548.
Colombo, F., Norton, E. G., & Cocucci, E. (2021). Microscopy approaches to study extracellular vesicles. *Biochimica et Biophysica Acta (BBA) - General Subjects*, *1865*, 129752.
Correll, V. L., Otto, J. J., Risi, C. M., Main, B. P., Boutros, P. C., Kislinger, T., Galkin, V. E., Nyalwidhe, J. O., Semmes, O. J., & Yang, L. (2022). Optimization of small extracellular vesicle isolation from expressed prostatic secretions in urine for in-depth proteomic analysis. *Journal of Extracellular Vesicles*, *11*, e12184.
Corrigan, L., Redhai, S., Leiblich, A., Fan, S. J., Perera, S. M., Patel, R., Gandy, C., Wainwright, S. M., Morris, J. F., Hamdy, F., Goberdhan, D. C., & Wilson, C. (2014). BMP-regulated exosomes from Drosophila male reproductive glands reprogram female behavior. *Journal of Cell Biology*, *206*, 671–688.
Corso, G., Heusermann, W., Trojer, D., Görgens, A., Steib, E., Voshol, J., Graff, A., Genoud, C., Lee, Y., Hean, J., Nordin, J. Z., Wiklander, O. P. B., El Andaloussi, S., & Meisner-Kober, N. (2019). Systematic characterization of extracellular vesicle sorting domains and quantification at the single molecule – single vesicle level by fluorescence correlation spectroscopy and single particle imaging. *Journal of Extracellular Vesicles*, *8*, 1663043.
Costa-Silva, B., Aiello, N. M., Ocean, A. J., Singh, S., Zhang, H., Thakur, B. K., Becker, A., Hoshino, A., Mark, M. T., Molina, H., Xiang, J., Zhang, T., Theilen, T. M., García-Santos, G., Williams, C., Ararso, Y., Huang, Y., Rodrigues, G., Shen, T. L., … Lyden, D. (2015). Pancreatic cancer exosomes initiate pre-metastatic niche formation in the liver. *Nature Cell Biology*, *17*, 816–826.
Coumans, F. A., van der Pol, E., Boing, A. N., Hajji, N., Sturk, G., van Leeuwen, T. G., & Nieuwland, R. (2014). Reproducible extracellular vesicle size and concentration determination with tunable resistive pulse sensing. *Journal of Extracellular Vesicles*, *3*, 25922.
Coumans, F. A. W., Brisson, A. R., Buzas, E. I., Dignat-George, F., Drees, E. E. E., El-Andaloussi, S., Emanueli, C., Gasecka, A., Hendrix, A., Hill, A. F., Lacroix, R., Lee, Y., van Leeuwen, T. G., Mackman, N., Mager, I., Nolan, J. P., van der Pol, E., Pegtel, D. M., Sahoo, S., … Nieuwland, R. (2017). Methodological guidelines to study extracellular vesicles. *Circulation Research*, *120*, 1632–1648.
Crescitelli, R., Lässer, C., Jang, S. C., Cvjetkovic, A., Malmhäll, C., Karimi, N., Höög, J. L., Johansson, I., Fuchs, J., Thorsell, A., Gho, Y. S., Bagge, R. O, & Lötvall, J. (2020). Subpopulations of extracellular vesicles from human metastatic melanoma tissue identified by quantitative proteomics after optimized isolation. *Journal of Extracellular Vesicles*, *9*, 1722433.
Crescitelli, R., Lasser, C., & Lotvall, J. (2021). Isolation and characterization of extracellular vesicle subpopulations from tissues. *Nature Protocols*, *16*, 1548–1580.
Crescitelli, R., Lässer, C., Szabó, T. G., Kittel, A., Eldh, M., Dianzani, I., Buzás, E. I., & Lötvall, J. (2013). Distinct RNA profiles in subpopulations of extracellular vesicles: Apoptotic bodies, microvesicles and exosomes. *Journal of Extracellular Vesicles*, *2*, 20677.
Cvjetkovic, A., Jang, S. C., Konečná, B., Höög, J. L., Sihlbom, C., Lässer, C., & Lötvall, J. (2016). Detailed analysis of protein topology of extracellular vesicles – Evidence of unconventional membrane protein orientation. *Scientific Reports*, *6*, 36338.
Czarniak, N., Kamińska, J., Matowicka-Karna, J., & Koper-Lenkiewicz, O. M. (2023). Cerebrospinal fluid-basic concepts review. *Biomedicines*, *11*, 1461.
Daaboul, G. G., Gagni, P., Benussi, L., Bettotti, P., Ciani, M., Cretich, M., Freedman, D. S., Ghidoni, R., Ozkumur, A. Y., Piotto, C., Prosperi, D., Santini, B., Unlu, M. S., & Chiari, M. (2016). Digital detection of exosomes by interferometric imaging. *Scientific Reports*, *6*, 37246.
Das, S., Ansel, K. M., Bitzer, M., Breakefield, X. O., Charest, A., Galas, D. J., Gerstein, M. B., Gupta, M., Milosavljevic, A., McManus, M. T., Patel, T., Raffai, R. L., Rozowsky, J., Roth, M. E., Saugstad, J. A., Van Keuren-Jensen, K., Weaver, A. M., & Laurent, L. C. (2019). The extracellular RNA communication consortium: Establishing foundational knowledge and technologies for extracellular RNA research. *Cell*, *177*, 231–242.
Singorenko, D. P., Chang, V., Whitcombe, A., Simonov, D., Hong, J., Phillips, A., Swift, S., & Blenkiron, C. (2017). Isolation of membrane vesicles from prokaryotes: A technical and biological comparison reveals heterogeneity. *Journal of Extracellular Vesicles*, *6*, 1324731.
de Jong, O. G., Murphy, D. E., Mäger, I., Willms, E., Garcia-Guerra, A., Gitz-Francois, J. J., Lefferts, J., Gupta, D., Steenbeek, S. C., van Rheenen, J., El Andaloussi, S., Schiffelers, R. M., Wood, M. J. A., & Vader, P. (2020). A CRISPR-Cas9-based reporter system for single-cell detection of extracellular vesicle-mediated functional transfer of RNA. *Nature Communications*, *11*, 1113.
de Rond, L., Coumans, F. A. W., Nieuwland, R., van Leeuwen, T. G., & van der Pol, E. (2018). Deriving extracellular vesicle size from scatter intensities measured by flow cytometry. *Current Protocols in Cytometry*, *86*, e43.
de Rond, L., van der Pol, E., Hau, C. M., Varga, Z., Sturk, A., van Leeuwen, T. G., Nieuwland, R., & Coumans, F. A. W. (2018). Comparison of generic fluorescent markers for detection of extracellular vesicles by flow cytometry. *Clinical Chemistry*, *64*, 680–689.
de Voogt, W. S., Tanenbaum, M. E., & Vader, P. (2021). Illuminating RNA trafficking and functional delivery by extracellular vesicles. *Advanced Drug Delivery Reviews*, *174*, 250–264.
de Vrij, J., Maas, S. L., van Nispen, M., Sena-Esteves, M., Limpens, R. W., Koster, A. J., Leenstra, S., Lamfers, M. L., & Broekman, M. L. (2013). Quantification of nanosized extracellular membrane vesicles with scanning ion occlusion sensing. *Nanomedicine (Lond)*, *8*, 1443–1458.

20013078, 2024, 2, Downloaded from https://isevjournals.onlinelibrary.wiley.com/doi/10.1002/jev2.12404 by Colorado State University, Wiley Online Library on [09/10/2024]. See the Terms and Conditions (https://onlinelibrary.wiley.com/terms-and-conditions) on Wiley Online Library for rules of use; OA articles are governed by the applicable Creative Commons License

Dhondt, B., Geeurickx, E., Tulkens, J., Van Deun, J., Vergauwen, G., Lippens, L., Miinalainen, I., Rappu, P., Heino, J., Ost, P., Lumen, N., De Wever, O., & Hendrix, A. (2020). Unravelling the proteomic landscape of extracellular vesicles in prostate cancer by density-based fractionation of urine. *Journal of Extracellular Vesicles*, *9*, 1736935.

Dhondt, B., Pinheiro, C., Geeurickx, E., Tulkens, J., Vergauwen, G., Van Der Pol, E., Nieuwland, R., Decock, A., Miinalainen, I., Rappu, P., Schroth, G., Kuersten, S., Vandesompele, J., Mestdagh, P., Lumen, N., De Wever, O., & Hendrix, A. (2023). Benchmarking blood collection tubes and processing intervals for extracellular vesicle performance metrics. *Journal of Extracellular Vesicles*, *12*, e12315.

Dixson, A. C., Dawson, T. R., Di Vizio, D., & Weaver, A. M. (2023). Context-specific regulation of extracellular vesicle biogenesis and cargo selection. *Nature Reviews Molecular Cell Biology*, *24*, 454–476.

Dogrammatzis, C., Saleh, S., Deighan, C., & Kalamvoki, M. (2021). Diverse populations of extracellular vesicles with opposite functions during herpes simplex virus 1 infection. *Journal of Virology*, *95*(6), e02357–20.

Dong, L., Zieren, R. C., Horie, K., Kim, C. J., Mallick, E., Jing, Y., Feng, M., Kuczler, M. D., Green, J., Amend, S. R., Witwer, K. W., de Reijke, T. M., Cho, Y. K., Pienta, K. J., & Xue, W. (2020). Comprehensive evaluation of methods for small extracellular vesicles separation from human plasma, urine and cell culture medium. *Journal of Extracellular Vesicles*, *10*, e12044.

Dooley, K., McConnell, R. E., Xu, K., Lewis, N. D., Haupt, S., Youniss, M. R., Martin, S., Sia, C. L., McCoy, C., Moniz, R. J., Burenkova, O., Sanchez-Salazar, J., Jang, S. C., Choi, B., Harrison, R. A., Houde, D., Burzyn, D., Leng, C., Kirwin, K., … Williams, D. E. (2021). A versatile platform for generating engineered extracellular vesicles with defined therapeutic properties. *Molecular Therapy*, *29*, 1729–1743.

Driedonks, T. A. P., Nijen Twilhaar, M. K., & Nolte-'t Hoen, E. N. M. (2019). Technical approaches to reduce interference of fetal calf serum derived RNA in the analysis of extracellular vesicle RNA from cultured cells. *Journal of Extracellular Vesicles*, *8*(1), 1552059.

Driedonks, T., Jiang, L., Carlson, B., Han, Z., Liu, G., Queen, S. E., Shirk, E. N., Gololobova, O., Liao, Z., Nyberg, L. H., Lima, G., Paniushkina, L., Garcia-Contreras, M., Schonvisky, K., Castell, N., Stover, M., Guerrero-Martin, S., Richardson, R., Smith, B., … Witwer, K. W. (2022). Pharmacokinetics and biodistribution of extracellular vesicles administered intravenously and intranasally to Macaca nemestrina. *Journal of Extracellular Biology*, *1*, e59.

Duijvesz, D., Versluis, C. Y., van der Fels, C. A., Vredenbregt-van den Berg, M. S., Leivo, J., Peltola, M. T., Bangma, C. H., Pettersson, K. S., & Jenster, G. (2015). Immuno-based detection of extracellular vesicles in urine as diagnostic marker for prostate cancer. *International Journal of Cancer*, *137*, 2869–2878.

Eldh, M., Lötvall, J., Malmhäll, C., & Ekström, K. (2012). Importance of RNA isolation methods for analysis of exosomal RNA: Evaluation of different methods. *Molecular Immunology*, *50*, 278–286.

Elgamal, S., Colombo, F., Cottini, F., Byrd, J. C., & Cocucci, E. (2020). Imaging intercellular interaction and extracellular vesicle exchange in a co-culture model of chronic lymphocytic leukemia and stromal cells by lattice light-sheet fluorescence microscopy. *Methods in Enzymology*, *645*, 79–107.

Enciso-Martinez, A., van der Pol, E., Lenferink, A. T. M., Terstappen, L., van Leeuwen, T. G., & Otto, C. (2020). Synchronized Rayleigh and Raman scattering for the characterization of single optically trapped extracellular vesicles. *Nanomedicine*, *24*, 102109.

Erdbrügger, U., Blijdorp, C. J., Bijnsdorp, I. V., Borràs, F. E., Burger, D., Bussolati, B., Byrd, J. B., Clayton, A., Dear, J. W., Falcón-Pérez, J. M., Grange, C., Hill, A. F., Holthöfer, H., Hoorn, E. J., Jenster, G., Jimenez, C. R., Junker, K., Klein, J., Knepper, M. A., … Martens-Uzunova, E. S. (2021). Urinary extracellular vesicles: A position paper by the Urine Task Force of the International Society for Extracellular Vesicles. *Journal of Extracellular Vesicles*, *10*, e12093.

Estrada, A. L., Valenti, Z. J., Hehn, G., Amorese, A. J., Williams, N. S., Balestrieri, N. P., Deighan, C., Allen, C. P., Spangenburg, E. E., Kruh-Garcia, N. A., & Lark, D. S. (2022). Extracellular vesicle secretion is tissue-dependent ex vivo and skeletal muscle myofiber extracellular vesicles reach the circulation in vivo. *American Journal of Physiology. Cell Physiology*, *322*, C246–C259.

EV-TRACK Consortium, van Deun, J., Mestdagh, P., Agostinis, P., Akay, O., Anand, S., Anckaert, J., Martinez, Z. A., Baetens, T., Beghein, E., Bertier, L., Berx, G., Boere, J., Boukouris, S., Bremer, M., Buschmann, D., Byrd, J. B., Casert, C., Cheng, L., … Hendrix, A. (2017). EV-TRACK: Transparent reporting and centralizing knowledge in extracellular vesicle research. *Nature Methods*, *14*, 228–232.

Evtushenko, E. G., Bagrov, D. V., Lazarev, V. N., Livshits, M. A., & Khomyakova, E. (2020). Adsorption of extracellular vesicles onto the tube walls during storage in solution. *PLoS ONE*, *15*, e0243738.

Fan, S. J., Kroeger, B., Marie, P. P., Bridges, E. M., Mason, J. D., McCormick, K., Zois, C. E., Sheldon, H., Khalid Alham, N., Johnson, E., Ellis, M., Stefana, M. I., Mendes, C. C., Wainwright, S. M., Cunningham, C., Hamdy, F. C., Morris, J. F., Harris, A. L., Wilson, C., & Goberdhan, D. C. (2020). Glutamine deprivation alters the origin and function of cancer cell exosomes. *Embo Journal*, *39*, e103009.

Feng, D., Zhao, W. L., Ye, Y. Y., Bai, X. C., Liu, R. Q., Chang, L. F., Zhou, Q., & Sui, S. F. (2010). Cellular internalization of exosomes occurs through phagocytosis. *Traffic (Copenhagen, Denmark)*, *11*, 675–687.

Foers, A. D., Chatfield, S., Dagley, L. F., Scicluna, B. J., Webb, A. I., Cheng, L., Hill, A. F., Wicks, I. P., & Pang, K. C. (2018). Enrichment of extracellular vesicles from human synovial fluid using size exclusion chromatography. *Journal of Extracellular Vesicles*, *7*, 1490145.

Foers, A. D., Dagley, L. F., Chatfield, S., Webb, A. I., Cheng, L., Hill, A. F., Wicks, I. P., & Pang, K. C. (2020). Proteomic analysis of extracellular vesicles reveals an immunogenic cargo in rheumatoid arthritis synovial fluid. *Clinical & Translational Immunology*, *9*, e1185.

Gaetani, L., Blennow, K., Calabresi, P., Di Filippo, M., Parnetti, L., & Zetterberg, H. (2019). Neurofilament light chain as a biomarker in neurological disorders. *Journal of Neurology, Neurosurgery, and Psychiatry*, *90*, 870–881.

Gallart-Palau, X., Serra, A., & Sze, S. K. (2016). Enrichment of extracellular vesicles from tissues of the central nervous system by PROSPR. *Molecular Neurodegeneration*, *11*, 41.

Gallego-Perez, D., Chang, L., Shi, J., Ma, J., Kim, S. H., Zhao, X., Malkoc, V., Wang, X., Minata, M., Kwak, K. J., Wu, Y., Lafyatis, G. P., Lu, W., Hansford, D. J., Nakano, I., & Lee, L. J. (2016). On-chip clonal analysis of glioma-stem-cell motility and therapy resistance. *Nano Letters*, *16*, 5326–5332.

Gámez-Valero, A., Monguió-Tortajada, M., Carreras-Planella, L., Franquesa, M. I., Beyer, K., & Borràs, F. E. (2016). Size-exclusion chromatography-based isolation minimally alters extracellular vesicles' characteristics compared to precipitating agents. *Scientific Reports*, *6*, 33641.

Gandham, S., Su, X., Wood, J., Nocera, A. L., Chandra Alli, S., Milane, L., Zimmerman, A., Amiji, M., & Ivanov, A. R. (2020). Technologies and standardization in research on extracellular vesicles. *Trends in Biotechnology*, *38*(10), 1066–1098.

Gao, H. N., Guo, H. Y., Zhang, H., Xie, X. L., Wen, P. C., & Ren, F. Z. (2019). Yak-milk-derived exosomes promote proliferation of intestinal epithelial cells in an hypoxic environment. *Journal of Dairy Science*, *102*, 985–996.

Gao, K., Zhu, W., Li, H., Ma, D., Liu, W., Yu, W., Wang, L., Cao, Y., & Jiang, Y. (2020). Association between cytokines and exosomes in synovial fluid of individuals with knee osteoarthritis. *Modern Rheumatology*, *30*, 758–764.

Gao, X., Ran, N., Dong, X., Zuo, B., Yang, R., Zhou, Q., Moulton, H. M., Seow, Y., & Yin, H. (2018). Anchor peptide captures, targets, and loads exosomes of diverse origins for diagnostics and therapy. *Science Translational Medicine*, *10*(444), eaat0195.

García-Silva, S., Benito-Martín, A., Nogués, L., Hernández-Barranco, A., Mazariegos, M. S., Santos, V., Hergueta-Redondo, M., Ximénez-Embún, P., Kataru, R. P., Lopez, A. A., Merino, C., Sánchez-Redondo, S., Graña-Castro, O., Matei, I., Nicolás-Avila, J. Á., Torres-Ruiz, R., Rodríguez-Perales, S., Martínez, L., Pérez-

20013078, 2024, 2, Downloaded from https://isevjournals.onlinelibrary.wiley.com/doi/10.1002/jev2.12404 by Colorado State University, Wiley Online Library on [09/10/2024]. See the Terms and Conditions (https://onlinelibrary.wiley.com/terms-and-conditions) on Wiley Online Library for rules of use; OA articles are governed by the applicable Creative Commons License

Martínez, M., … Peinado, H. (2021). Melanoma-derived small extracellular vesicles induce lymphangiogenesis and metastasis through an NGFR-dependent mechanism. *Nature Cancer*, *2*, 1387–1405.
García-Silva, S., Benito-Martín, A., Sánchez-Redondo, S., Hernández-Barranco, A., Ximénez-Embún, P., Nogués, L., Mazariegos, M. S., Brinkmann, K., Amor López, A., Meyer, L., Rodríguez, C., García-Martín, C., Boskovic, J., Letón, R., Montero, C., Robledo, M., Santambrogio, L., Sue Brady, M., Szumera-Ciećkiewicz, A., … Peinado, H. (2019). Use of extracellular vesicles from lymphatic drainage as surrogate markers of melanoma progression and BRAF (V600E) mutation. *Journal of Experimental Medicine*, *216*, 1061–1070.
Gardiner, C., Di Vizio, D., Sahoo, S., Théry, C., Witwer, K. W., Wauben, M., & Hill, A. F. (2016). Techniques used for the isolation and characterization of extracellular vesicles: Results of a worldwide survey. *Journal of Extracellular Vesicles*, *5*, 32945.
Gardiner, C., Shaw, M., Hole, P., Smith, J., Tannetta, D., Redman, C. W., & Sargent, I. L. (2014). Measurement of refractive index by nanoparticle tracking analysis reveals heterogeneity in extracellular vesicles. *Journal of Extracellular Vesicles*, *3*, 25361.
Gaurivaud, P., Ganter, S., Villard, A., Manso-Silvan, L., Chevret, D., Boulé, C., Monnet, V., & Tardy, F. (2018). Mycoplasmas are no exception to extracellular vesicles release: Revisiting old concepts. *PLoS ONE*, *13*, e0208160.
Gautron, J., Stapane, L., Roy, N. L., Nys, Y., Rodriguez-Navarro, A. B., & Hincke, M. T. (2021). Avian eggshell biomineralization: An update on its structure, mineralogy and protein tool kit. *BMC Molecular and Cell Biology*, *22*, 11.
Ge, X., Meng, Q., Wei, L., Liu, J., Li, M., Liang, X., Lin, F., Zhang, Y., Li, Y., Liu, Z., Fan, H., & Zhou, X. (2021). Myocardial ischemia-reperfusion induced cardiac extracellular vesicles harbour proinflammatory features and aggravate heart injury. *Journal of Extracellular Vesicles*, *10*, e12072.
Geeurickx, E., Tulkens, J., Dhondt, B., Van Deun, J., Lippens, L., Vergauwen, G., Heyrman, E., De Sutter, D., Gevaert, K., Impens, F., Miinalainen, I., Van Bockstal, P. J., De Beer, T., Wauben, M. H. M., Nolte-'t-Hoen, E. N. M., Bloch, K., Swinnen, J. V., van der Pol, E., Nieuwland, R., … Hendrix, A. (2019). The generation and use of recombinant extracellular vesicles as biological reference material. *Nature Communications*, *10*, 3288.
Gelibter, S., Marostica, G., Mandelli, A., Siciliani, S., Podini, P., Finardi, A., & Furlan, R. (2022). The impact of storage on extracellular vesicles: A systematic study. *Journal of Extracellular Vesicles*, *11*, e12162.
Ghoroghi, S., Mary, B., Larnicol, A., Asokan, N., Klein, A., Osmani, N., Busnelli, I., Delalande, F., Paul, N., Halary, S., Gros, F., Fouillen, L., Haeberle, A. M., Royer, C., Spiegelhalter, C., André-Grégoire, G., Mittelheisser, V., Detappe, A., Murphy, K., … Hyenne, V. (2021). Ral GTPases promote breast cancer metastasis by controlling biogenesis and organ targeting of exosomes. *Elife*, *10*, e61539.
Giddings, J. C., Yang, F. J., & Myers, M. N. (1976). Flow-field-flow fractionation: A versatile new separation method. *Science*, *193*, 1244–1245.
Gimona, M., Brizzi, M. F., Choo, A. B. H., Dominici, M., Davidson, S. M., Grillari, J., Hermann, D. M., Hill, A. F., de Kleijn, D., Lai, R. C., Lai, C. P., Lim, R., Monguió-Tortajada, M., Muraca, M., Ochiya, T., Ortiz, L. A., Toh, W. S., Yi, Y. W., Witwer, K. W., … Lim, S. K. (2021). Critical considerations for the development of potency tests for therapeutic applications of mesenchymal stromal cell-derived small extracellular vesicles. *Cytotherapy*, *23*, 373–380.
Gobbo, J., Marcion, G., Cordonnier, M., Dias, A. M. M., Pernet, N., Hammann, A., Richaud, S., Mjahed, H., Isambert, N., Clausse, V., Rébé, C., Bertaut, A., Goussot, V., Lirussi, F., Ghiringhelli, F., de Thonel, A., Fumoleau, P., Seigneuric, R., & Garrido, C. (2016). Restoring anticancer immune response by targeting tumor-derived exosomes with a HSP70 peptide aptamer. *JNCI: Journal of the National Cancer Institute*, *108*, 00–00.
Gomar-Vercher, S., Simón-Soro, A., Montiel-Company, J. M., Almerich-Silla, J. M., & Mira, A. (2018). Stimulated and unstimulated saliva samples have significantly different bacterial profiles. *PLoS ONE*, *13*, e0198021.
Gomes, D. E., & Witwer, K. W. (2022). L1CAM-associated extracellular vesicles: A systematic review of nomenclature, sources, separation, and characterization. *Journal of Extracellular Biology*, *1*(3), e35.
Gorgens, A., Bremer, M., Ferrer-Tur, R., Murke, F., Tertel, T., Horn, P. A., Thalmann, S., Welsh, J. A., Probst, C., Guerin, C., Boulanger, C. M., Jones, J. C., Hanenberg, H., Erdbrugger, U., Lannigan, J., Ricklefs, F. L., El-Andaloussi, S., & Giebel, B. (2019). Optimisation of imaging flow cytometry for the analysis of single extracellular vesicles by using fluorescence-tagged vesicles as biological reference material. *Journal of Extracellular Vesicles*, *8*, 1587567.
Görgens, A., Corso, G., Hagey, D. W., Jawad Wiklander, R., Gustafsson, M. O., Felldin, U., Lee, Y., Bostancioglu, R. B., Sork, H., Liang, X., Zheng, W., Mohammad, D. K., van de Wakker, S. I., Vader, P., Zickler, A. M., Mamand, D. R., Ma, L., Holme, M. N., Stevens, M. M., … El Andaloussi, S. (2022). Identification of storage conditions stabilizing extracellular vesicles preparations. *Journal of Extracellular Vesicles*, *11*, e12238.
Gori, A., Romanato, A., Greta, B., Strada, A., Gagni, P., Frigerio, R., Brambilla, D., Vago, R., Galbiati, S., Picciolini, S., Bedoni, M., Daaboul, G. G., Chiari, M., & Cretich, M. (2020). Membrane-binding peptides for extracellular vesicles on-chip analysis. *Journal of Extracellular Vesicles*, *9*, 1751428.
Gould, T. J., Hess, S. T., & Bewersdorf, J. (2012). Optical nanoscopy: From acquisition to analysis. *Annual Review of Biomedical Engineering*, *14*, 231–254.
Gradilla, A. C., González, E., Seijo, I., Andrés, G., Bischoff, M., González-Mendez, L., Sánchez, V., Callejo, A., Ibáñez, C., Guerra, M., Ortigão-Farias, J. R., Sutherland, J. D., González, M., Barrio, R., Falcón-Pérez, J. M., & Guerrero, I. (2014). Exosomes as Hedgehog carriers in cytoneme-mediated transport and secretion. *Nature Communications*, *5*, 5649.
Granvogl, B., Ploscher, M., & Eichacker, L. A. (2007). Sample preparation by in-gel digestion for mass spectrometry-based proteomics. *Analytical and Bioanalytical Chemistry*, *389*, 991–1002.
Gross, J. C., Chaudhary, V., Bartscherer, K., & Boutros, M. (2012). Active Wnt proteins are secreted on exosomes. *Nature Cell Biology*, *14*, 1036–1045.
Gualerzi, A., Kooijmans, S. A. A., Niada, S., Picciolini, S., Brini, A. T., Camussi, G., & Bedoni, M. (2019). Raman spectroscopy as a quick tool to assess purity of extracellular vesicle preparations and predict their functionality. *Journal of Extracellular Vesicles*, *8*, 1568780.
Gualerzi, A., Niada, S., Giannasi, C., Picciolini, S., Morasso, C., Vanna, R., Rossella, V., Masserini, M., Bedoni, M., Ciceri, F., Bernardo, M. E., Brini, A. T., & Gramatica, F. (2017). Raman spectroscopy uncovers biochemical tissue-related features of extracellular vesicles from mesenchymal stromal cells. *Scientific Reports*, *7*, 9820.
Gupta, D., Liang, X., Pavlova, S., Wiklander, O. P. B., Corso, G., Zhao, Y., Saher, O., Bost, J., Zickler, A. M., Piffko, A., Maire, C. L., Ricklefs, F. L., Gustafsson, O., Llorente, V. C., Gustafsson, M. O., Bostancioglu, R. B., Mamand, D. R., Hagey, D. W., Görgens, A., … El Andaloussi, S. (2020). Quantification of extracellular vesicles in vitro and in vivo using sensitive bioluminescence imaging. *Journal of Extracellular Vesicles*, *9*, 1800222.
Gyorgy, B., Modos, K., Pallinger, E., Paloczi, K., Pasztoi, M., Misjak, P., Deli, M. A., Sipos, A., Szalai, A., Voszka, I., Polgar, A., Toth, K., Csete, M., Nagy, G., Gay, S., Falus, A., Kittel, A., & Buzas, E. I. (2011). Detection and isolation of cell-derived microparticles are compromised by protein complexes resulting from shared biophysical parameters. *Blood*, *117*, e39–e48.
Gyorgy, B., Paloczi, K., Kovacs, A., Barabas, E., Beko, G., Varnai, K., Pallinger, E., Szabo-Taylor, K., Szabo, T. G., Kiss, A. A., Falus, A., & Buzas, E. I. (2014). Improved circulating microparticle analysis in acid-citrate dextrose (ACD) anticoagulant tube. *Thrombosis Research*, *133*, 285–292.
Hackley, V. A., & Clogston, J. D. (2011). Measuring the hydrodynamic size of nanoparticles in aqueous media using batch-mode dynamic light scattering. *Methods in Molecular Biology*, *697*, 35–52.
Han, C., Kang, H., Yi, J., Kang, M., Lee, H., Kwon, Y., Jung, J., Lee, J., & Park, J. (2021). Single-vesicle imaging and co-localization analysis for tetraspanin profiling of individual extracellular vesicles. *Journal of Extracellular Vesicles*, *10*(3), e12047.

20013078, 2024, 2, Downloaded from https://isevjournals.onlinelibrary.wiley.com/doi/10.1002/jev2.12404 by Colorado State University, Wiley Online Library on [09/10/2024]. See the Terms and Conditions (https://onlinelibrary.wiley.com/terms-and-conditions) on Wiley Online Library for rules of use; OA articles are governed by the applicable Creative Commons License

Han, P., Bartold, P. M., Salomon, C., & Ivanovski, S. (2021). Salivary outer membrane vesicles and DNA methylation of small extracellular vesicles as biomarkers for periodontal status: A pilot study. *International Journal of Molecular Sciences*, *22*, 2423.
He, B., Cai, Q., Qiao, L., Huang, C. Y., Wang, S., Miao, W., Ha, T., Wang, Y., & Jin, H. (2021). RNA-binding proteins contribute to small RNA loading in plant extracellular vesicles. *Nature Plants*, *7*, 342–352.
Hebisch, E., Wagner, E., Westphal, V., Sieber, J. J., & Lehnart, S. E. (2017). A protocol for registration and correction of multicolour STED superresolution images. *Journal of Microscopy*, *267*, 160–175.
Heddleston, J. M., Aaron, J. S., Khuon, S., & Chew, T. L. (2021). A guide to accurate reporting in digital image acquisition – can anyone replicate your microscopy data? *Journal of Cell Science*, *134*(6), jcs254144.
Hegyesi, H., Pallinger, É., Mecsei, S., Hornyák, B., Kovácsházi, C., Brenner, G. B., Giricz, Z., Pálóczi, K., Kittel, Á., Tóvári, J., Turiak, L., Khamari, D., Ferdinandy, P., & Buzás, E. I. (2022). Circulating cardiomyocyte-derived extracellular vesicles reflect cardiac injury during systemic inflammatory response syndrome in mice. *Cellular and Molecular Life Sciences*, *79*, 84.
Hell, S. W., & Wichmann, J. (1994). Breaking the diffraction resolution limit by stimulated emission: Stimulated-emission-depletion fluorescence microscopy. *Optics Letters*, *19*, 780–782.
Hendrix, A., Lippens, L., Pinheiro, C., Théry, C., Martin-Jaular, L., Lötvall, J., Lässer, C., Hill, A F., & Witwer, K. W. (2023). Extracellular vesicle analysis. *Nature Reviews Methods Primers*, *3*, 56.
Herrmann, I. K., Wood, M. J. A., & Fuhrmann, G. (2021). Extracellular vesicles as a next-generation drug delivery platform. *Nature Nanotechnology*, *16*, 748–759.
Hess, S. T., Girirajan, T. P. K., & Mason, M. D. (2006). Ultra-high resolution imaging by fluorescence photoactivation localization microscopy. *Biophysical Journal*, *91*, 4258–4272.
Heusermann, W., Hean, J., Trojer, D., Steib, E., von Bueren, S., Graff-Meyer, A., Genoud, C., Martin, K., Pizzato, N., Voshol, J., Morrissey, D. V., Andaloussi, S. E., Wood, M. J., & Meisner-Kober, N. C. (2016). Exosomes surf on filopodia to enter cells at endocytic hot spots, traffic within endosomes, and are targeted to the ER. *Journal of Cell Biology*, *213*, 173–184.
Higginbotham, J. N., Demory Beckler, M., Gephart, J. D., Franklin, J. L., Bogatcheva, G., Kremers, G. J., Piston, D. W., Ayers, G. D., McConnell, R. E., Tyska, M. J., & Coffey, R. J. (2011). Amphiregulin exosomes increase cancer cell invasion. *Current Biology*, *21*, 779–786.
Hill, A. F., Pegtel, D. M., Lambertz, U., Leonardi, T., O'Driscoll, L., Pluchino, S., Ter-Ovanesyan, D., & Nolte-'t Hoen, E. N. (2013). ISEV position paper: Extracellular vesicle RNA analysis and bioinformatics. *Journal of Extracellular Vesicles*, *2*, 00–00.
Hogg, W. R., & Coulter, W. H. (1967). Apparatus and method for measuring a dividing particle size of a particulate system. In United States.
Hole, P., Sillence, K., Hannell, C., Maguire, C. M., Roesslein, M., Suarez, G., Capracotta, S., Magdolenova, Z., Horev-Azaria, L., Dybowska, A., Cooke, L., Haase, A., Contal, S., Mano, S., Vennemann, A., Sauvain, J. J., Staunton, K. C., Anguissola, S., Luch, A., … Wick, P. (2013). Interlaboratory comparison of size measurements on nanoparticles using nanoparticle tracking analysis (NTA). *Journal of Nanoparticle Research*, *15*, 2101.
Hong, J., Dauros-Singorenko, P., Whitcombe, A., Payne, L., Blenkiron, C., Phillips, A., & Swift, S. (2019). Analysis of the *Escherichia coli* extracellular vesicle proteome identifies markers of purity and culture conditions. *Journal of Extracellular Vesicles*, *8*, 1632099.
Hood, R. R., DeVoe, D. L., Atencia, J., Vreeland, W. N., & Omiatek, D. M. (2014). A facile route to the synthesis of monodisperse nanoscale liposomes using 3D microfluidic hydrodynamic focusing in a concentric capillary array. *Lab on A Chip*, *14*, 2403–2409.
Hoog, J. L., & Lotvall, J. (2015). Diversity of extracellular vesicles in human ejaculates revealed by cryo-electron microscopy. *Journal of Extracellular Vesicles*, *4*, 28680.
Hoshino, A., Costa-Silva, B., Shen, T. L., Rodrigues, G., Hashimoto, A., Tesic Mark, M., Molina, H., Kohsaka, S., Di Giannatale, A., Ceder, S., Singh, S., Williams, C., Soplop, N., Uryu, K., Pharmer, L., King, T., Bojmar, L., Davies, A. E., Ararso, Y., … Lyden, D. (2015). Tumour exosome integrins determine organotropic metastasis. *Nature*, *527*, 329–335.
Hoshino, A., Kim, H. S., Bojmar, L., Gyan, K. E., Cioffi, M., Hernandez, J., Zambirinis, C. P., Rodrigues, G., Molina, H., Heissel, S., Mark, M. T., Steiner, L., Benito-Martin, A., Lucotti, S., Di Giannatale, A., Offer, K., Nakajima, M., Williams, C., Nogués, L., … Lyden, D. (2020). Extracellular vesicle and particle biomarkers define multiple human cancers. *Cell*, *182*, 1044–1061.e18.
Howell, J. C., Watts, K. D., Parker, M. W., Wu, J., Kollhoff, A., Wingo, T. S., Dorbin, C. D., Qiu, D., & Hu, W. T. (2017). Race modifies the relationship between cognition and Alzheimer's disease cerebrospinal fluid biomarkers. *Alzheimer's Research & Therapy*, *9*, 88.
Huang, Y., Cheng, L., Turchinovich, A., Mahairaki, V., Troncoso, J. C., Pletniková, O., Haughey, N. J., Vella, L. J., Hill, A. F., Zheng, L., & Witwer, K. W. (2020). Influence of species and processing parameters on recovery and content of brain tissue-derived extracellular vesicles. *Journal of Extracellular Vesicles*, *9*, 1785746.
Hühmer, A. F., Biringer, R. G., Amato, H., Fonteh, A. N., & Harrington, M. G. (2006). Protein analysis in human cerebrospinal fluid: Physiological aspects, current progress and future challenges. *Disease Markers*, *22*, 3–26.
Hurwitz, S. N., Olcese, J. M., & Meckes, D. G. Jr (2019). Extraction of extracellular vesicles from whole tissue. *Journal of Visualized Experiments: JoVE*, (144), https://doi.org/10.3791/59143
Hurwitz, S. N., Sun, L., Cole, K. Y., Ford, C. R. 3rd, Olcese, J. M., & Meckes, D. G. Jr (2018). An optimized method for enrichment of whole brain-derived extracellular vesicles reveals insight into neurodegenerative processes in a mouse model of Alzheimer's disease. *Journal of Neuroscience Methods*, *307*, 210–220.
Hyenne, V., Apaydin, A., Rodriguez, D., Spiegelhalter, C., Hoff-Yoessle, S., Diem, M., Tak, S., Lefebvre, O., Schwab, Y., Goetz, J. G., & Labouesse, M. (2015). RAL-1 controls multivesicular body biogenesis and exosome secretion. *Journal of Cell Biology*, *211*, 27–37.
Hyenne, V., Ghoroghi, S., Collot, M., Bons, J., Follain, G., Harlepp, S., Mary, B., Bauer, J., Mercier, L., Busnelli, I., Lefebvre, O., Fekonja, N., Garcia-Leon, M. J., Machado, P., Delalande, F., López, A. A., Silva, S. G., Verweij, F. J., van Niel, G., … Goetz, J. G. (2019). Studying the fate of tumor extracellular vesicles at high spatiotemporal resolution using the zebrafish embryo. *Developmental Cell*, *48*, 554–572.e7.
Ishida, T., Hashimoto, T., Masaki, K., Funabashi, H., Hirota, R., Ikeda, T., Tajima, H., & Kuroda, A. (2020). Application of peptides with an affinity for phospholipid membranes during the automated purification of extracellular vesicles. *Scientific Reports*, *10*, 18718.
Izumi, T. (2021). In vivo roles of Rab27 and its effectors in exocytosis. *Cell Structure and Function*, *46*, 79–94.
Jack, C. R. Jr., Bennett, D. A., Blennow, K., Carrillo, M. C., Dunn, B., Haeberlein, S. B., Holtzman, D. M., Jagust, W., Jessen, F., Karlawish, J., Liu, E., Molinuevo, J. L., Montine, T., Phelps, C., Rankin, K. P., Rowe, C. C., Scheltens, P., Siemers, E., Snyder, H. M., & Sperling, R. (2018). NIA-AA research framework: Toward a biological definition of Alzheimer's disease. *Alzheimers Dement*, *14*, 535–562.
Jang, S. C., Crescitelli, R., Cvjetkovic, A., Belgrano, V., Olofsson Bagge, R., Sundfeldt, K., Ochiya, T., Kalluri, R., & Lötvall, J. (2019). Mitochondrial protein enriched extracellular vesicles discovered in human melanoma tissues can be detected in patient plasma. *Journal of Extracellular Vesicles*, *8*, 1635420.
Jaqaman, K., Loerke, D., Mettlen, M., Kuwata, H., Grinstein, S., Schmid, S. L., & Danuser, G. (2008). Robust single-particle tracking in live-cell time-lapse sequences. *Nature Methods*, *5*, 695–702.

20013078, 2024, 2, Downloaded from https://isevjournals.onlinelibrary.wiley.com/doi/10.1002/jev2.12404 by Colorado State University, Wiley Online Library on [09/10/2024]. See the Terms and Conditions (https://onlinelibrary.wiley.com/terms-and-conditions) on Wiley Online Library for rules of use; OA articles are governed by the applicable Creative Commons License

Jeppesen, D. K., Fenix, A. M., Franklin, J. L., Higginbotham, J. N., Zhang, Q., Zimmerman, L. J., Liebler, D. C., Ping, J., Liu, Q., Evans, R., Fissell, W. H., Patton, J. G., Rome, L. H., Burnette, D. T., & Coffey, R. J. (2019). Reassessment of exosome composition. *Cell*, *177*, 428–445.e18.

Jeurissen, S., Vergauwen, G., Van Deun, J., Lapeire, L., Depoorter, V., Miinalainen, I., Sormunen, R., Van den Broecke, R., Braems, G., Cocquyt, V., Denys, H., & Hendrix, A. (2017). The isolation of morphologically intact and biologically active extracellular vesicles from the secretome of cancer-associated adipose tissue. *Cell Adhesion & Migration*, *11*, 196–204.

Jewett, K. A., Thomas, R. E., Phan, C. Q., Lin, B., Milstein, G., Yu, S., Bettcher, L. F., Neto, F. C., Djukovic, D., Raftery, D., Pallanck, L. J., & Davis, M. Y. (2021). Glucocerebrosidase reduces the spread of protein aggregation in a Drosophila melanogaster model of neurodegeneration by regulating proteins trafficked by extracellular vesicles. *Plos Genetics*, *17*, e1008859.

Jingami, N., Uemura, K., Asada-Utsugi, M., Kuzuya, A., Yamada, S., Ishikawa, M., Kawahara, T., Iwasaki, T., Atsuchi, M., Takahashi, R., & Kinoshita, A. (2019). Two-point dynamic observation of Alzheimer's disease cerebrospinal fluid biomarkers in idiopathic normal pressure hydrocephalus. *Journal of Alzheimer's Disease*, *72*, 271–277.

Jingushi, K., Uemura, M., Ohnishi, N., Nakata, W., Fujita, K., Naito, T., Fujii, R., Saichi, N., Nonomura, N., Tsujikawa, K., & Ueda, K. (2018). Extracellular vesicles isolated from human renal cell carcinoma tissues disrupt vascular endothelial cell morphology via azurocidin. *International Journal of Cancer*, *142*, 607–617.

Johnsen, K. B., Gudbergsson, J. M., Andresen, T. L., & Simonsen, J. B. (2019). What is the blood concentration of extracellular vesicles? Implications for the use of extracellular vesicles as blood-borne biomarkers of cancer. *Biochimica et Biophysica Acta (BBA) - Reviews on Cancer*, *1871*, 109–116.

Jones, R. R., Hooper, D. C., Zhang, L., Wolverson, D., & Valev, V. K. (2019). Raman techniques: Fundamentals and frontiers. *Nanoscale Research Letters*, *14*, 231.

Joshi, B. S., de Beer, M. A., Giepmans, B. N. G., & Zuhorn, I. S. (2020). Endocytosis of extracellular vesicles and release of their cargo from endosomes. *ACS Nano*, *14*, 4444–4455.

Joy, A. P., Ayre, D. C., Chute, I. C., Beauregard, A. P., Wajnberg, G., Ghosh, A., Lewis, S. M., Ouellette, R. J., & Barnett, D. A. (2018). Proteome profiling of extracellular vesicles captured with the affinity peptide Vn96: Comparison of Laemmli and TRIzol© protein-extraction methods. *Journal of Extracellular Vesicles*, *7*, 1438727.

Jurgielewicz, B. J., Yao, Y., & Stice, S. L. (2020). Kinetics and specificity of HEK293T extracellular vesicle uptake using imaging flow cytometry. *Nanoscale Research Letters*, *15*, 170.

Kaczor-Urbanowicz, K. E., Wei, F., Rao, S. L., Kim, J., Shin, H., Cheng, J., Tu, M., Wong, D. T. W., & Kim, Y. (2019). Clinical validity of saliva and novel technology for cancer detection. *Biochimica et Biophysica Acta (BBA) - Reviews on Cancer*, *1872*, 49–59.

Kahlert, C., Melo, S. A., Protopopov, A., Tang, J., Seth, S., Koch, M., Zhang, J., Weitz, J., Chin, L., Futreal, A., & Kalluri, R. (2014). Identification of double-stranded genomic DNA spanning all chromosomes with mutated KRAS and p53 DNA in the serum exosomes of patients with pancreatic cancer. *Journal of Biological Chemistry*, *289*, 3869–3875.

Kameli, N., Becker, H. E. F., Welbers, T., Jonkers, D., Penders, J., Savelkoul, P., & Stassen, F. R. (2021). Metagenomic profiling of fecal-derived bacterial membrane vesicles in Crohn's disease patients. *Cells*, *10*(10), 2795.

Kang, M., Jordan, V., Blenkiron, C., & Chamley, L. W. (2021). Biodistribution of extracellular vesicles following administration into animals: A systematic review. *Journal of Extracellular Vesicles*, *10*, e12085.

Karimi, N., Cvjetkovic, A., Jang, S. C., Crescitelli, R., Hosseinpour Feizi, M. A., Nieuwland, R., Lötvall, J., & Lässer, C. (2018). Detailed analysis of the plasma extracellular vesicle proteome after separation from lipoproteins. *Cellular and Molecular Life Sciences*, *75*, 2873–2886.

Karimi, N., Dalirfardouei, R., Dias, T., Lötvall, J., & Lässer, C. (2022). Tetraspanins distinguish separate extracellular vesicle subpopulations in human serum and plasma - Contributions of platelet extracellular vesicles in plasma samples. *Journal of Extracellular Vesicles*, *11*, e12213.

Karttunen, J., Heiskanen, M., Navarro-Ferrandis, V., Gupta, S. D, Lipponen, A., Puhakka, N., Rilla, K., Koistinen, A., & Pitkänen, A. (2019). Precipitation-based extracellular vesicle isolation from rat plasma co-precipitate vesicle-free microRNAs. *Journal of Extracellular Vesicles*, *8*, 1555410.

Keenan, J. I., & Allardyce, R. A. (2000). Iron influences the expression of *Helicobacter pylori* outer membrane vesicle-associated virulence factors. *European Journal of Gastroenterology & Hepatology*, *12*, 1267–1273.

Keremi, B., Beck, A., Fabian, T. K., Fabian, G., Szabo, G., Nagy, A., & Varga, G. (2017). Stress and salivary glands. *Current Pharmaceutical Design*, *23*, 4057–4065.

Kestens, V., Bozatzidis, V., De Temmerman, P. J., Ramaye, Y., & Roebben, G. (2017). Validation of a particle tracking analysis method for the size determination of nano- and microparticles. *Journal of Nanoparticle Research*, *19*, 271.

Khater, I. M., Nabi, I. R., & Hamarneh, G. (2020). A review of super-resolution single-molecule localization microscopy cluster analysis and quantification methods. *Patterns (N Y)*, *1*, 100038.

Khurshid, Z., Zohaib, S., Najeeb, S., Zafar, M. S., Slowey, P. D., & Almas, K. (2016). Human saliva collection devices for proteomics: An update. *International Journal of Molecular Sciences*, *17*, 846.

Klar, T. A., & Hell, S. W. (1999). Subdiffraction resolution in far-field fluorescence microscopy. *Optics Letters*, *24*, 954–956.

Klener, J., Hofbauerová, K., Bartoš, A., Říčný, J., Rípová, D., & Kopecký, V. (2014). Instability of cerebrospinal fluid after delayed storage and repeated freezing: A holistic study by drop coating deposition Raman spectroscopy. *Clinical Chemistry and Laboratory Medicine*, *52*, 657–664.

Klont, F., Bras, L., Wolters, J. C., Ongay, S., Bischoff, R., Halmos, G. B., & Horvatovich, P. (2018). Assessment of sample preparation bias in mass spectrometry-based proteomics. *Analytical Chemistry*, *90*, 5405–5413.

Kobayashi-Sun, J., Yamamori, S., Kondo, M., Kuroda, J., Ikegame, M., Suzuki, N., Kitamura, K. I., Hattori, A., Yamaguchi, M., & Kobayashi, I. (2020). Uptake of osteoblast-derived extracellular vesicles promotes the differentiation of osteoclasts in the zebrafish scale. *Communications Biology*, *3*, 190.

Koles, K., Nunnari, J., Korkut, C., Barria, R., Brewer, C., Li, Y., Leszyk, J., Zhang, B., & Budnik, V. (2012). Mechanism of evenness interrupted (Evi)-exosome release at synaptic boutons. *Journal of Biological Chemistry*, *287*, 16820–16834.

Kolhe, R., Owens, V., Sharma, A., Lee, T. J., Zhi, W., Ghilzai, U., Mondal, A. K., Liu, Y., Isales, C. M., Hamrick, M. W., Hunter, M., & Fulzele, S. (2020). Sex-specific differences in extracellular vesicle protein cargo in synovial fluid of patients with osteoarthritis. *Life (Basel)*, *10*(12), 337.

Koliha, N., Wiencek, Y., Heider, U., Jüngst, C., Kladt, N., Krauthäuser, S., Johnston, I. C., Bosio, A., Schauss, A., & Wild, S. (2016). A novel multiplex bead-based platform highlights the diversity of extracellular vesicles. *Journal of Extracellular Vesicles*, *5*, 29975.

Korkut, C., Li, Y., Koles, K., Brewer, C., Ashley, J., Yoshihara, M., & Budnik, V. (2013). Regulation of postsynaptic retrograde signaling by presynaptic exosome release. *Neuron*, *77*, 1039–1046.

Kowal, J., Arras, G., Colombo, M., Jouve, M., Morath, J. P., Primdal-Bengtson, B., Dingli, F., Loew, D., Tkach, M., & Théry, C. (2016). Proteomic comparison defines novel markers to characterize heterogeneous populations of extracellular vesicle subtypes. *PNAS*, *113*, E968–E977.

Kreimer, S., Belov, A. M., Ghiran, I., Murthy, S. K., Frank, D. A., & Ivanov, A. R. (2015). Mass-spectrometry-based molecular characterization of extracellular vesicles: lipidomics and proteomics. *Journal of Proteome Research*, *14*, 2367–2384.

20013078, 2024, 2, Downloaded from https://isevjournals.onlinelibrary.wiley.com/doi/10.1002/jev2.12404 by Colorado State University, Wiley Online Library on [09/10/2024]. See the Terms and Conditions (https://onlinelibrary.wiley.com/terms-and-conditions) on Wiley Online Library for rules of use; OA articles are governed by the applicable Creative Commons License

Krušić Alić, V., Malenica, M., Biberić, M., Zrna, S., Valenčić, L., Šuput, A., Kalagac Fabris, L., Wechtersbach, K., Kojc, N., Kurtjak, M., Kučić, N., & Grabušić, K. (2022). Extracellular vesicles from human cerebrospinal fluid are effectively separated by sepharose CL-6B-comparison of four gravity-flow size exclusion chromatography methods. *Biomedicines*, *10*, 785.

Kuehn, M. J., & Kesty, N. C. (2005). Bacterial outer membrane vesicles and the host-pathogen interaction. *Genes & Development*, *19*, 2645–2655.

Kumeda, N., Ogawa, Y., Akimoto, Y., Kawakami, H., Tsujimoto, M., & Yanoshita, R. (2017). Characterization of membrane integrity and morphological stability of human salivary exosomes. *Biological & Pharmaceutical Bulletin*, *40*, 1183–1191.

Kwizera, E. A., O'Connor, R., Vinduska, V., Williams, M., Butch, E. R., Snyder, S. E., Chen, X., & Huang, X. (2018). Molecular detection and analysis of exosomes using surface-enhanced Raman scattering gold nanorods and a miniaturized device. *Theranostics*, *8*, 2722–2738.

Lacroix, R., Judicone, C., Poncelet, P., Robert, S., Arnaud, L., Sampol, J., & Dignat-George, F. (2012). Impact of pre-analytical parameters on the measurement of circulating microparticles: Towards standardization of protocol. *Journal of Thrombosis and Haemostasis*, *10*, 437–446.

Lai, C. P., Kim, E. Y., Badr, C. E., Weissleder, R., Mempel, T. R., Tannous, B. A., & Breakefield, X. O. (2015). Visualization and tracking of tumour extracellular vesicle delivery and RNA translation using multiplexed reporters. *Nature Communications*, *6*, 7029.

Lamparski, H. G., Metha-Damani, A., Yao, J. Y., Patel, S., Hsu, D. H., Ruegg, C., & Le Pecq, J. B. (2002). Production and characterization of clinical grade exosomes derived from dendritic cells. *Journal of Immunological Methods*, *270*, 211–226.

Langer, J., Jimenez de Aberasturi, D., Aizpurua, J., Alvarez-Puebla, R. A., Auguie, B., Baumberg, J. J., Bazan, G. C., Bell, S. E. J., Boisen, A., Brolo, A. G., Choo, J., Cialla-May, D., Deckert, V., Fabris, L., Faulds, K., Garcia de Abajo, F. J., Goodacre, R., Graham, D., Haes, A. J., … Liz-Marzan, L. M. (2020). Present and future of surface-enhanced Raman scattering. *ACS Nano*, *14*, 28–117.

Lázaro-Ibáñez, E., Faruqu, F. N., Saleh, A. F., Silva, A. M., Tzu-Wen Wang, J., Rak, J., Al-Jamal, K. T., & Dekker, N. (2021). Selection of fluorescent, bioluminescent, and radioactive tracers to accurately reflect extracellular vesicle biodistribution in vivo. *ACS Nano*, *15*, 3212–3227.

Lázaro-Ibáñez, E., Lässer, C., Shelke, G. V., Crescitelli, R., Jang, S. C., Cvjetkovic, A., García-Rodríguez, A., & Lötvall, J. (2019). DNA analysis of low- and high-density fractions defines heterogeneous subpopulations of small extracellular vesicles based on their DNA cargo and topology. *Journal of Extracellular Vesicles*, *8*, 1656993.

Le Saux, S., Aarrass, H., Lai-Kee-Him, J., Bron, P., Armengaud, J., Miotello, G., Bertrand-Michel, J., Dubois, E., George, S., Faklaris, O., Devoisselle, J. M., Legrand, P., Chopineau, J., & Morille, M. (2020). Post-production modifications of murine mesenchymal stem cell (mMSC) derived extracellular vesicles (EVs) and impact on their cellular interaction. *Biomaterials*, *231*, 119675.

LeClaire, M., Wohlschlegel, J. A., Chang, H. C., Wadehra, M., Yu, W., Rao, J., Elashoff, D., Gimzewski, J. K., & Sharma, S. (2021). Nanoscale extracellular vesicles carry the mechanobiology signatures of breast cancer cells. *ACS Applied Nano Materials*, *4*, 9876–9885.

Lee, T. H., Chennakrishnaiah, S., Audemard, E., Montermini, L., Meehan, B., & Rak, J. (2014). Oncogenic ras-driven cancer cell vesiculation leads to emission of double-stranded DNA capable of interacting with target cells. *Biochemical and Biophysical Research Communications*, *451*, 295–301.

Lee, W., Nanou, A., Rikkert, L., Coumans, F. A. W., Otto, C., Terstappen, L., & Offerhaus, H. L. (2018). Label-free prostate cancer detection by characterization of extracellular vesicles using raman spectroscopy. *Analytical Chemistry*, *90*, 11290–11296.

Lehrich, B. M., Liang, Y., & Fiandaca, M. S. (2021). Foetal bovine serum influence on in vitro extracellular vesicle analyses. *Journal of Extracellular Vesicles*, *10*, e12061.

Lehrich, B. M., Liang, Y., Khosravi, P., Federoff, H. J., & Fiandaca, M. S. (2018). Fetal bovine serum-derived extracellular vesicles persist within vesicle-depleted culture media. *International Journal of Molecular Sciences*, *19*, 3538.

Lener, T., Gimona, M., Aigner, L., Börger, V., Buzas, E., Camussi, G., Chaput, N., Chatterjee, D., Court, F. A., del Portillo, H. A., O'Driscoll, L., Fais, S., Falcon-Perez, J. M., Felderhoff-Mueser, U., Fraile, L., Gho, Y. S., Görgens, A., Gupta, R. C., Hendrix, A., … Giebel, B. (2015). Applying extracellular vesicles based therapeutics in clinical trials – An ISEV position paper. *Journal of Extracellular Vesicles*, *4*, 30087.

Lennon, K. M., Wakefield, D. L., Maddox, A. L., Brehove, M. S., Willner, A. N., Garcia-Mansfield, K., Meechoovet, B., Reiman, R., Hutchins, E., Miller, M. M., Goel, A., Pirrotte, P., Van Keuren-Jensen, K., & Jovanovic-Talisman, T. (2019). Single molecule characterization of individual extracellular vesicles from pancreatic cancer. *Journal of Extracellular Vesicles*, *8*, 1685634.

Lewczuk, P., Beck, G., Ganslandt, O., Esselmann, H., Deisenhammer, F., Regeniter, A., Petereit, H. F., Tumani, H., Gerritzen, A., Oschmann, P., Schröder, J., Schönknecht, P., Zimmermann, K., Hampel, H., Bürger, K., Otto, M., Haustein, S., Herzog, K., Dannenberg, R., … Wiltfang, J. (2006). International quality control survey of neurochemical dementia diagnostics. *Neuroscience Letters*, *409*, 1–4.

Li, D., Shao, L., Chen, B. C., Zhang, X., Zhang, M., Moses, B., Milkie, D. E., Beach, J. R., Hammer, J. A. 3rd, Pasham, M., Kirchhausen, T., Baird, M. A., Davidson, M. W., Xu, P., & Betzig, E. (2015). ADVANCED IMAGING. Extended-resolution structured illumination imaging of endocytic and cytoskeletal dynamics. *Science*, *349*, aab3500.

Li, G., Shofer, J. B., Petrie, E. C., Yu, C. E., Wilkinson, C. W., Figlewicz, D. P., Shutes-David, A., Zhang, J., Montine, T. J., Raskind, M. A., Quinn, J. F., Galasko, D. R., & Peskind, E. R. (2017). Cerebrospinal fluid biomarkers for Alzheimer's and vascular disease vary by age, gender, and APOE genotype in cognitively normal adults. *Alzheimer's Research & Therapy*, *9*, 48.

Li-Hui, W., Chuan-Quan, L., Long, Y., Ru-Liu, L., Long-Hui, C., & Wei-Wen, C. (2016). Gender differences in the saliva of young healthy subjects before and after citric acid stimulation. *Clinica Chimica Acta*, *460*, 142–145.

Liangsupree, T., Multia, E., & Riekkola, M. L. (2021). Modern isolation and separation techniques for extracellular vesicles. *Journal of Chromatography A*, *1636*, 461773.

Liao, Z., Jaular, L. M., Soueidi, E., Jouve, M., Muth, D. C., Schøyen, T. H., Seale, T., Haughey, N. J., Ostrowski, M., Théry, C., & Witwer, K. W. (2019). Acetylcholinesterase is not a generic marker of extracellular vesicles. *Journal of Extracellular Vesicles*, *8*, 1628592.

Liebler, D. C., & Zimmerman, L. J. (2013). Targeted quantitation of proteins by mass spectrometry. *Biochemistry*, *52*, 3797–3806.

Liégeois, S., Benedetto, A., Garnier, J. M., Schwab, Y., & Labouesse, M. (2006). The V0-ATPase mediates apical secretion of exosomes containing Hedgehog-related proteins in Caenorhabditis elegans. *Journal of Cell Biology*, *173*, 949–961.

Ligtenberg, A. J., Liem, E. H., Brand, H. S., & Veerman, E. C. (2016). The effect of exercise on salivary viscosity. *Diagnostics (Basel)*, *6*, 40.

Lim, G. T., You, D. G., Han, H. S., Lee, H., Shin, S., Oh, B. H., Kumar, E. K. P., Um, W., Kim, C. H., Han, S., Lee, S., Lim, S., Yoon, H. Y., Kim, K., Kwon, I. C., Jo, D. G., Cho, Y. W., & Park, J. H. (2021). Bioorthogonally surface-edited extracellular vesicles based on metabolic glycoengineering for CD44-mediated targeting of inflammatory diseases. *Journal of Extracellular Vesicles*, *10*, e12077.

Limbutara, K., Chou, C. L., & Knepper, M. A. (2020). Quantitative proteomics of all 14 renal tubule segments in rat. *Journal of the American Society of Nephrology*, *31*, 1255–1266.

Linares, R., Tan, S., Gounou, C., Arraud, N., & Brisson, A. R. (2015). High-speed centrifugation induces aggregation of extracellular vesicles. *Journal of Extracellular Vesicles*, *4*, 29509.

20013078, 2024, 2, Downloaded from https://isevjournals.onlinelibrary.wiley.com/doi/10.1002/jev2.12404 by Colorado State University, Wiley Online Library on [09/10/2024]. See the Terms and Conditions (https://onlinelibrary.wiley.com/terms-and-conditions) on Wiley Online Library for rules of use; OA articles are governed by the applicable Creative Commons License

Lischnig, A., Bergqvist, M., Ochiya, T., & Lässer, C. (2022). Quantitative proteomics identifies proteins enriched in large and small extracellular vesicles. *Molecular & Cellular Proteomics*, *21*, 100273.

Liu, D., Kou, X., Chen, C., Liu, S., Liu, Y., Yu, W., Yu, T., Yang, R., Wang, R., Zhou, Y., & Shi, S. (2018). Circulating apoptotic bodies maintain mesenchymal stem cell homeostasis and ameliorate osteopenia via transferring multiple cellular factors. *Cell Research*, *28*, 918–933.

Liu, H., Tian, Y., Xue, C., Niu, Q., Chen, C., & Yan, X. (2022). Analysis of extracellular vesicle DNA at the single-vesicle level by nano-flow cytometry. *Journal of Extracellular Vesicles*, *11*, e12206.

Liu, Q., Rojas-Canales, D. M., Divito, S. J., Shufesky, W. J., Stolz, D. B., Erdos, G., Sullivan, M. L., Gibson, G. A., Watkins, S. C., Larregina, A. T., & Morelli, A. E. (2016). Donor dendritic cell-derived exosomes promote allograft-targeting immune response. *Journal of Clinical Investigation*, *126*, 2805–2820.

Liu, X., Yang, X., Sun, W., Wu, Q., Song, Y., Yuan, L., & Yang, G. (2019). Systematic evolution of ligands by exosome enrichment: A proof-of-concept study for exosome-based targeting peptide screening. *Advanced Biosystems*, *3*, e1800275.

Liu, Y., Li, H., Wang, J., Xue, Q., Yang, X., Kang, Y., Li, M., Xu, J., Li, G., Li, C., Chang, H. C., Su, K. P., & Wang, F. (2020). Association of cigarette smoking with cerebrospinal fluid biomarkers of neurodegeneration, neuroinflammation, and oxidation. *JAMA Network Open*, *3*, e2018777.

Liu, Z., Cauvi, D. M., Bernardino, E. M. A., Lara, B., Lizardo, R. E., Hawisher, D., Bickler, S., & De Maio, A. (2018). Isolation and characterization of human urine extracellular vesicles. *Cell Stress & Chaperones*, *23*, 943–953.

Lobb, R. J., Becker, M., Wen, S. W., Wong, C. S., Wiegmans, A. P., Leimgruber, A., & Möller, A. (2015). Optimized exosome isolation protocol for cell culture supernatant and human plasma. *Journal of Extracellular Vesicles*, *4*, 27031.

Long, Q., Upadhya, D., Hattiangady, B., Kim, D. K., An, S. Y., Shuai, B., Prockop, D. J., & Shetty, A. K. (2017). Intranasal MSC-derived A1-exosomes ease inflammation, and prevent abnormal neurogenesis and memory dysfunction after status epilepticus. *PNAS*, *114*, E3536–E3545.

López-Guerrero, J. A., Valés-Gómez, M., Borrás, F. E., Falcón-Pérez, J. M., Vicent, M. J., & Yáñez-Mó, M. (2023). Standardising the preanalytical reporting of biospecimens to improve reproducibility in extracellular vesicle research – A GEIVEX study. *Journal of Extracellular Biology*, *2*, e76.

Lőrincz, Á. M., Timár, C. I., Marosvári, K. A., Veres, D. S., Otrokocsi, L., Kittel, Á., & Ligeti, E. (2014). Effect of storage on physical and functional properties of extracellular vesicles derived from neutrophilic granulocytes. *Journal of Extracellular Vesicles*, *3*, 25465.

Lotvall, J., Hill, A. F., Hochberg, F., Buzas, E. I., Di Vizio, D., Gardiner, C., Gho, Y. S., Kurochkin, I. V., Mathivanan, S., Quesenberry, P., Sahoo, S., Tahara, H., Wauben, M. H., Witwer, K. W., & Thery, C. (2014). Minimal experimental requirements for definition of extracellular vesicles and their functions: A position statement from the International Society for Extracellular Vesicles. *Journal of Extracellular Vesicles*, *3*, 26913.

Lucas, M., Ryan, J. M., Watkins, J., Early, K., Kruh-Garcia, N. A., Mehaffy, C., & Dobos, K. M. (2021). Extraction and separation of mycobacterial proteins. *Methods in Molecular Biology*, *2314*, 77–107.

Lucey, B. P., Fagan, A. M., Holtzman, D. M., Morris, J. C., & Bateman, R. J. (2017). Diurnal oscillation of CSF Aβ and other AD biomarkers. *Molecular Neurodegeneration*, *12*, 36.

Lucien, F., Gustafson, D., Lenassi, M., Li, B., Teske, J. J., Boilard, E., Clemm von Hohenberg, K., Falcón-Perez, J. M., Gualerzi, A., Reale, A., Jones, J. C., Lässer, C., Lawson, C., Nazarenko, I., O'Driscoll, L., Pink, R., Siljander, P. R.-M., Soekmadji, C., Hendrix, A., … Nieuwland, R. (2023). MIBlood-EV: Minimal information to enhance the quality and reproducibility of blood extracellular vesicle research. *Journal of Extracellular Vesicles*, *12*(12), e12385.

Lunavat, T. R., Cheng, L., Einarsdottir, B. O., Olofsson Bagge, R., Veppil Muralidharan, S., Sharples, R. A., Lässer, C., Gho, Y. S., Hill, A. F., Nilsson, J. A., & Lötvall, J. (2017). BRAF(V600) inhibition alters the microRNA cargo in the vesicular secretome of malignant melanoma cells. *PNAS*, *114*, E5930–E5939.

Lundy, S. K., Klinker, M. W., & Fox, D. A. (2015). Killer B lymphocytes and their fas ligand positive exosomes as inducers of immune tolerance. *Frontiers in Immunology*, *6*, 122.

Luo, W., Dai, Y., Chen, Z., Yue, X., Andrade-Powell, K. C., & Chang, J. (2020). Spatial and temporal tracking of cardiac exosomes in mouse using a nano-luciferase-CD63 fusion protein. *Communications Biology*, *3*, 114.

Ma, D., Huang, C., Zheng, J., Tang, J., Li, J., Yang, J., & Yang, R. (2018). Quantitative detection of exosomal microRNA extracted from human blood based on surface-enhanced Raman scattering. *Biosensors & Bioelectronics*, *101*, 167–173.

Mackenzie, K., Foot, N. J., Anand, S., Dalton, H. E., Chaudhary, N., Collins, B. M., Mathivanan, S., & Kumar, S. (2016). Regulation of the divalent metal ion transporter via membrane budding. *Cell Discovery*, *2*, 16011.

Maire, C. L., Fuh, M. M., Kaulich, K., Fita, K. D., Stevic, I., Heiland, D. H., Welsh, J. A., Jones, J. C., Görgens, A., Ricklefs, T., Dührsen, L., Sauvigny, T., Joosse, S. A., Reifenberger, G., Pantel, K., Glatzel, M., Miklosi, A. G., Felce, J. H., Caselli, M., … Ricklefs, F. L. (2021). Genome-wide methylation profiling of glioblastoma cell-derived extracellular vesicle DNA allows tumor classification. *Neuro-oncol*, *23*, 1087–1099.

Marie, P. P., Fan, S. J., Mason, J., Wells, A., Mendes, C. C., Wainwright, S. M., Scott, S., Fischer, R., Harris, A. L., Wilson, C., & Goberdhan, D. C. I. (2023). Accessory ESCRT-III proteins are conserved and selective regulators of Rab11a-exosome formation. *Journal of Extracellular Vesicles*, *12*, e12311.

Martin-Jaular, L., Nevo, N., Schessner, J. P., Tkach, M., Jouve, M., Dingli, F., Loew, D., Witwer, K. W., Ostrowski, M., Borner, G. H. H., & Théry, C. (2021). Unbiased proteomic profiling of host cell extracellular vesicle composition and dynamics upon HIV-1 infection. *Embo Journal*, *40*, e105492.

Martinez-Bartolome, S., Deutsch, E. W., Binz, P. A., Jones, A. R., Eisenacher, M., Mayer, G., Campos, A., Canals, F., Bech-Serra, J. J., Carrascal, M., Gay, M., Paradela, A., Navajas, R., Marcilla, M., Hernaez, M. L., Gutierrez-Blazquez, M. D., Velarde, L. F., Aloria, K., Beaskoetxea, J., … Albar, J. P. (2013). Guidelines for reporting quantitative mass spectrometry based experiments in proteomics. *Journal of Proteomics*, *95*, 84–88.

Mateescu, B., Kowal, E. J., van Balkom, B. W., Bartel, S., Bhattacharyya, S. N., Buzas, E. I., Buck, A. H., de Candia, P., Chow, F. W., Das, S., Driedonks, T. A., Fernandez-Messina, L., Haderk, F., Hill, A. F., Jones, J. C., Van Keuren-Jensen, K. R., Lai, C. P., Lasser, C., Liegro, I. D., … Nolte-'t Hoen, E. N. (2017). Obstacles and opportunities in the functional analysis of extracellular vesicle RNA – An ISEV position paper. *Journal of Extracellular Vesicles*, *6*, 1286095.

Mathieu, M., Martin-Jaular, L., Lavieu, G., & Théry, C. (2019). Specificities of secretion and uptake of exosomes and other extracellular vesicles for cell-to-cell communication. *Nature Cell Biology*, *21*, 9–17.

Mathieu, M., Névo, N., Jouve, M., Valenzuela, J. I., Maurin, M., Verweij, F. J., Palmulli, R., Lankar, D., Dingli, F., Loew, D., Rubinstein, E., Boncompain, G., Perez, F., & Théry, C. (2021). Specificities of exosome versus small ectosome secretion revealed by live intracellular tracking of CD63 and CD9. *Nature Communications*, *12*, 4389.

Mattsson, N., Andreasson, U., Persson, S., Arai, H., Batish, S. D., Bernardini, S., Bocchio-Chiavetto, L., Blankenstein, M. A., Carrillo, M. C., Chalbot, S., Coart, E., Chiasserini, D., Cutler, N., Dahlfors, G., Duller, S., Fagan, A. M., Forlenza, O., Frisoni, G. B., Galasko, D., … Blennow, K. (2011). The Alzheimer's Association external quality control program for cerebrospinal fluid biomarkers. *Alzheimers Dement*, *7*, 386–395.e6.

Matusek, T., Wendler, F., Polès, S., Pizette, S., D'Angelo, G., Fürthauer, M., & Thérond, P. P. (2014). The ESCRT machinery regulates the secretion and long-range activity of Hedgehog. *Nature*, *516*, 99–103.

McCann, J. V., Bischoff, S. R., Zhang, Y., Cowley, D. O., Sanchez-Gonzalez, V., Daaboul, G. D., & Dudley, A. C. (2020). Reporter mice for isolating and auditing cell type-specific extracellular vesicles in vivo. *Genesis (New York, N.Y.: 2000)*, *58*, e23369.

20013078, 2024, 2, Downloaded from https://isevjournals.onlinelibrary.wiley.com/doi/10.1002/jev2.12404 by Colorado State University, Wiley Online Library on [09/10/2024]. See the Terms and Conditions (https://onlinelibrary.wiley.com/terms-and-conditions) on Wiley Online Library for rules of use; OA articles are governed by the applicable Creative Commons License

McKenzie, A. J., Hoshino, D., Hong, N. H., Cha, D. J., Franklin, J. L., Coffey, R. J., Patton, J. G., & Weaver, A. M. (2016). KRAS-MEK signaling controls Ago2 sorting into exosomes. *Cell Reports*, *15*, 978–987.
McMillan, H. M., & Kuehn, M. J. (2023). Proteomic profiling reveals distinct bacterial extracellular vesicle subpopulations with possibly unique functionality. *Applied and Environmental Microbiology*, *89*, e0168622.
Mehanny, M., Kroniger, T., Koch, M., Hoppstädter, J., Becher, D., Kiemer, A. K., Lehr, C. M., & Fuhrmann, G. (2022). Yields and immunomodulatory effects of pneumococcal membrane vesicles differ with the bacterial growth phase. *Advanced Healthcare Materials*, *11*, e2101151.
Michael, B. N. R., Kommoju, V., Ganapathy, C. K, & Negi, V. S. (2019). Characterization of cell-derived microparticles in synovial fluid and plasma of patients with rheumatoid arthritis. *Rheumatology International*, *39*, 1377–1387.
Mihaly, J., Deak, R., Szigyarto, I. C., Bota, A., Beke-Somfai, T., & Varga, Z. (2017). Characterization of extracellular vesicles by IR spectroscopy: Fast and simple classification based on amide and CH stretching vibrations. *Biochimica et Biophysica Acta (BBA) - Biomembranes*, *1859*, 459–466.
Mittelbrunn, M., Gutiérrez-Vázquez, C., Villarroya-Beltri, C., González, S., Sánchez-Cabo, F., González, M. Á., Bernad, A., & Sánchez-Madrid, F. (2011). Unidirectional transfer of microRNA-loaded exosomes from T cells to antigen-presenting cells. *Nature Communications*, *2*, 282.
Möhrmann, L., Huang, H. J., Hong, D. S., Tsimberidou, A. M., Fu, S., Piha-Paul, S. A., Subbiah, V., Karp, D. D., Naing, A., Krug, A., Enderle, D., Priewasser, T., Noerholm, M., Eitan, E., Coticchia, C., Stoll, G., Jordan, L. M., Eng, C., Kopetz, E. S., … Janku, F. (2018). Liquid biopsies using plasma exosomal nucleic acids and plasma cell-free DNA compared with clinical outcomes of patients with advanced cancers. *Clinical Cancer Research*, *24*, 181–188.
Mondal, A., Ashiq, K. A., Phulpagar, P., Singh, D. K., & Shiras, A. (2019). Effective visualization and easy tracking of extracellular vesicles in glioma cells. *Biological Procedures Online*, *21*, 4.
Montero Llopis, P., Senft, R. A., Ross-Elliott, T. J., Stephansky, R., Keeley, D. P., Koshar, P., Marqués, G., Gao, Y. S., Carlson, B. R., Pengo, T., Sanders, M. A., Cameron, L. A., & Itano, M. S. (2021). Best practices and tools for reporting reproducible fluorescence microscopy methods. *Nature Methods*, *18*(12), 1463–1476.
Morales-Kastresana, A., Musich, T. A., Welsh, J. A., Telford, W., Demberg, T., Wood, J. C. S., Bigos, M., Ross, C. D., Kachynski, A., Dean, A., Felton, E. J., van Dyke, J., Tigges, J., Toxavidis, V., Parks, D. R., Overton, W. R., Kesarwala, A. H., Freeman, G. J., Rosner, A., … Jones, J. C. (2019). High-fidelity detection and sorting of nanoscale vesicles in viral disease and cancer. *Journal of Extracellular Vesicles*, *8*, 1597603.
Morikawa, Y., Takahashi, N., Kamiyama, K., Nishimori, K., Nishikawa, Y., Morita, S., Kobayashi, M., Fukushima, S., Yokoi, S., Mikami, D., Kimura, H., Kasuno, K., Yashiki, T., Naiki, H., Hara, M., & Iwano, M. (2019). Elevated levels of urinary extracellular vesicle fibroblast-specific protein 1 in patients with active crescentic glomerulonephritis. *Nephron*, *141*, 177–187.
Mukhopadhya, A., Santoro, J., Moran, B., Useckaite, Z., & O'Driscoll, L. (2021). Optimisation and comparison of orthogonal methods for separation and characterisation of extracellular vesicles to investigate how representative infant milk formula is of milk. *Food Chemistry*, *353*, 129309.
Mukhopadhya, A., Santoro, J., & O'Driscoll, L. (2021). Extracellular vesicle separation from milk and infant milk formula using acid precipitation and ultracentrifugation. *STAR Protocols*, *2*, 100821.
Musicò, A., Zenatelli, R., Romano, M., Zendrini, A., Alacqua, S., Tassoni, S., Paolini, L., Urbinati, C., Rusnati, M., Bergese, P., Pomarico, G., & Radeghieri, A. (2023). Surface functionalization of extracellular vesicle nanoparticles with antibodies: A first study on the protein corona "variable". *Nanoscale Advances*, *5*, 4703–4717.
Mustonen, A. M., Capra, J., Rilla, K., Lehenkari, P., Oikari, S., Kääriäinen, T., Joukainen, A., Kröger, H., Paakkonen, T., Matilainen, J., & Nieminen, P. (2021). Characterization of hyaluronan-coated extracellular vesicles in synovial fluid of patients with osteoarthritis and rheumatoid arthritis. *BMC Musculoskeletal Disorders [Electronic Resource]*, *22*, 247.
Nakai, W., Yoshida, T., Diez, D., Miyatake, Y., Nishibu, T., Imawaka, N., Naruse, K., Sadamura, Y., & Hanayama, R. (2016). A novel affinity-based method for the isolation of highly purified extracellular vesicles. *Scientific Reports*, *6*, 33935.
Nakayasu, E. S., Gritsenko, M., Piehowski, P. D., Gao, Y., Orton, D. J., Schepmoes, A. A., Fillmore, T. L., Frohnert, B. I., Rewers, M., Krischer, J. P., Ansong, C., Suchy-Dicey, A. M., Evans-Molina, C., Qian, W. J., Webb-Robertson, B. M., & Metz, T. O. (2021). Tutorial: Best practices and considerations for mass-spectrometry-based protein biomarker discovery and validation. *Nature Protocols*, *16*, 3737–3760.
Navazesh, M. (1993). Methods for collecting saliva. *Annals of the New York Academy of Sciences*, *694*, 72–77.
Neckles, V. N., Morton, M. C., Holmberg, J. C., Sokolov, A. M., Nottoli, T., Liu, D., & Feliciano, D. M. (2019). A transgenic inducible GFP extracellular-vesicle reporter (TIGER) mouse illuminates neonatal cortical astrocytes as a source of immunomodulatory extracellular vesicles. *Scientific Reports*, *9*, 3094.
Newman, L A., Useckaite, Z., & Rowland, A. (2022). Addressing MISEV guidance using targeted LC-MS/MS: A method for the detection and quantification of extracellular vesicle-enriched and contaminant protein markers from blood. *Journal of Extracellular Biology*, *1*, e56.
Ngamchuea, K., Chaisiwamongkhol, K., Batchelor-McAuley, C., & Compton, R. G. (2017). Chemical analysis in saliva and the search for salivary biomarkers – A tutorial review. *Analyst*, *143*, 81–99.
Nguyen, V. V. T., Witwer, K. W., Verhaar, M. C., Strunk, D., & van Balkom, B. W. M. (2020). Functional assays to assess the therapeutic potential of extracellular vesicles. *Journal of Extracellular Vesicles*, *10*, e12033.
Nieuwland, R., Falcon-Perez, J. M., Thery, C., & Witwer, K. W. (2020). Rigor and standardization of extracellular vesicle research: Paving the road towards robustness. *Journal of Extracellular Vesicles*, *10*, e12037.
Nikonorova, I. A., Wang, J., Cope, A. L., Tilton, P. E., Power, K. M., Walsh, J. D., Akella, J. S., Krauchunas, A. R., Shah, P., & Barr, M. M. (2022). Isolation, profiling, and tracking of extracellular vesicle cargo in *Caenorhabditis elegans*. *Current Biology*, *32*(9), 1924–1936.e6.
Nizamudeen, Z., Markus, R., Lodge, R., Parmenter, C., Platt, M., Chakrabarti, L., & Sottile, V. (2018). Rapid and accurate analysis of stem cell-derived extracellular vesicles with super resolution microscopy and live imaging. *Biochimica et Biophysica Acta (BBA) - Molecular Cell Research*, *1865*, 1891–1900.
Nonaka, T., & Wong, D. T. W. (2022). Saliva diagnostics. *Annual Review of Analytical Chemistry*, *15*, 107–121.
Nørgård, M. Ø., Steffensen, L. B., Hansen, D. R., Füchtbauer, E. M., Engelund, M. B., Dimke, H., Andersen, D. C., & Svenningsen, P. (2022). A new transgene mouse model using an extravesicular EGFP tag enables affinity isolation of cell-specific extracellular vesicles. *Scientific Reports*, *12*, 496.
Norman, M., Ter-Ovanesyan, D., Trieu, W., Lazarovits, R., Kowal, E. J. K., Lee, J. H., Chen-Plotkin, A. S., Regev, A., Church, G. M., & Walt, D. R. (2021). L1CAM is not associated with extracellular vesicles in human cerebrospinal fluid or plasma. *Nature Methods*, *18*, 631–634.
Obeid, S., Sung, P. S., Roy, B. L., Chou, M. L., Hsieh, S. L., Elie-Caille, C., Burnouf, T., & Boireau, W. (2019). NanoBioAnalytical characterization of extracellular vesicles in 75-nm nanofiltered human plasma for transfusion: A tool to improve transfusion safety. *Nanomedicine*, *20*, 101977.
Ogawa, Y., Kanai-Azuma, M., Akimoto, Y., Kawakami, H., & Yanoshita, R. (2008). Exosome-like vesicles with dipeptidyl peptidase IV in human saliva. *Biological & Pharmaceutical Bulletin*, *31*, 1059–1062.
Oleksiuk, O., Abba, M., Tezcan, K. C., Schaufler, W., Bestvater, F., Patil, N., Birk, U., Hafner, M., Altevogt, P., Cremer, C., & Allgayer, H. (2015). Single-Molecule Localization Microscopy allows for the analysis of cancer metastasis-specific miRNA distribution on the nanoscale. *Oncotarget*, *6*, 44745–44757.

20013078, 2024, 2, Downloaded from https://isevjournals.onlinelibrary.wiley.com/doi/10.1002/jev2.12404 by Colorado State University, Wiley Online Library on [09/10/2024]. See the Terms and Conditions (https://onlinelibrary.wiley.com/terms-and-conditions) on Wiley Online Library for rules of use; OA articles are governed by the applicable Creative Commons License

Oliveira, D. L., Nakayasu, E. S., Joffe, L. S., Guimarães, A. J., Sobreira, T. J., Nosanchuk, J. D., Cordero, R. J., Frases, S., Casadevall, A., Almeida, I. C., Nimrichter, L., & Rodrigues, M. L. (2010). Characterization of yeast extracellular vesicles: evidence for the participation of different pathways of cellular traffic in vesicle biogenesis. *PLoS ONE*, *5*, e11113.

Osteikoetxea, X., Sodar, B., Nemeth, A., Szabo-Taylor, K., Paloczi, K., Vukman, K. V., Tamasi, V., Balogh, A., Kittel, A., Pallinger, E., & Buzas, E. I. (2015). Differential detergent sensitivity of extracellular vesicle subpopulations. *Organic & Biomolecular Chemistry*, *13*, 9775–9782.

Ostrowski, M., Carmo, N. B., Krumeich, S., Fanget, I., Raposo, G., Savina, A., Moita, C. F., Schauer, K., Hume, A. N., Freitas, R. P., Goud, B., Benaroch, P., Hacohen, N., Fukuda, M., Desnos, C., Seabra, M. C., Darchen, F., Amigorena, S., Moita, L. F., & Thery, C. (2010). Rab27a and Rab27b control different steps of the exosome secretion pathway. *Nature Cell Biology*, *12*, 19–30, 1–13.

Page, M. J., Kell, D. B., & Pretorius, E. (2022). The role of lipopolysaccharide-induced cell signalling in chronic inflammation. *Chronic Stress (Thousand Oaks)*, *6*, 24705470221076390.

Palma, J., Yaddanapudi, S. C., Pigati, L., Havens, M. A., Jeong, S., Weiner, G. A., Weimer, K. M., Stern, B., Hastings, M. L., & Duelli, D. M. (2012). MicroRNAs are exported from malignant cells in customized particles. *Nucleic Acids Research*, *40*, 9125–9138.

Palmieri, V., Lucchetti, D., Gatto, I., Maiorana, A., Marcantoni, M., Maulucci, G., Papi, M., Pola, R., De Spirito, M., & Sgambato, A. (2014). Dynamic light scattering for the characterization and counting of extracellular vesicles: A powerful noninvasive tool. *Journal of Nanoparticle Research*, *16*, 2583.

Palviainen, M., Saari, H., Kärkkäinen, O., Pekkinen, J., Auriola, S., Yliperttula, M., Puhka, M., Hanhineva, K., & Siljander, P. R. (2019). Metabolic signature of extracellular vesicles depends on the cell culture conditions. *Journal of Extracellular Vesicles*, *8*, 1596669.

Palviainen, M., Saraswat, M., Varga, Z., Kitka, D., Neuvonen, M., Puhka, M., Joenväärä, S., Renkonen, R., Nieuwland, R., Takatalo, M., & Siljander, P. R. M. (2020). Extracellular vesicles from human plasma and serum are carriers of extravesicular cargo-Implications for biomarker discovery. *PLoS ONE*, *15*, e0236439.

Panagopoulou, M. S., Wark, A. W., Birch, D. J. S., & Gregory, C. D. (2020). Phenotypic analysis of extracellular vesicles: A review on the applications of fluorescence. *Journal of Extracellular Vesicles*, *9*, 1710020.

Paolini, L., Federici, S., Consoli, G., Arceri, D., Radeghieri, A., Alessandri, I., & Bergese, P. (2020). Fourier-transform Infrared (FT-IR) spectroscopy fingerprints subpopulations of extracellular vesicles of different sizes and cellular origin. *Journal of Extracellular Vesicles*, *9*, 1741174.

Paolini, L., Zendrini, A., Di Noto, G., Busatto, S., Lottini, E., Radeghieri, A., Dossi, A., Caneschi, A., Ricotta, D., & Bergese, P. (2016). Residual matrix from different separation techniques impacts exosome biological activity. *Scientific Reports*, *6*, 23550.

Parisse, P., Rago, I., Ulloa Severino, L., Perissinotto, F., Ambrosetti, E., Paoletti, P., Ricci, M., Beltrami, A. P., Cesselli, D., & Casalis, L. (2017). Atomic force microscopy analysis of extracellular vesicles. *European Biophysics Journal*, *46*, 813–820.

Park, J., Hwang, M., Choi, B., Jeong, H., Jung, J. H., Kim, H. K., Hong, S., Park, J. H., & Choi, Y. (2017). Exosome classification by pattern analysis of surface-enhanced raman spectroscopy data for lung cancer diagnosis. *Analytical Chemistry*, *89*, 6695–6701.

"Particle size analysis — Dynamic light scattering (DLS).". (2017). In ISO.

Peinado, H., Alečković, M., Lavotshkin, S., Matei, I., Costa-Silva, B., Moreno-Bueno, G., Hergueta-Redondo, M., Williams, C., García-Santos, G., Ghajar, C., Nitadori-Hoshino, A., Hoffman, C., Badal, K., Garcia, B. A., Callahan, M. K., Yuan, J., Martins, V. R., Skog, J., Kaplan, R. N., … Lyden, D. (2012). Melanoma exosomes educate bone marrow progenitor cells toward a pro-metastatic phenotype through MET. *Nature Medicine*, *18*, 883–891.

Perez-Gonzalez, R., Gauthier, S. A., Kumar, A., & Levy, E. (2012). The exosome secretory pathway transports amyloid precursor protein carboxyl-terminal fragments from the cell into the brain extracellular space. *Journal of Biological Chemistry*, *287*, 43108–43115.

Perrin, P., Janssen, L., Janssen, H., van den Broek, B., Voortman, L. M., van Elsland, D., Berlin, I., & Neefjes, J. (2021). Retrofusion of intralumenal MVB membranes parallels viral infection and coexists with exosome release. *Current Biology*, *31*, 3884–3893.e4.

Pfeiler, S., Thakur, M., Grünauer, P., Megens, R. T. A., Joshi, U., Coletti, R., Samara, V., Müller-Stoy, G., Ishikawa-Ankerhold, H., Stark, K., Klingl, A., Fröhlich, T., Arnold, G. J., Wörmann, S., Bruns, C. J., Algül, H., Weber, C., Massberg, S., & Engelmann, B. (2019). CD36-triggered cell invasion and persistent tissue colonization by tumor microvesicles during metastasis. *Faseb Journal*, *33*, 1860–1872.

Pham, T. C., Jayasinghe, M. K., Pham, T. T., Yang, Y., Wei, L., Usman, W. M., Chen, H., Pirisinu, M., Gong, J., Kim, S., Peng, B., Wang, W., Chan, C., Ma, V., Nguyen, N. T. H., Kappei, D., Nguyen, X. H., Cho, W. C., Shi, J., & Le, M. T. N. (2021). Covalent conjugation of extracellular vesicles with peptides and nanobodies for targeted therapeutic delivery. *Journal of Extracellular Vesicles*, *10*, e12057.

Piontek, M. C., Lira, R. B., & Roos, W. H. (2021). Active probing of the mechanical properties of biological and synthetic vesicles. *Biochimica et Biophysica Acta (BBA) - General Subjects*, *1865*, 129486.

Pisitkun, T., Shen, R. F., & Knepper, M. A. (2004). Identification and proteomic profiling of exosomes in human urine. *PNAS*, *101*, 13368–13373.

Pleet, M. L., Cook, S., Tang, V. A., Stack, E., Ford, V. J., Lannigan, J., Do, N., Wenger, E., Fraikin, J. L., Jacobson, S., Jones, J. C., & Welsh, J. A. (2023). Extracellular vesicle refractive index derivation utilizing orthogonal characterization. *Nano Letters*, *23*(20), 9195–9202.

Pocsfalvi, G., Stanly, C., Vilasi, A., Fiume, I., Capasso, G., Turiak, L., Buzas, E. I., & Vekey, K. (2016). Mass spectrometry of extracellular vesicles. *Mass Spectrometry Reviews*, *35*, 3–21.

Pocsfalvi, G., Stanly, C., Fiume, I., & Vékey, K. (2016). Chromatography and its hyphenation to mass spectrometry for extracellular vesicle analysis. *Journal of Chromatography A*, *1439*, 26–41.

Polanco, J. C., Li, C., Durisic, N., Sullivan, R., & Götz, J. (2018). Exosomes taken up by neurons hijack the endosomal pathway to spread to interconnected neurons. *Acta Neuropathologica Communications*, *6*, 10.

Polanco, J. C., Scicluna, B. J., Hill, A. F., & Götz, J. (2016). Extracellular vesicles isolated from the brains of rTg4510 mice seed tau protein aggregation in a threshold-dependent manner. *Journal of Biological Chemistry*, *291*, 12445–12466.

Prados-Rosales, R., Baena, A., Martinez, L. R., Luque-Garcia, J., Kalscheuer, R., Veeraraghavan, U., Camara, C., Nosanchuk, J. D., Besra, G. S., Chen, B., Jimenez, J., Glatman-Freedman, A., Jacobs, W. R., Jr., Porcelli, S. A., & Casadevall, A. (2011). Mycobacteria release active membrane vesicles that modulate immune responses in a TLR2-dependent manner in mice. *Journal of Clinical Investigation*, *121*, 1471–1483.

Preußer, C., Stelter, K., Tertel, T., Linder, M., Helmprobst, F., Szymanski, W., Graumann, J., Giebel, B., Reinartz, S., Müller, R., Weber, G., & von Strandmann, E. P. (2022). Isolation of native EVs from primary biofluids—Free-flow electrophoresis as a novel approach to purify ascites-derived EVs. *Journal of Extracellular Biology*, *1*, e71.

Provencher, S. W. (1982). A constrained regularization method for inverting data represented by linear algebraic or integral equations. *Computer Physics Communications*, *27*, 213–227.

Puca, L., Chastagner, P., Meas-Yedid, V., Israël, A., & Brou, C. (2013). A-arrestin 1 (ARRDC1) and β-arrestins cooperate to mediate Notch degradation in mammals. *Journal of Cell Science*, *126*, 4457–4468.

Pucci, F., Garris, C., Lai, C. P., Newton, A., Pfirschke, C., Engblom, C., Alvarez, D., Sprachman, M., Evavold, C., Magnuson, A., von Andrian, U. H., Glatz, K., Breakefield, X. O., Mempel, T. R., Weissleder, R., & Pittet, M. J. (2016). SCS macrophages suppress melanoma by restricting tumor-derived vesicle-B cell interactions. *Science*, *352*, 242–246.

20013078, 2024, 2, Downloaded from https://isevjournals.onlinelibrary.wiley.com/doi/10.1002/jev2.12404 by Colorado State University, Wiley Online Library on [09/10/2024]. See the Terms and Conditions (https://onlinelibrary.wiley.com/terms-and-conditions) on Wiley Online Library for rules of use; OA articles are governed by the applicable Creative Commons License

Pužar Dominkuš, P., Stenovec, M., Sitar, S., Lasič, E., Zorec, R., Plemenitaš, A., Žagar, E., Kreft, M., & Lenassi, M. (2018). PKH26 labeling of extracellular vesicles: Characterization and cellular internalization of contaminating PKH26 nanoparticles. *Biochimica et Biophysica Acta (BBA) - Biomembranes*, *1860*, 1350–1361.

Qu, X., Li, Q., Yang, J., Zhao, H., Wang, F., Zhang, F., Zhang, S., Zhang, H., Wang, R., Wang, Q., Wang, Q., Li, G., Peng, X., Zhou, X., Hao, Y., Zhu, J., & Xiao, W. (2019). Double-stranded DNA in exosomes of malignant pleural effusions as a novel DNA source for EGFR mutation detection in lung adenocarcinoma. *Frontiers in Oncology*, *9*, 931.

Rad, M., Kakoie, S., Brojeni, F. N, & Pourdamghan, N. (2010). Effect of long-term smoking on whole-mouth salivary flow rate and oral Health. *Journal of Dental Research, Dental Clinics, Dental Prospects*, *4*, 110–114.

Radeghieri, A., Alacqua, S., Zendrini, A., Previcini, V., Todaro, F., Martini, G., Ricotta, D., & Bergese, P. (2022). Active antithrombin glycoforms are selectively physiosorbed on plasma extracellular vesicles. *Journal of Extracellular Biology*, *1*, e57.

Ragni, E., Perucca Orfei, C., De Luca, P., Lugano, G., Viganò, M., Colombini, A., Valli, F., Zacchetti, D., Bollati, V., & de Girolamo, L. (2019). Interaction with hyaluronan matrix and miRNA cargo as contributors for in vitro potential of mesenchymal stem cell-derived extracellular vesicles in a model of human osteoarthritic synoviocytes. *Stem Cell Research & Therapy*, *10*, 109.

Rahman, M. M., Shimizu, K., Yamauchi, M., Takase, H., Ugawa, S., Okada, A., & Inoshima, Y. (2019). Acidification effects on isolation of extracellular vesicles from bovine milk. *PLoS ONE*, *14*, e0222613.

Raj, A., Kato, C., Witek, H. A., & Hamaguchi, H. (2020). Toward standardization of Raman spectroscopy: Accurate wavenumber and intensity calibration using rotational Raman spectra of H-2, HD, D-2, and vibration-rotation spectrum of O-2. *Journal of Raman Spectroscopy*, *51*, 2066–2082.

Ramirez-Garrastacho, M., Bajo-Santos, C., Line, A., Martens-Uzunova, E. S., de la Fuente, J. M., Moros, M., Soekmadji, C., Tasken, K. A., & Llorente, A. (2022). Extracellular vesicles as a source of prostate cancer biomarkers in liquid biopsies: A decade of research. *British Journal of Cancer*, *126*, 331–350.

Rao, P., Benito, E., & Fischer, A. (2013). MicroRNAs as biomarkers for CNS disease. *Frontiers in Molecular Neuroscience*, *6*, 39.

Raposo, G., Nijman, H. W., Stoorvogel, W., Liejendekker, R., Harding, C. V., Melief, C. J., & Geuze, H. J. (1996). B lymphocytes secrete antigen-presenting vesicles. *Journal of Experimental Medicine*, *183*, 1161–1172.

Razzauti, A., & Laurent, P. (2021). Ectocytosis prevents accumulation of ciliary cargo in *C. elegans* sensory neurons. *Elife*, *10*, e67670.

Ridder, K., Keller, S., Dams, M., Rupp, A. K., Schlaudraff, J., del Turco, D., Starmann, J., Macas, J., Karpova, D., Devraj, K., Depboylu, C., Landfried, B., Arnold, B., Plate, K. H., Höglinger, G., Sültmann, H., Altevogt, P., & Momma, S. (2014). Extracellular vesicle-mediated transfer of genetic information between the hematopoietic system and the brain in response to inflammation. *Plos Biology*, *12*, e1001874.

Ridolfi, A., Brucale, M., Montis, C., Caselli, L., Paolini, L., Borup, A., Boysen, A. T., Loria, F., van Herwijnen, M. J. C., Kleinjan, M., Nejsum, P., Zarovni, N., Wauben, M. H. M., Berti, D., Bergese, P., & Valle, F. (2020). AFM-based high-throughput nanomechanical screening of single extracellular vesicles. *Analytical Chemistry*, *92*, 10274–10282.

Ridolfi, A., Caselli, L., Baldoni, M., Montis, C., Mercuri, F., Berti, D., Valle, F., & Brucale, M. (2021). Stiffness of fluid and gel phase lipid nanovesicles: Weighting the contributions of membrane bending modulus and luminal pressurization. *Langmuir*, *37*, 12027–12037.

Riekse, R. G., Li, G., Petrie, E. C., Leverenz, J. B., Vavrek, D., Vuletic, S., Albers, J. J., Montine, T. J., Lee, V. M., Lee, M., Seubert, P., Galasko, D., Schellenberg, G. D., Hazzard, W. R., & Peskind, E. R. (2006). Effect of statins on Alzheimer's disease biomarkers in cerebrospinal fluid. *Journal of Alzheimer's Disease*, *10*, 399–406.

Rikkert, L. G., Nieuwland, R., Terstappen, L., & Coumans, F. A. W. (2019). Quality of extracellular vesicle images by transmission electron microscopy is operator and protocol dependent. *Journal of Extracellular Vesicles*, *8*, 1555419.

Roberts-Dalton, H. D., Cocks, A., Falcon-Perez, J. M., Sayers, E. J., Webber, J. P., Watson, P., Clayton, A., & Jones, A. T. (2017). Fluorescence labelling of extracellular vesicles using a novel thiol-based strategy for quantitative analysis of cellular delivery and intracellular traffic. *Nanoscale*, *9*, 13693–13706.

Rodrigues, A. D., van Dyk, M., Sorich, M. J., Fahmy, A., Useckaite, Z., Newman, L. A., Kapetas, A. J., Mounzer, R., Wood, L. S., Johnson, J. G., & Rowland, A. (2021). Exploring the use of serum-derived small extracellular vesicles as liquid biopsy to study the induction of hepatic cytochromes P450 and organic anion transporting polypeptides. *Clinical Pharmacology & Therapeutics*, *110*, 248–258.

Rojalin, T., Koster, H. J., Liu, J., Mizenko, R. R., Tran, D., Wachsmann-Hogiu, S., & Carney, R. P. (2020). Hybrid nanoplasmonic porous biomaterial scaffold for liquid biopsy diagnostics using extracellular vesicles. *ACS Sensors*, *5*, 2820–2833.

Romanò, S., Di Giacinto, F., Primiano, A., Gervasoni, J., Mazzini, A., Papi, M., Urbani, A., Serafino, A., De Spirito, M., Krasnowska, E. K., & Ciasca, G. (2022). Label-free spectroscopic characterization of exosomes reveals cancer cell differentiation. *Analytica Chimica Acta*, *1192*, 339359.

Rostgaard, N., Olsen, M. H., Ottenheijm, M., Drici, L., Simonsen, A. H., Plomgaard, P., Gredal, H., Poulsen, H. H., Zetterberg, H., Blennow, K., Hasselbalch, S. G., MacAulay, N., & Juhler, M. (2023). Differential proteomic profile of lumbar and ventricular cerebrospinal fluid. *Fluids Barriers CNS*, *20*, 6.

Roux, Q., Van Deun, J., Dedeyne, S., & Hendrix, A. (2020). The EV-TRACK summary add-on: Integration of experimental information in databases to ensure comprehensive interpretation of biological knowledge on extracellular vesicles. *Journal of Extracellular Vesicles*, *9*, 1699367.

Royo, F., Cossío, U., Ruiz de Angulo, A., Llop, J., & Falcon-Perez, J. M. (2019). Modification of the glycosylation of extracellular vesicles alters their biodistribution in mice. *Nanoscale*, *11*, 1531–1537.

Royo, F., Théry, C., Falcón-Pérez, J. M., Nieuwland, R., & Witwer, K. W. (2020). Methods for separation and characterization of extracellular vesicles: results of a worldwide survey performed by the ISEV rigor and standardization subcommittee. *Cells*, *9*, 1955.

Rufino-Ramos, D., Lule, S., Mahjoum, S., Ughetto, S., Cristopher Bragg, D., Pereira de Almeida, L., Breakefield, X. O., & Breyne, K. (2022). Using genetically modified extracellular vesicles as a non-invasive strategy to evaluate brain-specific cargo. *Biomaterials*, *281*, 121366.

Russell, A. E., Sneider, A., Witwer, K. W., Bergese, P., Bhattacharyya, S. N., Cocks, A., Cocucci, E., Erdbrügger, U., Falcon-Perez, J. M., Freeman, D. W., Gallagher, T. M., Hu, S., Huang, Y., Jay, S. M., Kano, S. I., Lavieu, G., Leszczynska, A., Llorente, A. M., Lu, Q., … Vader, P. (2019). Biological membranes in EV biogenesis, stability, uptake, and cargo transfer: an ISEV position paper arising from the ISEV membranes and EVs workshop. *Journal of Extracellular Vesicles*, *8*, 1684862.

Russell, J. C., Kim, T. K., Noori, A., Merrihew, G. E., Robbins, J. E., Golubeva, A., Wang, K., MacCoss, M. J., & Kaeberlein, M. (2020). Composition of *Caenorhabditis elegans* extracellular vesicles suggests roles in metabolism, immunity, and aging. *Geroscience*, *42*, 1133–1145.

Rust, M. J., Bates, M., & Zhuang, X. W. (2006). Sub-diffraction-limit imaging by stochastic optical reconstruction microscopy (STORM). *Nature Methods*, *3*, 793–795.

Rüwald, J. M., Randau, T. M., Hilgers, C., Masson, W., Irsen, S., Eymael, R. L., Kohlhof, H., Gravius, S., Burger, C., Wirtz, D. C., & Schildberg, F. A. (2020). Extracellular vesicle isolation and characterization from periprosthetic joint synovial fluid in revision total joint arthroplasty. *Journal of Clinical Medicine*, *9*, 516.

Saari, H., Pusa, R., Marttila, H., Yliperttula, M., & Laitinen, S. (2023). Development of tandem cation exchange chromatography for high purity extracellular vesicle isolation: The effect of ligand steric availability. *Journal of Chromatography A*, *1707*, 464293.

Saari, H., Turunen, T., Lõhmus, A., Turunen, M., Jalasvuori, M., Butcher, S. J., Ylä-Herttuala, S., Viitala, T., Cerullo, V., Siljander, P. R. M., & Yliperttula, M. (2020). Extracellular vesicles provide a capsid-free vector for oncolytic adenoviral DNA delivery. *Journal of Extracellular Vesicles*, *9*, 1747206.

20013078, 2024, 2, Downloaded from https://isevjournals.onlinelibrary.wiley.com/doi/10.1002/jev2.12404 by Colorado State University, Wiley Online Library on [09/10/2024]. See the Terms and Conditions (https://onlinelibrary.wiley.com/terms-and-conditions) on Wiley Online Library for rules of use; OA articles are governed by the applicable Creative Commons License

Saludes, J. P., Morton, L. A., Ghosh, N., Beninson, L. A., Chapman, E. R., Fleshner, M., & Yin, H. (2012). Detection of highly curved membrane surfaces using a cyclic peptide derived from synaptotagmin-I. *Acs Chemical Biology*, *7*, 1629–1635.
Sanada, T., Hirata, Y., Naito, Y., Yamamoto, N., Kikkawa, Y., Ishida, Y., Yamasaki, C., Tateno, C., Ochiya, T., & Kohara, M. (2017). Transmission of HBV DNA mediated by ceramide-triggered extracellular vesicles. *Cellular and Molecular Gastroenterology and Hepatology*, *3*, 272–283.
Sandau, U. S., Duggan, E., Shi, X., Smith, S. J., Huckans, M., Schutzer, W. E., Loftis, J. M., Janowsky, A., Nolan, J. P., & Saugstad, J. A. (2020). Methamphetamine use alters human plasma extracellular vesicles and their microRNA cargo: An exploratory study. *Journal of Extracellular Vesicles*, *10*, e12028.
Sansone, P., Savini, C., Kurelac, I., Chang, Q., Amato, L. B., Strillacci, A., Stepanova, A., Iommarini, L., Mastroleo, C., Daly, L., Galkin, A., Thakur, B. K., Soplop, N., Uryu, K., Hoshino, A., Norton, L., Bonafé, M., Cricca, M., Gasparre, G., … Bromberg, J. (2017). Packaging and transfer of mitochondrial DNA via exosomes regulate escape from dormancy in hormonal therapy-resistant breast cancer. *PNAS*, *114*, E9066–E9075.
Santoro, J., Mukhopadhya, A., Oliver, C., Brodkorb, A., Giblin, L., & O'Driscoll, L. (2023). An investigation of extracellular vesicles in bovine colostrum, first milk and milk over the lactation curve. *Food Chemistry*, *401*, 134029.
Schioppo, T., Ubiali, T., Ingegnoli, F., Bollati, V., & Caporali, R. (2021). The role of extracellular vesicles in rheumatoid arthritis: a systematic review. *Clinical Rheumatology*, *40*, 3481–3497.
Scott, A., Sueiro Ballesteros, L., Bradshaw, M., Tsuji, C., Power, A., Lorriman, J., Love, J., Paul, D., Herman, A., Emanueli, C., & Richardson, R. J. (2021). In vivo characterization of endogenous cardiovascular extracellular vesicles in larval and adult zebrafish. *Arteriosclerosis, Thrombosis, and Vascular Biology*, *41*, 2454–2468.
Shah, S. S., Ebberson, J., Kestenbaum, L. A., Hodinka, R. L., & Zorc, J. J. (2011). Age-specific reference values for cerebrospinal fluid protein concentration in neonates and young infants. *Journal of Hospital Medicine*, *6*, 22–27.
Sharma, A., Mariappan, M., Appathurai, S., & Hegde, R. S. (2010). In vitro dissection of protein translocation into the mammalian endoplasmic reticulum. *Methods in Molecular Biology*, *619*, 339–363.
Sharma, S., Gillespie, B. M., Palanisamy, V., & Gimzewski, J. K. (2011). Quantitative nanostructural and single-molecule force spectroscopy biomolecular analysis of human-saliva-derived exosomes. *Langmuir*, *27*, 14394–14400.
Sharma, S., LeClaire, M., & Gimzewski, J. K. (2018). Ascent of atomic force microscopy as a nanoanalytical tool for exosomes and other extracellular vesicles. *Nanotechnology*, *29*, 132001.
Sharma, S., LeClaire, M., Wohlschlegel, J., & Gimzewski, J. (2020). Impact of isolation methods on the biophysical heterogeneity of single extracellular vesicles. *Scientific Reports*, *10*, 13327.
Shekari, F., Alibhai, F. J., Baharvand, H., Börger, V., Bruno, S., Davies, O., Giebel, B., Gimona, M., Salekdeh, G. H., Martin-Jaular, L., Mathivanan, S., Nelissen, I., Hoen, E. N.-T., O'Driscoll, L., Perut, F., Pluchino, S., Pocsfalvi, G., Salomon, C., Soekmadji, C., … Nieuwland, R. (2023). Cell culture-derived extracellular vesicles: Considerations for reporting cell culturing parameters. *Journal of Extracellular Biology*, *2*, e115.
Shen, S., Shen, Z., Wang, C., Wu, X., Wang, L., Ye, L., Zhang, S., & Cheng, X. (2023). Effects of lysate/tissue storage at −80°C on subsequently extracted EVs of epithelial ovarian cancer tissue origins. *Iscience*, *26*, 106521.
Shlomovitz, I., Erlich, Z., Arad, G., Edry-Botzer, L., Zargarian, S., Cohen, H., Manko, T., Ofir-Birin, Y., Cooks, T., Regev-Rudzki, N., & Gerlic, M. (2021). Proteomic analysis of necroptotic extracellular vesicles. *Cell Death & Disease*, *12*, 1059.
Silva, A. M., Lázaro-Ibáñez, E., Gunnarsson, A., Dhande, A., Daaboul, G., Peacock, B., Osteikoetxea, X., Salmond, N., Friis, K. P., Shatnyeva, O., & Dekker, N. (2021). Quantification of protein cargo loading into engineered extracellular vesicles at single-vesicle and single-molecule resolution. *Journal of Extracellular Vesicles*, *10*, e12130.
Simonsen, J. B. (2017). What are we looking at? Extracellular vesicles, lipoproteins, or both? *Circulation Research*, *121*, 920–922.
Simonsen, J. B. (2019). Pitfalls associated with lipophilic fluorophore staining of extracellular vesicles for uptake studies. *Journal of Extracellular Vesicles*, *8*, 1582237.
Singh, P., Szigyártó, I. C., Ricci, M., Zsila, F., Juhász, T., Mihály, J., Bősze, S., Bulyáki, É., Kardos, J., Kitka, D., Varga, Z., & Beke-Somfai, T. (2020). Membrane active peptides remove surface adsorbed protein corona from extracellular vesicles of red blood cells. *Frontiers in Chemistry*, *8*, 703.
Sitar, S., Kejžar, A., Pahovnik, D., Kogej, K., Tušek-Žnidarič, M., Lenassi, M., & Žagar, E. (2015). Size characterization and quantification of exosomes by asymmetrical-flow field-flow fractionation. *Analytical Chemistry*, *87*, 9225–9233.
Skliar, M., Chernyshev, V. S., Belnap, D. M., Sergey, G. V., Al-Hakami, S. M., Bernard, P. S., Stijleman, I. J., & Rachamadugu, R. (2018). Membrane proteins significantly restrict exosome mobility. *Biochemical and Biophysical Research Communications*, *501*, 1055–1059.
Skotland, T., Iversen, T. G., Llorente, A., & Sandvig, K. (2022). Biodistribution, pharmacokinetics and excretion studies of intravenously injected nanoparticles and extracellular vesicles: Possibilities and challenges. *Advanced Drug Delivery Reviews*, *186*, 114326.
Smith, E., & Dent, G. (2005). Modern raman spectroscopy: A practical approach. 1–210.
Smith, Z. J., Lee, C., Rojalin, T., Carney, R. P., Hazari, S., Knudson, A., Lam, K., Saari, H., Ibanez, E. L., Viitala, T., Laaksonen, T., Yliperttula, M., & Wachsmann-Hogiu, S. (2015). Single exosome study reveals subpopulations distributed among cell lines with variability related to membrane content. *Journal of Extracellular Vesicles*, *4*, 28533.
Sódar, B. W., Kittel, Á., Pálóczi, K., Vukman, K. V., Osteikoetxea, X., Szabó-Taylor, K., Németh, A., Sperlágh, B., Baranyai, T., Giricz, Z., Wiener, Z., Turiák, L., Drahos, L., Pállinger, É., Vékey, K., Ferdinandy, P., Falus, A., & Buzás, E. I. (2016). Low-density lipoprotein mimics blood plasma-derived exosomes and microvesicles during isolation and detection. *Scientific Reports*, *6*, 24316.
Sodar, B. W., Kovacs, A., Visnovitz, T., Pallinger, E., Vekey, K., Pocsfalvi, G., Turiak, L., & Buzas, E. I. (2017). Best practice of identification and proteomic analysis of extracellular vesicles in human health and disease. *Expert Review of Proteomics*, *14*, 1073–1090.
Soekmadji, C., Hill, A. F., Wauben, M. H., Buzás, E. I., Di Vizio, D., Gardiner, C., Lötvall, J., Sahoo, S., & Witwer, K. W. (2018). Towards mechanisms and standardization in extracellular vesicle and extracellular RNA studies: Results of a worldwide survey. *Journal of Extracellular Vesicles*, *7*, 1535745.
Somiya, M., & Kuroda, S. (2021a). Real-time luminescence assay for cytoplasmic cargo delivery of extracellular vesicles. *Analytical Chemistry*, *93*, 5612–5620.
Somiya, M., & Kuroda, S. (2021b). Reporter gene assay for membrane fusion of extracellular vesicles. *Journal of Extracellular Vesicles*, *10*, e12171.
Somiya, M., Yoshioka, Y., & Ochiya, T. (2018). Biocompatibility of highly purified bovine milk-derived extracellular vesicles. *Journal of Extracellular Vesicles*, *7*, 1440132.
Sorkin, R., Huisjes, R., Bošković, F., Vorselen, D., Pignatelli, S., Ofir-Birin, Y., Freitas Leal, J. K., Schiller, J., Mullick, D., Roos, W. H., Bosman, G., Regev-Rudzki, N., Schiffelers, R. M., & Wuite, G. J. L. (2018). Nanomechanics of extracellular vesicles reveals vesiculation pathways. *Small*, *14*, e1801650.
Stam, J., Bartel, S., Bischoff, R., & Wolters, J. C. (2021). Isolation of extracellular vesicles with combined enrichment methods. *Journal of Chromatography. B, Analytical Technologies in the Biomedical and Life Sciences*, *1169*, 122604.
Steenbeek, S. C., Pham, T. V., de Ligt, J., Zomer, A., Knol, J. C., Piersma, S. R., Schelfhorst, T., Huisjes, R., Schiffelers, R. M., Cuppen, E., Jimenez, C. R., & van Rheenen, J. (2018). Cancer cells copy migratory behavior and exchange signaling networks via extracellular vesicles. *Embo Journal*, *37*, e98357.

20013078, 2024, 2, Downloaded from https://isevjournals.onlinelibrary.wiley.com/doi/10.1002/jev2.12404 by Colorado State University, Wiley Online Library on [09/10/2024]. See the Terms and Conditions (https://onlinelibrary.wiley.com/terms-and-conditions) on Wiley Online Library for rules of use; OA articles are governed by the applicable Creative Commons License

Stetefeld, J., McKenna, S. A., & Patel, T. R. (2016). Dynamic light scattering: a practical guide and applications in biomedical sciences. *Biophysical Reviews*, *8*, 409–427.

Stoner, S. A., Duggan, E., Condello, D., Guerrero, A., Turk, J. R., Narayanan, P. K., & Nolan, J. P. (2016). High sensitivity flow cytometry of membrane vesicles. *Cytometry Part A: the journal of the International Society for Analytical Cytology*, *89*, 196–206.

Sung, B. H., Ketova, T., Hoshino, D., Zijlstra, A., & Weaver, A. M. (2015). Directional cell movement through tissues is controlled by exosome secretion. *Nature Communications*, *6*, 7164.

Sung, B. H., & Weaver, A. M. (2017). Exosome secretion promotes chemotaxis of cancer cells. *Cell Adhesion & Migration*, *11*, 187–195.

Suwatthanarak, T., Thiodorus, I. A., Tanaka, M., Shimada, T., Takeshita, D., Yasui, T., Baba, Y., & Okochi, M. (2021). Microfluidic-based capture and release of cancer-derived exosomes via peptide-nanowire hybrid interface. *Lab on A Chip*, *21*, 597–607.

Taha, E. A., Sogawa, C., Okusha, Y., Kawai, H., Oo, M. W., Elseoudi, A., Lu, Y., Nagatsuka, H., Kubota, S., Satoh, A., Okamoto, K., & Eguchi, T. (2020). Knockout of MMP3 weakens solid tumor organoids and cancer extracellular vesicles. *Cancers (Basel)*, *12*, 1260.

Taher, S., Borja, Y., Cabanela, L., Costers, V. J., Carson-Marino, M., Bailes, J. C., Dhar, B., Beckworth, M. T., Rabaglino, M. B., Post Uiterweer, E. D., & Conrad, K. P. (2019). Cholecystokinin, gastrin, cholecystokinin/gastrin receptors, and bitter taste receptor TAS2R14: Trophoblast expression and signaling. *American Journal of Physiology. Regulatory, Integrative and Comparative Physiology*, *316*, R628–R639.

Takov, K., Yellon, D. M., & Davidson, S. M. (2017). Confounding factors in vesicle uptake studies using fluorescent lipophilic membrane dyes. *Journal of Extracellular Vesicles*, *6*, 1388731.

Tassetto, M., Kunitomi, M., & Andino, R. (2017). Circulating immune cells mediate a systemic RNAi-based adaptive antiviral response in drosophila. *Cell*, *169*, 314–325.e13.

Taylor, C. F., Paton, N. W., Lilley, K. S., Binz, P. A., Julian R. K., Jr, Jones, A. R., Zhu, W., Apweiler, R., Aebersold, R., Deutsch, E. W., Dunn, M. J., Heck, A. J., Leitner, A., Macht, M., Mann, M., Martens, L., Neubert, T. A., Patterson, S. D., Ping, P., … Hermjakob, H. (2007). The minimum information about a proteomics experiment (MIAPE). *Nature Biotechnology*, *25*, 887–893.

Ter-Ovanesyan, D., Gilboa, T., Budnik, B., Nikitina, A., Whiteman, S., Lazarovits, R., Trieu, W., Kalish, D., Church, G. M., & Walt, D. R. (2023). Improved isolation of extracellular vesicles by removal of both free proteins and lipoproteins. *Elife*, *12*, e86394.

Ter-Ovanesyan, D., Norman, M., Lazarovits, R., Trieu, W., Lee, J. H., Church, G. M., & Walt, D. R. (2021). Framework for rapid comparison of extracellular vesicle isolation methods. *Elife*, *10*, e70725.

Teunissen, C. E., Petzold, A., Bennett, J. L., Berven, F. S., Brundin, L., Comabella, M., Franciotta, D., Frederiksen, J. L., Fleming, J. O., Furlan, R., Hintzen, R. Q., Hughes, S. G., Johnson, M. H., Krasulova, E., Kuhle, J., Magnone, M. C., Rajda, C., Rejdak, K., Schmidt, H. K., … Deisenhammer, F. (2009). A consensus protocol for the standardization of cerebrospinal fluid collection and biobanking. *Neurology*, *73*, 1914–1922.

Thakur, B. K., Zhang, H., Becker, A., Matei, I., Huang, Y., Costa-Silva, B., Zheng, Y., Hoshino, A., Brazier, H., Xiang, J., Williams, C., Rodriguez-Barrueco, R., Silva, J. M., Zhang, W., Hearn, S., Elemento, O., Paknejad, N., Manova-Todorova, K., Welte, K., … Lyden, D. (2014). Double-stranded DNA in exosomes: A novel biomarker in cancer detection. *Cell Research*, *24*, 766–769.

Théry, C., Amigorena, S., Raposo, G., & Clayton, A. (2006). Isolation and characterization of exosomes from cell culture supernatants and biological fluids. *Current Protocols in Cell Biology*, Chapter 3, Unit 3.22.

Théry, C., Witwer, K. W., Aikawa, E., Alcaraz, M. J., Anderson, J. D., Andriantsitohaina, R., Antoniou, A., Arab, T., Archer, F., Atkin-Smith, G. K., Ayre, D. C., Bach, J. M., Bachurski, D., Baharvand, H., Balaj, L., Baldacchino, S., Bauer, N. N., Baxter, A. A., Bebawy, M., … Zuba-Surma, E. K. (2018). Minimal information for studies of extracellular vesicles 2018 (MISEV2018): A position statement of the International Society for Extracellular Vesicles and update of the MISEV2014 guidelines. *Journal of Extracellular Vesicles*, *7*(1), 1535750. https://doi.org/10.1080/20013078.2018.1535750

Thomas, R. E., Vincow, E. S., Merrihew, G. E., MacCoss, M. J., Davis, M. Y., & Pallanck, L. J. (2018). Glucocerebrosidase deficiency promotes protein aggregation through dysregulation of extracellular vesicles. *Plos Genetics*, *14*, e1007694.

Tian, T., Wang, Y., Wang, H., Zhu, Z., & Xiao, Z. (2010). Visualizing of the cellular uptake and intracellular trafficking of exosomes by live-cell microscopy. *Journal of Cellular Biochemistry*, *111*, 488–496.

Tian, Y., Gong, M., Hu, Y., Liu, H., Zhang, W., Zhang, M., Hu, X., Aubert, D., Zhu, S., Wu, L., & Yan, X. (2020). Quality and efficiency assessment of six extracellular vesicle isolation methods by nano-flow cytometry. *Journal of Extracellular Vesicles*, *9*, 1697028.

Tian, Y., Ma, L., Gong, M., Su, G., Zhu, S., Zhang, W., Wang, S., Li, Z., Chen, C., Li, L., Wu, L., & Yan, X. (2018). Protein profiling and sizing of extracellular vesicles from colorectal cancer patients via flow cytometry. *ACS Nano*, *12*, 671–680.

Toda, H., Diaz-Varela, M., Segui-Barber, J., Roobsoong, W., Baro, B., Garcia-Silva, S., Galiano, A., Gualdron-Lopez, M., Almeida, A. C. G., Brito, M. A. M., de Melo, G. C., Aparici-Herraiz, I., Castro-Cavadia, C., Monteiro, W. M., Borras, E., Sabido, E., Almeida, I. C., Chojnacki, J., Martinez-Picado, J., … del Portillo, H. A. (2020). Plasma-derived extracellular vesicles from Plasmodium vivax patients signal spleen fibroblasts via NF-kB facilitating parasite cytoadherence. *Nature Communications*, *11*, 2761.

Tóth, E. Á., Turiák, L., Visnovitz, T., Cserép, C., Mázló, A., Sódar, B. W., Försönits, A. I., Petővári, G., Sebestyén, A., Komlósi, Z., Drahos, L., Kittel, Á., Nagy, G., Bácsi, A., Dénes, Á., Gho, Y. S., Szabó-Taylor, K. É., & Buzás, E. I. (2021). Formation of a protein corona on the surface of extracellular vesicles in blood plasma. *Journal of Extracellular Vesicles*, *10*, e12140.

Toyofuku, M., Schild, S., Kaparakis-Liaskos, M., & Eberl, L. (2023). Composition and functions of bacterial membrane vesicles. *Nature Reviews Microbiology*, *21*, 415–430.

Trajkovic, K., Hsu, C., Chiantia, S., Rajendran, L., Wenzel, D., Wieland, F., Schwille, P., Brügger, B., & Simons, M. (2008). Ceramide triggers budding of exosome vesicles into multivesicular endosomes. *Science*, *319*, 1244–1247.

Trenkenschuh, E., Richter, M., Heinrich, E., Koch, M., Fuhrmann, G., & Friess, W. (2022). Enhancing the stabilization potential of lyophilization for extracellular vesicles. *Advanced Healthcare Materials*, *11*, e2100538.

Tsai, Y. W., Sung, H. H., Li, J. C., Yeh, C. Y., Chen, P. Y., Cheng, Y. J., Chen, C. H., Tsai, Y. C., & Chien, C. T. (2019). Glia-derived exosomal miR-274 targets Sprouty in trachea and synaptic boutons to modulate growth and responses to hypoxia. *PNAS*, *116*, 24651–24661.

Tulkens, J., Vergauwen, G., Van Deun, J., Geeurickx, E., Dhondt, B., Lippens, L., De Scheerder, M. A., Miinalainen, I., Rappu, P., De Geest, B. G., Vandecasteele, K., Laukens, D., Vandekerckhove, L., Denys, H., Vandesompele, J., De Wever, O., & Hendrix, A. (2020). Increased levels of systemic LPS-positive bacterial extracellular vesicles in patients with intestinal barrier dysfunction. *Gut*, *69*, 191–193.

Turner, L., Bitto, N. J., Steer, D. L., Lo, C., D'Costa, K., Ramm, G., Shambrook, M., Hill, A. F., Ferrero, R. L., & Kaparakis-Liaskos, M. (2018). *Helicobacter pylori* outer membrane vesicle size determines their mechanisms of host cell entry and protein content. *Frontiers in Immunology*, *9*, 1466.

Vagner, T., Spinelli, C., Minciacchi, V. R., Balaj, L., Zandian, M., Conley, A., Zijlstra, A., Freeman, M. R., Demichelis, F., De, S., Posadas, E. M., Tanaka, H., & Di Vizio, D. (2018). Large extracellular vesicles carry most of the tumour DNA circulating in prostate cancer patient plasma. *Journal of Extracellular Vesicles*, *7*, 1505403.

20013078, 2024, 2, Downloaded from https://isevjournals.onlinelibrary.wiley.com/doi/10.1002/jev2.12404 by Colorado State University, Wiley Online Library on [09/10/2024]. See the Terms and Conditions (https://onlinelibrary.wiley.com/terms-and-conditions) on Wiley Online Library for rules of use; OA articles are governed by the applicable Creative Commons License

Valcz, G., Buzas, E. I., Kittel, A., Krenacs, T., Visnovitz, T., Spisak, S., Torok, G., Homolya, L., Zsigrai, S., Kiszler, G., Antalffy, G., Paloczi, K., Szallasi, Z., Szabo, V., Sebestyen, A., Solymosi, N., Kalmar, A., Dede, K., Lorincz, P., … Molnar, B. (2019). En bloc release of MVB-like small extracellular vesicle clusters by colorectal carcinoma cells. *Journal of Extracellular Vesicles*, *8*(1), 1596668.

Valkov, N., Das, A., Tucker, N. R., Li, G., Salvador, A. M., Chaffin, M. D., Pereira de Oliveira Junior, G., Kur, I., Gokulnath, P., Ziegler, O., Yeri, A., Lu, S., Khamesra, A., Xiao, C., Rodosthenous, R., Srinivasan, S., Toxavidis, V., Tigges, J., Laurent, L. C., … Das, S. (2021). SnRNA sequencing defines signaling by RBC-derived extracellular vesicles in the murine heart. *Life Science Alliance*, *4*, e202101048.

van der Pol, E., Coumans, F. A., Grootemaat, A. E., Gardiner, C., Sargent, I. L., Harrison, P., Sturk, A., van Leeuwen, T. G., & Nieuwland, R. (2014). Particle size distribution of exosomes and microvesicles determined by transmission electron microscopy, flow cytometry, nanoparticle tracking analysis, and resistive pulse sensing. *Journal of Thrombosis and Haemostasis*, *12*, 1182–1192.

van der Pol, E., Coumans, F. A., Sturk, A., Nieuwland, R., & van Leeuwen, T. G. (2014). Refractive index determination of nanoparticles in suspension using nanoparticle tracking analysis. *Nano Letters*, *14*, 6195–6201.

van der Pol, E., de Rond, L., Coumans, F. A. W., Gool, E. L., Boing, A. N., Sturk, A., Nieuwland, R., & van Leeuwen, T. G. (2018). Absolute sizing and label-free identification of extracellular vesicles by flow cytometry. *Nanomedicine*, *14*, 801–810.

van der Pol, E., Sturk, A., van Leeuwen, T., Nieuwland, R., Coumans, F., & Isth-Ssc-Vb Working group. (2018). Standardization of extracellular vesicle measurements by flow cytometry through vesicle diameter approximation. *Journal of Thrombosis and Haemostasis*, *16*, 1236–1245.

van der Pol, E., Welsh, J. A., & Nieuwland, R. (2022). Minimum information to report about a flow cytometry experiment on extracellular vesicles: Communication from the ISTH SSC subcommittee on vascular biology. *Journal of Thrombosis and Haemostasis*, *20*, 245–251.

van Deun, J., Jo, A., Li, H., Lin, H. Y., Weissleder, R., Im, H., & Lee, H. (2020). Integrated dual-mode chromatography to enrich extracellular vesicles from plasma. *Advanced Biology*, *4*, e1900310.

van Royen, M. E., Soekmadji, C., Grange, C., Webber, J. P., Tertel, T., Droste, M., Buescher, A., Giebel, B., Jenster, G. W., Llorente, A., Blijdorp, C. J., Burger, D., Erdbrügger, U., & Martens-Uzunova, E. S. (2023). The quick reference card "Storage of urinary EVs" – A practical guideline tool for research and clinical laboratories. *Journal of Extracellular Vesicles*, *12*, e12286.

Vella, L. J., Scicluna, B. J., Cheng, L., Bawden, E. G., Masters, C. L., Ang, C. S., Willamson, N., McLean, C., Barnham, K. J., & Hill, A. F. (2017). A rigorous method to enrich for exosomes from brain tissue. *Journal of Extracellular Vesicles*, *6*, 1348885.

Vergauwen, G., Dhondt, B., Van Deun, J., De Smedt, E., Berx, G., Timmerman, E., Gevaert, K., Miinalainen, I., Cocquyt, V., Braems, G., Van den Broecke, R., Denys, H., De Wever, O., & Hendrix, A. (2017). Confounding factors of ultrafiltration and protein analysis in extracellular vesicle research. *Scientific Reports*, *7*, 2704.

Vergauwen, G., Tulkens, J., Pinheiro, C., Avila Cobos, F., Dedeyne, S., De Scheerder, M. A., Vandekerckhove, L., Impens, F., Miinalainen, I., Braems, G., Gevaert, K., Mestdagh, P., Vandesompele, J., Denys, H., De Wever, O., & Hendrix, A. (2021). Robust sequential biophysical fractionation of blood plasma to study variations in the biomolecular landscape of systemically circulating extracellular vesicles across clinical conditions. *Journal of Extracellular Vesicles*, *10*, e12122.

Verweij, F. J., Balaj, L., Boulanger, C. M., Carter, D. R. F., Compeer, E. B., D'Angelo, G., El Andaloussi, S., Goetz, J. G., Gross, J. C., Hyenne, V., Krämer-Albers, E. M., Lai, C. P., Loyer, X., Marki, A., Momma, S., Nolte-'t Hoen, E. N. M., Pegtel, D. M., Peinado, H., Raposo, G., … van Niel, G. (2021). The power of imaging to understand extracellular vesicle biology in vivo. *Nature Methods*, *18*(9), 1013–1026.

Verweij, F. J., Revenu, C., Arras, G., Dingli, F., Loew, D., Pegtel, D. M., Follain, G., Allio, G., Goetz, J. G., Zimmermann, P., Herbomel, P., Del Bene, F., Raposo, G., & van Niel, G. (2019). Live tracking of inter-organ communication by endogenous exosomes in vivo. *Developmental Cell*, *48*, 573–589.e4.

Verwilt, J., Trypsteen, W., Van Paemel, R., De Preter, K., Giraldez, M. D., Mestdagh, P., & Vandesompele, J. (2020). When DNA gets in the way: A cautionary note for DNA contamination in extracellular RNA-seq studies. *PNAS*, *117*, 18934–18936.

Vestad, B., Llorente, A., Neurauter, A., Phuyal, S., Kierulf, B., Kierulf, P., Skotland, T., Sandvig, K., Haug, K. B. F., & Ovstebo, R. (2017). Size and concentration analyses of extracellular vesicles by nanoparticle tracking analysis: A variation study. *Journal of Extracellular Vesicles*, *6*, 1344087.

Visnovitz, T., Osteikoetxea, X., Sodar, B. W., Mihaly, J., Lorincz, P., Vukman, K. V., Toth, E. A., Koncz, A., Szekacs, I., Horvath, R., Varga, Z., & Buzas, E. I. (2019). An improved 96 well plate format lipid quantification assay for standardisation of experiments with extracellular vesicles. *Journal of Extracellular Vesicles*, *8*, 1565263.

Vorselen, D., MacKintosh, F. C., Roos, W. H., & Wuite, G. J. (2017). Competition between bending and internal pressure governs the mechanics of fluid nanovesicles. *ACS Nano*, *11*, 2628–2636.

Vorselen, D., van Dommelen, S. M., Sorkin, R., Piontek, M. C., Schiller, J., Döpp, S. T., Kooijmans, S. A. A., van Oirschot, B. A., Versluijs, B. A., Bierings, M. B., van Wijk, R., Schiffelers, R. M., Wuite, G. J. L., & Roos, W. H. (2018). The fluid membrane determines mechanics of erythrocyte extracellular vesicles and is softened in hereditary spherocytosis. *Nature Communications*, *9*, 4960.

Walker, J. G. (2012). Improved nano-particle tracking analysis. *Measurement Science and Technology*, *23*, 065605.

Walsh, R. B., Dresselhaus, E. C., Becalska, A. N., Zunitch, M. J., Blanchette, C. R., Scalera, A. L., Lemos, T., Lee, S. M., Apiki, J., Wang, S., Isaac, B., Yeh, A., Koles, K., & Rodal, A. A. (2021). Opposing functions for retromer and Rab11 in extracellular vesicle traffic at presynaptic terminals. *Journal of Cell Biology*, *220*, e202012034.

Wang, C., Ding, Q., Plant, P., Basheer, M., Yang, C., Tawedrous, E., Krizova, A., Boulos, C., Farag, M., Cheng, Y., & Yousef, G. M. (2019). Droplet digital PCR improves urinary exosomal miRNA detection compared to real-time PCR. *Clinical Biochemistry*, *67*, 54–59.

Wang, J., Kaletsky, R., Silva, M., Williams, A., Haas, L. A., Androwski, R. J., Landis, J. N., Patrick, C., Rashid, A., Santiago-Martinez, D., Gravato-Nobre, M., Hodgkin, J., Hall, D. H., Murphy, C. T., & Barr, M. M. (2015). Cell-specific transcriptional profiling of ciliated sensory neurons reveals regulators of behavior and extracellular vesicle biogenesis. *Current Biology*, *25*, 3232–3238.

Wang, J., Silva, M., Haas, L. A., Morsci, N. S., Nguyen, K. C., Hall, D. H., & Barr, M. M. (2014). *C. elegans* ciliated sensory neurons release extracellular vesicles that function in animal communication. *Current Biology*, *24*, 519–525.

Wang, Q., & Lu, Q. (2017). Plasma membrane-derived extracellular microvesicles mediate non-canonical intercellular NOTCH signaling. *Nature Communications*, *8*, 709.

Wang, X., Shen, H., Zhangyuan, G., Huang, R., Zhang, W., He, Q., Jin, K., Zhuo, H., Zhang, Z., Wang, J., Sun, B., & Lu, X. (2018). 14-3-3zeta delivered by hepatocellular carcinoma-derived exosomes impaired anti-tumor function of tumor-infiltrating T lymphocytes. *Cell Death & Disease*, *9*, 159.

Wang, Z. T., Li, K. Y., Tan, C. C., Xu, W., Shen, X. N., Cao, X. P., Wang, P., Bi, Y. L., Dong, Q., Tan, L., & Yu, J. T. (2021). Associations of alcohol consumption with cerebrospinal fluid biomarkers of Alzheimer's disease pathology in cognitively intact older adults: The CABLE Study. *Journal of Alzheimer's Disease*, *82*, 1045–1054.

Wehman, A. M., Poggioli, C., Schweinsberg, P., Grant, B. D., & Nance, J. (2011). The P4-ATPase TAT-5 inhibits the budding of extracellular vesicles in *C. elegans* embryos. *Current Biology*, *21*, 1951–1959.

20013078, 2024, 2, Downloaded from https://isevjournals.onlinelibrary.wiley.com/doi/10.1002/jev2.12404 by Colorado State University, Wiley Online Library on [09/10/2024]. See the Terms and Conditions (https://onlinelibrary.wiley.com/terms-and-conditions) on Wiley Online Library for rules of use; OA articles are governed by the applicable Creative Commons License

Welsh, J. A., Killingsworth, B., Kepley, J., Traynor, T., Cook, S., Savage, J., Marte, J., Lee, M., Maeng, H. M., Pleet, M. L., Magana, S., Gorgens, A., Maire, C. L., Lamszus, K., Ricklefs, F. L., Merino, M. J., Linehan, W. M., Greten, T., Cooks, T., … Jones, J. C. (2022). MPAPASS software enables stitched multiplex, multidimensional EV repertoire analysis and a standard framework for reporting bead-based assays. *Cell Reports Methods*, *2*, 100136.

Welsh, J. A., Arkesteijn, G. J. A., Bremer, M., Cimorelli, M., Dignat-George, F., Giebel, B., Görgens, A., Hendrix, A., Kuiper, M., Lacroix, R., Lannigan, J., van Leeuwen, T. G., Lozano-Andrés, E., Rao, S., Robert, S., de Rond, L., Tang, V. A., Tertel, T., Yan, X., … van der Pol, E. (2023). A compendium of single extracellular vesicle flow cytometry. *Journal of Extracellular Vesicles*, *12*, e12299.

Welsh, J. A., Horak, P., Wilkinson, J. S., Ford, V. J., Jones, J. C., Smith, D., Holloway, J. A., & Englyst, N. A. (2020). FCMPASS software aids extracellular vesicle light scatter standardization. *Cytometry Part A: The Journal of the International Society for Analytical Cytology*, *97*, 569–581.

Welsh, J. A., Jones, J. C., & Tang, V. A. (2020). Fluorescence and light scatter calibration allow comparisons of small particle data in standard units across different flow cytometry platforms and detector settings. *Cytometry Part A: The Journal of the International Society for Analytical Cytology*, *97*, 592–601.

Welsh, J. A., Killingsworth, B., Kepley, J., Traynor, T., McKinnon, K., Savage, J., Appel, D., Aldape, K., Camphausen, K., Berzofsky, J. A., Ivanov, A. R., Ghiran, I. H., & Jones, J. C. (2021). A simple, high-throughput method of protein and label removal from extracellular vesicle samples. *Nanoscale*, *13*, 3737–3745.

Welsh, J. A., Tang, V. A., van der Pol, E., & Görgens, A. (2021). MIFlowCyt-EV: The next chapter in the reporting and reliability of single extracellular vesicle flow cytometry experiments. *Cytometry Part A: The Journal of the International Society for Analytical Cytology*, *99*, 365–368.

Welsh, J. A., Van Der Pol, E., Arkesteijn, G. J. A., Bremer, M., Brisson, A., Coumans, F., Dignat-George, F., Duggan, E., Ghiran, I., Giebel, B., Gorgens, A., Hendrix, A., Lacroix, R., Lannigan, J., Libregts, S., Lozano-Andres, E., Morales-Kastresana, A., Robert, S., de Rond, L., … Jones, J. C. (2020). MIFlowCyt-EV: A framework for standardized reporting of extracellular vesicle flow cytometry experiments. *Journal of Extracellular Vesicles*, *9*, 1713526.

Welsh, J. A., van der Pol, E., Bettin, B. A., Carter, D. R. F., Hendrix, A., Lenassi, M., Langlois, M. A., Llorente, A., van de Nes, A. S., Nieuwland, R., Tang, V., Wang, L., Witwer, K. W., & Jones, J. C. (2020). Towards defining reference materials for measuring extracellular vesicle refractive index, epitope abundance, size and concentration. *Journal of Extracellular Vesicles*, *9*, 1816641.

Wen, S. W., Sceneay, J., Lima, L. G., Wong, C. S., Becker, M., Krumeich, S., Lobb, R. J., Castillo, V., Wong, K. N., Ellis, S., Parker, B. S., & Möller, A. (2016). The biodistribution and immune suppressive effects of breast cancer-derived exosomes. *Cancer Research*, *76*, 6816–6827.

Whitehead, B., Wu, L., Hvam, M. L., Aslan, H., Dong, M., Dyrskjøt, L., Ostenfeld, M. S., Moghimi, S. M., & Howard, K. A. (2015). Tumour exosomes display differential mechanical and complement activation properties dependent on malignant state: Implications in endothelial leakiness. *Journal of Extracellular Vesicles*, *4*, 29685.

Wiklander, O. P. B., Bostancioglu, R. B., Welsh, J. A., Zickler, A. M., Murke, F., Corso, G., Felldin, U., Hagey, D. W., Evertsson, B., Liang, X. M., Gustafsson, M. O., Mohammad, D. K., Wiek, C., Hanenberg, H., Bremer, M., Gupta, D., Bjornstedt, M., Giebel, B., Nordin, J. Z., … Gorgens, A. (2018). Systematic methodological evaluation of a multiplex bead-based flow cytometry assay for detection of extracellular vesicle surface signatures. *Frontiers in Immunology*, *9*, 1326.

Wiklander, O. P., Nordin, J. Z., O'Loughlin, A., Gustafsson, Y., Corso, G., Mäger, I., Vader, P., Lee, Y., Sork, H., Seow, Y., Heldring, N., Alvarez-Erviti, L., Smith, C. I., Blanc, K. Le, Macchiarini, P., Jungebluth, P., Wood, M. J., & Andaloussi, S. E. (2015). Extracellular vesicle in vivo biodistribution is determined by cell source, route of administration and targeting. *Journal of Extracellular Vesicles*, *4*, 26316.

Willy, N. M., Colombo, F., Huber, S., Smith, A. C., Norton, E. G., Kural, C., & Cocucci, E. (2021). CALM supports clathrin-coated vesicle completion upon membrane tension increase. *PNAS*, *118*, e2010438118.

Witwer, K. W., Buzas, E. I., Bemis, L. T., Bora, A., Lasser, C., Lotvall, J., Nolte-'t Hoen, E. N., Piper, M. G., Sivaraman, S., Skog, J., Thery, C., Wauben, M. H., & Hochberg, F. (2013). Standardization of sample collection, isolation and analysis methods in extracellular vesicle research. *Journal of Extracellular Vesicles*, *2*, 20360.

Witwer, K. W., Goberdhan, D. C., O'Driscoll, L., Théry, C., Welsh, J. A., Blenkiron, C., Buzás, E. I., di Vizio, D., Erdbrügger, U., Falcón-Pérez, J. M., Fu, Q. L., Hill, A. F., Lenassi, M., Lötvall, J., Nieuwland, R., Ochiya, T., Rome, S., Sahoo, S., & Zheng, L. (2021). Updating MISEV: Evolving the minimal requirements for studies of extracellular vesicles. *Journal of Extracellular Vesicles*, *10*, e12182.

Wolf, M., Poupardin, R. W., Ebner-Peking, P., Andrade, A. C., Blöchl, C., Obermayer, A., Gomes, F. G., Vari, B., Maeding, N., Eminger, E., Binder, H. M., Raninger, A. M., Hochmann, S., Brachtl, G., Spittler, A., Heuser, T., Ofir, R., Huber, C. G., Aberman, Z., … Strunk, D. (2022). A functional corona around extracellular vesicles enhances angiogenesis, skin regeneration and immunomodulation. *Journal of Extracellular Vesicles*, *11*, e12207.

Wombacher, R., Heidbreder, M., van de Linde, S., Sheetz, M. P., Heilemann, M., Cornish, V. W., & Sauer, M. (2010). Live-cell super-resolution imaging with trimethoprim conjugates. *Nature Methods*, *7*, 717–719.

Wong, M., Schlaggar, B. L., Buller, R. S., Storch, G. A., & Landt, M. (2000). Cerebrospinal fluid protein concentration in pediatric patients: Defining clinically relevant reference values. *Archives of Pediatrics & Adolescent Medicine*, *154*, 827–831.

Wong, V. (2007). Medication use as a confounding factor in the use of the cerebrospinal fluid tau/beta-amyloid42 ratio. *Archives of Neurology*, *64*, 1357–1359.

Wood, C. R., Huang, K., Diener, D. R., & Rosenbaum, J. L. (2013). The cilium secretes bioactive ectosomes. *Current Biology*, *23*, 906–911.

Woud, W. W., Hesselink, D. A., Hoogduijn, M. J., Baan, C. C., & Boer, K. (2022). Direct detection of circulating donor-derived extracellular vesicles in kidney transplant recipients. *Scientific Reports*, *12*, 21973.

Wu, Y., Deng, W., & Klinke, D. J. 2nd (2015). Exosomes: Improved methods to characterize their morphology, RNA content, and surface protein biomarkers. *Analyst*, *140*, 6631–6642.

Xiang, H., Jin, S., Tan, F., Xu, Y., Lu, Y., & Wu, T. (2021). Physiological functions and therapeutic applications of neutral sphingomyelinase and acid sphingomyelinase. *Biomedicine & Pharmacotherapy*, *139*, 111610.

Xu, F., Laguna, L., & Sarkar, A. (2019). Aging-related changes in quantity and quality of saliva: Where do we stand in our understanding? *Journal of Texture Studies*, *50*, 27–35.

Yang, C., Chalasani, G., Ng, Y. H., & Robbins, P. D. (2012). Exosomes released from Mycoplasma infected tumor cells activate inhibitory B cells. *PLoS ONE*, *7*, e36138.

Yang, K., Jia, M., Cheddah, S., Zhang, Z., Wang, W., Li, X., Wang, Y., & Yan, C. (2022). Peptide ligand-SiO(2) microspheres with specific affinity for phosphatidylserine as a new strategy to isolate exosomes and application in proteomics to differentiate hepatic cancer. *Bioactive Materials*, *15*, 343–354.

Ye, S., Li, W., Wang, H., Zhu, L., Wang, C., & Yang, Y. (2021). Quantitative nanomechanical analysis of small extracellular vesicles for tumor malignancy indication. *Advanced Science*, *8*, e2100825.

Yelamanchili, S. V., Lamberty, B. G., Rennard, D. A., Morsey, B. M., Hochfelder, C. G., Meays, B. M., Levy, E., & Fox, H. S. (2015). MiR-21 in extracellular vesicles leads to neurotoxicity via TLR7 signaling in SIV neurological disease. *Plos Pathogens*, *11*, e1005032.

Yerneni, S. S., Solomon, T., Smith, J., & Campbell, P. G. (2022). Radioiodination of extravesicular surface constituents to study the biocorona, cell trafficking and storage stability of extracellular vesicles. *Biochimica et Biophysica Acta (BBA) - General Subjects*, *1866*, 130069.

You, J. S., Gelfanova, V., Knierman, M. D., Witzmann, F. A., Wang, M., & Hale, J. E. (2005). The impact of blood contamination on the proteome of cerebrospinal fluid. *Proteomics*, *5*, 290–296.

20013078, 2024, 2, Downloaded from https://isevjournals.onlinelibrary.wiley.com/doi/10.1002/jev2.12404 by Colorado State University, Wiley Online Library on [09/10/2024]. See the Terms and Conditions (https://onlinelibrary.wiley.com/terms-and-conditions) on Wiley Online Library for rules of use; OA articles are governed by the applicable Creative Commons License

Young, G., Hundt, N., Cole, D., Fineberg, A., Andrecka, J., Tyler, A., Olerinyova, A., Ansari, A., Marklund, E. G., Collier, M. P., Chandler, S. A., Tkachenko, O., Allen, J., Crispin, M., Billington, N., Takagi, Y., Sellers, J. R., Eichmann, C., Selenko, P., … Kukura, P. (2018). Quantitative mass imaging of single biological macromolecules. *Science*, *360*, 423–427.

Yuana, Y., Koning, R. I., Kuil, M. E., Rensen, P. C., Koster, A. J., Bertina, R. M., & Osanto, S. (2013). Cryo-electron microscopy of extracellular vesicles in fresh plasma. *Journal of Extracellular Vesicles*, *2*, https://doi.org/10.3402/jev.v2i0.21494

Zavan, L., Bitto, N. J., Johnston, E. L., Greening, D. W., & Kaparakis-Liaskos, M. (2019). *Helicobacter pylori* growth stage determines the size, protein composition, and preferential cargo packaging of outer membrane vesicles. *Proteomics*, *19*, e1800209.

Zavan, L., Fang, H., Johnston, E. L., Whitchurch, C., Greening, D., Hill, A. F., & KaparakisLiaskos, M. (2023). The mechanism of *Pseudomonas aeruginosa* outer membrane vesicle biogenesis determines their protein composition. *Proteomics*, e2200464.

Zhang, H., Freitas, D., Kim, H. S., Fabijanic, K., Li, Z., Chen, H., Mark, M. T., Molina, H., Martin, A. B., Bojmar, L., Fang, J., Rampersaud, S., Hoshino, A., Matei, I., Kenific, C. M., Nakajima, M., Mutvei, A. P., Sansone, P., Buehring, W., … Lyden, D. (2018). Identification of distinct nanoparticles and subsets of extracellular vesicles by asymmetric flow field-flow fractionation. *Nature Cell Biology*, *20*, 332–343.

Zhang, H., Lu, J., Liu, J., Zhang, G., & Lu, A. (2020). Advances in the discovery of exosome inhibitors in cancer. *Journal of Enzyme Inhibition and Medicinal Chemistry*, *35*, 1322–1330.

Zhang, J., Goodlett, D. R., Peskind, E. R., Quinn, J. F., Zhou, Y., Wang, Q., Pan, C., Yi, E., Eng, J., Aebersold, R. H., & Montine, T. J. (2005). Quantitative proteomic analysis of age-related changes in human cerebrospinal fluid. *Neurobiology of Aging*, *26*, 207–227.

Zhang, K., Yue, Y., Wu, S., Liu, W., Shi, J., & Zhang, Z. (2019). Rapid capture and nondestructive release of extracellular vesicles using aptamer-based magnetic isolation. *ACS Sensors*, *4*, 1245–1251.

Zhang, Q., Higginbotham, J. N., Jeppesen, D. K., Yang, Y. P., Li, W., McKinley, E. T., Graves-Deal, R., Ping, J., Britain, C. M., Dorsett, K. A., Hartman, C. L., Ford, D. A., Allen, R. M., Vickers, K. C., Liu, Q., Franklin, J. L., Bellis, S. L., & Coffey, R. J. (2019). Transfer of functional cargo in exomeres. *Cell Reports*, *27*, 940–954.e6.

Zhang, Q., Jeppesen, D. K., Higginbotham, J. N., Graves-Deal, R., Trinh, V. Q., Ramirez, M. A., Sohn, Y., Neininger, A. C., Taneja, N., McKinley, E. T., Niitsu, H., Cao, Z., Evans, R., Glass, S. E., Ray, K. C., Fissell, W. H., Hill, S., Rose, K. L., Huh, W. J., … Coffey, R. J. (2021). Supermeres are functional extracellular nanoparticles replete with disease biomarkers and therapeutic targets. *Nature Cell Biology*, *23*, 1240–1254.

Zhang, S., Wear, D. J., & Lo, S. (2000). Mycoplasmal infections alter gene expression in cultured human prostatic and cervical epithelial cells. *Fems Immunology and Medical Microbiology*, *27*, 43–50.

Zhang, X., Baht, G. S., Huang, R., Chen, Y. H., Molitoris, K. H., Miller, S. E., & Kraus, V. B. (2022). Rejuvenation of neutrophils and their extracellular vesicles is associated with enhanced aged fracture healing. *Aging Cell*, *21*, e13651.

Zhang, X., Borg, E. G. F., Liaci, A. M., Vos, H. R., & Stoorvogel, W. (2020). A novel three step protocol to isolate extracellular vesicles from plasma or cell culture medium with both high yield and purity. *Journal of Extracellular Vesicles*, *9*, 1791450.

Zhao, K., Bleackley, M., Chisanga, D., Gangoda, L., Fonseka, P., Liem, M., Kalra, H., Al Saffar, H., Keerthikumar, S., Ang, C. S., Adda, C. G., Jiang, L., Yap, K., Poon, I. K., Lock, P., Bulone, V., Anderson, M., & Mathivanan, S. (2019). Extracellular vesicles secreted by *Saccharomyces cerevisiae* are involved in cell wall remodelling. *Communications Biology*, *2*, 305.

Zhu, S., Ma, L., Wang, S., Chen, C., Zhang, W., Yang, L., Hang, W., Nolan, J. P., Wu, L., & Yan, X. (2014). Light-scattering detection below the level of single fluorescent molecules for high-resolution characterization of functional nanoparticles. *ACS Nano*, *8*, 10998–11006.

Zomer, A., Maynard, C., Verweij, F. J., Kamermans, A., Schäfer, R., Beerling, E., Schiffelers, R. M., de Wit, E., Berenguer, J., Ellenbroek, S. I. J., Wurdinger, T., Pegtel, D. M., & van Rheenen, J. (2015). In vivo imaging reveals extracellular vesicle-mediated phenocopying of metastatic behavior. *Cell*, *161*, 1046–1057.

Zomer, A., Steenbeek, S. C., Maynard, C., & van Rheenen, J. (2016). Studying extracellular vesicle transfer by a Cre-loxP method. *Nature Protocols*, *11*, 87–101.

Zong, S., Zong, J., Chen, C., Jiang, X., Zhang, Y., Wang, Z., & Cui, Y. (2018). Single molecule localization imaging of exosomes using blinking silicon quantum dots. *Nanotechnology*, *29*, 065705.

Zonneveld, M. I., Brisson, A. R., van Herwijnen, M. J., Tan, S., van de Lest, C. H., Redegeld, F. A., Garssen, J., Wauben, M. H., & Nolte-'t Hoen, E. N. (2014). Recovery of extracellular vesicles from human breast milk is influenced by sample collection and vesicle isolation procedures. *Journal of Extracellular Vesicles*, *3*, https://doi.org/10.3402/jev.v3.24215

How to cite this article: Welsh, J. A., Goberdhan, D. C. I., O'Driscoll, L., Buzas, E. I., Blenkiron, C., Bussolati, B., Cai, H., Di Vizio, D., Driedonks, T. A. P., Erdbrügger, U., Falcon-Perez, J. M., Fu, Q.-L., Hill, A. F., Lenassi, M., Lim, S. K., Mahoney, M. G., Mohanty, S., Möller, A., Nieuwland, R., … Witwer, K. W. (2024). Minimal information for studies of extracellular vesicles (MISEV2023): from basic to advanced approaches. *Journal of Extracellular Vesicles*, *13*, e12404. https://doi.org/10.1002/jev2.12404

20013078, 2024, 2, Downloaded from https://isevjournals.onlinelibrary.wiley.com/doi/10.1002/jev2.12404 by Colorado State University, Wiley Online Library on [09/10/2024]. See the Terms and Conditions (https://onlinelibrary.wiley.com/terms-and-conditions) on Wiley Online Library for rules of use; OA articles are governed by the applicable Creative Commons License

Menjivar *et al. Biological Procedures Online* (2024) 26:14
https://doi.org/10.1186/s12575-024-00241-6

Biological Procedures Online

REVIEW

Open Access

MicroRNA Nano-Shuttles: Engineering Extracellular Vesicles as a Cutting-Edge Biotechnology Platform for Clinical Use in Therapeutics

Nico G. Menjivar[1†], Jaiden Oropallo[2,3†], Samuel Gebremedhn[1,4], Luca A. Souza[1,5], Ahmed Gad[1,6], Christian M. Puttlitz[2] and Dawit Tesfaye[1*]

Abstract

Extracellular vesicles (EVs) are nano-sized, membranous transporters of various active biomolecules with inflicting phenotypic capabilities, that are naturally secreted by almost all cells with a promising vantage point as a potential leading drug delivery platform. The intrinsic characteristics of their low toxicity, superior structural stability, and cargo loading capacity continue to fuel a multitude of research avenues dedicated to loading EVs with therapeutic and diagnostic cargos (pharmaceutical compounds, nucleic acids, proteins, and nanomaterials) in attempts to generate superior natural nanoscale delivery systems for clinical application in therapeutics. In addition to their well-known role in intercellular communication, EVs harbor microRNAs (miRNAs), which can alter the translational potential of receiving cells and thus act as important mediators in numerous biological and pathological processes. To leverage this potential, EVs can be structurally engineered to shuttle therapeutic miRNAs to diseased recipient cells as a potential targeted 'treatment' or 'therapy'. Herein, this review focuses on the therapeutic potential of EV-coupled miRNAs; summarizing the biogenesis, contents, and function of EVs, as well as providing both a comprehensive discussion of current EV loading techniques and an update on miRNA-engineered EVs as a next-generation platform piloting benchtop studies to propel potential clinical translation on the forefront of nanomedicine.

Keywords Extracellular vesicles, miRNAs, Cargo carriers, Drug-delivery, Cancer, Therapies, Clinical studies

†Nico G. Menjivar and Jaiden Oropallo these authors equally contributed to this manuscript.

*Correspondence:
Dawit Tesfaye
dawit.tesfaye@colostate.edu
[1] Animal Reproduction and Biotechnology Laboratory (ARBL), Department of Biomedical Sciences, College of Veterinary Medicine and Biomedical Sciences, Colorado State University, Fort Collins, CO 80523, USA
[2] Orthopaedic Bioengineering Research Laboratory (OBRL), Translational Medicine Institute (TMI), Department of Mechanical Engineering, Colorado State University, Fort Collins, CO 80523, USA
[3] Orthopaedic Research Center (ORC), Translational Medicine Institute (TMI), Department of Clinical Sciences, College of Veterinary Medicine and Biomedical Science, Colorado State University, Fort Collins, CO 80523, USA
[4] J.R. Simplot Company, 1099 W. Front St, Boise, ID 83702, USA
[5] Department of Veterinary Medicine, College of Animal Science and Food Engineering, University of São Paulo, 225 Av. Duque de Caxias Norte, Pirassununga, SP 13635-900, Brazil
[6] Department of Animal Production, Faculty of Agriculture, Cairo University, Giza 12613, Egypt

© The Author(s) 2024. **Open Access** This article is licensed under a Creative Commons Attribution 4.0 International License, which permits use, sharing, adaptation, distribution and reproduction in any medium or format, as long as you give appropriate credit to the original author(s) and the source, provide a link to the Creative Commons licence, and indicate if changes were made. The images or other third party material in this article are included in the article's Creative Commons licence, unless indicated otherwise in a credit line to the material. If material is not included in the article's Creative Commons licence and your intended use is not permitted by statutory regulation or exceeds the permitted use, you will need to obtain permission directly from the copyright holder. To view a copy of this licence, visit http://creativecommons.org/licenses/by/4.0/. The Creative Commons Public Domain Dedication waiver (http://creativecommons.org/publicdomain/zero/1.0/) applies to the data made available in this article, unless otherwise stated in a credit line to the data.

Introduction

The field of EV research has grown exponentially in recent decades due to their functional association as pertinent nano-shuttles to transfer bioactive molecules [1]. Extracellular vesicle, is an all-encompassing term underwritten by the International Society for Extracellular Vesicles (ISEV) to broadly connect lipid-encapsulated, secreted cellular particles to include exosomes, microvesicles (MVs), and apoptotic bodies (ApoBDs) [2, 3]. From the perspective as cargo carriers, EVs are intriguingly similar to liposomes, paralleling their dense phospholipid nature. Of specific distinction, dependent upon their biogenesis, EVs are constructed with a blend of lipids and surface membrane proteins, ultimately aiding in their downstream functions [4]. As tags for precise sites both locally and distant, intracellular molecules entertain the capacity to traffic through extracellular spaces, as effective drug carriers for therapeutic applications and novel scientific research avenues at the forefront of discovery.

Here, we discuss effective loading techniques to precisely harness EVs with miRNAs as bioactive compounds for the application as a cutting-edge platform for drug discovery and delivery. Previous attempts to review miRNA-enriched EVs focused primarily on the composition of EVs and the functional basis of miRNAs as future therapeutic prospects [5]. In this review, we largely focus on mechanisms of targeted loading miRNAs into EVs, with a principal element of incorporating recently published and impactful articles that include functionally relevant preclinical, clinical, and therapeutic involvement of engineered and/or modified EVs with specific nanomedicinal application.

Biological role and EV uptake

EV Biogenesis

Extracellular vesicles possess heterogeneous structural and biochemical properties, which reflect their cellular origin and biogenesis pathways. According to their origin, biogenesis, shape, and molecular constituents, EVs are broadly categorized as exosomes, microvesicles, and apoptotic bodies [6]. Exosomes comprise the smallest and rather homogenous size of EVs with a range in diameter from 30-150 nm and originate from the inward invagination of late endosomal membranes forming multivesicular bodies (MVBs), released into the extracellular space as exosomes upon fusion with the plasma membrane [7, 8]. Conceptually, during EV biogenesis, early endosomes are formed from the inward budding of the plasma membrane and mature to form intraluminal vesicles (ILVs) and MVBs. Frequently, the lysosomal fusion of MVBs results in its degradation. However, when MVBs contain CD63 in conjunction with lysosome-associated membrane proteins (LAMPs; LAMP1 and LAMP2), as well as MHC class II molecules, their contents are then released into the extracellular space upon fusion with the plasma membrane [9]. The formation of ILVs and MVBs are largely commissioned by the endosomal sorting complex required for transport (ESCRT)-dependent [10] or the ESCRT-independent pathways via the tetraspanin protein, CD63 [11]. Alternative pathways regulating ILV and MVB formation are associated with the sorting of cargo into exosomes [12]. On the other hand, microvesicles are often termed as shedding vesicles being comparatively irregularly shaped and a relatively heterogeneous population, with a size ranging from 100-1000 nm in diameter and generated via the outward budding of the plasma membrane [13]. Nevertheless, the largest fraction in size of EVs are apoptotic bodies, which range from 1–5 μm in diameter and are released during cellular disintegration preceding apoptosis [14, 15]. In addition to differing from their modes of biogenesis, EVs collectively can be differentiated based on their encapsulated molecular cargo contents. For instance, exosomes and MVs are more commonly preferentially enriched with a multitude of cytoplasmic components, including RNAs, proteins, and lipids. Alternatively, ApoBDs are largely enriched with cellular organelles and nuclear components [16, 17].

Ensuing biogenesis, EV release into the surrounding extracellular space is predominately facilitated by several subclasses of Rab family-GTPase proteins including RAB11, RAB35, and RAB27. For instance, exosomes are released from MVBs upon fusion with the plasma membrane through the facilitation of the RAB35 protein [18]. Moreover, exosomes are enriched with specific proteins including Wnt, PLP, TfR and flotillin [19]. The presence of highly-conserved and identifiable proteins, primarily membrane-associated proteins such as CD63, CD81, CD9, Alix, and TSG101 encompass hallmark characterization probes anchored amidst EVs [20]. These proteins also serve as marker proteins during EV processing and verification within EV preparations for functional studies as set forth by the guidelines in the Minimal Information for Studies of Extracellular Vesicles (MISEV), a position statement of the ISEV [2, 3]. All in all, crucial factors including the type and physiological status of varying cell types, ultimately determine facets of EV biogenesis, affecting their selection and packaging of key regulatory proteins [4].

Unpacking EV cargo

In their infancy, EVs were assumed to be merely mediators that shuttle cellular toxicants into the extracellular space for the maintenance of cellular fitness and homeostasis [21]. However, studies have more recently shown the critical role of these nanovesicles in facilitating communication with neighboring cells, which are capable of

posing both beneficial and deleterious effects. Phenotypic changes undergone by naïve recipient cells arise from the transfer of functionally active biomolecular components including lipids, proteins, mRNAs [22], and miRNAs [23], that subsequently interact with the ensuing extracellular matrix of naïve cells. Initial attempts to profile the protein contents of EVs have revealed their capacity to conceal both integrated proteins and proteins attached to their bilipid membranes. Although there is a clear divergence in the biogenesis pathways of both exosomes and MVs, no distinctive proteins have been reported that clearly differentiate the two EV subpopulations. This could in part be a result of the shared features of the endosomal and plasma membranes. Reports have shown that proteins necessary for exosome biogenesis such as ESCRT proteins are highly abundant in the proteome profile of exosomes [24]. Due to the amplified nuclease activity amidst the extracellular environment, it can be assumed that secreted EVs are potentially vulnerable and subject to degradation. Therefore, EV structural composition is integral in protecting their harnessed bioactive cargo from degradation upon release into the extracellular space [25]. The multifaceted structural characteristics that allow EVs to withstand adverse extracellular conditions poise them as attractive vehicles to shuttle therapeutic proteins and RNAs as a potential drug delivery platform [26, 27]. Various forms of EV interactions with recipient cells underpin their functional delivery of bioactive molecules [28]. Once integrated within recipient cells, EVs are capable of evading lysosomal degradation as a means to release their functional cargo molecules. Here we focus on miRNAs, which exert functional regulatory impacts on gene expression through post-transcriptional regulation of target mRNAs. It is well-documented that the expression level of particular miRNAs are key during development [29, 30] and stress responses [31, 32], and that EVs play an important role in transferring miRNA cargoes between cells [33]. Alterations in the release and uptake of EVs are associated with pathologies including cancer [34] and cellular stress [32, 35–39].

Mechanisms of EV uptake

The uptake of EVs by recipient cells can be confirmed either via direct or indirect evidence. EVs can be directly visualized by labeling their bilipid membranes using lipophilic fluorescent dyes, including the commonly used PKH67 and PKH26, Rhodamine B (R18) and DIL [40]. Alternatively, EVs can be stained using permeable dyes like CFSE and CFDA, amidst the confines of their cytoplasmic lumen [41]. The incorporation of fluorescently labeled EVs can then be verified either using microscopy [42] or via cellular sorting technologies in recipient cells using flow cytometry [28, 40]. In vivo, various mechanisms of EV internalization into recipient cells and/or tissues are discussed within the literature across many fields of study. Among those mechanisms commonly represented, clathrin-mediated endocytosis, phagocytosis, micropinocytosis, lipid raft-mediated internalization, and direct fusion with the plasma membrane of the receiving cell are among the most widely reported. Specific physiological uptake mechanisms of EVs are largely dependent upon their molecular composition, most commonly the surface protein and/or glycoprotein configurations of both the EVs membrane and the plasma membrane of the receiving cell [43]. This has in part been confirmed where tetraspanin proteins CD9 and CD81, which are present on the surface of EVs, were evidenced to play important roles in the cellular uptake of EVs. Cells treated with anti-CD9 and anti-CD81 antibodies showed similar reductions in EV uptake [44]. Additionally, a study using EVs treated with proteinase K (broad-spectrum serine protease used for protein digestion), resulted in the reduced uptake of EVs in recipient cells [45]. Conceptually, the dominant mechanisms of EV uptake can vary greatly amongst cells of differing pathophysiological conditions.

Extracellular miRNAs and their incorporation within EVs

miRNAs

As implied by their name, miRNAs are short, single-stranded RNA molecules of ~ 22 nucleotides, initially discovered by Lee and colleagues in 1993, while studying the nematode *Caenorhabditis elegans* [46]. MicroRNAs function to effectively modulate the stability of mRNA, most commonly inhibiting the translational potential and/or inducing degradation to respective mRNA targets via a sequence-specific complementarity mechanism [47, 48]. Focusing primitively on canonical miRNAs, their biogenesis primarily initiates from DNA sequences called miRNA genes, which are then transcribed into primary miRNAs (pri-miRNA; ~ 150 nt) by RNA polymerase III, and further processed via a microprocessing system into precursor miRNA (pre-miRNAs; ~ 70 nt). Pre-miRNAs are then shuttled from the nucleus of the donor cell into the cytoplasm via a complex of exportin5 and RAS-related nuclear protein-guanosine-5'-triphosphate-ase [49]. Amid the cytoplasm, the terminal loop of pre-miRNAs are sequestered via the RNase III endonuclease, Dicer [50], molding miRNA duplexes that are then catalyzed by Argonaute RISC Catalytic Component 2, responsible for leaving and/or removing one strand of the duplex to propagate the directionality of a mature miRNA strand [51, 52] with the capacity to be packaged into EVs for potential functional alterations upon its effective release amidst receptor cells (Fig. 1).

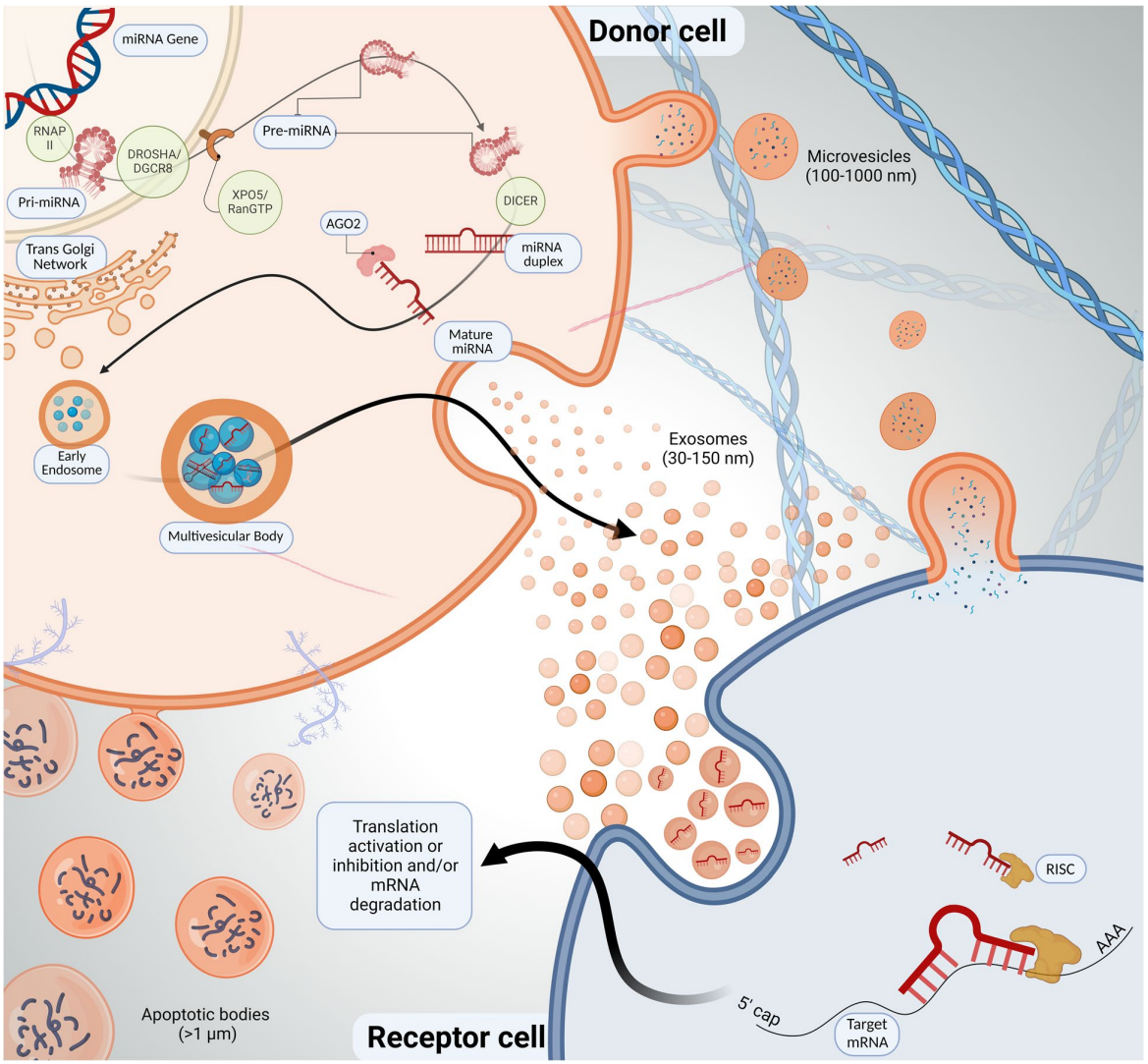


Fig. 1 Diagrammatic Overview of Extracellular Vesicle Biogenesis and miRNA Processing. Extracellular vesicles (EVs) are a heterogeneous collection of membrane-enveloped nanoparticles that serve as a mass transit mechanism for the packaging and release of complex cargos, including miRNAs. Exosomes (30-150 nm), are commonly spherical in shape and arise via the endocytic pathway via exocytosis from the fusion of the vesicular membrane into the plasma membrane. Microvesicles (100-1000 nm), notably irregularly shaped, are the byproduct of the outward budding/pinching of the plasma membrane. Apoptotic bodies (> 1 μm) are formed through apoptotic cell disassembly or programmed cell death, and released through cell blebbing. The cargo 'selection' or 'sorting' process that ensues, specifically the local enrichment of miRNA cargo molecules during nascent EV formation is largely propagated through the miRNA processing enzymes Drosha and Dicer, required for the maturation of miRNAs that lead to the translational repression or degradation of target mRNAs

Initial studies reporting that EVs carry miRNAs [23, 53, 54] have fueled further research efforts to unpack the all-inclusive nature of EVs and their biological cargoes. It has been previously reported that over 60% of all mammalian mRNAs are predicted to be post-transcriptionally regulated by miRNAs [55], indicating that miRNAs functionally constitute a significant class of pervasive regulators of various cellular processes, outnumbering kinases and phosphatases [56]. Collated data generated from small RNA sequencing reports have indicated that miRNAs comprise anywhere from < 1% to 30% of the total read counts within EVs of diverse origins [57]. Extracellular miRNAs encapsulated within EVs are progressively being explored as promising circulating biomarkers for many

cancers and diseases [58], and their ability to remain predominantly stable while evading degradation from external nucleases, underpins their significance, and the basis for studying EVs as cargo carriers for downstream therapeutic usage. However, the precise mechanisms by which specific miRNAs are packaged and released and/or enriched into EVs still largely remains unknown.

Encasing selective miRNAs into EVs

Attempts to pinpoint the explicit processing mechanisms leading to extracellular miRNAs export into EVs versus their cellular retention have been predominantly inconclusive. Many studies exist to suggest that collectively, RNAs are primarily shuttled into EVs selectively via the interaction of specific RNA sequence motifs [59] or lipid interactions [60] in association with RNA-binding proteins (RBPs) [61–63], or possibly through non-selective measures as evidenced previously [64, 65]. In more recent efforts and extending past the initial observations of single tetranucleotide motifs connected to miRNA export [61, 66, 67], Garcia et al. has shown up to an 80-fold enrichment of specific RNA sequence motifs (CGGGAG) identified by 'reader' proteins Alyref and Fus, which function to promote the sorting of sequence motif-bearing miRNAs into EVs for potential downstream delivery [59]. Still, a range of other EV-sorting signals including RNA and/or RBP modifications that inherently impact RNA stability and miRNA biogenesis also exist [68], such as ubiquitylation, sumoylation, phosphorylation, and uridylation, which likely involve regulatory processing machinery that implicate miRNA packaging into EVs. Together, these studies along with many others suggest an overabundance of influences that likely labor interchangeably, and coalesce in the packaging of various forms of RNAs into EVs. A more detailed understanding of RNA incorporation mechanisms is discussed in a recent review by Dellar and colleagues [57].

Methods of miRNA cargo loading for incorporation into EVs

Primitive compositional and nano-mechanical properties of EVs including their admirable biocompatibility and stability, non-cytotoxic and low immunogenic traits, high loading ability and lengthy life span, and their intrinsic aptness to cross biological barriers make them ideal drug delivery candidates that natively carry cargo components, easily modifiable to contain therapeutic agents of interest (*e.g.*, nucleic acids). Recent evidence in mice using engineered EVs with small interfering RNAs (siRNAs), indicated more than a tenfold improvement in functional siRNA delivery in contrast to synthetic lipid nanocarriers [69]. Compared to EVs, to date, a multitude of hindrances exist in developing synthetic nanocarriers for downstream clinical usage in drug delivery [70], specifically involving their toxicity and immunogenic responses, lack of specificity, and preferential aggregation amidst the liver and spleen [71]. All things considered, copious evidence suggests that the advantageous and distinct features of EVs are likely the eminent angle catalyzing their integration as a mainstream effort at the forefront of nanomedicinal discovery.

Complexities in EV sample heterogeneity combined with the variability in encapsulated molecular cargoes primitively pose an inherent need in EV loading mechanism optimization in producing cargo-modified EVs for downstream therapeutic applications. Conceptually, EV loading techniques can be categorized into two main approaches: indirect modification to donor cell physiology ('endogenous' or 'passive' cell-based alterations) or through the direct modification of EVs ('exogenous' or 'active' cargo harnessing), each of which, with varying degrees in efficiency. Utilizing 'endogenous' or 'passive' loading measures, molecular constituents act upon and are taken up via donor cells, and subsequent excess cargo can then be shuttled into EVs prior to formation, resulting in the subsequent secretion of indirectly modified EVs with an increased abundance of the molecular component of interest. Assuming a more natural role in cargo loading, the enriched EVs can then be utilized as a delivery platform to recipient cells [72]. Alternatively, 'exogenous' or 'active' loading measures, primarily draw a focus on implementing catalytic reagents post-EV isolation to induce a permeable bilipid membrane to bolster cargo loading with precision molecules of interest [73]. In spite of the fact it is a more direct approach, such re-engineering of EVs heavily influences the composition of their bilipid membrane, which serves as the primary contact point in cell-to-cell communication propagating the various mechanistic routes of their ensuing uptake [74] (Fig. 2). The following sections offer a more comparative approach of multiple loading techniques in greater depths, focused on cargo loading efficiency with an emphasis on loading selective miRNAs into EVs.

Endogenous (Passive) pre-loading of EVs

Pre-loading miRNAs as potential therapeutic cargoes into EVs is a method widely executed across many disciplines, largely accomplished through donor cell manipulation via incubation and transfection with synthetic miRNAs (also known as miRNA mimics) and/or with miRNA-expressing plasmids/viral vectors, to increase endogenous levels of selective miRNAs that can then be passively incorporated into EVs during their biogenesis [75]. Although, current attempts in manipulating donor cells to secrete therapeutic-miRNA enriched EVs largely bypass the structural and/or compositional alternations of miRNA loading post-isolation, recent reports also

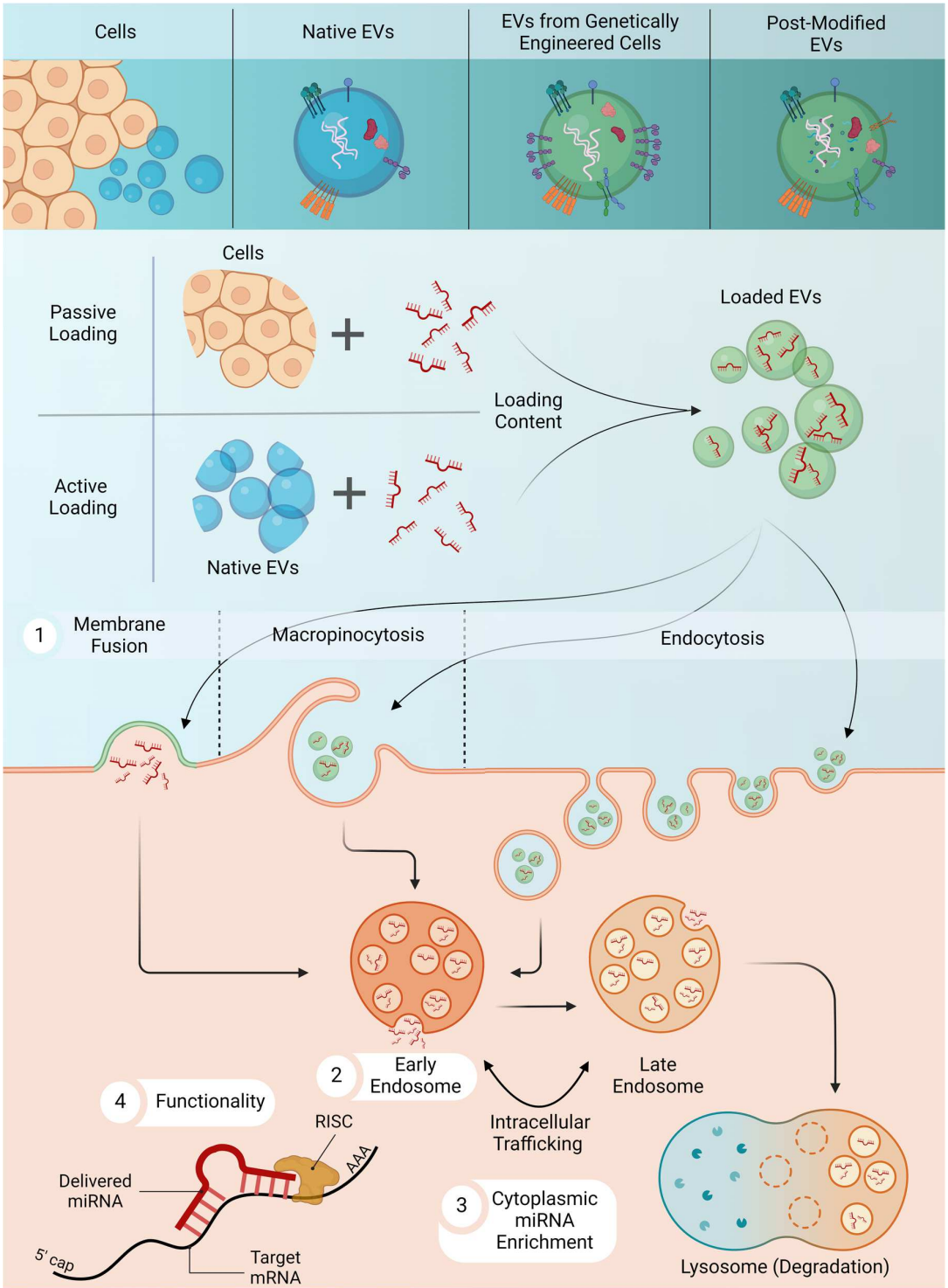


Fig. 2 Schematic Representation of Methodological Approaches in Extracellular Vesicle Loading for Functional Uptake in Target Cells. Lipid bilayer-delimited particles (EVs) serve as an effective novel drug delivery system for endless pharmaceutical compounds, including miRNAs. Thus, the method of incorporation for enriching miRNA cargoes into EVs can be segmented into two main sub-types: passive (donor cell manipulation) and active (direct EV alterations) loading methods

suggest that circumjacent transfection reagents critically affect downstream RNA cargo delivery [76–78]. Nevertheless, methods of endogenous cargo loading are still widely used, warranting further discussion of specific loading techniques.

Donor cell manipulation and genetic engineering

Direct transfection of EV-secreting cells as a means to modulate their cargo content is a rather straightforward and simple method to enrich or deplete EVs, prior to their inception. The use of chemical transfection reagents to load synthetic mimics and/or precisely designed vectors/plasmids effectively transduced into donor cells, are the two predominant methods utilized in overexpressing desired molecules (therapeutic drugs), such as small nucleic acids to include miRNAs. Assimilating and concentrating miRNAs within the cytosol of naïve cells following assisted passage across the cell defining plasma membrane, miRNAs have the potential to escape the endolysosomal system, and withstand dynamic and degradative ribonucleases. If successful, assimilated miRNAs typically favor incorporation into ILVs, which foregoes their exocytosis within EVs. Endogenous RNA modulations have been reported using commercialized transfection reagents such as Lipofectamine™ 2000 (Thermo Fisher Scientific; Waltham, MA, USA) and HiPerFect® (Qiagen; Hilden, Germany), artificially designed constructs/vectors [79], RNA aptamer–protein interactions and reversible light-inducible protein–protein interaction modules [80], EXOtic RNA-packaging devices [81], and the TAMEL loading platform [82]. To this point, the generation of stably modified HEK293T cell lines designed to express miR-21, have been reported to produce modified EVs for downstream therapeutic use in glioblastoma rat models [83]. In addition, the development and delivery of CRISPR-Cas9 technologies as a novel gene editing molecular tool has also been shown to be applied to living cells through electroporation for the establishment of manipulated parent cells designed for the production of EVs bearing specific cargoes [84–86]. Although extensive damage to the physiochemical properties of EVs using passive loading measures is largely averted, preserving their integrity, the endogenous preloading of EVs is predominantly unmanageable due to the elusive disparities in RNA incorporation within EVs [63], and the presence of residual contaminants such as transfection reagents that ultimately affect RNA cargo delivery [76–78]. Given the regulatory properties of miRNAs, the low loading efficiencies of this method likely induce some level of cytotoxicity in donor cells, promoting ensuing cellular damage that hinders a natural homeostatic condition, thus altering the function of subsequent EV secretions under basal conditions of homeostasis [87, 88]. Moreover, a major drawback of this approach is the lack of control over the incorporation of other cargoes, including non-selective miRNAs, mRNAs, lipids, and proteins. Furthermore, the contribution of specific miRBPs in functionally regulating in part the efficiencies of passive loading of target miRNAs into EVs, is not yet fully investigated or understood, ultimately preventing a more specific and controlled method of cargo loading.

Exogenous (Active) post-loading of EVs

Post-isolation loading of EVs with exogenous biomolecules has been principally achieved through incubation strategies promoting a close-knit association of the cargo of interest with the EV lipid bilayer membrane [89], harnessing therapeutic cargo interests to the EVs surface [90], or most regularly through the diffusion of biomolecules into EVs employing techniques to mechanically and/or chemically stimulate a porous membrane [91]. Despite initial reports indicating a low cargo loading efficiency and an ineffective delivery of active RNA cargos [92], more recent reports have shown a robust miRNA upregulation (> 1000-fold) into EVs via exogenous manipulation [93]. However, mechanistic follow-up studies to evaluate the compositional surface of EVs in supporting the delivery of targeted cargo, effectively need to be further elucidated to unlock the full translational potential of EVs as carriers of therapeutic agents. The following subsections review precisely in greater depth, common methods of exogenous cargo loading, elucidating both their strengths and drawbacks as a serviceable EV loading system.

Provisional membrane permeabilization

Understanding the compositional elements encompassing the structure of EVs is quintessential to conceptualizing progressive approaches for therapeutic alterations in cargo packaging. Broadly speaking, bi-lipid encapsulated nanoparticles (EVs) principally express surface ligands and receptors from their source cells, all while encircling a hydrophilic core [94]. Early attempts of miRNA cargo loading into EVs post-isolation, all followed a common and relatively simple method of incubation. Under specialized conditions, cationic lipid formulations like Lipofectamine™ RNAiMAX Transfection Reagent (Thermo Fisher Scientific; Waltham, MA, USA) have been shown to successfully incorporate miR-335-5p into EVs for functional therapeutic delivery in vivo to desmoplastic cancers [95]. Pending the cargo of interest, incorporation into isolated EVs is targetedly achieved through simple diffusion across the EVs bilipid membrane, while its stunted loading efficiencies are generally restricted via the concentration gradient within the solution and the hydrophobicity of the loading compounds [91]. Other direct mechanistic approaches

to destabilize the bilipid membrane of EVs are predominantly performed through sonication and electroporation. For instance, recent reports from Pottash et al. used sonication-mediated EV loading techniques to incorporate anti-inflammatory miRNAs (miR-146a, miR-155, and miR-223) into HEK293T EVs for downstream use in inflammation-related diseases [96]. The focus of sonication is on disrupting the membrane rigidity and microviscosity through ultrasound waves, while the electroporation of EVs is highly dependent upon their subjection to a high-voltage pulsing that dismembers its pores. Taken together, central technical adversities exist involving both methods including the destabilization of the membrane and the preservation of EV integrity, which regulate and affect downstream cellular uptake [97]. Additionally, the electroporation of EVs with uncommitted nucleic acids have been described to manifest large cargo aggregates, which have partially been attempted to have been offset by incorporating EDTA in conjunction with an electroporation buffer [98]. Aside, recent reports have suggested that sonication-assisted loading (28%) is comparably more efficient than both incubation (1%) and electroporation (5%), respectively [99].

Various other techniques exist to include: calcium chloride transfection, freeze–thaw cycles, pH gradient modifications, as well as kit-based assays like the Exo-Fect™ siRNA/miRNA Transfection Kit (System Biosciences; Palo Alto, CA, USA) that secure the potential application to targetedly load precision molecules into EVs as a new and promising frontier among established drug delivery systems. Exogenous loading of miRNA molecules using calcium chloride transfection has been evidenced and slightly modified via heat shock, which alters the fluidity of the exosomal membrane to promote the incorporation of miRNA into EVs with similar efficiencies in loading to electroporation [100]. Additionally, the notion of EVs as nanocarriers has also been evidenced through the successful accumulation of carrier RNA complexes using repeated freeze–thaw cycles (10 times), from room temperature to -80 °C [101]. Although, recent evidences have duly suggested that repeated freeze–thaw cycles leads to a reduction in the number of EVs, as well as a cycle-dependent increase in their particle size, suggesting the phenomena of EVs subsequent fusion during storage [102]. Aside, given the structure and composition of EVs, pH gradients between the intravesicular and extravesicular environments have also been studied to mechanistically load negatively charged cargos via dehydration/rehydration using 70% ethanol and acidic citrate buffer (pH 2.5) followed by dialysis in HEPES-buffered saline (HBS; pH 7), respectively. The same study revealed decreased levels of Alix and TSG101 following mechanistic measures of pH gradient modifications, suggesting potential surface protein and lipid rearrangements amid the EVs surface [103]. Of particular ineterst in terms of loading efficiencies, recent reports have indicated that EV cargo modulations via the Exo-Fect™ system (System Biosciences; Palo Alto, CA, USA) have revealed a > 1000-fold upregulation of specific miRNA moleculaes of interest. In the same study, it was also shown that Exo-Fect™ miRNA-modified EVs contained altered membranes that catalyzed their internalization within target cells, while duly minimizing their lysosomal colocalization compared to native EVs, underpinning a very promising method of incorporation for loading therapeutic miRNAs into EVs [93]. These summarized findings elucidate useful technical advancements in developing an efficient platform to produce therapeutic miRNA-enriched EVs capable of downstream clinical usage.

Therapeutic and clinical translation of miRNA Cargo-Enriched EVs for disease treatment

EVs hold great therapeutic and clinical potential, owing partially to their ability to be used in allogeneic and/or xenogeneic applications without eliciting signs of cytotoxicity and/or immune reaction [104–106]. As such, they are routinely investigated as both a stand-alone therapy and as carriers for a variety of drug-based therapeutic compounds. Of these applications, miRNA loading into EVs has gained significant popularity within the last decade, given the proven regulatory properties of miRNAs becoming more widely recognized within a variety of tissues [107]. The first results of miRNA loading into EVs quickly followed such discoveries, with Katakowksi et al. 2013 demonstrating that engineered mesenchymal stem cell (MSC) exosomes loaded with miR-146b, having the ability to significantly reduce glioma xenograft growth within a rat model of primary brain tumor [108]. That same year, Ohno et al. adapted measures to transfect HEK293 cells with Let-7a, revealing that the purified exosomes resulting from the cell culture were able to effectively, translationally inhibit tumor formation in a murine model of xenograft breast cancer [109], while Bryniarski et al. duly used exosome-like nanovesicles to deliver miR-150, as a means to regulate T-cell tolerance, which also in a murine model showed to inhibit allergic contact dermatitis [110]. Agreeingly, these discoveries provided early evidence of the therapeutic application and clinical potential, which has since aided in helping to shape the steadily increasing interest in miRNA-enriched EV therapies spanning multiple disciplines, as evidenced in the provided schematic (Fig. 3).

Recent research into the clinical application of miRNA cargo-enriched EVs have been heavily driven by their oncological appeal, notably in breast, lung, liver, colorectal, ovarian, and brain tissues, given that cancer

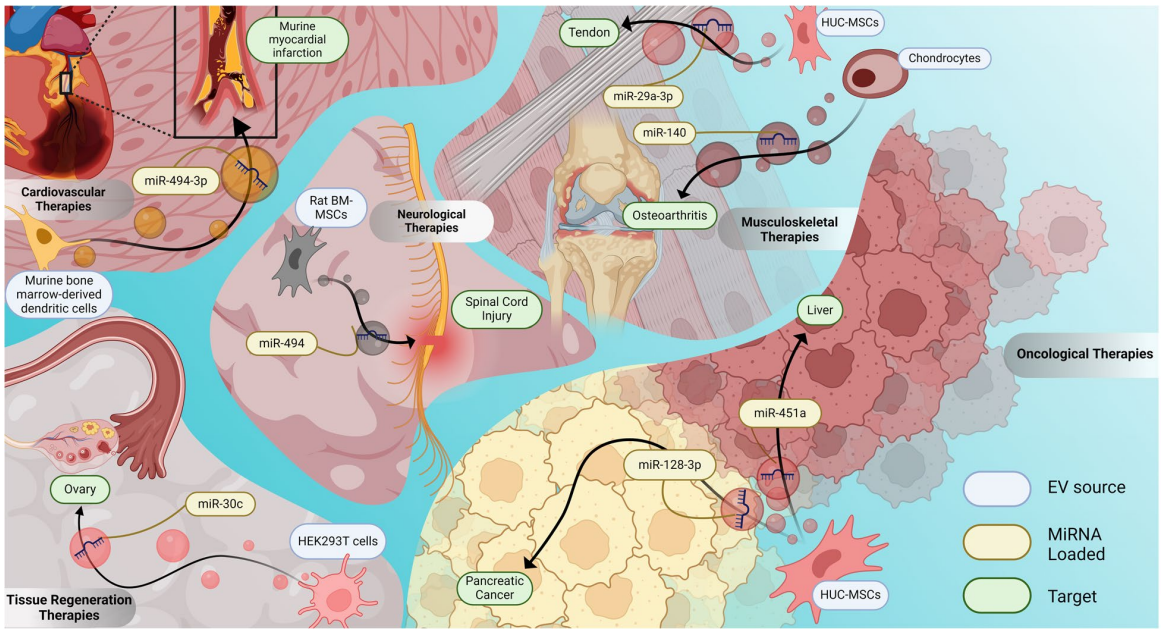


Fig. 3 Conceptual Illustration of EV-miRNAs Regulatory Role in Intercellular Communication Among Selected Reviewed Studies. Collectively, EV treatments have been implicated as a targeted approach in combating disease, as therapeutically-enhanced tiny particles with immense therapeutic potential in nanomedicine. Major areas of therapeutic interest include: tissue regeneration, oncology, as well as within various musculoskeletal, cardiovascular, and neurological disorders

progression and metastasis are intently connected with the repressed expression of tumor-suppressing miRNAs [111]. In addition, the therapeutic applicability of miRNA-enriched EVs are under investigation regarding tissue regeneration and amelioration of chronic illnesses in nearly every tissue in the body (Table 1); most prominently in the musculoskeletal, cardiopulmonary, and nervous systems. Research studies involving the potential clinical translation of miRNA-enriched EVs encompasses a large body of literature/number of publications, spanning a lengthy list of high-impact scientific journals amidst diverse fields, previously summarized by other groups [5]. With the rapid growth of miRNA-enriched EV research enhancing our basic scientific knowledge of EVs for downstream application, this review largely focuses on previously undiscussed publications with the substantial translational potential to feasibly favor the journey from benchtop to clinic.

Oncology

Globally, nearly 20 million people are diagnosed with cancer every year, with that number predicted to rise to nearly 30 million by 2040 [116]. Given the steady increase in the global cancer burden, it is imperative that new therapeutic strategies are developed to reduce cancer deaths. Trends in miRNA-engineered EV therapies for cancer treatment have catapulted studies amidst some of the most commonly diagnosed and deadliest cancers, with a strong focus on breast, lung, liver, and colorectal cancers. Significant research has also been conducted on ovarian and brain cancers, likely due to their high mortality rates [117].

Breast cancer has recently surpassed lung cancer as the most commonly diagnosed cancer, with an estimated 2.3 million new cases every year, globally [116]. As such, it has become the target of multiple potential miRNA-engineered EV therapies. Largely, targeted therapies for breast cancer can be bisected into two groups, with a focus either on the activation of the immune system to inhibit malignant growth or through the direct tumor suppression via miRNA-mediated cellular apoptosis. Case in point, a previously reported attempt using exosomes derived from M1 macrophages, loaded with miR-511-3p were opportunely surface-modified to include interleukin-4 receptor-binding peptide and subsequently showed to successfully induce M1 polarization through the downregulation of M2 markers in vitro, showing greater homing properties to tumors in a murine model using 4T1 breast cancer cells. In vivo experiments duly confirmed the inhibition of tumor growth and decreased levels of M2 cytokines and immune-suppressive cells, increasing levels of M1 cytokines and

Table 1 miRNA-engineerd EVs as an advanced drug delivery system in *Tissue Regeneration Therapies*

Therapeutic miRNA	miRNA Enrichment	Incorporation method	Source of EVs	Target	in vitro Cell Lines Utilized	in vitro Findings	in vivo Model	in vivo Findings	Source
miR-21-5p	Exogenous	Electroporation	Human ADSCs	Diabetic cutaneous wound healing	HaCaT human keratinocytes	Promotion of cell proliferation and migration via Wnt/b-catenin pathway	Rat diabetic cutaneous wound model	Significant promotion of wound closure, increased re-epithelialization, and increases in both total blood vessel count and mature blood vessel count	Lv, Qijun, et al. [112]
miR-31-5p	Exogenous	Electroporation	Raw milk	Diabetic wound healing	HUVECs	Increased cell proliferation, migration, and angiogenesis	Rat diabetic cutaneous wound model	Decrease in unclosed wound rate, increased collagen deposition and re-epithelialization rate, and improved vascular network formation	Yan, Chengqi, et al. [113]
miR-30c	Endogenous	Transfection	Ectopic endometrial endothelial cells	Ovarian endometriosis	N/A	N/A	Murine endometrial model	Decrease in ectopic nodules and attenuation of metastatis via BCL9/Wnt/CD44 regulatory cascade	Zhang, Mengmeng, et al. [114]
miR-31-5p	Endogenous	Lentiviral Transduction	HEK293T cells	Diabetic wound healing	HaCaT human keratinocytes, HFF-1 human foreskin fibroblast, EA.hy926 human endothelial cells	Promotion of cell proliferation and migration; as well as increased capillary-like construction activity of endothelial cells	Rat diabetic cutaneous wound model	Increases in cutaneous wound closure rate, blood vessel density, and number of mature blood vessels, as well as increased collagen deposition	Huang, Jinghuan, et al. [115]

immune-stimulatory cells [118]. In addition, other groups have also reported the successful targeting of breast cancer cells with miRNA-loaded EVs, namely miR-34a-enriched exosomes, which were shown to dose-dependently induce breast cancer cell death, visibly increasing the inhibition of cell migration and invasion, compared to unloaded-exosomes [119]. Conversely, lung cancer, now the second most prevalent cancer worldwide, is reported as the leading cause of cancer death [116]. Implemented strategies to actively inhibit non-small cell lung cancer have been predominantly focused on promoting tumor cell apoptosis in both human cancer cell lines and murine models. For example, Zhou et al. tested the efficacy of miRNA-enriched exosomes on both A549 cells, as well as in a murine xenograft model. The application of miR-449a-loaded exosomes to A549 cells, revealed their ability to effectively inhibit proliferation and promote apoptosis, while duly decreasing tumor volume, nearly doubling the survival time of the mice in vivo [120]. Although these studies demonstrate the modulatory effects and the significance of selected candidate miRNAs as a targeted treatment to combat several types of aggressive cancers, further in-depth studies are required to explicitly evaluate their encompassing functions and off-target effects in order to ultimately apply these therapeutics to in vivo human models as EV-based miRNA therapies.

Apart from breast and lung cancers, liver cancers are currently the third leading cause of cancer-related deaths, accounting for approximately 8.3% of all cancer-related deaths worldwide [116]. Given miRNAs' powerful use as both biomarkers and mediators of physiology and disease, miRNA-enriched EV therapies for liver cancers have predominantly focused on identifying candidate miRNAs downregulated in hepatocyte cancer progression, prior to designing potential strategic EV-based therapies. Yu et al. tested the anti-tumor capacity of lowly expressed miR-375 in human hepatocellular carcinoma (HCC), revealing miR-375-loaded exosomes ability to reduce proliferation, increase apoptosis, and decrease the number of migratory and invasive HCC cells in vitro. Employing the use of an in vivo murine model, the anti-tumor effects of miR-375-loaded exosomes injected with Huh-7 cells were shown to result in a significant inhibition of Huh-7 tumor growth, with reductions in the proportion of KI67-positive proliferative cells [121]. Alongside liver cancers inimical effects, colorectal cancer (CRC), the third most commonly diagnosed cancer and the second leading cause of cancer death [116], has also positionally implemented broad utilization of EV-based treatments using a numerous amount of cell lines for both in vitro and in vivo work. Alike, a representative study from Hosseini et al. aimed to investigate the anti-tumor effects of CT-26 murine CRC-derived exosomes loaded with miR-34a in an in vivo murine model, disclosing miR-34a-loaded-exosomes ability to greatly reduce tumor size, prolonging the survival time of mice. Additionally, miR-34a-enriched exosomes were shown to aptly induce T cell polarization towards the cytotoxic T cell subtype, which is in part responsible for targeting and destroying cancerous growths [122]. In addition to those aforementioned cancerous subtypes, ovarian cancer (OC), accounts for 5% of female cancer deaths and approximately 2.5% of all malignancies among women, despite its 1.3% lifetime risk of development in the United States [117]. Despite the immense amount of research in the field, a massive shortage persists for promising screening tools given OCs high morbidity and low survival rates. In the case of miRNA-engineered EV therapies, two predominant strategies are commonly utilized and explored for OC: (1) comparing the miRNA expression patterns between healthy and cancerous ovarian tissues aimed in identifying potentially therapeutic miRNAs, or (2) selecting miRNAs capable of reducing cancer cell sensitivity to chemotherapeutics. A previous attempt by Zhao et al. aimed to combine both approaches through first selecting a candidate miRNA (miR-484) post-comparison of the miRNA expression patterns of ovarian cell lines and tissues, denoting the significant downregulation of miR-484 in cancerous tissue types. Aimed to unveal its functional relevance in a murine model revealed, miR-484-loaded HEK293T-derived exosomes improved vascular normalization and the chemotherapeutic sensitization of ovarian tumors [123]. Collectively, these studies suggest the broad efficacy of identifying potential targeting therapies through the investigation of differentially regulated miRNAs amidst cancerous tissues, a technique that could be more broadly applied to create therapeutics for both cancerous and non-cancerous illnesses.

Alas, brain cancers, including gliomas and meningiomas, constitute fairly rare types of cancers, but otherwise have one of the lowest survival rates. Alongside, such cancers persist and are particularly prevalent in areas embodying a high Human Development Index (i.e. North America, Europe, Russia, China), composing double the incidence and mortality per 100,000 people, compared to areas with a low Human Development Index [116]. These statistics undeviatingly underpin just why brain cancers are a common target for miRNA-engineered EV therapeutics, with glioma treatments being actively investigated by multiple groups. From initial attempts screening glioma stem cell lines, Lang et al. found that miR-124a packaged into BM-MSC exosomes showed significant reductions in glioma stem cell viability and clonogenicity. Using an i*n vivo* murine model, glioma stem cell lines were exposed to miR-124a-loaded exosomes prior to intracranial xenograft, revealing a 50%

survival rate over a 120-day period, whereas both the PBS and unloaded-exosome control treatments plummeted to a 0% survival rate by day 70 [124]. In short, initial piloting efforts in the development of cancer therapies for implementation in mainstream medicine by use of miRNA-engineered EVs are currently being explored both using in vitro and in vivo models, as an effective nanodelivery system (Table 2).

Musculoskeletal disorders

Musculoskeletal disorders affect the motor organs, muscles, tendons, bones, cartilage, ligaments, and nerves, which are characterized by varying forms of discomfort to irreversible and disabling injury [157]. Moreover, the prevention and treatment of musculoskeletal disorders is a global concern, fueled primarily through government and private company efforts. More recently, in several classified musculoskeletal disorders, adipose-derived mesenchymal stromal cell EVs have been shown to improve tissue healing as a primary paracrine effector, providing yet another potential alternative therapeutic solution [158–162]. While the underlying mechanisms of EV-mediated repair are not explicitly and/or fully understood, studies entailing aspects of bone, intervertebral disc degeneration (IVDD), and cartilage therapies have begun to focus on aspects of deciphering EV-mediated cargo and subsequent RNA manipulation for the generation of miRNA-engineered EVs for downstream therapeutic applications.

Therapies involving miRNA-engineered EVs in bone tissue profile two main categories; (1) the treatment of osteoporosis and (2) attempts to increase osteogenesis for larger defects. In this respect, miRNA-loaded EV approaches using miR-19b-3p applied to osteoporotic BMMSCs resulted in the promotion of osteogenic differentiation and potential, evidenced by the significant upregulation of *ALP*, *collagen type 1*, and *RUNX2* expression, compared to the unloaded control exosome treatment [163]. Subsequent investigations of miRNA-loaded EV therapies in the intervertebral disc have followed a similar pattern in accordance to bone regenerative strategies, primarily using miRNA sequencing analysis techniques, as a means to identify potentially therapeutic miRNAs. Indeed, Zhang et al. identified a potential candidate miRNA by first recognizing six major proteinases that drive IVDD. Through functional use of IL-1β as a means to mimic degenerative conditions, miR-27a-loaded EVs were applied to degenerated rat nucleus pulposus cells and showed significant protein alterations, such as upregulated collagen type II and aggrecan, and conversely correlated decreases in their potent degradative molecule, MMP-13 [164]. Apart from IVDD, investigations involving cartilage tissue have almost exclusively honed in on the alleviation of osteoarthritis (OA), a habitual disease affecting the joints. Using similar approaches to those aforementioned, multiple groups have focused on miRNA-loaded EV strategies in orthopaedic tissue through the comparison of miRNA expression profiles of normal and OA-afflicted tissues. In vitro, exosomes from synovial fibroblasts isolated from knee joints of Sprague–Dawley rats loaded with miR-126-3p, have been shown to decrease chondrocyte apoptosis and suppress inflammation through decreased levels of IL-1β, IL-6, and TNF-α. Furthermore, using an OA rat model in vivo, miR-126-3p-loaded exosomes were also shown to decrease the occurrence of abnormal lesion- or edema-like inflammation, restore bone volume fraction levels, and to increase the articular cartilage thickness and surface regularity [165]. Nevertheless, the breadth of studies in this regard (Table 3) contain a wide-array of interfacial engineering strategies that require extensive investigation in further developing this technology, as both a promising diagnostic and an effective therapeutic system.

Cardiovascular disorders

Accounting for almost a third of all deaths, cardiovascular disease is the leading, predominant, and principal underlying cause of death worldwide [179]. Aside from established cardiac care and continued advancements in certain aspects of applied research, calls for novel and strategic alternatives, such as therapeutically-enriched, miRNA-engineered EVs, are imperative in pushing the threshold on the forefront of nanomedicine. Initially emerging as a promising diagnostic tool, the noninvasive nature of EV collection has propagated their exploitation for disease prevention, intervention, and palliation in cardiovascular disease and repair [180]. Repair strategies for the heart entailing miRNA-engineered EV therapies have largely focused on aspects of regeneration post-heart attack, either through the investigation of ischemia–reperfusion (I/R) injury or via myocardial infarction. As such, parameters for healing in these models are generally characterized by reduced inflammation and rates of apoptosis (Table 4). Hence, Chen et al. showed that in vitro, miR-125b loaded exosomes applied to rat myocardium cells derived from an I/R injury model led to the restoration of cell viability (similar values to the sham rat myocardium cells), as well as decreased apoptosis and levels of inflammatory proteins IL-1β, IL-6 and TNF-α. Moreover, the same group showed that in vivo, the cardiac function of I/R rats was restored following the administration of miR-125b loaded exosomes through lowered infarct size, reduced ratios of inflammatory cells, and restored left ventricular function [181]. Collectively, this suggests in part, the role of miR-125b in contributing to the remission of I/R in myocardium and its functional

Table 2 miRNA-engineerd EVs as an advanced drug delivery system in *Oncology*

Therapeutic miRNA	miRNA Enrichment	Incorporation method	Source of EVs	Cancer Target	in vitro Model	in vitro Findings	in vivo Model	in vivo Findings	Source
miR-130	Exogenous	Electroporation	4T1 breast cancer cells	Breast	Peritoneal macrophages from female C57BL/6 mice	Repolarization of M2 macrophages to M1 phenotype; reprogrammed macrophages then showed the ability to reduce 4T1 breast cancer cell proliferaion, migration, and invasion abilities	N/A	N/A	Moradi-Chaleshtori M, et al. [125]
miR-33	Exogenous	Electroporation	4T1 breast cancer cells	Breast	Peritoneal macrophages from female BALB/c mice	Repolarization of M2 macrophages to M1 phenotype	N/A	N/A	Moradi-Chaleshtori M, et al. [126]
miR-511-3p	Exogenous	Exo-Fect™	Murine M1 macropahges from bone marrow-derived monocytes	Breast	M2 macropahges and 4T1 breast cancer cells	Repolarization of M2 macrophages to M1 phenotype	Murine 4T1-luc xenograft model	Exosome homing to tumors, inhibition of tumor growth and increased presence of M1 marcophages and immune-stimulatory cells	Gunassekaran GR, et al. [127]
let-7i, miR-142, miR-155	Exogenous	Electroporation	4T1 breast cancer cells	Breast	Bone marrow-derived dendritic cells, T cells, and 4T1 cells	Promotion of dendritic cell maturation and increased T cell proliferation and colony formation around tumor cells	Murine 4T1 xenograft model	Significant reduction in tumor size and increase in percent survival over a 50 day period	Khani AT, et al. [128]
miR-34a	Endogenous	Lentiviral Transduction	Genetically modified dental pulp MSCs	Breast	MDA-MB-231 breast carcinoma cells	Breast cancer cell death in a dose-dependent manner and increased inhibition of cell migration and invasion	N/A	N/A	Vakhshiteh F, et al. 211

Table 2 (continued)

Therapeutic miRNA	miRNA Enrichment	Incorporation method	Source of EVs	Cancer Target	in vitro Model	in vitro Findings	in vivo Model	in vivo Findings	Source
let7c-5p	Exogenous	Lipofectamine™ Transfection	HEK293T cells	Breast	MDA-MB-231 breast carcinoma cells	Inhibition of breast cancer cell proliferation and migration	N/A	N/A	Kim, Haneul, and Won Jong Rhee. [129]
miR-1296	Exogenous	Incubation/Rehydration	Nanoliposomes	Breast	MDA-MB-231 breast carcinoma cells	Significant reduction of cell viability in a dose-dependent manner and increased sensitization to cisplatin	N/A	N/A	Albakr, Lamyaa, et al. [130]
miR-3182	Exogenous	Electroporation	Human umbilical cord mesenchymal stem cells (HUCMSCs)	Breast	MDA-MB-231 breast carcinoma cells	Reduction of cell proliferation and migration and induction of apoptosis via the downregulation of the mTOR and RPS6K1 genes	N/A	N/A	Khazaei-Poul, Yalda, et al. [131]
miR-381-3p	Exogenous	Electroporation	Adipose-derived mesenchymal stem cells	Breast	MDA-MB-231 breast carcinoma cells	Inhibited proliferation, migration, and invasion capacity of cancer cells, as well as significant downregulation of genes and proteins related to the epithelial to mesenchymal transition that gives cancer cells increased motility	N/A	N/A	Shojaei, Samaneh, et al. [132]
miR-449a	Endogenous	Recombinant Plasmid Transfection	A549 human non-small cell lung cancer (NSCLC) cells	Lung	A549 human NSCLC cells	Inhibition of cell proliferation and promotion of apoptosis	Murine A549 xenograft model	Significantly decreased tumor volume and increased survival time of the treated mice	Zhou, Wen, et al. [120]

Table 2 (continued)

Therapeutic miRNA	miRNA Enrichment	Incorporation method	Source of EVs	Cancer Target	in vitro Model	in vitro Findings	in vivo Model	in vivo Findings	Source
miR-126	Exogenous	ExoFectin®	MDA-MB-231 breast carcinoma cells	Lung	A549 human non-small cell lung cancer (NSCLC) cells	Higher internalization by A549 cells compared to human embryonic lung fibroblast cells and strongly suppressed A549 cell proliferation and migration	Murine A549 xenograft model	Successful lung homing after intravenous injection followed by inhibition of lung metastasis formation	Nie, Huifang, et al. [133]
miR-497	Exogenous	Transfection	HEK293T cells	Lung	A549 human NSCLC cells and human umbilical vein endothelial cells (HUVECs)	Suppression of tumor growth and downregulation of related genes. Additionally, in the 3D microfluidic system, a decrease of both endothelial cell tube formation and migration of tumor cells	N/A	N/A	Jeong, Kyeongsoo, et al. [134]
miR-375	Endogenous	Lipofectamine™ Transfection	Bone marrow-derived MSCs (BM-MSCs)	Liver	SNU-449 and Huh7 human HCC cell lines	Reduction of proliferation rate, elevated levels of apoptosis, and decrease in the number of migratory and invasive HCC cells	Murine Huh-7 xenograft model	Significant inhibition of Huh-7 tumor growth and reduction in the number of Kl67-positive cells	Yu, Zhaoxia, et al. [135]

Table 2 (continued)

Therapeutic miRNA	miRNA Enrichment	Incorporation method	Source of EVs	Cancer Target	in vitro Model	in vitro Findings	in vivo Model	in vivo Findings	Source
miR-125b	Both	Transfection	Huh7 human hepatocellular carcinoma (HCC) cells	Liver	SK-HEP1 adenocarcinoma and SNU-449 hepatocellular carcinoma cells	Inhibition of migration and invasion, downregulation of mRNA expression of MMPs -2, 9 and 14, disruption of TGF-β1-induced epithelial to mesenchymal transition, and SMAD2 protein expression	N/A	N/A	Kim, Hye Seon, et al. [136]
miR-451a	Endogenous	Lipofectamine™ Transfection	HUCMSCs	Liver	Hep3B and SMMC-7721 HCC cells	Reduction in cell survival rate and viability and promotion of apoptosis by downregulating ADAM10 gene expression	N/A	N/A	Xu, Yunxiuxiu, et al. [137]
miR-30a-3p	Exogenous	Lipofectamine™ Transfection	Human hepatic stellate cells LX-2	Liver	SK-Hep-1 and SMMC-7721 HCC cell lines	Inhibition of HCC cell migration, invasion and metastasis by targeting SNAP23	Murine SK-Hep-1 xenograft model	Fewer metastatic colonies	Liu, Chengdong, et al. [138]
miR-199a	Endogenous	Lentivirus Infection	Adipose tissue-derived MSCs	Liver	PLC/PRF/5 cells	Increased cancer cell sensitivity to doxorubicin and reduction in cell proliferation and viability	Murine PLC/PRF/5 xenograft model	Inhibition of tumor growth and increased effectiveness of doxorubicin	Lou, Guohua, et al. [139]
miR-34a	Exogenous	CaCl2 Transfection	CT-26 murine colon cancer cell line	Colorectal	CT-26 murine colon cancer cell line	Efficient delivery of functional miR-34a mimic	Murine CT-26 xenograft model	Significantly reduced tumor size and prolonged survival time. Induction of T cell polarization towards CD8 + T subtypes	Hosseini, Maryam, et al. [140]

Table 2 (continued)

Therapeutic miRNA	miRNA Enrichment	Incorporation method	Source of EVs	Cancer Target	in vitro Model	in vitro Findings	in vivo Model	in vivo Findings	Source
miR-375-3p	Exogenous	CaCl2 Transfection	HT-29 and SW480 human colon cancer cell lines	Colorectal	T-29 and SW480 EMT-induced cells	Inhibition of cancer cell migration and invasion as well as reversed epithelial to mesenchymal transition via the downregulation of mesenchymal markers and upregulation of epithelial markers	N/A	N/A	Rezaei, Ramazan, et al. [141]
miR-124-3p	Exogenous	CaCl2 Transfection	CT-26 murine colon cancer cell line	Colorectal	CT-26 murine colon cancer cell line	Efficient delivery of functional miR-124-3p mimic	Murine CT-26 xenograft model	Significant tumor growth inhibition and increased median survival time	Rezaei, Ramazan, et al. [142]
miR-181c	Endogenous	Lentiviral Transduction	Bone marrow stromal cells	Ovarian	A2780 human ovarian cancer cell line and A2780/DDP, a DDP-resistant cell line	Suppression of cisplatin resistance in OC cells via downregulation of mesoderm-specific transcript and subsequent inactivation of the Wnt/β-catenin signaling pathway	Murine A2780/DDP xenograft model	Significant reduction in tumor growth, mass and volume	Ruan, Zhengyi, et al. [143]
miR-484	Exogenous	Electroporation	HEK293T cells	Ovarian	HUVEC cells	Inhibition of angiogenesis	Murine OVCAR-3-Luc xenograft model	Improved vascular normalization and sensitization of ovarian tumors to chemotherapeutics	Zhao, Zongxia, et al. [123]

Table 2 (continued)

Therapeutic miRNA	miRNA Enrichment	Incorporation method	Source of EVs	Cancer Target	in vitro Model	in vitro Findings	in vivo Model	in vivo Findings	Source
miR-424	Endogenous	Lipofectamine™ Transfection	Bone marrow-derived mesenchymal stem cells from tibias and femurs of C57BL/6 mice	Ovarian	Normal human ovarian epithelial cell line (HOSEpiC), human ovarian cancer cell lines (SKOV-3, HO8910, A2780), and human umbilical vein endothelial cells (HUVECs)	Repress proliferation, migration, and invasion of ovarian cancer cells, reducing the expression of VEGF and VEGFR. Furthermore, inhibit the proliferation, migration, and tube formation of human umbilical vein endothelial cells	Murine SKOV-3 xenograft model	Suppressed tumorigenesis and angiogenesis	Li, Ping, et al. [144]
miR-494-3p	Exogenous	Electroporation	SKOV3 ovarian cancer cells	Ovarian	OVCAR3 and SKOV3 ovarian cancer cell lines	Reduction of OC cell growth and promotion of apoptosis	N/A	N/A	Wang, Suli, et al. [145]
miR-199a-3p	Exogenous	Electroporation	Fibroblasts derived from the normal omentum of patients	Ovarian	CaOV3, OVCAR3 and SKOV3 ovarian cancer cell lines	Inhibiton of cell proliferation and invasion	Murine SKOV3-13 xenograft model	Drastically inhibited peritoneal dissemination and reduced expression of c-Met expression, ERK phosphorylation, and MMP-2	Kobayashi, Masaki, et al. [146]
miR-124a	Endogenous	Lentiviral Transduction	BM-MSCs	Brain	Five Glioma stem cell lines (GSC267, GSC20, GSC6-27, GSC8-11, and GSC2-14)	Significant reduction in viability and clonogenicity of glioma stem cells	Mnurine intracranial GSC267 xenograft model	50% survival rate over a 120 day period, whereas both the PBS and unloaded-exosome treatments had a 0% survival rate by day 70	Lang, Frederick M., et al. [124]

Table 2 (continued)

Therapeutic miRNA	miRNA Enrichment	Incorporation method	Source of EVs	Cancer Target	in vitro Model	in vitro Findings	in vivo Model	in vivo Findings	Source
miR-124	Exogenous	Lipofectamine™ Transfection	HEK293T cells	Brain	Human glioblastoma cell lines U373MG and U87MG and immortalized SV40 microglial cell line	Anti-tumor effects via the decreased expression levels of genes associated with tumor progression, as well as decreased M2 microglial polarization markers. Additionally, the use of the 3D microfluidics experiments showed decreased migration of both cell types, as well as increased tumor suppression via altered cytokine levels	N/A	N/A	Hong, Soohyun, et al. [147]
miR-100, anti-miR-21	Endogenous	Lipofectamine™ Transfection	Control neural stem cells (NSCs) and CXCR4- engineered NSCs	Brain	U87 glioma cells	Increased chemosensitization to temozolomide	Murine miRNA-loaded mpEVs intranasal delivery model	Increased glioblastoma cell sensitivity to the chemotherapeutic temozolomide, resulting in significant tumor regression and improved survival of the mice	Wang, Kai, et al. [148]
miR-744-5p	Endogenous	Lipofectamine™ Transfection	Human MSCs	Brain	U87 and U251 Human glioma cell lines	Delayed cell proliferative, invasive, and migration capabilities	Murine U87/THP-1 + PMA xenograft model	Reduced rate of cancer cell growth and reduction of tumor nodules in lung tissue	Liu, Ling, et al. [149]

Table 2 (continued)

Therapeutic miRNA	miRNA Enrichment	Incorporation method	Source of EVs	Cancer Target	in vitro Model	in vitro Findings	in vivo Model	in vivo Findings	Source
miR-1252-5p	Exogenous	Electroporation	HEK293T cells	Multiple myeloma	RPMI-8226 B Lymphocyte cancer cells	Increased sensitization of RPMI-8226 cells to Bortezomib, leading to decreased cell viability	N/A	N/A	Rodrigues-Junior, Dorival Mendes, et al. [150]
miR-128-3p	Endogenous	Lipofectamine™ Transfection	HUCMSCs	Pancreatic	PANC-1 pancreatic carcinoma cells	Suppression of proliferation, invasion, and migration via targeting Galectin 3	N/A	N/A	Xie, X., et al. [151]
miR-142-5p	Endogenous	Lentiviral Infection	5-8F and CNE-3 nasopharyngeal carcinoma cells	Nasopharyngeal carcinoma	Radiotherapy-resistant 5-8F and CNE-3 nasopharyngeal carcinoma cells	Inhibition of cell proliferation and radioresistance	Murine 5-8FR xenograft model	Inhibition of tumor growth and radioresistance and acceleration of apoptosis in radiotherapy-resistant cells via inhibition of HGF/c-Met and EGF/EGFR pathways	Zhu, Changyu, et al. [152]
miR-144-3p	Endogenous	Plasmid Transfection/ Lentiviral Transduction	BM-MSCs	Cervical	SiHA squamous carcinoma cells	Suppression of cancer cell migration, invasion, proliferation, and colony formation	Murine SiHA xenograft model	Increased tumor cell apoptosis and significant decrease in tumor growth rate and size via downregulation of CEP55	Meng, Qin, et al. [153]

Table 2 (continued)

Therapeutic miRNA	miRNA Enrichment	Incorporation method	Source of EVs	Cancer Target	in vitro Model	in vitro Findings	in vivo Model	in vivo Findings	Source
miR-371b-5p	Exogenous	Electroporation	HEK293T cells	Osteosarcoma	143B osteosarcoma, A549 lung carcinoma, and HeLa cervical cancer cells	Osteosarcoma cells took up loaded-EVs at a much higher rate as compared to other cancer cell types and showed significantly decreased cell viability while HeLA and A549 cell viability did not significantly change	Murine 143B xenograft model	Greatly decreased tumor volume as compared to unloaded exosomes and controls as well as significantly increased survival time of mice	Xue, Qiang, et al. [154]
miR-7-5p	Endogenous	Lipofectamine™ Transfection	BM-MSCs	Acute myeloid leukemia	HL60 and MOLM13 Myeloid Leukemia cells	Significantly decreased proliferation rate and increased apoptosis rate via downregulation of OSBPL11 gene	Murine MOLM13 xenograft model	Significantly decreased cancer load of splenic leukemia, increase in cancer cell apoptosis and decreased cancer cell proliferation	Jiang, Duanfeng, et al. [155]
miR-21	Exogenous	Electroporation	Blood plasma from mice	Heart	N/A	N/A	Murine Chemotherapy-related cardiotoxicity model	Reduction in cardiotoxicity after doxorubicin administration and restored cardiac function via increase in left ventricular ejection fraction and increased E wave/A wave ratio	Sun, Wenqi, et al. [156]

Table 3 miRNA-engineerd EVs as an advanced drug delivery system in *Musculoskeletal Disorders*

Therapeutic miRNA	miRNA Enrichment	Incorporation method	Source of EVs	Target	in vitro Cell Lines Utilized	in vitro Findings	in vivo Model	in vivo Findings	Source
miR-19b-3p	Exogenous	HiPerfect® Transfection	Serum from 1-month-old rats	Osteoporosis	Osteoporotic BM-MSCs	Higher osteogenic potential through increased expression of osteogenic genes (ALP, collagen type I, and RUNX2) and greatly increased collagen type 1 expression	N/A	N/A	Xun, Jingqiong, et al. [166]
miR-101	Endogenous	Lentiviral Transduction	Human BMSCs (hBMSCs)	Osteoporosis	hBMSCs	Increase in both osteogenic activity and osteogenic differentiation of MSCs as demonstrated by increased alkaline phosphatase activity and expression of osteogenic markers RUNX2, Osterix, OCN, and osteopontin	N/A	N/A	Li, Yanhong, et al. [167]
miR-935	Endogenous	Lipofectamine™ Transfection	hBMSCs	Osteoporosis	hFOB1.19 human osteoblast cells	Improved osteoblast cell proliferation and differentiation as seen through increased RUNX2 and activating transcription factor 4 protein levels	N/A	N/A	Zhang, Ying, et al. [168]
miR-20a	Endogenous	Lipofectamine™ Transfection	hBMSCs	Osteoporosis	hBMSCs	Successful promotion of in vitro migration and osteogenesis of BM-MSCs as seen through upregulation of ALP, RUNX2, and OCN genes	Rat osteoporosis model	Significantly increased bone volume fraction, total bone volume, and bone mineral density	Liu, Wei, et al. [169]

Table 3 (continued)

Therapeutic miRNA	miRNA Enrichment	Incorporation method	Source of EVs	Target	in vitro Cell Lines Utilized	in vitro Findings	in vivo Model	in vivo Findings	Source
miR-27a	Endogenous	riboFECT Transfection	Autophagy Activated Nucleus pulposus cells (NPCs)	Intervertebral disc degeneration (IVDD)	NPCs	Protein analysis indicated significantly upregulated collagen type II and aggrecan levels, coinciding with a significant decrease in MMP-13 levels	N/A	N/A	Zhang, Qi-Chen, et al. [164]
miR-129-5p	Endogenous	Lipofectamine™ Transfection	hBMSCs	IVDD	Human NPCs	Increased cell viability combined with increased collagen type II and aggrecan production	Rat IVDD model	Successfully inhibited M1 polarization, reversed cellular apoptosis and extracellular matrix degradation	Cui, Shaoqian, and Lei Zhang. [170]
miR-15a	Endogenous	Lipofectamine™ Transfection	Human NP-MSCs	IVDD	Dedifferentiated MSCs from human NP tissue	Significantly increased MSC proliferation and colony formation as well as increased MSC chondrogenic differentiation shown through upregulation of aggrecan and collagen type II mRNA levels coupled with the downregulation of multiple proteinase mRNAs	N/A	N/A	Zhang, Qiang, et al. [171]

Table 3 (continued)

Therapeutic miRNA	miRNA Enrichment	Incorporation method	Source of EVs	Target	in vitro Cell Lines Utilized	in vitro Findings	in vivo Model	in vivo Findings	Source
miR-17-5p	Endogenous	Lipofectamine™ Transfection	BMSC-bm	IVDD	Human NP cells	Increase in human NP cell proliferation, decrease in apoptosis rate, and significant increase in collagen type II and aggrecan protein levels coupled with significantly decreased MMP-13 and ADAMTS5 levels	Rat IVDD model	Similar changes in protein levels to in vitro studies, coupled with lower histological grading score of IVDD	Zhou, Zhi-Min, et al. [172]
miR-125b-5p	Endogenous	Lipofectamine™ Transfection	Cartilage endplate stem cells	IVDD	Tert-buty l hydroperoxide (TBHP) induced NPCs	Inhibited the apoptosis of TBHP-NPCs as well as the expression of bax, MMP13, and p62 while increased the expression of bcl2, ACAN, and LC3-II/I	Rat IVDD model	Upregulation of BCL2 apoptosis regulator, ACAN, and LC3-II/I coupled with the downregulation of SUV39H1 histone lysine methyltransferase, bax, MMP-13, and ubitquitin-binding protein p62. Histological analysis revealed decreased NP cell apoptosis and reduced fibrotic remodeling of the NP	Chen, Dong, and Xin Jiang. [173]

Table 3 (continued)

Therapeutic miRNA	miRNA Enrichment	Incorporation method	Source of EVs	Target	in vitro Cell Lines Utilized	in vitro Findings	in vivo Model	in vivo Findings	Source
miR-126-3p	Endogenous	Transfection	Synovial fibroblasts	Osteoarthritis (OA)	Rat chondrocytes	Decrease in apoptosis in chondrocytes and suppression of their inflammation as seen through decreased IL-1b, IL-6, and TNF-a	Rat OA model	Anti-apoptotic and anti-inflammatory effects on cartilage, suppression of osteophyte formation, decreased occurrence of abnormal lesion- or edema-like inflammation, restoration of bone volume fraction levels, and increased articular cartilage thickness and surface regularity as seen through histological analysis	Zhou, Yan, et al. [174]
miR-361-5p	Exogenous	Electroporation	hBMSCs	OA	IL-1β-treated chondrocytes	Significantly increased cell viability and downregulation of proteinases involved in OA progression	Rat OA model	Downregulation of proteinases involved in OA as well as increased synovial tissue hyperplasia and decreased OA pathological scoring	Tao, Yunxia, et al. [175]
miR-140	Exogenous	Electroporation	Human Chondrocytes	OA	IL-1β-treated chondrocytes	Downregulated MMP-13 and ADAMTS-5 gene expression	Rat OA model	Downregulation of MMP-13 and ADAMTS-5, while cartilage tissue repair was nearly identical to the sham surgical group as evidenced by histological scoring	Liang, Yujie, et al. [176]

Table 3 (continued)

Therapeutic miRNA	miRNA Enrichment	Incorporation method	Source of EVs	Target	in vitro Cell Lines Utilized	in vitro Findings	in vivo Model	in vivo Findings	Source
miR-140	Exogenous	Freeze and Thaw Method	Rabbit serum	Cartilage regeneration	Rabbit BM-MSC and chondrocytes	Exhibited chondrogenic differentiation through changes in BM-MSC morphology, as well as the upregulation of collagen type II, Sox9, and ACAN genes in BM-MSCs	N/A	N/A	Won Lee, Gi, et al. [101]
miR-29a-3p	Endogenous	Agonist	HUCMSCs	Tendon regeneration	N/A	N/A	Rat achilles tendon defect model	Significantly increased expression of tendon markers TNMD and SCXA, elevated COL1A1 gene expression and higher average ultimate tensile strength, stiffness, and Young's modulus in treated tendons	Yao, Zhixiao, et al. [177]
miR-24	Endogenous	Lentiviral Transduction	HMSCs	Bone repair	HMSCs, macrophages	Enhanced osteoinductive function by activating SMAD1/5/8 phosphorylation and MSC differentiation	Rat calvarial bone defect model	Enhanced bone repair and anti-inflammatory activity	Huang CC, et al. [178]

Table 4 miRNA-engineerd EVs as an advanced drug delivery system in *Cardiovascular Disorders*

Therapeutic miRNA	miRNA Enrichment	Incorporation method	Source of EVs	Target	in vitro Cell Lines Utilized	in vitro Findings	in vivo Model	in vivo Findings	Source
miR-125b	Endogenous	Lipofectamine™ Transfection	Rat BM-MSCs	Ischemia reperfusion (I/R) injury model	Rat I/R myocardium cells	Restoration of cell viability coupled with a decease in the apoptotic ratio. Additionally, the levels of IL-1b, IL-6 and TNF-a proteins were significantly reduced, indicating reduced cellular inflammation	Rat Ischemia reperfusion (I/R) model	Restored cardiac function as seen through significantly lower infarct size, reduced ratio of inflammatory cells, and restored left ventricular function	Chen, Qi, et al. [181]
miR-494-3p	Endogenous	RiboFECTTM Transfection	Murine bone marrow-derived dendritic cells	Murine myocardial infarction	Cardiac microvascular endothelial cells	Enhanced tube formation	Murine myocardial infarction model	Increased VEGF expression and a significant increase in the mean number of vessels in the myocardium	Liu, Haibo, et al. [182]
miR-210	Endogenous	Transfection	Human Adipose Derived Stem Cells	Ischemia heart disease	Hypoxic endothelial cells and H9C2 cardiomyocyte cells	Inhibition of EFNA3 in endothelial cells and a significant increase in VEGF expression combined with an increase in viability for cardiomyocyte cells	Rat I/R injury model	Significant increase in cardiac function and no significant changes in fibrotic area ratio	Song, Byeong-Wook, et al. [183]
miR-144-3p	Exogenous	Exo-Fect™ Transfection	HEK293 cells	Murine myocardial infarction	H9C2 rat myoblast cells	Increased cell viability, decreased lactate dehydrogenase release, and decreased cellular apoptosis after H2O2-induced cellular injury	Murine myocardial infarction model	Reduction of infarct size, significantly reduced cell death, and no systemic toxicity	Kang, Ji-Young, et al. [184]

Table 4 (continued)

Therapeutic miRNA	miRNA Enrichment	Incorporation method	Source of EVs	Target	in vitro Cell Lines Utilized	in vitro Findings	in vivo Model	in vivo Findings	Source
miR-126	Endogenous	Lipofectamine™ Transfection	Human BM-MSCs	Nonspecific angiogenesis	HUVECs	Enhanced proliferation, migration, and tube formation	Murine full-thickness cutaneous wound model	Significantly increased wound closure rate, reduction of scar formation, and enhancement of angiogenesis	Zhang, Lei, et al. [185]
miR-186	Endogenous	Lipofectamine™ Transfection	Human BM-MSCs	Idiopathic pulmonary fibrosis	LL29 human lung fibroblasts	Suppression of lung fibroblast activation and reduced fibroblast viability and invasion	Murine pulmonary fibrosis model	Reduced expression of myofibroblastic markers, reduction in collagen fibers, impaired fibroblast activation, and suppression of idiopathic pulmonary fibrosis	Zhou, Jing, et al. [186]
miR-146a, miR-370, miR-126a	Endogenous	Trans-IT TKO (Mirus)	NHDF-EVs	Ischemic heart disease	C57BL/6 mouse primary neonatal cardiomyocytes	Therapeutic miRNA cluster acts synergistically to reduce cardiomyocyte apoptosis	N/A	N/A	Euscher LM, et al. [187]

applicability to serve as a potential therapeutic agent for myocardial I/R. MicroRNA-engineered EV therapies for cardiovascular repair have thus far shown in vivo promise for the treatment of several prominent and deadly cardiac pathologies, however, additional work is needed to exclusively translate these therapeutic applications bedside for the implementation in human patients.

Neurological disorders

The brain is an infinitely complex, temporally, and spatially multiscale structure that is far from well understood. The development of new treatments and therapies for brain-related diseases are furthermore hindered due to epithelial-like tight junctions within the brain capillary endothelium that compose the blood–brain barrier (BBB), preventing the uptake of most pharmaceutical compounds [188]. Fortunately, EVs effectively traverse this restriction via the bidirectional BBB transendothelial transport, both from the blood into the brain and from the brain into the blood [189]. Hence, treatments for neurodegenerative afflictions using miRNA-engineered EVs compose a strategic and novel system to combat ailments like subarachnoid hemorrhage, alzheimer's disease, and depression (Table 5).

Implementation of miRNA-engineered EVs to treat brain illnesses inherently provoke query on their capacity to reach targets in effective concentrations after systemic/intranasal administration, or targeted deposition. Comparing the global miRNA profiles from plasma exosomes of subarachnoid hemorrhage (SAH) and healthy patients, followed by extrapolation to a murine model of SAH, Lai et al. functionally revealed the role of miR-193-3b-loaded BM-MSC-derived exosomes in reducing inflammatory cytokine levels, improving neurological scoring, and decreasing brain edema post-SAH treatment, all of which indicate neurobehavioral impairment alleviation [199]. This study, along with others denoted previously, precisely specify the value of using multi-omics analysis to accurately identify differentially regulated miRNAs that govern health and disease. Such studies unveiling the functional applicability of miRNA-engineered EVs using small animal models suggest their preeminent role as future clinical therapeutic treatments. Additionally, at minimum, rigorous and in-depth studies are still needed to optimize various aspects of EV production, loading, and administration, prior to potential clinical EV-based therapy commercialization.

Therapeutic use of miRNA-loaded EVs under clinical trial

EV therapies have been investigated amid multiple clinical trials, demonstrating acceptable safety profiles and therapeutic proof of efficacy in humans [200–203]. While promising, at least 1 miRNA-engineered EV therapy exists under clinical trial, although its results have yet to be substantiated and published. Additionally, phase I/II testing of allogenic MSC-derived exosomes loaded with miR-124 for the treatment of acute ischemic stroke is also currently in the recruiting phase, with the trial expected to consist of 5 patients (NCT03384433). Aside from EVs, several miRNA-based therapies have already undergone and completed clinical trials. In the past several years, in total, at least 4 miRNAs (miR-16, miR-29, miR-34a, and miR-124) have shown clinical relevance for subsequent translation to EV-based therapeutics.

A multicenter phase 1 clinical trial completed several years back used miR-16 to treat mesothelioma and non-small cell lung cancer (NCT02369198). Twenty-six pleural mesothelioma patients received weekly doses of miR-16 loaded into non-living bacterial minicells (TargomiRs), which revealed an acceptable safety profile, producing an objective response in 1 of 22 patients. The foremost side-effect observed was a heightened inflammatory response, although unable to pinpoint and decipher its origins as the delivery of miR-16, the bacterial origin of the TargomiRs, or an antitumor effect [204, 205]. Aside, the confirmation of an acceptable safety profile is conclusively promising for miR-16's clinical use, which has also shown effects in the attenuation of lung inflammation and the reduction of lung injury in mice, when targetly delivered via ADSC-derived exosomes [206]. Moreover, a phase 1 clinical trial was also conducted on MRG-201, a synthetic drug designed to mimic the bioactivity of miR-29 (NCT02603224). In total 54 healthy volunteers were enrolled to the study and assigned to either intact or incised skin groups. Volunteers received intradermal injections of either a single or multiple doses of MRG-201, considered safe and well-tolerated at all levels, with a total of 139 doses given to 47 subjects. Collectively, it was shown that MRG-201 treatment decreased wound fibroplasia with no evidence of wound dehiscence [207]. Efficacy and tolerance of MRG-201 permits significant credibility to the clinical potential of miR-29-engineered-EVs, which have recently shown promising results as a strategic effort in tendon regeneration [177].

To date, miR-34a delivered intravenously to patients with solid tumors refractory to standard treatment has been investigated within two phase 1 clinical trials (NCT01829971 and NCT02862145). The first trial aimed to establish and optimize miR-34a dosing associated with its acceptable safety. One patient with HCC evidenced the confirmation of a prolonged response (at minimum a 30% decrease in the longest diameter sum of the target lesions), while four others experienced the persistence of stable disease (neither sufficient shrinkage, nor sufficient increase in the longest diameter sum) [208]. The second

Table 5 miRNA-engineerd EVs as an advanced drug delivery system in *Neurological Disorders*

Therapeutic miRNA	miRNA Enrichment	Incorporation method	Source of EVs	Target	in vitro Cell Lines Utilized	in vitro Findings	in vivo Model	in vivo Findings	Source
miR-194	Endogenous	Lentiviral Infection	Murine BM-MSCs	Neurovascular endothelial cell injury	Human brain microvascular endothelial cells	Restoration of cell viability and migratory ability after oxygen–glucose deprivation/reoxygenation treatment and inhibition of ferroptosis	N/A	N/A	Li, Xu, et al. [190]
miR-223-3p	Endogenous	Lentiviral Infection	Murine BM-MSCs	Cerebral ischemic injury	Murine BV-2 microglia cells	Promotion of M1 to M2 phenotypic conversion of microglia cells as well as modulation of inflammatory cytokine expression, indicating a shift towards an anti-inflammatory remodeling phenotype	Rat middle cerebral artery occlusion and reperfusion model	Improved neurological dysfunction and decreased infarct volume over a 28-day period	Zhao, Yangmin, et al. [191]
miR-17-5p	Endogenous	Lipofectamine™ Transfection	Rat primary astrocytes	Hypoxic-ischemic brain damage	Immortalized H19-7 microglial cell line	Promotion of cell viability and reduced inflammation after OGD-induced damage	Neonatal rat model of hypoxic-ischemic brain damage	Treatment alleviated brain damage and coincided with high expression of miR-17-5p. Additionally increased the healing by reducing neuronal apoptosis and inflammation	Du, Lin, et al. [192]

Table 5 (continued)

Therapeutic miRNA	miRNA Enrichment	Incorporation method	Source of EVs	Target	in vitro Cell Lines Utilized	in vitro Findings	in vivo Model	in vivo Findings	Source
miR-210	Endogenous	DharmaFECT Transfection	Human endothelial progenitor cells	Ischemia-induced neuronal damage	SH-SY5Y human neuroblastoma cells	Reduced hypoxia and reoxygenation (H/R) induced apoptosis, attenuation of intracellular reactive oxygen species levels, and increased neuroblastoma proliferation	N/A	N/A	Yerrapragada, Sri Meghana, et al. [193]
miR-193-3b	Exogenous	Electroporation	Murine BM-MSCs	Neuroinflammation following subarachnoid hemorrhage	N/A	N/A	Murine subarachnoid hemorrhage (SAH) model	Reduced inflammatory cytokine levels, improved neurological scoring, and decreased brain edema after SAH treatment, which indicates alleviation of neurobehavioral impairments	Lai, Niansheng, et al. [194]
miR-22	Endogenous	HiPerfect® Transfection	Mouse Adipose-derived MSCs	Alzheimer's disease	PC12 rat adrenal medulla cells	Inhibition of apoptosis and significantly decreased release rate of inflammatory factors	Murine APP/PS1 model	Increased nerve function and motor ability, improved survival of nerve cells, and decreased expression of inflammatory factors	Zhai, Liping, et al. [195]

Table 5 (continued)

Therapeutic miRNA	miRNA Enrichment	Incorporation method	Source of EVs	Target	in vitro Cell Lines Utilized	in vitro Findings	in vivo Model	in vivo Findings	Source
miR-26a	Endogenous	Lipofectamine™ Transfection	Human BM-MSCs	Depression	Neonatal rat hippocampal neurons	Elevated superoxide dismutase levels and inhibition of inflammatory factors in hippocampal neurons as well as increased hippocampal neuron proliferation and restriction of apoptosis	N/A	N/A	Guo, Huirong, et al. [196]
miR-146a	Endogenous	Lipofectamine™ Transfection	Murine BM-MSCs	Diabetic peripheral neuropathy	Human dermal microvascular endothelial cells	Inhibition of inflammatory activation	Murine diabetic peripheral neuropathy model	Significantly increased intraepidermal nerve fiber density, restoration of nerve fiber diameter, increased axonal remyelination, and inhibition of inflammatory effects	Fan, Baoyan, et al. [197]
miR-494	Exogenous	Exo-Fect™ Transfection	Rat BM-MSCs	Spinal cord injury	Rat dorsal root ganglion cells and alveolar macrophages	Significantly increased ganglion cell viability and promotion of M2 macrophage polarization	Rat spinal cord injury model	Homing to spinal cord lesion, reduction of lesion volume, regeneration of neurofilaments, and recovery of rat behavioral function	Huang, Wei, et al. [198]

trial was abruptly closed early due to serious immune-mediated adverse events within four patients, yet demonstrated a manageable toxicity profile in the majority [209]. These studies corroborate the proof-of-concept required in establishing miR-34a therapeutics, while engineered-EV treatments have been recently studied in light of breast [119], and colorectal [122] cancer suppression. Alas, a phase IIa clinical trial has also been conducted on ABX464, an orally administered small molecule that induces the splicing of miR-124 (NCT03093259). A total of 32 participants with moderate to severe ulcerative colitis were recruited to the study and enrolled in an 8-week induction phase, followed by an optional long-term extension phase. ABX464 was shown to be safe and well-tolerated, while also greatly increasing both the clinical remission and response amid the treatment group over the initial 8-week period. During the extension phase, a high maintenance of remission rates persisted, with the majority of patients remaining in clinical remission to the 12 and 24-month time points. Currently, the safety and efficacy of ABX464 is ongoing and being further investigated within a phase IIb clinical trial, with 254 recruited participants (NCT03760003). Preliminary results aid in the promising perspective for miR-124-engineered-EV therapeutics, which have duly recently been investigated in glioblastomas [124, 147], colorectal cancer [210], and spinal cord ischemia–reperfusion injury [211] treatment. Taken together, the clinical evaluation of miRNA-engineered EV therapies is still in its relative infancy. However, with one therapy under clinical trial thus far, and multiple successful proposed examples of miRNA-loaded EV strategies published, it is highly likely that the number of proposed miRNA-engineered EVs for therapeutic use will steadily rise within the next decade.

miRNA loaded EVs: limitations hindering clinical progression in nanomedicine

Outlined in Fig. 4, the premise to move miRNA-engineered EV therapeutics from benchtop and small animal models, to clinical trials is a time and resource-intensive process. In order to produce a potential therapeutic treatment for clinical testing, standards in EV purity must be met. In addition, such therapeutics require the isolation of a large number of EVs, underscoring the need for reproducible and scalable methods. To meet purity standards set forth for EV-based treatments, several methodologies have been developed to meet Good Manufacturing Practices (GMP), a system of processing, standardized procedures, and documentation that establishes quality standards. This includes GMP strategies for the production and isolation of EVs from MSCs [212–214], HEK293 human embryonic kidney cells [215], and cardiac progenitor cells [216]. Established methodologies have helped to lay the groundwork for EV-based therapeutics in achieving GMP standards, not only in terms of isolation and purification, but duly in their scale-up production. To further scale-up the production of EVs in a controlled manner, a number of bioreactor systems have been developed [217–219], which have resulted in high-yields of EVs, while also serving as a platform to mechanically or chemically stimulate cells, as a means to augment the cargo of EVs. A full review was recently published focusing on large-scale cell culture platforms to increase EV yields, which further details the use of scale-up strategies currently being implemented in clinical trials [220].

Several groups have also attempted to generate clinically relevant numbers of EVs through the isolation of common biologics such as blood and milk. These methods drastically reduce the amount of time needed to obtain large amounts of EVs, removing the production time necessary to expand large quantities of cells in vitro. In addition, this method also avoids the need in standardizing cell culture strategies, by instead utilizing pre-existing GMP protocols for the standardized collection of biologics. Large-scale EV isolation from blood has been developed by several groups, either through the isolation of large quantities of cells to rapidly farm EVs or through direct isolation of the EVs themselves. A novel method developed to induce rapid EV production over a 48-h window has duly been established via isolating natural killer cells from 30-50 mL of donor blood [221]. Alternatively, direct isolation of EVs from blood plasma has equitably demonstrated high EV yields and purities [222]. Moreover, timely isolation methods also exist that were originally designed for the rapid and efficient isolation of EVs for proteomic analysis, which yield ~ $1^{*}10^{11}$ EVs per milliliter of serum in 15 min, a promising method to generate clinically relevant numbers of EVs to be successfully scaled-up or scaled-out [223]. Combining established large-scale EV isolation methods from blood with the partnerships of blood banks and hospitals, further the applicability of such methods in collecting large quantities of GMP-grade EVs in the advancement of future clinical trials. On the other hand, milk-derived exosomes are even more readily available offering an alternative promising source of GMP-grade EVs for clinical trials. Marsh et al. developed protocols for the scalable production of EVs from bovine milk, creating ultra-dense isolates of sEVs that accounted for 10–15% of the total starting milk volume, resulting in incredibly high concentrations of EVs isolatable from an additional common biologic [224]. The use of milk-derived EVs for miRNA delivery have also recently been investigated, finding that hsa-miR148a-3p, can be successfully loaded into raw bovine milk derived-exosomes with confirmed uptake by hepatic and interstitial cell lines [225]. Although miRNA loading into milk-derived EVs has not yet been widely investigated, such studies effectively outline an additional,

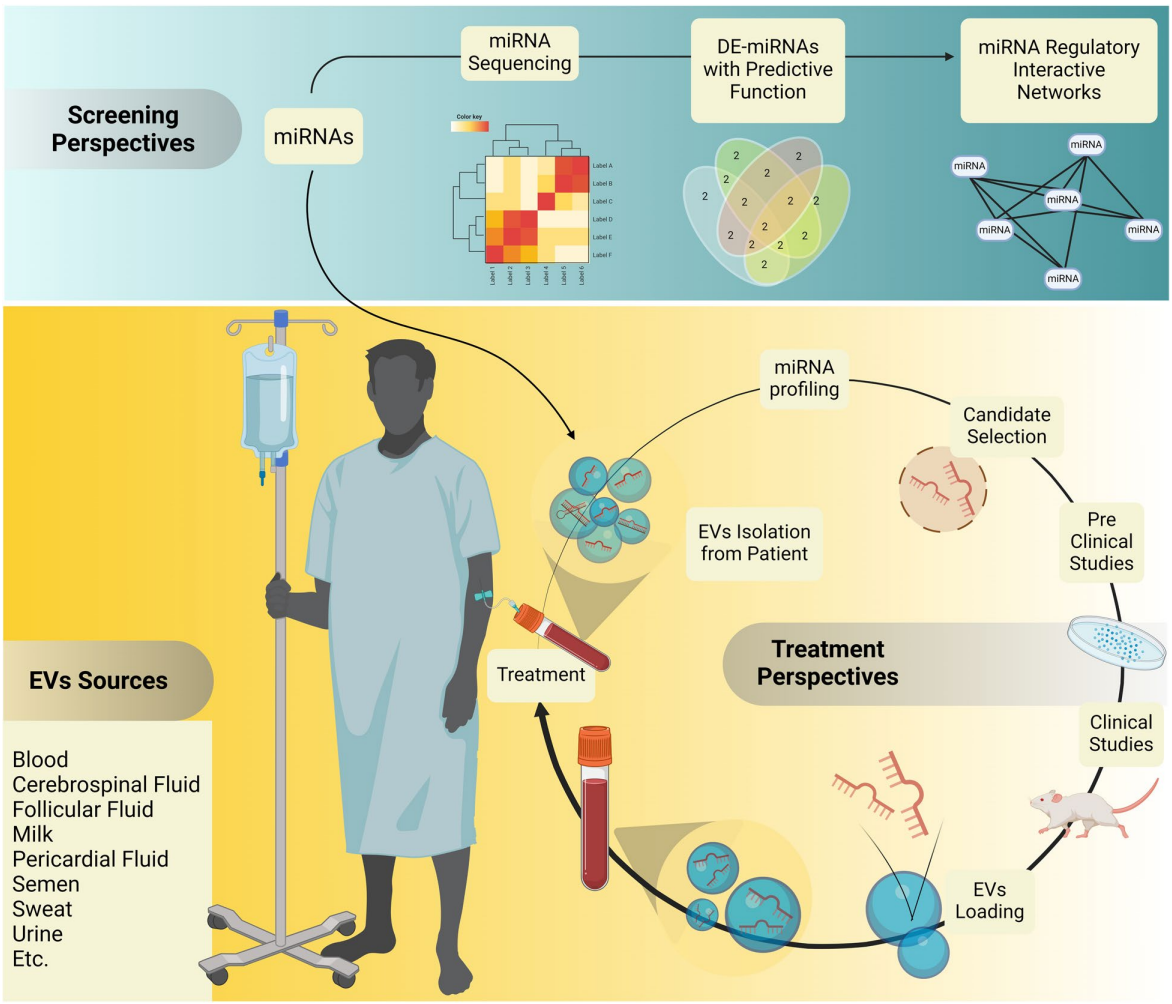


Fig. 4 Treatment Perspective of EV-miRNAs for Clinical Use as Therapeutics. EVs carrying host molecules, readily isolated from systemic fluids, propagate EVs as an effective screening perspective or diagnostic tool in the identification of biomarkers for many diseases and their potential application as an effective therapeutic treatment

potentially promising, strategy to propagate miRNA-loaded EV therapies on a large scale that caters to satisfactory purities and reproducibility standards. Albeit therapeutically promising studies exist and in part, some of the prominent hurdles are currently being overcome, plausible concern still remains regarding the efficacy/dose optimization, biodistribution, and the target site bioavailability and engagement, which all require an increased and more developed understanding of EV biology prior to wide-scale clinical implementation.

Concluding remarks and future perspectives

Over the past decade compounding knowledge of the structure of EVs, as well as their biogenesis and function, have catapulted advancements for their novel potential in pharmaceuticals as a next-generation drug delivery system. Functional studies denoting the roles of EV-coupled miRNAs continue to accumulate aiding in their incorporation in preclinical and clinical settings alike. Given the complex effects of miRNAs in post-transcriptional gene regulation, in combination with the additonal ambiguities that undermine their precise functions, a need to further elucidate such systems both in vitro and in vivo still persist. Moreover, predetermined mechanistic approaches to modify EVs for the incorporation of therapeutic miRNAs requires further technical optimization in managing dosage and other pharmacokinetic factors, prior to their large-scale distribution as a new frontier drug delivery platform. Further advancements in EV biology and the mechanistic

approaches to effectively modify EVs with repeatability will favor the clinical translation of miRNA-engineered EVs for precise therapeutic application in treating a number of disease pathologies, continuing to push their implementation as novel payers on the forefront of nanomedicine.

Abbreviations

EV	Extracellular vesicle
miRNA	MicroRNA
ISEV	International society for extracellular vesicles
MV	Microvesicle
ApoBD	Apoptotic body
MVB	Multivesicular body
ILV	Intraluminal vesicle
LAMP	Lysosome-associated membrane proteins
ESCRT	Endosomal sorting complex required for transport
MISEV	Minimal information for studies of extracellular vesicles
pri-miRNA	Primary miRNA
pre-miRNA	Precursor miRNA
siRNA	small interfering RNA
RBP	RNA-binding protein
HBS	HEPES-buffered saline
MSC	Mesenchymal stem cell
HCC	Hepatocellular carcinoma
CRC	Colorectal cancer
OC	Ovarian cancer
IVDD	Intervertebral disc degeneration
OA	Osteoarthritis
I/R	Ischemia-reperfusion
BBB	Blood brain barrier
SAH	Subarachnoid hemorrhage
GMP	Good manufacturing practices

Acknowledgements
The authors acknowledge the collaborative efforts of the Animal Reproduction and Biotechnology Laboratory and the Translational Medicine Institute of Colorado State University.

Authors' contributions
Idea Conceptualization: N.M., J. O., Literature Review N.M., J.O., S.G., Illustrations: N.M., L.S., Writing of original draft: N.M., J.O., S.G., Manuscript editing: N.M., J.O., S.G., L.S., A.G., C. P., D.T., Supervision: D.T., All authors have read and agreed to the published version of this manuscript.

Funding
NGM is financially supported by grant funds from USDA-NIFA-AFRI Predoctoral Fellowship grant number 2023–67011-40511.

Availability of data and materials
No datasets were generated or analysed during the current study.

Declarations

Ethics approval and consent to participate
Not applicable.

Consent for publication
Not applicable.

Competing interests
The authors declare no competing interests.

Received: 4 April 2024 Accepted: 30 April 2024
Published online: 21 May 2024

References

1. Tesfaye D, Menjivar N, Gebremedhn S. Current knowledge and the future potential of extracellular vesicles in mammalian reproduction. Reprod Fertil Dev. 2021;34:174–89. https://doi.org/10.1071/RD21277.
2. Théry C, Witwer KW, Aikawa E, Alcaraz MJ, Anderson JD, Andriantsitohaina R, et al. Minimal information for studies of extracellular vesicles 2018 (MISEV2018): a position statement of the International Society for Extracellular Vesicles and update of the MISEV2014 guidelines. J Extracell Vesicles. 2018;7:1535750. https://doi.org/10.1080/20013078.2018.1535750.
3. Welsh JA, Goberdhan DCI, O'Driscoll L, Buzas EI, Blenkiron C, Bussolati B, et al. Minimal information for studies of extracellular vesicles (MISEV2023): From basic to advanced approaches. J Extracell Vesicles. 2024;13:e12404. https://doi.org/10.1002/jev2.12404.
4. Mathieu M, Martin-Jaular L, Lavieu G, Théry C. Specificities of secretion and uptake of exosomes and other extracellular vesicles for cell-to-cell communication. Nat Cell Biol. 2019;21:9–17. https://doi.org/10.1038/s41556-018-0250-9.
5. Munir J, Yoon JK, Ryu S. Therapeutic miRNA-Enriched Extracellular Vesicles: Current Approaches and Future Prospects. Cells. 2020. https://doi.org/10.3390/cells9102271.
6. Taylor DD, Gercel-Taylor C. The origin, function, and diagnostic potential of RNA within extracellular vesicles present in human biological fluids. Front Genet. 2013;4:142. https://doi.org/10.3389/fgene.2013.00142.
7. Schorey JS, Bhatnagar S. Exosome function: from tumor immunology to pathogen biology. Traffic. 2008;9:871–81. https://doi.org/10.1111/j.1600-0854.2008.00734.x.
8. Pioltine EM, Costa CB, Barbosa Latorraca L, Franchi FF, Dos Santos PH, Mingoti GZ, et al. Treatment of in vitro-Matured Bovine Oocytes With Tauroursodeoxycholic Acid Modulates the Oxidative Stress Signaling Pathway. Front Cell Dev Biol. 2021;9:623852. https://doi.org/10.3389/fcell.2021.623852.
9. Jaiswal JK, Andrews NW, Simon SM. Membrane proximal lysosomes are the major vesicles responsible for calcium-dependent exocytosis in nonsecretory cells. J Cell Biol. 2002;159:625–35. https://doi.org/10.1083/jcb.200208154.
10. Stuffers S, Sem Wegner C, Stenmark H, Brech A. Multivesicular endosome biogenesis in the absence of ESCRTs. Traffic. 2009;10:925–37. https://doi.org/10.1111/j.1600-0854.2009.00920.x.
11. Edgar JR, Eden ER, Futter CE. Hrs- and CD63-dependent competing mechanisms make different sized endosomal intraluminal vesicles. Traffic. 2014;15:197–211. https://doi.org/10.1111/tra.12139.
12. Carayon K, Chaoui K, Ronzier E, Lazar I, Bertrand-Michel J, Roques V, et al. Proteolipidic composition of exosomes changes during reticulocyte maturation. J Biol Chem. 2011;286:34426–39. https://doi.org/10.1074/jbc.M111.257444.
13. Tricarico C, Clancy J, D'Souza-Schorey C. Biology and biogenesis of shed microvesicles. Small GTPases. 2017;8:220–32. https://doi.org/10.1080/21541248.2016.1215283.
14. Atkin-Smith GK, Poon IKH. Disassembly of the Dying: Mechanisms and Functions. Trends Cell Biol. 2017;27:151–62. https://doi.org/10.1016/j.tcb.2016.08.011.
15. Caruso S, Poon IKH. Apoptotic Cell-Derived Extracellular Vesicles: More Than Just Debris. Front Immunol. 2018;9:1486. https://doi.org/10.3389/fimmu.2018.01486.
16. Lee Y, El Andaloussi S, Wood MJA. Exosomes and microvesicles: extracellular vesicles for genetic information transfer and gene therapy. Hum Mol Genet. 2012;21:R125–34. https://doi.org/10.1093/hmg/dds317.
17. Poon IKH, Lucas CD, Rossi AG, Ravichandran KS. Apoptotic cell clearance: basic biology and therapeutic potential. Nat Rev Immunol. 2014;14:166–80. https://doi.org/10.1038/nri3607.
18. Hsu C, Morohashi Y, Yoshimura S-I, Manrique-Hoyos N, Jung S, Lauterbach MA, et al. Regulation of exosome secretion by Rab35 and its GTPase-activating proteins TBC1D10A-C. J Cell Biol. 2010;189:223–32. https://doi.org/10.1083/jcb.200911018.
19. Laulagnier K, Grand D, Dujardin A, Hamdi S, Vincent-Schneider H, Lankar D, et al. PLD2 is enriched on exosomes and its activity is correlated to the release of exosomes. FEBS Lett. 2004;572:11–4. https://doi.org/10.1016/j.febslet.2004.06.082.

20. Kumar D, Gupta D, Shankar S, Srivastava RK. Biomolecular characterization of exosomes released from cancer stem cells: Possible implications for biomarker and treatment of cancer. Oncotarget. 2015;6:3280–91. https://doi.org/10.18632/oncotarget.2462.
21. Baixauli F, López-Otín C, Mittelbrunn M. Exosomes and autophagy: coordinated mechanisms for the maintenance of cellular fitness. Front Immunol. 2014;5:403. https://doi.org/10.3389/fimmu.2014.00403.
22. Valadi H, Ekström K, Bossios A, Sjöstrand M, Lee JJ, Lötvall JO. Exosome-mediated transfer of mRNAs and microRNAs is a novel mechanism of genetic exchange between cells. Nat Cell Biol. 2007;9:654–9. https://doi.org/10.1038/ncb1596.
23. Sohel MMH, Hoelker M, Noferesti SS, Salilew-Wondim D, Tholen E, Looft C, et al. Exosomal and Non-Exosomal Transport of Extra-Cellular microRNAs in Follicular Fluid: Implications for Bovine Oocyte Developmental Competence. PLoS ONE. 2013;8:e78505. https://doi.org/10.1371/journal.pone.0078505.
24. Villarroya-Beltri C, Baixauli F, Gutiérrez-Vázquez C, Sánchez-Madrid F, Mittelbrunn M. Sorting it out: regulation of exosome loading. Semin Cancer Biol. 2014;28:3–13. https://doi.org/10.1016/j.semcancer.2014.04.009.
25. Keller S, Ridinger J, Rupp A-K, Janssen JWG, Altevogt P. Body fluid derived exosomes as a novel template for clinical diagnostics. J Transl Med. 2011;9:86. https://doi.org/10.1186/1479-5876-9-86.
26. Alvarez-Erviti L, Seow Y, Yin H, Betts C, Lakhal S, Wood MJA. Delivery of siRNA to the mouse brain by systemic injection of targeted exosomes. Nat Biotechnol. 2011;29:341–5. https://doi.org/10.1038/nbt.1807.
27. Tang K, Zhang Y, Zhang H, Xu P, Liu J, Ma J, et al. Delivery of chemotherapeutic drugs in tumour cell-derived microparticles. Nat Commun. 2012;3:1282. https://doi.org/10.1038/ncomms2282.
28. Mulcahy LA, Pink RC, Carter DRF. Routes and mechanisms of extracellular vesicle uptake. J Extracell Vesicles. 2014. https://doi.org/10.3402/jev.v3.24641.
29. Gebremedhn S, Salilew-Wondim D, Ahmad I, Sahadevan S, Hossain MM, Hoelker M, et al. MicroRNA Expression Profile in Bovine Granulosa Cells of Preovulatory Dominant and Subordinate Follicles during the Late Follicular Phase of the Estrous Cycle. PLoS ONE. 2015;10:e0125912. https://doi.org/10.1371/journal.pone.0125912.
30. Gebremedhn S, Gad A, Ishak GM, Menjivar NG, Gastal MO, Feugang JM, et al. Dynamics of extracellular vesicle-coupled microRNAs in equine follicular fluid associated with follicle selection and ovulation. Mol Hum Reprod. 2023. https://doi.org/10.1093/molehr/gaad009.
31. Jacobs LA, Bewicke-Copley F, Poolman MG, Pink RC, Mulcahy LA, Baker I, et al. Meta-analysis using a novel database, miRStress, reveals miRNAs that are frequently associated with the radiation and hypoxia stress-responses. PLoS ONE. 2013;8:e80844. https://doi.org/10.1371/journal.pone.0080844.
32. Gebremedhn S, Gad A, Aglan HS, Laurincik J, Prochazka R, Salilew-Wondim D, et al. Extracellular vesicles shuttle protective messages against heat stress in bovine granulosa cells. Sci Rep. 2020;10:15824. https://doi.org/10.1038/s41598-020-72706-z.
33. Al-Mayah AHJ, Irons SL, Pink RC, Carter DRF, Kadhim MA. Possible role of exosomes containing RNA in mediating nontargeted effect of ionizing radiation. Radiat Res. 2012;177:539–45. https://doi.org/10.1667/rr2868.1.
34. Ogorevc E, Kralj-Iglic V, Veranic P. The role of extracellular vesicles in phenotypic cancer transformation. Radiol Oncol. 2013;47:197–205. https://doi.org/10.2478/raon-2013-0037.
35. Bewicke-Copley F, Mulcahy LA, Jacobs LA, Samuel P, Akbar N, Pink RC, Carter DRF. Extracellular vesicles released following heat stress induce bystander effect in unstressed populations. J Extracell Vesicles. 2017;6:1340746. https://doi.org/10.1080/20013078.2017.1340746.
36. Gebremedhn S, Ali A, Gad A, Prochazka R, Tesfaye D. Extracellular Vesicles as Mediators of Environmental and Metabolic Stress Coping Mechanisms During Mammalian Follicular Development. Front Vet Sci. 2020;7:602043. https://doi.org/10.3389/fvets.2020.602043.
37. Menjivar NG, Gad A, Gebremedhn S, Ghosh S, Tesfaye D. Granulosa cell-derived extracellular vesicles mitigate the detrimental impact of thermal stress on bovine oocytes and embryos. Front Cell Dev Biol. 2023;11:1142629. https://doi.org/10.3389/fcell.2023.1142629.
38. Gad A, Joyce K, Menjivar NG, Heredia D, Rojas CS, Tesfaye D, Gonella-Diaza A. Extracellular vesicle-microRNAs mediated response of bovine ovaries to seasonal environmental changes. J Ovarian Res. 2023;16:101. https://doi.org/10.1186/s13048-023-01181-7.
39. Menjivar NG, Gad A, Thompson RE, Meyers MA, Hollinshead FK, Tesfaye D. Bovine oviductal organoids: a multi-omics approach to capture the cellular and extracellular molecular response of the oviduct to heat stress. BMC Genomics. 2023;24:646. https://doi.org/10.1186/s12864-023-09746-y.
40. Feng D, Zhao W-L, Ye Y-Y, Bai X-C, Liu R-Q, Chang L-F, et al. Cellular internalization of exosomes occurs through phagocytosis. Traffic. 2010;11:675–87. https://doi.org/10.1111/j.1600-0854.2010.01041.x.
41. Temchura VV, Tenbusch M, Nchinda G, Nabi G, Tippler B, Zelenyuk M, et al. Enhancement of immunostimulatory properties of exosomal vaccines by incorporation of fusion-competent G protein of vesicular stomatitis virus. Vaccine. 2008;26:3662–72. https://doi.org/10.1016/j.vaccine.2008.04.069.
42. Lai CP, Tannous BA, Breakefield XO. Noninvasive in vivo monitoring of extracellular vesicles. Methods Mol Biol. 2014;1098:249–58. https://doi.org/10.1007/978-1-62703-718-1_19.
43. Horibe S, Tanahashi T, Kawauchi S, Murakami Y, Rikitake Y. Mechanism of recipient cell-dependent differences in exosome uptake. BMC Cancer. 2018;18:47. https://doi.org/10.1186/s12885-017-3958-1.
44. Morelli AE, Larregina AT, Shufesky WJ, Sullivan MLG, Stolz DB, Papworth GD, et al. Endocytosis, intracellular sorting, and processing of exosomes by dendritic cells. Blood. 2004;104:3257–66. https://doi.org/10.1182/blood-2004-03-0824.
45. Escrevente C, Keller S, Altevogt P, Costa J. Interaction and uptake of exosomes by ovarian cancer cells. BMC Cancer. 2011;11:108. https://doi.org/10.1186/1471-2407-11-108.
46. Lee RC, Feinbaum RL, Ambros V. The C. elegans heterochronic gene lin-4 encodes small RNAs with antisense complementarity to lin-14. Cell. 1993;75:843–54. https://doi.org/10.1016/0092-8674(93)90529-y.
47. Bushati N, Cohen SM. microRNA functions. Annu Rev Cell Dev Biol. 2007;23:175–205. https://doi.org/10.1146/annurev.cellbio.23.090506.123406.
48. Fabian MR, Sonenberg N, Filipowicz W. Regulation of mRNA translation and stability by microRNAs. Annu Rev Biochem. 2010;79:351–79. https://doi.org/10.1146/annurev-biochem-060308-103103.
49. Okada C, Yamashita E, Lee SJ, Shibata S, Katahira J, Nakagawa A, et al. A high-resolution structure of the pre-microRNA nuclear export machinery. Science. 2009;326:1275–9. https://doi.org/10.1126/science.1178705.
50. Cullen BR. Transcription and processing of human microRNA precursors. Mol Cell. 2004;16:861–5. https://doi.org/10.1016/j.molcel.2004.12.002.
51. Liu J, Carmell MA, Rivas FV, Marsden CG, Thomson JM, Song J-J, et al. Argonaute2 is the catalytic engine of mammalian RNAi. Science. 2004;305:1437–41. https://doi.org/10.1126/science.1102513.
52. Rivas FV, Tolia NH, Song J-J, Aragon JP, Liu J, Hannon GJ, Joshua-Tor L. Purified Argonaute2 and an siRNA form recombinant human RISC. Nat Struct Mol Biol. 2005;12:340–9. https://doi.org/10.1038/nsmb918.
53. Skog J, Würdinger T, van Rijn S, Meijer DH, Gainche L, Sena-Esteves M, et al. Glioblastoma microvesicles transport RNA and proteins that promote tumour growth and provide diagnostic biomarkers. Nat Cell Biol. 2008;10:1470–6. https://doi.org/10.1038/ncb1800.
54. Ekström K, Valadi H, Sjöstrand M, Malmhäll C, Bossios A, Eldh M, Lötvall J. Characterization of mRNA and microRNA in human mast cell-derived exosomes and their transfer to other mast cells and blood CD34 progenitor cells. J Extracell Vesicles. 2012. https://doi.org/10.3402/jev.v1i0.18389.
55. Friedman RC, Farh KK-H, Burge CB, Bartel DP. Most mammalian mRNAs are conserved targets of microRNAs. Genome Res. 2009;19:92–105. https://doi.org/10.1101/gr.082701.108.
56. Leung AKL, Sharp PA. MicroRNA functions in stress responses. Mol Cell. 2010;40:205–15. https://doi.org/10.1016/j.molcel.2010.09.027.
57. Dellar ER, Hill C, Melling GE, Carter DR, Baena-Lopez LA. Unpacking extracellular vesicles: RNA cargo loading and function. Journal of Extracellular Biology. 2022;1:e40. https://doi.org/10.1002/jex2.40.
58. Turchinovich A, Weiz L, Langheinz A, Burwinkel B. Characterization of extracellular circulating microRNA. Nucleic Acids Res. 2011;39:7223–33. https://doi.org/10.1093/nar/gkr254.
59. Garcia-Martin R, Wang G, Brandão BB, Zanotto TM, Shah S, Kumar Patel S, et al. MicroRNA sequence codes for small extracellular vesicle release and cellular retention. Nature. 2022;601:446–51. https://doi.org/10.1038/s41586-021-04234-3.

60. Janas T, Janas MM, Sapoń K, Janas T. Mechanisms of RNA loading into exosomes. FEBS Lett. 2015;589:1391–8. https://doi.org/10.1016/j.febslet.2015.04.036.
61. Villarroya-Beltri C, Gutiérrez-Vázquez C, Sánchez-Cabo F, Pérez-Hernández D, Vázquez J, Martin-Cofreces N, et al. Sumoylated hnRNPA2B1 controls the sorting of miRNAs into exosomes through binding to specific motifs. Nat Commun. 2013;4:2980. https://doi.org/10.1038/ncomms3980.
62. McKenzie AJ, Hoshino D, Hong NH, Cha DJ, Franklin JL, Coffey RJ, et al. KRAS-MEK Signaling Controls Ago2 Sorting into Exosomes. Cell Rep. 2016;15:978–87. https://doi.org/10.1016/j.celrep.2016.03.085.
63. Shurtleff MJ, Temoche-Diaz MM, Karfilis KV, Ri S, Schekman R. Y-box protein 1 is required to sort microRNAs into exosomes in cells and in a cell-free reaction. Elife. 2016. https://doi.org/10.7554/eLife.19276.
64. Tosar JP, Gámbaro F, Sanguinetti J, Bonilla B, Witwer KW, Cayota A. Assessment of small RNA sorting into different extracellular fractions revealed by high-throughput sequencing of breast cell lines. Nucleic Acids Res. 2015;43:5601–16. https://doi.org/10.1093/nar/gkv432.
65. Gámbaro F, Li Calzi M, Fagúndez P, Costa B, Greif G, Mallick E, et al. Stable tRNA halves can be sorted into extracellular vesicles and delivered to recipient cells in a concentration-dependent manner. RNA Biol. 2020;17:1168–82. https://doi.org/10.1080/15476286.2019.1708548.
66. Santangelo L, Giurato G, Cicchini C, Montaldo C, Mancone C, Tarallo R, et al. The RNA-Binding Protein SYNCRIP Is a Component of the Hepatocyte Exosomal Machinery Controlling MicroRNA Sorting. Cell Rep. 2016;17:799–808. https://doi.org/10.1016/j.celrep.2016.09.031.
67. Temoche-Diaz MM, Shurtleff MJ, Nottingham RM, Yao J, Fadadu RP, Lambowitz AM, Schekman R. Distinct mechanisms of microRNA sorting into cancer cell-derived extracellular vesicle subtypes. Elife. 2019. https://doi.org/10.7554/eLife.47544.
68. Liu X, Zheng Q, Vrettos N, Maragkakis M, Alexiou P, Gregory BD, Mourelatos Z. A MicroRNA precursor surveillance system in quality control of MicroRNA synthesis. Mol Cell. 2014;55:868–79. https://doi.org/10.1016/j.molcel.2014.07.017.
69. Reshke R, Taylor JA, Savard A, Guo H, Rhym LH, Kowalski PS, et al. Reduction of the therapeutic dose of silencing RNA by packaging it in extracellular vesicles via a pre-microRNA backbone. Nat Biomed Eng. 2020;4:52–68. https://doi.org/10.1038/s41551-019-0502-4.
70. Witwer KW, Wolfram J. Extracellular vesicles versus synthetic nanoparticles for drug delivery. Nat Rev Mater. 2021;6:103–6. https://doi.org/10.1038/s41578-020-00277-6.
71. Cataldi M, Vigliotti C, Mosca T, Cammarota M, Capone D. Emerging Role of the Spleen in the Pharmacokinetics of Monoclonal Antibodies, Nanoparticles and Exosomes. Int J Mol Sci. 2017. https://doi.org/10.3390/ijms18061249.
72. Kanada M, Bachmann MH, Hardy JW, Frimannson DO, Bronsart L, Wang A, et al. Differential fates of biomolecules delivered to target cells via extracellular vesicles. Proc Natl Acad Sci U S A. 2015;112:E1433–42. https://doi.org/10.1073/pnas.1418401112.
73. Familtseva A, Jeremic N, Tyagi SC. Exosomes: cell-created drug delivery systems. Mol Cell Biochem. 2019;459:1–6. https://doi.org/10.1007/s11010-019-03545-4.
74. Camussi G, Deregibus MC, Bruno S, Cantaluppi V, Biancone L. Exosomes/microvesicles as a mechanism of cell-to-cell communication. Kidney Int. 2010;78:838–48. https://doi.org/10.1038/ki.2010.278.
75. Wu Q, Sun S, Li Z, Yang Q, Li B, Zhu S, et al. Breast cancer-released exosomes trigger cancer-associated cachexia to promote tumor progression. Adipocyte. 2019;8:31–45. https://doi.org/10.1080/21623945.2018.1551688.
76. McCann J, Sosa-Miranda CD, Guo H, Reshke R, Savard A, Zardini Buzatto A, et al. Contaminating transfection complexes can masquerade as small extracellular vesicles and impair their delivery of RNA. J Extracell Vesicles. 2022;11:e12220. https://doi.org/10.1002/jev2.12220.
77. McConnell RE, Youniss M, Gnanasambandam B, Shah P, Zhang W, Finn JD. Transfection reagent artefact likely accounts for some reports of extracellular vesicle function. J Extracell Vesicles. 2022;11:e12253. https://doi.org/10.1002/jev2.12253.
78. Nordin JZ. Transfection reagents affect Extracellular Vesicle cargo transfer to recipient cells: The importance of appropriate controls in EV research. J Extracell Vesicles. 2022;11:e12227. https://doi.org/10.1002/jev2.12227.
79. Hagiwara K, Katsuda T, Gailhouste L, Kosaka N, Ochiya T. Commitment of Annexin A2 in recruitment of microRNAs into extracellular vesicles. FEBS Lett. 2015;589:4071–8. https://doi.org/10.1016/j.febslet.2015.11.036.
80. Huang L, Gu N, Zhang X-E, Wang D-B. Light-Inducible Exosome-Based Vehicle for Endogenous RNA Loading and Delivery to Leukemia Cells. Adv Funct Mater. 2019;29:1807189. https://doi.org/10.1002/adfm.201807189.
81. Kojima R, Bojar D, Rizzi G, Hamri GC-E, El-Baba MD, Saxena P, et al. Designer exosomes produced by implanted cells intracerebrally deliver therapeutic cargo for Parkinson's disease treatment. Nat Commun. 2018;9:1305. https://doi.org/10.1038/s41467-018-03733-8.
82. Hung ME, Leonard JN. A platform for actively loading cargo RNA to elucidate limiting steps in EV-mediated delivery. J Extracell Vesicles. 2016;5:31027. https://doi.org/10.3402/jev.v5.31027.
83. Monfared H, Jahangard Y, Nikkhah M, Mirnajafi-Zadeh J, Mowla SJ. Potential Therapeutic Effects of Exosomes Packed With a miR-21-Sponge Construct in a Rat Model of Glioblastoma. Front Oncol. 2019;9:782. https://doi.org/10.3389/fonc.2019.00782.
84. Shi J, Ma Y, Zhu J, Chen Y, Sun Y, Yao Y, et al. A Review on Electroporation-Based Intracellular Delivery. Molecules. 2018. https://doi.org/10.3390/molecules23113044.
85. Kostyushev D, Kostyusheva A, Brezgin S, Smirnov V, Volchkova E, Lukashev A, Chulanov V. Gene Editing by Extracellular Vesicles. Int J Mol Sci. 2020. https://doi.org/10.3390/ijms21197362.
86. Yan B, Liang Y. New Therapeutics for Extracellular Vesicles: Delivering CRISPR for Cancer Treatment. Int J Mol Sci. 2022. https://doi.org/10.3390/ijms232415758.
87. Fu S, Wang Y, Xia X, Zheng JC. Exosome engineering: Current progress in cargo loading and targeted delivery. NanoImpact. 2020;20:100261. https://doi.org/10.1016/j.impact.2020.100261.
88. Kimiz-Gebologlu I, Oncel SS. Exosomes: Large-scale production, isolation, drug loading efficiency, and biodistribution and uptake. J Control Release. 2022;347:533–43. https://doi.org/10.1016/j.jconrel.2022.05.027.
89. Fuhrmann G, Serio A, Mazo M, Nair R, Stevens MM. Active loading into extracellular vesicles significantly improves the cellular uptake and photodynamic effect of porphyrins. J Control Release. 2015;205:35–44. https://doi.org/10.1016/j.jconrel.2014.11.029.
90. de Jong OG, Kooijmans SAA, Murphy DE, Jiang L, Evers MJW, Sluijter JPG, et al. Drug Delivery with Extracellular Vesicles: From Imagination to Innovation. Acc Chem Res. 2019;52:1761–70. https://doi.org/10.1021/acs.accounts.9b00109.
91. Herrmann IK, Wood MJA, Fuhrmann G. Extracellular vesicles as a next-generation drug delivery platform. Nat Nanotechnol. 2021;16:748–59. https://doi.org/10.1038/s41565-021-00931-2.
92. Sutaria DS, Jiang J, Elgamal OA, Pomeroy SM, Badawi M, Zhu X, et al. Low active loading of cargo into engineered extracellular vesicles results in inefficient miRNA mimic delivery. J Extracell Vesicles. 2017;6:1333882. https://doi.org/10.1080/20013078.2017.1333882.
93. de Abreu RC, Ramos CV, Becher C, Lino M, Jesus C, da Costa M, Paula A, et al. Exogenous loading of miRNAs into small extracellular vesicles. J Extracell Vesicles. 2021;10:e12111. https://doi.org/10.1002/jev2.12111.
94. Dreyer F, Baur A. Biogenesis and Functions of Exosomes and Extracellular Vesicles. Methods Mol Biol. 2016;1448:201–16. https://doi.org/10.1007/978-1-4939-3753-0_15.
95. Wang F, Li L, Piontek K, Sakaguchi M, Selaru FM. Exosome miR-335 as a novel therapeutic strategy in hepatocellular carcinoma. Hepatology. 2018;67:940–54. https://doi.org/10.1002/hep.29586.
96. Pottash AE, Levy D, Jeyaram A, Kuo L, Kronstadt SM, Chao W, Jay SM. Combinatorial microRNA Loading into Extracellular Vesicles for Increased Anti-Inflammatory Efficacy. Noncoding RNA. 2022. https://doi.org/10.3390/ncrna8050071.
97. Haney MJ, Klyachko NL, Zhao Y, Gupta R, Plotnikova EG, He Z, et al. Exosomes as drug delivery vehicles for Parkinson's disease therapy. J Control Release. 2015;207:18–30. https://doi.org/10.1016/j.jconrel.2015.03.033.
98. Kooijmans SAA, Stremersch S, Braeckmans K, de Smedt SC, An H, Wood MJA, et al. Electroporation-induced siRNA precipitation obscures the efficiency of siRNA loading into extracellular vesicles. J Control Release. 2013;172:229–38. https://doi.org/10.1016/j.jconrel.2013.08.014.
99. Kim MS, Haney MJ, Zhao Y, Mahajan V, Deygen I, Klyachko NL, et al. Development of exosome-encapsulated paclitaxel to overcome MDR

in cancer cells. Nanomedicine. 2016;12:655–64. https://doi.org/10.1016/j.nano.2015.10.012.
100. Zhang D, Lee H, Zhu Z, Minhas JK, Jin Y. Enrichment of selective miRNAs in exosomes and delivery of exosomal miRNAs in vitro and in vivo. Am J Physiol Lung Cell Mol Physiol. 2017;312:L110–21. https://doi.org/10.1152/ajplung.00423.2016.
101. Won Lee G, Thangavelu M, Joung Choi M, Yeong Shin E, Sol Kim H, Seon Baek J, et al. Exosome mediated transfer of miRNA-140 promotes enhanced chondrogenic differentiation of bone marrow stem cells for enhanced cartilage repair and regeneration. J Cell Biochem. 2020;121:3642–52. https://doi.org/10.1002/jcb.29657.
102. Gelibter S, Marostica G, Mandelli A, Siciliani S, Podini P, Finardi A, Furlan R. The impact of storage on extracellular vesicles: A systematic study. J Extracell Vesicles. 2022;11:e12162. https://doi.org/10.1002/jev2.12162.
103. Jeyaram A, Lamichhane TN, Wang S, Zou L, Dahal E, Kronstadt SM, et al. Enhanced Loading of Functional miRNA Cargo via pH Gradient Modification of Extracellular Vesicles. Mol Ther. 2020;28:975–85. https://doi.org/10.1016/j.ymthe.2019.12.007.
104. Chen K-H, Chen C-H, Wallace CG, Yuen C-M, Kao G-S, Chen Y-L, et al. Intravenous administration of xenogenic adipose-derived mesenchymal stem cells (ADMSC) and ADMSC-derived exosomes markedly reduced brain infarct volume and preserved neurological function in rat after acute ischemic stroke. Oncotarget. 2016;7:74537–56. https://doi.org/10.18632/oncotarget.12902.
105. Chang C-L, Sung P-H, Chen K-H, Shao P-L, Yang C-C, Cheng B-C, et al. Adipose-derived mesenchymal stem cell-derived exosomes alleviate overwhelming systemic inflammatory reaction and organ damage and improve outcome in rat sepsis syndrome. Am J Transl Res. 2018;10:1053–70.
106. Banfai K, Garai K, Ernszt D, Pongracz JE, Kvell K. Transgenic Exosomes for Thymus Regeneration. Front Immunol. 2019;10:862. https://doi.org/10.3389/fimmu.2019.00862.
107. Cai Y, Yu X, Hu S, Yu J. A brief review on the mechanisms of miRNA regulation. Genomics Proteomics Bioinformatics. 2009;7:147–54. https://doi.org/10.1016/S1672-0229(08)60044-3.
108. Katakowski M, Buller B, Zheng X, Lu Y, Rogers T, Osobamiro O, et al. Exosomes from marrow stromal cells expressing miR-146b inhibit glioma growth. Cancer Lett. 2013;335:201–4. https://doi.org/10.1016/j.canlet.2013.02.019.
109. Ohno S, Takanashi M, Sudo K, Ueda S, Ishikawa A, Matsuyama N, et al. Systemically injected exosomes targeted to EGFR deliver antitumor microRNA to breast cancer cells. Mol Ther. 2013;21:185–91. https://doi.org/10.1038/mt.2012.180.
110. Bryniarski K, Ptak W, Jayakumar A, Püllmann K, Caplan MJ, Chairoungdua A, et al. Antigen-specific, antibody-coated, exosome-like nanovesicles deliver suppressor T-cell microRNA-150 to effector T cells to inhibit contact sensitivity. J Allergy Clin Immunol. 2013;132:170–81. https://doi.org/10.1016/j.jaci.2013.04.048.
111. Otmani K, Lewalle P. Tumor Suppressor miRNA in Cancer Cells and the Tumor Microenvironment: Mechanism of Deregulation and Clinical Implications. Front Oncol. 2021;11:708765. https://doi.org/10.3389/fonc.2021.708765.
112. Lv Q, Deng J, Chen Y, Wang Y, Liu Bo, Liu J. Engineered Human Adipose Stem-Cell-Derived Exosomes Loaded with miR-21-5p to Promote Diabetic Cutaneous Wound Healing. Mol Pharm. 2020;17(5):1723–33. https://doi.org/10.1021/acs.molpharmaceut.0c00177.
113. Yan C, Chen J, Wang C, Yuan M, Kang Yu, Wu Z, et al. Milk exosomes-mediated miR-31-5p delivery accelerates diabetic wound healing through promoting angiogenesis. Drug Delivery. 2022;29(1):214–28. https://doi.org/10.1080/10717544.2021.2023699.
114. Zhang M, Wang Xi, Xia X, Fang X, Zhang T, Huang F. Endometrial epithelial cells-derived exosomes deliver microRNA-30c to block the BCL9/Wnt/CD44 signaling and inhibit cell invasion and migration in ovarian endometriosis. Cell Death Discovery. 2022;8(1):151. https://doi.org/10.1038/s41420-022-00941-6.
115. Huang J, Yu M, Yin W, Liang Bo, Li A, Li J, et al. Development of a novel RNAi therapy: Engineered miR-31 exosomes promoted the healing of diabetic wounds. In Bioactive materials. 2021;6(9):2841–53. https://doi.org/10.1016/j.bioactmat.2021.02.007.
116. Sung H, Ferlay J, Siegel RL, Laversanne M, Soerjomataram I, Jemal A, Bray F. Global Cancer Statistics 2020: GLOBOCAN Estimates of Incidence and Mortality Worldwide for 36 Cancers in 185 Countries. CA Cancer J Clin. 2021;71:209–49. https://doi.org/10.3322/caac.21660.
117. Torre LA, Trabert B, DeSantis CE, Miller KD, Samimi G, Runowicz CD, et al. Ovarian cancer statistics, 2018. CA Cancer J Clin. 2018;68:284–96. https://doi.org/10.3322/caac.21456.
118. Gunassekaran GR, Poongkavithai Vadevoo SM, Baek M-C, Lee B. M1 macrophage exosomes engineered to foster M1 polarization and target the IL-4 receptor inhibit tumor growth by reprogramming tumor-associated macrophages into M1-like macrophages. Biomaterials. 2021;278:121137. https://doi.org/10.1016/j.biomaterials.2021.121137.
119. Vakhshiteh F, Rahmani S, Ostad SN, Madjd Z, Dinarvand R, Atyabi F. Exosomes derived from miR-34a-overexpressing mesenchymal stem cells inhibit in vitro tumor growth: A new approach for drug delivery. Life Sci. 2021;266:118871. https://doi.org/10.1016/j.lfs.2020.118871.
120. Zhou W, Xu M, Wang Z, Yang M. Engineered exosomes loaded with miR-449a selectively inhibit the growth of homologous non-small cell lung cancer. Cancer Cell Int. 2021;21:485. https://doi.org/10.1186/s12935-021-02157-7.
121. Yu Z, Liu J, Fan Q, Yu J, Ren X, Wang X. Extracellular Vesicle-Encapsulated MicroRNA-375 from Bone Marrow-Derived Mesenchymal Stem Cells Inhibits Hepatocellular Carcinoma Progression through Regulating HOXB3-Mediated Wnt/β-Catenin Pathway. Anal Cell Pathol (Amst). 2022;2022:9302496. https://doi.org/10.1155/2022/9302496.
122. Hosseini M, Baghaei K, Hajivalili M, Zali MR, Ebtekar M, Amani D. The anti-tumor effects of CT-26 derived exosomes enriched by MicroRNA-34a on murine model of colorectal cancer. Life Sci. 2022;290:120234. https://doi.org/10.1016/j.lfs.2021.120234.
123. Zhao Z, Shuang T, Gao Y, Lu F, Zhang J, He W, et al. Targeted delivery of exosomal miR-484 reprograms tumor vasculature for chemotherapy sensitization. Cancer Lett. 2022;530:45–58. https://doi.org/10.1016/j.canlet.2022.01.011.
124. Lang FM, Hossain A, Gumin J, Momin EN, Shimizu Y, Ledbetter D, et al. Mesenchymal stem cells as natural biofactories for exosomes carrying miR-124a in the treatment of gliomas. Neuro Oncol. 2018;20:380–90. https://doi.org/10.1093/neuonc/nox152.
125. Moradi-Chaleshtori M, Shojaei S, Mohammadi-Yeganeh S, Hashemi SM. Transfer of miRNA in tumor-derived exosomes suppresses breast tumor cell invasion and migration by inducing M1 polarization in macrophages. In Life sciences. 2021;282:119800. https://doi.org/10.1016/j.lfs.2021.119800.
126. Moradi-Chaleshtori M, Bandehpour M, Heidari N, Mohammadi-Yeganeh S, MahmoudHashemi S. Exosome-mediated miR-33 transfer induces M1 polarization in mouse macrophages and exerts antitumor effect in 4T1 breast cancer cell line. Int Immunopharmacol. 2021;90:107198. https://doi.org/10.1016/j.intimp.2020.107198.
127. Gunassekaran GR, Poongkavithai Vadevoo SM, Baek M-C, Lee B. M1 macrophage exosomes engineered to foster M1 polarization and target the IL-4 receptor inhibit tumor growth by reprogramming tumor-associated macrophages into M1-like macrophages. In Biomaterials. 2021;278:121137. https://doi.org/10.1016/j.biomaterials.2021.121137.
128. Khani A, Sharifzad F, Mardpour S, Hassan ZM, Ebrahimi M. Tumor extracellular vesicles loaded with exogenous Let-7i and miR-142 can modulate both immune response and tumor microenvironment to initiate a powerful anti-tumor response. In Cancer letters. 2021;501:200–9. https://doi.org/10.1016/j.canlet.2020.11.014.
129. Kim H, Rhee WJ. Exosome-mediated Let7c-5p Delivery for Breast Cancer Therapeutic Development. In Biotechnol Bioproc E. 2020;25(4):513–20. https://doi.org/10.1007/s12257-020-0002-0.
130. Albakr L, Alqahtani FY, Aleanizy FS, Alomrani A, Badran M, Alhindas H, Al-Mohanna F. Improved delivery of miR-1296 loaded cationic nanoliposomes for effective suppression of triple negative breast cancer. In Saudi pharmaceutical journal : SPJ : the official publication of the Saudi Pharmaceutical Society. 2021;29(5):446–55. https://doi.org/10.1016/j.jsps.2021.04.007.
131. Khazaei-Poul Y, Shojaei S, Koochaki A, Ghanbarian H, Mohammadi-Yeganeh S. Evaluating the influence of Human Umbilical Cord Mesenchymal Stem Cells-derived exosomes loaded with miR-3182 on metastatic performance of Triple Negative Breast Cancer cells. In Life sciences. 2021;286:120015. https://doi.org/10.1016/j.lfs.2021.120015.

132. Shojaei S, HashemiMahmoudGhanbarianSharifiSalehiMohammadi-Yeganeh SHKMS. Delivery of miR-381-3p Mimic by Mesenchymal Stem Cell-Derived Exosomes Inhibits Triple Negative Breast Cancer Aggressiveness; an In Vitro Study. Stem Cell Rev Rep. 2021;17(3):1027–38. https://doi.org/10.1007/s12015-020-10089-4.
133. Nie H, Xie X, Zhang D, Zhou Yu, Li B, Li F, et al. Use of lung-specific exosomes for miRNA-126 delivery in non-small cell lung cancer. In Nanoscale. 2020;12(2):877–87. https://doi.org/10.1039/c9nr09011h.
134. Jeong K, Yu YJ, You JY, Rhee WJ, Kim JA. Exosome-mediated microRNA-497 delivery for anti-cancer therapy in a microfluidic 3D lung cancer model. In Lab on a chip. 2020;20(3):548–57. https://doi.org/10.1039/c9lc00958b.
135. Yu Z, Liu Ju, Fan Q, Yu J, Ren X, Wang X. Extracellular Vesicle-Encapsulated MicroRNA-375 from Bone Marrow-Derived Mesenchymal Stem Cells Inhibits Hepatocellular Carcinoma Progression through Regulating HOXB3-Mediated Wnt/β-Catenin Pathway. Anal Cellular Pathology (Amsterdam). 2022;2022:9302496. https://doi.org/10.1155/2022/9302496.
136. Kim HS, Kim JS, Park NR, Nam H, Sung PS, Bae SH, et al. Exosomal miR-125b Exerts Anti-Metastatic Properties and Predicts Early Metastasis of Hepatocellular Carcinoma. In Frontiers in oncology. 2021;11:637247. https://doi.org/10.3389/fonc.2021.637247.
137. Xu Y, Lai Yu, Cao L, Li Y, Chen G, Chen L, et al. Human umbilical cord mesenchymal stem cells-derived exosomal microRNA-451a represses epithelial-mesenchymal transition of hepatocellular carcinoma cells by inhibiting ADAM10. In RNA biology. 2021;18(10):1408–23. https://doi.org/10.1080/15476286.2020.1851540.
138. Liu C, Zhou X, Long Q, Zeng H, Sun Q, Chen Y, et al. Small extracellular vesicles containing miR-30a-3p attenuate the migration and invasion of hepatocellular carcinoma by targeting SNAP23 gene. In Oncogene. 2021;40(2):233–45. https://doi.org/10.1038/s41388-020-01521-7.
139. Lou G, Chen L, Xia C, Wang W, Qi J, Li A, et al. MiR-199a-modified exosomes from adipose tissue-derived mesenchymal stem cells improve hepatocellular carcinoma chemosensitivity through mTOR pathway. J Exp Clin Cancer Res. 2020;39(1):4. https://doi.org/10.1186/s13046-019-1512-5.
140. Hosseini M, Baghaei K, Hajivalili M, Zali MR, Ebtekar M, Amani D. The anti-tumor effects of CT-26 derived exosomes enriched by MicroRNA-34a on murine model of colorectal cancer. In Life sciences. 2022;290:120234. https://doi.org/10.1016/j.lfs.2021.120234.
141. Rezaei R, Baghaei K, Amani D, Piccin A, Hashemi SM, Asadzadeh Aghdaei H, Zali MR. Exosome-mediated delivery of functionally active miRNA-375-3p mimic regulate epithelial mesenchymal transition (EMT) of colon cancer cells. Life Sci. 2021;269:119035. https://doi.org/10.1016/j.lfs.2021.119035.
142. Rezaei R, Baghaei K, Hashemi SM, Zali MR, Ghanbarian H, Amani D. Tumor-Derived Exosomes Enriched by miRNA-124 Promote Anti-tumor Immune Response in CT-26 Tumor-Bearing Mice. Frontiers Med. 2021;8:619939. https://doi.org/10.3389/fmed.2021.619939.
143. Ruan Z, Lu L, Zhang Li, Dong M. Bone marrow stromal cells-derived microRNA-181-containing extracellular vesicles inhibit ovarian cancer cell chemoresistance by downregulating MEST via the Wnt/β-catenin signaling pathway. In Cancer gene therapy. 2021;28(7–8):785–98. https://doi.org/10.1038/s41417-020-0195-6.
144. Li P, Xin H, Lu L. Extracellular vesicle-encapsulated microRNA-424 exerts inhibitory function in ovarian cancer by targeting MYB. In Journal of translational medicine. 2021;19(1):4. https://doi.org/10.1186/s12967-020-02652-x.
145. Wang S, Li K. Engineered exosomes loaded with miR-494–3p suppress homologous ovarian cancer. 2022.
146. Kobayashi M, Sawada K, Miyamoto M, Shimizu A, Yamamoto M, Kinose Y, et al. Exploring the potential of engineered exosomes as delivery systems for tumor-suppressor microRNA replacement therapy in ovarian cancer. In Biochemical and biophysical research communications. 2020;527(1):153–61. https://doi.org/10.1016/j.bbrc.2020.04.076.
147. Hong S, You JY, Paek K, Park J, Kang SJ, Han EH, et al. Inhibition of tumor progression and M2 microglial polarization by extracellular vesicle-mediated microRNA-124 in a 3D microfluidic glioblastoma microenvironment. Theranostics. 2021;11:9687–704. https://doi.org/10.7150/thno.60851.
148. Wang K, Kumar US, Sadeghipour N, Massoud TF, Paulmurugan R. A Microfluidics-Based Scalable Approach to Generate Extracellular Vesicles with Enhanced Therapeutic MicroRNA Loading for Intranasal Delivery to Mouse Glioblastomas. ACS Nano. 2021. https://doi.org/10.1021/acsnano.1c07587.
149. Liu L, Cheng M, Zhang T, Chen Y, Wu Y, Wang Qi. Mesenchymal stem cell-derived extracellular vesicles prevent glioma by blocking M2 polarization of macrophages through a miR-744-5p/TGFB1-dependent mechanism. In Cell biology and toxicology. 2022;38(4):649–65. https://doi.org/10.1007/s10565-021-09652-7.
150. Rodrigues-Junior DM, de PelarinAndrade MF, Nader HB, Vettore AL, Pinhal MAS. MicroRNA-1252-5p Associated with Extracellular Vesicles Enhances Bortezomib Sensitivity in Multiple Myeloma Cells by Targeting Heparanase. In OncoTargets and therapy. 2021;14:455–67. https://doi.org/10.2147/OTT.S286751.
151. Xie X, Ji J, Chen X, Xu W, Chen H, Zhu S, et al. Human umbilical cord mesenchymal stem cell-derived exosomes carrying hsa-miRNA-128-3p suppress pancreatic ductal cell carcinoma by inhibiting Galectin-3. Clinical & translational oncology : official publication of the Federation of Spanish Oncology Societies and of the National Cancer Institute of Mexico. 2022;24(3):517–31. https://doi.org/10.1007/s12094-021-02705-7.
152. Zhu C, Jiang X, Xiao H, Guan J. Tumor-derived extracellular vesicles inhibit HGF/c-Met and EGF/EGFR pathways to accelerate the radiosensitivity of nasopharyngeal carcinoma cells via microRNA-142-5p delivery. Cell Death Discovery. 2022;8(1):17. https://doi.org/10.1038/s41420-021-00794-5.
153. Meng Q, Zhang B, Zhang Y, Wang S, Zhu X. Human bone marrow mesenchymal stem cell-derived extracellular vesicles impede the progression of cervical cancer via the miR-144-3p/CEP55 pathway. J Cellular Mol Med. 2021;25(4):1867–83. https://doi.org/10.1111/jcmm.15573.
154. Xue Q, Yang Y, Yang L, Yan X, Shen Z, Liu J, et al. miR-371b-5p-Engineered Exosomes Enhances Tumor Inhibitory Effect. Frontiers Cell Develop Biology. 2021;9:750171. https://doi.org/10.3389/fcell.2021.750171.
155. Jiang D, Wu X, Sun X, Tan W, Dai X, Xie Y, et al. Bone mesenchymal stem cell-derived exosomal microRNA-7-5p inhibits progression of acute myeloid leukemia by targeting OSBPL11. J Nanobiotechnol. 2022;20(1):29. https://doi.org/10.1186/s12951-021-01206-7.
156. Sun W, Zhao P, Zhou Y, Xing C, Zhao L, Li Z, Yuan L. Ultrasound targeted microbubble destruction assisted exosomal delivery of miR-21 protects the heart from chemotherapy associated cardiotoxicity. Biochem Biophys Res Commun. 2020;532(1):60–7. https://doi.org/10.1016/j.bbrc.2020.05.044.
157. Gómez-Galán M, Pérez-Alonso J, Callejón-Ferre Á-J, López-Martínez J. Musculoskeletal disorders: OWAS review. Ind Health. 2017;55:314–37. https://doi.org/10.2486/indhealth.2016-0191.
158. Wang C, Zhang Y, Zhang G, Yu W, He Y. Adipose Stem Cell-Derived Exosomes Ameliorate Chronic Rotator Cuff Tendinopathy by Regulating Macrophage Polarization: From a Mouse Model to a Study in Human Tissue. Am J Sports Med. 2021;49:2321–31. https://doi.org/10.1177/03635465211020010.
159. Huber J, Griffin MF, Longaker MT, Quarto N. Exosomes: A Tool for Bone Tissue Engineering. Tissue Eng Part B Rev. 2022;28:101–13. https://doi.org/10.1089/ten.TEB.2020.0246.
160. Aktas E, Chamberlain CS, Saether EE, Duenwald-Kuehl SE, Kondratko-Mittnacht J, Stitgen M, et al. Immune modulation with primed mesenchymal stem cells delivered via biodegradable scaffold to repair an Achilles tendon segmental defect. J Orthop Res. 2017;35:269–80. https://doi.org/10.1002/jor.23258.
161. Chamberlain CS, Saether EE, Aktas E, Vanderby R. Mesenchymal Stem Cell Therapy on Tendon/Ligament Healing. J Cytokine Biol. 2017;2(1):112.
162. Saether EE, Chamberlain CS, Aktas E, Leiferman EM, Brickson SL, Vanderby R. Primed Mesenchymal Stem Cells Alter and Improve Rat Medial Collateral Ligament Healing. Stem Cell Rev Rep. 2016;12:42–53. https://doi.org/10.1007/s12015-015-9633-5.
163. Xun J, Li C, Liu M, Mei Y, Zhou Q, Wu B, et al. Serum exosomes from young rats improve the reduced osteogenic differentiation of BMSCs in aged rats with osteoporosis after fatigue loading in vivo. Stem Cell Res Ther. 2021;12:424. https://doi.org/10.1186/s13287-021-02449-9.
164. Zhang Q-C, Hu S-Q, Hu A-N, Zhang T-W, Jiang L-B, Li X-L. Autophagy-activated nucleus pulposus cells deliver exosomal miR-27a to prevent extracellular matrix degradation by targeting MMP-13. J Orthop Res. 2021;39:1921–32. https://doi.org/10.1002/jor.24880.

165. Zhou Y, Ming J, Li Y, Li B, Deng M, Ma Y, et al. Exosomes derived from miR-126-3p-overexpressing synovial fibroblasts suppress chondrocyte inflammation and cartilage degradation in a rat model of osteoarthritis. Cell Death Discov. 2021;7:37. https://doi.org/10.1038/s41420-021-00418-y.
166. Xun J, Li C, Liu M, Mei Y, Zhou Q, Wu Bo, et al. Serum exosomes from young rats improve the reduced osteogenic differentiation of BMSCs in aged rats with osteoporosis after fatigue loading in vivo. Stem Cell Res Therapy. 2021;12(1):424. https://doi.org/10.1186/s13287-021-02449-9.
167. Li Y, Wang J, Ma Y, Du W, Feng K, Wang S. miR-101-loaded exosomes secreted by bone marrow mesenchymal stem cells requires the FBXW7/HIF1α/FOXP3 axis, facilitating osteogenic differentiation. In Journal of cellular physiology. 2021;236(6):4258–72. https://doi.org/10.1002/jcp.30027.
168. Zhang Y, Cao X, Li P, Fan Y, Zhang L, Ma X, et al. microRNA-935-modified bone marrow mesenchymal stem cells-derived exosomes enhance osteoblast proliferation and differentiation in osteoporotic rats. Life Sci. 2021;272:119204. https://doi.org/10.1016/j.lfs.2021.119204.
169. Liu W, Huang J, Chen F, Xie D, Wang L, Ye C, et al. MSC-derived small extracellular vesicles overexpressing miR-20a promoted the osteointegration of porous titanium alloy by enhancing osteogenesis via targeting BAMBI. Stem Cell Res Therapy. 2021;12(1):348. https://doi.org/10.1186/s13287-021-02303-y.
170. Cui S, Zhang L. microRNA-129-5p shuttled by mesenchymal stem cell-derived extracellular vesicles alleviates intervertebral disc degeneration via blockade of LRG1-mediated p38 MAPK activation. In Journal of tissue engineering. 2021;12:20417314211021680. https://doi.org/10.1177/20417314211021679.
171. Zhang Q, Shen Y, Zhao S, Jiang Y, Zhou D, Zhang Y. Exosomes miR-15a promotes nucleus pulposus-mesenchymal stem cells chondrogenic differentiation by targeting MMP-3. Cellular Signalling. 2021;86:110083. https://doi.org/10.1016/j.cellsig.2021.110083.
172. Zhou Z-M, Bao J-P, Peng X, Gao J-W, Vlf C, Zhang C, et al. Small extracellular vesicles from hypoxic mesenchymal stem cells alleviate intervertebral disc degeneration by delivering miR-17-5p. Acta Biomaterialia. 2022;140:641–58. https://doi.org/10.1016/j.actbio.2021.11.044.
173. Chen D, Jiang X. Exosomes-derived miR-125-5p from cartilage endplate stem cells regulates autophagy and ECM metabolism in nucleus pulposus by targeting SUV38H1. In Experimental cell research. 2022;414(1):113066. https://doi.org/10.1016/j.yexcr.2022.113066.
174. Zhou Y, Ming J, Li Y, Li B, Deng M, Ma Y, et al. Exosomes derived from miR-126-3p-overexpressing synovial fibroblasts suppress chondrocyte inflammation and cartilage degradation in a rat model of osteoarthritis. Cell Death Discovery. 2021;7(1):37. https://doi.org/10.1038/s41420-021-00418-y.
175. Tao Y, Zhou J, Wang Z, Tao H, Bai J, Ge G, et al. Human bone mesenchymal stem cells-derived exosomal miRNA-361-5p alleviates osteoarthritis by downregulating DDX20 and inactivating the NF-κB signaling pathway. Bioorg chem. 2021;113:104978. https://doi.org/10.1016/j.bioorg.2021.104978.
176. Liang Y, Xu X, Li X, Xiong J, Li B, Duan Li, et al. Chondrocyte-Targeted MicroRNA Delivery by Engineered Exosomes toward a Cell-Free Osteoarthritis Therapy. In ACS applied materials & interfaces. 2020;12(33):36938–47. https://doi.org/10.1021/acsami.0c10458.
177. Yao Z, Li J, Xiong H, Cui H, Ning J, Wang S, et al. MicroRNA engineered umbilical cord stem cell-derived exosomes direct tendon regeneration by mTOR signaling. J Nanobiotechnology. 2021;19:169. https://doi.org/10.1186/s12951-021-00906-4.
178. Huang C-C, Kang M, Leung K, Lu Yu, Shirazi S, Gajendrareddy P, Ravindran S. Micro RNA based MSC EV engineering: Targeting the BMP2 cascade for bone repair. In Frontiers in cell and developmental biology. 2023;11:1127594. https://doi.org/10.3389/fcell.2023.1127594.
179. Benjamin EJ, Blaha MJ, Chiuve SE, Cushman M, Das SR, Deo R, et al. Heart Disease and Stroke Statistics-2017 Update: A Report From the American Heart Association. Circulation. 2017;135:e146–603. https://doi.org/10.1161/CIR.0000000000000485.
180. Gartz M, Strande JL. Examining the Paracrine Effects of Exosomes in Cardiovascular Disease and Repair. J Am Heart Assoc. 2018. https://doi.org/10.1161/JAHA.117.007954.
181. Chen Q, Liu Y, Ding X, Li Q, Qiu F, Wang M, et al. Bone marrow mesenchymal stem cell-secreted exosomes carrying microRNA-125b protect against myocardial ischemia reperfusion injury via targeting SIRT7. Mol Cell Biochem. 2020;465:103–14. https://doi.org/10.1007/s11010-019-03671-z.
182. Liu H, Zhang Y, Yuan J, Gao W, Zhong X, Yao K, et al. (2022): Corrigendum Dendritic cell derived exosomal miR 494 3p promotes angiogenesis following myocardial infarction. In International journal of molecular medicine 49 (4). https://doi.org/10.3892/ijmm.2022.5096.
183. Song B-W, Lee CY, Kim R, Kim WJ, Lee HW, Lee MY, et al. Multiplexed targeting of miRNA-210 in stem cell-derived extracellular vesicles promotes selective regeneration in ischemic hearts. Exp Mol Med. 2021;53(4):695–708. https://doi.org/10.1038/s12276-021-00584-0.
184. Kang J-Y, Kim H, Mun D, Yun N, Joung B. Co-delivery of curcumin and miRNA-144-3p using heart-targeted extracellular vesicles enhances the therapeutic efficacy for myocardial infarction. J Control Release. 2021;331:62–73. https://doi.org/10.1016/j.jconrel.2021.01.018.
185. Zhang L, Ouyang P, He G, Wang X, Song D, Yang Y, He X. Exosomes from microRNA-126 overexpressing mesenchymal stem cells promote angiogenesis by targeting the PIK3R2-mediated PI3K/Akt signalling pathway. J Cellular Mol Med. 2021;25(4):2148–62. https://doi.org/10.1111/jcmm.16192.
186. Zhou J, Lin Y, Kang X, Liu Z, Zhang W, Xu F. microRNA-186 in extracellular vesicles from bone marrow mesenchymal stem cells alleviates idiopathic pulmonary fibrosis via interaction with SOX4 and DKK1. Stem Cell Res Therapy. 2021;12(1):96. https://doi.org/10.1186/s13287-020-02083-x.
187. Euscher LM, Mentkowski KI, Tarvirdizadeh T, Julian I, Bhatt K, Eagler L, Lang JK. (2022): Extracellular vesicle microRNA cargo engineering reveals critical mechanisms underlying therapeutic efficacy. https://doi.org/10.1101/2022.01.31.478505.
188. Pardridge WM. Drug transport across the blood-brain barrier. J Cereb Blood Flow Metab. 2012;32:1959–72. https://doi.org/10.1038/jcbfm.2012.126.
189. Banks WA, Sharma P, Bullock KM, Hansen KM, Ludwig N, Whiteside TL. Transport of Extracellular Vesicles across the Blood-Brain Barrier: Brain Pharmacokinetics and Effects of Inflammation. Int J Mol Sci. 2020. https://doi.org/10.3390/ijms21124407.
190. Li Xu, Zhang X, Liu Y, Pan R, Liang X, Huang L, Yang C. Exosomes derived from mesenchyml stem cells ameliorate oxygen-glucose deprivation/reoxygenation-induced neuronal injury via transferring MicroRNA-194 and targeting Bach1. In Tissue & cell. 2021;73:101651. https://doi.org/10.1016/j.tice.2021.101651.
191. Zhao Y, Gan Y, Xu G, Hua K, Liu D. Exosomes from MSCs overexpressing microRNA-223-3p attenuate cerebral ischemia through inhibiting microglial M1 polarization mediated inflammation. Life Sci. 2020;260:118403. https://doi.org/10.1016/j.lfs.2020.118403.
192. Du L, Jiang Y, Sun Y. Astrocyte-derived exosomes carry microRNA-17-5p to protect neonatal rats from hypoxic-ischemic brain damage via inhibiting BNIP-2 expression. In Neurotoxicology. 2021;83:28–39. https://doi.org/10.1016/j.neuro.2020.12.006.
193. Yerrapragada SM (2021): The Protective Effects of miR-210 Modified Endothelial Progenitor Cells Released Exosomes in Hypoxia/Reoxygenation Injured Neurons. Master's dissertation. Wright State University, Dayton, OH. Pharmacology and Toxicology. Available online at http://rave.ohiolink.edu/etdc/view?acc_num=wright1629835915811575, checked on 8/2/2022.
194. Lai N, Wu D, Liang T, Pan P, Yuan G, Li X, et al. Systemic exosomal miR-193b-3p delivery attenuates neuroinflammation in early brain injury after subarachnoid hemorrhage in mice. In Journal of neuroinflammation. 2020;17(1):74. https://doi.org/10.1186/s12974-020-01745-0.
195. Zhai L, Shen H, Sheng Y, Guan Q. ADMSC Exo-MicroRNA-22 improve neurological function and neuroinflammation in mice with Alzheimer's disease. J Cellular Mol Med. 2021;25(15):7513–23. https://doi.org/10.1111/jcmm.16787.
196. Guo H, Huang B, Wang Y, Zhang Y, Ma Q, Ren Y. Bone marrow mesenchymal stem cells-derived exosomes improve injury of hippocampal neurons in rats with depression by upregulating microRNA-26a expression. In Int immunopharmacol. 2020;82:106285. https://doi.org/10.1016/j.intimp.2020.106285.
197. Fan B, Chopp M, Zhang ZG, Liu XS. Treatment of diabetic peripheral neuropathy with engineered mesenchymal stromal cell-derived exosomes enriched with microRNA-146a provide amplified therapeutic

efficacy. In Experimental neurology. 2021;341:113694. https://doi.org/10.1016/j.expneurol.2021.113694.
198. Huang W, Lin M, Yang C, Wang F, Zhang M, Gao J, Yu X. Rat Bone Mesenchymal Stem Cell-Derived Exosomes Loaded with miR-494 Promoting Neurofilament Regeneration and Behavioral Function Recovery after Spinal Cord Injury. In Oxidative medicine and cellular longevity. 2021;2021:1634917. https://doi.org/10.1155/2021/1634917.
199. Lai N, Wu D, Liang T, Pan P, Yuan G, Li X, et al. Systemic exosomal miR-193b-3p delivery attenuates neuroinflammation in early brain injury after subarachnoid hemorrhage in mice. J Neuroinflammation. 2020;17:74. https://doi.org/10.1186/s12974-020-01745-0.
200. Chen Y-S, Lin E-Y, Chiou T-W, Harn H-J. Exosomes in clinical trial and their production in compliance with good manufacturing practice. Ci Ji Yi Xue Za Zhi. 2020;32:113–20. https://doi.org/10.4103/tcmj.tcmj_182_19.
201. Ciferri MC, Quarto R, Tasso R. Extracellular Vesicles as Biomarkers and Therapeutic Tools: From Pre-Clinical to Clinical Applications. Biology (Basel). 2021. https://doi.org/10.3390/biology10050359.
202. Perocheau D, Touramanidou L, Gurung S, Gissen P, Baruteau J. Clinical applications for exosomes: Are we there yet? Br J Pharmacol. 2021;178:2375–92. https://doi.org/10.1111/bph.15432.
203. Pocsfalvi G, Mammadova R, Ramos Juarez AP, Bokka R, Trepiccione F, Capasso G. COVID-19 and Extracellular Vesicles: An Intriguing Interplay. Kidney Blood Press Res. 2020;45:661–70. https://doi.org/10.1159/000511402.
204. van Zandwijk N, Pavlakis N, Kao SC, Linton A, Boyer MJ, Clarke S, et al. Safety and activity of microRNA-loaded minicells in patients with recurrent malignant pleural mesothelioma: a first-in-man, phase 1, open-label, dose-escalation study. Lancet Oncol. 2017;18:1386–96. https://doi.org/10.1016/S1470-2045(17)30621-6.
205. Viteri S, Rosell R. An innovative mesothelioma treatment based on miR-16 mimic loaded EGFR targeted minicells (TargomiRs). Transl Lung Cancer Res. 2018;7:S1–4. https://doi.org/10.21037/tlcr.2017.12.01.
206. Tian J, Cui X, Sun J, Zhang J. Exosomal microRNA-16-5p from adipose mesenchymal stem cells promotes TLR4-mediated M2 macrophage polarization in septic lung injury. Int Immunopharmacol. 2021;98:107835. https://doi.org/10.1016/j.intimp.2021.107835.
207. Gallant-Behm CL, Piper J, Lynch JM, Seto AG, Hong SJ, Mustoe TA, et al. A MicroRNA-29 Mimic (Remlarsen) Represses Extracellular Matrix Expression and Fibroplasia in the Skin. J Invest Dermatol. 2019;139:1073–81. https://doi.org/10.1016/j.jid.2018.11.007.
208. Beg MS, Brenner AJ, Sachdev J, Borad M, Kang Y-K, Stoudemire J, et al. Phase I study of MRX34, a liposomal miR-34a mimic, administered twice weekly in patients with advanced solid tumors. Invest New Drugs. 2017;35:180–8. https://doi.org/10.1007/s10637-016-0407-y.
209. Hong DS, Kang Y-K, Borad M, Sachdev J, Ejadi S, Lim HY, et al. Phase 1 study of MRX34, a liposomal miR-34a mimic, in patients with advanced solid tumours. Br J Cancer. 2020;122:1630–7. https://doi.org/10.1038/s41416-020-0802-1.
210. Rezaei R, Baghaei K, Hashemi SM, Zali MR, Ghanbarian H, Amani D. Tumor-Derived Exosomes Enriched by miRNA-124 Promote Anti-tumor Immune Response in CT-26 Tumor-Bearing Mice. Front Med (Lausanne). 2021;8:619939. https://doi.org/10.3389/fmed.2021.619939.
211. Li R, Zhao K, Ruan Q, Meng C, Yin F. Bone marrow mesenchymal stem cell-derived exosomal microRNA-124-3p attenuates neurological damage in spinal cord ischemia-reperfusion injury by downregulating Ern1 and promoting M2 macrophage polarization. Arthritis Res Ther. 2020;22:75. https://doi.org/10.1186/s13075-020-2146-x.
212. Witwer KW, Van B, Bas WM, Bruno S, Choo A, Dominici M, Gimona M, et al. Defining mesenchymal stromal cell (MSC)-derived small extracellular vesicles for therapeutic applications. J Extracell Vesicles. 2019;8:1609206. https://doi.org/10.1080/20013078.2019.1609206.
213. Rohde E, Pachler K, Gimona M. Manufacturing and characterization of extracellular vesicles from umbilical cord-derived mesenchymal stromal cells for clinical testing. Cytotherapy. 2019;21:581–92. https://doi.org/10.1016/j.jcyt.2018.12.006.
214. Mendt M, Kamerkar S, Sugimoto H, McAndrews KM, Wu C-C, Gagea M, et al. Generation and testing of clinical-grade exosomes for pancreatic cancer. JCI Insight. 2018. https://doi.org/10.1172/jci.insight.99263.
215. Watson DC, Yung BC, Bergamaschi C, Chowdhury B, Bear J, Stellas D, et al. Scalable, cGMP-compatible purification of extracellular vesicles carrying bioactive human heterodimeric IL-15/lactadherin complexes. J Extracell Vesicles. 2018;7:1442088. https://doi.org/10.1080/20013078.2018.1442088.
216. Andriolo G, Provasi E, Lo Cicero V, Brambilla A, Soncin S, Torre T, et al. Exosomes From Human Cardiac Progenitor Cells for Therapeutic Applications: Development of a GMP-Grade Manufacturing Method. Front Physiol. 2018;9:1169. https://doi.org/10.3389/fphys.2018.01169.
217. Gobin J, Muradia G, Mehic J, Westwood C, Couvrette L, Stalker A, et al. Hollow-fiber bioreactor production of extracellular vesicles from human bone marrow mesenchymal stromal cells yields nanovesicles that mirrors the immuno-modulatory antigenic signature of the producer cell. Stem Cell Res Ther. 2021;12:127. https://doi.org/10.1186/s13287-021-02190-3.
218. Phelps J, Leonard C, Shah S, Krawetz R, Hart DA, Duncan NA, Sen A. Production of Mesenchymal Progenitor Cell-Derived Extracellular Vesicles in Suspension Bioreactors for Use in Articular Cartilage Repair. Stem Cells Transl Med. 2022;11:73–87. https://doi.org/10.1093/stcltm/szab008.
219. Kang H, Bae Y-H, Kwon Y, Kim S, Park J. Extracellular Vesicles Generated Using Bioreactors and their Therapeutic Effect on the Acute Kidney Injury Model. Adv Healthc Mater. 2022;11:e2101606. https://doi.org/10.1002/adhm.202101606.
220. Grangier A, Branchu J, Volatron J, Piffoux M, Gazeau F, Wilhelm C, Silva AKA. Technological advances towards extracellular vesicles mass production. Adv Drug Deliv Rev. 2021;176:113843. https://doi.org/10.1016/j.addr.2021.113843.
221. Jong AY, Wu C-H, Li J, Sun J, Fabbri M, Wayne AS, Seeger RC. Large-scale isolation and cytotoxicity of extracellular vesicles derived from activated human natural killer cells. J Extracell Vesicles. 2017;6:1294368. https://doi.org/10.1080/20013078.2017.1294368.
222. Onódi Z, Pelyhe C, Terézia Nagy C, Brenner GB, Almási L, Kittel Á, et al. Isolation of High-Purity Extracellular Vesicles by the Combination of Iodixanol Density Gradient Ultracentrifugation and Bind-Elute Chromatography From Blood Plasma. Front Physiol. 2018;9:1479. https://doi.org/10.3389/fphys.2018.01479.
223. Ji X, Huang S, Zhang J, Bruce TF, Tan Z, Wang D, et al. A novel method of high-purity extracellular vesicle enrichment from microliter-scale human serum for proteomic analysis. Electrophoresis. 2021;42:245–56. https://doi.org/10.1002/elps.202000223.
224. Marsh SR, Pridham KJ, Jourdan J, Gourdie RG. Novel Protocols for Scalable Production of High Quality Purified Small Extracellular Vesicles from Bovine Milk. Nanotheranostics. 2021;5:488–98. https://doi.org/10.7150/ntno.62213.
225. Del Pozo-Acebo L, Hazas, María-Carmen López de Las, Tomé-Carneiro J, Gil-Cabrerizo P, San-Cristobal R, Busto R, et al. Bovine Milk-Derived Exosomes as a Drug Delivery Vehicle for miRNA-Based Therapy. Int J Mol Sci 2021. https://doi.org/10.3390/ijms22031105.

Publisher's Note

Springer Nature remains neutral with regard to jurisdictional claims in published maps and institutional affiliations.

Biology of Reproduction, 2024, 1–15
https://doi.org/10.1093/biolre/ioae081
Research Article

Mapping the follicle-specific regulation of extracellular vesicle-mediated microRNA transport in the southern white rhinoceros (*Ceratotherium simum simum*)†

Ahmed Gad[1,2,‡], Nico G. Menjivar[1,‡], Rachel Felton[3], Barbara Durrant[3], Dawit Tesfaye[1,*] and Elena Ruggeri[3]

[1]Animal Reproduction and Biotechnology Laboratory (ARBL), Department of Biomedical Sciences, College of Veterinary Medicine and Biomedical Sciences, Colorado State University, Fort Collins, CO 80523, USA
[2]Department of Animal Production, Faculty of Agriculture, Cairo University, Giza 12613, Egypt
[3]Reproductive Sciences, Conservation Science Wildlife Health, San Diego Zoo Wildlife Alliance, Escondido, CA 92027, USA

*__Correspondence:__ Department of Biomedical Sciences, Animal Reproduction and Biotechnology Laboratory (ARBL), Colorado State University, Fort Collins, CO 80521, USA. E-mail: dawit.tesfaye@colostate.edu

†__Grant Support:__ This project was internally funded by the San Diego Zoo Wildlife Alliance Ocelots Donor Group. NGM is financially supported by grant funds from the USDA National Needs Fellowship grant number 2021-38420-34040 and USDA-NIFA-AFRI Predoctoral Fellowship grant number 2023-67011-40511.

‡Ahmed Gad and Nico G. Menjivar contributed equally to this work.

Abstract

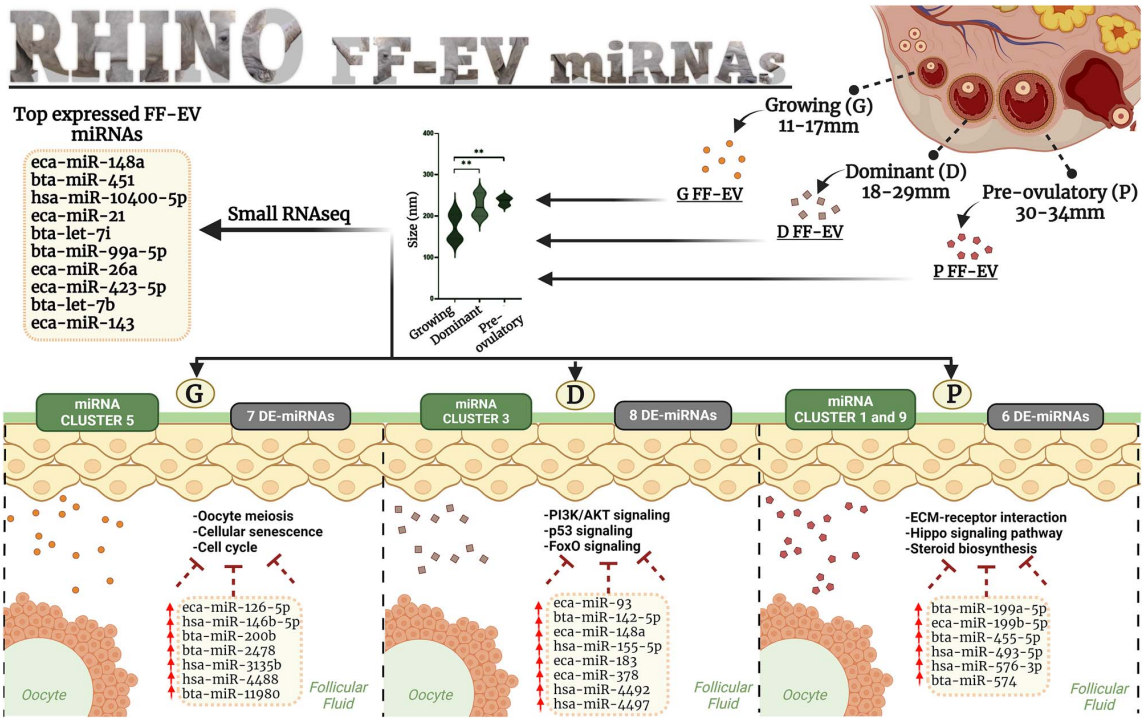
Efforts to implement effective assisted reproductive technologies (ARTs) for the conservation of the northern white rhinoceros (NWR; *Ceratotherium simum cottoni*) to prevent its forthcoming extinction, could be supported by research conducted on the closely related southern white rhinoceros (SWR; *Ceratotherium simum simum*). Within the follicle, extracellular vesicles (EVs) play a fundamental role in the bidirectional communication facilitating the crucial transport of regulatory molecules such as microRNAs (miRNAs) that control follicular growth and oocyte development. This study aimed to elucidate the dynamics of EV-miRNAs in stage-dependent follicular fluid (FF) during SWR ovarian antral follicle development. Three distinct follicular stages were identified based on diameter: Growing (G; 11–17 mm), Dominant (D; 18–29 mm), and Pre-ovulatory (P; 30–34 mm). Isolated EVs from the aspirated FF of segmented follicle stages were used to identify EV-miRNAs previously known via subsequent annotation to all equine (*Equus caballus*; eca), bovine *(Bos taurus*; bta), and human (*Homo sapiens*; hsa) miRNAs. A total of 417 miRNAs were detected, with 231 being mutually expressed across all three stages, including eca-miR-148a and bta-miR-451 as the top highly expressed miRNAs. Distinct expression dynamics in miRNA abundance were observed across the three follicular stages, including 31 differentially expressed miRNAs that target various pathways related to follicular growth and development, with 13 miRNAs commonly appearing amidst two different comparisons. In conclusion, this pioneering study provides a comprehensive understanding of the stage-specific expression dynamics of FF EV-miRNAs in the SWR. These findings provide insights that may lead to novel approaches in enhancing ARTs to catalyze rhinoceros conservation efforts.

Summary Sentence
Stage-specific miRNA cargo encapsulated within follicular fluid-derived extracellular vesicles possess intrinsic functions to modulate cell–cell communication during follicular growth in the rhinoceros.

Received: February 22, 2024. **Revised:** April 25, 2024. **Accepted:** May 20, 2024
© The Author(s) 2024. Published by Oxford University Press behalf of Society for the Study of Reproduction.
This is an Open Access article distributed under the terms of the Creative Commons Attribution License (https://creativecommons.org/licenses/by/4.0/), which permits unrestricted reuse, distribution, and reproduction in any medium, provided the original work is properly cited.

Downloaded from https://academic.oup.com/biolreprod/advance-article/doi/10.1093/biolre/ioae081/7679394 by Colorado State University user on 04 June 2024

Graphical Abstract



Key words: rhinoceros, ovarian follicle, follicular fluid, extracellular vesicles, miRNA.

Introduction

Wild rhinoceros populations are facing extinction due to constant threats; increased conservation measures are critically necessary to protect these species. As one of the few mega vertebrate herbivores living in the world, rhinoceros play a vital role as a keystone species of the African landscape. With just two non-reproductive living individuals, global attention has been focused on rescuing the northern white rhinoceros (NWR) from extinction [1, 2]. Conservation efforts have been focused on using the NWR's closest relative, the SWR to overcome rhinoceros population decline and to develop effective propagation strategies using assisted reproductive technologies (ARTs). Numerous ART procedures have been developed for different rhinoceros species, including ovum pickup (OPU), which enables oocytes to be retrieved for *in vitro* maturation and intracytoplasmic sperm injection, resulting in blastocyst production and cryopreservation for future use [2]. In addition, advanced ARTs, such as stem cell-associated techniques and artificial gamete production, could also pose promising strategies to support conservation efforts in rhinoceros [3].

Unfortunately, working with the rhinoceros comes with inherent management challenges and limited procedure opportunities. Therefore, to advance our reproductive knowledge and develop conservation technologies, domestic species are used to aid in the lesser accessible species, including the NWR and SWR. The domestic horse is phylogenetically related to the white rhinoceros, hence it can be a valuable model for reproductive studies [2]. Other domestic species, as well as humans, may also provide scientific context to advance rhinoceros reproductive knowledge and promote conservation efforts, although there is less comparative and translational work reported. Like the domestic horse, the white rhinoceros is a mono-ovulatory species, exhibiting a 3- to 5-day period of estrus behavior [4, 5], accompanied by the growth and ovulation of a single follicle (30–40 mm) [6], preceeded by a single pre-ovulatory LH surge. Throughout folliculogenesis, many antral follicles exist, segmented into multiple stages based on follicle diameter size (also known as selection, dominance, and ovulation). The nature of follicle dynamics and subsequent mechanisms of development are largely based on a series of systemic processes involving hormonal interaction and various intrafollicular constituents [7].

In the rhinoceros, serial ultrasound examinations have provided detailed characterizations of normal follicular growth and ovulation, as well as the documentation of anovulatory cycles amidst other irregularities. In captivity, cyclic females exhibit estrous cycles from 20 (similar to the horse) to 80 days in duration [8]. These two cycle lengths are deemed short (clustered around 30 days) and long (clustered around 70 days), but no mechanistic difference has been found to explain these differences in cycle length [4, 6, 9–13]. It was previously thought that the long cycle was either infertile or subfertile, but recent work has resulted in established pregnancies from long estrous cycles [8]. Regardless of the cycle length, the SWR cycle has been successfully manipulated with gonadotropin-releasing hormone (GnRH)

Downloaded from https://academic.oup.com/biolreprod/advance-article/doi/10.1093/biolre/ioae081/7673394 by Colorado State University user on 04 June 2024

to induce ovulation when follicles reach 30–35 mm [6, 8, 14, 15]. Moreover, in domesticated species like horses and cattle, GnRH treatment is correspondingly used to obtain high-quality oocytes and achieve greater pregnancy rates [16–18]. Ultimately, this unusual pattern of an irregular estrous cycle length, potentially complicates the development of ARTs in the SWR.

More recently, in a variety of domesticated species, including the horse, primary attention has focused on the role of EVs in governing intrafollicular communication, follicle dynamics, and reproductive function. Extracellular vesicles are lipid-bound nanoparticles secreted by cells [19] and encompass a heterogenous population of exosomes, microvesicles, and apoptotic bodies, which are primarily differentiated by their size and mode of biogenesis. These vesicles contain lipids, nucleic acids, and proteins, and are a functional system regulating the bidirectional communication between cells present within most body fluids. In addition, EVs are evolutionarily conserved structures secreted from a variety of cell types through exocytosis [20]. Previously discovered within the FF of various mammalian species and presiding over events including folliculogenesis and oogenesis [21–23], EVs of follicular, oviductal, and uterine fluid origin [24–28] have suitably proved to be beneficial in promoting oocyte competence and embryo development [29–31].

Recently, stage-specific expression profiles of follicular fluid EV-miRNAs during equine follicular development were performed using high-throughput miRNA sequencing to elucidate the patterns of EV-miRNAs and their association during specific stages of follicle development [24]. As such, in this study, critical miRNAs regulating follicular development were identified, proposing novel approaches using EV-mediated signaling to improve *in vitro* technological outcomes that span a multitude of species. These findings could be used for comparative approaches in understanding the potential role of EV-coupled miRNA dynamics in regulating follicular growth in the rhinoceros. Furthermore, the EV-miRNA patterns observed during follicle development could duly be used to distinguish physiological and pathological reproductive conditions, aid in defining fertility parameters, and to identify targets of future intervention, ultimately improving ART outcomes.

Materials and methods

Animal management and transrectal ovum pick up

Animals for this study were housed and managed at the San Diego Zoo Wildlife Alliance's Safari Park in Escondido, CA. All experimental procedures and methods involving the specific use of animals were reviewed and approved by the San Diego Zoo Wildlife Alliance's Institutional Animal Care and Use Committee (IACUC; protocol number #18-018, United States Department of Agriculture Certificate #93-R-0151).

For this study, two southern white rhinoceros females were stimulated prior to transrectal OPU similar to previous protocols [32, 33], facilitating the *in vivo* collections of FF aspirate from antral follicles of distinct sizes. Females orally received synthetic chlormadinone acetate (CMA) at 3 mg/day for 35 days. Two days after CMA withdrawal, both animals received 3 mg of Deslorelin (GnRH analog) followed by 2 mg of Deslorelin every 48 h prior to OPU (7 mg total) via injection. Both rhinoceroses were anesthetized using a combination of etorphine (2 mcg/kg), butorphanol (20–24 mcg/kg), medetomidine (23–25 mcg/kg), and azaperone (14–16 mcg/kg) administered intramuscularly using a remote drug delivery system. Propofol was administered intravenously during the initial positioning to facilitate intubation (0.5 mg/kg). Concluding collection procedures, anesthesia reversal was achieved using atipamezole delivered intramuscularly at a 5:1 ratio to medetomidine (116–125 mcg/kg) and naltrexone delivered intramuscularly at a target 50:1 ratio to etorphine (53–61 mcg/kg).

Following fecal removal, rinsing, and disinfection, OPU was achieved using a customized, ultrasound-guided probe enclosing three double-lumen needles. Follicle contents were aspirated, and each follicle was rinsed with a warmed (37°C) flushing solution (Vigro) containing 12.5 I.U./mL of heparin. The complete experimental design is illustrated in Figure 1.

Ovarian follicle grouping and FF collection

Prior to ultrasound-guided aspirations, antral follicles were assigned to one of three predetermined categories based on their diameters: growing (G; 11–17 mm), dominant (D; 18–29 mm), and pre-ovulatory (P; 30–34 mm), adapted from previous work [24]. Follicle aspirates were maintained at 37°C and immediately transported to the laboratory, where they were filtered through a 0.22-μm embryo filter (Professional Embryo Transfer Supply Inc.). Prior to storage, EV-bearing FF was centrifuged at 300 × g for 10 min, with the uppermost aqueous phase transferred and re-centrifuged at 2000 × g for 10 min, and 16 500 × g for 30 min. The final supernatant was passed through a 0.20-μm sterile syringe filter, removing particles larger than 200 nm in diameter, and stored at −80°C for further processing [34].

EV isolation and characterization

EVs were isolated using the dual-targeted approach of ultracentrifugation followed by precipitation and elution through size exclusion chromatography columns. Initially, in three technical replicates, frozen-thawed aliquots of 2 mL of FF aspirate from individual animals were subjected to ultracentrifugation using an SW 55Ti rotor on the Optima XE-90 Ultracentrifuge (Beckman Coulter; Pasadena, CA, USA) system at 120 000 × g for 70 min at 4°C, as previously described [28, 31]. Pelletized EVs were then washed with 3 mL of Dulbecco's Phosphate Buffered Saline without calcium and magnesium chloride [DPBS (1X)] (Sigma-Aldrich; St. Louis, MO, USA) and ultracentrifuged once more under the same parameters. Following ultracentrifugation, washed EV pellets were resuspended in Exo-spin™ Buffer and left to precipitate overnight at 4°C prior to processing through Exo-spin™ mini columns (CELL guidance systems; St. Louis, MO, USA) according to the manufacturer's protocol. Final 180-μL EV aliquots were then stored at −80°C for RNA extraction.

Identification and characterization methods of EVs (western blotting, transmission electron microscopy, and nanoparticle tracking analysis) were carried out as recommended by the International Society for Extracellular Vesicles in the proposed Minimal Information for Studies of Extracellular Vesicles ("MISEV") guidelines [35, 36]. Detailed experimental procedures have been submitted to the EV-TRACK knowledgebase (https://evtrack.org/) (EVTRACK ID: EV240017) [37].

Western blot

Isolated EV samples suspended in DPBS (1X) were combined with RIPA Ready to use [RIPA-RTU; 890-μL RIPA Buffer (Sigma R0278), 10-μL phosphatase inhibitor cocktail (Fisher 78420), 100-μL10X protease inhibitor cocktail (Sigma

Downloaded from https://academic.oup.com/biolreprod/advance-article/doi/10.1093/biolre/ioae081/7679394 by Colorado State University user on 04 June 2024

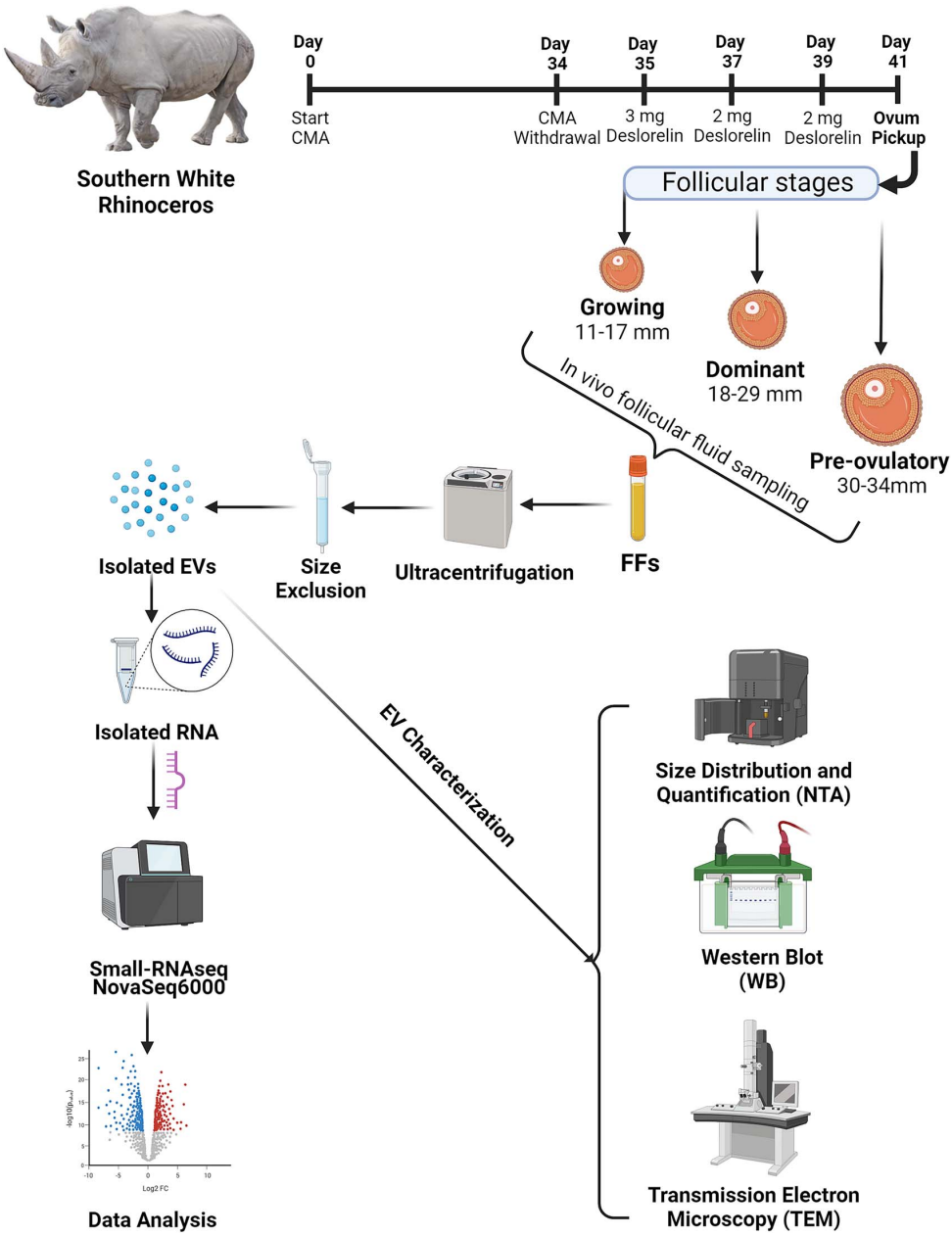


Figure 1. Schematic experimental illustration of the data analysis pipeline. Experimental pipeline outlining the design and workflow for the analysis of extracellular vesicle-coupled miRNAs from stage-specific rhinoceros FF. Given the rarity of the sample collections, following *in vivo* FF collections and subsequent EV isolation, the first-factor variable of differences in individual animals were removed. Total RNA including small RNAs were isolated from equal volumes of pooled EV technical replicates of two biologically dissimilar females (three pooled replicates/follicle stage, pool consisting of two animals).

11836170001)] to detect EV and cellular marker proteins. Protein lysate mixtures were vortexed for 30 s and kept on ice prior to suspension in 4x Laemmli Sample Buffer (Bio-Rad 1610747) and 2-Mercaptoethanol (Bio-Rad 1610710). Loading mixtures were then boiled at 95°C for 5 min, and protein samples were separated using Sodium Dodecyl Sulfate-PolyAcrylamide Gel Electrophoresis on a gradient (4–15%) Mini-PROTEAN TGX Stain-Free Precast Gels (Bio-Rad 4568084) and transferred to a 0.20-μm pore nitrocellulose membrane (Bio-Rad 1620112). Membranes were blocked for 1 h at room temperature in 5% (w/v) Non-Fat Dry Milk (Bio-Rad 1706404) in 1X Tris-buffered saline-Tween 20 (TBS-T) buffer and further incubated overnight at 4°C with respective primary antibodies. Membranes were then incubated with the suitable secondary antibody conjugated with horseradish peroxidase (System Biosciences; Goat

Downloaded from https://academic.oup.com/biolreprod/advance-article/doi/10.1093/biolre/ioae081/7679394 by Colorado State University user on 04 June 2024

anti-Rabbit HRP, 1:200 dilution) for 1 h at room temperature. Membranes were each probed and developed once with SuperSignal™ West Pico PLUS Chemiluminescent Substrate (ThermoFisher Scientific 34,579) and imaged using the ChemiDoc XRS+ chemiluminescence system with Image Lab™ Software (version 6.0.1 build 34) (Bio-Rad).

The following rabbit anti-human antibodies were used for western blot: rabbit polyclonal TSG101 (System Biosciences; EXOAB-TSG101-1; 1:100 dilution), rabbit polyclonal HSP70 (System Biosciences; EXOAB-Hsp70A-1; 1:100 dilution), and rabbit polyclonal Cytochrome C (Sino Biological; 102139-T42; 1:200 dilution). All antibodies were diluted in 5% (w/v) Non-Fat Dry Milk (Bio-Rad 1706404) in TBS-T.

Transmission electron microscopy

The morphological shape and size of EVs were determined using a particle beam of electrons for visualization on a FEI/TFS Tecnai T12 Spirit transmission electron microscope (FEI Company; Hillsboro, OR, USA), operating at 100 kV, with an AMT CCD. Briefly, a small volume of isolated EV samples (6-8 μL) was applied to a carbon-coated, copper mesh grid for 1–2 min., followed by negative staining with 2% aqueous uranyl acetate. After fixing, samples were allowed to dry prior to imaging. Multiple frames were visualized per sample with approximately 15–20 captured for assessment.

Nanoparticle tracking analysis

The size distribution and collective particle concentration in isolated EV samples were analyzed using a ZetaView® QUATT 4 Nanosight Instrument (Particle Metrix). Briefly, isolated EVs were diluted in sterile DPBS (1X) and injected into the device for analysis. Measurements were taken at 11 positions via scatter mode using a 488-nm laser. Analysis of EV concentrations was calculated using the Zetaview Software (version 8.05.12 SP1) and re-analyzed based on the dilution factors to reveal the approximate number of particles/mL for each sample.

Exosomal RNA extraction, library preparation, and sequencing

Total RNA to include miRNAs were isolated from equal volumes of pooled EV technical replicates of two biologically dissimilar females (three pooled replicates/follicle stage, pool from 2 animals) using the Norgen Exosomal RNA Isolation kit (Norgen Biotek Corp.; Thorold, ON, CA.) following the instructions for the Mini Kit provided by the manufacturer, and as carried out previously [24, 38]. Objective measurements for RNA quality using RINs (RNA Integrity Number), concentration, and size distribution were characterized using an Agilent RNA 6000 Pico kit in an Agilent 2100 Bioanalyzer (Agilent Technologies; Santa Clara, CA, USA). Small-RNA library preparations for Next Generation Sequencing were prepared by Novogene Co., LTD (Sacramento, CA, USA) using a TruSeq Small RNA Library Prep Kit (Illumina RS-200) according to the manufacturer's instructions. Library quantity and quality assessments were performed using a Qubit® DNA HS Assay Kit on a Qubit® 2.0 Fluorometer and an Agilent DNA High Sensitivity Kit in an Agilent 2100 Bioanalyzer, respectively. Explicit library concentrations were calculated using quantitative PCR measures then pooled in equimolar ratios and sequenced in a NovaSeq6000 sequencing instrument (Illumina) as single-end (50 bases) reads.

Bioinformatic analysis and identification of miRNA clustering

FASTQ files were generated for individual samples using the software bcl2fastq (Illumina) with quality assurance performed using FastQC tool version 0.11.9. Raw FASTQ files and processed comma-separated value (CSV) files have been deposited into NCBI's Gene Expression Omnibus (GEO) and are accessible through the GEO Series accession number (GSE246260). Formal analysis of the data was conducted using the CLC Genomics Workbench software, version 21 (www.qiagenbioinformatics.com). After removing adapter sequences, raw sequencing reads were trimmed based on quality score (Q-score > 30), ambiguous nucleotides (maximum two nucleotides allowed), and read length (≥15 nucleotides). As miRNAs have not been sequenced for the rhinoceros species, reads were annotated against the equine, bovine, and human precursor and mature miRNAs listed in the mirBase database (release 22) using the CLC Genomics Workbench Quantify miRNA tool after applying default software parameters and allowing a maximum of two mismatches within the read. We used these three species to annotate the rhinoceros's sequence reads as they have well-annotated genomes and miRNAs and well-developed ARTs, with equine given priority based on the phylogenetic relationship [39]. Normalization of raw expression data was conducted using the trimmed mean of the M-values method (TMM normalization) [40] and correspondingly presented as TMM-adjusted Counts Per Million (CPM). Any miRNA with a CPM value greater than 10 in a minimum of two out of the three biological replicates of each group was considered as expressed. Additionally, the expression analysis comparison was performed using the CLC Genomics Workbench Differential Expression tool. Differentially expressed (DE) miRNAs were determined on the criteria of exhibiting a fold change (FC) ≥ 2 and p-adjusted value (FDR) < 0.1 [41]. miRNAs were grouped in different cluster patterns according to their expression profiles among the different developmental stages using the Mfuzz Bioconductor package [42].

miRNA-target gene prediction and ontological classification

Target genes of the DE-miRNAs were identified using the human DE-miRNAs and the human homologous miRNAs for the equine and bovine DE-miRNAs to cover all possible validated and predicted target genes appearing in the miRWalk database [43]. Validated target genes from miRTarBase (version 7.0) and predicted commonly targeted genes by TargetScan (version 7.1) and miRDB (release 5.0) were selected for ontological classification analysis using the DAVID bioinformatics web tool (https://david.abcc.ncifcrf.gov/). Significant pathways and biological processes were determined from the KEGG pathway database [44], and the GOTERM_BP_DIRECT annotation set, respectively. The interaction network of the DE-miRNAs from the different comparisons were constructed using Cytoscape [45].

Results

Rhinoceros EVs bear conventional EV-like physical and biochemical traits

Stage-specific FF was collected from two female rhinoceros' and subjected to a dual-targeted approach to isolate high-grade EVs for small RNA sequencing, as outlined

Downloaded from https://academic.oup.com/biolreprod/advance-article/doi/10.1093/biolre/ioae081/7679394 by Colorado State University user on 04 June 2024

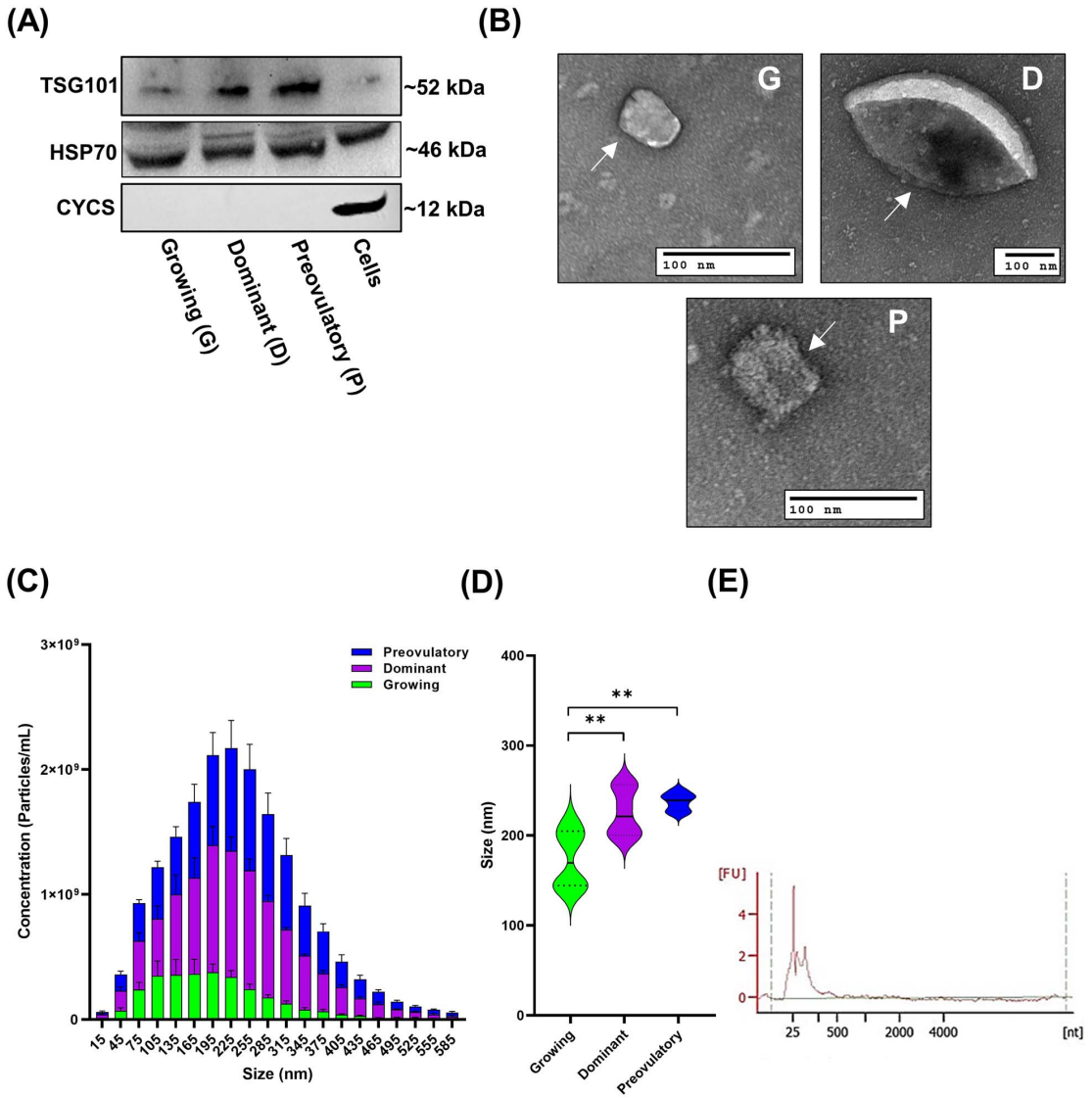


Figure 2. Rhinoceros extracellular vesicle morphological and biochemical validation. (A) Immunoblots indicating traditionally expressed EV-associated marker proteins (TSG101 and HSP70), and the absence of cellular contamination marker (CYCS). (B) Representative transmission electron microscopy images revealing the ultrastructure cup-like morphology of rhinoceros FF-derived EVs, indicated by arrows. Scale bars: 100 nm. Nanoparticle tracking analysis of the concentration (C) and size distribution (D) of rhinoceros FF-derived EVs from diverging stages. (E) Representative graphical overview of the quality and integrity of exosomal RNA samples used for small RNA sequencing.

in the workflow diagram (Figure 1). The analysis of the isolated EVs and independent rhinoceros granulosa cells revealed the presence of EV markers (TSG101 and HSP70) in all samples, assessed by western blot analysis, as well as the absence of cellular mitochondrial protein marker cytochrome c (CYCS) from the EV samples (Figure 2A). Transmission electron microscopy images captured of pooled EV samples from each respective stage, revealed that rhinoceros EVs exhibit hallmark cup-like morphology, characteristics indicative of long-established EVs (Figure 2B). Additionally, we evaluated six technical replicates of EVs [three per follicle stage, per individual animal ($n = 2$)], and according to nanoparticle tracking analysis, EVs collected from stage-specific FF differ in concentration (Avg. Conc.: G = 2.93E ± 09, D = 8.17E ± 09, P = 7.05E ± 09) and differ in size [G = 173.78 nm, D = 225.76 nm ($p = 0.0072$), P = 237.41 nm ($p = 0.0015$)], compared to those EVs collected from growing follicles (Figure 2C and D). The quality and integrity of the isolated exosomal RNA samples were used to sequence small RNAs (n = 9) and were additionally analyzed with a representative electropherogram revealing peaks for small RNAs amid EVs with the absence of 18S and 28S cellular ribosomal RNAs (Figure 2E).

Expression profiles and DE miRNAs

A total of nine small-RNA libraries were constructed with an average of 18 million reads per library that passed the QC parameters. An average of 0.4% of reads were annotated

Downloaded from https://academic.oup.com/biolreprod/advance-article/doi/10.1093/biolre/ioae081/7679394 by Colorado State University user on 04 June 2024

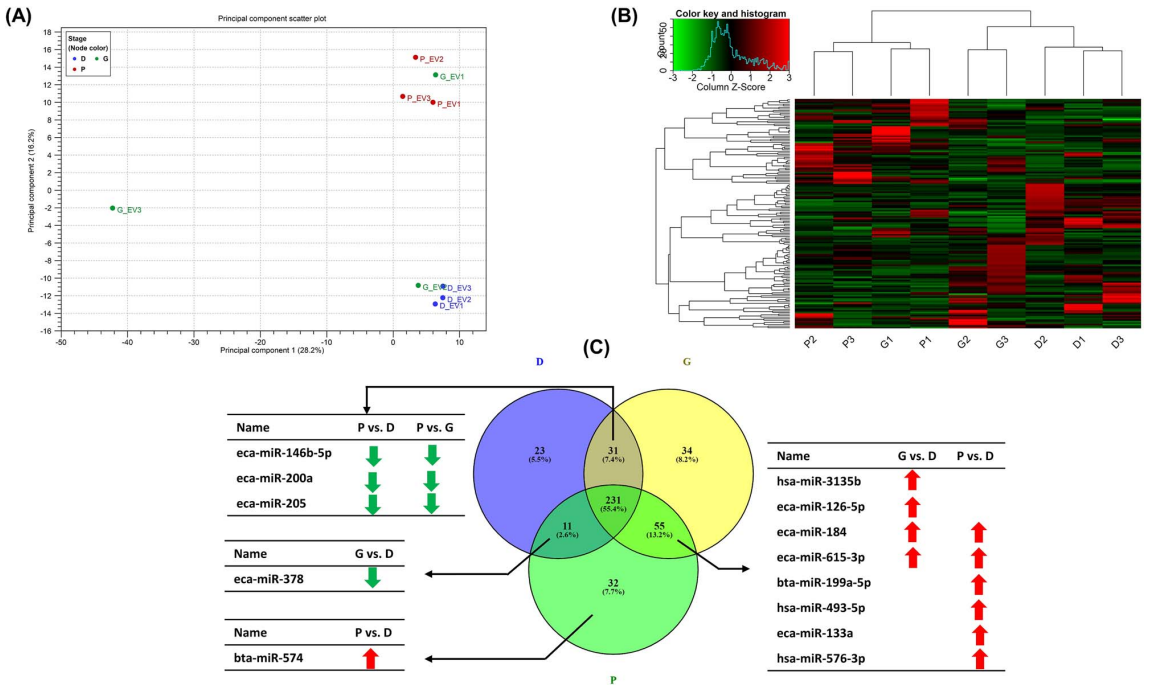


Figure 3. Small-RNA sequencing data overview. (A) Principal component analysis. (B) Heatmap and hierarchical clustering of expressed miRNAs. (C) Venn diagram for commonly and exclusively expressed miRNAs in the FF EVs at different stages of follicular development. MicroRNAs with a value of CPM >10 in at least two replicates of the three biological replicates was considered detected. Exclusively expressed miRNAs that exhibited a significant difference are presented in the Venn diagram with arrows indicating significantly up or downregulated miRNAs in the corresponding comparison. G: Growing; D: dominant; P: preovulatory.

to the equine, bovine, and human miRNAs from the mirBase database (Supplementary Table S1). Principal component analysis (PCA) and hierarchical heatmap exhibited clear clusterings of the D and P replicates, while this was not the case for the replicates of the G group (Figure 3A and B). A total of 351, 296, and 329 miRNAs were expressed (>10 CPM in at least two replicates) in the G, D, and P groups, respectively, with 231 miRNAs being commonly expressed across the three groups (Figure 3C). The top 20 highly expressed miRNAs are presented in Table 1 and the complete list of all expressed miRNAs is presented in Supplementary Table S2. Among the top 20 expressed miRNAs, 13 miRNAs were commonly detected in the three groups. Interestingly, eca-miR-148a and bta-miR-451 were among the top three miRNAs in the three groups (Table 1). Among the exclusively expressed miRNAs, or the ones that were expressed in only two groups, 13 miRNAs exhibited differences in either one or two comparisons, as shown in Figure 3(C).

In addition, a total of 31 miRNAs, among the 231 commonly expressed miRNAs, were DE (FC $\geq$ 2, FDR $<$ 0.1) in the three different comparisons (Figure 4A). The DE-miRNAs in the G vs. D, P vs. G, and P vs. D comparisons are presented in Figure 4(B), (C), and (D), respectively and in the Supplementary Table S3. Out of the 31 DE-miRNAs, 13 commonly appeared in atleast two different comparisons. Three miRNAs, eca-miR-486-5p, eca-miR-31, and bta-miR-142-5p were downregulated in the P group compared to both the G and D groups. In the G group, bta-miR-215, hsa-miR-4492, and hsa-miR-4497 were downregulated, while bta-miR-2478 and bta-miR-11980 were upregulated compared to both the P and D groups. In the D group, bta-miR-9-5p, eca-miR-9a, and eca-miR-381 were downregulated, while eca-miR-148a and hsa-miR-155-5p were upregulated compared to both the G and P groups (Figure 4).

miRNA cluster analysis

The abundance of EV-coupled miRNAs across the stages of follicular development was sorted according to the abundance in each stage of development and shown to have distinct clustering patterns. Cluster analysis showed that the miRNAs expressed in the FF-EVs were clustered into nine different patterns (Figure 5A, Supplementary Table S4). Each cluster pattern was composed of a variable number of miRNAs, as well as, DE-miRNAs, in which, clusters 3, 5, and 6 contained the highest numbers of DE-miRNAs compared to the other clusters (Figure 5B).

Cluster 3 comprises a group of 67 miRNAs that exhibited an increase in their expression from the G until the D stage and then a reduction at the P stage (Figure 6A). Among this cluster, eight miRNAs, including eca-miR-148a, were differentially or exclusively expressed amidst the different groups (Figure 6B). Pathways associated with the exclusive and DE-miRNA target genes of this cluster exhibited that several signaling pathways (including RAS, P13K-Akt, P53, mTOR, and MAPK), focal adhesion, cellular senescence, and endocrine resistance were among the top significantly targeted pathways (Figure 6C). Cluster 5 comprises a group of 53 miRNAs that exhibited a sharp reduction in their expression in the D and P stages but not in the G stage (Figure 7A). Among this cluster, seven

Downloaded from https://academic.oup.com/biolreprod/advance-article/doi/10.1093/biolre/ioae081/7679394 by Colorado State University user on 04 June 2024

Table 1. List of the top 20 most abundant miRNAs amidst EVs obtained from rhinoceros FFs at different follicular stages

miRNA	G CPM	miRNA	D CPM	miRNA	P CPM
bta-miR-11980	185 839.3	eca-miR-148a	872 829.2	eca-miR-148a	94 882.4
eca-miR-148a	85 922.45	bta-miR-451	96 984.29	hsa-miR-10400-5p	54 664.73
bta-miR-451	83 159.52	hsa-miR-10400-5p	91 187.32	bta-miR-451	38 476.65
bta-miR-2478	50 026.85	eca-miR-21	45 580.34	bta-miR-99a-5p	38 245.91
hsa-miR-3168	47 238.03	eca-miR-122	32 587.91	eca-miR-99a	30 796.38
eca-miR-21	34 231.73	eca-miR-486-5p	30 169.45	bta-let-7i	24 071.29
bta-let-7i	29 962.76	bta-let-7i	28 037.44	eca-miR-21	23 430.8
hsa-miR-10400-5p	24 243.74	hsa-miR-3168	26 703.2	eca-miR-10b	21 032.38
bta-miR-99a-5p	24 046.17	bta-miR-99a-5p	23 336.02	eca-miR-143	20 767.12
eca-miR-26a	20 774.92	eca-miR-26a	21 300.4	eca-miR-26a	18 064.75
eca-miR-1	20 262.69	bta-miR-192	17 449.7	bta-let-7b	17 731.89
eca-let-7g	16 584.2	eca-let-7g	14 136.19	eca-let-7a	16 031.34
eca-let-7f	16 230.58	eca-miR-423-5p	13 883.41	bta-miR-192	15 927.29
eca-miR-486-5p	16 206.56	bta-let-7b	13 142.76	eca-miR-122	15 727.23
bta-miR-151-3p	15 349.26	eca-miR-126-3p	12 884.64	eca-miR-100	15 330.03
eca-miR-143	13 270.89	eca-miR-143	11 875.72	eca-miR-1	13 948.54
eca-miR-423-5p	12 834.61	eca-let-7f	11 162.91	eca-miR-128	12 321.1
bta-let-7b	12 829.24	eca-miR-128	10 955.84	eca-let-7f	12 199.41
eca-miR-122	12 587.2	bta-miR-151-3p	10 827	bta-miR-151-3p	11 359.67
eca-miR-100	11 683.97	eca-miR-10b	10 642.12	eca-miR-423-5p	9912.52

miRNA: microRNA; CPM: counts per million; G: growing; D: dominant; P: pre-ovulatory.

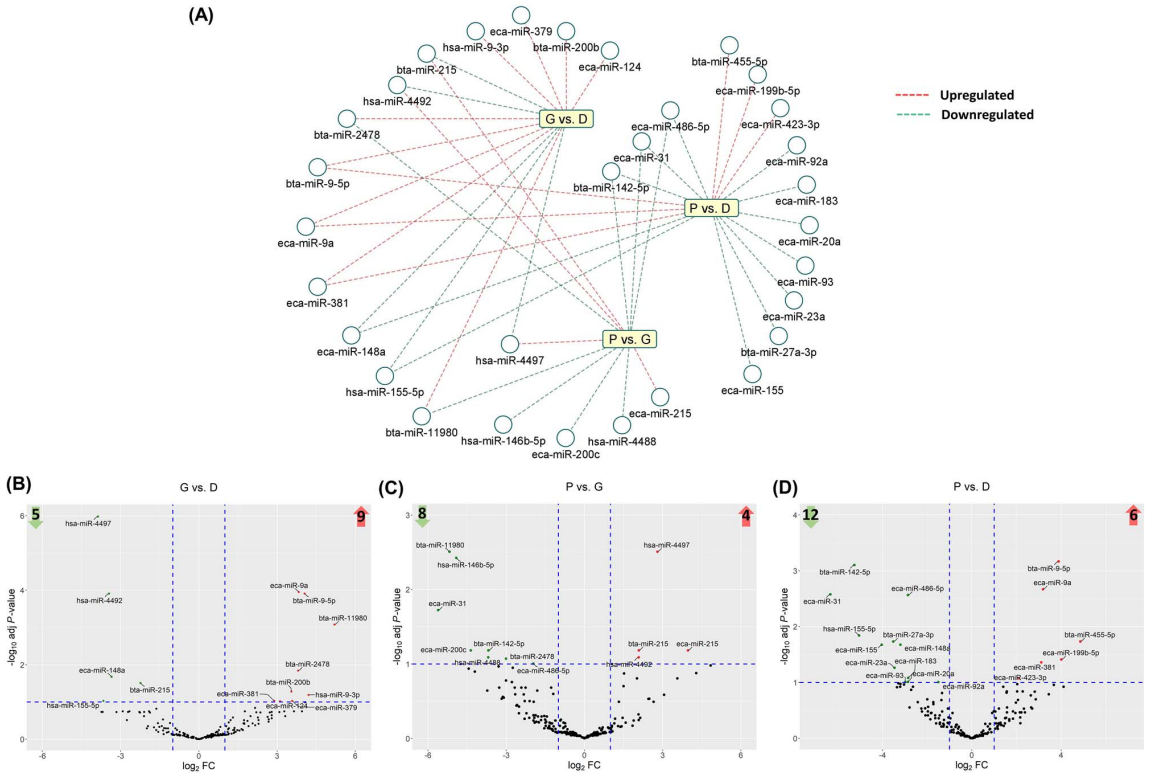
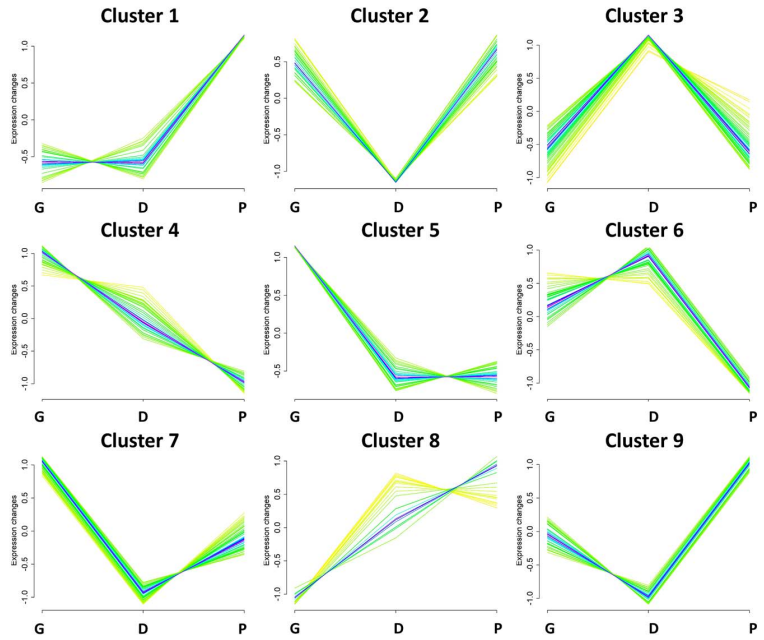


Figure 4. DE miRNAs. (A) All DE-miRNAs from the three different comparisons. Up- and down regulated miRNAs from each comparison are presented as red and green lines, respectively. Volcano plots of expressed miRNAs. Up- (upper right), and downregulated (upper left) miRNAs in (B) G vs. D, (C) P vs. G, and (D) P vs. D comparisons. The number of up and downregulated miRNAs in each comparison are presented on the up and down arrows, respectively. G: growing; D: dominant; P: preovulatory.

miRNAs were differentially or exclusively expressed amidst the different groups, including bta-miR-11980 with approximately a 36-fold increase in the G groups compared to both the D and P groups (Figure 7B). Pathways associated with the exclusive and DE-miRNA target genes of this cluster showed that oocyte meiosis, cellular senescence, and cell cycle were among the top significantly targeted pathways (Figure 7C). Cluster 6 comprises a group of 47 miRNAs that exhibited a high expression level at the G and D stages and then a sharp reduction at the P stage. Among this cluster, 10 miRNAs,

Downloaded from https://academic.oup.com/biolreprod/advance-article/doi/10.1093/biolre/ioae081/7679394 by Colorado State University user on 04 June 2024

(A)



(B)

Cluster	#miRNAs	Exclusive and DE-miRNAs
1	41	2
2	40	6
3	67	8
4	47	1
5	53	7
6	47	10
7	56	4
8	24	2
9	42	4
Total	**417**	**44**

Figure 5. Clustering analysis of EV-coupled miRNAs across the stages of follicular development. (A) Nine different miRNA expression patterns in the FF EVs during follicular development. (B) The counts of total and DE miRNAs in each cluster. G: growing; D: dominant; P: preovulatory.

including eca-miR-486-5p and eca-miR-31, were differentially or exclusively expressed amidst the different comparisons. Pathways associated with the exclusive and DE-miRNA target genes of this cluster showed similar pathways as in cluster 3, including several signaling pathways and endocrine resistance (Figure 8C).

Discussion

Recent achievements in ARTs in the white rhinoceros [1, 16–18] have elucidated numerous aspects of reproduction and improved *in vitro* technologies for this species. Ovum pick up, *in vitro* oocyte maturation, fertilization, and embryo culture, as well as embryo transfer [1] have been implemented in the white rhinoceros, providing hope for the successful restoration of the genetic diversity necessary for a self-sustainable population. However, with very few scientific groups working on this challenging task worldwide, innovative approaches to increase the efficiency of *in vitro* technologies are imperative. Molecular mechanisms of follicle dynamics and ovarian function are still unmapped in the rhinoceros, hence the need to develop more sophisticated tools used in other model species.

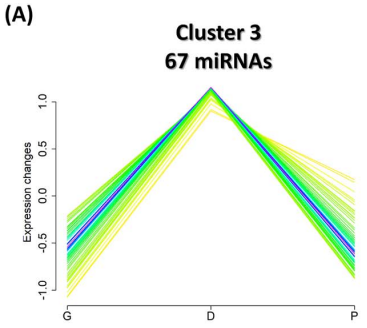
At their core, EVs establish and liaise the molecular dialog between the growing oocyte and maternal tissues, through which miRNAs are the essential elements regulating follicular maturation [46, 47]. Previous studies from our group have implicated the role of EV-coupled miRNAs from FF in mediating the strictly coordinated and intricate crosstalk of follicular cells to ultimately ensure the ovulation of a competent oocyte [21]. Given that EVs [31] containing miRNAs [48] are readily uptaken by growing oocytes and embryos, and that FF-EVs categorically have been shown to stimulate cumulus expansion (morphologic and via gene regulation) *in vitro* [49], the aim of this study encompasses elucidating the dynamics and potential roles of EV-miRNAs from stage-specific FF amidst follicle growth for the first time in the SWR.

The presented data identify deviations among groups in miRNA expression levels from FF-EVs implying the probable regulatory machinery affecting the developing oocyte and the circumambient microenvironment. Due to the nature and rarity of the sample collections, to our knowledge, this is the first comparative analysis of FF-EVs and miRNAs, aimed toward a better understanding of the reproductive complexities and the prospective preservation of the rhinoceros species through potential improvements in ART efficiencies. Although the differences in individual animals were the first-factor variable removed, the PCA of quantified miRNAs clearly segments group D from P, which are more defined and structured in stage, while the fate of group G remains undifferentiated at the time of collection. This is a clear indication revealing that the EV-coupled miRNA fingerprint within the rhinoceros FF is directly associated with their follicular differentiation. Overall, a total of 231 miRNAs (55.4%) were identified to be commonly expressed among the three groups, while 34 (8.2%), 23 (5.5%), and 32 (7.7%), represent those exclusively expressed within the G, D, and P groups, respectively. These data suggest prominent alterations in the EV-miRNA cargo during different stages of follicle development, in accordance with previous work in bovine [21], humans [46], goats [50], and equine [24].

Functional implications of miRNA expression and DE-miRNAs during segmented early stages of follicular development

Amidst the top highly expressed miRNAs, based on read counts, from the top 20 most abundant miRNAs (Table 1) in all groups include, eca-miR-148a, bta-miR-451, eca-miR-21,

Downloaded from https://academic.oup.com/biolreprod/advance-article/doi/10.1093/biolre/ioae081/7679394 by Colorado State University user on 04 June 2024



(B)

Differentially and exclusively expressed miRNAs (Fold Change)

Name	G vs. D	P vs. D	P vs. G
eca-miR-148a	-10.16	-9.20	
hsa-miR-4492	-10.90		4.24
hsa-miR-155-5p	-12.68	-33.17	
hsa-miR-4497	-14.64		6.95
eca-miR-378	Not in G		
eca-miR-183		-7.21	
eca-miR-93		-7.91	
bta-miR-142-5p		-38.27	-12.88

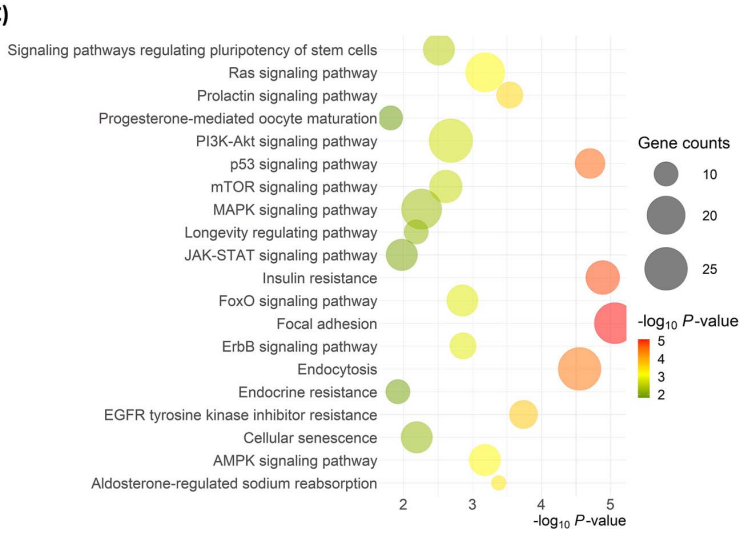
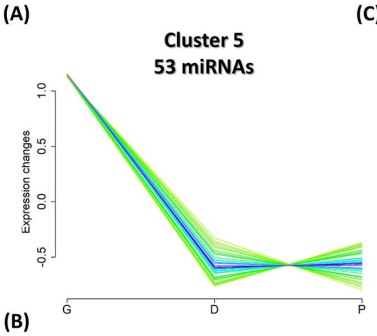


Figure 6. Cluster 3 consists of 67 miRNAs. (A) A group of 67 miRNAs exhibited an increase in their expression from the G until the D stage and then a reduction at the P stage. (B) Among this cluster, eight miRNAs were differentially or exclusively expressed amidst the different comparisons. (C) Pathways associated with the exclusive and DE-miRNA target genes of this cluster. G: growing; D: dominant; P: preovulatory.



(B)

Differentially and exclusively expressed miRNAs (Fold Change)

Name	G vs. D	P vs. G
hsa-miR-3135b	Not in D	
bta-miR-11980	36.77	-36.30
eca-miR-126-5p	Not in D	
bta-miR-2478	13.96	-8.07
bta-miR-200b	11.71	
hsa-miR-4488		-12.93
hsa-miR-146b-5p		-30.27

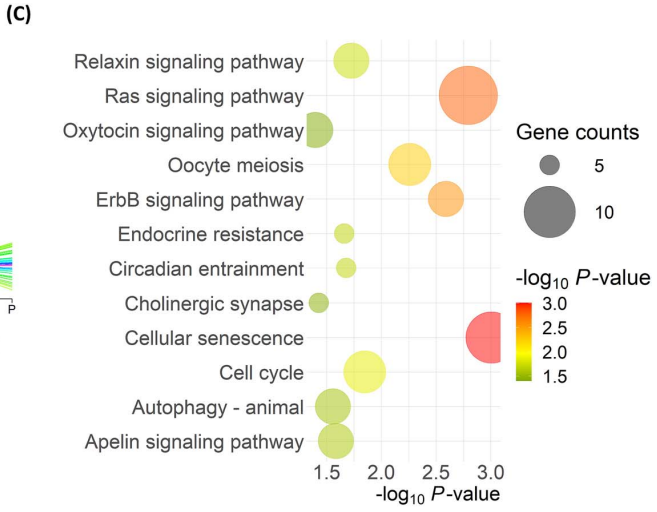
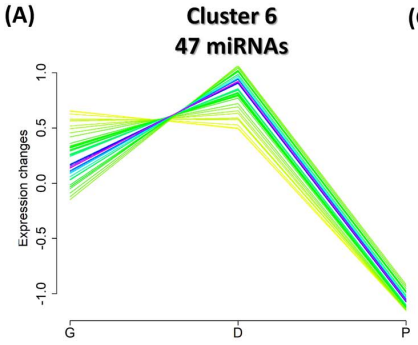


Figure 7. Cluster 5 consists of 53 miRNAs. (A) A group of 53 miRNAs exhibited a sharp reduction in their expression in the D and P stages, however, not in the G stage. (B) Among this cluster, seven miRNAs were differentially or exclusively expressed in different comparisons. (C) Pathways associated with the exclusive and DE-miRNA target genes of this cluster. G: growing; D: dominant; P: preovulatory.

and bta-let-7i. To this point, the abundant expression patterns of eca-miR-148a and eca-miR-21, harmoniously follow suit with our previous publication of FF-EVs from stage-specific follicles in the mare, an adjacent representative model for reproduction in the rhinoceros [24]. Furthermore, a similar approach using FF-EVs in humans demonstrated the correlation of hsa-miR-148a with Day-3 embryo quality [51], and miR-21 in mouse oocyte maturation, blastocyst formation, and pre-implantation embryo development [52]. Analogously, the low expression of miR-451 in FF from endometriosis patients has been suggested to significantly affect oocyte competence for fertilization and pre-implantation embryo development via the aberrant expression of genes regulating the WNT signaling pathway [53]. Thus, it is likely that the integrative roles of these highly abundant EV-miRNAs may play critical function in regulating the timely undertaking needed to ovulate a competent gamete with the high-yielding capacity to develop past the blastocyst stage. Additionally, and

Downloaded from https://academic.oup.com/biolreprod/advance-article/doi/10.1093/biolre/ioae081/7679394 by Colorado State University user on 04 June 2024



(B) **Differentially and exclusively expressed miRNAs (Fold Change)**

Name	P vs. D	P vs. G
eca-miR-92a	-2.83	
eca-miR-486-5p	-7.26	-3.90
eca-miR-20a	-7.28	
eca-miR-23a	-11.05	
bta-miR-27a-3p	-11.51	
eca-miR-155	-16.44	
eca-miR-146b-5p	Not in P	Not in P
eca-miR-31	-80.70	-49.05
eca-miR-200a	Not in P	Not in P
eca-miR-205	Not in P	Not in P

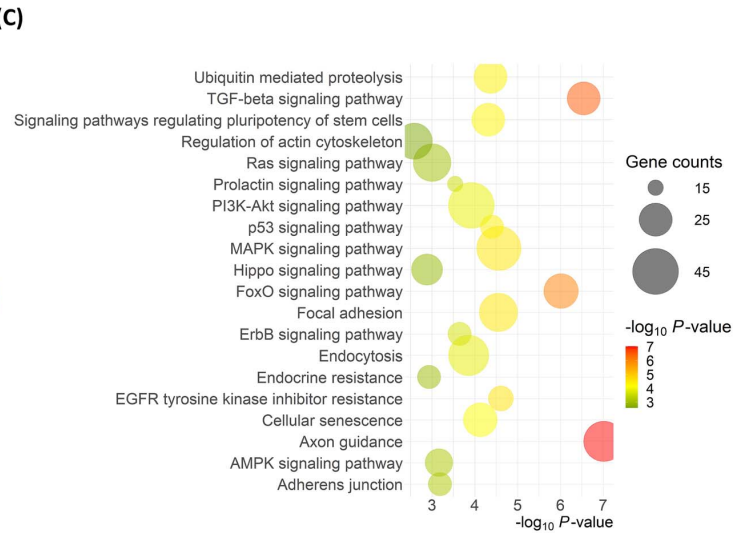


Figure 8. Cluster 6 consists of 47 miRNAs. (A) A group of 47 miRNAs exhibited a slight increase in their expression from the G to the D stage and then a sharp reduction at the P stage. (B) Among this cluster, 10 miRNAs were differentially or exclusively expressed in the different comparisons. (C) Pathways associated with the exclusive and DE-miRNA target genes of this cluster. G: growing; D: dominant; P: preovulatory.

consistent with our results, a previous study in cattle from different-sized follicles noted stable expression patterns of bta-let-7i in cumulus-oocyte complexes (COCs), denuded oocytes, and granulosa cells, albeit, a tendency for an increased expression of *DICER1* (miRNA processing machinery) in COCs from larger follicles [54]. These results suggest that during oogenesis, as follicles increase in size, the interaction between the oocyte and the surrounding follicular somatic cells may trigger miRNA machinery that directly involves the process of follicular maturation and ovulation. Further studies warrant the necessity to unveil the expression of such candidate miRNAs in biologically divergent samples collected from individual follicles based on size and subsequent maturation capacity *in vitro*.

Investigation of the effect of follicle size on the abundance of EV-miRNAs permitted the venture to transitionally decipher the alterations in small RNA cargoes governing follicle growth. The significant and exclusively expressed miRNAs in the D and G groups that don't meet the expression threshold in the P group include eca-miR-146b-5p, eca-miR-200a, and eca-miR-205, as observed by the green arrows in Figure 3(C). Recent studies found that EVs collected from failed embryonic development (non-blastocyst) contained high expression of bta-miR-146b [48], while the use of synthetic bta-miR-146b mimics revealed its transcriptional regulatory role in inducing apoptosis and encumbering embryo development and quality [55]. On the other hand, the absence of miR-378 in the G group may be dually regulated by the precise stage of the developing follicle. MicroRNA-378 has been posed to regulate intrafollicular estradiol production by targeting aromatase (*CYP19A1*) during specific stages of follicular development [56–58]. In accordance, levels of FF estradiol are increased in larger follicles further participating in the selection of a dominant preovulatory follicle [59], whereas the fate of growing follicles may be undetermined to this point.

Numerous DE-miRNAs amidst the three comparisons (G vs. D, P vs. G, and P vs. D; Figure 4) involve critical regulatory roles in the potential to govern follicular growth. Case in point, bta-miR-200b and eca-miR-379 upregulated in the G vs. D group, have been previously shown to be essential for ovulation and fertility in mice [60, 61], while granulosa cell-secreted exosomal miR-379-5P was shown as a proliferative response to androgenic stimulation in preantral stage follicular development [62]. Taken together, these data suggest a firmly integrated association between the EV-miRNA intrafollicular response and follicle growth/size. MicroRNA-200c downregulated in the P vs. G comparison, aligns in accordance with a study in humans where diminished expression of hsa-miR-200c-5p positively correlated with embryos permitting successful pregnancy [63]. Also in this study, eca-miR-423-3p (up-), eca-miR-155 (down-), were DE (P vs. D), and have been shown to inhibit granulosa cell apoptosis [64] and negatively regulate cumulus cell function, oocyte maturation, and blastocyst formation [65]. Whether the aforementioned DE-miRNAs serve as potential biomarkers governing follicle status for ovulation of a competent gamete remains to be determined.

miRNA cluster involvement via pathway regulation in developing follicles

The miRNA cluster analysis identified nine different expression patterns during the three follicular developmental stages.

Downloaded from https://academic.oup.com/biolreprod/advance-article/doi/10.1093/biolre/ioae081/7679394 by Colorado State University user on 04 June 2024

Three out of the nine clusters involved a higher number of DE-miRNAs. Clusters 3 and 6 shared a similar pattern, in which the miRNAs exhibited peak expression at the D stage compared to the G and P stages. Although both clusters include different DE-miRNAs, they showed similar targeted signaling pathways. Several studies have demonstrated the role of signaling pathways in coordinating ovarian follicle development [66]. During follicle development, primordial follicle activation and oocyte growth are under the control of PI3K/AKT/FOXO3 signaling pathways [67]. Targeting *PI3K* via the abundant expression of miR-214-3p disrupts PI3K/AKT/FOXO3 signaling pathways, leading to the inhibition of primordial follicle development [68]. Additionally, miRNAs are known to be involved in regulating the proliferation and apoptosis of granulosa cells [69, 70], and follicular development [71]. In bovine, a cluster of miRNAs, including miR-183-96-182, was among the top most significantly upregulated miRNAs in granulosa cells of dominant follicles compared to subordinate follicles [72]. In that study, we suggested that this miRNA cluster regulates and promotes granulosa cell proliferation by targeting the proapoptotic gene *FOXO1*. Similarly, in the current study, miR-183 was among cluster 3 with a significantly higher expression in the D compared to the P stage. Another interesting miRNA in cluster 6 is miR-92a, which exhibited the same pattern as miR-183. Previously, it has been reported that miR-92 coordinately regulates granulosa cell proliferation and differentiation by targeting *PTEN* and *BMPR2* genes [73]. The upregulation of miR-92 promoted granulosa cell proliferation, while its downregulation increased differentiation.

Cluster 5 exhibited a consistent declining expression pattern from the G toward the D and P stage groups. Interestingly, oocyte meiosis, cellular senescence, and cell cycle were among the top pathways targeted by the miRNAs of this cluster. In most mammals, it is well known that antral follicles maintain the first meiotic arrest of the oocytes during the diplotene stage of prophase I through the elevation of the intracellular cAMP levels that inactivate the oocyte maturation-promoting factor [74]. Additionally, several studies have demonstrated the potential role of miRNAs in regulating oocyte meiosis [75]. In yak oocytes, miR-342-3p was reported to play an important role in meiotic maturation by targeting *DNMT1* [76]. The same miRNA is involved in different biological processes to include inducing cancer cell proliferation arrest [77, 78]. Moreover, the role of miRNAs in regulating several biological functions in granulosa cells including cell cycle and senescence has been reported [79]. Among these miRNAs, miR-200b, one of the DE-miRNAs in cluster 5, was recently reported to suppress proliferation and induce senescence in ovine granulosa cells [80], indicating its role in follicular atresia. This may explain the pattern of this miRNA cluster with a higher abundance during the G phase, in which follicular atresia will take place, compared to the D and P phases. These findings together with our results, indicate the potential crucial role of EV-coupled miRNAs in folliculogenesis, atresia, and oocyte maturation in the rhinoceros, as it has been reported in various other domestic species [38, 71, 81]. Comprehensive studies on the precise roles of miRNAs in ovarian follicular development and oocyte meiosis will provide important insights into female reproductive fertility aiding to improving ARTs in this near-threatened species. Although *in vitro* maturation and culture systems have been developed for the SWR [1, 32], *in vitro* results remain largely suboptimal compared to domestic species, and improvements are necessary to have a large scale impact on the outcome of assisted reproduction. The possibility of using EVs to better understand EV-coupled miRNA dynamics regulating follicular growth to aide in improving the *in vitro* development of SWR embryos provides an uncharted and novel approach to support and facilitate conservation efforts in this species. Moreover, potential crossovers of EV-coupled molecular signaling during folliculogenesis in the SWR, could also provide valuable input to the identification of physiological and pathological reproductive conditions propagating abnormal fertility, and ultimately to the development of new reproductive strategies to improve ART outcomes for this species and many others.

Supplementary material

Supplementary data are available at *BIOLRE* online.

Acknowledgment

We thank the University of Colorado, Boulder EM Services Core Facility in the MCDB Department, for their knowledge and support with transmission electron microscopy imaging. Additionally, we acknowledge Ms. Mindy A. Meyers from the Department of Clinical Sciences at Colorado State University for her assistance with nanoparticle tracking analysis.

Author contributions

Project conceptualization: B.D., E.R.; Sample collections: R.F., B.D., E.R.; Sample processing: N.M.; Data analysis: A.G., N.M.; Writing—original draft: A.G., N.M., E.R.; Writing—review & editing: A.G., N.M., R.F., B.D., D.T., E.R.; Funding acquisition: B.D., D.T., E.R. All authors have read and approved the published version of this manuscript.

Conflict of interest: The authors have declared that no conflict of interest exists.

Data availability

Raw FASTQ files and the processed CSV files of the miRNA sequencing data were deposited in the National Center for Biotechnology Information (NCBI) Gene Expression Omnibus (GEO) database (https://www.ncbi.nlm.nih.gov/geo/) and can be accessed with the accession number GSE246260. Reported details on the experimental procedures concerning EVs have been submitted to the EV-TRACK knowledgebase with open access under (EV-TRACK ID: EV240017). Additional information regarding the findings of this study is available upon request from the corresponding author.

References

1. Hildebrandt TB, Hermes R, Colleoni S, Diecke S, Holtze S, Renfree MB, Stejskal J, Hayashi K, Drukker M, Loi P, Göritz F, Lazzari G, *et al.* Embryos and embryonic stem cells from the white rhinoceros. *Nat Commun* 2018; **9**:2589.
2. Hildebrandt TB, Holtze S, Colleoni S, Hermes R, Stejskal J, Lekolool I, Ndereeh D, Omondi P, Kariuki L, Mijele D, Mutisya S, Ngulu S, *et al.* In vitro fertilization (IVF) program in white rhinoceros. *Reproduction* 2023; **166**:383–399.
3. Hildebrandt TB, Hermes R, Goeritz F, Appeltant R, Colleoni S, de Mori B, Diecke S, Drukker M, Galli C, Hayashi K, Lazzari G, Loi P, *et al.* The ART of bringing extinction to a freeze - history and future of species conservation, exemplified by rhinos. *Theriogenology* 2021; **169**:76–88.
4. Radcliffe RW, Czekala NM, Osofsky SA. Combined serial ultrasonography and fecal progestin analysis for reproductive

Downloaded from https://academic.oup.com/biolreprod/advance-article/doi/10.1093/biolre/ioae081/7679394 by Colorado State University user on 04 June 2024

evaluation of the female white rhinoceros (Ceratotherium simum simum): Preliminary results. *Zoo Biol* 1997; **16**:445–456.
5. Pryor P, Tibary A. Management of estrus in the performance mare. *Clin Tech Equine Pract* 2005; **4**:197–209.
6. Roth TL, Schook MW, Stoops MA. Monitoring and controlling ovarian function in the rhinoceros. *Theriogenology* 2018; **109**: 48–57.
7. Komatsu K, Masubuchi S. Observation of the dynamics of follicular development in the ovary. *Reprod Med Biol* 2017; **16**:21–27.
8. Pennington PM, Marshall KL, Capiro JM, Howard L, Durrant BS. Pregnancies following long luteal phases in southern white rhinoceros (Ceratotherium simum simum). *Zoo Biol* 2020; **39**: 141–144.
9. Brown JL, Bellem AC, Fouraker M, Wildt DE, Roth TL. Comparative analysis of gonadal and adrenal activity in the black and white rhinoceros in North America by noninvasive endocrine monitoring. *Zoo Biol* 2001; **20**:463–486.
10. Hindle JE, Möstl E, Hodges JK. Measurement of urinary oestrogens and 20 alpha-dihydroprogesterone during ovarian cycles of black (Diceros bicornis) and white (Ceratotherium simum) rhinoceroses. *J Reprod Fertil* 1992; **94**:237–249.
11. Patton ML, Swaisgood RR, Czekala NM, White AM, Fetter GA, Montagne JP, Rieches RG, Lance VA. Reproductive cycle length and pregnancy in the southern white rhinoceros (Ceratotherium simum simum) as determined by fecal pregnane analysis and observations of mating behavior. *Zoo Biol* 1999; **18**:111–127.
12. Schwarzenberger F, Walzer C, Tomasova K, Vahala J, Meister J, Goodrowe KL, Zima J, Strauss G, Lynch M. Faecal progesterone metabolite analysis for non-invasive monitoring of reproductive function in the white rhinoceros (Ceratotherium simum). *Anim Reprod Sci* 1998; **53**:173–190.
13. van der Goot A, Catharina MGB, Millar RP, Paris MCJ, Ganswindt A. Profiling patterns of fecal 20-oxopregnane concentrations during ovarian cycles in free-ranging southern white rhinoceros (Ceratotherium simum simum). *Anim Reprod Sci* 2015; **161**:89–95.
14. Pennington PM, Durrant BS. Assisted reproductive technologies in captive rhinoceroses. *Mammal Rev* 2019; **49**:1–15.
15. Pennington PM, Marshall KL, Capiro JM, Felton RG, Durrant BS. Ovulation induction in anovulatory southern white rhinoceros (Ceratotherium simum simum) without altrenogest. *Conserv Physiol* 2019; **7**:coz033.
16. Bordignon V, Morin N, Durocher J, Bousquet D, Smith LC. GnRH improves the recovery rate and the in vitro developmental competence of oocytes obtained by transvaginal follicular aspiration from superstimulated heifers. *Theriogenology* 1997; **48**:291–298.
17. Ogata Y, Yu G-M, Hidaka T, Matzushige T, Maeda T. Effective embryo production from Holstein cows treated with gonadotropin-releasing hormone during early lactation. *Theriogenology* 2016; **86**:1421–1426.
18. Squires EL, Carnevale EM, McCue PM, Bruemmer JE. Embryo technologies in the horse. *Theriogenology* 2003; **59**:151–170.
19. Doyle LM, Wang MZ. Overview of extracellular vesicles, their origin, composition, purpose, and methods for exosome isolation and analysis. *Cells* 2019; **8**:727.
20. György B, Szabó TG, Pásztói M, Pál Z, Misják P, Aradi B, László V, Pállinger E, Pap E, Kittel A, Nagy G, Falus A, *et al.* Membrane vesicles, current state-of-the-art: emerging role of extracellular vesicles. *Cell Mol Life Sci* 2011; **68**:2667–2688.
21. Sohel MMH, Hoelker M, Noferesti SS, Salilew-Wondim D, Tholen E, Looft C, Rings F, Uddin MJ, Spencer TE, Schellander K, Tesfaye D. Exosomal and non-exosomal transport of extra-cellular microRNAs in follicular fluid: implications for bovine oocyte developmental competence. *PloS One* 2013; **8**:e78505.
22. Noferesti SS, Sohel MMH, Hoelker M, Salilew-Wondim D, Tholen E, Looft C, Rings F, Neuhoff C, Schellander K, Tesfaye D. Controlled ovarian hyperstimulation induced changes in the expression of circulatory miRNA in bovine follicular fluid and blood plasma. *J Ovarian Res* 2015; **8**:81.
23. Hailay T, Hoelker M, Poirier M, Gebremedhn S, Rings F, Saeed-Zidane M, Salilew-Wondim D, Dauben C, Tholen E, Neuhoff C, Schellander K, Tesfaye D. Extracellular vesicle-coupled miRNA profiles in follicular fluid of cows with divergent post-calving metabolic status. *Sci Rep* 2019; **9**:12851.
24. Gebremedhn S, Gad A, Ishak GM, Menjivar NG, Gastal MO, Feugang JM, Prochazka R, Tesfaye D, Gastal EL. Dynamics of extracellular vesicle-coupled microRNAs in equine follicular fluid associated with follicle selection and ovulation. *Mol Hum Reprod* 2023; **29**:gaad009.
25. Tesfaye D, Hailay T, Salilew-Wondim D, Hoelker M, Bitseha S, Gebremedhn S. Extracellular vesicle mediated molecular signaling in ovarian follicle: Implication for oocyte developmental competence. *Theriogenology* 2020; **150**:70–74.
26. Gervasi MG, Soler AJ, González-Fernández L, Alves MG, Oliveira PF, Martín-Hidalgo D. Extracellular vesicles, the road toward the improvement of ART outcomes. *Animals (Basel)* 2020; **10**:2171.
27. Liu C, Wang M, Yao H, Cui M, Gong X, Wang L, Sui C, Zhang H. Inhibition of oocyte maturation by follicular extracellular vesicles of nonhyperandrogenic PCOS patients requiring IVF. *J Clin Endocrinol Metab* 2023; **108**:1394–1404.
28. Menjivar NG, Gad A, Thompson RE, Meyers MA, Hollinshead FK, Tesfaye D. Bovine oviductal organoids: a multi-omics approach to capture the cellular and extracellular molecular response of the oviduct to heat stress. *BMC Genomics* 2023; **24**:646.
29. Da Silveira JC, Andrade GM, Del Collado M, Sampaio RV, Sangalli JR, Silva LA, Pinaffi FVL, Jardim IB, Cesar MC, Nogueira MFG, Cesar ASM, Coutinho LL, *et al.* Supplementation with small-extracellular vesicles from ovarian follicular fluid during in vitro production modulates bovine embryo development. *PloS One* 2017; **12**:e0179451.
30. Asaadi A, Dolatabad NA, Atashi H, Raes A, Van Damme P, Hoelker M, Hendrix A, Pascottini OB, Van Soom A, Kafi M, Pavani KC. Extracellular vesicles from follicular and ampullary fluid isolated by density gradient ultracentrifugation improve bovine embryo development and quality. *Int J Mol Sci* 2021; **22**:578.
31. Menjivar NG, Gad A, Gebremedhn S, Ghosh S, Tesfaye D. Granulosa cell-derived extracellular vesicles mitigate the detrimental impact of thermal stress on bovine oocytes and embryos. *Front Cell Dev Biol* 2023; **11**:1142629.
32. Ruggeri E, Young C, Ravida N, Sirard MA, Krisher R, de la Rey M, Herbst C, Durrant B. Glucose consumption and gene expression in granulosa cells collected before and after in vitro oocyte maturation in the southern white rhinoceros (Ceratotherium simum simum). *Reprod Fertil Dev* 2022; **34**:875–888.
33. Ruggeri E, Klohonatz K, Sirard M-A, Durrant B, Coleman S. Genomic insights into southern white rhinoceros (Ceratotherium simum simum) reproduction: Revealing granulosa cell gene expression. *Theriogenology Wild* 2023; **3**:100055.
34. Klohonatz KM, Cameron AD, Hergenreder JR, Da Silveira JC, Belk AD, Veeramachaneni DNR, Bouma GJ, Bruemmer JE. Circulating miRNAs as potential alternative cell signaling associated with maternal recognition of pregnancy in the mare. *Biol Reprod* 2016; **95**:124.
35. Théry C, Witwer KW, Aikawa E, Alcaraz MJ, Anderson JD, Andriantsitohaina R, Antoniou A, Arab T, Archer F, Atkin-Smith GK, Ayre DC, Bach J-M, *et al.* Minimal information for studies of extracellular vesicles 2018 (MISEV2018): a position statement of the International Society for Extracellular Vesicles and update of the MISEV2014 guidelines. *J Extracell Vesicles* 2018; **7**:1535750.
36. Welsh JA, Goberdhan DCI, O'Driscoll L, Buzas EI, Blenkiron C, Bussolati B, Cai H, Di Vizio D, Driedonks TAP, Erdbrügger U, Falcon-Perez JM, Fu Q-L, *et al.* Minimal information for studies of extracellular vesicles (MISEV2023): From basic to advanced approaches. *J Extracell Vesicles* 2024; **13**:e12404.
37. van Deun J, Mestdagh P, Agostinis P, Akay Ö, Anand S, Anckaert J, Martinez ZA, Baetens T, Beghein E, Bertier L, Berx G,

Downloaded from https://academic.oup.com/biolreprod/advance-article/doi/10.1093/biolre/ioae081/7679394 by Colorado State University user on 04 June 2024

Boere J, *et al.* EV-TRACK: transparent reporting and centralizing knowledge in extracellular vesicle research. *Nat Methods* 2017; **14**: 228–232.
38. Gad A, Joyce K, Menjivar NG, Heredia D, Rojas CS, Tesfaye D, Gonella-Diaza A. Extracellular vesicle-microRNAs mediated response of bovine ovaries to seasonal environmental changes. *J Ovarian Res* 2023; **16**:101.
39. Leiberich M, Marais HJ, Naidoo V. Phylogenetic analysis of the cytochrome P450 (CYP450) nucleotide sequences of the horse and predicted CYP450s of the white rhinoceros (Ceratotherium simum) and other mammalian species. *PeerJ* 2018; **6**:e5718.
40. Robinson MD, Oshlack A. A scaling normalization method for differential expression analysis of RNA-seq data. *Genome Biol* 2010; **11**:R25.
41. Benjamini Y, Drai D, Elmer G, Kafkafi N, Golani I. Controlling the false discovery rate in behavior genetics research. *Behav Brain Res* 2001; **125**:279–284.
42. Kumar L, Futschik ME. Mfuzz: a software package for soft clustering of microarray data. *Bioinformation* 2007; **2**:5–7.
43. Sticht C, De La Torre C, Parveen A, Gretz N. miRWalk: an online resource for prediction of microRNA binding sites. *PloS One* 2018; **13**:e0206239.
44. Ogata H, Goto S, Sato K, Fujibuchi W, Bono H, Kanehisa M. KEGG: Kyoto Encyclopedia of Genes and Genomes. *Nucleic Acids Res* 1999; **27**:29–34.
45. Shannon P, Markiel A, Ozier O, Baliga NS, Wang JT, Ramage D, Amin N, Schwikowski B, Ideker T. Cytoscape: a software environment for integrated models of biomolecular interaction networks. *Genome Res* 2003; **13**:2498–2504.
46. Santonocito M, Vento M, Guglielmino MR, Battaglia R, Wahlgren J, Ragusa M, Barbagallo D, Borzì P, Rizzari S, Maugeri M, Scollo P, Tatone C, *et al.* Molecular characterization of exosomes and their microRNA cargo in human follicular fluid: bioinformatic analysis reveals that exosomal microRNAs control pathways involved in follicular maturation. *Fertil Steril* 2014; **102**:1751–61.e1.
47. Qasemi M, Amidi F. Extracellular microRNA profiling in human follicular fluid: new biomarkers in female reproductive potential. *J Assist Reprod Genet* 2020; **37**:1769–1780.
48. Pavani KC, Meese T, Pascottini OB, Guan X, Lin X, Peelman L, Hamacher J, van Nieuwerburgh F, Deforce D, Boel A, Heindryckx B, Tilleman K, *et al.* Hatching is modulated by microRNA-378a-3p derived from extracellular vesicles secreted by blastocysts. *Proc Natl Acad Sci U S A* 2022; **119**:e2122708119.
49. Hung W-T, Hong X, Christenson LK, McGinnis LK. Extracellular vesicles from bovine follicular fluid support cumulus expansion. *Biol Reprod* 2015; **93**:117.
50. Ding Q, Jin M, Kalds P, Meng C, Wang H, Zhong J, Wang X, Chen Y. Comparison of microRNA profiles in extracellular vesicles from small and large goat follicular fluid. *Animals (Basel)* 2021; **11**:3190.
51. Martinez RM, Liang L, Racowsky C, Dioni L, Mansur A, Adir M, Bollati V, Baccarelli AA, Hauser R, Machtinger R. Extracellular microRNAs profile in human follicular fluid and IVF outcomes. *Sci Rep* 2018; **8**:17036.
52. Dehghan Z, Mohammadi-Yeganeh S, Rezaee D, Salehi M. MicroRNA-21 is involved in oocyte maturation, blastocyst formation, and pre-implantation embryo development. *Dev Biol* 2021; **480**:69–77.
53. Li X, Zhang W, Fu J, Xu Y, Gu R, Qu R, Li L, Sun Y, Sun X. MicroRNA-451 is downregulated in the follicular fluid of women with endometriosis and influences mouse and human embryonic potential. *Reprod Biol Endocrinol* 2019; **17**:96.
54. Miles JR, McDaneld TG, Wiedmann RT, Cushman RA, Echternkamp SE, Vallet JL, Smith TPL. MicroRNA expression profile in bovine cumulus-oocyte complexes: possible role of let-7 and miR-106a in the development of bovine oocytes. *Anim Reprod Sci* 2012; **130**:16–26.
55. Pavani KC, XueFeng G, Chunduru J, Meese T, Peelman LJ, Van Nieuwerburgh F, Deforce D, Hendrix A, Tilleman K, Van Soom A, Smits K. MicroRNA-146b negatively affects bovine embryo development and quality. *Reproduction* 2023; **167**: e230155.
56. Xu S, Linher-Melville K, Yang BB, de Wu LJ, Li J. Micro-RNA378 (miR-378) regulates ovarian estradiol production by targeting aromatase. *Endocrinology* 2011; **152**:3941–3951.
57. Schauer SN, Sontakke SD, Watson ED, Esteves CL, Donadeu FX. Involvement of miRNAs in equine follicle development. *Reproduction* 2013; **146**:273–282.
58. Pan B, Toms D, Shen W, Li J. MicroRNA-378 regulates oocyte maturation via the suppression of aromatase in porcine cumulus cells. *Am J Physiol Endocrinol Metab* 2015; **308**:E525–E534.
59. Hutz RJ, Dierschke DJ, Wolf RC. Estradiol-induced follicular atresia in rhesus monkeys is not prevented by exogenous gonadotropins. *Am J Primatol* 1991; **23**:247–255.
60. Hasuwa H, Ikawa M, Okabe M. Disruption of miR-200b leads to female infertility. *Biol Reprod* 2008; **78**:213.
61. Hasuwa H, Ueda J, Ikawa M, Okabe M. miR-200b and miR-429 function in mouse ovulation and are essential for female fertility. *Science* 2013; **341**:71–73.
62. Salehi R, Wyse BA, Asare-Werehene M, Esfandiarinezhad F, Abedini A, Pan B, Urata Y, Gutsol A, Vinas JL, Jahangiri S, Xue K, Xue Y, *et al.* Androgen-induced exosomal miR-379-5p release determines granulosa cell fate: cellular mechanism involved in polycystic ovaries. *J. Ovarian Res.* 2023; **16**:74.
63. Fang F, Li Z, Yu J, Long Y, Zhao Q, Ding X, Wu L, Shao S, Zhang L, Xiang W. MicroRNAs secreted by human embryos could be potential biomarkers for clinical outcomes of assisted reproductive technology. *J Adv Res* 2021; **31**:25–34.
64. Li Y, Zhang Z, Wang S, Du X, Li Q. miR-423 sponged by lncRNA NORHA inhibits granulosa cell apoptosis. *J Anim Sci Biotechnol* 2023; **14**:154.
65. Dehghan Z, Mohammadi-Yeganeh S, Salehi M. MiRNA-155 regulates cumulus cells function, oocyte maturation, and blastocyst formation. *Biol Reprod* 2020; **103**:548–559.
66. Li L, Shi X, Shi Y, Wang Z. The signaling pathways involved in ovarian follicle development. *Front Physiol* 2021; **12**:730196.
67. John GB, Gallardo TD, Shirley LJ, Castrillon DH. Foxo3 is a PI3K-dependent molecular switch controlling the initiation of oocyte growth. *Dev Biol* 2008; **321**:197–204.
68. Zeng J, Sun Y, Li X, Zhu J, Zhang W, Lu W, Weng Y, Liu J. 2,5-Hexanedione influences primordial follicular development in cultured neonatal mouse ovaries by interfering with the PI3K signaling pathway via miR-214-3p. *Toxicol Appl Pharmacol* 2020; **409**:115335.
69. Yao G, Yin M, Lian J, Tian H, Liu L, Li X, Sun F. MicroRNA-224 is involved in transforming growth factor-beta-mediated mouse granulosa cell proliferation and granulosa cell function by targeting Smad4. *Mol Endocrinol* 2010; **24**:540–551.
70. Zhang Q, Sun H, Jiang Y, Ding L, Wu S, Fang T, Yan G, Hu Y. MicroRNA-181a suppresses mouse granulosa cell proliferation by targeting activin receptor IIA. *PloS One* 2013; **8**:e59667.
71. Gebremedhn S, Pandey HO, Salilew-Wondim D, Hoelker M, Schellander K, Tesfaye D. Dynamics and role of microRNAs during mammalian follicular development. *Anim Reprod* 2016; **13**: 257–263.
72. Gebremedhn S, Salilew-Wondim D, Hoelker M, Rings F, Neuhoff C, Tholen E, Schellander K, Tesfaye D. MicroRNA-183-96-182 cluster regulates bovine granulosa cell proliferation and cell cycle transition by coordinately targeting FOXO1. *Biol Reprod* 2016; **94**:127.
73. Andreas E, Hoelker M, Neuhoff C, Tholen E, Schellander K, Tesfaye D, Salilew-Wondim D. MicroRNA 17-92 cluster regulates proliferation and differentiation of bovine granulosa cells by targeting PTEN and BMPR2 genes. *Cell Tissue Res* 2016; **366**: 219–230.
74. Pan B, Li J. The art of oocyte meiotic arrest regulation. *Reprod Biol Endocrinol* 2019; **17**:8.
75. Li Y, Adur MK, Hale BJ, Ross JW. Regulation of oogenesis by noncoding RNAs. In: Skinner MK (ed.), *Encyclopedia of Reproduction*, 2nd ed. Amsterdam: Elsevier; 2018: 190–196.

Downloaded from https://academic.oup.com/biolreprod/advance-article/doi/10.1093/biolre/ioae081/7679394 by Colorado State University user on 04 June 2024

76. Xiong X, Yang M, Yu H, Hu Y, Yang L, Zhu Y, Fei X, Pan B, Xiong Y, Fu W, Li J. MicroRNA-342-3p regulates yak oocyte meiotic maturation by targeting DNA methyltransferase 1. *Reprod Domest Anim* 2022; **57**:761–770.
77. Wang H, Wu J, Meng X, Ying X, Zuo Y, Liu R, Pan Z, Kang T, Huang W. MicroRNA-342 inhibits colorectal cancer cell proliferation and invasion by directly targeting DNA methyltransferase 1. *Carcinogenesis* 2011; **32**:1033–1042.
78. Zhao L, Zhang Y. miR-342-3p affects hepatocellular carcinoma cell proliferation via regulating NF-κB pathway. *Biochem Biophys Res Commun* 2015; **457**:370–377.
79. Xu Y, Zhang A, Zhang Z, Yuan X, Chen Z, Zhang H, Li J. MicroRNA-34c regulates porcine granulosa cell function by targeting forkhead box O3a. *J Integr Agric* 2017; **16**:2019–2028.
80. Song P, Chen X, Zhang P, Zhou Y, Zhou R. miR-200b/MYBL2/CDK1 suppresses proliferation and induces senescence through cell cycle arrest in ovine granulosa cells. *Theriogenology* 2023; **207**:19–30.
81. Da Silveira JC, de Ávila A, Clara FCM, Garrett HL, Bruemmer JE, Winger QA, Bouma GJ. Cell-secreted vesicles containing microRNAs as regulators of gamete maturation. *J Endocrinol* 2018; **236**:R15–R27.

Downloaded from https://academic.oup.com/biolreprod/advance-article/doi/10.1093/biolre/ioae081/7679394 by Colorado State University user on 04 June 2024

Feugang *et al.*
Journal of Animal Science and Biotechnology (2024) 15:137
https://doi.org/10.1186/s40104-024-01097-2

Journal of Animal Science and Biotechnology

RESEARCH Open Access

Seasonal influence on miRNA expression dynamics of extracellular vesicles in equine follicular fluid

Jean M. Feugang[1*], Ahmed Gad[2,3], Nico G. Menjivar[2], Ghassan M. Ishak[4,5], Samuel Gebremedhn[6], Melba O. Gastal[5], Notsile H. Dlamini[1], Radek Prochazka[7], Eduardo L. Gastal[5] and Dawit Tesfaye[2]

Abstract

Background Ovarian follicular fluid (FF) is a dynamic environment that changes with the seasons, affecting follicle development, ovulation, and oocyte quality. Cells in the follicles release tiny particles called extracellular vesicles (EVs) containing vital regulatory molecules, such as microRNAs (miRNAs). These miRNAs are pivotal in facilitating communication within the follicles through diverse signaling and information transfer forms. EV-coupled miRNA signaling is implicated to be associated with ovarian function, follicle and oocyte growth and response to various environmental insults. Herein, we investigated how seasonal variations directly influence the ovulatory and anovulatory states of ovarian follicles and how are they associated with follicular fluid EV-coupled miRNA dynamics in horses.

Results Ultrasonographic monitoring and follicular fluid aspiration of preovulatory follicles in horses during the anovulatory (spring: non-breeding) and ovulatory (spring, summer, and fall: breeding) seasons and subsequent EV isolation and miRNA profiling identified significant variation in EV-miRNA cargo content. We identified 97 miRNAs with differential expression among the groups and specific clusters of miRNAs involved in the spring transition (miR-149, -200b, -206, -221, -328, and -615) and peak breeding period (including miR-143, -192, -451, -302b, -100, and let-7c). Bioinformatic analyses showed enrichments in various biological functions, e.g., transcription factor activity, transcription and transcription regulation, nucleic acid binding, sequence-specific DNA binding, p53 signaling, and post-translational modifications. Cluster analyses revealed distinct sets of significantly up- and down-regulated miRNAs associated with spring anovulatory (Cluster 1) and summer ovulation–the peak breeding season (Clusters 4 and 6).

Conclusions The findings from the current study shed light on the dynamics of FF-EV-coupled miRNAs in relation to equine ovulatory and anovulatory seasons, and their roles in understanding the mechanisms involved in seasonal shifts and ovulation during the breeding season warrant further investigation.

Keywords Extracellular vesicle, Follicle growth, Follicular fluid, Horse, Mare, Ovulation, Pre-ovulation, Seasonal breeding

*Correspondence:
Jean M. Feugang
j.feugang@msstate.edu
Full list of author information is available at the end of the article

© The Author(s) 2024. **Open Access** This article is licensed under a Creative Commons Attribution 4.0 International License, which permits use, sharing, adaptation, distribution and reproduction in any medium or format, as long as you give appropriate credit to the original author(s) and the source, provide a link to the Creative Commons licence, and indicate if changes were made. The images or other third party material in this article are included in the article's Creative Commons licence, unless indicated otherwise in a credit line to the material. If material is not included in the article's Creative Commons licence and your intended use is not permitted by statutory regulation or exceeds the permitted use, you will need to obtain permission directly from the copyright holder. To view a copy of this licence, visit http://creativecommons.org/licenses/by/4.0/. The Creative Commons Public Domain Dedication waiver (http://creativecommons.org/publicdomain/zero/1.0/) applies to the data made available in this article, unless otherwise stated in a credit line to the data.

Introduction

Folliculogenesis is a well-orchestrated regulatory process involving autocrine, paracrine, and endocrine signaling steadily influenced by intrinsic and extrinsic factors in the female body [1–3]. Seasonal variations in temperature extremes, daylight duration, and relative humidity are among the many extrinsic factors that disrupt intrafollicular molecular interactions, leading to impaired fertility in livestock species [1, 4, 5]. Numerous studies have reported the negative impacts of seasonal variation at the cellular (e.g., cell proliferation and apoptosis) and endocrine (e.g., increased production of steroids) levels, affecting tissue organization (e.g., reduction in follicle diameter and luteolytic failure) in farm animals [6–8]. Consistent with these observations, in vitro studies have demonstrated such adverse effects on ovarian follicle growth, oocyte maturation, and embryo production [9–11]. Understanding how environmental factors affect the reproductive capabilities of animals like horses can help improve animal husbandry practices.

The mare is considered a seasonal breeder and is often studied to understand potential changes in fertility during different seasons of the year [1, 12]. The mare typically experiences a major ovulatory wave every 21 to 24 d. During this time, one large follicle of the wave, typically at least 28 mm in diameter, becomes the dominant follicle [13, 14], eventually growing to preovulatory size (around 30–45 mm in diameter) and ovulating in the spring (SOV), summer (SUM), and/or fall (FOV) ovulatory seasons. Meanwhile, homologous dominant follicles regress during the non-breeding seasons, such as the transient spring (SAN) and fall anovulatory seasons. The mare enters deep anestrus during the winter with follicles less than 20 mm in diameter [1, 15, 16]. Previous research suggests that during anovulatory seasons and low ovarian activity, the difference in ovarian activities between small and large follicles influences the potential for exogenous gonadotropin-releasing hormone to induce ovulation [1, 17]. These findings underscore the importance of studying preovulatory follicles in the context of seasonal variations, as it has the potential to significantly enhance our understanding and thereby improve female fertility in seasonally inactive species.

Various studies have demonstrated continuous changes in ovarian activity of non-pregnant mares throughout the year, with periods of high activity during the summer, low activity during the winter, and irregular and interspaced activity during the spring and fall transitional seasons [1, 18, 19]. Additionally, aberrant blood flow, hormonal levels, and gene expression changes have previously been observed among follicles from different seasons [19–21]. Recent studies in horses focusing on the effects of seasons demonstrated further aberrations in the gene expression profiles of follicular cells [22], as well as the proteomic profiles [23, 24] and miRNA signatures [25] from follicular fluid (FF) and follicular fluid-derived extracellular vesicles (FF-EVs), respectively. The miRNA, the small noncoding RNA molecules of approximately 22 nucleotides long, are expressed in the ovary to regulate various aspects of follicle growth post-transcriptionally. This includes miR-224, miR-378, and miR-383 in follicle growth, miR-34 in atresia, miR-21 in ovulation, miR-175p and let-7b in angiogenesis, and miR-23a, miR-92, and miR-143 in steroidogenesis [26, 27]. The detection of miRNAs encapsulated in EVs in the ovarian FF of livestock such as cows, pigs, sheep, and mares and their profiles were associated with long-term effects during in vitro fertilization [28]. Research also shows that these miRNAs have effects during heat stress [29, 30] and seasonal changes [31]. Together, these studies conclude that season-specific factors comprising the FF may inherently affect follicle function and oocyte maturation, and the understanding of miRNA dynamics in FF-EVs provides insights into reproductive health and potential therapies.

This study aims to explore the miRNAs associated with equine FF-EVs, which are small lipid-enclosed particles released by various cell types and classified as exosomes (30–130 nm) and microvesicles (50–1,000 nm). These particles are essential in cell-to-cell communication and transferring genetic information within the follicular environment [32, 33]. They transport and shuttle regulatory molecules such as lipids, proteins, and small RNAs to the target cells in a timely delivery system [34, 35]. A recent study observed changes in the miRNA profiles of bovine FF-EVs collected during summer and winter, suggesting the possible role of EV-coupled miRNAs in regulating ovarian response to environmental variations and controlling follicular activity [31]. Here, we hypothesize that the miRNA content of equine FF-EVs varies depending on the ovulatory and anovulatory seasons and influences follicular activity during seasonal variations, which can impact mares' fertility. Our study aims to investigate the expression and dynamics of the equine FF-EV miRNA profiles in preovulatory follicles during ovulatory (SOV, SUM, and FOV) and anovulatory (SAN) seasons.

Materials and methods

See Additional file 1 for further details.

Animals, transrectal ultrasonography and seasonal grouping

The study used 19 multiparous Quarter Horse mares, weighing between 400 and 600 kg and aged 8 to 14 years, grazed freely in the northern hemisphere (latitude, 37.7° N) under natural light conditions with unlimited access to fresh water and trace-mineralized salt. During the

non-ovulatory season (SAN) and ovulatory seasons (SOV, SUM, and FOV), transvaginal ultrasound-guided ablations of all ovarian follicles were carried out 10–11 d after the ovulation of the previous cycle to induce a new follicular wave [36]. Then, daily ultrasonographic tracking was performed until the dominant follicle reached a preovulatory diameter. Only animals showing continuous ultrasonographic follicle growth for at least three consecutive days, uterine edema (estrus-like), and the absence of a corpus luteum at the time of FF aspiration were used for sample collection.

Follicular-fluid sample collection

All mares were adequately prepared and sedated before follicular ablation and FF sampling procedures, as described in previous studies [37, 38]. Preovulatory follicles with a diameter of 30–35 mm were aspirated into sterile vials during specific seasons: SAN (March), SOV (April and May), SUM (June to July), and FOV (September). Following the abovementioned restrictions, only 6 to 12 mares per seasonal group were used, resulting in 42 clear FF samples collected throughout the year. These FF samples were promptly centrifuged (1,600 × *g* for 10 min at 4 °C), and the supernatants were then subjected to subsequent centrifugation (3,200 × *g* for 15 min at 4 °C) and stored at −80 °C for downstream analysis.

Isolation of extracellular vesicles from follicular fluid

The experiment combined two to three FF samples of individual mares (0.5 mL) to create four biological replicates (1.0–1.5 mL/replicate) for isolating extracellular vesicles (EVs). The FF samples underwent a series of centrifugation steps to remove cells (500 × *g* for 5 min) and debris (4,000 × *g* for 5 min) and were then filtered (0.22 μm) to exclude large particles. The EVs were then isolated using centrifugation (25,000 × *g* for 30 min at 4 °C) and ultracentrifugation (120,000 × *g* for 70 min at 4 °C) procedures. Finally, the isolated EVs were washed, resuspended in PBS, and stored at −80 °C for further analysis.

Morphological and molecular characterization of FF-EVs

Specific proteins of frozen-thawed EVs were analyzed using the JESS Simple Western™ instrument (ProteinSimple®, Bio-Techne, Minneapolis, MN, USA). Proteins CD81, FLOT-1, and TSG101 were checked, while the absence of cytochrome C (CYCS) was ensured. Protein lysate (10 μL) was extracted using RIPA lysis buffer and run under JESS's Assay Module for Protein Normalization (AM-PN001). The analysis used 25 capillary cartridges and specific antibodies, followed by detection and analysis using Compass for Simple Western software. *The size distribution and concentration of EVs* were measured using the Zetaview Particle Metrix (Particle Metrix, Germany). EV samples were diluted (1,000×) in sterile PBS and analyzed using the ZetaView Laser scattering microscope with an LM14C laser. For each sample, 11 independent video measurements were recorded at 11 independent positions, and video files were analyzed using ZetaView software version 8.05.12. *The morphology of EVs* was analyzed using a transmission electron microscope (TEM) according to the methods previously reported [39]. Purified EVs were placed on grids, stained, and viewed using an FEI/TFS Tecnai T12 Spirit TEM. All relevant data have been submitted to the EV-TRACK knowledgebase (https://evtrack.org) with the EV-TRACK ID EV231010 [40].

Total RNA extraction, library preparation, and sequencing

The EV samples from different experimental groups were used to isolate total RNA, including miRNAs, using a Norgen Exosomal RNA Isolation kit (Norgen, Canada). Genomic DNA contaminants were eliminated using on-column DNA digestion, and RNA concentration and size distribution were assessed using an Agilent 2100 Bioanalyzer (Agilent Technologies, Santa Clara, CA, USA). Small-RNA libraries were prepared for next-generation sequencing with Illumina's TruSeq Small RNA Library Prep Kit. Library quantity and quality were assessed using a Qubit 2.0 Fluorometer and an Agilent 2100 Bioanalyzer. The libraries were then sequenced using a NovaSeq6000 instrument (Illumina, Inc., San Diego, CA, USA), as single-end reads (50 bases).

Small RNAseq data analysis

The FASTQ files for each sample were generated using the bcl2fastq software. Data analysis was performed using CLC Genomics Workbench version 21. Raw sequencing reads were trimmed based on quality score (Q-score > 30), ambiguous nucleotides (≤ 2 nucleotides), read length (≥ 15 nucleotides), and removal of adapter sequences. The reads were mapped to the equine reference genome (EquCab3.0) and annotated against equine precursor and mature miRNAs (miBase database, release 22). Raw expression data were normalized using the TMM normalization method [41] and presented as TMM-adjusted Counts Per Million (CPM). MiRNAs exhibiting a fold change (FC) ≥ 2 and a *P*-adjusted value (FDR) < 0.05 [42] were considered differentially expressed (DE). The raw FASTQ and processed CSV files have been deposited in the NCBI's Gene Expression Omnibus (GEO) under accession number GSE249220.

Cluster analysis, target gene prediction, and ontological classification

The expressed miRNAs were grouped into different clusters based on their expression profiles during different seasons using the Mfuzz Bioconductor package [43]. The genes targeted by the DE-miRNAs were identified using the human homologous miRNAs in the miRWalk database [44]. Validated target genes from miRTarBase (version 7.0) and standard target gene predictions by TargetScan (version 7.1) and miRDB (release 5.0) within miRWalk were chosen for pathway analysis using the DAVID bioinformatics web tool (https://david.ncifcrf.gov/) and the KEGG pathway database [45]. Furthermore, a network of all DE-miRNAs from different comparisons was created using Cytoscape [46].

Results

Seasonal alterations dynamically impact the intrafollicular secretion of EVs

The FF-EVs isolated from mares in SAN, SOV, SUM, and FOV underwent thorough morphological and molecular characterization, strictly following the guidelines of the International Society of Extracellular Vesicles (ISEV) [47]. A detailed summary of the FF-EVs' characterization is presented in Fig. 1, highlighting the use of TEM

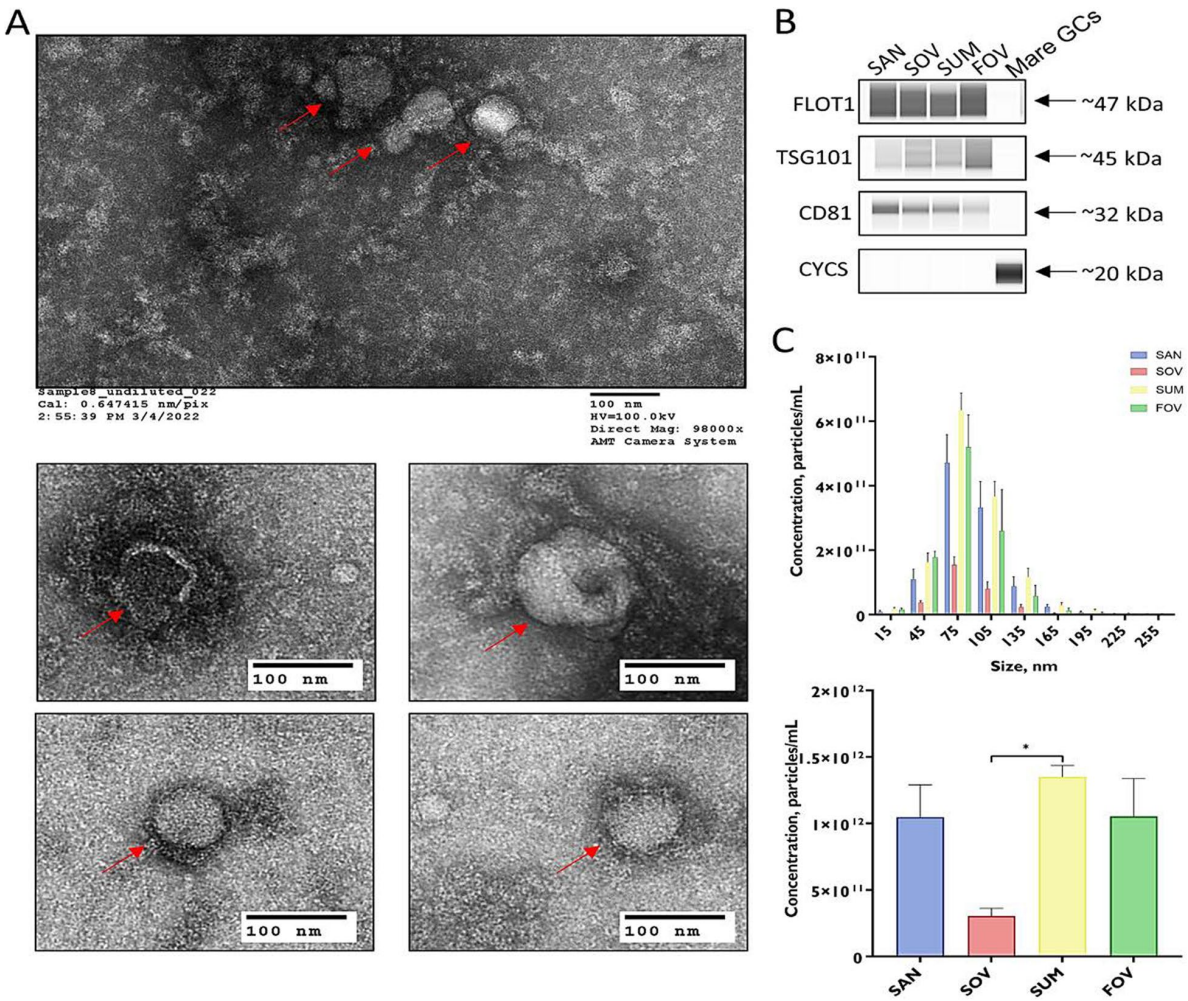


Fig. 1 EV characterization. **A** Transmission electron microscope (TEM) imaging shows EVs with typical structure (red arrow), scale bar = 100 nm. **B** Western blot analysis of EVs marker proteins CD81, FLOT-1, and TSG101 and cellular protein contamination indicator CYCS. **C** The NTA analysis reveals the size distribution (upper panel) and concentration (lower panel) of the isolated EVs, with the asterisk indicating a significant difference between groups. Data were analyzed and graphs were generated using GraphPad Prism version 8.4.2 (GraphPad; San Diego, CA, USA). Statistical differences were assessed between the mean values of more than two groups using One-way Analysis of Variance (ANOVA) followed by Tukey's Multiple Comparisons tests. Data are presented as the Mean ± SEM of biological replicates. Statistical significance was identified at $P \leq 0.05$

(A), immunoblotting (B), and NTA (C) techniques for all samples. The isolated FF-EVs exhibited nanoscale, spherical structures with high purity and expressed typical exosomal protein markers, including CD81, FLOT-1, and TSG101, while showing the absence of the mitochondrial cellular contamination marker CYCS. Each seasonal group displayed varying EV sizes, averaging 85.9 nm for SAN, 81.2 nm for SOV, 84.4 nm for SUM, and 79.6 nm for FOV. The SOV-derived samples had the lowest EV concentration, averaging 3.03×10^{11} particles/mL, which significantly differed from the EV concentration in the SUM samples, averaging 1.35×10^{12} particles/mL ($P<0.05$). Nevertheless, the EV concentration in the SOV samples did not significantly differ from that of the SAN and FOV groups.

Sequencing and miRNA expression profiles

The small RNA sequencing analysis revealed an average of 23 million raw reads, resulting in nearly 22 million clean reads after QC trimming per sample. On average, 70% of the reads are successfully mapped to the equine reference genome. In Fig. 2, the principal component analysis (Fig. 2A) and heatmap (Fig. 2B) display distinct miRNA expression profiles and sample clustering for each seasonal group, excluding the FOV_1 sample from further analysis. A total of 282 unique miRNAs were expressed (>10 CPM), with 235 in the SAN, 231 in the SOV, 238 miRNAs in the SUM, and 249 in the FOV group (Fig. 2C). Around 72% (203) of total detected miRNAs were found in all groups, and 13 of the 20 most abundant miRNAs were common to all datasets (Table 1). Among these, six miRNAs (miR-148a, miR-143, miR-99a, miR-192, miR-21, and miR-10b) accounted for 61%–72% of all 20 miRNA expressions. MiR-143 had the lowest expression level in the SUM group (3.8%) compared to 32.1% in the other groups, while miR-192 showed a similar pattern with 7.2% in the SAN group versus 31% in the others (Table 1). A detailed list of all expressed miRNAs per season is provided in Additional file 2.

Differential expression, target gene prediction, and bioinformatic analyses

The volcano plots in Figs. 3 and 4 depict the results of pairwise comparisons. A total of 97 unique miRNAs were

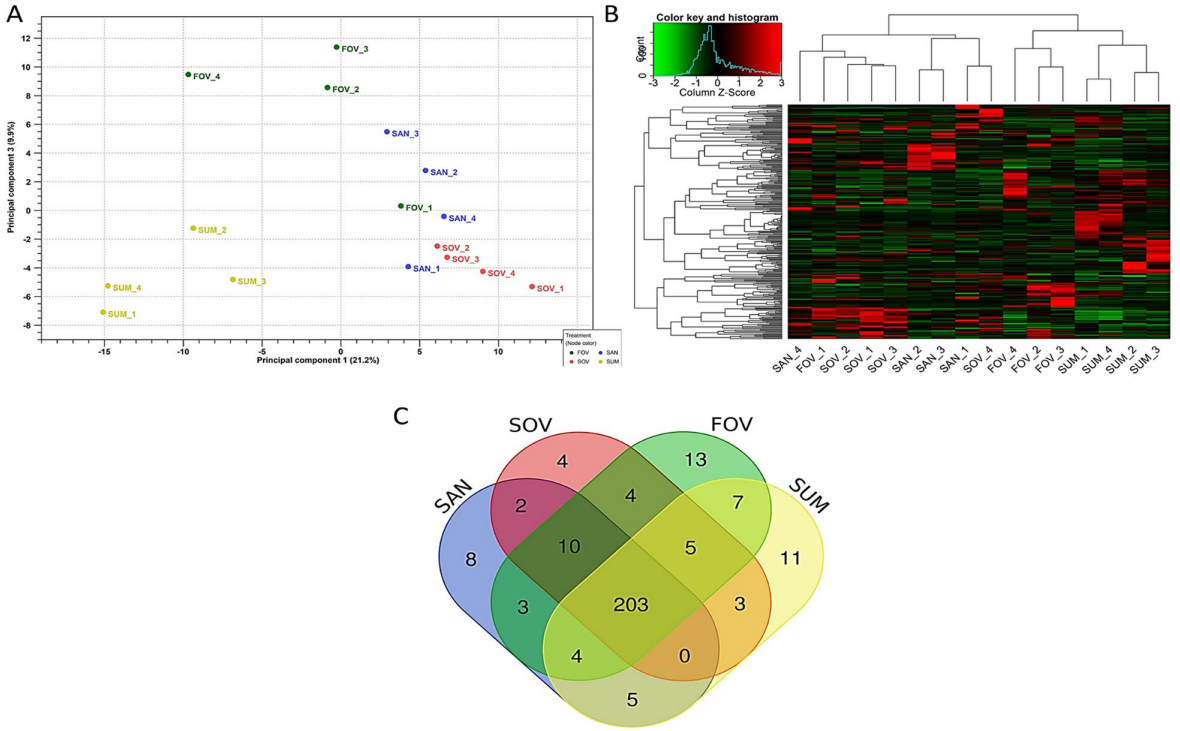


Fig. 2 Principal component analysis (PCA), heatmap, and miRNA expression profiles. Small-RNA sequence data and miRNA expression profile overviews. **A** Principal component analysis. **B** Heatmap and hierarchical clustering of expressed miRNAs. Red and green colors represent high and low expressed miRNAs, respectively. **C** miRNA expression profiles in each seasonal group. Experimental groups are represented as SAN (Spring Anovulatory), SOV (Spring Ovulatory), SUM (Summer), and FOV (Fall Ovulatory) seasons. EVs and miRNAs were obtained from four independent samples, harboring different suffices (1, 2, 3, or 4) in each group. In the FOV group, however, FOV_1 was removed from further analyses (Fig. 2B and 2C) due to similarity to the SAN group (PCA analysis)

Table 1 List of top 20 most abundant FF-EV miRNAs from different seasonal groups

Name	SAN	Name	SOV	Name	SUM	Name	FOV
eca-miR-148a	153217.5	**eca-miR-143**	220236.4	**eca-miR-148a**	185229.96	**eca-miR-148a**	130802.1
eca-miR-99a	152297.6	**eca-miR-99a**	139358.2	**eca-miR-21**	110374.93	**eca-miR-143**	124999.3
eca-miR-143	148564.7	**eca-miR-148a**	127656.7	**eca-miR-99a**	88377.861	**eca-miR-99a**	85233.95
eca-miR-21	66253.57	**eca-miR-21**	112097.5	**eca-miR-192**	61590.064	**eca-miR-192**	59664.31
eca-miR-10b	32721.78	**eca-miR-26a**	41150.8	**eca-miR-10b**	59013.673	**eca-miR-21**	47142.89
eca-let-7c	32308.23	**eca-miR-10b**	31779.63	**eca-miR-423-5p**	47375.737	eca-miR-100	33616.31
eca-miR-26a	31335.63	**eca-let-7 g**	27746.73	**eca-miR-10a**	38047.633	**eca-miR-10b**	27615.29
eca-miR-10a	27625.71	**eca-miR-423-5p**	25721.44	eca-miR-486-5p	28771.487	**eca-miR-423-5p**	27610.03
eca-let-7 g	23924.93	**eca-let-7f**	23289.82	eca-miR-218	27141.321	**eca-miR-10a**	24416.9
eca-miR-423-5p	20638.59	**eca-miR-27b**	23034.01	eca-miR-215	22536.951	**eca-miR-26a**	23407.8
eca-let-7a	18658.87	**eca-miR-192**	19979.72	**eca-let-7 g**	21758.141	eca-miR-215	22890.12
eca-miR-100	17932.95	**eca-let-7a**	18330.15	eca-miR-128	21423.475	eca-miR-24	18177.65
eca-let-7f	16062.56	eca-let-7c	16168.63	**eca-miR-26a**	19879.521	**eca-let-7 g**	17308.86
eca-miR-27b	14922.12	eca-miR-100	14713.95	**eca-miR-143**	19513.78	**eca-miR-27b**	16276.16
eca-miR-9a	14392.11	**eca-miR-10a**	13075.2	**eca-miR-27b**	19296.781	eca-miR-128	14358.85
eca-miR-1	13990.02	eca-miR-215	12377.61	**eca-miR-7f**	18443.203	eca-miR-27a	12482.74
eca-miR-192	10933.04	eca-miR-1	9928.538	eca-miR-22	18431.73	eca-miR-451	12127.98
eca-miR-30d	10138.15	eca-miR-126-3p	9608.478	eca-miR-24	17516.918	**eca-let-7f**	12126.65
eca-miR-24	9319.776	eca-miR-199a-3p	9071.105	eca-let-7c	14230.575	**eca-let-7a**	11556.09
eca-miR-128	7818.761	eca-miR-30d	8234.176	**eca-let-7a**	12710.04	eca-miR-486-5p	10986.71

The 20 most abundant miRNAs are listed from the highly to the lesser abundant in each season, measured as Count Per Million (CPM). The 13 commonly shared miRNAs are bolded. Experimental groups are represented as SAN (Spring Anovulatory), SOV (Spring Ovulatory), SUM (Summer), and FOV (Fall Ovulatory) seasons

found to be differentially expressed (FC > 2.0, FDR < 0.05, CPM > 10), with 11, 14, 74, 06, 67, and 8 miRNAs identified in SOV vs. FOV (Fig. 3A), SUM vs. FOV (Fig. 3B), SOV vs. SUM (Fig. 3C), SAN vs. SOV (Fig. 4A), SAN vs. SUM (Fig. 4B), and SAN vs. FOV (Fig. 4C), respectively. Venn diagrams in Figs. 3D and 4D illustrate the list of differentially expressed miRNAs shared between two comparisons. These miRNAs were either downregulated (in green) or upregulated (in red) in the joint seasonal group of both comparisons. Additionally, all differentially expressed miRNAs in the six comparisons are presented in Fig. 5 and Additional file 3. Among the findings, miR-143 and miR-192 were the two most abundant dysregulated in pairwise comparisons. For example, miR-143 was significantly downregulated in the SUM group compared to SOV (−11.33 FC, FDR = 7.3×10^{-18}), SAN (−7.64 FC, FDR = 2.78×10^{-12}), and FOV (−6.43 FC, FDR = 1.62×10^{-8}). Similarly, miR-192 expression was downregulated in the SAN group compared to SUM (−5.63 FC, FDR = 3.9×10^{-4}) and FOV (−5.46 FC, FDR = 5.97×10^{-3}), as well as in the SOV group compared to SUM (−3.08 FC, FDR = 2.02×10^{-2}). Additionally, several miRNAs appeared unique (e.g., miR-328 and miR-451) or paired (e.g., 302b and miR-429) in different comparisons, such as SAN vs. SOV, SUM vs. FOV, and SOV vs. FOV.

The subsets of differentially expressed miRNAs, including miR-143 and miR-192 (among the top 20 most abundant), as well as miR-149, miR-200b, miR-206, miR-221, miR-328, and miR-615 (spring transition), were chosen for target gene prediction and bioinformatic analyses. Results in Table 2, miR-143, targeting 74 genes, are mainly associated with post-translation modifications like phosphoprotein, isopeptide bound, Ubl conjugation, and methylation. Conversely, miR-192, targeting 49 genes, did not show significant enrichments. All six miRNAs upregulated in SAN vs. SOV targeted 634 genes, significantly enriched in diverse biological functions including DNA-, RNA-, and miRNA- "binding", "transcription factor activity", "sequence-specific DNA binding", and post-translation modifications such as acetylation and methylation. The specific upregulation of miR-328 in SAN (vs. SOV; +3.48 FC), targeting 46 genes, showed significant enrichment in the "endoplasmic reticulum" cellular components. Additionally, the specific upregulation of miR-302b in SUM (vs. FOV; −68.13 FC) targeted 118 genes, enriched in various biological pathways related to cellular component (i.e., "nucleoplasm"), molecular function (i.e., "DNA-binding," "transcription factor activity," and "sequence-specific DNA binding"), and biological process (i.e., transcription and transcription

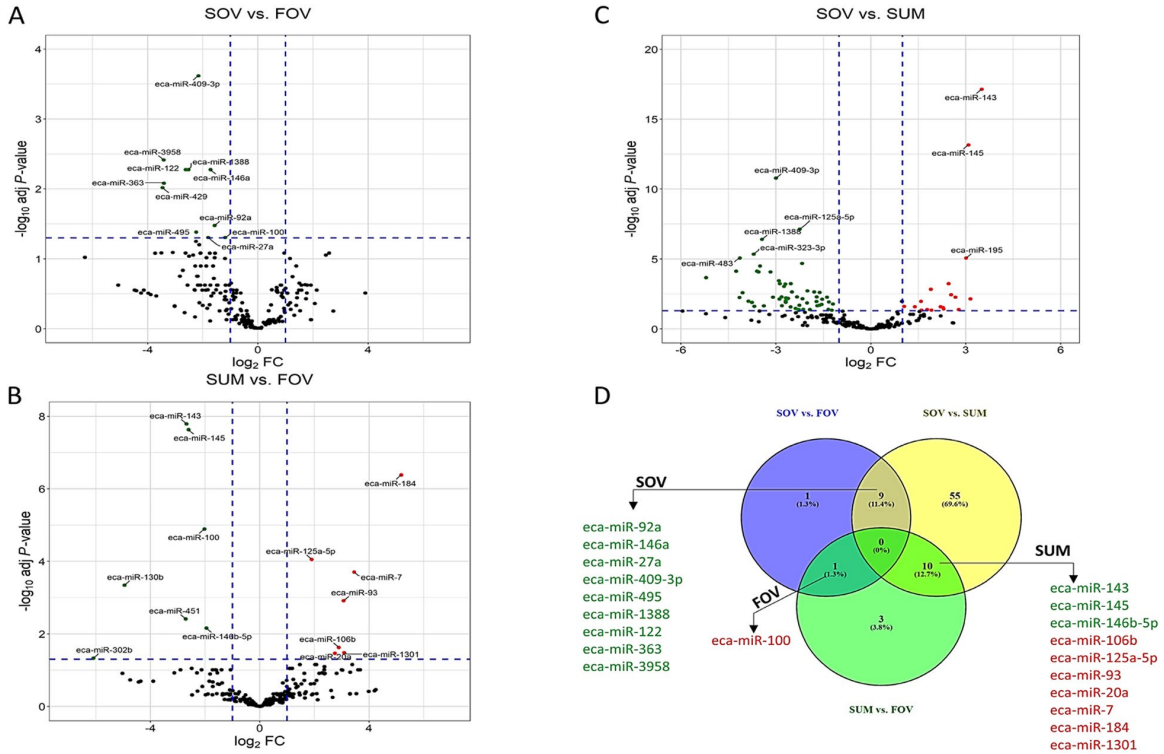


Fig. 3 Differential expression and group comparisons. Volcano representations of pairwise comparisons between SOV and FOV (**A**), SUM and FOV (**B**), and SOV and SUM (**C**) are shown. The Venn diagram (**D**) provides the lists of miRNAs that are shared between pairwise comparisons (Red = downregulation and Green = upregulation). Experimental groups are represented as SAN (Spring Anovulatory), SOV (Spring Ovulatory), SUM (Summer), and FOV (Fall Ovulatory) seasons

regulation). Both miR-100 and let-7c were significantly dysregulated in multiple comparisons. MiR-100 was downregulated in SOV vs. FOV (−2.28 FC) and SUM vs. FOV (−4.06 FC) and upregulated in SAN vs. SUM (+2.17 FC), targeting 20 genes significantly enriched for "protein binding". Meanwhile, let-7c was upregulated in SAN vs. FOV (+3.2 FC) and vs. SUM (+2.27 FC), targeting 311 genes enriched in various biological pathways, including the "p53 signaling pathway", "glutamatergic synapse", "response to gamma radiation", and "endoplasmic reticulum."

Cluster analysis revealed nine distinct patterns of miRNA expression across seasons (Fig. 6A), with a substantial number of miRNAs associated with each cluster (Fig. 6B). Three clusters demonstrating critical seasonal patterns displayed significant numbers of DE-miRNA (12, 25, and 19 for Clusters 1, 4, and 6, respectively), thereby allowing for further pathway analyses. Cluster 1 exhibited the highest expression levels of 37 miRNAs in the SAN group (Fig. 7A). In contrast, both Cluster 4 (Fig. 8A) and Cluster 6 (Fig. 9A) displayed similar highest expressions of 43 and 48 miRNAs, respectively, in the SUM group. DE-miRNAs were found in 4 (Clusters 1 and 4; Figs. 7B and 8B) and 3 (Cluster 6; Fig. 9B) different comparisons, leading to significant enrichments of various pathways (Figs. 7C, 8C, and 9C).

Discussion

The molecular mechanisms governing ovarian dynamics during different seasons remain mysterious. Extracellular vesicles in follicular fluid are crucial in causing functional adjustments in target cells [48, 49]. A previous study demonstrated that mares' follicular fluid-derived extracellular vesicles' miRNA profiles are closely associated with follicle development, selection, and ovulation. However, little is known about EVs and their effectual miRNA profiles during the ovulatory and anovulatory seasons. This study compares miRNA cargo of extracellular vesicles collected from mares' follicular fluid during ovulatory and anovulatory seasons, and significant seasonal variations are unveiled. These findings enhance our understanding of extracellular vesicle–coupled miRNA control over ovarian activity during seasonal reproductive changes.

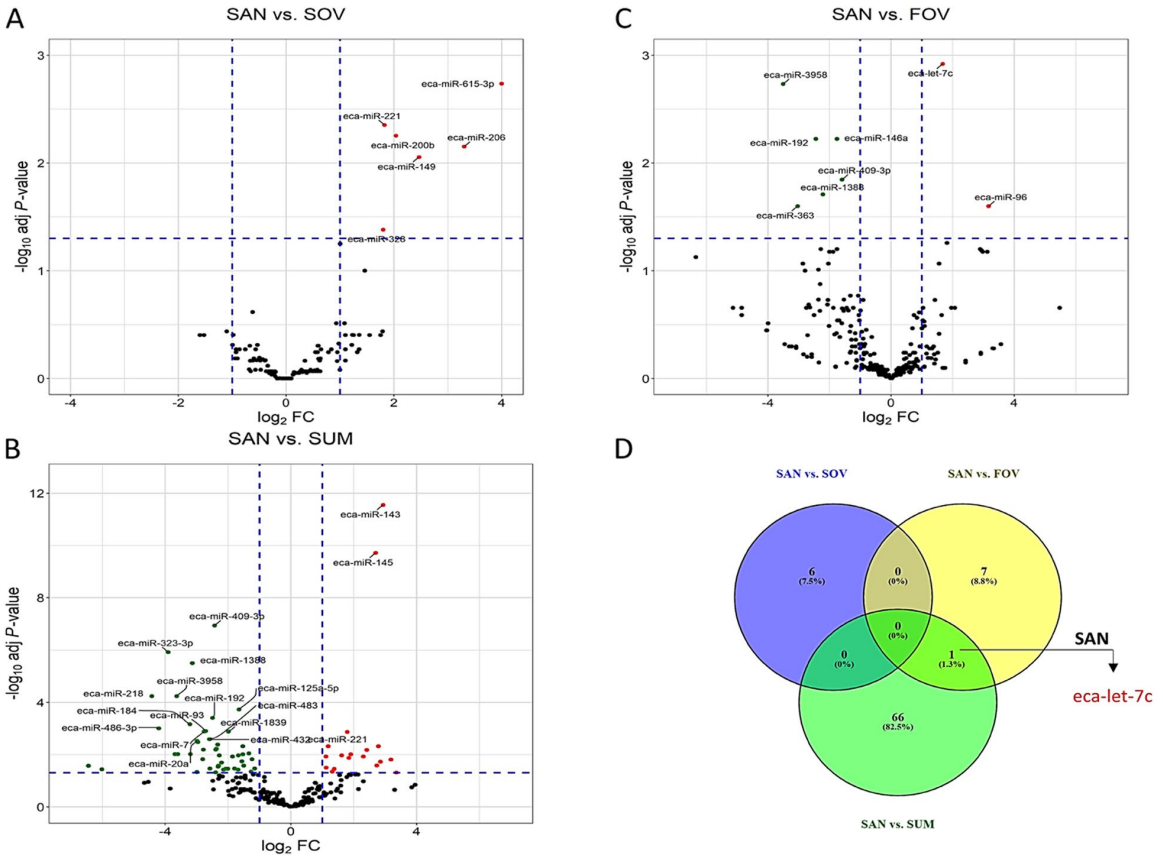


Fig. 4 Differential expression and group comparisons. Volcano representations of pairwise comparisons between SAN and SOV (**A**), SAN and SUM (**B**), and SAN and FOV (**C**) are shown. The Venn diagram (**D**) shows the miRNAs that are shared between pairwise comparisons (Red = downregulation and Green = upregulation). Experimental groups are represented as SAN (Spring Anovulatory), SOV (Spring Ovulatory), SUM (Summer), and FOV (Fall Ovulatory) seasons

EV identification, total and abundant miRNA in equine follicular fluid across seasons

The follicular fluid contains vital components for oocyte and follicular maturation and cellular communication. Studies have shown that FF-EV–derived miRNAs are crucial in mediating cellular communication [50] and responding to stress within the follicle [51–53]. Our findings revealed a higher accumulation of EVs in the SUM group, which may implicate an increased EV release from the follicular cells in response to high environmental temperature. Previous in vivo and in vitro studies have demonstrated these EVs can shuttle protective signals in the form of miRNAs, which can induce tolerance to high temperatures if delivered to recipient cells [30, 31, 39, 54], indicating their potential to regulate the response to elevated thermal temperatures for maintaining intrafollicular homeostasis.

Our analysis found that 203 out of 282 (72%) of the uniquely detected miRNAs were shared across seasons, indicating that they may represent the core miRNA profile of equine FF-EVs, which may have a housekeeping role in follicular dynamics in mares irrespective of the season. During the winter-to-summer comparison, a similar core miRNA profile was observed in bovine FF-EV–derived miRNAs (89.6%: 232/259) [31]. Studies on equine [25] and porcine [55] follicle development also reported high percentages of shared miRNA across follicle developmental stages (82% and 86%, respectively). The expression levels of the number of these FF-EV–coupled miRNAs were altered across seasons (Cluster analysis), which observation was in agreement with previous reports in short-day breeder sheep [56, 57] and buffalo oocyte- and follicular cell-derived miRNAs [58]. Considering their involvement in various cancers, miRNAs have been suggested as potent regulators of follicular atresia and degeneration [59], playing a crucial role in follicular development, meiotic resumption, and ovulation by targeting genes involved in signaling pathways such as *AKT*,

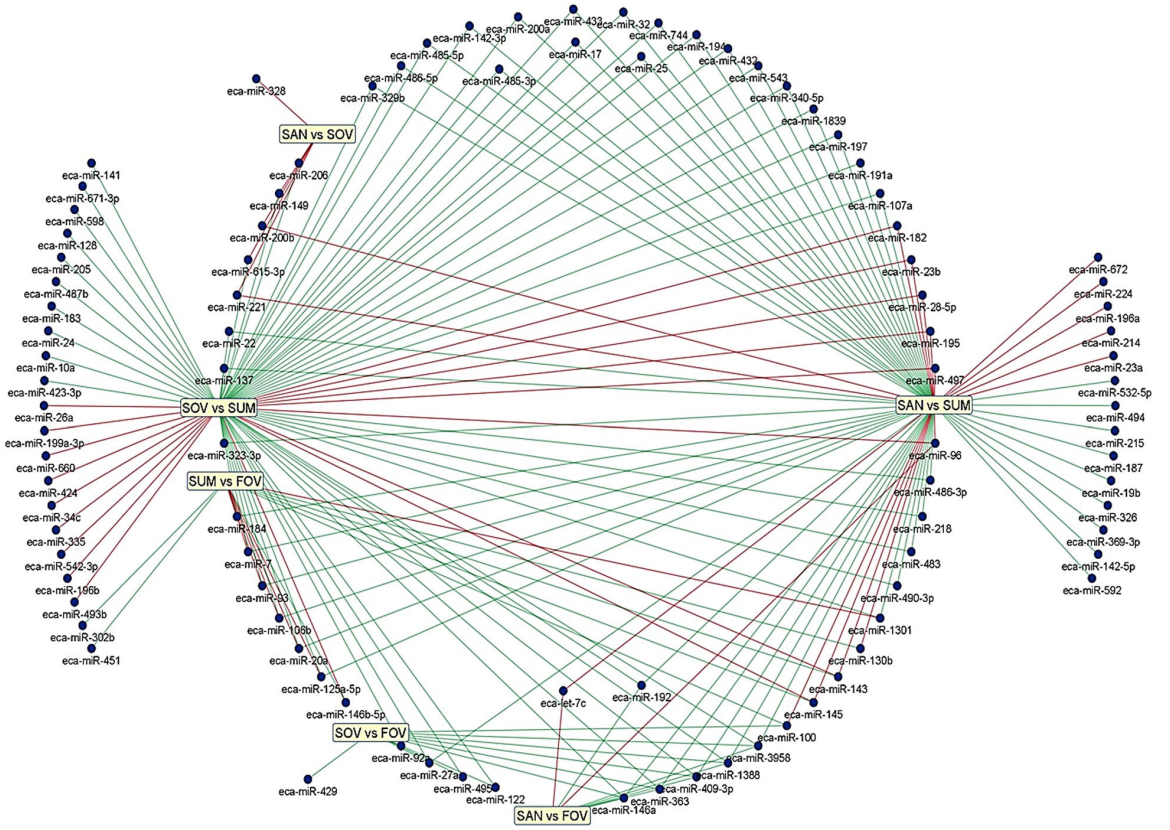


Fig. 5 All differentially expressed (DE) miRNAs. All DE-miRNAs from the six different comparisons. Up- and down-regulated miRNAs from each comparison are presented as red and green lines, respectively. Experimental groups are represented as SAN (Spring Anovulatory), SOV (Spring Ovulatory), SUM (Summer), and FOV (Fall Ovulatory) seasons

WNT1, *GDF9*, *BMP15*, *MAPK*, *ErbB*, *PTEN*, *PI3K-Akt*, *P53*, *mTOR*, *FOXO1*, and *TGFβ1* [60–62].

The current study found that miR-148a, miR-143, miR-192, miR-99a, miR-21, miR-10a, and miR-10b are abundant miRNAs across all seasons. These miRNAs regulate ovarian development, including ovarian cell proliferation and steroidogenesis [63–65]. They have been shown to have diverse beneficial effects on livestock species, such as sheep [66, 67] and pigs [68, 69], with reported effects on embryo quality [28]. High expression levels of these miRNAs were found in FF-EVs of large antral follicles, granulosa, and luteal cells throughout folliculogenesis, and their upregulation in late corpus luteum and atretic follicles during SAN, SUM, and FOV was observed in various livestock species, including sheep [70], cows [31, 71], horses [25], and pigs [33]. Previous studies have indicated positive correlations between these miRNAs and oocyte maturation [72] and IVF outcomes [28], highlighting the potential of these abundant miRNAs as essential molecules in regulating ovarian function throughout all seasons and as potential markers for improving female fertility.

Seasonal variations in FF-EV–coupled miRNAs

The cluster analysis found that about 34% of all detected miRNAs are differentially expressed across seasons, likely impacting follicular function and ovulatory capacity in various seasons. The discussion will focus on selected miRNAs with high abundance and significant differential expression, especially those related to spring (SAN vs. SOV) and fall (SUM vs. FOV) transitions or involved in selected clusters (1, 4, and 6) or comparisons across multiple seasons.

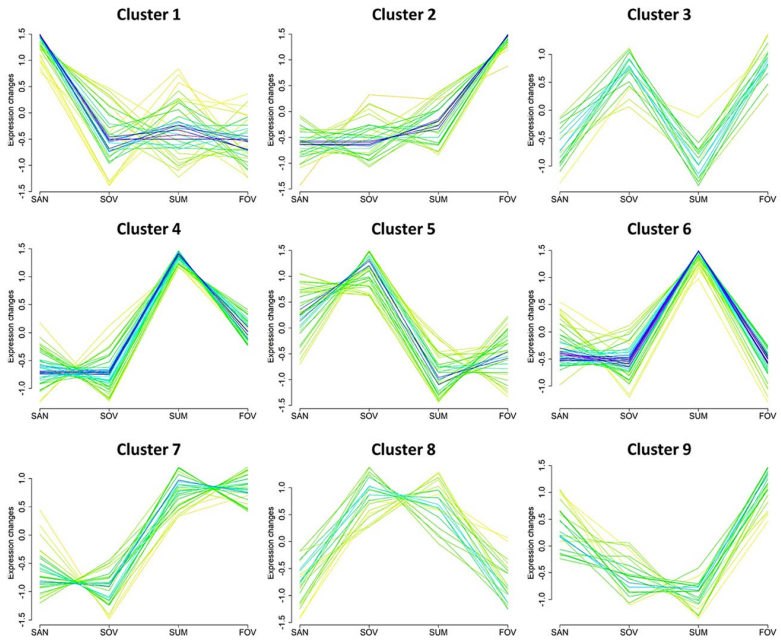
Two abundant miRNAs, miR-192 and miR-143, varied significantly across seasons. Despite no significant pathway enrichment of the miR-192 gene targets, its higher expression during SUM (vs. SAN and SOV) and FOV (vs. SAN) suggests a link to ovulation. Noteworthy, the miR-192 has been proposed as a potential biomarker for early pregnancy screening in sows due to its higher

Table 2 Enrichment analysis of selected miRNA clusters

miRNA			Seasonal comparisons	Biological pathways ($P < 0.1$)
Expression status		**IDs (# of Gene targets)**	**(Expression in 1st stated group)**	
Abundant	DE	miR-143 (74)	SUM-SOV (Down) SUM-SAN (Down) SUM-FOV (Down)	➢ KW-1017 ~ Isopeptide bond (PTM) ➢ KW-0832 ~ Ubl conjugation (PTM) ➢ KW-0597 ~ Phosphoprotein (PTM) ➢ KW-0488 ~ Methylation (PTM)
		miR-192 (49)	SAN-FOV (Down) SOV-SUM (Down) SAN-SUM (Down)	No significant enrichments
Transitional	Spring (DE)	miR-149 miR-200b miR-206 miR-221 miR-328 miR-615 (Total of 634)	SAN-SOV (Up)	➢ KW-0832 ~ Ubl conjugation (PTM) ➢ KW-1017 ~ Isopeptide bond (PTM) ➢ GO:0000381 ~ Regulation of alternative mRNA splicing (BP) ➢ KW-0694 ~ RNA-binding (MF) ➢ KW-0227 ~ DNA damage (BP) ➢ KW-0238 ~ DNA-binding (MF) ➢ GO:0000785 ~ chromatin (CC) ➢ GO:0003700 ~ transcription factor activity, sequence-specific DNA binding (MF) ➢ GO:0008139 ~ nuclear localization sequence binding (MF) ➢ GO:0035198 ~ miRNA binding (MF) ➢ KW-0597 ~ Phosphoprotein (PTM) ➢ KW-0007 ~ Acetylation (PTM) ➢ KW-0488 ~ Methylation (PTM)
	Spring (Specific)	miR-328 (46)	SAN-SOV	➢ KW-0256 ~ Endoplasmic reticulum (CC)
	Fall (Specific)	miR-451 (1)	SUM-FOV	➢ Interleukin 6 receptor (IL6R)
		miR-302b (118)	SUM-FOV	➢ KW-0010 ~ Activator (MF) ➢ KW-0805 ~ Transcription regulation (BP) ➢ KW-0804 ~ Transcription (BP) ➢ KW-0597 ~ Phosphoprotein (PTM) ➢ GO:0003700 ~ transcription factor activity, sequence-specific DNA binding (MF) ➢ GO:0003677 ~ DNA binding (MF) ➢ GO:0005654 ~ Nucleoplasm (CC) ➢ GO:0005634 ~ Nucleus (CC) ➢ GO:0000978 ~ RNA polymerase II core promoter proximal region sequence-specific DNA binding (MF) ➢ GO:0003682 ~ chromatin binding (MF) ➢ GO:0001228 ~ transcriptional activator activity, RNA polymerase II transcription regulatory region sequence-specific binding (MF)
		miR-429 (none)	SOV-FOV	N/A
Multi-seasonal		Let-7c (311)	SAN-FOV SAN-SUM	➢ GO:0098978 ~ glutamatergic synapse (CC) ➢ GO:0005783 ~ endoplasmic reticulum (CC) ➢ GO:0010332 ~ response to gamma radiation (BP) ➢ KW-0597 ~ Phosphoprotein (PTM) ➢ hsa04115: p53 signaling pathway (KEGG) ➢ GO:0005739 ~ mitochondrion (CC) ➢ GO:0005829 ~ cytosol (CC) ➢ GO:0005654 ~ nucleoplasm (CC) ➢ GO:0005737 ~ cytoplasm (CC)
		miR-100 (20)	SOV-FOV SUM-FOV SAN-SUM	➢ GO:0005515 ~ protein binding (MF)

DE Differentially expressed or Differential expression, *Down* Downregulated, *Up* Upregulated, *CC* Cellular component, *MF* Molecular function, *BP* Biological process, *PTM* Post-translational modification, *GO* Gene Ontology, *KW* Key word, *KEGG* Kyoto Encyclopedia of Genes and Genomes. Experimental groups are represented as *SAN* Spring Anovulatory, *SOV* Spring Ovulatory, *SUM* Summer, and *FOV* Fall Ovulatory seasons

A



B

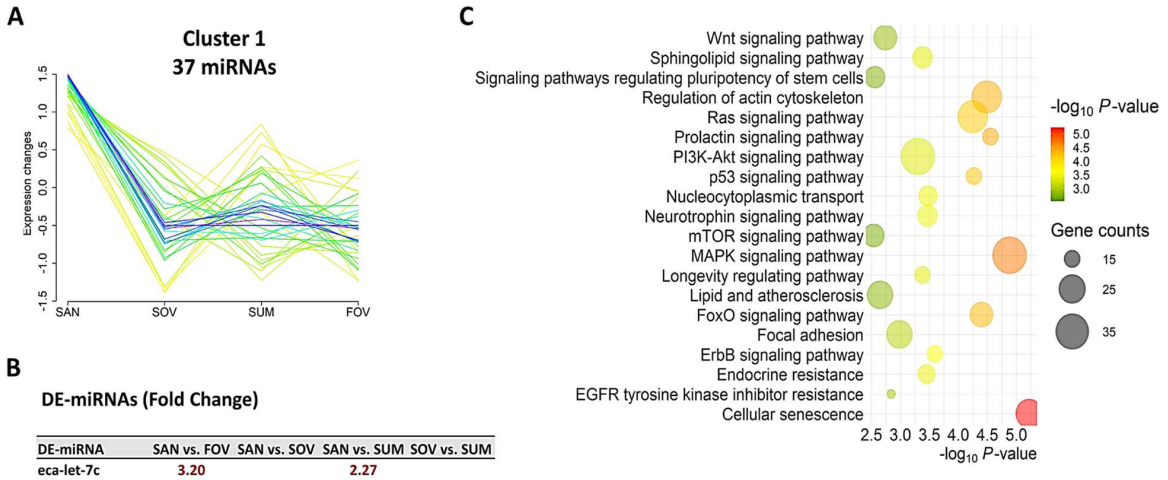
Cluster	miRNA counts	%	DE-miRNAs	Comparisons
1	37	13.12	12	4
2	31	10.99	4	5
3	17	6.03	4	2
4	43	15.25	25	4
5	34	12.06	13	3
6	48	17.02	19	3
7	30	10.64	16	4
8	20	7.09	0	0
9	22	7.80	4	3
Total	282		97	

Fig. 6 Clustering analysis of extracellular vesicle–coupled microRNAs across the different seasons. **A** Nine different miRNA expression patterns in the follicular fluid extracellular vesicles across the seasons. **B** The counts and percentages of expressed microRNAs (miRNAs) and the differentialy expressed (DE) miRNAs from the different comparisons in each cluster. Each line represents one miRNA that fits (better: red, purple, and blue lines; lesser: yellow or green lines) with its pattern of expression within the cluster. Experimental groups are represented as SAN (Spring Anovulatory), SOV (Spring Ovulatory), SUM (Summer), and FOV (Fall Ovulatory) seasons

detection in blood serum [73]. On the other hand, the downregulation of miR-143 in SUM (vs. SAN, SOV, and FOV) is associated with post-translational modifications impacting protein functions, especially apoptosis. Overexpression of miR-143-3p has been found to have steroidogenesis inhibitory and pro-apoptotic effects, targeting intracellular signaling factors like *TGF-β* in porcine granulosa cells and follicular atresia [74], as well as *BMPR1A/SMAD1/5/8* in polycystic ovary syndrome (PCOS). This endocrine disorder leads to abnormal follicular development, chronic anovulation, and infertility [75]. Higher levels of miR-143-3p expression have also been reported in FF-EVs of women with PCOS [76]. Therefore, the contrasting expressions of miR-192 (upregulation) and miR-143 (downregulation) in healthy equine preovulatory follicles during summer could potentially serve as predictive markers for successful ovulation and promise improved early pregnancy screening methods in mammalian reproduction.

Spring transition

In this study, the principal component analysis (PCA) comparing the spring anovulatory season (SAN) and the spring ovulatory season (SOV) showed minimal overlap, regardless of the PC1/PC2 (Additional file 4) and PC1/PC3 combination. The factors contributing to the onset of normal ovarian cyclicity during the spring transition remain unknown. Here, we found that during this transition, specific miRNAs (miR-149, miR-200b, miR-206, miR-221, miR-328, and miR-615) were overexpressed in the SAN compared to the SOV season, suggesting their role in maintaining oocyte meiotic arrest and regulating the cell cycle. These miRNAs are identified in Cluster 1, characterizing the expression profiles of the anovulatory or non-breeding season. Twelve related differentially expressed miRNAs may promote cellular senescence over apoptosis by influencing pathways that regulate stable cell cycle arrest and/or cell survival. The overexpression of these miRNAs may contribute to maintaining oocytes in a meiotic arrest state (e.g., miR-206) through ERα targeting [77, 78], regulating the cell cycle by promoting proliferation or inducing arrest (e.g., miR-221, miR-149, and miR-615) via targets such as *FoxO*, *MAPK*, and estrogen signaling pathways [61], and ensuring the developmental transition from the follicular to luteal phase (e.g., miR-221-5p) through targeting genes associated with *Ras* and *PI3K-Akt* signaling pathways [79]. These differentially expressed miRNAs significantly enrich these signaling



B

DE-miRNAs (Fold Change)

DE-miRNA	SAN vs. FOV	SAN vs. SOV	SAN vs. SUM	SOV vs. SUM
eca-let-7c	3.20		2.27	
eca-miR-96	8.95		6.87	4.59
eca-miR-200b		4.10	2.60	
eca-miR-328		3.48		
eca-miR-221		3.54	3.45	
eca-miR-615-3p		15.96		-8.53
eca-miR-206		9.85		-6.45
eca-miR-149		5.51		-5.05
eca-miR-672			10.23	
eca-miR-214			2.49	
eca-miR-23a			2.18	
eca-miR-224			7.18	

Fig. 7 Cluster 1 of microRNAs (miRNAs). A group of 37 miRNAs exhibited a sharp reduction in their expression from the SAN till the FOV seasons (**A**). Among this cluster, 12 miRNAs were differentially expressed (DE) in four comparisons (**B**). Top 20 pathways associated with the DE-miRNAs target genes of this cluster (**C**). Experimental groups are represented as SAN (Spring Anovulatory), SOV (Spring Ovulatory), SUM (Summer), and FOV (Fall Ovulatory) seasons

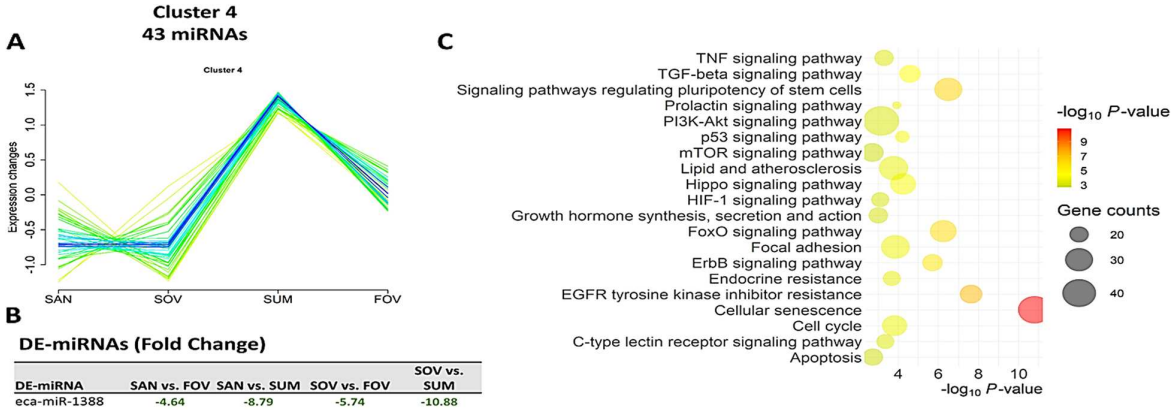
pathways during the spring transition and have been identified in the preovulatory follicle cells and FF-EVs of humans [80, 81], pigs [68, 82], and sheep [83, 84], playing a crucial role in regulatory processes. In the current study, these miRNAs exert their impacts through regulating target genes affecting biological functions such as post-translational modifications, RNA- and DNA-binding, DNA damage, chromatin, transcription activity, nuclear localization sequence binding, and miRNA binding, all associated with steroidogenesis and/or cell cycle [33, 81, 83]. These intricate regulatory roles are key to their function during follicular development and oocyte maturation [33, 85, 86], with the potential to positively influence female reproductive performance [85, 87, 88]. Nutritional studies have reported dysregulations of miR-328 and miR-200 impacting fertility outcomes [28], and miR-200 inspires further research through appropriate nutritional measures during the non-breeding season, as reported in sheep [83, 89].

Summer ovulatory season, the peak of breeding

Our research has identified 2 key Clusters, 4 and 6, shedding light on the distinct roles of miRNAs during the summer ovulatory season (SUM). The biological functions within both clusters converge on sustaining cell proliferation, growth, and survival processes in ovarian follicles. Cluster 4 is linked to cellular senescence, while Cluster 6 is linked to the MAPK signaling pathway and the regulation of pluripotency in stem cells, especially within the oocyte. These findings underscore the intricate balance between non-dividing oocytes and dividing somatic cells in the ovarian follicle during the peak of breeding. Understanding these clusters could enhance the sustainability of cell proliferation, growth, and survival processes in the follicles, potentially positively influencing seasonal fertility.

Fall transition

Preovulatory follicles in various species, including humans [90, 91], horses [20], cows [60], pigs [82], chickens [92], and mice [93, 94], have been found to contain specific miRNAs such as miR-302b, 429, and 451. The expression of miR-302b was specific to the transition from summer to fall ovulation, showing higher levels in the summer compared to the fall. In chickens, reduced expression of miR-302b in primordial germ cells has been linked to decreased cell proliferation and increased apoptosis, potentially



B

DE-miRNAs (Fold Change)

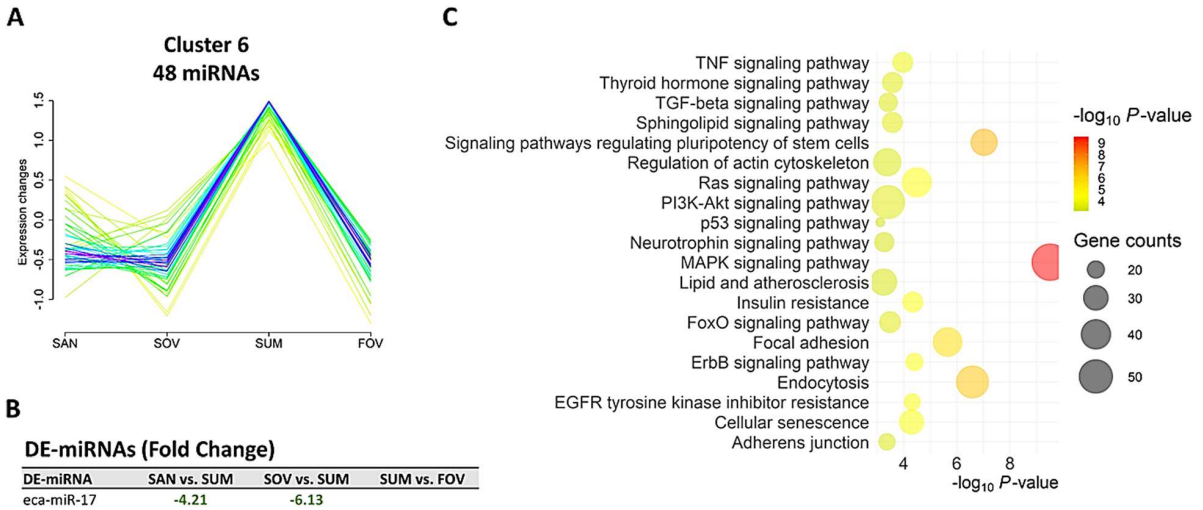
DE-miRNA	SAN vs. FOV	SAN vs. SUM	SOV vs. FOV	SOV vs. SUM
eca-miR-1388	-4.64	-8.79	-5.74	-10.88
eca-miR-409-3p	-3.02	-5.40	-4.47	-8.00
eca-miR-485-3p		-7.82		-7.07
eca-miR-486-5p		-5.26		-7.37
eca-miR-323-3p		-15.01		-13.03
eca-miR-485-5p		-5.04		-7.51
eca-miR-142-3p		-12.14		-7.03
eca-miR-744		-4.64		-4.80
eca-miR-25		-2.89		-4.51
eca-miR-197		-2.95		-2.54
eca-miR-326		-5.27		
eca-miR-1839		-3.97		-3.28
eca-miR-218		-21.56		-19.15
eca-miR-22		-4.87		-11.33
eca-miR-369-3p		-5.97		
eca-miR-329b		-4.94		-7.41
eca-miR-187		-4.98		
eca-miR-19b		-5.19		
eca-miR-432		-6.02		-4.05
eca-miR-423-3p				-2.61
eca-miR-671-3p				-16.58
eca-miR-128				-6.51
eca-miR-183				-3.28
eca-miR-205				-4.88
eca-miR-10a				-2.91

Fig. 8 Cluster 4 of microRNAs (miRNAs). A group of 43 miRNAs exhibited a sharp increase in their expression during the summer and then a slight reduction during the fall ovulatory season (**A**). Among this cluster, 25 miRNAs were differentially expressed (DE) in four comparisons (**B**). Top 20 pathways associated with the DE-miRNAs target genes of this cluster (**C**). Experimental groups are represented as SAN (Spring Anovulatory), SOV (Spring Ovulatory), SUM (Summer), and FOV (Fall Ovulatory) seasons

contributing to the decline in intrafollicular processes leading to the end of the ovulatory season [92]. On the other hand, miR-429 expression was detected in both the spring and fall ovulatory seasons and has been associated with luteinizing hormone synthesis in the pituitary gland [62, 94], likely linked to the transition from the follicular phase to the luteal phase. Similarly, the overexpression of miR-451 in the summer compared to the fall suggests potential benefits during ovulation. In cows, miR-451 is overexpressed in large healthy follicles (12–17 mm) [95], while in women with endometriosis, decreased miR-451 expression in FF and oocytes is associated with reduced fertility potential such as decreased number of oocytes, fertilization rate, and embryo quality compared to healthy women [93]. Altogether, these findings emphasize the importance of further exploring these miRNAs' functional roles and practical applications in reproductive health, especially the overexpression of miR-302b and miR-451 in the SUM group (compared to FOV) during ovulation.

Comparing multiple seasons

It was found that miR-100 and let-7c are significant miRNAs that are present in various ovarian cell types, FF, and FF-EVs and play a role in promoting follicle development and regulating ovarian follicle pathways in different species, including human [96], horses [25], and cows [31, 60]. MiR-100 has multiple roles in cells and may affect oocyte reprogramming through its interaction with SMARCA5, a key regulator of global chromatin structure [97, 98]. Previous studies showed that miR-100 triggers the resumption of meiosis in human oocytes by negatively regulating genes encoding inhibitory factors of follicular maturation via *mTOR* [96, 99, 100] or supports tumor suppression in ovarian cancer via *mTOR*, inducing apoptosis [99]. Thus, controlling the *mTOR* by reduced expression of miR-100 during SOV and SUM could maintain the oocyte in meiosis arrest for further cytoplasmic maturation to optimal developmental competence acquisition and the survival of other follicular cells. On the other hand, the overexpression of let-7 family members (let-7c, let-7a-5p, and



B

DE-miRNAs (Fold Change)

DE-miRNA	SAN vs. SUM	SOV vs. SUM	SUM vs. FOV
eca-miR-17	-4.21	-6.13	
eca-miR-7	-6.77	-9.03	10.94
eca-miR-1301	-6.90	-13.54	8.48
eca-miR-184	-9.31	-12.10	36.12
eca-miR-490-3p	-12.97	-14.61	
eca-miR-125a-5p	-3.14	-4.76	3.73
eca-miR-93	-6.58	-5.64	8.36
eca-miR-20a	-7.99	-6.41	6.70
eca-miR-592	-64.73		
eca-miR-340-5p	-2.89	-3.46	
eca-miR-137	-87.24	-12.90	
eca-miR-106b	-4.03	-3.80	7.39
eca-miR-32	-7.02	-5.20	
eca-miR-142-5p	-7.99		
eca-miR-483	-6.04	-17.64	
eca-miR-486-3p	-18.48	-36.89	
eca-miR-107a	-2.41	-2.35	
eca-miR-598		-10.43	
eca-miR-141		-17.76	

Fig. 9 Cluster 6 of microRNAs (miRNAs). A group of 48 miRNAs exhibited a sharp increase in their expression during the summer compared to the other seasons (**A**). Among this cluster, 19 miRNAs were differentially expressed (DE) in three different comparisons (**B**). Top 20 pathways associated with the DE-miRNAs target genes of this cluster (**C**). Experimental groups are represented as SAN (Spring Anovulatory), SOV (Spring Ovulatory), SUM (Summer), and FOV (Fall Ovulatory) seasons

let-7 g-5p) in FF-EVs is directly linked to human oocyte failure to fertilize [28, 101], with significantly higher expressions in developmentally arrested oocytes at the GV stage, as compared to their MI and MII counterparts [102]. These reports support the findings of the present study, which identifies the upregulation of let-7c during anovulatory (SAN) versus ovulatory seasons (SUM and FOV) as potentially contributing to oocyte meiotic arrest during SAN.

Conclusions

This study presents the miRNA profiles of equine FF-EVs collected during anovulatory or non-breeding (SAN) and ovulatory or breeding (SOV, SUM, and FOV) seasons. The EVs were isolated from dominant 30–34 mm follicle sizes, which are absent in ovaries during deep winter anestrus (contain only follicles < 20 mm in diameter). The study has unveiled seasonal dynamic patterns of FF-EV–coupled miRNAs, which are pivotal for advancing fertility research. A group of miRNAs appeared as potential regulators of spring transition (SAN-SOV), with specific miRNAs upregulated in the SAN season (miR-149, miR-200b, miR-206, miR-221, miR-328, and miR-615). Furthermore, the study has revealed that specific miRNAs play a crucial role in maintaining continued folliculogenesis, leading up to ovulation during the ovulatory seasons (SOV, SUM, and FOV), with consistent downregulation compared to SAN (miR-100, let-7c, and miR-143) and FOV (miR-302b) and upregulation compared to SAN (miR-192). These findings shed light on the potential involvement of EV-coupled miRNAs in seasonal variations on breeding and fertility, offering insights into ovulatory failure mechanisms.

Abbreviations

BMPR1A	Bone morphogenetic protein receptor type 1A
CPM	Count per million
DE	Differential expression
DNA	Deoxyribonucleic acid
EV	Extracellular vesicles
FF	Follicular fluid
FOV	Fall ovulatory
HRP	Horseradish peroxidase
LH	Luteinizing hormone
MI	Metaphase I
MII	Metaphase II
PCOS	Polycystic ovary syndrome
RNA	Ribonucleic acid
SAN	Spring anovulatory
SMARCA5	SWI/SNF-related matrix-associated actin-dependent regulator of chromatin A5
SOV	Spring ovulatory
SUM	Summer
TEM	Transmission electron microscope
TGF-b	Transforming growth factor-beta
Ubl	Ubiquitin-like

Supplementary Information

The online version contains supplementary material available at https://doi.org/10.1186/s40104-024-01097-2.

Additional file 1. Detailed materials and methods.

Additional file 2. Expressed miRNAs in each seasonal group represented as the average CPM value.

Additional file 3. Total differentially expressed miRNAs.

Additional file 4. Principal component analysis: P1/P2.

Acknowledgements

The authors acknowledge the University of Colorado, Boulder EM Services Core Facility in the MCDB Department for their help and support with TEM imaging. Ms. Melinda Meyers from the Department of Clinical Sciences at Colorado State University performed nanoparticle tracking analysis.

Authors' contributions

Conceptualization: JMF, ELG, and DT. Experimental work: JMF, AG, NGM, GMI, SG, MOG, and ELG. Data analysis: JMF, AG, NGM, NHD, RP, and GMI. Interpretation of data: JMF, GMI, AG, NHD, and NGM. Writing of original draft: JMF, AG, NGM, and GMI. Manuscript editing: JMF, AG, NGM, GMI, SG, ELG, and DT. Supervision: JMF, ELG, and DT. Funding acquisition: ELG, JMF, and DT. All authors have read and agreed to the published version of this manuscript.

Funding

This research was supported in part by Southern Illinois University, Carbondale, IL; Ministry of Higher Education & Scientific Research, Baghdad, Iraq; NIFA-USDA Hatch project accession #1016077 (Multistate # W4171); USDA-ARS project 6066-31000-015-00D; and NIH MS-IDeA network of Biomedical Research Excellence award 5P20GMI03476-19. GMI received a PhD scholarship from the Ministry of Higher Education & Scientific Research, Baghdad, Iraq.

Availability of data and materials

The miRNA sequencing dataset generated during the current study, including the raw FASTQ files and processed CSV files, was deposited in the National Center for Biotechnology Information (NCBI) Gene Expression Omnibus (GEO) database (https://www.ncbi.nlm.nih.gov/geo/) for open-access using the accession number GSE249220. Experimental procedures related to EV experiments have been submitted to the EV-TRACK knowledgebase (https://evtrack.org/) (EVTRACK ID: EV231010). Additional data are included in Additional file 1 (Detailed materials and methods), Additional file 2 (Expressed miRNAs in each seasonal group represented as the average CPM value), Additional file 3 (Differentially expressed miRNAs in all comparisons), and Additional file 4 (Principal component analysis: P1/P2).

Declarations

Ethics approval and consent to participate

All experimental procedures were performed in accordance with the United States Department of Agriculture Guide for Care and Use of Agricultural Animals in Research and were approved by the Institutional Animal Care and Use Committee (IACUC) of Southern Illinois University.

Consent for publication

Not applicable.

Competing interests

The authors declare that they have no competing interests.

Author details

[1]Department of Animal and Dairy Sciences, Mississippi State University, Mississippi State, MS 39762, USA. [2]Animal Reproduction and Biotechnology Laboratory (ARBL), Department of Biomedical Sciences, College of Veterinary Medicine and Biomedical Sciences, Colorado State University, Fort Collins, CO 80523, USA. [3]Department of Animal Production, Faculty of Agriculture, Cairo University, Giza 12613, Egypt. [4]Department of Surgery and Obstetrics, College of Veterinary Medicine, University of Baghdad, Baghdad 10011, Iraq. [5]Animal Science, School of Agricultural Sciences, Southern Illinois University, Carbondale, IL 62901, USA. [6]J.R. Simplot Company, Kuna, ID 83634, USA. [7]Institute of Animal Physiology and Genetics, Czech Academy of Sciences, Liběchov 27721, Czech Republic.

Received: 30 April 2024 Accepted: 27 August 2024
Published online: 09 October 2024

References

1. Donadeu F, Watson E. Seasonal changes in ovarian activity: lessons learnt from the horse. Anim Reprod Sci. 2007;100(3–4):225–42.
2. Donadeu F, Pedersen H. Follicle development in mares. Reprod Domest Anim. 2008;43:224–31.
3. Matsuda F, Inoue N, Manabe N, Ohkura S. Follicular growth and atresia in mammalian ovaries: regulation by survival and death of granulosa cells. J Reprod Dev. 2012;58(1):44–50.
4. De Rensis F, Scaramuzzi RJ. Heat stress and seasonal effects on reproduction in the dairy cow—a review. Theriogenology. 2003;60(6):1139–51.
5. Habeeb AA, Osman SF, Teama FEI, Gad AE. The detrimental impact of high environmental temperature on physiological response, growth, milk production, and reproductive efficiency of ruminants. Trop Anim Health Prod. 2023;55(6):388.
6. Wolfenson D, Thatcher W, Badinga L, Savio J, Meidan R, Lew B, et al. Effect of heat stress on follicular development during the estrous cycle in lactating dairy cattle. Biol Reprod. 1995;52(5):1106–13.
7. Dobson H, Smith R. What is stress, and how does it affect reproduction? Anim Reprod Sci. 2000;60:743–52.
8. Roth Z. Heat stress, the follicle, and its enclosed oocyte: mechanisms and potential strategies to improve fertility in dairy cows. Reprod Domest Anim. 2008;43:238–44.
9. Wilson S, Marion R, Spain J, Spiers D, Keisler D, Lucy M. Effects of controlled heat stress on ovarian function of dairy cattle. 1. Lactating cows. J Dairy Sci. 1998;81(8):2124–31.
10. Ju J-C, Jiang S, Tseng J-K, Parks JE, Yang X. Heat shock reduces developmental competence and alters spindle configuration of bovine oocytes. Theriogenology. 2005;64(8):1677–89.
11. Paes V, Vieira L, Correia H, Sa N, Moura A, Sales A, et al. Effect of heat stress on the survival and development of in vitro cultured bovine preantral follicles and on in vitro maturation of cumulus–oocyte complex. Theriogenology. 2016;86(4):994–1003.
12. Ginther OJ. The mare: a 1000-pound guinea pig for study of the ovulatory follicular wave in women. Theriogenology. 2012;77(5):818–28.
13. Gastal E. Recent advances and new concepts on follicle and endocrine dynamics during the equine periovulatory period. Anim Reprod. 2009;6(1):144–58.

14. Ginther O, Beg MA, Bergfelt D, Donadeu F, Kot K. Follicle selection in monovular species. Biol Reprod. 2001;65(3):638–47.
15. Ginther O. Folliculogenesis during the transitional period and early ovulatory season in mares. J Reprod Fertil. 1990;90(1):311–20.
16. Ginther O. Reproductive biology of the mare: basic and applied aspects. J Equine Vet Sci. 1992;12(2):71.
17. Bergfelt D, Ginther O. Embryo loss following GnRH-induced ovulation in anovulatory mares. Theriogenology. 1992;38(1):33–43.
18. Nagy P, Guillaume D, Daels P. Seasonality in mares. Anim Reprod Sci. 2000;60:245–62.
19. Ginther O, Gastal E, Gastal M, Beg M. Seasonal influence on equine follicle dynamics. Anim Reprod. 2004;1(1):31–44.
20. Donadeu F, Schauer S. Differential miRNA expression between equine ovulatory and anovulatory follicles. Domest Anim Endocrinol. 2013;45(3):122–5.
21. Acosta T, Beg MA, Ginther O. Aberrant blood flow area and plasma gonadotropin concentrations during the development of dominant-sized transitional anovulatory follicles in mares. Biol Reprod. 2004;71(2):637–42.
22. Ishak GM, Dutra GA, Gastal GD, Gastal MO, Feugang JM, Gastal EL. Transition to the ovulatory season in mares: an investigation of antral follicle receptor gene expression in vivo. Mol Reprod Dev. 2019;86(12):1832–45.
23. Dutra G, Ishak G, Pechanova O, Pechan T, Peterson D, Jacob J, et al. Seasonal variation in equine follicular fluid proteome. Reprod Biol Endocrinol. 2019;17(1):29.
24. Ishak GM, Feugang JM, Pechanova O, Pechan T, Peterson DG, Willard ST, et al. Follicular-fluid proteomics during equine follicle development. Mol Reprod Dev. 2022;89(7):298–311.
25 Gebremedhn S, Gad A, Ishak GM, Menjivar NG, Gastal MO, Feugang JM, et al. Dynamics of extracellular vesicle-coupled microRNAs in equine follicular fluid associated with follicle selection and ovulation. Mol Hum Reprod. 2023;29(4):gaad009.
26. Donadeu FX, Schauer SN, Sontakke SD. Involvement of miRNAs in ovarian follicular and luteal development. J Endocrinol. 2012;215(3):323–34.
27. Li Y, Fang Y, Liu Y, Yang X. MicroRNAs in ovarian function and disorders. J Ovarian Res. 2015;8:51.
28. Martinez RM, Liang L, Racowsky C, Dioni L, Mansur A, Adir M, et al. Extracellular microRNAs profile in human follicular fluid and IVF outcomes. Sci Rep. 2018;8:17036.
29. Dalanezi FM, Garcia HDM, de Andrade FR, Franchi FF, Fontes PK, de Souza Castilho AC, et al. Extracellular vesicles of follicular fluid from heat-stressed cows modify the gene expression of in vitro-matured oocytes. Anim Reprod Sci. 2019;205:94–104.
30. Gebremedhn S, Gad A, Aglan HS, Laurincik J, Prochazka R, Salilew-Wondim D, et al. Extracellular vesicles shuttle protective messages against heat stress in bovine granulosa cells. Sci Rep. 2020;10:15824.
31. Gad A, Joyce K, Menjivar NG, Heredia D, Rojas CS, Tesfaye D, et al. Extracellular vesicle-microRNAs mediated response of bovine ovaries to seasonal environmental changes. J Ovarian Res. 2023;16:101.
32. Di Pietro C. Exosome-mediated communication in the ovarian follicle. J Assist Reprod Genet. 2016;33:303–11.
33. Yuan C, Li Z, Zhao Y, Wang X, Chen L, Zhao Z, et al. Follicular fluid exosomes: Important modulator in proliferation and steroid synthesis of porcine granulosa cells. FASEB J. 2021;35(5):e21610.
34. Shao H, Im H, Castro CM, Breakefield X, Weissleder R, Lee H. New technologies for analysis of extracellular vesicles. Chem Rev. 2018;118(4):1917–50.
35 Yáñez-Mó M, Siljander PRM, Andreu Z, BedinaZavec A, Borràs FE, Buzas EI, et al. Biological properties of extracellular vesicles and their physiological functions. J Extracell Vesicles. 2015;4(1):27066.
36. Gastal EL, Gastal MO, Bergfelt DR, Ginther OJ. Role of diameter differences among follicles in selection of a future dominant follicle in mares. Biol Reprod. 1997;57(6):1320–7.
37. Haag K, Magalhaes-Padilha D, Fonseca G, Wischral A, Gastal M, King S, et al. Quantification, morphology, and viability of equine preantral follicles obtained via the Biopsy Pick-Up method. Theriogenology. 2013;79(4):599–609.
38. Ishak G, Bashir S, Dutra G, Gastal G, Gastal M, Cavinder C, et al. In vivo antral follicle wall biopsy: a new research technique to study ovarian function at the cellular and molecular levels. Reprod Biol Endocrinol. 2018;16:71.
39. Menjivar NG, Gad A, Gebremedhn S, Ghosh S, Tesfaye D. Granulosa cell-derived extracellular vesicles mitigate the detrimental impact of thermal stress on bovine oocytes and embryos. Front Cell Dev Biol. 2023;11:1142629.
40. Van Deun J, Mestdagh P, Agostinis P, Akay Ö, Anand S, Anckaert J, et al. EV-TRACK: transparent reporting and centralizing knowledge in extracellular vesicle research. Nat Methods. 2017;14(3):228–32.
41. Robinson MD, Oshlack A. A scaling normalization method for differential expression analysis of RNA-seq data. Genome Biol. 2010;11(3):R25.
42. Benjamini Y, Hochberg Y. Controlling the false discovery rate: a practical and powerful approach to multiple testing. J Roy Stat Soc: Ser B (Methodol). 1995;57(1):289–300.
43. Kumar L, Futschik M. Mfuzz: a software package for soft clustering of microarray data. Bioinformation. 2007;2(1):5–7.
44. Sticht C, De La Torre C, Parveen A, Gretz N. miRWalk: an online resource for prediction of microRNA binding sites. PLoS One. 2018;13(10):e0206239.
45. Ogata H, Goto S, Sato K, Fujibuchi W, Bono H, Kanehisa M. KEGG: Kyoto Encyclopedia of Genes and Genomes. Nucleic Acids Res. 1999;27(1):29–34.
46. Shannon P, Markiel A, Ozier O, Baliga NS, Wang JT, Ramage D, et al. Cytoscape: a software environment for integrated models of biomolecular interaction networks. Genome Res. 2003;13(11):2498–504.
47. Théry C, Witwer KW, Aikawa E, Alcaraz MJ, Anderson JD, Andriantsitohaina R, et al. Minimal information for studies of extracellular vesicles 2018 (MISEV2018): a position statement of the International Society for Extracellular Vesicles and update of the MISEV2014 guidelines. J Extracell Vesicles. 2018;7(1):1535750.
48. Godakumara K, Dissanayake K, Hasan MM, Kodithuwakku SP, Fazeli A. Role of extracellular vesicles in intercellular communication during reproduction. Reprod Domest Anim. 2022;57:14–21.
49. Thomou T, Mori MA, Dreyfuss JM, Konishi M, Sakaguchi M, Wolfrum C, et al. Adipose-derived circulating miRNAs regulate gene expression in other tissues. Nature. 2017;542(7642):450–5.
50 da Silveira JC, Veeramachaneni DNR, Winger QA, Carnevale EM, Bouma GJ. Cell-secreted vesicles in equine ovarian follicular fluid contain miRNAs and proteins: a possible new form of cell communication within the ovarian follicle. Biol Reprod. 2012;86(3):71.
51. Leung AK, Sharp PA. MicroRNA functions in stress responses. Mol Cell. 2010;40(2):205–15.
52. Nehammer C, Podolska A, Mackowiak SD, Kagias K, Pocock R. Specific microRNAs regulate heat stress responses in *Caenorhabditis elegans*. Sci Rep. 2015;5:8866.
53. Li Q, Yang C, Du J, Zhang B, He Y, Hu Q, et al. Characterization of miRNA profiles in the mammary tissue of dairy cattle in response to heat stress. BMC Genomics. 2018;19:975.
54. Gebremedhn S, Ali A, Gad A, Prochazka R, Tesfaye D. Extracellular vesicles as mediators of environmental and metabolic stress coping mechanisms during mammalian follicular development. Front Vet Sci. 2020;7:602043.
55. Inoue Y, Munakata Y, Shinozawa A, Kawahara-Miki R, Shirasuna K, Iwata H. Prediction of major microRNAs in follicular fluid regulating porcine oocyte development. J Assist Reprod Genet. 2020;37:2569–79.
56. Di R, He J, Song S, Tian D, Liu Q, Liang X, et al. Characterization and comparative profiling of ovarian microRNAs during ovine anestrus and the breeding season. BMC Genomics. 2014;15:899.
57. Zhai M, Xie Y, Liang H, Lei X, Zhao Z. Comparative profiling of differentially expressed microRNAs in estrous ovaries of Kazakh sheep in different seasons. Gene. 2018;664:181–91.
58. Capra E, Lazzari B, Russo M, Kosior MA, Valle GD, Longobardi V, et al. Seasonal effects on miRNA and transcriptomic profile of oocytes and follicular cells in buffalo (*Bubalus bubalis*). Sci Rep. 2020;10:13557.
59. Li Y, Deng X, Zeng X, Peng X. The role of Mir-148a in cancer. J Cancer. 2016;7(10):1233–41.
60. Nagata S, Inoue Y, Sato T, Tanaka K, Shinozawa A, Shirasuna K, et al. Age-associated changes in miRNA profile of bovine follicular fluid. Reproduction. 2022;164(5):195–206.
61. Wei C, Xiang S, Yu Y, Song J, Zheng M, Lian F. MiR-221-3p regulates apoptosis of ovarian granulosa cells via targeting FOXO1 in older

women with diminished ovarian reserve (DOR). Mol Reprod Dev. 2021;88(4):251–60.
62. da Silveira JC, Winger QA, Bouma GJ, Carnevale EM. Effects of age on follicular fluid exosomal microRNAs and granulosa cell transforming growth factor-β signalling during follicle development in the mare. Reprod Fertil Dev. 2015;27(6):897–905.
63. Noferesti SS, Sohel MMH, Hoelker M, Salilew-Wondim D, Tholen E, Looft C, et al. Controlled ovarian hyperstimulation induced changes in the expression of circulatory miRNA in bovine follicular fluid and blood plasma. J Ovarian Res. 2015;8:81.
64. Hilker RE, Pan B, Zhan X, Li J. MicroRNA-21 enhances estradiol production by inhibiting WT1 expression in granulosa cells. J Mol Endocrinol. 2022;68(1):11–22.
65. Ding Q, Jin M, Kalds P, Meng C, Wang H, Zhong J, et al. Comparison of microRNA profiles in extracellular vesicles from small and large goat follicular fluid. Animals. 2021;11(11):3190.
66. Dai T, Kang X, Yang C, Mei S, Wei S, Guo X. Integrative analysis of miRNA-mRNA in ovarian granulosa cells treated with kisspeptin in Tan sheep. Animals. 2022;12(21):2989.
67. Xie L, Li A, Huang W, Zhang X, Miao X. Identification and analysis of miRNAs at different developmental stages in Hu sheep ovaries. Acta Vet Zootech Sin. 2019;50(7):1396–404.
68. Zhang X, Chen Y, Yang M, Shang J, Xu Y, Zhang L, et al. MiR-21-5p actions at the Smad7 gene during pig ovarian granulosa cell apoptosis. Anim Reprod Sci. 2020;223:106645.
69. Xu G, Hu Y, Yu D, Chen X, Li X, Duan S, et al. Discovery of differentially expressed microRNAs in porcine ovaries with smaller and larger litter size. Front Genet. 2022;13:762124.
70. Zhang T, Huo S, Wei S, Cui S. miR-21, miR-125b, and let-7b contribute to the involution of atretic follicles and corpus lutea in Tibetan sheep ovaries. Anim Sci J. 2022;93(1):e13756.
71. Sohel MMH, Hoelker M, Noferesti SS, Salilew-Wondim D, Tholen E, Looft C, et al. Exosomal and non-exosomal transport of extra-cellular microRNAs in follicular fluid: implications for bovine oocyte developmental competence. PLoS One. 2013;8(11):e78505.
72. Dehghan Z, Mohammadi-Yeganeh S, Rezaee D, Salehi M. MicroRNA-21 is involved in oocyte maturation, blastocyst formation, and pre-implantation embryo development. Dev Biol. 2021;480:69–77.
73. Gao R, Li Q, Qiu M, Xie S, Sun X, Huang T. Serum exosomal miR-192 serves as a potential detective biomarker for early pregnancy screening in sows. Anim Biosci. 2023;36(9):1336.
74. Du X, Zhang L, Li X, Pan Z, Liu H, Li Q. TGF-β signaling controls FSHR signaling-reduced ovarian granulosa cell apoptosis through the SMAD4/miR-143 axis. Cell Death Dis. 2016;7(11):e2476–576.
75. Zhao Y, Pan S, Li Y, Wu X. Exosomal miR-143-3p derived from follicular fluid promotes granulosa cell apoptosis by targeting BMPR1A in polycystic ovary syndrome. Sci Rep. 2022;12:4359.
76. Jarrett BY, Vanden Brink H, Oldfield AL, Lujan ME. Ultrasound characterization of disordered antral follicle development in women with polycystic ovary syndrome. J Clin Endocrinol Metab. 2020;105(11):e3847–61.
77 Lu S, Tang Y, Yao R, Xu R, Zhang H, Liu J, et al. E2/ER signaling mediates the meiotic arrest of goat intrafollicular oocytes induced by follicle-stimulating hormone. J Anim Sci. 2023;101:skad351.
78. Liu W, Xin Q, Wang X, Wang S, Wang H, Zhang W, et al. Estrogen receptors in granulosa cells govern meiotic resumption of pre-ovulatory oocytes in mammals. Cell Death Dis. 2017;8(3):e2662–762.
79. Zhang X, Zhang L, Shang J, Tao Q, Tian M, Ma Y, et al. Combined microRNAome and transcriptome analysis of follicular phase and luteal phase in porcine ovaries. Reprod Domest Anim. 2019;54(7):1018–25.
80. Andrei D, Nagy RA, van Montfoort A, Tietge U, Terpstra M, Kok K, et al. Differential miRNA expression profiles in cumulus and mural granulosa cells from human pre-ovulatory follicles. MicroRNA. 2019;8(1):61–7.
81. Martinez RM, Baccarelli AA, Liang L, Dioni L, Mansur A, Adir M, et al. Body mass index in relation to extracellular vesicle–linked microRNAs in human follicular fluid. Fertil Steril. 2019;112(2):387-96. e3.
82. Hu J, Dong J, Zeng Z, Wu J, Tan X, Tang T, et al. Using exosomal miRNAs extracted from porcine follicular fluid to investigate their role in oocyte development. BMC Vet Res. 2020;16:485.
83. Song P, Chen X, Zhang P, Zhou Y, Zhou R. miR-200b/MYBL2/CDK1 suppresses proliferation and induces senescence through cell cycle arrest in ovine granulosa cells. Theriogenology. 2023;207:19–30.
84. Yang J, Li X, Cao Y-H, Pokharel K, Hu X-J, Chen Z-H, et al. Comparative mRNA and miRNA expression in European mouflon (*Ovis musimon*) and sheep (*Ovis aries*) provides novel insights into the genetic mechanisms for female reproductive success. Heredity. 2019;122(2):172–86.
85. Tesfaye D, Gebremedhn S, Salilew-Wondim D, Hailay T, Hoelker M, Grosse-Brinkhaus C, et al. MicroRNAs: tiny molecules with a significant role in mammalian follicular and oocyte development. Reproduction. 2018;155(3):R121–35.
86. Zhang D, Lv J, Tang R, Feng Y, Zhao Y, Fei X, et al. Association of exosomal microRNAs in human ovarian follicular fluid with oocyte quality. Biochem Biophys Res Commun. 2021;534:468–73.
87. Machtinger R, Rodosthenous RS, Adir M, Mansour A, Racowsky C, Baccarelli AA, et al. Extracellular microRNAs in follicular fluid and their potential association with oocyte fertilization and embryo quality: an exploratory study. J Assist Reprod Genet. 2017;34:525–33.
88. Liu Y, Zhou Z, He X, Tao L, Jiang Y, Lan R, et al. Integrated analyses of miRNA-mRNA expression profiles of ovaries reveal the crucial interaction networks that regulate the prolificacy of goats in the follicular phase. BMC Genomics. 2021;22:812.
89. Yang H, Liu X, Hu G, Xie Y, Lin S, Zhao Z, et al. Identification and analysis of microRNAs-mRNAs pairs associated with nutritional status in seasonal sheep. Biochem Biophys Res Commun. 2018;499(2):321–7.
90. Eisenberg I, Nahmias N, Novoselsky Persky M, Greenfield C, Goldman-Wohl D, Hurwitz A, et al. Elevated circulating micro-ribonucleic acid (miRNA)-200b and miRNA-429 levels in anovulatory women. Fertil Steril. 2017;107(1):269–75.
91 Salas-Huetos A, James ER, Aston KI, Jenkins TG, Carrell DT, Yeste M. The expression of miRNAs in human ovaries, oocytes, extracellular vesicles, and early embryos: a systematic review. Cells. 2019;8(12):1564.
92. Lázár B, Szabadi NT, Anand M, Tóth R, Ecker A, Urbán M, et al. Effect of miR-302b microRNA inhibition on chicken primordial germ cell proliferation and apoptosis rate. Genes. 2021;13(1):82.
93. Li X, Zhang W, Fu J, Xu Y, Gu R, Qu R, et al. MicroRNA-451 is downregulated in the follicular fluid of women with endometriosis and influences mouse and human embryonic potential. Reprod Biol Endocrinol. 2019;17:96.
94. Hasuwa H, Ueda J, Ikawa M, Okabe M. miR-200b and miR-429 function in mouse ovulation and are essential for female fertility. Science. 2013;341(6141):71–3.
95. Sontakke SD, Mohammed BT, McNeilly AS, Donadeu FX. Characterization of microRNAs differentially expressed during bovine follicle development. Reproduction. 2014;148(3):271–83.
96. Assou S, Al-Edani T, Haouzi D, Philippe N, Lecellier C-H, Piquemal D, et al. MicroRNAs: new candidates for the regulation of the human cumulus–oocyte complex. Hum Reprod. 2013;28(11):3038–49.
97. Bhushan L, Kandpal RP. EphB6 receptor modulates micro RNA profile of breast carcinoma cells. PLoS One. 2011;6(7):e22484.
98. Assou S, Cerecedo D, Tondeur S, Pantesco V, Hovatta O, Klein B, et al. A gene expression signature shared by human mature oocytes and embryonic stem cells. BMC Genomics. 2009;10:10.
99. Nagaraja AK, Creighton CJ, Yu Z, Zhu H, Gunaratne PH, Reid JG, et al. A link between mir-100 and FRAP1/mTOR in clear cell ovarian cancer. Mol Endocrinol. 2010;24(2):447–63.
100. Kharazi U, Badalzadeh R. A review on the stem cell therapy and an introduction to exosomes as a new tool in reproductive medicine. Reprod Biol. 2020;20(4):447–59.
101. Machtinger R, Laurent LC, Baccarelli AA. Extracellular vesicles: roles in gamete maturation, fertilization and embryo implantation. Hum Reprod Update. 2016;22(2):182–93.
102. Wei L, Yang X, Gao L, Liang Z, Yu H, Zhang N, et al. Comparison of miRNA landscapes between the human oocytes with or without arrested development. J Assist Reprod Genet. 2022;39(10):2227–37.

Joyce *et al. Journal of Ovarian Research* (2024) 17:201
https://doi.org/10.1186/s13048-024-01530-0

Journal of Ovarian Research

RESEARCH Open Access

Seasonal environmental fluctuations alter the transcriptome dynamics of oocytes and granulosa cells in beef cows

Kamryn Joyce[1], Ahmed Gad[2,3], Nico G. Menjivar[2], Samuel Gebremedhn[2,4], Daniella Heredia[1], Georgia Dubeux[1], Maria Camila Lopez-Duarte[1], Joao Bittar[5], Angela Gonella-Diaza[1*] and Dawit Tesfaye[2]

Abstract

Background Examining the mechanistic cellular responses to heat stress could aid in addressing the increasing prevalence of decreased fertility due to elevated ambient temperatures. Here, we aimed to study the differential responses of oocytes and granulosa cells to thermal fluctuations due to seasonal differences. Dry beef cows ($n = 10$) were housed together, synchronized and subjected to a stimulation protocol to induce follicular growth before ovum pick-up (OPU). Two OPU's were conducted (summer and winter) to collect cumulus-oocyte-complexes (COCs) and granulosa cells. In addition, rectal temperatures and circulating blood samples were collected during OPU. Oocytes were separated from the adherent cumulus cells, and granulosa cells were isolated from the collected OPU fluid. RNA was extracted from pools of oocytes and granulosa cells, followed by library preparation and RNA-sequencing. Blood samples were further processed for the isolation of plasma and leukocytes. The transcript abundance of *HSP70* and *HSP90* in leukocytes was evaluated using RT-qPCR, and plasma cortisol levels were evaluated by immunoassay. Environmental data were collected daily for three weeks before each OPU session. Data were analyzed using MIXED, Glimmix or GENMOD procedures of SAS, according to each variable distribution.

Results Air temperatures (27.5 °C vs. 11.5 °C), average max air temperatures (33.7 °C vs. 16.9 °C), and temperature-humidity indexes, THI (79.16 vs. 53.39) were shown to contrast significantly comparing both the summer and winter seasons, respectively. Rectal temperatures (Summer: 39.2 ± 0.2 °C; Winter: 38.8 ± 0.2 °C) and leukocyte *HSP70* transcript abundance (Summer: 4.18 ± 0.47 arbitrary units; Winter: 2.69 ± 0.66 arbitrary units) were shown to increase in the summer compared to the winter. No visual differences persisted in *HSP90* transcript abundance in leukocytes and plasma cortisol concentrations during seasonal changes. Additionally, during the summer, 446 and 940 transcripts were up and downregulated in oocytes, while 1083 and 1126 transcripts were up and downregulated in the corresponding granulosa cells, respectively (Fold Change ≤ -2 or ≥ 2 and FDR ≤ 0.05). Downregulated transcripts in the oocytes were found to be involved in ECM-receptor interaction and focal adhesion pathways, while the upregulated transcripts were involved in protein digestion and absorption, ABC transporters, and oocyte meiosis pathways. Downregulated transcripts in the granulosa cells were shown to be involved in cell adhesion molecules, chemokine

*Correspondence:
Angela Gonella-Diaza
a.gonelladiaza@ufl.edu

Full list of author information is available at the end of the article

© The Author(s) 2024. **Open Access** This article is licensed under a Creative Commons Attribution 4.0 International License, which permits use, sharing, adaptation, distribution and reproduction in any medium or format, as long as you give appropriate credit to the original author(s) and the source, provide a link to the Creative Commons licence, and indicate if changes were made. The images or other third party material in this article are included in the article's Creative Commons licence, unless indicated otherwise in a credit line to the material. If material is not included in the article's Creative Commons licence and your intended use is not permitted by statutory regulation or exceeds the permitted use, you will need to obtain permission directly from the copyright holder. To view a copy of this licence, visit http://creativecommons.org/licenses/by/4.0/.

signaling, and cytokine-cytokine receptor interaction pathways, while those upregulated transcripts were involved in protein processing and metabolic pathways.

Conclusion In conclusion, seasonal changes dramatically alter the gene expression profiles of oocytes and granulosa cells in beef cows, which may in part explain the seasonal discrepancies in pregnancy success rates during diverging climatic weather conditions.

Keywords Oocytes, Granulosa cells, Heat stress, Seasonality, Transcriptome, Beef cows

Background

With the rise of climate change becoming more prevalent over the years, it has been postulated that the duration and severity of heat stress will continually increase, posing detrimental impacts to the livestock industry, notably the beef and dairy sectors [1]. Excessive heat loads on animals negatively impact animal welfare and performance, with evident reductions in reproductive efficiencies, as one of the leading heat stress-related impacts affecting livestock productivity [2]. Additionally, it is well-documented that heat stress negatively impacts the reproductive performance of dairy and beef cattle through alterations in follicular development, oocyte maturation, and granulosa cells' function [3, 4]. Therefore, understanding the molecular changes in oocytes and follicular cells associated with environmental heat stress in beef cows could provide a unique opportunity to identify molecular targets for future managerial interventions and the development of therapeutic strategies.

Seasonal studies in cattle have shown that elevated temperatures compromise oocyte development [5]. Rocha et al. [6] observed the effects of environmental temperatures and humidity on the quality and developmental capacity of bovine oocytes from Holstein cows [6]. Results from this study showed that a higher percentage of morphologically normal oocytes were produced during the cooler season than during the warmer season, while the percentage of fertilized oocytes that developed to the 2-cell, 8-cell, and morula stages, were also greater during the cooler season. Moreover, previous studies have duly indicated that altered oocyte developmental competence from direct exposure to heat stress also negatively hampers their mitochondrial function by impacting ATP levels and redox regulation [7].Furthermore,, heat stress also has negative impacts on the function of granulosa cells. Disturbances in granulosa cells' quality and impairments to their proliferation capacity may indirectly affect follicular development and oocyte maturation, resulting in impaired embryo development and subsequent failures in pregnancy establishment [4]. Furthermore, in mice, it was shown that the exposure to heat stress increased the proportion of granulosa cells undergoing apoptosis and the number of atretic follicles, while reducing the intrafollicular aromatase activity, as well as circulating estradiol concentrations [8]. Additional studies are required to examine the molecular mechanisms underlying the response of oocytes and granulosa cells to heat stress, specifically in beef cattle.

A recent study from our group [9] investigated the encapsulated microRNA cargo of extracellular vesicles (EVs) derived from the follicular fluid of beef cows in response to seasonal environmental changes. In that study, several miRNAs were differentially expressed in EVs derived from the summer versus the winter, with precise candidates like miR-10a, miR-10b, miR-184, miR-19b, and miR-452 upregulated and miR-1246, miR-199b, and miR-370 downregulated during summer compared to the winter groups. Interestingly, those DE-miRNAs were found to be involved in the regulation of signaling pathways including WNT-, p53-, mTOR-, Hippo, and FoxO-signaling pathways, which are the dominant regulatory pathways involved in mammalian follicular development. As follicular fluid EV molecular cargos are direct determinants and a reflection of the physiology of the cells amidst the follicular microenvironment including cumulus cells, granulosa cells, and theca cells, the results of our previous study led us to hypothesize that the oocytes and the surrounding granulosa cells respond to environmental seasonal fluctuations in heat stress via altering their transcriptome profile. Therefore, in the present study, we aimed to investigate the transcriptome dynamics of GV-stage oocytes and granulosa cells, determining their response to fluctuating environmental temperatures during summer and winter seasons.

Materials and methods

Animals

This experiment was conducted at the UF/IFAS North Florida Research and Education Center in Marianna, FL, and was approved by the Institutional Animal Care and Use Committee (IACUC ID: IACUC202200000706). Eleven non-pregnant and non-lactating, multiparous *Bos taurus* cows crossbreed were clinically examined via transrectal ultrasound to evaluate their reproductive tract and cyclicity status. Only animals without clinical abnormalities showing at least one corpus luteum were enrolled in the study. Cows remained together for the duration of the experiment (February-August) and were maintained in outdoor pens with Bahia grass and fed bermudagrass hay to meet the nutritional requirements of

mature cows with ad libitum access to water and mineralized salt during the duration of the study. One cow died before the second OPU session and therefore, was completely removed from the study.

Synchronization, follicular stimulation, and ovum pick-up

Cows were subjected to a synchronization and FSH-based stimulation protocol to induce follicular growth as indicated in the hormonal experimental design outlined in Fig. 1. On day 0, an intravaginal P4 device (Eazi-Breed™ CIDR®; 1.38 gr P4; Zoetis Animal Health; Kalamazoo, MI, USA) was inserted and an intramuscular injection of a GnRH analog (100 µg of synthetic gonadorelin hydrochloride; Factrel; Zoetis Animal Health; Kalamazoo, MI, USA) was administrated. Follicular growth was stimulated by administering exogenous FSH (porcine pituitary-derived follicle-stimulating hormone; Folltropin®; Vetoquinol; Canada). Briefly, on day 3, 105 IU of FSH were administrated intramuscularly twice, once in the morning (7 am) and once in the afternoon (6 pm). Next, on day 4, one injection of 70 IU of FSH was administered in the morning (7 am). Finally, the CIDR was removed on day 5 (morning), and rectal temperature was collected. Transrectal ultrasounds were then conducted to assess the number of antral follicles and the presence of a CL. OPU was performed as previously reported [9] using a real-time B-mode ultrasound scanner (Mindray 2200; Mindray Bio-Medical Electronics, Shenzhen, China) equipped with a 5-MHz micro-convex transducer (Mindray model 65C15EAV, Mindray Bio-Medical Electronics, Shenzhen, China) and coupled to a follicular aspiration guide (WTA, São Paulo, Brazil) and a stainless-steel guide. The follicular puncture was performed using a disposable 18 G hypodermic needle connected to a 50-mL conical tube via a suitable silicon tubing system (WTA). The pressure for aspiration was maintained using a vacuum pump (WTA model BV-003, WTA) with negative pressure adjusted between 60 and 80 mmHg. Only follicles from ~4 mm to ≤8 mm were aspirated. Follicles ≥ to 9 mm were starting a dominance phase and were not aspirated. After the OPU of both ovaries, the aspiration system was replaced with a new one before conducting OPU for the next cow. OPUs from winter and summer were conducted in February and August, respectively by the same operator.

Sample collections

Collection of cumulus-oocyte-complexes and oocyte isolation

Following OPU procedures for each animal, COCs were allowed to settle to the bottom of the collection tube. The uppermost aqueous fluid above the pelleted aspirate was then collected with a pipette and transferred to a new tube. Following searching the dense collection of cellular debris and tissue remnants, COCs were washed three times with holding media (ABT complete flush; ABT 360, LLC; Pullman, WA, USA). Grading of COCs was performed based on the criteria set by the International Embryo Technology Society [10]. Grade 1: >5 layers of even cumulus cells with even cytoplasm; Grade 2: three to five layers of cumulus cells, mostly even distributed, and even cytoplasm; Grade 3: < 3 layers of dense compact cumulus cells, often uneven, and abnormally small oocytes with clear, granular, and uneven cytoplasm; Grade 4: degenerated. Grade 3 and 4 COCs were discarded and not included in further analyses of this study.

Collected grades 1 and 2 COCs were immediately subjected to enzymatic and mechanical efforts to remove adhered cumulus cells using 10,000 units/mL hyaluronidase (Sigma H-4272) and a high-speed vortex. One ml of holding medium was added to each tube, and the contents were transferred to a separate petri dish. Denuded oocytes (germinal vesicle stage, GV) were then isolated and washed twice in PBS. Every oocyte was closely checked for the presence of somatic cells under a stereomicroscope. Finally, the oocytes were transferred individually to a new tube with minimal volume of PBS and immediately snap-frozen in liquid nitrogen. All samples were stored at -80°C until further analysis.

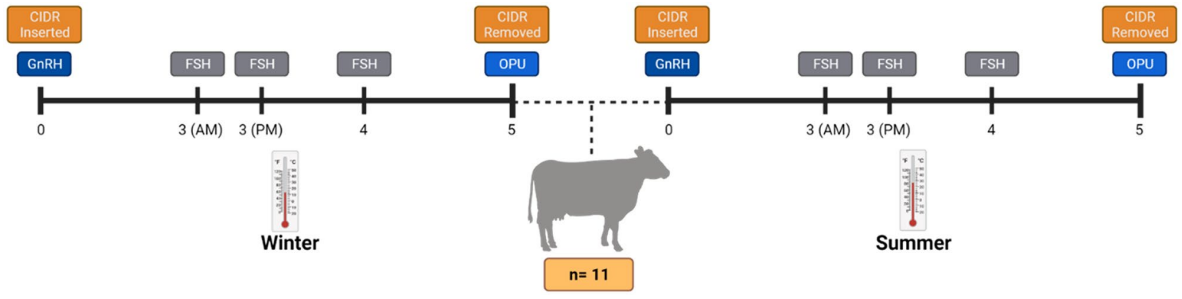


Fig. 1 Hormonal protocol used in the present study. Briefly, a 5-day CIDR and FSH synchronization and stimulation protocol was used to induce follicular growth before each OPU session (Winter and Summer). Created with BioRender.com

Collection of granulosa cells

For individual animals, the uppermost aqueous phase of the OPU collection fluid was transferred to a new 15 ml falcon tube and centrifuged at 750 ×g for 5 min to pelletize the cells. Granulosa cells were then immediately snap-frozen and stored at -80°C until further use.

Collection of plasma samples

At the time of each OPU, blood samples were collected using EDTA blood collection tubes (K2 EDTA BD Vacutainer®; Ref. 366643; BD Vacutainer; United Kingdom). OPU session happened in the morning period for both, summer and winter collections. Collection tubes containing the blood samples were centrifuged at 3000 ×g for 15 min to separate the plasma from the blood cells. The plasma was pipetted into microtubes and stored at -80°C for downstream analysis.

Leukocytes isolation

The white blood cell layer resulting from harvesting the plasma was then used to harvest the buffy coat. Briefly, the white layer was transferred into a 15 ml falcon tube using a sterile pipette and diluted in 3x the volume (~6 ml) of distilled water. Cells were mechanically suspended via pipetting, followed by centrifugation at 500×g for 15 min at 18°C. The supernatant was removed, and the pellets were scraped against a rack to unstick the cells. This step was repeated until the pellet was cleared of all red blood cells (2–3 times). Finally, the resuspended cells were transferred to a 2 ml microtube and centrifuged at 4000 ×g for 10 min. Without disturbing the cell pellet, the supernatant was removed, and the ensuing leukocytes were then immediately snap-frozen and stored at -80°C for downstream application.

Climatic conditions

Data for climatic conditions were collected daily for three weeks before each OPU session using the Florida Automated Weather Network (FAWN) [11]. The following weather measurements were taken from FAWN: temperature (average and maximum) and relative humidity. The temperature humidity index (THI) was calculated using the following equation: $THI = (1.8 \times T + 32) - [(0.55 - 0.0055 \times RH) \times (1.8 \times T - 26)]$. Where T = air temperature (°C) and RH = relative humidity (%) [12].

Plasma cortisol assay

Circulating plasma cortisol concentrations were quantified using the automated IMMULITE® 2000 Xpi cortisol Immunoassay kit (Cat. No. L2KCO2, Siemens Healthcare, CA, USA). Briefly, per the manufacturer's recommendations, the cortisol kit was adjusted for each lot number with a calibration range of 10 to 500 ng/mL. Commercially available tri-level (26.8, 149, and 254 ng/mL) quality control samples (Lyphocheck Immunoassay Plus Control, Cat. No. 370, Bio-Rad, Hercules, CA, USA) were run daily before the experimental samples. Quality control samples were considered to pass if the coefficient of variation (CV) was below 10% for each level and the replicates were within the manufacturer's reported range. Before analysis, samples were thawed at room temperature and run in duplicates. An internal calculation of quantification was reported for each duplicate, and these values were averaged to determine the CV. All concentrations reported have a CV of less than 10%.

Total RNA extraction, reverse transcription, and quantitative real-time PCR of leukocytes

Total RNA was extracted from leukocytes using the PureLink™ RNA Mini Kit (Cat. No. 12183025; Thermo Fisher Scientific™; Austin, TX, USA) according to the manufacturer's instruction. Samples were homogenized in 600 µL of lysis buffer containing 1% mercaptoethanol. The "On-Column PureLink® DNase Treatment Protocol" from the PureLink™ DNase Set (Cat. No. 12185010; Thermo Fisher Scientific™) was performed on individual samples to remove DNA contaminants. RNA yield and purity were analyzed using the NanoDrop™ One Spectrophotometer (Thermo Fisher Scientific™) with criteria set that the yield (>20 ng/µL) and the purity (absorbance 260/280 ratio ~ 2). Cows containing valid samples from summer and winter, were keep for further analysis. Samples were then stored at -80 °C until further use.

RNA samples ($n=7$ in summer and $n=7$ in winter) were reverse transcribed to cDNA using the High-Capacity cDNA Reverse Transcription Kit (Cat. No. 4368814; Thermo Fisher Scientific™) following the manufacturer's instruction. Briefly, 500 ng of RNA and ensuing reagents were combined and subjected to incubation in a Bio-Rad C1000 Touch™ Thermal Cycler at an initial temperature of 25°C for 10 min, followed by 37°C for 120 min, 85°C for 5 min, and then 4°C. The final output volume of 20 µL of cDNA was then diluted 1:80 with DEPC-treated water and stored at -20 °C for further qRT-PCR reactions.

Primers used for quantitative real-time PCR (qPCR) are indicated in Supplementary Table 1. The characteristics of the primers were checked in The OligoAnalyzer™ Tool software, (Integrated DNA Technologies, Biodynamics, https://www.idtdna.com/pages/tools/oligoanalyzer?returnurl=%2Fcalc%2Fanalyzer), while the specificity was compared by BLAST1 (NCBI, http://blast.ncbi.nlm.nih.gov). each primer pair were previously validated to establish primer pair efficiency (standard curves) and optimal primer concentration (concentration test). For all reactions (target and reference genes), a master mix containing SYBR Green (Cat. No. 1725274; SsoAdvanced Universal SYBR Green Supermix; Bio-Rad), forward and reverse primers, and DEPC-treated water were prepared

in a 2 ml microtube. qPCR reactions were conducted in triplicates and prepared in a 96-well PCR plate (Cat. No. HSP9601; Bio-Rad) containing 16 µL of the master mix and 4 µL of the diluted cDNA samples. No template controls (NTC) without cDNA were run in each PCR plate. The Bio-Rad CFX software was used to run the protocol as follows: denaturation at 95°C for 3 min, followed by 40 cycles of 95°C for 10 s, and 60°C for 30 s, and finally, annealing/extension and plate read at 65°C for 5 s and then melting curve analysis at 95°C+0.5°C. No amplification was detected in NTC. RefFinder [13, 14] was used to determine the stability of the reference genes, and according to their Cq, *ACT-B*, and *RPL15* were the most stable reference genes. Analysis to determine the relative expression of the genes of interest was done using the PFAFFL equation [15], considering each primer's efficiency and following normalization using the geometric mean of the selected reference genes (*ACT-B* and *RPL15*). qPCR products from reactions containing target and reference genes primers were submitted to agarose gel electrophoresis and sequencing and identities were confirmed.

Preparation of RNA from oocytes and granulosa cells for sequencing

Total RNA extraction of oocytes was performed after pooling 2–4 oocytes from a single cow and using the Arcturus™ PicoPure™ RNA (Thermo Fisher Scientific™) according to the manufacturer's instruction Total RNA from granulosa cells was extracted using the miRNeasy mini kit (Qiagen, Hilden, Germany). For both types of samples (oocytes and granuloma cells), on-column DNA digestion was performed using the RNase-Free DNase Set (Qiagen) to remove genomic DNA contaminants. The concentration and integrity of the isolated samples were then assessed with NanoDrop 8000 spectrophotometer (Thermo Fisher Scientific™) and Agilent 2100 Bioanalyzer (Agilent Technologies, CA), respectively. RNA samples were pooled from two individual animals to create five biological replicates ($n=2$ cows/pool, 5 pools per season) for both oocytes and granulosa cells, collected during the summer and winter. RNA samples were stored at -80 °C until sequencing.

Library preparation and RNA-sequencing

For library preparation, messenger RNA was purified from total RNA using poly-T oligo-attached magnetic beads. After fragmentation, the first strand of cDNA was synthesized using random hexamer primers, followed by the second strand of cDNA synthesis. The library was ready after the end repair, A-tailing, adapter ligation, size selection, amplification, and purification. The libraries were checked with a Qubit DNA HS Assay Kit in a Qubit 2.0 Fluorometer (Thermo Fisher Scientific™) for concentration, qPCR for quantification, and a bioanalyzer (Agilent Technologies) for the size distribution. Quantified libraries were pooled and sequenced using a NovaSeq6000 sequencing instrument (Illumina, Inc., San Diego, CA, USA) as paired end reads (150 bases).

Sequencing data analysis

FASTQ files were generated for each sample using the software bcl2fastq (Illumina Inc., San Diego, CA), and their quality was checked using the FastQC tool version 0.11.9. Data were analyzed using the CLC Genomics Workbench, version 21 (Qiagen). Raw sequencing reads were trimmed based on quality score (Q-score > 30), ambiguous nucleotides (maximum two nucleotides allowed), read length (≥ 15 nucleotides), and after removing adapter sequences. One replicate from oocyte/summer group didn't pass the quality control check. Therefore, we decided to exclude this replicate and its corresponding oocyte/winter and granulosa cell replicates from further analysis. Reads were mapped to the bovine reference genome (ARS-UCD1.3) applying the default software parameters. Data were normalized using the trimmed mean of the M-values normalization method (TMM normalization) [16] and presented as transcripts per million (TPM). The expression threshold was determined by the zFPKM method using the zFPKM R package v.1.16.0 [17]. Genes with zFPKM > −3 in all replicates were considered expressed. Differential expression analysis was done using the Differential Expression tool based on a negative binomial Generalized Linear Model (GLM) function. Differentially expressed genes (DEGs) were filtered based on fold change (FC ≥ 2) and the P-adjusted value (FDR < 0.05) [18]. The raw FASTQ files and processed CSV files have been deposited into NCBI's Gene Expression Omnibus (GEO) with the accession numbers (GSE235170, GSE235171) for the oocytes and granulosa cells, respectively.

After the identification of the DEGs in each cell type separately, a comparative analysis has been conducted to elucidate the unique and shared molecular responses of oocytes and granulosa cells to elevated environmental temperatures. Specifically, we focused on genes that were commonly dysregulated in both cell types during the summer followed by pathway enrichment analysis to identify the biological pathways impacted by these DEGs.

Pathways and ontological classification analysis

The DEGs were submitted to the Database for Annotation, Visualization, and Integrated Discovery (DAVID) Bioinformatics web tool v. 2021 [19] for pathways and ontological classification enrichment analysis. Pathways and biological processes (BP) were determined from the KEGG database [20] and GOTERM_BP_DIRECT annotation set, respectively.

Statistical analysis

Rectal temperature, plasma cortisol concentration, and HSP70 and HSP90 transcript abundance in leukocytes were analyzed using the MIXED procedure of SAS version 9.3 (SAS/STAT®, SAS Inst. Inc., Cary, NC) with cow as a random effect. The number of follicles and oocytes were analyzed by negative binomial regression analyses using the GENMOD procedure. The proportion of grade 1, 2, 3, and 4 oocytes were analyzed by ANOVA using the GLIMMIX procedure with logit function. Square-root transformation was applied when residuals were not normally distributed according to the Shapiro-Wilk and Kolmogorov-Smirnov tests. For all models, cow was considered the experimental unit, and data are presented as mean ± standard error of the mean. We set the significance level for rejecting the null hypothesis to $P \leq 0.05$ and considered trends significant at $0.05 \leq P \leq 0.10$.

Results

Climatic conditions

As expected, the average air temperature (27.5 °C vs. 11.5 °C), average maximum air temperature (33.7 °C vs. 16.9 °C), and relative humidity (82.3% vs. 83.5%) during the summer and winter, respectively, differed considerably (Fig. 2). After using the equation to calculate the THI for the 3 weeks prior to each sample collection, the summer estimate was 79.2, while the winter was 53.4 (Fig. 2; Table 1). Accordingly, the Livestock Safety Weather Index [21], a common resource used to classify the intensity of the THI values, recognizes four primary categories: normal, alert, danger, and emergency. Based on this criterion, over the three weeks preceding the OPU collections, the winter had 100.0% normal THI days, while the summer had 59.1% of the days considered as 'alert' and 40.9% considered as 'danger' THI thresholds (Table 1).

Rectal temperature and plasma cortisol concentration

Average rectal temperatures were higher ($P=0.03$) in the summer (39.2±0.2 °C) than in the winter (38.8±0.2 °C; Fig. 3A). However, plasma cortisol concentrations did not differ when comparing collections from the summer (29.4±3.0 ng/mL) and winter (34.4±4.2 ng/mL) seasons (Fig. 3B).

HSP70 and HSP90 transcript abundance in leukocytes

Quantitative analysis of *HSP70* and *HSP90* in leukocytes isolated from cows during the summer and winter seasons revealed that *HSP70* tended to have a higher abundance during the summer season, with no difference in the expression of *HSP90* (Fig. 3C and D).

Follicular observations and oocyte recovery

No significant difference in the total number of follicles (summer 23.9±3.9 vs. winter 18.9±4.8) and the total number of oocytes recovered (summer 13.0±3.6 vs. winter 9.0±1.6) between seasonal collections was observed (Table 2). However, oocyte quality differed when comparing the seasons. In summer, both the number (summer 1.09±0.5 vs. winter 6.4±1.7; P=<0.01) and the proportion (summer 7.1% ± 2.5 vs. winter 57.8% ± 12.0; P=<0.01) of grade 1 oocytes decreased, while the number (summer 4.1±1.1 vs. winter 1.2±0.7; $P=0.09$) and the proportion (summer 30.5% ± 5.5 vs. winter 12.3% ± 5.2; $P=0.04$) of grade 4 oocytes increased or tended to increased. The number of grade 2 and grade 3 oocytes did not differ significantly between seasonal collections, however, the proportion of grade 2 (summer 26.3% ± 8.4 vs. winter 11.4% ± 5.6; $P=0.05$) and grade 3 (summer 36.1% ± 5.4 vs. winter 8.3% ± 8.3; P=<0.01) oocytes was higher from collections during the summer compared to the winter (Table 2).

Oocyte transcriptome analysis

After quality control, data from 8 libraries ($n=4$ for summer and $n=4$ for winter) were used for the bioinformatic analyses. The eight cDNA libraries had an approximate average of 53 million clean reads per library, with an average of 98.4% of the reads mapped to the bovine reference genome. The principal component analysis (PCA) in Fig. 4A and hierarchical heatmap in Fig. 4B displayed clear separation and distribution based on the expression of genes for each group. A total of 12,489 and 13,129 genes were expressed (zFPKM > -3 in the four replicates) in the summer and winter groups, respectively with 12,239 genes being mutually expressed during both seasons. Alternatively, 250 genes were expressed exclusively in the summer, while 890 genes were expressed exclusively in the winter (Fig. 4C). Among the top 20 expressed genes, 16 were detected in both groups, including Ubiquitin B *(UBB)*, Serglycin *(SRGN)*, Inhibin Subunit Alpha *(INHA)*, Cytochrome C Oxidase I *(COX1)*, Cytochrome C Oxidase III *(COX3)*, and Heat Shock Protein Family B (Small) Member 1 *(HSPB1)* (Table 3).

Differential expression analysis indicated a total of 1,386 genes differentially expressed between the two groups (FC≥2; FDR=≤0.05; zFPKM>-3) in all biological replicates of the enriched group (Supp Table 2). During the summer, there was an up-regulation of 446 genes and a downregulation of 940 genes compared to the winter (Fig. 4D). Matrix Metallopeptidase 2 (*MMP2) was the* top downregulated gene (FC = -1628.99) and Tumor necrosis factor Receptor Superfamily Member 13B (*TNFRSF13B)* was among the top upregulated genes; (FC=213.56; Table 4).

Gene enrichment analysis of the oocytes identified protein digestion and absorption, ABC transporters, oocyte meiosis, and progesterone-mediated oocyte maturation as the top significant pathways upregulated

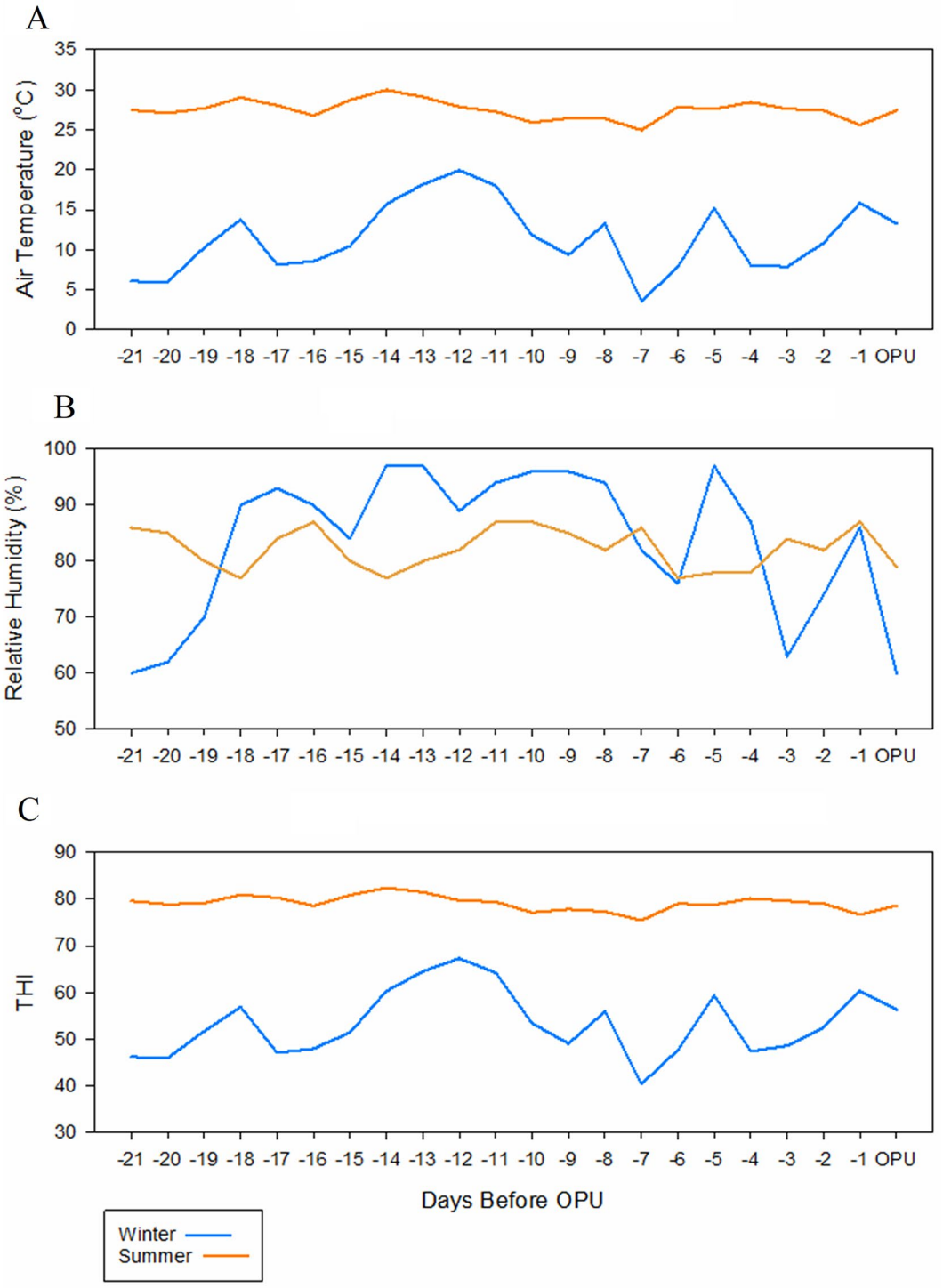


Fig. 2 Climatic conditions were collected for twenty-one days before each OPU session. **A**) Average air temperature, **B**) Relative humidity, **C**) Temperature humidity index (THI). Data were collected using the Florida Automated Weather Network (FAWN; https://fawn.ifas.ufl.edu/data/reports/)

Table 1 Descriptive statistics for the temperature humidity index (THI) average values for 21 days before each OPU session

Season	Mean	SD	Min	Max	CV, %	% Days THI normal	% Days THI alert	% Days THI danger
Winter	53.4	7.1	40.4	67.3	13.3	100.00	0	0
Summer	79.2	1.6	75.5	82.4	2.0	0	59.1	40.9

SD, Standard deviation; Min, Minimum; Max, Maximum; CV, Coefficient of variation

Thresholds cutoff points from *Livestock Weather Safety Index (LCI, 1970)*: THI ≤ 74 = Normal, 74 > THI ≤ 79 = Alert, 79 > THI ≤ 84 = Danger, and THI 84 = Emergency

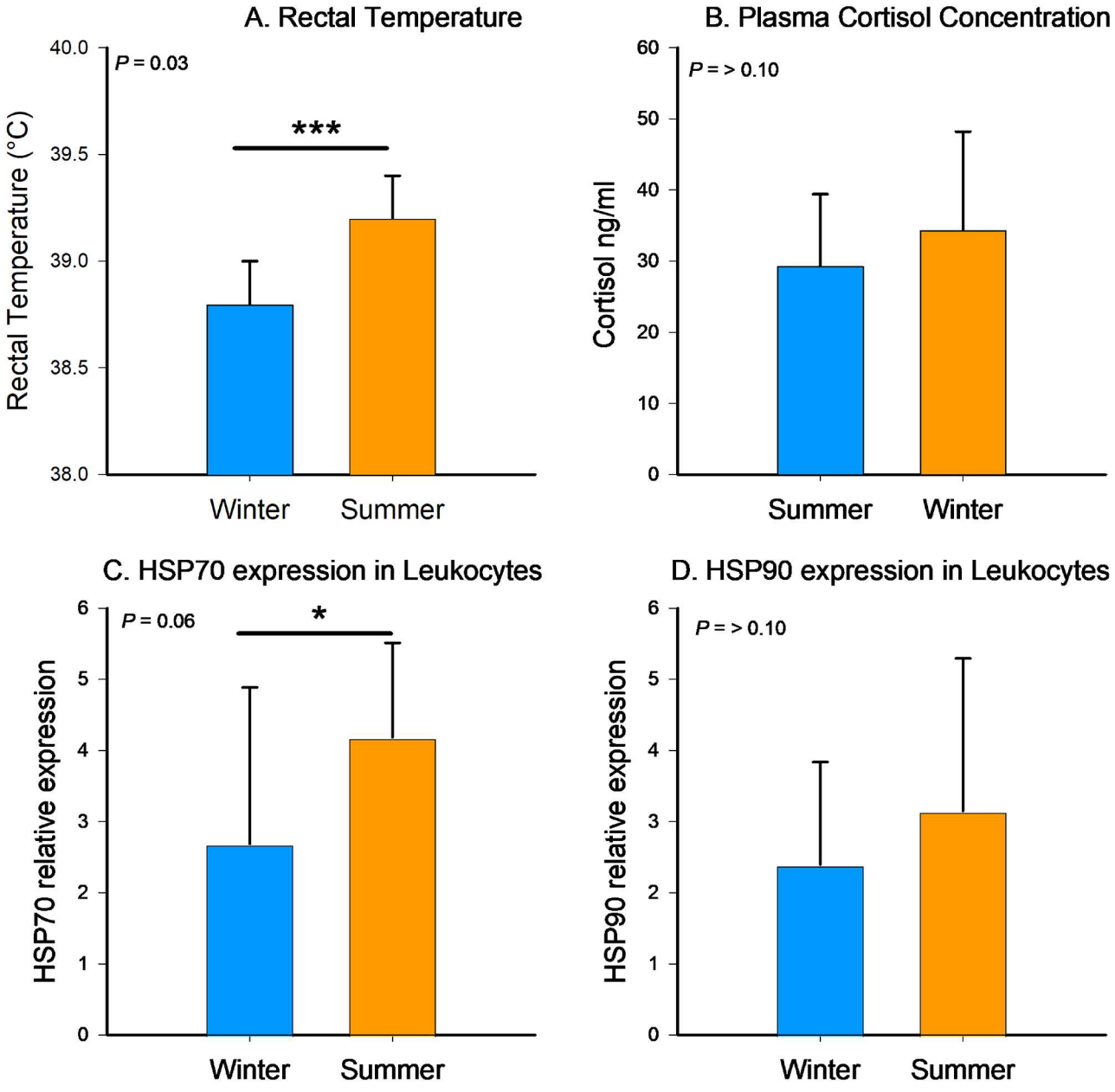


Fig. 3 Mean ± SEM of rectal temperature (**A**), plasma cortisol concentration (**B**), and *HSP70* (**C**) and *HSP90* (**D**) transcript abundance from beef cows during the summer and winter ($n = 11$). *** Denotates statistical differences when $P \leq 0.05$ and * denotates statistical tendencies when $P \geq 0.05$ still $P < 0.1$

Table 2 Number of follicles visualized at OPU and of recovered oocytes and their quality in summer and winter

Variables (Mean ± SEM)	SUM	WIN	*P* value
	Numbers		
Total follicles	23.9 ± 3.9	18.9 ± 4.	0.57
Total oocytes	13.5 ± 0.2	9.3 ± 1.6	0.36
Grade 1	1.09 ± 0.5	6.4 ± 1.7	< 0.01
Grade 2	3.2 ± 1.3	1.4 ± 0.7	0.13
Grade 3	5.1 ± 1.5	0.6 ± 0.6	0.64
Grade 4	4.1 ± 1.1	1.2 ± 0.7	0.09
	Percentage		
Grade 1	7.1 ± 2.5	57.8 ± 12.0	< 0.01
Grade 2	26.3 ± 8.4	11.4 ± 5.6	0.05
Grade 3	36.1 ± 5.4	8.3 ± 8.3	< 0.01
Grade 4	30.5 ± 5.5	12.3 ± 5.2	0.04

in summer (Fig. 5A). While ECM receptor interaction, phosphoinositide 3-kinase (*PI3K*)–*AKT* (*PI3K-AKT*) signaling, and focal adhesion pathways were the top-significant pathways downregulated (Fig. 5B). Moreover, the meiotic cycle and DNA methylation involved in gamete generation were the top significant biological processes upregulated in summer and extracellular matrix organization was the top downregulated (Fig. 5C & D).

Granulosa cells transcriptome analysis

Data from 8 libraries ($n=4$ for summer and $n=4$ for winter) were used in the bioinformatic analyses following quality control. The eight cDNA libraries had an approximate average of 42 million clean reads per library, with an

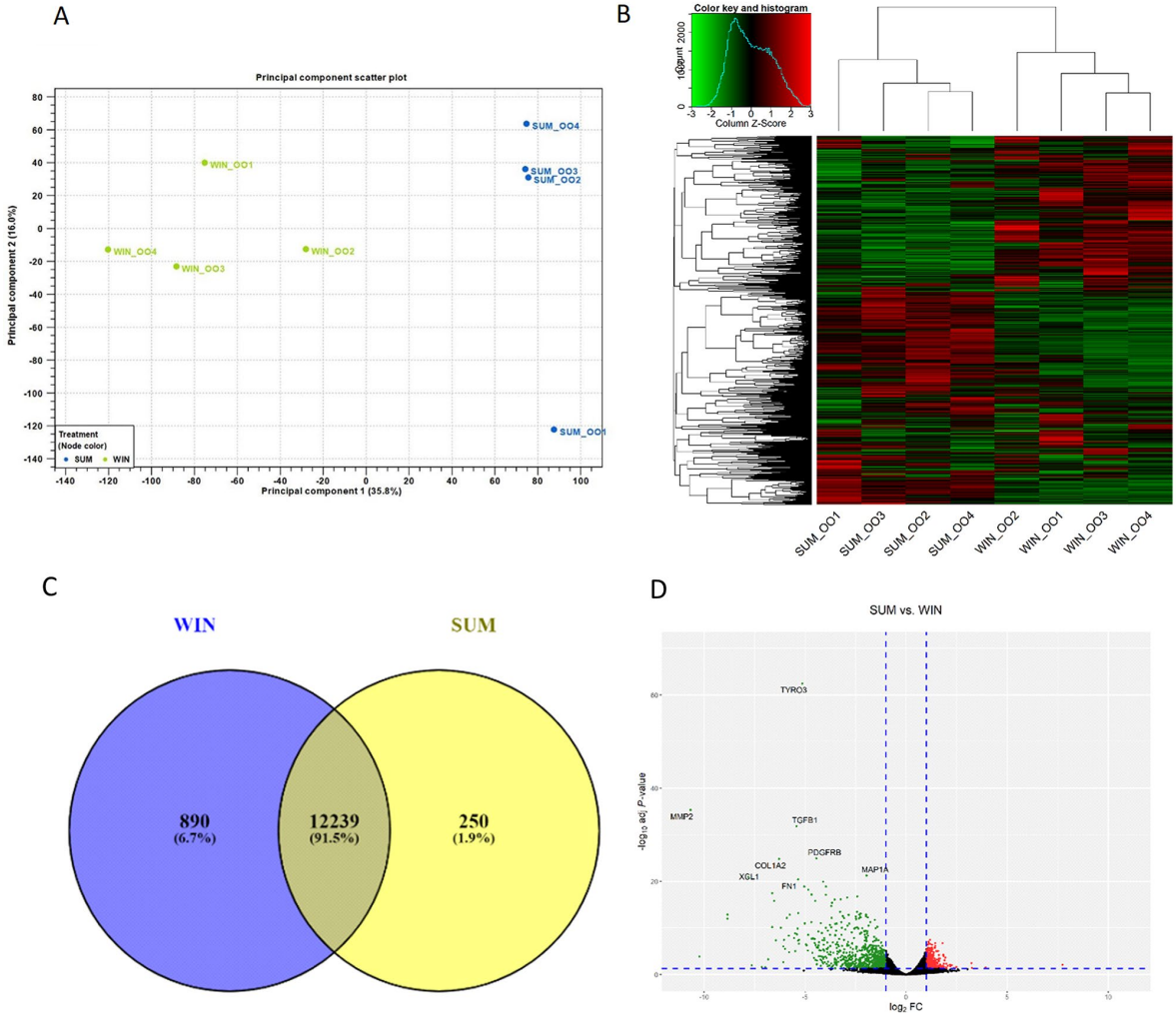


Fig. 4 Transcriptomic analyses and differentially expressed genes (DEGs) during summer and winter of oocytes in beef cows. Principal component analysis (PCA; **A**) and hierarchical heatmap (**B**) indicating the expression of genes in oocyte's during summer and winter. Venn diagram (**C**) showing exclusively and mutually expressed genes between summer and winter and Volcano plot (**D**) indicating the differentially expressed genes from summer compared to the winter [Individual red and green dots represent the number of up- and downregulated genes, respectively (FC ≥ 2; FDR p-value ≤ 0.05)]. Summer = SUM ($n=4$) and Winter = WIN ($n=4$)

Table 3 The top 20 most abundant expressed genes in the oocytes from the summer (SUM) and the winter (WIN), represented as the mean of TPM. Common genes in SUM and WIN are bolded

Gene symbol	SUM, TPM	Gene symbol	WIN, TPM
UBB	8675.86	***SRGN***	7458.34
SRGN	6404.08	***INHA***	6818.34
HSPB1	4652.46	***COX3***	6490.96
VIM	4635.51	***VIM***	6143.22
ACTG1	4398.71	***UBB***	5878
COX3	4098.08	***ACTG1***	5643.2
RPLP0	4082.57	***COX1***	5413.63
RPS15	4031.76	***HSPB1***	5185.75
RPLP1	3724.83	***RPS15***	4297.18
ACTB	3655.07	***RPLP0***	4251.25
RPS5	3647.72	*ATP6*	4164.03
ACCSL	3629.19	***ACTB***	4132.6
COX1	3460.1	***RPLP1***	4119.52
INHA	3214.14	***TPT1***	4013.41
GAPDH	3181.01	***ENO1***	3948.27
TPT1	3156.35	*ND3*	3906.64
RPL7A	3153.91	***GAPDH***	3719.85
ENO1	2934.14	*SERPINE2*	3687.72
RPL18A	2807.29	***RPS5***	3619.45
ZP3	2770.11	*ND2*	3455.46

TPM-Transcript per million

Table 4 Top 10 up- and downregulated, genes in the oocytes from the summer (SUM) compared to the winter (WIN) groups

Name	FC	FDR
TNFRSF13B	213.56	0.008224
ENSBTAG00000050942	15.23	0.033098
GAST	9.56	0.040492
ENSBTAG00000030892	9.41	0.003428
DRD5	5.62	0.023822
PPYR1	5.18	0.038289
EFNA3	4.82	0.009969
VSX1	4.57	0.016235
TLX3	4.52	0.008296
ENSBTAG00000018583	4.20	0.013834
COL3A1	-98.37	3.38E-18
TEAD4	-113.22	0.000543
TNFRSF8	-124.88	0.028745
TNFSF4	-141.01	0.023035
C1QTNF5	-200.22	0.011001
XCL1	-223.48	1.18E-21
EMP1	-456.81	1.04E-12
ANXA8L1	-457.97	1.34E-13
TMEM26	-1198.66	0.000143
MMP2	-1628.99	4.78E-36

FC-Fold change, FDR-False discovery rate

average of 98.57% of the reads mapped to the bovine reference genome. The PCA (Fig. 6A) and hierarchical heatmap (Fig. 6B) displayed clear separation and distribution based on the expression of genes for each group. A total of 12,504 and 12,030 genes were expressed (zFPKM > -3 in the four replicates) in the summer and winter groups, respectively, with 11,488 genes being mutually expressed in both groups. Alternatively, 1016 genes were expressed exclusively in the summer, while 542 genes were expressed exclusively in the winter (Fig. 6C). Among the top 20 expressed genes, 16 genes were also mutually represented amongst both groups (Table 5), including *COX1-3*, *ND1-6*, *ATP6*, and *ATP8* with *COX1* and *COX3* represented as the top 2 genes in both seasons.

Differential expression analysis indicated a total of 2,209 genes significantly differentially expressed between the two seasons (FC≥2; FDR=≤0.05; zFPKM>-3) in all replicates of the enriched group; Supp Table 3). Comparing the granulosa cells collected during the summer and the winter groups, there was an up-regulation of 1083 genes and a down-regulation of 1126 genes (Fig. 6D). Table 6 represents the top 10 up- and downregulated DEGs. Gene enrichment analysis of DEGs in granulosa cell samples identified protein processing in the endoplasmic reticulum and cell cycle as the top-significant upregulated pathways in summer, while chemokine signaling and Th17 cell differentiation were the top downregulated (Fig. 7A & B). When analyzing biological processes enrichment, microtubule-based movement and cell division were the top upregulated, while the inflammatory response was the top downregulated in summer (Fig. 7C & D).

Comparative gene expression analysis of oocyte and granulosa cells

Differential expression analysis revealed a set of 270 genes commonly dysregulated in both oocyte and granulosa cell datasets (Fig. 8). Within this set, 127 genes exhibited a similar expression pattern in which 13 were upregulated and 114 were downregulated in both oocytes and granulosa cells during summer compared to winter conditions. Conversely, 101 genes were upregulated in granulosa cells and downregulated in oocytes while 42 genes showed the opposite pattern, being upregulated in oocytes, and downregulated in granulosa cells (Fig. 8). Pathway analysis of these 270 common DEGs identified several pathways including transforming growth factor-β (*TGF-beta*), TNF, mitogen-activated protein kinase (*MAPK*), and *PI3K-Akt* signaling pathways, as well as cytokine-cytokine receptor interaction, *Th1* and *Th2* cell differentiation, focal adhesion, ECM-receptor interaction, and protein digestion and absorption pathways as the top affected pathways. The interaction network of these pathways and their corresponding DEGs

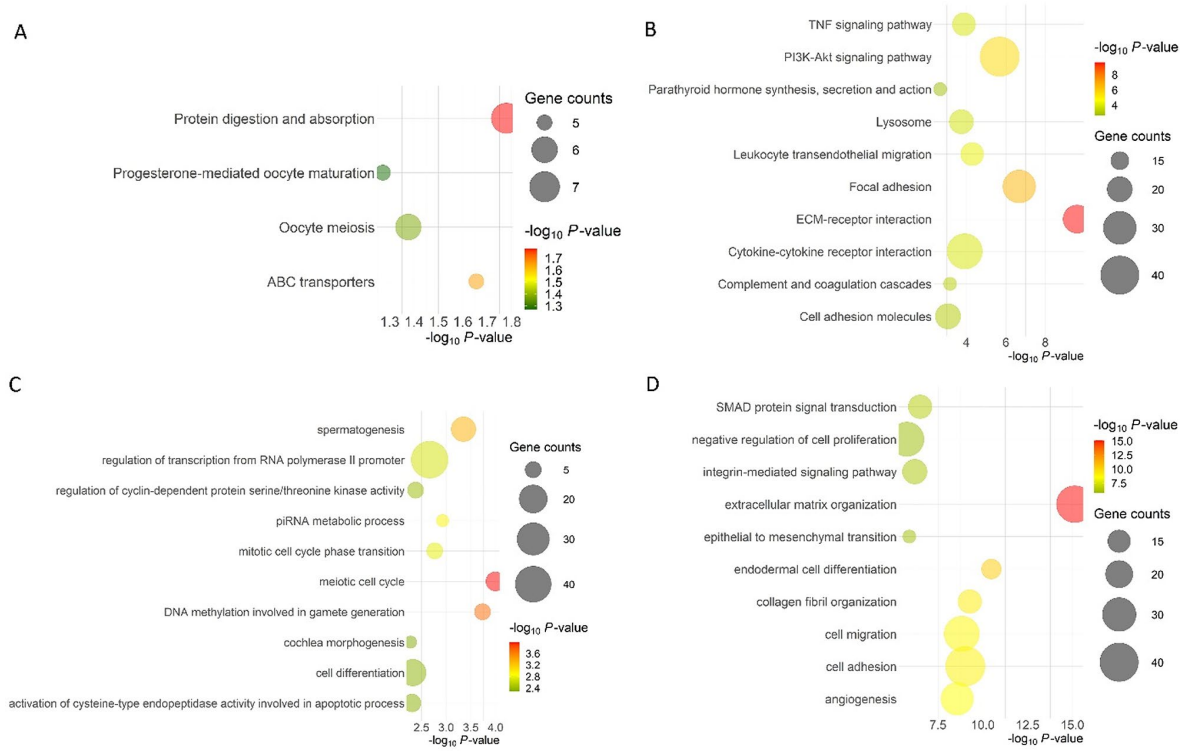


Fig. 5 Top 20 enriched pathways (**A**. Upregulated pathways; **B**. Downregulated pathways) and biological processes (BP; **C**. Upregulated BP; **D**. Downregulated BP) in oocytes collected during summer (SUM) and winter (WIN) in beef cows

is presented in Fig. 9. Most of these pathways involved genes that were mutually downregulated in both datasets, as depicted in Fig. 10.

Discussion

Our study aimed to identify differences in the transcriptome of oocytes and granulosa cells collected from beef cows during the summer and winter months. Throughout our study, the THI during the summer period continually deviated from normal levels, likely indicating that the animals within the study were exposed to environmental heat stress as evidenced by their increased rectal temperatures. In *Bos taurus* beef cattle, a THI over 75 signifies a level of heat stress [22], which was replicated in the present study with the average summer THI being 79.2. While THI has been commonly used as an indicator of heat stress in livestock [23, 24], it does come with certain limitations given that other factors, such as solar radiation and wind speed, are not included in its calculation [25, 26]. In our study, plasma cortisol concentrations did not differ between collections during the summer and winter. Cortisol is a steroid hormone regulated by the hypothalamic-pituitary-adrenal axis [27], in which previous studies in dairy cattle [28–30] have found a significant increase in plasma cortisol concentrations in animals exposed to heat stress. Such discrepancies in cortisol results might be due to the fact that our observations included chronic (long-term) rather than acute (short-term) exposure to levels of heat stress. Additionally, in our study the transcript abundance of *HSP70* in leukocytes tended to increase in the summer ($P=0.06$), while levels of *HSP90* remained stable during both seasons. In peripheral blood mononuclear cells of beef calves, Kim et al. [31] found that *HSP70* expression was higher during conditions of heat stress, while the expression of *HSP90* showed no differences, concluding that *HSP70* exhibits a more sensitive mechanism than *HSP90*, aiding in the adaptation to heat stress. A major function of HSPs are via their role as indicators of thermotolerance [32], defined as an animal's ability to balance heat production/dissipation under ambient temperatures above the thermoneutral zone [33]. Therefore, the combination of increased rectal temperatures and the tendency of increased *HSP70* expression in leukocytes during the summer, may indicate that our experimental animals have experienced heat stress prior to the summer OPU collections.

Heat stress affects oocyte quality and subsequently oocyte competence [34], nuclear maturation rate [35], fertilization rate [35], and blastocyst production in vitro

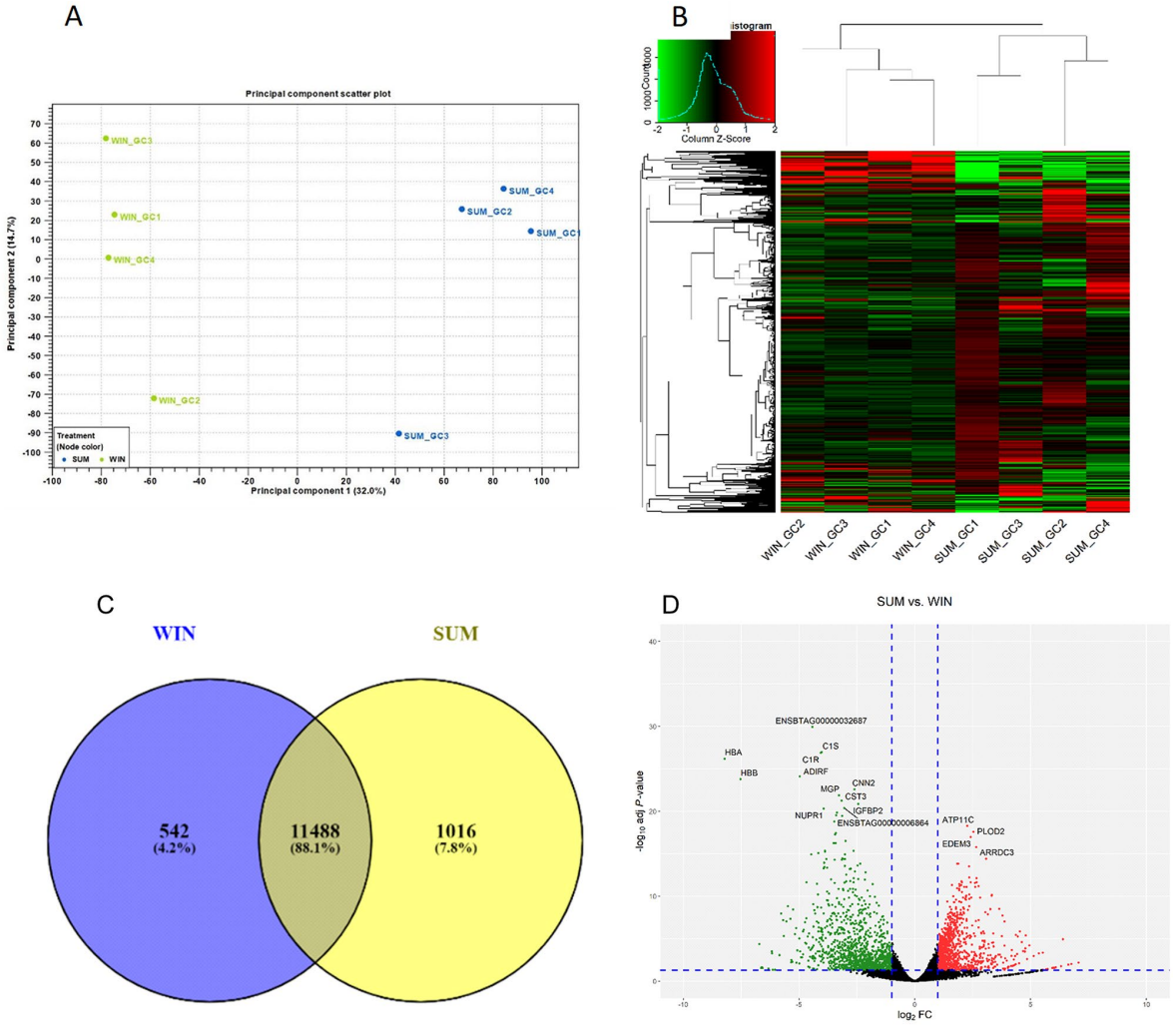


Fig. 6 Transcriptomic analyses and differentially expressed genes (DEGs) during summer and winter of granulosa cells in beef cows. Principal component analysis (PCA; **A**) and hierarchical heatmap (**B**) indicating the expression of genes in granulosa cells during summer and winter. Venn diagram (**C**) showing exclusively and mutually expressed genes between summer and winter and Volcano plot (**D**) indicating the differentially expressed genes from summer compared to the winter [Individual red and green dots represent the number of up- and downregulated genes, respectively (FC ≥ 2; FDR p-value ≤ 0.05)]. Summer = SUM ($n = 4$) and Winter = WIN ($n = 4$)

[34]. Similarly, in the present study while a higher proportion of grade 1 oocytes was collected during winter, the proportion of grade 4 oocytes was higher in summer collections. In addition, heat stress disturbs the synthesis of steroid hormones (i.e., decrease estradiol although increase progesterone concentration in the follicular fluid) [36] which are directly involved in the mechanisms regulating oocyte maturation. The consistency in these results among different studies should be a concern for the beef industry, where there is low adoption of reproductive biotechnologies that would help improve fertility and pregnancy rates in the summer (such as in vitro embryo production and embryo transfer programs) and where reproductive programs consisting of natural mating with no controlled breeding season (i.e., bulls are allowed to breed cows continuously during the year) are predominantly used [37].

In the current study we showed that oocytes and granulosa cells respond to environmental fluctuations between the summer and winter seasons through the activation or inhibition of genes involved in several pathways associated with ovarian function. We reported here that 1,386 genes were differently expressed in oocytes during the summer and winter. The top upregulated protein-coding genes for oocytes collected during the summer were *TNFRSF13B*, Gastrin (*GAST*), Dopamine Receptor D5

Table 5 The top 20 most abundantly expressed genes in the granulosa cells of the summer (SUM) and the winter (WIN) groups, represented as the mean of TPM. Common genes in SUM and WIN are bolded

Gene symbol	SUM, Avg TPM	Gene symbol	WIN, Avg TPM
COX1	193,132	***COX1***	212,379
COX3	125,826	***COX3***	165,935
ATP6	72772.2	***ND3***	126,366
ND1	53169.8	***ATP6***	83449.6
CYTB	51791.2	***COX2***	72552.4
COX2	48233.7	***ND1***	59318.4
ND3	45521.3	***CYTB***	54185.6
ND4	43397.3	***ND4***	39361.5
ND2	32595.8	***ND2***	24648.4
ND5	22146.8	***ND6***	19,144
ND6	14126.5	***ND5***	18328.2
INHA	10505.2	***ND4L***	9892.43
SRGN	5114.24	***ENSBTAG00000043570***	9711.51
ENSBTAG00000043570	5063.53	*ENSBTAG00000043567*	5481.22
ND4L	4927.43	***ATP8***	2139.79
GSTA1	4899.34	***GSTA1***	1694.48
SERPINE2	4193.81	*RPLP1*	1181.72
ATP8	3699.33	***INHA***	1064.28
HSPB1	3475.47	*RPL18A*	1023.44
INHBA	2863.98	*HBA*	868.832

TPM-Transcript per million

Table 6 Top 10 up- and downregulated genes in the granulosa cells from the summer (SUM) compared to the winter (WIN)

Name	FC	FDR
ENSBTAG00000050418	134.88	0.006551
DNAH10	108.88	0.009549
LRRC71	98.71	0.011828
DNAH11	84.21	1.19E-05
ACCSL	79.89	0.018649
DNAH6	68.15	0.024894
TMEM151B	65.44	0.028451
PLEKHS1	63.40	0.027665
ZP2	61.61	0.029016
CCDC13	61.03	0.030493
NKX2-3	-70.50	0.046237
CABLES1	-71.73	0.000577
WNT2	-72.44	0.000320
CIDEC	-79.70	0.035243
ZNF831	-95.60	0.028134
GASK1A	-98.00	0.024834
NRN1	-100.16	0.027999
RNASE1_2	-104.72	4.51E-05
HBB	-185.26	1.68E-24
HBA	-296.61	6.38E-27

FC-Fold change, FDR-False discovery rate

(*DRD5*), Pancreatic Polypeptide Receptor 1 *(PPYR1)*, Ephrin A3 *(EFNA3)*, Visual System Homeobox 1 *(VSX1)*, and T Cell Leukemia Homeobox 3 *(TLX3)*. On the other hand, Collagen Type III Alpha 1 Chain *(COL3A1)*, TEA Domain Transcription Factor 4 *(TEAD4)*, TNF Receptor Superfamily Member 8 (*TNFRSF8*), TNF Superfamily Member 4 (*TNFSF4*), C1q and TNF Related 5 (*C1QTNF5*), X-C Motif Chemokine Ligand 1 (*XCL1*), Epithelial Membrane Protein 1 (*EMP1*), Annexin A8 Like 1 (*ANXA8L1*), Transmembrane Protein 26 (*TMEM26*), and Matrix Metallopeptidase 2 (*MMP2*) were among the top downregulated genes in summer. These dramatic differences in the transcriptome of oocytes collected during the summer and winter seasons indicate both oocytes response to elevated environmental THI and its subsequent impact on the physiology of the oocyte.

Genes involved in regulating cellular proliferation were upregulated in oocytes collected during the summer season. Among the transcripts upregulated, *TNFRSF13B* is a tumor necrosis factor receptor superfamily member previously identified in human and mouse oocytes [38]. *GAST*, which encodes for a peptide hormone key in gastric acid secretion in stomach G cells, was reported to be associated with positive regulation of cell proliferation [39–41]. *EFNA3* is a member of the ephrin (*EPH*) family, a group of molecules known for playing a role in embryonic development, cellular proliferation, migration, and adhesion [42–44]. *DRD5* is expressed in several types of cancers, and treatment with *DRD5* agonists can induce apoptosis and autophagy [45]. These upregulated genes are members of the meiotic cell cycle and cell differentiation pathways, enriched in oocytes collected during the summer season. The upregulation of cellular proliferation markers in immature oocytes from summer compared to winter could be a protective response to the challenging conditions caused by heat stress. However, it can also disrupt the normal developmental process of the oocyte which relies on the balance between proliferation and apoptosis in the COCs, leading to suboptimal maturation or developmental competence [46]. Additionally, the cumulus cells surrounding the oocyte normally undergo a shift from proliferation to differentiation as the oocyte matures. Persistent proliferation markers could suggest incomplete differentiation of these supporting cells [47].

Interestingly, Gendelman and Roth (2012) described an abundance of Proto-Oncogene C-Mos (*C-MOS)*, Growth Differentiation Factor 9 *(GDF9)*, POU Class 5 Homeobox 1 *(POU5F1)*, and Glyceraldehyde-3-Phosphate Dehydrogenase *(GAPDH)* transcripts as higher in MII-stage oocytes collected in the cold season than in those from the hot season [48]. However, in their study, this seasonal variation was not present in GV-stage oocytes [48]. In contrast, our study found that *MOS* and *GDF9* were upregulated in oocytes during the summer

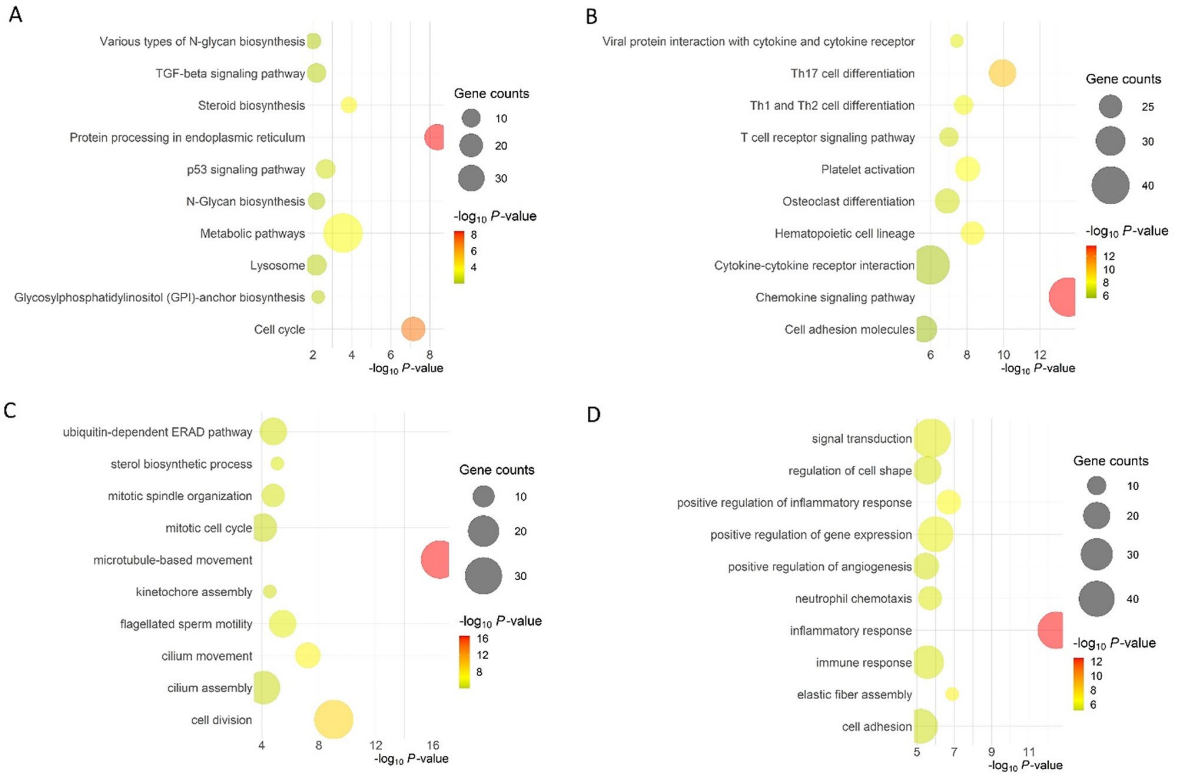


Fig. 7 Top 20 enriched pathways (**A**. Upregulated pathways; **B**. Downregulated pathways) and biological processes (BP; **C**. Upregulated BP; **D**. Downregulated BP) in granulosa cells collected during summer (SUM) and winter (WIN) in beef cows

season (GV-stage). Also, similar to Ferreira et al. [49], we found an upregulation of Fibroblast Growth Factor 16 (*FGF16)* and *GDF9* in oocytes collected during the summer months compared to those in the winter months. This may signify the fact that oocytes respond to thermal stress in stage dependent manner.

Among the genes downregulated in oocytes collected during the summer season, transmembrane protein 26 (*TMEM26*) and matrix metalloproteinase 2 (*MMP2*) were suppressed by more than a thousand-fold. The latter, i.e., *MMP2*, levels in human follicular fluid were found to be a reliable marker for oocyte maturation in in vitro fertilization and intracytoplasmic sperm injection cycles [50]. Moreover, a recent study by Latorraca et al. [51] identified *MMP2* to be present at all phases of oocyte growth (common to all oocyte size groups, from <60 µm to >120 µm). Therefore, the significant reduction of such transcripts in oocytes collected during the summer season implies the negative impact of thermal stress on oocytes' developmental competence by suppressing transcripts critical for their growth and development. Collectively, double the number of transcripts were found to be downregulated in oocytes collected during the summer compared to their winter counterparts. This fact evidenced the potential impact of elevated environmental temperatures on oocytes competence is via the suppression of the expression of transcripts important for their growth and maturation. This has also been evidenced in the type of pathways in which the downregulated transcripts participate (Fig. 5B). A significant proportion of downregulated transcripts were found to be involved in *PI3K-Akt* signaling and focal adhesion pathways. The *PI3K-Akt* signaling pathway is reported to be a key regulator of many cellular processes associated with cell proliferation, survival, growth, cytoskeletal rearrangement, and metabolism [52], which makes the pathway to be a potential predictor for the developmental competence of oocytes and successful embryo implantation [53]. Similarly, studies in bovine oocytes revealed that follicular granulosa cells' expression of the *PI3K-Akt* signaling pathway to be correlated with the developmental competence of oocytes after parthenogenetic activation [54]. Therefore, our results demonstrate that one of the mechanisms by which environmental thermal stress impacts oocyte competence is via the suppression of transcripts involved in various key pathways regulating follicular development, oocyte maturation, and further embryonic developmental potential.

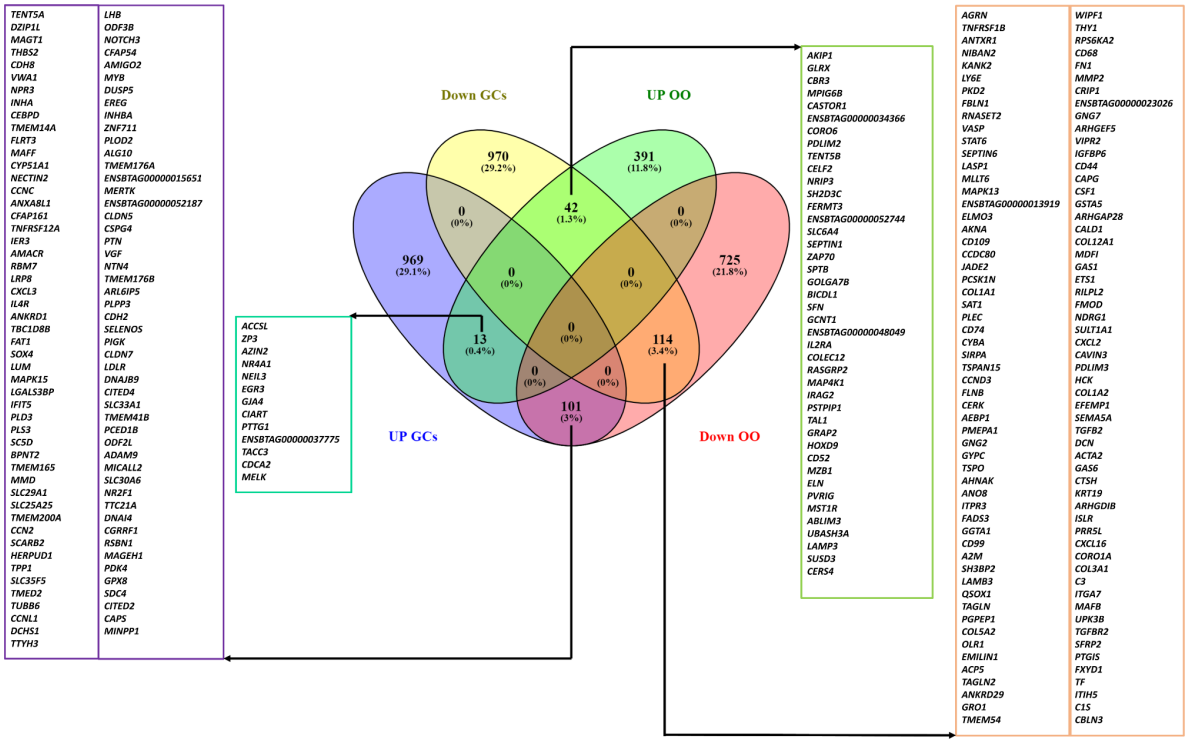


Fig. 8 Commonly and exclusively differentially expressed genes from summer compared to winter collected oocytes (OO) and granulosa cells (GCs)

Granulosa cells are known to mediate oocyte developmental process via an active bidirectional communication with the oocyte [55, 56]. Therefore, any significant negative impact of environmental seasonal changes on granulosa cell physiology would have a direct impact on ovarian function and oocyte developmental processes. Transcriptome analysis of granulosa cells form summer and winter seasons revealed that among the 2,209 differentially expressed genes, several members of the Heat Shock proteins family (Heat Shock Protein Family A *(Hsp70)* Member 5 (*HSPA5*), Heat Shock Protein 90 Beta Family Member 1 (*HSP90B1*), DnaJ Heat Shock Protein Family (*Hsp40*) Member B9 (*DNAJB9*), B11 (*DNAJB11*), B14 (*DNAJB14*), B13 (*DNAJB13)*, and C5 (*DNAJC25*) were found to be upregulated in granulosa cells during the summer season as a response to higher environmental temperatures. These genes have been previously described as components of the Heat Shock Protein cascade in response to heat stress [57, 58], and have been shown to be elevated in granulosa cells after in vitro exposure to acute heat stress [59, 60]. In addition, here we report that several members of the axonemal dynein complex members including Dynein Axonemal Heavy Chains 1 (*DNAH1*), 5 (*DNAH5*), 6 (*DNAH6*), 7 (*DNAH7*), 9 (*DNAH9*), 10 (*DNAH10*), 11 (*DNAH11*), and 12 (*DNAH12*) to be upregulated in the summer months. Moreover, *DNAH6*, *DNAH10*, and *DNAH11* were in the top 10 upregulated genes in the granulosa cells during summer. Dyneins are a family of cytoskeletal motor proteins that form the microtubules in cells. Dyneins have been localized in follicles (granulosa cells and oocytes) [61, 62], and in mice, the inhibition of dynein proteins significantly increased the number of growing follicles [63].

Other class of transcripts related to Zona Pellucida Glycoprotein 2 (*ZP2*), a critical component of the Zona Pellucida, was in the top 10 upregulated genes in the granulosa cells during summer. Similar studies have also previously indicated that heat stress impacts the ZP function and therefore disrupts the anti-polyspermy system of the oocyte, which resulted in increasing polyspermy [64] and increased number of pores and a more significant percentage of oocytes with amorphous ZPs [65] as a result of thermal stress. Collectively, our data and also from others suggest that in vivo, granulosa cells are also susceptible to seasonal heat stress provoking changes in cell transcriptome dynamics, which could be possibly related to the decrease in oocyte quality in the summer.

As observed in oocytes, granulosa cells collected during summer showed upregulation of genes involved in protein processing in endoplasmic reticulum, while downregulated genes are involved in chemokine signaling

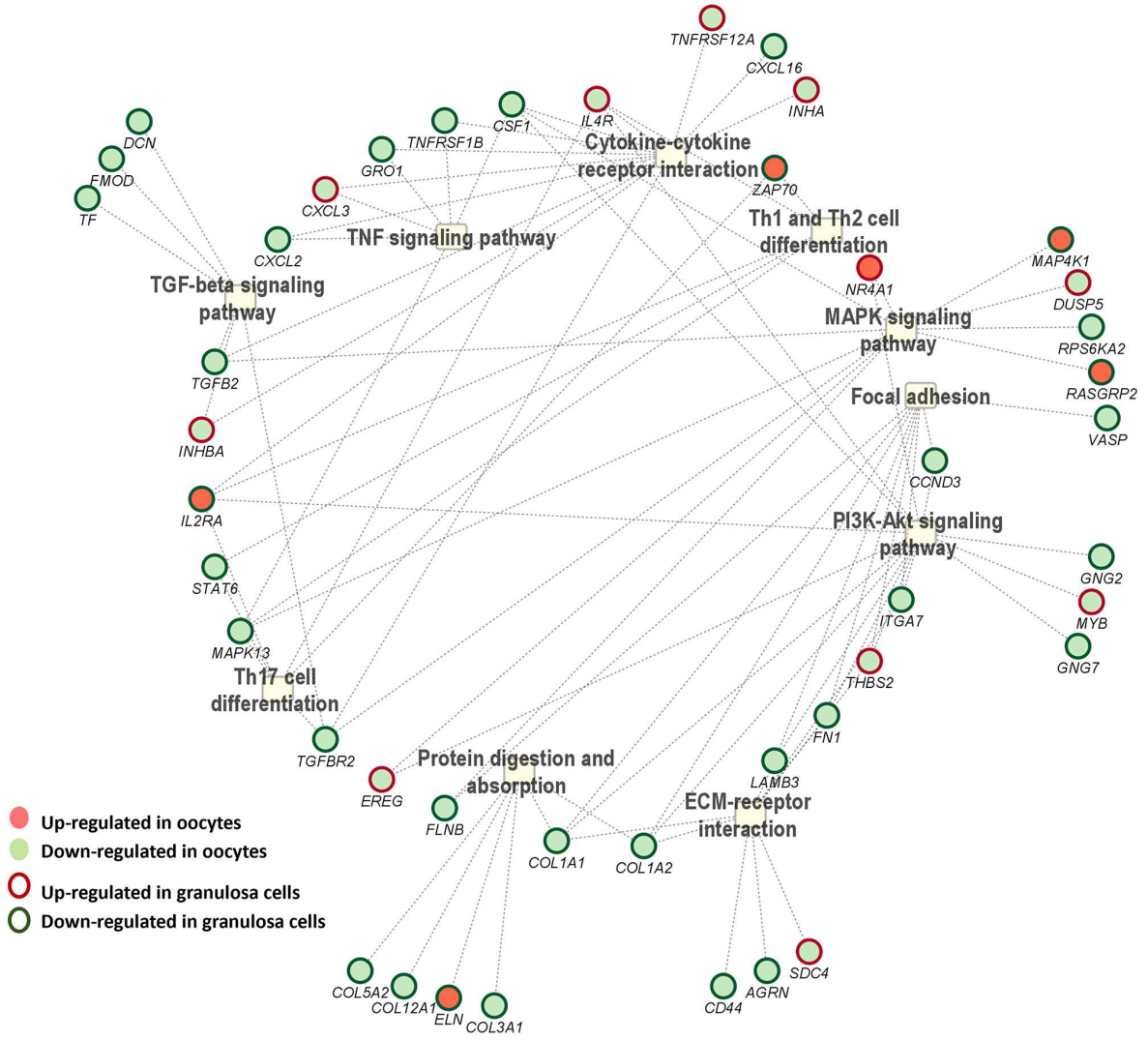


Fig. 9 Top pathways and the related commonly DEGs in the oocytes and granulosa cells in summer compared to winter groups

pathways. Accumulation of unfolded or misfolded proteins in the endoplasmic reticulum due to various environmental stressors induced the onset of ER stress, which ultimately leads to cellular apoptosis [66]. One of the coordinated responses to accumulated unfolded protein in the ER is called unfolded protein response (UPR). Therefore, the upregulation of genes associated with protein processing in ER in the current study revealed that increased protein processing in the ER is one of the mechanisms in which granulosa cells respond to elevated environmental temperature.

Integration of the oocyte and granulosa cells transcriptome data revealed differential regulation of 127 genes in common with a similar direction of expression in both oocytes and granulosa cells in response to environmental temperature. The majority of the transcripts (114 genes) were found to be suppressed in both oocytes and granulosa cells collected during the summer season compared to the winter. Pathway analysis for these commonly suppressed transcripts due to thermal stress in oocytes and granulosa cells revealed their enrichment in several pathways associated with ovarian function, follicle and oocyte development (Fig. 10). The involvement of the *TGF-beta* and *PI3K-Akt* pathways suggests alterations in cell growth, apoptosis, and metabolic processes, which are critical for follicular maturation and oocyte quality [53, 67]. Additionally, changes in focal adhesion and ECM-receptor interactions indicate potential disruptions in oocyte-follicle communication and intracellular signaling [68] due to the elevated summer temperature.

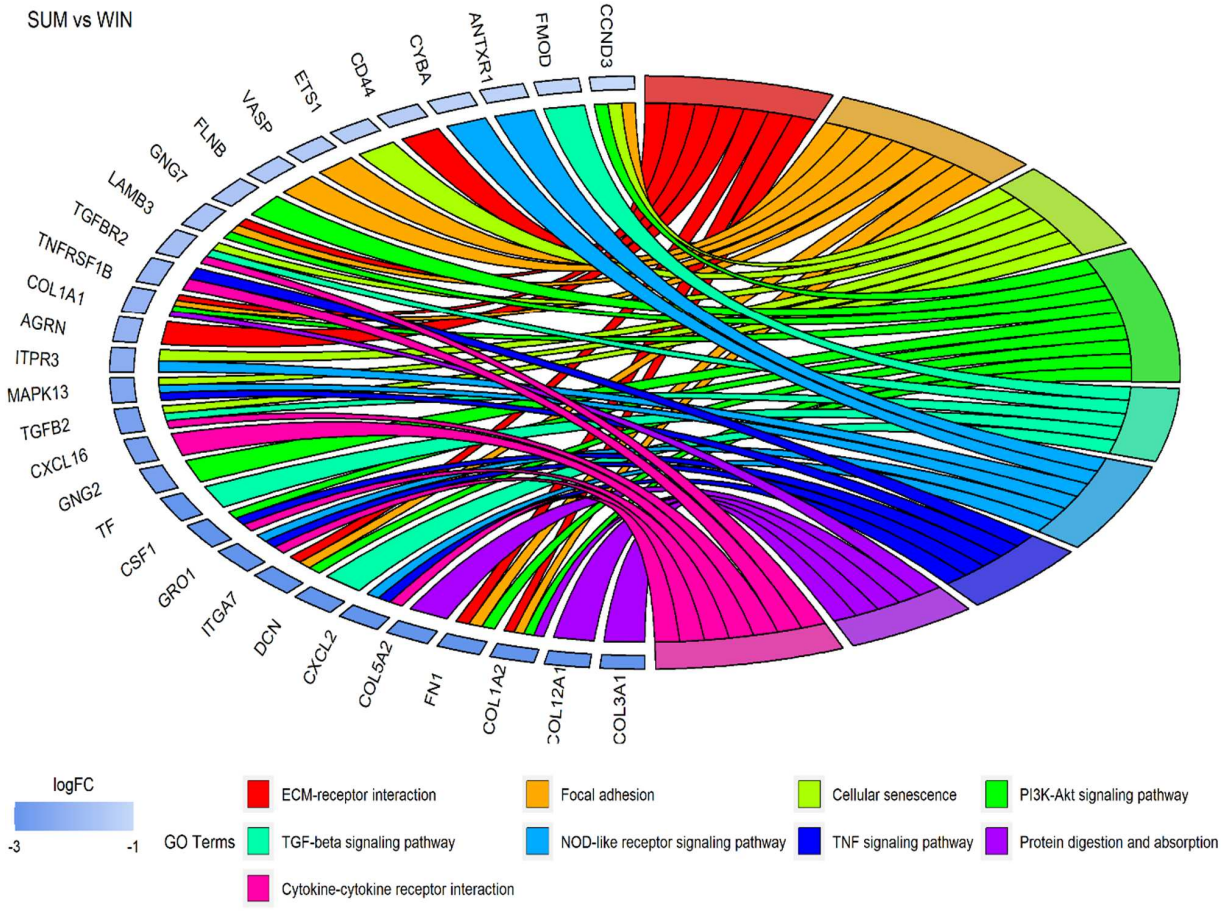


Fig. 10 Top pathways and the related DEGs which exhibited a downregulation in oocytes and granulosa cells in summer compared to winter groups

Investigating the functional consequences of these gene expression changes on further embryonic development in vivo could provide deeper insights into how environmental stressors affect reproductive efficiency. This is the first evidence indicating how follicular cells (granulosa cells) and gametes (oocytes) are affected by or respond to environmental elevated temperature in the ovarian follicle.

Conclusion

Our results indicate that cows exposed to seasonal fluctuations of heat stress dramatically alter their granulosa cells and oocytes transcriptome, which may in part be responsible for negatively impacting follicular physiology. Specified genes and their associated pathways and biological processes pose an essential function in bovine granulosa cells and oocytes' response to heat stress, potentially serving as mechanisms for future targets to mitigate the impact of heat stress within the intrafollicular environment.

Abbreviations

ANXA8L1	Annexin A8 Like 1
ATP6	Mitochondrially Encoded ATP Synthase Membrane Subunit 6
ATP8	Mitochondrially encoded ATP synthase membrane subunit 8
BP	Biological processes
C1QTNF5	C1q and TNF Related 5
C-MOS	Proto-Oncogene C-Mos
COCs	Cumulus-oocyte-complexes
COL3A1	Collagen Type III Alpha 1 Chain
COX1	Cytochrome C Oxidase I
COX3	Cytochrome C Oxidase III
CV	Coefficient of variation
DEGs	Differentially expressed genes
DNAH 1, 1, 5, 6, 7, 9, 10, 11, and 12	Dynein Axonemal Heavy Chains 1, 5, 6, 7, 9, 10, 11, and 12
DNAJB 11, 13, 14, and 90	DnaJ Heat Shock Protein Family (Hsp40) Members B11 B13, B14, and B90
DNAJC25	DnaJ Heat Shock Protein Family (Hsp40) Member C25
DRD5	Dopamine Receptor D5
ECM	Extracellular Matrix
EFNA3	Ephrin A3
EMP1	Epithelial Membrane Protein 1
EVs	Extracellular vesicles
FAWN	Florida Automated Weather Network

FDR	False discovery rate
FGF16	Fibroblast Growth Factor 16
GAPDH	Glyceraldehyde-3-Phosphate Dehydrogenase
GAST	Gastrin
GDF9	Growth Differentiation Factor 9
GEO	NCBI's Gene Expression Omnibus
GLM	Generalized Linear Model
GV	Germinal vesicle
Hsp40	DnaJ Heat Shock Protein Family
HSP70	Heat shock protein 70
HSP90	Heat shock protein 90
HSP90B1	Heat Shock Protein 90 Beta Family Member 1
HSPA5	Heat Shock Protein Family A (Hsp70) Member 5
HSPB1	Heat Shock Protein Family B (Small) Member 1
INHA	Inhibin Subunit Alpha
MAPK	Mitogen-activated protein kinase
MMP2	Matrix Metallopeptidase 2
ND1-6	NADH dehydrogenase subunits 1–6
OPU	Ovum Pick up
PCA	Principal component analysis
PI3K-AKT	Phosphoinositide 3-kinase (PI3K)–AKT pathway
POU5F1	POU Class 5 Homeobox 1
PPYR1	Pancreatic Polypeptide Receptor 1
qPCR	Quantitative real-time PCR
SRGN	Serglycin
TEAD4	TEA Domain Transcription Factor 4
TGF-beta	Transforming growth factor-β
THI	Temperature humidity index
TLX3	T Cell Leukemia Homeobox 3
TMEM26	Transmembrane Protein 26
TMM normalization	Trimmed mean of the M-values normalization method
TNF	Tumor necrosis factor
TNFRSF13B	TNF Receptor Superfamily Member 13B
TNFRSF8	TNF Receptor Superfamily Member 8
TNFSF4	TNF Superfamily Member 4
TPM	Transcripts per million
UBB	Ubiquitin B
UPR	Unformed protein response
VSX1	Visual System Homeobox 1
XCL1	X-C Motif Chemokine Ligand 1
ZP2	Zona Pellucida Glycoprotein 2

Supplementary Information

The online version contains supplementary material available at https://doi.org/10.1186/s13048-024-01530-0.

Supplementary Material 1

Acknowledgements
Kamryn Joyce was supported by a National Needs Fellowship from USDA (NIFA Grant 2021-38420-34067). The authors thank Jhon Fredy Rodriguez and Edna Ballesteros from Breeding Tech LLC (Madisonville – Texas) for their technical assistance in conducting the OPU procedures. Additionally, the authors thank the NFREC's Beef Unit crew for their assistance with this experiment.

Author contributions
Conceptualization: D.T., A.G.D.; Experimental work: K.J., A.G., N.G.M., S.G., D.H., G.D., M.C.L.D., J.B.; Data analysis: K.J., A.G, N.G.M., Interpretation of data: K.J., A.G., N.G.M. A.G.D.; Writing of original draft: K.J., A.G., N.G.M.; Manuscript editing: A.G., N.G.M., D.T., A.G.D.; Supervision: D.T., A.G.D.; Funding acquisition: D.T., A.G.D.; All authors have read and agreed to the published version of this manuscript.

Funding
Nothing to declare.

Data availability
The raw FASTQ files and processed CSV files of the RNA sequencing data have been deposited in the NCBIs Gene Expression Omnibus (GEO) repository with the accession numbers GSE235170 and GSE235171.

Declarations

Ethics approval and consent to participate
All procedures involving cows were approved by the Animal Care and Use committee of the University of Florida (Approval Number: IACUC202200000706).

Consent for publication
Not applicable.

Clinical trial number
Not applicable.

Footnotes
N/A.

Disclaimer
We declare that in part some of the results described in this manuscript were adapted from Kamryn Joyce's Master's Thesis.

Competing interests
The authors declare no competing interests.

Author details
[1]North Florida Research and Education Center, University of Florida, Marianna, FL 32446, USA
[2]Animal Reproduction and Biotechnology Laboratory, Department of Biomedical Sciences, Colorado State University, Fort Collins, CO 80523, USA
[3]Department of Animal Production, Faculty of Agriculture, Cairo University, Giza 12613, Egypt
[4]J.R. Simplot Company, 1099 W. Front St, Boise, ID 83702, USA
[5]Large Animal Clinical Sciences, College of Veterinary Medicine, University of Florida, Gainesville, FL 32610, USA

Received: 31 July 2024 / Accepted: 5 October 2024
Published online: 14 October 2024

References

1. Thornton P, Nelson G, Mayberry D, Herrero M. 2022. Impacts of heat stress on global cattle production during the 21st century: a modelling study. Lancet Planet Health. 2022;6:e192–e201. https://doi.org/10.1016/S2542-5196(22)00002-X
2. Fernandez-Novo A, Pérez-Garnelo SS, Villagrá A, Pérez-Villalobos N, Astiz S. The effect of stress on Reproduction and Reproductive Technologies in Beef Cattle-A review. Animals. 2020;10:2096–119. https://doi.org/10.3390/ani10112096.
3. Badinga L, Thatcher WW, Diaz T, Drost M, Wolfenson D. Effect of environmental heat stress on follicular development and steroidogenesis in lactating Holstein cows. Theriogenology. 1993;39:797–810. https://doi.org/10.1016/0093-691x(93)90419-6.
4. Khan A, Khan MZ, Umer S, Khan IM, Xu H, Zhu H, Wang Y. Cellular and molecular adaptation of bovine granulosa cells and oocytes under heat stress. Animals. 2020b;10:110. https://doi.org/10.3390/ani10010110.
5. Roth Z. Effect of heat stress on Reproduction in dairy cows: insights into the Cellular and molecular responses of the oocyte. Annu Rev Anim Biosci. 2017;5:151–70. https://doi.org/10.1146/annurev-animal-022516-022849.
6. Rocha A, Randel RD, Broussard JR, Lim JM, Blair RM, Roussel JD, Hansel W. High environmental temperature and humidity decrease oocyte quality in Bos taurus but not in Bos indicus cows. Theriogenology. 1998;49:657–65. https://doi.org/10.1016/s0093-691x(98)00016-8.

7. Payton RR, Rispoli LA, Nagle KA, Gondro C, Saxton AM, Voy BH, Edwards JL. Mitochondrial-related consequences of heat stress exposure during bovine oocyte maturation persist in early embryo development. J Reprod Dev. 2018;64:243–51. https://doi.org/10.1262/jrd.2017-160.
8. Li J, Gao H, Tian Z, Wu Y, Wang Y, Fang Y, Lin L, Han Y, Wu S, Haq IU, Zang S. Effects of chronic heat stress on granulosa cell apoptosis and follicular atresia in mouse ovary. J Anim Sci Biotechnol. 2016;7:57. https://doi.org/10.1186/s40104-016-0116-6.
9. Gad A, Joyce K, Menjivar NG, Heredia D, Rojas CS, Tesfaye D, Gonella-Diaza A. Extracellular vesicle-microRNAs mediated response of bovine ovaries to seasonal environmental changes. J Ovarian Res. 2023;16:101. https://doi.org/10.1186/s13048-023-01181-7.
10. International Embryo Technology Society. https://www.iets.org. Accessed 13 March 2023.
11. Florida Automated Weather Network (FAWN). https://fawn.ifas.ufl.edu/data/reports/. Accessed 10 January 2022.
12. NRC. A guide to environmental research on animals - National Research Council (US). Committee on Physiological Effects of Environmental Factors on Animals. Natl. Acad. Sci., Washington,DC; 1971.
13. Xie F, Xiao P, Chen D, Xu L, Zhang B. miRDeepFinder: a miRNA analysis tool for deep sequencing of plant small RNAs. Plant Mol Biol. 2012;80:75–84. https://doi.org/10.1007/s11103-012-9885-2.
14. Xie F, Wang J, Zhang B. RefFinder: a web-based tool for comprehensively analyzing and identifying reference genes. Funct Integr Genomics. 2023;23:125. https://doi.org/10.1007/s10142-023-01055-7.
15. Pfaffl MW. A new mathematical model for relative quantification in real-time RT-PCR. Nucleic Acids Res. 2001;29:e45. https://doi.org/10.1093/nar/29.9.e45.
16. Robinson MD, Oshlack A. A scaling normalization method for differential expression analysis of RNA-seq data. Genome Biol. 2010;11:R25. https://doi.org/10.1186/gb-2010-11-3-r25.
17. Hart T, Komori HK, LaMere S, Podshivalova K, Salomon DR. Finding the active genes in deep RNA-seq gene expression studies. BMC Genomics. 2013;14:778. https://doi.org/10.1186/1471-2164-14-778.
18. Benjamini Y, Hochberg Y. Controlling the false discovery rate: a practical and powerful approach to multiple testing. Royal Stati Soci: Ser B. 1995;57:289–300. https://doi.org/10.1111/j.2517-6161.1995.tb02031.x.
19. Database. for Annotation, Visualization, and Integrated Discovery (DAVID) Bioinformatics. http://david.abcc.ncifcrf.gov/. Accessed 23 May 2022.
20. Ogata H, Goto S, Sato K, Fujibuchi W, Bono H, Kanehisa M. KEGG: Kyoto Encyclopedia of genes and genomes. Nucleic Acids Res. 1999;27:29–34. https://doi.org/10.1093/nar/27.1.29.
21. LCI. Patterns of transit losses. Livestock Conservation, Inc. Omaha, NE; 1970.
22. St-Pierre NR, Cobanov B, Schnitkey G. Economic losses from heat stress by US livestock industries. J Dairy Sci. 2003;86:E52–77. https://doi.org/10.3168/jds.S0022-0302(03)74040-5.
23. Ingraham RH, Gillette DD, Wagner WD. Relationship of temperature and humidity to conception rate of Holstein cows in subtropical climate. J Dairy Sci. 1974;57:476–81. https://doi.org/10.3168/jds.S0022-0302(74)84917-9.
24. Dikmen S, Hansen PJ. Is the temperature-humidity index the best indicator of heat stress in lactating dairy cows in a subtropical environment? J Dairy Sci. 2009;92:109–16. https://doi.org/10.3168/jds.2008-1370.
25. Gaughan JB, Mader TL, Holt SM, Lisle A. A new heat load index for feedlot cattle. J Anim Sci. 2008;86:226–34. https://doi.org/10.2527/jas.2007-0305.
26. Brown-Brandl TM. Understanding heat stress in beef cattle. R Bras Zootec. 2018;47:e20160414. https://doi.org/10.1590/rbz4720160414.
27. Brown EJ, Vosloo A. The involvement of the hypothalamopituitary-adrenocortical axis in stress physiology and its significance in the assessment of animal welfare in cattle. Onderstepoort J Vet Res. 2017;84:e1–9. https://doi.org/10.4102/ojvr.v84i1.1398.
28. Christison GI, Johnson HD. Cortisol turnover in heat-stressed cows. J Anim Sci. 1972;35:1005–10. https://doi.org/10.2527/jas1972.3551005x.
29. Abilay TA, Mitra R, Johnson HD. Plasma cortisol and total progestin levels in Holstein steers during acute exposure to high environmental temperature (42 C) conditions. J Anim Sci. 1975;41:113–7. https://doi.org/10.2527/jas1975.411113x.
30. Chen S, Wang J, Peng D, Li G, Chen J, Gu X. Exposure to heat-stress environment affects the physiology, circulation levels of cytokines, and microbiome in dairy cows. Sci Rep. 2018. https://doi.org/10.1038/s41598-018-32886-1.
31. Kim WS, Ghassemi Nejad J, Peng DQ, Jung US, Kim MJ, Jo YH, Jo JH, Lee JS, Lee HG. Heat-shock proteins gene expression in peripheral blood mononuclear cells as an indicator of heat stress in beef calves. Animals. 2020;10:895. https://doi.org/10.3390/ani10050895.
32. Lindquist S. The heat-shock response. Annu Rev Biochem. 1986;55:1151–91. https://doi.org/10.1146/annurev.bi.55.070186.005443.
33. Hassan FU, Nawaz A, Rehman MS, Ali MA, Dilshad SMR, Yang C. Prospects of HSP70 as a genetic marker for thermo-tolerance and immuno-modulation in animals under climate change scenario. Anim Nutr. 2019;5:340–50. https://doi.org/10.1016/j.aninu.2019.06.005.
34. Al-Katanani YM, Paula-Lopes FF, Hansen PJ. Effect of season and exposure to heat stress on oocyte competence in Holstein cows. J Dairy Sci. 2002;85:390–6. https://doi.org/10.3168/jds.s0022-0302(02)74086-1.
35. Lenz RW, Ball GD, Leibfried ML, Ax RL, First NL. In vitro maturation and fertilization of bovine oocytes are temperature-dependent processes. Biol Reprod. 1983;29:173–9. https://doi.org/10.1095/biolreprod29.1.173.
36. Roth Z, Meidan R, Shaham-Albalancy A, Braw-Tal R, Wolfenson D. Delayed effect of heat stress on steroid production in medium-sized and preovulatory bovine follicles. Reproduction. 2001;121:745–51. https://doi.org/10.1530/rep.0.1210745.
37. NAHMS. Beef 2017: Beef Cow-Calf Management Practices in the United States. https://www.aphis.usda.gov/animal_health/nahms/beefcowcalf/downloads/beef2017/Beef2017_dr_PartI.pdf (2017). Accessed 1 Nov 2021.
38. Haouzi D, Boumela I, Chebli K, Hamamah S. Global, Survival, and apoptotic transcriptome during mouse and human early embryonic development. Biomed Res Int. 2018;2018:5895628. https://doi.org/10.1155/2018/5895628.
39. De Hauwer C, Camby I, Darro F, Migeotte I, Decaestecker C, Verbeek C, Danguy A, Pasteels JL, Brotchi J, Salmon I, Van Ham P. Gastrin inhibits motility, decreases cell death levels, and increases proliferation in human glioblastoma cell lines. J Neurobiol. 1998;37:373–82. https://doi.org/10.1002/(sici)1097-4695(19981115)37:3%3C373::aid-neu3%3E3.3.co;2-8.
40. Dockray G, Dimaline R, Varro A. Gastrin: old hormone, new functions. Pflügers Archiv. 2005;449:344–55. https://doi.org/10.1007/s00424-004-1347-5.
41. Meng S, Shi C, Jia Y, Fu M, Zhang T, Wu N, Han H, Shen H. A combined clinical and specific genes' model to predict live birth for in vitro fertilization and embryo transfer patients. BMC Pregnancy Childbirth. 2023;23:702. https://doi.org/10.1186/s12884-023-05988-6.
42. Frisén J, Holmberg J, Barbacid M. Ephrins and their eph receptors: multitalented directors of embryonic development. EMBO J. 1999;18:5159–65. https://doi.org/10.1093/emboj/18.19.5159.
43. Vihanto MM, Plock J, Erni D, Frey BM, Frey FJ, Huynh-Do U. Hypoxia upregulates expression of eph receptors and ephrins in mouse skin. FASEB J. 2005;19:1689–91. https://doi.org/10.1096/fj.04-3647fje.
44. Buensuceso AV, Deroo BJ. The Ephrin Signaling Pathway regulates morphology and adhesion of mouse granulosa cells in Vitro. Biol Reprod. 2013;88:1–12. https://doi.org/10.1095/biolreprod.112.100123.
45. Wang X, Wang ZB, Luo C, Mao XY, Li X, Yin JY, Zhang W, Zhou HH, Liu ZQ. The prospective value of dopamine receptors on bio-behavior of tumor. J Cancer. 2019;10:1622–32. https://doi.org/10.7150/jca.27780.
46. Chermuła B, Brązert M, Jeseta M, Ożegowska K, Sujka-Kordowska P, Konwerska A, Bryja A, Kranc W, Jankowski M, Nawrocki MJ, Kocherova I, Celichowski P, Borowiec B, Popis M, Budna-Tukan J, Antosik P, Bukowska D, Brussow KP, Pawelczyk L, Bruska M, Zabel M, Nowicki M, Kempisty B. The Unique mechanisms of Cellular Proliferation, Migration and apoptosis are regulated through Oocyte Maturational Development-A Complete Transcriptomic and histochemical study. Int J Mol Sci. 2018;20(1):84. https://doi.org/10.3390/ijms20010084. PMID: 30587792; PMCID: PMC6337548.
47. Turathum B, Gao EM, Chian RC. The function of Cumulus cells in Oocyte Growth and Maturation and in subsequent ovulation and fertilization. Cells. 2021;10(9):2292. https://doi.org/10.3390/cells10092292. PMID: 34571941; PMCID: PMC8470117.
48. Gendelman M, Roth Z. In vivo vs. in vitro models for studying the effects of elevated temperature on the GV-stage oocyte, subsequent developmental competence and gene expression. Anim Reprod Sci. 2012;134:125–34. https://doi.org/10.1016/j.anireprosci.2012.07.009.
49. Ferreira RM, Chiaratti MR, Macabelli CH, Rodrigues CA, Ferraz ML, Watanabe YF, Smith LC, Meirelles FV, Baruselli PS. The infertility of repeat-breeder cows during summer is associated with decreased mitochondrial DNA and increased expression of mitochondrial and apoptotic genes in oocytes. Biol Reprod. 2016;94(3):66–1.
50. Yang WJ, Liu FC, Hsieh JS, Chen CH, Hsiao SY, Lin CS. Matrix metalloproteinase 2 level in human follicular fluid is a reliable marker of human oocyte maturation in in vitro fertilization and intracytoplasmic sperm injection cycles. Reprod Biol Endocrinol. 2015;13:102. https://doi.org/10.1186/s12958-015-0099-8.

51. Latorraca LB, Galvão A, Rabaglino MB, D'Augero JM, Kelsey G, Fair T. Single-cell profiling reveals transcriptome dynamics during bovine oocyte growth. BMC Genomics. 2024;25:335. https://doi.org/10.1186/s12864-024-10234-0.
52. Makker A, Mati Goel M, Mahdi AA. PI3K/PTEN/Akt and TSC/mTOR signaling pathways, ovarian dysfunction, and infertility: an update. J Mol Endocrinol. 2014;53(3):R102–18.
53. Kalous J, Aleshkina D, Anger M. A role of PI3K/Akt signaling in oocyte maturation and early embryo development. Cells. 2023;12(14):1830.
54. Andrade GM, Da Silveira JC, Perrini C, Del Collado M, Gebremedhn S, Tesfaye D, Meirelles FV, Perecin F. The role of the PI3K-Akt signaling pathway in the developmental competence of bovine oocytes. PLoS ONE. 2017;12(9):e0185045.
55. Eppig JJ. Intercommunication between mammalian oocytes and companion somatic cells. BioEssays. 1991;13:569–74. https://doi.org/10.1002/bies.950131105.
56. Kidder GM, Vanderhyden BC. Bidirectional communication between oocytes and follicle cells: ensuring oocyte developmental competence. Can J Physiol Pharmacol. 2010;88:399–413. https://doi.org/10.1139/y10-009.
57. Kampinga HH, Hageman J, Vos MJ, Kubota H, Tanguay RM, Bruford EA, Cheetham ME, Chen B, Hightower LE. Guidelines for the nomenclature of the human heat shock proteins. Cell Stress Chaperones. 2009;14:105–11. https://doi.org/10.1007/s12192-008-0068-7.
58. Hu C, Yang J, Qi Z, Wu H, Wang B, Zou F, Mei H, Liu J, Wang W, Liu Q. Heat shock proteins: Biological functions, pathological roles, and therapeutic opportunities. MedComm. 2022;3:e161. https://doi.org/10.1002/mco2.161.
59. Khan A, Dou J, Wang Y, Jiang X, Khan MZ, Luo H, Usman T, Zhu H. Evaluation of heat stress effects on cellular and transcriptional adaptation of bovine granulosa cells. J Anim Sci Biotechnol. 2020a;11:25. https://doi.org/10.1186/s40104-019-0408-8.
60. Sammad A, Luo H, Hu L, Zhu H, Wang Y. Transcriptome reveals granulosa cells coping through redox, inflammatory and metabolic mechanisms under acute heat stress. Cells. 2022;11:1443. https://doi.org/10.3390/cells11091443.
61. Li MG, McGrail M, Serr M, Hays TS. Drosophila cytoplasmic dynein, a microtubule motor that is asymmetrically localized in the oocyte. J Cell Biol. 1994;126:1475–94. https://doi.org/10.1083/jcb.126.6.1475.
62. Kehoe S, Jewgenow K, Johnston PR, Mbedi S, Braun BC. Signalling pathways and mechanistic cues highlighted by transcriptomic analysis of primordial, primary, and secondary ovarian follicles in domestic cat. Sci Rep. 2021;11:2683. https://doi.org/10.1038/s41598-021-82051-4.
63. Nagamatsu G, Shimamoto S, Hamazaki N, Nishimura Y, Hayashi K. Mechanical stress accompanied with nuclear rotation is involved in the dormant state of mouse oocytes. Sci Adv. 2019;5:eaav9960. https://doi.org/10.1126/sciadv.aav9960.
64. Sakatani M, Yamanaka K, Balboula AZ, Takenouchi N, Takahashi M. Heat stress during in vitro fertilization decreases fertilization success by disrupting anti-polyspermy systems of the oocytes. Mol Reprod Dev. 2015;82:36–47. https://doi.org/10.1002/mrd.22441.
65. Báez F, Camargo Á, Reyes AL, Márquez A, Paula-Lopes F, Viñoles C. Time-dependent effects of heat shock on the zona pellucida ultrastructure and in vitro developmental competence of bovine oocytes. Reprod Biol. 2019;19(2):195–203.
66. Tabas I, Ron D. Integrating the mechanisms of apoptosis induced by endoplasmic reticulum stress. Nat Cell Biol. 2011;13(3):184–90.
67. Patton BK, Madadi S, Pangas SA. Control of ovarian follicle development by TGF-β family signaling. Curr Opin Endocr Metabolic Res. 2021;18:102–10.
68. McGinnis LK, Kinsey WH. Role of focal adhesion kinase in oocyte-follicle communication. Mol Reprod Dev. 2015;82(2):90–102.
69. Hooper HB, Titto CG, Gonella-Diaza AM, Henrique FL, Pulido-Rodríguez LF, Longo ALS, Leme-Dos-Santos TMDC, Geraldo ACAPM, Pereira AMF, Binelli M, Balieiro JCC, Titto ELA. Heat loss efficiency and HSP gene expression of Nellore cows in tropical climate conditions. Int J Biometeorol. 2019;63:1475–86. https://doi.org/10.1007/s00484-018-1576-5.
70. Bettegowda A, Patel OV, Ireland JJ, Smith G. Quantitative analysis of messenger RNA abundance for ribosomal protein L-15, cyclophilin-A, phosphoglycerokinase, β-glucuronidase, glyceraldehyde 3-phosphate dehydrogenase, β-actin, and histone H2A during bovine oocyte maturation and early embryogenesis. Mol Reprod Dev. 2006;73:267–78. https://doi.org/10.1002/mrd.20333.

Publisher's note

Springer Nature remains neutral with regard to jurisdictional claims in published maps and institutional affiliations.